XXVIII Congress of the Polish Physiological Society

Gdańsk, September 15-17 2021

Poster book

HONORARY PATRONAGE

Prof. dr Marcin Gruchała
Rector of the Medical University of Gdansk

Uniwersytet Gdański

Prof. dr Piotr Stepnowski
Rector of the University of Gdansk

WOJEWODA POMORSKI
DARIUSZ DRELICH

Dariusz Drelich
Governor of the Pomeranian Voivodeship

HONORARY PATRONAGE
Mayor of the City of Gdańsk

Aleksandra Dulkiewicz
Mayor of Gdansk

Mieczysław Struk
Marshal of the Pomeranian Voivodeship

PARTNER

PAN
POLSKA AKADEMIA NAUK

ANIMA LAB
animal facility and laboratory equipment • animal research models

FUNDACJA LOTOS

Medical University of Gdansk
Department of Physiology

XXVIII Congress of the Polish Physiological Society

Gdańsk, September 15-17 2021

Poster book

SESSION I

MUSCLE FUNCTION. MUSCLE EXERCISE

HONORARY PATRONAGE

Prof. dr Marcin Gruchała
Rector of the Medical University of Gdansk

Uniwersytet Gdański

Prof. dr Piotr Stepnowski
Rector of the University of Gdansk

WOJEWODA POMORSKI
DARIUSZ DRELICH

Dariusz Drelich
Governor of the Pomeranian Voivodeship

HONORARY PATRONAGE
Mayor of the City of Gdańsk

Aleksandra Dulkiewicz
Mayor of Gdansk

Mieczysław Struk
Marshal of the Pomeranian Voivodeship

PARTNER

PAN
POLSKA AKADEMIA NAUK

ANIMA LAB
animal facility and laboratory equipment • animal research models

FUNDACJA LOTOS

Medical University of Gdansk
Department of Physiology

THE FACTORS THAT MODULATE GROWTH HORMONE RESPONSES TO A PHYSICAL EFFORT

Benedykt H. Opaszowski
Department of Endocrinology, Institute of Sport-National Research Institute, Warsaw.

Exercise is a strong stimulator of growth hormone secretion (GH). Its increase release takes place during increased anaerobic processes, large O_2 deficit and oxygen debt. The GH response mechanism is complex. Data indicate, that a crucial contribution to exercise response of GH have the adrenergic and cholinergic systems. This research aimed to assess an impact of “warm up” and cholinergic preparation on the GH response to exercise.

Material & methods

Eight students of age 22-25 and VO_2 max 5,019±0,301 l O_2/min volunteered in this study. They performed 3 separated supramaximal runs on a treadmill (22 km/h) until exhaustion, without information about the time completing of the effort. On the first visit the effort was preceded by 10-min warm-up. On the two next visits prior to the efforts without warm-up, placebo or cholinergic preparation (DMAE) were administered in a randomized order. Physiological parameters, such as: like heart rate (HR), oxygen uptake (VO_2), O_2 deficit and oxygen debt were recorded. Pre- and post-effort capillary blood were sampled for determination of lactate and GH levels.

Results

Run “ad maximum” lasted on average 132 s with placebo, 146 s with cholinergic preparation and 149 s with warm-up. It was found, that the longer the time, the higher contribution the aerobic processes. The effort with warm up was characterized by the lower O_2 deficit as compared to two other runs. The highest lactate peak was recorded after run with cholinergic preparation - 14,8 mm, followed by placebo - 13,7 mM and with warm up - 12,6 mM. GHmax concentration. after the "ad maximum" run without warm-up was 63,4 µU/ml, with cholinergic preparation 47,4 µU/ml and with the warm-up 32 µU/ml and appropriate areas under curves (AUCs) were 2462, 2055 and 1597 µU×min × ml^{-1}. GH correlated with O_2 deficit (r = 0,656), with LA (r = 0,866) and GHmax with time of run. (r = - 0,880).

Results are expressed in terms of mean

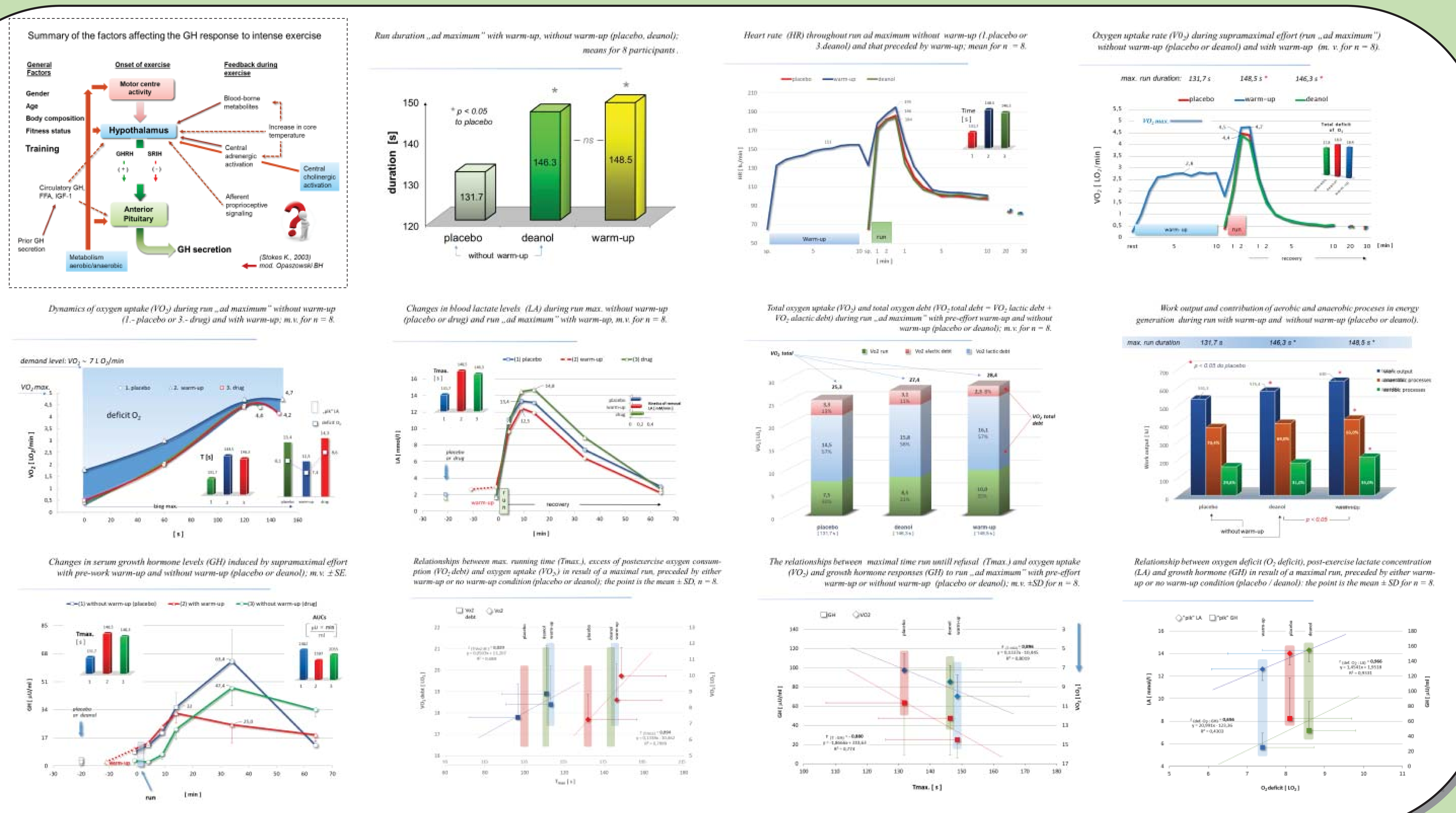

Summary & conclusion

Warm-up and DMAE reduce the exercise response of growth hormone after supramaximal exertion. Submaximal warm-up performed prior to supramaximal effort increases oxygen availability, activates oxidative processes and cholinergic system, thus in turn moderates GH response to supramaximal effort and protects the "secretory reserve" of the pituitary gland.

1. *Stokes K.*, Growth Hormone & IGF Research, vol. 13, Issue 5., *October 2003.* ***2.*** *Eugenio E. Muller, Physiol. Reviews, vol. 67, No 8, July 1987.* ***3.*** *Truls Raastad at all, Eur J. Appl Physiol (2000) 82.* ***4.*** *Hunter WM, Proc. Nutr. Soc. (1972), 31,199.*

EFFECT OF S-EQUOL, SELECTIVE ESTROGEN RECEPTOR β AGONISTS, ON MDX MUSCLE FIBERS

[1]Felipe Figueiredo, [1]Fabio Yoshimura, [1]João Suh, [1]Arthur Silva Neto, [2]Fernando Fonseca, [1]David Feder, [1]Monica Sato, [3]Tulio Hermes

[1]Dept. Morphology and Physiology, Centro Universitario FMABC, Santo Andre, SP, Brazil, [2]Laboratory of Clinical Analysis, Centro Universitario FMABC, Santo Andre, SP, Brazil, [3]Dept. Anatomy, Federal University of Alfenas (UNIFAL-MG), Alfenas, MG, Brazil. tulio.ah13@gmail.com

Session I: Muscle Function. Muscle Exercise

INTRODUCTION

Duchenne muscular dystrophy (DMD) is the most prevalent human dystrophinopathy. It is a recessive disease characterized by progressive and irreversible degeneration of the skeletal striated musculature. As a X chromosome-linked disease, it is more common in males, affecting approximately 1 in every 3500-6000 live births.

AIM

We investigated the effects of S-equol, a selective ligand for estrogen receptor (ER)- β, on muscle fibers of mdx mice.

METHODS

Mdx mice (14-days-old) were randomly divided in groups: treated with S-equol (20 mg/kg dissolved in DMSO, i.p.), DMSO (vehicle, i.p.), and control group (without drug treatment). After 14 days of daily treatment, the animals were euthanized with an overdose of isoflurane for morphological analyzes of different skeletal muscles.

Skeletal muscles analysed: brachial biceps (BB), quadriceps (QUA), long digital extender (EDL), anterior tibial (TA), sternocleidomastoid (STN), diaphragram (DIA).

Histological analysis: the skeletal muscles were frozen and maintained in an ultrafreezer at -80º C. The tissues were sliced in a cryostat (8 µm) and stained with hematoxylin-eosin. The different skeletal muscle slices were analysed in a light field microscope (Eclipse E-200, Nikon, Tokyo, Japan).

EXPERIMENTAL PROTOCOL

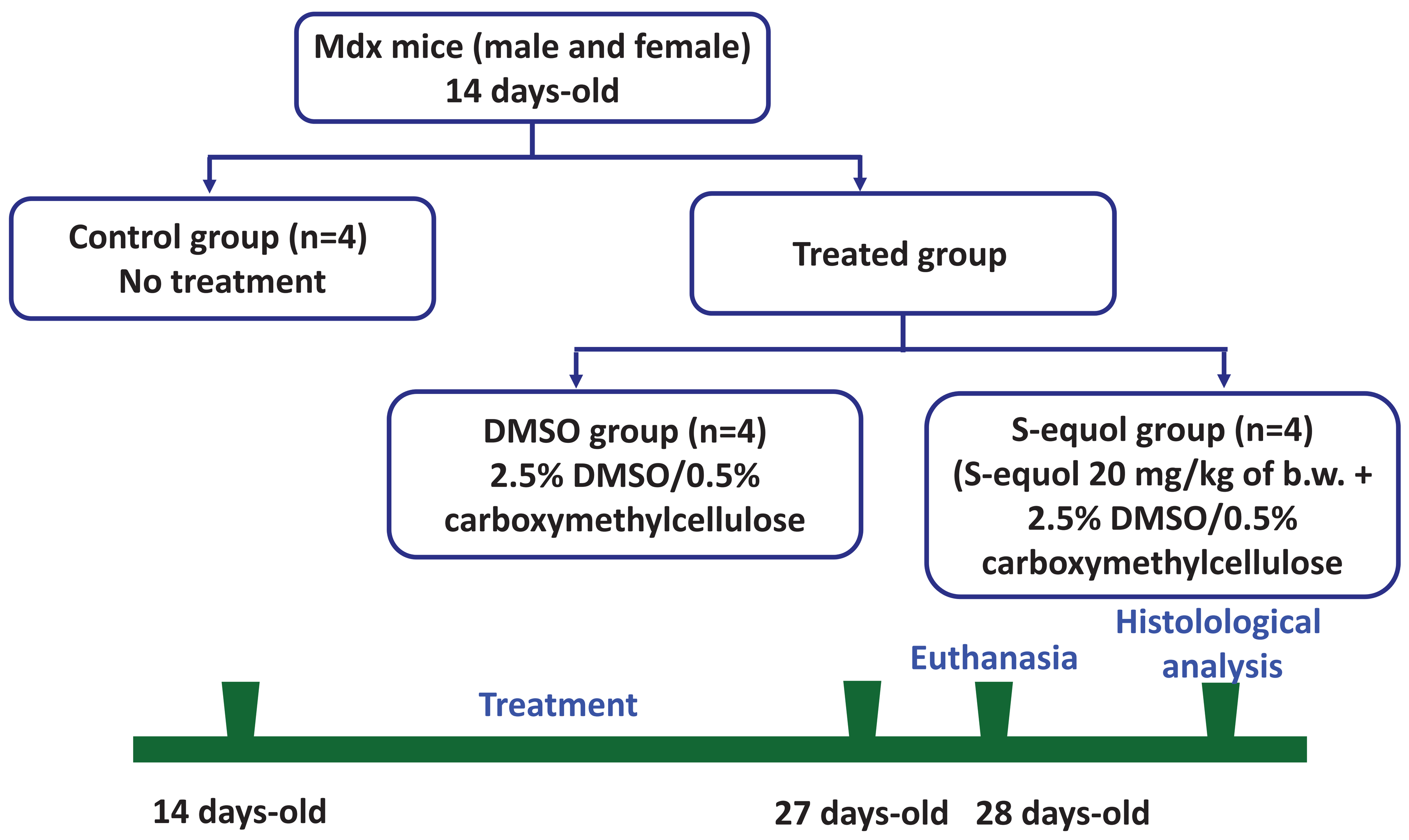

RESULTS

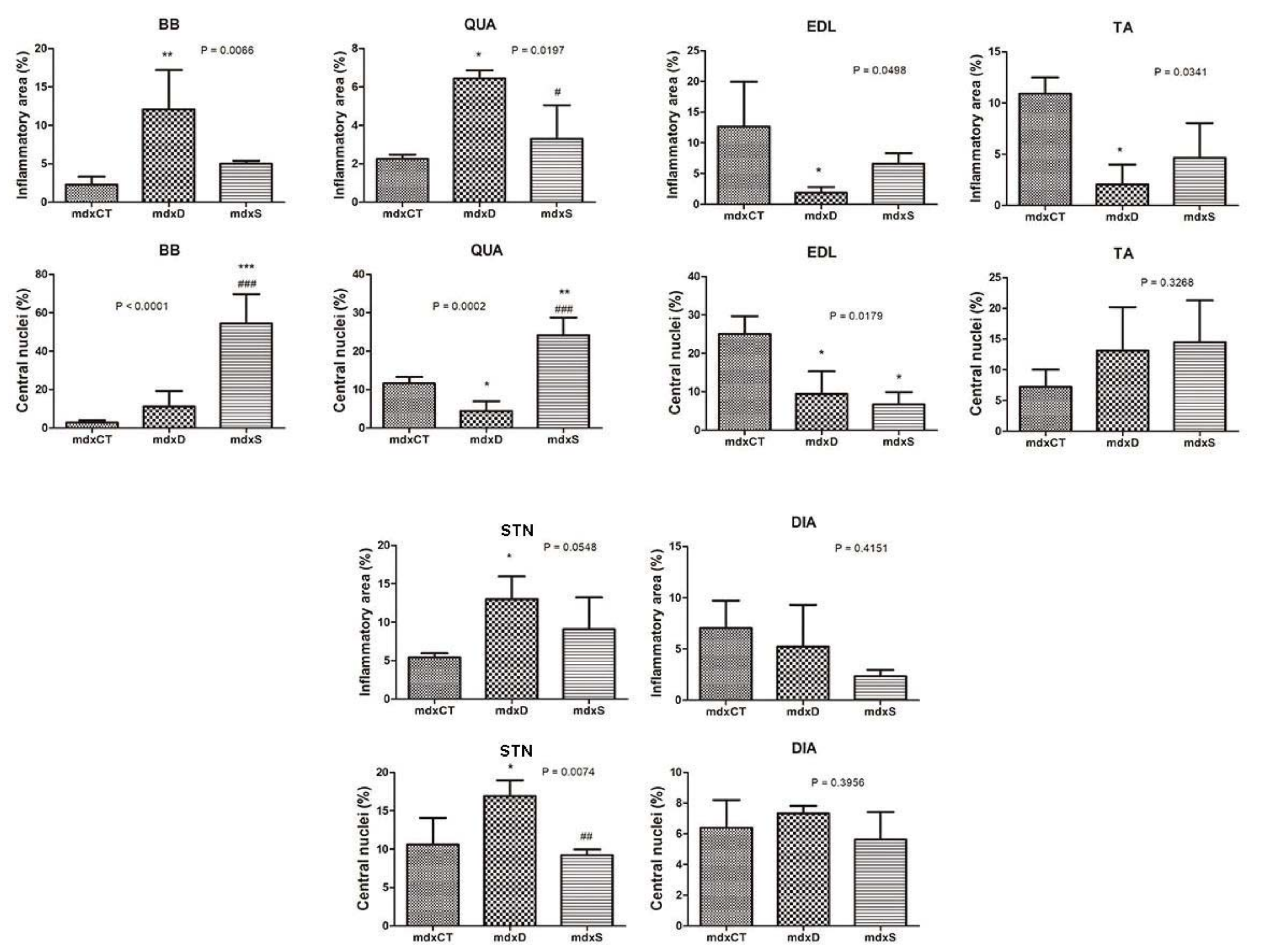

Figure 1: Percentage of inflammatory area (%) and central nuclei (%) in the brachial biceps (BB), quadriceps (QUA), long digital extender (EDL), anterior tibial (TA), sternocleidomastoid (STN), diaphragram (DIA) muscles slices in control mdx (mdx CT), treated with DMSO (mdx D) and treated with S-equol (mdx S).

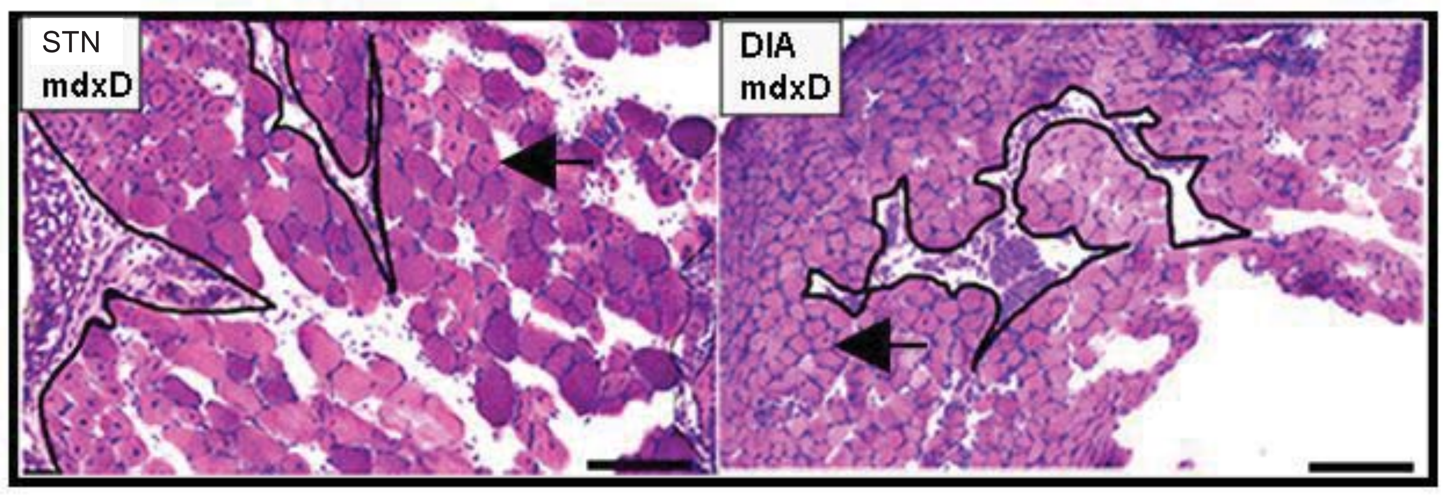

Figure 2: Photomicrograph showing the central nucleus in the sternocleidomastoid (STN) and diaphragram (DIA) muscles slices in a mdx treated with DMSO (mdx D). Bar 100um.

CONCLUSION

Both S-Equol and DMSO treatments reduced muscle fiber degeneration. Although the positive results were not observed in all skeletal muscle studied, either S-equol or DMSO can be promising in the treatment of DMD, suggesting a possible novel therapeutic approach, given the current lack of satisfactory treatments and its several adverse effects

REFERENCES

1. Schmalbruch, H. (1982). "Skeletal muscle fibers of newborn rats are coupled by gap junctions." Dev Biol **91**(2): 485-490.
2. Biggar, W. D., H. J. Klamut, P. C. Demacio, D. J. Stevens and P. N. Ray (2002). "Duchenne muscular dystrophy: current knowledge, treatment, and future prospects." Clin Orthop Relat Res(401): 88-106.
3. Ohlendieck, K. and K. P. Campbell (1991). "Dystrophin constitutes 5% of membrane cytoskeleton in skeletal muscle." FEBS Lett **283**(2): 230-234
4. Bogdanovich, S., K. J. Perkins, T. O. Krag and T. S. Khurana (2004). "Therapeutics for Duchenne muscular dystrophy: current approaches and future directions." J Mol Med (Berl) **82**(2): 102-11.
5. Engel, A. G., M. Yamamoto and K. H. Fischbeck (1998). Distrophinopathies. Myology: Basic and Clinical. A. G. Engel and C. Franzini-Armstrong. New York, McGraw-Hill. **2:** 1133-1187.

ACKNOWLEDGMENTS

NEPAS (Núcleo de Estudos, Pesquisa e Assessoria à Saúde)

Functional outcomes of distal radius fractures managed with various methods of fracture stabilization

Jarosław Olech[1], Grzegorz Konieczny[2], Piotr Morasiewicz[3]

1 - Provincial Specialist Hospital in Legnica, Orthopedic Surgery Department, Legnica, Poland
2 - Faculty of Health Sciences and Physical Education, The Witelon State University of Applied Sciences in Legnica, Legnica, Poland
3 - University of Opole, Department of Orthopaedic and Trauma Surgery, University Hospital in Opole, Institute of Medical Sciences, Opole, Poland

Introduction and objective

Distal radius fractures (DRF) pose a serious problem due to their high incidence. The risk of distal radius fracture has been reported as 9–139/10,000 people per year. Depending on fracture morphology, distal fractures of the radius can be treated with various methods. The purpose of our study was to assess the functional parameters following distal radius fractures treatment with three different fracture stabilization methods.

Material and methods

50 patients (33 women and 17 men), the mean age at the beginning of treatment was 56.5years. The mean duration of follow-up was 2 years and 8 months. The first subgroup (n=14) were **the patients treated with volar plating**, another subgroup (n=23) were **the patients with cast immobilization** and the third subgroup (n=13) were **the patients treated with closed reduction and K-wire fixation**.

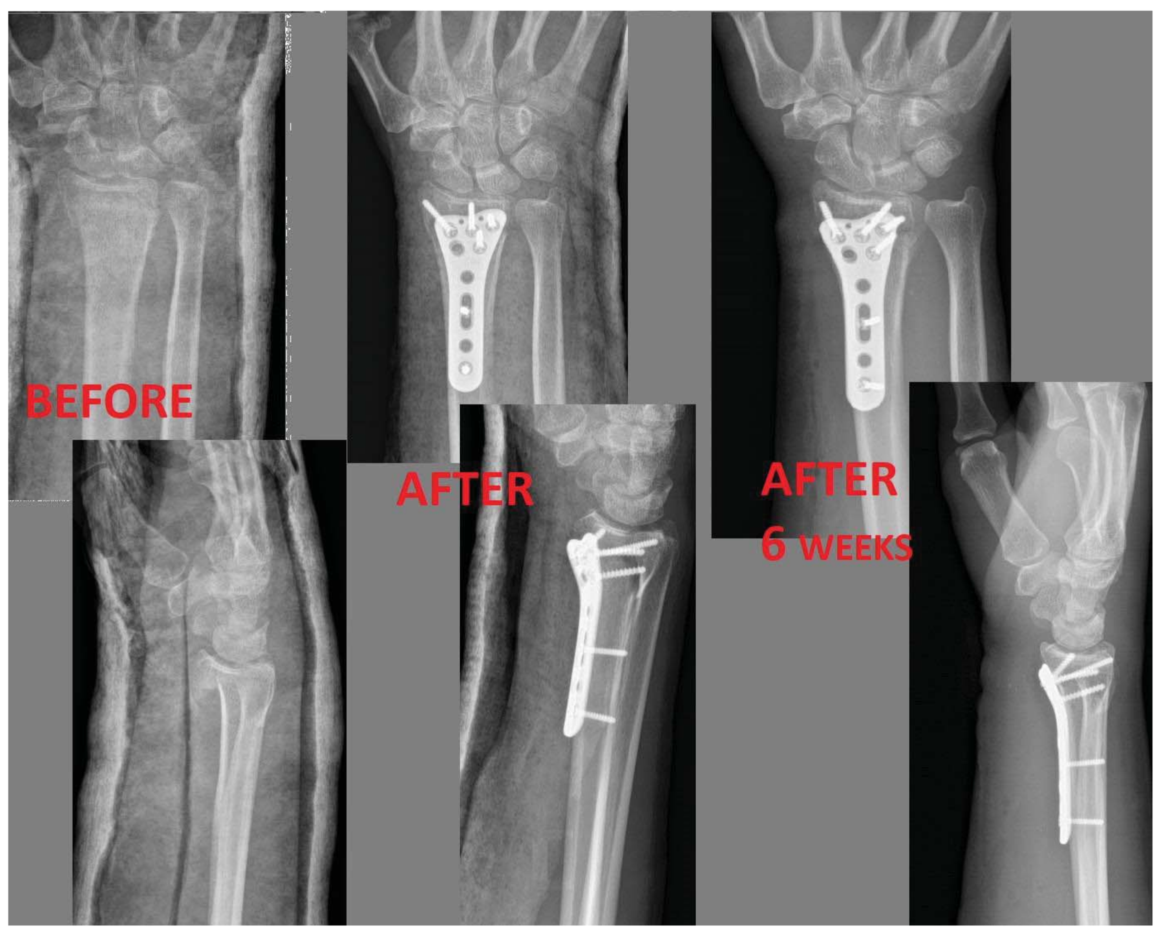

Fig. 1. Patient with volar plate fixation.

Fig. 2. Patient with K-wire fixation.

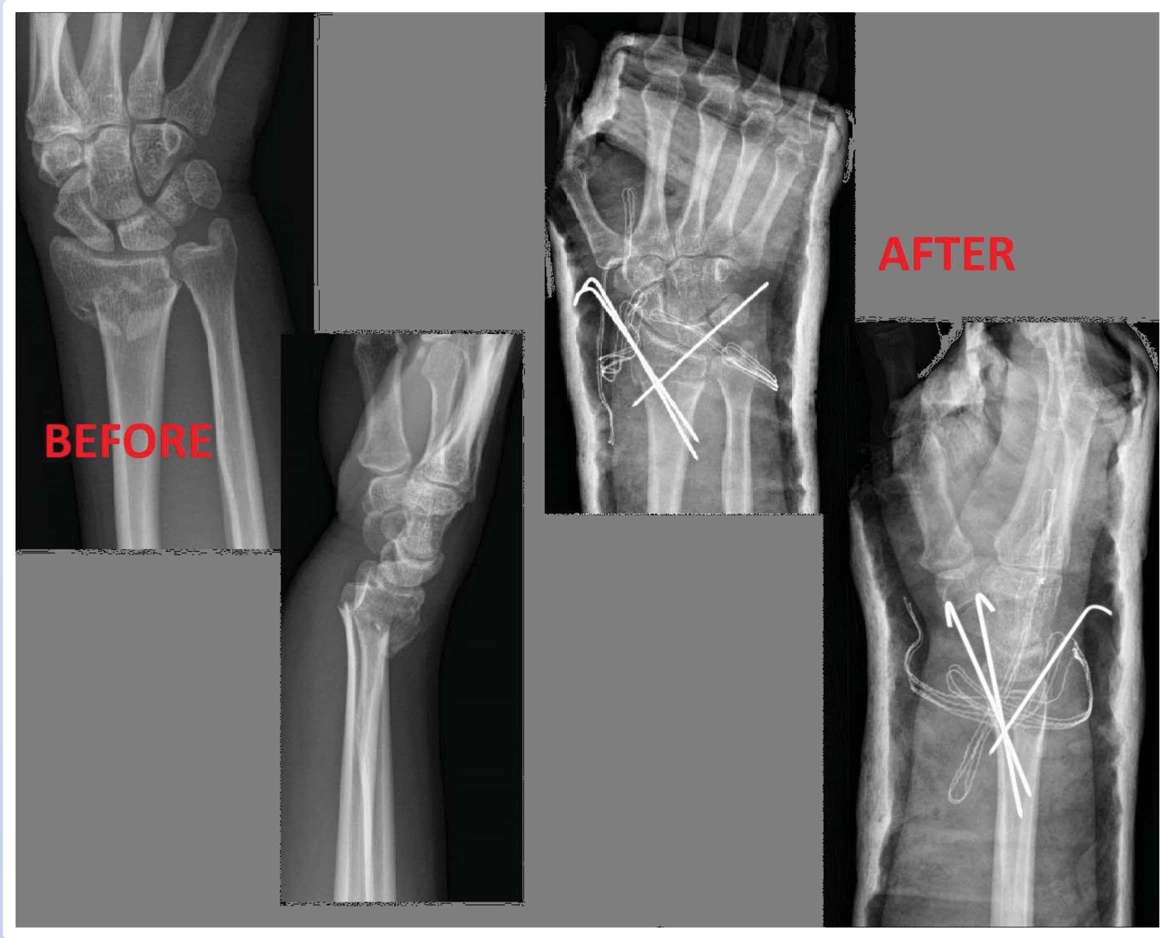

Fig. 3. Patient with cast stabilization.

We assessed: 1) **muscle strength** (dynamometer), 2) **range of motion** (digital inclinometr), 3) **pain severity** (VAS).

Fig. 4.Hand dynamometer.

Fig. 5. Digital inclinometer.

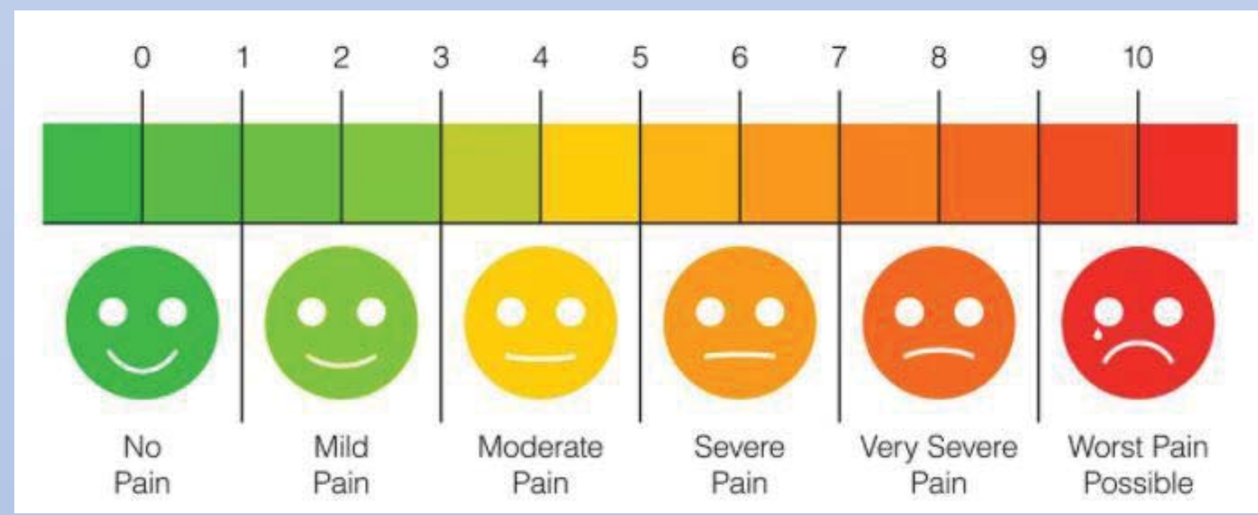

Fig. 6. Visual Analogue Scale.

Results

The mean relative grip power values in the volar-plate, cast and K-wire subgroups were 56%, 79% and 56% respectively. These differences were statistically significant (p = 0.0028). The best range of flexion (75.7°) was achieved in the cast subgroup and the most limited flexion (59.9°) was observed in the volar-plate subgroup. By far the lowest pain severity was reported by patients in the volar-plate subgroup (VAS score of 1.9). The most severe pain was reported by patients from the K-wire group (score 4.1), whereas the patients from the cast subgroup rated their pain severity as 3.

Conclusions

The greatest muscle strength in the affected limb, similar to that in the uninjured limb and the greatest mean range of wrist flexion was achieved in the cast subgroup. The lowest pain severity was reported in the volar-plate subgroup. **The best functional outcomes were achieved in the cast subgroup**.

References

1. Kwon HY, Kim HH, Sung YK, Ha YC. Incidence and Mortality of Osteoporotic Fracture in Rheumatoid Arthritis in South Korea Using Nationwide Claims Data. J Bone Metab. 2019, 97-104. doi: 10.11005/jbm.2019.26.2.97. **2.** Ogunleye AA, Mullner DF, Skochdopole A, Armstrong M, Herrera FA. Remote Injuries and Outcomes After Distal Radius Fracture Management. Hand (N Y). 2019, 1, 102-6. doi: 10.1177/1558944718798838. **3.** Ochi K, Go Y, Furuya T, Ikari K, Taniguchi A, Yamanaka H, Momohara S. Risk factors associated with the occurrence of distal radius fractures in Japanese patients with rheumatoid arthritis: a prospective observational cohort study. Clin Rheumatol. 2014, 33, 477-83. doi: 10.1007/s10067-013-2415-z. **4.** Ali M, Eiriksdottir A, Murtadha M, Åkesson A, Atroshi I. Incidence of distal radius fracture in a general population in southern Sweden in 2016 compared with 2001. Osteoporos Int. 2020, Jan 13. doi: 10.1007/s00198-020-05282-7. **5.** Talmaç MA, Görgel MA, Kanar M, Tok O, Özdemir HM. Comparison of three surgical methods in the treatment of intraarticular comminuted distal radius fractures: Volar locking plate, non-bridging external fixator, and bridging external fixator. Eklem Hastalik Cerrahisi. 2019, 30, 224-32. doi: 10.5606/ehc.2019.66955. **6.** Chung KC, Malay S, Shauver MJ, Kim HM. WRIST Group. Assessment of Distal Radius Fracture Complications Among Adults 60 Years or Older: A Secondary Analysis of the WRIST Randomized Clinical Trial. JAMA Netw Open. 2019, 2:e187053. doi: 10.1001/jamanetworkopen.2018.7053. **7.** Katayama T, Ono H, Omokawa S. Comparison of Five Years Clinical and Radiological Outcomes between Progressive and Non-Progressive Wrist Osteoarthritis after Volar Locking Plate Fixation of Distal Radius Fractures. J Hand Surg Asian Pac Vol. 2019, 24, 30-5. doi: 10.1142/S2424835519500061. **8.** Lameijer CM, Ten Duis HJ, Dusseldorp IV, Dijkstra PU, van der Sluis CK. Prevalence of posttraumatic arthritis and the association with outcome measures following distal radius fractures in non-osteoporotic patients: a systematic review. Arch Orthop Trauma Surg. 2017, 137,1499-513. doi: 10.1007/s00402-017-2765-0. **9.** Toon DH, Premchand RAX, Sim J, Vaikunthan R. Outcomes and financial implications of intra-articular distal radius fractures: a comparative study of open reduction internal fixation (ORIF) with volar locking plates versus nonoperative management. J Orthop Traumatol.2017, 18,229-34. doi: 10.1007/s10195-016-0441-8. **10.** Rundgren J, Bojan A, Mellstrand Navarro C, Enocson A. Epidemiology, classification, treatment and mortality of distal radius fractures in adults: an observational study of 23,394 fractures from the national Swedish fracture register. BMC Musculoskelet Disord. 2019, 21, 88. doi: 10.1186/s12891-020-3097-8. **11.** Hevonkorpi TP, Launonen AP, Huttunen TT, Kannus P, Niemi S, Mattila VM. Incidence of distal radius fracture surgery in Finns aged 50 years or more between 1998 and 2016 - too many patients are yet operated on? BMC Musculoskelet Disord. 2018, 19, 70. doi: 10.1186/s12891-018-1983-0. 12. Jennifer L. Kelsey, PhD and Elizabeth J. Samelson. Variation in Risk Factors for Fractures at Different Sites. Curr Osteoporos Rep. 2009, 7, 127–33. **13.** Ardouin L, Durand A, Gay A, Leroy M . Why do we use arthroscopy for distal radius fractures? Eur J Orthop Surg Traumatol.2018, 28, 1505-14. doi: 10.1007/s00590-018-2263-2. **14.** Lameijer CM, Ten Duis HJ, Vroling D, Hartlief MT, El Moumni M, van der Sluis CK. Prevalence of posttraumatic arthritis following distal radius fractures in non-osteoporotic patients and the association with radiological measurements, clinician and patient-reported outcomes. Arch Orthop Trauma Surg.2018, 138, 1699-712. doi: 10.1007/s00402-018-3046-2. **15.** Saving J, Enocson A, Ponzer S, Mellstrand Navarro C. External Fixation Versus Volar Locking Plate for Unstable Dorsally Displaced Distal Radius Fractures-A 3-Year Follow-Up of a Randomized Controlled Study. J Hand Surg Am.2019, 44, 18-26. doi: 10.1016/j.jhsa.2018.09.015. **16.** Shimura H, Nimura A, Fujita K, Miyamoto T. Mid-Term Functional Outcome after Volar Locking Plate Fixation of Distal Radius Fractures in Elderly Patients. J Hand Surg Asian Pac Vol. 2018, 23, 238-42. doi: 10.1142/S2424835518500273. **17.** Fan J, Jiang B, Yuan F, Li SZ, Zhou JQ, Mei J, Cheng LM, Yu GR. Clinical effect of compound internal fixations in treating extreme distal radial fractures. Zhonghua Wai Ke Za Zhi.2016, 54, 766-71. doi: 10.3760/cma.j.issn.0529-5815.2016.10.009. **18.** Karantana A, Scammell BE, Davis TR, Whynes DK. Cost-effectiveness of volar locking plate versus percutaneous fixation for distal radial fractures: Economic evaluation alongside a randomised clinical trial. Bone Joint J. 2015, 97-B, 1264-70. doi: 10.1302/0301-620X.97B9.35560. **19.** Erhart S, Schmoelz W, Lutz M. Clinical and biomechanical investigation of an increased articular cavity depth after distal radius fractures: effect on range of motion, osteoarthrosis and loading patterns. Arch Orthop Trauma Surg.2013, 133, 1249-55. doi: 10.1007/s00402-013-1787-5.

CHANGES IN SERUM LIPID PROFILE CAUSED BY FASTING AND PHYSICAL EXERCISE

KAROL PILIS, ADRIANNA KOSIOR-LARA, KAROL LESZCZYŃSKI, ANNA PILIS
Department of Health Sciences, Jan Dlugosz University in Czestochowa, Poland; corresponding- author-k.pilis@ujd.edu.pl

Introduction

The serum lipid profile is most often performed to predict the risk of cardiovascular disease (CVD) in patients (Louter et al. 2020). It should be noted that this profile should always be considered together as a complete lipid profile and less attention is paid to the analysis of the individual fractions, although it is indicated that only an increased concentration of high-density lipoprotein cholesterol (Ch-HDL) leads to a reduction in the risk of CVD and a reduction in mortality due to cerebrovascular. (Wood et al. 2006, Freedman et al. 2001). It is also postulated that total cholesterol/ high-density lipoprotein cholesterol (Ch-T / Ch-HDL), low-density lipoprotein cholesterol/ high-density lipoprotein cholesterol (Ch-LDL / Ch-HDL) ratios are better CVD risk indicators than Ch-T or Ch-LDL concentrations (Mensink et al. 2006, Natarajan et al. 2003). It was also noted that the type of diet and exercise used had a significant impact on endothelial disfunction (Tyldum et al. 2009). However, there are no studies conducted on people subjected to a specific type of fasting and physical activity in whom a comprehensive classification of the lipid profile has been made (Santos, Macedo 2018).

Objective

The aim of the presented study is to show whether and to what extent 8 days of water-only fasting and laboratory exercise of maximum intensity affect the changes in the serum lipid profile in apparently healthy middle-aged men.

Material and methods

Subjects

Thirteen seemingly healthy middle-aged men volunteered to 8 days of water-only fasting during which they consumed only any amount of moderately mineralized water individually. Before the study, during the 8 days of water-only fasting and 3 days after its completion, the studied men were under medical supervision. Their basic demographic characteristics are presented in Table 1.

Table 1. Age and somatic variables of the studied men (n = 13) before and after 8 days of water-only fasting

Variables	Before X ±SD	After X ±SD	Significance (p)
Age [lat]	50,25±14,18	50,25±14,18	NS
BW [kg]	79,38±10,79	73,42±10,26	p<0,001
BH [cm]	178,67±4,54	178,67±4,54	NS
BF [%]	18,68±5,04	17,37±5,72	p<0,001
BF [kg]	15,27±5,42	13,21±5,33	p<0,001
FFM [%]	81,31±5,06	82,38±5,63	p<0,01
FFM [kg]	64,11±5,87	60,07±5,88	p<0,001
TBW [%]	59,54±3,71	60,50±4,21	p<0,001
TBW [kg]	46,94±4,29	44,08±4,11	p<0,001
BMI [kg/m^2]	24,89±3,52	23,02±3,35	p<0,001
BSA [m^2]	1,98±0,12	1,90±0,13	p<0,001

NS - not statistically significant; BW (body weight); BH (body height); BF (body fat); FFM (fat-free mass); TBW (total body water); BMI (body mass index); BSA (body surface area)

The surveyed men never smoked cigarettes and did not consume alcohol 3 days before, during and 3 days after the end of this dietary restriction. All participants had current medical examinations and showed no contraindications that would exclude them from the study. They stated that they had not taken any medications or dietary supplements at least one month prior to the study. Before the described study, all participants had previously participated in voluntary fasting sessions of various duration. The longest fasting previously used by one participant was 42 days and the shortest 3 days. The number of fasts previously performed by these people ranged from 3 to 10 (6.50 ± 0.93, median: 6.23) days. None of the surveyed men used the practice of fasting for at least the last 6 months. The participants were informed about the nature of the study, with a clearly defined purpose, and about the possible health risks of participating in this study. Each of them could withdraw from the experiment at any time. Each of the men signed a written informed consent to participate in the study before its commencement. The protocol of the experiment was approved by the Scientific Research Ethics Committee of the Jan Długosz University in Częstochowa and was in line with the principles set out in the Helsinki Declaration.

Protocol

Participants were instructed to change and enrich their diets as much as possible with fresh raw fruit and vegetables and steamed vegetables for 3 days prior to the study. The men under study came to the laboratory in the morning between 8:00 and 9:30 am after 12 hours of fasting. In the first stage of the study, basic demographic (age) and somatic data (body height - BH, body weight - BM, body fat - BF, fat-free mass - FFM, total body water - TBW and body mass index - BMI) were recorded using the Tanita TBF 300A body composition analyzer (Tanita, Amsterdam, The Netherlands). The body surface area-BSA of the men was also calculated. Blood samples were then taken from a vein in the arm while the patient was seated. Blood was allowed to clot at room temperature and then centrifuged at 1500 g for 15 minutes. The obtained serum was aliquoted and stored at -80 ° C until later analysis. The following variables were measured in serum samples: total cholesterol (Ch-T), high-density lipoprotein cholesterol (Ch-HDL), low-density lipoprotein cholesterol (Ch-LDL), and triglycerides (TG). Moreover, the concentration of β-hydroxybutyrate (β-HB) was also determined. The following coefficients were also calculated: R1 = Ch-T / Ch-HDL, R2 = Ch-LDL / Ch-HDL, R3 = TG / Ch-HDL. Then, a cycloergometric test was performed with a gradually increasing load up to the individual maximum, starting from 60 W, which was increased every 3 minutes by 30 W. Immediately after the end of the exercise, venous blood was collected again, in which the concentrations of the above-mentioned biochemical variables were determined according to the procedure described above. After this study, the men began an 8 days of water-only fasting during which they consumed only any amount of moderately mineralized mineral water. After this fasting intervention was completed, the above-described rest and exercise tests were performed again.

Statistics

The obtained results were expressed as arithmetic means, standard deviations and medians. The distributions of the variables determined in the research were examined using the Shapiro-Wilk statistics, then the Friedman test was used to determine the differences between and within groups, and the Dunn-Bonferroni formula was considered as a post hoc test. P value of 0.05 or less was considered statistically significant. The statistical procedure was performed with the use of the Statistica program.

Results

Table. 2. The lipid profile and β-hydroxybutyrate concentration of the serum of the studied men modified with 8 days of water-only fasting and physical exertion

Variables	Rest, before fasting (1)	Rest, after fasting (2)	Physical exertion, before fasting (3)	Physical exertion, after fasting (4)	Test rang Friedman, significance (p)	Post hoc (Dunn-Bonferroni), significance (p)
Ch-T(x) [mg/dl]	213,54	226,92	236,69	246,31	0,00038	1 vs 2; ns
Ch-T(±SD)	62,24	79,06	63,61	81,21		1vs 3; 0,0085
Ch-T (M)	203,0	194,0	231,0	212,0		3 vs 4; ns
						2 vs 4; ns
Ch-HDL(x) [mg/dl]	52,00	53,15	57,15	58,62	0,00002	1 vs 2; ns
Ch-HDL(±SD)	9,35	9,68	10,37	11,06		1 vs 3; 0,0038
Ch-HDL(M)	53,00	52,00	58,00	56,00		3 vs 4; ns
;						2 vs 4; 0,0111
Ch-LDL (x) [mg/dl]	143,49	151,26	158,45	160,45	0,01767	1 vs 2; ns
Ch-LDL (±SD)	55,67	73,52	57,39	73,30		1 vs 3; 0,0375
Ch-LDL (M)	138,80	125,40	156,40	136,60		3vs 4; ns
						2 vs 4; ns
TG (x) [mg/dl]	90,23	112,54	105,46	136,23	0,0001	1 vs 2; ns
TG (±SD)	33,75	28,1	36,68	27,17		1 vs 3; ns
TG (M)	91,00	111,00	103,00	131,00		3 vs 4; ns
						2 vs 4; 0,0375
R1=Ch-T/Ch-HDL (x)	4,13	4,30	4,18	4,21	0,91720	1vs2; ns
R1 (±SD)	0,99	1,19	0,95	0,95		1vs3; ns
R1 (M)	4,20	4,40	4,17	4,32		3vs4; ns
						2vs4; ns
R2=Ch-LDL/Ch-HDL (x)	2,78	2,86	2,80	2,73	0,42097	1vs2; ns
R2 (±SD)	0,93	1,14	0,90	0,92		1vs3; ns
R2 (M)	2,66	2,87	2,63	2,67		3vs4; ns
						2vs4; ns
R3=TG/Ch-HDL (x)	1,78	2,19	1,89	2,39	0,03610	1vs2; ns
R3 (±SD)	0,65	0,66	0,69	0,57		1vs3; ns
R3 (M)	1,63	2,22	1,82	2,50		3vs4; ns
						2vs4; ns
β-HB (x) [mmol/l]	0,31	4,55	0,21	3,86	0,000001	1 vs2; 0,0002
β-HB(±SD)	0,21	1,04	0,16	1,06		1 vs 3; ns
β-HB (M)	0,35	4,54	0,19	4,24		3 vs 4; 0,0009
						2 vs 4; ns

In relation to the serum lipid profile, statistical changes were observed, which were caused by the influence of the applied fasting and physical effort in the following variables: Ch-T (p <0.001), Ch-HDL (p <0.001), Ch-LDL (p = 0.018), TG (p <0.001) and the R3 coefficient (p =0.036), with the upper limits of the reference values being exceeded in relation to Ch-T, Ch-LDL and the R1 coefficient (Table 2). 8 days of water-only fasting did not change the serum lipid profile, but exercise caused such changes. Ch-T (p = 0.009), Ch-HDL (p = 0.004), Ch-LDL (p = 0.038) concentrations obtained after exercise under the conditions of a standard diet, as well as post-exercise Ch-HDL (p = 0.011) and TG concentrations (p = 0.038) measured after 8 days of water-only fasting were significantly higher than the values determined under resting conditions, respectively. It should be noted that the applied fasting caused severe ketosis, as the concentration of β-HB in the serum under these conditions increased several times in relation to the physiological nutritional status of the body, both under the conditions of rest and exercise (p <0.001).

Conclusion

8 days of water-only fasting together with physical exercise increased the concentration of total cholesterol, HDL, LDL TG and the R3 coefficient, which proves the increased metabolism of these fat bodies. It seems that physical exercise had a greater impact onthese changes than the applied dietary restriction.

References

1. Louter L. , Visseren F.L.J , Roeters van Lennep J.E. [A fasting lipid profile is not a necessity in majority of cases] [Article in Dutch]. Ned Tijdschr Geneeskd. 2020 May 20;164:D4394.
2. Wood R.J., Volek J.S., Davis S.R., Dell'Ova C., Fernandez L.M. Effects of a carbohydrate-restricted diet on emerging plasma markers for cardiovascular disease. Nutr Metab (Lond). 2006 May 4;3:19. doi: 10.1186/1743-7075-3-19.
3. Freedman M.R., King J., Kennedy E. Popular diets: a scientific review. Obes Res . 2001 Mar;9 Suppl 1:1S-40S. doi: 10.1038/oby.2001.113.
4. Mensink R.P. , Zock P.L., Kester A.D., Katan M.B. Effects of dietary fatty acids and carbohydrates on the ratio of serum total to HDL cholesterol and on serum lipids and apolipoproteins: a meta-analysis of 60 controlled trials. Am J Clin Nutr. 2003 May;77(5):1146-55. doi: 10.1093/ajcn/77.5.1146.
5. Natarajan S. , Glick H., Criqui M., Horowitz D., Lipsitz S.R., Kinosian B. Cholesterol measures to identify and treat individuals at risk for coronary heart disease. Am J Prev Med . 2003 Jul;25(1):50-7. doi: 10.1016/s0749-3797(03)00092-8.
6. Tyldum G.A. , Schjerve I.E., Tjønna A.E. , Kirkeby-Garstad I., Stølen T.O., Richardson R.S., Wisløff U. Endothelial dysfunction induced by post-prandial lipemia: complete protection afforded by high-intensity aerobic interval exercise. J Am Coll Cardiol . 2009 Jan 13;53(2):200-6. doi: 10.1016/j.jacc.2008.09.033.
7. Santos H.O., , Macedo R.C.O. Impact of intermittent fasting on the lipid profile: Assessment associated with diet and weight loss. Clin Nutr ESPEN. 2018 Apr;24:14-21. doi: 10.1016/j.clnesp.2018.01.002.

Relation between Rectus femoris and Vastus medialis passive mechanical properties and body mass index after total knee replacement

Identifier: orthopaedics

Daiva Lenčiauskienė

Klaipeda State University of Applied Sciences, Physiotherapy and Beauty Therapy Department

Introduction and objectives

- More than 50 percent patients undergoing total knee replacement are obese[2].
- Obesity has influence on healing process complications after surgery of tendons[1]. There is deficit of studies justifying correlation between BMI and Rectus femoris and Vastus medialis muscles passive mechanical properties after knee replacement.
- The aim of the study was to to determine the relationship between Rectus femoris and Vastus medialis muscles passive mechanical properties and BMI after total knee replacement.

Cross-sectional observational study.

Methods

- Cross sectional observational study of 21 patients, mean age 68,2±4,6 year was carried out one week after knee replacement.
- BMI calculation was used to assign participants to overweight, obesity class I and obesity class II groups. Rectus femoris and Vastus medialis muscles myotonometric characteristics: tone, elasticity and stiffness were recorded using the hand-held myotonometer Myoton –PRO.
- Statistical data analysis was carried out using SPSS 25.0 statistical analysis package. Data compliance with the normal distribution was verified using Kolmogorov-Smirnov test. Non-parametric Spearmen correlation coefficient *r* was used to determine relation between parameters. The outcome results were interpreted according to the degree of association as strong /r/ (≥0.7), moderate 0.3 ≤/r/<0.7, weak /r/ <0.3 after taking significant correlation (p<0.01) or (p<0.05) values into consideration[3].

Results

- The results of present study has revealed that overweight was strongly inversely related to RF muscle tone (r=-0.82 p<0,05) and elasticity (r=-0.75 p<0.05).
- Obesity class I was strongly inversely related to RF muscle stiffness (r=-0.75 p<0.05).
- We have not detected relation between obesity class II and RF and VM muscles passive mechanical properties (p>0,05).
- BMI was strongly inversely related to RF muscle stiffness (r=-0,79 p<0,01), moderately related to RF musle tone (r=-0,66 p<0,01), elasticity (r=-0,50 p<0,05), VM muscle tone (r=-0,48 p<0,05), stiffness (r=-0,56 p<0,05) Table 1.

Table 1. The relation between RF and VM passive mechanical properties and BMI after TKA

	RF (T)	RF (S)	RF (D)	VM (T)	VM (S)	VM (D)
Overweight group (n=7)						
r	-0.82*	-0.46	-0.75*	-0.57	-0.46	0.64
p	**0.02**	0.29	**0.03**	0.18	0.29	0.12
Obesity class I group (n=7)						
r	-0.57	-0.75*	-0.25	-0.29	-0.36	-0.43
p	0.18	**0.03**	0.59	0.53	0.43	0.34
Obesity class II group (n=7)						
r	0.33	-0.46	0.61	0.18	-0.04	-0.29
p	0.47	0.29	0.15	0.70	0.94	0.53
All groups (n=21)						
r	-0.66**	-0.79**	-0.50*	-0.48*	-0.56**	0.05
p	**0.00**	**0.00**	**0.02**	**0.03**	**0.00**	0.83

*Remark: RF- rectus femoris muscle; VM- vastus medialis muscle; D- decrement; T-tone; S- stiffness. *Correlation coefficient significant p<0.05. **Correlation coefficient significant p<0.01*

Conclusion

BMI satistically significantly inversely related to RF and VM muscles tone, stiffness and RF elasticity after total knee replacement, therefore the relation between obesity class and passive mechanical RF and VM muscles properties should be further investigated involving larger sample size.

References

1. Macchi, M., Spezia, M., Elli, S. (2020). Obesity Increases the Risk of Tendinopathy, Tendon Tear and Rupture, and Postoperative Complications: A Systematic Review of Clinical Studies, *Clinical Orthopaedics and Related Research,* 478(8), 1703-1705.

2. Odum, M., Springer, D., Dennos, C., Fehring, T. K. (2013). National Obesity Trends in Total Knee Arthroplasty. *The Journal of Arthroplasty,* 28 (8), 148–151.

3. Venclovienė J. (2010). *Statistiniai metodai medicinoje:bendrasis vadovėlis aukštosioms mokykoms.* Kaunas: Vytauto Didžiojo universiteto leidykla.

Effect of sodium bicarbonate supplementation on muscle performance and damage: a double blind, randomized crossover study

C. LEITE[1], R. BATTAZZA[2], M. KALYTCZAK[2], M. LAMOLHA[2], R. RICA[3] , J. BAKER[4] , F. POLITTI[2] , D. BOCALINI[1]

[1]Federal University of Espirito Santo, Vitoria, Brazil; [2]Nove de Julho University, São Paulo, Brazil, [3]Estácio de Sá University, Espírito Santo, Brazil, [4]Hong Kong Baptist University Kowloon Tong, Hong Kong, China.

Introduction and objectives

Sodium bicarbonate ($NaHCO^3$) is the most studied alkaline substance in several sports and performance protocols with high energy demand, so this study investigated the effects of $NaHCO3$ supplementation on parameters related to the external and internal exercise load in trained individuals submitted to fatigue induction using an isokinetic dynamometer.

Methods

Sample

Ten physically healthy and independent men were tested on two occasions: after ingesting 0,3 g.Kg of body mass of $NaHCO^3$ or placebo in double-blind, randomized *cross over* study. The subects' biometric parameters assessed are: a) body mass of approximately 85 Kg; b) aged between 22 and 42 years; c) minimum experience of one year in strength training; d) workout routines exercises for lower limbs.

Exercise session

Maximum voluntary isometric contraction (MVIC) tests were performed before and after a dynamic protocol consisted of 10 series of 10 movements of unilateral extension (concentric phase) and flexion (eccentric phase) of the knee extensors at 120^0 s^{-1} at an interval of 60 seconds between series. For the dynamic test, a total amplitude of 90^0 was requested with a maximum limit of 15^0 for knee extension.

Parameters evaluated

Mechanical analysis: Performance parameter was performed using PT (the point of greatest torque in the range of motion) values throughout the experimental procedure. PT was measured in Newton-meter (Nm).

Biochemical analysis: Blood was collected for analysis of pH, Lactate concentrations (La) and CK.

Determination of blood pH: Blood samples were taken under vacuum in tubes dried and analyzed using the pHmeter. pH analyzes occurred at different times: pre-ingestion of $NaHCO^3$ and during the dynamic protocol (intervals between the 10 series).

Determination of blood lactate concentrations: Blood samples were taken under vacuum in tubes dried and analyzed using the portable lactimeter. La analyzes occurred at diferente times: pre-ingestion of $NaHCO3$ and during the dynamic protocol.

Determination of blood CK concentrations: Blood samples were taken under vacum in dry tubes and centrifuged at 9000 RPM for 30 minutes and the sérum was used for the spectrophotometric reading in duplicate using comercial kits. CK was analyzed pre intake of $NaHCO^3$ and 24 hours after the experimental protocol.

Analysis of perceptions of effort, pain and recovery: The perception of effort was evaluated using the OMNI – RES scale, which consists of a graduated scale from zero to 10 with verbal anchors related to RPE. The RPP (local) was assessed using a visual analog scale (VAS) which consists of a 10 cm line barred at the left end by the expression. "no pain" and at the right end by the expression "greatest pain possible". The RPR was mensured with a scale raging 6 to 20. The closer to 20 the better the perception of recovery. The OMNI-RES and VAS scales were Applied immediately after MVIC tests and along the dynamic protocol. The RPR scale was Applied one minute post MVIC tests.

Training load: The internal load of the session was evaluated by calculation trough multiplication of the total number of repetitions of the session (100 repetitions) by the value of the exercise intensity provided from the RPE scale.

Statistical Analyses

Values are expressed as the mean ± standard deviation (mean ± SD) with the level of significance p ≤0.05. One-way ANOVA was used for repeated measures followed by the Tukey's post hoc test and 95% confidence intervals (95% CI) were calculated. All statistical analyses were performed using the GraphPad Prism 5 program

Results

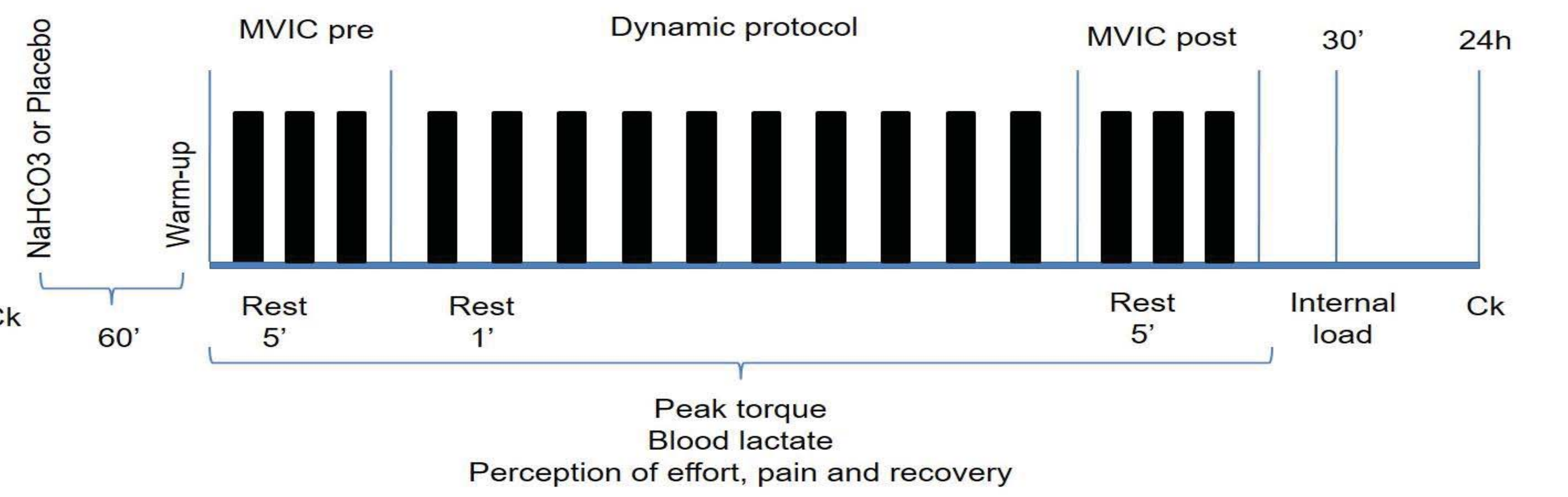

Figure 1. Outline of experimental protocol.

Table 1: Parameters related to the performances

Parameters	Pre	Post	%	d Cohen (ES)	ANOVA Time effect F	ANOVA Time effect p	ANOVA time*condition effect F	ANOVA time*condition effect p
IPT(Nm)								
Placebo	259 ± 58	211 ± 51*	-18 ± 10	0.87 (0.40)	30.49	0.0004	0.8082	0.3921
$NaHCO_3$	264 ± 52	210 ± 53*	-20 ± 13	1.02 (045)				
Lactate (mmMol/L)								
Placebo	1.16 ± 0.32	6.22 ± 1.48*	482 ± 227	4.72 (0.92)	176.70	0.0001	0.2380	0.6373
$NaHCO_3$	1.28 ± 0.42	6.69 ± 1.73*	497 ± 336	4.29 (0.90)				
RPE (0-10)								
Placebo	3.90 ± 1.91	7.40 ± 1.78*	157 ± 187	1.89 (0.68)	55.73	0.0001	0.0117	0.9162
$NaHCO_3$	3.50 ± 2.01	6.70 ± 2.45*	147 ± 149	1.42 (0.58)				
Pain (0-10)								
Placebo	2.70 ± 1.57	7.57 ± 2.13*	253 ± 230	140.25 (0.99)	35.33	0.0002	0.1525	0.7052
$NaHCO_3$	2.80 ± 1.69	7.00 ± 2.54*	251 ± 247	126.54 (0.99)				
Recovery (0-20)								
Placebo	16.30 ± 2.54	11.40 ± 1.65*	-29 ± 14†	2.28 (0.75)	65.00	0.0001	5.5980	0.0422
$NaHCO_3$	17.20 ± 2.10	14.40 ± 1.65*	-16 ± 3	1.48 (0.59)				
CK ($u.L_1$)								
Placebo	238.00 ± 94.03	486.02 ± 336.57*	118 ± 119	1.00 (0.44)	6.21	0.0373	0.6594	0.4403
$NaHCO_3$	225.31 ± 135.94	418.39 ± 318.42*	110 ± 133	0.85 (0.39)				

Values expressed as mean ± standard deviation. IPT: isometric peak torque. RPE: rating of perceived effort. CK: creatine kinase. *p<0.05 vs pre. †p<0.05 vs $NaHCO^3$.

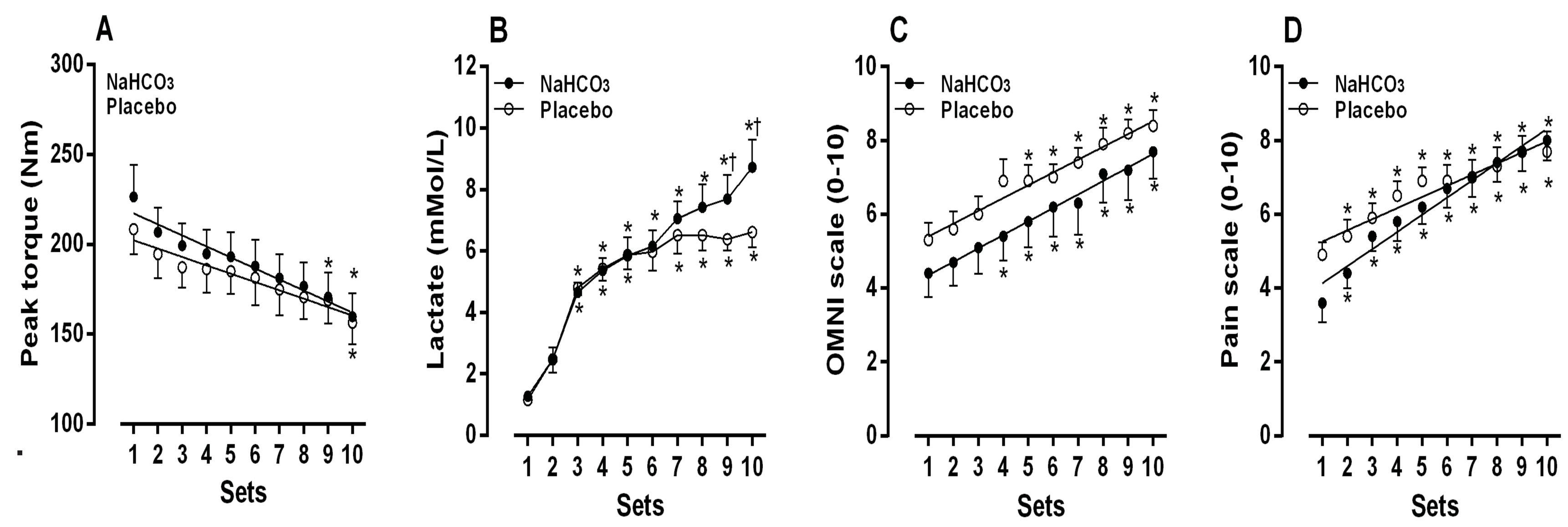

Figure 2. Values expressed as mean ± standard deviation for peak torque (Panel A), lactate concentrations (Panel B), perception of effort (Panel C) and pain (Panel D) over 10 series of 10 isokinetic contractions for extension of the knee joint at a speed of 120^0 s^{-1} in $NaHCO^3$ and placebo.

Conclusion

$NaHCO^3$ supplementation did not attribute benefits on exercise performance (although it increased blood lactate levels in the last series of the dynamic protocol) or in parameters related to the internal load of the exercise.

Identifier/Topic: Fatigue. Adaptation to environment. Thermoregulation.

Reference

1. Amann, M. Central and peripheral fatigue: interaction during cycling exercise in humans. *M. Sci. Sport Exerc. Online* **43**, 2039–45 (2011).
2. Ament, W, Verkerke, G.J. Exercise and fatigue. *Sports Med.* **5,** 389-422 (2009).
3. Artioli, GG, Gualano, B, Coelho, DF, et al. Does sodium-bicarbonate ingestion improve simulated judo performance? *Int .J. Sport. Nutr. Exerc. Metab.* **17,** 206-217 (2007).
4. Baker, JS, Mccormick, MC, Robergs, RA. Interaction among skeletal muscle metabolic energy systems during intense exercise. *J. Nutr. Metabol.* **1**-13 (2010).

KATP CHANNELS OPENING IS CRITICAL FOR ENERGY METABOLISM UNDER PHYSICAL STRESS

O. AKOPOVA, I. MANKOVSKA, V. NOSAR, L. KOLCHINSKAYA, V. SAGACH
Circulation Department of A.A. Bogomoletz Institute of Physiology, NAS of Ukraine, Kiev, Ukraine
e-mail: ov_akopova@ukr.net; olga-akopova@biph.kiev.ua

Introduction and Objectives: The modulation of mKATP channel activity by pharmacological means is known to have a great impact on energy metabolism in a living organism. In multiple studies it was shown that mKATP channels openers were effective for the recovery of cardiac and neuronal tissues from ischemia and the risks of oxidative damadge after reperfusion [Garlid et al., 2009; Kowaltowski et al., 2021]. ATP-sensitive K^+ transport was shown to take part in the regulation of mitochondrial volume, respiration, Ca^{2+} transport, ROS production and ATP synthesis; however its direct effects on mitochondrial functions still remain controversial. As we observed earlier [Akopova et al., 2016], mKATP channel blocker glibenclamide dramatically reduced physical endurance of animals, which required mechanistic explanation. So, the aim of this work was to examine the impact of endogenous activity of mKATP channel on physical endurance of the rats subject to compulsory swimming with a load.

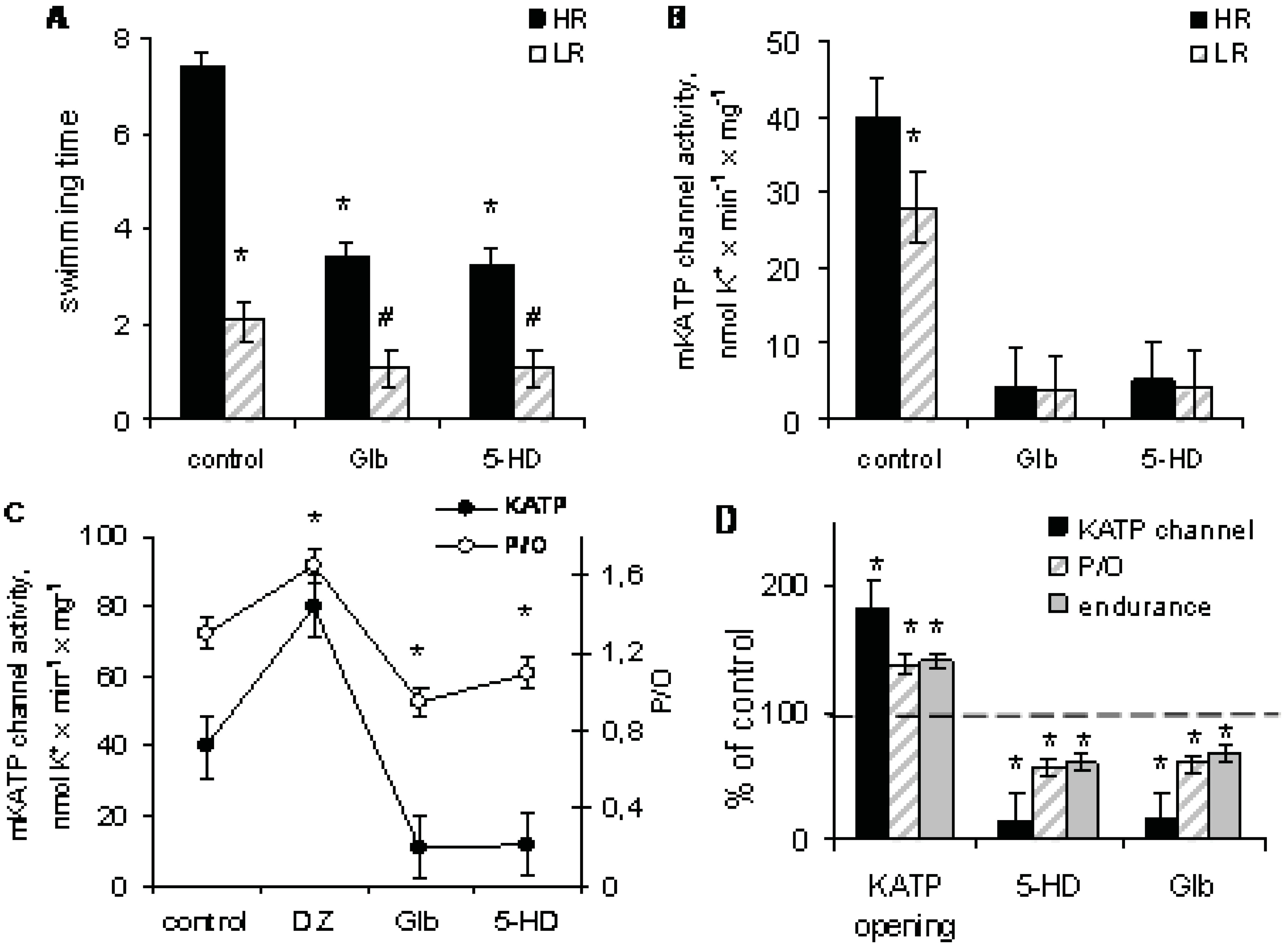

Methods: Male Wistar rats were subject to compulsory swimming with a load till fatigue and separated in two groups with high and low resistance to physical stress based on their swimming time (ST): HR and LR. Mitochondrial functions were assessed polarographically in a medium:. 120 mM KCl, 0.5 mM EDTA, 5 mM sodium glutamate, 1 mM KH2PO4, 20 mM Tris-HCl buffer (pH 7.4). KATP channel activity was determined with K+-selective microelectrode [4baranova et al]. Statistical analysis was performed using paired Student's t-test; P<0.05 was taken as the level of significance

	Respiration rate, ng-at. O·min^{-1}·mg^{-1}			RCR	P/O	J_p, nmol·min^{-1}·mg^{-1}
	J_4^S	J_3	J_4^{ATP}			
control	11.5±1.0	92.0±3.0	16.7±1.2	5.5±0.7	1.23±0.08	154.0±6.0
DZ	26.7±1.1 *	65.0±4.0 *	23.8±1.2 *	3.6±0.4 *	1.58±0.12 *	107.0±5.5 *
Glb	8.0±0.9*#	67.0±4.5*	20.0±0.6*	3.3±0.3*	1.0±0.1*#	73.0±8.0*#

Results: higher ST in HR group reliably coincided with higher endogenous mKATP channels activity. mKATP channels blockers dramatically reduced ST in both groups, and completely blocked mKATP channel *in vivo*, which indicated the dependence of physical endurance on mKATP channel activity (Fig. 1). To find a mechanistic basis for this, we studied the direct effects of mKATP channel opening by diazoxide and blocking by glibenclamide on mitochondrial functions *in vitro*. Mild uncoupling of mitochondria by diazoxide (Table) reduced the rate of phosphorylation (Jp), but increased its efficiency (P/O). Glibenclamide inhibited respiration, and dramatically reduced both P/O and Jp (Table). Physical endurance strongly correlated with P/O, both dependent on mKATP channels activity (Fig. 1C, D). Dramatic fall of P/O by mKATP channels blockers indicated dramatic increase of energy expense for ATP synthesis, which correlated with extremely low endurance.

Conclusions: OxPhos is one of the primary targets of mKATP channel opening *in vivo*. mKATP channels opening increased phosphorylation efficiency and reduced oxygen consumption by OxPhos, which helped to avoid oxygen depletion under the conditions of oxygen shortage under physical loading. Our results provide an explanation for the improvement of the endurance in the animals with elevated endogenous mKATP channel activity.

Effect of loss of miR-23-27-24 cluster microRNAs on muscle regeneration

Tatsuya Kato[1], Minjung Lee[2], Satoshi Oikawa[2] , Takayuki Akimoto[2]

[1]Graduate school of Sport Sciences, Waseda University. [2]Faculty of Sports sciences, Waseda University.

Introduction/objective

Skeletal muscle exhibits remarkable regeneration capacity in response to injury on myofibers. Research on mechanisms of muscle regeneration can lead to quicker recovery from the injury and better improvement of myopathies.

Muscle regeneration capacity depends on muscle satellite cells（SCs）expressing Pax7. After myofibers get injured, SCs start proliferation and differentiation into myoblasts with the expression of MyoD, then become myocytes expressing Myogenin. Myocytes form myofiber with expression of myosin heavy chain（MyHC）.

microRNA（miRNA: miR）is a class of small non-cording RNAs that represses translation through targeting 3' UTR of mRNA or promotes decay of the mRNA. In fact, some miRNAs play important roles in muscle development and regeneration.

Our laboratory has been investigating miR-23 cluster miRNAs which are highly expressed in skeletal muscle. It has been revealed that miR-27 targets Pax3 and promoting myogenesis（**1**）. miR-23 and miR-24 promote C2C12 differentiation by increasing the expression of Myogenin and fast MyHC isoforms through targeting Trxr1 and Acvr1b respectively according to in vitro study（**2, 3, 4**）.

However, function of miR-23 cluster miRNAs in vivo muscle regeneration remains unclear.

In this study we aimed to reveal the role of miR-23 cluster miRNA in muscle regeneration.

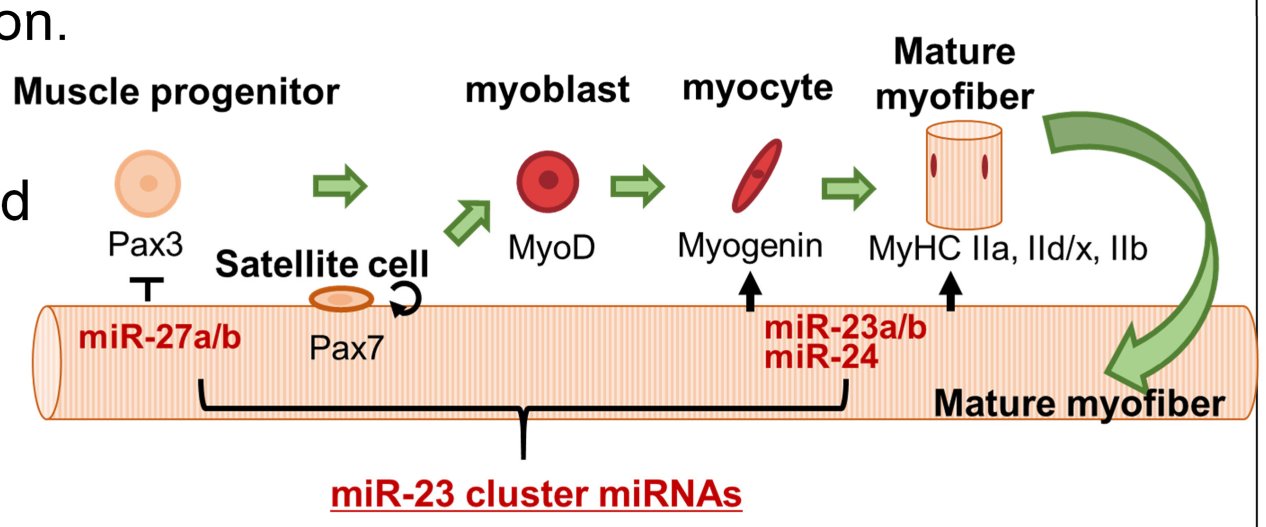

Methods

Cre-loxP system: MyoD-mediated miR-23 cluster miRNA KO（dKO mice）
Muscle regeneration: Cardiotoxin injection into TA muscle

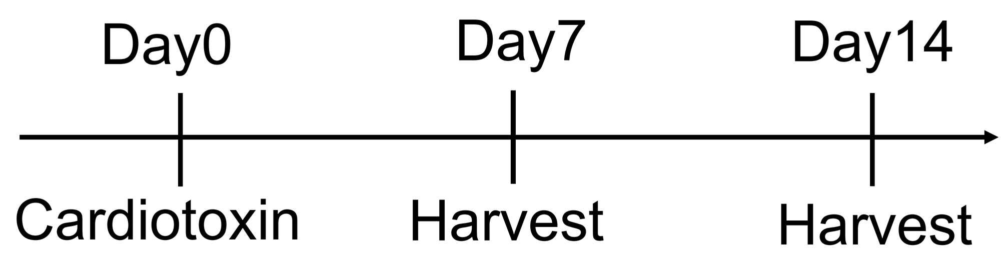

Results

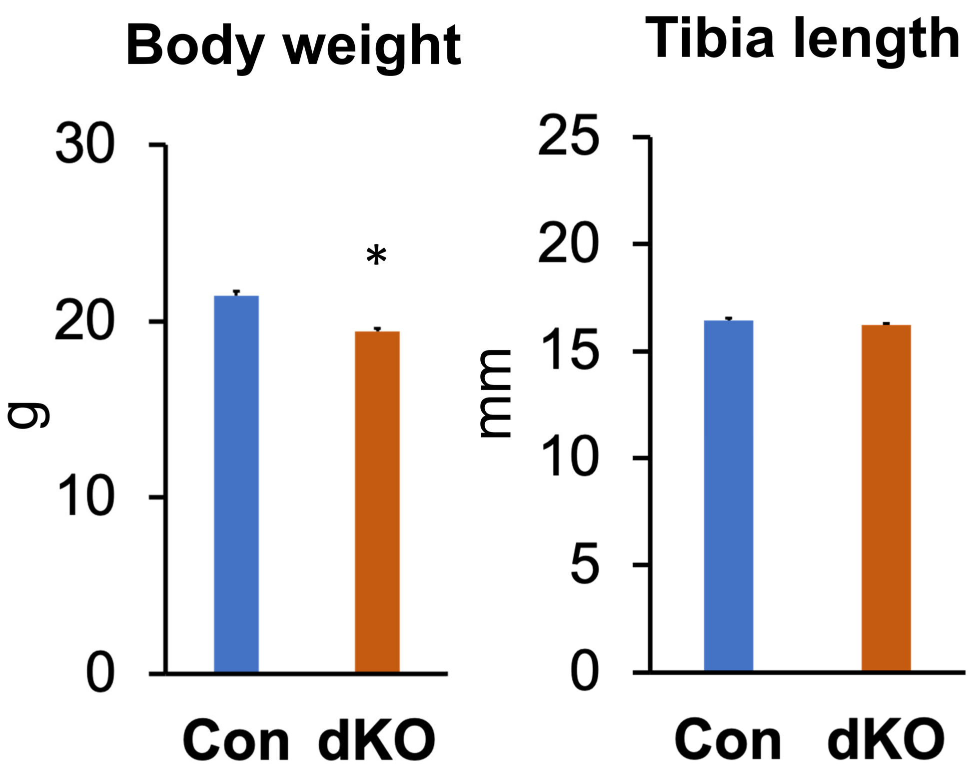

Fig1: Body weight and Tibia length
Left: Body weight of Control and dKO mice（Mean + SEM. *P<0.05）.
Right: Tibia length of Control and dKO mice. Tibia length represents the body size（n = 6, Mean + SEM）.

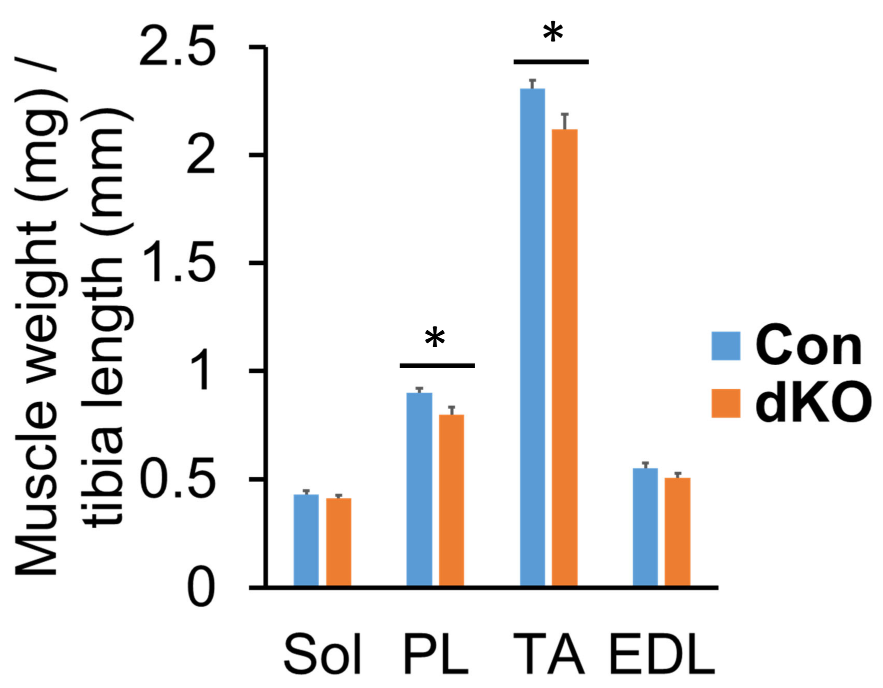

Fig2: Muscle weight
Normalized muscle weight of soleus（Sol）, plantaris（PL）, tibialis anterior（TA）, extensor digitorum muscle（EDL）. Each muscle weight was normalized by tibia length（n = 6, Mean+SEM, *P < 0.05）.

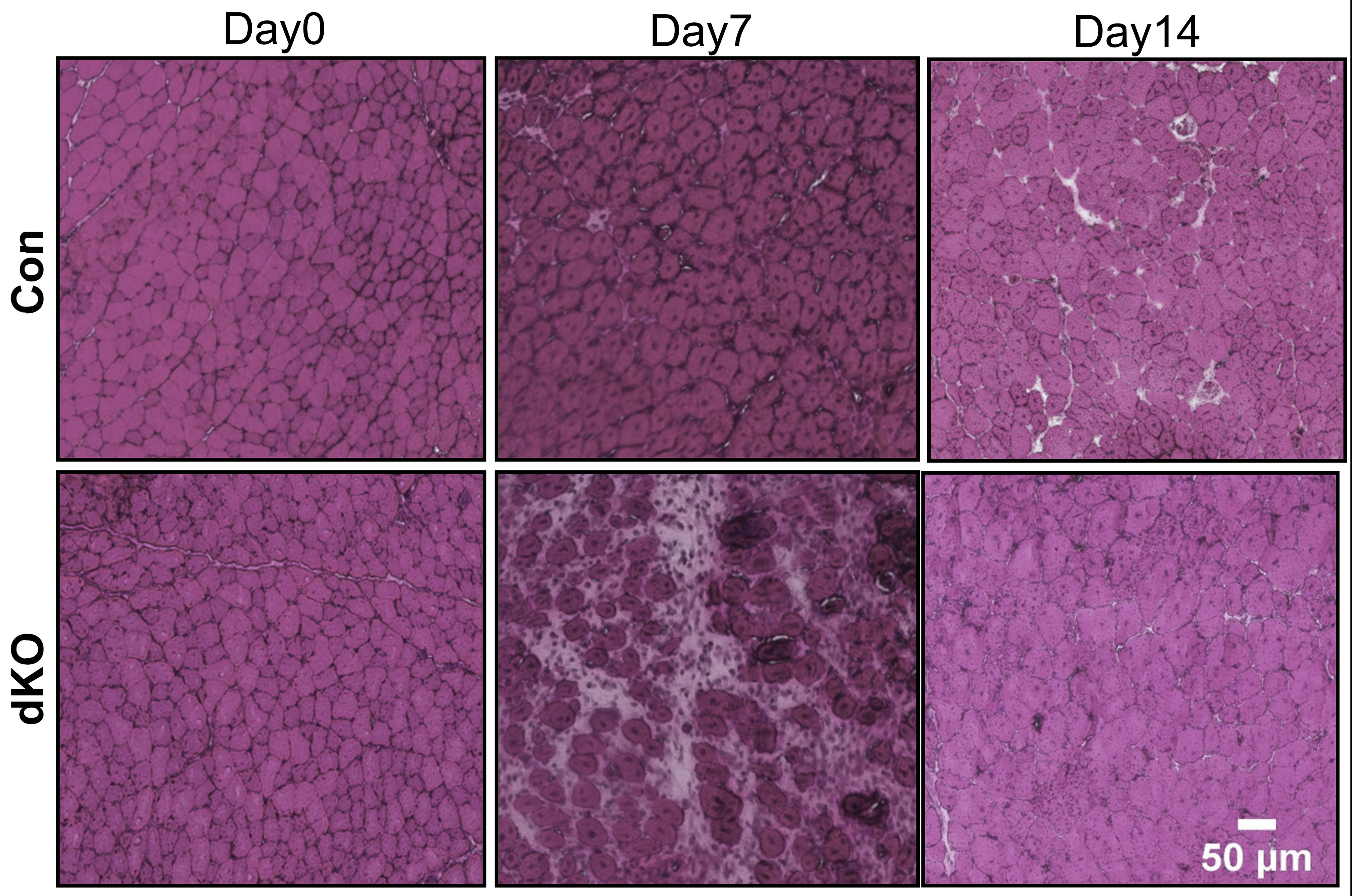

Fig3: Muscle cross section
TA was harvested at Day0, Day7 and Day14 after injury and were stained with Hematoxylin and Eosin（HE）. Scale bar = 50 μm.

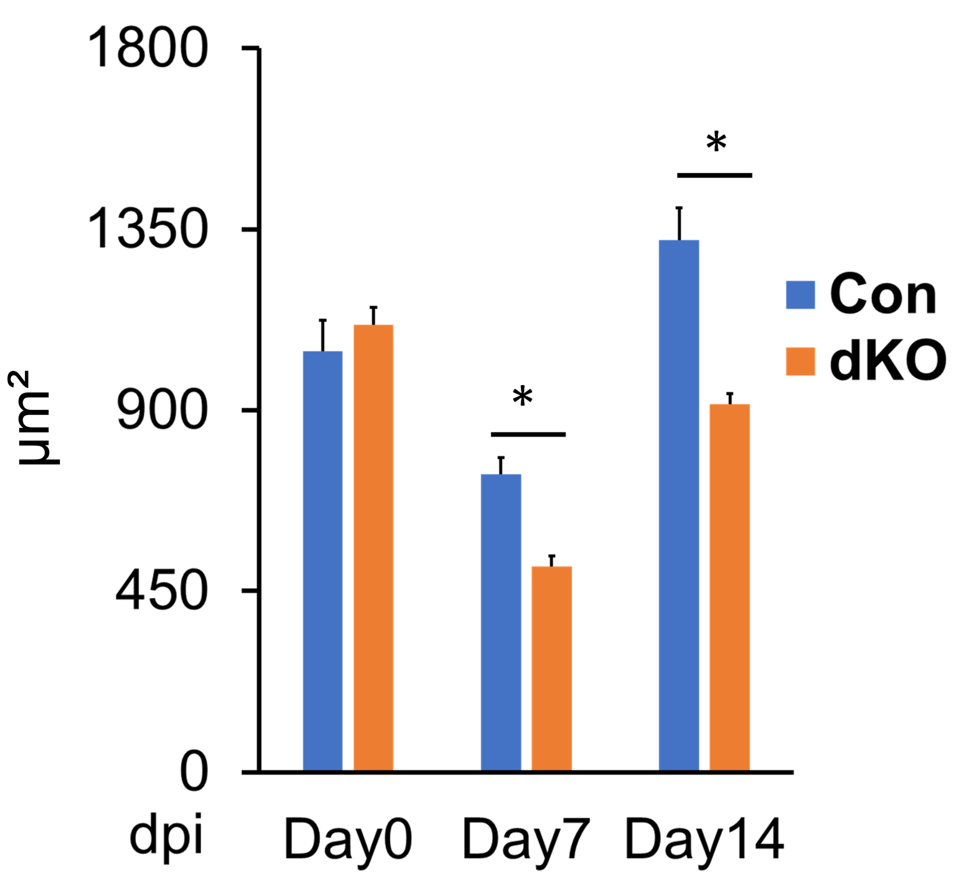

Fig4: Cross sectional area
Cross sectional area of TA muscle 7 days and 14 days after the injury. Day0 represents intact TA muscle（n = 5, Mean + SEM, *P < 0.05）.

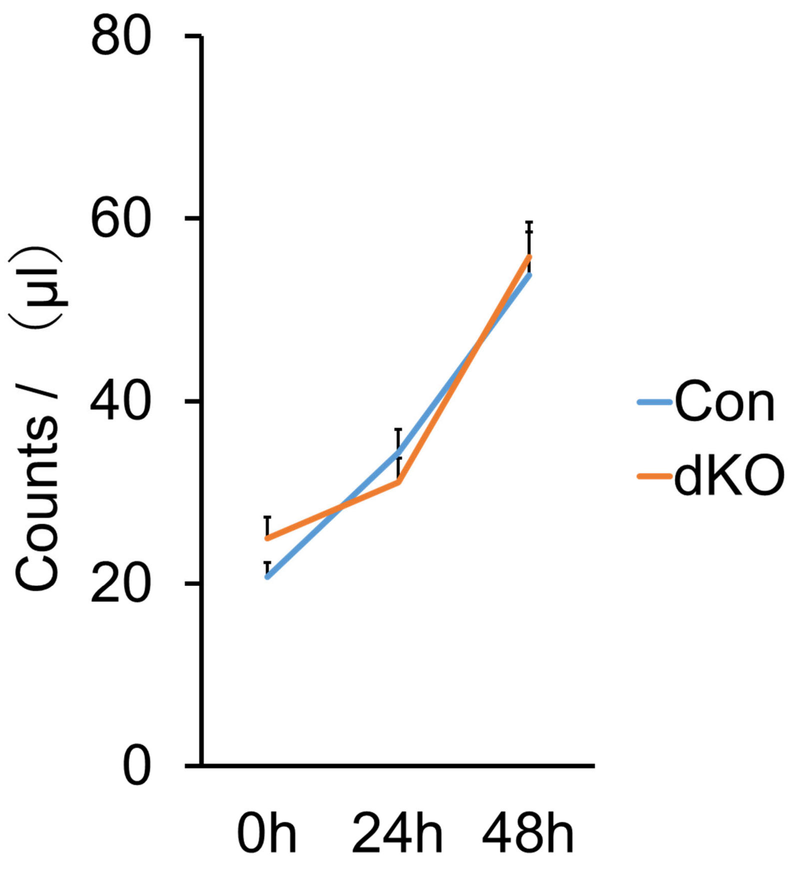

Fig5: Myoblast proliferation
Number of myoblast at 0h, 24h, 48h（n = 6, Mean + SEM）

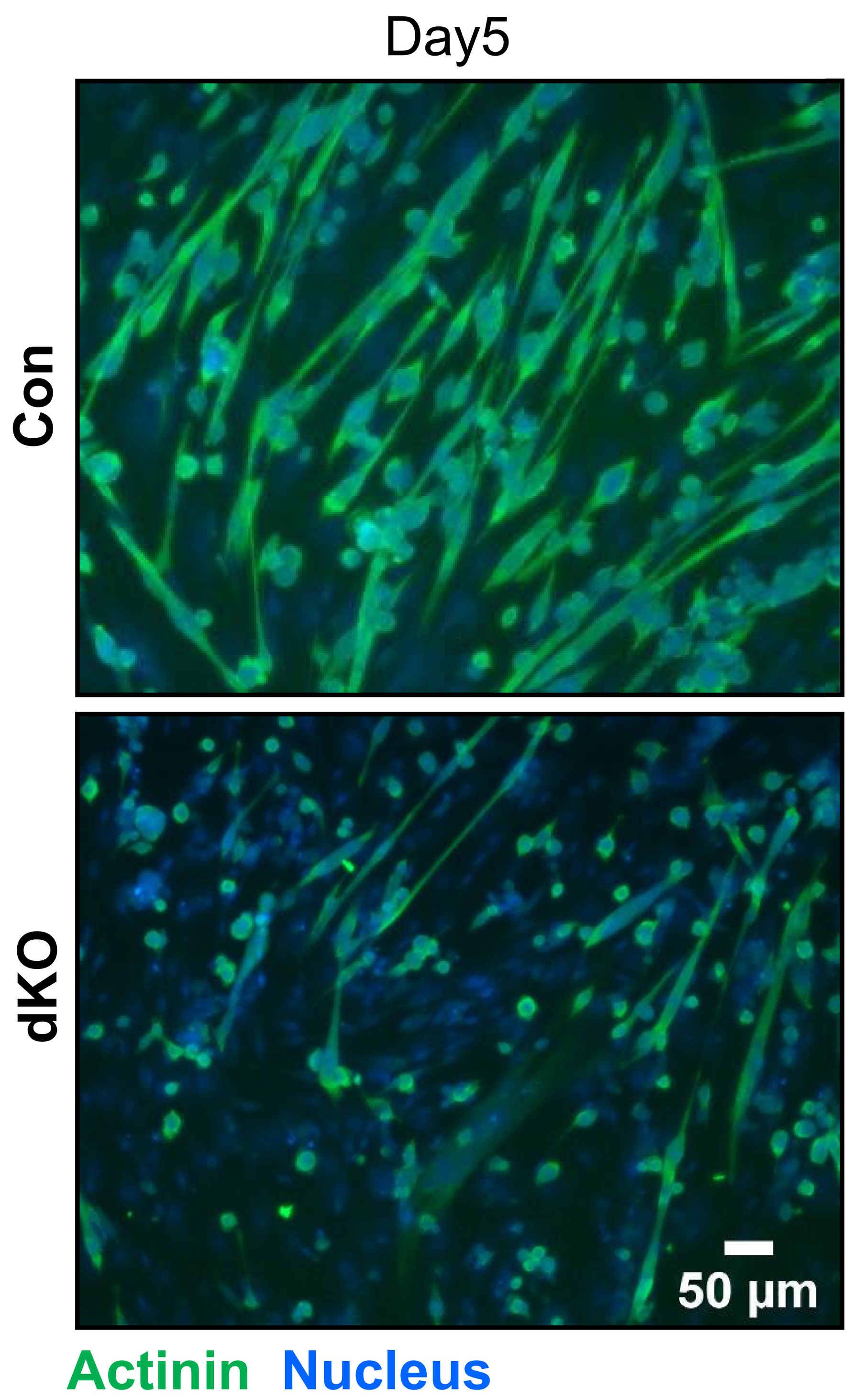

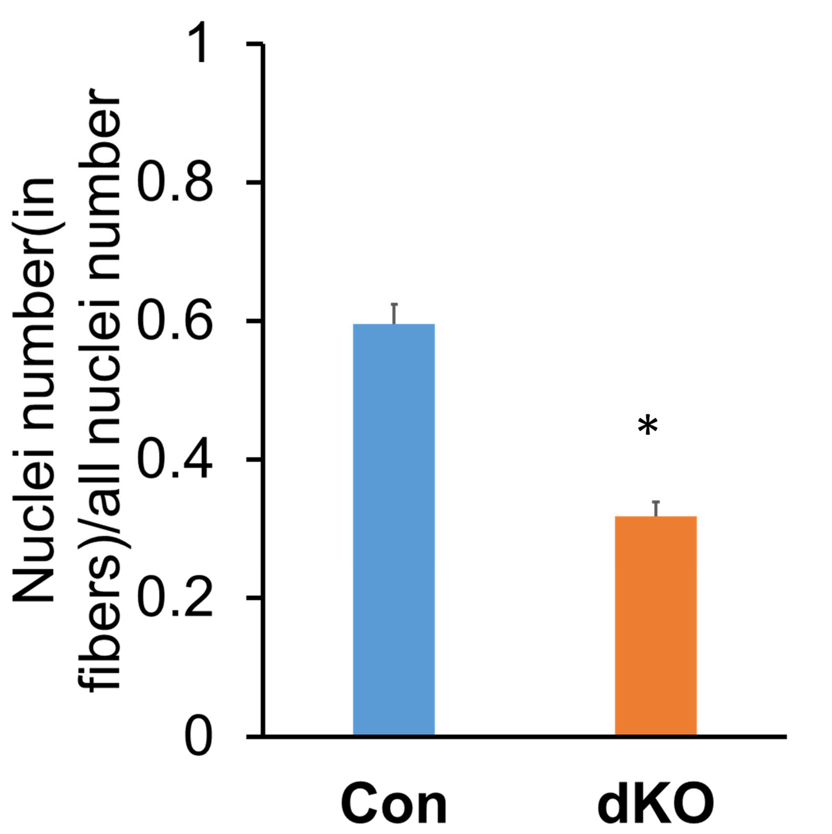

Fig6: Myoblast differentiation
Left: Primary myoblasts were harvested from Con and dKO mice. Myotubes were stained with anti-actinin antibody and Hoechst.
Graph: Fusion index indicating the degree of differentiation（n=6, mean+SEM, *P<0.05、Scale bar = 50 μm）

Conclusion

The miR-23 cluster miRNAs KO mice showed:

1. Decrease of body weight & muscle weight.
2. Inhibited or delayed muscle regeneration
3. Inhibited myoblast differentiation

Reference

（**1**）Crist et al., Proc Natl Acad Sci USA. 2009.
（**2**）Sun et al., Nucleic Acids Res. 2008.
（**3**）Mercatelli et al., Sci Rep. 2017.
（**4**）Hu et al., Animals. 2019.

XXVIII Congress of the Polish Physiological Society

Gdańsk, September 15-17 2021

Poster book

SESSION II

CENTRAL NERVOUS SYSTEM. NEUROPHYSIOLOGY.

PLASTICITY OF NEURAL FUNCTION

HONORARY PATRONAGE

Prof. dr Marcin Gruchała
Rector of the Medical University of Gdansk

Uniwersytet Gdański

Prof. dr Piotr Stepnowski
Rector of the University of Gdansk

WOJEWODA POMORSKI
DARIUSZ DRELICH

Dariusz Drelich
Governor of the Pomeranian Voivodeship

HONORARY PATRONAGE
Mayor of the City of Gdańsk

Aleksandra Dulkiewicz
Mayor of Gdansk

Mieczysław Struk
Marshal of the Pomeranian Voivodeship

PARTNER

PAN
POLSKA AKADEMIA NAUK

ANIMA LAB
animal facility and laboratory equipment • animal research models

FUNDACJA LOTOS

Medical University of Gdansk
Department of Physiology

INHIBITION OR STIMULATION OF SHELL NUCLEUS ACCUMBENS CHANGES INTRAVESICAL PRESSURE AND CARDIOVASCULAR PARAMETERS IN WISTAR RATS.

RODRIGO DE CARVALHO[1], BRUNO ANTONIO[1], NUHA DSOUKI[1], BARBARA DO VALE[1], PATRIK ARONSSON[2], LAURIVAL DE LUCA JR[3]., MONICA SATO[1]

[1]Dept. Morphology and Physiology, Centro Universitario FMABC, Santo Andre, SP, Brazil, [2]Dept Pharmacology, Institute of Neuroscience and Physiology, Sahlgrenska Academy, University of Gothenburg, Gothenburg, Sweden, [3]Dept. of Pathology and Physiology, Dentistry School, Sao Paulo State University (UNESP), Araraquara, SP, Brazil. monica.akemi.sato@gmail.com

SESSION II: CENTRAL NERVOUS SYSTEM. NEUROPHYSIOLOGY. PLASTICITY OF NEURAL FUNCTION

INTRODUCTION AND OBJECTIVE

- Neuroanatomical studies have shown that rostral regions of the dorsomedial shell Nucleus Accumbens (NAcc) project to the lateral preoptic area (LPA). Injections of angiotensin-(1-7) into the LPA evokes a huge increase in intravesical pressure (IP). It is still unknown whether the shell NAcc has any role in micturition control or not. This study aimed to investigate the possible involvement of shell NAcc in the micturition control.

MATERIALS AND METHODS

- Adult male Wistar rats (~470 g) with stainless steel guide cannulas implanted bilaterally in the shell NAcc 7 days prior to the experiments were anesthetized with 2% isoflurane in 100% O_2 and subjected to cannulation of the femoral artery and vein for pulsatile arterial pressure (PAP), mean arterial pressure (MAP) and heart rate recordings (HR) and infusion of drugs, respectively. The urinary bladder was cannulated for intravesical pressure (IP) measurement. A miniaturized Doppler flow probe was placed around the left renal arterial for renal blood flow (RBF) recordings. After the baseline MAP, HR, IP and RBF recordings for 15 min, GABA (50 mM, 1 µL) or L-glutamate (50 mM, 1 µL) or saline (vehicle, 1 µL) injections were made bilaterally into the shell NAcc and the variables were measured for additional 30 min. Data are as mean±SEM and submitted to Student´s t test (P<0.05).

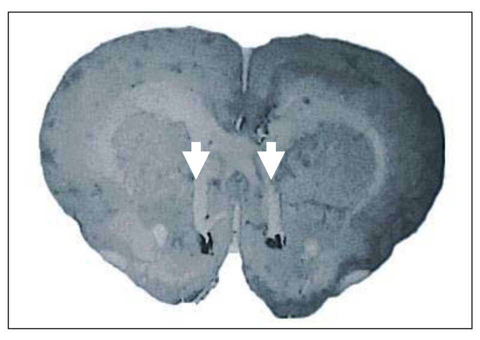

Figure 1: Histological section showing the sites of injections into the shell nucleus Accumbens (white arrows).

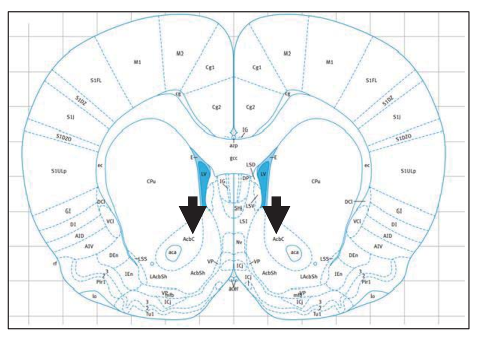

Figure 2: Schematic representation of "The Rat Brain in Stereotaxic Coordinates - Paxinos &Watson" showing the location of the shell nucleus Accumbens (black arrow).

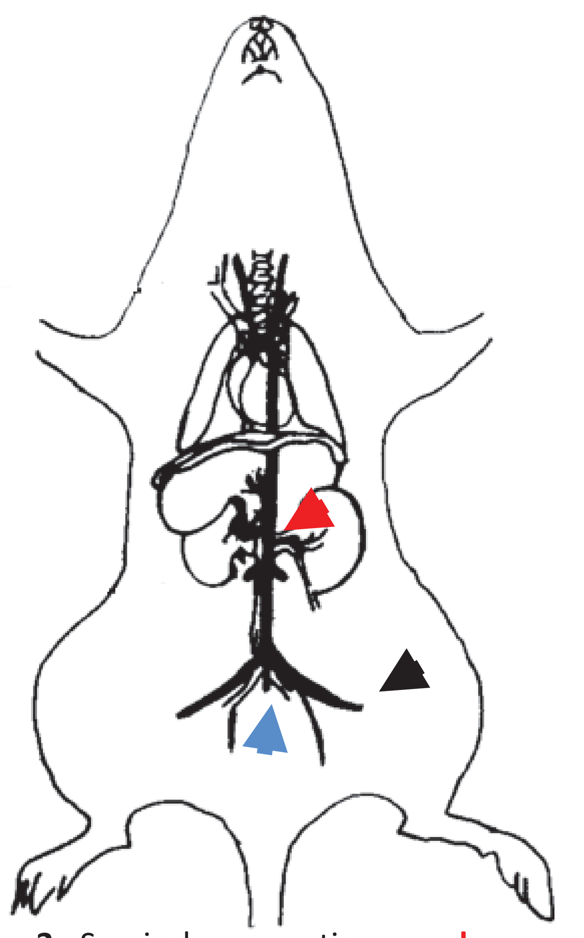

Figure 3: Surgical preparation - red arrow indicates the left renal artery where a miniaturized Doppler flow probe was placed; blue arrow represents the urinary bladder cannulation region and the **black arrow** shows the femoral artery and vein, which were submitted to catheterization.

EXPERIMENTAL PROTOCOL

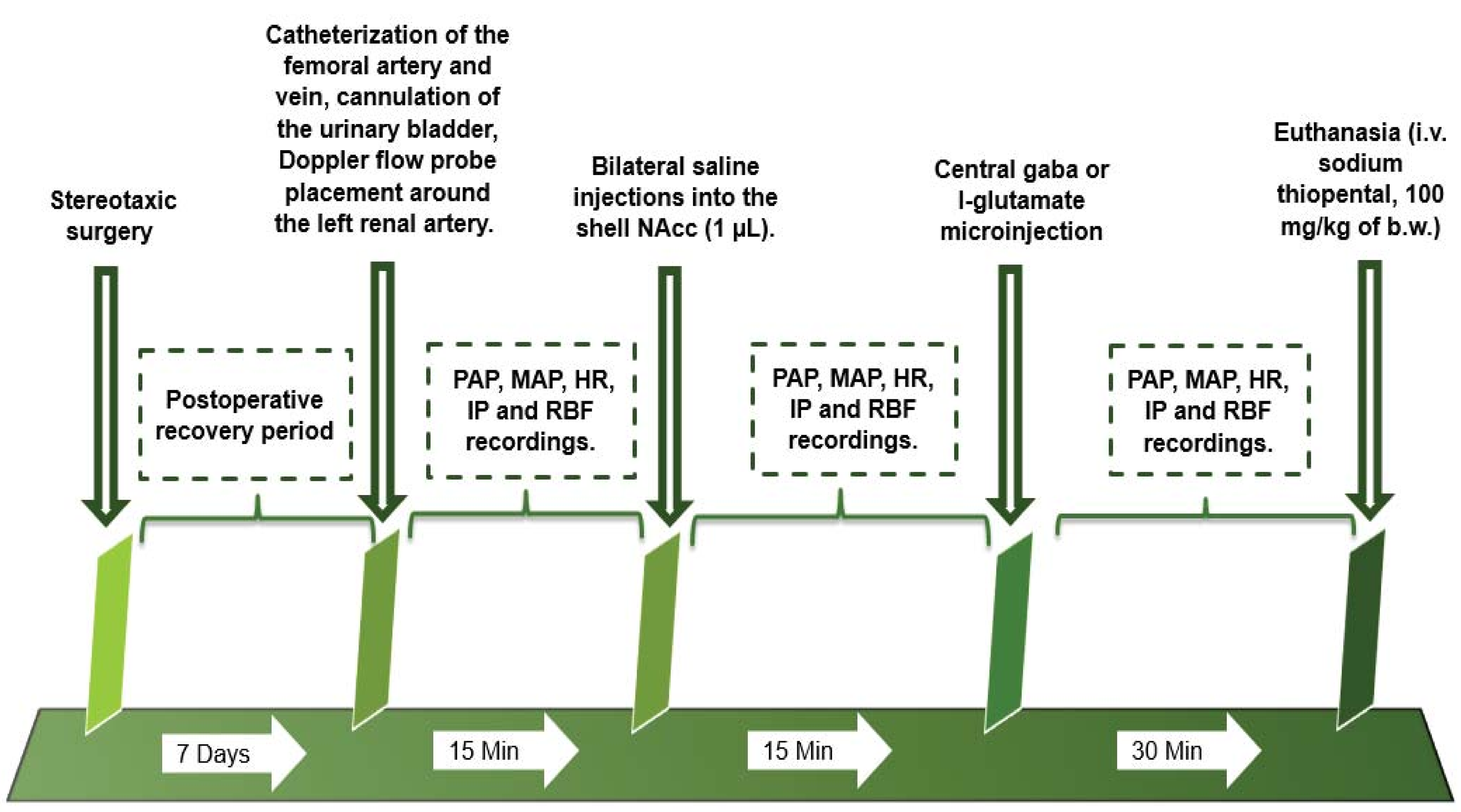

RESULTS

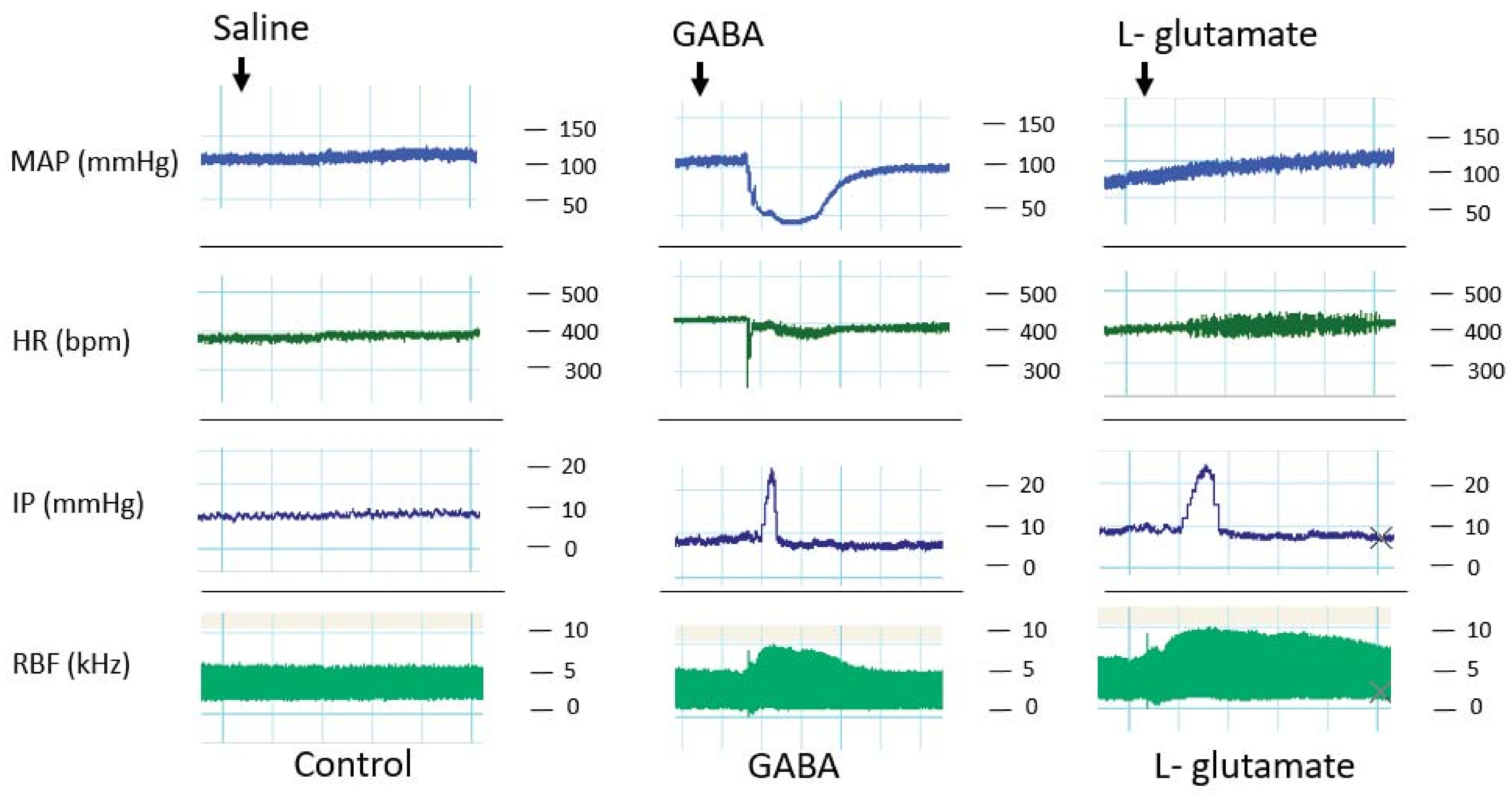

Figure 4: Tracings showing the mean arterial pressure (MAP, mmHg), heart rate (HR,bpm), intravesical pressure (IP) and renal blood flow (RBF) responses evoked by bilateral injections of saline (vehicle, control), or GABA or L-glutamate into the shell Nucleus Accumbens (NAcc). Arrows indicate the moment of injection into the shell NAcc.

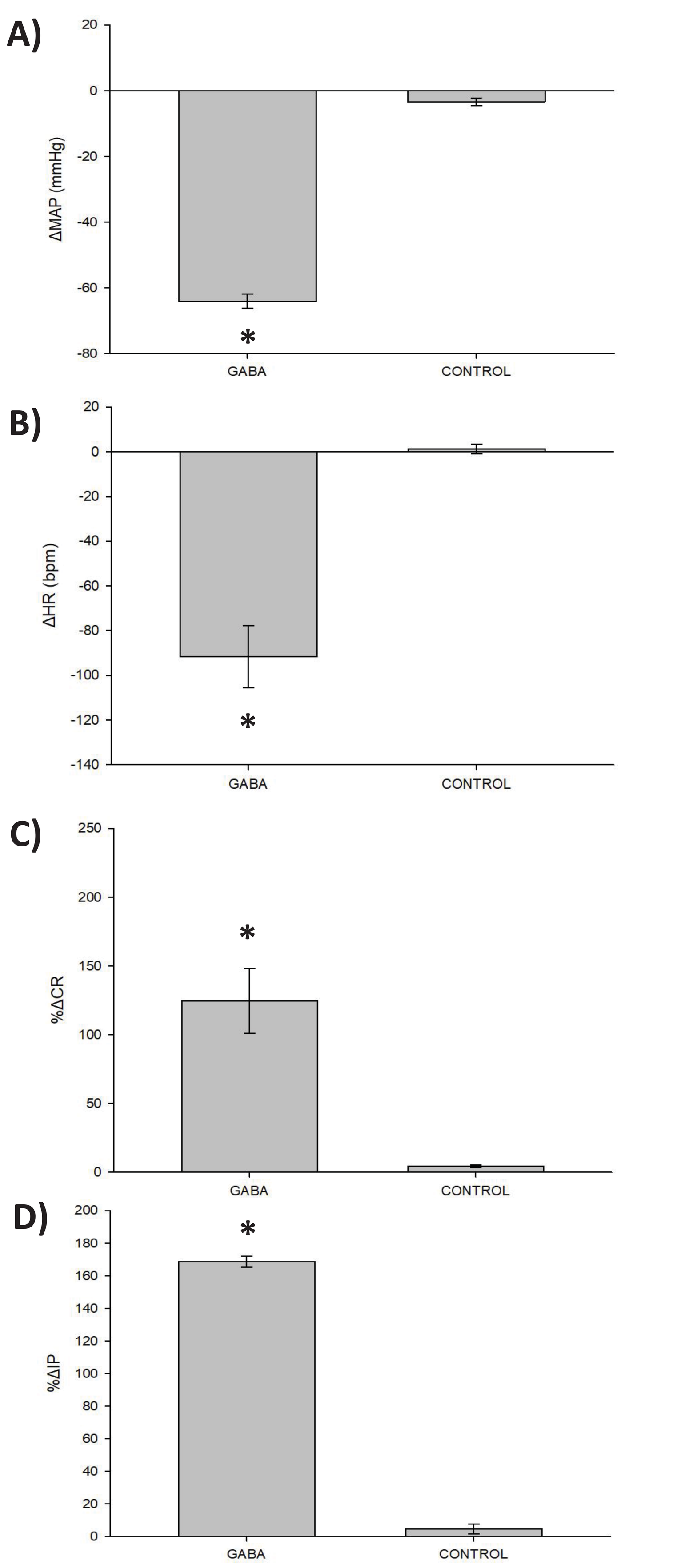

Figure 5: A) Change in mean arterial pressure (ΔMAP, mmHg), B) Change heart rate (ΔHR, bpm), C) Percent change in renal conductance (%ΔRC), and D) Percent change in intravesical pressure (%ΔIP) evoked by bilateral injections of GABA or saline (control) into the shell NAcc. *P<0.05 vs. control

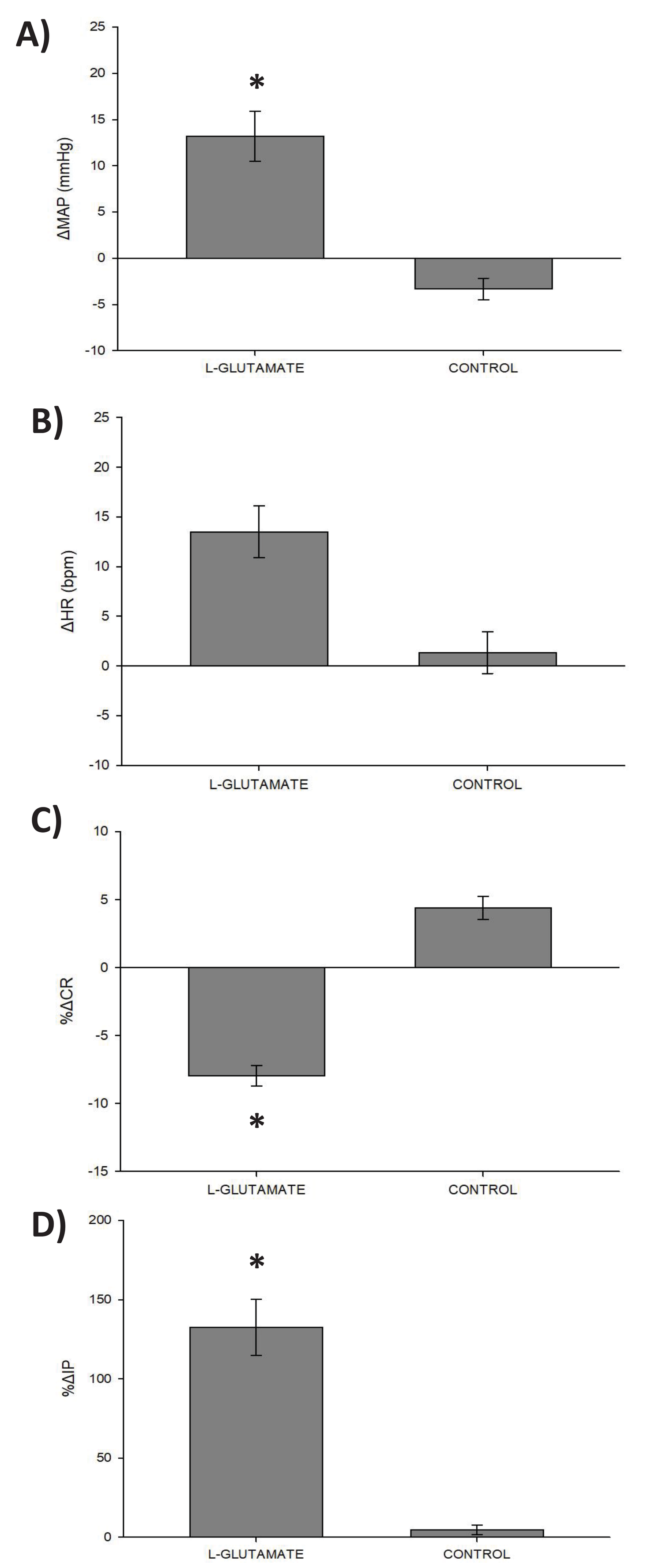

Figure 6: A) Change in mean arterial pressure (ΔMAP, mmHg), B) Change heart rate (ΔHR, bpm), C) Percent change in renal conductance (%ΔRC), and D) Percent change in intravesical pressure (%ΔIP) evoked by bilateral injections of L-glutamate or saline (control) into the shell NAcc. *P<0.05 vs. control

CONCLUSION

- The shell NAcc participates in the neural circuitry involved in micturition control and plays a possible tonic role in the arterial pressure regulation.

REFERENCES

- Ding, Y.Q, Wang, D., Xu, J.Q., Ju, G. Direct projections from the medial preoptic area to spinally-projecting neurons in Barrington's nucleus: an electron microscope study in the rat. Neuroci Lett. 271 (3): 175-178, 1999.
- Fowler, C.L., Griffiths, D., DE Groat, W.C. The neural control of micturition. Nat. Ver. Neurosc. 9(6): 453-466, 2008. Doi: 1038/nrn2401.

ACKNOWLEDGMENTS

- NEPAS and FAPESP

BIDIRECTIONAL EFFECT OF THE EXTREMELY LOW-FREQUENCY ELECTROMAGNETIC FIELD (50 HZ) ON BDNF LEVEL

Angelika Klimek, Hanna Kletkiewicz, Agnieszka Siejka, Maciej Klimiuk, Justyna Maliszewska, Milena Jankowska, Anna Nowakowska, Joanna Wyszkowska, Maria Stankiewicz, Justyna Rogalska

Department of Animal Physiology and Neurobiology, Faculty of Biological and Veterinary Sciences, Nicolaus Copernicus University in Toruń, Poland

TOPIC

Central nervous system- Neurophysiology. Plasticity of neural function.

INTRODUCTION

The impact of the extremely low-frequency electromagnetic field (ELF-EMF) on living organisms is still intensively and widely evaluated. Although many reports suggest a negative impact of ELF-EMF on human health, including the nervous system (e.g. sleep and mood disorders, oxidative stress), ELF-EMF is used in the therapy of brain injuries. Some authors consider ELF-EMF to be a mild stress factor causing changes in the levels of neurotransmitters as well as in stress hormones concentrations. On the other hand, ELF-EMF treatment contributes to increased antioxidant protection and levels of growth factors as well as improvement of functional and mental status in post-stroke patients. The exact effects of ELF-EMF interaction with the organism and the mechanism of its action remain insufficiently described.

OBJECTIVES

We hypothesized that the effects of ELF-EMF is dependent on the value of magnetic induction. Exposure to weak field (low magnetic induction) triggers compensatory mechanisms, while strong field (high magnetic induction) causes harmful changes in the brain. We decided to determine the level of brain derived neurotrophic factor- BDNF in hippocampus to evaluate the influence of ELF-EMF exposure on brain plasticity processes.

MATERIALS AND METHODS

Adult (3 months old), male Wistar rats were used in the experiment. Animals were divided into three groups: control, exposed to 1 mT 50 Hz ELF-EMF or to 7 mT 50 Hz ELF-EMF. Rats were exposed to ELF-EMF 1 hour a day for 7 days. Control animals were subjected to the same experimental procedure as the exposed groups, except ELF-EMF exposure. The exposure was repeated three times with three week intervals. After the end of each exposure the part of rats was sacrificed and brains were collected. The level of BDNF was determined in hippocampus.

Fig. 1. ELF-EMF exposure set. Coil generating ELF-EMF with the plastic box.

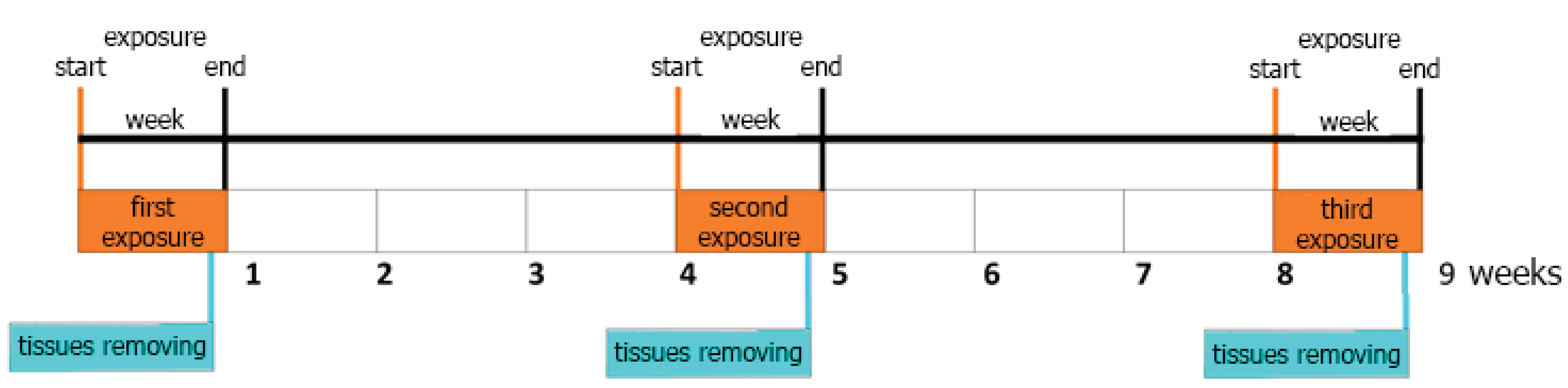

Fig. 2. The scheme of the experiment.

RESULTS

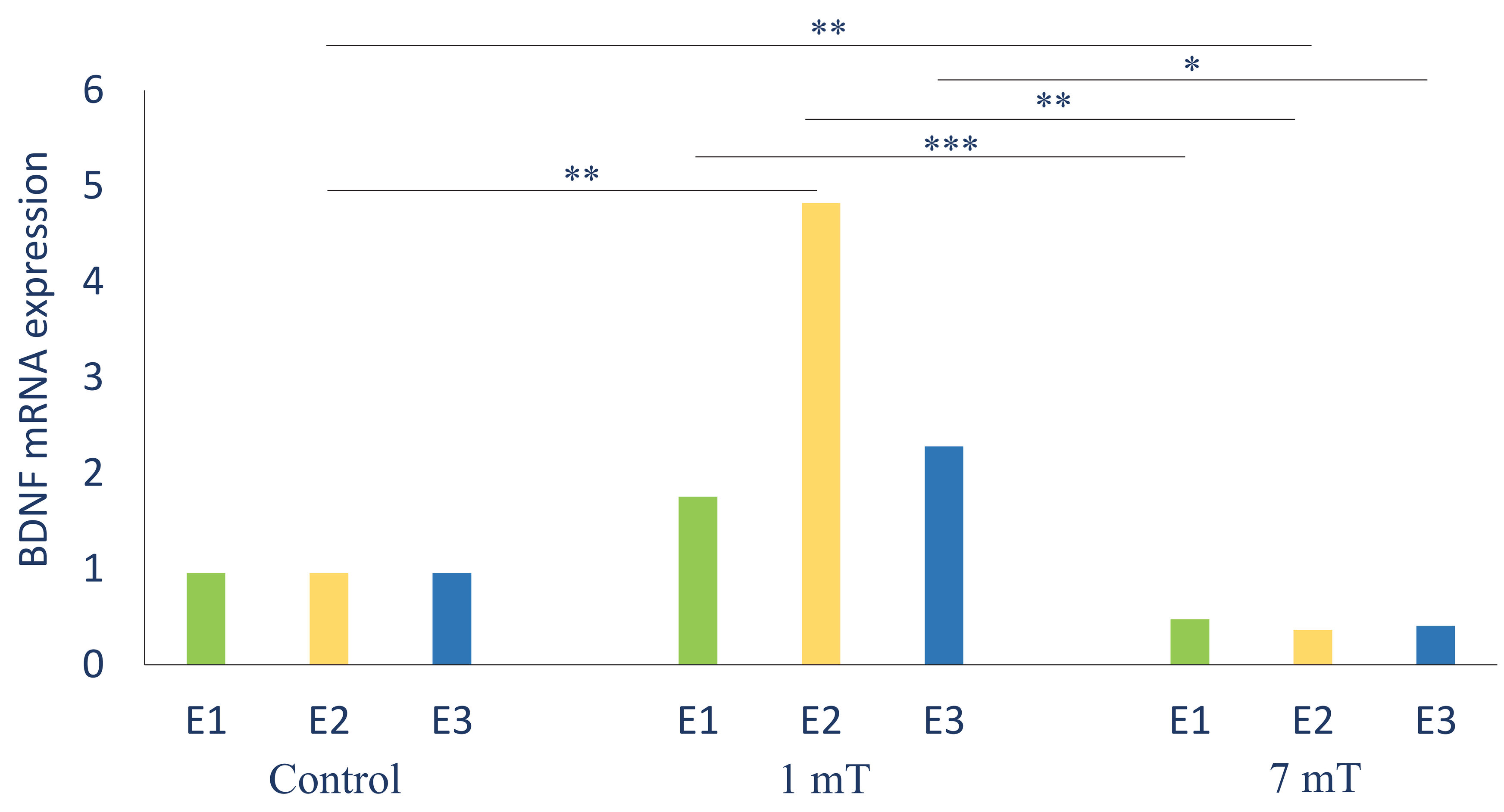

Fig. 3. Level of BDNF expression in hippocampus.

Exposure to 1 mT ELF-EMF significantly increased the level of BDNF after the second exposure. The level of BDNF after second exposure to 7 mT ELF-EMF was significantly lower compared to control group level. Moreover, the level of expression of BDNF was significantly lower in 7 mT group compared to 1 mT group after each exposure.

CONCLUSIONS

Our results suggest that the effect of ELF-EMF is bidirectional and depends on the value of magnetic induction. 1 mT ELF-EMF is a stimulus activating brain plasticity processes by increasing BDNF level, while exposure to 7 mT ELF-EMF decreases BDNF level.

REFERENCES

- Szemerszky R., Zelena D., Barna I., Bárdos G. Stress-related endocrinological and psychopathological effects of short- and long-term 50Hz electromagnetic field exposure in rats, 2010, Brain Res Bull, p. 92-99
- Mahdavi S.M., Sahraei H., Yaghmaei P., Tavakoli H., Effects of electromagnetic radiation exposure on stress-related behaviors and stress hormones in male wistar rats, 2014, Biomol Ther (Seoul), p. 570–576
- El-Helaly M., Abu-Hashem E., Oxidative stress, melatonin level, and sleep insufficiency among electronic equipment repairers, 2010, Indian J Occup Environ Med., p. 66-70
- Cichoń N., Bijak M., Miller E., Saluk J. Extremely low frequency electromagnetic field (ELF-EMF) reduces oxidative stress and improves functional and psychological status in ischemic stroke patients, 2017, Bioelectromagnetics, p. 386-396
- Cichoń N., Bijak M., Czarny P., Miller E., Synowiec E., Sliwinski T., Saluk-Bijak J. Increase in Blood Levels of Growth Factors Involved in the Neuroplasticity Process by Using an Extremely Low Frequency Electromagnetic Field in Post-stroke Patients, 2018, Front Aging Neurosci.

FUNDING

grant from National Science Centre, Poland, no. 2017/25/B/NZ7/00638 and project no. POWR.03.05.00-00-Z302/17 Universitas Copernicana Thoruniensis In Futuro, a part of the programme Knowledge Education Development

EARLY-LIFE STRESS AFFECTS PERIPHERAL AND BRAIN RESPONSE TO IMMUNE CHALLENGE IN FEMALE RATS

ANNA SOLARZ, IWONA MAJCHER-MAŚLANKA, JOANNA KRYST, AGNIESZKA CHOCYK

Maj Institute of Pharmacology, Polish Academy of Sciences, Department of Pharmacology, Laboratory of Pharmacology and Brain Biostructure, 31-343 Kraków, Smetna street 12, Poland

solarz@if-pan.krakow.pl

INTRODUCTION

Early-life stress (ELS) is considered as relevant etiological factor in mental and neurodegenerative disorders. Those disorders can occur later in life, despite the fact that they might have developmental origins. Nowadays coexistence of blood-brain barrier (BBB) disturbances and inflammation appears to play an important role in the etiology, development and progression of those diseases. Our previous study revealed small-scale effects of ELS, modeled by maternal separation (MS), on BBB, which could reflect both adaptive or maladaptive changes within the BBB depending on sex, age and brain region. Moreover, ELS-induced changes in the expression of key regulators of BBB function, such as tight junctions proteins (TJPs), may result in maladaptation of the BBB specifically in response to other environmental factors. ELS may result in impaired functioning of the medial prefrontal cortex (mPFC) and hippocampus (HP), therefore structures selected for this study seem to be crucial for ELS as well as for mental and neurodegenerative disorders. Clinical data suggest that mentioned diseases exhibit different prevalence in-between sexes, however data on females are still insufficient in this regard. This seems to be especially important due to the fact that BBB is less permeable in females than in males..

OBJECTIVES

In the present study we investigated if, ELS may modulate BBB functions and inflammatory processes in response to acute infection in later life

RESULTS

- **LPS induced proinflammatory response on the periphery and in consequence increased BBB permeability, TJPs (*Cldn5*, *Ocln*) and *Icam1* mRNA expression in the mPFC and HP**
- **LPS enhanced mRNA expression of neuroinflammation mediators *Tlr4*, microglial markers (*Aif1*, *Itgam*) and proinflammatory cytokines (*Il-1β*, *Tnfα*)**
- **MS enhanced LPS-induced upregulation of TJPs expression in the HP**
- **MS blunted LPS-induced mRNA expression of *Icam1*, *Tlr4*, microglial markers (*Aif1*, *Itgam*) and proinflammatory cytokines (*Il-1β*, *Tnfα*) in the mPFC and HP**
- **MS-triggered changes in response to LPS were more pronounced in adulthood (PND70) than in preadolescence period (PND22)**
- **Especially in adult females, TNFα serum levels and the mRNA level of *Tlr4* and *Aif1* in the HP were significantly lower in the MS group**

MATERIALS & METHODS

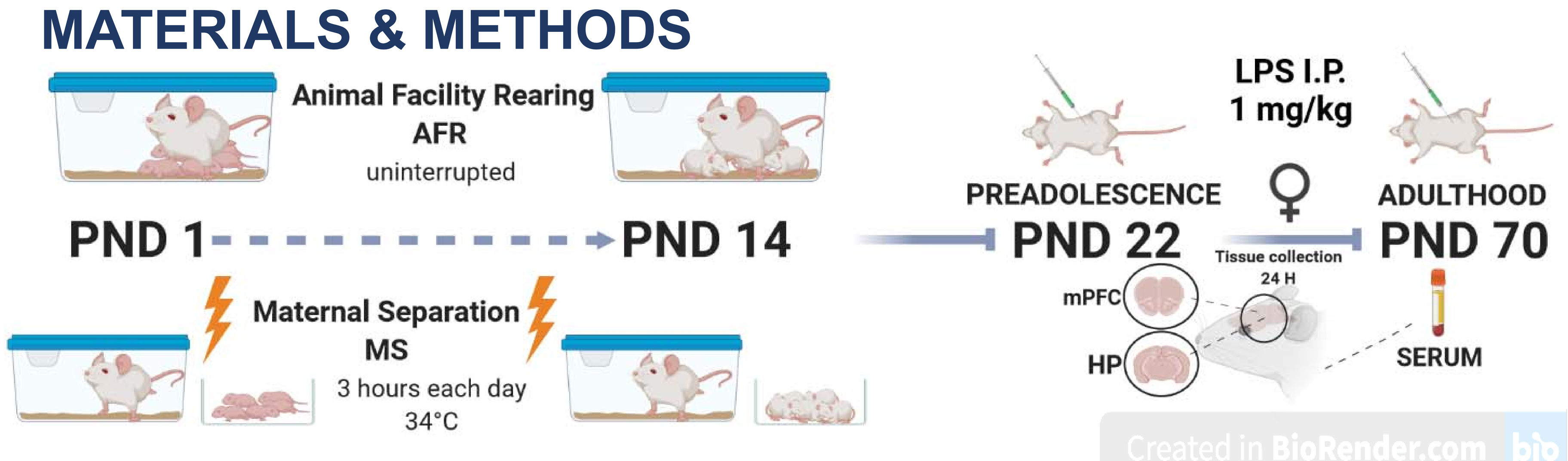

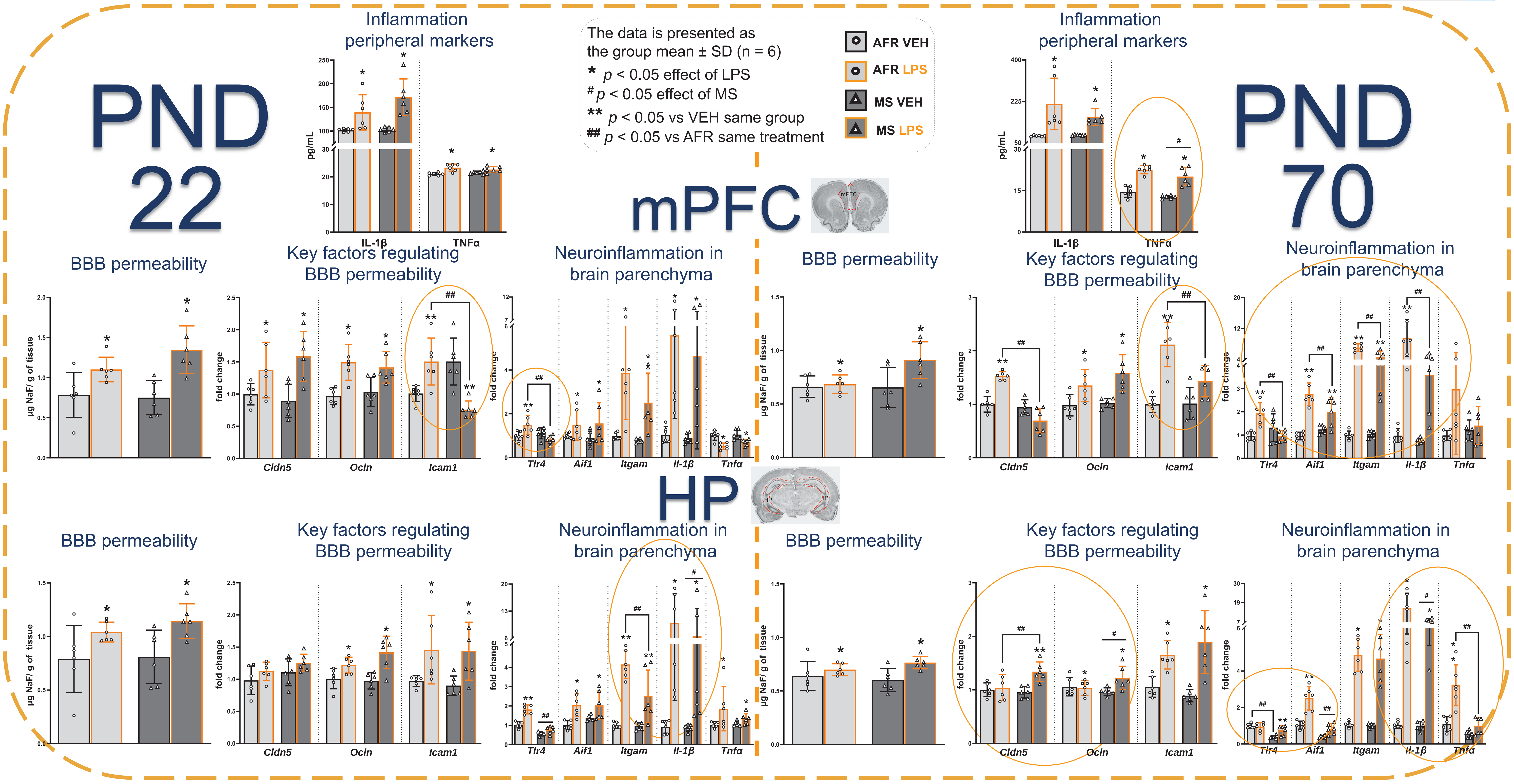

CONCLUSIONS

- **ELS may permanently affect BBB integrity during brain maturation leading to lifelong consequences**
- **ELS may trigger adaptive response counteracting the impact of acute immune challenge in females**
- **Such ELS-triggered effects may underlie susceptibility or resilience to mental and neurodegenerative disorders**

REFERENCES

1. Solarz A, Majcher-Maślanka I, Chocyk A. Effects of early-life stress and sex on blood-brain barrier permeability and integrity in juvenile and adult rats. Dev Neurobiol. 2021 Jul 28. doi: 10.1002/dneu.22846. Epub ahead of print. PMID: 34320279.

2. Created with BioRender.com

ACKNOWLAGMENTS: *Supported by grant NCN PRELUDIUM 12 2016/23/N/NZ4/01148 and partially by statutory activity of the Maj Institute of Pharmacology, Polish Academy of Sciences, 31-343 Kraków, Smetna street 12, Poland*

NATIONAL SCIENCE CENTRE POLAND

MATERIALS & METHODS

Model of acute infection: Acute intraperitoneal injection (I.P.) of lipopolysaccharide (LPS; 1 mg/kg; Sigma Aldrich) or vehicle (VEH, saline) at postnatal day (PND) 22 and 70

ELISA: The concentration of the proinflammatory cytokines in the serum was determined using commercially available kits for rat interleukin 1 beta (IL-1β) and tumor necrosis factor alpha (TNF-α) (R&D Systems)

Assessment of BBB permeability: Fluorescent tracer administration: 4% sodium fluorescein (NaF; 2 ml/kg; i.p.; Sigma Aldrich); tracer circulation time: 30 min; Transcardial perfusion with saline; Brain tissue homogenization (TissueLyser II, Qiagen); Fluorescence determination: excitation/emission 440/525 nm (Tecan)

RT-qPCR: Brain tissue homogenization (TissueLyser II, Qiagen). Total RNA extraction (RNAeasy Mini Kit, Qiagen); RNA reverse transcription (High-Capacity cDNA Reverse Transcription Kit, ThermoFisher Scientific). The TaqMan® Gene Expression Assays (ThermoFisher Scientific) used: *Cldn5* Rn01753146_s1, *Ocln* Rn00580064_m1, *Icam1* Rn00564227_m1, Tlr4 Rn00569848_m1, *Aif1* Rn00574125_g1, *Itgam* Rn00709342_m1, *Il-1β* Rn00580432_m1, *Tnfα* Rn99999017_m1. The amplification using the TaqMan® Gene Expression PCR Master Mix (ThermoFisher Scientific) was conducted by the Quant Studio Flex 12K (ThermoFisher Scientific). The expression of housekeeping gene (*Gapdh* Rn01775763_g1) was quantified to control for variations in cDNA levels.

Statistics: Data was analyzed by two-way ANOVA followed by post-hoc analysis. $p < 0.05$ was considered statistically significant

THE ACTIVATED MICROGLIA IN HIPOCAMPUS AS A CHARACTERISTIC OF STREPTOZOTOCIN INDUCED MODEL OF ALZHEIMER DISEASE IN RATS

S2.P7

CENTRAL NERVOUS SYSTEM. NEUROPHYSIOLOGY. PLASTICITY OF NEURAL FUNCTION

JOANNA DUNACKA[1], GRZEGORZ ŚWIĄTEK[1], IRENA MAJKUTEWICZ[1], PAWEŁ MATULEWICZ[1], BEATA GREMBECKA[1], WOJCIECH GLAC[1], DANUTA WRONA[1]

[1] University of Gdansk, Faculty of Biology, Department of Animal and Human Physiology; joanna.dunacka@ug.edu.pl

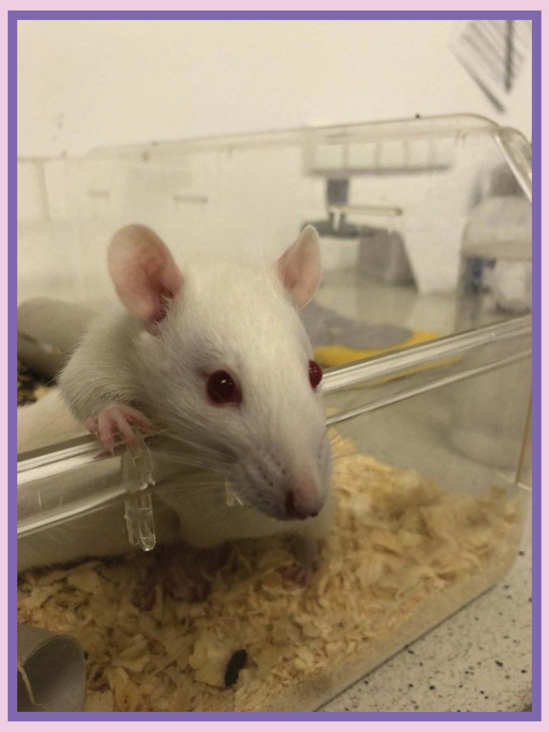

Introduction and Objectives

Sporadic form of Alzheimer's disease (sAD) accounts for 95 % of AD cases. Due to the unknown etiology of sAD, it is only possible to model by reproducing its symptoms. One of the models used is the administration of streptozotocin to the lateral ventricles of the brain. The application of this substance causes: methylation or alkylation of DNA, increased presence of β-amyloid and tau protein, neuronal death, neuroinflammation, oxidative stress, impartment of IR expression and glucose metabolism, damage insulin signaling, insulin resistance, cholinergic deficits, impairment functioning of working and spatial memory (Nazem et al., 2015; Grieb, 2016; Kamat el al., 2016). The aim of the study was to determine whether there is activation of microglia in the various parts of hippocampus (structure responsible for consolidation of memory trace), which may affect the neurodegenerative changes observed in this model of the disease.

Methods

Animals

In experiment were used male Wistar Han rats (n=11 (STZ=5, VEH=6)) with initial weight 200±20g. After handling, the animals were separated into individual cages with constant olfactory and visual contact with other animals. The cages with the animals were located in the animal house throughout the entire experiment (12h:12h-light:dark cycle; lights on at 6 a.m.). Rodents had access to food and water *ad libitium*.

Induction of sAD model

Streptozotocin (STZ) dissolved in citratte buffer (VEH-pH 4,5; 0,02M) was administrated by intracerebroventricular microinjections (AP-1,3mm, L±2mm, D-3,6mm). The substance served through the cannulae implanted on the surface of the skull. STZ applied twice, with one day interval, about total dose 3 mg/kg. The volume of 1 imicroinjections totals 2 µl/lateral ventrice. The control group received VEH in the same volume (Majkutewicz et. al., 2016).

Immunohistochemistry

The fixed brains were cut into coronal sections of 20 µm thickness with the use of cryostat (CM1850, Leica Germany). Slices between 2.8 and 3.14 mm posterior to the bregma were collected and blocked for 2h in 5% bovine serum albumin (BSA) in 0.3% Triton X. After triple rinsing in PBS slices were incubated for 48h in 4°C in primary antibody: mouse anti-macrophages/monocytes (Sigma Aldrich, MAB1435, 1:250) in PBS with 2% BSA and 0.3% Triton X. After triple rinse in PBS sections were incubated for 2h in secondary antibody solution (goat anti mouse IgG H&L Alexa Fluor 488, Abcam, ab150113, 1:500 in PBS). Slices were placed on gelatin-coated slides, dried, immersed in xylene and mounted using DPX.

Microglia counting

The slides were analyzed on fluorescence microscope (Zeiss Axio Scope A1) coupled with Axio Vision software. After collection of images from various part of hippocampus, a calibrated frame for cell counting (0.01 mm2) was imposed on the photographs and labelled microglia were identified and counted by an observer blinded to the experimental group allocation.

Analysis of results

For statistical analysis U-Manna-Whitney test was used in Statistica program. The graphes were created in Graphpad program.

Results and Conclusions

Samples photo

CA1 VEH

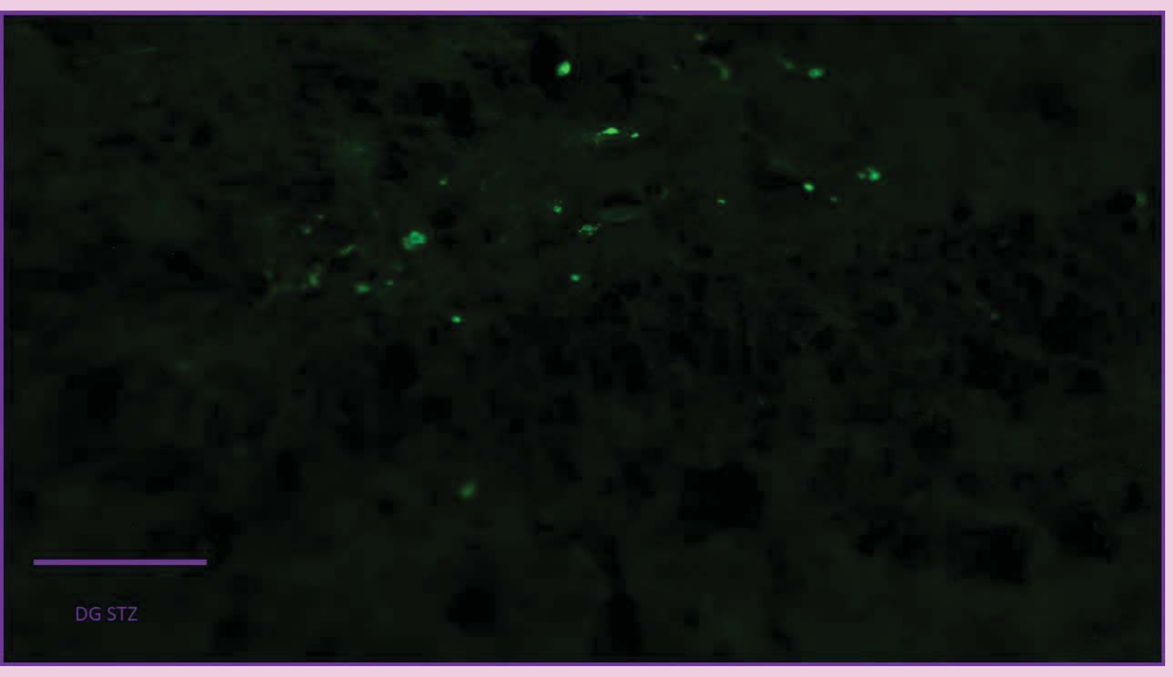

DG STZ

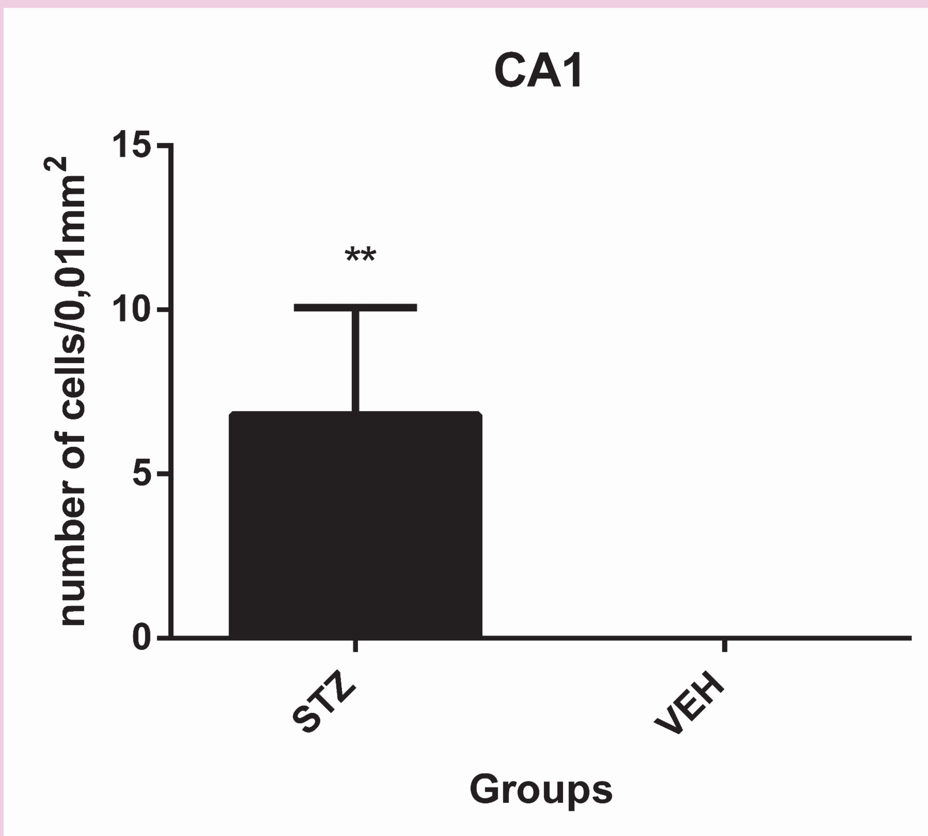

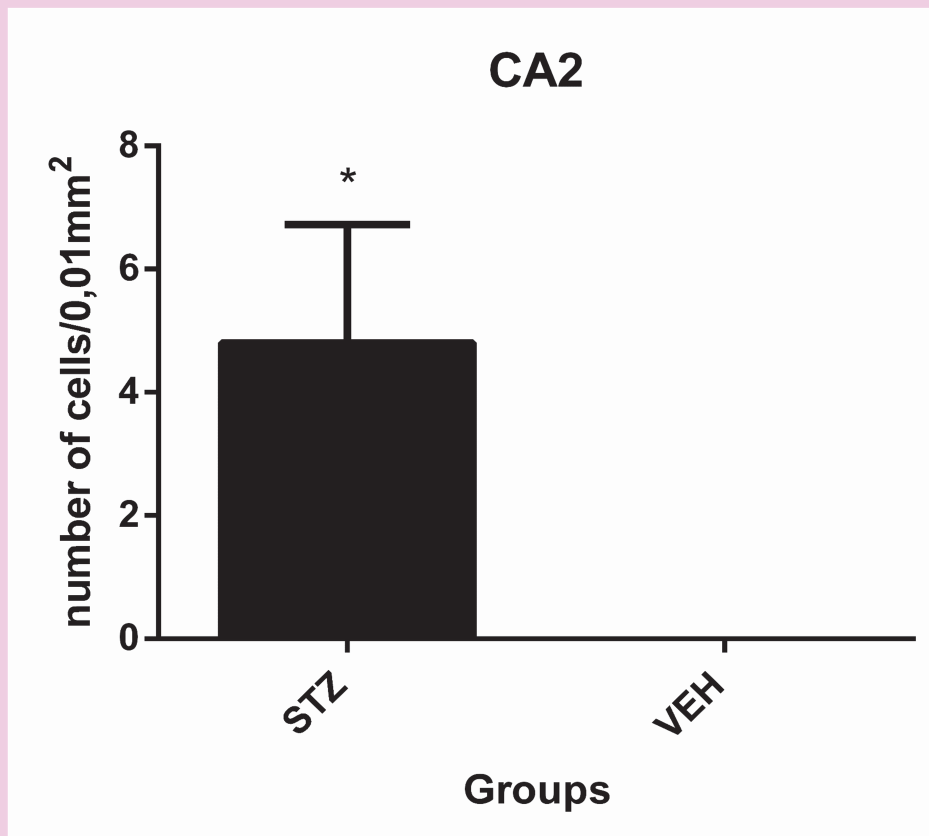

The numer of activated microglia cells in various parts of hippocampus

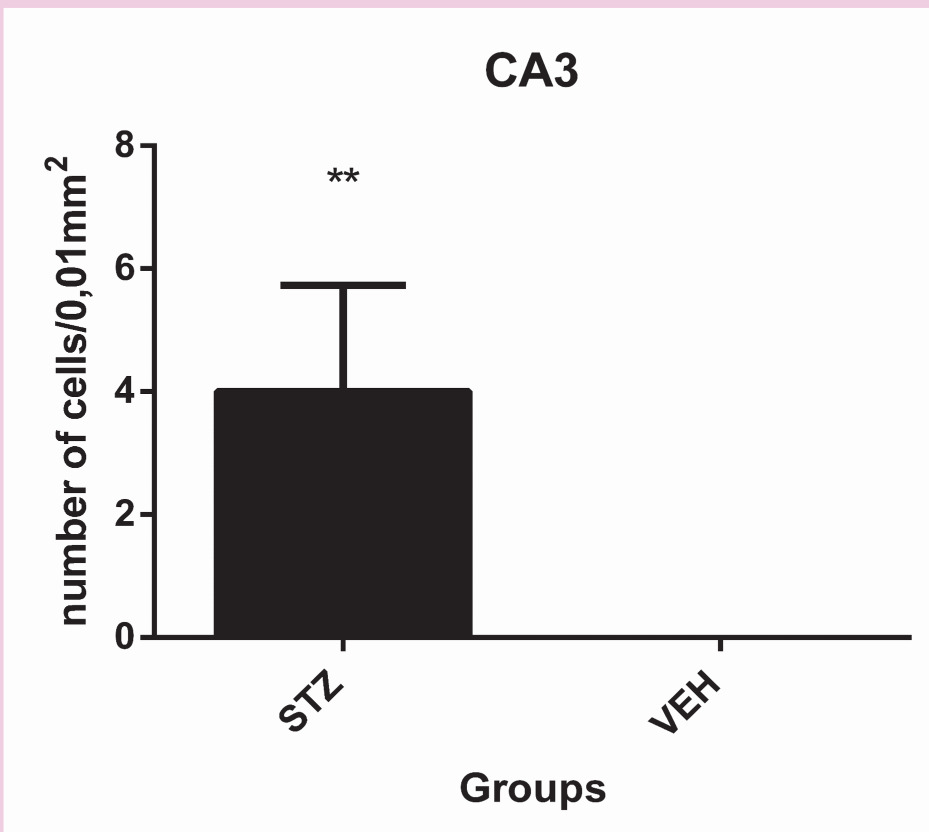

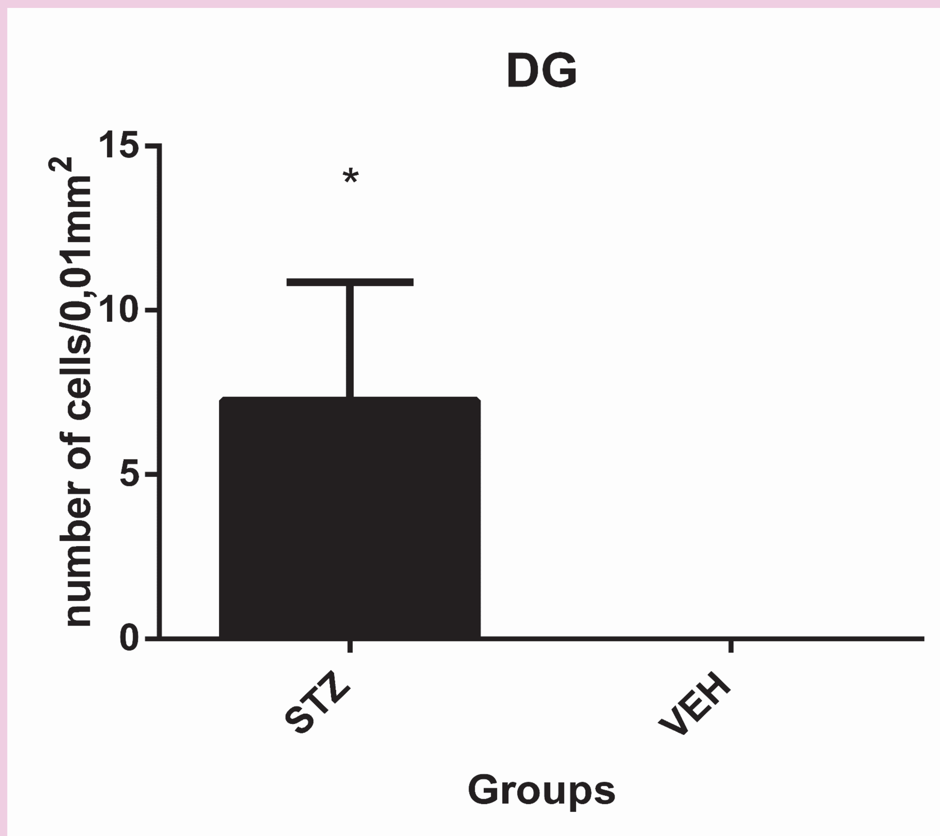

* p<0,05 compare to VEH, ** p<0,01 compare to VEH

The activated microglia cells has been observed in different parts of the hippocampus only in rats with sAD model. Activation of these cells may contribute to neurodegeneration, and thus memory disorders observed in this model of disease (Majkutewicz et.al, 2016).

Bibliography

Grieb P. Intracerebroventricular Streptozotocin Injections as a Model of Alzheimer's Disease: in Search of a Relevant Mechanism. Mol Neurobiol. 2016 Apr;53(3):1741-1752. doi: 10.1007/s12035-015-9132-3. Epub 2015 Mar 7. PMID: 25744568; PMCID: PMC4789228.

Kamat PK, Kalani A, Rai S, Tota SK, Kumar A, Ahmad AS. Streptozotocin Intracerebroventricular-Induced Neurotoxicity and Brain Insulin Resistance: a Therapeutic Intervention for Treatment of Sporadic Alzheimer's Disease (sAD)-Like Pathology. Mol Neurobiol. 2016 Sep;53(7):4548-62. doi: 10.1007/s12035-015-9384-y. Epub 2015 Aug 23. PMID: 26298663.

Majkutewicz I, Kurowska E, Podlacha M, Myślińska D, Grembecka B, Ruciński J, Plucińska K, Jerzemowska G, Wrona D. Dimethyl fumarate attenuates intracerebroventricular streptozotocin-induced spatial memory impairment and hippocampal neurodegeneration in rats. Behav Brain Res. 2016 Jul 15;308:24-37. doi: 10.1016/j.bbr.2016.04.012. Epub 2016 Apr 12. PMID: 27083302.

Nazem A, Sankowski R, Bacher M, Al-Abed Y. Rodent models of neuroinflammation for Alzheimer's disease. J Neuroinflammation. 2015 Apr 17;12:74. doi: 10.1186/s12974-015-0291-y. PMID: 25890375; PMCID: PMC4404276.

INFLUENCE OF CAFFEINE ON THE GENE EXPRESSION OF PROINFLAMMATORY CYTOKINES AND THEIR RECEPTORS IN THE HYPOTHALAMIC-PITUITARY UNIT

M. Wójcik[1], M. Tomczyk[1], J. Bochenek[1], D. Tomaszewska-Zaremba[1], A. Antushevich[1], A. Krawczyńska[1], A. Herman[2], A.P. Herman[1]*

1 The Kielanowski Institute of Animal Physiology and Nutrition Polish Academy of Sciences, Poland;
2 Faculty of Health Sciences, Warsaw School of Engineering and Health, Warsaw, Poland
**a.herman@ifzz.pl*

Introduction: Inflammatory cytokines are considered to be important mediators modulating neuroendocrine system at the level of the brain. The origin of these cytokines are differentiated. Some of them reach the brain parenchyma from periphery or are produced in the cells of choroid plexus; however these cytokines and their corresponding receptors are also expressed in the hypothalamic and pituitary cells both during homeostasis millau and inflammation. Caffeine is one of the most widely consumed pharmacologically active substances which receptors are also widespread in the hypothalamic-pituitary unit. There are reports suggesting that caffeine may influence secretion of pituitary hormones however, this mechanism is not fully elucidated.

Aim: The aim of the study was to determine the influence of caffeine on the expression of proinflammatory cytokines and their receptors in the hypothalamus and pituitary

Material and methods: The study was performed on sheep model. The experiment was carried out on 12 ewes intravenously injected with caffeine at the dose of 40 mg/kg (n = 6) or saline (n = 6). Animals were euthanized 3 hours after caffeine or saline injection. Hypothalamic tissue and anterior pituitary (AP) was dissected. The gene expression of cytokines such as: interleukin (IL)-1, IL-6 and tumor necrosis factor (TNF) α and their receptors IL-1R1, IL-1R2, IL-6R, gp-130, TNFR1, TNFR2.

Results:

HYPOTHALAMUS

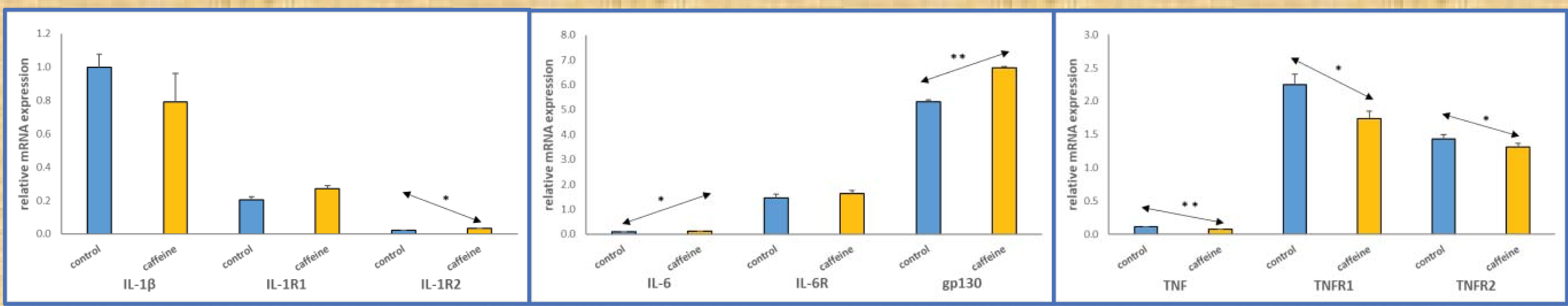

PITUITARY

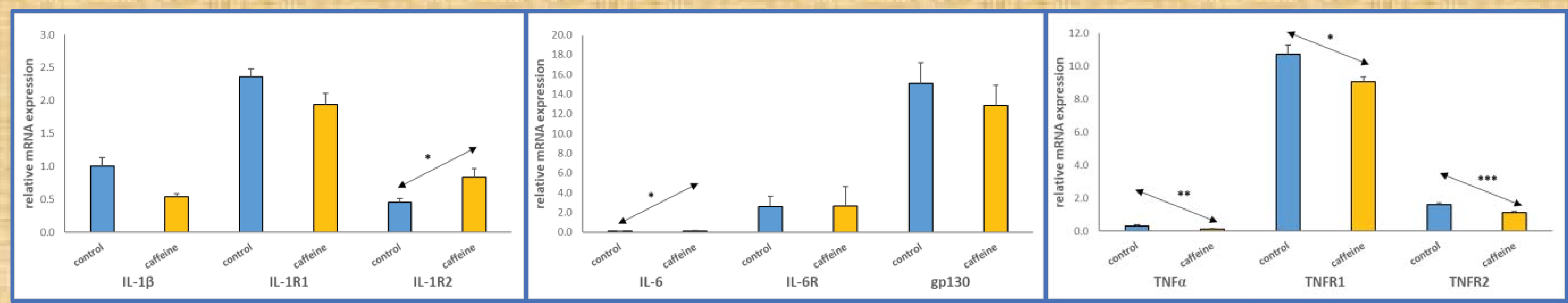

*Asterisks indicate statistical significance according to U Mann-Whitney test; * p<0,05; ** p<0,01; *** P<0,001*

Conclusion: Our study showed that caffeine exerted both stimulatory and suppressory effect on the gene expression of proinflammatory cytokines and some of these cytokines receptors in the hypothalamic-pituitary unit. This suggests that one of the mechanisms via caffeine influences the secretory activity of the hypothalamic-pituitary unit may be modulation of proinflammatory cytokines synthesis in these brain tissues.

***Acknowledgments**: This work was supported by the funds granted by National Science Centre, Poland based on the decision no DEC-2017/25/B/NZ9/00225*

The CB_1 receptor antagonist reduces the pressor response of Ang II and Ang 1-7 injected into paraventricular nucleus of the hypothalamus (PVN) in conscious normotensive and hypertensive rats.

Krzysztof Mińczuk[1], Barbara Malinowska[1]

1. Medical University of Bialystok, Department of Experimental Physiology and Patophysiology

Introduction

Previous experiments performed on anesthetized normotensive rats, have shown that intravenous injection of AT_1 antagonist losartan reverses the pressor response to stimulation of CB_1 cannabinoid receptors (CB_1-R) in the paraventricular nucleus of the hypothalamus (PVN) (1).

Aim

The aim of our study was to determine the interaction between CB_1-R and Ang II as well as the Ang 1-7 in the regulation of blood pressure in conscious rats with **spontaneous hypertension** (**SHR**) and their **normotensive control** - Wistar Kyoto (**WKY**).

Materials and Methods

All the experiments were performed on __conscious__ rats.

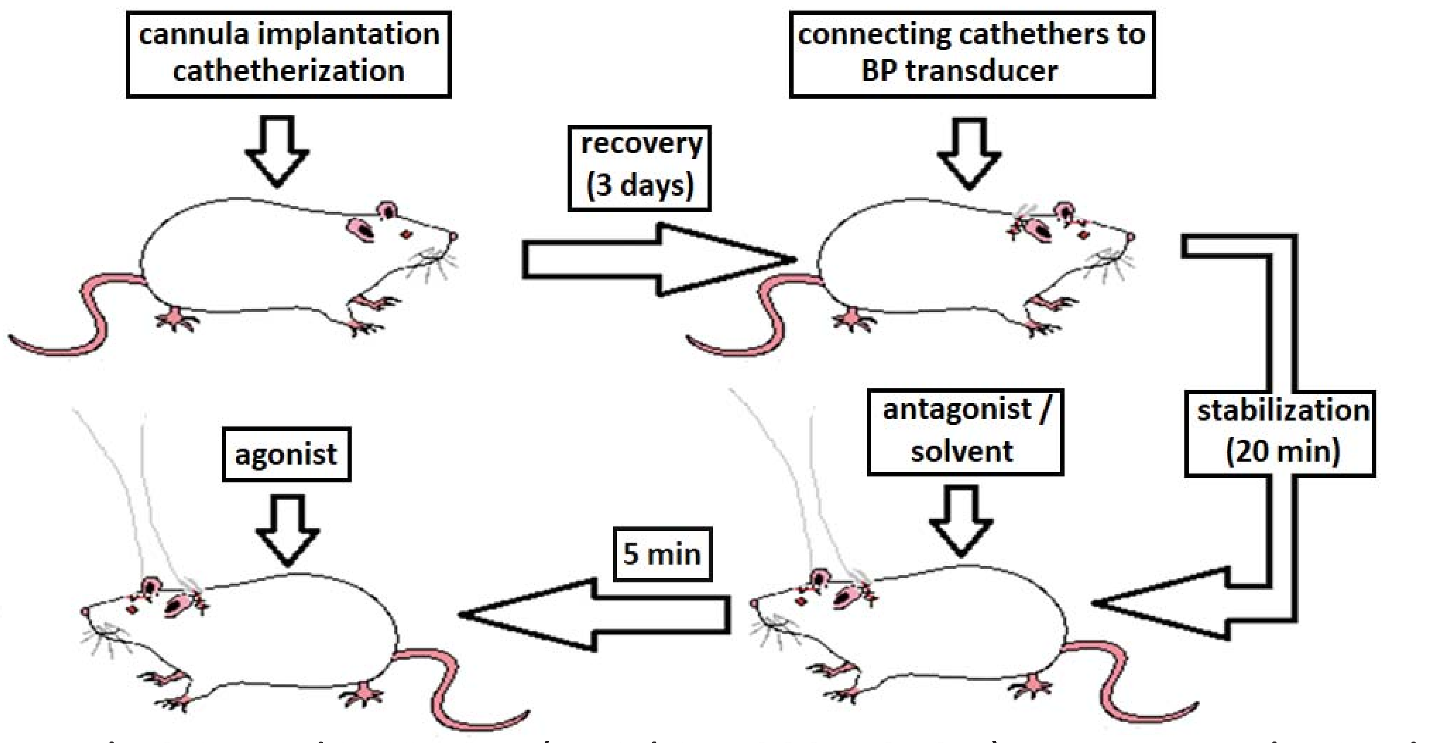

Male SHR and WKY rats (weighing 280 – 350 g) were anaesthetized with intraperitoneal *(i.p.)* injection of pentobarbitone sodium (300 µmol/kg) and placed in a stereotaxic instrument. Stainless steel cannulae (outer and inner diameter of 0.5 and 0.3 mm, respectively) were implanted on the right side, using established coordinates obtained from the Paxinos and Watson rat brain atlas (2) (1.5 mm caudal to the bregma; 0.5 mm lateral to the midline and 8 mm below the skull surface). Next, catheters were placed in left carotid artery, which then were guided under skin and protruded in the neck area.

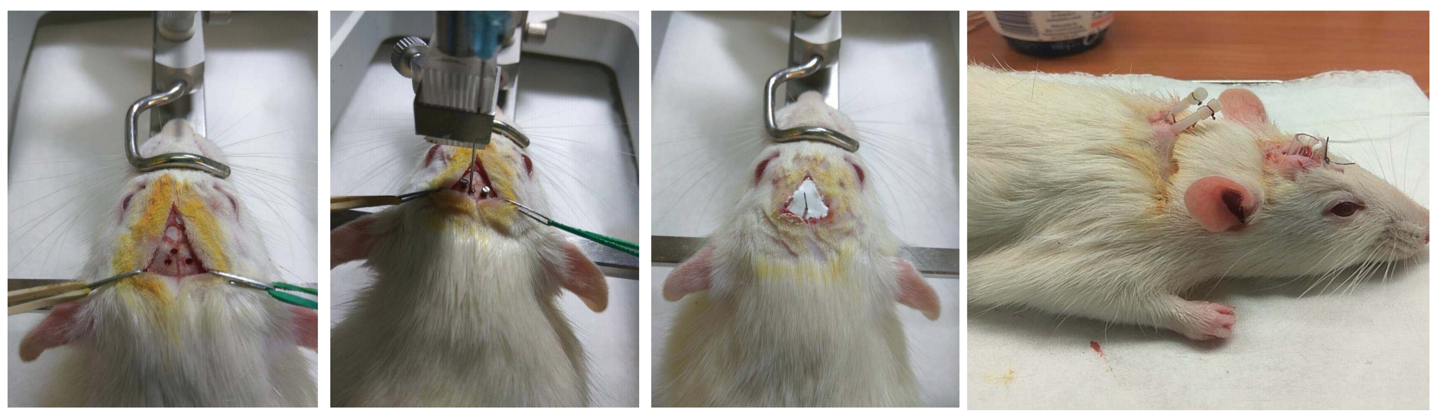

3 days later **PVN** microinjections were administered slowly in a volume of 200 nl per rat. Correct cannula placement was confirmed by light microscopy at the end of the experiment. Only animals for which the correct placement of the guide cannula to the PVN was confirmed were included in this study.

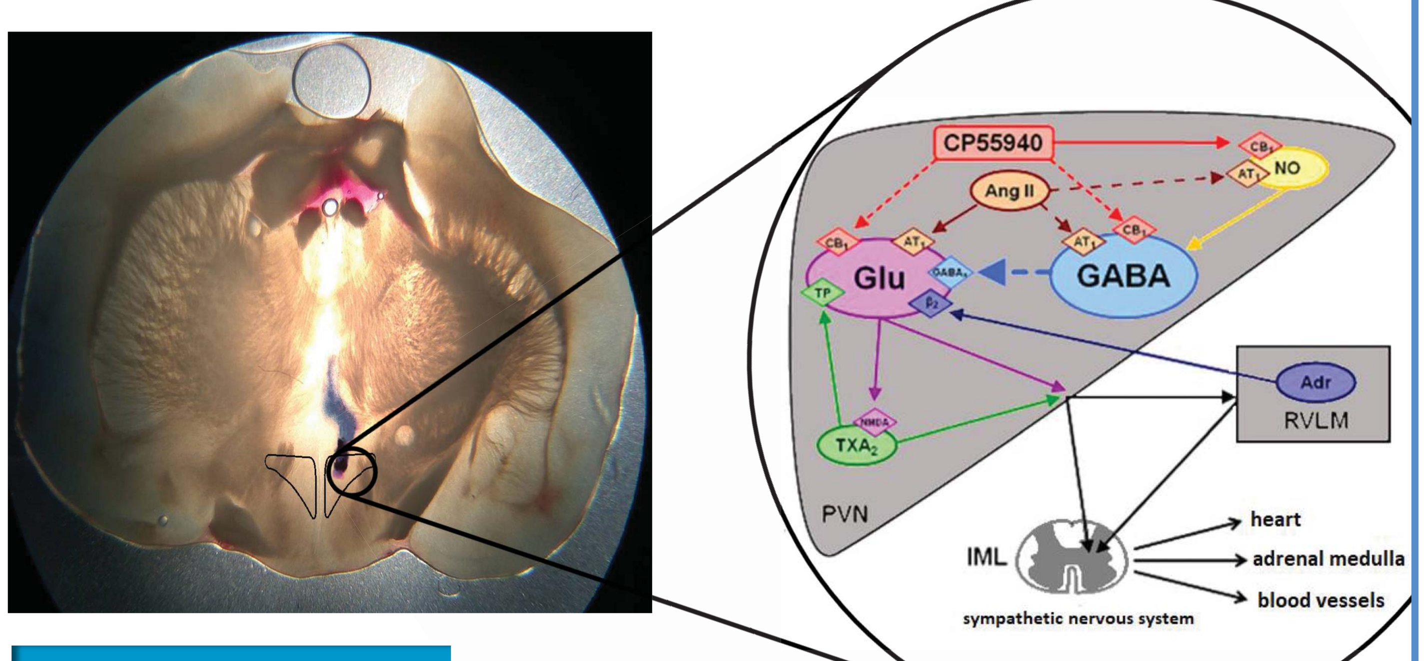

[1] Grzęda et al., 2017

Results

Base systolic (SBP), diastolic (DBP) and mean (MAP) pressures were approximately 60% lower in WKY compared to SHR.

	n	WKY	SHR	p
SBP (mmHg)	40	128 ± 2	196 ± 5	***
DBP (mmHg)	40	105 ± 3	164 ± 3	***
MAP (mmHg)	40	117 ± 3	180 ± 4	***
HR (BPM)	40	366 ± 8	385 ± 3	*

Results presented as means ± SEM

Angiotensin II (0.3 nmol) increases BP via AT_1 and AT_2 receptors

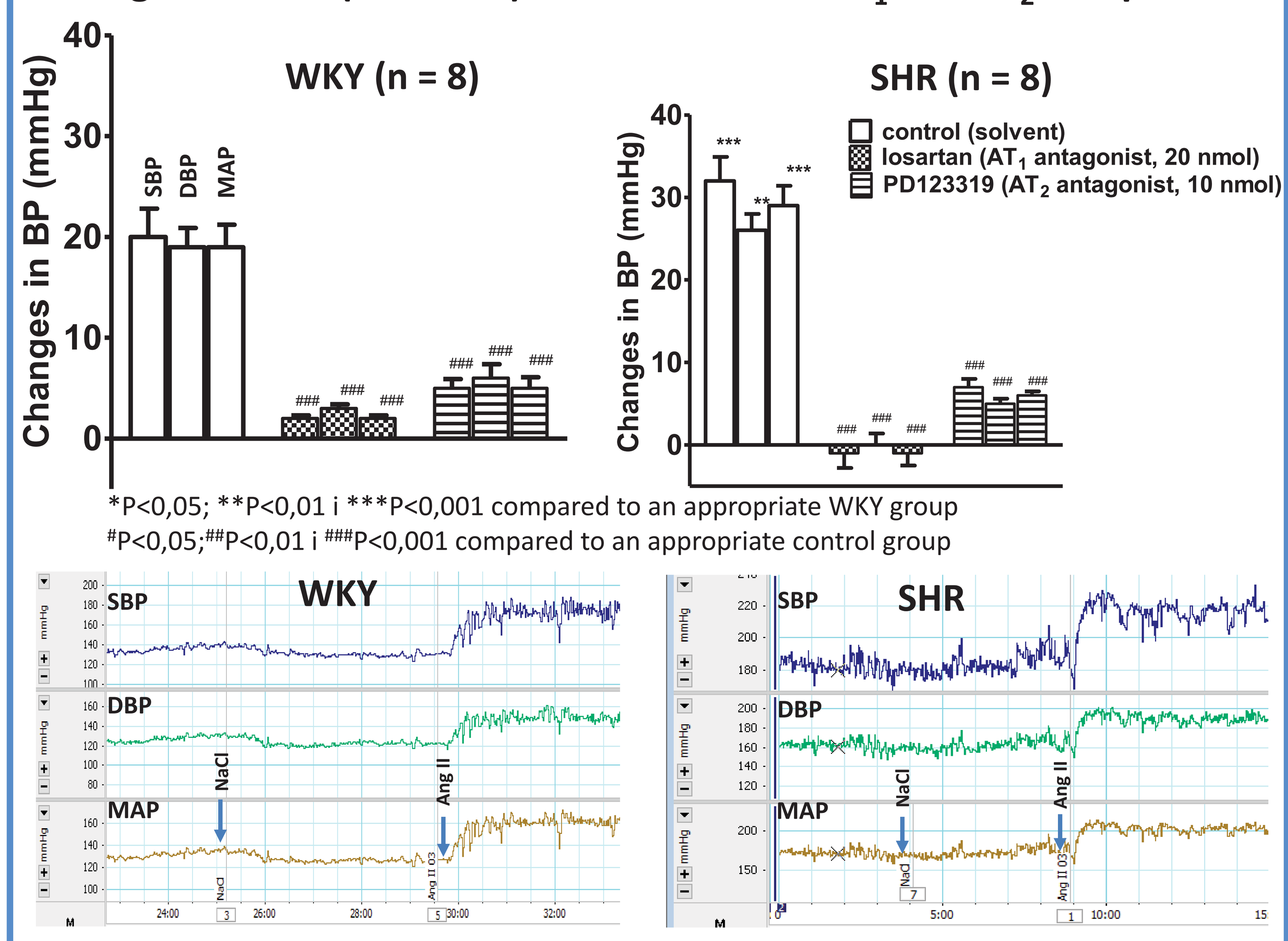

Angiotensin 1-7 (0.3 nmol) increases BP via MAS receptor

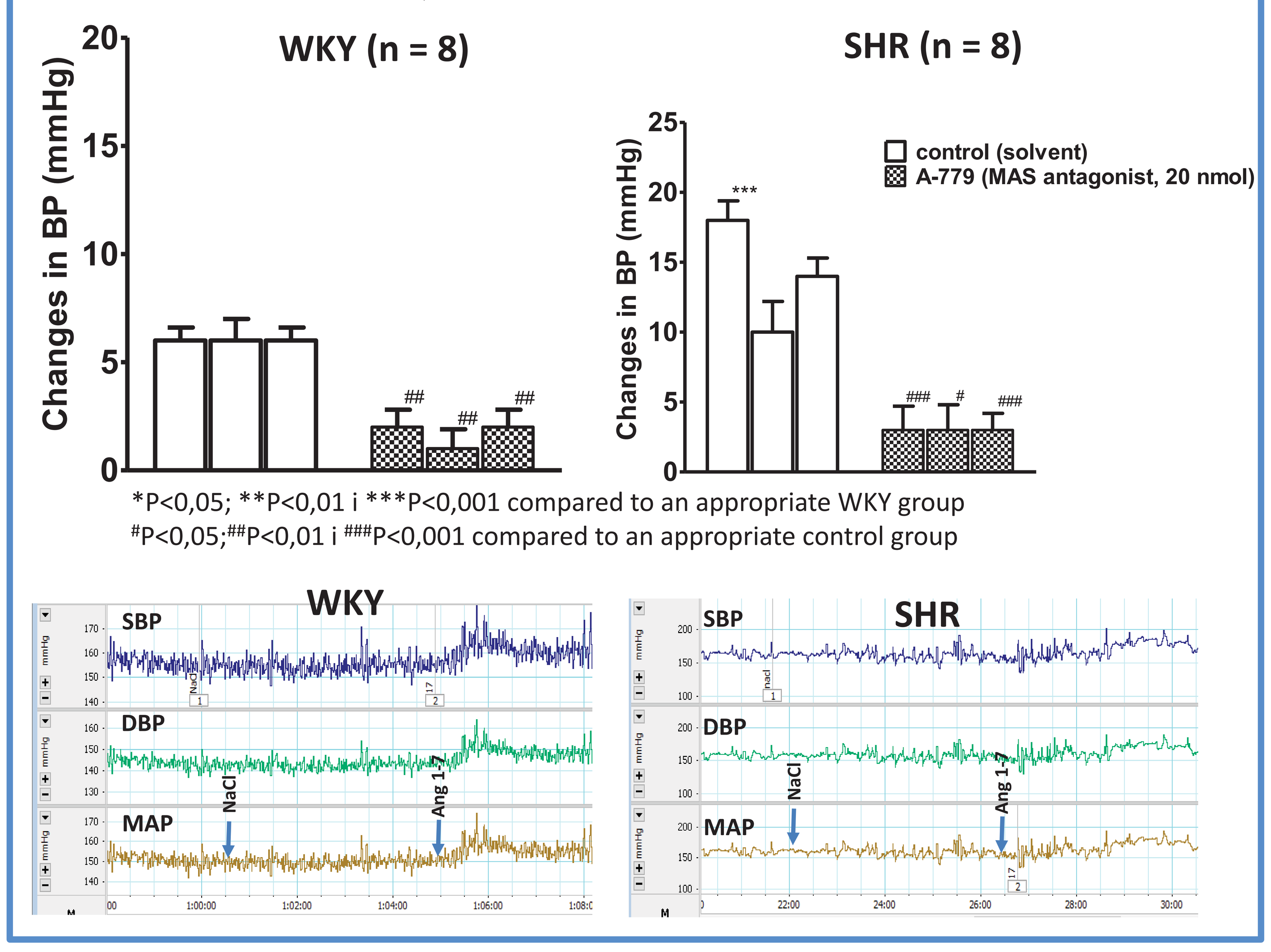

CB_1 receptor antagonist reduces the pressor effects of angiotensin II

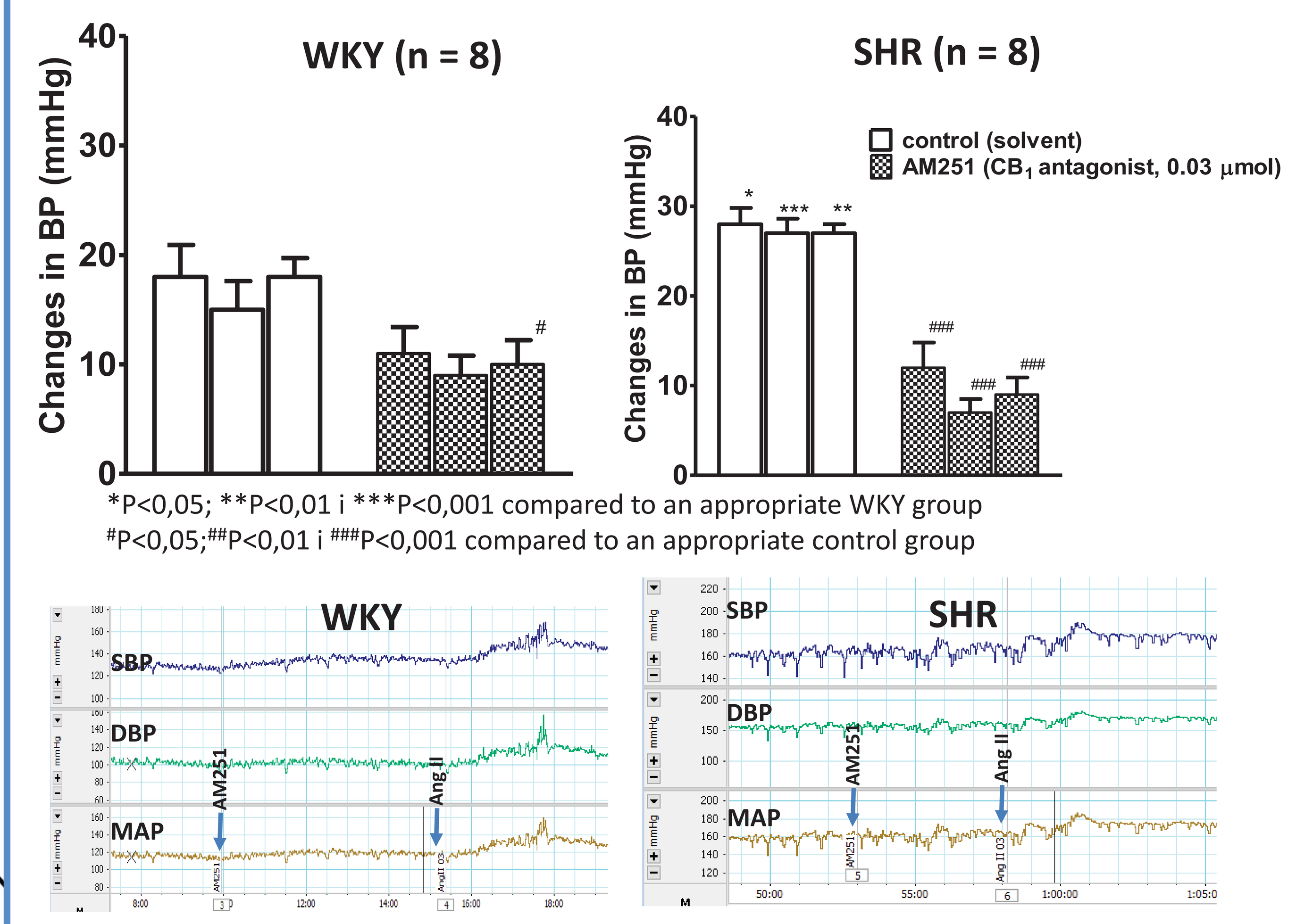

CB_1 receptor antagonist __reverses__ the pressor effects of angiotensin 1-7

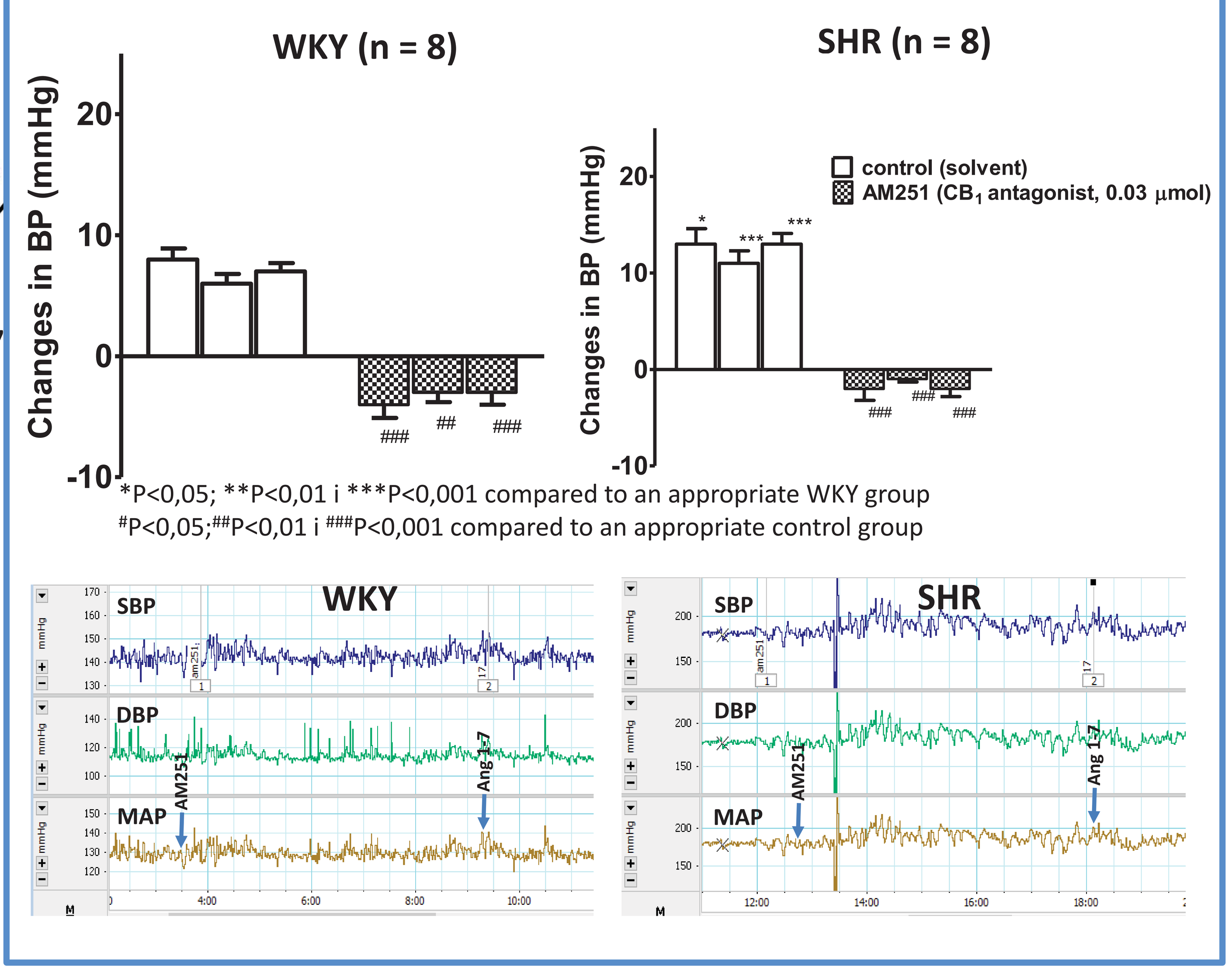

Results cont.

- Centrally administered angiotensin II (0.3 nmol) and angiotensin 1-7 (0.3 nmol), acting through AT_1 and AT_2 receptors, increased blood pressure significantly greater in SHR rats compared to WKY rats.
- Centrally administered angiotensin 1-7 acting through MAS receptor, produces a pressor effect, significantly stronger in SHR rats compared to WKY rats.
- The increase in blood pressure stimulated by Ang II and Ang 1-7 was inhibited by the antagonists AT_1 losartan (8 nmol), AT_2 PD123319 (10 nmol) and Mas A779 (3 nmol) in WKY and SHR, respectively.

- The CB_1-R antagonist AM251 (0.03 µmol) significantly inhibited the effect of Ang II, and __**reversed**__ the pressure response of Ang 1-7 in SHR and WKY. None of the solvents (DMSO, NaCl) nor antagonists caused a significant effect on blood pressure on its own.

Conclusions

- Angiotensin II, with involvement of AT_1 and AT_2 receptors induces a pressor effect significantly greater in SHR rats compared to WKY rats.
- Angiotensin 1-7, with involvement of MAS receptors, induces a pressor effect significantly stronger in SHR rats compared to WKY rats.
- Cannabinoid CB_1-Rs in the PVN modify the pressor effects of Ang II and Ang 1-7 injected into the PVN.

References

[1] Grzęda E, Schlicker E, Toczek M, Zalewska I, Baranowska-Kuczko M, Malinowska B. *CB_1 receptor activation in the rat paraventricular nucleus induces bi-directional cardiovascular effects via modification of glutamatergic and GABAergic neurotransmission*. **Naunyn Schmiedebergs Arch Pharmacol. 2017 Jan;390(1):25-35**

[2] Paxinos G and Watson C. *The Rat Brain in Stereotaxic Coordinates*–**The New Coronal Set, 5th Edn. 2004**

Acknowledgements

The work has been supported by the Medical University of Białystok (SUB/2/DN/21/004/2213).

THE EFFECT OF NIACIN, VITAMIN B3, ON THE β-AMYLOID-ASSOCIATED PROCESS OF NEURODEGENERATION.

Anna Litwiniuk[1], Małgorzata Kalisz[1], Lidia Martyńska[1], Magdalena Chmielowska[1], Anita Domańska[1,2], Wojciech Bik[1]

[1]Department of Neuroendocrinology, Centre of Postgraduate Medical Education, Warsaw;

[2] Department of Physiological Sciences, Warsaw University of Life Sciences (SGGW), Warsaw

Introduction Alzheimer's disease (AD) is the most common form of dementia. Mechanisms of synaptic damage in AD are related to the neurotoxic effects of soluble forms of β-amyloid oligomers (AβO). AβOs attach to the synapses, inhibit synaptic plasticity, damage synaptic cytoskeletal proteins, and ultimately leads to synapse loss. The current direction of research is focused on identifying factors that protect neurons from the toxic effects of AβO. Because niacin is associated with energy metabolism, mitochondrial function, cell death, and aging, it could affect Aβ-dependent neurodegeneration.

The aim of the study We aimed to assess the effect of two different forms of niacin: nicotinic acid (NA) and nicotinamide (N) on the Aβ-dependent neurodegeneration process. The second aim was to investigate whether NA and N could stimulate the neuroprotective effects of astrocytes.

Materials and Methods Experiments were performed on human cell lines: SH-SY5Y (neuroblastoma) and NHA astrocytes. The SH-SY5Y cells were differentiated for 10 days. 24h before the end of the experiment, the SH-SY5Y cells were incubated with CM (Conditioned Medium) derived from NHA astrocyte cultures: the control (CM), and treated with NA (CM-NA) or N (CM-N). After 1h preincubation with CM, CM-NA or CM-N differentiated SH-SY5Y cells were incubated for another 24h with Aβ [5μM]. The MTT test was used to assess the cytotoxicity of the tested factors. The expression level of PSD95 (Postsynaptic density protein 95, which plays an important role in synaptic plasticity) mRNA in neurons was assessed by qRT-PCR. Microscopic observation of autophagolysosomes (Acidic vesicular organelles, AVO) in neurons was also performed.

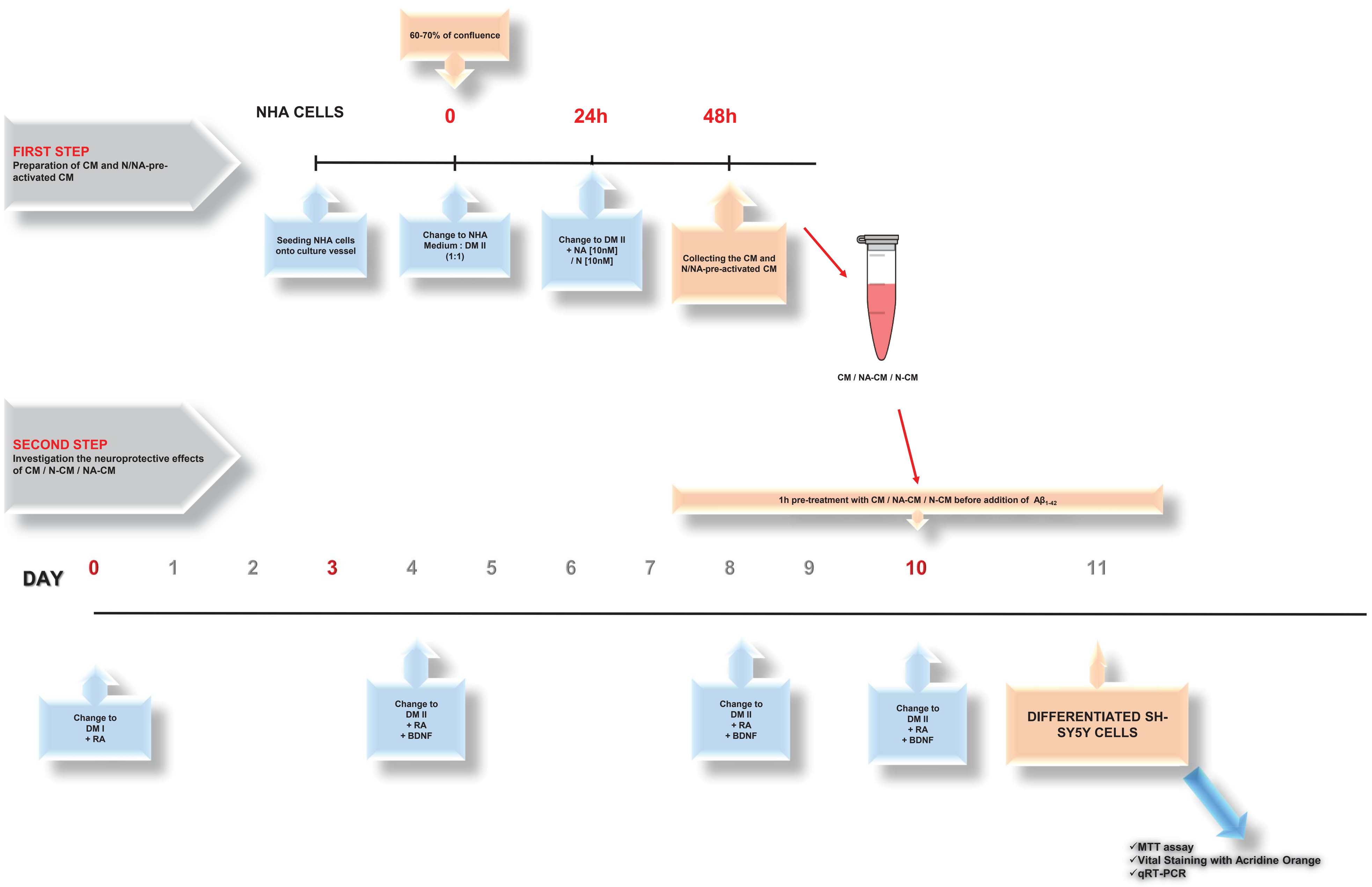

Figure 1. The scheme of the experimental procedures

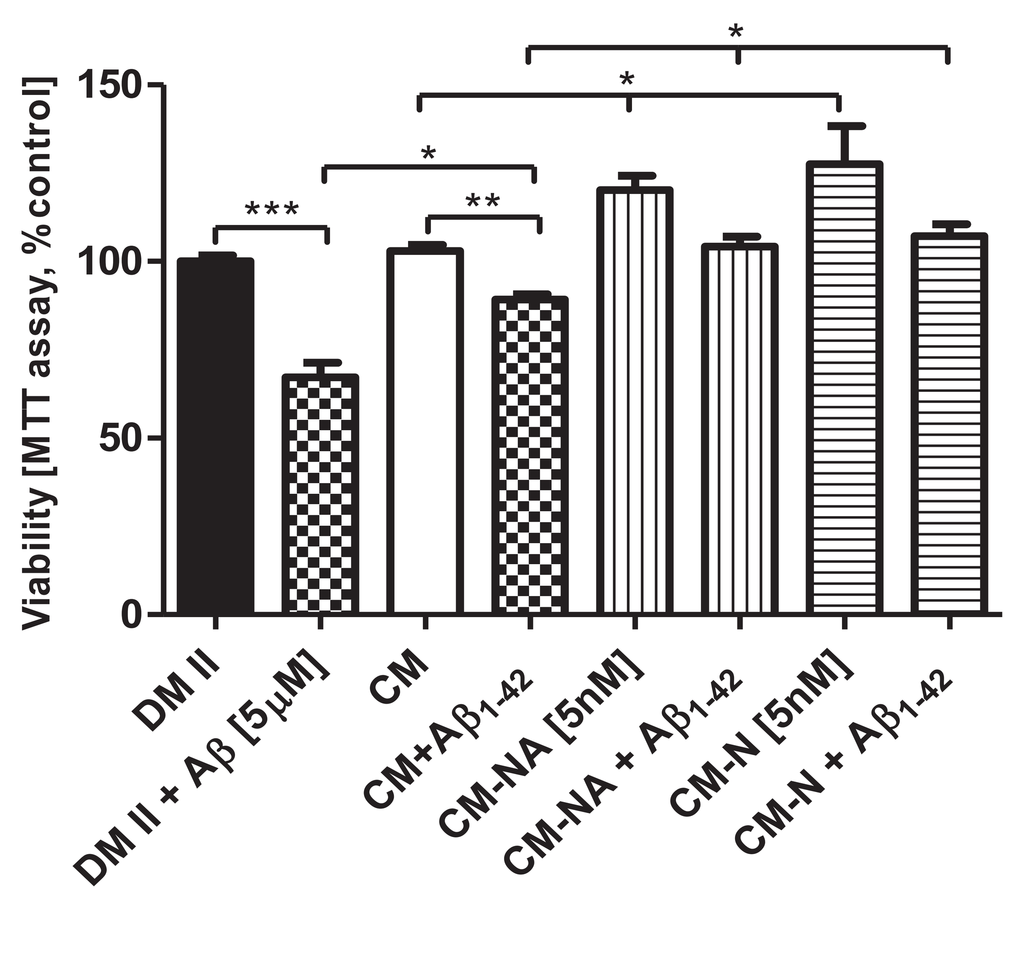

Figure 2. Analysis of cell viability of differentiated SH-SY5Y cells by used MTT assay. On the day 10th, the SH-SY5Y cells (differentiated) were pre-treated for 1 h with CM, CM-NA or CM-N before the addition of 5 μM $A\beta_{1-42}$ for the next 24 h. The obtained results are presented as a percentage of the control value. One-way ANOVA test for viability followed by Tukey's multiple comparisons was used to analyse data. Statistical differences between the treated cells and untreated control cells are indicated by asterisks (* for $p < 0.05$; ** for $p < 0.01$; *** for $p < 0.001$). Results are means ± SEM of three independent experiments.

Figure 3. Measurement of mRNA expression of PSD95 (Postsynaptic density protein 95) by qRT-PCR. One-way ANOVA followed by Tukey's multiple comparisons test at the 0.05 level was used to determine differences between the treated cells and untreated control cells. Results are presented as means ± SEM (n = 3-8). qRT-PCR fold increase was calculated according to the formula described in the Materials and Methods section. Statistical differences between the treated cells and untreated control cells are indicated by asterisks (** for $p < 0.01$).

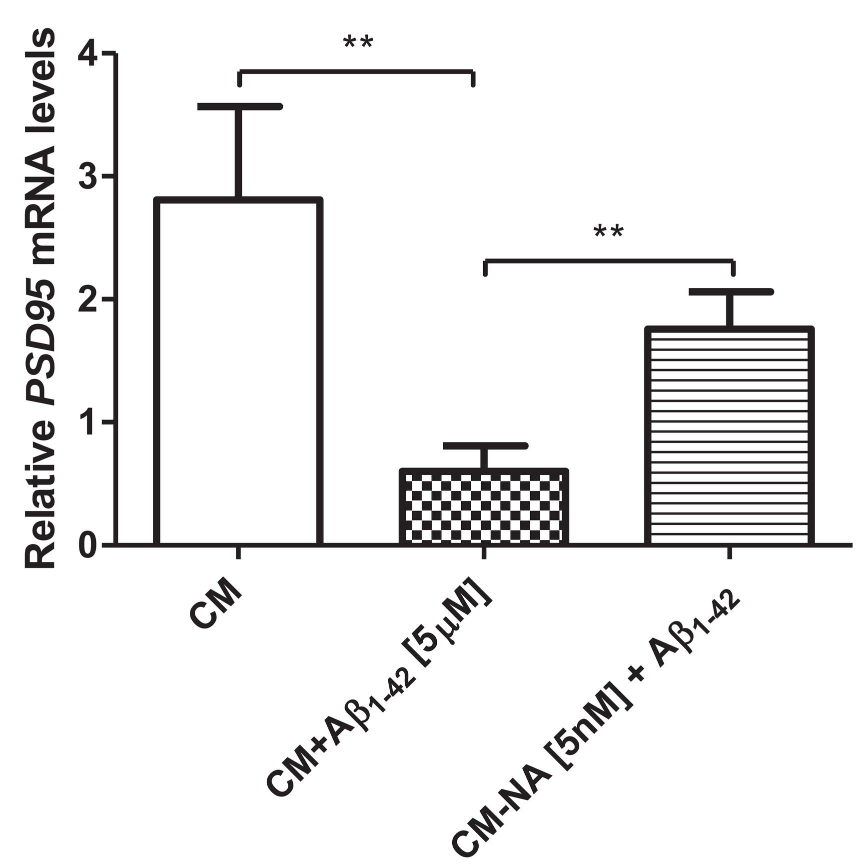

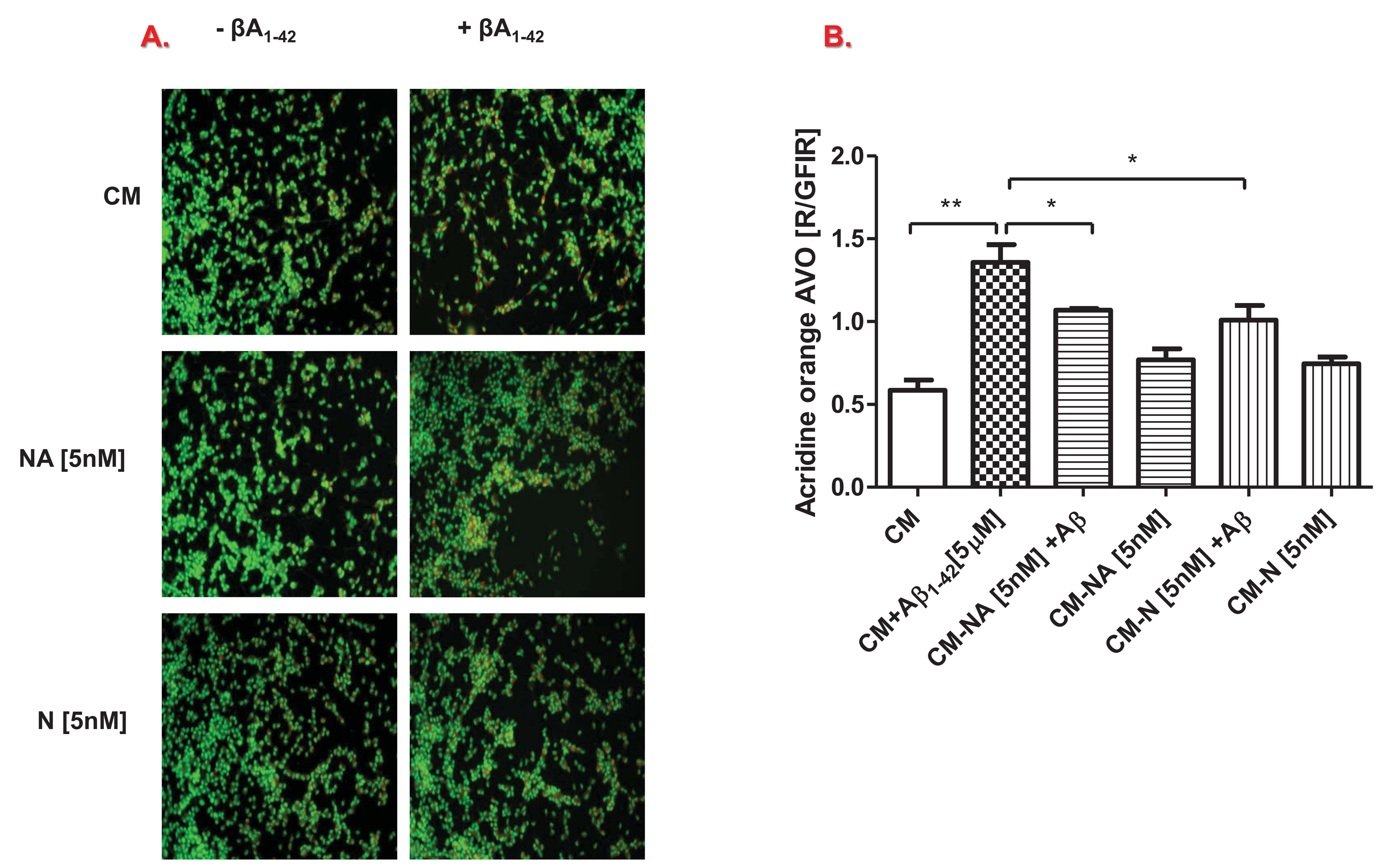

Figure 4. The microscopic evaluation of the effect of CM, CM-NA, CM-N on Amyloid β ($A\beta_{1-42}$)-induced formation of acidic vesicular organelles (AVO). The CM-NA and CM-N pre-treatment reduced AVOs production in the SH-SY5Y cells treated with $A\beta_{1-42}$. Representative fluorescence microscopy images of acridine orange (AO) staining (A) and the ratio of red to green fluorescence intensity ratio (R/GFIR) (B) were used to measure the late state of autophagy, which is characterized by AVOs production. One-way ANOVA followed by Tukey's multiple comparisons test at the 0.05 level was used to determine differences between the treated cells and untreated control cells. Results are presented as means ± SEM. Statistical differences between the treated cells and untreated control cells are indicated by asterisks (* for $p < 0.05$; ** for $p < 0.01$; *** for $p < 0.001$).

Conclusions CM from astrocyte cultures protects neurons from the toxic effects of Aβ. The use of two different forms of niacin: CM-NA or CM-N enhances this effect.

Acknowledgements: This study was supported by CMKP grants No 501-1-31-22-20 and 501-1-31-22-21

Swim training ameliorates oxidative stress in the spinal cord of ALS mice

Katarzyna P. Dzik[1], Damian J. Flis[1,2], Zofia K. Bytowska[2], Mateusz J. Karnia[1], Wiesław Ziółkowski[2], Jan J. Kaczor[1]

[1]Gdansk University of Physical Education and Sport, Poland; [2]Medical University of Gdansk, Poland

Introduction and objectives

- Amyotrophic lateral sclerosis (ALS) is a chronic motoneuron disease characterized by progressive motor weakness, muscle atrophy, and selective motoneuron loss (1).
- A recent meta-analysis suggests that exercise, especially endurance/ aerobic activity, can be a beneficial and safe option for patients with ALS. However, the condition to recommend a specific type of exercise for ALS patients is a low cost of exercise (2).
- Previously published data shown the swim training to undoubtedly improve handgrip strength in ALS mice in the early symptomatic stage of the disease (3) and increase survival in ALS mice (4).
- **Objectives**: swim training will influence the concentration of oxidative stress markers and antioxidant and energy metabolism enzymes activities in the spinal cord of SOD1-G93A mice.

Methods

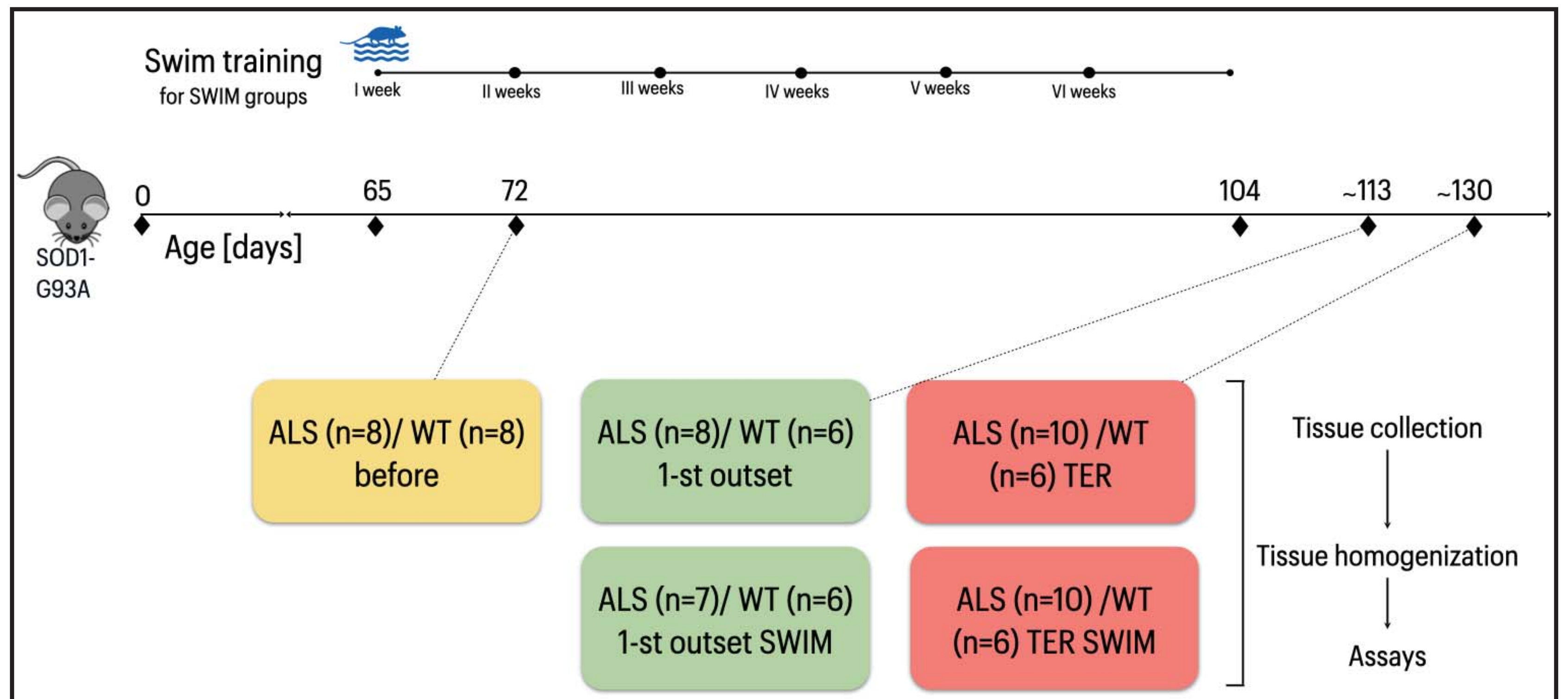

- **Swim training protocol:** 30 min swim, five times per week, in the water at the temperature 30°C, without additional weight, in the swimming pool with an adjustable flow (max. 5 l min^{-1}).
- **Measurement of enzymes activities**: the citrate synthase (CS), lactate dehydrogenase (LDH), catalase (CAT), gluthatione peroxidase (GPx) and superoxide dismutase (SOD, SOD1, SOD2) activities were measured in the spinal cord homogenates using spectrophotometric methods.
- **Measurement of oxidative stress markers:** 8-isoprostanes, 8-(OH)guanosine were measured in the spinal cord homogenates with specific ELISA kits.

Results and Conclusion

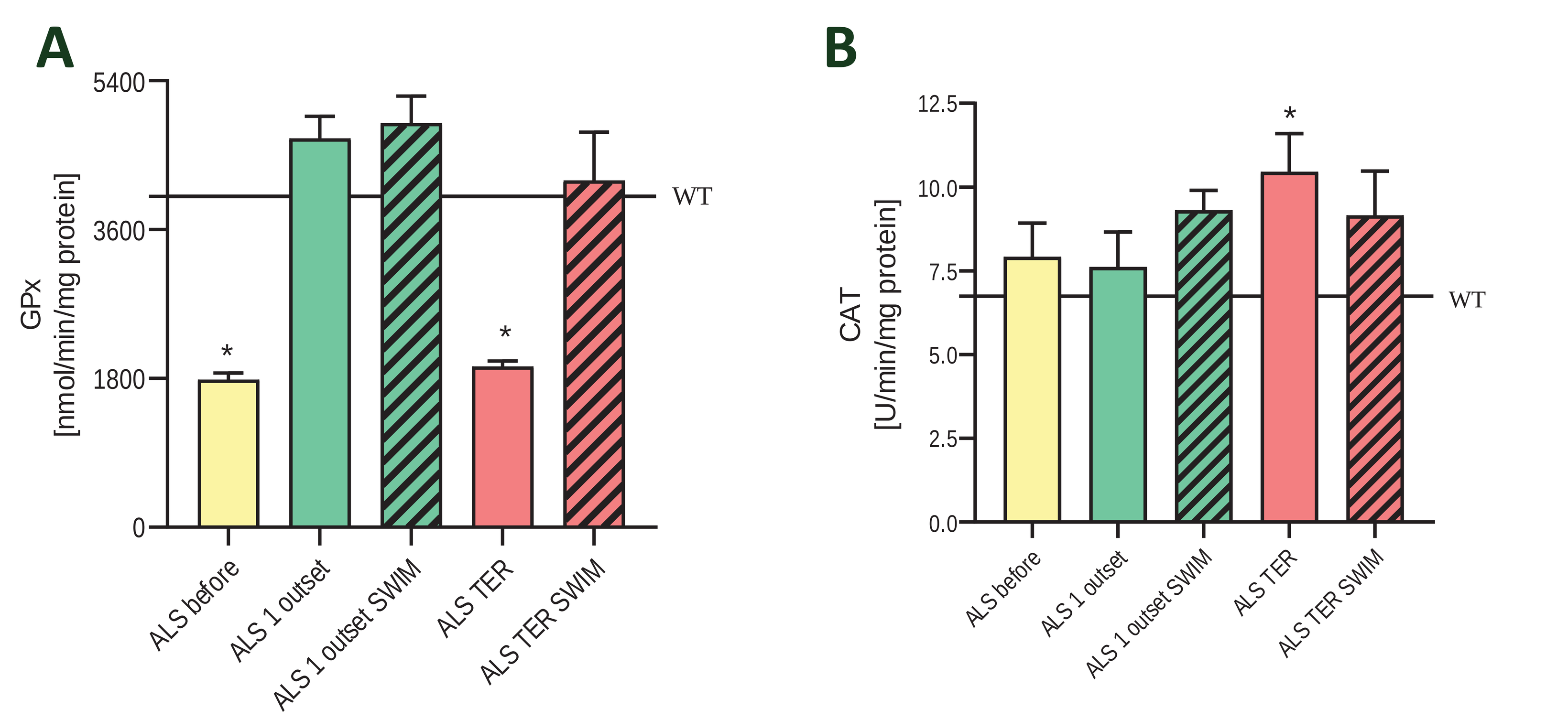

Figure 1 (**A**) glutathione peroxidase activity, * p<0.05 versus WT and the rest of the ALS groups (**B**) catalase activity * p<0.05 versus the WT group, LSD *post hoc* tests after one-way ANOVA

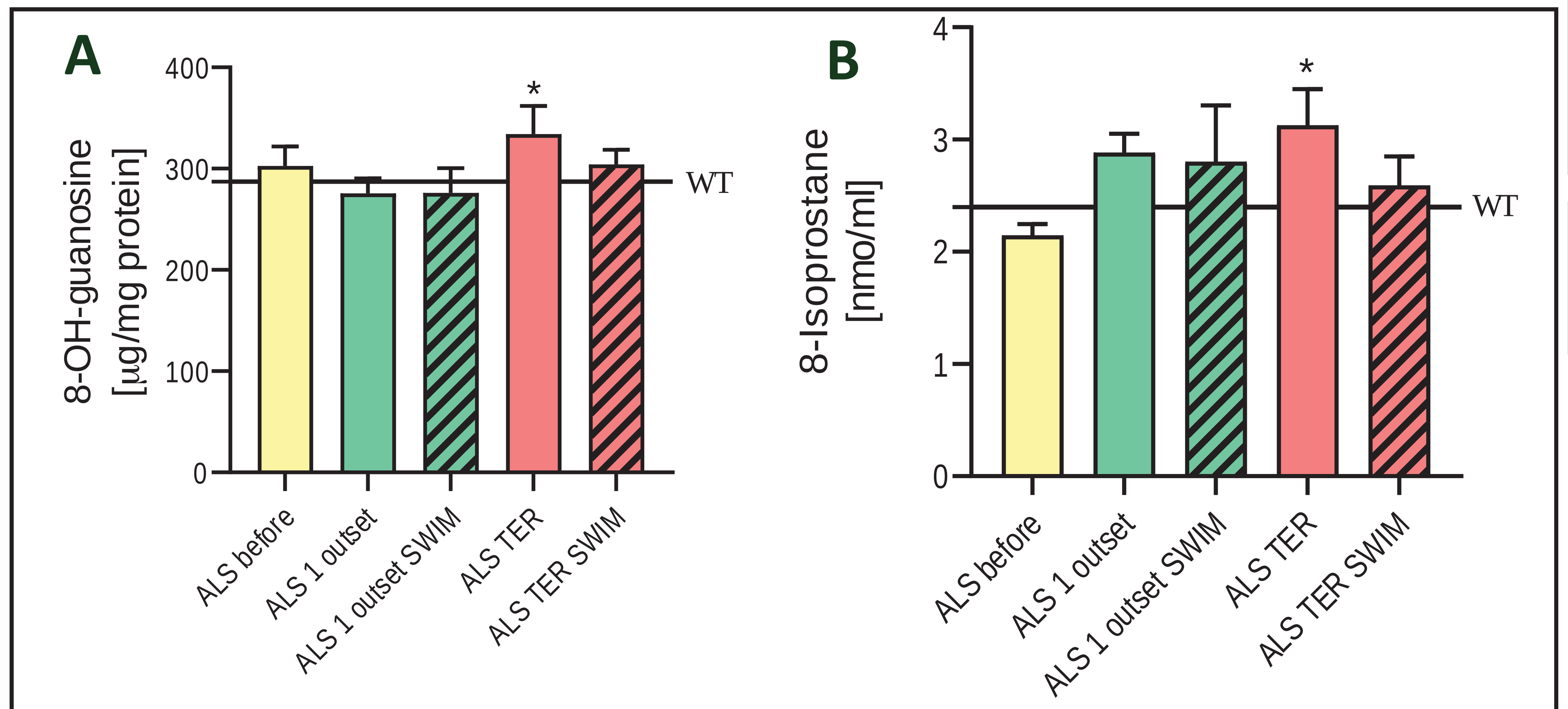

Figure 2 (**A**) The 8-Isoprostanes concentration, * p<0.05 versus the ALS before group; (**B**) 8-OH guanosine concentration, * p<0.05 versus the ALS 1 outset group; For A and B was used LSD *post hoc* test after one-way ANOVA

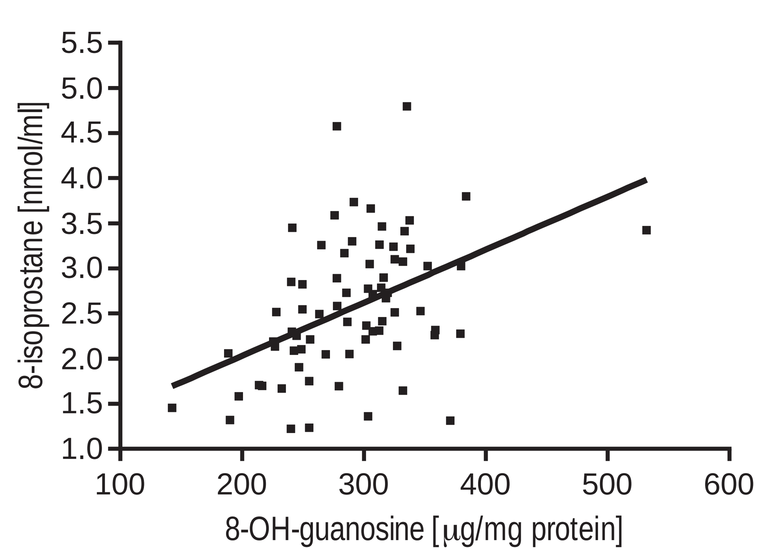

Figure 3 The positive correlation of 8-OH guanosine with 8-Isoprostanes, p<0.05, r=0.447.

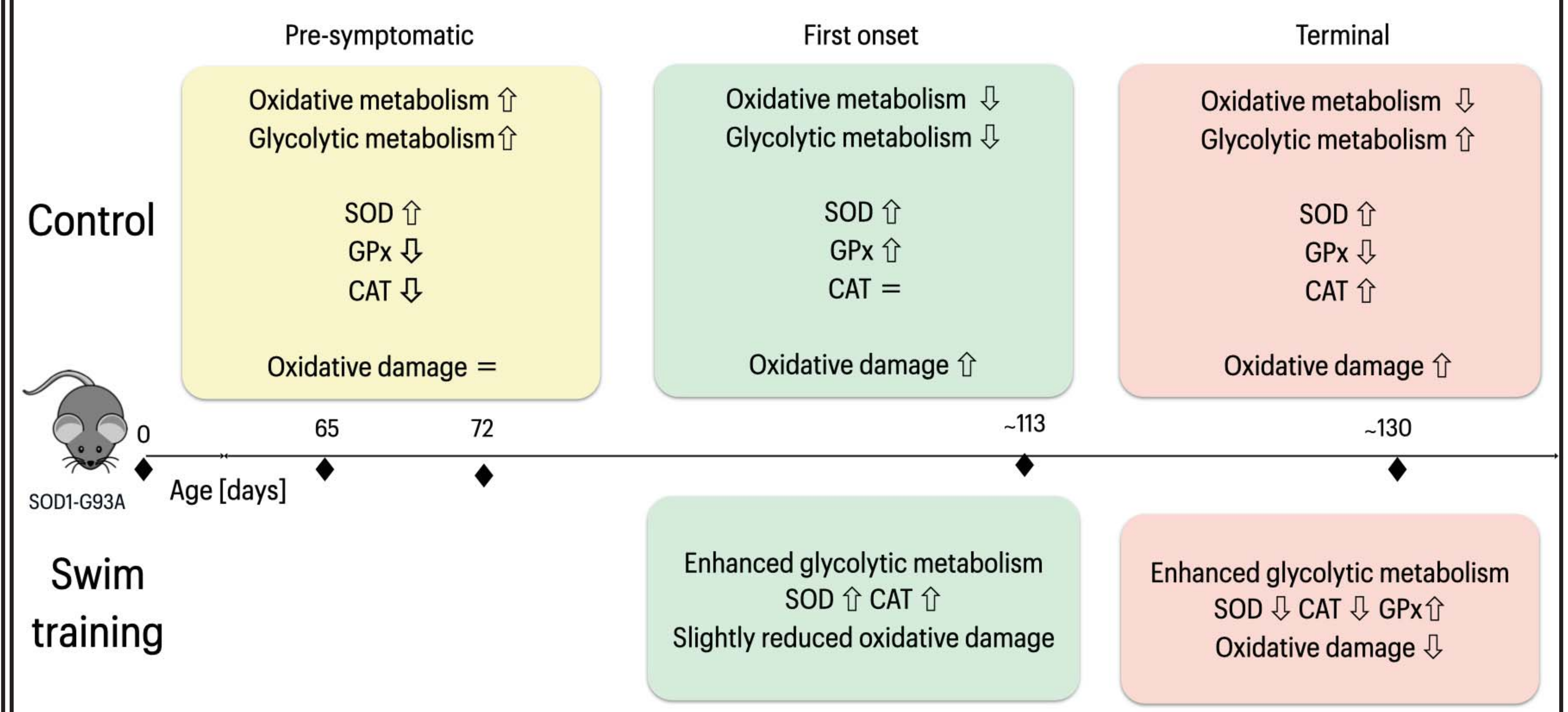

The adaptation to swim training includes the increase of glycolytic energy metabolism and ameliorates the destructive effects of oxidative stress, which is associated with a better compensatory antioxidative defense in the spinal cord.

References

1. Martin LJ. Biology of mitochondria in neurodegenerative diseases. Research Support, N.I.H., Extramural Review. Progress in molecular biology and translational science. 2012;107
2. Meng L, Li X, Li C, et al. Effects of Exercise in Patients With Amyotrophic Lateral Sclerosis: A Systematic Review and Meta-Analysis. Meta-Analysis Research Support, Non-U.S. Gov't Systematic Review. *American journal of physical medicine & rehabilitation*. Sep 2020;99(9):801-810. doi:10.1097/PHM.0000000000001419
3. Flis DJ, Dzik K, Kaczor JJ, et al. Swim Training Modulates Mouse Skeletal Muscle Energy Metabolism and Ameliorates Reduction in Grip Strength in a Mouse Model of Amyotrophic Lateral Sclerosis. *International journal of molecular sciences*. Jan 9 2019;20(2). doi:10.3390/ijms20020233
4. Flis DJ, Dzik K, Kaczor JJ, et al. Swim Training Modulates Skeletal Muscle Energy Metabolism, Oxidative Stress, and Mitochondrial Cholesterol Content in Amyotrophic Lateral Sclerosis Mice. *Oxidative medicine and cellular longevity*. 2018;2018:5940748. doi:10.1155/2018/5940748

Acknowledgement: research supported by grant from Polish National Science Centre (2018/29/N/NZ7/01627).

S2.P13

CENTRAL NERVOUS SYSTEM. NEUROPHYSIOLOGY.
PLASTICITY OF NEURAL FUNCTION

THE EFFECT OF BENZO[A]PYRENE ON OXIDATIVE STRESS IN CHICKEN EMBRYOS BRAIN

RENATA MUCHACKA, ŁUKASZ KOŁODZIEJCZYK, GRZEGORZ FORMICKI, AGNIESZKA GREŃ
Institute of Biology, Pedagogical University of Krakow, Poland

INTRODUCTION

Benzo[a]pyrene (BaP) is a compound commonly found in the environment and belongs to the group of polycyclic aromatic hydrocarbons (PAHs), which are made up of several condensed aromatic rings. There is an electron-dense region in the benzo[a]pyrene molecule that allows adducts to form in DNA, which can adversely affect cell replication. PAHs, i.e. also BaP, are formed naturally in the environment or as a result of human activities, for example by pyrolysis or incomplete combustion of organic substances such as wood, coal, oil. The factors contributing to the formation of PAHs are: widely understood food processing (smoking, frying, grilling), smoking, petrochemical processes. The development of civilization, and above all technological development have contributed to an increase in the amount of these compounds in the environment, and thus to the exposure of both humans and animals to its negative impact, because they can be introduced into the body both through the respiratory tract, skin, digestive tract and with breast milk. Benzo[a]pyrene readily penetrates all tissues of organisms containing fat and has a high accumulation capacity, primarily in adipose tissue, but also in the liver, kidneys, ovaries and spleen. During oxidation, it undergoes metabolic activation, which results in the formation of reactive metabolites that bind to DNA or lipids. This process also promotes the formation of reactive oxygen species (ROS). In the presence of polyunsaturated fatty acids such as arachidonic acid, BaP undergoes oxidative transformations and the resulting oxidized PAH products exhibit mutagenic potential.

The aim of the study was to show whether early exposure to benzo[a]pyrene affects the antioxidant system in the brain during the embryonic development of the bird.

MATERIALS AND METHODS

For this purpose, 100 fertile eggs of Ross 308 broiler parent stock were used. The eggs were divided into 5 groups as control (I), vehicle control (II), 0,1 (III), 0,5 (IV), and 1 (V) mg BaP/kg of egg weight. The eggs were injected to the yolk on day 6 of incubation. At day 14 of incubation, eggs were opened until 6 living embryos were obtained from each group. The activity of CAT, GPx, SOD and the level of GSH and MDA were determined in the collected tissues.

RESULTS AND CONCLUSIONS

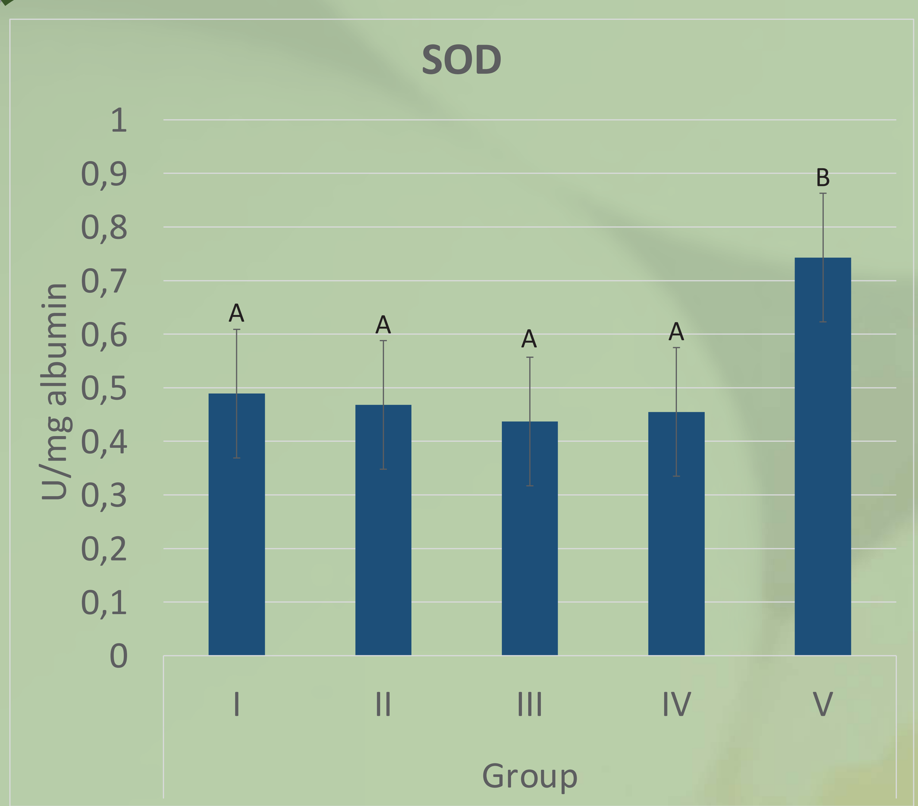

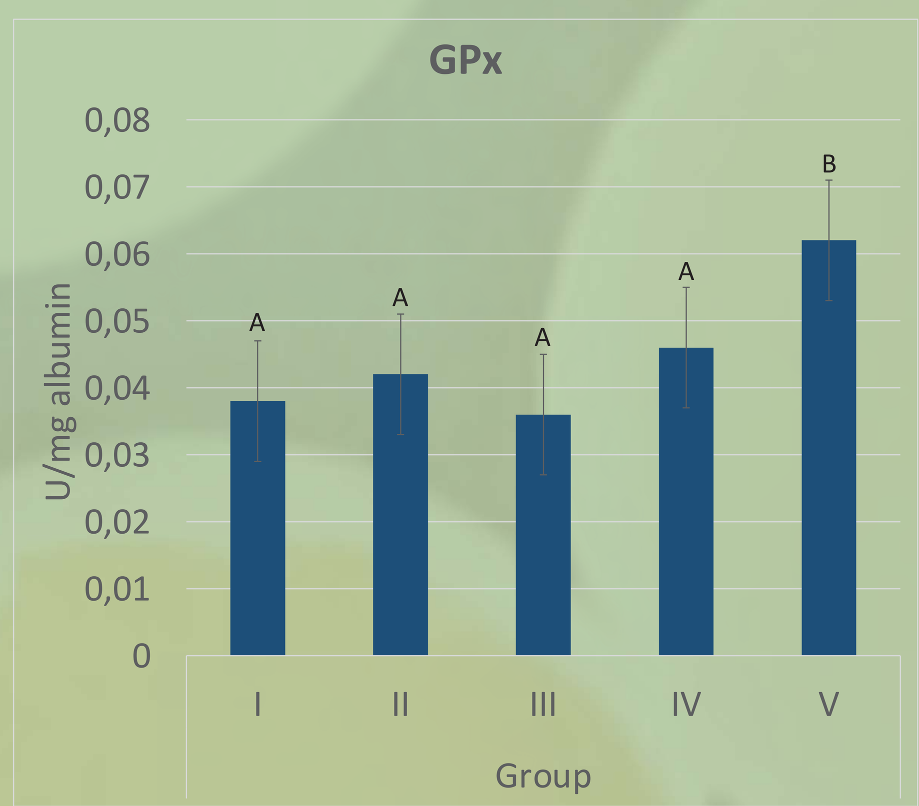

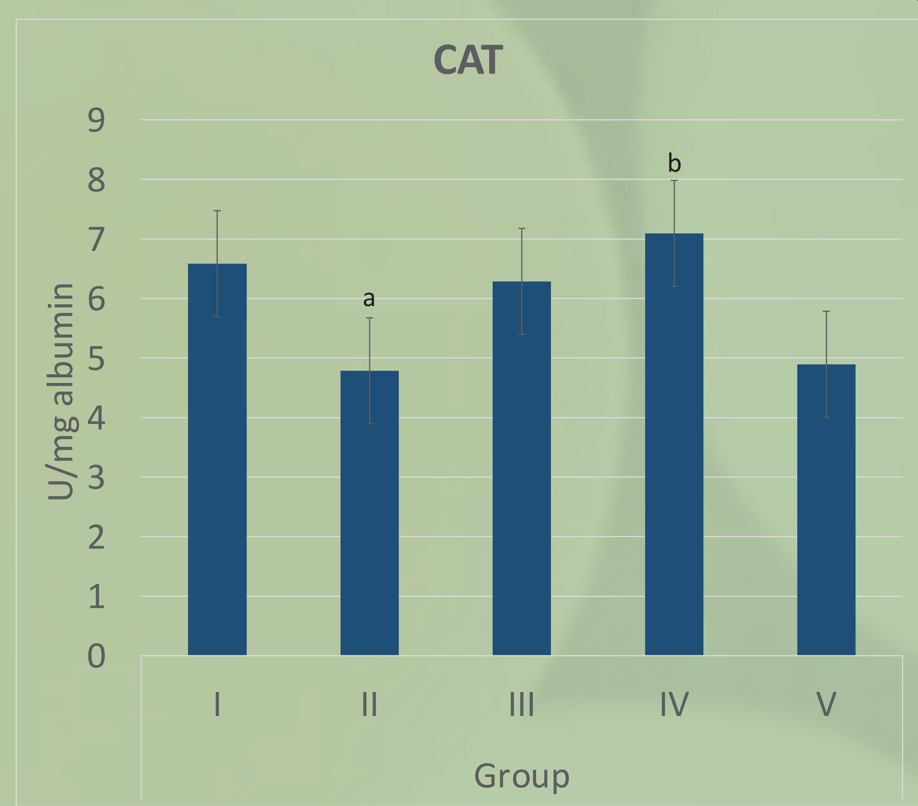

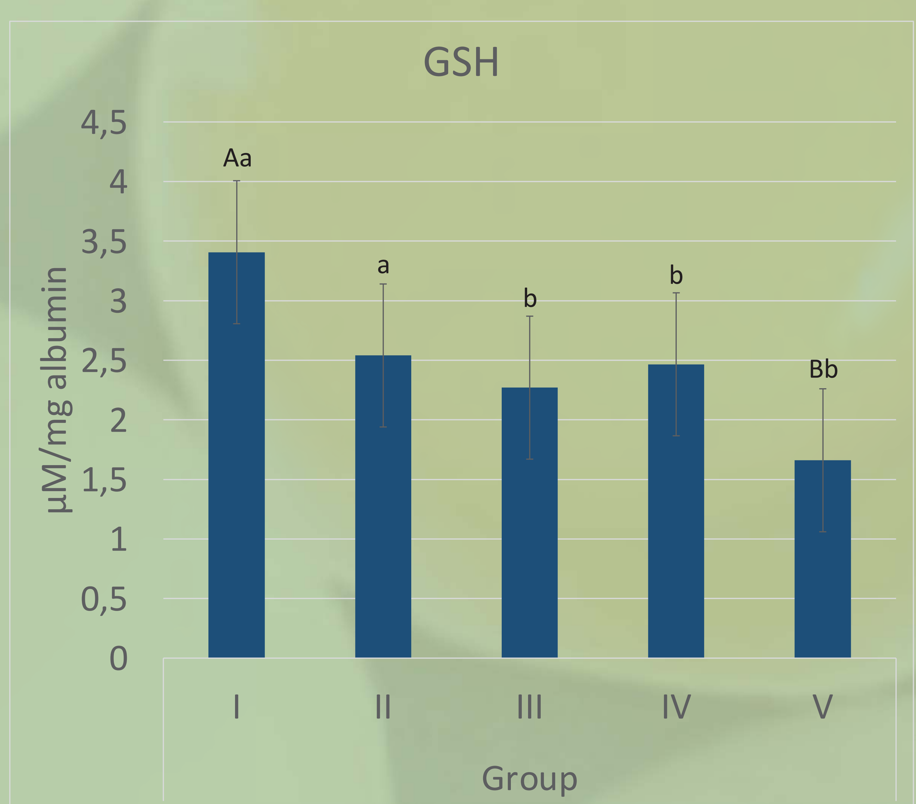

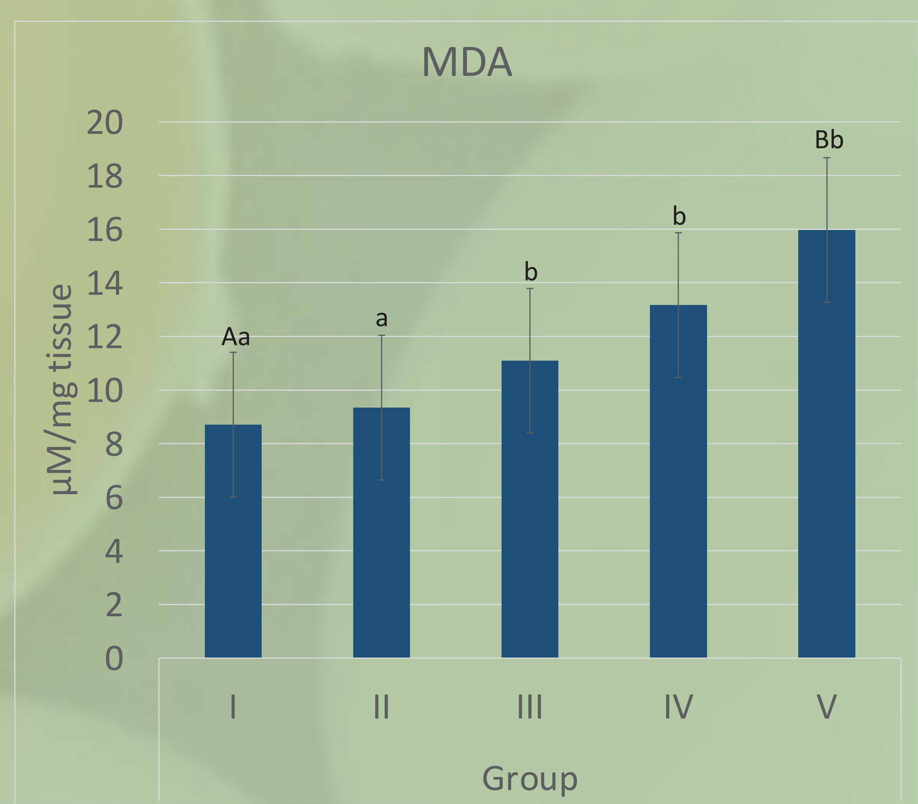

It was observed that, in benzo[a]pyrene-treated groups, the activity of SOD and GPx was increased. It was also indicated that the level of GSH was significantly decreased and the level of MDA - significantly increased. The greatest changes in the examined parameters were observed in the group of eggs injected with the dose of 1 mg BaP/kg of egg weight.
These results indicate that *in ovo* administration of benzo[a]pyrene causes oxidative stress in the brains of chicken embryos.

Effect of dimethyl fumarate on disorders of the olfactory bulb neurogenesis in the streptozotocin-induced rat model of Alzheimer's disease

WYDZIAŁ BIOLOGII
UNIWERSYTET GDAŃSKI

Ewelina Kurowska, I. Majkutewicz, J. Ruciński, D. Myślińska, K. Sawicka, N. Piekarczyk
Department of Animal and Human Physiology, Faculty of Biology, University of Gdansk

KATEDRA FIZJOLOGII ZWIERZĄT I CZŁOWIEKA • Uniwersytet Gdański •

S2.P15 Central Nervous System. Neurophysiology. Plasticity of neural function.

email: ewelina.kurowska@ug.edu.pl

Background and aim

The sporadic late-onset form of Alzheimer's disease (sAD) affects 90% of AD patients and it is associated mainly with environmental factors. The intracerebroventricular injection of streptozotocin (STZ-icv) rat model of the sAD is widely used in basic research for understanding of the sAD pathophysiology and testing new therapeutic methods [1]. One of the mechanisms contributing to memory impairment in AD is disruption of the postnatal neurogenesis in both the hippocampus and the olfactory bulb (OB) [2]. New neurons in the OB determine the proper functioning of perceptual and memory processes related to smell, which in adults may be associated with adaptive mechanisms in response to environmental changes [3]. It has been shown that patients with mild cognitive impairment and olfactory deficits are at higher risk of developing AD [4]. In our previous study, we found that dimethyl fumarate (DMF) – registered drug in multiple sclerosis treatment, with antioxidant and anti-inflammatory properties alleviates hippocampal neurodegeneration and memory deficits in young and old rats in the STZ-icv model of sAD [5, 6]. **The present study aims to determine if the STZ-icv impairs adult neurogenesis in the olfactory bulb in rats and whether the DMF treatment attenuates these disruptions. The second purpose of this study is to determine whether the animals age affects the level of the OB neurogenesis by influence on STZ and DMF action in the rat model of sAD.**

Material and methods

Young (n=20) and old (n=20) male Wistar rats were randomly divided into four groups (in each young n=5 and old n=5): **1)** STZ+DMF with STZ-icv injection (3 mg/kg) and fed with chow containing DMF (0.4% by weight), **2)** STZ with STZ-icv injection and fed with standard chow, **3)** Sham+DMF with icv injection of vehicle (citrate buffer) and fed with DMF chow, **4)** Sham – vehicle-icv and fed with standard chow. One week after STZ/vehicle icv rats were subjected to intraperitoneal (ip.) injection of 5-bromo-2'deoksyurydine (BrdU) (50 mg/kg, once daily for three days) - a marker of cells undergoing cell division. Rats were sacrificed 9 days after the third BrdU injection and brain were subjected to immunofluorescent BrdU and doublecortin (DCX, marker of immature neurons) labelling. Microphotographs of the olfactory bulb were taken with the fluorescent microscope (Zeiss Axio Scope.A1). The calibrated frame of counting area (0.1 mm^2) was imposed on the photographs and labelled cells were counted manually.

Fig. 1. Experimental procedure. ICV 1/ICV 2 – STZ-ICV (1.5mg/kg STZ in 2µl of buffer per brain lateral ventricle) or VEH-ICV (2µl of buffer/ventricle); 1 – first ICV, 2 – second ICV; BrdU ip. - intraperitoneal injection of BrDU (50 mg/kg body weight) for 3 consecutive days

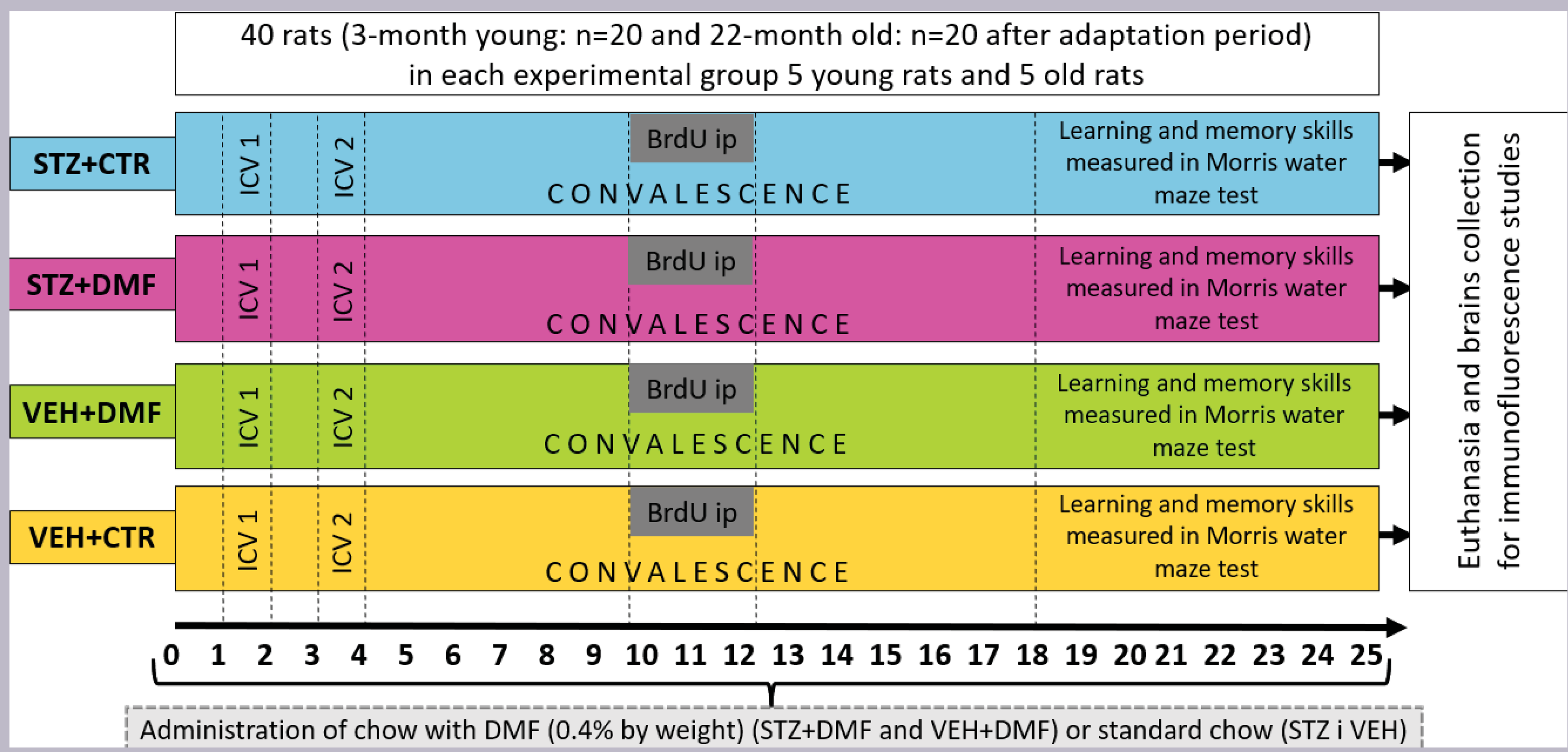

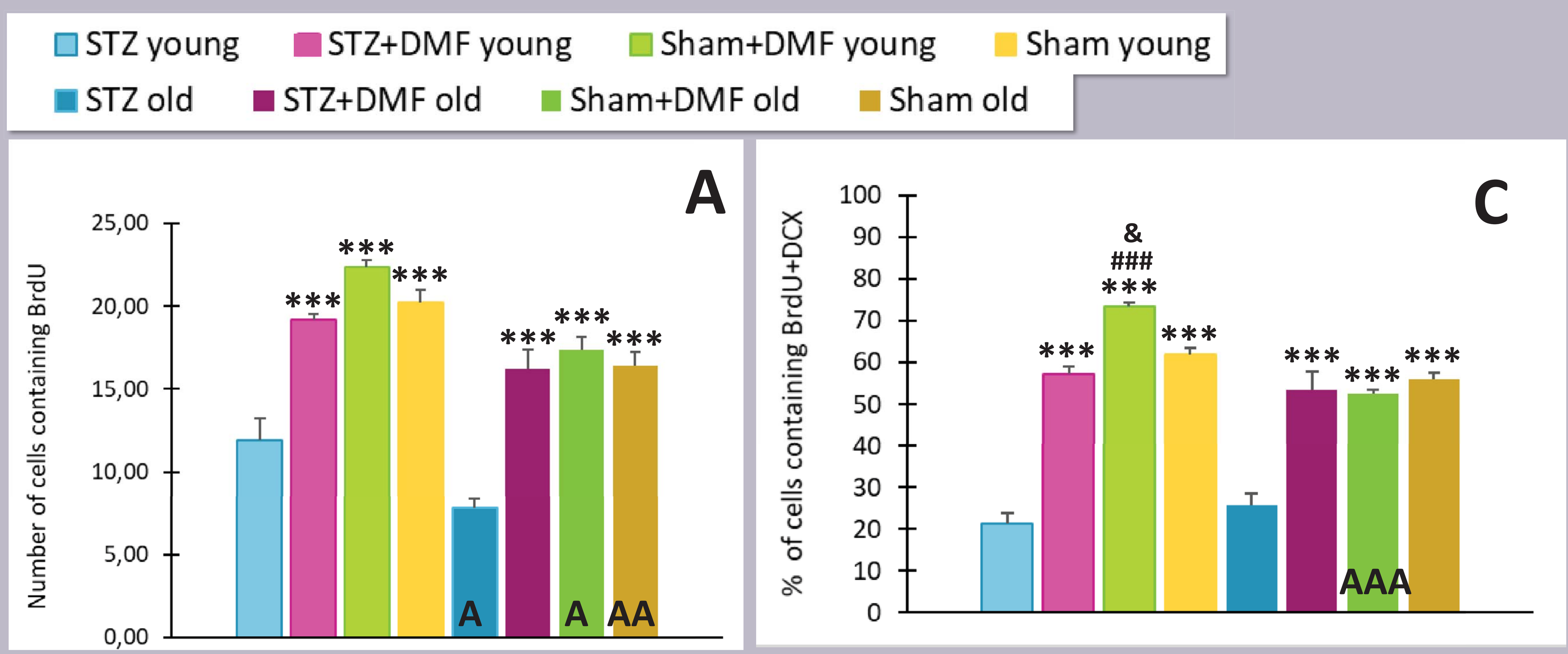

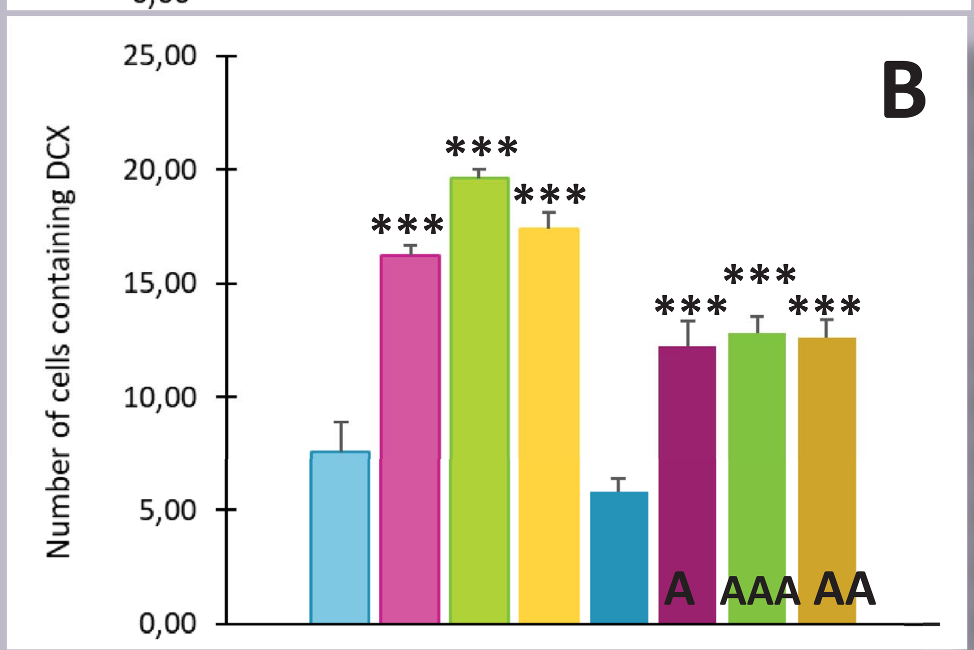

Fig. 2. Number of cells containing BrdU (**A**) or DCX (**B**) and percentage of newly born immature neurons (BrdU+DCX) (**C**) in the olfactory bulb. Three-way ANOVA, Tukey's post-hoc test.
*** - p<0.001 STZ+CTR group vs. other groups at the same age;
- p<0.001 Sham+DMF vs. STZ DMF group at the same age;
& - p<0.05 Sham+DMF vs. Sham at the same age;
A – p<0.05; AA - p<0.01 young vs. old rats within the experimental group; @ - statistical tendency

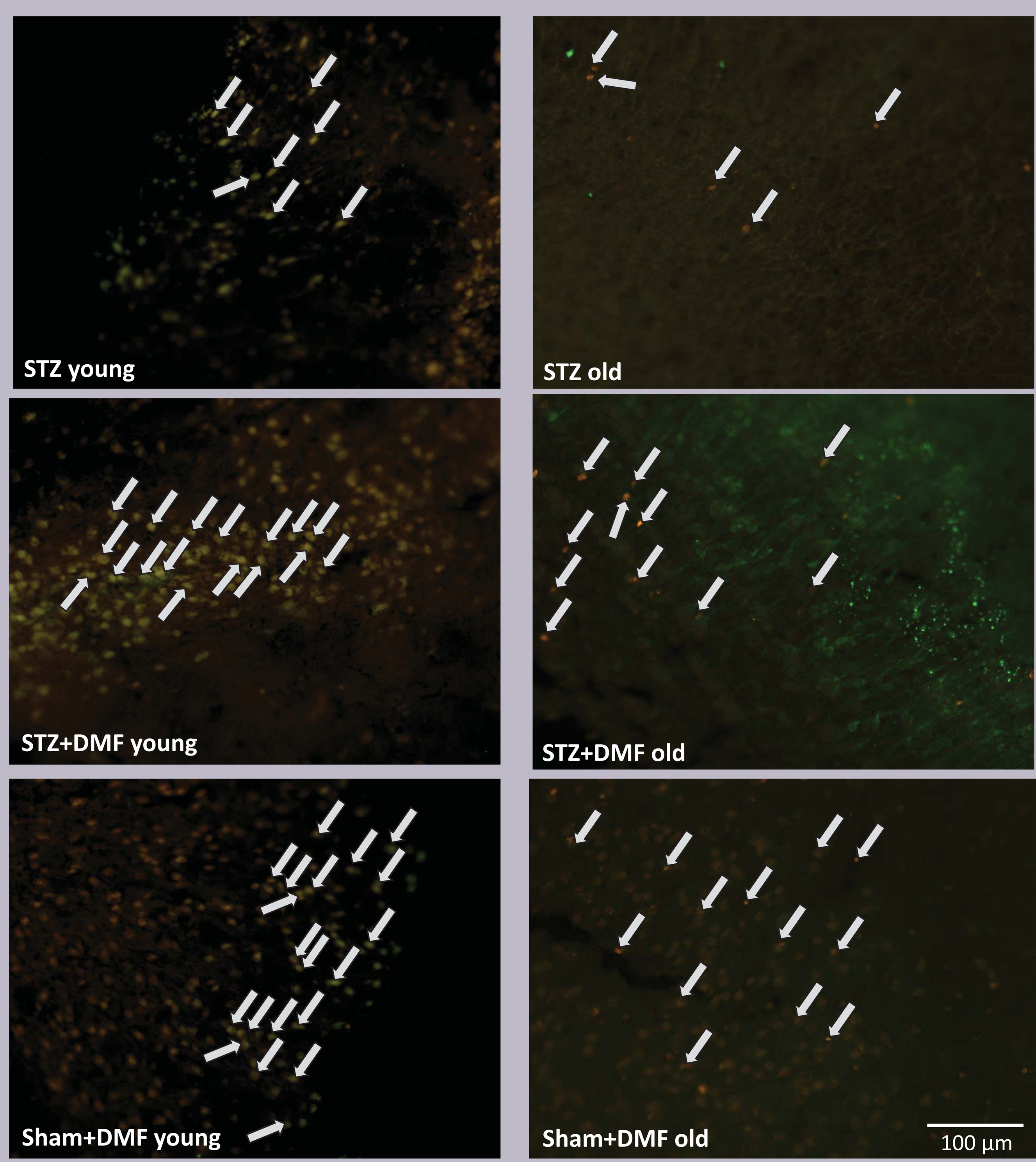

Fig. 3. Representative microphotographs of BrdU+DCX-containing cells (arrows) in the olfactory bulb of rats.

Results and conclusion

Both young and aged STZ rats were characterized by the lowest number of new immature neurons (BrdU+DCX containing cells) in the olfactory bulb (p<0.001 STZ vs. other groups). STZ+DMF young and aged rats showed higher density of newly born neurons in the OB (p<0.001) compared to STZ group. The highest percentage of immature neurons was observed in the OB of Sham+DMF rats in both age groups compared to the other experimental groups. STZ-icv causes significant disorders of neurogenesis in the OB. DMF therapy improved disruptions of adult neurogenesis in the OB induced by STZ-icv treatment.

References

[1] Salkovic-Petrisic M., et al., 2013. What have we learned from the streptozotocin-induced animal model of sporadic Alzheimer's disease, about the therapeutic strategies in Alzheimer's research. J. Neural. Transm., 120, 233-252. **[2]** Vivar C. 2015. Adult hippocampal neurogenesis, aging and neurodegenerative diseases: possible strategies to prevent cognitive impairment. Curr. Top. Med. Chem., 15, 2175-2192. **[3]** Rochefort C., et al., 2002. Enriched odor exposure increases the number of newborn neurons in the adult olfactory bulb and improves odor memory. J. Neurosci., 22, 2679-289. **[4]** Devanand D.P., et al., 2015. Olfactory deficits predict cognitive decline and Alzheimer dementia in an urban community. Neurology, 84, 182-189. **[5]** Majkutewicz I., Kurowska E., et al., 2016. Dimethyl fumarate attenuates intracerebroventricular streptozotocin-induced spatial memory impairment and hippocampal neurodegeneration in rats. Behav. Brain Res., 308, 24-37. **[6]** Majkutewicz I., Kurowska E., et al., 2018. Age-dependent effects of dimethyl fumarate on cognitive and neuropathological features in the streptozotocin-induced rat model of Alzheimer's disease. Brain Res., 1686, 19-33.

The work is the result of the research project No 2013/09/D/NZ4/01658 funded by the National Science Center.

Effect of prebiotics supplementation on social behaviour and plasma TNF-α level disturbances in high- and low responders rats with central amygdala hyperactivation

WYDZIAŁ BIOLOGII
UNIWERSYTET GDAŃSKI

Jan Ruciński, E. Kurowska, N. Piekarczyk, I. Majkutewicz, J. Ruciński, D. Myślińska
Department of Animal and Human Physiology, Faculty of Biology, University of Gdansk

KATEDRA FIZJOLOGII ZWIERZĄT I CZŁOWIEKA • Uniwersytet Gdański •

S2.P16 Central Nervous System. Neurophysiology. Plasticity of neural function.
email: jan.rucinski@ug.edu.pl

Background and aim

Amygdala (Amg) hyperactivity as well as higher TNF-α plasma concentration occurs in patients with PTSD, anxiety disorders or depression [1]. Long-term electrical stimulation (ES) induces abnormal hyperactivation of the Amg and can be used as an animal model of mentioned disorders [2]. The central nucleus of the Amg (CeA) contribute to neural and endocrine responses to stress and it's functioning is associated with anxiety and social behaviour. Moreover Amg is considered to have a crucial role in the microbiota signals processing and integration [3]. Between the gut microbiota and central nervous system exists a functional bidirectional communication. Manipulating the gut microbiome may improve host mental health and reduce inflammatory processes [4]. Galactooligosaccharides (GOS) are prebiotics - non-digestable polysaccharides that increase the growth and activity of health-promoting microorganisms [5]. Individual differences in the neuronal, endocrine and immune responses to stress may result in different susceptibility to the development of anxiety disorders in humans. The rat model in which male rats are divided into high responders (HRs) and low responders (LRs) - based on their locomotor activity during exposure to the novel environment - is well-described and reflects differences observed in humans [6]. **The present study aims to determine if the long- term ES of the CeA induces social behaviour disruptions and proinflammatory processes in rats, and whether the GOS supplementation can reverse these changes. The second purpose of this study is to determine whether the animals behavioural profile (HRs/LRs) influences on severity of ES-induced disturbances and influences the level of therapeutic efficacy of GOS.**

Material and methods

28 male Wistar rats categorized as HRs or LRs in the novelty test were subjected to 14-day electrical stimulation of the CeA and 21-day supplementation with GOS. Three chamber sociability test was used to assess social behaviour. One hour after the test blood samples were collected and centrifuged to obtain plasma. TNF-α plasma concentration was determined by ELISA test.

Fig. 1. Experimental procedure with timeline

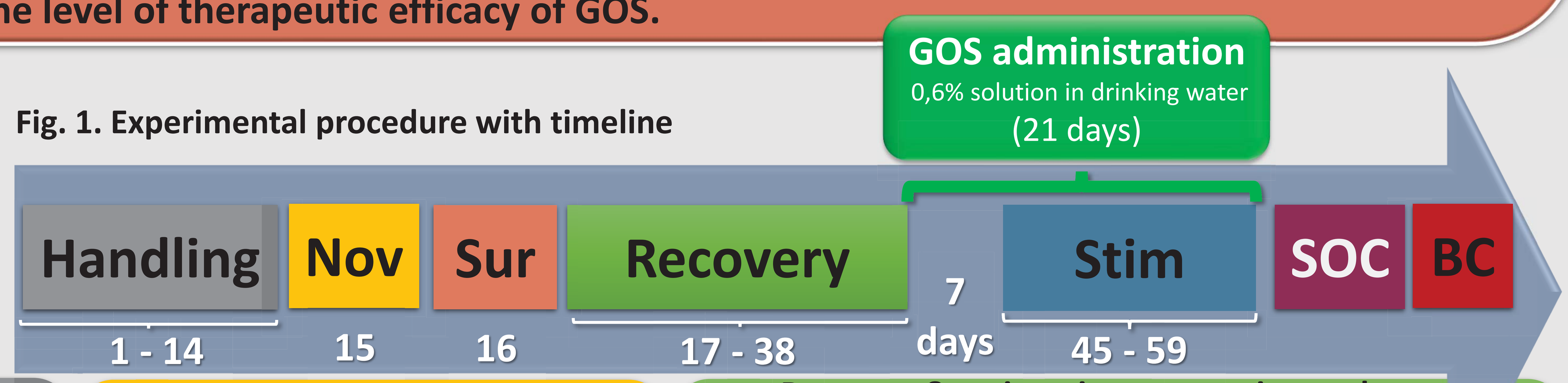

Handling
Habituation to a new environment and experimenter

Novelty test
Division of rats into high responders (HRs) with high horizontal locomotor actvity and low responders (LRs) with lower locomotor activity

Recovery & assignation to experimental group
Sham – without CeA stimulation and GOS supplementation
Stim – CeA stimulation, without GOS Sham+GOS - without CeA stimulation, with GOS
Stim+GOS - CeA stimulation, without GOS supplementation

Stereotaxic surgery
Electrodes implantation into the CeA (isoflurane inhalation anesthesia)

Electrical stimulation
14-day electrical stimulation of the CeA (30 trials/day: 30s stimulation + 20s rest; frequency 50Hz, current from 60 to 150 μA). In Sham animals – identical procedure with current switched off

Blood collection
Blood samples were collected by heart puncture to determine plasma TNF-α concentration using commercially available ELISA kit according to the manufacturer's instructions

Three-chamber social test

Tested animal was placed in a chamber adjacent to two other chambers. Each of these compartments contained a small wire cage that allowed an animal to see and smell.

Phase I – **Habituation**: tested rat allowed to freely explore whole apparatus for 10 min

Phase II – **Sociability**: an unfamiliar sex-matched rat (novel rat 1, NO1) was placed in one of the small cages and the other was empty.

Phase III – **Social novelty** (social recognition memory assessment): a new unfamiliar rat (novel rat 2, NO2) was placed in the small cage that had been empty during the sociability phase. The NO1 (a familiar rat in this phase) localization was the same as in the phase II.

The time spent in each chamber and time spent exploring enclosed novel rat or empty cages (novel objects) was measured (each phase lasted 10 min) using the EthoVision XT software.

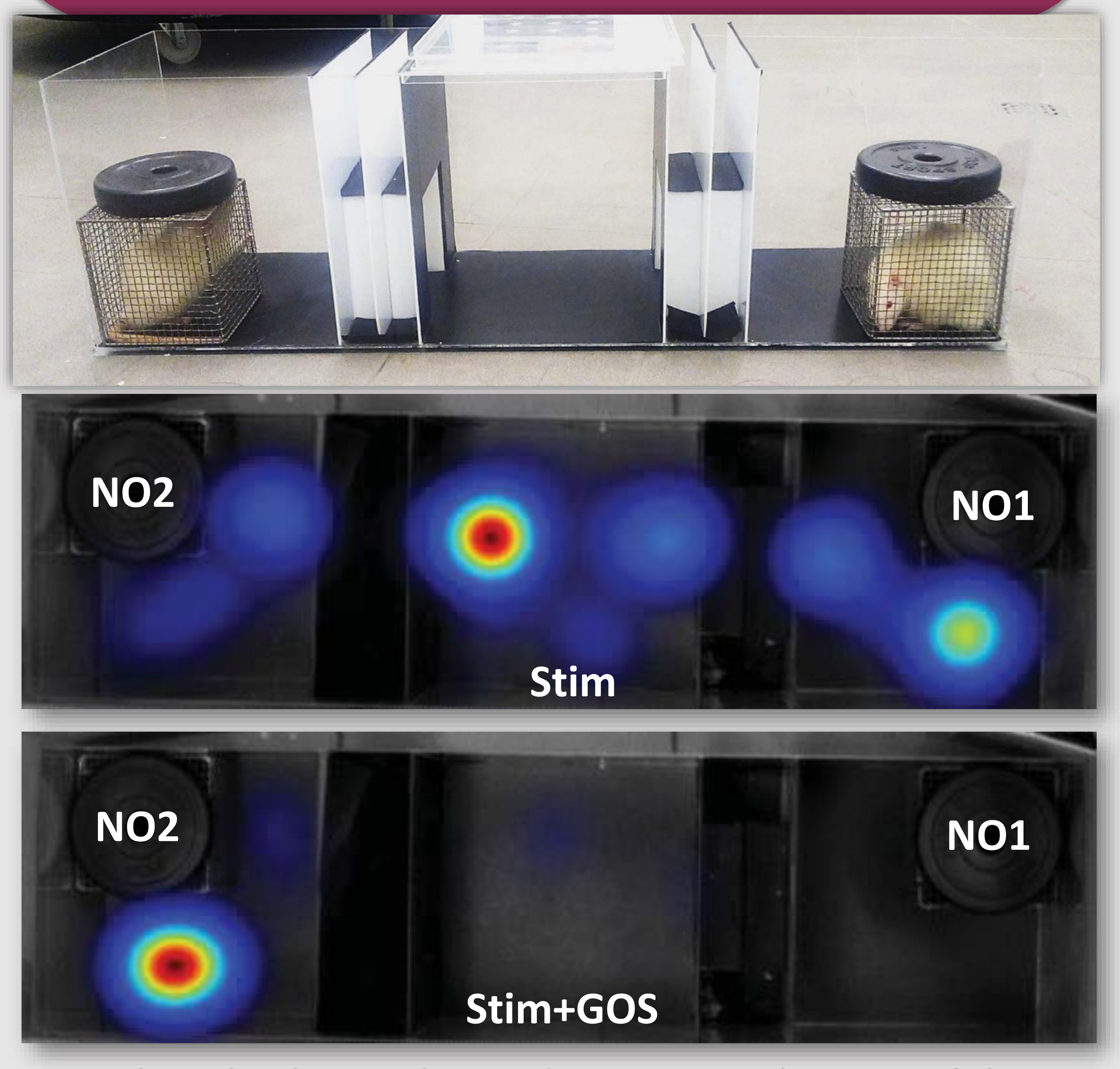

Fig. 2. Three-chamber social test and representative heatmaps of phase III (social novelty)

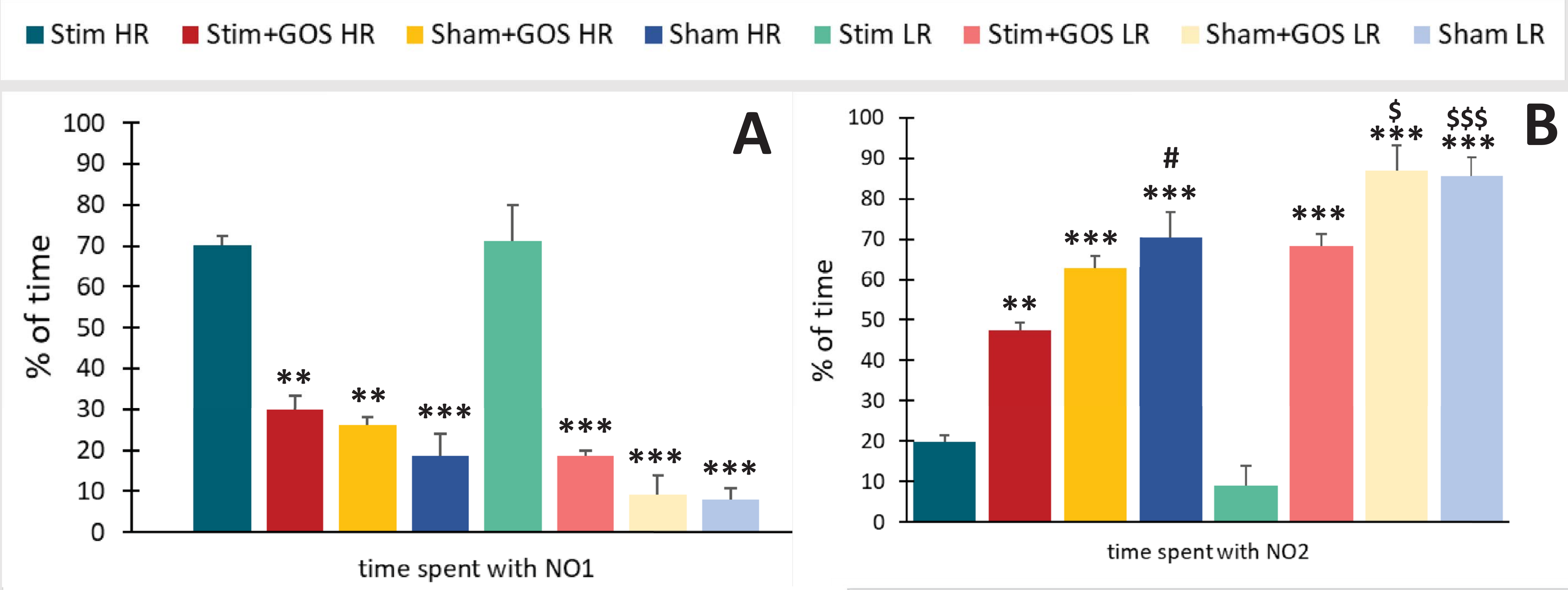

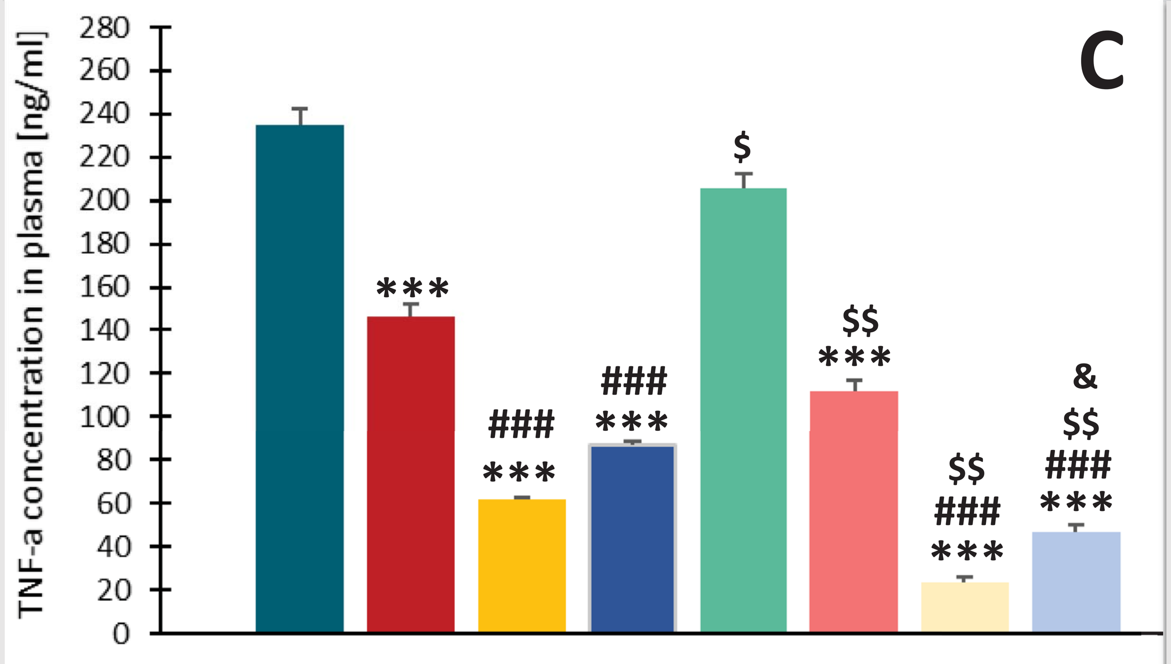

Fig. 3. Effects of electrical stimulation of the CeA and GOS supplementation on % of time spent in chamber with familiar rat, NO1 (A) or in chamber with unfamiliar rat, NO2 (B) in three-chamber social test and on plasma TNF-α concentration (C) in rats with different stress-related vulnerability (HR – high responders = stress-sensitive, LR – low responders = stress-resistant).
Three-way ANOVA, Tukey's post-hoc test.

** p<0.01; *** p<0.001 as compared to the Stim group within the same behavioural profile
# p<0.05; ### p<0.001 as compared to the Stim+GOS group within the same behavioural profile
$ p<0.05; $$ p<0.01; $$$ p<0.001 HRs vs. LRs within the same experimental group
& p<0.05 Sham vs. Sham+GOS within the same behavioural profile

Results and conclusion

The long-term ES of the CeA caused deficits in social behaviour (avoiding interaction with a non-familiar rat and spending more time with the familiar rat; p<0,01). It also led to a significant increase in plasma TNF-α level (p<0,001). In HRs rats these effects were enhanced. GOS supplementation improved disturbances induced by the ES of the CeA as stimulated and supplemented rats exhibited more prosocial behaviour and lower TNF-α plasma concentration (p<0,05). GOS therapeutic effects were more pronounced in LRs rats.

References

[1] Mukhara D., Oh U., Neigh G.N. (2020). Neuroinflammation. Handb. Clin. Neurol., 175, 235-259. **[2]** Reznikov R., Binko M., Nobrega J.N., Hamani C. (2016). Deep brain stimulation in animal models of fear, anxiety, and posttraumatic stress disorder. Neuropsychopharmacology, 41, 2810-2817. **[3]** Cowan C. S., Hoban A. E., Ventura-Silva A. P., Dinan T. G., Clarke G., Cryan J. F. (2018). Gutsy moves: the amygdala as a critical node in microbiota to brain signaling. BioEssays, 40, 1700172. **[4]** Cryan J.F., Dinan T.G. (2012). Mind-altering microorganisms: the impact of the gut microbiota on brain and behaviour. Nat. Rev. Neurosci., 13, 701-712. **[5]** Śliżewska K., Nowak A., Barczynska R., Libudzisz Z. (2013). Prebiotyki - definicja, właściwości i zastosowanie w przemyśle. Żywn. Nauka Technol. Jakość, 1, 5-20. **[6]** Dellu F., Piazza P.V., Mayo W., Le Moal M., Simon H. (1996). Novelty-seeking in rats - biobehavioral characteristics and possible relationship with the sensation-seeking trait in man. Neuropsychobiology, 34, 136-145.

The work is the result of the research project No 2019/35/N/NZ4/00908 funded by the National Science Center.

IMPROVED MOTOR FUNCTION AS A RESULT OF THE INFLUENCE OF MINOCYCLINE ON MOTOR CORTEX NEURONS IN CORTICAL MODEL OF PHOTOTHROMBOTIC ISCHEMIC STROKE IN RATS

Katarzyna Pawletko[1], Aniela Grajoszek [1,2], Halina Jędrzejowska-Szypułka[1]

[1] *Department of Physiology, School of Medicine in Katowice, Medical University of Silesia, ul. Medyków 4, 40-752 Katowice, Poland. Correspondence : kpawletko@sum.edu.pl*

[2] *Department for Experimental Medicine Medical University of Silesia, 4, Medyków Street 40-752 Katowice*

MEDICAL UNIWERSITY OF SILESIA
SCHOOL OF MEDICINE IN KATOWICE

Contact with us:
kpawletko@sum.edu.pl

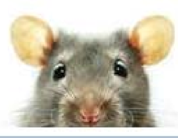

Introduction: Development a repeatable, very precise and minimally invasive animal model of ischemic stroke is necessary. Cerebrovascular diseases are the principal causes of mortality and disability worldwide. About 87% of all strokes are ischemic. Cellular survival and restoration of correct circulation are the goals of ischemic stroke therapy.

A well-designed model will facilitate future research on new possibilities of treatment of ischemic stroke and allows animals to participate in behavioral tests

Protein HuR is a member of the ELAVL protein family. This protein has one of best-known functions is stabilize mRNAs in order to regulate gene expression. The role of HuR protein during ischemic stroke is not yet well understood. Minocycline, by launching plethora of neuroprotective mechanisms may be beneficial as the treatment which has been confirmed in many research models of acute brain damage. HuR protein stabilize mRNAs by translocation to cytoplasm from nucleus. Thus, HuR is considered as a potential target for neuroprotection during stress.

Aims: The first aim of our research was to develop, test and select the most favourable parameters in model of photothrombotic ischemic stroke in rat (the first part of the experiment). The second goal was to testing the effect of minocycline on state of penumbra and functional outcomes after ischemic stroke with evaluation whether regulation of HuR protein is involved in this treatment. We have also performed a number of behavioral tests, helpfull in evaluation.

Methods: All procedures were performed in accordance to the EU animal protection law and were approved by the Local Animal Research Ethics Committee.

Phototrombotic ischemia was produced in 72 male Long-Evans rats by evoking the clotting of blood inside the cerebral vessels of the rat, through activation of Bengali rose (tetracholor-tetraiodofluorescein) with the light of 3200 K energy. In all groups exposure to light was 15 min. We give Bengal rose (Sigma, St. Louis, MO, U.S.A) solution 20mg/1 ml PBS in dose of 1 ml / kg b.w. Was administered by intravenous injection into the tail vein. Small stereotactic cortical ischemia, 3 mm left from bregma, was induced.

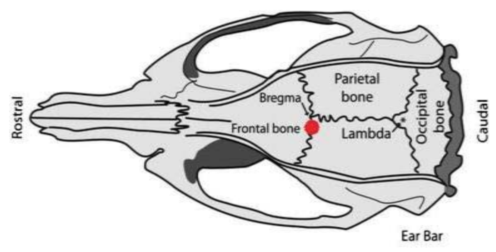

Fig.1. The graphic shows the radiation locations on the Long-Evans rat skull

We use a special mask to limit the area of exposure

Fig.2. Photo of the mask used during the exposure (foto.K.Pawletko)

We tested different time windows: 24h, 48h and 7 days after stroke induction. Half of the experimental groups received an intravenous dose of minocycline (1 mg / 1 kg b.w /1ml solution/ Sigma, St. Louis, MO, U.S.A). A dose of minocycline was given 10 minutes after induction of ischemic stroke. All animals form „minocycline groups", receive only one dose of minocycline after the stroke.

CatWalk XT, Grip Strength-test and elevated runway tests were performed. These functional tests were applied before and after ischemic stroke. After a specified period (24h, 48h, 7 days) from the onset of stroke, the animals were euthanized, and the brains of the animals were taken for immunohistochemical and biochemical tests. Elevated runway tests takes place over six consecutive days: 4 days of training, on the 5th day, the measurement was taken before the stroke and the sixth measurement on the day of euthanasia.

Results: We present the results of the analysis the elevated runway tests. In the groups without minocycline, we observed a tendency for the time required to passage the beam to be longer compared to the group treated with minocycline. The passage time on day 6 in um-groups was similar to the value of day 1.

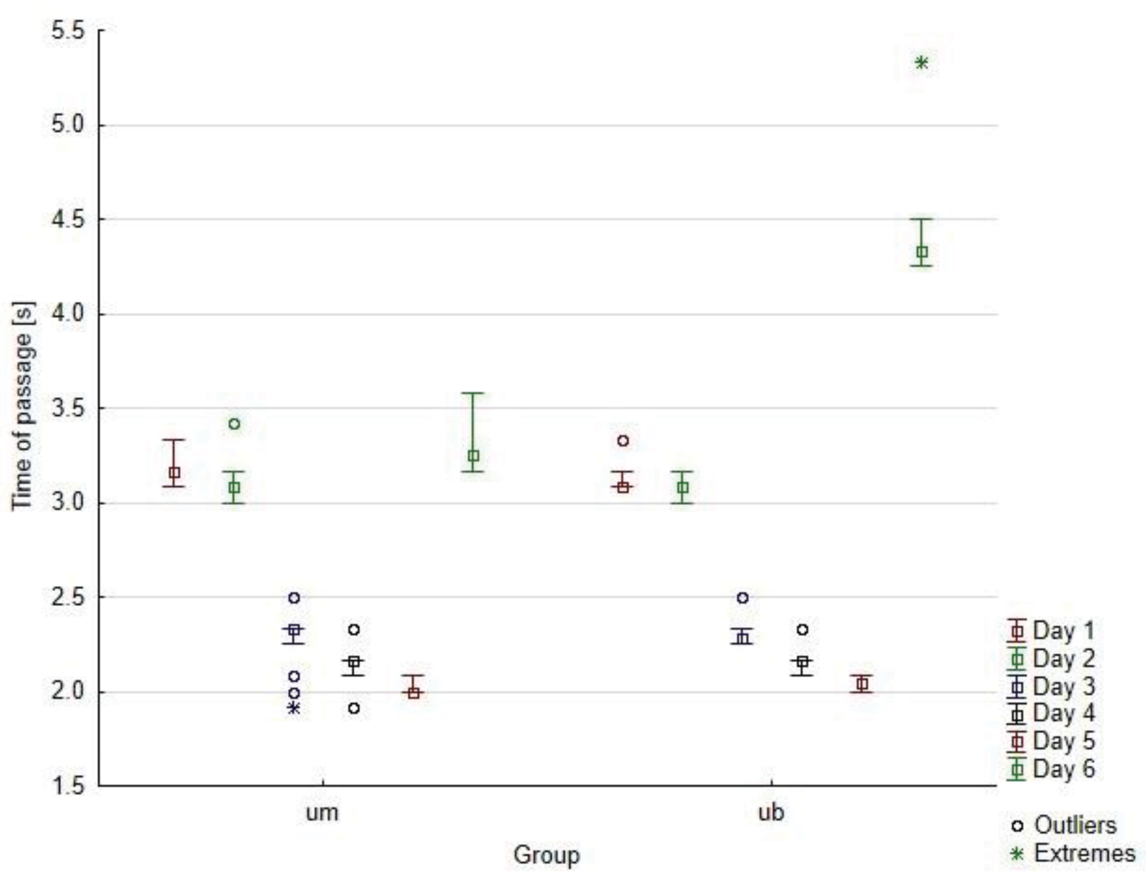

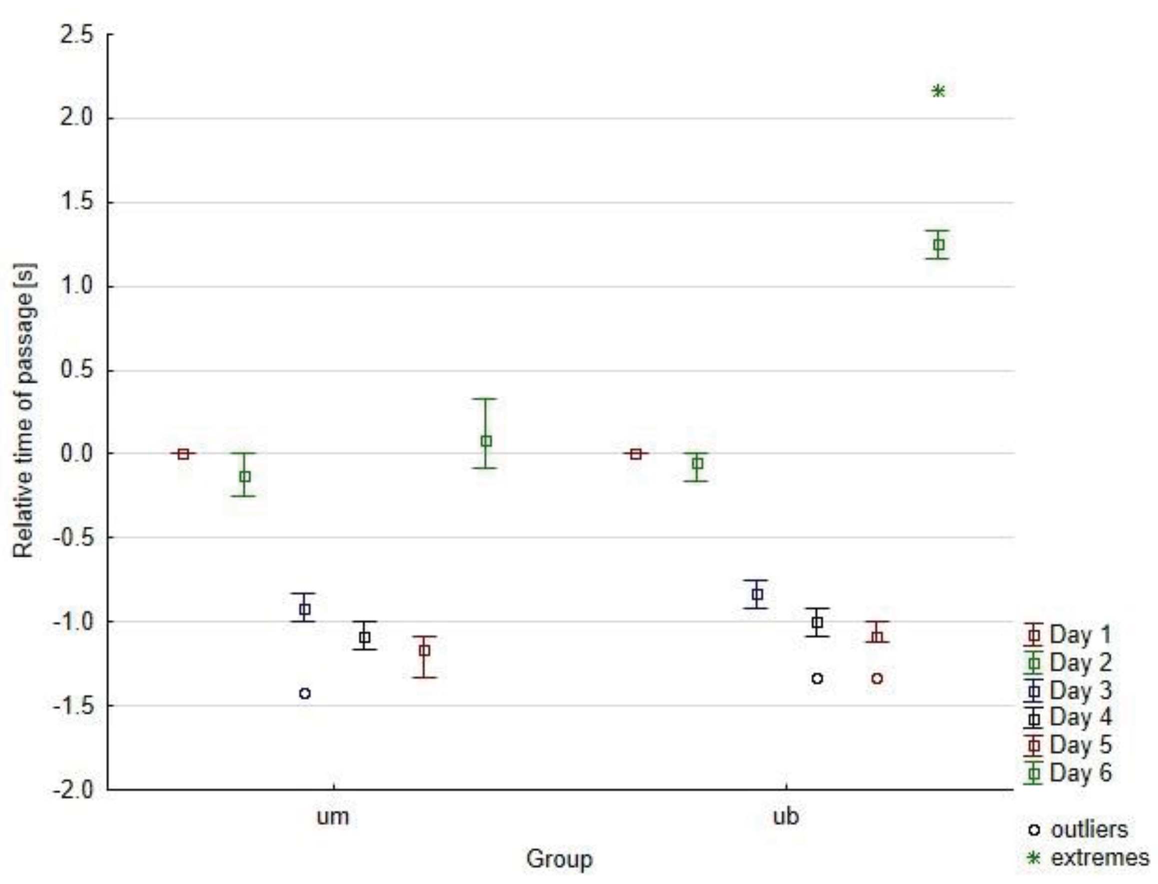

um- groups with treatment with minocycline
ub - groups without treatment

Conclusion:
Minocycline improves motor function and general condition in ischemic rats. It's action could correlates with HuR protein in penumbra, but determining the exact relationship between minocycline and HuR protein requires in-depth studies.
We are in the process of last biochemical analysis.

Bibliography:
- Minocycline for Acute Neuroprotection. Hazem F. Elewa et al. Pharmacotherapy. 2006 April ; 26(4): 515–521.
- Photochemically induced ischemic stroke in rats.Antje Schmidt. Schmidt et al. Experimental & Translational Stroke Medicine 2012, 4:13
- SMALL SYNTHETIC HYALURONAN DISACCHARIDES AFFORD NEUROPROTECTION IN BRAIN ISCHEMIA-RELATED MODELS. J. EGEA et al. Neuroscience 265 (2014) 313–322

Changes in the responsiveness of the rat Dorsomedial Hypothalamus to different metabolic conditions under high-fat diet

POSTER SESSION II
Central Nervous System.
Neurophysiology.
Plasticity of Neural Function.

Sanetra AM, Palus-Chramiec K, Chrobok L, Jeczmien-Lazur JS, Klich JD, Lewandowski MH
Department of Neurophysiology and Chronobiology, Faculty of Biology, Jagiellonian University in Krakow

Introduction and objectives

Food intake and metabolism are coordinated by a set of brain structures, most of which are located within the hypothalamus. Among these, the Dorsomedial Hypothalamic Nucleus (DMH) is involved especially in the modulation of the regularity of feeding behaviour. It has been shown, that DMH neurons respond to restricted feeding (RF; 1,2), which causes an enhancement of the rhythmicity in clock gene expression, both when the feeding occurs during daytime (3) and when the animals are fed at night-time (4).
The DMH receives information about the metabolic states from the digestive system via various hunger and satiety peptides, and processes them in order to affect animals' feeding behaviour, as well as autonomic functions related to metabolism and thermoregulation. Changes in its physiological functioning have been observed in high-fat diet (HFD)-induced obesity (5), which provokes a question whether the DMH could be partially responsible for the excessive weight gain under HFD.
The aim of this study was to investigate into the responsiveness of DMH neurons to different metabolic states, such as hunger and satiety, and whether this changes under short-term HFD (before the development of obesity). Here we compare two experiments, in which hunger/satiety states were induced on animals previously fed *ad libitum*, or could have been anticipated (due to prolonged restricted feeding).

Methods

In the study we used 8-week old, male Sprague-Dawley rats. At 1 month of age (weaning) they were put on either control or high-fat diet for the following 4 weeks. Two separate protocols were applied:
- 1st protocol - food deprivation.
After 4 weeks of *ad libitum* feeding, two groups of rats were food deprived for 48h, after which one group was given access to food for the next 2h (control group continued being fed *ad libitum*). Following, all rats were perfused transcardially with 4% paraformaldehyde, the brains were extracted and slices containing the DMH were immunostained for cFOS protein (an early-response gene, used as a marker of neuronal activity).
- 2nd protocol - restricted feeding.
Rats were fed *ad libitum* for the first 2 weeks on a diet, after which they were given access to food for 6h every day during night-time (ZT14-ZT20, where ZT0 is lights on). The perfusion was then performed either 0.5h before, 1.5h after or 3.5h after the scheduled meal, and the immunostaining performed as in the 1st protocol.
cFOS positive cells were counted manually, and their number divided by the total area of the structure.

Results and conclusions

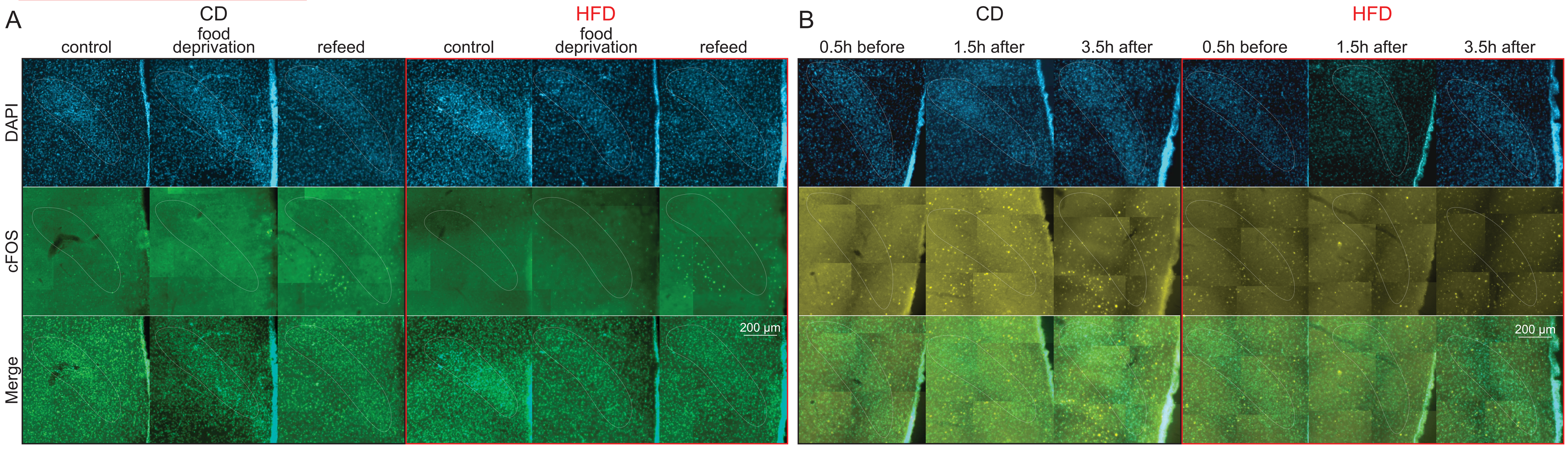

Fig. 1. Representative photographs of brain slices containing DMH, taken from rats under different metabolic conditions after food deprivation protocol (A) or the RF protocol (B). White dotted lines indicate the compact part of the DMH, which separates the structure into ventral and dorsal parts.

In both experiments we observed low cFOS immunoreactivity during hunger and high cFOS after food intake (1st protocol: $F_{2,60}=30.633$, $p<0.0001$; 2nd protocol: $F_{2,27}=28.2544$, $p<0.0001$). Interestingly, depending on the protocol, there was a difference in the the effect of HFD on cFOS immunoreactivity. In the food deprivation/refeed experiment, the density of cFOS-positive cells was higher for animals fed HFD (diet: $F_{1,60}=4.217$, $p=0.0444$, interaction: $F_{2,60}=0.571$, $p=0.5682$; Fig. 2A), whereas the neuronal responsiveness to analogical metabolic states during RF was diminished under HFD (diet: $F_{1,27}=3.2124$, $p=0.0843$, interaction: $F_{2,27}=3.3931$, $p=0.0485$; Fig. 2B), especially at the first time point after the scheduled meal (after 1.5h of food availability, $p=0.0112$).
Keeping in mind, that these differences might have been related to the amount of food eaten by the rats, we have collected and weighed their stomachs. As expected, the stomach weight was highly dependent on the treatment ($p<0.0001$ in both cases), confirming the validity of the applied procedures. Stomachs collected from HFD-fed animals were lighter than the those of the control group (for the 1st protocol- diet: $F_{1,30}=4.461$, $p=0.0164$, interaction: $F_{2,30}=0.08483$, $p=0.9189$; Fig. 2C) which was also anticipated, as HFD is more callorically dense, therefore less of it is required to meet the metabolic demands.
Most importantly, data from the collected stomachs denied the hypothesis, that changes in the effect of the diet between experiments is due to different feeding behaviour of the animals. Even though in both cases HFD-fed animals ate no more than the control group, unexpected changes in food availability caused a higher cFOS immunoreactivity, whereas anticipated meal resulted in a diminished response, comparing to the control group.
Our results show that the DMH responsiveness to metabolic states changes under HFD, which might be an important contributing factor in the development of obesity.

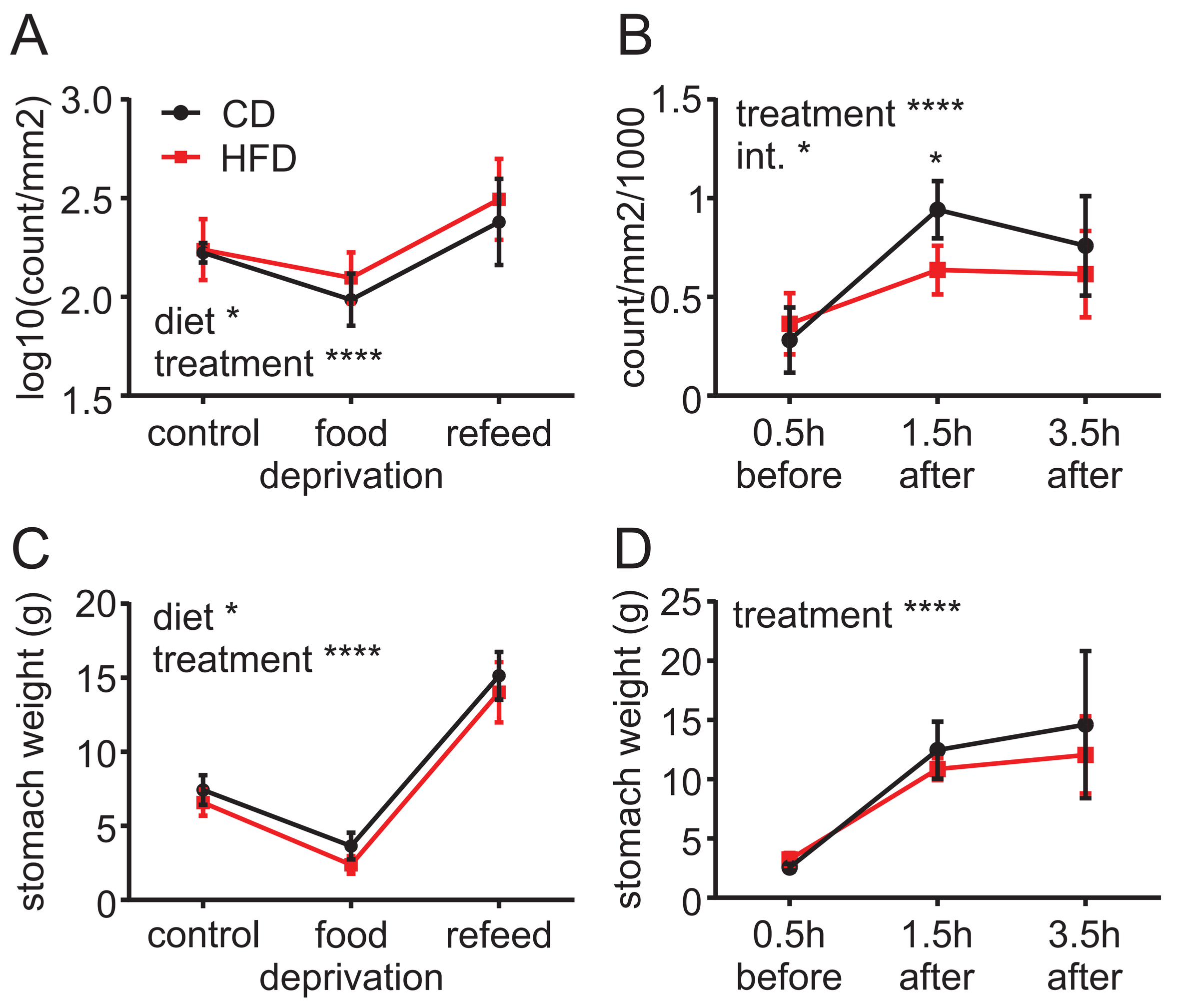

Fig. 2. Comparison of the neuronal response in the DMH to hunger and satiety states following different experimental conditions. (A) Density of cFOS - positive cells after 48h- food deprivation and 2-refeed. (B) cFOS immunoreactivity in the RF protocol. (C-D) Weight of the stomachs collected from the animals after the end of protocol 1 (food deprivation; C) or protocol 2 (restricted feeding; D). *p<0.05, ****p<0.0001; data presented as mean ± SD.

References

1. Minana-Solis, M. C., Angeles-Castellanos, M., Feillet, C., Pevet, P., Challet, E., & Escobar, C. (2009). Differential effects of a restricted feeding schedule on clock-gene expression in the hypothalamus of the rat. Chronobiology international, 26(5), 808-820. **2.** Mieda, M., Williams, S. C., Richardson, J. A., Tanaka, K., & Yanagisawa, M. (2006). The dorsomedial hypothalamic nucleus as a putative food-entrainable circadian pacemaker. Proceedings of the National Academy of Sciences, 103(32), 12150-12155. **3.** Verwey, M., Khoja, Z., Stewart, J., & Amir, S. (2007). Differential regulation of the expression of Period2 protein in the limbic forebrain and dorsomedial hypothalamus by daily limited access to highly palatable food in food-deprived and free-fed rats. Neuroscience, 147(2), 277-285. **4.** Verwey, M., Khoja, Z., Stewart, J., & Amir, S. (2008). Region-specific modulation of PER2 expression in the limbic forebrain and hypothalamus by nighttime restricted feeding in rats. Neuroscience letters, 440(1), 54-58. **5.** Zhang, C., Barkholt, P., Nielsen, J. C., Thorbek, D. D., Rigbolt, K., Vrang, N., ... & Jelsing, J. (2020). The dorsomedial hypothalamus and nucleus of the solitary tract as key regulators in a rat model of chronic obesity. Brain research, 1727, 146538.

Funding: Polish National Science Centre, grant: 2017/25/B/NZ4/01433 ('OPUS13').

NATIONAL SCIENCE CENTRE
POLAND

Modulation of Pain in Brain Limbic Areas: Role of Opioid and Cannabinoid Systems

Nana Tsiklauri[1], Natia Tsagareli[1,2], Irina Kvachadze[2], Merab G. Tsagareli[1,2]

[1]Lab of Pain and Analgesia, Ivane Beritashvili Center for Experimental Biomedicine, Tbilisi;
[2]Department of Physiology, Tbilisi State Medical University, Tbilisi; GEORGIA

Introduction

The most important means of signaling imminent harm is the pain system. Studies of the emotional and motivational basis of pain reveal a diverse and complex set of processes by which the affective experience of pain is realized [1]. Pain has a strong emotional component, and negative emotions can exacerbate chronic pain. We have recently shown that microinjections of commonly used non-steroidal anti-inflammatory drugs (NSAIDs) separately, into the agranular insular cortex (AIC), anterior cingulate cortex (ACC), or central nucleus of amygdala (CeA), induce strong antinociception in rats. Repeated administration of the analgesics in these limbic structures develops tolerance to them [2,3,4,5].

Opioids remain the drug of choice for the clinical management of moderate to severe pain and play a large role in the pain modulatory system. Studies over the past decade have shed light on the influence of endocannabinoids on the opioid system. Evidence from both animal and clinical researches point toward an interaction between these two opioid and cannabinoid systems, and suggest that targeting the endocannabinoid system may provide novel interventions for managing morphine addiction, opiate dependence and tolerance, and of withdrawal reactions [6,7]. Here we report the role of endogenous opioid and cannabinoid receptors in modulation pain sensation by injection their antagonists into the brain limbic areas, – such as the AIC, the rostral part of the ACC, and the CeA of rats.

Methods

The study was carried out on adult male rats. Under anesthesia with intramuscular administration of ketamine, stainless steel guide cannula was stereotaxically implanted into three limbic areas for injection NSAIDs (diclofenac, ketorolac, ketoprofen and lornoxicam) and pre- or post-administration of separetely non-specific opioid receptor antagonist (naloxone) and CTOP, and cannabinoid receptor 1 (CB1) antagonist (AM-251). Thermal paw withdrawal latencies and mechanical thresholds were measured in experimental and control (saline) rats. Here we used the formalin test that is related to models of chronic inflammatory pain.

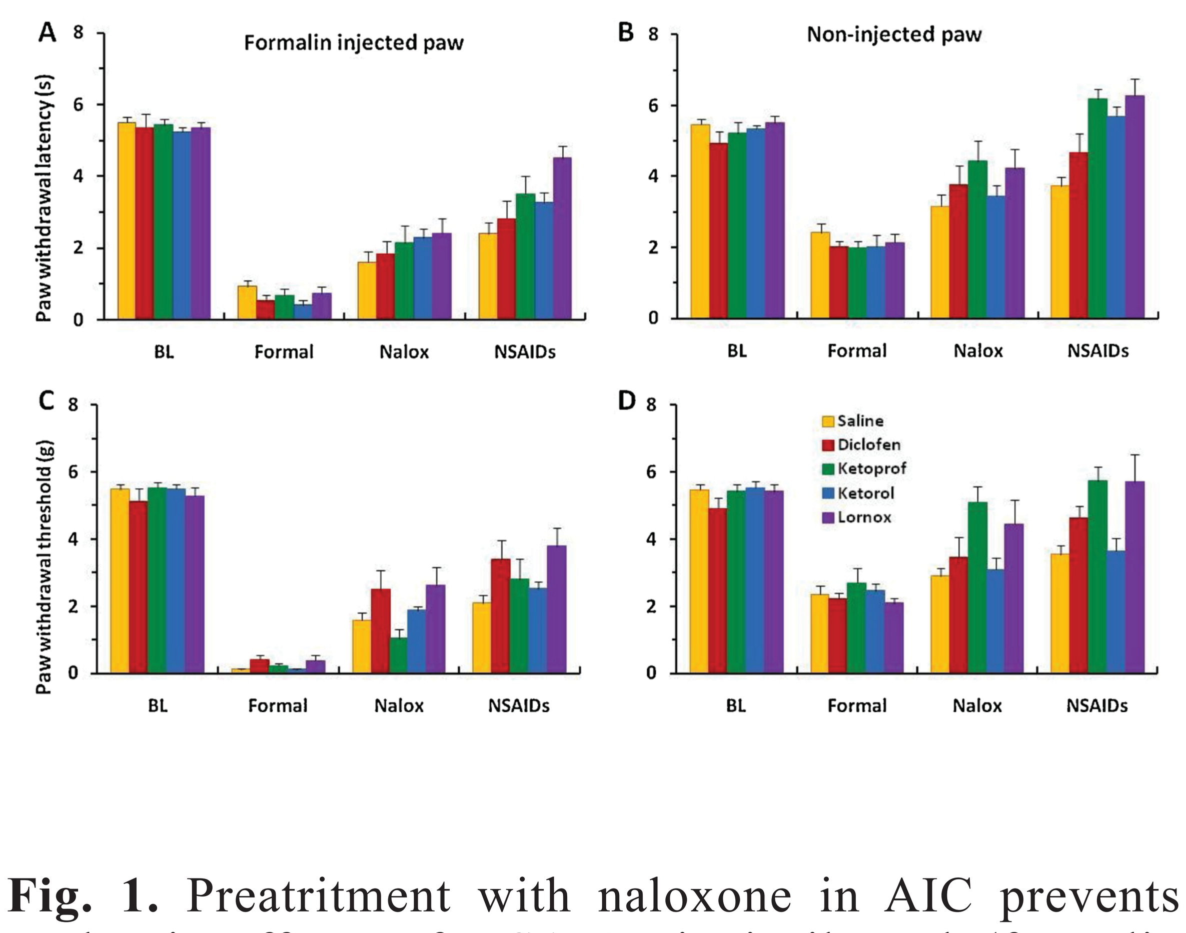

Fig. 1. Preatritment with naloxone in AIC prevents analgesic effects of NSAIDs in ipsilateral (formalin injected) paw (A, C) and contralateral (non-injected) paw (B, D) in latencies of the thermal paw withdrawal reflex (s) (A, B) and thresholds of the mechanical paw withdrawal reflex (g) (C, D) for post-formalin phase II (30 min), respectively.

Results

Five min following intraplantar formalin injection all animals showed a significant reduction in thermal paw withdrawal latency and mechanical withdrawal threshold compared to pre-baseline values. Fifteen minutes after formalin injection, NSAIDs injected into the ACC, the AIC or the CeA clearly showed antinociceptive effects of withdrawals. However, when pretreated with naloxone or AM-251 we found a significant reduction of analgesic effects of NSAIDs as well as post-treatment of these antagonists completely abolished NSAIDs-induced antinociception.

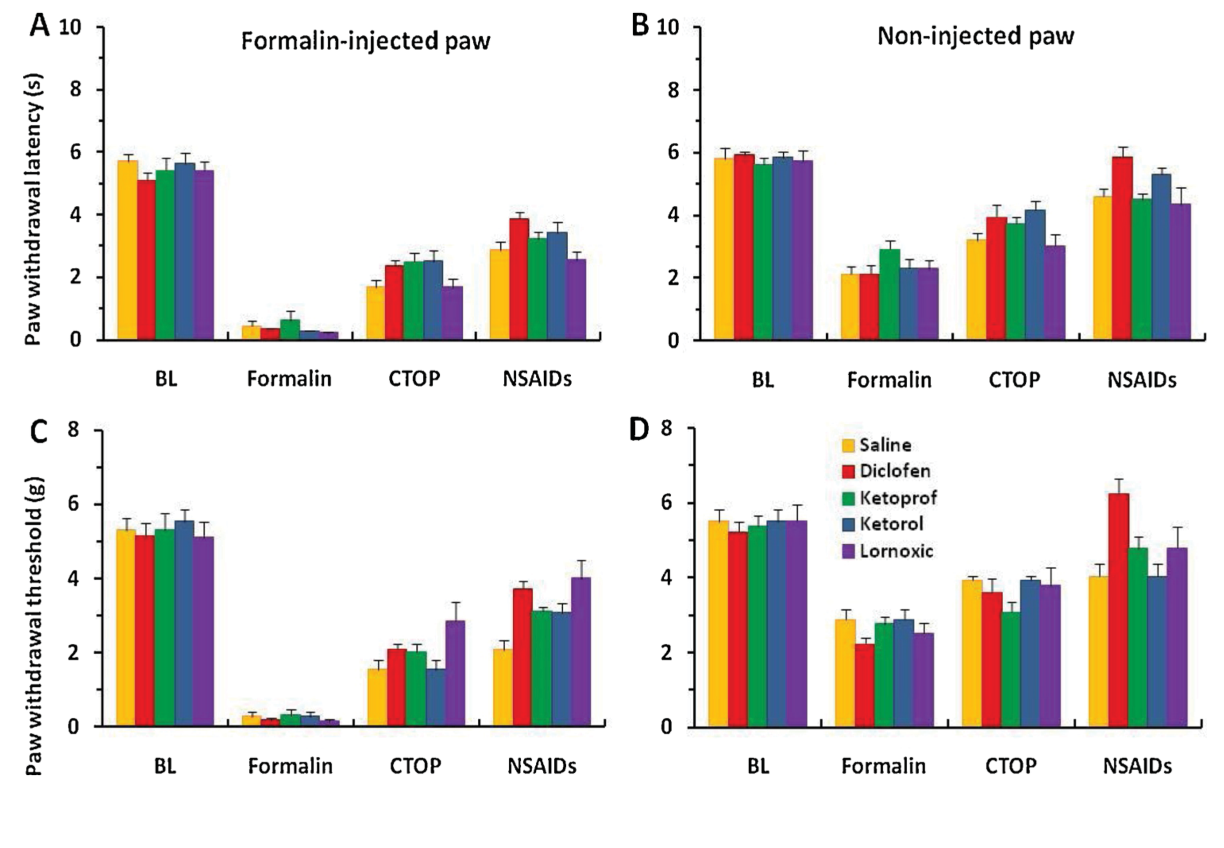

Fig. 2. Pretreatment with mu opioid receptor antagonist CTOP into the AIC significantly reduces analgesic effects of NSAIDs in ipsilateral (formalin injected) paw (A, C) and contralateral (non-injected) paw (B, D) in latencies of the thermal paw withdrawal reflex (s) (A, B) and thresholds of the mechanical paw withdrawal reflex (g) (C, D) for post-formalin phase II (30 min), respectively.

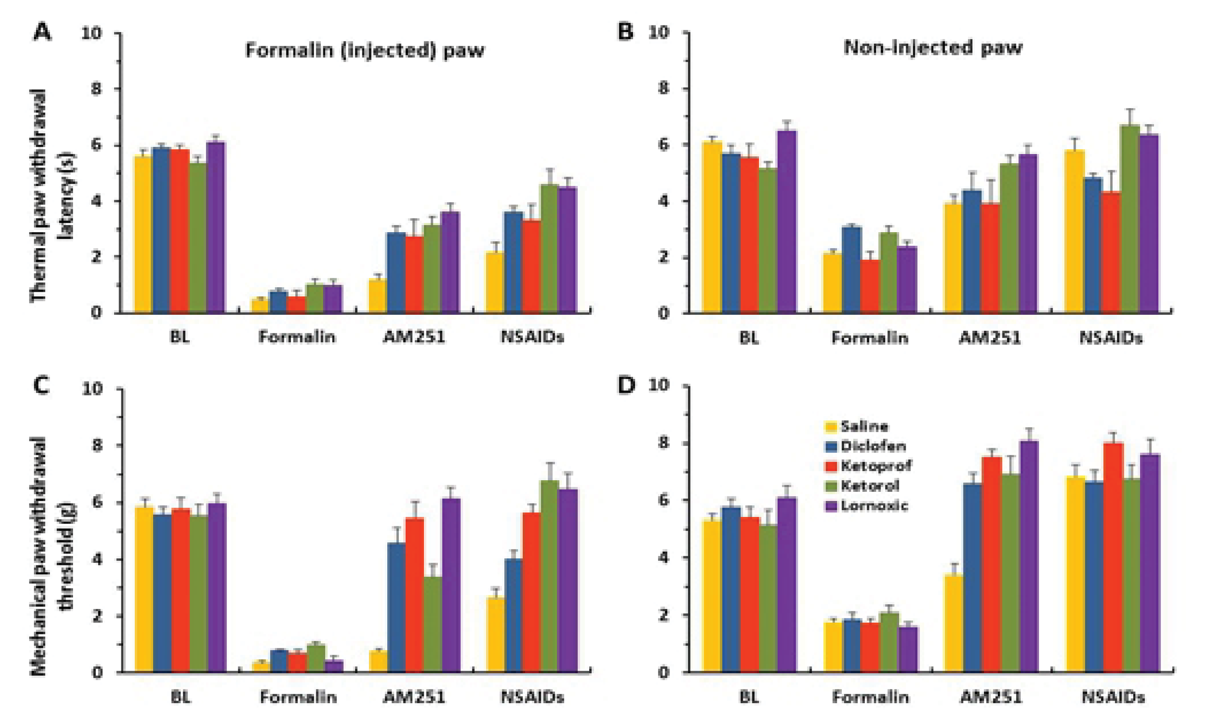

Fig. 3. Pretreatment with CB1 receptor antagonist AM-251 into the ACC completely prevents analgesic effects of NSAIDs in ipsilateral (formalin injected) paw (A, C) and contralateral (non-injected) paw (B, D) in latencies of the thermal paw withdrawal reflex (s) (A, B) and thresholds of the mechanical paw withdrawal reflex (g) (C, D) for post-formalin phase II (30 min), respectively.

Discussion

The present data have demonstrated that microinjections of commonly used NSAIDs, diclofenac, ketorolac, ketoprofen and lornoxicam (xefocam) into the ACC, AIC and CeA result in antinociception in the formalin test model of rats. These data are similar to our previous findings in an acute pain model with tail flick and hot plate tests, and in which metamizol (analgin), diclofenac, ketorolac or lornoxicam were given systemically, or microinjected into the PAG, the CeA, the nucleus raphe magnus (NRM) or the dorsal hippocampus [4,5,6].

These new findings confirmed the concept that antinociception and the development of tolerance to NSAIDs are mediated via endogenous opioid and cannabinoid systems involving the descending pain modulatory circuits attenuating pain behavior in rats – defensive withdrawal reflexes at the spinal cord level.

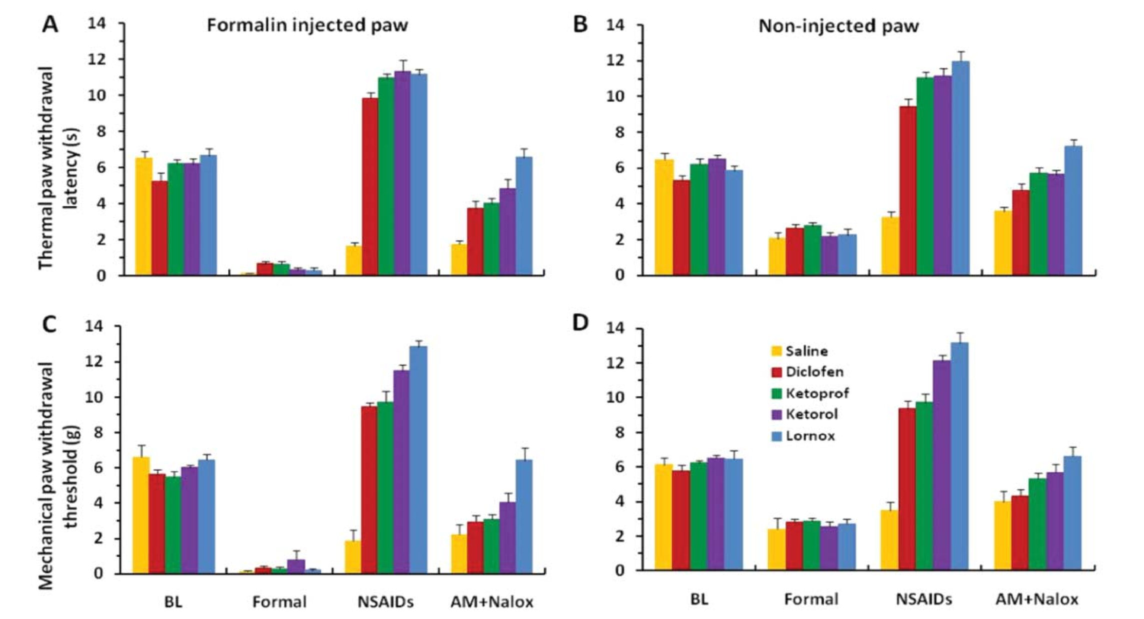

Fig. 4. Post-treatment with a combined CB1 receptor antagonist AM-251 and opioid receptor antagonist naloxon into the CeA completely reduces analgesic effects of NSAIDs injected into CeA in ipsilateral (formalin injected) paw (A, C) and contralateral (non-injected) paw (B, D) in latencies of the thermal paw withdrawal reflex (s) (A, B) and thresholds of the mechanical paw withdrawal reflex (g) (C, D) for post-formalin phase II (30 min), respectively.

Conclusions

We have shown thus that microinjection of commonly used NSAIDs in the CeA induces antinociception in the formalin test. Furthermore, we have revealed that pre- or post-treatment with naloxone and AM-251 injected into the AIC, the ACC or CeA significantly prevented or diminished NSAIDs-induced antinociception. In addition, separate pre- or post-injection AM-251 into the periaquaductal grey (PAG) also showed attenuation of NSAIDs-induced antinociception injected into CeA. Overall, the present findings support the concept that NSAIDs-evoked antinociception is mediated *via* descending endogenous opioid and cannabinoid modulatory systems with the central position of the PAG.

References

1. Seymour B, Dolan RJ. Emotion, motivation, and pain. In: *Wall and Melzacks' Textbook of Pain.* Elsevier, 2013, pp. 248-255.
2. Pirkulashvili N, Tsiklauri N, Tsagareli MG. Antinociceptive tolerance to NSAIDs in the agranular insular cortex is mediated by opioid mechanism. *J. Pain Res.*, 2017, 1561–1568.
3. Tsiklauri N, Nozadze I, Gurtskaia G, Tsagareli MG. Antinociceptive tolerance to NSAIDs in the anterior cingulate cortex is mediated by an opioid mechanism. *BMC Pharmacol. Toxicol.*, 2018, 19(1), art. 2.
4. Tsiklauri N, Nozadze I, Tsagareli N, Gurtskaia G, Tsagareli MG. Brain limbic areas involved in the tolerance of NSAIDs via opioid mechanism. In: *Systemic, Cellular and Molecular Mechanisms of Physiological Functions and Their Disorders.* Chapter 23. New York, Nova, 2018, pp. 281-299.
5. Tsagareli N, Tsiklauri N, Kvachadze I, Tsagareli MG. Endogenous opioid and cannabinoid systems contribute to antinociception produced by administration of NSAIDs into the insular cortex of rats. *Biomed & Pharmacother,* 2020, 131, art: 110722.
6. Tsagareli MG, Tsiklauri N. *Behavior Study of 'Non-opioid Tolerance.'* New York, Nova, 2012.
7. Tsagareli N, Tsiklauri N, Tsagareli MG. *Modulation of Pain in Brain Limbic Areas: Role of Opioid and Cannabinoid Systems.* New York, Nova, 2021.

Funding: Shota Rustaveli National Science Foundation of Georgia (# 217148).

MINOCYCLINE AFFECTS SPLEEN T AND B LYMPHOCYTES PERCENTAGE IN STREPTOZOTOCIN-INDUCED MODEL OF ALZHEIMER'S DISEASE IN RATS

G. Świątek, J. Dunacka, W. Glac, B. Grembecka, I. Majkutewicz, D. Wrona
Departament of Animal and Human Physiology, Faculty of Biology, University of Gdańsk, Poland grzegorz.swiatek@phdstud.ug.edu.pl

University of Gdańsk

WYDZIAŁ BIOLOGII UNIWERSYTET GDAŃSKI

01. BACKGROUND

The sporadic form of Alzheimer's disease (sAD) accounts for more than 90% disease cases and effective treatment is yet to be developed. Main morphological features of sAD - β-amyloid plaques and tau protein tangles in CNS result in neuroinflammation, severe neural damage and cognitive functions impairment. Novel therapy approaches suggest usage of non-steroidal anti-inflammatory drugs (NSAIDs)[1]. We previously demonstrated that NSAID - dimethyl fumarate (DMF) decreased expression of IL-6 and IL-10 [2,3] in hippocampal tissue and attenuated production of IL-10 by spleen T lymphocytes [4] in rats with streptozotocin (STZ)-induced sAD. Here, to broaden the understanding of therapeutic potential of non-steroidal anti-inflammatory drugs we used minocycline (MINO) – synthetic tetracycline, that was shown to have anti-inflammatory and neuroprotective effect in neurodegenerative diseases [5].

02. OBJECTIVE

In present study, to investigate immunomodulatory effect of minocycline, administered intraperitonealy (i.p.) for 7 consecutive days, on immune system in rats with STZ-induced animal model of sAD, we examined lymphocytes percentages in spleen .

03. METHODOLOGY

Thirty Male Wistar rats were divided into four groups: STZMINO (subjected to intracerebroventricular, i.c.v., microinjection of streptozotocine (STZ) and, injections of minocycline 35 mg/kg b.w. i.p.), VEHMINO (subjected to i.c.v. microinjection of vehicle and, injections of minocycline 35 mg/kg b.w. i.p.), STZ (subjected to i.c.v. micorinjection of STZ), VEH (subjected to i.c.v. microinjection of vehicle). Spleens were collected and homogenized. Flow cytometry with a three-color combination of fluorescent monoclonal antibodies was used to identify T (CD3+), B (CD45RA+), NK (CD161a+) lymphocytes and T lymphocyte subsets of CD4+ and CD8+ lymphocyte percentages in spleen supernatants, according to the method that we previously described [6]. Statistical significance was ascertained by U Mann-Whitney test and the results were considered significant at p ≤0.05. Data is presented as mean percentage (%) of cells ± SD.

04. RESULTS

Significantly (p<0,05) increased T lymphocytes (STZMINO: 40,82 ± 9,61; VEHMINO: 42,13 ± 3,71) and B lymphocytes (STZMINO: 17,05 ± 2,64; VEHMINO: 24,2 ± 8,29) percentages were observed in minocycline-treated groups relative to corresponding T lymphocytes (STZ: 20,4 ± 1,16, VEH: 17,75 ± 3,65) and B lymphocytes (STZ: 7,35 ± 1,71, VEH: 11,87 ± 1,97) percentages in non-treated animal groups. Moreover, percentages of T lymphocytes subsets TCD4+ (39,5 ± 7,18) and TCD8+ (16,09 ± 3,16) in STZMINO group were significantly (p<0,05) increased as compared to corresponding STZ (TCD4+: 15,58 ± 3,4; TCD8+: 9,09 ± 1,45) groups.

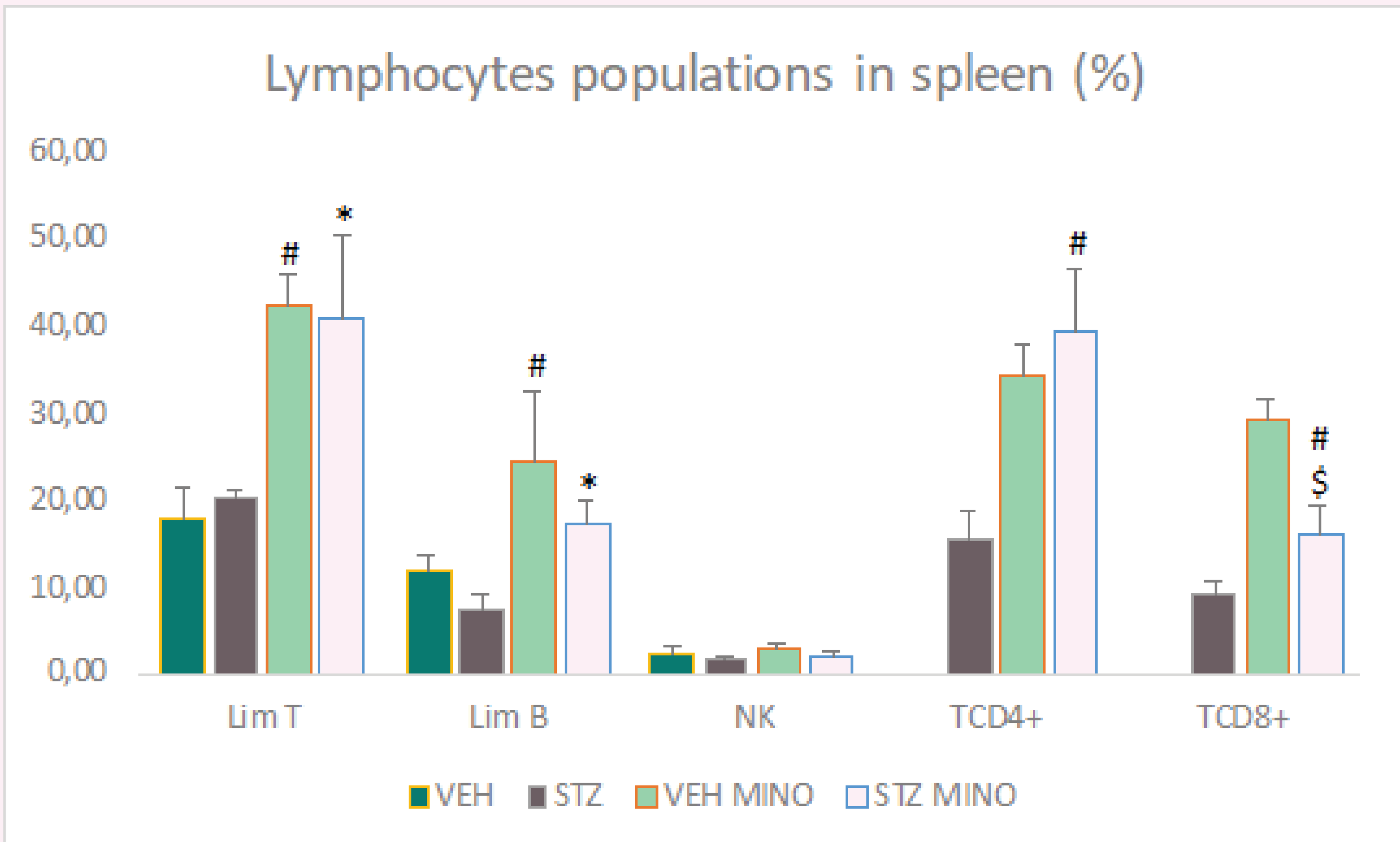

Fig. 1 Percentages of lymphocytes in spleen of rats subjected to chronic i.p . injections of minocycline (saline for control) and i.c.v . microinjections of STZ (VEH for control)
Explanations: * - p ≤ 0.05 significance of differences in comparison to VEH-treated group; # - p ≤ 0.05 significance of differences in comparison to STZ-treated controls; $ - p ≤ 0.05 significance of differences in comparison VEH MINO group

06. CONCLUSION

The results indicate that minocycline changes spleen lymphocyte distribution, including TCD4+/TCD8+cell ratio in the sAD model.

REFERENCES

[1] Moore, A. H., Bigbee, M. J., Boynton, G. E., Wakeham, C. M., Rosenheim, H. M., Staral, C. J. Morrissey, J. L., & Hund, A. K. (2010). Non-Steroidal Anti-Inflammatory Drugs in Alzheimer's Disease and Parkinson's Disease: Reconsidering the Role of Neuroinflammation. Pharmaceuticals (Basel, Switzerland), 3(6), 1812–1841. https://doi.org/10.3390/ph3061812
[2] Majkutewicz, I., Kurowska, E., Podlacha, M., Myslinska, D.,Grembecka, B., Rucinski, J., Plucinska, K., Jerzemowska, G.,Wrona, D., 2016. Dimethyl fumarate attenuates intracerebroventricular streptozotocin-induced spatial memory impairment and hippocampal neurodegeneration in rats. Behav Brain Res 308, 24–37.
[3] Majkutewicz, I., Kurowska, E., Podlacha, M., Myslinska, D.,Grembecka, B., Rucinski, J., Pierzynowska, K., Wrona, D., 2018.Age-dependent effects of dimethyl fumarate on cognitive and neuropathological features in the streptozotocin-induced rat model of Alzheimer's disease. Brain Res 1686, 19–33.
[4] Świątek G., Dunacka J., Wyroślak M., Gratek M., Marchewka J., Majkutewicz I., Grembecka B., Glac W., Wrona D. Dimethyl fumarate affects spleen lymphocyte production of interleukin 10 in streptozotocin-induced model of Alzheimer's disease in rats. European Neuropsychopharmacology, 2019, 29,1, 154-155.
[5] Garrido-Mesa N, Zarzuelo A, Gálvez J. Minocycline: far beyond an antibiotic. Br J Pharmacol. 2013 May; 169(2):337-52
[6] Glac W, Dunacka J, Grembecka B, Świątek G, Majkutewicz I, Wrona D Prolonged Peripheral Immunosuppressive Responses as Consequences of Random Amphetamine Treatment, Amphetamine Withdrawal and Subsequent Amphetamine Challenges in Rats J Neuroimmune Pharmacol 2021 Feb 13

EFFECT OF KETOGENIC DIET ON NEURODEVELOPMENTAL

JAGIELLONIAN UNIVERSITY IN KRAKÓW

Wojciech Kosiek, Zuzanna Rauk, Zuzanna Setkowicz-Janeczko
Institute of Zoology and Biomedical Studies, Jagiellonian University, Crakow, Poland

CENTRAL NERVOUS SYSTEM. NEUROPHYSIOLOGY. PLASTICITY OF NEURAL FUNCTION
S2.P21

INTRODUCTION OBJECTIVES

The ketogenic diet is a type of nutritional system based on deriving energy from fats while minimising carbohydrate intake and maintaining an adequate amount of protein in the diet. It is currently used for the treatment of drug-resistant epilepsy with very good results. There are many studies showing the positive effect of diet on the nervous system in the case of neurodegenerative disorders, endocrine immune disorders, obesity, diabetes and certain types of cancer, while there is a lack of data on the effect of diet on the development of the nervous system. This is an important consideration for pregnant women who are concerned about the safety of the fetus.

METHODS

In order to test the effect of diet on neurodevelopment, a series of experiments were carried out on Wistar rats. These tests aimed to check reflexes such as forelimb grasp, hindlimb grasp, righting, hindlimb placing, cliff avoidance, gait, auditory startle, posture, eye openings and accelerated righting. The rats were divided into three study groups: a control group on a normal diet (ND) , rats prenatally on a ketogenic diet (KD/ND) and a group on a ketogenic diet until P21 (KD). Each reflex had to be recorded on two consecutive days to exclude confusion.

RESULTS AND CONCLUSION

The first finding is a significant difference in weight and weight gain between the groups. For young rats, weight differences are greatest and rats raised on the ketogenic diet have 40-50% of the weight of control rats. At a later stage, the weight difference between ND and KD/ND groups disappears, while adults on the ketogenic diet reach about 51% of the weight of the control group. Rats on ketosis are also less hairy and around day 60 develop full hair which is less stiff than the control group. Studies show that there is an average of 1-2 days difference in the development of individual developmental reflexes. The difference correlates with the length of time spent on the ketogenic diet.

The obtained results show significant differences in the development of rats raised on a ketogenic diet, however, further studies investigating behavioural, histological and metabolomic-lipidomic changes should be carried out, because the current state of knowledge does not allow for a precise statement on the degree to which a diet influences the development of the nervous system.

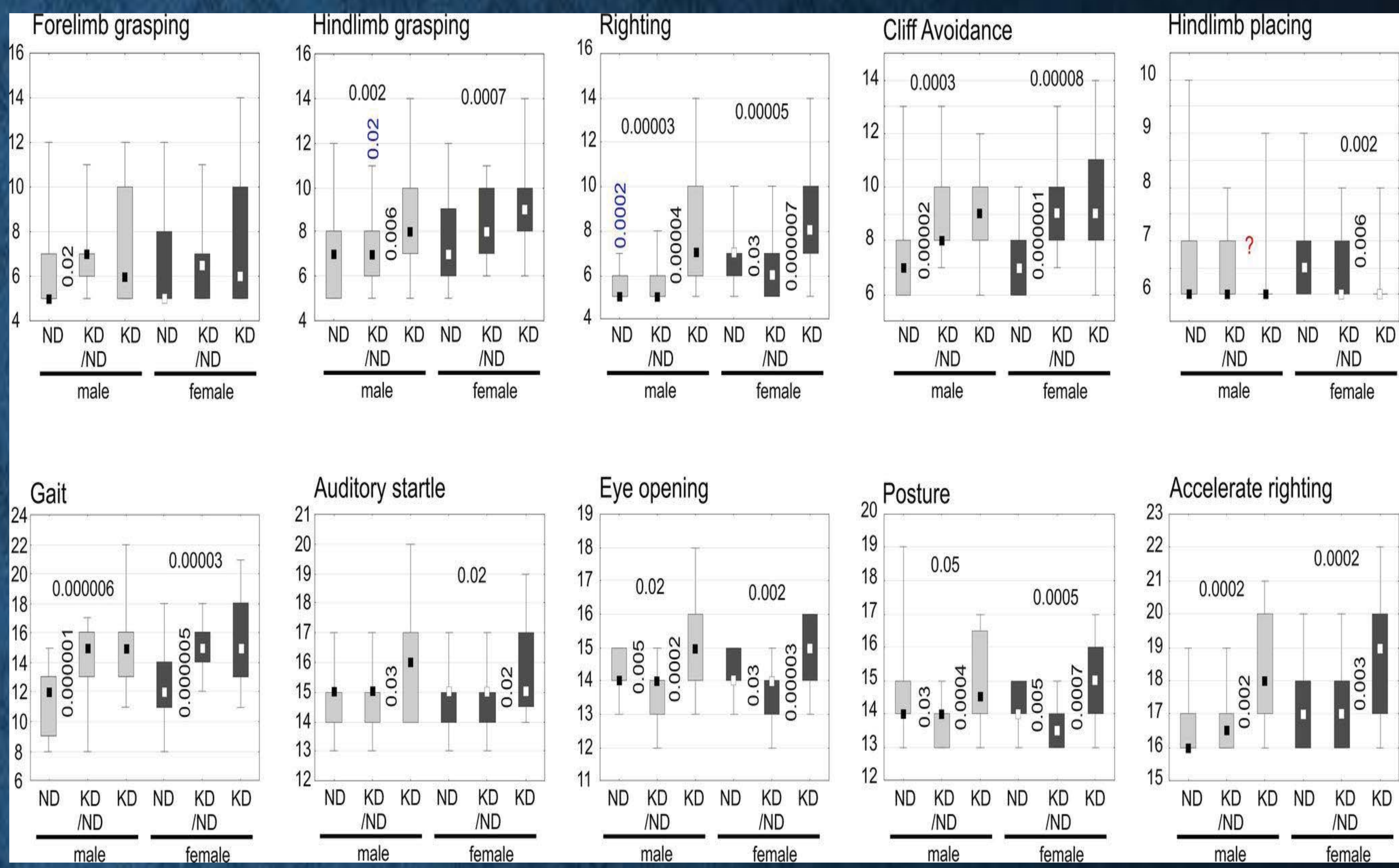

Grapf 1. Overview of the occurrence of the various reflexes on particular days.

Pic. 1. Rat at P30 raised on a normal diet.

Pic.21. Rat at P30 raised on a ketogenic diet.

REFERENCES

1. Sussman D, Germann J, Henkelman M (2015) Gestational ketogenic diet programs brain structure and susceptibility to depression & anxiety in the adult mouse offspring. Brain Behav 5:e00300. doi 10.1002/brb3.300

2. Nguyen AT, Armstrong EA, Yager JY (2017) Neurodevelopmental Reflex Testing in Neonatal Rat Pups. J Vis Exp 122:55261. doi 10.3791/55261

3. Kirkpatrick CF, Bolick JP, Kris-Etherton PM, Sikand G, Aspry KE, Soffer DE, Willard KE, Maki KC (2019) Review of current evidence and clinical recommendations on the effects of low-carbohydrate and very-low-carbohydrate (including ketogenic) diets for the management of body weight and other cardiometabolic risk factors: a scientific statement from the National Lipid Association Nutrition and Lifestyle Task Force. J Clin Lipidol 13:689–711. https://doi.org/10.1016/j.jacl.2019.08.003

ARCHITECTURE OF A FUNCTIONAL SYSTEM OF THE SAGITTAL BALANCE MAINTAINING

A. GONCHAROVA, PhD
Kharkiv National Medical University, Physiology Department, Kharkiv, Ukraine

Body balance is required for a static position and locomotor function. Its maintaining means alignment of the different levels structures of the body in space with respect to each other for organizing the skeleton geometry and locomotor apparatus structure so as to ensure their correspondence to gravity. In the form of mechanical stress this environmental factor affects the processes of adaptive remodeling of bone tissue, and a number of other structures with it.

An integrative indicator characterizing the balance of the body in space is the sagittal balance of the spine - the vertical alignment of the trunk above the pelvis. Its quantitative characteristic is the horizontal distance between the centers of the body of the VII cervical vertebra (C7) and the posterosuperior border of the sacrum on lateral radiographs of the spine in full growth.

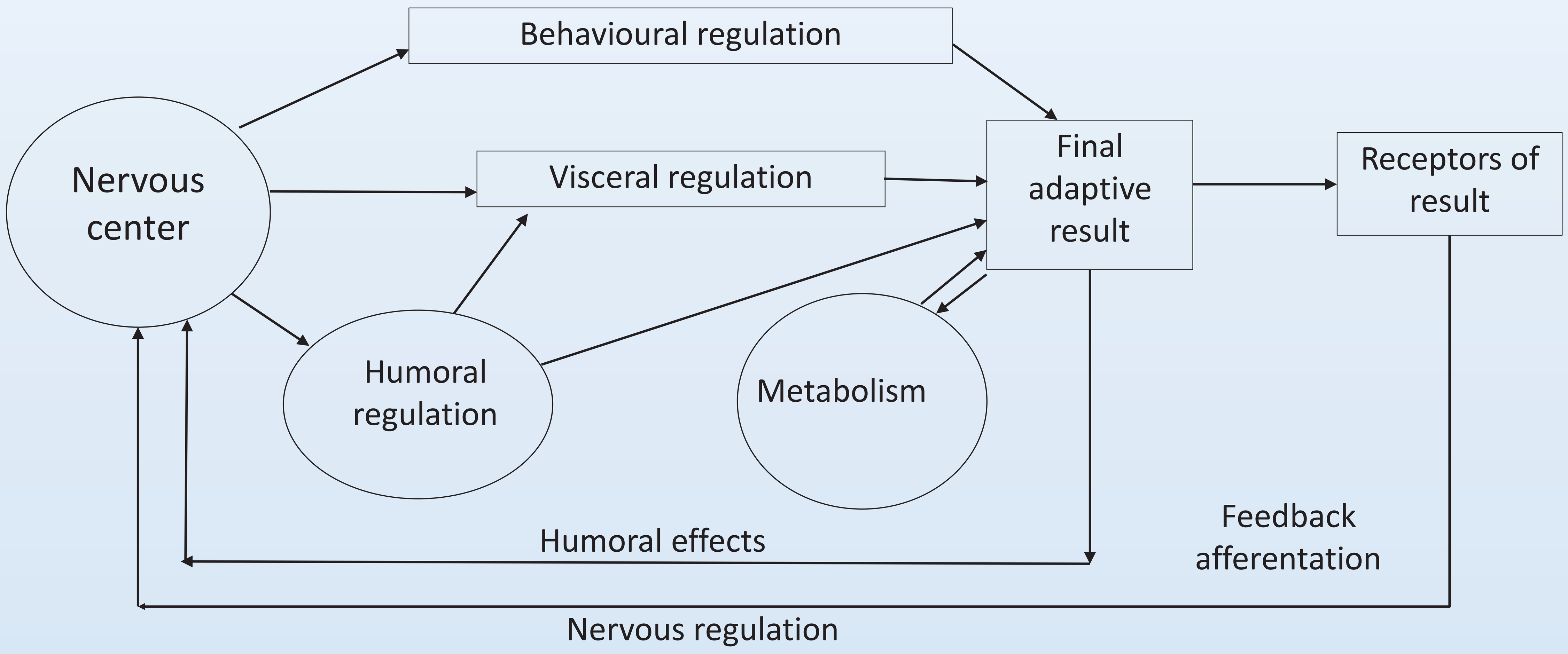

General scheme of functional system (after P. Anokhin)

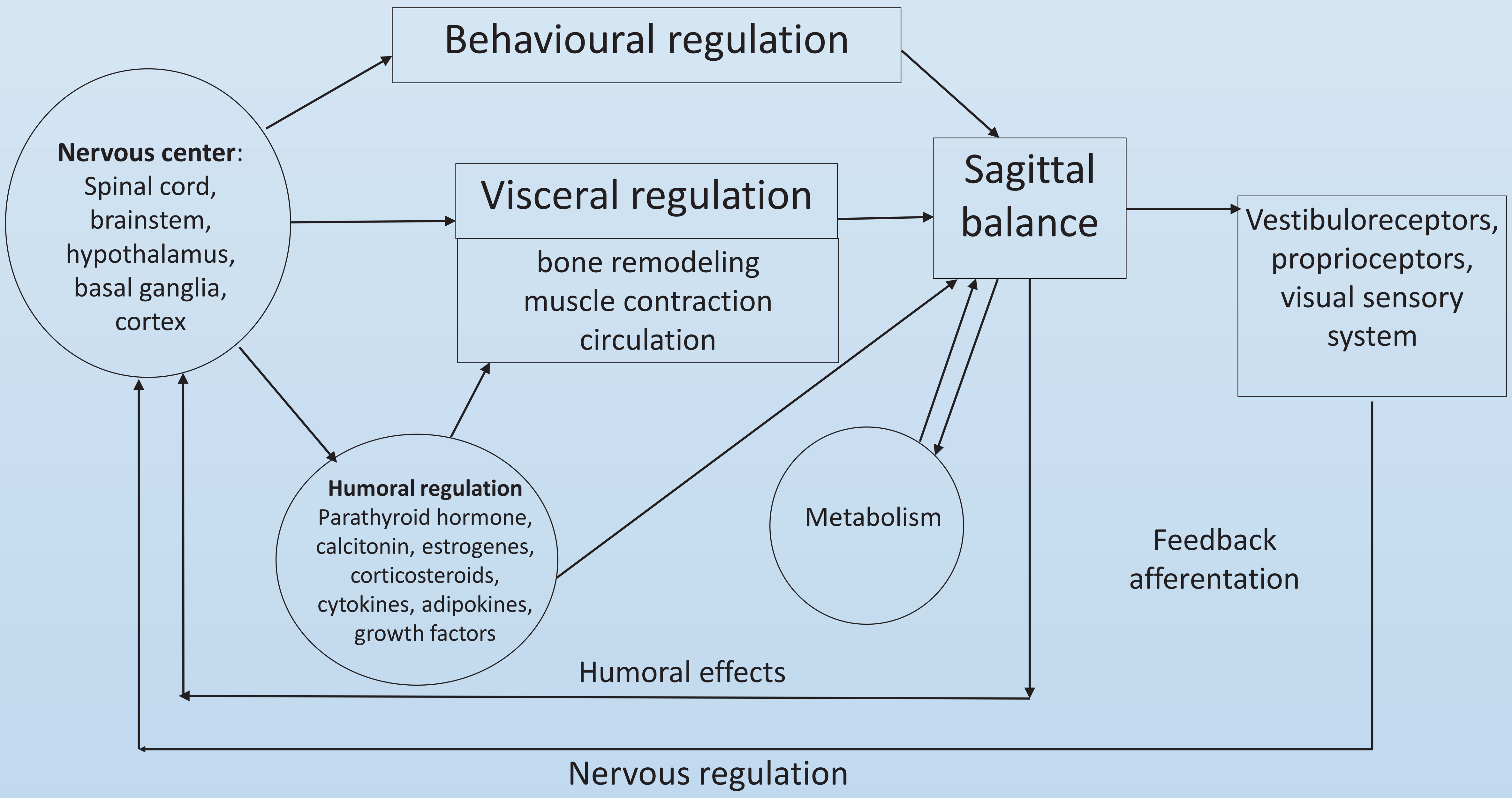

Functional system of the sagittal balance maintaining

To understand the mechanisms of maintaining the sagittal balance within physiological borders, it is important to consider it within the P.K. Anokhin's concept of functional system. In this case, the sagittal balance should take a central place forming the functional system, being the final adaptive result of functioning, that is, one of the parameters of homeostasis, for the maintenance of which all functional systems of the body are formed. In the architecture of such a functional system, it is necessary to distinguish functional blocks - structures that interact with each other to maintain this parameter and perform a certain role, for further multilateral study of such systems.

The receptors that determine homeostasis parameter (sagittal balance) deviations and trigger the functional system are vestibuloreceptors, proprioceptors, and the visual sensory system. In the physiological center, which includes a number of central nervous system structures, the resulting afferentation is integrated in the creation of motor programs. At each current moment, there are changes in the state of the body's executive structures involved in maintaining the sagittal balance. Such efferent structures are not only skeletal and muscle macrostructures, but also elements of bone microarchitecture. They undergo changes in a shorter time interval during remodeling, ensuring the body adaptation with the external environment at higher levels of interaction.

Consideration of the structures involved in maintaining the sagittal balance from this point of view will allow us to determine the possible causes of its displacement and methods of its correction.

References

1. Анохин П. К. Анохин П.К. Узловые вопросы теории функциональной системы. М.: Наука, 1980; 197 с.
2. Судаков К.В. Общая теория функциональных систем. М.: Медицина, 1984; 224 с.
3. Rauch F, Schönau E. The developing bone: slave or master of its cells and molecules? Pediatr Res 2001; 50:309-314.
4. Frost HM Bone "mass" and the "mechanostat": a proposal. Anat Rec 1987; 219:1–9.
5. Mallau S, Vaugoyeau M, Assaiante C. Postural strategies and sensory integration: no turning point between childhood and adolescence. PLoS One. 2010 29;5(9):e13078.
6. Cohen, L., Kobayashi, S., Simic, M., Dennis, S., Refshauge, K., Pappas, E. Non-radiographic methods of measuring global sagittal balance: a systematic review. Scoliosis and spinal disorders, 2017; *12*, 30.

EFFECT OF PROCAINE BLOCKADE OF THE VENTRAL TEGMENTAL AREA ON THETA RHYTHM INDUCED BY PHARMACOLOGICAL ACTIVATION OF THE PEDUNCULOPONTINE NUCLEUS

CENTRAL NERVOUS SYSTEM. NEUROPHYSIOLOGY. PLASTICITY OF NEURAL FUNCTION

S2.P23

WYDZIAŁ BIOLOGII UNIWERSYTET GDAŃSKI

KATEDRA FIZJOLOGII ZWIERZĄT I CZŁOWIEKA • Uniwersytet Gdański •

A. PIWKA, J. ORZEŁ-GRYGLEWSKA
UNIVERSITY OF GDAŃSK – FACULTY OF BIOLOGY, DEPARTMENT OF ANIMAL AND HUMAN PHYSIOLOGY, GDAŃSK, POLAND.

INTRODUCTION

The ventral tegmental area (VTA) and the pedunculopontine nucleus (PPN) are structures that have important influence on the induction and regulation of hippocampal theta rhythm – activity, which plays a key role in important processes such as memory and REM sleep. PPN is one of the initial structures of an extensive theta rhythm induction network, additionally – one of the nuclei that sends cholinergic projections to the VTA. Recent studies has also shown that VTA stimulation is accompanied by the theta rhythm in the hippocampus. However, the functional relationships between these structures and hippocampal theta rhythm is still not fully understood.

THE AIM

of the experiment was to investigate the effect of pharmacological cholinergic activation (carbachol) of PPN and inactivation (procaine) of VTA on the formation and regulation of hippocampal theta rhythm.

METHODS

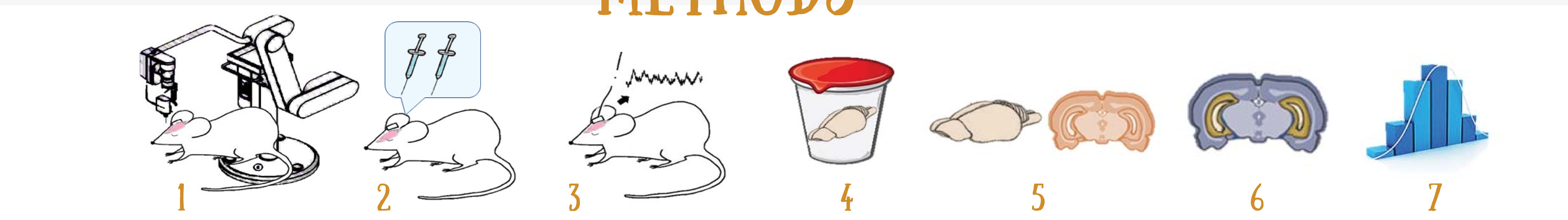

1. STEREOTAXIC OPERATION2 2. INJECTION 3. EEG REGISTRATION 4. PERFUSION AND TISSUE ISOLATION 5. CUTTING THE TISSUE 6. STAINING AND VERIFICATION 7. ANALYSIS

The experiments were performed on 11 male Wistar rats. Animals were divided into groups, each receiving: intra - PPN microinjection (0.5 µl) of cholinergic receptors agonist - carbachol (3.5µg) and intra - VTA microinjection (0.5 µl) of procaine (20%) (PPNkarbVTApro, *n=7*) or intra - PPN microinjection (0.5 µl) of cholinergic receptors agonist - carbachol (3.5µg) and intra - VTA microinjection of either solvent (0.5 µl) (PPNkarbVTAH2O, *n=4*). Surgery and EEG recordings were performed under deep urethane anesthesia maintained at a constant depth by careful monitoring of respiration. The animals were implanted with recording electrodes in HPC and guides for infusions to the VTA and PPN. Local field potential (LFP) was recorded from the hippocampal electrodes during the whole experiment with the use of Spike-2 software. Total power in the hippocampal signal was analyzed. Changes in local field potential were assessed on the basis of peak power (Pmax) for the delta and theta bands.

RESULTS

PPN_KARB_VTA_PRO PPN_KARB_VTA_H2O

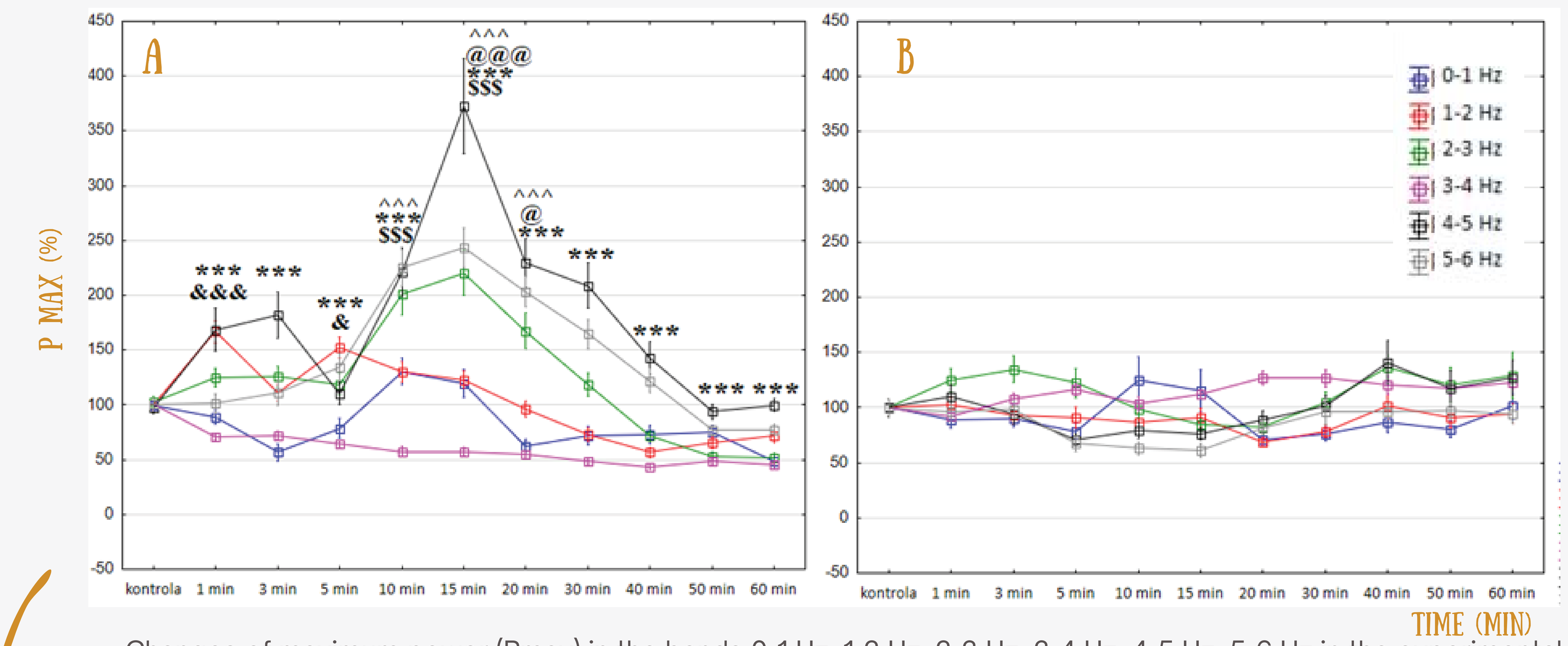

Changes of maximum power (Pmax) in the bands 0-1 Hz, 1-2 Hz, 2-3 Hz, 3-4 Hz, 4-5 Hz, 5-6 Hz in the experimental group (A) and control group (B) before and after injection of procaine (A) and solvent (B) into the VTA.
Explanations: ***& - 1-2 Hz:*** *& - p<0,05, &&& - p<0,001;* ***$ - 2-3 Hz:*** *$$$ - p<0,001;* ****- 3-4 Hz:*** ****- p<0,001;* ***@ - 4-5 Hz,*** *@ - <0,05, @@@ - p<0,001;* ***^ - 5-6 Hz:*** *^^^ - p<0,001. Significant difference in comparison with the control.*
control - theta rhythm analyzed 2 min after injection of carbachol into the PPN

Pmax values in the theta frequency band (3-4 Hz) temporarily decreased after intra-VTA injection of procaine during carbachol-induced theta episodes in comparison to control group. Pmax values in the delta frequency band (1-2 Hz and 2-3 Hz) temporarily increased after intra-VTA injection of procaine during carbachol-induced theta episodes in comparison to control group. In control group with solvent injection to VTA there was no effect in the signal power in theta and delta bands during carbachol-induced theta rhythm episodes.

1-2 HZ 2-3 HZ 3-4 HZ 4-5 HZ 5-6 HZ

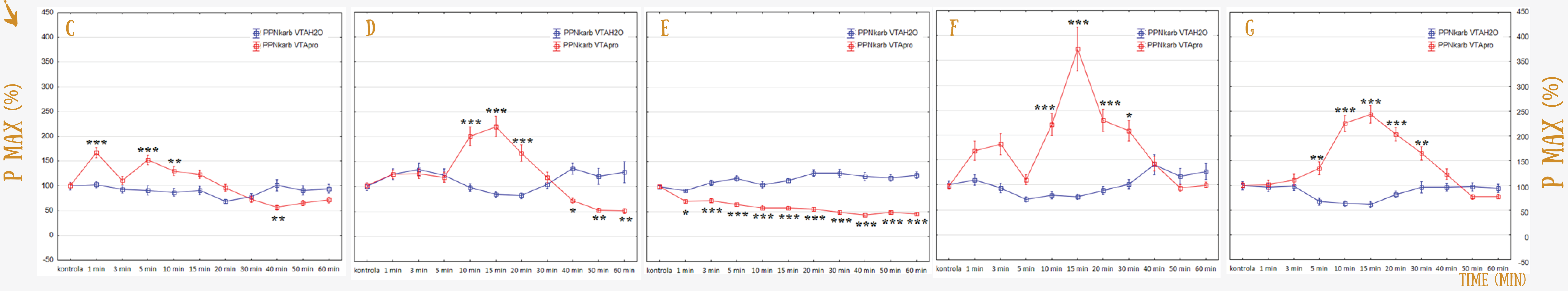

The value of the maximum power (Pmax) in the 1-2 Hz, 2-3 Hz, 3-4 Hz, 4-5 Hz, 5-6 Hz bands in the PPNkarbVTApro group after the injection of procaine into the VTA and the PPNkarbVTAH2O group after the injection of water into the VTA.
*Explanations: * - p<0,05; **-p<0,01;***-p<0,001; control - theta rhythm analyzed 2 min after injection of carbachol into the PPN*

CONCLUSIONS

The results suggest that the a small fraction of the neuronal activation ascending from the PPN into the hippocampus and resulting in theta rhythm in this structure probably may be transmitted through the neural pathways leading through the VTA.

MET-ENKEPHALIN INVOLVEMENT IN THE PROTECTION OF CEREBELLAR AND FRONTAL CORTEX IN VAGOTOMIZED RAT

K.PIERZCHAŁA-KOZIEC[1], M.WIECZOREK[2], ANNA KOBRZYCKA[2], PAWEŁ NAPORA[2]

WYDZIAŁ BIOLOGII I OCHRONY ŚRODOWISKA
Uniwersytet Łódzki

[1]Department of Animal Physiology and Endocrinology, University of Agriculture in Kraków, Poland;
[2]Department of Neurobiology, University of Lodz, Poland;
corresponding author-email: rzkoziec@cyf-kr.edu.pl

INTRODUCTION

Met-enkephalin, one of the opioids peptide, exerts protective effects on the pain sensation, mood, modulation of all endocrines axis and dopamine activity in the brain.

Dopamine and other monoamines are involved in depressive disorders in parkinsonians and epileptic patients. Moreover, evidences were found, that vagus nerve which is connected with the gastrointestinal system, is affected very early in the Parkinson disease. Recently, it was also postulated that opioids and cholinergic systems interacts (via vagus nerve) at the level of brain-gastrointestinal axis. The question arises about the role of opioids in the regulation of vagus nerve effect on the brain structures connected with movement and mental disorders.

AIM OF THE STUDY

The aim of this study was to examine the effect of vagotomy on the activity of Met-enkephalin in the cerebellar cortex (CBR) and frontal cortex (FCTX) in rats during control and inflammation conditions.

MATERIALS AND METHODS

Animals: Adult, male Wistar rats divided into seven groups:
1. CNT – control group,
2. NaCl – injection of NaCl,
3. Sham – sham surgery and injection with NaCl,
4. Vgax – subdiaphragmatic vagotomy,
5. NaCl+LPS – NaCl treated with lipopolysaccharide,
6. Sham+LPS,
7. Vags+LPS.

Tissues: cerebellar cortex (CBR), frontal cortex (FCTX) taken 30 days after Vags

Methods: RIA for Met-enkephalin concentration

RESULTS

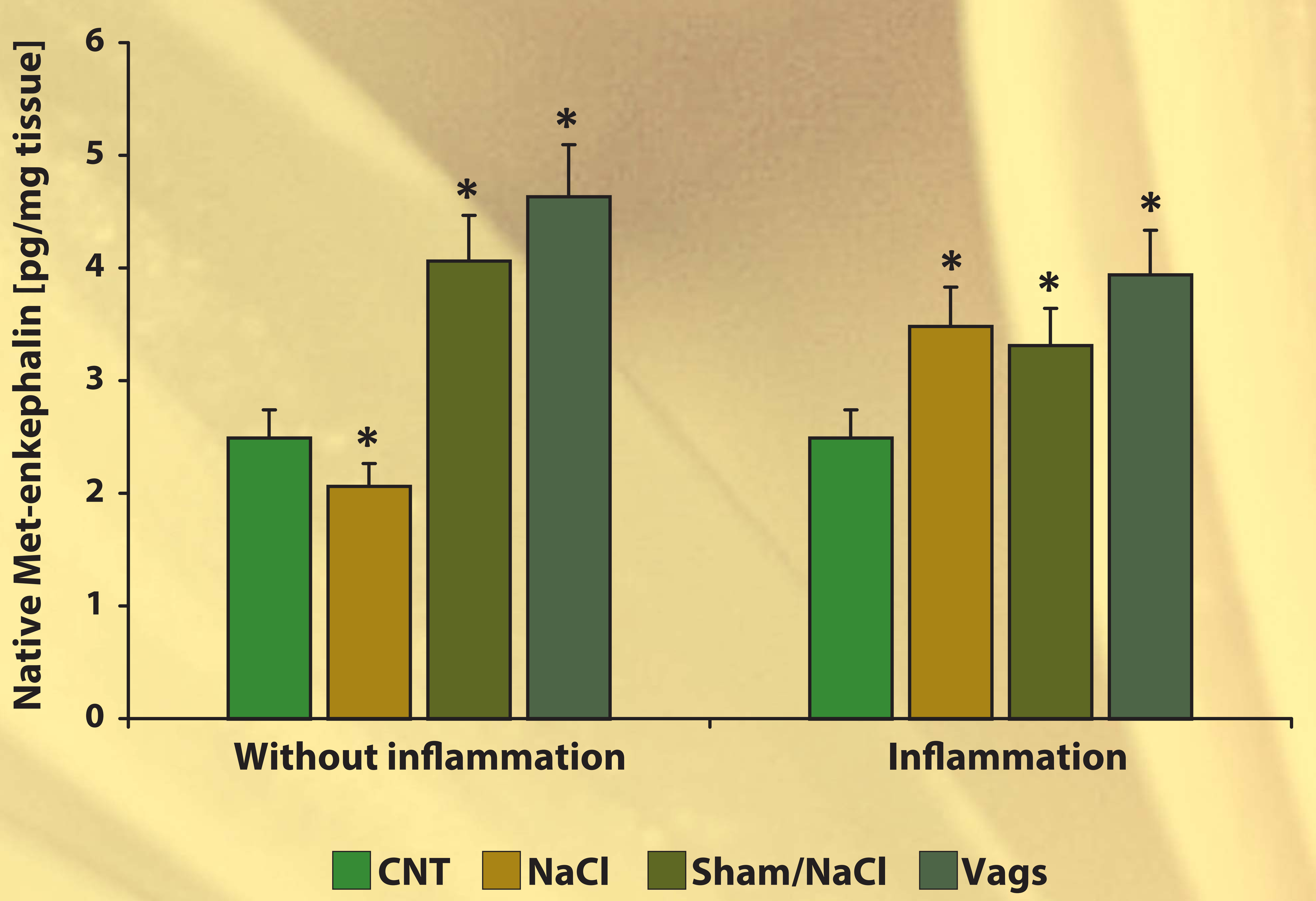

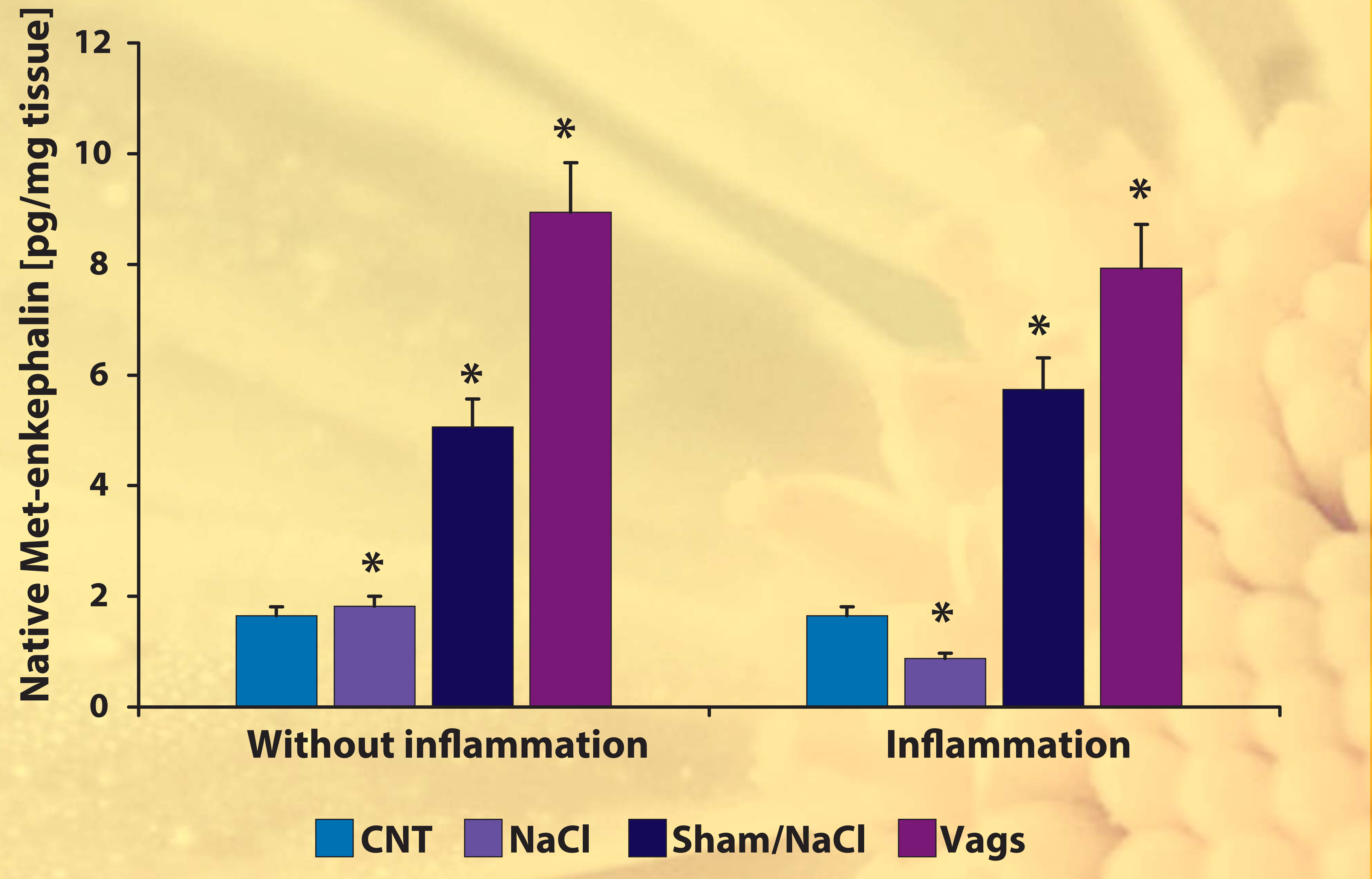

CONCLUSIONS

1. CBR and FCTX opioid system similarly responded to vagotomy (increase) but showed different sensitivity to inflammation.
2. Met-enkephalin protective effect on cholinergic system under inflammation condition in vagotomized rats was significantly higher in frontal cortex than in cerebellar cortex.

Acknowledgements: Research was financed by the Ministry of Science and Education, No Sub-020002-D015

XXVIII Congress of the Polish Physiological Society, Gdańsk, September 15-17 2021

FREQUENCY-DEPENDENT PLASTICITY OF SPONTANEOUS ACTION POTENTIALS WITHIN IDENTIFIED LYMNAEA'S NEURONS

S2. P25

Zeynep SEVAL, Alexander V. SIDOROV *

Department of Physiology , Belarusian State University

Nezalezhnastsi Av., 4, Minsk 220030, Republic of Belarus

*e-mail: sidorov@bsu.by

Introduction

Action potential (AP or spike) is a key reaction of neuronal membrane underlying the responses of the nervous cells on any type of irritation. Some neurons are able to generate spontaneous AP independently from external impact (pacemaker neurons and pacemaker potentials). There is no doubt that AP duration can determine the total excitability of the neuronal membrane due to ability to regulate a time course of it refractory period, i.e. defines a firing rate of the neurons which is critically important for correct operation of neuronal networks. In our days, an initial point of view on AP as "all-or-none", permanent-type event is considerably revised. The plastic nature of AP has been described in various neuronal types both in vertebrates and invertebrates. As a rule it is talking about frequency-dependent broadening of neuron soma spikes, evoked by intracellular current injection. From the other hand, AP variability during spontaneous activity is less described. We report about frequency-dependent changes in the duration of various AP phases: depolarization (DP), repolarization (RP) and undershoot (US) in identified central neurons of mollusk Lymnaea stagnalis.

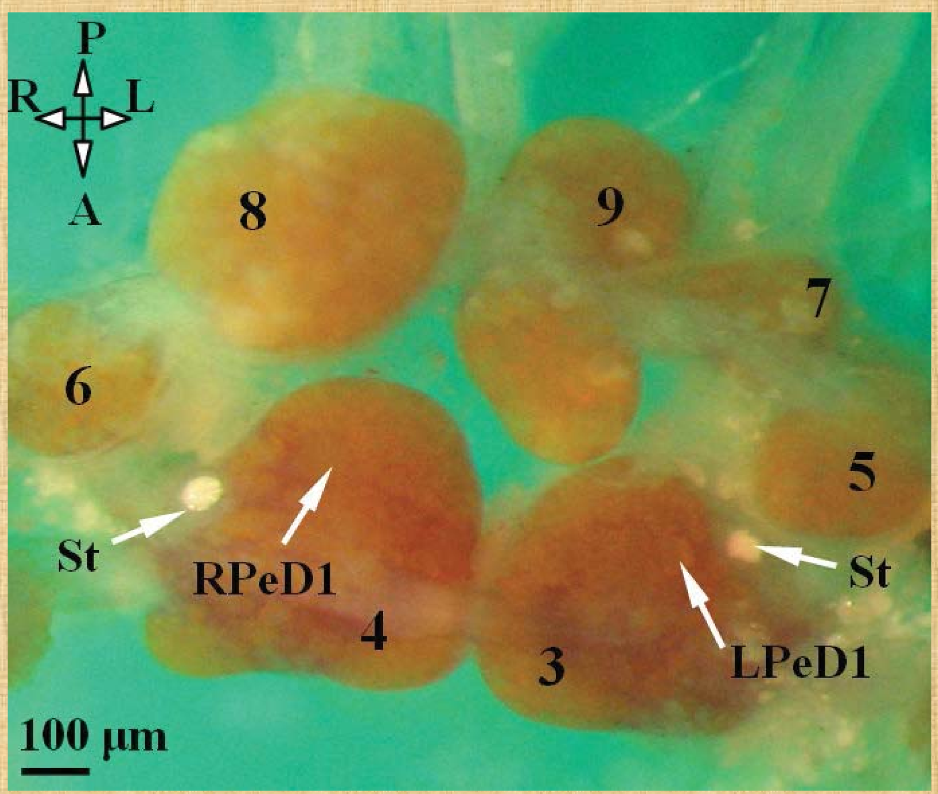

Fig. 1. Representation of the nervous system of *Lymnaea* and the location of the neurons used in the present study

The figure shows the dorsal view of the nervous system. Buccal ganglia have been omitted and the cerebral commisure has been sectioned. 1,2 - left and right cerebral; 3,4 - left and right pedal; 5,6 - left and right pleural; 7,8 - left and right parietal ganglia; 9 – visceral ganglion. St – statocyst, A,P,R,L – anterior, posterior, right and left body sides respectively. **RPeD1** – dopamine- and **LPeD1** – serotonine-containing neurons, identified by their location, size, color and electrophysiological pattern.

Materials & Methods

Specimens of Lymnaea stagnalis were collected locally (Dzerzhinsky district, Minsk region), kept for up to 4 weeks in tap water at 20–22 °C and fed on lettuce. All experiments were conducted on snails weighing 4-6 g.

Animals were anaesthetized in 0.2 M $MgCl_2$ and isolated brains (CNS) of mollusks were put in Ringer's saline (in mM: NaCl 44.0, KCl 1.7, $CaCl_2$ 4.0, $MgCl_2$ 1.5 and HEPES 10, pH 7.5. Individual neurons (**fig. 1**), giant dopaminergic (RPeD1, n=6) and serotonergic (LPeD1, n=4) were impaled with glass microelectrodes filled with 2.5 M KCl (electrode resistance 10–20 MOhm).

Spontaneous electrical activity of mentioned above cells was recorded for 10 min periods and then analyzed by conventional electrophysiological (InputWin) and statistical (Statistica 6.0) tools. Based on initial data distribution of frequencies (**fig. 2**), all spikes in a record were combine in 3 groups – low (first quartile or less), base (between first and third quartiles), high (third quartile or more) and then their time characteristics (**fig. 3**) within those groups were analyzed.

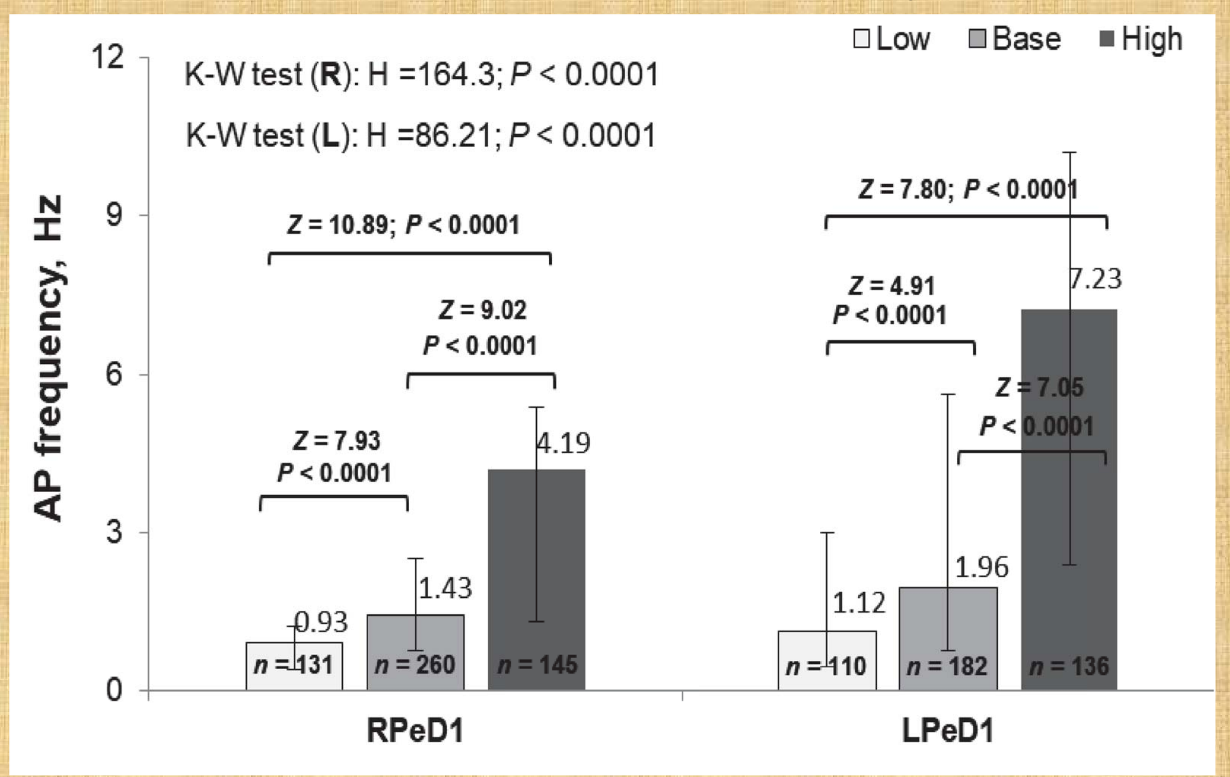

Fig. 2. Frequency grouping for RPeD1 and LPeD1 action potentials (AP)

Numbers above the columns – median, error bars – lower and upper quartiles, n – amount of action potentials analyzed. K-W – Kruskal-Wallis ANOVA test, Z and P values are presented for Mann-Whitney test

Results

For RPeD1 we were able to observe a slight AP broadening both for DP and RP phases at high frequencies, while for LPeD1 about two-time decrease of duration in all AP phases under the study was determined, meaning compression of the signal (**fig. 4, 6**). AP amplitude is also varied in frequency-dependent manner in RPeD1 and LPeD1 – both a positive (an area above) and a negative (an area below rest potential value) phases of AP decline with spike frequency rise (**fig. 5, left pair; 6**). However, total time of neuronal membrane depolarization and hyperpolarization state was significantly increased at high frequencies in both cells (**fig. 5, right pair**).

Fig. 3. Time characteristics of RPeD1 and LPeD1 action potentials (AP)

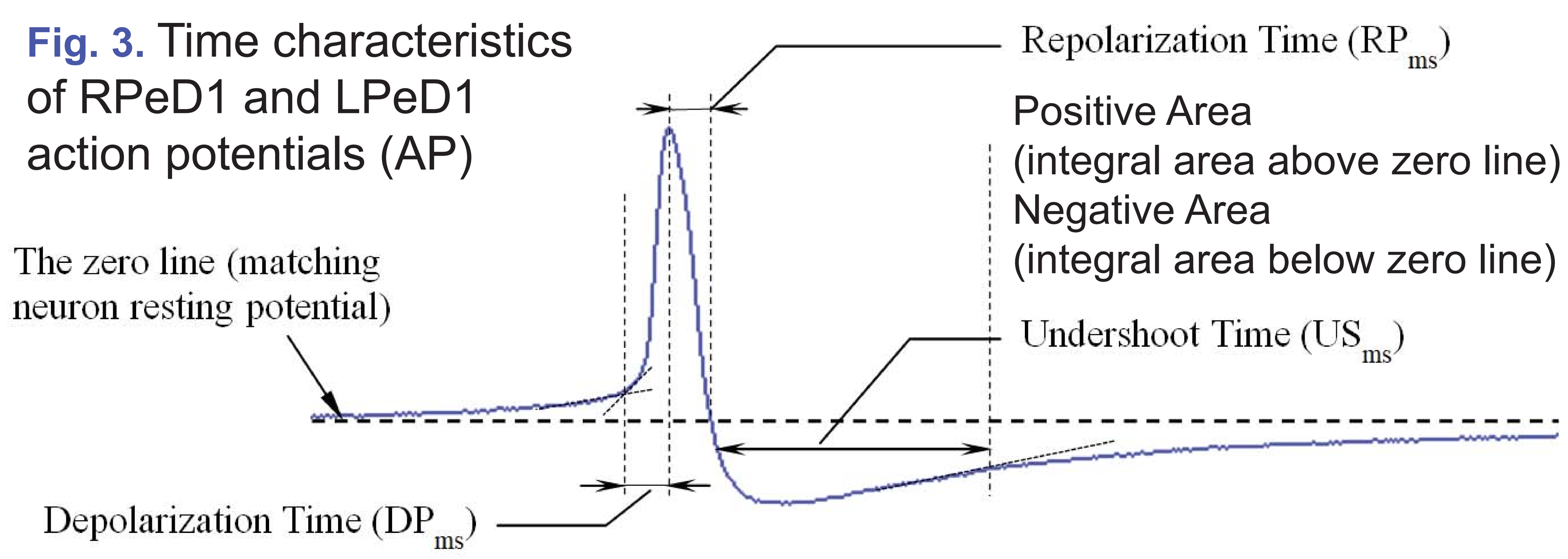

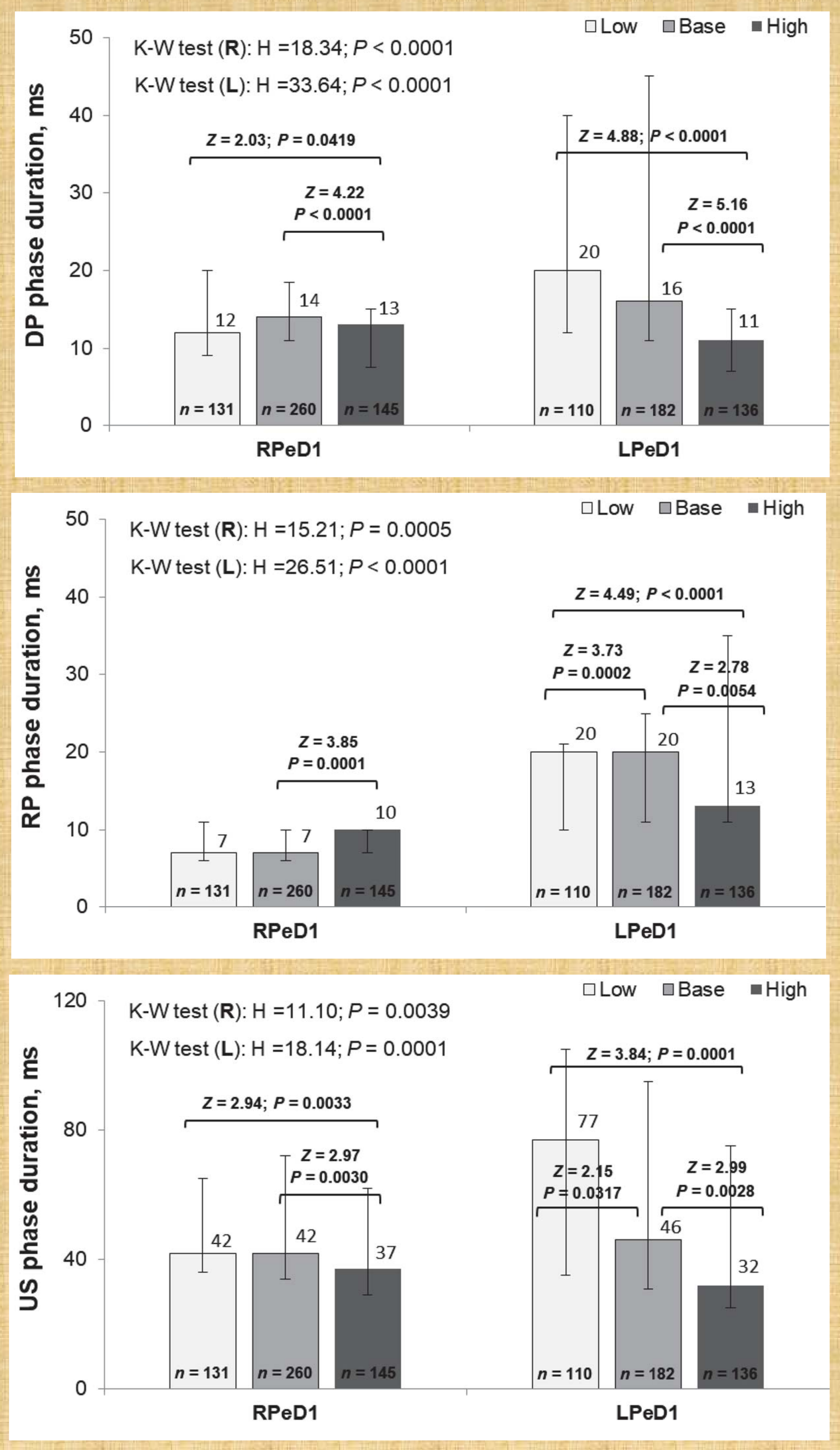

Fig. 4. Dependence of AP phases (DP, RP, US) duration from neuron firing rate

Legend is the same as on fig. 2

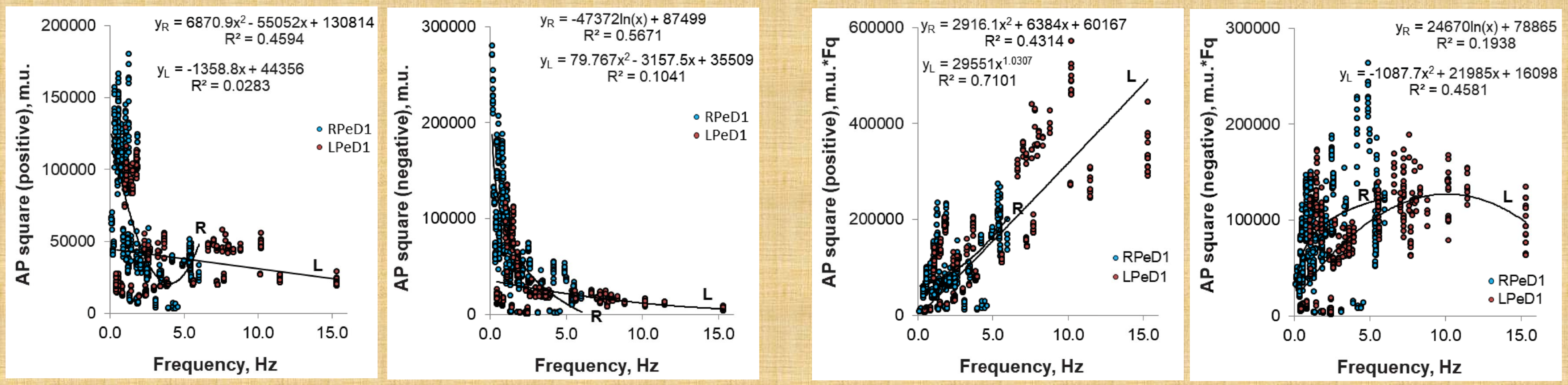

Fig. 5. Dependence of action potential (AP) phases characteristics from neuron firing rate

Left pair - for positive and negative phases (over and under rest potential level) respectively, right – total time for membrane de- or repolarization. Blue dots – RPeD1 data (n = 536), orange dots – LPeD1 data (n = 428). Equation (y) and approximation value (R^2) are presented for the trend line separately for RPeD1 (R) and LPeD1 (L). Fq – spiking frequency, m.u. – machine units.

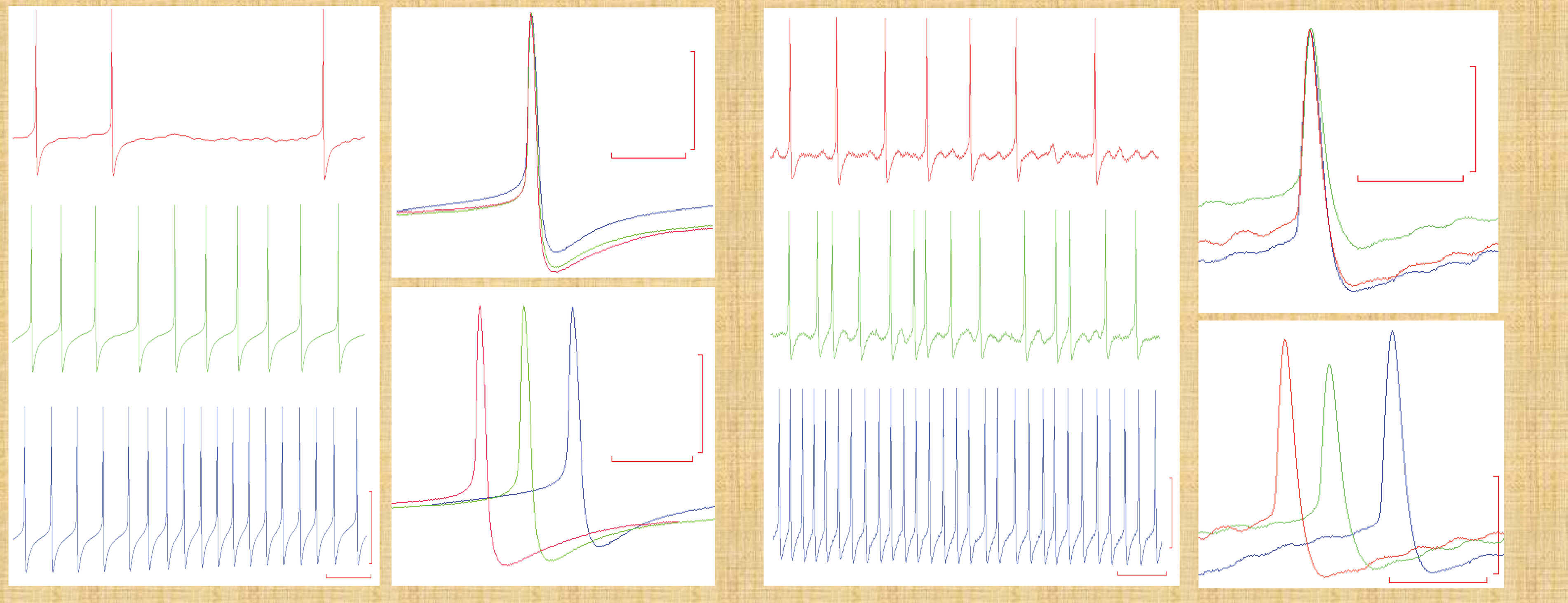

Fig. 6. Examples of AP shape within RPeD1 (left column) and LPeD1 (right column)

Low, base and high frequencies are colorized by red, green and blue lines respectively. Superposition of AP images by depolarization peak (top) or threshold level (bottom) presented. Calibration bars: time – 500 (frequency record) or 50 (individual spikes) ms, amplitude – 25 mV.

Conclusions

We hypothesize that mentioned above differences in AP frequency-dependent plasticity can underlie variations in the efficiency of interneuronic communication in dopamine- and serotoninergic networks of molluscan brain.

Acknowledgements

•This work was supported by State Program for Scientific Research "Convergence-2020" (project 3.10.2)

THANK YOU FOR ATTENTION !

XXVIII Congress of the Polish Physiological Society

Gdańsk, September 15-17 2021

Poster book

SESSION III

BIOLOGICAL RHYTHMS. SLEEP

HONORARY PATRONAGE

Prof. dr Marcin Gruchała
Rector of the Medical University of Gdansk

Uniwersytet Gdański

Prof. dr Piotr Stepnowski
Rector of the University of Gdansk

WOJEWODA POMORSKI
DARIUSZ DRELICH

Dariusz Drelich
Governor of the Pomeranian Voivodeship

HONORARY PATRONAGE
Mayor of the City of Gdańsk

Aleksandra Dulkiewicz
Mayor of Gdansk

Mieczysław Struk
Marshal of the Pomeranian Voivodeship

PARTNER

PAN
POLSKA AKADEMIA NAUK

ANIMA LAB
animal facility and laboratory equipment • animal research models

FUNDACJA LOTOS

Medical University of Gdansk
Department of Physiology

THE SLOW OSCILLATION (<1 HZ) BEFORE SLEEP IN THALAMO – CORTICAL NEURONS

V. TSOMAIA, N. NACHKEBIA

I. BERITASHVILI CENTER OF EXPERIMENTAL BIOMEDICINE, TBILISI, GEORGIA

VTSOMAIA@GMAIL.COM

S3.P1

Introduction:

The slow oscillation (<1 Hz) is an EEG hallmark of the resting state. The Thalamus is involved in several types of oscillatory activity including slow (<1 Hz) rhythms that are considered as the forerunner of the deeper stages of sleep during the transition from wakefulness to sleep as well as the faster activity that occurs during awakening. In order to examine the involvement of muscarinic acetylcholine receptors in slow oscillatory activities, it was interesting for us to investigate the effects of muscarinic combined agonist, carbochol, on the extracellular unitary and field activities and intracellular discharges in brain slice preparations of the rat and cat Lateral geniculate nucleus and Ventrobasal Thalamus.

Methods:

Extracellular recordings were performed using glass pipettes filled with 0.5 M NaCl (resistance: 1-5 MΩ) connected to a Neurolog 104 differential amplifier and bandpass filtered at 0.1-20 kHz. Intracellular recordings, using the current clamp technique, were performed with standard-wall glass microelectrodes filled with 1M potassium acetate (resistance: 80-120 MΩ), and in some cases 2% biocytin or neurobiotin, and connected to an Axoclamp-2A amplifier (Axon Instruments, Foster City, USA) operating in bridge mode. Impaled cells were identified as TC neurons using established electrophysiological and morphological criteria (Williams et al., 1996, Hughes et al., 2002a). All neurons recorded in the VB (cat, rat) were from the ventral posterior lateral nucleus (VPL) whereas all cells assessed in the MGB (cat only) were from the dorsal subdivision. A small proportion (<20%) of the cat LGN TC neurons included for analysis in this study were also included in a previous paper (Hughes et al., 2002b). The apparent input resistance (RN) was estimated from voltage responses evoked at -60 mV by small (20-50 pA) hyperpolarizing current steps. Statistical significance was assessed using Student's t-test.

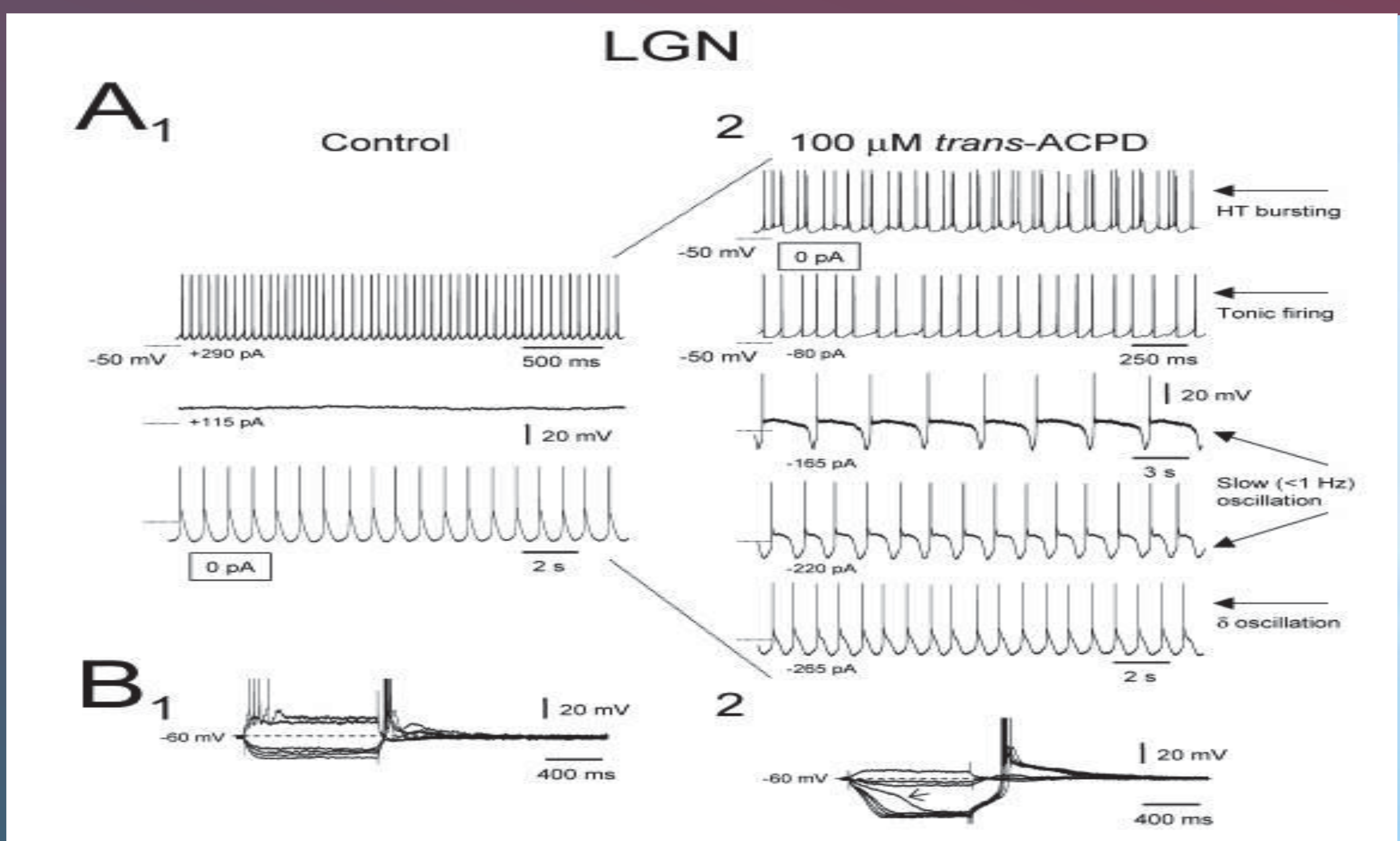

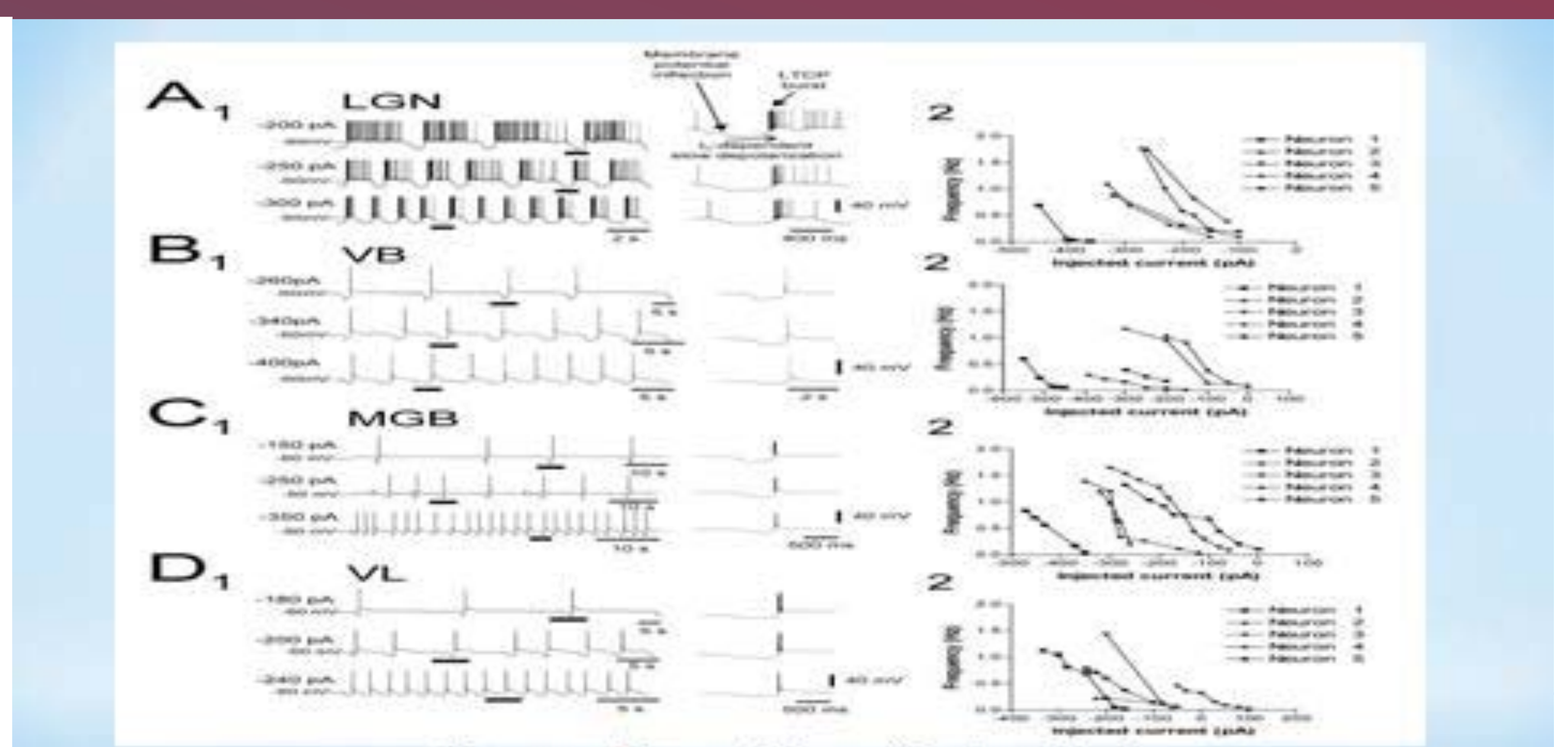

Comparison of the relationship between injected d.c. current and slow oscillation frequency in TC neurons of the cat LGN, VB, MGB and Vl

Results:

We suggest that the presence of an LTCP-mediated burst at the commencement of each UP state may be a mechanism whereby the thalamus is sending a specific priming signal to the cortex that the 'activated' or 'processing' phase of the slow oscillation is about to begin. Of course, the idea that the LTCP-mediated bursts of the slow oscillation signal the upcoming transmission of high-priority information is essentially equivalent to that which has been suggested for the role of LTCP-mediated bursts in TC neurons during wakefulness. Indeed, we have recently postulated that similar cellular mechanisms may underlie both the slow oscillation and the ability to generate LTCP-mediated bursts from depolarized membrane potentials during the wake state.

Conclusions:

Thus these results suggest that whilst moderate activation of muscarinic acetylcholine receptors on Thalamocortical neurons mediates a natural change from sleep to wake-related electrical activity.

References / Bibliography:

Achermann P, Borbely AA. Low-frequency (< 1 Hz) oscillations in the human sleep electroencephalogram. Neuroscience. 1997; 81:213–222. [PubMed: 9300413]

Amzica F, Steriade M. The K-complex: its slow (<1-Hz) rhythmicity and relation to delta waves. Neurology. 1997; 49:952–959. [PubMed: 9339673]

Amzica F, Steriade M. Cellular substrates and laminar profile of sleep K-complex. Neuroscience. 1998; 82:671–686. [PubMed: 9483527]

Blethyn KL, Hughes SW, Cope DW, Crunelli V. Nucleus-specific properties of the slow (<1 Hz) oscillation in thalamic neurones in vitro. Society for Neuroscience Abstracts. 2002; 28:352.4.

Contreras D, Steriade M. Cellular basis of EEG slow rhythms: a study of dynamic corticothalamic relationships. J Neurosci. 1995; 15:604–622. [PubMed: 7823167]

Crunelli V, Cope DW, Hughes SW. Thalamic T-type calcium channels and NREM sleep. Cell Calcium. 2006 In Press.

Crunelli V, Toth TI, Cope DW, Blethyn K, Hughes SW. The 'window' T-type calcium current in brain dynamics of different behavioral states. J Physiol. 2005; 562:121–129. [PubMed: 15498803]

ANTIBACTERIAL ACTIVITY OF ANTIDEPRESSANTS, INHIBITORS OF MONOAMINE'S REUPTAKE, DEPENDS FROM THEIR ANTIDEPRESSIVE EFICACY ON SLEEP DISORDERS

N. ROGAVA 1,2, Z. LOMTATIDZE 2, N. MAGLAKELIDZE 1, KH. BEZHANISHVILI 1, N. NACHKEBIA 1

[1]I. BERITASHVILI CENTER OF EXPERIMENTAL BIOMEDICINE,[2]SOKHUMI STATE UNIVERSITY, TBILISI, GEORGIA

NINO.ROGAVA24@GMAIL.COM

S3.P2

Introduction.

Unlimited uses of antimicrobial agents, frequently applied arbitrarily, contributed to the development of "antibiotic resistance" and new infectious diseases. Therefore searching for non-antibiotic agents with antimicrobial activity, antidepressants among them, is very topical. No less important is the question of whether the antimicrobial activity of antidepressants can be dependent on their effectiveness in restoring sleep disturbances in animal models of depression. Problem is important because antidepressants are supposed to restore disturbances characteristic for major depressive disorder (MDD) - sleep disorders among them, and effective drugs mustn't additionally worsen sleep and general condition of depressive patients.

Methods.

Study was aimed to investigate the antibacterial action of tricyclic, non-selective (Melipramin, Group I) and selective (Fluoxetine, Group II), antidepressants and the possible dependence of antimicrobial activity on their anti-depressive efficacy to sleep disturbances in animal models of depression. Wild white rat pups (n=5 in each group) received a subcuteneous injection of antidepressantas, 30 mg/kg, two times daily, from postnatal day 7 to 28. Control rat pups received saline. Sleep EEG registration have been started 8-12 weeks after the drug discontinuation. Continuous sleep registration in each control rat was made for three consecutive days, 10.00 a.m. – 20.00 p.m. In experimental groups, EEG registration of SWC, with the same duration, was started after intraperitoneal injection of Melipramin and /or Fluoxetine (10 mg/kg and/or 15 mg/kg).

Escherichia coli, Bacillus subtilis, Staphylococcus aureus and Mycobacterium phlei were used as test cultures. Melipramin, (0.01; 0.1 and 1 g/L) and Fluoxetine (0.01; 0.1 and 1 g/L) were used for the studying of antibacterial spectrum.

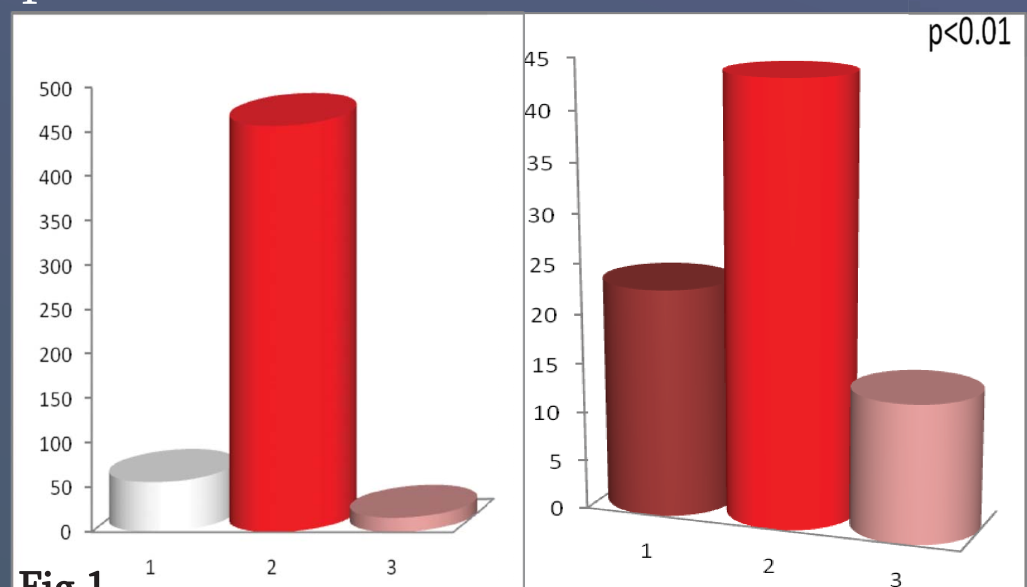

Fig.1.

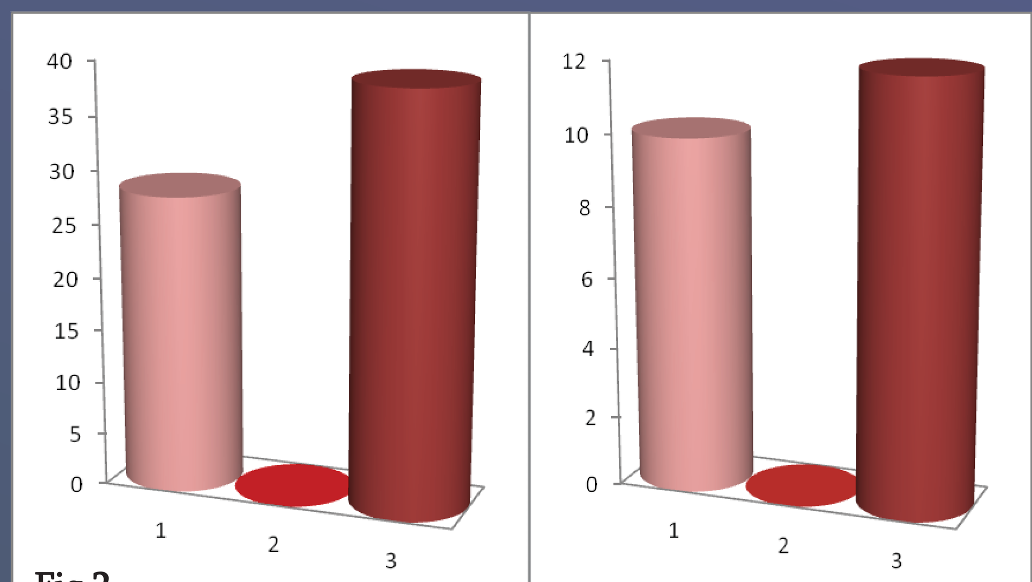

Fig.2.

Fig.1 The effect of melipramine on latent and paradoxical sleep in control animal
Fig. 2 The effect of melipramine on the frequency and total percentage of paradoxical sleep onset in control animal

Microorganisms	Control	Antidepressants					
		Fluoxetine			Molypremine		
		Concentration G / L					
		1	0,1	0,01	1	0,1	0,01
		The size of the suppression zone, mm					
Escherichia coli	0	3,0	0	0	0	0	0
Bacillus subtilis	0	5,5	0	0	0	0	0
Staphylococcus aureus	0	3,0	0	0	0	0	0
Mycobacterium phlei	0	5,0	0	0	0	0	0

Antibacterial spectrum of fluteoxetine and molypremine

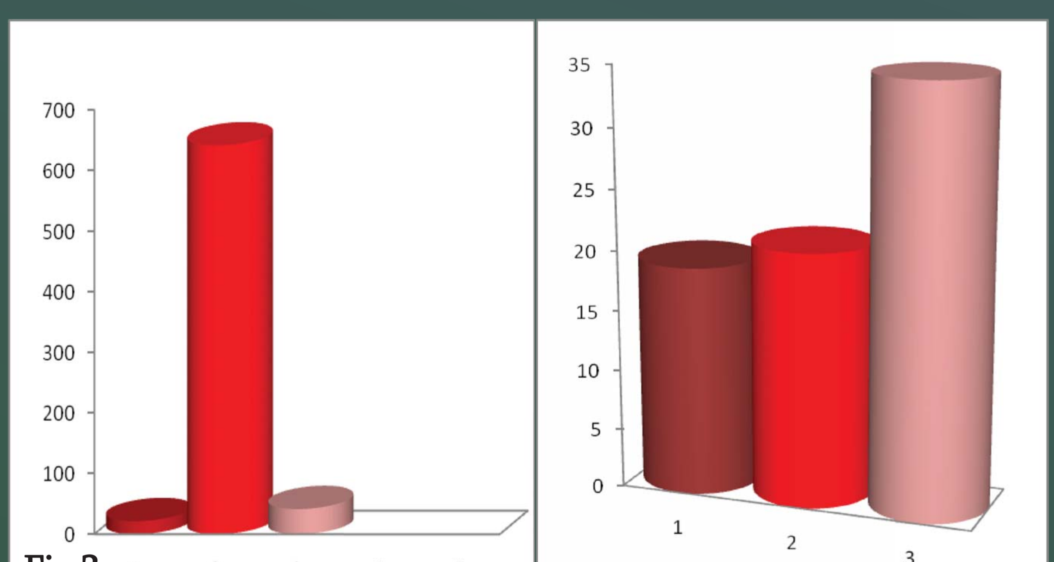

Fig.3.

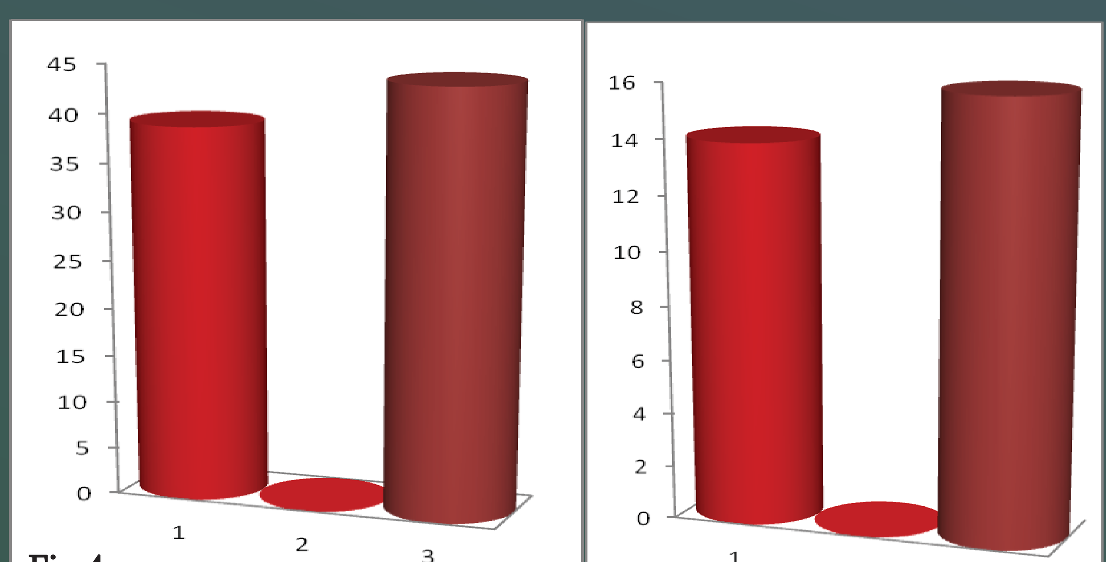

Fig.4.

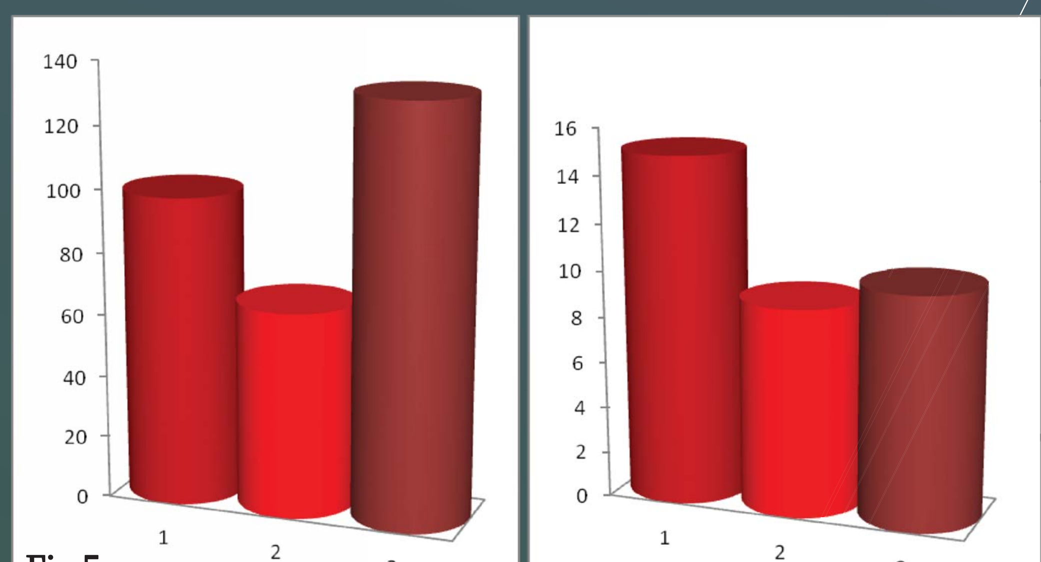

Fig.5.

Fig. 3 The effect of melipramine on latent and paradoxical sleep in animal models of depression
First bar – Background data; Second bar - Effects of dose of 15 mg / kg dose of melipramine; Third bar- Data 24 hours after drug administration
On the ordinate – time in min.
Fig. 4 The effect of melipramine on the frequency and total percentage of paradoxical sleep onset in animal models of depression
Fig. 5 The effect of melipramin on the frequency and total percentage of slow wave sleep, in animal models of depression

Results.

In adult rats, with postnatal exposure to Melipramin and/or Fluoxetine, sleep was disturbed significantly. Single-dose Melipramin produced worsening of sleep quality and whole inhibition of REM sleep during 4-5 h after drug injection. Sleep disorders like depression were developed in the recovery period (24 h after drug injection) – sleep quality becomes deteriorated, sleep interruptions increases, REM sleep latency diminishes, but its incidence rise. The influence of Fluoxetine on SWC was relatively weaker and short-term indicating to higher anti-depressive efficacy of the drug.

Conclusions:

Antimicrobial activity of Melipramin and/or Fluoxetine on growth-development of Escherichia coli, Bacillus subtilis, Staphylococcus aureus and Mycobacterium phlei was dependent on their anti-depressive efficacy on sleep disturbances which has been only revealed by the selective inhibitor of serotonin reuptake, Fluoxetine.

S13P3

S3.P3

BLOOD LUEKOCYTES IN YUONG AND OLD RATS UNDER DESYNCRONOSIS INITIATION ON THE BACKGROUND OF WHOLE BODY CRYOSTIMULATION

V.V. LOMAKO, O.V. SHYLO

Institute for Problems of Cryobiology and Cryomedicine of National Academy of Sciences of Ukraine, Department of Cryophysiology; st. Pereyaslavskaya, 23, Kharkiv, Ukraine, 61016.

Introduction

•It is known that prolonged inconsistency (desynchronization) between endogenous and exogenous circadian rhythms contributes to the development of a number of functional disorders in the body, especially in aging [2]. Recently, the whole body cryostimulation (WBC) have become widespread in medicine and reabilitation [3]. We assumed that WBC can be used to prevent the consequences of desynchronosis development.

•Since each type of leukocyte performs a specific, unique function (protective, trophic, trigger, regulatory, regenerative and others), their quantitative-qualitative ratio largely reflects nearly any change in the mammalian organism [1], the severity of which depends on the level of its reactivity. Integral leukocyte indices (ILIs) are used for a more complete view of the status of the blood system. They are reliable diagnostic and prognostic indicators that make it possible to evaluate the dynamics of the activity of various parts of the immune system and the level of nonspecific resistance of the organism without the involvement of special research methods [4].

•**The aim of the work** was to study the effect of whole body cryostimulation on leukocyte blood parameters in rats of different ages with a model of circadian desynchronosis (CD).

Methods

•***Experiments on animals.*** The work was carried out on young and old (6 and 18 months) male outbred white rats according to biotic requirements.

•CD was initiated by single prolongation the light period by 12 hrs [5].

•One WBC (-120ºC, 90 s) session was applied the day before CD initiation.

•The leukocyte types were quantitatively and qualitatively assessed in blood smears fixed with May-Grunwald and stained with hematological dye according to Romanowsky, by counting 100-200 cells in each sample. The total leukocyte number was determined in Goryaev chamber.

•The integral leukocyte indices (ILIs), allowing to assess the state of certain links of immune system and body resistance without using special methods, were calculated [4] such as: the nuclear shift index ((MCs + MMCs + Bls)/SLs); the leukocyte index (L/N); the leukocyte index of intoxication by Kalf-Kalif ((4MCs + 3MMCs + 2BLs + SLs) × (PCs + 1)/(L + M) × (E + 1)); the leukocyte shift index ((E + B + SLs + BLs)/L + M); the lymphocyte-granulocyte index (10L/(MCs + MMCs + BLs + SLs + E + B)); the index of neutrophils to lymphocytes ratio (BLs + SLs/L); the index of lymphocytes toeosinophils ratio (L/E); the index of neutrophils to monocytes ratio (N/M); the index of lymphocytes to monocytes ratio (L/M); the indices of allergization (L + 1 – (E + 1)/(BLs + SLs + M)) and Garkavi adaptation index (L/SLs). The abbreviations in the above formulae mean the cell types such as: BLs – band and SLs – segmented neutrophils; L – lymphocytes; M – monocytes; N – neutrophils; E – eosinophils; B – basophils; MCs – myelocytes; MMCs – metamyelocytes (immature cells), PCs – plasmatic cells (expressed in percentage).

•***Statistical analysis.*** The obtained results were statistically processed using the non-parametric Kruskal-Wallis statistic method with Statistica 6.0 software (MatStat Inc., USA) , *M ± SE*

Results

•CD increased the band neutrophils number as well as cause leukocytosis and leukopenia in young and old rats correspondingly (Table 1 and 2). Segmented neutrophils decreased in young animals and increased in old animals, but the change in lymphocyte number had the opposite direction. Eosinophils decreased only in young animals. Changes in ILIs indicate an increase in young neutrophils, activation of cells of specific protection and hypersensitivity of the immediate type, strengthening of humoral immunity, intoxication, lack of inflammation and impaired immunoreactivity, and also increase adaptation ability in young animals.

Results

• Changes in ILIs indicate an increase in young neutrophils, activation of cells of specific protection and hypersensitivity of the immediate type, strengthening of humoral immunity, intoxication, lack of inflammation and impaired immunoreactivity, and also increase adaptation ability in young animals. In old rats, immunoreactivity was impaired, inflammation and non-specific defence cells increased. CD initiation on the background of WBC caused to an increase in the total number of leukocytes and monocytes in young animals, and to decrease its in old rats; segmented neutrophils, on the contrary. The lymphocytes and eosinophils decreased only in old rats. Band neutrophils increased, more significantly in young animals. ILIs revealed a predominance of young neutrophils, macrophages and effector immune system activity, decreased immunoreactivity in young rats. The predominance of cellular immunity, increased intoxication, activation of inflammation and impaired immunoreactivity, predominance of nonspecific defence cells, microphages and allergy reduction were noted in old rats.

Table 1

Indices	Control (n=15)	CD (n=5)	WBC+CD (n=5)
Young rats			
Total leukocyte number, 10^9/L	6.5±0,1	**15.2±0.3***	**8.0±1.0***
Band neutrophils, %	1.9±0.4	**7.0±0.4***	**7.8±0.5***
Segmented neutrophils,%	27.1±1.5	**16.9±2.2***	**20.0±2.0***
Lymphocytes, %	65.5±1.3	**73.2±2.2***	65.2±2.5
Eosinophils, %	3.5±0.7	**1.5±0.2***	2.8±0.8
Monocytes, %	1.3±0.2	1.4±0.2	**3.8±0.3***
Nuclear shift index	0,1±0,0	**0,6±0,1***	**0,7±0,1***
Leukocyte index	2,5±0,2	**3,2±0,4***	2,4±0,3
Leukocyte index of intoxication by Kalf-Kalif	0,1±0,0	0,2±0,0	0,1±0,0
Leukocyte shift index	0,5±0,0	**0,3±0,0***	0,5±0,0
Lymphocyte-granulocyte index	20,1±1,3	**30,9±3,6***	22,2±2,6
Index of neutrophils to lymphocytes ratio	0,4±0,0	**0,3±0,0***	0,4±0,0
Index of lymphocytes to eosinophils ratio	17,8±2,9	**58,6±7,7***	30,3±9,6
Index of neutrophils to monocytes ratio	23,6±2,4	19,7±3,3	**7,4±0,6***
Index of lymphocytes to monocytes ratio	54,2±4,9	59,1±6,5	**17,7±1,9***
Index of allergization	3,9±0,4	4,1±0,4	3,4±0,3
Garkavi adaptation index	2,6±0,2	**5,0±0,8***	3,5±0,6
Immuno reactivity index	59,5±5,8	59±6,3	**21,2±3,1***

* - statistically significant data

Data increase

Data decrease

Table 2

Indices	Control (n=8)	CD (n=5)	WBC+CD (n=5)
Old rats			
Total leukocyte number, 10^9/L	7.3±0.3	**5.7±0.1***	**3.7±0.3***
Band neutrophils, %	2.5±0.5	**5.5±0.3***	**5.5±0.3***
Segmented neutrophils, %	32.6±2.0	**40.7±2.3***	**49.0±1.5***
Lymphocytes,%	56.2±4.8	**46.2±1.0***	**39.2±1.1***
Eosinophils,%	6.9±0.7	**1.5±1.2***	**3.0±1.6***
Monocytes,%	2.4±0.4	2.0±0.4	**1.5±0.3***
Nuclear shift index	0,2±0,1	0,2±0,0	0,1±0,0
Leukocyte index	2,4±0,6	**1,0±0,1***	**0,7±0,0***
Leukocyte index of intoxication by Kalf-Kalif	0,1±0,0	0,2±0,1	**0,7±0,3***
Leukocyte shift index	0,8±0,15	**1,1±0,0***	**1,5±0,1***
Lymphocyte-granulocyte index	16,4±3,7	**8,9±0,3***	**6,6±0,3***
Index of neutrophils to lymphocytes ratio	0,7±0,1	**1,0±0,1***	**1,4±0,1***
Index of lymphocytes to eosinophils ratio	9,2±1,2	12,2±4,2	13,2±8,5
Index of neutrophils to monocytes ratio	20,6±5,7	26,2±5,3	**40,2±8,3***
Index of lymphocytes to monocytes ratio	28,5±5,5	27,3±7,4	29,4±5,9
Index of allergization	4,4±1,0	**2,4±0,5***	**1,4±0,3***
Garkavi adaptation index	2,4±0,7	**1,2±0,2***	**0,8±0,0***
Immuno-reactivity index	31,9±5,6	31,1±9,2	31,6±6,8

Conclusion

CD in young rats causes more significant changes in leukocyte indices, but the protective effect of preventive WBC compared to older animals is more pronounced, because after the initiation of CD on the background of WBC the total number of leukocytes, percentage of lymphocytes, eosinophils and segmented neutrophils (trend) correspond to control levels. The reduction index allergization were noted only in old rats.

References

- 1.Abdulkadyrov KM, editor. [Hematology, the newest guidance]. Moscow: EKSMO; 2004: 928 p. Russian.
- 2.Gubin DG. [Molecular basis of circadian rhythms and principles of circadian disruption] Usp Fiziol Nauk. 2013; 44(4): 65–87. Russian
- 3.Lombardi G, Ziemann E, Banfi G. Whole-Body Cryotherapy in Athletes: From Therapy to Stimulation. An Updated Review of the Literature. Front. Physiol. Front Physiol. 2017 May 2; 8: 258.
- 4. Speranskii II, Samoilenko GE, Lobacheva MV. Possibilities of general blood analysis. Integral intoxication indices as assessment criteria of the severity of endogenous intoxication, its complications, and the treatmentefficiency, Zdorov'e Ukr. 2009; 19(6): 51–7.
- 5.Sudo A, Miki K. Circadian rhythm of catecholamine excretion in rats after phase shift of light-dark cycle. Indust Health. 1995; 33 (2): 57–66.

Contact Information

Victoria V. Lomako: victoria0regia@gmail.com

S3.P4

PITUITARY-THYROID SYSTEM IN YOUNG AND OLD RATS UNDER PREVENTIVE WHOLE-BODY CRYOSTIMULATION AND CIRCADIAN DISRUPTION

O.SHYLO[1], V. LOMAKO[1], D.LUTSENKO[1], L.SAMOKHINA[2]

[1]Institute for Problems of Cryobiology and Cryomedicine, NAS of Ukraine, department of Cryophysiology, Kharkiv, Ukraine;
oleksandr.v.shylo@gmail.com;

[2]GD "National Institute of Therapy of L.T. Malaya name of National Academy of Medical Sciences of Ukraine",
Laboratory of Immuno-biochemical and Molecular Genetic Studies, Kharkiv, Ukraine

Introduction and objectives

Perturbation of fluctuation of the endocrine system that occurs due to chronic circadian disruption, resulted from shift-work, jet lag or irregular sleep-wake cycle, is recognized as the main mechanism of increasing the risk of cardiovascular, autoimmune and metabolic disorders as well as a number of psychological disorders [1]. Thyroid hormones (TH) are necessary for normal differentiation and growth of the body, metabolism and thermoregulation, etc. Their synthesis and secretions from thyroid follicular cells are controlled by the thyroid-stimulating hormone (TSH), which level depends on the TH concentration in the blood. The main circadian pacemaker of the body located in the suprachiasmatic nuclei (SCN) of the anterior hypothalamus affects the TSH level as well, which is manifested in its daily fluctuations in the blood [2]. Moreover, TSH amount is modulated by the sleep-wake cycle, the quality of which is altered to some extent under the whole-body cryostimulation [3].

We **aimed** to study the preventive effect of whole-body cryostimulation (WBC) on activity of the pituitary-thyroid system in rats with the model of circadian disruption (CD).

Methods

In young and old (6- and 18 months) males of white outbred rats, CD was modelled by a 12 hrs single prolongation of the light period [5]. One WBC session was performed in a cryochamber [4] (at a temperature of -120 °C, 90 sec) the day before the initiation of CD. The content of total (T4) and free thyroxine (T4f), total (T3) and free triiodothyronine (T3f) as well as TSH in blood serum (BS) was determined by enzyme-linked immunosorbent assay. The data were statistically processed by the Kruskal-Wallis method.

Cryochamber

CD initiation (+12 h)

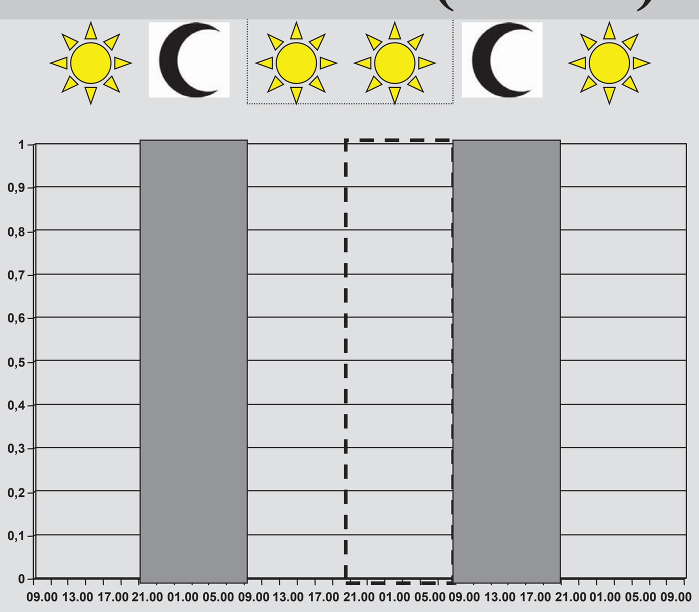

WBC (-120 °C, 90 sec)

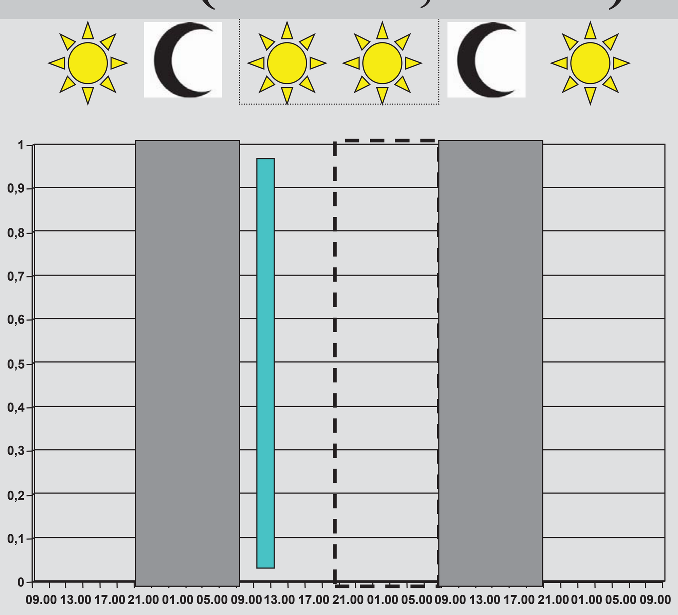

Blood sampling

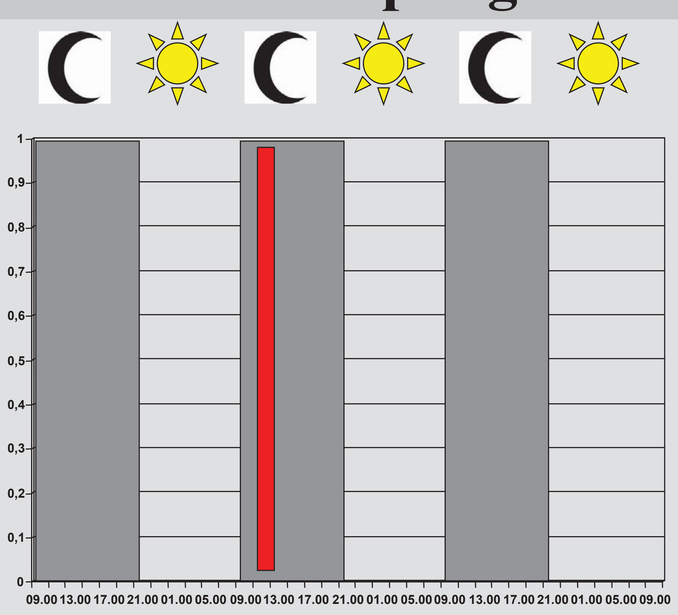

Results and Conclusions

Initiation of CD led to a decrease in TSH in BS in both young (5.35±0.66 vs 1.47±0.07 nM/L) and old rats (3.38±1.42 vs 0.81±0.01 nM/L, $p < 0.05$) (Table 1 and 2). The preventive WBC application before CD initiation helped to maintain the level of TSH in the BS at the level of control values (4.64±1.8 and 1.91±0.11 nM/L, in young and old animals, respectively). No significant differences in the levels of total or free T3 and T4 in BS after CD and preventive WBC application were found (with exception for a decrease in fT3 in old rats with WBC).

Table 1	Young (6 months) rats				
	TSH	T3	fT3	T4	fT4
Control	5,35±0,66	1,34±0,08	6,82±0,36	25,3±7,07	12,17±1,79
DC	1,47±0,07*	1,39±0,05	6,2±0,1	26,5±3,5	13,35±1,35
WBC	3,34±0,22*	1,48±0,17	6,0±0,35	28,92±5,49	15,47±2,03
WBC+DC	4,64±1,8	1,32±0,06	6,0±0,15	16,0±0,76	9,8±0,41

Table 2	Old (18 months) rats				
	TSH	T3	fT3	T4	fT4
Control	3,38±1,42	1,4±0,07	5,96±0,1	25,0±5,98	10,3±0,64
DC	0,81±0,01*	1,43±0,06	5,8±0,1	22,0±1,5	9,65±0,24
WBC	2,06±0,44	1,41±0,14	6,28±0,5	15,62±0,5*	7,43±0,6*
WBC+DC	1,91±0,11	1,29±0,09	5,4±0,06*	15,8±6,2	9,65±1,05

Thus, the preventive WBC application stabilizes the response of the pituitary-thyroid system of young and old rats to the CD initiation.

References / Bibliography

1. Kryger M., Roth T., Dement W. Principles and practice of sleep medicine. – Philadelphia.: Elsevier, Saunders, 2011. – P. 1766.
2. Ottenweller J. E., Hedge G. A. Diurnal Variations of Plasma Thyrotropin, Thyroxine, and Triiodothyronine in Female Rats Are Phase Shifted after Inversion of the Photoperiod // Endocrinology, 1982. - Vol. 111. - No. 2. - P. 509-514
3. Douzi W., O Dupuy., Tanneau M., Boucard G., Bouzigon R., Dugué B. 3-min whole body cryotherapy/cryostimulation after training in the evening improves sleep quality in physically active men // Eur J Sport Sci. – 2019. – Vol. 19. – No. 6. – P. 860-867
4. Babiychuk G.O., Kozlov O.V., Lomakin I.I. et al. Cryochamber for experimental cooling of laboratory animals. Patent of Ukraine N 40168. 2009 March 25.
5. Sudo A., Miki K. Circadian rhythm of catecholamine excretion in rats after phase shift of light-dark cycle // Indust. Health. – 1995. – Vol. 33, No. 2 – P. 57–66.

XXVIII Congress of the Polish Physiological Society

Gdańsk, September 15-17 2021

Poster book

SESSION IV

FATIGUE. ADAPTATION TO ENVIRONMENT. THERMOREGULATION

HONORARY PATRONAGE

Uniwersytet Gdański

Prof. dr Marcin Gruchała
Rector of the Medical University of Gdansk

Prof. dr Piotr Stepnowski
Rector of the University of Gdansk

WOJEWODA POMORSKI
DARIUSZ DRELICH

Dariusz Drelich
Governor of the Pomeranian Voivodeship

HONORARY PATRONAGE
Mayor of the City of Gdańsk

Aleksandra Dulkiewicz
Mayor of Gdansk

Mieczysław Struk
Marshal of the Pomeranian Voivodeship

PARTNER

PAN POLSKA AKADEMIA NAUK

ANIMA LAB
animal facility and laboratory equipment • animal research models

FUNDACJA LOTOS

Medical University of Gdansk
Department of Physiology

DO ELITE ATHLETES HAVE DIFFERENT LEVELS OF PHYSIOLOGICAL STRAIN (PSI) IN RESPONSE TO A SIMILAR SUBMAXIMAL EXERCISE PERFORMED UNDER TEMPERATE CONDITIONS AFTER MEDIUM-TERM ACCLIMATION TO WHOLE BODY HYPERTHERMIA (MWBH) AND WHOLE BODY CRYOSTIMULATION (MWBC)?

[1]POKORA, I., [2]WOLOWSKI, Ł., [2]WYDERKA, P.

[1]The Jerzy Kukuczka Academy of Physical Education in Katowice, Institute of Sport Sciences, Department of Physiological-Medical Sciences, Katowice, Poland.

[2]The Jerzy Kukuczka Academy of Physical Education in Katowice, Doctoral Studies, Katowice, Poland.

Background

A characteristic feature of adaptation is an increase in the ability to tolerate stress or a margin of safety during stress loading [Taylor, 2006]. Strategies that use adaptation to heat stress or cold are often used in sport to reduce thermal stress, improve endurance, and protect against overload. The Physiological Strain Index (PSI) [Moran et al., 1998] has been proposed as a method for assessing the combined effect of cardiovascular and thermal stress and was used to assess the physiological stress in various experimental models [Moran et al., 1998; Pokora and Żebrowska, 2016; Pokora et al., 2021].

This study aimed to examine the differences in the physiological strain (PSI) in response to exercise performed under temperate conditions after medium-term sauna-based heat acclimation (MWBH) and after a series of whole-body cryostimulation (MWBC) in athletes.

Research methods and organization

1. Ten elite cross-country skiers participated in four exercise trials, (2) before and after a series of ten sauna baths (MWBH) or (2) before and after a series of ten whole-body cryostimulations (MWBC).
2. Thermal and physiological variables were measured before and after the exercise tests.

Table 1. Participants' baseline characteristics

Characteristic	Mean ± SD
Age (yr)	21.2 ± 2.99
Height (cm)	178.8 ± 4.12
Body mass (kg)	70.6 ± 6.0
V O$_2$peak,kg (mL kg^{-1} min^{-1})	64.5 ± 6.33

SD standard deviation, V O$_2$peak,kg maximum oxygen uptake relative to body mass

Experimental Design

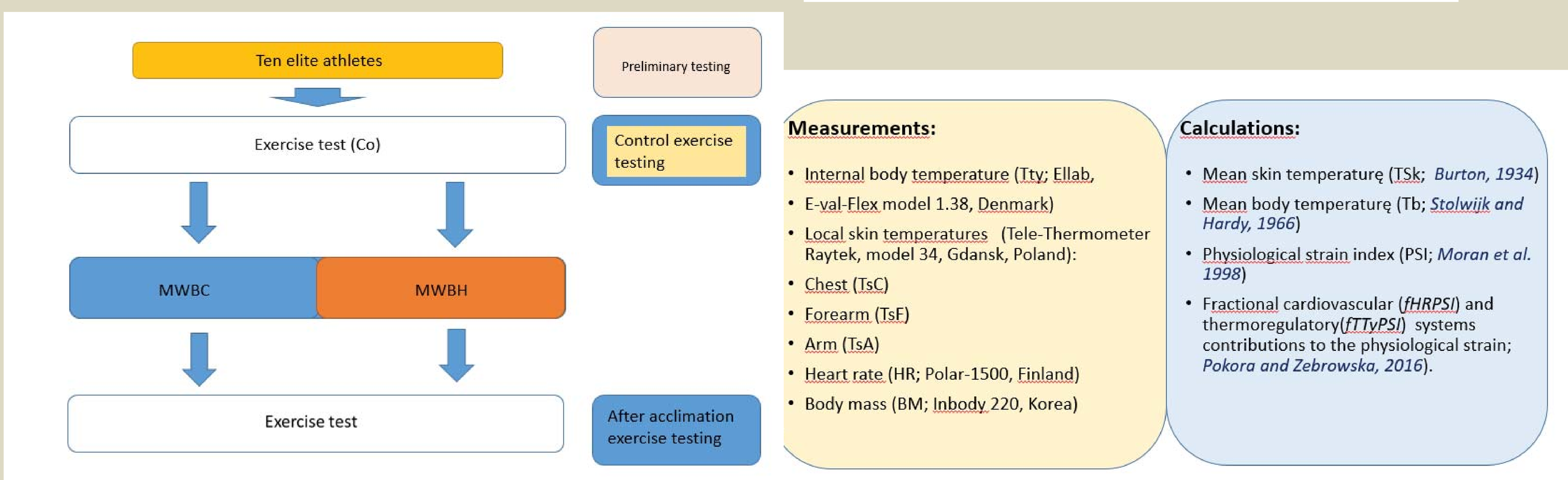

3. Statistical analysis was performed using Statistica 13, PL software.

Results

The series of ten sauna baths induced a moderate decrease in the heart rate (HR) at rest, but did not influence the baseline internal (Tty; p=0.31), body ($\bar{\bar{T}}$b; p=0.53) and skin ($\bar{\bar{T}}$sk; p=0.38) temperatures. The series of MWBC did not induce an either change in the heart rate (HR) at rest or the baseline internal (Tty; p=0.31) and body ($\bar{\bar{T}}$b; p=0.38) temperatures but influenced on the local and mean skin temperature ($\bar{\bar{T}}$sk; p=0.008) [fig. 1, 2]. In response to exercise, physiological strain index (PSI) tended to be lower (p=0.31) after MWBH but not after MWBC (p=0.88) [fig. 3]. There was a significant difference in fHR PSI (p=0.02) and fTty PSI (p=0.02) in response to exercise between MWBH and MWBC groups. The MWBC and MWBH did not induce changes in the relationship between metabolic rate and PSI [fig.4] although there was a noticeable change in the slope of this relationship after MWBC.

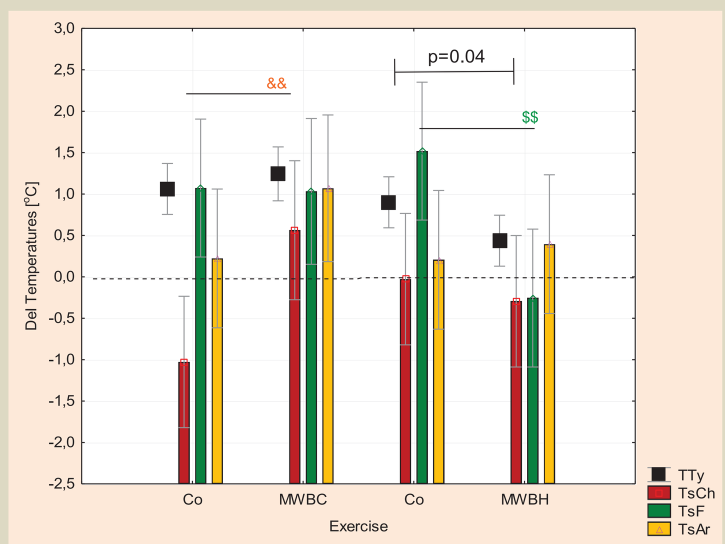

Fig. 1 Differences (Δ) in internal temperature (TTy), local skin temperatures (Ts) in response to the exercise test before (Co) and after MWBC and MWBH procedures.

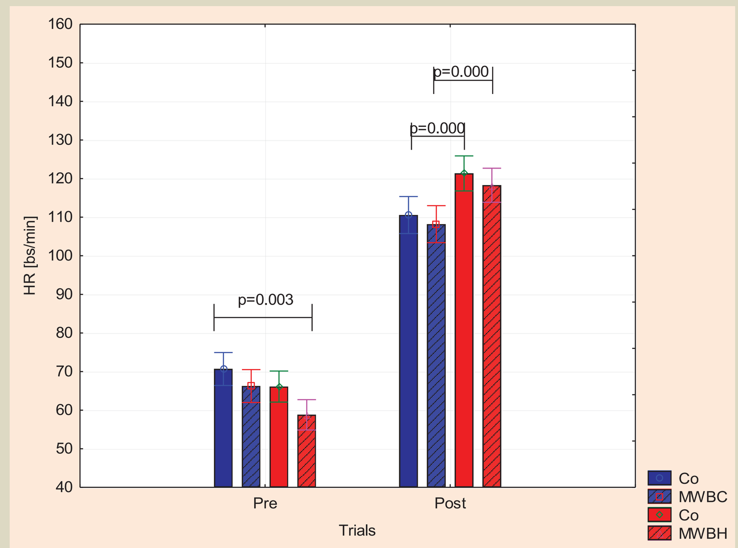

Fig. 2 Average of heart rate (HR) at rest (Pre) and at the end (Post) of the exercise test before (Co) and after MWBC and MWBH procedures.

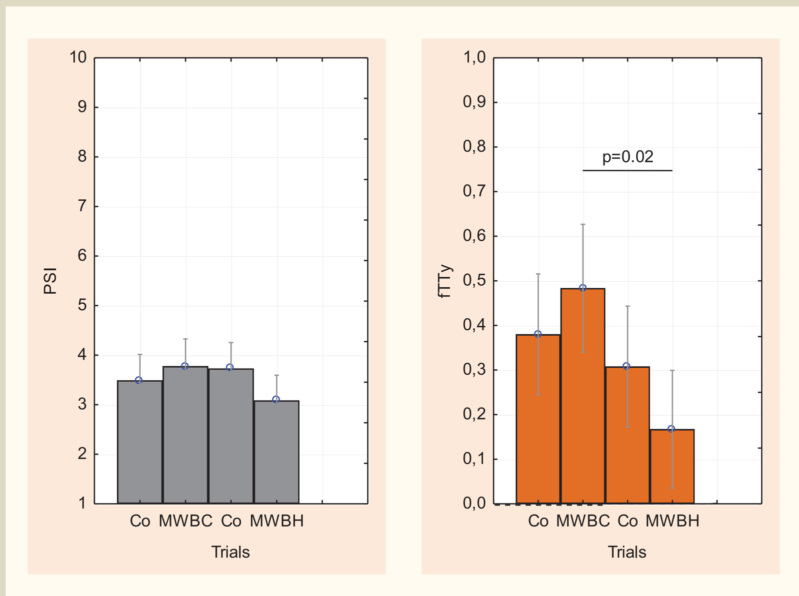

Fig. 3 The physiological strain (PSI) and thermal fraction of physiological strain (fTTyPSI) in response to the exercise test before (Co) and after MWBC and MWBH procedures.

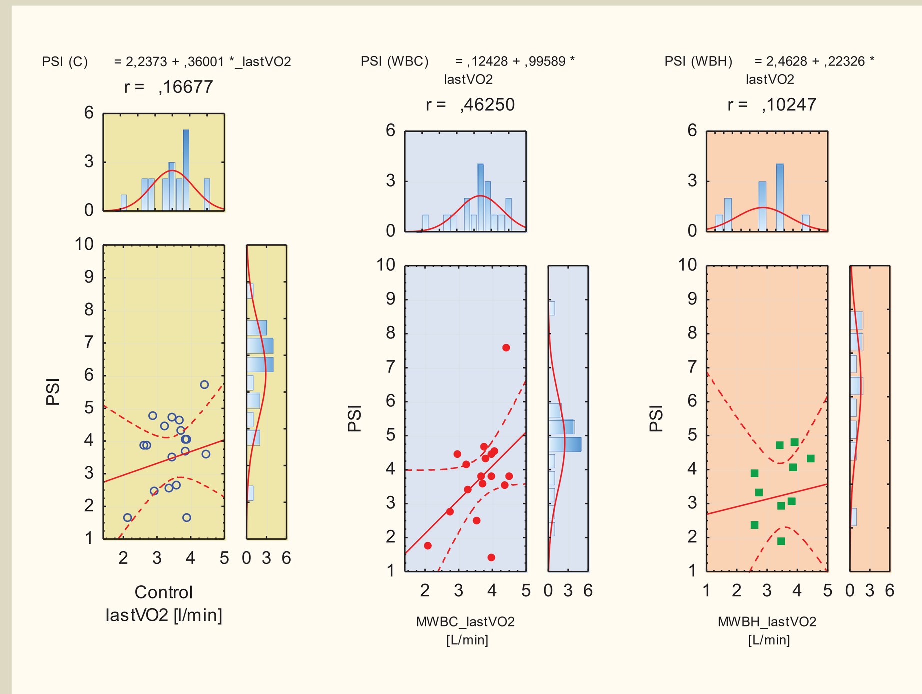

Fig. 4 Relationship between metabolic rate (VO2) during exercise and PSI before (Control) and after MWBC and MWBH programs.

Conclusions

1. The results of this study indicated that level of physiological strain index was similar during exercise test performed after MWBH and MWBC acclimations.
2. There were differences in the share of contribution of the cardiovascular fraction and the thermoregulatory fraction to the PSI (circulatory strain, thermoregulatory strain) during exercise trials performed in this study after heat and cold adaptations, respectively.

References

Stolwijk, J.A.J.; Hardy, J.D. *Pflügers Arch.* 1966, 291, 129–162.

Burton, A. J. Nutr. 1934, 7, 497–533.

Pokora, I.; Zebrowska, A. J. *Hum. Kinet.* 2016, 50, 103–114.

Moran, D.S.; Montain, S.J.; Pandolf, K.B. *Am. J. Physiol. Integr. Comp. Physiol.* 1998, 275, 854–860.

Taylor, Nigel A.S. *Journal of Thermal Biology* 31 (1-2 SPEC. ISS.): 2006, 90–104.

Pokora, I., Sadowska-Krępa, E., Wolowski, Ł., Wyderka, P., Michnik, A., Drzazga, Z. *International Journal of Environmental Research and Public Health.* 2021, 18, 1-21.

THE INFLUENCE OF REGULAR PROFESSIONAL TRAINING ON THE RESTING TEMPERATURE DISTRIBUTION OF THE BODY SKIN

M. Binek[1);2)], I. Pokora[1)] , Z. Drzazga[2)]

1) The Jerzy Kukuczka Academy of Physical Education in Katowice, Institute of Sport Sciences, Department of Physiological-Medical Sciences, Poland

2) The Silesian Centre for Education and Interdisciplinary Research, University of Silesia in Katowice, A. Chełkowski Institute of Physics, Department of Medical Physics, Poland

Introduction:

Infrared imaging is a non-invasive method of studying body temperature that is widely used in sports medicine.

Aim:

The aim of our preliminary research was to evaluate the effect of continuous, professional training on the distribution of skin temperature at rest.

Material and Method:

1. Infrared imaging is a non-invasive method of studying body temperature that is widely used in sports medicine The study gruop consisted of 20 healthy man divided into two subgroups. Groups A consisted of 10 professional cross-country skiers, while group B consisted of 10 people who did not train professionally.
2. For each of them series of 4 thermo images were performed in suitable, thermoneutral conditions, without any stressors, using thermal imaging camera FLIR E95. [1]
3. Thermal images were analysed using ThermaCAMResaecherPro 2.10, statistical analysis was performed in Statistica 13.

Professional athletes   Casual Man

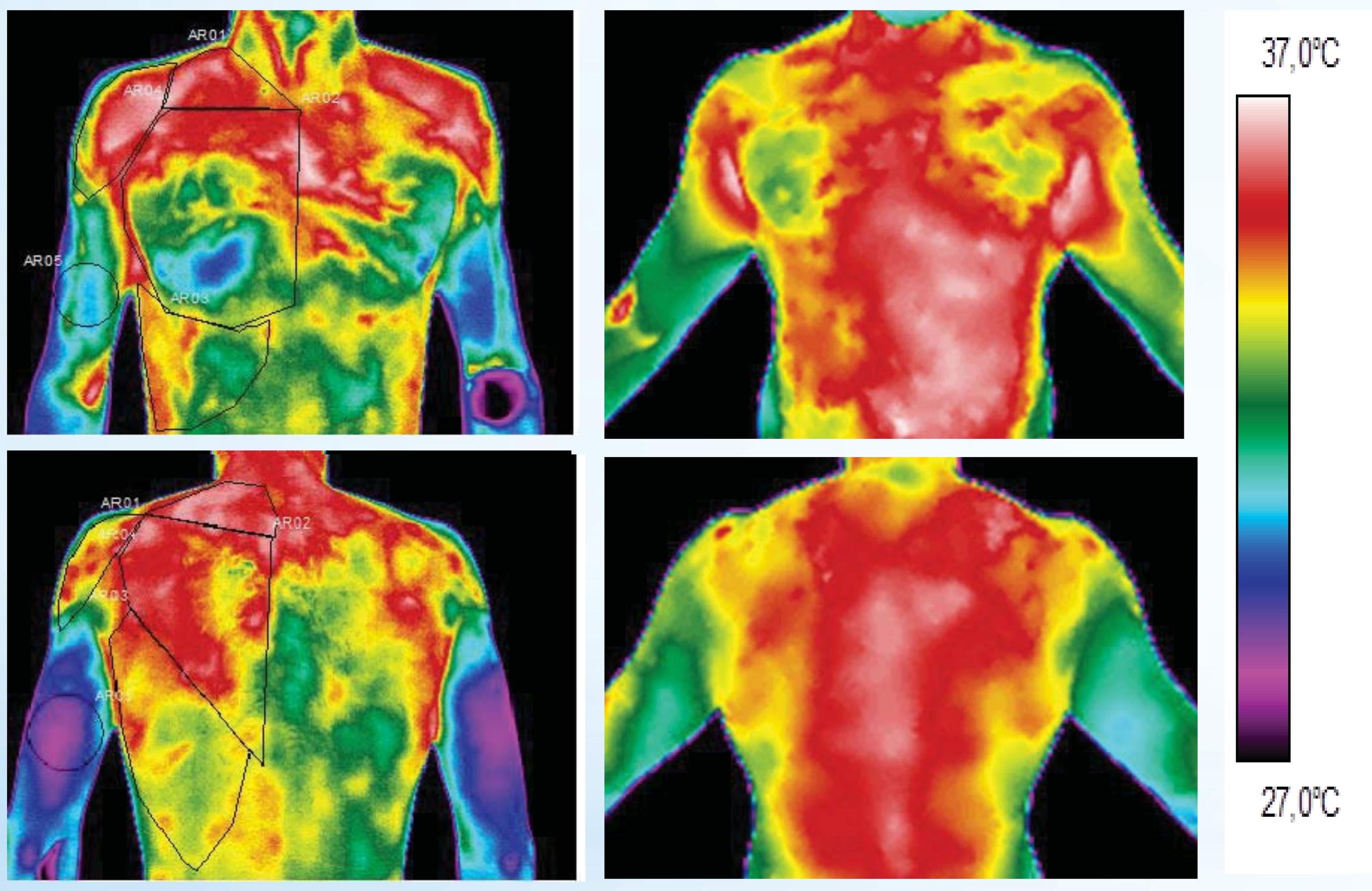

Fig. 1. Examples of thermal images of the upper body of an exemplary member of each group; on the left there are examples of muscle zones selected for analysis.

Table 1. Mean temperatures over selected muscle zones for selected groups, respectively. Red font color mark statistically significant changes.

Muscle zone	Professional Cross-Country Skiers		Control Group - no professional training		P Eta
	Temperature[°C]	St. Dev.	Temperature [°C]	St. Dev.	
Trapezius muscle	34.38	0.64	34.91	0.47	P=0.05 Eta=0.19
Deltoid	33.72	0.61	34.63	0.62	P=0.00 Eta=0.37
Pectoralis Major	33.59	0.49	34.66	0.73	P=0.00 Eta=0.45
Serratus anterior	33.80	0.72	34.72	0.72	P=0.01 Eta=0.31
Abdomen	33.49	0.67	34.37	0.89	P=0.02 Eta=0.25
Biceps	33.56	0.71	33.94	0.67	P=0.24 Eta=0.07
Trapezius (neck)	34.01	0.69	35.57	0.63	P=0.00 Eta=0.61
Trapezious (back)	33.95	0.35	34.76	1.05	P=0.03 Eta=0.23
Deltoid (rear)	33.15	0.49	34.07	0.63	P=0.00 Eta=0.42
Latissimus Dorsi	33.42	0.55	34.22	0.82	P=0.02 Eta=0.27
Triceps	31.57	0.83	32.26	0.51	P=0.03 Eta=0.21
Vastus lateralis	31.62	0.70	32.5	0.86	P= 0.02 Eta= 0.25
Rectus femoris	32.16	0.60	32.75	0.82	P= 0.08 Eta=0.15
Vastus medialis	32.32	0.72	32.54	1.07	P=0.59 Eta=0.01
Knee (at front)	29.77	0.81	31.17	1.09	P=0.00 eta=0.37
Tibialis anterior	31.6	0.75	32.17	0.86	P=0.13 Eta=0.13
Soleus	31.6	0.69	32.22	0.85	P=0.09 Eta=0.15
Biceps Femoris	32.03	0.75	32.28	1.2	P=0.57 Eta=0.02
Rest of thigh muscle	32.36	0.67	32.71	1.05	P=0.39 Eta= 0.04
Knee (rear)	32.95	0.48	33.09	0.82	P=0.64 Eta= 0.01
Gastrocnemius caput laterale	32.1	0.51	31.92	0.93	P=0.59 Eta= 0.01
Gastrocnemius caput mediale	32.03	0.70	32.23	0.97	P=0.59 Eta= 0.02

Results:

Generally, lower temperatures for each muscle zones were obtained for group of professional cross-country skiers. Values of mean temperatures measured over muscles were listed in table. Statistic analysis shows that in upper part of body differences between skiers and control group were significant. In lower extremities differences are smaller however still visible.

The confirmation of such differences in the skin temperature distribution is also visible in the exemplary thermal images obtained for representatives of each group. On left side(skiers) of Fig 1 one can see much more cold points than on right side(control group).

Conclusions:

Practicing professional sport has an impact on the distribution of skin body temperature. In our research group, the skin temperature of the upper parts of the body was significantly lower than in the control group, the trend is also maintained in the lower parts of the body, but to a lesser extent.

References:

1. Binek M., et al. „Do exist gender differences in skin temperature of lower limbs following exercise test in male and female cross-country skiers?", Journal of thermal Analysis and Calorimetry (in print), DOI:10.1007/s10973-021-11055-z

GEOGRAPHICAL ORIGIN REFLECTED IN PHYSIOLOGY – DIFFERENCES IN THERMAL BEHAVIOUR OF THREE HONEYBEE *APIS MELLIFERA* SUBSPECIES

UNIWERSYTET MIKOŁAJA KOPERNIKA W TORUNIU
Wydział Nauk Biologicznych i Weterynaryjnych

Joanna Bacia [1] and Przemysław Grodzicki [1]

[1]Nicolaus Copernicus University, Faculty of Biological and Veterinary Sciences, Department of Animal Physiology and Neurobiology, Toruń, Poland; grodzick@umk.pl

INTRODUCTION

Originally, honeybees (*Apis mellifera* L). inhabited in Europe, Africa, Arabia and Western Asia. They did not occur in both Americas occupied by stingless bees then. Due to wide-spreading and the need to cope with various environmental conditions, *A. mellifera* species became different in morphology and behaviour, e.g. nest defence, foraging and wintering.

Based on morphometric, zoological and geographical conditions Ruttner (1992) enumerated 25 various honeybee populations that could be qualified to subspecies or geographical races divided into four main groups: The dark bees of North and West Europe and North Africa, including *A. mellifera mellifera*; Balkan and related bees (incl. *A.m. carnica*), oriental bees (incl. *A.m. caucasia*) and African bees (See Table I).

We suspect geographic origin influences the honeybees physiology.

OBJECTIVES

- To compare the thermoregulatory behaviour of honeybee Queens with their retinues, who represent three subspecies reared in Poland, differentiated regarding their geographical origin.
- To check out:
  - Do the thermal preferences depend on affiliation to given honeybee subspecies?
  - Do the thermal preferences for those three honeybee subspecies the same, characteristic of the whole *Apis mellifera* L. species?

Table I. Honeybee subspecies reared in Poland and their affiliation to geographical groups

Species	Honeybee (*Apis mellifera* L.)			
Geographic group of honeybees	**Balcan** and related Honeybees	**Oriental** Honeybees	**Black** Honeybees from Nothern and Western Europe and Nothern Africa	**African** Honeybees
Honeybee subspecies reared in Poland	Carniolan Honeybee	Caucasian Honeybee	Eastern European Honeybee	They do not exist in Poland

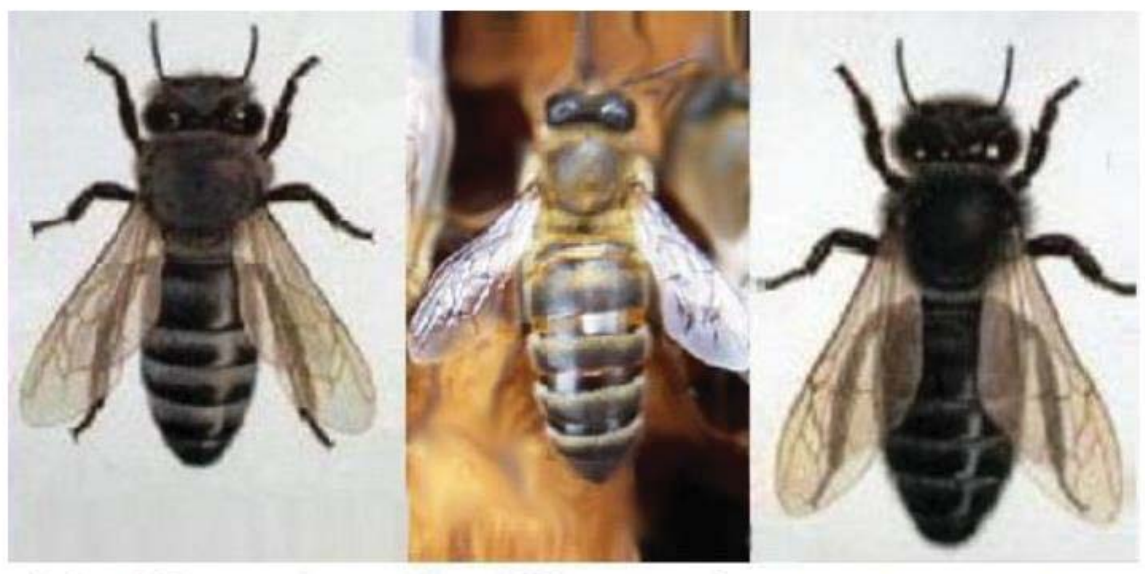

Apis mellifera carnica *Apis mellifera caucasica* *Apis mellifera mellifera*

METHODS

Thermal preferences of Caucasian, Carniolan and Central European Honeybees were studied using the thermal gradient (Figure 2). Eighteen virgin honeybee Queens (six repetitions for each subspecies experimental group) with their retinues, counting 5-12 workers (3-14 day-aged), originated from that year's breeding (2019) in breeding apiaries.

The location of the bees in the temperature gradient (Figure 1) was recorded with the use of a video camera connected to a computer, which enabled immediate recording of movies in AVI format on its disk. At the same time with thermocouples, temperature distribution in gradient chambers was recorded using the Grad_K.exe program. After analyzing the videos, the position of each bee relative to the temperature was recorded in a specially created Excel worksheet.

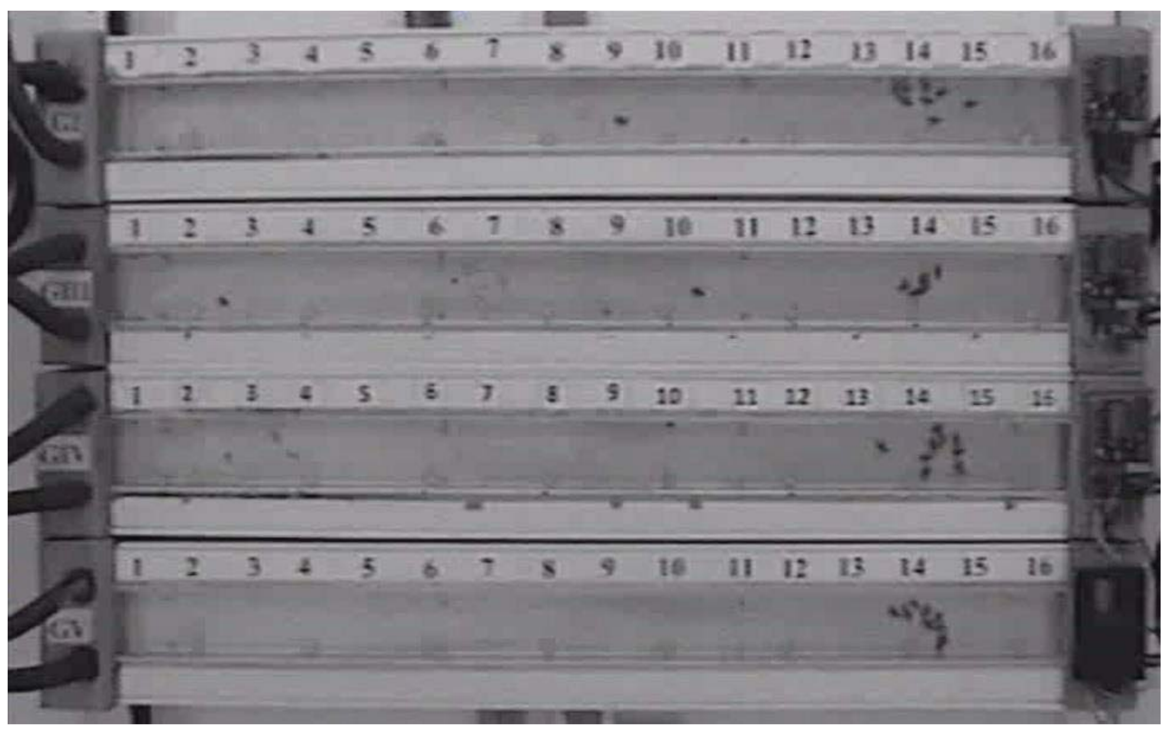

Figure 1. Surveyed honeybee Queens with retinues (accopmanying worker bees) in thermal gradient chambers (freeze frame from video recording).

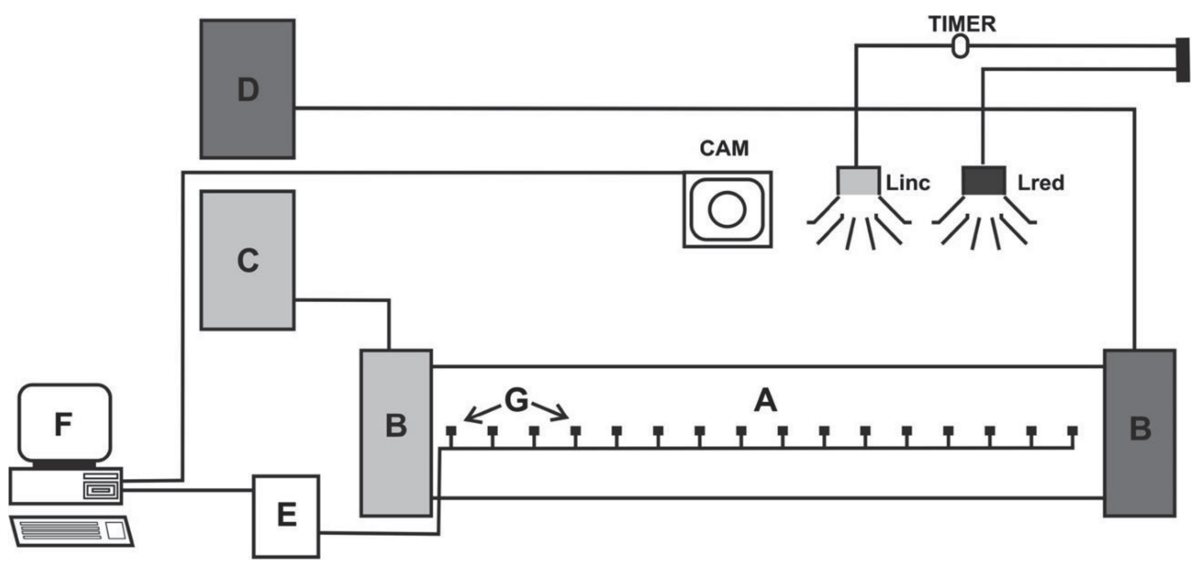

Figure 2. Experimental set-up for recording of thermoregulatory behaviour. A—thermal gradient chamber; B—fluid chambers; C—cryostat; D—thermostat; E—recording-keeper; F—computer; G—thermocouples; L_{inc}—white light; L_{red}—red light and CAM—video camera. (Grodzicki and Caputa, 2012)

The obtained data were statistically analyzed and graphs (Figures 3, 4, and 5) were prepared on their basis. We determined the daily average temperature selected and temperatures selected during the day (16 hours of the highest activity) and at night (8 hours of the lowest activity level of bees).

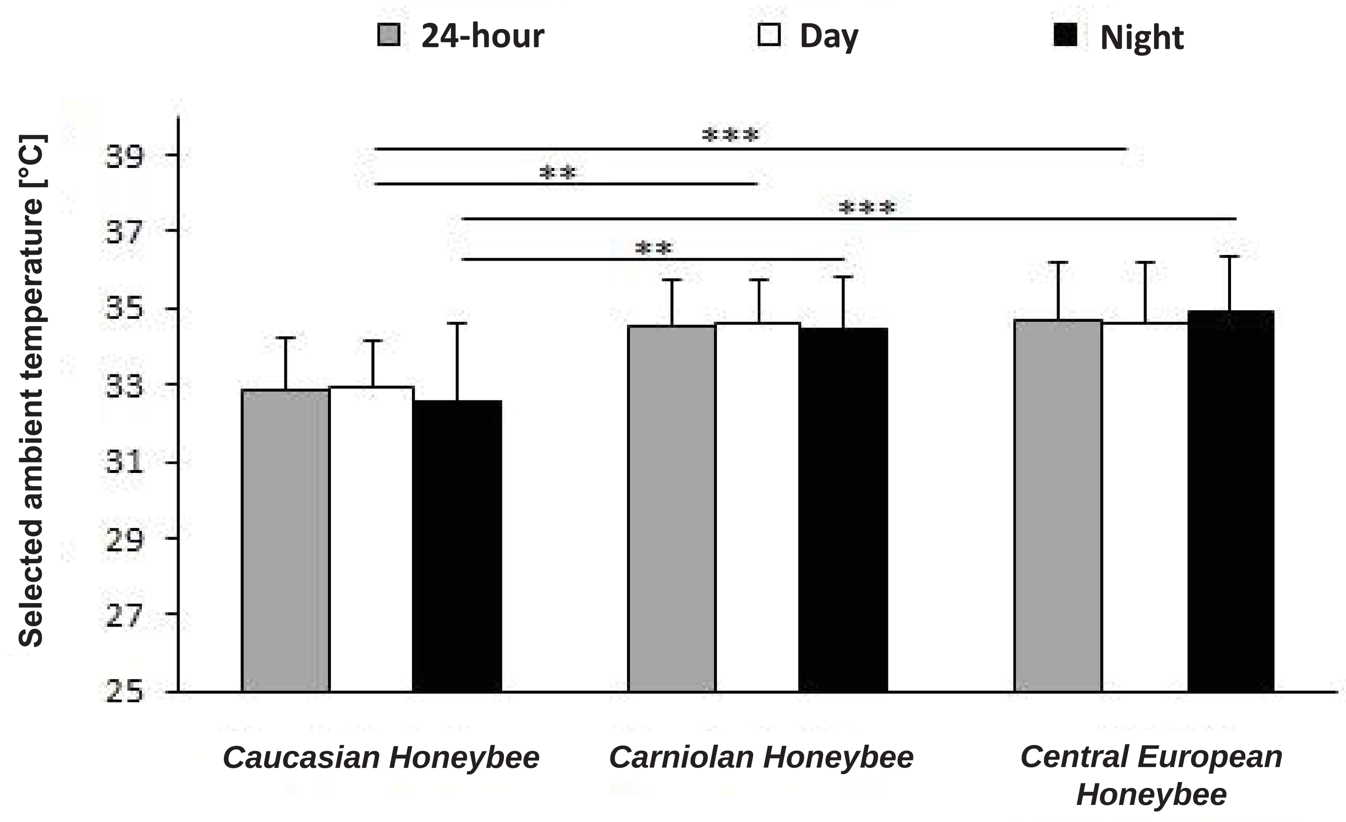

Figure 3. 24-hour, day and night average ambient temperatures selected by the studied honeybee subspecies

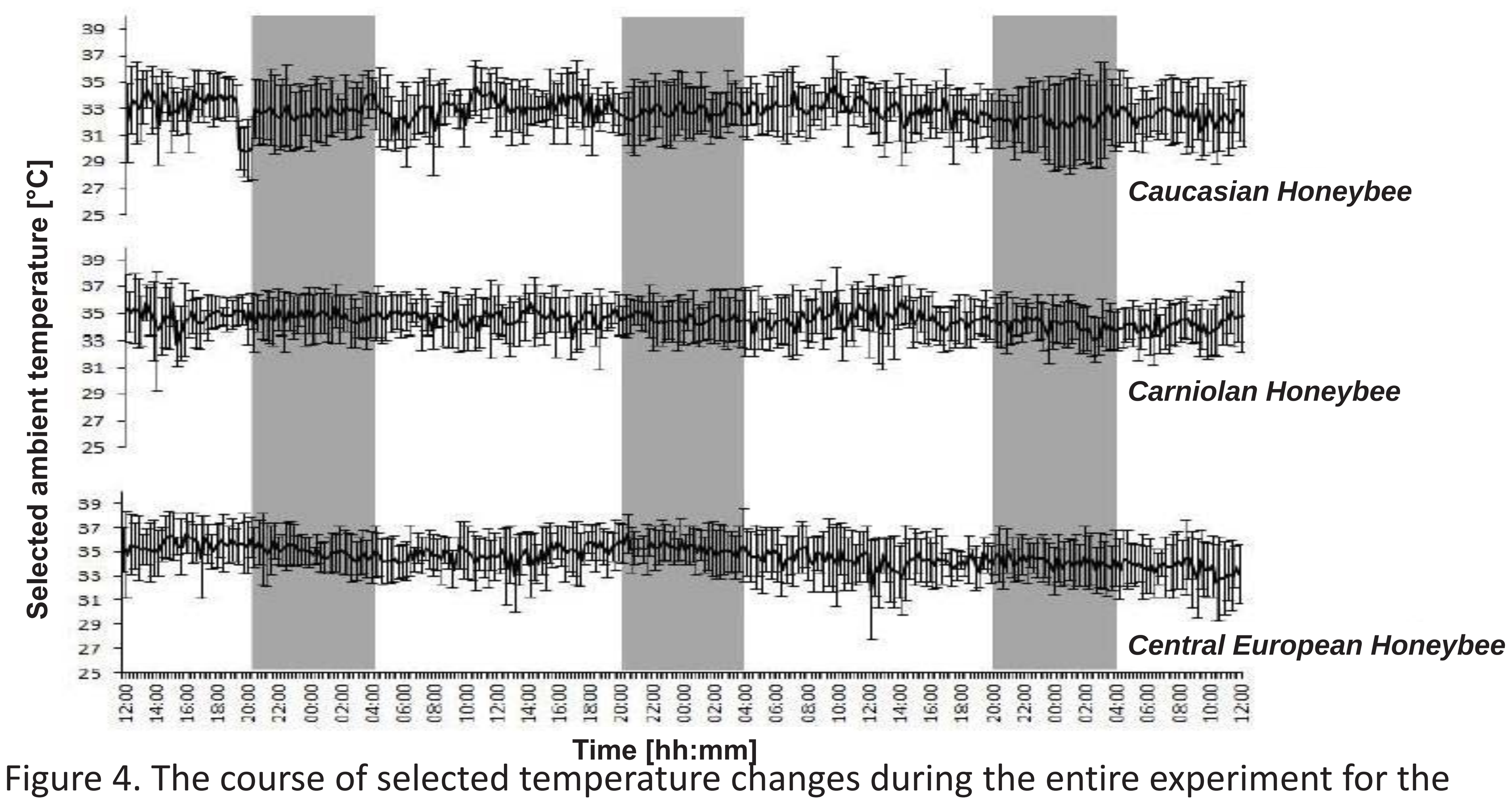

Figure 4. The course of selected temperature changes during the entire experiment for the studied honeybee subspecies

RESULTS

- The 24-hour average selected ambient temperature (Figure 3) is slightly, statistically not significantly lower in the Caucasian bee, compared to the Carniolan bee and the Central European bee.
- The Caucasian bee prefers significantly lower ambient temperatures both during the period of daily activity and night rest than the Carniolan and Central European bees (Figures 3 and 5).
- During the entire registration period (Figure 4), Caucasian bees experienced more pronounced oscillations of the selected ambient temperature than in the remaining breeds studied, most likely due to differences in body size and size of colonies.

CONCLUSION

- Differences in thermal behaviour between Caucasian and other bee subspecies might indicate the influence of the geographical origin of the honey bee subspecies (Apis mellifera L.) on the thermoregulation of these insects.

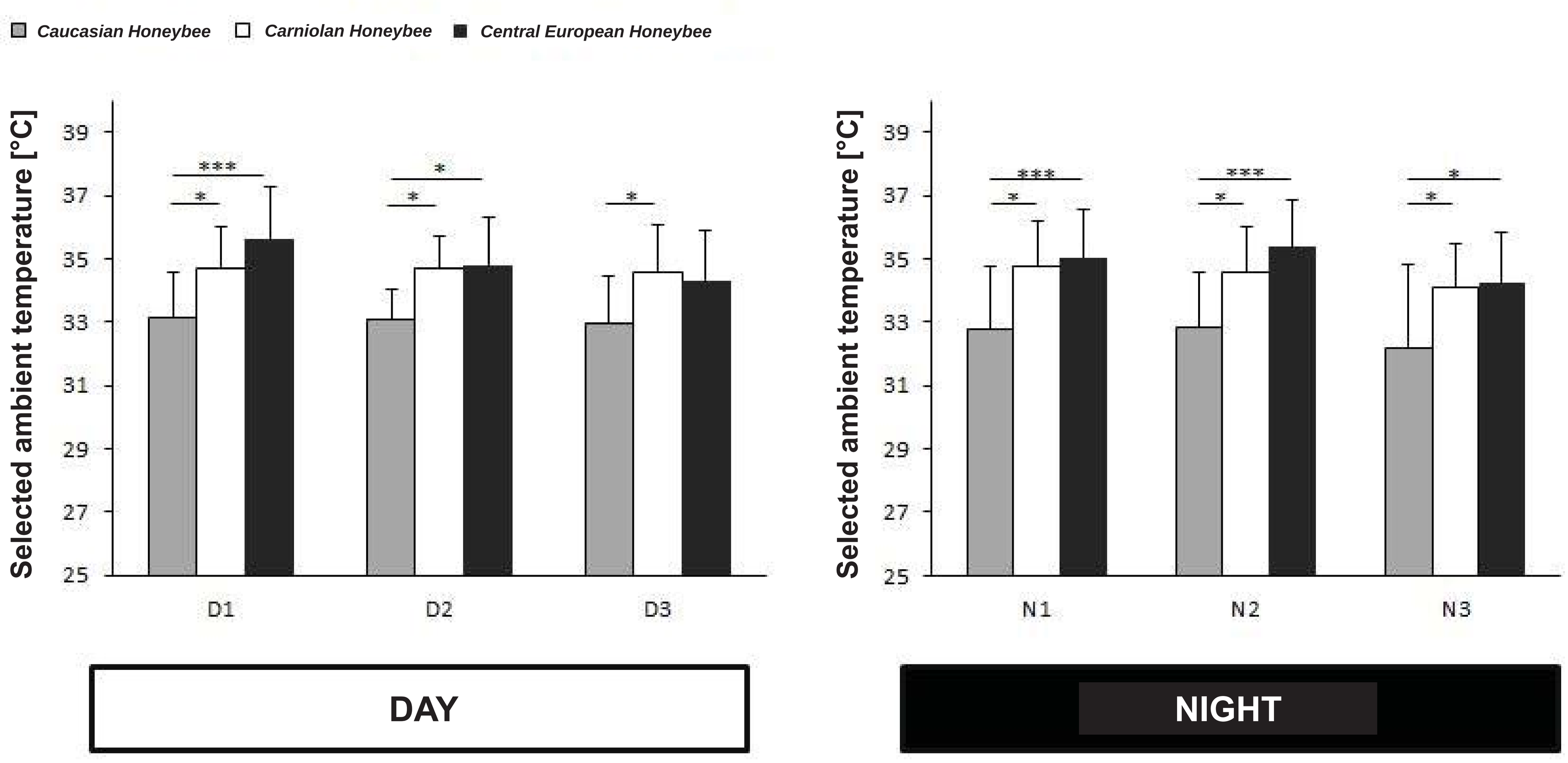

Figure 5. Average ambient temperatures selected by the studied subspecies during the consecutive days (D1, D2, D3) and nights (N1, N2, N3) of the experiment

Grodzicki, P., Caputa, M., 2012. Photoperiod influences endogenous rhythm of ambient temperature selection by the honeybee Apis mellifera. J. Therm. Biol. 37, 587–594. https://doi.org/10.1016/j.jtherbio.2012.07.005
Ruttner, F., 1992. Naturgschichte der Honigbienen. Ehrenwirth Verlag, München.

A NEW VIEW ON OVERWINTERING IN SNAILS: THE ROLE OF MICROBIOTA IN FREEZE TOLERANCE

UNIWERSYTET MIKOŁAJA KOPERNIKA W TORUNIU

PAULINA IDCZAK[1], ANNA NOWAKOWSKA[1], AGNIESZKA KALWASIŃSKA[2]

[1]Department of Animal Physiology and Neurobiology, [2]Department of Environmental Microbiology and Biotechnology, Nicolaus Copernicus University in Toruń, Poland; pidczak@doktorant.umk.pl

SESSION IV: FATIGUE. ADAPTATION TO ENVIRONMENT. THERMOREGULATION

INTRODUCTION

Snails of temperate zone are seasonally subjected to extreme climatic situations: temperature below freezing point of their body fluids. Therefore, they are equipped with many mechanisms to respond and adapt to extreme temperature. Before entering into winter torpor snails lose water and produce cryoprotectant substances that prevent ice crystals forming inside their cells. Moreover, they stop eating and emptying their gut. But it is interesting that snails which had a poor bacterial community did not enter hibernation despite being exposed to winter conditions.

AIM OF THE RESEARCH

Gut bacteria in snails are involved in multiple physiological processes, assisting their hosts with digestion, disease resistance, and environmental resistance [2-3] Thus, the main aim of this work was to examine changes in the gut microbiome during the year. We expected significant turnover in the microbial community composition between individuals before and after winter torpor which enable survival at low temperature (below freezing point of body fluids).

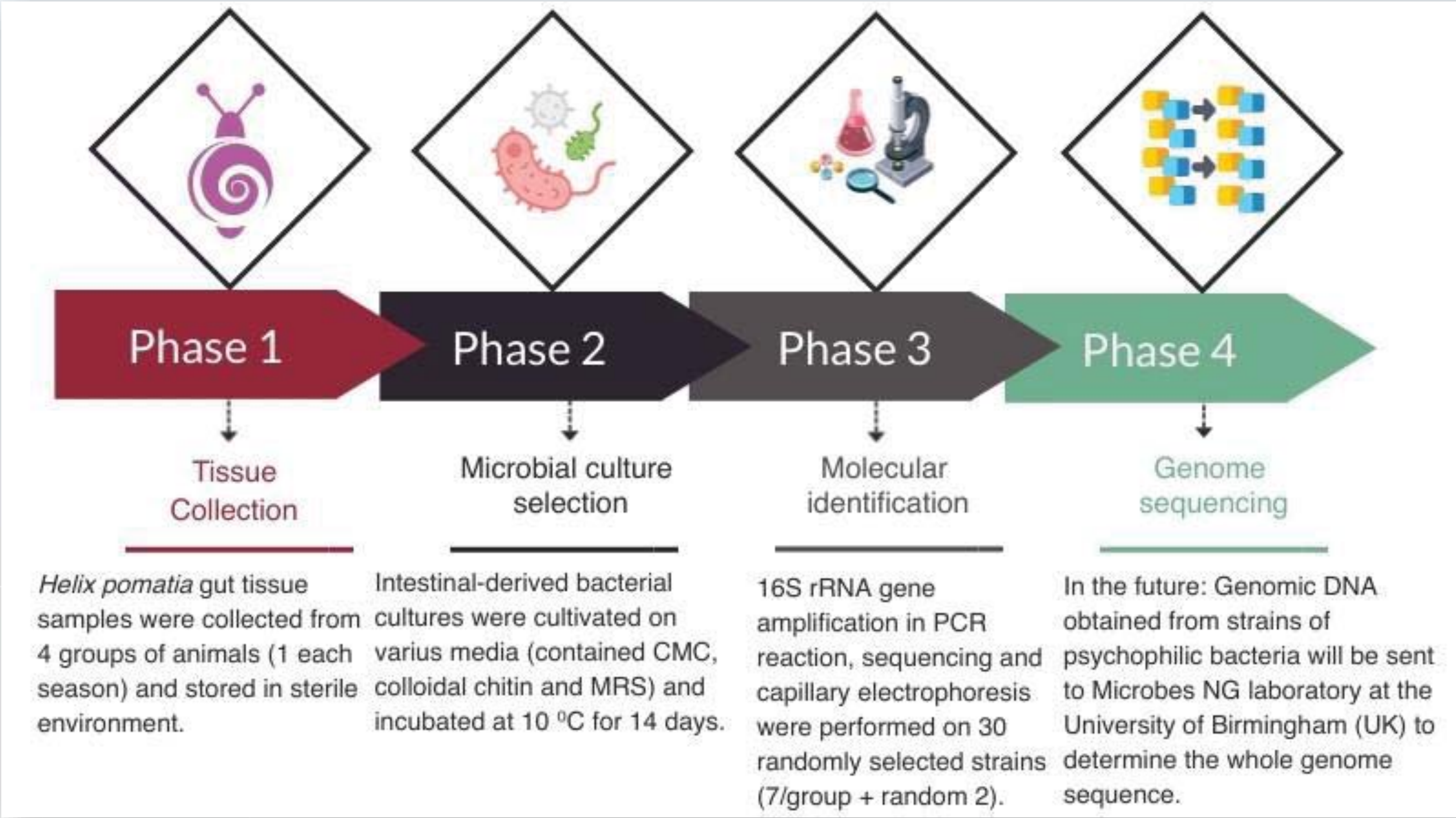

Fig. 1 Workflow chart

PHYLUM	
Actinobacteria	3%
Bacteroidetes	27%
Firmicutes	13%
Proteobacteria	57%

CLASS	
Actinomycetia	3%
Alphaproteobacteria	3%
Bacilli	13%
Flavobacteriia	17%
Gammaproteobacteria	57%
Sphingobacteriia	10%

ORDER	
Bacillales	13%
Enterobacterales	57%
Lysobacterales	3%
Microbacteriales	3%
Moraxellales	3%
Pseudomonadales	7%
Rhizobiales	3%
Sphingobacteriales	10%

FAMILY	
Bacillaceae	13%
Enterobacteriaceae	33%
Erwiniaceae	7%
Flavobacteriaceae	13%
Lysobacteraceae	3%
Microbacteriaceae	3%
Moraxellaceae	3%
Pseudomonadaceae	7%
Rhizobiaceae	3%
Sphingobacteriaceae	10%
Weeksellaceae	3%

Table 1.Bacterial isolates diversity at various taxonomy levels

GROUP 1	
Alphaproteobacteria	12,5%
Flavobacteriia	50%
Gammaproteobacteria	12,5%
Sphingobacteriia	25%

GROUP 2	
Actinomycetia	14,3 %
Gammaproteobacteria	71,4%
Sphingobacteriia	14,3%

GROUP 3	
Flavobacteriia	14,3 %
Gammaproteobacteria	85,7%

GROUP 4	
Bacilli	50%
Gammaproteobacteria	50%

Table 2. Diversity of bacterial strains at the class level in each group of snails

MATERIALS & METHODS

The snails *Helix pomatia* were collected from their natural habitat over the period of their annual activity at two-month intervals starting from fall, prior to winter torpor. There were 4 groups: 1 - fall before hibernation, 2 - early and 3 - late stage during the hibernation and 4 - spring, after their arousal. Gut samples obtained from the intestinal tract were homogenized and used for culturing on selective media containing colloidal chitine, carboxymethylcellulose and on MRS medium at 10°C for 14 days, followed by 16S rRNA gene sequencing.

RESULTS & CONCLUSIONS

- We identified cultivable psychrophilic snail gut bacteria belonging mostly to *Gammaproteobacteria* in all groups.
- Group 1 was the most diverse, groups 2-4 were less diverse. which means that their gut culturable microbiota was most diverse before the hibernation, and that during the winter torpor their microbial diversity continued to decline.
- Overall, results have shown high individual variation in bacterial composition of *H. pomatia* snails right before and after the winter torpor. All of the samples/strains are still in use for further investigation.
- In addition, in each group we have found at least 1 unidentified strain, which may be as yet undescribed species, which we intend to investigate as soon as possible.

This work was supported by grant number 90-SIDUB.6102.38.2021.G4NCUS1 from Inicjatywa Doskonałości Uczelnia Badawcza – Grants4NCUstudents.

We want to express our gratitude to dr hab. Maria Swiontek-Brzezinska prof. UMK for technical assistance of the project.

REFERENCES

1. *Lind H*, 1988. Videnskabelige Meddelelser Dansk Naturhistorisk Forening; 2. *Ansart A*, et al., 2010. Cryoletters, 31: 329–340; 3. *Cardoso AM*, et al., 2012. PLOS One, 7(11): e48505;

XXVIII Congress of the Polish Physiological Society

Gdańsk, September 15-17 2021

Poster book

SESSION V

BODY FLUID HOMEOSTASIS. RENAL FUNCTION

HONORARY PATRONAGE

Prof. dr Marcin Gruchała
Rector of the Medical University of Gdansk

Prof. dr Piotr Stepnowski
Rector of the University of Gdansk

WOJEWODA POMORSKI
DARIUSZ DRELICH

Dariusz Drelich
Governor of the Pomeranian Voivodeship

HONORARY PATRONAGE
Mayor of the City of Gdańsk

Aleksandra Dulkiewicz
Mayor of Gdansk

Mieczysław Struk
Marshal of the Pomeranian Voivodeship

PARTNER

Medical University of Gdansk
Department of Physiology

URINARY EXCRETION OF EXTRACELLULAR VESICLES IN PATIENTS IN THE EARLY PERIOD AFTER KIDNEY TRANSPLANTATION

K. SAŁAGA-ZALESKA[1], A. KUCHTA[1], B. BZOMA[2], A. PŁOSKA[3], L. KALINOWSKI[3], A. DĘBSKA-ŚLIZIEŃ[2], M. JANKOWSKI[1]

[1] Department of Clinical Chemistry
[2] Department of Nephrology, Transplantology and Internal Diseases
[3] Department of Medical Laboratory Diagnostics - Biobank Fahrenheit BBMRI.pl
Medical University of Gdansk, Poland

www.mug.edu.pl

Introduction and objectives:

Extracellular vesicles (EV) have a size about 30-300 nm and can be found in various body fluids, including urine. Increased excretion of extracellular vesicles may have a diagnostic value in the initial early stages of renal dysfunction. The aim of the study was to investigate the urinary excretion of extracellular vesicles (uEV) in patients in the early period after kidney transplantation.

Method:

The preliminary study involved adult Patients from the Department of Nephrology, Transplantology and Internal Diseases at the University Clinical Centre in Gdansk, Poland in the early period after kidney transplantation (n=3; 9, 19 and 28 days) and healthy volunteers (n=3). Urinary extracellular vesicles were isolated by ultracentrifugation-based method from the same volume of each first morning urine sample.

The expressions of the specific marker CD63, nephrin and podocin were verificated by Western blot. The total number of extracellular vesicles per miligram of creatinine was determined by Nanoparticle Tracking Analysis (NTA).

The study was approved by the Medical Ethics Committee of Medical University of Gdansk and the director of University Clinical Center in Gdansk. All values are expressed as mean ± SEM. Statistical significance between the two group was determined by unpaired t test.

Results:

Human urinary extracellular vesicles were identified by showing the expression of the exosomal marker CD63 in all samples (Figure 1).

In early period after kidney transplantation the urinary excretion of extracellular vesicles was 1.5-fold higher compared to healthy volunteers ($2.6*10^{10} \pm 4.4*10^{9}$ vs. $3.9*10^{10} \pm 5.0*10^{9}$ particles/mg creatinine, $p = 0.1218$), however this difference was not statistically significant (Figure 2).

The presence of nephrin and podocin were confirmed on isolated extracellular vesicles (Figure 3).

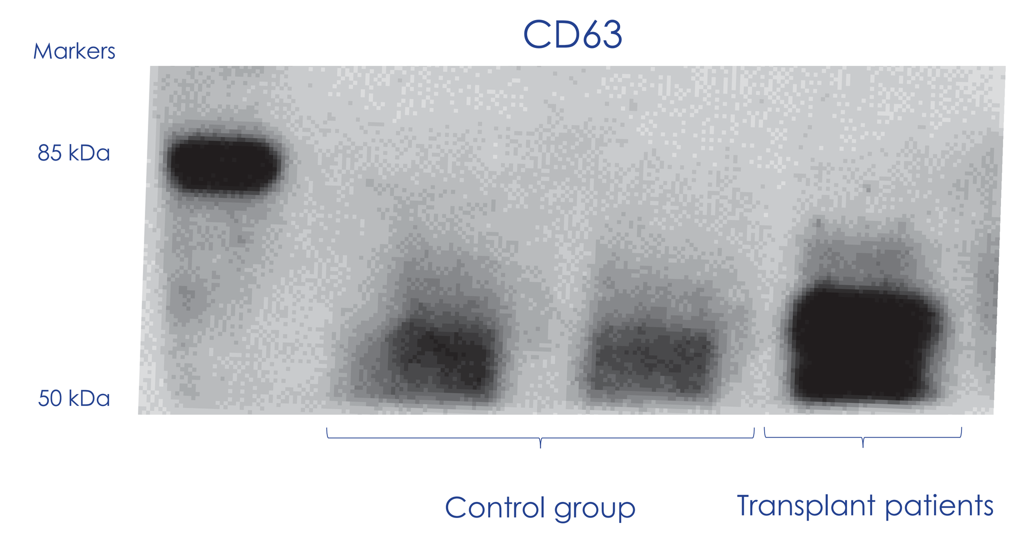

Fig. 1. Expression of the specific marker CD 63 in uEVs detected by western blot analysis.

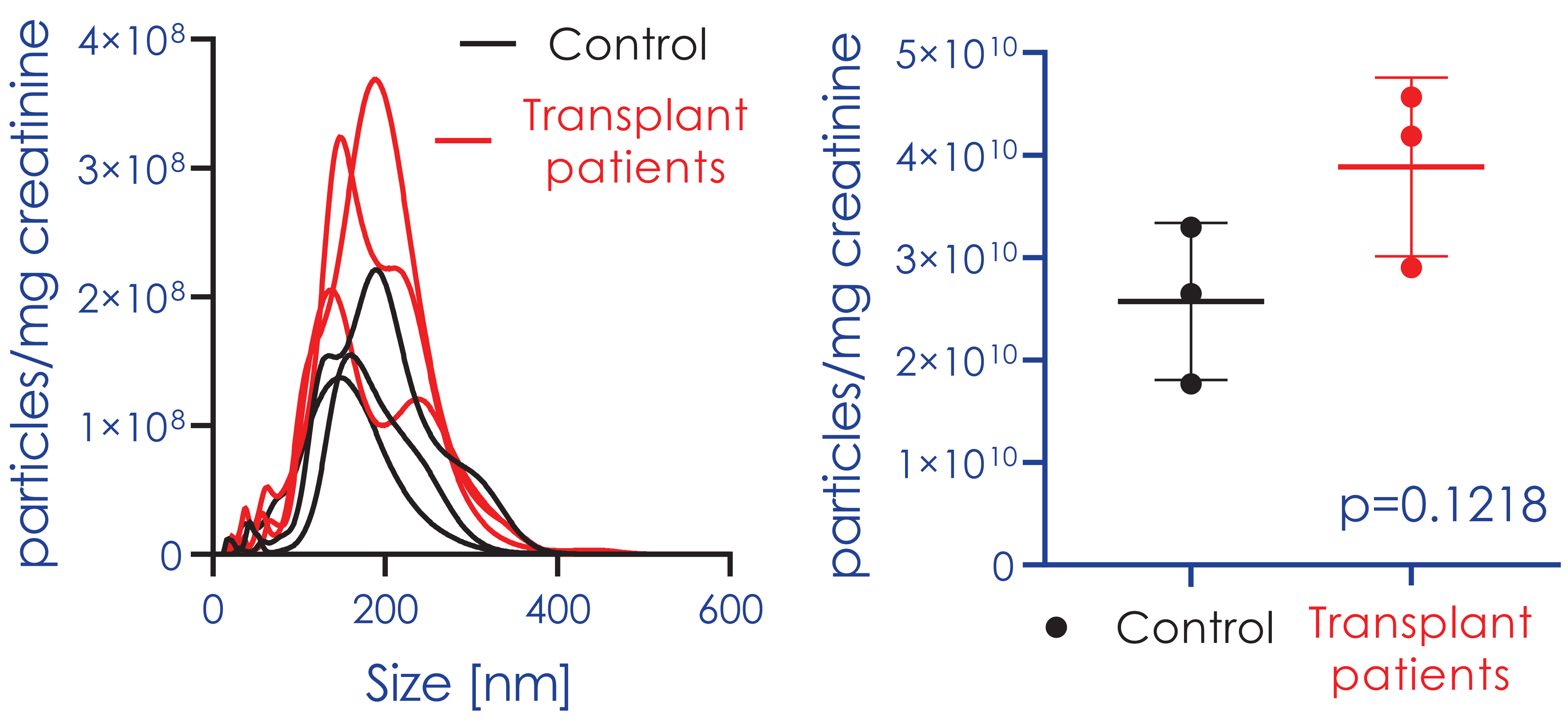

Fig. 2. NTA analysis of urinary extracellular vesicles: determination of the creatinine-standardized number of uEVs, dilution factor 1:100, laser 405 nm.

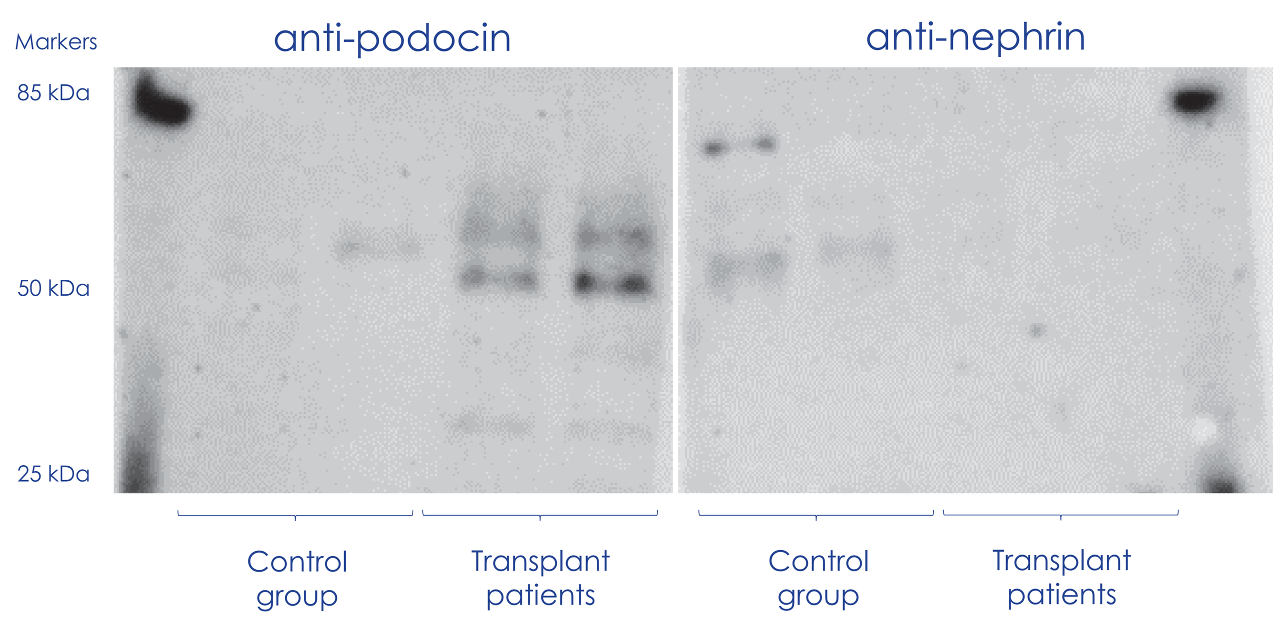

Fig. 2. Expression of the podocin and nephrin in uEVs detected by western blot analysis.

Conclusion:

The research is preliminary and prompted us to further analyze of urinary excretion of extracellular vesicles proteins in a larger group of patients, looking for early markers of renal graft function.

References / Bibliography:

Erdbrügger, Uta, et al. Urinary extracellular vesicles: A position paper by the Urine Task Force of the International Society for Extracellular Vesicles. Journal of Extracellular Vesicles, 2021, 10.7: e12093.

The study was supported by the project POWR.03.02.00-00-I014/17-00 co-financed by the European Union through the European Social Fund under the Operational Programme Knowledge Education Development 2014–2020.

Aging affects urinary bladder reactivity in female Wistar rats: an in vivo preparation

Vinicius Correia1, Cristiane Magaldi2, Monise Moreno2, Fernanda Magaldi2, Bárbara do Vale1, Laura Maifrino2, Monica Sato1, Eduardo Cafarchio1

1Dept. Morphology and Physiology, Centro Universitario FMABC, Santo Andre, SP, Brazil; 2Universidade Sao Judas Tadeu, Sao Paulo, SP, Brazil.

Sessions V: Body Fluid Homeostasis. Renal Function.

INTRODUCTION

Urinary bladder diseases affect mostly women worldwide and the number of patients with bladder disorders increases with aging.

OBJECTIVES

This study aimed to investigate the urinary bladder reactivity to the neurotransmitters of the autonomic nervous system in elderly female rats.

MATERIALS AND METHODS

- Female nulliparous Wistar rats with 8, 15 and 18 months-old were anesthetized with 2% isoflurane in 100% O_2 (300- 320 g).
- The rats were submitted to the catheterization of the femoral artery and vein for pulsatile arterial pressure (PAP), mean arterial pressure (MAP), heart rate (HR) in a data acquisition system (PowerLab 16 SP, ADInstruments), and infusion of drugs, respectively.
- The urinary bladder was canullated for intravesical pressure (IP) recording.
- After a baseline recording of MAP, HR and IP, acetylcholine (Ach, 2.0 µg/mL, 0.1 mL), or noradrenaline (Nor, 2.0 µg/mL, 0.1 mL), or saline (vehicle, 0.1 mL) were topically *(in situ*) administrated onto the urinary bladder, and all the parameters were recorded for additional 15 min. Data are expressed as mean±SEM and were submitted to paired Student´s t-test or One-way ANOVA (P<0.05).

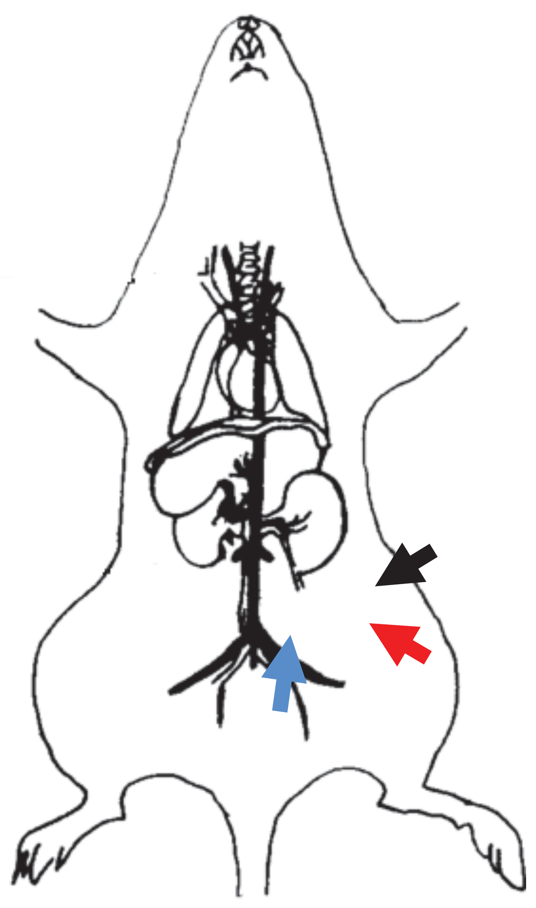

Figure 1: Surgical preparation under isoflurane anestesia. Blue arrow indicates the urinary bladder cannulation region. **Black** and **red** arrows show the femoral arterial and vein cannulation, respectively.

EXPERIMENTAL PROTOCOL

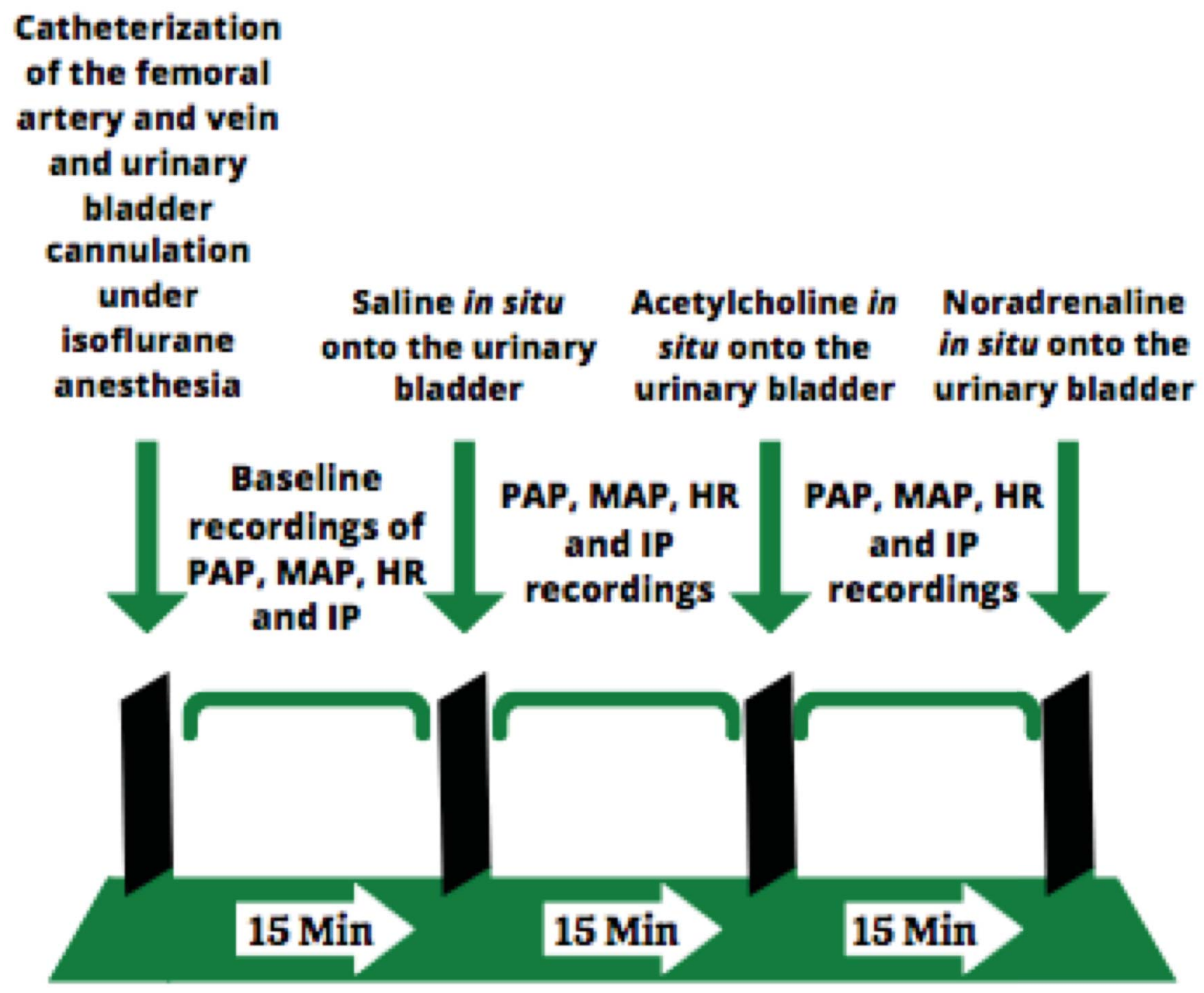

RESULTS

The rats with 8, 15 and 18 months-old (n=6/group) showed significant increases in IP after Ach (500.00±22.81%, 174.55± 20.88%, and 83.01±0.80%, respectively) and significant decreases in IP after Nor (-67±12%, -27.83±12.69%, and -31.41±0.28%, respectively) compared to saline (-0.97±2.54%, 3.71±0.68%, and -1.69±1.97%, respectively). The IP responses to Ach were significantly attenuated in 15 and 18 months-old compared to 8 months-old female rats. No changes were observed in MAP and HR after Ach or Nor or saline *in situ* onto the urinary bladder in all groups.

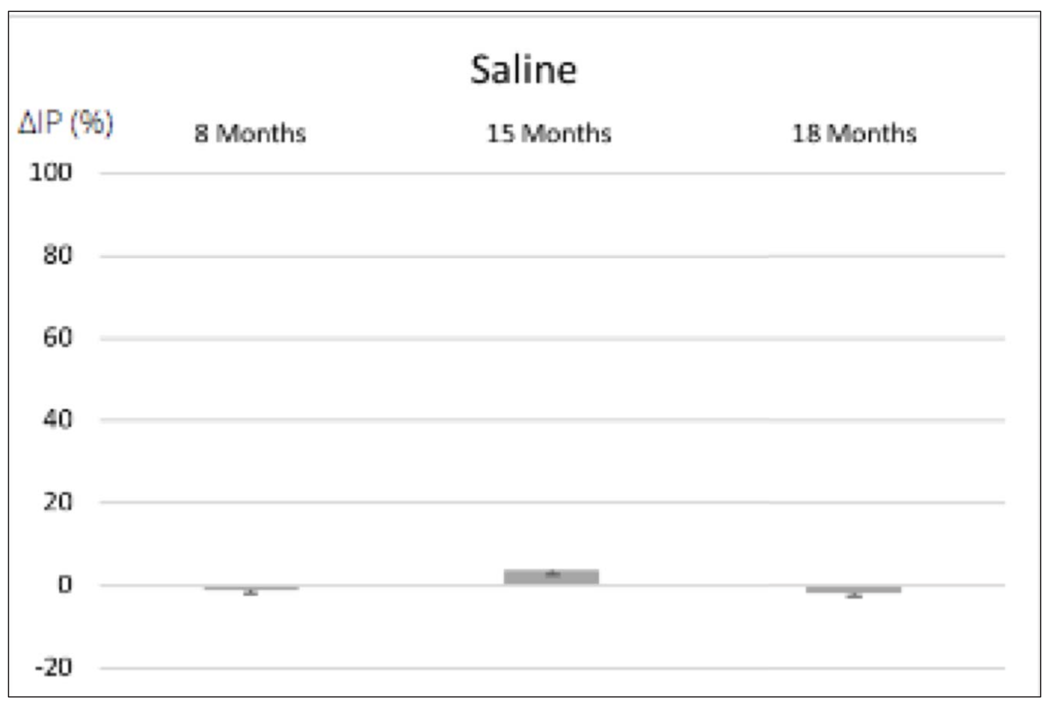

Figure 2: Percent changes in intravesical pressure (%ΔIP) elicited by saline (vehicle) *in situ* onto the urinary bladder in female rats with 8, 15 and 18 months-old.

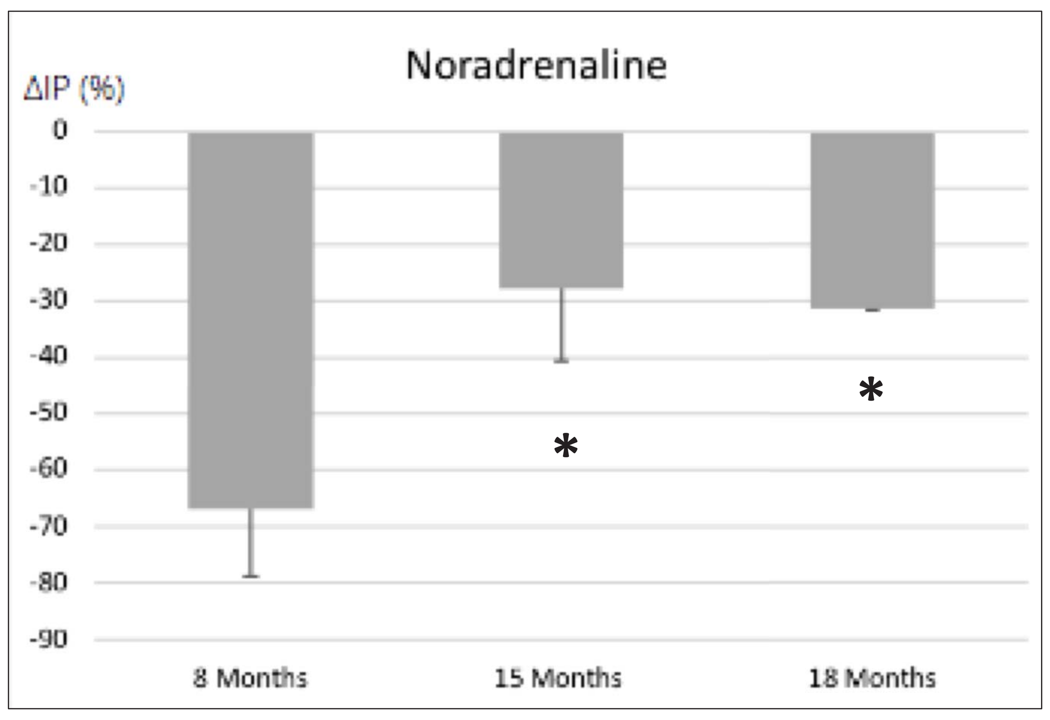

Figure 3: Percent changes in intravesical pressure (%ΔIP) evoked by noradrenaline *in situ* onto the urinary bladder in female rats with 8, 15 and 18 months-old. *P<0.05 vs. 8 months-old.

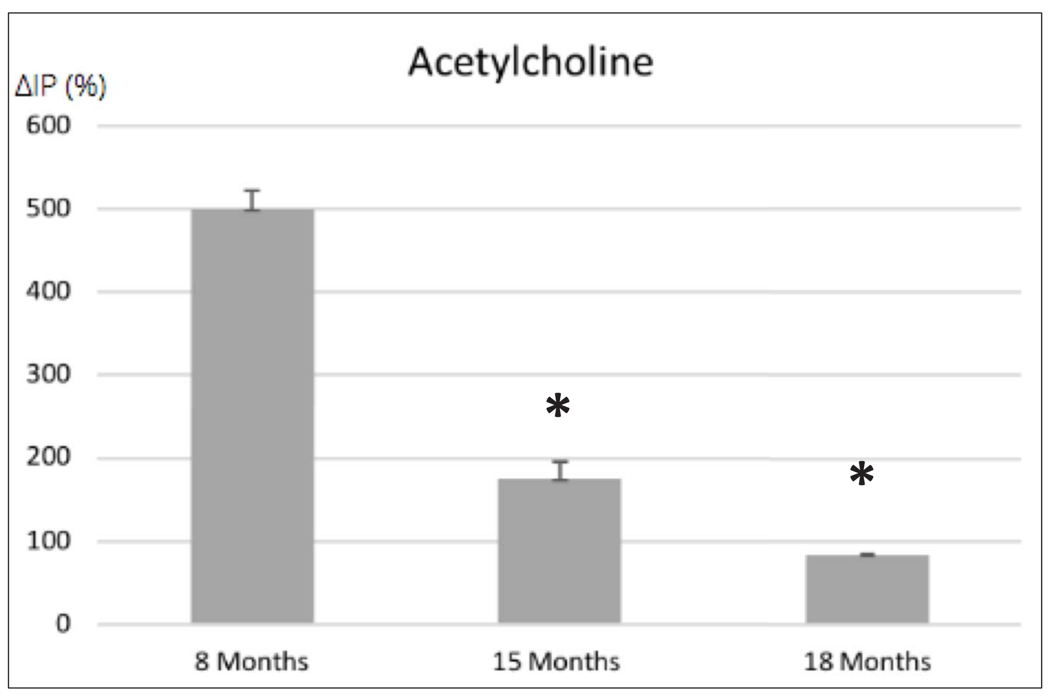

Figure 4: Percent changes in intravesical pressure (%ΔIP) induced by acetylcholine *in situ* onto the urinary bladder in female rats with 8, 15 and 18 months-old. *P<0.05 vs. 8 months-old.

CONCLUSION

The findings suggest that aging reduces the urinary bladder reactivity to Ach and Nor, which are the neurotransmitters of the autonomic nervous system. In addition, the bladder reactivity to Ach was the most affected by elderly.

ACKNOWLEDGMENTS

NEPAS scholarship and FAPESP for the financial support.

SODIUM APPETITE IS INDUCED BY SWIMMING EXERCISE IN WISTAR RATS

[1]Davi Vantini, [2]Giuliana Petri, [2]Jose F. R. Dos Santos, [3]Jessica O. Santana, [3]Fernando L.A. Fonseca, [1]Roberto L. de Almeida, [1]Monica A. Sato.

[1]Dept. Morphology and Physiology, Faculdade de Medicina do ABC, Centro Universitario FMABC, Santo André, SP, Brazil, [2]Animals Care of Dept. Technical Surgery and Experimental Surgery, Faculdade de Medicina do ABC, Centro Universitario FMABC, Santo André, SP, Brazil, [3]Laboratory of Clinical Analysis, Faculdade de Medicina do ABC, Centro Universitario FMABC, Santo André, SP, Brazil.

SESSION V: BODY FLUID HOMEOSTASIS. RENAL FUNCTION

INTRODUCTION AND OBJECTIVE

Regulation of body fluid volume and plasma osmolarity is a fundamental condition for cell survival and maintenance of body homeostasis. Sodium ion (Na+) is an essential mineral for the maintenance of extracellular fluid and blood volume. Thirst, which is a sensation described as a desire to drink, is a regulatory mechanism of the body to increase water consumption in response to the perception of deficiencies in body fluids. Sodium appetite is a motivated behavior observed in a number of species that arises in response to sodium deficiency.[1]

Excessive consumption of sodium in the diet, and sedentary lifestyle have been associated with cardiovascular diseases, which among are the main causes of death in the world.[2]

Situations as in the physical exercise, in which changes in the volume of body water and sodium occur, the activation of thirst sensation and sodium intake helps the maintenance of normal plasma osmolarity levels.[3] In this study, we aimed to investigate if chronic swimming exercise induces sodium appetite in rats.

MATERIALS AND METHODS

Animals. Adult male Wistar rats (14-16 wks-old, ~ 320 g, n=24) were housed in individual plastic cages or in individual metabolic cages at the days of urine collection. The humidity of the animal room was maintained at ~ 70% and the room temperature was set at 22–24° C with a 12:12-h light-dark cycle. Animal Ethics Committee Approval 02/2019 - Centro Universitario FMABC.

Feed. The rats had access to standard chow pellets and two bottles containing tap water and 0.3 M NaCl *ad libitum*. Daily water and 0.3 M NaCl intakes were measured using drinking bottles, in swimming exercise (SE) and sedentary (SED) rats.

Swimming. Rats were submitted to swimming exercise or maintained sedentary after the gradual adaptation period in the individual tanks with warmed water. Afterwards, the animals were submitted to daily bouts of exercise, with 1 h of duration, 5 consecutive days/wk, for 6 wks with 5% of body weight (b.w.) load (Figure 1). At the end of the 6 wks of swimming, the animals were left in a recovery period for 3 wks. Daily water and 0.3 M NaCl intakes were measured using drinking bottles.

Electrolyte dosage. Urine sodium and potassium were analyzed at the adaptation period, after 3 and 6 wks of exercise, and after 3 wks of recovery from the exercise bouts in all groups. In those weeks the rats were in metabolic cages. Plasma sodium and potassium were evaluated in blood samples of all animals at the end of the experiment protocol.

Statistics. Data area as mean±SEM and submitted to Two-way ANOVA followed by Tukey post-test ($P<0.05$).

Figure 1: Individual tank with warmed water in which the rats were submitted to daily bouts of swimming exercise.

EXPERIMENTAL PROTOCOL

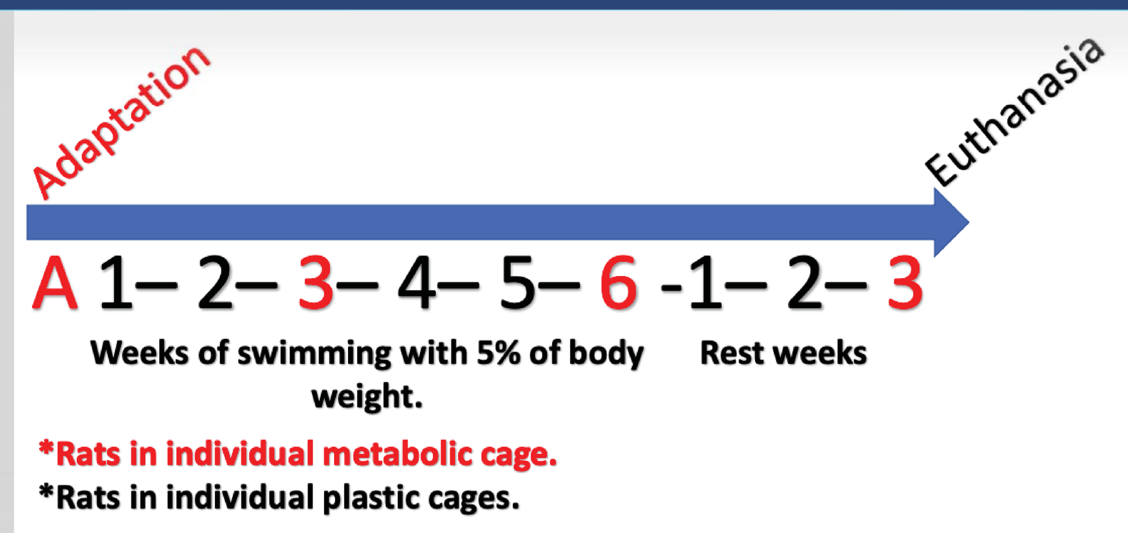

RESULTS

We observed a significant higher sodium intake in SE rats compared to SED rats after 2wks (4.6±0.7 vs 1.1±0.4 mL/100 g of bw), 4wks (5.7±0.7 vs 1.8±0.3 mL/100 g of bw) , 5 wks (6.3±1.0 vs 2.0±0.3 mL/100 g of bw) and during the 2 wks of recovery from SE bouts (fig. 2), without corresponding increase in water intake (fig. 3). No difference was observed in water intake in rats without 0.3 M NaCl comparing SE and SED groups.

Urine and plasma sodium showed no difference in all groups. Urine potassium only reduced after 6 wks of SE in rats with access to 0.3 M NaCl (189.4±22.9 mEq/L) compared to SED animals (260.5±9.6 mEq/L) (Fig. 4).

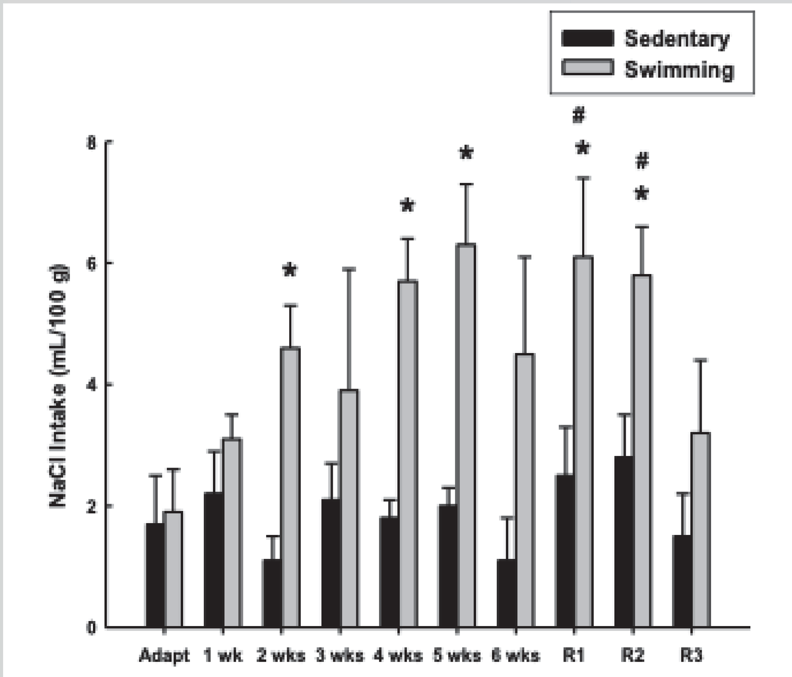

Figure 2- NaCl intake (mL/100 g) in rats with access to 0.3 M NaCl in the adaptation period, after 1, 2, 3, 4, 5, and 6 wks of swimming exercise or sedentarism, and after 1, 2, and 3 wks of recovery from exercise bouts or remaining sedentary. Two-way ANOVA followed by Tukey post-test. *P<0.05 vs. sedentary, # P<0.05 vs, adaptation period.

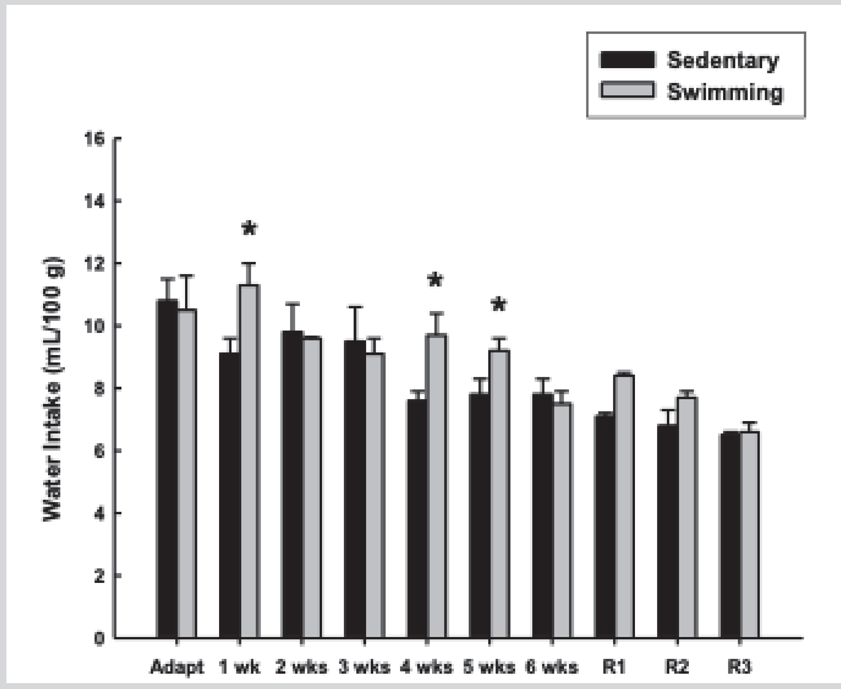

Figure 3- water intake (mL/100 g) in rats with access to 0.3 M NaCl in the adaptation period, after 1, 2, 3, 4, 5, and 6 wks of swimming exercise or sedentarism, and after 1, 2, and 3 wks of recovery from exercise bouts or remaining sedentary. Two-way ANOVA followed by Tukey post-test. *P<0.05 vs. sedentary, # P<0.05 vs, adaptation period.

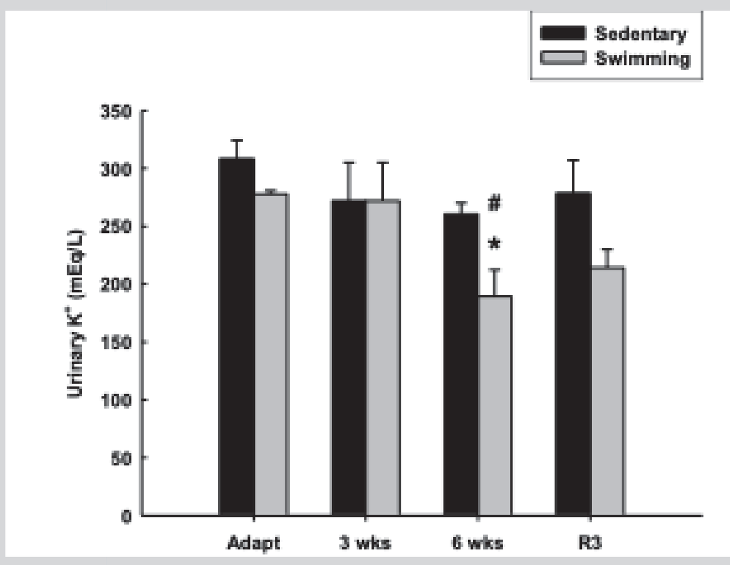

Figure 4 - Urine potassium (mEq/L) in rats with access 0.3 M NaCl in the adaptation period, after 3 and 6 wks or swimming exercise or maintained sedentary; and C) Plasma potassium in rats with and without access to 0.3 M NaCl at the end of the experiment. Two-way ANOVA followed by Tukey post-test for comparisons of urine sodium. Unpaired Student´s t-test for comparisons intra-group. *P<0.05 vs. sedentary, # P<0.05 vs, adaptation period.

CONCLUSION

Our data demonstrated that SE with 5% b.w. load for 6 wks increases sodium appetite in rats, which remained higher even after the cessation of the exercise bouts, suggesting that long-term mechanisms activated by this approach of exercise can mediate the change in this ingestive behavior.

ACKNOWLEDGEMENTS

FAPESP and NEPAS.

REFERENCES

1. Geerling JC, Loewy AD. Central regulation of sodium appetite. Exp Physiol. 2008;93(2):177–209.

2. Campbell NR, Willis KJ, L'Abbe M, Strang R, Young E. Canadian initiatives to prevent hypertension by reducing dietary sodium. Nutrients. 2011;3(8):756–64.

3. Leshem M, Abutbul A, Eilon R. Exercise increases the preference for salt in humans. Appetite. 1999;32(2):251–60.

4. Gobatto CA, de Mello MA., Gobatto FD., Papoti M, Voltarelli FA, Contarteze, RV, de Araujo GG. Avaliações fisiológicas adaptadas a roedores: aplicações ao treinamento em diferentes modelos experimentais. Revista Mackenzie de Educação Física e Esporte. 2009 7(1).

CORRESPONDING AUTHOR

Davi Vantini
davi@davivántini.com.br.

The role of purine P1 receptors in control of the renal excretion depends on rat's age and Duration of Streptozotocin induced hyperglycaemia

Leszek Dobrowolski, Marta Kuczeriszka, Agnieszka Walkowska, Joanna D. Sitek

Department of Renal and Body Fluid Physiology, Mossakowski Medical Research Institute, Polish Academy of Sciences, Warsaw, Poland

Introduction and objectives

Chronic hyperglycaemia (DM) could affect adenosine concentration and its P1 receptors (P1-R) density in the kidney. The impact of these modifications on renal excretion (RE) alterations may reflect a direct influence on tubular transport by P1-R located along the nephron.

To examine if the role of P1-R on kidney function depends on the DM duration we examined effects on RE with: **a)** THEO, a nonselective P1-R antagonist and **b)** CSC, selective for A2a type of P1-R antagonist, using a pharmacological model of DM induced by streptozotocin (STZ) during: **i)** short- 2-wks, (DM-14) or **ii)** long-term (8-wks, DM-60) after STZ injection to compare with the effects in NG age-matched male Sprague Dawley (SD) rats.

Methods

Observation after *diabetes* induction: for 14 or 60 days following STZ (60 mg/kg *i.p.*) or solvent injection in male SD rats (Tac:Cmd:SD) body weight (Bwt) and glycaemia were monitored (Fig. 1).

<u>**Acute experiments:**</u> **Anaesthesia -** sodium thiopental, 100 mg/kg Bwt *i.p.* N = 7-8, each experimental group.

Measurements: in hyper- (**DM**) or normoglycaemic (**NG**) age-matched rats we measured:

<u>Renal excretion (RE) parameters</u>: Urine flow - V, urine osmolality - U_{osm}, total solute excretion - $U_{osm}V$, Na^+ or K^+ excretion - $U_{Na}V$ or U_KV.

<u>Haemodynamic:</u> mean arterial blood pressure (MBP).

P1-R antagonists and dosages: Theophylline (THEO) given at 14 mg/kg/h *i.v.* and 8-(3-Chlorostyryl)caffeine (CSC) at 1.7 µmol/kg/h infused into renal artery. Solvent of THEO or CSC did not alter renal excretion in both NG and DM rats.

Statistics: parametric and non-parametric tests were performed, respectively, using STATISTICA; significance level at P<0.05.

Fig. 1

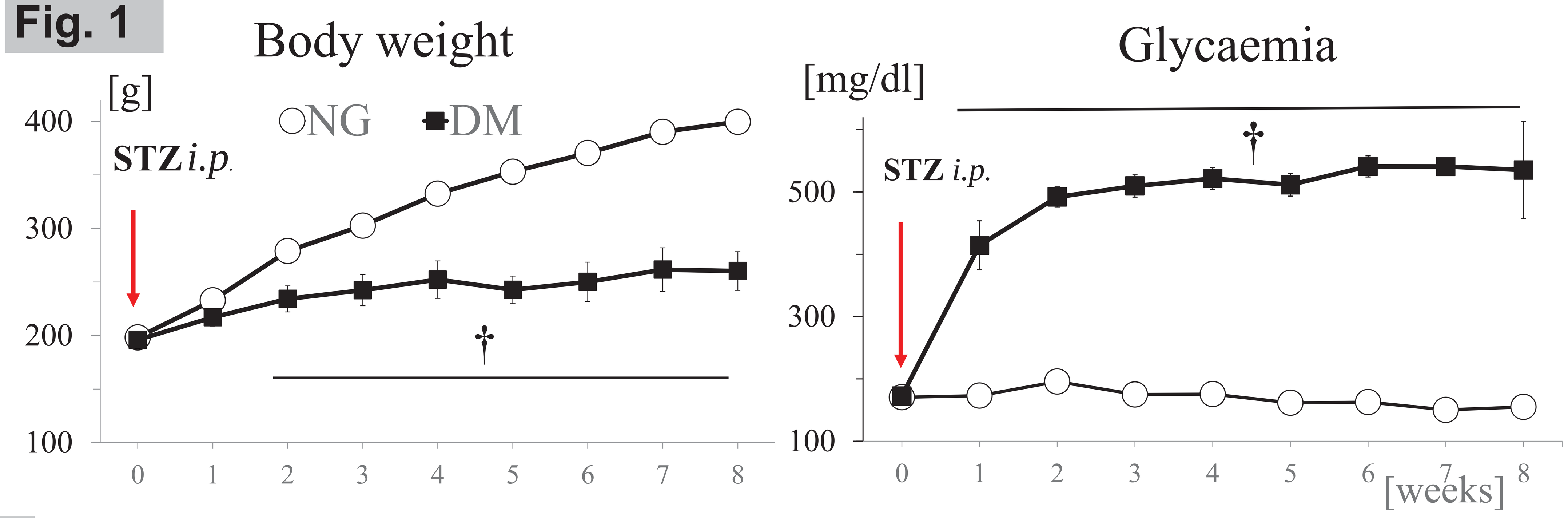

Results and Conclusions

Fig. 2 THEO effects on renal excretion

14 days **60 days**

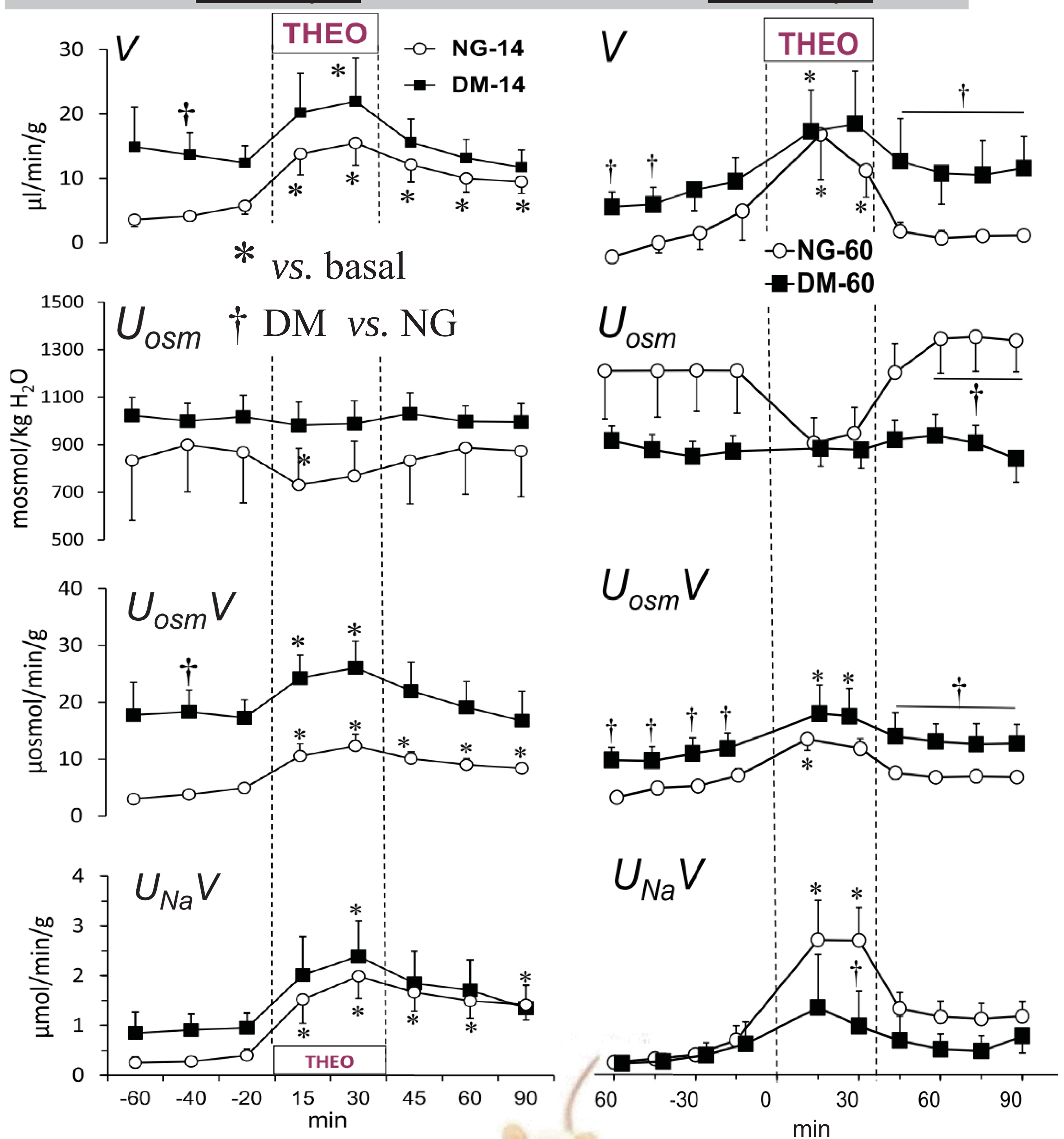

Fig. 3 CSC effects on renal excretion

14 days **60 days**

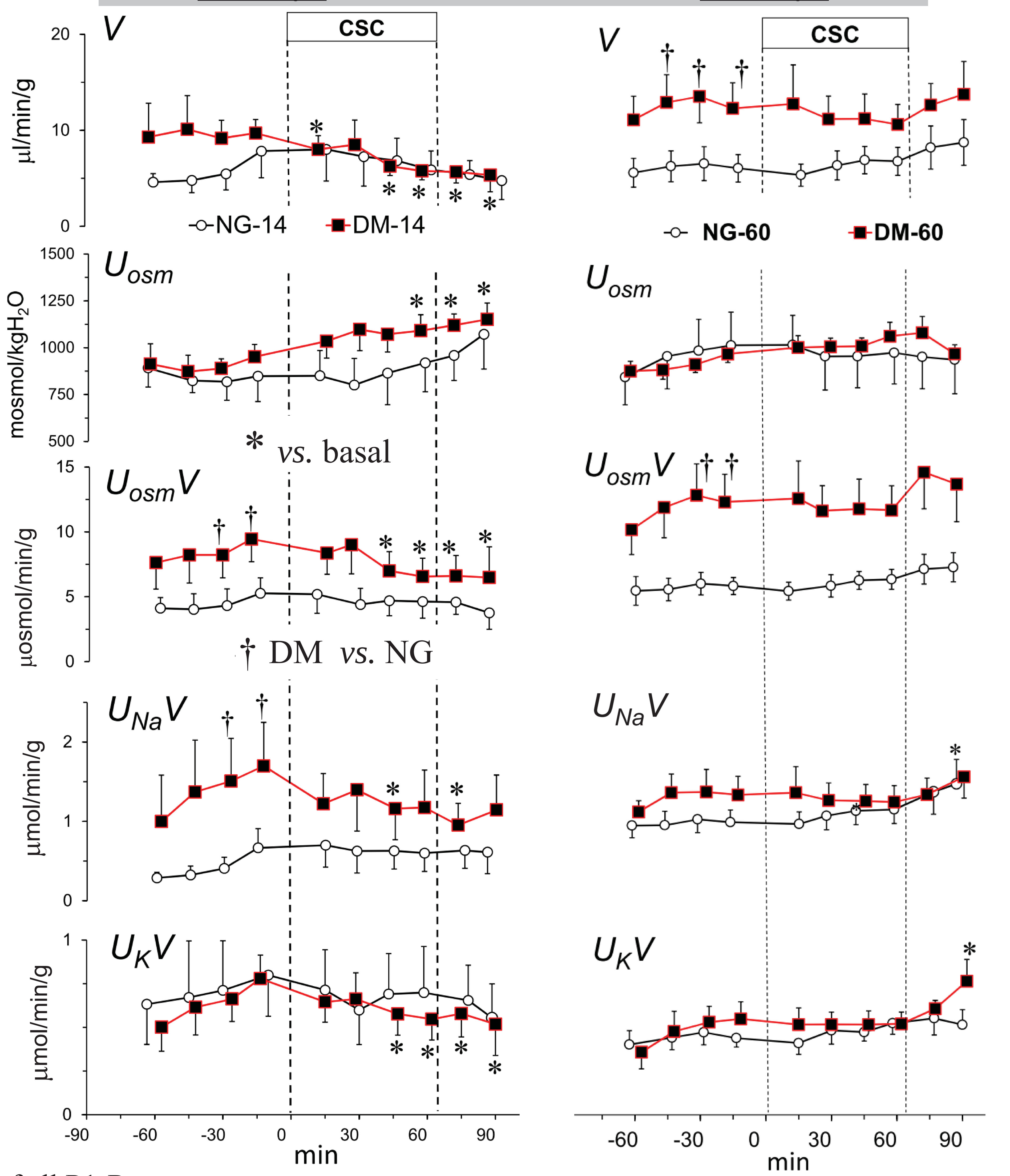

Our data indicate:

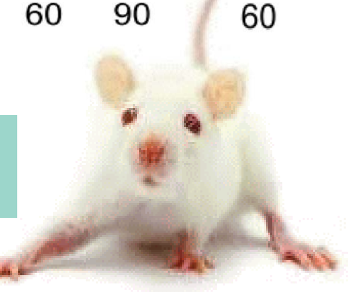

- The effects of THEO and CSC on RE depended mainly on direct action on the tubular transport because neither P1-R antagonist affected MBP.
- **Short-term diabetes** (2 weeks, DM-14) did not modify the joint effect of all P1-R on renal excretion but could alter the contribution of individual subtypes, such as P1-RA2a.
- **Long-term diabetes** (8 weeks, DM-60) blunted the P1-R impact on sodium excretion and urine concentration and abolished P1-RA2a contribution to the control of renal excretory function.

J.D.S. is POWEROch!DOK" project participant.

Study supported by National Science Centre, Poland: grant # 2017/25/B/NZ5/01292.

Session V: BODY FLUID HOMEOSTASIS. RENAL FUNCTION

The role of Ang1-7 in control of blood pressure, renal haemodynamics, and excretion in rats model of STZ-induced diabetes

Leszek Dobrowolski, Agnieszka Walkowska, Elżbieta Kompanowska-Jezierska, Joanna D. Sitek, Marta Kuczeriszka

Department of Renal & Body Fluid Physiology, Mossakowski Medical Research Institute,
Polish Academy of Sciences, Warsaw, Poland

Introduction

Diabetes mellitus causes multiple morphological and functional changes, ultimately leading to the end stage damage of many organs, including kidney. It is well known that longlasting hyperglycaemia is accompanied by endothelial dysfunction due to decreased NO bioavailability. Contribution of angiotensin 1-7 (Ang1-7) to control of extrarenal and renal function may be modified in diabetes. Ang1-7 could modulate blood pressure and renal function in diabetes. The impact of these modifications on renal function remains unclear.

Aim of the study

To examine if chronic Ang1-7 supplementation would affect blood pressure and improve kidney function in rats with streptozotocin-induced diabetes.

Methods

In Sprague Dawley diabetic (DM) and normoglycaemic (NG) rats, three weeks after streptozotocin (STZ, 60 mg/kg *i.p.*) or solvent injection (citrate buffer), Ang1-7 was given (400 ng/min by subcaneously implanted osmotic minipumps) for next two weeks.
Along five weeks blood pressure (BP, tail cuff method), 24 hours' water intake and renal excretion were determined weekly.
Thereafter in anaesthetized animals (sodium thiopental, 100 mg/kg Bwt *i.p.*) arterial blood pressure and renal function were evaluated:

Haemodynamics

- MABP - mean blood pressure, [mmHg]
- RBF - whole kidney blood flow, [ml/min]
- CBF - cortical laser-Doppler (l-D) flux, [PU]
- OMBF - outer-medullary l-D flux, [PU]
- IMBF - inner-medullary l-D flux, [PU]

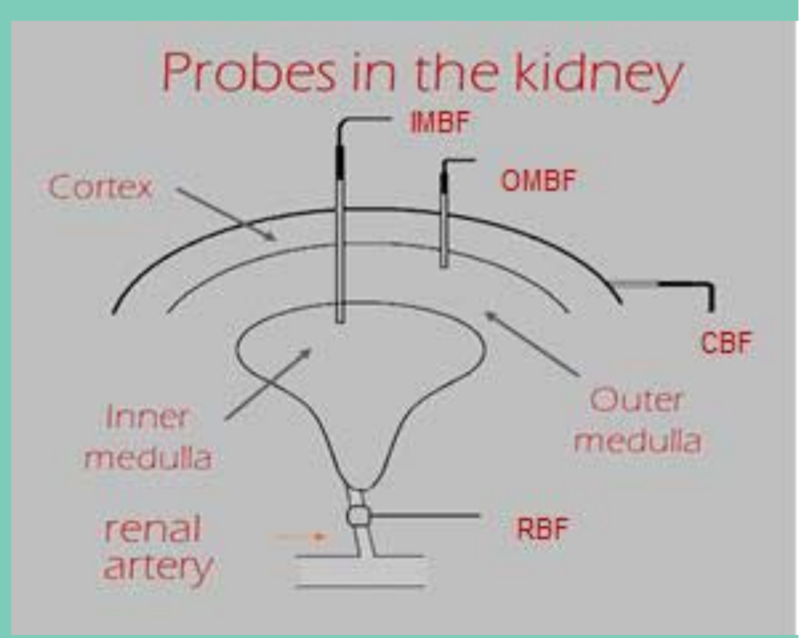

Renal excretion

- urine flow,
- UosmV - urine solute excretion,
- UNaV - urine sodium excretion.

Protocol of acute experiments:
all the parameters were measured simultaneously during Ringer solution infusion.

Results

Effects of Ang1-7 in normoglycaemic (NG) and diabetic (DM) rats

	body weight [g]			glycaemia [mg/dL]			Posm [mosmol/kgH2O]			Hct [%]		
	0	3	5 weeks	0	3	5 weeks	0	3	5 weeks	0	3	5 weeks
NG (n=8-12)	227±12	319±8 *	352±9 *	164±8	146±6	139±4	299±2	314±5 *	306±4	43±1	46±1*	45±0
NG+Ang1-7 (n=8)	230±18	304±14	333±12	182±7	161±9	164±11	299±4	302±4	309±5 *	41±1	44 ±0*	46±0 *
DM (n=11-13)	243±10	266±10 #	264±9 #	165±5	455±25 *#	501±20 *#	302±3	323±3*	325±2 *#	44±1	48±1 *	47±0*#
DM+Ang1-7 (n=9-12)	255±12	273±7 *	281±8 *	179±13	530±21 *	520±31 *	301±3	325±4 *	327±2*	44±1	50±2*	47±1 *

	PNa [mmol/l]			urine flow [ml/24h]			UosmV [mosmol/24h]			water intake [ml/24h]		
	0	3	5 weeks	0	3	5 weeks	0	3	5 weeks	0	3	5 weeks
NG	126±2	137±1	139±3	12±1	16±2	27±12	22±2	26±2	26±1 *	32±1	32±3	35±3
NG+Ang1-7	137±3	132±2	133±2	10±1	11±1	10±1	21±1	22±2	21±2	33±1	33±2	31±3
DM	133±2	125±1	124±2	11±1	89±14 *#	85±14*#	21±2	107±2 *	97±15 *#	36±3	118±16 *;	110±15 *#
DM+Ang1-7	133±2	122±2	126±1	10±1	90±13 *	111±12 *	19±1	106±15 *	120±15 *	37±4	90±18*	125±11*

Body weight, blood and plasma and renal excretion parameters for Tac:Cmd:SD rats before ("0") and 3 or 5 weeks after vehicle or streptozotocin (STZ) administration in rats untreated or with chronic Ang1-7 treatment.
Glycaemia (blood glucose level), Posm - plasma osmolality, Hct - haematocrit, PNa - plasma sodium, UosmV - total solute excretion.
The Ang1-7 treatment was started three weeks after vehicle/STZ injection (the shaded values depict effects shown in the last week of Ang1-7).* - vs. day 0, # - vs. NG.

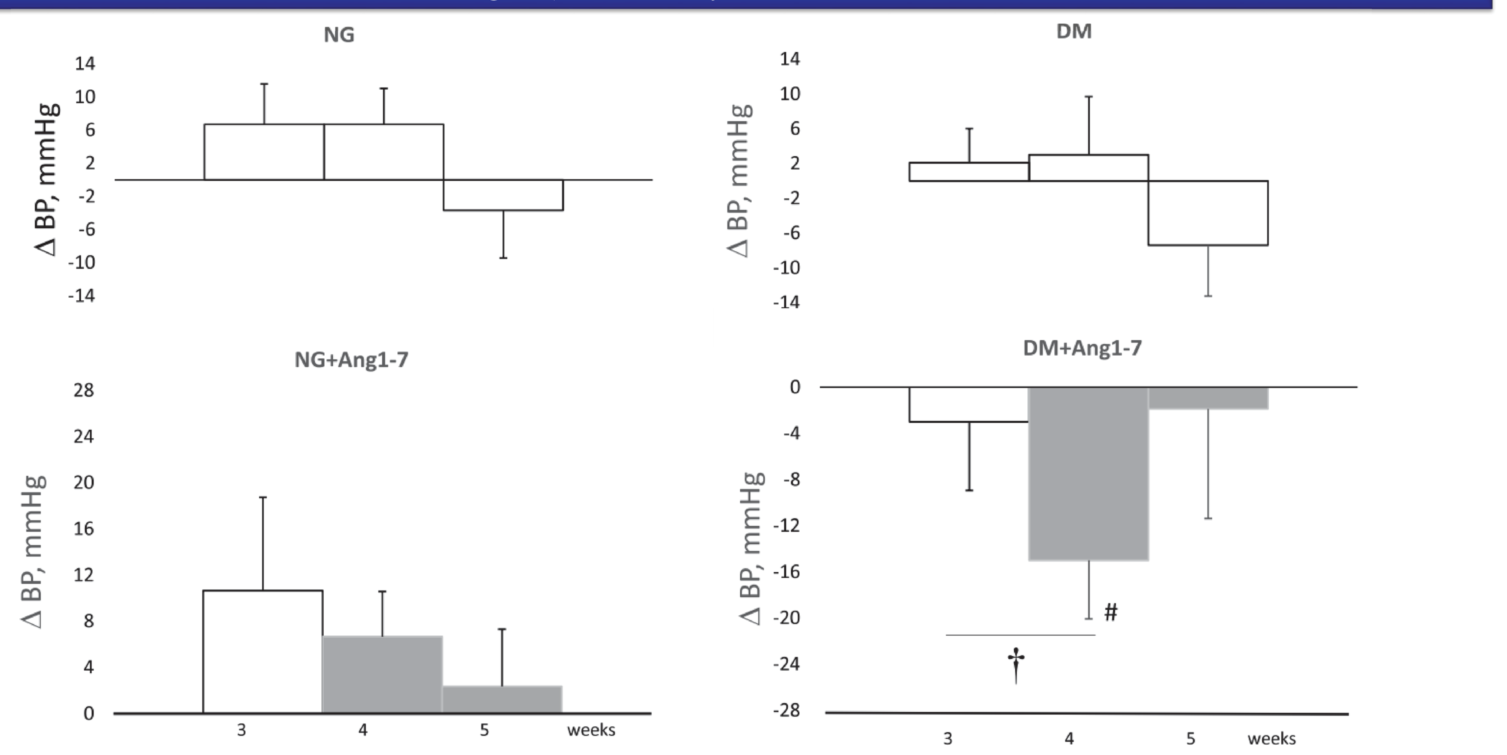

Blood pressure changes measured 3, 4 or 5 weeks after vehicle/STZ injection in NG (n=10) and DM rats (n=8), untreated or treated with Ang1-7 (NG+Ang1-7, n=5; DM+Ang1-7, n=6).
The Ang1-7 treatment was started three weeks after vehicle/STZ injection (the shaded bars depict the values seen after Ang1-7). Means ± SEM. † - vs. the value measured 3 weeks after STZ injection, # - vs. the corresponding values in all the other groups.

	MABP mmHg	RBF ml/min/g	CBF PU	OMBF PU	IMBF PU	urine flow μl/min	UosmV μosmol/min	UNaV μmol/min
NG (n=12)	128±7	2.9±0.5	575±44	135±16	226±40	11.5±1.9	9.0±1.4	1.22±0.23
NG+Ang1-7 (n=7)	127±7	3.0±0.8	590±48	155±20	221±33	4.6±1.4 *	4.4±1.1	0.48±0.22 *
DM (n=12)	123±3	3.3±0.4	473±44	158±22	160±30 *	16.3±2.5	15.2±2.2 *	0.91±0.14
DM+Ang1-7 (n=8)	121±5	2.6±0.3	539±49	115±9	121±24 $	23.4±2.8 $	19.1±2.9 # $	0.98±0.28

Baseline values for systemic and renal haemodynamic: RBF, CBF, OMBF, IMBF and renal excretion: urine flow, UosmV and UNaV in anaesthetized normoglycaemic and diabetic male Sprague Dawley rats without or with Ang1-7 treatment.
* - vs. NG, # - vs. untreated, $ - vs. NG+Ang1-7.

Summary and Conclusions

- MABP, RBF, CBF and OMBF did not differ among groups.
- Regardless Ang1-7 treatment IMBF was significantly higher in NG than in DM rats.
- Urine flow was significantly decreased by Ang1-7 in NG, but increased in DM rats.

Data from the study with conscious and anaesthetized animals indicate:

❖ **Chronic studies:**
Ang1-7 could modify blood pressure in DM rats, however transiently, while water intake and urine excretion longlasting.

❖ **Acute studies:**
Ang1-7 rather not contribute to systemic (no MABP changes) and renal haemodynamics independent of glycaemia.
Ang1-7 can modify tubular water and solutes reabsorption but the final effect depends on glycaemia – it improves in normo- and impairs in hyperglycaemia.

➢ **We postulate the renal excretion effects could depend on the selective affinity of Ang1-7 to the AT-1 receptors, which density is simultaneously increased in diabetes as was shown in several studies.**

IMDiK POLSKA AKADEMIA NAUK

The study was supported by 217/01/X/NZ4/02053 Miniatura M. Kuczeriszka. J.D. Sitek – "POWEROch!DOK" project participant.

HYPERGLICAEMIA MODULATES P1 RECEPTORS IMPACT ON THE RENAL CIRCULATION AND URINE EXCRETION BUT NOT TISSUE NO.

Walkowska Agnieszka, Kuczeriszka Marta, Sitek Joanna D., Dobrowolski Leszek

Department of Renal & Body Fluid Physiology,
Mossakowski Medical Research Institute, Polish Academy of Sciences, Warsaw, Poland

Background

Chronic hyperglicaemia could affect in the kidney paracrine factors like adenosine (Ado), their P1 receptor (P1R) density and nitric oxide (NO) bioavailability. The impact of these modifications on renal function remains unclear.

Ado can induce either vasoconstriction or vasodilation, depending on the dominant stimulation of A1 or A2 receptors (A1R, A2R). The changes in renal excretion induced by Ado may be due to its direct effect on tubular transport or be secondary to haemodynamic changes, both could be mediated by fluctuated intrarenal NO activity.

Aim of the study

To find out if hyperglicaemia alters P1-R effects on renal function and if this could be mediated by intrarenal NO activity in streptozotocin-induced diabetic rat model

Materials and methods

The effects of theophylline (Theo, A1R/A2R antagonist) in anaesthetized male SD rats, two weeks after streptozotocin - induced (60 mg/kg *i.p.*) hyperglicaemia (DM) was investigated.

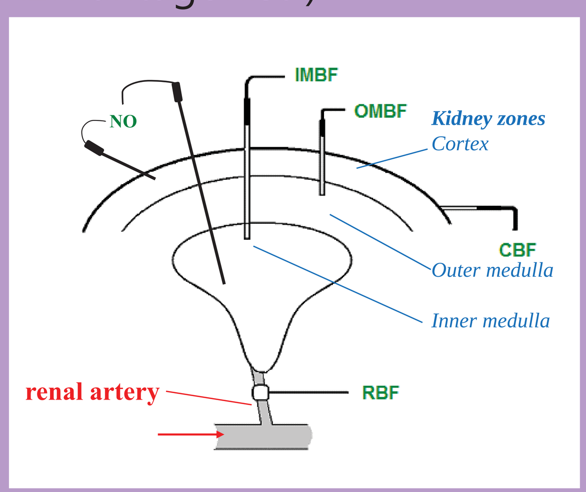

Measurements in anaesthesia

(sodium thiopental,100 mg/kg Bwt *i.p.*)

Haemodynamics

- MBP (mean blood pressure) [mmHg]
- RBF (whole kidney blood flow) [ml/min]
- CBF (cortical laser-Doppler flux) [PU]
- OMBF (outer-medullary laser-Doppler flux) [PU]
- IMBF (inner-medullary laser-Doppler flux) [PU]

Renal excretion

- urine flow (V), urine solute excretion (UosmV), sodium excretion (UNaV)

Tissue NO

- *In situ* measurement with NO selective sensors

Protocol of acute experiments:

- All the parameters were measured simultaneously during drug infusion or solvent infusion
- After control period the drug solvent i.v. infusion was replaced by Theo (12mg/kg/h), later replaced by solvent again - recovery period
- In another (control for DM and NG) groups only drug solvent was infused

Results

Theo effects in DM and those in normoglicaemic (NG) rats

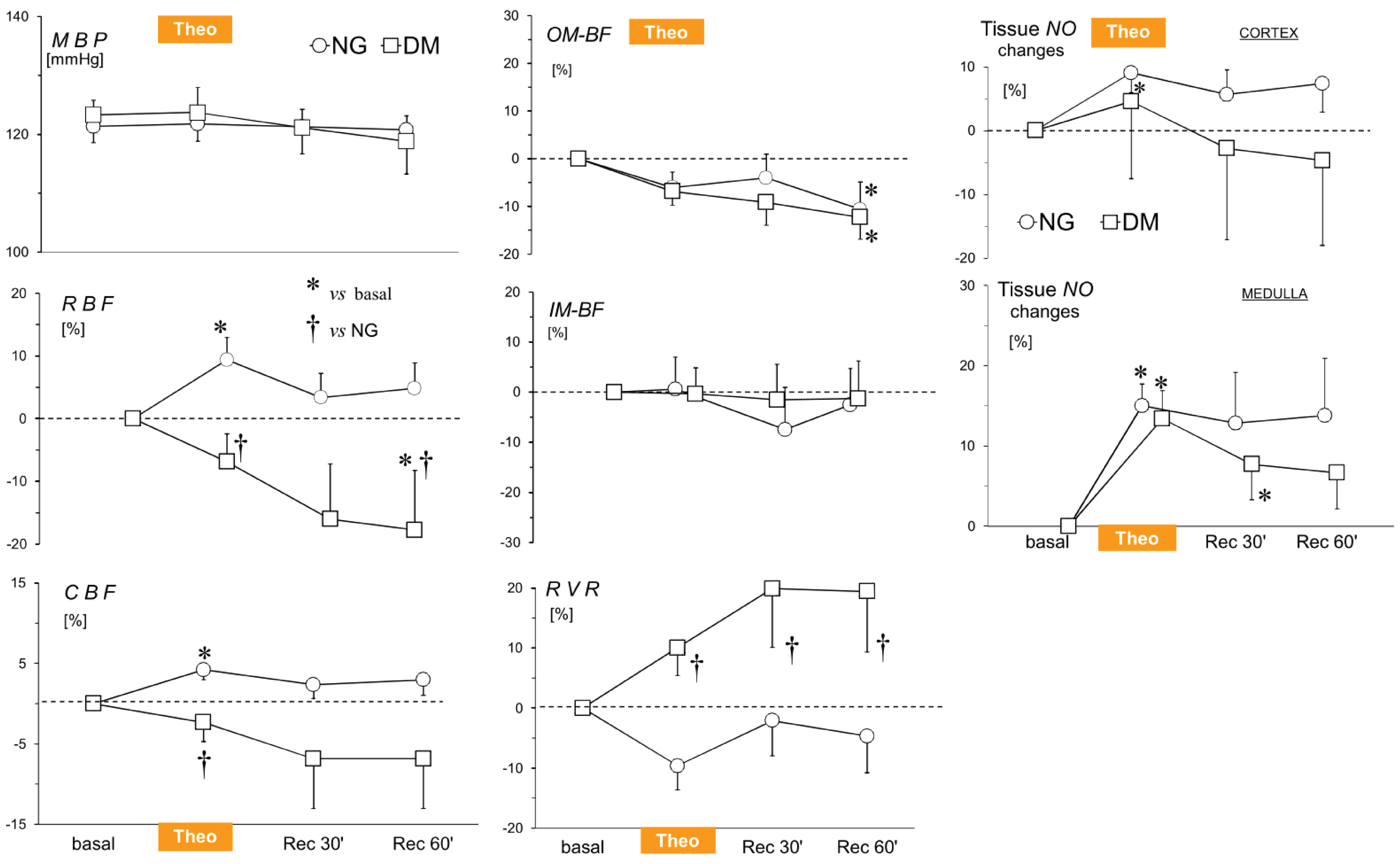

Fig 1. Effects of Theo on MBP, renal haemodynamics, renal vascular resistance (RVR) and tissue NO in DM rats and their normoglicaemic control (NG).
*** significantly different vs basal value; † significantly different from the change in NG rats.**

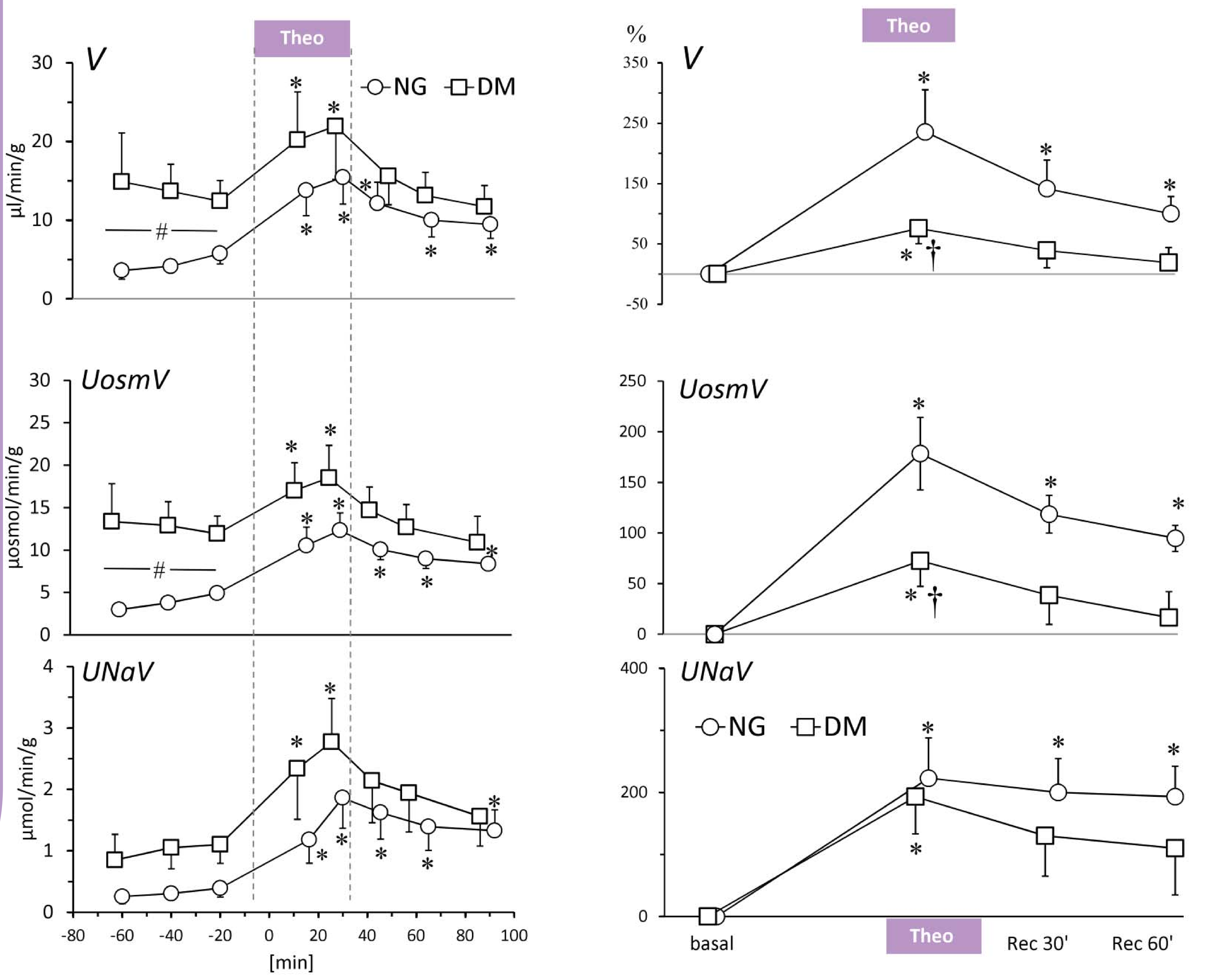

Fig 2. Effects of Theo renal excretion in hyperglicaemic (DM) rats and their normoglicaemic control (NG).
*** significantly different from the baseline value before Theo infusion; † significantly different from the NG;**
 # significantly different between DM and NG rats.

Summary and Conclusion

- Theo did not affect systemic blood pressure both in DM and NG rats.
- RBF significantly decreased in DM rats in contrast to the increase in NG rats.
- Significant OM-BF decrease without IMBF alteration were shown in both groups.
- Renal tissue NO signal increased similarly in the cortex and medulla, independent of glycaemia.
- Increases of V, UosmV were lower in DM than NG rats (51% and 76%vs. 178% and 236%, respectively), while UNaV increase did not differ between both groups (193% vs. 223%, respectively).

- **Thus, in DM, in opposite to NG, within the cortex A2R prevails over A1R effects, reflected by RP1 antagonist vasoconstriction, whereas within medulla a balance between receptors persisted. A1R/A2R impact on tubular transport of water and solutes (but not sodium) were also modify by hyperglicaemia. However, these alterations of P1R action on renal haemodynamics and excretion seems to be not dependent on *NO* bioavailability.**

The study was supported by the National Science Centre, Poland, project No. 2017/25/B/NZ5/01292,
Joanna D. Sitek – "POWEROch!DOK" project participant

XXVIII Congress of the Polish Physiological Society

Gdańsk, September 15-17 2021

Poster book

SESSION VI

HEART. CARDIOVASCULAR AND RESPIRATORY REGULATION

HONORARY PATRONAGE

Prof. dr Marcin Gruchała
Rector of the Medical University of Gdansk

Uniwersytet Gdański

Prof. dr Piotr Stepnowski
Rector of the University of Gdansk

WOJEWODA POMORSKI
DARIUSZ DRELICH

Dariusz Drelich
Governor of the Pomeranian Voivodeship

HONORARY PATRONAGE
Mayor of the City of Gdańsk

Aleksandra Dulkiewicz
Mayor of Gdansk

Mieczysław Struk
Marshal of the Pomeranian Voivodeship

PARTNER

PAN
POLSKA AKADEMIA NAUK

ANIMA LAB
animal facility and laboratory equipment • animal research models

FUNDACJA LOTOS

Medical University of Gdansk
Department of Physiology

CHEMOSENSITIVITY DURING MECHANO AND METABOREFLEX ACTIVATION IN HEALTHY SUBJECTS CHARACTERIZED BY LOW AND HIGH EXERCISE CAPACITY

WOJCIECH ŁOPUSIEWICZ[1], A.LIS[1], T.OKUPNIK[1], B.PALECZNY[1], B.PONIKOWSKA[1]

[1]Department of Physiology and Pathophysiology, Wroclaw Medical University, Poland;

Introduction and objectives

The behavior of the peripheral chemoreceptor reflex during: (i) concomitant stimulation of the muscle mechanoreceptors alone, or (ii) combined stimulation of mechano- and metaboreceptors remains poorly known and the nature of the interaction between these reflexive mechanisms is likely to be influenced by the level of aerobic and/or anaerobic capacity.

Methods

Study aimed to explore this issue in a group of 19 healthy, young volunteers (9 men; age: 28.5±3.8 years, body mass index: 24.0±3.7 kg/m2 [mean±SD]). Anaerobic fitness was tested by the Wingate test, while aerobic fitness was tested with the progressive RAMP test. A bicycle ergometer was used for both tests. Peripheral chemoreflex sensitivity ($PChS_{REST}$) was assessed by the transient hypoxia method at rest, during passive cycling ($PChS_{PC}$; activation of muscle mechanoreflex), and passive cycling with circulatory occlusion of the lower limbs ($PChS_{PC+CO}$; simultaneous activation of muscle mechano- and metaboreflex). Subjects were divided into the low- and high-anaerobic fitness groups and the low- and high-aerobic fitness groups according to medians of the Wingate test and the RAMP test, respectively, and the PChS at rest, during passive pedaling and passive pedaling with circulatory occlusion of the lower limbs were compared between low- vs. high-fitness groups.

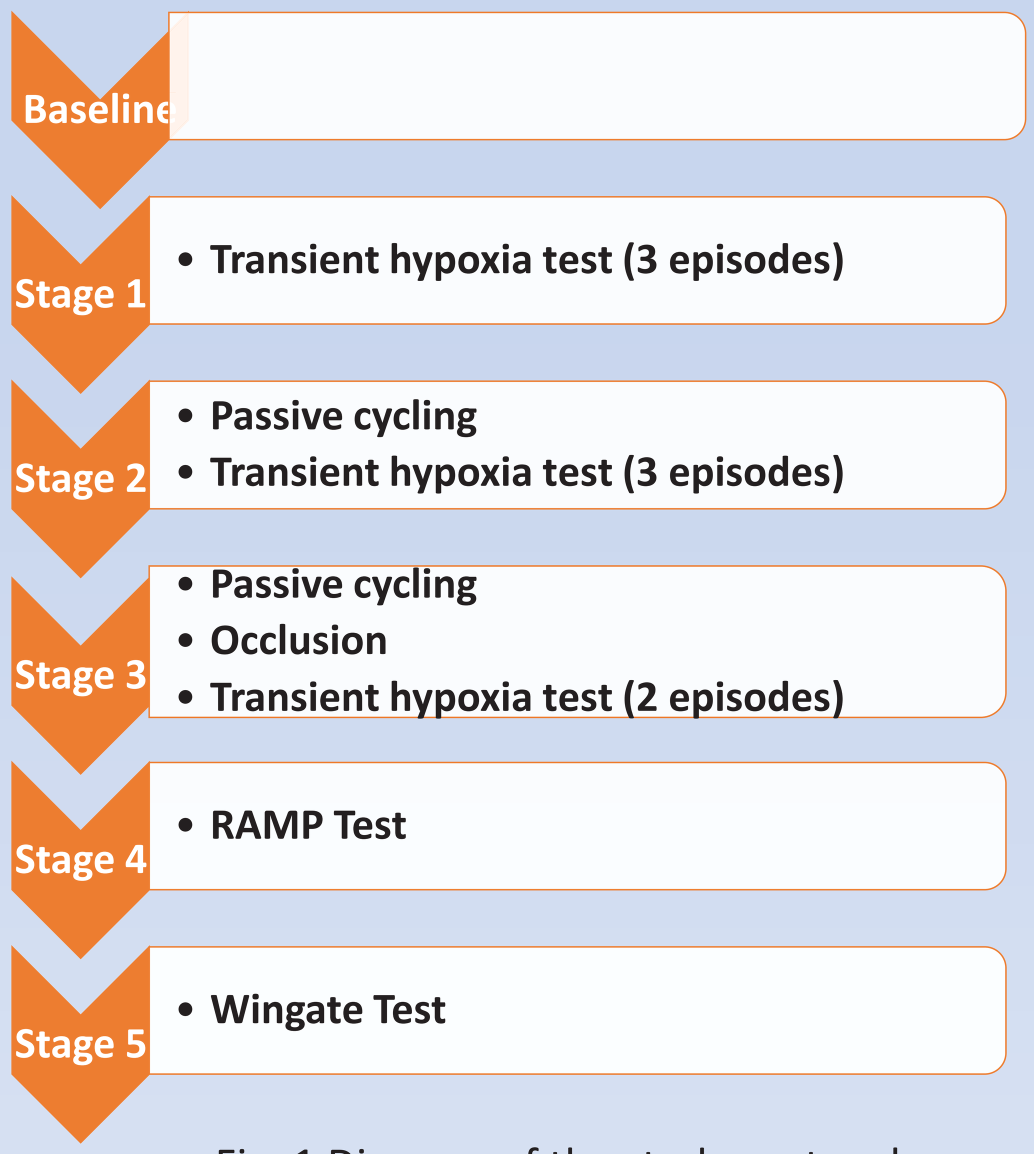

Fig. 1 Diagram of the study protocol.

Fig. 2 Results of ventilation response to transient hypoxia in the low - and high - fitness group. Dark blue dots - $PChS_{REST}$; Orange dots - $PChS_{PC}$; Gray dots – $PChS_{PC+CO}$; Yellow dots – $PChS_{REST}$; Light blue dots - $PChS_{PC}$; Green dots - $PChS_{PC+CO}$. Dotted lines - trend lines.

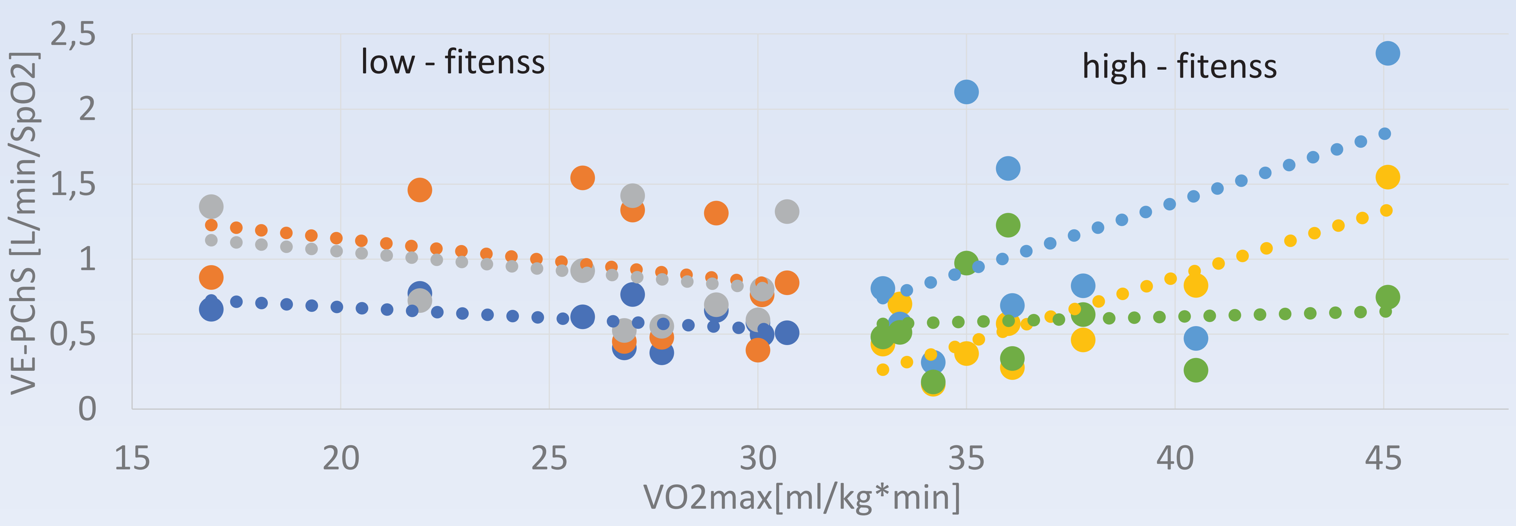

Fig. 3 Results of heart rate response to transient hypoxia in the low - and high - fitness group. Dark blue dots - $PChS_{REST}$; Orange dots - $PChS_{PC}$; Gray dots – $PChS_{PC+CO}$; Yellow dots – $PChS_{REST}$; Light blue dots - $PChS_{PC}$; Green dots - $PChS_{PC+CO}$. Dotted lines - trend lines.

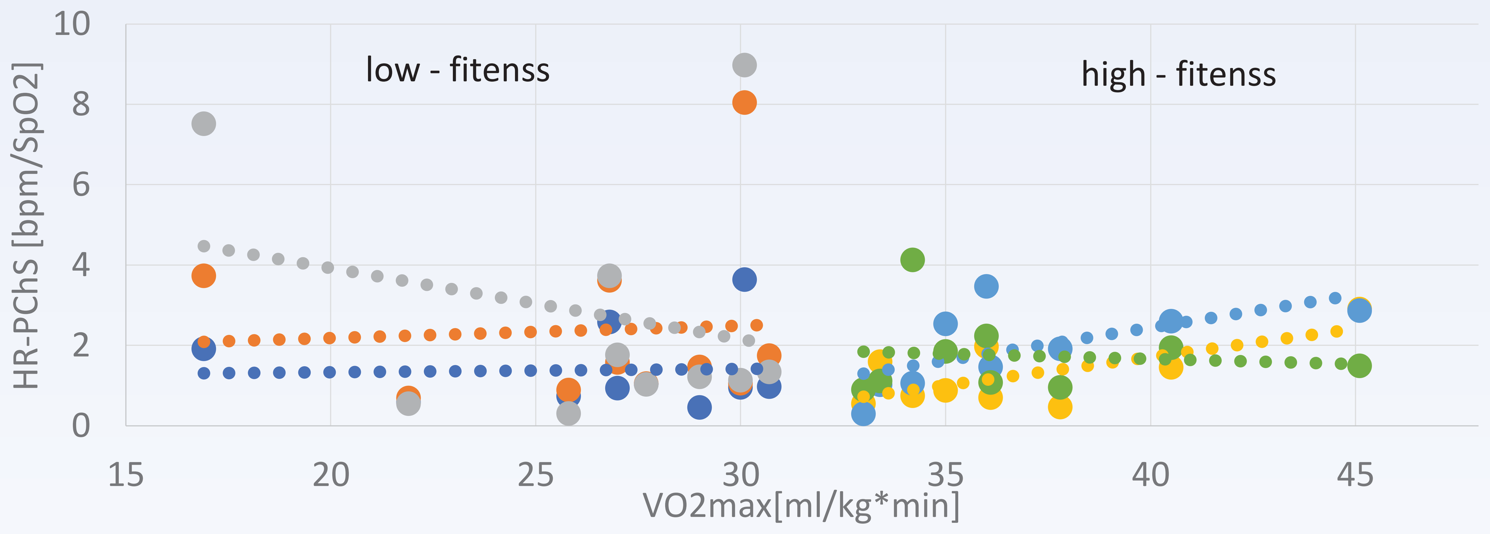

Fig. 5 Results of ventilation response to transient hypoxia in the low - and high - anaerobic group. Dark blue dots - $PChS_{REST}$; Orange dots - $PChS_{PC}$; Gray dots – $PChS_{PC+CO}$; Yellow dots – $PChS_{REST}$; Light blue dots - $PChS_{PC}$; Green dots - $PChS_{PC+CO}$. Dotted lines - trend lines.

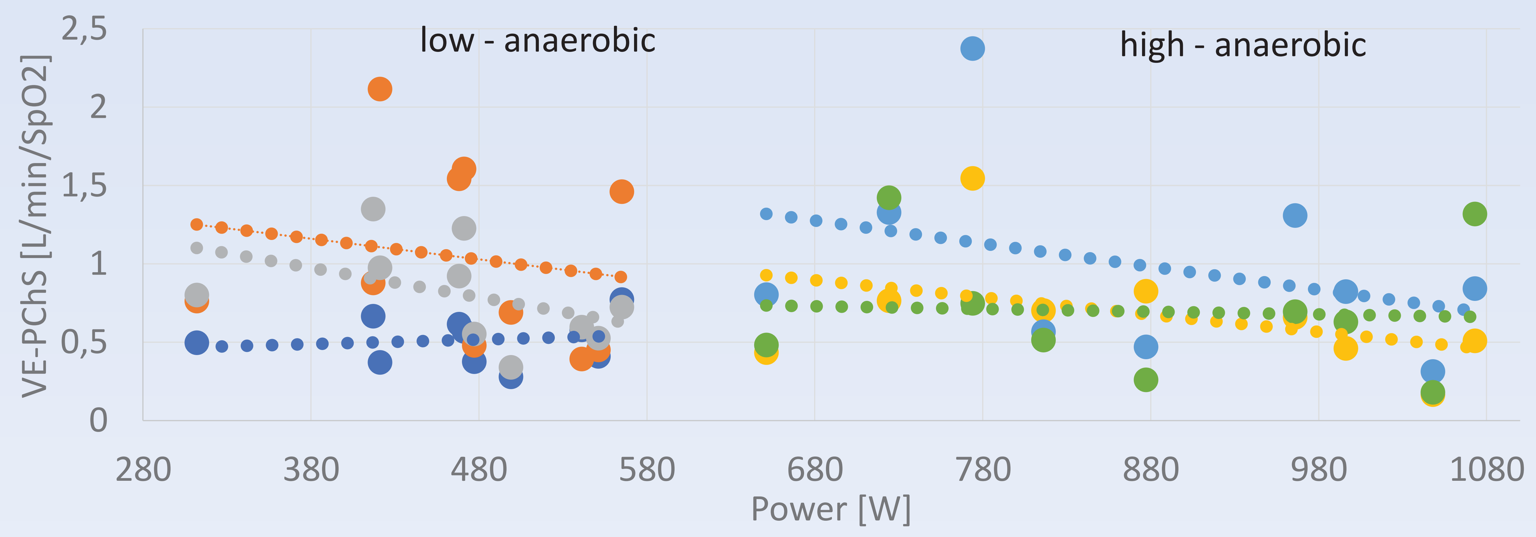

Fig. 6 Results of heart rate response to transient hypoxia in the low - and high - anaerobic group. Dark blue dots - $PChS_{REST}$; Orange dots - $PChS_{PC}$; Gray dots – $PChS_{PC+CO}$; Yellow dots – $PChS_{REST}$; Light blue dots - $PChS_{PC}$; Green dots - $PChS_{PC+CO}$. Dotted lines - trend lines.

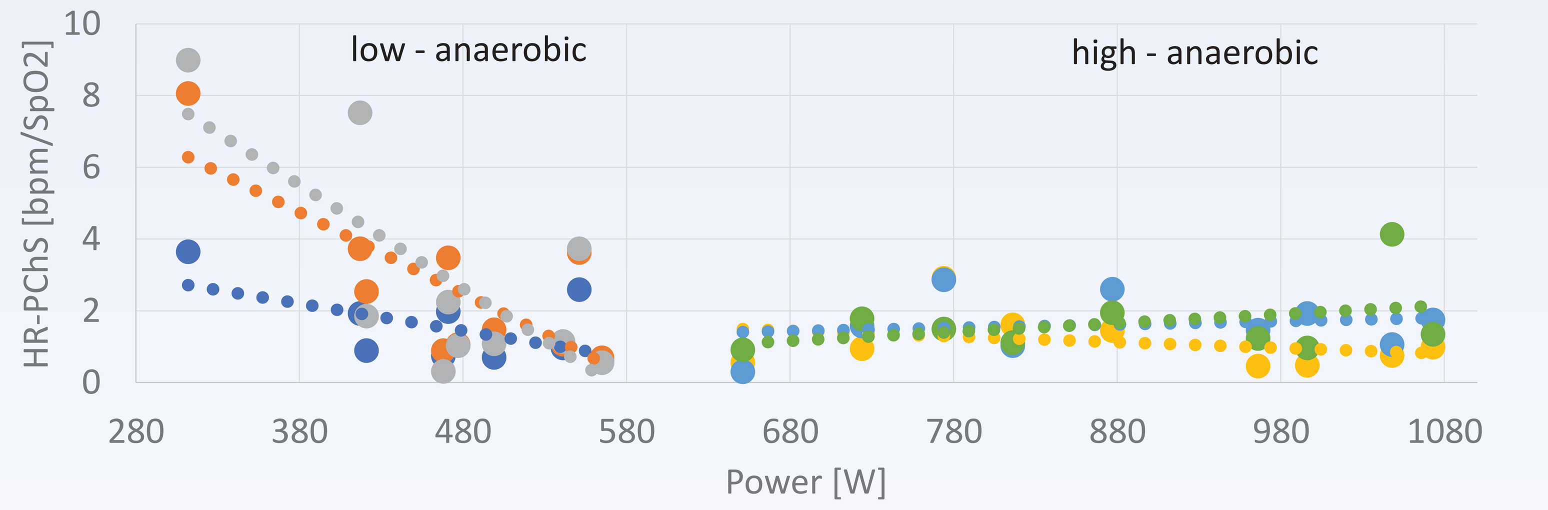

Fig. 4 The mean values of ventilation response in low - and high - fitness group.

Fig. 4 The mean values of ventilation response in low - and high - anaerobic group.

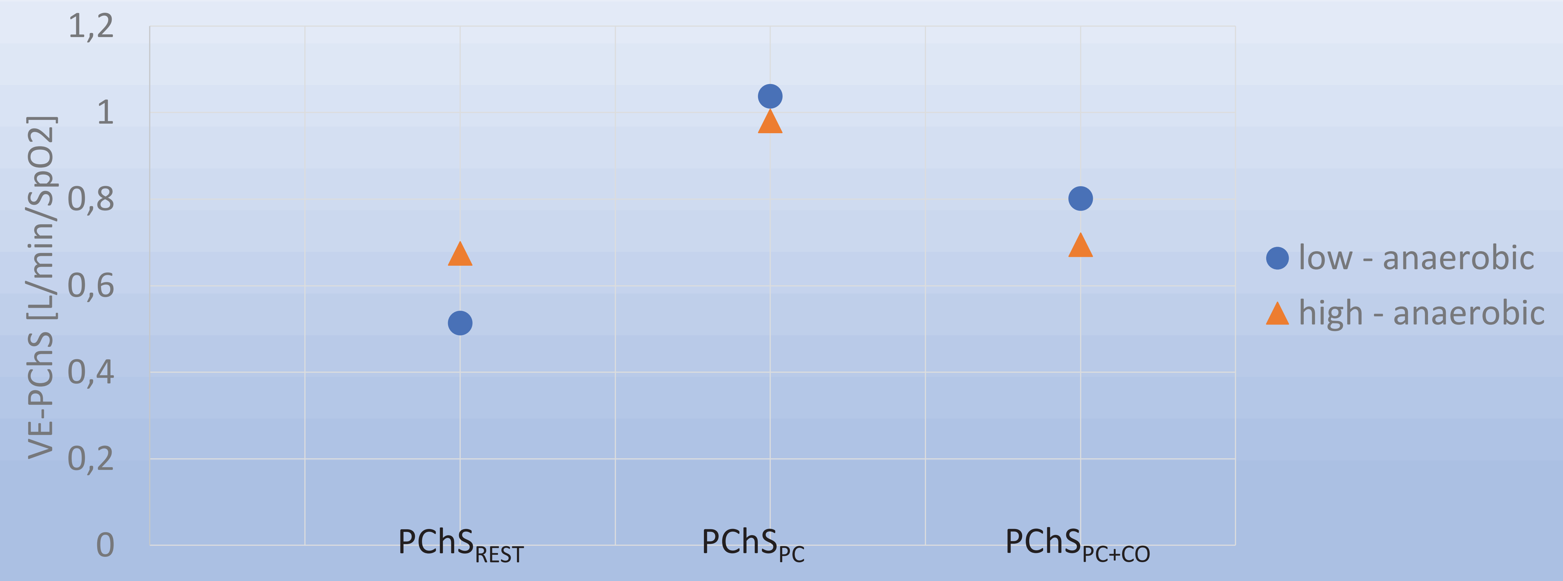

Results and Conclusion

We found no difference in the PChS at rest, during passive cycling and passive cycling with circulatory occlusion of the lower limbs between the high- and low-fitness groups. It can be concluded that the level of the aerobic and anaerobic capacity does not affect the nature of the interaction between the peripheral chemoreflex and the mechano- and metaboreflexes in humans.

CARDIAC PHYSIOLOGY AFTER OSTARINE TREATMENT – *IN VITRO* STUDY ON H9C2 CARDIOMYOCYTES AND FIBROBLASTS

N. Leciejewska[1], P. A. Kołodziejski[1], E. Małek[2], K. Mielnik[1], E. Pruszyńska-Oszmałek[1]

[1]Department of Animal Physiology, Biochemistry and Biostructure, Poznań University of Life Sciences, Poznan, Poland; [2]Department of Preclinical Sciences and Infectious Diseases, Faculty of Veterinary Medicine and Animal Science, Poznań University of Life Sciences, Poznan, Poland; natalia.Leciejewska@up.poznan.pl

Introduction

Selective androgen receptor modulators (SARMs) are anabolic compounds that bind to androgen receptors. They have been studied as potential treatment for cancer, osteoporosis, sexual dysfunction and muscle wasting. Due to their anabolic effects, they have become popular as performance-enhancing supplements. In 2017, the FDA issued a public advisory stating that SARMs were being included in bodybuilding products and that these compounds posed an increased risk for heart attack, stroke, and liver damage.

The aim of the study was to investigate the influence of the most popular SARM - ostarine on the functioning of the heart using in vitro techniques.

Material and methods

H9C2 cardiomyocyte cells and isolated rat cardiac fibroblasts (CF) were used. Fibroblasts were isolated from the ventricles by collagenase digestion. Viability and proliferation at different doses of ostarine were assessed using the MTT and BrdU ELISA test.

ERK phosphorylation was tested at 5, 10, 15, 30 and 45 min and analyzed by Western Blot. αsmooth muscle actin(αSMA) was tested after 72h in cardiac fibroblasts using Western Blots.

Expression of the androgen receptor in cardiac fibroblast and in undifferentiated and differentiated H9C2 myoblasts was assessed by Western Blot.

Results and conclusions

We have shown that ostarine regulate cells by phosphorylate ERK in male CF and H9C2 cell line. We have also shown that in these models, ostarine affects survival and proliferation. No effect was observed on female fibroblasts.

Additionally, we observed that after 72h there was an increase in αSMA protein expression in male CF.

Low-dose ostarine treatment has no significant effect on the heart cells. However, high doses of ostarine can promote the processes of fibrosis in fibroblast cells. Ostarine as one of the most popular SARMs used by athletes as well as a potential drug candidate may be a potential risk factor in the development of cardiovascular disease, but more research is needed.

References

1. Christiansen, A.R.; Lipshultz, L.I.; Hotaling, J.M.; Pastuszak, A.W. Selective androgen receptor modulators: The future of androgen therapy? *Transl. Androl. Urol.* 2020, *9*, S135–S148

2. Leciejewska, N.; Pruszynska-Oszmalek, E.; Bien, J.; Nogowski, L.; Kolodziejski, P.A. Effect of ostarine (Enobosarm/gtx024), a selective androgen receptor modulator, on adipocyte metabolism in wistar rats. *J. Physiol. Pharmacol.*

3. Thevis M, Schänzer W Detection of SARMs in doping control analysis. Mol Cell Endocrinol. 2018 Mar 15;464:34-45

Results and conclusions

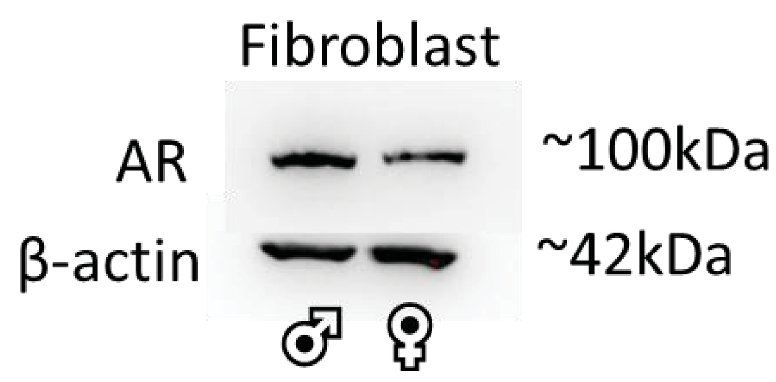

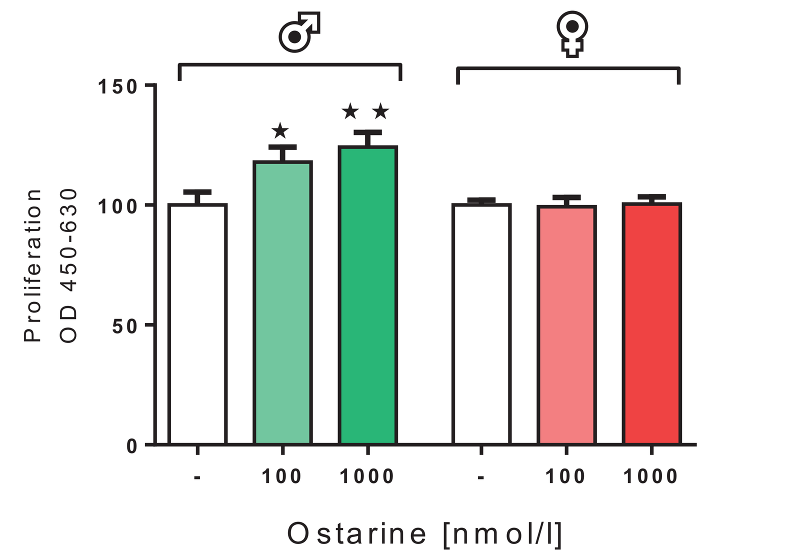

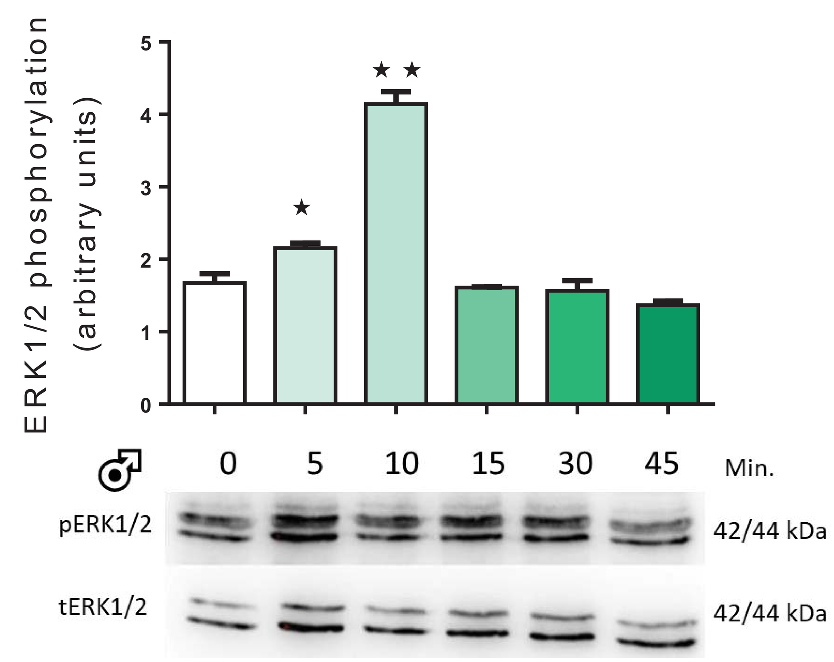

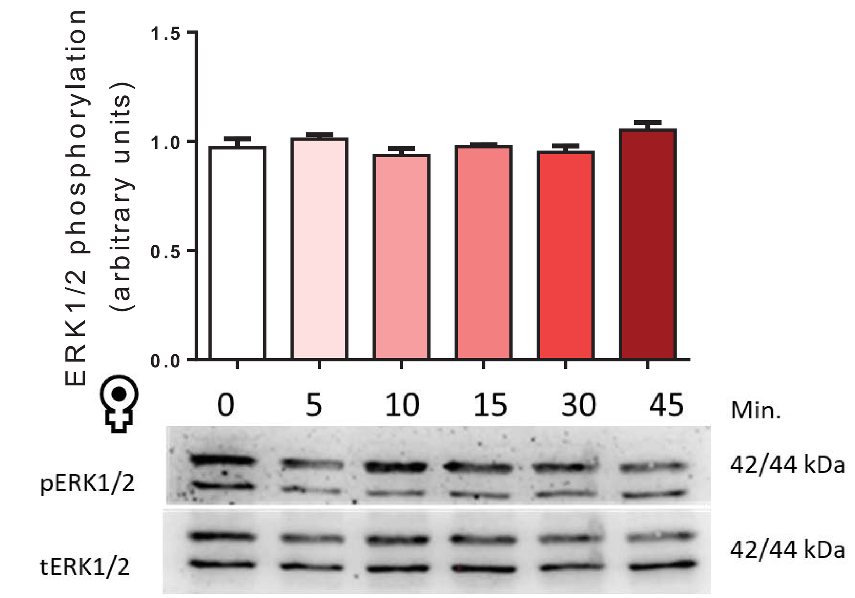

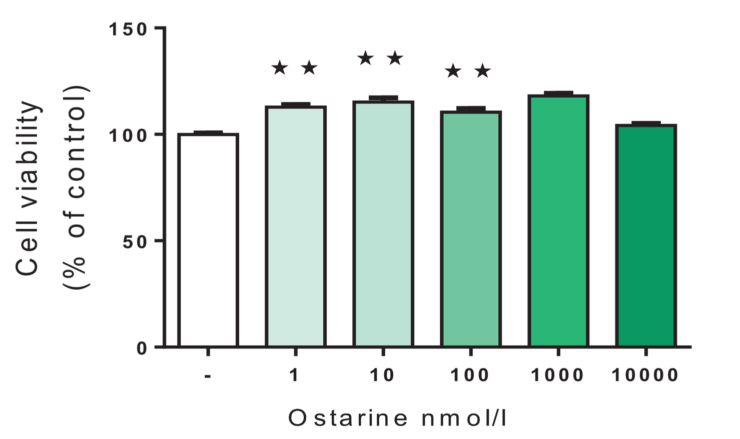

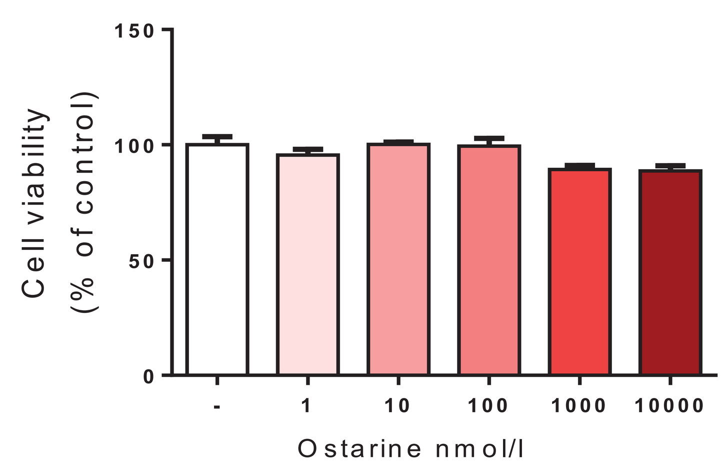

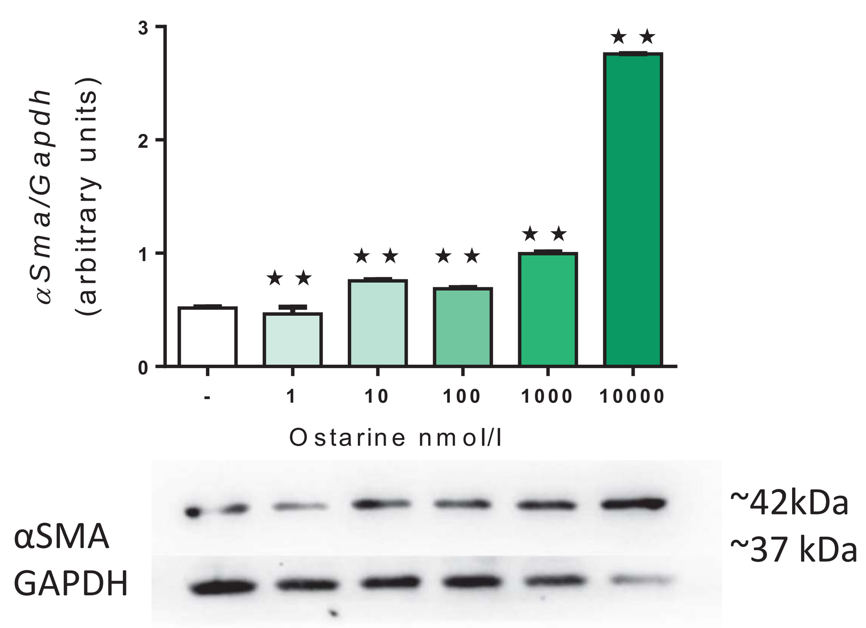

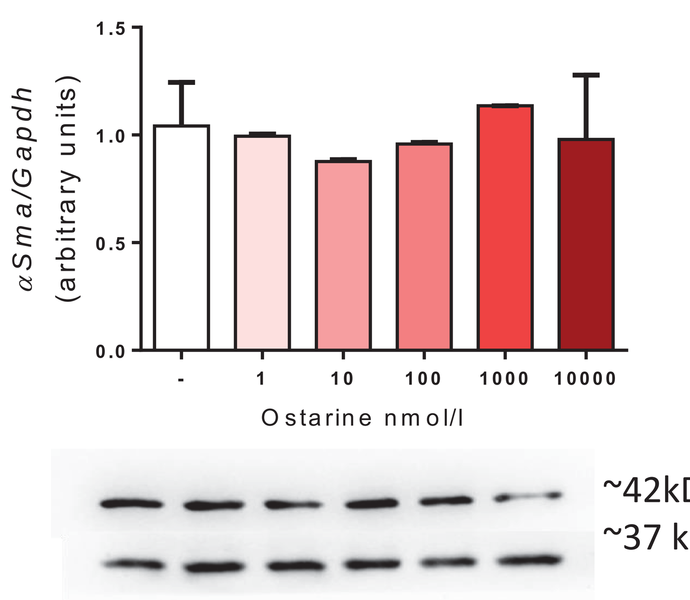

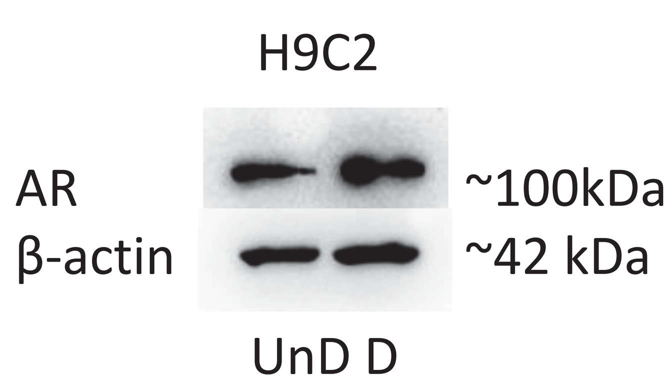

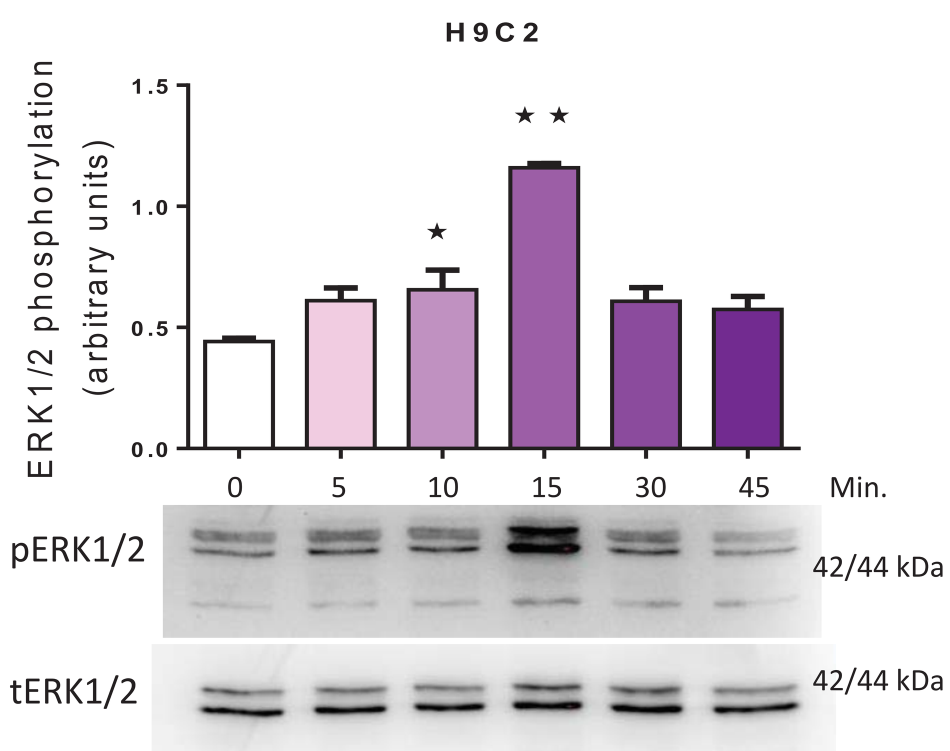

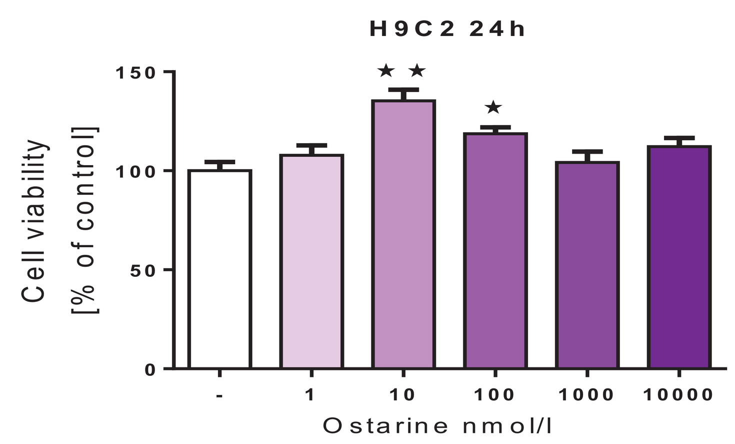

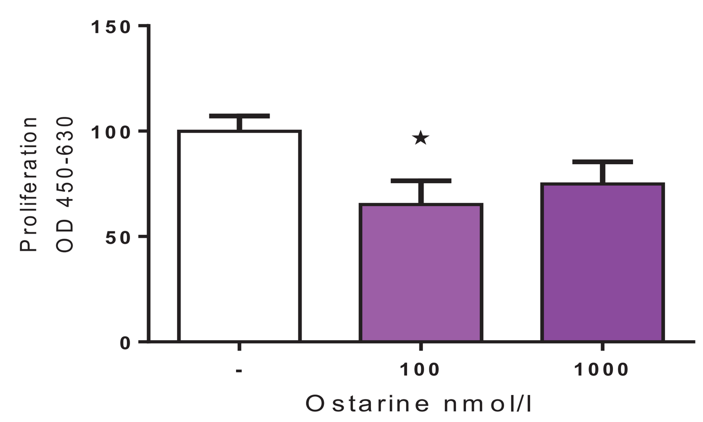

The work was financed by the National Science Centre (project number 2019/35/N/NZ7/00738)

Evaluation of the anti-inflammatory and anti-proliferative properties of cannabidiol in an experimental model of monocrotaline-induced pulmonary hypertension

A. KRZYŻEWSKA[1]*, M. BARANOWSKA-KUCZKO[1,2], I. KASACKA[3], H. KOZŁOWSKA[1]

[1]Department of Experimental Physiology and Pathophysiology, [2]Department of Clinical Pharmacy, [3]Department of Histology and Cytophysiology, Medical University of Bialystok, Poland.

INTRODUCTION

PULMONARY HYPERTENSION (PH)

- leads to right ventricular failure and the patients' death,
- mean pulmonary artery pressure, determined by right heart catheterization ≥25 mmHg,
- small pulmonary arteries (40-100 µm) remodelling
- inflammation plays an important role in the pathogenesis,
- no effective treatment [1].

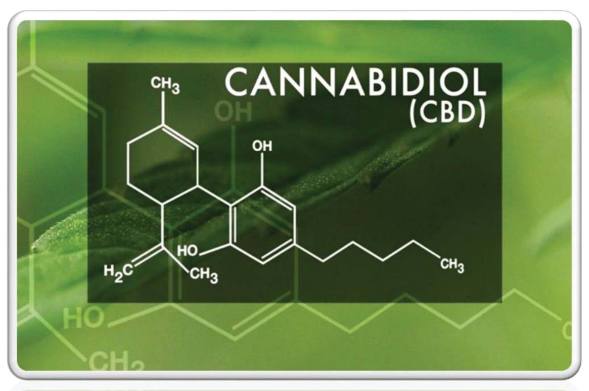

- the relaxant effect in isolated systemic and pulmonary vessels, including human pulmonary arteries,
- decrease right ventricular systolic pressure (RVSP) and pulmonary arterial hypertrophy,
- no psychoactive effect,
- anti-inflammatory effect [2,3].

AIM

The aim of the study was to evaluate the effect of CBD on the selected parameters of inflammation and remodelling in the lungs of rats with PH induced with the plant alkaloid - monocrotaline (MCT) - MCT rats.

MATERIALS and METHODS

Once, MCT *s.c.* at a dose of 60 mg/kg or MCT solvent

CBD *i.p.* at a dose of 10 mg/kg, once daily over a period of 3 weeks

day 21 - end of the experiment

Wistar rats 5-8 weeks old (150-250g)

Day 0 Day 1 Day 21

The rats were divided into the following research groups: two groups without PH: 1/ control (CTR), 2/ control+CBD (CTR+CBD) and analogously two groups with PH: 3/ MCT, 4/ MCT+CBD. Rats' lungs were perfused, frozen at temp. <-80 ^{0}C, and then pulverized in liquid nitrogen. RVSP was determined by right heart catheterization. The galectin-3 (Gal-3), cluster of differentiation 68 (CD68), and interleukin-1β (IL-1β) expression in rat lungs was assessed by immunohistochemistry. Western blot method showed the expression of Gal-3 and CD68 parameters in lung tissue. The concentrations of tumor necrosis factor-alpha (TNF-α), IL1-β and nuclear factor kappa-light-chain-enhancer of activated B cells (NF-κB) parameters in lung tissue as well as macrophage colony-stimulating factor (M-CSF) in serum were performed using ELISA method. Results are shown as means ± SEM of n animals. Statistical comparisons were made using one-way ANOVA followed by Bonferroni's post hoc test. P<0.05 was considered as statistically significant.

RESULTS

Table 1. The effect of chronic administration of CBD on the RVSP.

	CTR	CTR+CBD	MCT	MCT+CBD
RVSP [mmHg]	20.0 ± 1.0 n=6	21.4 ± 1.0 n=6	43.4 ± 4.0 n=6*** vs CTR	28.4 ± 1.0 n=6### vs MCT

***P<0.001; ### P<0.001 compared to the respective group.

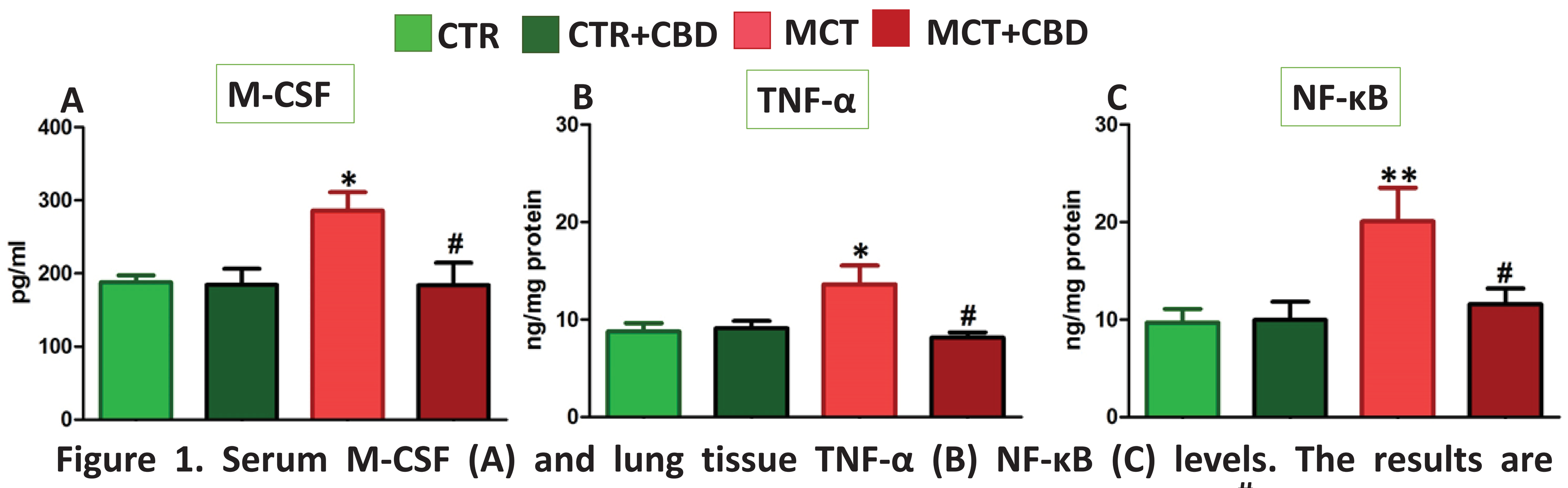

Figure 1. Serum M-CSF (A) and lung tissue TNF-α (B) NF-κB (C) levels. The results are presented as the mean ± SEM of n=6 for each bar. *P<0.05, **P<0.01, #P<0.05 compared to *CTR or #MCT group, respectively.

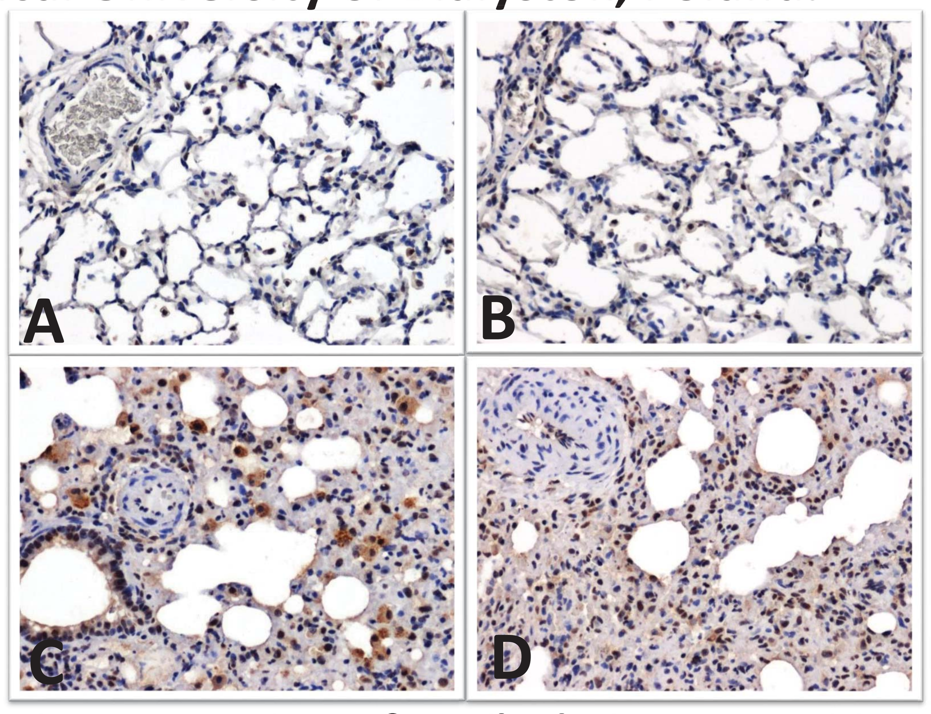

Figure 2. Anti- IL-1β antibody immunopositive staining images in rat lungs; magnification x200. No significant differences were observed in IL-1β immunoreactivity in CTR (A) and CTR+CBD groups (B). A much stronger immunoreactivity of IL-1β was demonstrated in the MCT rats (C). CBD-treated MCT group showed a reduction of the IL-1β-immunoreaction (D).

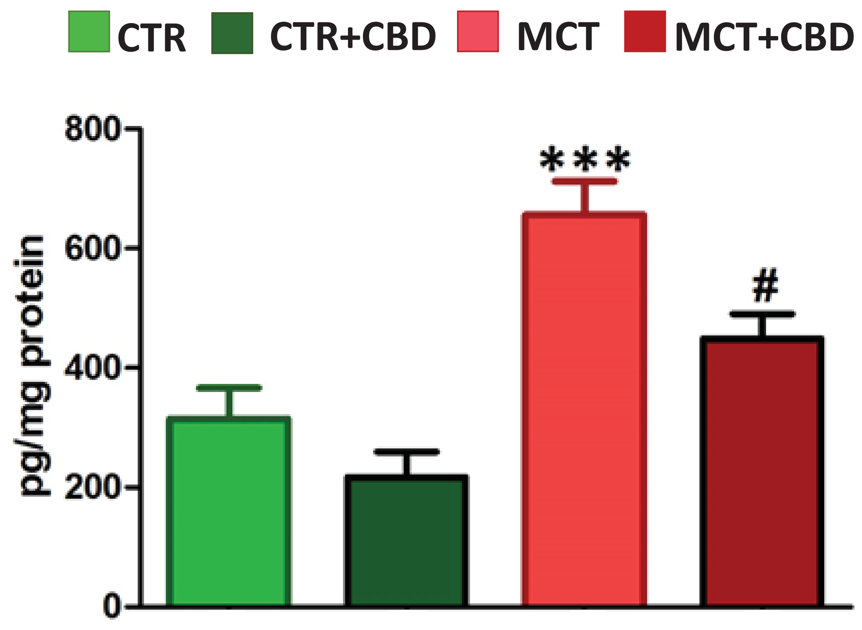

Figure 3. Lung tissue IL-1β levels. The results are presented as the mean ± SEM of n=6 for each bar. ***P<0.001, #P<0.05 compared to *CTR or #MCT group, respectively.

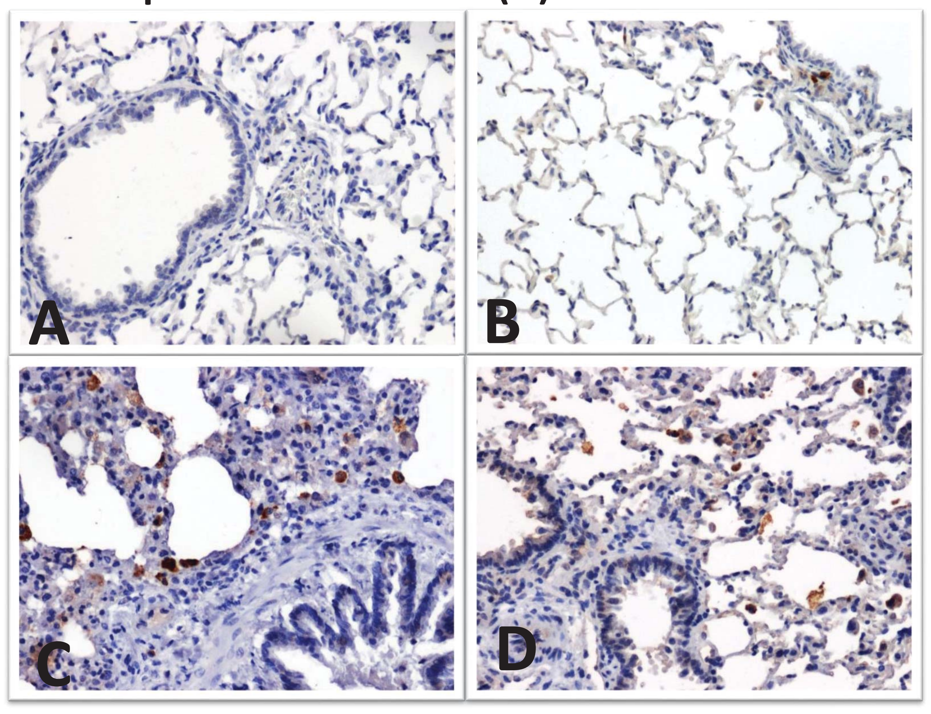

Figure 4. Anti-CD68 antibody immunopositive staining images in rat lung; magnification x200. Immunohistochemical staining revealed the presence of CD68 only in single cells in the lungs of CTR (A) and CTR+CBD (B) groups. MCT rats showed a strong CD68 immunoreactivity (C). Administration of CBD to MCT group lowered the immunoreactivity of CD68 (D).

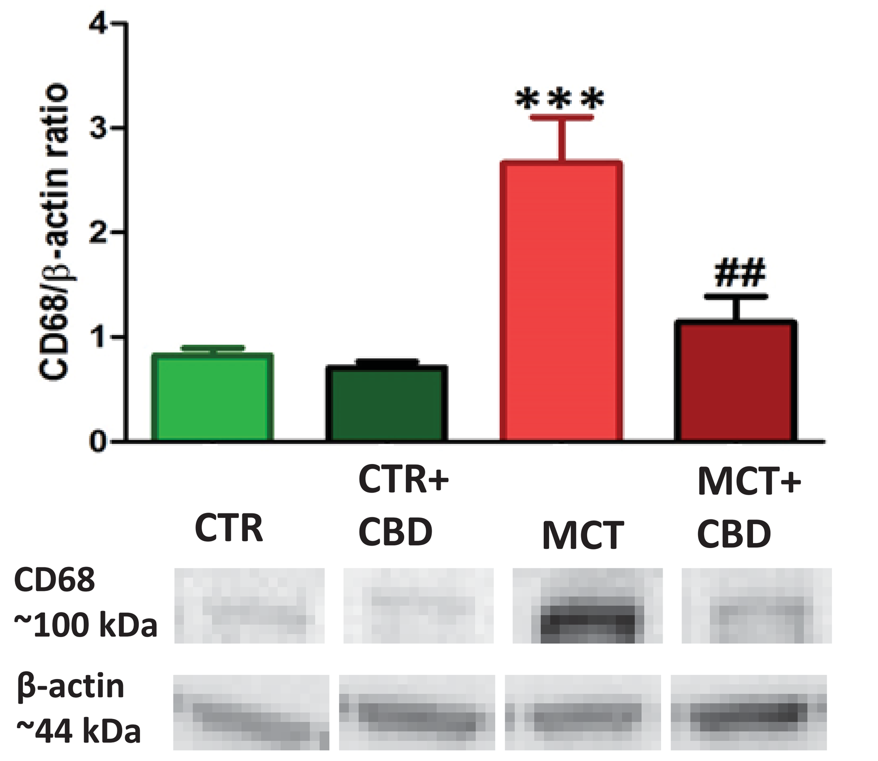

Figure 5. Western blots of CD68 normalized to β-actin. The results are presented as the mean ± SEM of n=6 lung tissues for each bar. ***P<0.001, ##P<0.01 compared to *CTR or #MCT group, respectively.

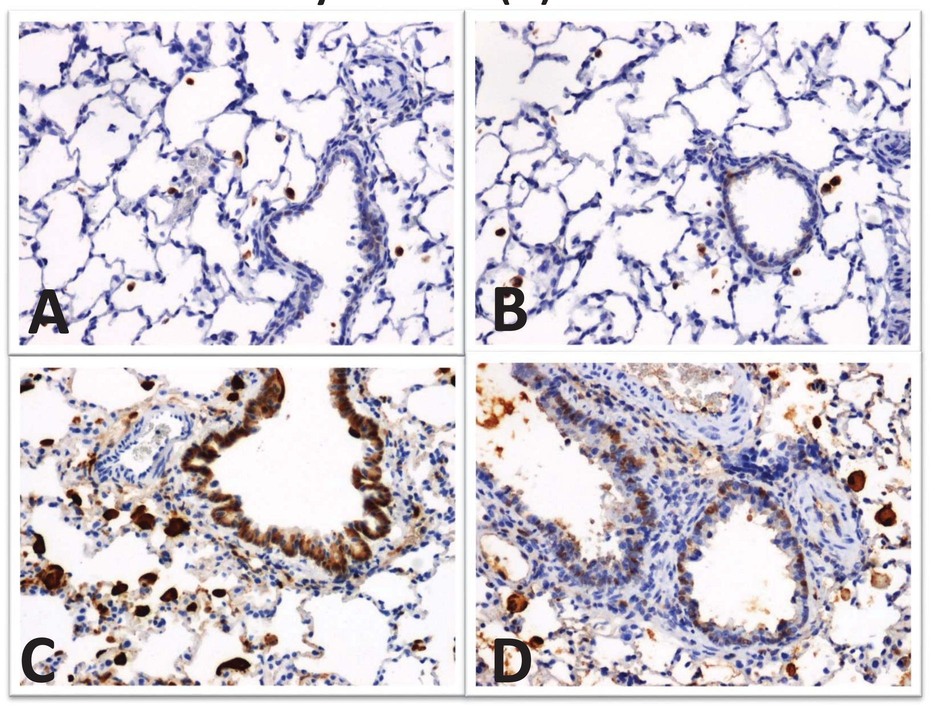

Figure 6. Gal-3 immunostaining images in rat lungs; magnification x200. No significant differences were observed in Gal-3 immunoreactivity in CTR (A) and CTR+CBD groups (B). A strong expression of Gal-3 was found in MCT group (C). Administration of CBD to MCT rats resulted in a reduction in Gal-3 immunoreactivity (D).

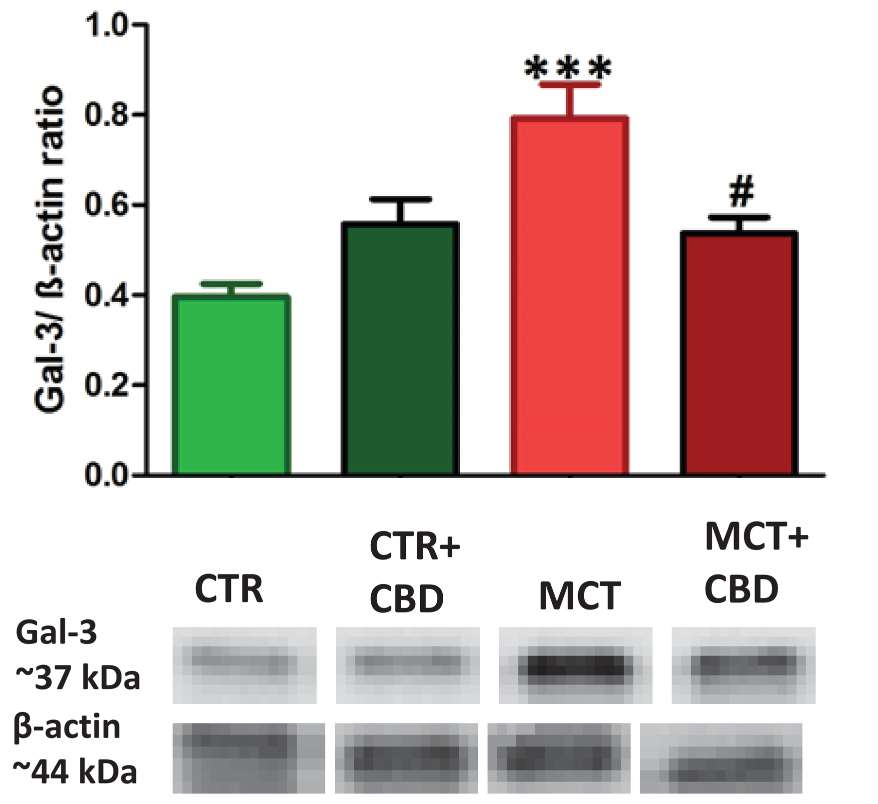

Figure 7. Western blots of Gal-3 normalized to β-actin. The results are presented as the mean ± SEM of n=6 lung tissues for each bar. ***P<0.001, #P<0.05 compared to *CTR or #MCT group, respectively.

CONCLUSION

(1) CBD reduces inflammation (TNF-α, IL-1β, NF-κB, CD68) and remodeling (Gal-3) in the lungs of MCT rats.
(2) Due to the presented properties, CBD may be used as an adjuvant therapy in the treatment of PH. The potential therapeutic effect of CBD should be confirmed in clinical trials.

REFERENCES

[1] Mandras, S.A. et al. Pulmonary Hypertension: A Brief Guide for Clinicians. Mayo. Clin. Proc. 2020, 95, 1978-1988, doi: 10.1016/j.mayocp.2020.04.039.
[2] Kicman, A.; Toczek, M. The Effects of Cannabidiol, a Non-Intoxicating Compound of Cannabis, on the Cardiovascular System in Health and Disease. Int. J. Mol. Sci. 2020, 21, 6740, doi: 10.3390/ijms21186740.
[3] Sadowska O. et al. Cannabidiol Ameliorates Monocrotaline-Induced Pulmonary Hypertension in Rats. Int J Mol Sci. 2020 Sep 25;21(19):7077. doi: 10.3390/ijms21197077.

ACKNOWLEDGEMENTS

This work was supported by Medical University of Bialystok (SUB/1/DN/21/003).

THE EFFECT OF CHOLESTERYL ESTER TRANSFER PROTEIN (CETP) INHIBITORS ANACETRAPIB AND TORCETRAPIB ON LIVER DDAH1 ACTIVITY AND EXPRESSION IN RATS WITH FRUCTOSE INDUCED DYSLIPIDEMIA

EWA KRZEWICKA-ROMANIUK, DAGNA SIEDLECKA, ANNA PRADIUCH, GRAŻYNA WÓJCICKA

Department of Pathophysiology, Medical University of Lublin, Poland, ewakrzewicka@gmail.com

INTRODUCTION: Dimethylarginine dimethylaminohydrolase (DDAH) is an enzyme found in all mammalian cells. There are two isoforms of DDAH – DDAH1 and DDAH2, with some differences in tissue distribution of the two isoforms. DDAH1 predominates in tissues that express neuronal NOS (nitric oxide synthases), while DDAH 2 predominates in tissues expressing endothelial NOS. DDAH degrades methylarginines, specifically asymmetric dimethylarginine (ADMA) and NG-monomethyl-L-arginine (MMA).

Inhibition of DDAH activity causes methylarginines to accumulate, blocking nitric oxide(NO) synthesis and causing vasoconstriction. An impairment of DDAH activity appears to be involved in the elevation of plasma ADMA, and impairment of vascular relaxation observed in humans with cardiovascular disease or risk factors. The activity of DDAH is impaired by oxidative stress.

The cholesteryl ester transfer protein (CETP) inhibitors have ability to elevate high density lipoprotein (HDL) level. It is supposed that protective effect of CETP inhibitors on endothelial function may be HDL-independent and related to its effect on DDAH/ADMA/NO pathway. The present study was undertaken in order to answer the question whether the treatment of anacetrapib or torcetrapib affect liver DDAH1 activity/expression and therefore modulate endothelial function.

Fig. 1

↓DDAH → ↑methylarginines → blocking nitric oxide(NO) synthesis → vasoconstriction

METHODS: The study was carried out on 40 Wistar rats. Dyslipideamia was induced by administration of 20% fructose in drinking water ad libitum for 8 weeks.. Fructose – induced (FRU) dyslipidemic rats were treated for 1 week with anacetrapib (ANA) (3.0mg/kg p.o) or with torcetrapib (TOR) (10mkgg/, p.o).

Study groups:

I. (KON): control group
II. (FRU): receiving 20% fructose solution
III. (FRU + ANA): receiving anacetrapib at a dose of 3 mg / kg / day and 20% fructose solution
IV. (FRU + TOR): receiving torcetrapib at a dose of 10 mg / kg / day and 20% fructose solution

Liver activity of DDAH1 and plasma NO concentration were measured spectrophotometrically. The expression of DDAH1 protein was determined by ELISA method

RESULTS: The administration of both drugs increased plasma NO level in fructose-fed rats. Both ANA and TOR had no effect on liver DDAH1 activity. The significant increase of DDAH1 expression was found in liver of fructose-fed rats treated with torcetrapib (FRU+TOR) vs fructose-fed rats (FRU) and fructose-fed rats treated with anacetrapib (FRU+ANA).

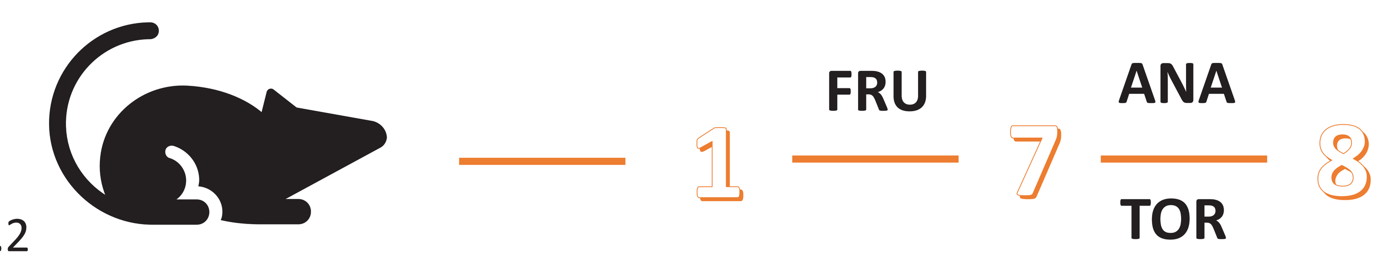

Fig.2

CONCLUSIONS: Treatment with CETP inhibitors increases plasma NO level and affects DDAH1 expression in rats' liver. Therefore, treatment with CETPi –most probably modulate endothelial function in dyslipidemia.

REFERENCES:

1. Leiper JM, Santa Maria J, Chubb A et al. Identification of two human dimethylarginine dimethylaminohydrolases with distinct tissue distributions and homology with microbial arginine deiminases. Biochem J. 1999; 343: 209-214
2. MacAllister RJ, Parry H, Kimoto M, Ogawa T, Russell RJ, Hodson H, Whitley GS, Vallance P (December 1996). "Regulation of nitric oxide synthesis by dimethylarginine dimethylaminohydrolase„. *Br. J. Pharmacol*. **119** (8): 1533–40. doi:10.1111/j.1476-5381.1996.tb16069.x. PMC 1915783. PMID 8982498
3. Simic B, Mocharla P, Crucet M, Osto E, Kratzer A, Stivala S, Kühnast S, Speer T, Doycheva P, Princen HM, van der Hoorn JW, Jukema JW, Giral H, Tailleux A, Landmesser U, Staels B, Lüscher TF. Anacetrapib, but not evacetrapib, impairs endothelial function in CETP-transgenic mice in spite of marked HDL-C increase. Atherosclerosis. 2017, 257:186-194.

THE CHARACTERISTICS OF A SUB-CHRONIC MODEL OF NON-ATOPIC ASTHMA

D. ZAJAC, E. RUSSJAN, AND K. KACZYNSKA

Department of Respiration Physiology, Mossakowski Medical Research Institute, Polish Academy of Sciences, Warsaw, Poland

Introduction

Non-atopic asthma is, contrary to the allergy-related form of the disease, more severe and more difficult to treat as it is less responsive to corticosteroids. It is characterized not only by airway hyperresponsiveness but also by neutrophilia and not, like the allergic one, by eosinophilia. New medications are needed and to develop and test them, good, reliable and stable chronic or sub-chronic animal models of the disease are sought.

Methods

The DNFB/DNS model of non-atopic asthma was used. Mice aged 7-8 weeks weighting 25-30 g were skin-sensitized with DNFB (1-fluoro-2,4-dinitrobenzene) in olive oil:acetone on two consecutive days. 4 days later, the animals were intratracheally challenged with the water-soluble hapten DNS (2,4-dinitrobenzenesulfonic acid). 24hs later, the mice underwent a methacholine (MCh) challenge test in a plethysmographic chamber (Buxco, Fig. 4) using increasing concentrations of MCh of 0, 5, 10, 20 and 40 mg/ml (Day 7, Week 0). During the next two weeks, the animals stayed in the local animal facility under standard conditions. Afterwards, the animals were challenged once again with DNS. 24 hours later, the methacholine test was repeated, and the animals were sacrificed for BALF collection (Day 21, week 2). A scheme of the experiment is shown in Fig. 1.

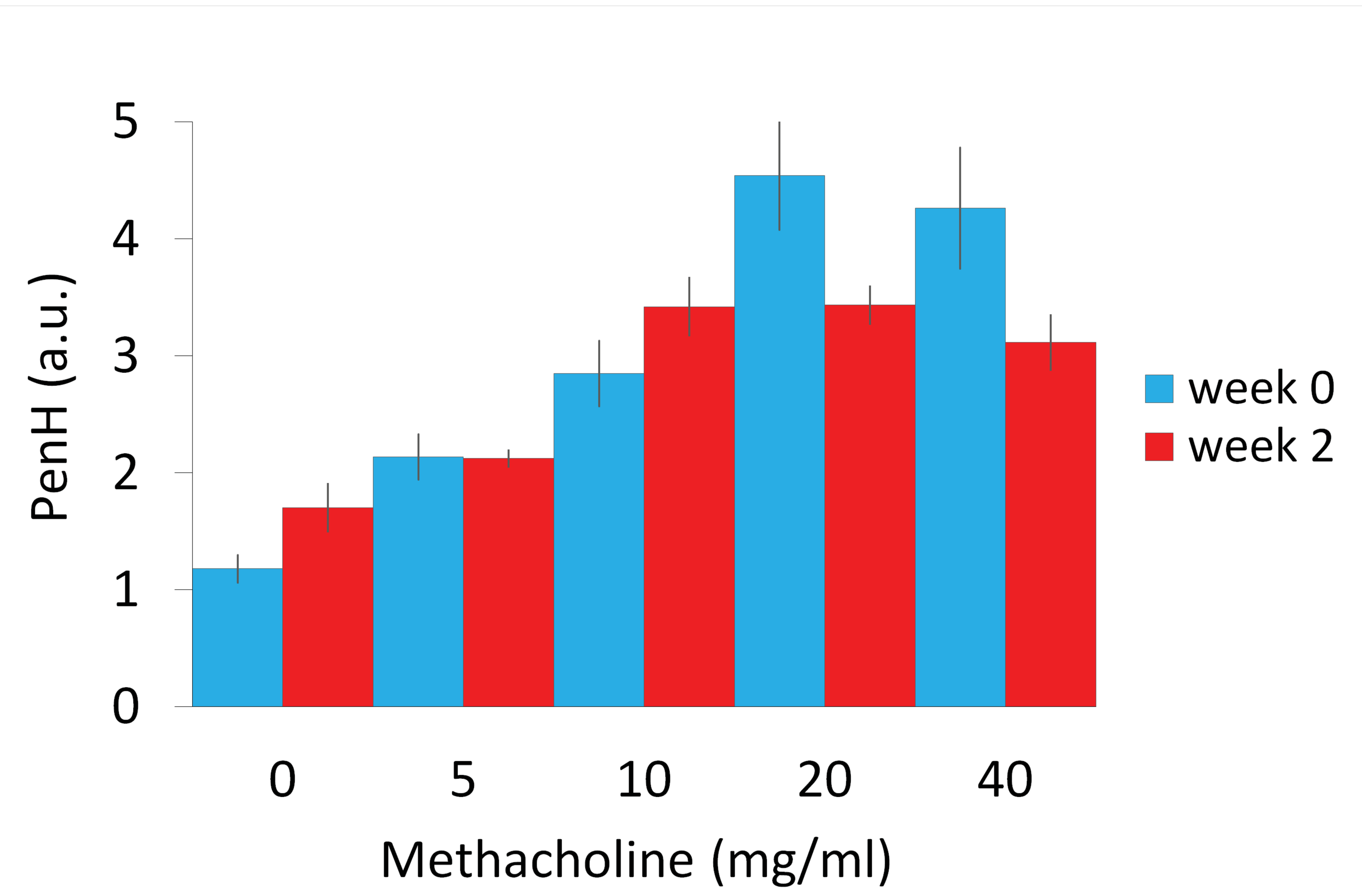

Fig. 2. Airway hyperreactivity measured in the methacholine test

Aim

The aim of the study was to prove if the DNFB/DNS murine model of non-atopic asthma remains stable for two weeks and thus, can be regarded as a good sub-chronic model of the disease.

Results

Basic ventilatory parameters including breathing frequency, tidal volume and minute ventilation did not change within the two weeks (Table 1). Control recordings of airway hyperreactivity showed a typical pattern with growing PenH values in response to increasing concentrations of methacholine (Fig 2, in blue). After two weeks, airway hyperreactivity decreased at higher methacholine concentrations (Fig 2, in red). The total number of cells in BALF increased (Fig. 3 left) but the number of neutrophils, a hallmark of non-atopic asthma, decreased (Fig. 3 right).

Table 1. Basic ventilatory parameters

	Week 0	Week 2
Breathing frequency (1/min)	459.94 ± 16.20	472.73 ± 9.80
Tidal volume (ml)	0.342 ± 0.013	0.344 ± 0.017
Minute ventilation (ml /min)	149.50 ± 8.08	154.35 ± 8.18
Inspiratory time (s)	0.0509 ± 0.0016	0.0506 ± 0.0012
Expiratory time (s)	0.1273 ± 0.0196	0.1388 ± 0.0134
Penh	1.181 ± 0.118	1.702 ± 0.212 #

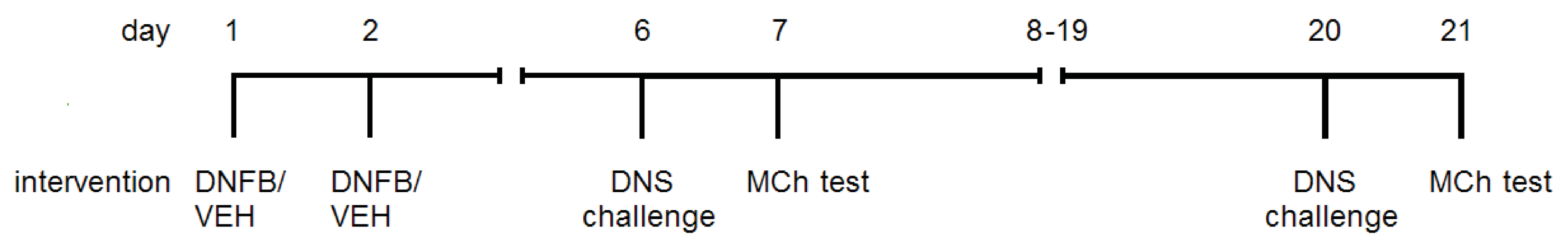

Fig. 1. Experimental procedure

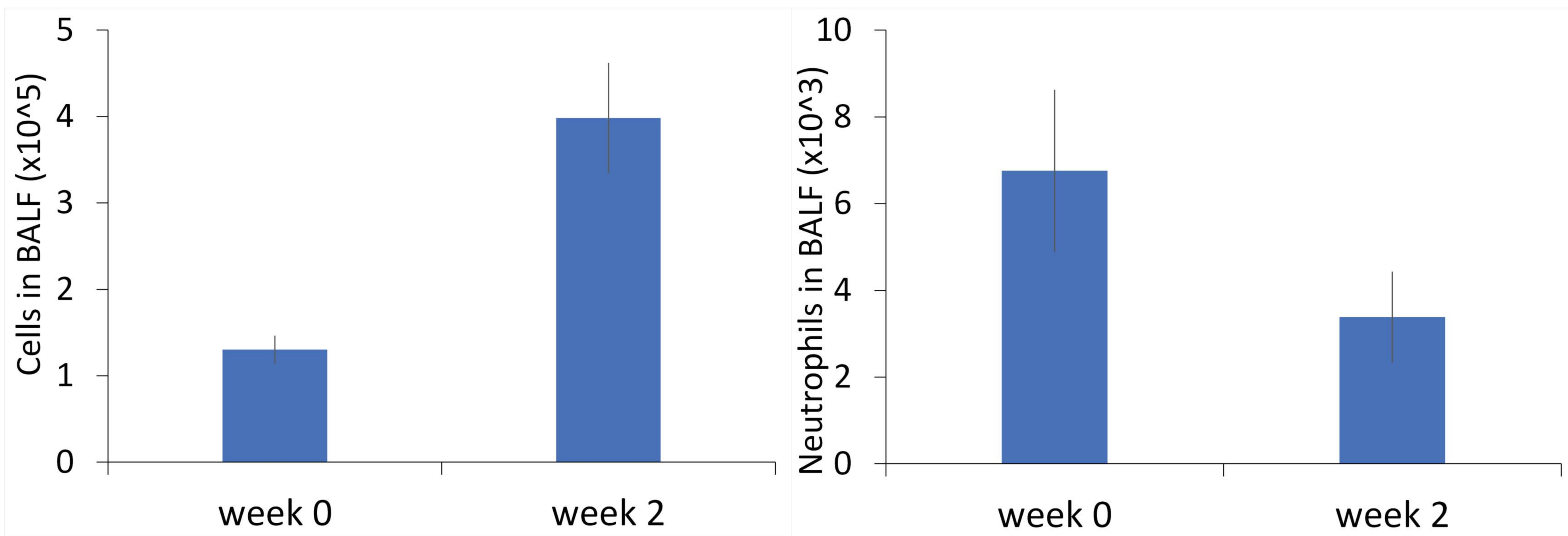

Fig. 3. Number of cells (left) and neutrophils (right) in BALF

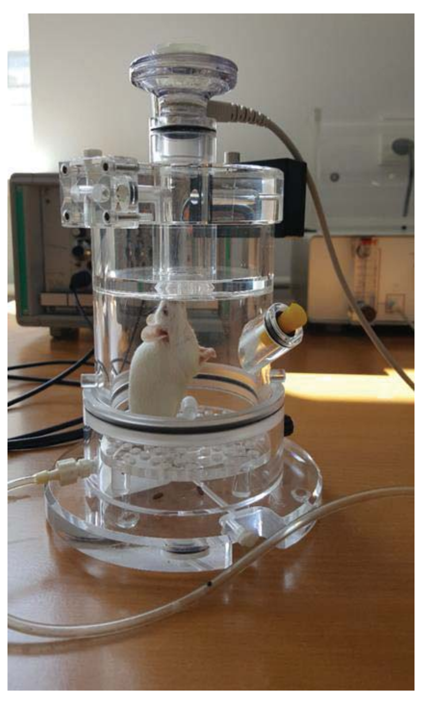

Fig. 4. Methacholine test

Conclusions

Airway hyperreactivity decreases in this DNFB/DNS model with time despite persistent inflammation at the level of cellular influx. Because of the fading of neutrophils, the type of asthma seems to change into a non-neutrophilic one. In consequence, the DNFB/DNS model of non-atopic asthma cannot be seen as a sub-chronic model of the disease without additional interventions including re-sensitization.

Acknowledgments

The research was partially financed by the Polish National Research Centre, MINIATURA research grant 2017/01/X/NZ5/00325 and was partially published in *Int. J. Mol. Sci.* **2020**, *21*, 4798

The effect of cholesteryl ester transfer protein (CETP) inhibitors, anacetrapib and torcetrapib, on plasma and liver Paraoxonase 1 (PON 1) activity and expression in rats with fructose induced dyslipidemia.

D.Siedlecka[1], E.Krzewicka-Romaniuk[1], A.Pradiuch[1], G.Wójcicka[1]
[1] Department of Pathophysiology, Medical University of Lublin, Poland

Introduction and objectives

The paraoxonase family consists of three proteins: PON1, PON2 and PON3. They are differentially expressed and have different functions. PON1 is an antioxidant glycoprotein synthesized in the liver and secreted to the bloodstream. It binds high-density lipoproteins (HDL) and therefore potentiates their antioxidant and antiatherogenic properties.

The cholesteryl ester transfer protein (CETP) inhibitors are a new class of lipid-lowering drugs that can elevate HDL level. However, the development of various cardiovalscular diseases is related to HDL function, rather than HDL level. The present study was undertaken in order to answer the question whether the treatment of anacetrapib or torcetrapib can modulate PON1 activity and expression, the HDL-associated antioxidant enzyme.

Methods

The study was carried out on 40 Wistar rats. Insulin resistance was induced by administration of 20% fructose in drinking water ad libitum for 8 weeks. Fructose – induced (FRU) dyslipidemic rats were treated for 1 week with anacetrapib (ANA) (3.0mg/kg p.o)[1] or with torcetrapib (TOR) (10mg/kg, p.o)[2] (Fig. 1).

Study groups:

I. (KON): control group
II. (FRU): receiving 20% fructose.
III. (FRU + ANA): receiving anacetrapib at a dose of 3 mg / kg / day and 20% fructose.
IV. (FRU + TOR): receiving torcetrapib at a dose of 10 mg / kg / day and 20% fructose.

Plasma and liver activity of PON1 was measured spectrophotometrically. PON1 protein expression was assessed by enzyme immunoassay technique[3,4].

Fig. 1

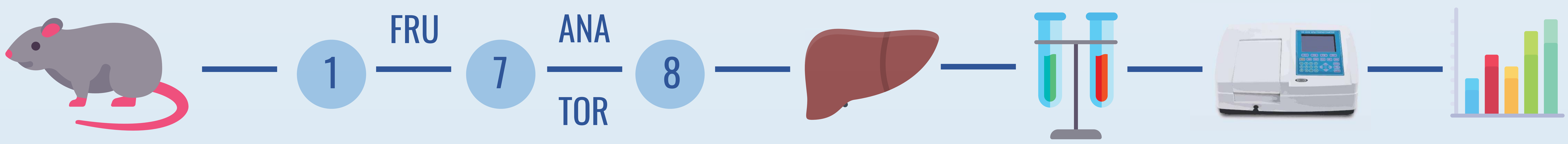

Results

8 weeks of fructose administration resulted in decrease of plasma PON1 activity. By contrast, the significant increase of PON1 activity was found in the liver of fructose-fed rats (FRU). The treatment with anacetrapib and torcetrapib resulted in the significant reduction in PON1 activity in the liver. Moreover, TOR increased the PON1 expression in the liver. Both drugs did not affect PON1 plasma PON1 activity and concentration.

Conclusions

CETP inhibitors can impact PON1 activity and expression in the liver but they had no effect on and HDL antioxidant function.

References

1. Simic B, Mocharla P, Crucet M, Osto E, Kratzer A, Stivala S, Kühnast S, Speer T, Doycheva P, Princen HM, van der Hoorn JW, Jukema JW, Giral H, Tailleux A, Landmesser U, Staels B, Lüscher TF. Anacetrapib, but not evacetrapib, impairs endothelial function in CETP-transgenic mice in spite of marked HDL-C increase. Atherosclerosis. 2017, 257:186-194.
2. Rios FJ, Lopes RA, Neves KB, Camargo LL, Montezano AC, Touyz RM. Off-Target Vascular Effects of Cholesteryl Ester Transfer Protein Inhibitors Involve Redox-Sensitive and Signal Transducer and Activator of Transcription 3-Dependent Pathways. J Pharmacol Exp Ther. 2016, 357(2):415-22
3. Ayub A, Mackness MI, Arrol S, Mackness B, Patel J, Durrington PN. Serum paraoxonase after myocardial infarction. Arterioscler Thromb Vasc Biol. 1999, 19: 330-5.
4. Billecke S, Draganov D, Counsell R, Stetson P, Watson C, Hsu C, La Du BN. Human serum paraoxonase (PON1) isozymes Q and R hydrolyze lactones and cyclic carbonate esters. Drug Metab Dispos. 2000, 28(11):1335-42.

XXVIII Congress of the Polish Physiological Society, Gdańsk, September 15-17 2021, Session VI, Heart. Cardiovascular And Respiratory Regulation

Long-term effect of peripartum depression on the cardiovascular system observed in the adult rat offspring

Jagoda Kruszewska MD[1], Dorota Sztechman DVM[1], Veronica Skital[1], Jasmin Malik[1],
Agnieszka Segiet-Święcicka MD[1], Katarzyna Czarzasta PhD[1], Prof. Elżbieta Sajdel Sułkowska PhD[2]

[1] Department of Experimental and Clinical Physiology, Laboratory of Centre for Preclinical Research, Medical University of Warsaw, Warsaw, Poland
[2] Department of Psychiatry, Harvard Medical School, Boston MA, USA.

INTRODUCTION AND OBJECTIVE

Prenatal depression may affect up to 9.2-19.2% pregnant women. Maternal stress may provide a suboptimal intrauterine environment for the development of the offspring and exposure to such chronic mild stress (CMS) and increased levels of glucocorticoids in utero may lead to dysregulation of fetal hypothalamic-pituitary-adrenal axis and autonomic nervous system, as well as to increased proinflammatory response, all of which may have an impact on the offspring's cardiac development. In our former studies we investigated cardiovascular abnormalities in adolescent (35 days old) rats, born to dams with experimentally induced depression.

The purpose of this study was to assess the function of the cardiovascular system of the adult (six months old) offspring exposed prenatally to pregestational maternal stress.

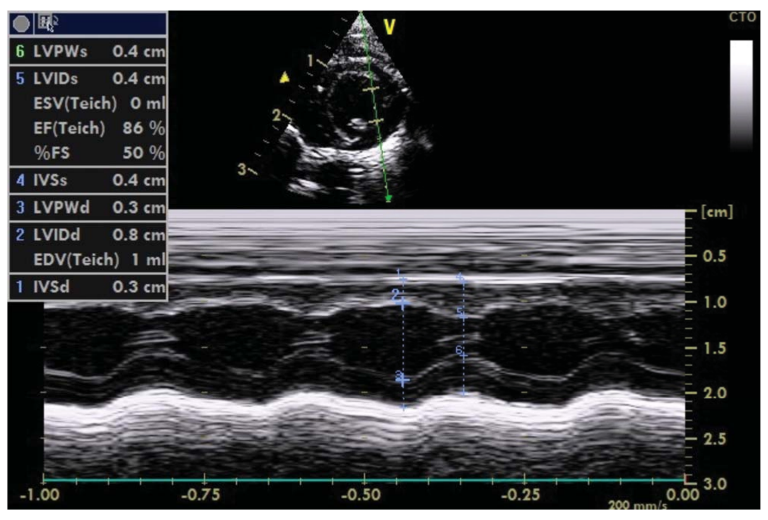

Fig. 2 Echocardiographical assessment of left ventricular (LV) hypertrophy and function in DO

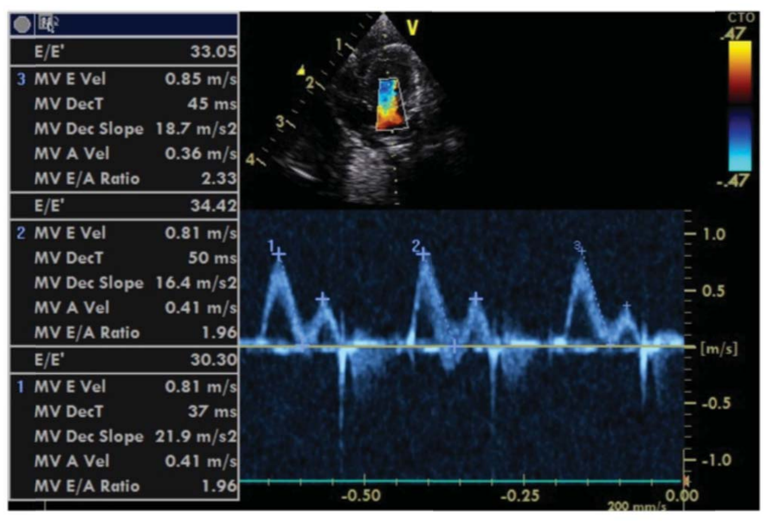

Fig. 3 Echocardiographical assessment of mitral valve (MV) flow in DO

METHODS

Sprague Dawley rat females were randomized into two groups: stress-exposed dams (SD, n=7) subjected to pregestational CMS with repeated restraint paradigm for 8 consecutive weeks, and seven control dams (CD, n=7) handled daily. Afterwards, females from both SD and CD groups were mated with Sprague Dawley males, formerly not subjected to CMS. Prior to and during pregnancy, the development of depression in dams was being assessed by a self-care test (splash test), urinary corticosterone (CORT) concentration and body weight (BW) monitoring (Fig.1). Subsequent studies were carried out on the offspring derived from CD (control offspring; CO, n=12) and SD dams (depressed offspring; DO, n=12). The offspring was examined in terms of cardiovascular health: blood pressure was measured on 216 postnatal day (PD216) and echocardiography (ECHO) was performed on PD225 (Fig. 2,3). The study was approved by the Local Animal Ethics Committee in Warsaw (WAW2/022/2019 and WAW2/090/2019).

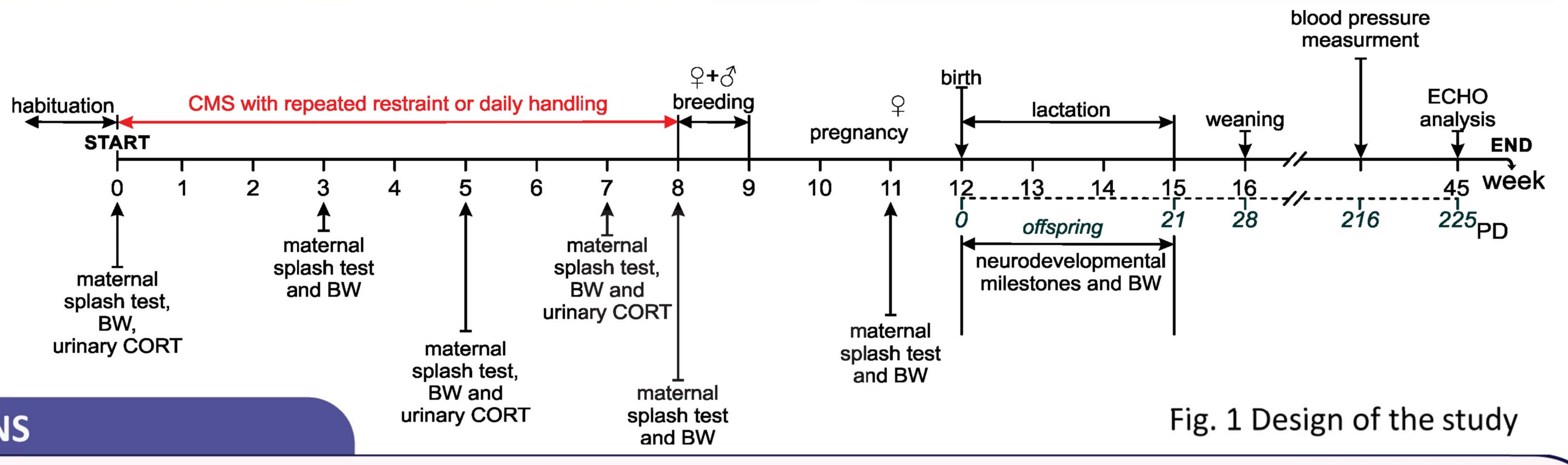

Fig. 1 Design of the study

RESULTS AND CONCLUSIONS

In stressed dams (SD) decreased body mass, as well as increased plasma corticosterone level and weight of adrenal glands were observed, what confirmed the depressive state development. In their offspring (DO) exposure to maternal stress in utero contributed to higher values of blood pressure than in CO (Fig. 4), mild left ventricular (LV) hypertrophy (Fig. 5) and diastolic dysfunction (Fig.6). CMS did not significantly affect the body weight, heart rate, LV weight and systolic function of the depressed offspring (data not shown).

These results suggest that peripartum depression can have a long-term effect on the offspring's cardiovascular system, persisting until adulthood.

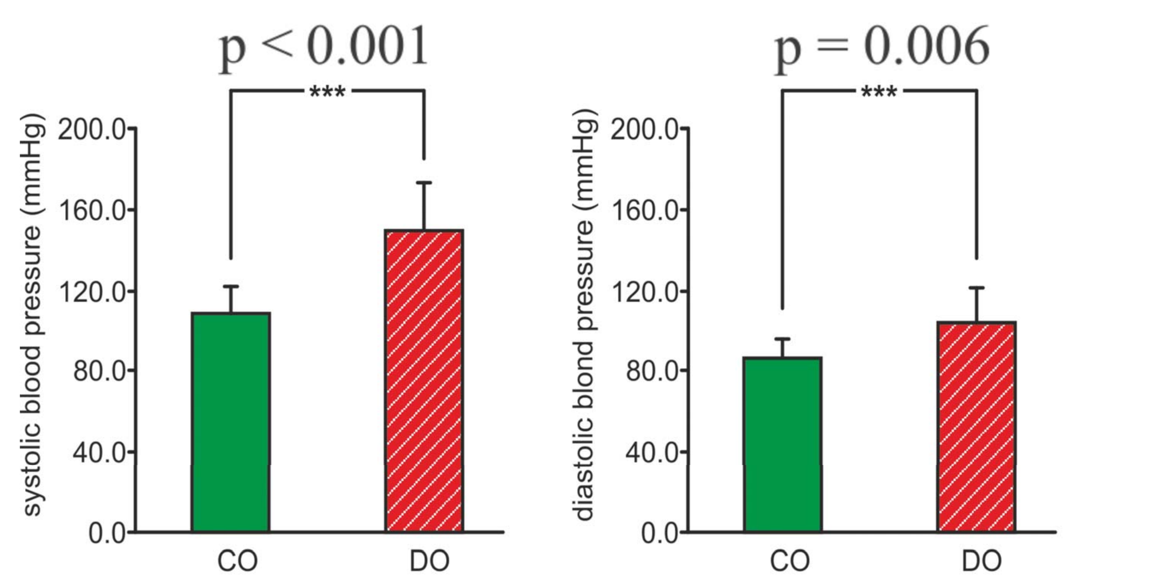

Fig. 4 DO had significantly higher values of both systolic and diastolic blood pressure compared to the CO

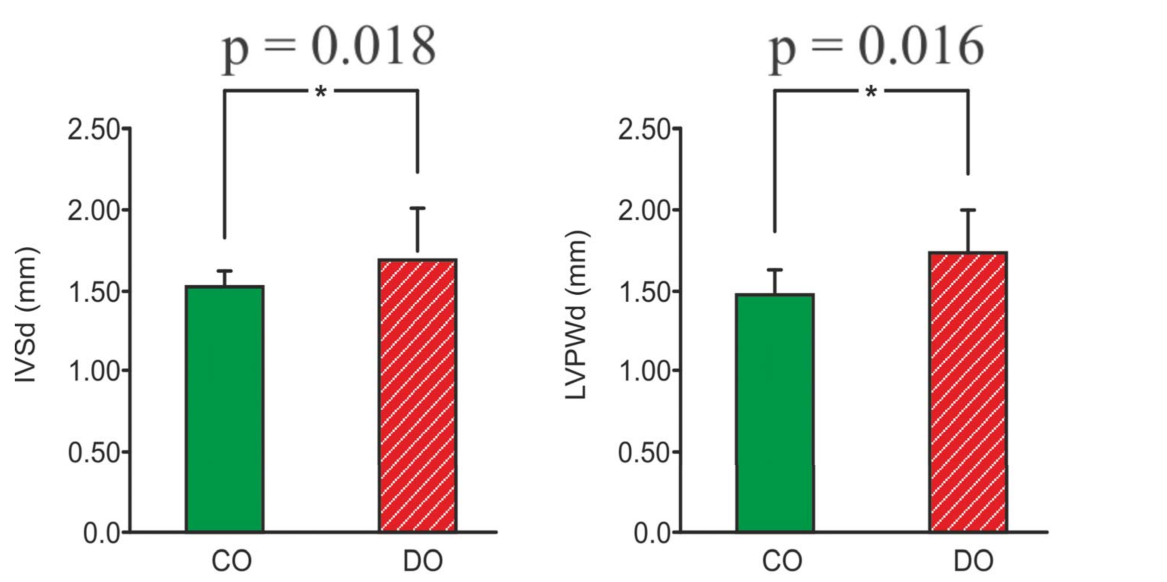

Fig. 5 The interventricular septum thickness at end-diastole (IVSd) and LV posterior wall thickness at end-diastole (LVPWd) were both increased in the DO.

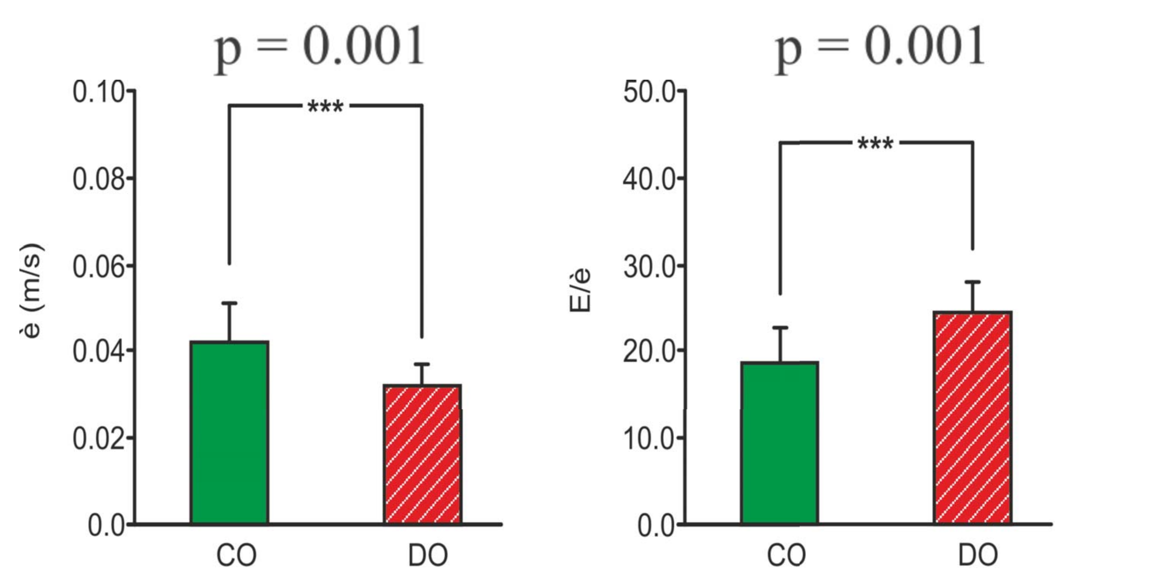

Fig. 6 Significant decrease in the speed of the wave e' and the increased ratio of E/e' was observed in the DO compared to CO.

This project was supported by the Grant Medical University of Warsaw for Young Researcher (1MA/PM2/18), and Grant Medical University of Warsaw for Students (MG/M/8/8/20(1)).

REFERENCES

Woody CA, et al. J Affect Disord. 2017 Sep;219:86-92. doi: 10.1016/j.jad.2017.05.003.
Silva CCV,et al. s. Nutr Metab Cardiovasc Dis. 2019 Jun;29(6):572-579. doi: 10.1016/j.numecd.2019.02.008.
Czarzasta K et al. Stress. 2021 Sep;24(5):652-658. doi: 10.1080/10253890.2020.1845646.
Czarzasta K,et al. Physiol Behav. 2019 Feb 1;199:258-264. doi: 10.1016/j.physbeh.2018.11.024.

ELECTROPHYSIOLOGICAL, HEART RATE VARIABILITY, AND BIOCHEMICAL DISTURBANCES IN A RAT MODEL OF 5-FLUOROURACIL INDUCED CARDIOTOXICITY ARE PARTIALLY REVERSED BY CHRONIC VITAMIN D SUPPLEMENTATION.

Authors: M. Jurczyk[1], P. Stach[1], V. Aleksandrovych[1], A. Midro[1], M. Król[1], B. Kuśnierz-Cabala[2], P. Mazur[3], K. Jasiński[4], A. Poniatowski[1], K. Gil[1]

[1] Department of Pathophysiology, Jagiellonian University Medical College, Cracow, Poland; [2]Department of Diagnostics, Chair of Clinical Biochemistry, Jagiellonian University Medical College, Poland; [3]Department of Medical Diagnostics, Faculty of Pharmacy, Jagiellonian University Medical College, Cracow, Poland; [4]Institute of Nuclear Physics of the Polish Academy of Sciences, Department of Magnetic Resonance Imaging, Cracow, Poland.

Introduction: 5-fluorouracil (5-FU) is one of the most commonly used drug belonging to the fluoropyrimidines. Disturbances of cardiac muscle are common and dangerous side effects of fluoropyrimidines, including: chest pain, arrhythmias, heart failure, and myocardial infarction. Cardiovascular complications most commonly occur during the first dose.

Aim: The aim of the study was to evaluate electrophysiological, heart rate variability (HRV), and biochemical changes observed after subsequent doses of 5-fluorouracil and after attempting to reduce cardiotoxicity using vitamin D supplementation.

Methods: 60 adult male Wistar rats were included in the study. The rats were randomized into four groups:
In group 1, the rats received 0.9% saline p.o. daily;
In group 2, the rats received vitamin D (500IU/kg) p.o. daily;
In group 3, the rats received up to 4 doses of 5-FU (150mg/kg) i.p. injection every two weeks with 0.9% saline p.o. daily;
In group 4, the rats received up to 4 doses of 5-FU (150mg/kg) i.p. every two weeks with vitamin D (500IU/kg) p.o. daily.
Vitamin D or water p.o. administration began four weeks before the first dose of 5-FU.

Results and Conclusions

The first dose of 5-FU decreased both mean heart rate (289 vs 275, p=0.22) and systolic blood pressure (sBP)(119 vs 103, p=0.02), meanwhile SDNN (3.22 vs 4.08, p=0.13) and HRV triangular index (1.51 vs 1.72, p=0.03) were increased.

After the third dose of 5-FU heart rate decreased promptly (292 vs 253, p=0.01), and at the same time indicators of sympathetic activity were decreased.

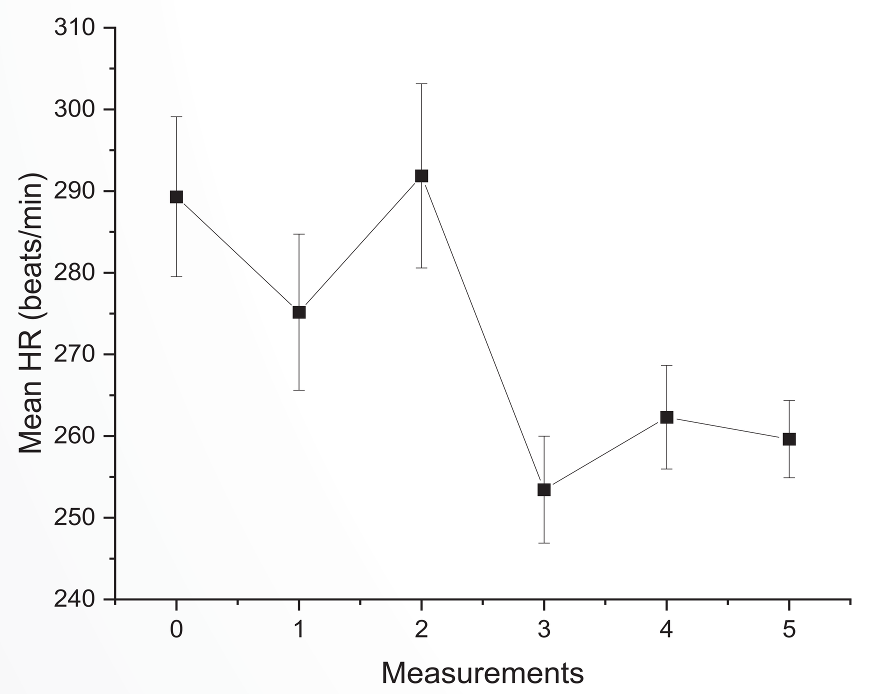

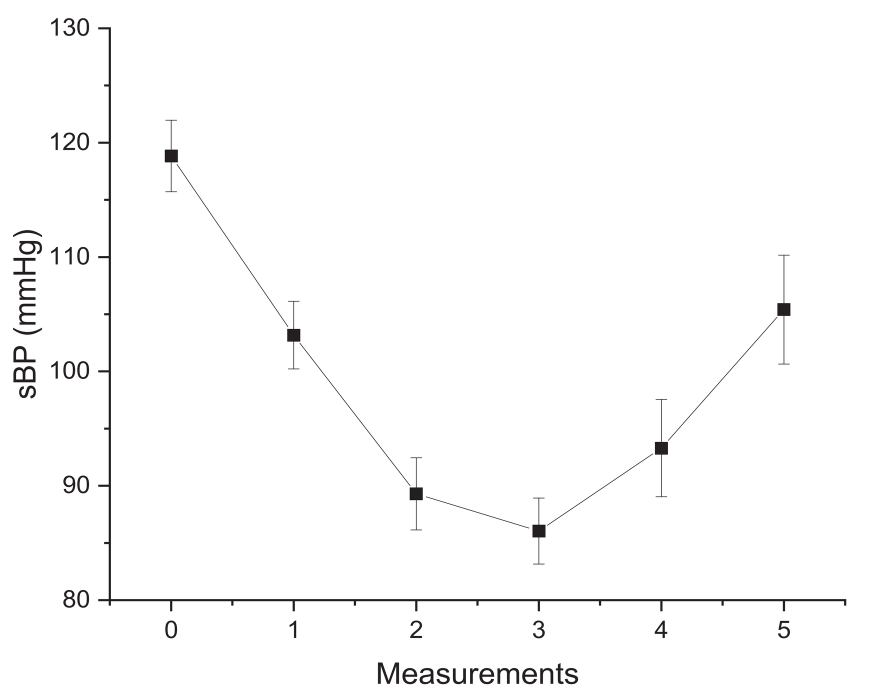

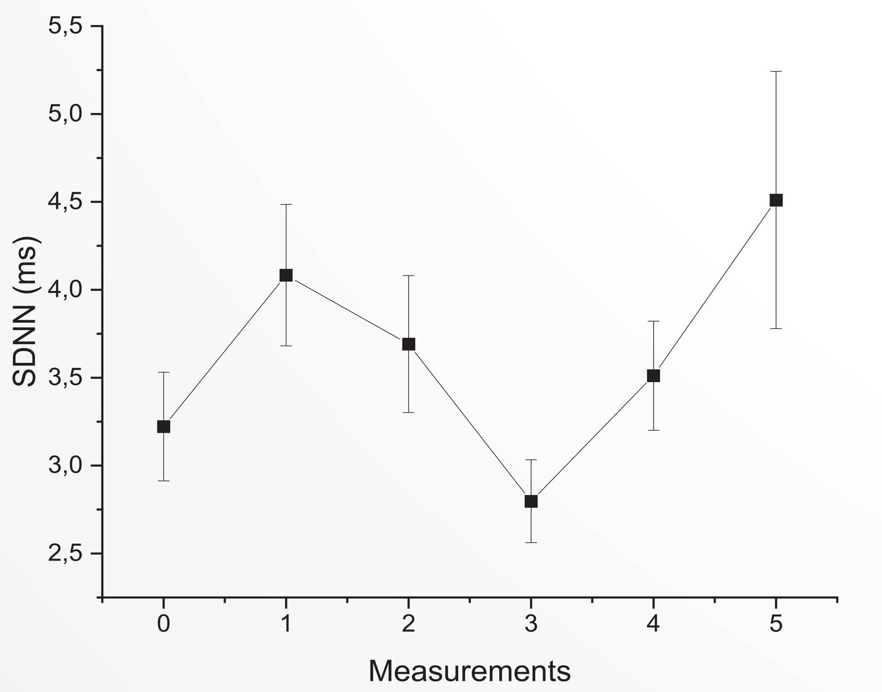

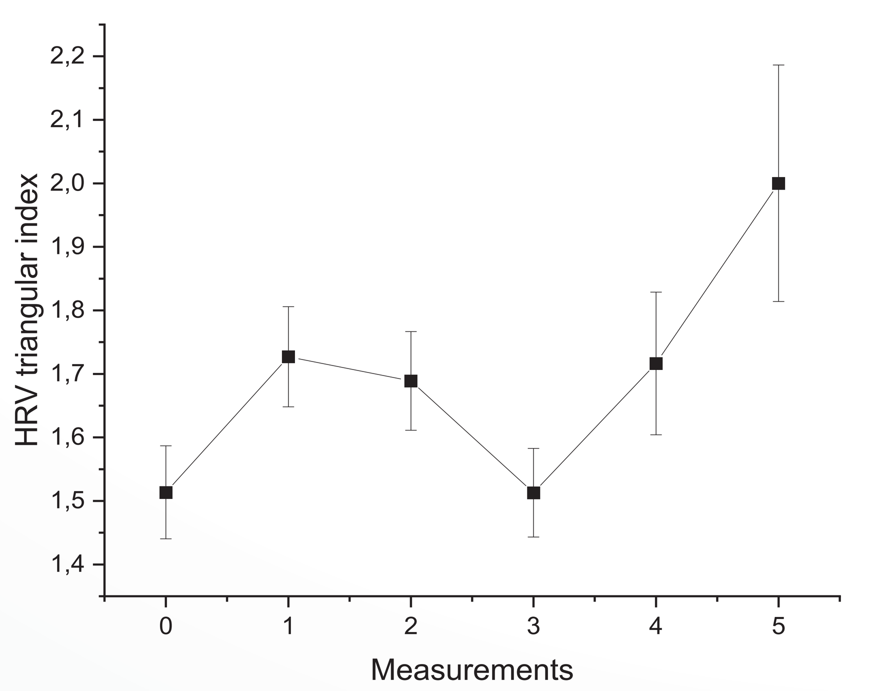

First dose of 5-FU increased duration of QRS (34.4 vs 40.1, p=0.13) and QT (55.8 vs 62.1, p=0.08). Interestingly, the lowest HR was observed after the third dose and did not correlate with the longest QRS and QT. 5-FU administration affected TnI concentration after the first dose (0 vs 6.65, p=0.049) and after four doses (0 vs 11.92, p<0.01).

In groups 1 and 2 such significant changes were not observed.

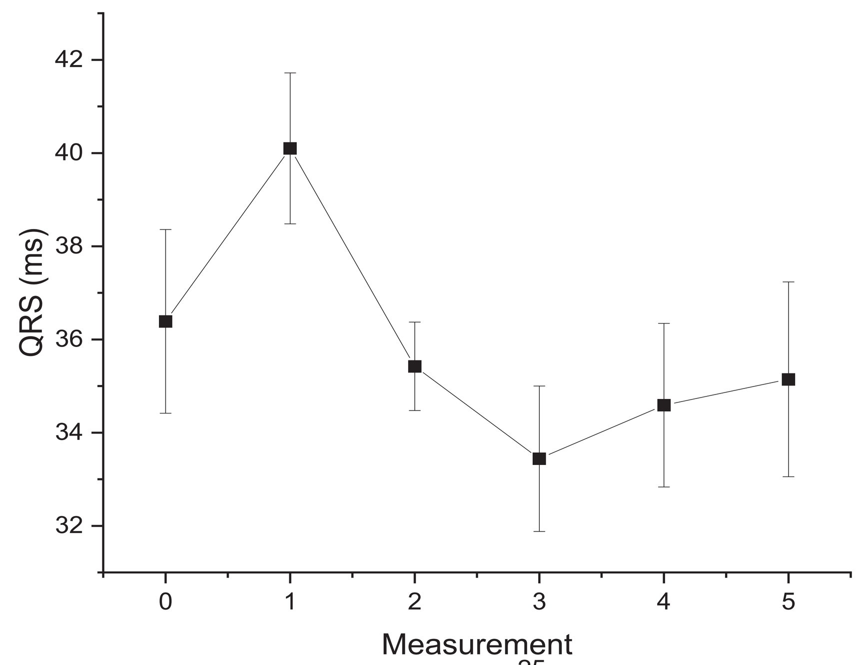

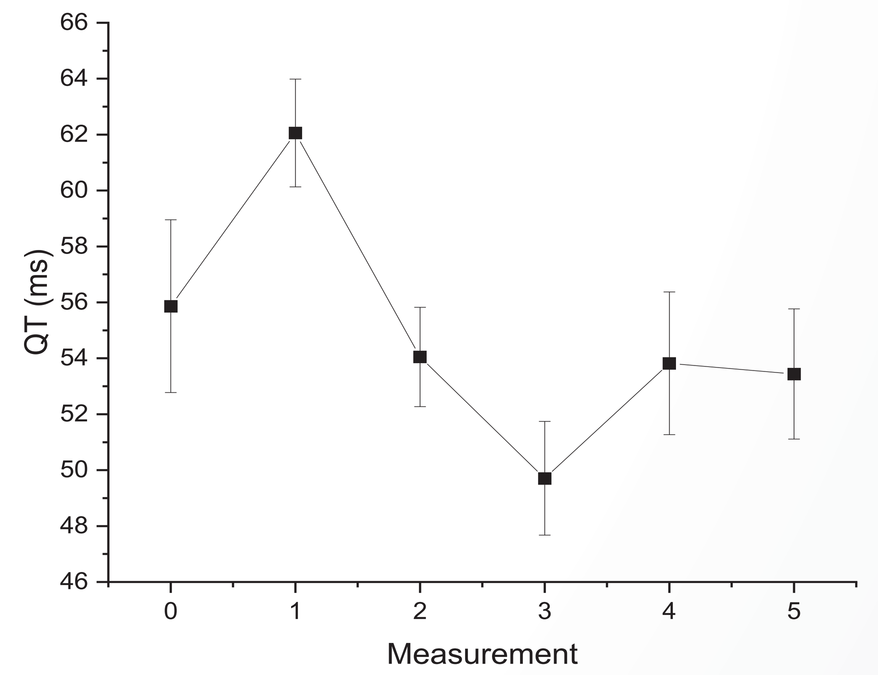

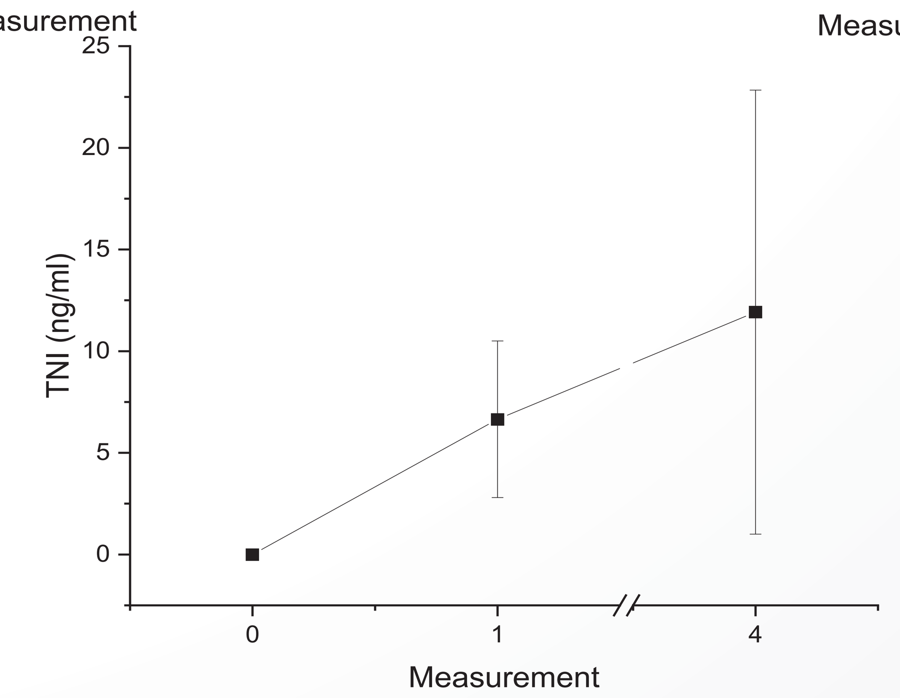

The most of 5-FU associated cardiotoxicity occurs during first administration. Vitamin D chronić administration partially prevented decrease in heart rate (260 vs 292, p=0.14) and sBP (100 vs 107, p=0.19).

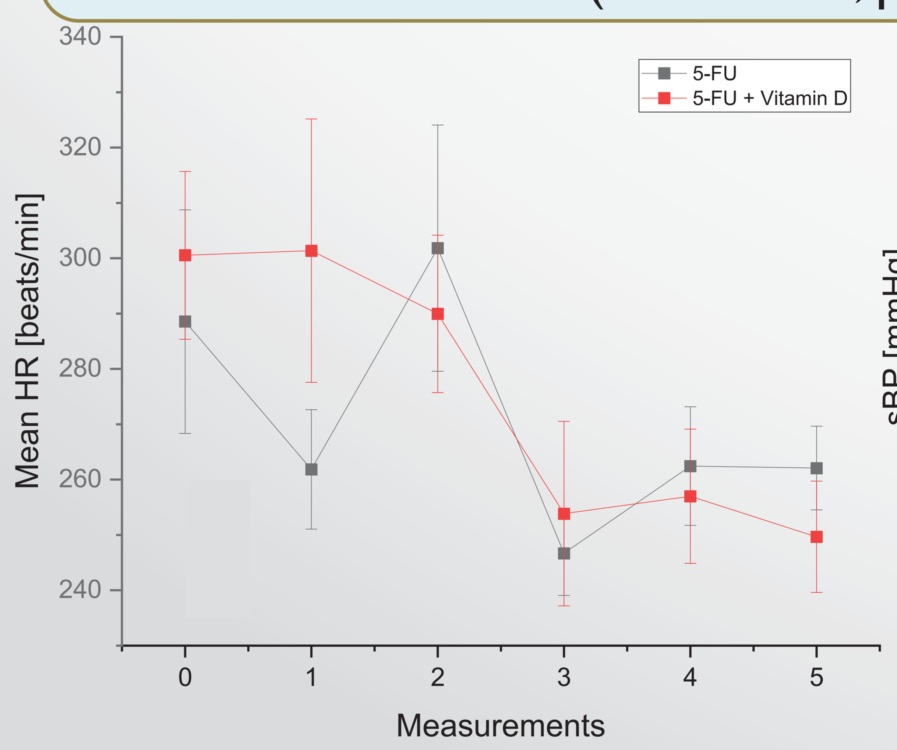

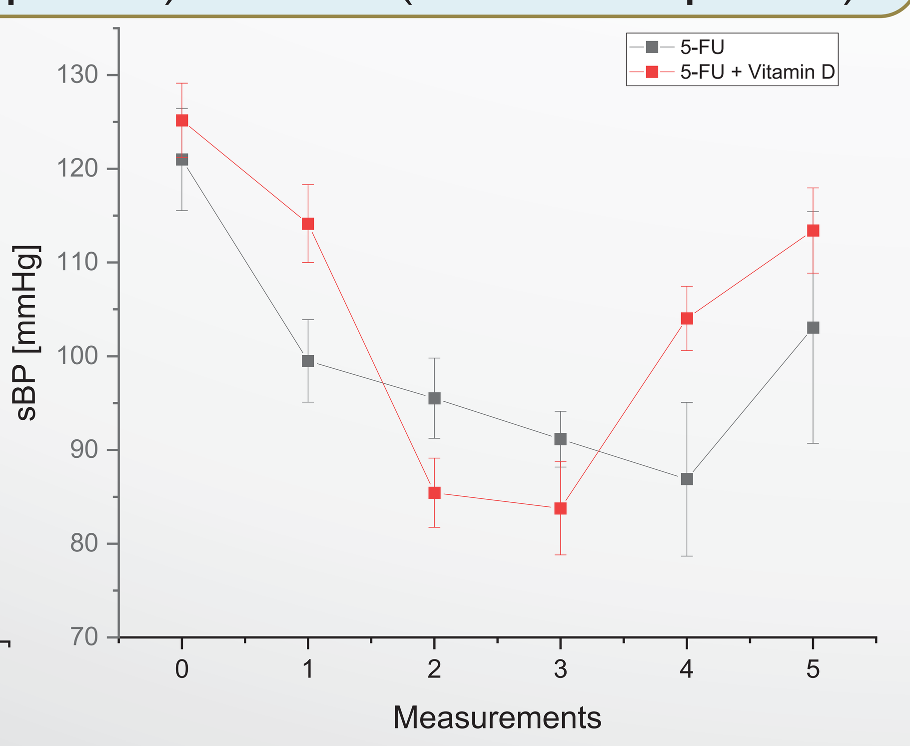

Conclusions: Repeated 5-FU administrations, predominantly the first dose, influenced heart rate variability, electrophysiological and biochemical heart parameters.
Chronic vitamin D supplementation partially prevented 5-FU evoked effects.

UNIWERSYTET JAGIELLOŃSKI
COLLEGIUM MEDICUM

Tumour necrosis factor receptors type 1 and type 2 are expressed in the brainstems of normotensive and hypertensive rats

Agnieszka Segiet-Święcicka, Katarzyna Czarzasta, Tymoteusz Żera

Chair and Department of Experimental and Clinical Physiology
Laboratory of Centre for Preclinical Research
Medical University of Warsaw, Poland

Introduction

1) Tumour necrosis factor (TNF) is a pleiotropic cytokine involved in the regulation of the cardiovascular system. TNF exerts its proinflammatory effects via TNF type 1 receptors (TNFR1), whereas anti-inflammatory effects are mediated by TNF type 2 receptors (TNFR2).

2) Increased level of TNF in the brain has been implicated in arterial hypertension.

3) The evidence of expression of TNFR1 and TNFR2 in the cardiovascular centres of the brainstem is limited.

Objectives

We aimed to determine the expression of TNFR1 and TNFR2 in the brain regions encompassing cardiovascular centres in normotensive Wistar-Kyoto (WKY) and spontaneously hypertensive (SHR) rats.

Methods

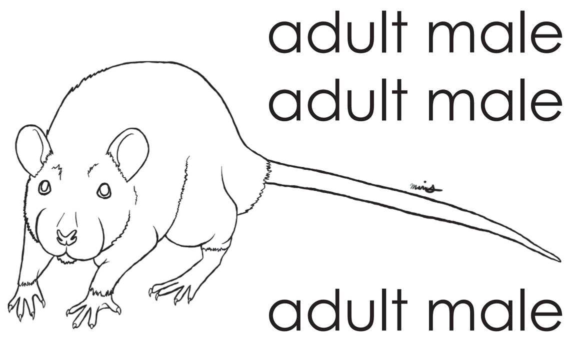

adult male SHR (n=6)
adult male WKY (n=6)

- non-invasive systolic blood pressure (SBP) measurement (tail-cuff method)
- brains harvesting

TNFR1 and TNFR2 mRNA expression (RT-PCR) in:
- dorsal medulla (containing NTS)
- ventral medulla (containing RVLM)
- hypothalamus

adult male SHR (n=2)
adult male WKY (n=2)

- non-invasive SBP measurement (tail-cuff method)
- brains harvesting

immunostaining of TNFR1 and TNFR2 in the brainstem and in the hypothalamus

Results

TNFR1 and TNFR2 mRNA expression

There were no significant differences in the mRNA expression of TNFR1 and of TNFR2 between SHR and WKY rats in the dorsal medulla (DM) containing NTS, ventral medulla (VM) containing RVLM and hypothalamus (HTH).

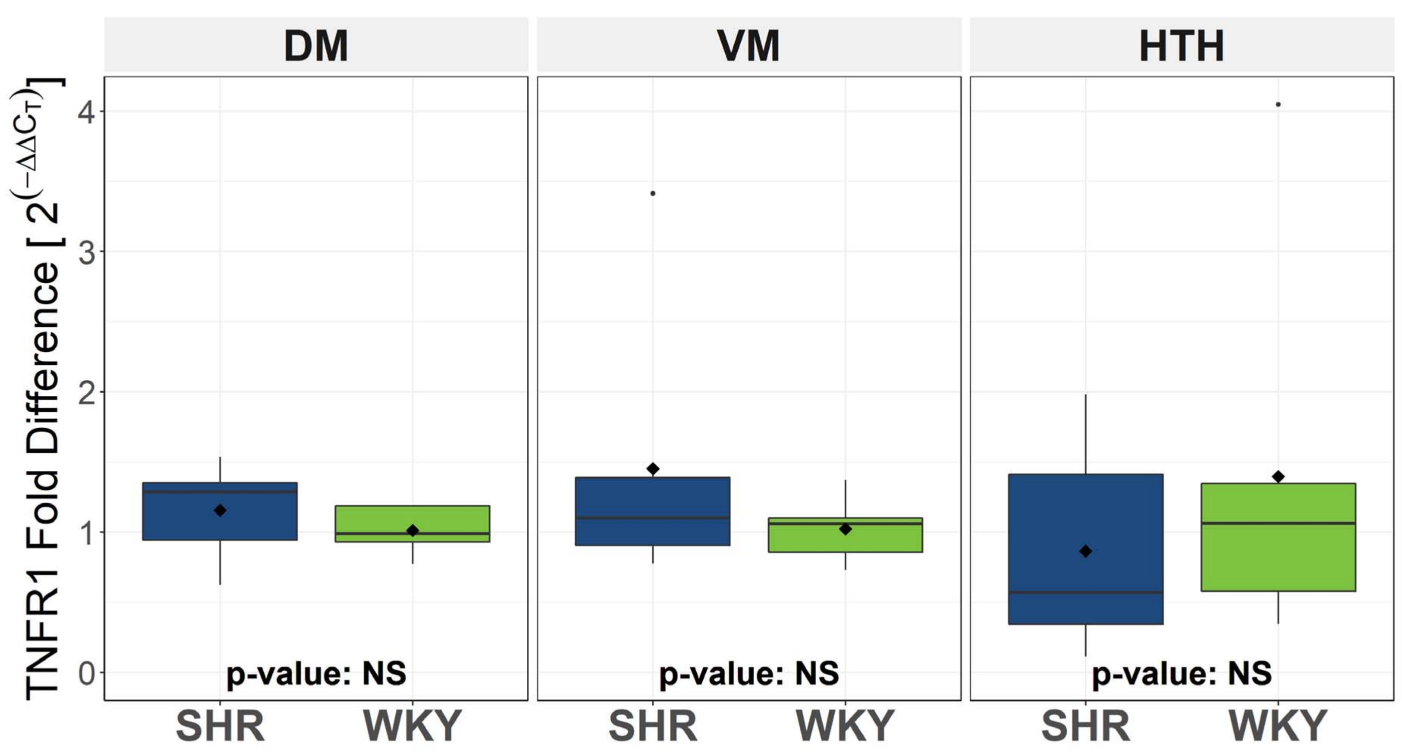

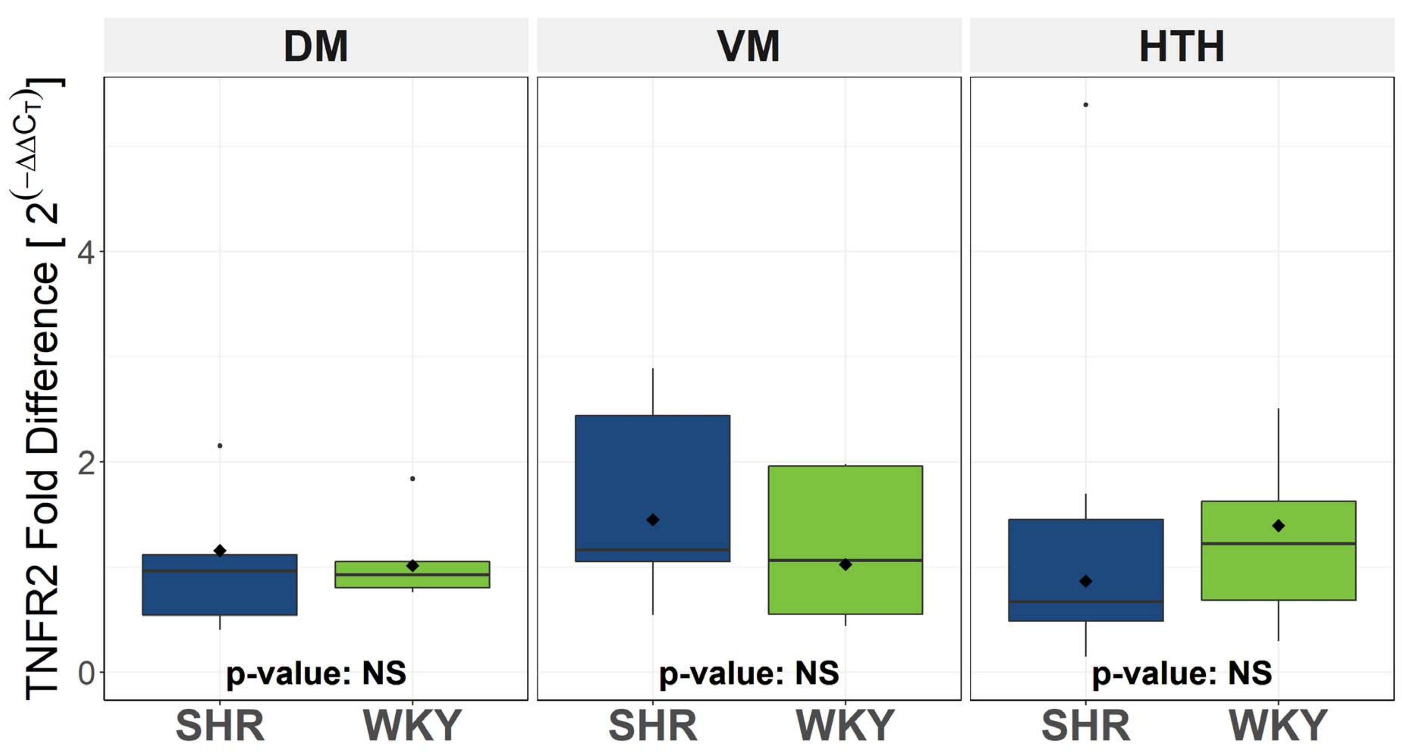

Immunostaining of TNFR1 and TNFR2

Immunostaining revealed presence of both subtypes of TNF receptors in the brainstem and in the hypothalamus in both SHR and WYK rats.

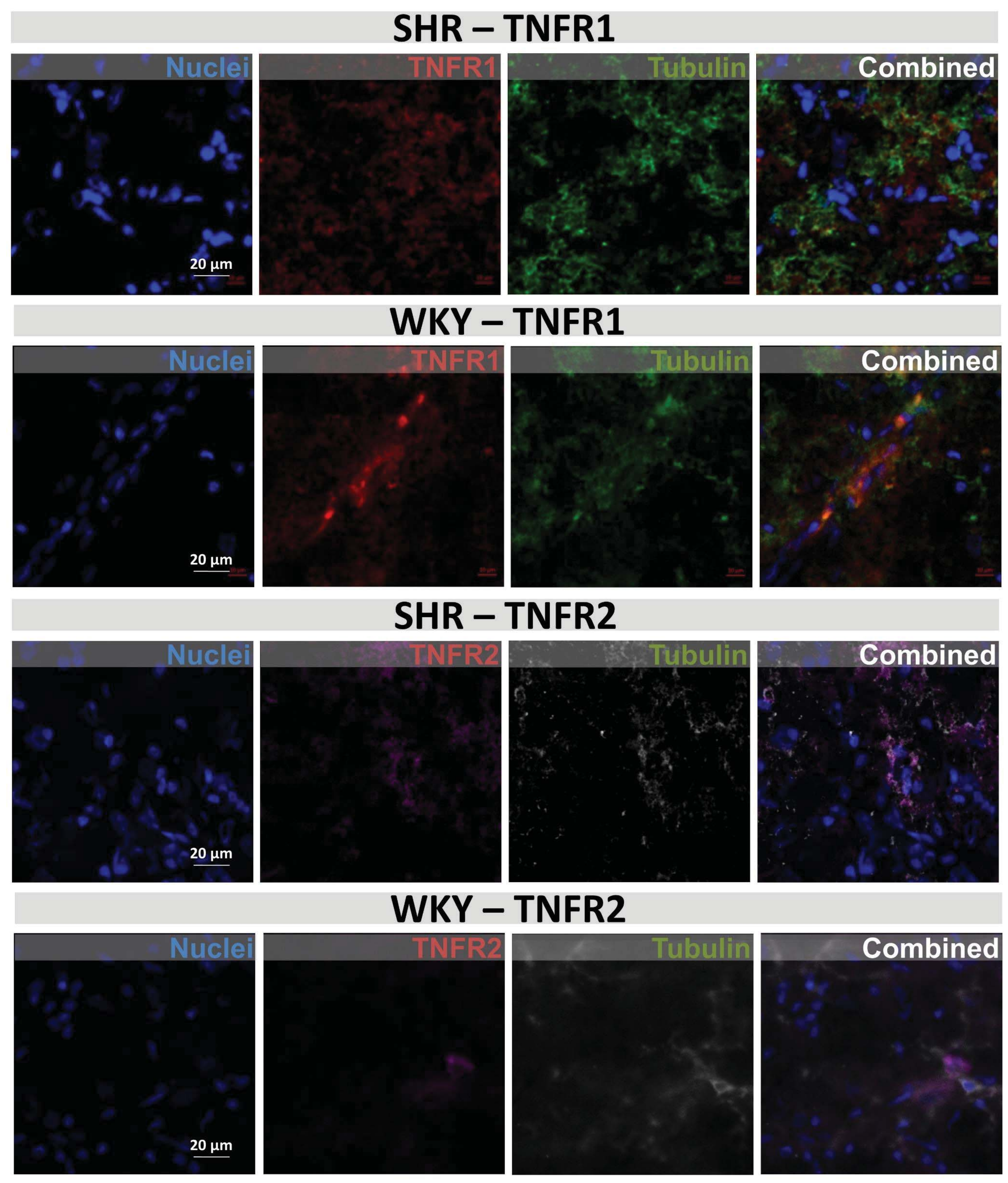

Conclusions

TNF type 1 and type 2 receptors are expressed in the regions of brain containing cardiovascular centres of normotensive WKY and hypertensive SHR rats, however, surprisingly mRNA levels of these receptors are similar between SHR and WKY rats.

References:

1. Shi P, Raizada MK, Sumners C. Brain cytokines as neuromodulators in cardiovascular control. Clin Exp Pharmacol Physiol. 2010; 37(2):e52-7.
2. Zera T, Ufnal M, Szczepanska-Sadowska E. TNF and angiotensin type 1 receptors interact in the brain control of blood pressure in heart failure. Cytokine. 2015; 71(2):272-7.
3. Winklewski PJ, Radkowski M, Wszedybyl-Winklewska M, Demkow U. Brain inflammation and hypertension: the chicken or the egg? J Neuroinflammation. 2015; 12:85.
4. Idris-Khodja N, Mian MO, Paradis P, Schiffrin EL. Dual opposing roles of adaptive immunity in hypertension. Eur Heart J. 2014; 35(19):1238–1244.
5. Shi P, Diez-Freire C, Jun J et al. Brain microglial cytokines in neurogenic hypertension. Hypertension. 2010; 56:297–303.
6. Probert L. TNF and its receptors in the CNS: The essential, the desirable and the deleterious effects. Neuroscience. 2015; 302:2-22.

Acknowledgements:

The study was supported by the Medical University of Warsaw, grant no. 1MA/NM2/18/18

Contact details: Agnieszka Segiet-Święcicka, asegiet@wum.edu.pl, fizjologia.wum.edu.pl

XXVIII Congress of the Polish Physiological Society, Gdańsk 15 - 17 September 2021, Session: HEART. CARDIOVASCULAR AND RESPIRATORY REGULATION, Poster Session, Poster S6.P9

DEVELOPMENT OF HEART FAILURE IN SPONTANEOUSLY HYPERTENSIVE RATS (SHR)

O. KROL[1], P. MIERZEJEWSKA[1], M. ZABIELSKA-KACZOROWSKA[1,2], T. BORKOWSKI[3], A. JEDRZEJEWSKA[1], E. M. SLOMINSKA[1], R.T. SMOLENSKI[1]

[1]Department of Biochemistry, Medical University of Gdansk, Poland;
[2] Department of Physiology, Medical University of Gdansk, Poland;
[3] Department of Medical Laboratory Diagnostics, Medical University of Gdansk, Poland

Corresponding author e-mail@address; ewa.slominska@gumed.edu.pl

www.mug.edu.pl

Introduction and objectives: Spontaneously hypertensive rats (SHR) rats are an animal model that strictly reflects to the one of the most common cardiovascular diseases in humans- hypertension. SHR rats are characterized by the development of spontaneous arterial hypertension from 5-6 weeks of age. This study aimed to test whether SHR rats will develop heart failure based on long-term hypertension.

Methods: Rats were housed in a conventional animal facility. Wistar Kyoto (WKY) rats were the control group, the test group was SHR rats. The studies were conducted after the rats were 6-, 12- and 18-month-old. Rats were anesthetized with ketamine (20 mg/kg) and xylazine (10 mg/kg) intraperiteneally. Transthoracic echocardiography was performed on each animal. The obtained acquired images were used to calculate hemodynamic parameters. Blood pressure parameters were mesured using the tail-cuff system.

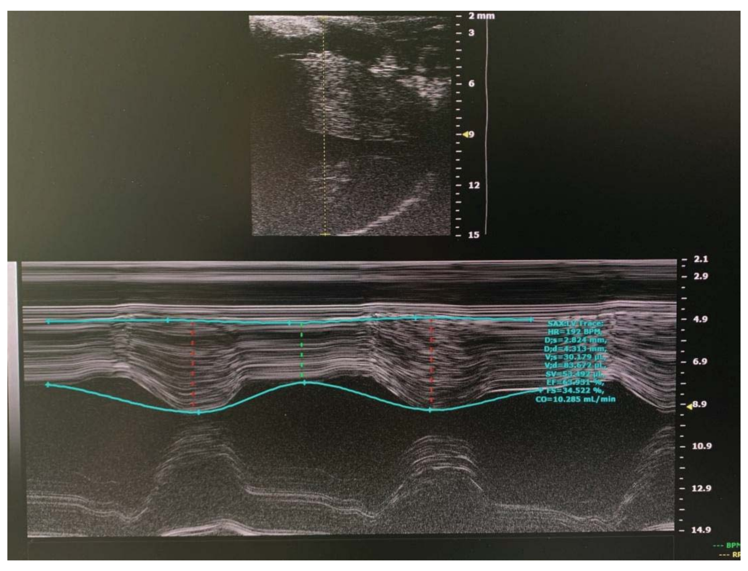

Pic.1. Rat echocardiography, long axis parasternal projection, left ventricular imaging

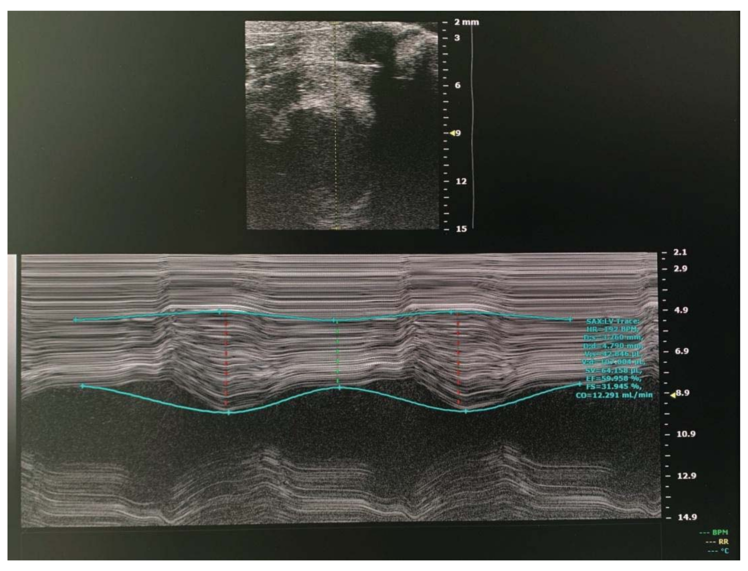

Pic.2. Rat echocardiography, short axis parasternal projection, left ventricular imaging

Results and conclusions: Based on a statistical analysis of hemodynamic parameters, changes in heart function in SHR rats over time were observed. Left ventricular systolic dysfunction was not observed based on the Ejection Fraction (EF) in 6-month-old SHR rats (74,26 ± 4,34 vs 70,32 ± 2,88 [%]). However, in the group of 12-months-old SHR rats, a statistical decrease of this parameter was observed compared to the WKY group (68,86 ± 3,17 vs 78,73 ± 1,97 [%]). Moreover, in a group of 18-month-old rats, this occurrence was even more pronounced (61,83 ± 1,3 vs 75,29 ± 2,24 [%]). Another important parameter describing the systolic function of the left ventricle is Fractional Shortening (FS). The deterioration trend of left ventricular function based on FS was the same as in the of EF (WKY vs SHR - 6-mth: 45,02 ± 3,02 vs 39,73 ± 2,17; 12-mth: 47,36 ± 1,81 vs 39,06 ± 2,48; 18-mth: 44,21 ± 2,16 vs 32,99 ± 0,85 [%]). All examined SHR rats developed advanced arterial hypertension (systolic/diastolic BP: 198 ± 6/145 ± 8 [mm Hg]; heart rate: 354 ± 11 [bpm]).

The presented results indicate the development of left ventricular heart failure based on long-term hypertension in SHR rats. This allows the SHR model to be used in experimental in-vivo studies in the field of heart failure.

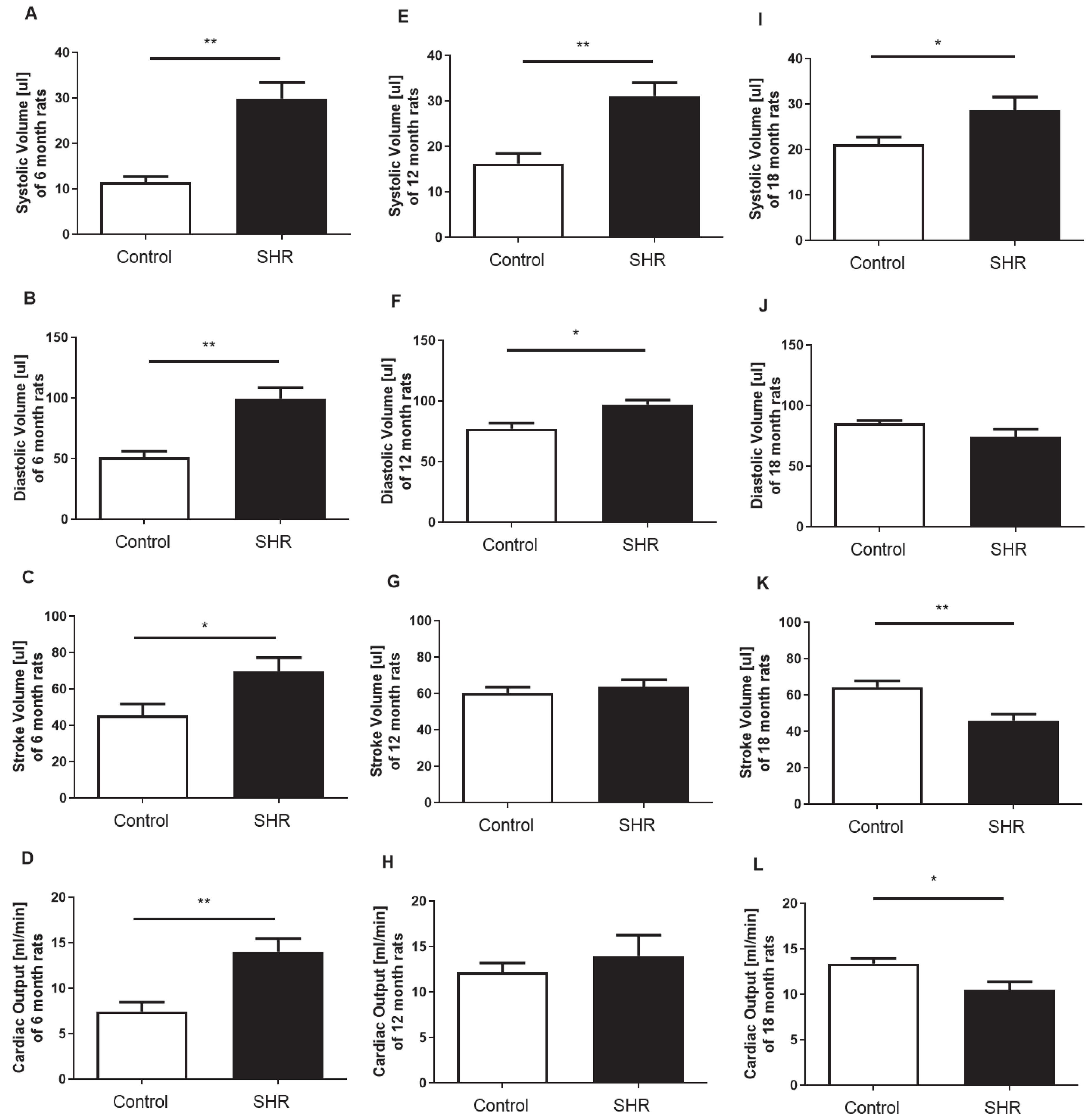

Fig.1. Cardiac function of 6- (A-D), 12- (E-H) and 18-month (I-L) SHR and control (WKY) rats. Echocardiographic parameters: Systolic Volume (**A, E, I**), Diastolic Volume (**B, F, J**), Stroke Volume (**C, G, K**), Cardiac Output (D, H, L). Values are shown as mean ± SEM (n=5; Student t test: *p<0.05; **p<0.01)

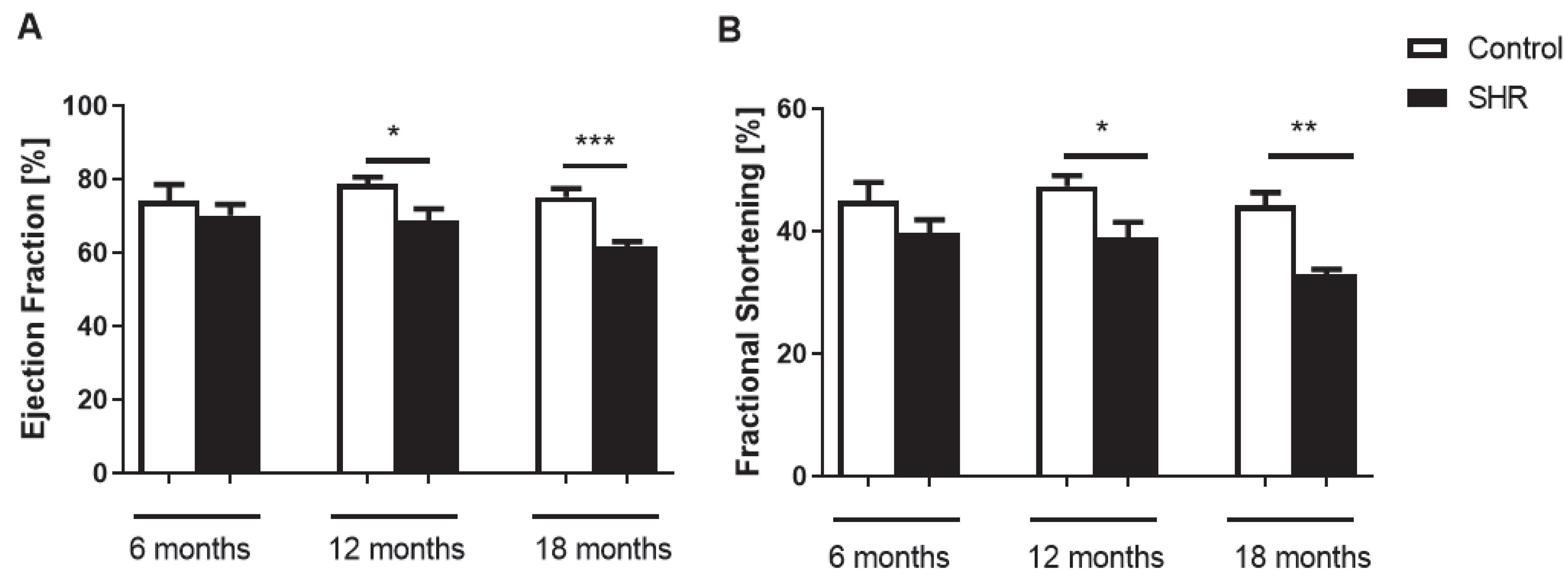

Fig.2. Age-dependent disturbance of heart function of SHR rats. Changes in echocardiographic parameters: Ejection Fraction **(A)** and Fractional Shortening **(B)** of 18-, 12- and 6 - month – old SHR and WKY rats. Values are shown as mean ± SEM (n=5; ANOVA: *p<0.05; **p<0.01; ***p<0.001)

Acknowledgements: HARMONIA 2016/22/M/NZ4/00678

Contact:

Department of Biochemistry, Medical University of Gdansk
ul. Debinki 1
80-211 Gdańsk, Poland

oliwia.krol@gumed.edu.pl
+48 58 349 1460

STEAROYL-COA DESATURASE 4 DEFICIENCY PROTECTS AGAINST HIGH FAT DIET-INDUCED HEART DYSFUNCTION IN MOUSE

[1]MARCIN WOLOSIEWICZ, [1]ANNA FILIP, [2]MONIKA DUDA, [1]ADAM OLICHWIER, [1]VIKTOR NAVRULIN, [1]PAWEL DOBRZYN
1. LABORATORY OF MOLECULAR MEDICAL BIOCHEMISTRY, NENCKI INSTITUTE OF EXPERIMENTAL BIOLOGY, POLISH ACADEMY OF SCIENCES, WARSAW, POLAND;
2. DEPARTMENT OF CLINICAL PHYSIOLOGY, POSTGRADUATE MEDICAL SCHOOL, WARSAW, POLAND;

nencki institute of experimental biology

Introduction and objectives

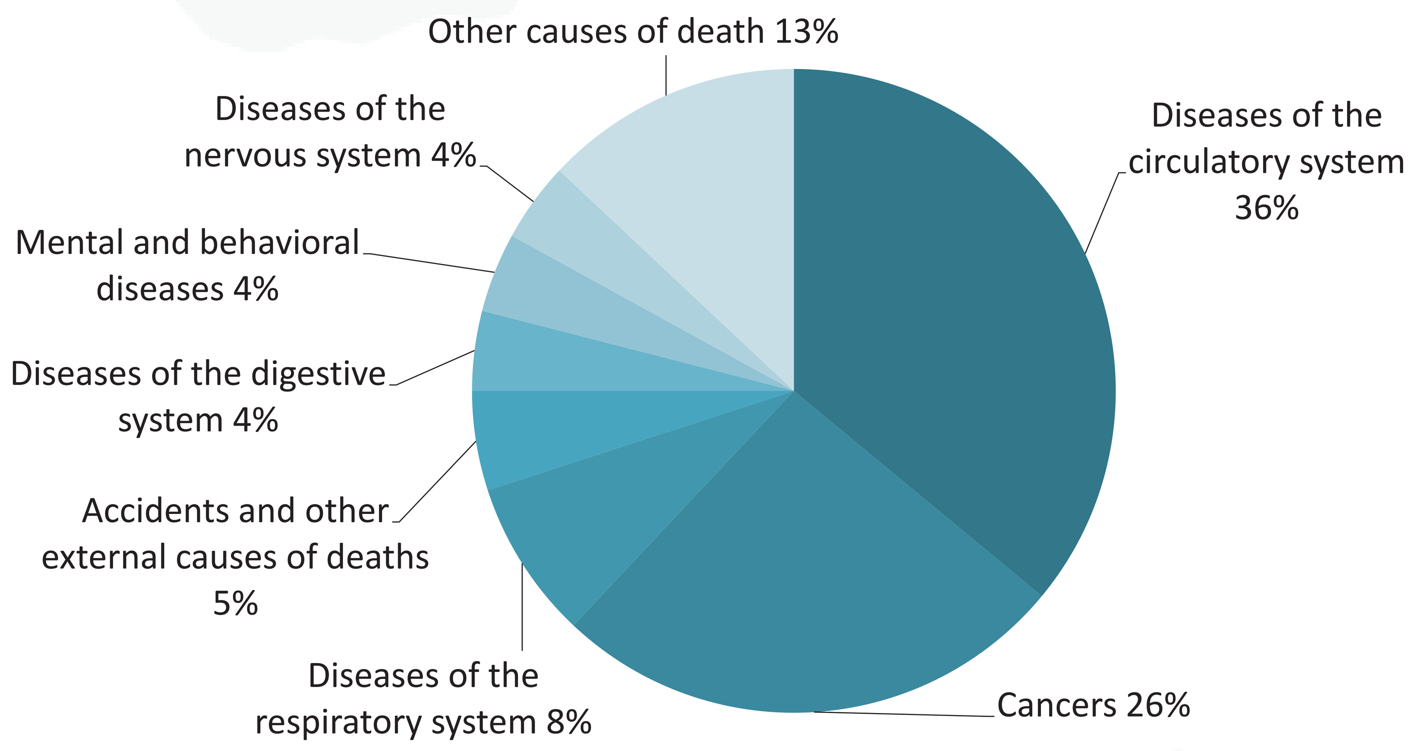

Fig. 1. Percentage of causes of death in European Union.

Cardiovascular disease (CVD) is the reason of every third death in Europe, which makes it **the most common cause of death**. Fat or carbohydrates reach diet, physical inactivity, **obesity**, type 2 diabetes are examples of risk factors leading to CVD development (O'Donnell, Elosua 2008). Fat oversupply result in aberrations in cardiac lipid metabolism and heart steatosis, what in turn causes cardiomyopathies (Lopaschuk et al. 2010). **Stearoyl-CoA desaturase (SCD)** is an enzyme localized in endoplasmatic reticulum (ER) and is involved in biosynthesis of monounsaturated fatty acids, what was shown as a crucial point in the **regulation of cardiac metabolism** (Dobrzyn et al. 2015). SCD4 is the heart-specific isoform, which expression is induced by SCD1 deficiency, liver X receptor agonists and a high carbohydrate fat-free diet (Miyazaki et al. 2003), however little is known about its physiological role in the heart.

THE AIM of the present study was to determine the impact of heart-specific isoform SCD4 deficiency on heart metabolism and function in high-fat diet-induced dysfunction.

Methods

In our study we used SCD4 knock-out (SCD4-/-) and wild type (WT) mice. Animals were assigned to groups fed regular laboratory diet (chow) or high-fat diet (HFD) for 8 weeks. At the end of the experiment echocardiography was performed. Total RNA was isolated, cDNA synthesized and real-time qPCR was performed using gene specific primers: alpha myosin heavy chain (α-MHC), beta myosin heavy chain (β-MHC), B-type natriuretic peptide (BNP) and 60S ribosomal protein L32 (Rpl32). For Western Blot proteins were isolated by homogenization of tissue fragment in a buffer and after centrifugation supernatant was collected for further proceedings. We used antibodies against protein kinase A (PKA), Ca^{2+}/calmodulin-dependent protein kinase II (CaMKII), phospholamban (PLN), sarcoplasmic reticulum Ca^{2+}-ATPase 2 (SERCA2a) and glyceraldehyde-3-phosphate dehydrogenase (GAPDH).

Results

SCD4-/- mice maintain proper heart function and structure

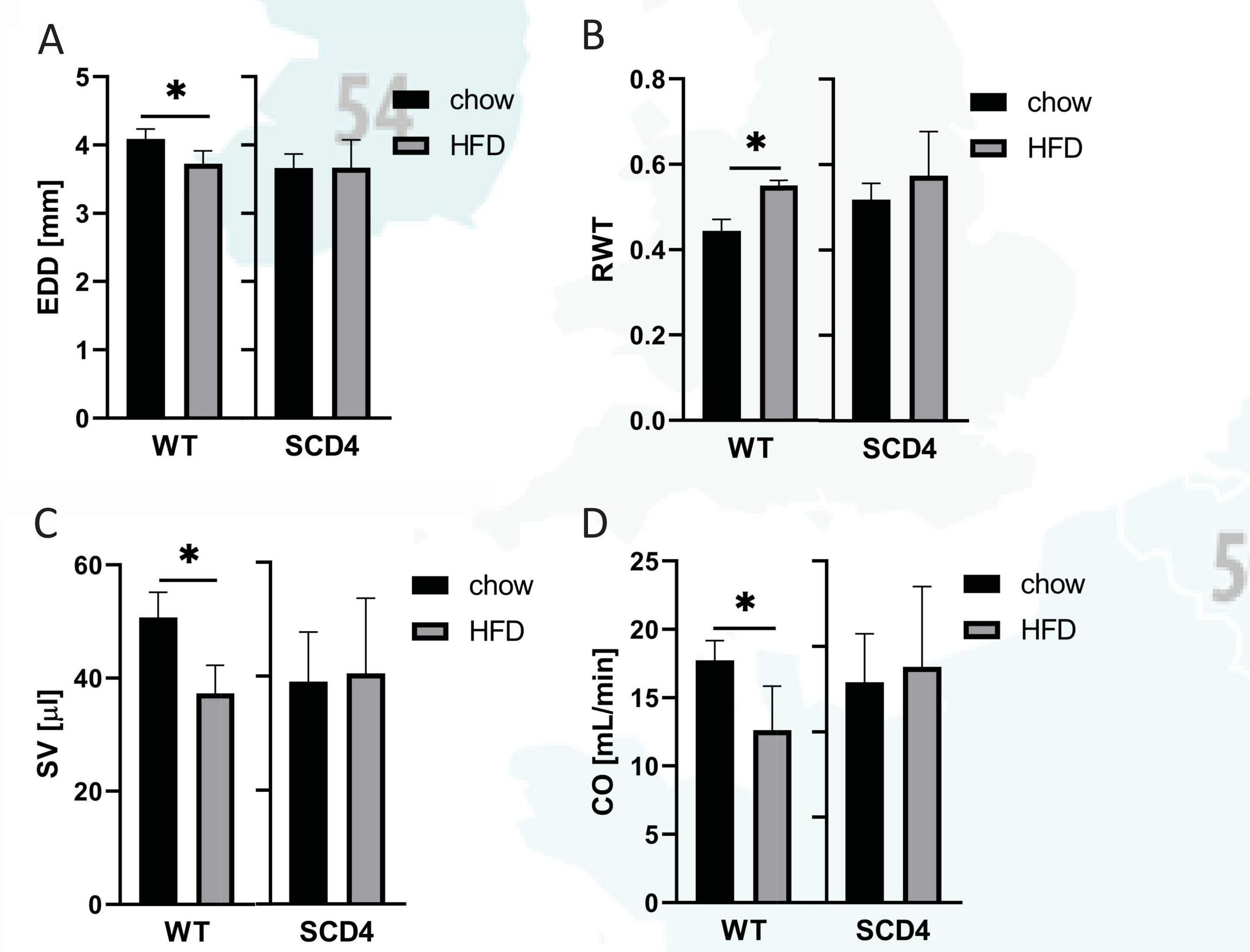

Fig. 2. Results from echocardiographic analysis: (A) end-diastolic diameter (EDD), (B) relative wall thickness (RWT), (C) stroke volume (SV), (D) cardiac output (CO). * p-value < 0.05 vs chow.

SCD4 deficiency prevents from decreased Ca^{2+} transport

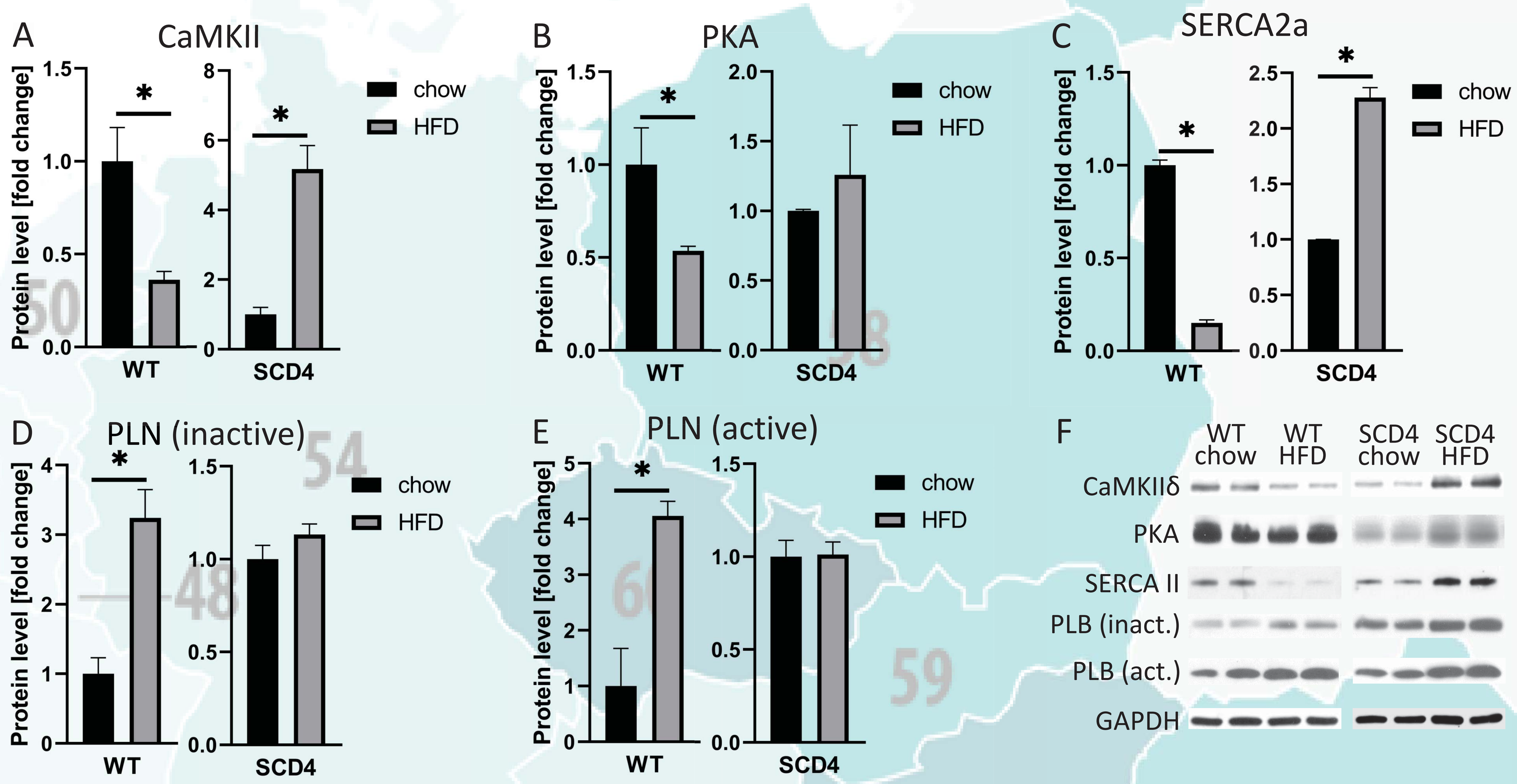

Fig. 3. Protein levels of: (A) Ca^{2+}/calmodulin-dependent protein kinase II (CaMKII), (B) protein kinase A (PKA), (C) sarcoplasmic reticulum Ca^{2+}-ATPase 2 (SERCA2a), (D) and (E) phospholamban (PLN) pentameric and monomeric respectively, (F) representative Western Blots of analysed proteins. * p-value < 0.05 vs. chow.

SCD4-/- mice preserve expression of BNP

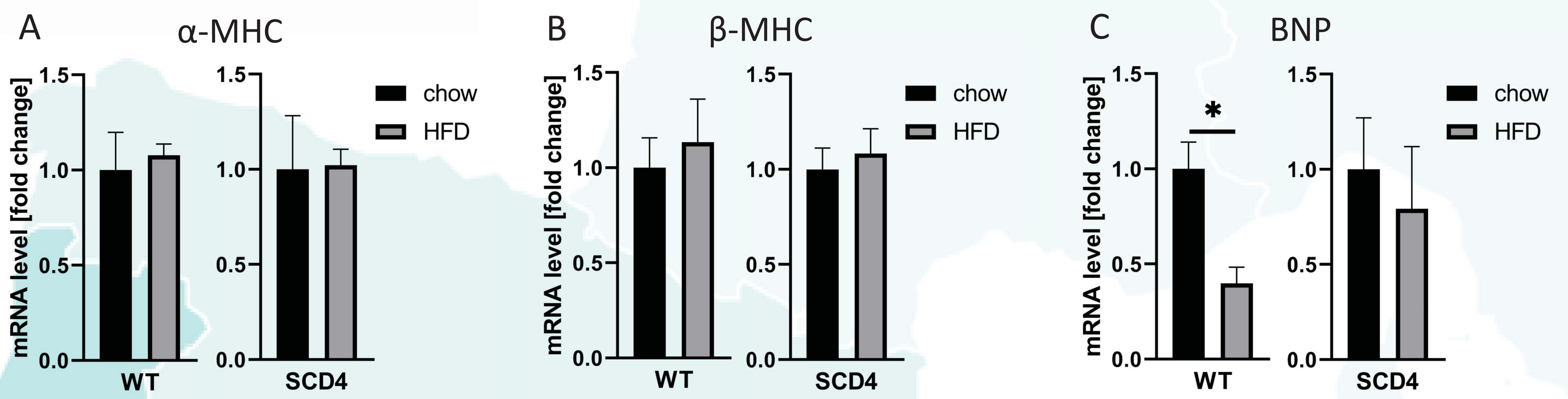

Fig. 4. Expression of (A) alpha myosin heavy chain (α-MHC), (B) beta myosin heavy chain (β-MHC) and (C) B-type natriuretic peptide (BNP). * p-value < 0.05 vs. chow.

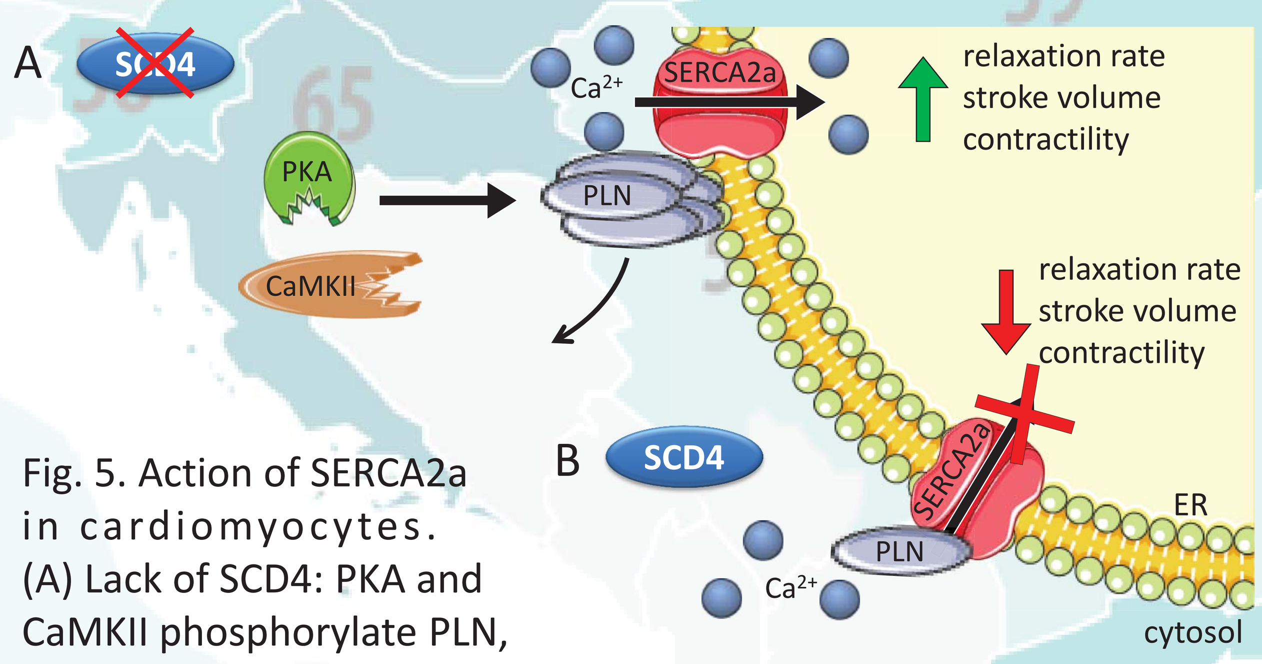

Fig. 5. Action of SERCA2a in cardiomyocytes.
(A) Lack of SCD4: PKA and CaMKII phosphorylate PLN, inactive pentamer is formed and Ca^{2+} transport is maintained.
(B) Presence of SCD4: PLN phosphorylation rate is lower, active monomer blocks SERCA2a and Ca^{2+} transport is impaired.

Conclusions

- SCD4 deficiency protects against HFD-induced heart dysfunction and concentric hypertrophy.
- Despite heart remodeling in WT mice expression of α-MHC and β-MHC is unaffected.
- SCD4-/- mice maintain mRNA level of BNP, which is involved in inhibition of hypertrophy and cardiac steatosis.
- Lack of SCD4 protects against HFD-induced impairment in Ca^{2+} transport.

References

1. Dobrzyn P, Bednarski T, Dobrzyn A. Metabolic reprogramming of the heart through stearoyl-CoA desaturase. Prog Lipid Res. 2015;57:1-12.
2. Lopaschuk GD, Ussher JR, Folmes CD, Jaswal JS, Stanley WC. Myocardial fatty acid metabolism in health and disease. Physiol Rev. 2010;90(1):207-58.
3. Miyazaki M, Jacobson MJ, Man WC, Cohen P, Asilmaz E, Friedman JM, Ntambi JM. Identification and characterization of murine SCD4, a novel heart-specific stearoyl-CoA desaturase isoform regulated by leptin and dietary factors. J Biol Chem. 2003;278(36):33904-11.
4. O'Donnell CJ, Elosua R. Cardiovascular risk factors. Insights from Framingham Heart Study. Rev Esp Cardiol. 2008; 61(3):299-310.

Funding: This work was supported by grant from the National Science Centre, Poland (no. UMO-2016/22/E/NZ4/00650).

Post-exercise hypotension in elderly: the effect of single session of water based exercise

C. REIS[1], W. BARBOSA[1], L. BARCELLOS[1], P. ZOVICO[1], C. LEITE[1], R. RICA[2], D. BOCALINI[1]

[1]Federal University of Espirito Santo, Vitoria, Brazil; [2]Estácio de Sá University, Vitória, Espirito Santo, Brazil.

Introduction and objectives

Among cardiovascular diseases, hypertension has been considered with high prevalence. In this way, countless treatments are often attributed as disease management strategies, in this way, the physical activity is highlighted above all for being able to reduce blood pressure. However, the hypotensive effect in acute sessions performed in an aquatic environment still remains inconclusive. Thus, the objective of the study was to verify the hypotensive effect of a water based exercise in normotensive and hypertensive elderly people.

Methods

Sample

After the research ethics committee approval. Eight physically healthy and independent men (26 ±2 years) were randomly submitted to three sessions of HIIT-C with the influence of preferred music (PM), non-preferred music (NPM) and no music (NM). Each subject signed an approved informed consent document.

Exercise session

For exercise training the session was led by the same trained fitness instructors and supervised by the researchers. This providence was adopted because differences of effectiveness between instruction and encouragement.

The WE program consisted of 45-min of a single session. The water level was fixed at xiphoid or near xiphoid level, with the water temperature at 29ºC. The session was divided into three stages. The first stage was warming-up for 5 min, composed of stretching and warm-up movements. The second stage was of endurance-type exercise for 35 min, composed of races, movements of arms and legs, resistance exercises using water-resistance products that included soft-cushioned hand-bars, leg pads and aquatubes. Dumbbell- and barbell-type devices were used to perform upper body resistance exercises (chest press, biceps curl, and lumber rotation) and leg pads were used to perform lower body exercises (knee extension and flexion, leg press and leg curl, calf press, leg abduction and adduction). Finally, the third stage was cooling-down/relaxation exercise for 5 min, composed of slow walking and stretching.

The intensity was monitored by the subjective perception of effort, indicating that throughout the main part the exercises were performed between 6 and 7 on the 0-10 scale.

Parameters evaluated

The following parameters were analyzed before and after 60 minutes of the exercise session using an automated non-invasive blood pressure monitor (Microlife 3AC1-1PC, Microlife, Widnau, Switzerland): systolic blood pressure (SBP), diastolic blood pressure (DBP), mean arterial blood pressure (MBP = DBP + [SBP - DBP]/3), heart rate and heart pressure product (RPP) was evaluated according to the following equation: RPP = HR*SBP.

Statistical Analyses

Values are expressed as the mean ± standard deviation (mean ± SD) for all variables. One-way ANOVA was used for repeated measures followed by the Tukey's post hoc test and 95 % confidence intervals (95 % CI) were calculated. Statistical significance was established at p ≤0.05. All statistical analyses were performed using the SPSS® software (v.15.0) on Windows.

Table 1. Anthropometric parameters.

Parameters	Normotensive	Hypertensive	95% CI	Dif M	p
Age (years)	61.70 ± 7.08 (11.49%)	65.33 ± 7.96 (12.19%)	-2.58 - 9.85	3.63 ± 3.02	= 0.240
Body mass (kg)	71.40 ± 13.19 (18.48%)	73.44 ± 11.06 (15.06%)	-7.55 - 11.65	2.04 ± 4.67	= 0.665
Height (m)	1.59 ± 0.10 (6.42%)	1.61 ± 0.11 (6.88%)	-0.07 - 0.10	0.01 ± 0.04	= 0.751
BMI (kg*m^2)	28.10 ± 4.90 (17.47%)	28.67 ± 5.52 (19.26%)	-3.74 - 4.87	0.56 ± 2.09	= 0.789
Fat body (%)	32.40 ± 5.58 (17.23%)	29.39 ± 4.28 (14.58%)	-6.88 - 0.85	-3.01 ± 1.88	= 0.121
Fat mass (kg)	39.00 ± 13.75 (35.26%)	44.06 ± 12.06 (27.37%)	-5.21 - 15.33	-5.05 ± 4.99	= 0.321
Fat free mass (kg)	32.40 ± 5.58 (17.23%)	29.39 ± 4.28 (14.58%)	-6.88 - 0.85	-3.01 ± 1.88	= 0.121

Values expressed as mean ± standard deviation (coefficient of variation). Confidence interval (95% CI).

Table 2. Comparison of hemodynamic parameters at land and water immersion condition.

Parameters	Land	Water	%	ES	ANOVA Time		Group		Interaction	
					F	P	F	P	F	P
HR (bpm)										
Normotensive	79 ± 9	77 ± 10	2.12 ± 4.57	0.17	0.194	=0.662	3.676	=0.066	0.288	=0.595
Hypertensive	85 ± 9	85 ± 10	-1.48 ± 6.38	0.11						
SBP (mmHg)										
Normotensive	122 ± 7	118 ± 5	-1.60 ± 5.28	0.27	1.685	=0.205	119.5	<0.0001	0.7509	=0.394
Hypertensive	151 ± 9	149 ± 8	-1.29 ± 4.21	0.18						
DBP (mmHg)										
Normotensive	80 ± 8	81 ± 6	-1.00 ± 4.85	0.10	2.51	=0.125	19.08	=0.001	1.08	=0.308
Hypertensive	88 ± 5	90 ± 5	-3.10 ± 5.59	0.53						
MBP (mmHg)										
Normotensive	93 ± 5	109 ± 4	-1.21 ± 4.39	0.22	1.54	=0.225	24.90	<0.001	0.617	=0.439
Hypertensive	94 ± 4	110 ± 4	-1.02 ± 3.02	0.24						
*RPP (mmHg*bpm)*										
Normotensive	9497 ± 1222	9580 ± 1284	-0.65 ± 5.34	0.07	2.02	=0.166	112.40	<0.001	0.199	=0.658
Hypertensive	12577 ± 1680	12948 ± 2091	-2.84 ± 8.50	0.17						

Values expressed as mean ± standard deviation of heart rate (HR), systolic blood pressure (SBP), diastolic blood pressure (DBP), mean blood pressure (MBP), rate pressure product (RPP). ES: effect size.

Table 3. Hypotension post exercise after water based exercise.

Parameters	Before	After	%	ES	ANOVA Time		Group		Interaction	
					F	P	F	P	F	P
HR (bpm)										
Normotensive	77 ± 8	76 ± 7	0.63 ± 1.98	0.06	0.786	=0.383	6.23	=0.019	0.322	=0.575
Hypertensive	86 ± 10	84 ± 9	-1.48 ± 6.38	0.11						
SBP (mmHg)										
Normotensive	123 ± 7	121 ± 5	-1.65 ± 3.48	0.29	12.74	=0.001	77.96	<0.001	7.25	=0.012
Hypertensive	147 ± 7	135 ± 8‡	-9.57 ± 8.96*	1.66						
DBP (mmHg)										
Normotensive	80 ± 7	80 ± 6	-3.10 ± 5.59	0.13	1.40	=0.246	16.95	=0.001	3.65	=0.066
Hypertensive	90 ± 4	88 ± 5‡	-0.98 ± 3.09	0.53						
MBP (mmHg)										
Normotensive	95 ± 4	93 ± 3	-1.26 ± 2.10	0.29	11.09	=0.002	118.7	<0.001	3.21	=0.084
Hypertensive	109 ± 3	105 ± 4‡	-4.37 ± 5.00*	1.14						
*RPP (mmHg*bpm)*										
Normotensive	9539 ± 12124	9313 ± 884	-2.28 ± 3.71	0.20	9.65	=0.004	22.05	<0.001	4.52	=0.043
Hypertensive	12620 ± 1938	11412 ± 1480	11.27 ± 12.29*	0.64						

Values expressed as mean ± standard deviation of heart rate (HR), systolic blood pressure (SBP), diastolic blood pressure (DBP), mean blood pressure (MBP), rate pressure product (RPP). ES: effect size.

Conclusion

An acute session of water based exercise was able to promote a reduction in systolic, diastolic and mean and rate pressure product in hypertensive elderly women.

Identifier/Topic: Heart. Cardiovascular and respiratory Regulation

Reference

1. Barroso W K S , Roberts C I S , Bortolotto L A , Mota Gomes, M A , Brandao The A , Feitosa The D M , Machado C A , et al. Brazilian Guidelines on Arterial Hypertension – 2020. Arq. Bras. Cardiol. 2021;116(3):516-658.

2. Memon W, Rodriguez D, Jonato Prestes, Rica R, Serra AJ, Bocalini D, et al. Hypotensive response after water-walking and land-walking exercise sessions in healthy trained and untrained women. International Journal of General Medicine. Informa UK Limited; 2011 Aug;549. Available from: http://dx.doi.org/10.2147/ijgm.s23094

3. Nogueira IC, Santos ZM de SA, Mont'Alverne DGB, Martins ABT, Magalhães CB de A. Effects of physical exercise on hypertension control in the elderly: a systematic review. Brazilian Journal of Geriatrics and Gerontology. 2012 Sep;15(3):587–601. Available from: http://dx.doi.org/10.1590/s1809-98232012000300019

4. Rica RL, Carneiro RMM, Serra AJ, Rodriguez D, Pontes Junior FL, Bocalini DS. Effects of water-based exercise in obese older women: Impact of short-term follow-up study on anthropometric, functional fitness and quality of life parameters. Geriatrics & Gerontology International. Wiley; 2012 Jun 14;13(1):209–14. Available from: http://dx.doi.org/10.1111/j.1447-0594.2012.00889.

The effects of enhanced endocannabinoid tone induced by chronic administration of dual FAAH/MAGL inhibitor JZL195 in spontaneously hypertensive rats

M. TOCZEK, A. KICMAN, B. MALINOWSKA

Department of Experimental Physiology and Pathophysiology, Medical University of Białystok, Poland

corresponding author: marektoczek@interia.eu

INTRODUCTION AND OBJECTIVES

Endocannabinoids (e.g. AEA and 2-AG) affect many physiological functions, including cardiovascular, hepatic, pulmonary and renal functions, body mass regulation and glucose homeostasis. Two major endocannabinoid degrading enzymes are fatty acid amide hydrolase (FAAH) and monoacylglycerol lipase (MAGL) [1,2]. We have previously demonstrated that chronic administration of FAAH inhibitor induced different (also positive) age- and model-dependent effects on various cardiovascular parameters in normotensive and hypertensive rats [3,4,5]. The therapeutic potential of stronger enhancement of endocannabinoid tone by dual FAAH/MAGL blockade in hypertension is unknown. Thus, the aim of our study was to examine the influence of dual FAAH/MAGL inhibitor JZL195 on the cardiovascular system in spontaneously hypertensive rats (SHR).

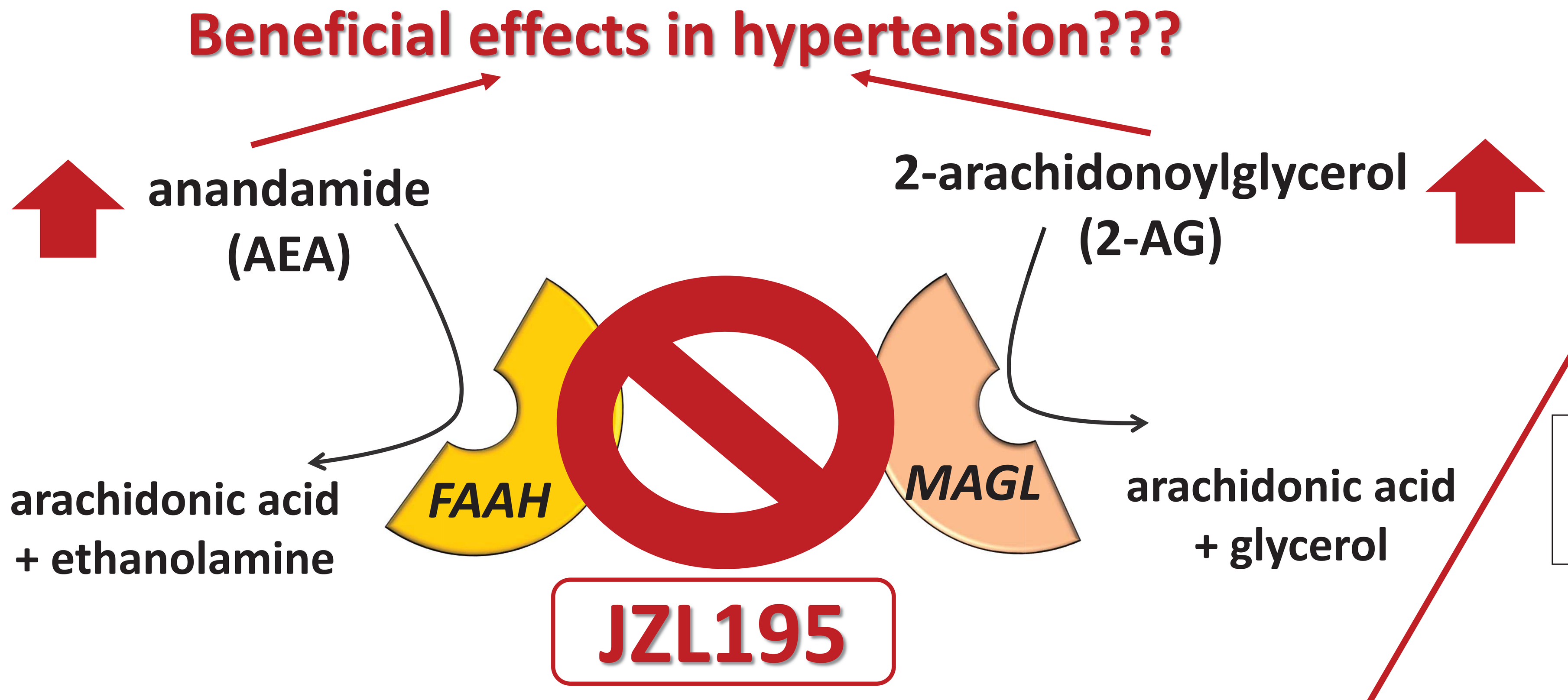

10 mg/kg (or vehicle Et0H:Tween80:saline 2:1:17) i.p.; 14 days

MATERIAL AND METHODS

8-11 weeks old

SHR (spontaneously hypertensive rats)
PRIMARY HYPERTENSION

WKY (Wistar-Kyoto rats)
NORMOTENSIVE CONTROL

MEASUREMENTS

- systolic (SBP), diastolic (DBP), mean (MBP) blood pressure and heart rate (HR) by tail cuff method or radiotelemetry system
- body weight

conscious

- blood glucose in tail capillary blood
- rectal temperature
- organ weight expressed as organ weight to body weight (BW) or tibia length (TL) ratio

pentobarbitone anaesthesia

0 — 14 days — 14

RESULTS

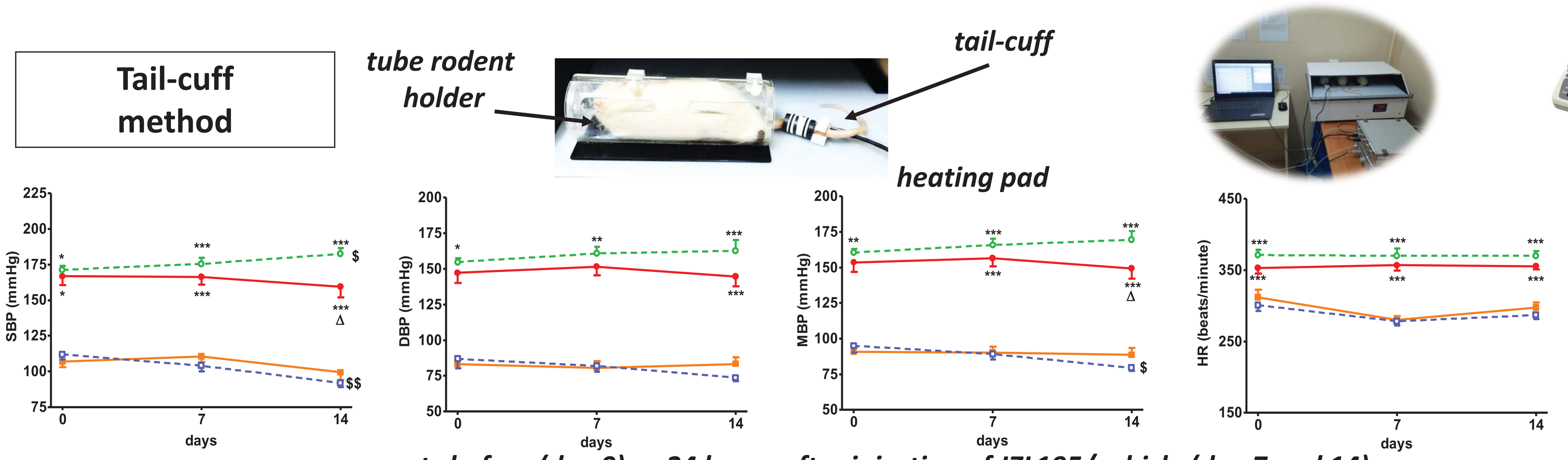

measurements before (day 0) or 24 hours after injection of JZL195/vehicle (day 7 and 14)

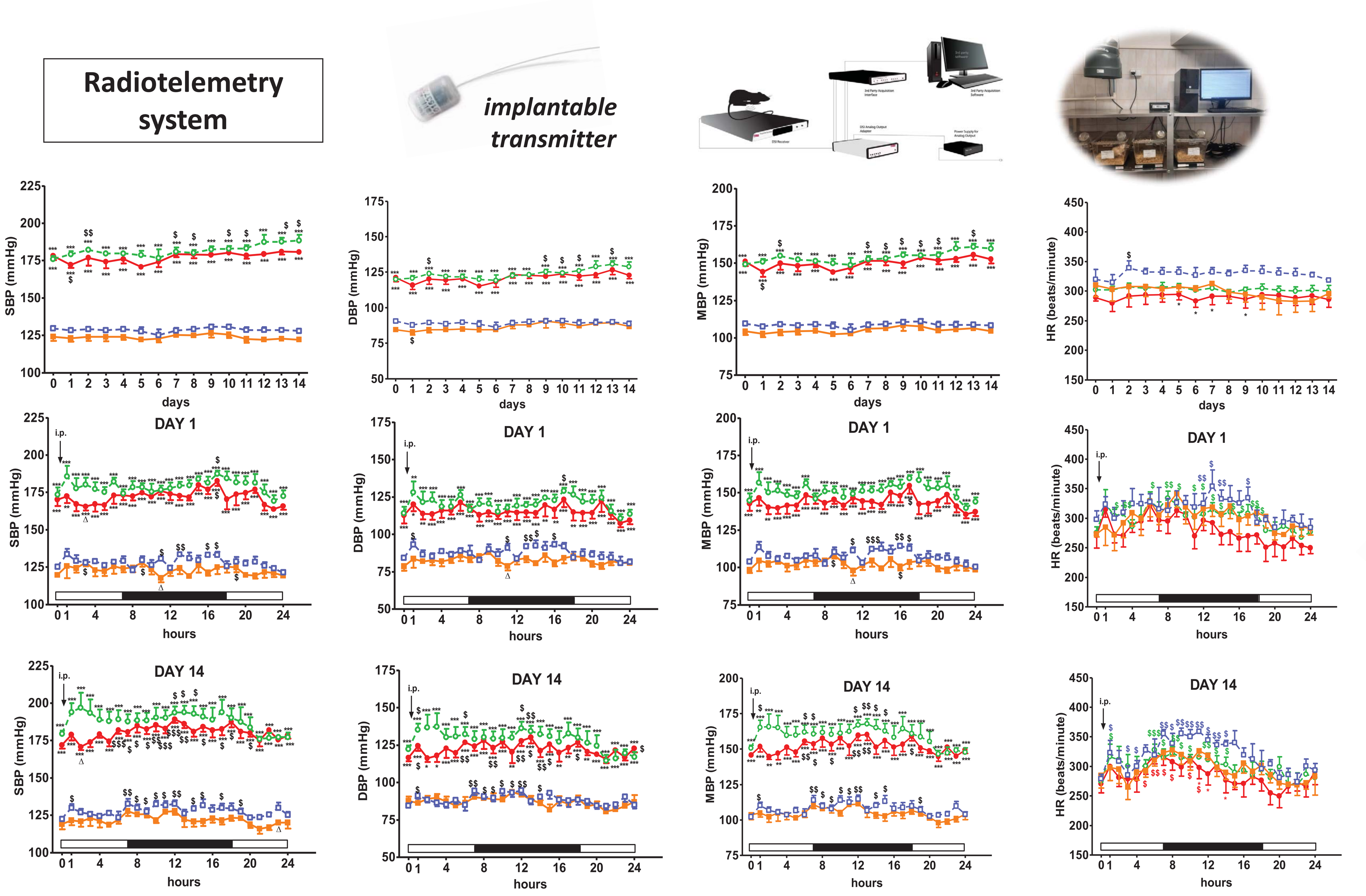

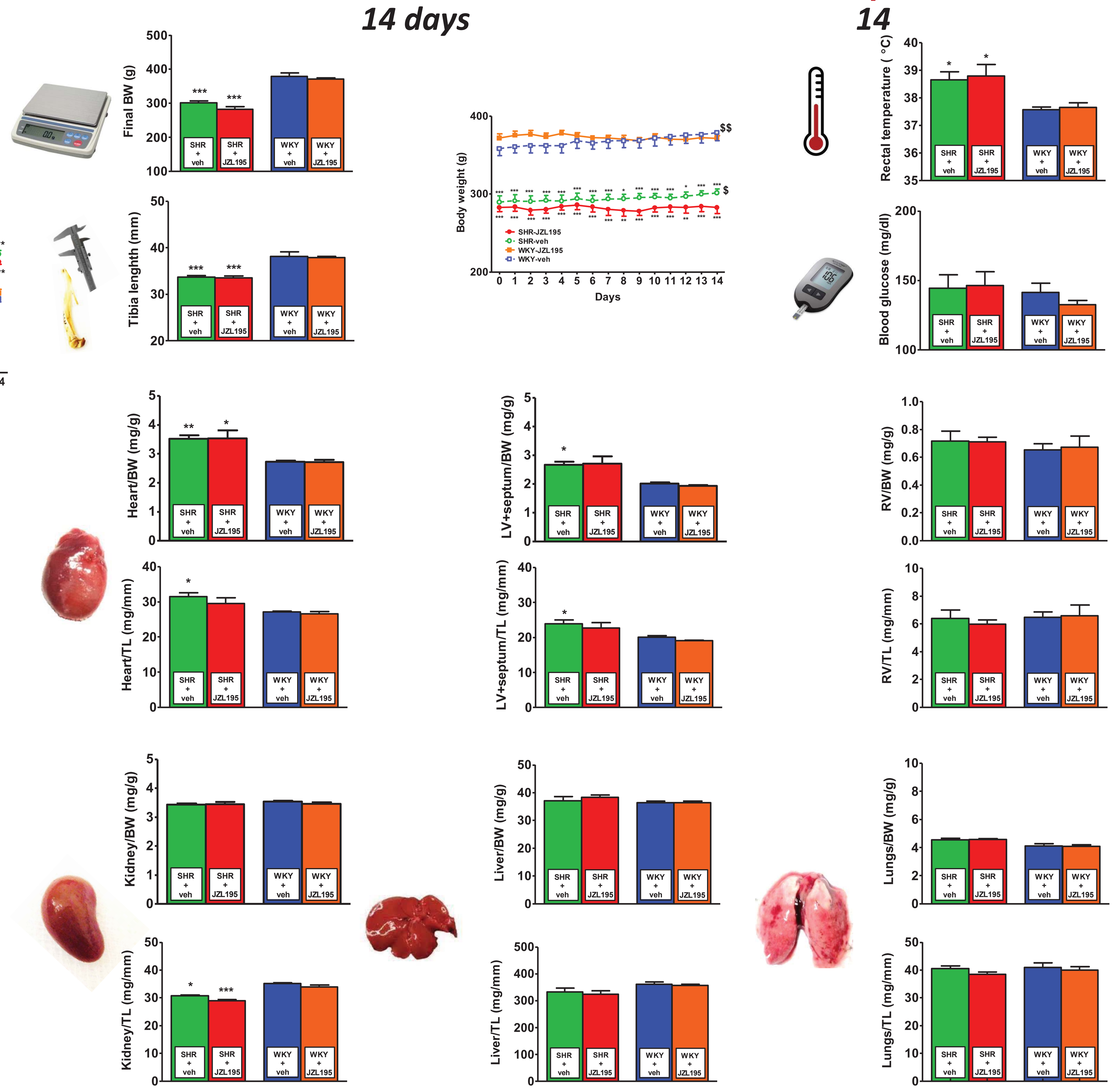

*means ± SEM; n=4-6; ***P<0.001, **P<0.01, *P<0.05 vs normotensive control group (WKY); ΔΔΔP<0.001, ΔP<0.05, ΔP<0.05 vs respective vehicle control groups (SHR or WKY); $$$P<0.001, $$P<0.01, $P<0.05 vs day/hour 0*

- SHR+JZL195
- SHR+veh
- WKY+JZL195
- WKY+veh

CONCLUSIONS

Chronic (14 days) administration of JZL195 evoked only slight beneficial influences on hemodynamic parameters in hypertension, so further investigations (other dose, period of administration, stage of hypertension, model of hypertension) are necessary to determine its real antihypertensive potential. Dual FAAH/MAGL blockade seems to be safe with respect to measured physiological parameters in hypertensive and normotensive rats.

REFERENCES:

1. Malinowska B, Toczek M, Pędzińska-Betiuk A, Schlicker E. Cannabinoids in arterial, pulmonary and portal hypertension - mechanisms of action and potential therapeutic significance. Br J Pharmacol. 2019; 176:1395-1411
2. Toczek M, Malinowska B. Enhanced endocannabinoid tone as a potential target of pharmacotherapy. Life Sci. 2018; 204:20-45.
3. Biernacki M, Malinowska B, Timoszuk M, Toczek M, Jastrząb A, Remiszewski P, Skrzydlewska E. Hypertension and chronic inhibition of endocannabinoid degradation modify the endocannabinoid system and redox balance in rat heart and plasma. Prostaglandins Other Lipid Mediat. 2018; 138:54-63.
4. Pędzińska-Betiuk A, Weresa J, Toczek M, Baranowska-Kuczko M, Kasacka I, Harasim-Symbor E, Malinowska B. Chronic inhibition of fatty acid amide hydrolase by URB597 produces differential effects on cardiac performance in normotensive and hypertensive rats. Br J Pharmacol. 2017; 174:2114-2129.
5. Toczek M, Baranowska-Kuczko M, Grzęda E, Pędzińska-Betiuk A, Weresa J, Malinowska B. Age-specific influences of chronic administration of the fatty acid amide hydrolase inhibitor URB597 on cardiovascular parameters and organ hypertrophy in DOCA-salt hypertensive rats. Pharmacol Rep. 2016; 68:363-9.

The work was supported by the National Science Centre, Poland, research grant No. 2016/21/N/NZ7/02338

Effect of music on training parameters and mood state in HIIT body work sessions

P.V.C. ZOVICO[1], R.A.A. FILHO[1], J.J.G. OLIVEIRA[1], W.A BARBOSA[1], R.L. RICA[2] and D.S. BOCALINI[1]
[1]Federal University of Espirito Santo, Vitoria, Brazil; [2]Estácio de Sá University, Vitória, Espirito Santo, Brazil.

Introduction and objectives

Use of music in exercise sessions has been considered an interesting strategy for both psychophysical and psychophysiological effects. However, considering the high intensity interval training (HIIT), the effects of music remain inconclusive. In this way, the objective of the study was to evaluate the influence of music in HIIT sessions using body weight (HIIT-C) in internal training load parameters and in the mood of university students

Methods

Sample

After the research ethics committee approval. Eight physically healthy and independent men (26 ±2 years) were randomly submitted to three sessions of HIIT-C with the influence of preferred music (PM), non-preferred music (NPM) and no music (NM). Each subject signed an approved informed consent document.

Exercise session

The HIIT body weight session consisted 5 min warm-up followed by 20 sets of 30 seconds of all-out intensity, and 30 seconds of passive recovery. The following exercise order (5 sets for each exercise) used jumping jack, burpee, mountain climb, and a squat jump. Additionally, all sessions were monitored by professionals and the influence of music were randomized.

Parameters evaluated

Total movement capacity: The total exercise movement amount realized on each set was used as external training load.

Heart rate: Heart rate (HR) was recorded continuously throughout the training session using HR monitors (Polar Electro Oy S810i, Kempele, Finland). The maximal and percentage of heart rate was estimated using the Tanaka equation.

Blood lactate: Capillary blood samples were taken from a sterile fingertip using a sterile lancet. The first drop of blood was discarded, and free flowing blood was collected in glass capillary tubes. All blood samples for lactate analysis were evaluated using an Accutrend® (Roche – Basel, Switzerland).

Rate of perceived exertion: Subjects reported their rating of perceived exertion (RPE, scale 1-10) immediately at the end and before each exercise set.

Feeling scale: The feeling scale (FS) is an 11-point bipolar scale ranging from +5 to -5, commonly used to measure the affective response (pleasure/displeasure) during exercise. The subjects received standard instructions regarding the use of the FS in the initial screening and before of boot exercise.

Mood State: The subjects responded to the Profile of Mood States (BRUMS) questionnaire based on a test that assessed 7 transient mood states: tension, depression, anger, stamina, fatigue, mental confusion and mood disorder. The questionnaire is used to evaluate the subjects' mood profile before and after exercise, and it can be used as a trace or state measure.

Statistical Analyses

Values are expressed as the mean ± standard deviation (mean ± SD) for all variables. One-way ANOVA was used for repeated measures followed by the Tukey's post hoc test and 95 % confidence intervals (95 % CI) were calculated. Statistical significance was established at p ≤0.05. All statistical analyses were performed using the SPSS® software (v.15.0) on Windows.

Results

Table 1. Parameters related to HIIT session

Parameters	NM	NPM	PM	F	p
HR (bpm)	165.10 ± 7.93 4.80%	167.80 ± 9.14 5.45%	170.40 ± 10.97 6.44%	2.052	=0.182
HR (% max)	88.46 ± 3.44 3.89%	89.21 ± 4.05 4.54%	89.80 ± 5.40 6.02%	0.448	=0.583
Movements (n)	672.40 ± 58.69† 8.73%	624.50 ± 71.28 11.41%	713.00 ± 52.28†‡ 7.33%	17.57	=0.001
RPE (0-10)	8.25 ± 1.03 12.55%	7.62 ± 1.40 18.46%	8.50 ± 1.30 15.40%	1.993	=0.192

Values expressed as mean ± standard deviation. NM (no music). PM (preferred music). NPM (no-preferred music). HR (heart rate). Rate of perceived exertion (RPE). †p<0.0001 vs NPM. ‡p<0.0001 vs NM.

Table 2. Parameters of HIIT session-related training load

Parameters	Before	After	MD	95% IC	ANOVA Time effect	ANOVA Time*protocol F	ANOVA Time*protocol p
HR (bpm)							
NM	76.50 ± 11.38 14.88%	169.02 ± 7.48 4.42%	-92.53	-105.2 to -79.89	< 0.0001		
NPM	77.25 ± 11.13 14.41%	169.65 ± 11.03 6.50%	-92.40	-112.4 to -72.43	< 0.0001	0.40	=0.6714
PM	71.87 ± 7.79 10.83%	166.00 ± 16.19 9.75%	-94.13	-114.1 to -74.16	< 0.0001		
Lactate (mMol.L⁻¹)							
NM	1.17 ± 0.29 24.81%	13.88 ± 3.00 21.64%	-12.71	-15.93 to -9.49	< 0.0001		
NPM	1.20 ± 0.30 25.58%	15.12 ± 3.65 24.16%	-13.93	-17.14 to -10.71	< 0.0001	0.34	=0.7127
PM	1.07± 0.16 15.52%	14.98 ± 3.18 21.25%	-13.91	-17.13 to -10.70	< 0.0001		
Feeling scale							
NM	3.25 ± 0.88 27.27%	1.25 ± 1.98 158.56%	2.00	0.36 to 3.63	= 0.0151		
NPM	2.87 ± 1.35 47.17%	-1.12 ± 2.41 -214.79	4.00	2.36 to 5.63	< 0.0001	15.45	=0.0003
PM	3.00 ± 1.06 35.63%	3.62 ± 0.74 20.52%	-0.62	-2.26 to 1.01	= 0.9502		

Values expressed as mean ± standard deviation. NM (no music). PM (preferred music). NPM (no-preferred music). *p<0.0001 vs before. †p<0.0001 vs NM. ‡p<0.0001 vs NPM.

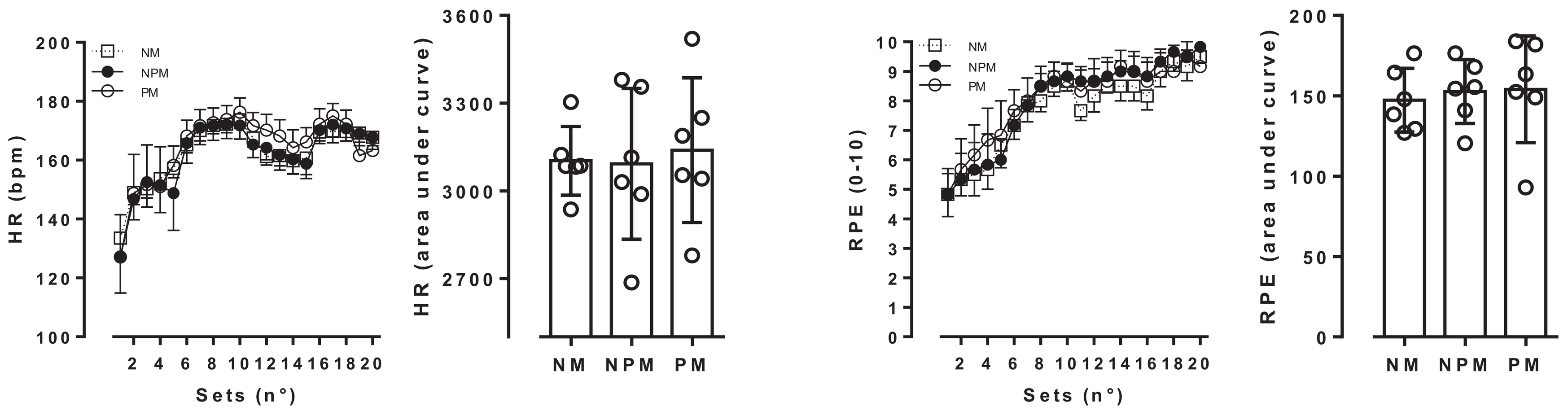

Figure 1. Values expressed as mean ± standard deviation. HR (heart rate). RPE (Rate of perceived exertion). NM (no music). PM (preferred music). NPM (no-preferred music). *p<0.0001 vs before. †p<0.0001 vs NM. ‡p<0.0001 vs NPM.

Table 3. Parameters of HIIT session-related mood state

Parameters	Before	After	MSD	95% CI	ANOVA Time effect F	Time effect p	Protocol effect F	Protocol effect p	Time*protocol F	Time*protocol p
Tension										
NM	2,12 ± 1,88	0,62 ± 0,74*	1,50	0,03 to 2,97						
NPM	2,50 ± 2,20	1,25 ± 1,38	1,25	-0,21 to 2,72	4,43	=0,0733	2,35	=0,1311	0,12	=0,8837
PM	1,87 ± 2,16	0,25 ± 0,46*	0,62	0,15 to 3,09						
Depression										
NM	0,62 ± 0,91	0,25 ± 0,46	0,37	-0,87 to 1,62						
NPM	1,25 ± 1,16	0,87 ± 1,72	0,37	-0,87 to 1,62	0,23	=0,6430	1,82	=0,1980	0,09	=0,9067
PM	0,87 ± 0,99	0,75 ± 1,75	0,12	-1,12 to 1,37						
Anger										
NM	0,50 ± 0,75	0,37 ± 0,74	0,12	0,51 to 0,76						
NPM	0,25 ± 0,70	0,50 ± 0,53	-0,25	-0,89 to 0,39	0,05	=0,8264	0,04	=0,9548	1,21	=0,3266
PM	0,50 ± 0,53	0,25 ± 0,46	0,25	0,25 to 0,89						
Stamine										
NM	7,50 ± 4,40	6,37 ± 3,88	1,12	-4,55 to 6,80						
NPM	6,62 ± 3,58	5,87 ± 5,08	0,75	-4,93 to 6,43	1,09	=0,3301	0,94	=0,4105	0,25	=0,7756
PM	8,87 ± 3,04	6,12 ± 2,69	2,75	-2,93 to 8,43						
Fatigue										
NM	2,25 ± 2,25	6,00 ± 2,13*	-3,70	-7,23 to -0,26						
NPM	2,75 ± 1,58	6,37 ± 3,62*	-3,62	-7,11 to -0,13	15,79	=0,0054	0,25	=0,7747	0,00	=0,9968
PM	2,75 ± 2,12	6,50 ± 3,58*	-3,70	-7,23 to -0,26						
Mental confusion										
NM	0,25 ± 0,46	0,75 ± 1,16	-0,50	-1,50 to 0,50						
NPM	0,50 ± 0,75	1,00 ± 1,41	-0,50	-1,50 to 0,50	1,37	=0,2802	0,51	=0,6064	0,00	>0,9999
PM	0,25 ± 0,70	0,75 ± 1,03	-0,50	-1,50 to 0,50						
Mood disorder										
NM	-1,37 ± 5,09	2,87 ± 5,91*	-3,75	-9,93 to 2,43						
NPM	-1,37 ± 3,42	5,62 ± 9,51*	-6,00	-12,19 to 0,18	27,41	=0,0012	1,22	=0,3247	1,68	=0,2211
PM	-2,12 ± 3,39	1,25 ± 5,36	-3,37	-9,56 to 2,81						

Values expressed as mean ± standard deviation. NM (no music). PM (preferred music). NPM (no-preferred music). *p<0.0001 vs before.

Conclusion

HIIT-C sessions using PM presented a higher NMO and positive PP when compared to sessions with NPM and NM without promoting changes in internal training load parameters. Although all sessions of HIIT-C increased the feeling of fatigue, the sessions of HIIT-C that use PM and NM showed less tension when compared to the session with NPM. In addition, the NM and NPM sessions were able to increase the mood disorder, with no effect for the PM session.

Identifier/Topic: Miscellaneous

Reference

1. Evangelista AL. *et al.* Effects of high-intensity calisthenic training on mood and affective responses. *J. Exerc. Physiol. Online* **20**, 15–23 (2017).
2. Machado AF *et al.* Energy expenditure and intensity of HIIT bodywork® session. *Motriz. Rev. Educ. Fis.* **26**, (2020).
3. Ballmann CG. The Influence of Music Preference on Exercise Responses and Performance: A Review. *J. Funct. Morphol. Kinesiol.* **6**, (2021).
4. Rasteiro FM *et al.* Effects of preferred music on physiological responses, perceived exertion, and anaerobic threshold determination in an incremental running test on both sexes. *PLoS One* **15**, e0237310 (2020).

The effect of genetically altered AMP deaminase activity in experimental isoproterenol- induced heart failure

M. A. ZABIELSKA-KACZOROWSKA[1,2], P. MIERZEJEWSKA[1], E. M. SLOMINSKA[1], R.T. SMOLENSKI[1]

[1]Department of Biochemistry, Medical University of Gdansk, Poland;
[2] Department of Physiology, Medical University of Gdansk, Poland;

Corresponding author e-mail@address; ryszard.smolenski@gumed.edu.pl

www.mug.edu.pl

Introduction and objectives: Studies on the influence of AMP deaminase (AMPD) activity on the progression of heart disease are conflicting, possibly due to the diverse effect in different clinical conditions. Isoproterenol is a non-selective β-adrenergic agonist that has been used widely to mimic the heart failure state. Our study aims to investigate the effect of isoproterenol (ISO)-induced heart failure on cardiac function in murine hearts lacking AMPD3.

Methods: : In this study we used male wild type and AMPD3 knockout mice (n=6-8). We injected intra-peritoneally ISO in the experimental animals at a dose of 100 mg/kg body weight/day for 12 days. ISO-treated and control mice (saline) from each group were examined with echocardiography. At the age of 12 months old, mice were anesthetized intraperitoneally with ketamine (100 mg/kg) and xylazine (10 mg/kg). After chest hair removal, animals were placed on a heated platform to maintain the body temperature at 37°C. The transthoracic echocardiography was performed using the Vevo 1100 (VisualSonics Inc, Canada) equipped with a 40-MHz linear array transducer. Images were acquired at a frame rate consistently above 200 frames/s. The transducer was placed above the anterior chest wall and hemodynamic parameters, including Stroke Volume (SV), LV Ejection Fraction (EF) and Fractional Shortening (FS) as well as Cardiac Output (CO) and LV Mass were collected. The statistical analysis was performed using Graph Pad Prism 7 (Graph Pad Software). Paired Student t-test was used for comparisons between two groups. A p-value < 0.05 was considered as a significant difference.

Results and conclusions: To characterize the implications of the AMPD KO for the ISO-induced development of cardiac dysfunction, we conducted two-dimensional echocardiographic measurements. The measurement of SV and CO did not differ in the studied groups, both WT and AMPD KO and after the treatment with ISO. A significant decrease in EF was observed in WT mice treated with isoproterenol compared to WT. Interestingly, the effect of ISO on EF was abolished in AMPD KO mice. EF was not different between WT and AMPD KO mice not treated with ISO. Moreover, a similar effect was observed with the FS measurement. There was a considerable reduction in FS in the WT group treated with ISO compared to the WT group and a suppression of the ISO impact on FS in the AMPD KO group. FS measurement did not differ between the non-treated WT and AMPD KO groups. Furthermore, a significant increase in left ventricular mass was observed in ISO-treated WT mice compared to WT. In turn, ISO did not affect left ventricular mass in AMPD KO mice. LV Mass did not differ between the untreated animals, WT and AMPD .

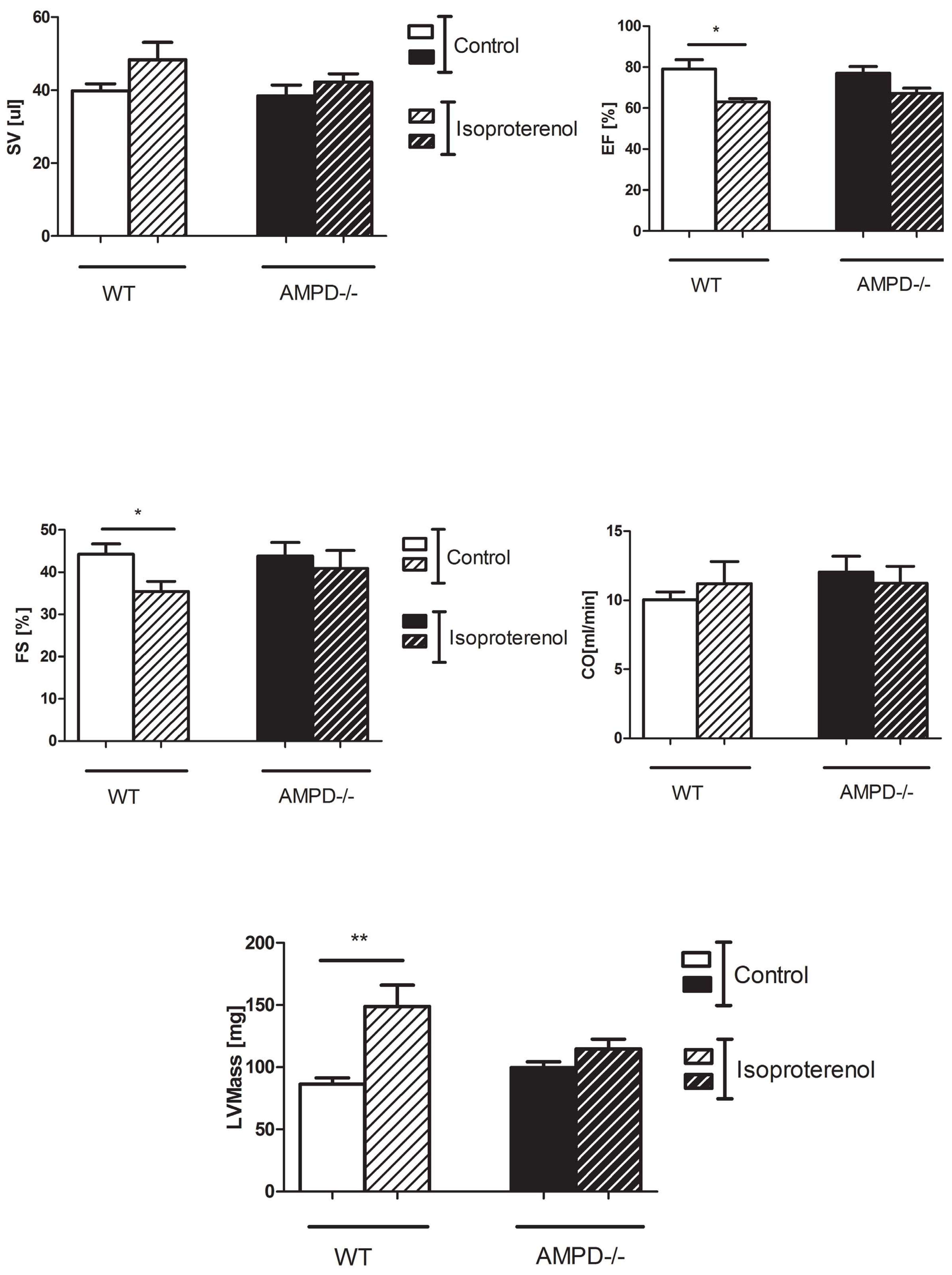

Fig.1. Cardiac function of 12-month-old wild type and AMPD3 knockout mice after 12 days isoproterenol administration. Echocardiographic parameters: Stroke Volume (SV), LV Ejection Fraction (EF), Fractional Shortening (FS) and Cardiac Output (CO) and LV Mass . Values are shown as mean ± SEM (n=-;- Student t test: *p<0.05; **p<0.01)

This study shows that reduced AMPD activity has a beneficial effect on cardiac function in isoproterenol- induced heart failure. Possibly the enhanced activation of protective AMPK cascade is likely to be the mechanism. The use of specific AMPD inhibitors may offer significant therapeutic potential.

Acknowledgements: Preludium 2018/29/N/NZ4/02259, HARMONIA 2016/22/M/NZ4/00678

Contact:

Department of Biochemistry, Medical University of Gdansk
ul. Debinki 1
80-211 Gdańsk, Poland
magdalena.zabielska@gumed.edu.pl
+48 58 349 1460

The influence of cannabidiol on isolated rat atria under normoxic, hypoxic and reoxygenation conditions

S6.P18

A. PĘDZIŃSKA-BETIUK[1], J. WERESA[1], B. MALINOWSKA[1]

[1]Department of Experimental Physiology and Pathophysiology, Medical University of Bialystok, Poland

INTRODUCTION

- Cannabidiol (CBD) is a non-psychoactive component of marijuana.
- CBD has a protective action in the brain hypoxia [1] and in rat model of cardiac ischemia [2, 3].
- In hypoxic cardiac damage, the antioxidant, anti-inflammatory and antiapoptotic properties as well as the comprehensive mechanism of CBD may play potential cardioprotective role [4].
- The most common causes of myocardial hypoxia:

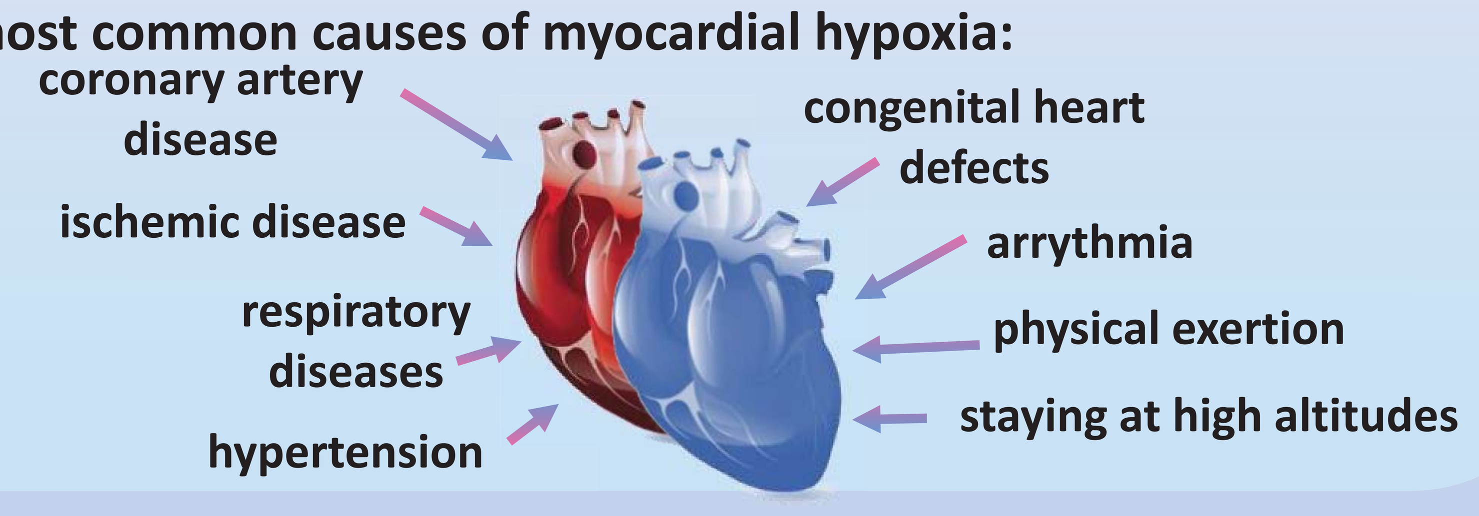

AIM

The aim of this study was to examine the potential cardioprotecive effect of CBD on the rate and force of contractions of isolated rat atria under hypoxic conditions. The experiments were conducted in basal conditions and after β-adrenoceptors stimulation with a non-selective agonist isoprenaline (ISO).

MATERIALS AND METHODS

Male Wistar rats (350 – 450 g) were anesthetized with 300 μg/kg of sodium pentobarbital (i.p). After deep anesthesia was reached, atria were isolated and immediately mounted into bath system and incubated with an oxygenated Krebs-Henseleit solution at 37.4°C (normoxia). Hypoxia was achieved by replacement of carbogen gas by 95 % N_2 and 5 % CO_2 in the organ baths (Figure 1).

Figure 1. The organ bath system.

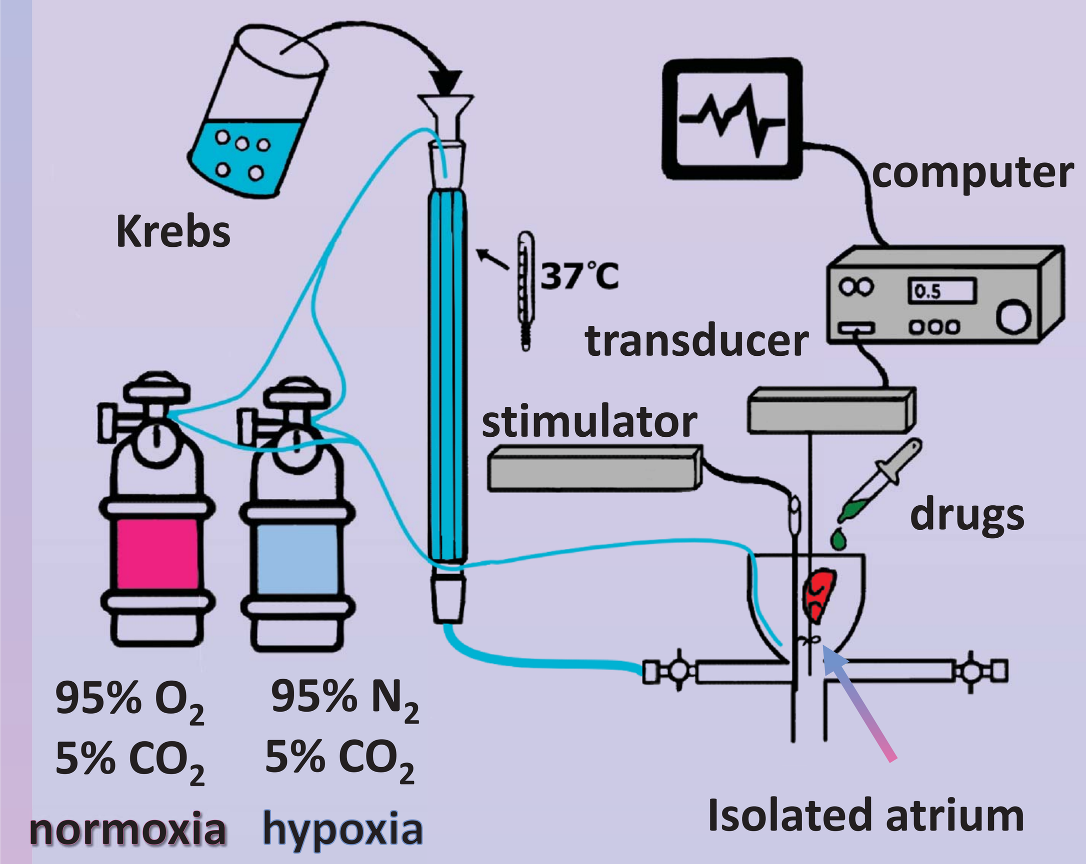

Both, positive chronotropic (spontaneously beating right atria) and inotropic (electrically stimulated left atria) effects were evaluated. After 30-min incubation with 1 μM CBD (or its vehicle DMSO, control) atria were exposed to 30 min hypoxia (H) followed by 30 min reoxygenation (R). The increasing concentrations of ISO (0.01 nM - 10 μM) were administered before or after H/R.

The influence of CBD on H/R-induced changes in atrial rate and force of contractions were determined according following protocols:

Protocol 1. hypoxia under basal conditions:

ISOPRENALINE 0.01 nM – 10 μM

STABILIZATION 60 min	CBD 1 μM 30 min	HYPOXIA 30 min	REOXYGENATION 30 min	ISOPRENALINE

Figure 2, 3 (A, B)

Protocol 2. hypoxia after adrenergic stimulation:

ISOPRENALINE 0.01 nM – 10 μM

STABILIZATION 60 min	CBD 1 μM 30 min	ISOPRENALINE	HYPOXIA 30 min	REOXYGENATION 30 min

Figure 2, 3 (C, D)

RESULTS

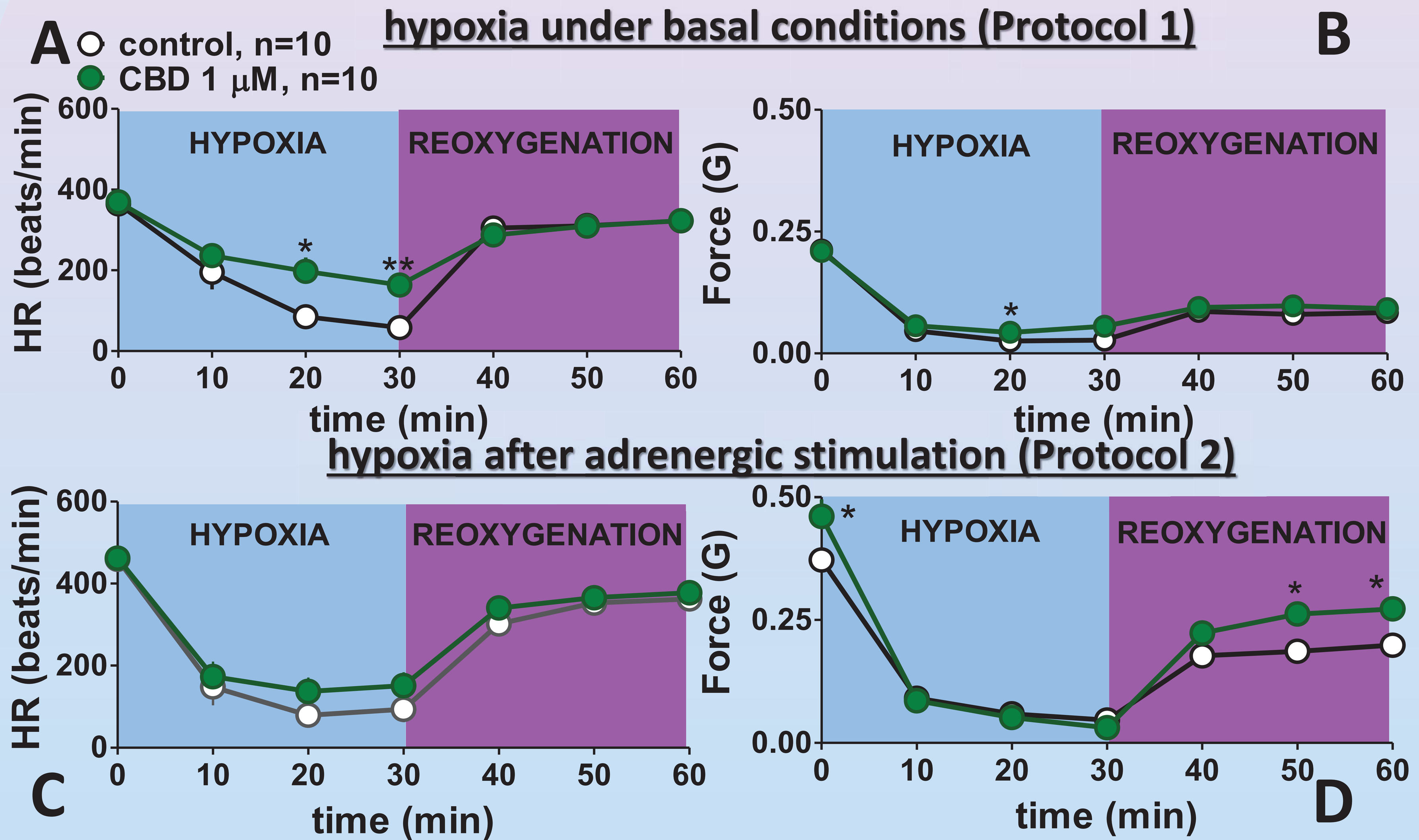

Figure 2. Influence of CBD (1 μM) on heart rate (HR, beats/min, right atria, A, C) and force (G, left atria, B, D) of contractions during hypoxia occured under basal conditons and after adrenergic stimulation. t – test ($p<0.05$* vs control).

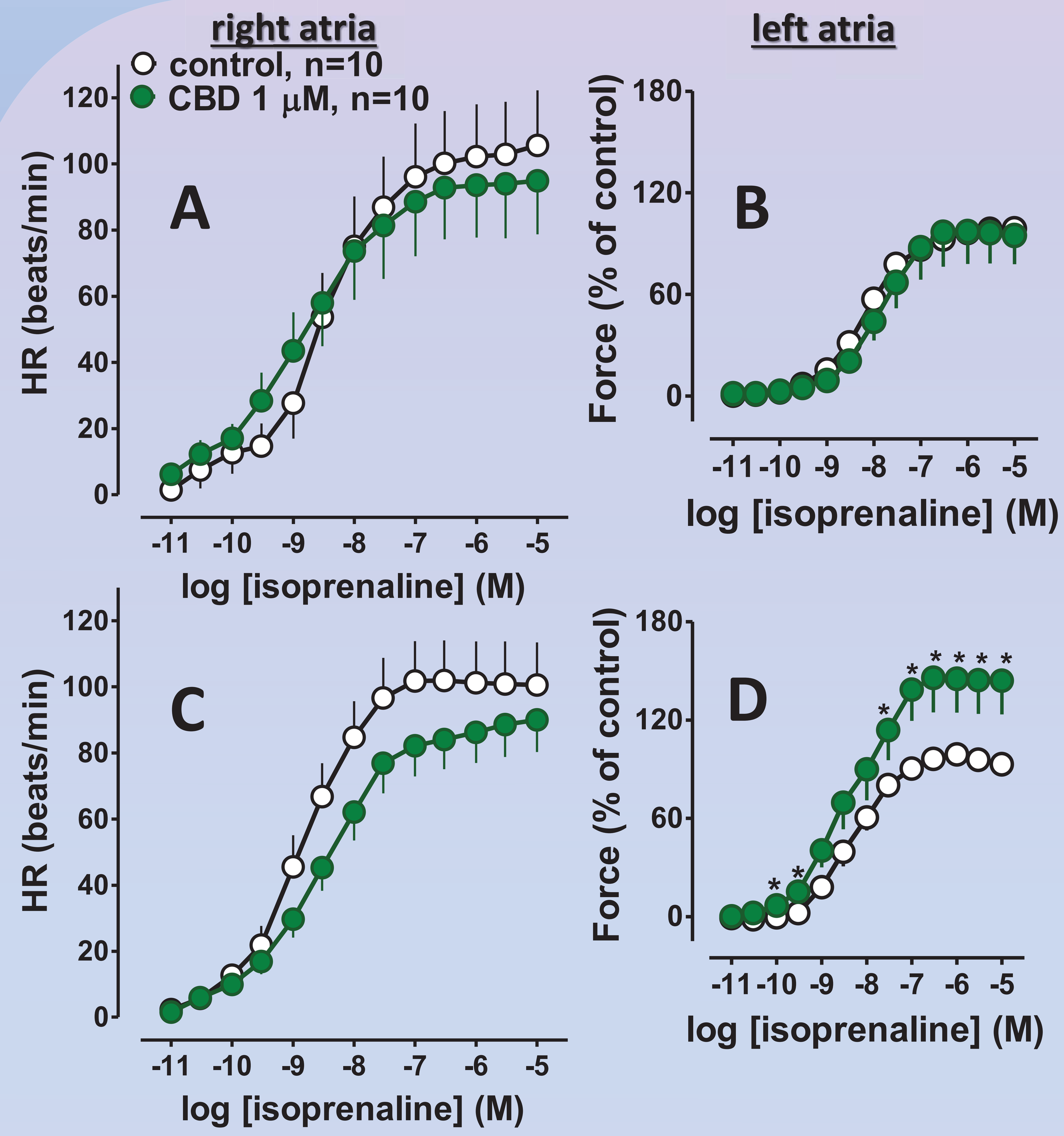

Figure 3. The influence of CBD (1 μM) on isprenaline-dependent (0.01 nM – 10 μM) increase in heart rate and force of contractions of right and left rat atria. Isoprenaline was given after H/R. (A, B) and on basal conditions (C, D) t – test ($p<0.05$* vs control).

	ISO was given after H/R (Protocol 1)				ISO was given on basal conditions (Protocol 2)			
	RIGHT ATRIUM		LEFT ATRIUM		RIGHT ATRIUM		LEFT ATRIUM	
n=10	control	CBD	control	CBD	control	CBD	control	CBD
basal	364±11	369±17	2.1±0.1	2.1±0.1	359±15	373±12	2.2±0.1	2.2±0.1
E_{max}	106±17	95±16	99±1	97±19	111±16	90±10	99±1	146±21*
pEC_{50}	8.5±0.2	8.7±0.2	8.2±0.1	7.9±0.2	8.8±0.2	8.5±0.1	8.3±0.1	8.4±0.2

Table 1. Basal values and influence of CBD (1 μM) on isprenaline-dependent (0.01 nM – 10 μM) increase in rate and force of contractions of right and left rat atria, respectively. Isoprenaline was given before and after hypoxia. t – test ($p<0.05$* vs control).

CONCLUSION

CBD influences atrial response to hypoxia and reoxygenation but in a different manner in right and left rat atria. Additionally, CBD potentiates inotropic effects of adrenergic stimulation.

AKNOWLEDGEMENTS

The work has been supported by the National Science Centre (Poland), research grant 2019/03/X/NZ7/00446.

REFERENCES

[1] Sagredo et al. Biochem Pharmacol. 2018;157:85
[2] Walsh et al. Br J Pharmacol 2010;160:1234
[3] Franco-Vadillo et al., Pharmacol Res Perspect. 2021; 9:e00784.
[4] Shayesteh et al., Curr Pharm Des 2019;25(22):2499-2507.

NEUROPEPTIDE FF COUNTERACTS OPIOID INDUCED RESPIRATORY DEPRESSION

P. Wojciechowski, K. Andrzejewski, K. Kaczyńska

Department of Respiration Physiology, Mossakowski Medical Research Institute Polish Academy of Sciences, Warsaw, Poland

Introduction and objectives

The activity of opioids undergoes the regulation by a homeostatic anti-opioid system involving i.a. neuropeptide FF (NPFF) – a member of RF-amidated neuropeptides.

Phe - Leu - Phe - Gln - Pro - Gln - Arg - Phe-NH_2
(FLFQPQRF-NH_2)

This peptide does not bind to opioid receptors.

The share of this peptide to the modulation of pain perception, opioid-induced tolerance, and dependence seems to be well documented while there is limited information about its effect on respiratory pattern and opioid-induced respiratory depression.

Hence the aim of the present study was to examine the influence of intracerebroventricular (icv) administration of NPFF on respiration and its effect on post-opioid cessation of breathing (apnea).

Methods

Object: Male Wistar rat

n: 5-7 per group

Weight: 262 ± 24 g

Anaesthesia: urethane + α-chloralose

Surgery:

- Tracheostomy tube connected to a pneumotach head to measure respiratory variables
- Arthery and vein cannulation for blood pressure monitoring and drug administration
- Bipolar electrode placed in sternal part of the diaphragm to monitor its activity
- Right lateral ventricle injected drugs (coordinates adjusted according to Paxinos and Watson stereotactic atlas, 2006)

Drugs:

- IV: Saline; EM-1 50 ug/kg; 1 ml/kg
- ICV: Saline, NPFF 1, 10, 20 ug; NPFF+RF9 (NPFF antagonist) 20+20 ug; 5 ul per rat

Results and Conclusions

The icv pre-treatment with NPFF dose-dependently limited the number of EM-1 -induced apneas and at the dose of 20 μg abolished its presence completely (Fig. 1ab Fig.2a) reducing the T_E test/T_E control ratio from 16.2 ± 8.6 s in saline group to the 1.0 ± 0.1 s (Fig. 2b). 20 μg of NPFF together with the smaller dose of 10 μg reduced maximal drop in MAP and HR (Tab. 1).

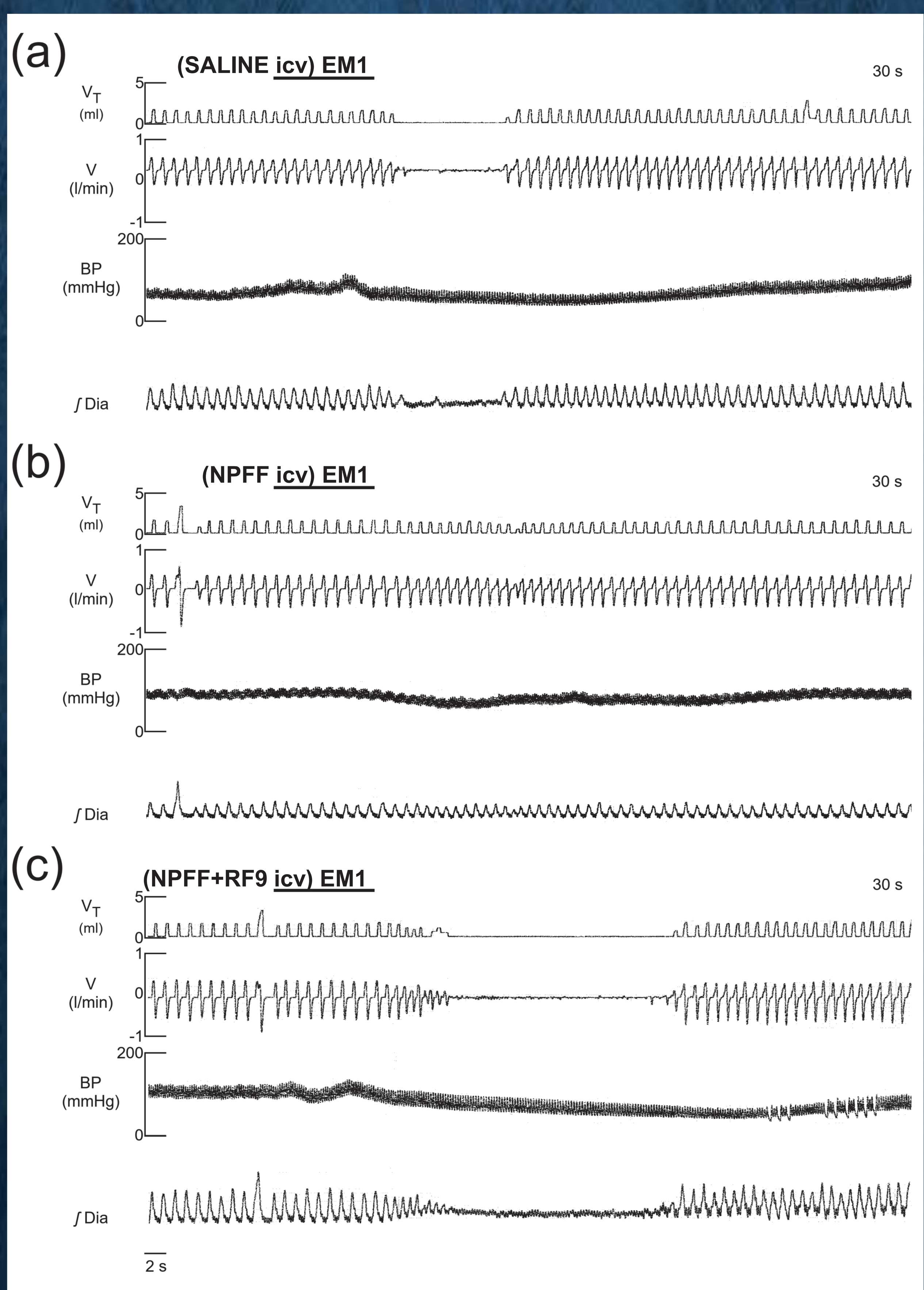

Fig. 1 Exemplary responses to intravenous EM-1 injection in:

(a) control rat; (b) after icv pre-treatment with 20 μg NPFF and (c) a mixture of 20 μg of NPFF and 20 μg RF9 (an antagonist of NPFF receptors). The line above top traces shows the injection of EM-1.

(a) – present apneic spell and a drop in arterial blood pressure after EM-1 injection, and recovered breathing and blood pressure
(b) – icv injection of NPFF abolished the apnea and hypotensive effect of EM-1 injection.
(c) – co-administration of NPFF and RF9 restored the EM-1 ability to induce apnea and drop in arterial blood pressure.

V_T – tidal volume; V – airflow; BP – blood pressure; ∫DIA – integrated electromyogram of the diaphragm

		Saline	NPFF 1 μg	NPFF 10 μg	NPFF 20 μg	NPFF 20 μg RF9 20 μg
	n	7	5	7	5	6
HR 1/min	Baseline	428 ± 39	410 ± 32	430 ± 31	459 ± 15	413 ± 56
	MIN 0–30 s	**387 ± 11** *	**394 ± 34** *	398 ± 33	400 ± 5 #	**354 ± 33** *
	Recovery (1 min)	412 ± 18	426 ± 12	455 ± 20 *	456 ± 23	432 ± 31
MAP mmHg	Baseline	81 ± 4	75 ± 15	77 ± 6	76 ± 7	73 ± 7
	MIN 0–30 s	**51 ± 2** *	**43 ± 3** *#	68 ± 21	66 ± 5	**52 ± 16** *
	Recovery (1 min)	81 ± 7	67 ± 15	89 ± 10	85 ± 7 *	73 ± 9

Median ± QD; Wilcoxon test: * $p < 0.05$ vs. Baseline; Mann–Whitney test: # $p < 0.05$ vs. control (saline) group.

Tab.1 Modulation of cardiovascular effects of intravenous EM-1 by icv administration of NPFF FF

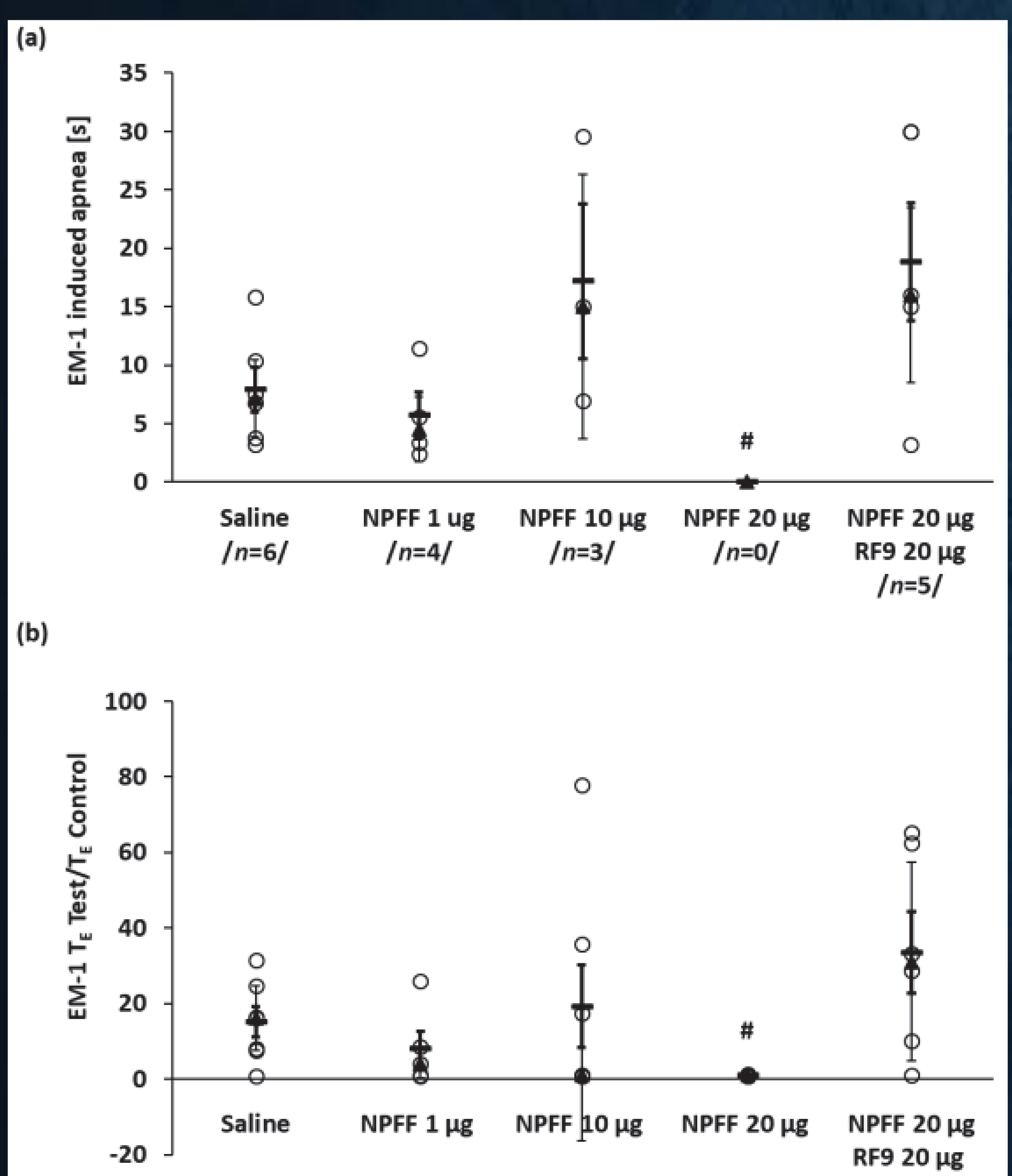

Fig. 2 The dose dependent effect of icv NPFF administration on the number and duration of EM-1-induced apneas (a) and TE test/TE control ratio (b)

The above mentioned effects of icv NPFF on EM-1-induced cardiovascular and respiratory pattern were completely blocked by icv pre-tretreatment with NPFF receptor antagonist – RF9 (20 μg) (Fig. 1c Fig. 2, Tab. 1)

Our experiments showed that centrally administered neuropeptide FF weakens the respiratory depression induced by iv EM-1 injection. This suggests the important role of NPFF and its receptors localized centrally in the manifestation of vagally mediated opioid-induced apnea.

References / Bibliography:
Wojciechowski et al., 2020

Polish National Science Center MINIATURA 1 Program
(2017/01/X/NZ4/00465)

INFLUENCE OF CANNABINOID CB_1 AND CB_2 RECEPTOR ANTAGONISTS ON CARDIOSTIMULATORY EFFECTS OF ISOPRENALINE IN HUMAN ATRIAL TRABECULAE

S6.P20

J. WERESA[1], A. PĘDZIŃSKA-BETIUK[1], G. HIRNLE[2], M. MITROSZ[2], B. MALINOWSKA[1]
[1]Department of Experimental Physiology and Pathophysiology, [2]Department of Cardiac Surgery, Medical University of Białystok, Poland

INTRODUCTION

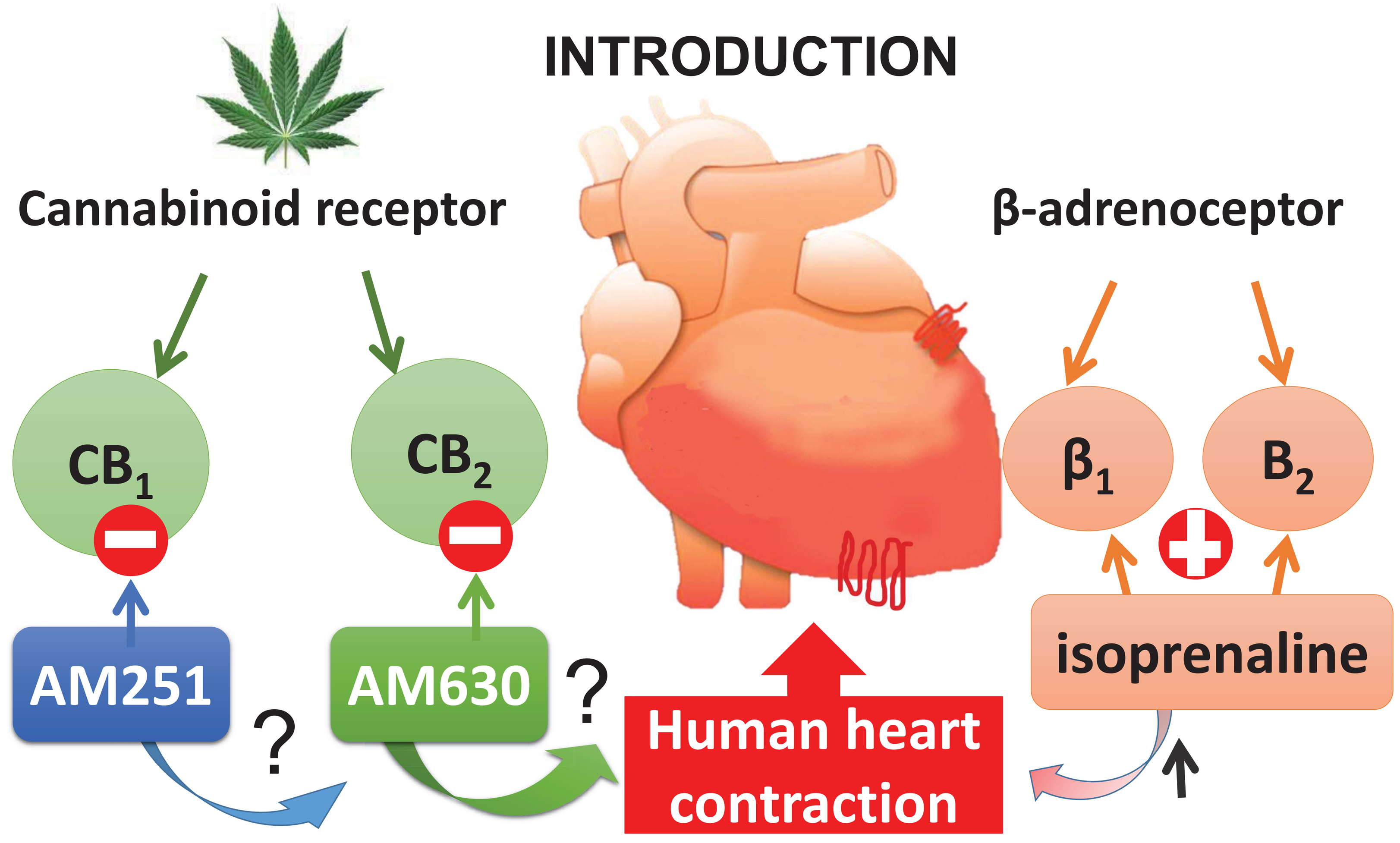

- CB_1 and CB_2 cannabinoid receptors are present in the human heart [2].
- Cannabinoid receptor antagonists, AM251 (CB_1) and AM630 (CB_2) modulate cardiostimulatory effects of isoprenaline in atria of Wistar rats [1].
- Cannabinoids acting on CB_1 receptors dose - dependently decrease contractile function in human atrial myocardium [3].

AIM

The aim of our study was to examine the influence of cannabinoid receptor antagonists CB_1 AM251 and CB_2 AM630 on isoprenaline-induced positive inotropic effect in the trabeculae from human right atrium.

METHODS

1. Dissection of the right atrial appendages from patients undergoing coronary artery bypass grafting, valve surgery, combination of both or ascending aorta surgery procedures.
2. Isolated trabeculae from human right atrium (diameter, 1-3 mm; length, 4-8 mm).
3. Connection to isometric force transducers.
4. Electrical stimulation (5 ms duration, 1 Hz).

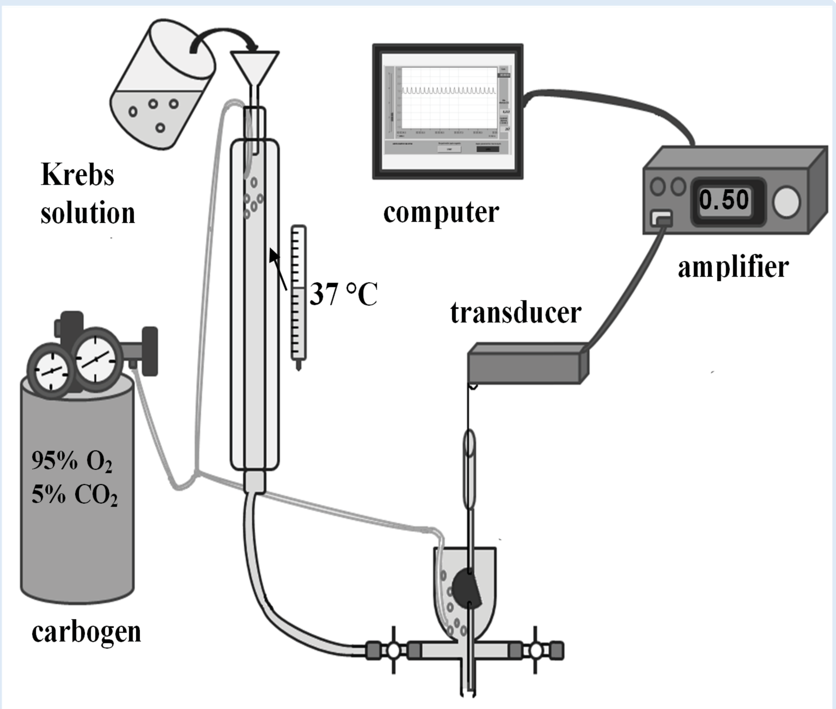

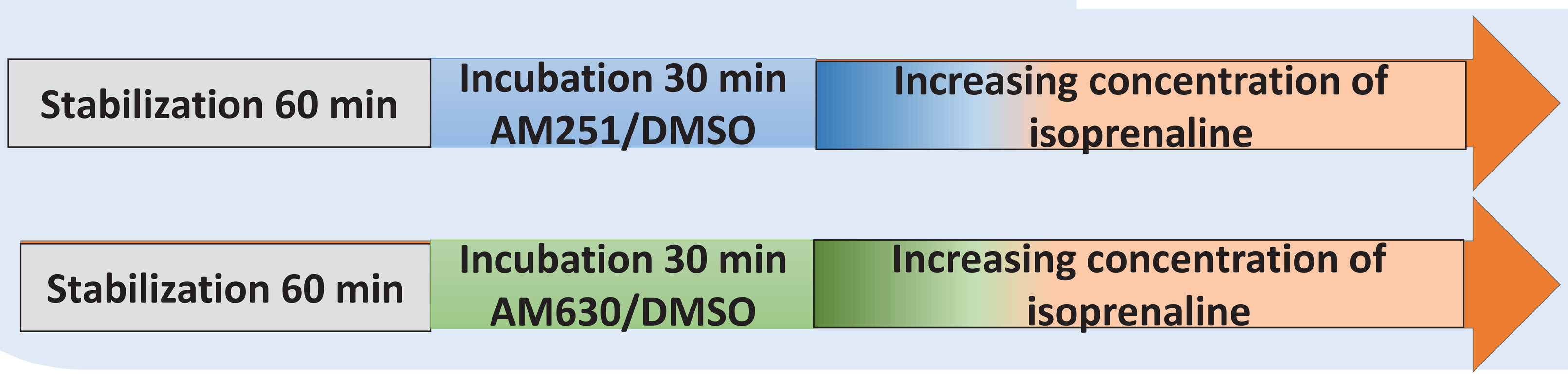

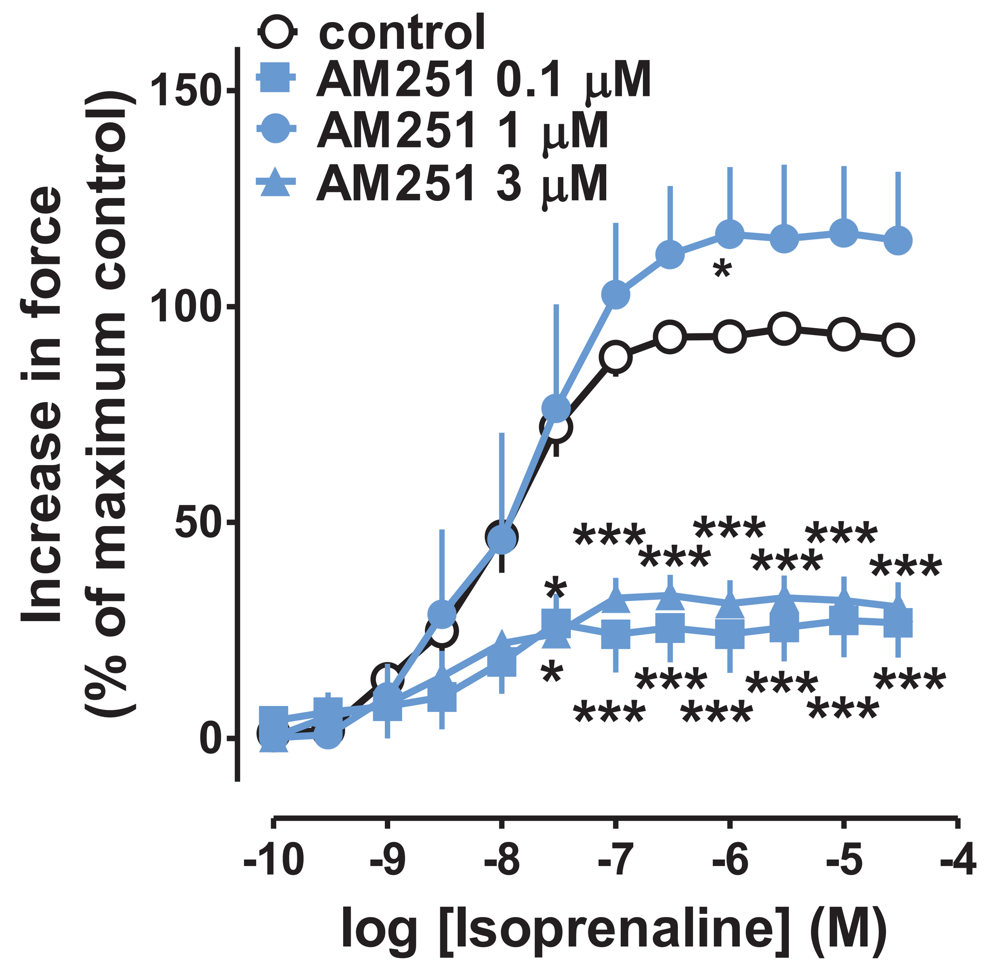

Figure 1. Influence of AM251 or their vehicle (control-DMSO) on the positive inotropic effects of isoprenaline in isolated human right atrial appendages. Data are presented as means ± SEM of 5-15 experiments. *$P < 0.05$; **$P < 0.01$; ***$P < 0.001$, compared to the respective values in control groups.

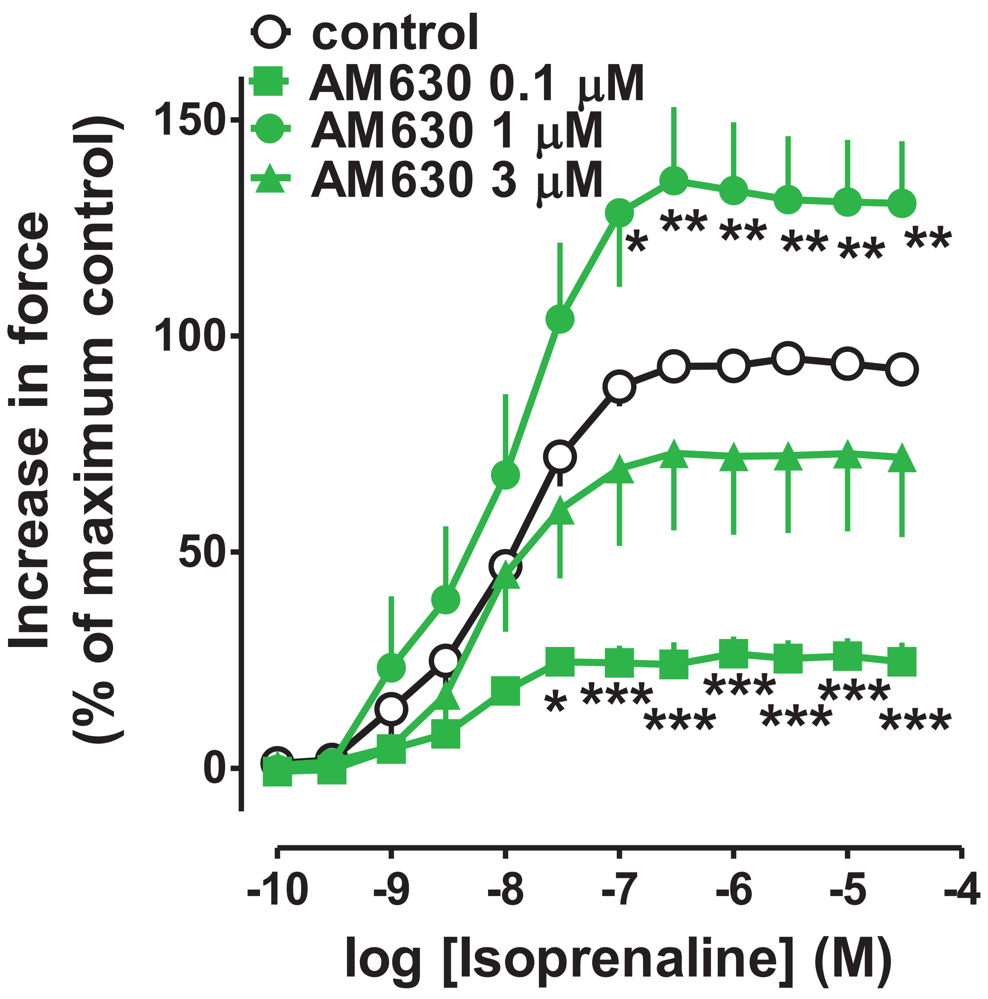

Figure 2. Influence of AM630 or their vehicle (control-DMSO) on the positive inotropic effects of isoprenaline in isolated human right atrial appendages. Data are presented as means ± SEM of 5-15 experiments. *$P < 0.05$; **$P < 0.01$; ***$P < 0.001$, compared to the respective values in control groups.

TABLE 1 Patient characteristics

General		
Total patients, n	30	
Age (years) (mean ± SEM)	67±1	
Gender, male/female, n (%)	21 (70)/9 (30)	
BMI (kg/m^2) (mean ± SEM)	30±1	
LVEF % (mean ± SEM)	49±2	
Diseases	**n**	**%**
Smokers	4	13
Atrial fibrillation	6	20
History of infarction	11	37
Coronary artery disease (CAD)	10	33
Valvular heart disease (VHD)	3	10
Ascending aorta disease	6	20
CAD+VHD	11	37
Hypertension	26	87
Hyperlipidaemia	29	97
Diabetes mellitus	12	40
Kidney disease	7	23
Lung disease	3	10
Prostate disease	4	13
Thyroid disease	3	10

Drugs	n	%
β-Blockers	26	87
Bisoprolol	15	50
Metoprolol	6	20
Nebivolol	4	13
Sotalol	1	3
Calcium channel blockers	13	43
ACE inhibitors	18	60
AT_1 receptor antagonists	10	33
α_1-Adrenoceptor antagonists	6	20
Hypoglycemic medication	12	40
Lipid lowering drugs	29	97
Diuretics	17	57
Protein pump inhibitors	15	50
Acetylsalicylic acid	16	53

TABLE 2. Effects of AM251 and AM630 on the concentration-response curves of isoprenaline in isolated human right atrial appendages.

	μM	n	Basal force (mN)	pEC_{50}	E_{max} (%)
control		15	2.4±0.1	8.0±0.1	95±2
AM251	0.1	6	2.5±0.2	8.3±0.4	**27±9*** **
	1	6	2.1±0.3	7.8±0.2	117±15
	3	5	2.4±0.1	8.4±0.2	**33±5*** **
AM630	0.1	5	2.2±0.2	8.3±0.2	**27±4*** **
	1	6	2.2±0.2	8.1±0.2	**136±17** **
	3	5	2.3±0.2	8.1±0.2	73±18

Data are presented as means ± SEM. *$P < 0.05$; **$P < 0.01$; ***$P < 0.001$, compared to the respective values in control groups.

CONCLUSION

1. Cannabinoid CB_1 and CB_2 receptor antagonists AM251 and AM630 exert concentration-dependent beneficial and harmful effects on inotropic effects related to atrial β-adrenoceptor activation in humans.
2. Caution should be taken with their potential therapeutic application.

REFERENCES
[1]. Weresa J, Pędzińska-Betiuk A, Kossakowski R, Malinowska B. Cannabinoid CB_1 and CB_2 receptors antagonists AM251 and AM630 differentially modulate the chronotropic and inotropic effects of isoprenaline in isolated rat atria. *Pharmacol Rep*. 2019;71(1):82-89. doi:10.1016/j.pharep.2018.09.008
[2]. Weis F, Beiras-Fernandez A, Sodian R, et al. Substantially altered expression pattern of cannabinoid receptor 2 and activated endocannabinoid system in patients with severe heart failure. *J Mol Cell Cardiol*. 2010;48(6):1187-1193. doi:10.1016/j.yjmcc.2009.10.025
[3]. Bonz A, Laser M, Küllmer S, et al. Cannabinoids acting on CB_1 receptors decrease contractile performance in human atrial muscle. *J Cardiovasc Pharmacol*. 2003;41(4):657-664. doi:10.1097/00005344-200304000-00020

ACKNOWLEDGEMENTS SUB/2/DN/19/002/2213.

CHANGES IN ARTERIAL OXYGEN SATURATION IN HEALTHY PERSONS DURING BACK MASSAGE PROCEDURE

Paweł Radziejowski[1], Maria Radziejowska[1], Vladyslav Dychko[2], Olha Romaniv[1]

[1]Department of Innovations and Safety Management Systems, Faculty of Management, Czestochowa University of Technology, Poland;

[2]Department of Physical Therapy, Physical Education and Biology, Donbass State Pedagogical University, Slavyansk, Ukraine;

maria.radziejowska@pcz.pl

SESSION VII   FUNCTION OF BLOOD. HEMOSTASIS.   S7.P7   16:12 – 16:18

Introduction

- In late December 2019, a new wariant of coronavirus called SARS-CoV-2 emerged in China and spread rapidly around the world (Huang i wsp., 2020). Early descriptive reports of the clinical presentation of the disease resulting from SARS-CoV-2 infection, called the 2019 Coronavirus Disease (COVID-19) revealed that a third of patients were not suffering from breathlessness (Zhou i wsp., 2020; Guan i wsp., 2020). Further more, many patients who later developed respiratory failure experienced hypoxemia and hypercapnia without signs of respiratory failure, especially the elderly. This was called "silent hypoxemia" and was reported in patients during the initial Wuhan epidemic (Xie i wsp., 2020).

- The cause of this asymptomatic hypoxia is not yet clear. The condition has been described as a common clinical symptom in COVID-19 (Boudjema i in., 2020). Some researchers justify the occurrence of this hypoxemia with the development of thrombi in the pulmonary vascular system (Couzin-Frankel, 2020).
- The current goal of arterial oxygen saturation for COVID-19 patients recommended by the National Institutes of Health is92-96% (Luks AM, Swenson ER, 2020). In the light of these data, it seems that after COVID-19 arraved control of S_aO_2 level and other breathing parameters may be of particular importance in assessing the effectiveness of using physiotherapeutic methods, which include, among others, classic massage.

Hypothesis

The use of the thermovision method (for the standardization of the influence of massage techniques) and blood saturation measurement in the assessment of the effectiveness of classic massage used in humans during convalescence after COVID-19 will allow to increase the knowledge about the degree of activation of the system's compensation mechanisms, which are involved in the recovery of the organism infected with the virus Sars-CoV-2. We believe that before starting such research, you should know how the massage treatment will affect healthy people, because there is not much such data and they mainly concern infants and professional athletes (Mirzarahimi M. , Nasrin M. , Sahife S. , Nasrin S., Firouz A., 2013; Gatterer, H., Schenk, K., Wille, M., Murnig, P., & Burtscher, M. ; 2013) .

- The aim of this study was to assess changes in arterial oxygen saturation (S_aO_2) in healthy persons during a procedure of back massage. Relevance of this studies is justified by the fact that it is crucial to control the level of S_aO_2 when massaging persons who recovered from COVID-19 in order to assess efficiency of any therapeutic measures, including physiotherapy, for instance massage therapy.

- The studies included 3 women and 3 men aged 43.5±1.5 years, BMI = 24.84±2.03 kg/m^2. All subjects signed a written consent to take part in the study (permission of the Kazimiera Milanowska College of Education and Therapy Bioethical Commission – Resolution No. 006/2018/2019 of 10.05.2019).

The intensity of the classical back massage was controlled with thermovision pictures (thermovision camera Flir E6, Estonia) taken before and after the procedure what enabled, through the assessment of temperature distribution in the massaged area, to even out the level of stimulation caused by the mechanical influence of manual massage (the increase in the massaged area temperature was 3.02±0.38°C).

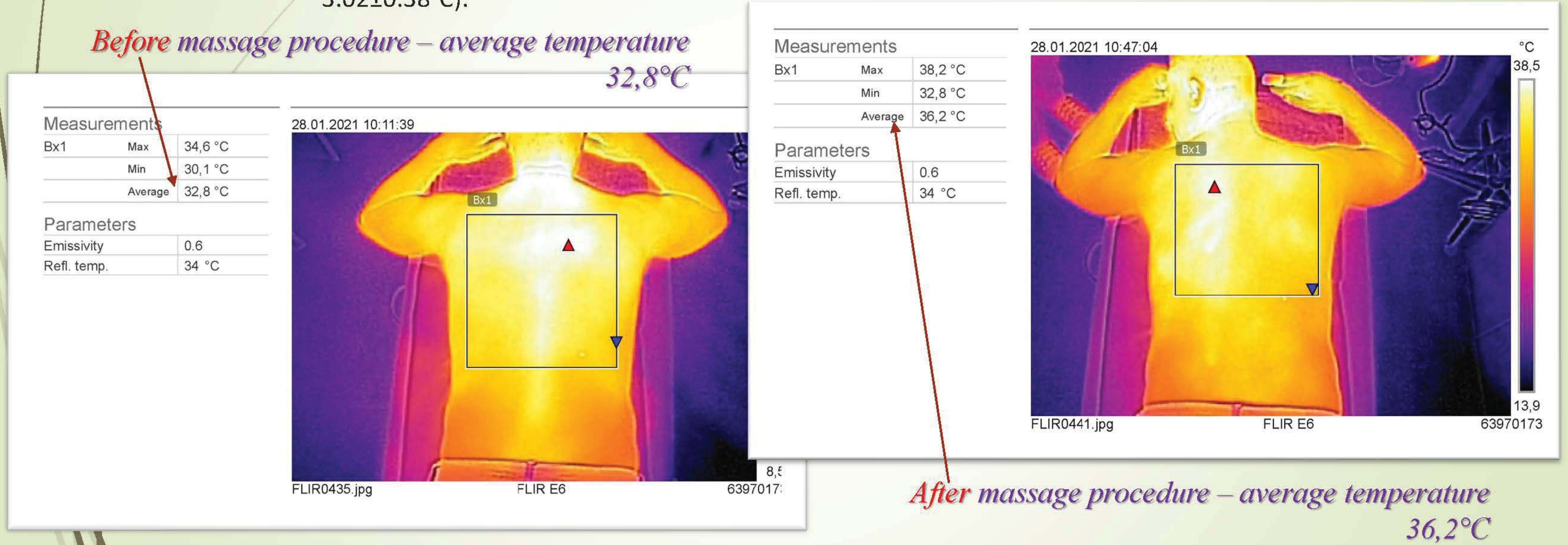

- The procedure lasted for 20 minutes. The massage was conducted according to the rules of the safe classical massage methodology (Zborowski, 2010).

Oxygen saturation and heart rate were measured with pulse oximeter (OxyShuttle, USA) before the procedure, with a patient lying down, during the procedure, and within 5 minutes after the procedure was completed. The baseline S_aO_2 was 96.83±0.75% (1). The highest deviation from the baseline was observed during the massage of left and right side intercostal muscles (7th and 14th minute of the procedure, respectively); S_aO_2 decreased to 94.0±0.63% (2 - 7th minute, left side) and 94.16±0.75% (3 - 14th minute, right side). Decrease in S_aO_2 to 94.5±0.55% was also noted at the completion of the procedure, after employing the tapotement techniques (hacking and cupping) (4). 5 minutes after the massage, the level of S_aO_2 increased to 97.0±0.63% (5).

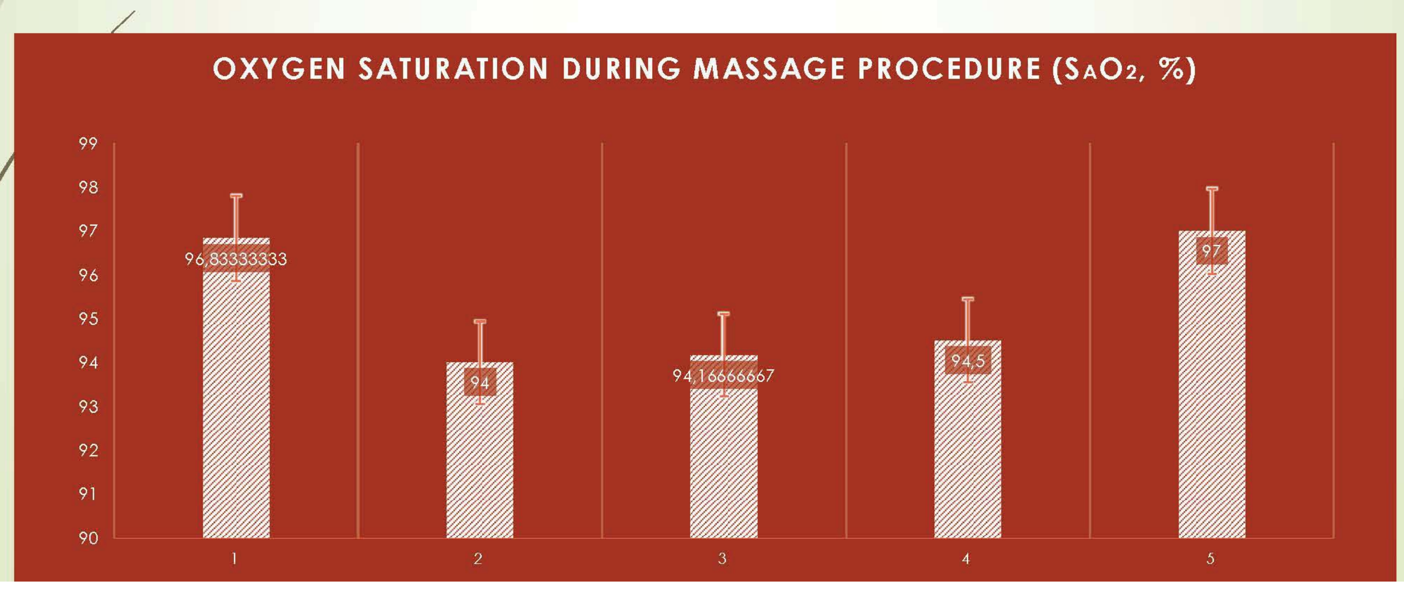

Changes in S_aO_2 observed during the massage procedure can indicate that during the massage the vesicular ventilation to blood flow velocity ratio changes similarly to low intensity physical activity due to increased temperature of the massaged area.

Noting such changes in healthy people should be treated as preliminary results and when adding the massage treatment to the comprehensive therapy after COVID-19, cautiously use strike techniques (tapotement), which even in healthy people may temporarily reduce the level of blood saturation. This data is still not enough for final conclusions, we will continue them with the inclusion of more measurements in the research.

References

1. Bauer J., E. Boerner, H. Podbielska: *Termowizyjna ocena kolejności stosowania zabiegów fizykalnych*, [w:] *Biomedyczne zastosowania termowizji*, H. Podbielska, A. Skrzek (red.), Oficyna Wydawnicza Politechniki Wrocławskiej ukaże się w 3 kwartale 2014r.
2. Boudjema S., Finance J., Coulibaly F., Meddeb L., Tissot-Dupont H., Michel M. et al. Olfactory and gustative disorders for the diagnosis of COVID-19. *Travel Med Infect Dis.* 2020; : 101875.
3. Couzin-Frankel J. The mystery of the pandemic's 'happy hypoxia'. *Science.* 2020; 368: 455-456.
4. Elsagh, A., Lotfi, R., Amiri, S., & Gooya, H. H. (2019). Comparison of Massage and Prone Position on Heart Rate and Blood Oxygen Saturation Level in Preterm Neonates Hospitalized in Neonatal Intensive Care Unit: A Randomized Controlled Trial. *Iranian journal of nursing and midwifery research, 24*(5), 343–347. https://doi.org/10.4103/ijnmr.IJNMR_34_18
5. Gatterer, H., Schenk, K., Wille, M., Murnig, P., & Burtscher, M. (2013). Effects of massage under hypoxic conditions on exercise-induced muscle damage and physical strain indices in professional soccer players. Biology of Sport, 30(2), 81-83.
6. Guan W.J., Ni Z.Y., Hu Y., Liang W.H., Ou C.Q., He J.X. et al. Clinical characteristics of coronavirus disease 2019 in China. *N Engl J Med.* 2020; 382: 1708-1720
7. Huang C., Wang Y., Li X., Ren L., Zhao J., Hu Y. et al. Clinical features of patients infected with 2019 novel coronavirus in Wuhan, China. *Lancet.* 2020; 395: 497-506.
8. Luks AM, Swenson ER (September 2020). "Pulse Oximetry for Monitoring Patients with COVID-19 at Home. Potential Pitfalls and Practical Guidance". *Annals of the American Thoracic Society.* ***17** (9): 1040–1046.* doi:10.1513/AnnalsATS.202005-418FR. PMC 7462317. PMID 32521167.
9. Mirzarahimi Mehrdad , Nasrin Mehrnoush , Sahife Shahizadeh , Nasrin Samadi, Firouz Amani Effect of non-nutritive sucking and leg massage on physiological and behavioral indicators of pain following heel blood sampling in term neonates International Journal of Advanced Nursing Studies, 2 (2) (2013) 74-79 ©Science Publishing Corporation www.sciencepubco.com/index.php/IJANS
10. Radziejowska Maria, Paweł Radziejowski, Kinga Rutkowska Effectiveness of Chinese cupping massage during the initial stage of lipodystrophy (case report) // Journal og Physical Education and Sport (JPES), Vol. 20 (Supplement issue 3), Art 300, pp 2239 – 2245, 2020 online ISSN: 2247 - 806X; p-ISSN: 2247 – 8051; ISSN - L = 2247 – 8051 (DOI:10.7752/jpes.2020.s3300).
11. Radziejowska Maria, Paweł Radziejowski, Olha Romaniv Effects of massaging upper limb parts in different order on changing the level of blood circulation in the massaged area // Journal og Physical Education and Sport (JPES), Vol. 20 (Supplement issue 6), Art 444 pp 3273 – 3279, 2020 online ISSN: 2247 - 806X; p-ISSN: 2247 – 8051; ISSN - L = 2247 – 8051 (DOI:10.7752/jpes.2020.s6444).
12. Ring E.F., H. McEvoy, A. Jung, J. Zuber, G. Machin: *New standards for devices used for the measurement of human body temperature*, Journal of Medical Engineering & Technology, vol. 34(4), 2010, s. 249–253.
13. Xie J., Tong Z., Guan X., Du B., Qiu H., Clinical characteristics of patients who died of coronavirus disease 2019 in China. *JAMA Netw Open.* 2020; 3e205619
14. Zborowski. *Masaż w wybranych jednostkach chorobowych.* Kraków 2010.
15. Zhou F., Yu T., Du R., Fan G., Liu Y., Liu Z., et al. Clinical course and risk factors for mortality of adult inpatients with COVID-19 in Wuhan, China: a retrospective cohort study. *Lancet.* 2020

XXVIII Congress of the Polish Physiological Society

Gdańsk, September 15-17 2021

Poster book

SESSION VII

FUNCTION OF BLOOD. HEMOSTASIS

HONORARY PATRONAGE

Prof. dr Marcin Gruchała
Rector of the Medical University of Gdansk

Uniwersytet Gdański

Prof. dr Piotr Stepnowski
Rector of the University of Gdansk

WOJEWODA POMORSKI
DARIUSZ DRELICH

Dariusz Drelich
Governor of the Pomeranian Voivodeship

HONORARY PATRONAGE
Mayor of the City of Gdańsk

Aleksandra Dulkiewicz
Mayor of Gdansk

Mieczysław Struk
Marshal of the Pomeranian Voivodeship

PARTNER

PAN
POLSKA AKADEMIA NAUK

ANIMA LAB
animal facility and laboratory equipment • animal research models

FUNDACJA LOTOS

Medical University of Gdansk
Department of Physiology

CONTRIBUTION OF GASEOUS TRANSMITTERS TO THE OZONE EFFECT ON BLOOD OXYGEN TRANSPORT FUNCTION UNDER HYPOCAPNIC CONDITIONS

V.ZINCHUK [1], E.BILETSKAYA [1], A. MURAVYOV[2]

zinchuk@grsmu.by, biletskaya.e@inbox.ru, alexei.47@mail.ru

[1] Grodno State Medical University, Department of Normal Physiology, Grodno, Belarus
[2] Yaroslavl State Pedagogical University named after K.D. Ushinsky, Department of Medical and Biological Foundations of Sports, Yaroslavl, Russia



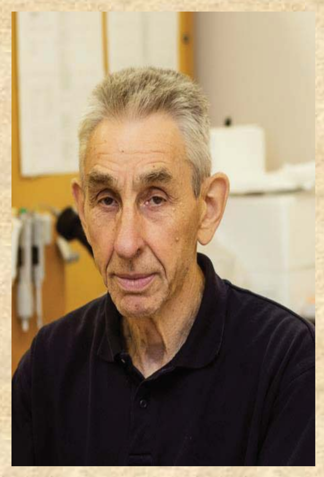

Introduction:

Ozone (O_3) is a physiological factor that can change hemoglobin oxygen affinity and the formation of gaseous transmitters (NO, H_2S) [1]. O_3 improves tissue oxygenation that enable to use it in hypoxic conditions, which are often accompanied by hypocapnia [2].

Objectives:

To study the contribution of gaseous transmitters to the effect of ozone (6 mg/L) on blood oxygen transport function under hypocapnic conditions (4,2% CO_2; 5,3% O_2, 90,5% N_2) *in vitro* experiments at exposure of 30 minutes was studied.

Methods:

The following parameters of blood oxygen transport function were determined: oxygen partial pressure (pO_2), blood oxygen saturation (SO_2), hemoglobin affinity for oxygen according p50 value (with pO_2 equal 50%). Ozonized isotonic sodium chloride solution in a volume of 1 ml and donors of nitrogen monoxide and hydrogen sulfide gaseous transmitters were added to blood samples (nitroglycerin at a final concentration of 0.05 mmol / L and sodium hydrosulfide at a final concentration of 0.38 mmol / L) .

Results:

Introducing O_3 into the blood samples led to an increase in the main parameters of the blood oxygen transport function, such as SO_2, pO_2, $p50_{real}$, $p50_{stand}$ and the shift of the oxyhemoglobin dissociation curve to the right compared to control group. When treated with hypocapnic gas mixture, these parameters decreased compared to the control. Incubation of the blood samples in hypocapnic conditions enhanced the effect of O_3 on blood oxygen transport function parameters. Nitroglycerin caused a significant increase in this effect under given conditions of pO_2 and SO_2 that is parameters increased compared to the group of preliminary hypocapnia with the ozone addition. The $p50_{real}$ parameter increased and the shift of the oxyhemoglobin dissociation curve to the right became more pronounced. Sodium hydrosulfide did not have this effect. Concentration of NO_3^-/NO_2^- and H_2S in blood plasma at action of O_3 under conditions of hypocapnia did not change compared to the group in which only ozone was administered. The addition of nitroglycerin and sodium hydrosulfide under these conditions led to a significant increase of NO_3^-/NO_2^- and H_2S compared with group ozonised under hypocapnic conditions.

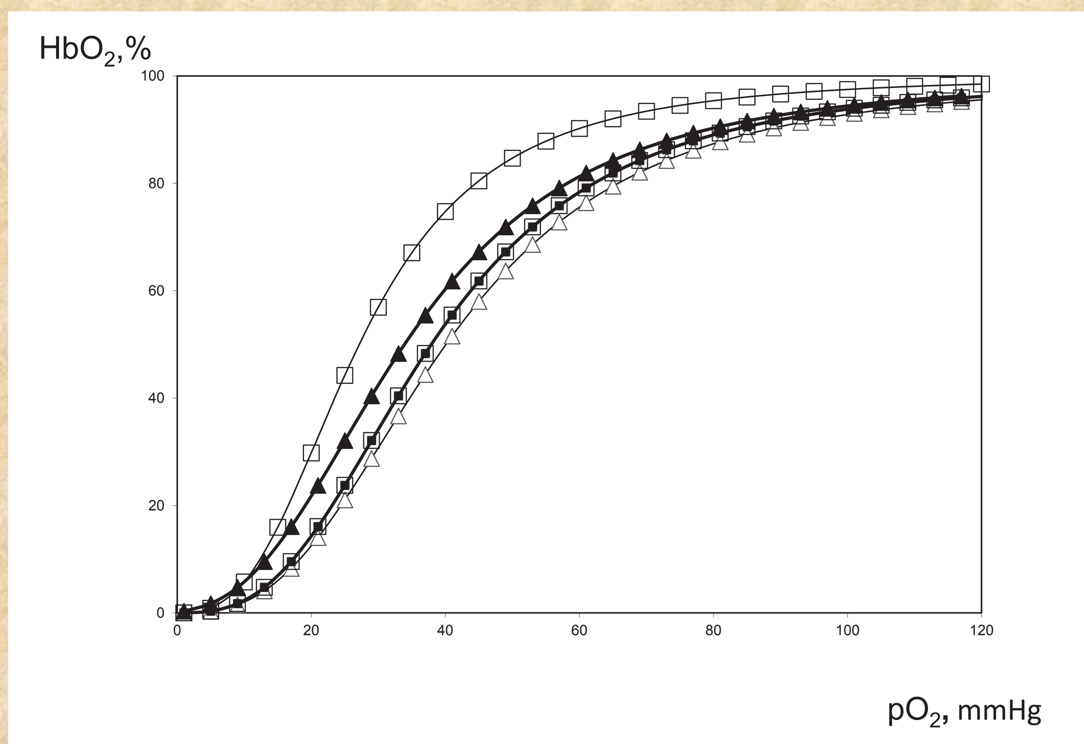

The effect of ozone on the position of the oxyhemoglobin dissociation curve at real pH and PCO_2 values: □ - control; ▲ - ozone; ■ - hypocapnia + ozone, △ - hypocapnia + nitroglycerin + ozone.

A

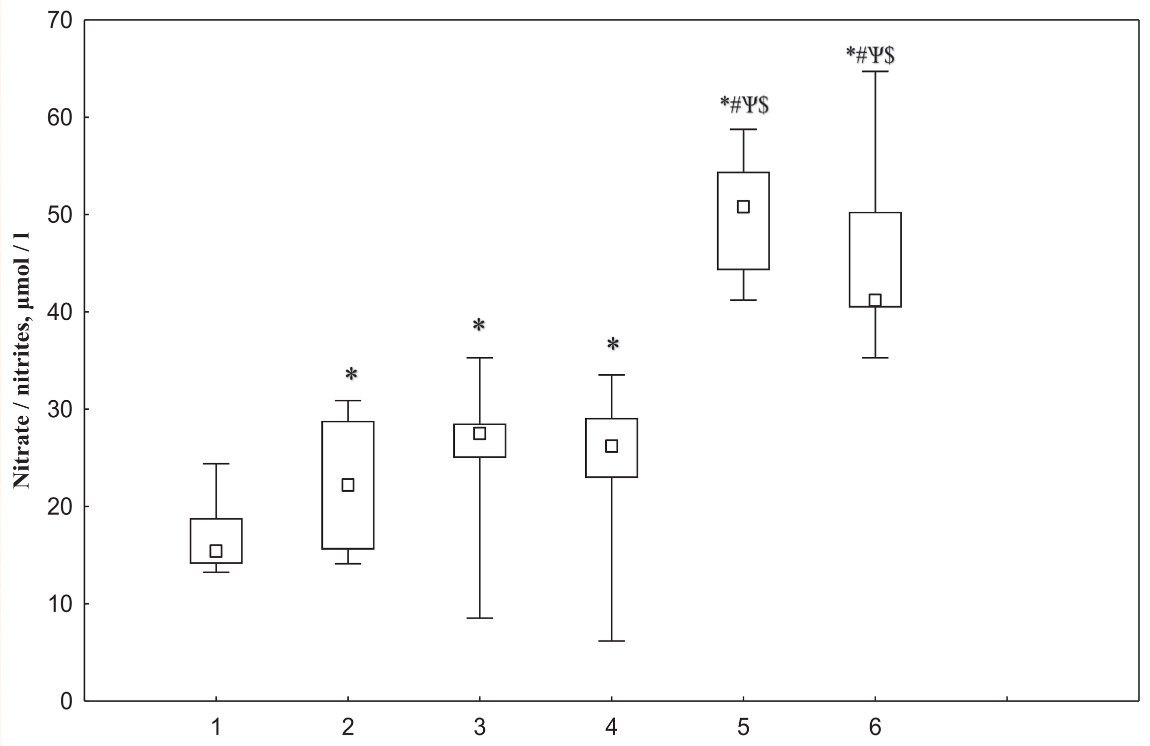

B

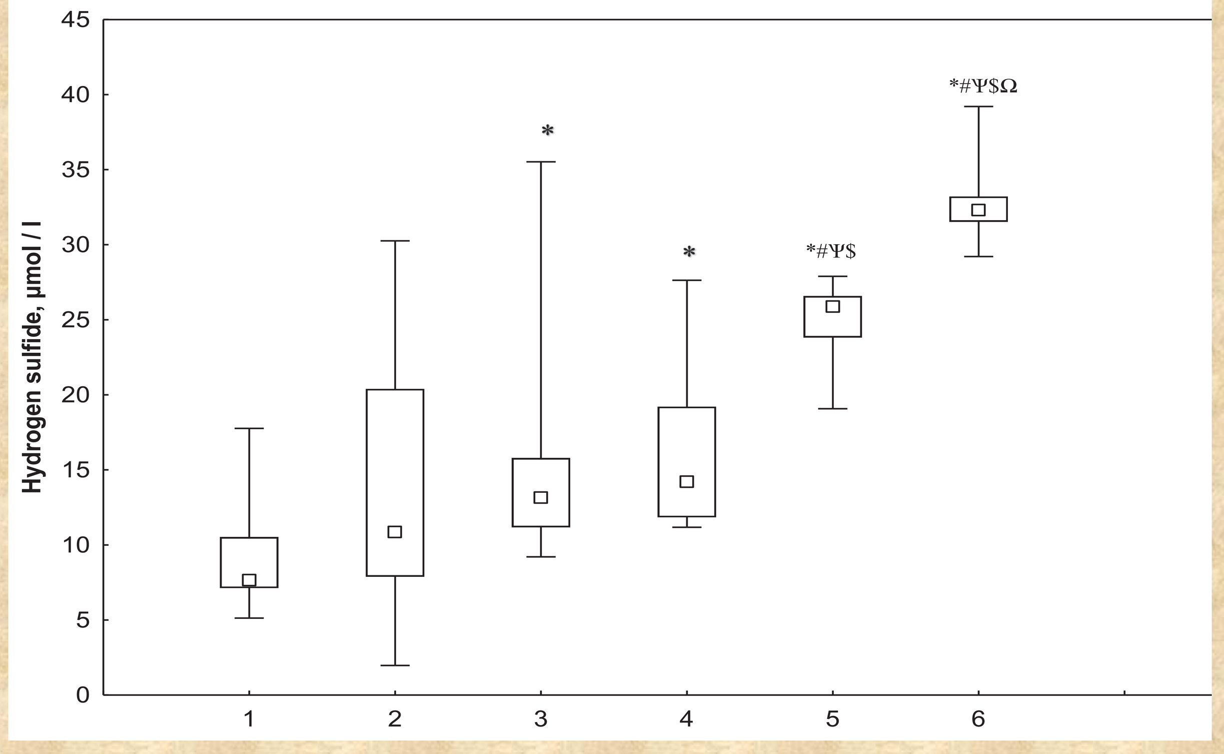

The concentration of nitrate / nitrite (A) and hydrogen sulfide (B) in blood plasma
Control (*), hypocapnia (#), ozone (Ψ), hypocapnia + ozone ($), hypocapnia + nitroglycerin + ozone (Ω).

Conclusions:

1. Under conditions of pretreatment with a hypocapnic gas mixture, the effect of ozone of the blood oxygen transport function increases significantly, which manifests itself in an increase in the following indicators: pO_2, SO_2, $p50_{real}$, $p50_{stand}$ and a shift of the oxyhemoglobin dissociation curve to the right.
2. The addition of nitroglycerin under these conditions leads to an even more pronounced intensification of the effect of ozone of the blood oxygen transport function, accompanied by an increase in the content of NO_3^- / NO_2^- and H_2S. Sodium hydrosulfide does not have a similar effect on the oxygen-binding properties of blood, despite an increase in the concentrations of NO_3^- / NO_2^- and H_2S.
3. Preliminary hypocapnia with ozone, as well as the addition of nitroglycerin or sodium hydrosulfide, do not significantly affect the state of the prooxidant-antioxidant balance of the blood under study.

References:

1. Yılmaz O, Bilge A, Erken HY, Kuru T. The effects of systemic ozone application and hyperbaric oxygen therapy on knee osteoarthritis: an experimental study in rats. Int Orthop. 2021 Feb;45(2):489-496. doi: 10.1007/s00264-020-04871-9. Epub 2020 Nov 13. PMID: 33185724
2. Scassellati C, Galoforo AC, Bonvicini C, Esposito C, Ricevuti G. Ozone: a natural bioactive molecule with antioxidant property as potential new strategy in aging and in neurodegenerative disorders. Ageing Res Rev. 2020;63:101138. doi:10.1016/j.arr.2020.101138

Acknowledgements: This work was supported by international projects No. M20P-428 – BRFFR and No. 20-515-00019- RFBR.

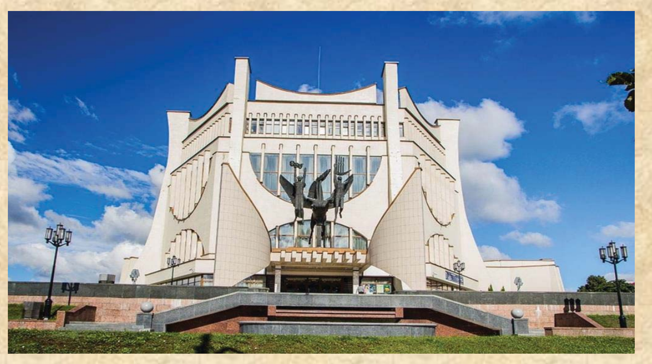

NEUTROPHIL-TO-LYMPHOCYTE RATIO AS A FACTOR PREDICTING RADIOTHERAPY INDUCED ORAL MUCOSITIS AND OVERALL SURVIVAL IN HEAD NECK CANCER PATIENTS TREATED WITH RADIOTHERAPY

Iwona Homa-Mlak[1], Anna Brzozowska[2] , Radosław Mlak[1], Aneta Szudy-Szczyrek[3], Teresa Małecka-Massalska[1]

1Department of Human Physiology, Medical University of Lublin, Poland;
2II Department of Radiotherapy, Center of Oncology of the Lublin Region St. John of Dukla, Poland
3 Department of Hemato-Oncology and Bone Marrow Transplantation, Medical University of Lublin, Lublin, Poland

Introduction

Epithelial tumors in the head and neck area (head and neck cancer-HNC) are ones of the most frequently tumors with as many as 650,000 new cases every year [1]. Despite comprehensive, highly specialized treatment of HNC patients, including surgery, radiotherapy (RT), chemotherapy (CTH) or the combination of these methods, we still achieve moderate rates of 5-year survival (from 27% up to 67%, depending on tumor location and degree of progression) [2,3].

Radical RT, often combined with chemotherapy (C-RT), leads to complications including severe acute radiation reaction in the area of mucosa (oral mucositis - OM). OM occurs in the majority of irradiated patients (80%), which constitutes a serious problem in everyday clinical practice [4–6]. From the clinical point of view, severe OM is particularly important, referred to as grades 3 and 4 according to the RTOG/EORTC scale [4].

Acute toxicities due to irradiation (e.g. OM) usually relent after few weeks of the end of RT. Starting from few months after RT late toxicity may develop including eg. xerostomia, cavities (dental caries), trismus due to fibrosis. The typical clinical symptom of OM is inflammation. Its gradual development manifests itself by severe pain, ulceration, dysphagia and deterioration of the quality of life (QoL) [5-7].

One of the markers of inflammatory reaction in the body is neutrophil-to-lymphocyte ratio (NLR) [8]. In patients with elevated NLR values, high levels of pro-inflammatory cytokines and increased peri-tumor macrophage infiltration are observed [9,10]. The hypothesis of our study assumes that NLR as an exponent of the inflammatory process may be a predictor of more severe OM in HNC patients undergoing RT.

Objectives

The aim of the study was to assess pre-treatment NLR in HNC patients subjected to IMRT and to analyse the relationship between NRL and OM severity as well as overall survival (OS).

Methods and material

Patient and clinical data:

This retrospective study involved 207 HNC patients in advanced stages of disease: III-IV (2014-2017). The disease stage has been evaluated using VIIth-edition of TNM classification (UICC). Only patients without infection symptoms and a normal CRP value (<5 mg/l) were included in our study. To exclude patients with infection urinalysis, CRP level assessment, and chest X-ray was performed. Patients who receive corticosteroids therapy one month before commencement of RT were not included in the study.

NLR

Blood samples for routine control were collected 1 to 3 days before the commencement of RT.

Results

Patient characteristics

The study group consisted of 92.3% men. The median age was 62 years. Squamous-cell carcinoma was diagnosed in all patients. At the time of enrolment, all patients were in advanced stage of disease (III-IV). All enrolled patients were treated with RT and received a complete treatment dose (48.3% patients were treated with surgery followed by RT; 5.8% underwent neoadjuvant chemotherapy followed by RT; 32.4% patients were treated with C-RT (13.5% received RT alone and 8.7% were subjected to concurrent C-RT).

Comparison of NLR values according to demographic and clinical factors as well as OM grade after subsequent weeks of RT

Starting from the 2nd week we observed significantly higher median NLR values in patients with more severe OM grade in all subsequent weeks of RT. (after 2nd week: 1.94 vs 1.69, p=0.0225; after 3rd week: 4.76 vs 1.75, p=0.0005; after 4th week: 2.60 vs 1.72, p=0.0159; after 5th week: 2.80 vs 1.70, p<0.0001; after 6th week: 2.74 vs 1.60, p<0.0001; after 7th week: 2.35 vs 1.60, p<0.0001; during 7 weeks: 2.35 vs 1.60, p<0.0001). Figure 1

Survival analysis

Median OS in the study group was 27 months. 55.1% of patients died during follow-up. Among analysed demographic and clinical factors significantly higher risk of death was found in patients with more advanced disease stage (IVA-IVC vs III: medians: 24 vs 38 months; HR=1.78; p=0.0041) and higher NLR values (medians: 23 vs 36 months; HR=1.45; p=0.0433; Figure 2). Multivariate analysis (results adjusted for statistically significant variables from univariate analysis) revealed that both higher TNM stage (HR=1.84; p=0.0043) and high NLR values (HR=1.48; p=0.0395) were independent prognostic factors

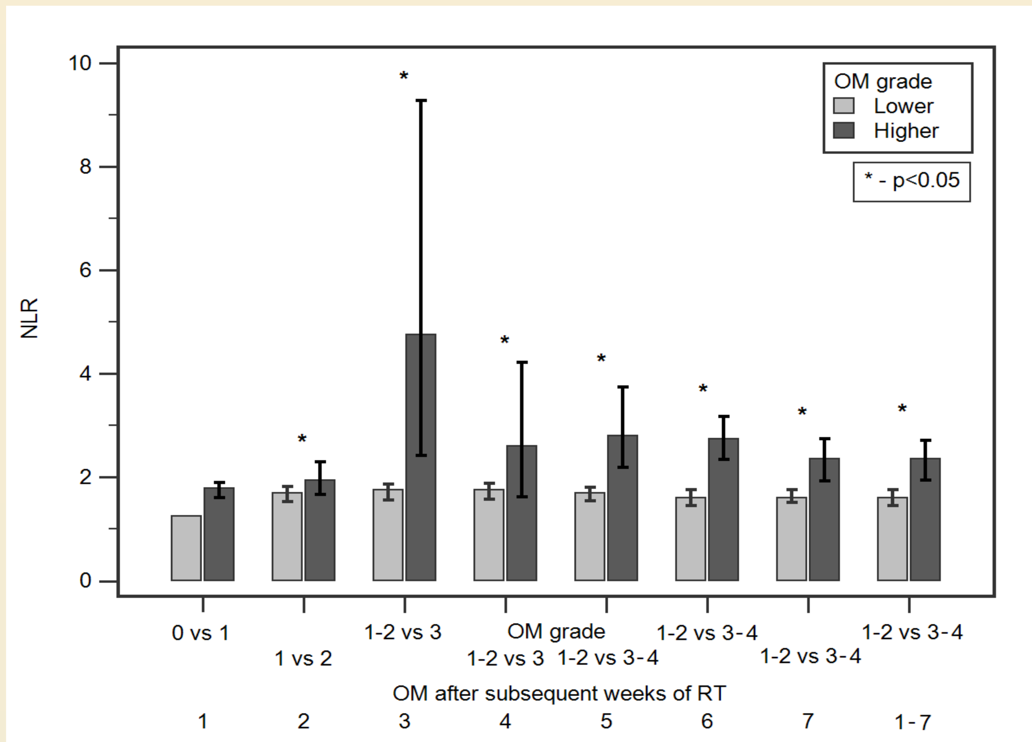

Figure 1. Comparisons of NLR values according to OM grade in subsequent weeks of RT.

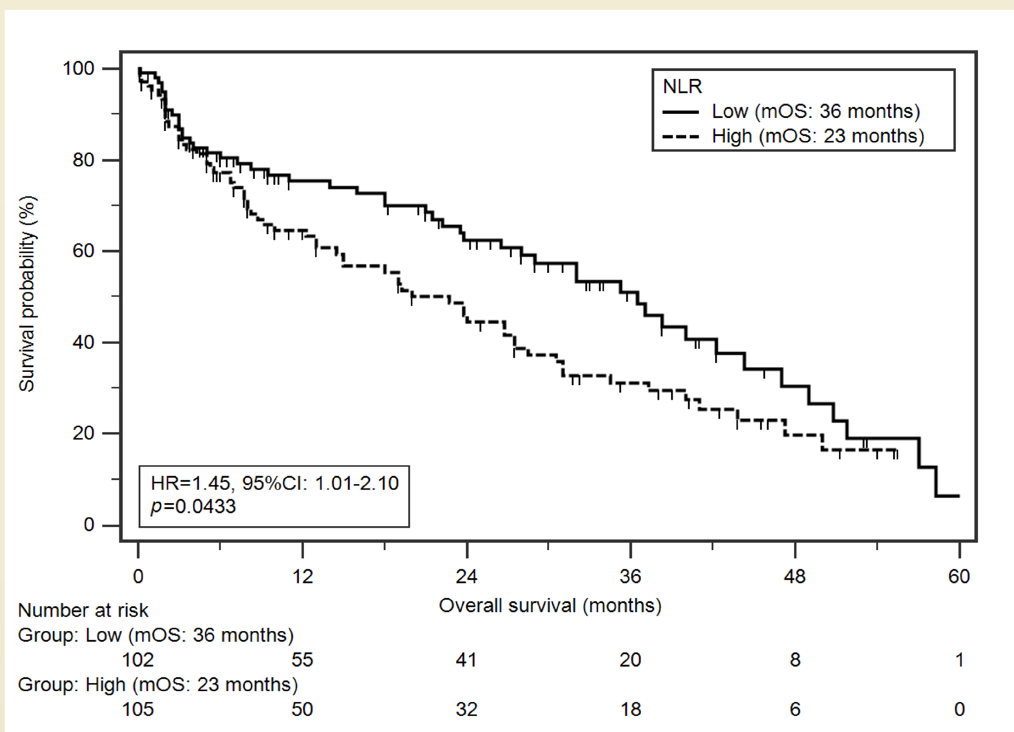

Figure 2. Kaplan-Meier curves illustrating death probability differences according to NLR values.

Conclusions

Our study demonstrated that the pre-treatment NLR may be an independent, significant predictor of OM as well as prognostic factor in HNC patients undergoing RT. Large prospective and validation studies are warranted to confirm the optimal NLR cut-off value and its predictive significance in that group of patients.

References

1. Siegel, R.L.; Miller, K.D.; Jemal, A. Cancer Statistics, 2017. CA. Cancer J. Clin. 2017, 67, 7–30, doi:10.3322/caac.21387.
2. Head and neck cancers survival statistics. Available online: http://www.cancerresearchuk.org/health-professional/cancer-statistics/statistics-by-cancer-type/head-and-neck-cancers/survival#heading-Zero.
3. Brockstein, B.; Haraf, D.J.; Rademaker, A.W.; Kies, M.S.; Stenson, K.M.; Rosen, F.; Mittal, B.B.; Pelzer, H.; Fung, B.B.; Witt, M.-E.; et al. Patterns of failure, prognostic factors and survival in locoregionally advanced head and neck cancer treated with concomitant chemoradiotherapy: a 9-year, 337-patient, multi-institutional experience. Ann. Oncol. Off. J. Eur. Soc. Med. Oncol. 2004, 15, 1179–1186, doi:10.1093/annonc/mdh308.
4. Sonis, S.T. Oral mucositis in head and neck cancer: risk, biology, and management. Am. Soc. Clin. Oncol. Educ. book. Am. Soc. Clin. Oncol. Annu. Meet. 2013, doi:10.1200/EdBook_AM.2013.33.e236.
5. Lalla, R. V; Saunders, D.P.; Peterson, D.E. Chemotherapy or radiation-induced oral mucositis. Dent. Clin. North Am. 2014, 58, 341–349, doi:10.1016/j.cden.2013.12.005.
6. Marcelo, B.; Katharine, B. Supportive Management of Mucositis and Metabolic Derangements in Head and Neck Cancer Patients. Cancers (Basel). 2015, 7, 1743-1757, doi: 10.3390/cancers7030862.
7. Adelstein, D.J.; Li, Y.; Adams, G.L.; Wagner, H.J.; Kish, J.A.; Ensley, J.F.; Schuller, D.E.; Forastiere, A.A. An intergroup phase III comparison of standard radiation therapy and two schedules of concurrent chemoradiotherapy in patients with unresectable squamous cell head and neck cancer. J. Clin. Oncol. Off. J. Am. Soc. Clin. Oncol. 2003, 21, 92–98, doi:10.1200/JCO.2003.01.008.
8. Lee, Y.H.; Choi, H.-S.; Jeong, H.; Kang, K.M.; Song, J.H.; Lee, W.S.; Lee, G.-W.; Song, H.-N.; Kim, H.-G.; Kang, M.H.; et al. Neutrophil-lymphocyte ratio and a dosimetric factor for predicting symptomatic radiation pneumonitis in non-small-cell lung cancer patients treated with concurrent chemoradiotherapy. Clin. Respir. J. 2018, 12, 1264–1273, doi:10.1111/crj.12660.
9. Masucci, M.T.; Minopoli, M.; Carriero, M.V. Tumor Associated Neutrophils. Their Role in Tumorigenesis, Metastasis, Prognosis and Therapy. Front. Oncol. 2019, 9, 1146, doi:10.3389/fonc.2019.01146.
10. Galdiero, M.R.; Varricchi, G.; Loffredo, S.; Mantovani, A.; Marone, G. Roles of neutrophils in cancer growth and progression. J. Leukoc. Biol. 2018, 103, 457–464, doi:10.1002/JLB.3MR0717-292R.

THE INFLUENCE OF ANTIMICROBIAL NEUTROPHIL EXTRACT AND PENTOXIFYLLINE ON OVINE NEUTROPHILS ISOLATED DURING THE INSERTION TITANIUM IMPLANT IN A SHEEP MODEL

J. Zdziennicka[1], J. Wessely-Szponer[1], T. Szponder[2], M. Latalski[3]

[1]Sub-Department of Pathophysiology, Department of Preclinical Veterinary Sciences, Faculty of Veterinary Medicine, University of Life Sciences, Lublin, Poland;

[2]Department and Clinic of Animal Surgery, Faculty of Veterinary Medicine, University of Life Sciences, Lublin, Poland;

[3]Department of Pediatric Orthopedics, Medical University, Lublin, Poland)

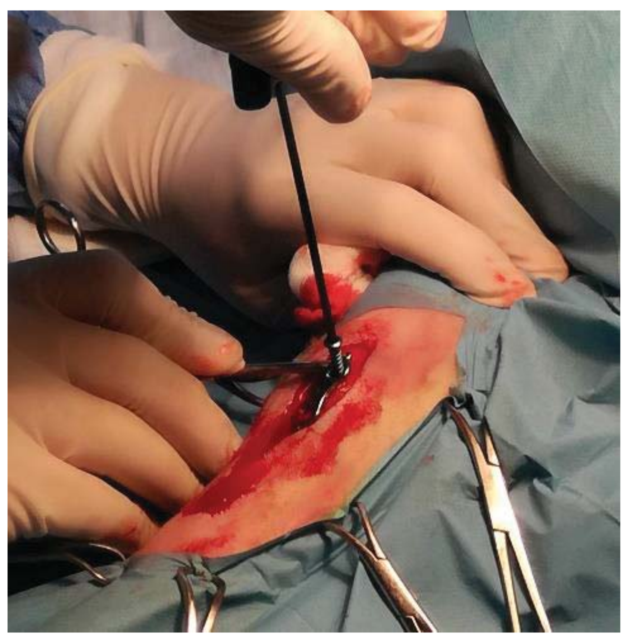

Figure 1. Implantation of a titanium implant into the proximal tibial physis

The aim of the study was to assess the effect two factors: autologous neutrophilic antimicrobial extract (ANE) and pentoxifylline (PTX) on ovine neutrophil activity as potential regulators of increased inflammatory response during implantation of titanium implants and long- term interactions between circulating neutrophils and Ti implants insertion in the area of growth cartilage of the tibia. Recalled ANE is a compound of peptides isolated from neutrophils with a broad spectrum of antibacterial, antiviral and antifungal activity. As estimated previously, AMP isolated from ovine blood contains cathelicidins, namely: SMAP-29, SMAP34, OaBac5, OaBac6, Oabac7.5, OaBac11 (2). The another stimulator used in this study is non-selective phosphodiesterase inhibitor-PTX with confirmed properties in promotion of microcirculation, enhancement of blood flow, tissue oxygenation and anti- inflammatory activity (3).

The study was conducted in a group of 12 sheep, females, BCP local breed, 4 months old. During the experiment animals were randomly divided into two groups: a control group (n=4) and an experimental group (n=8). All animals from the experimental group had a Ti implant inserted into the tibia directly into the proximal growth plate (Fig.1).The material necessary to obtain autologous product- neutrophilic antimicrobial extract (ANE) was collected into an anticoagulant tube (EDTA) 7 days before surgery from the jugular vein. For assessment of the circulating neutrophils during the inflammatory phase response, blood samples were collected at the two time points: T0 – 7 days before surgery and T1 – 24 hrs after surgery. Isolated neutrophils were stimulated with phosphate-buffered saline (PBS) as a control group (marked as unstimulated) and experimental groups were stimulated with ANE at a concentration of 20 μg/mL (marked as stimulated). At the next step cultures were incubated for 30 min and for 20 hrs at 37°C in the presence of 5% CO_2. The second stimulator, namely PTX (Polfillin Polpharma Poland) was used during experiment in concentrations of 0, 1, and 100 μg/mL of culture. These suspensions were incubated for 1 hour in the same temperature and presence of 5% CO_2 as culture with ANE and PBS.

The results show that the addition of ANE to neutrophil culture didn't cause significant differences between activity of neutrophils in group isolated 24 hrs after implantation compared to control group. Our study shown that addition ANE cause decrease release enzymatic activity and RNI (nitrite) generation. The insignificant inhibitory ANE effect was observed in the case of elastase and MPO release. Decrease of NO concentration was observed in all time points after 30 min incubation and after 20 hrs incubation in second time point in experimental group (Figure 2). As a result of stimulation with PTX, after treatment of neutrophils in all time points (T0,T1) PTX with 1 μg/mL we observed diminished release of elastase, MPO and ALP. Similar effects were seen in release of NO. Stimulation with 100 μg/mL didn't caused significant different compared to unstimulated group (Fig. 3).

These results shown that Ti implant insertion into the ovine growth cartilage of the tibia did not evoke any side effects neither at the inflammatory phase of repair process. Moreover, we also evaluated PTX and ANE extract as potential modifiers of immune cells response. Our study revealed that these factors acted anti- inflammatory and decreased neutrophil response. Thanks to these findings we know that ANE and PTX are applicable in modulation of inflammatory process during implantation of biomaterial.

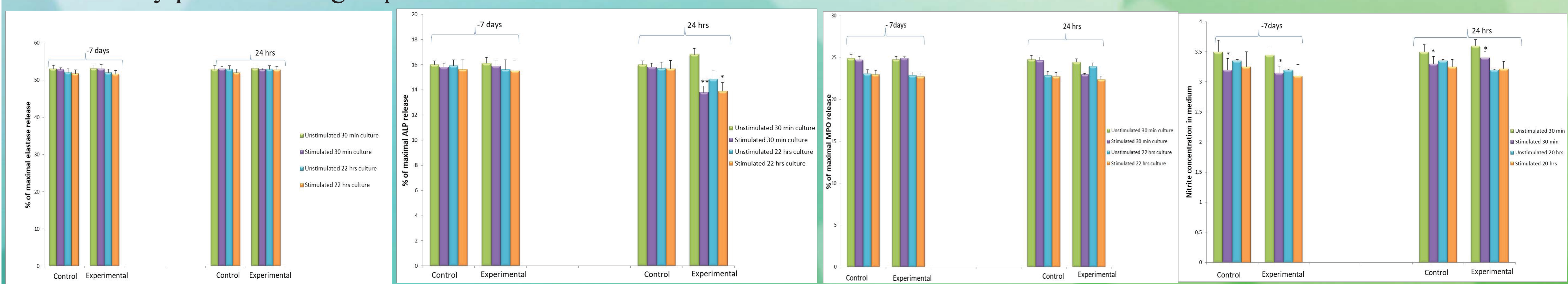

Figure 2 . Activity of neutrophils with or without stimulation with ANE extract, isolated 7 days before and 24 hrs after implantation in both groups: experimental and control after 30 min and 20 hrs incubation at 37°C and 5% CO_2. The neutrophil response to Ti implant insertion; A - elastase release from neutrophils, B - MPO release, C - ALP release, D - NO generation in the inflammatory phase of the repair process.

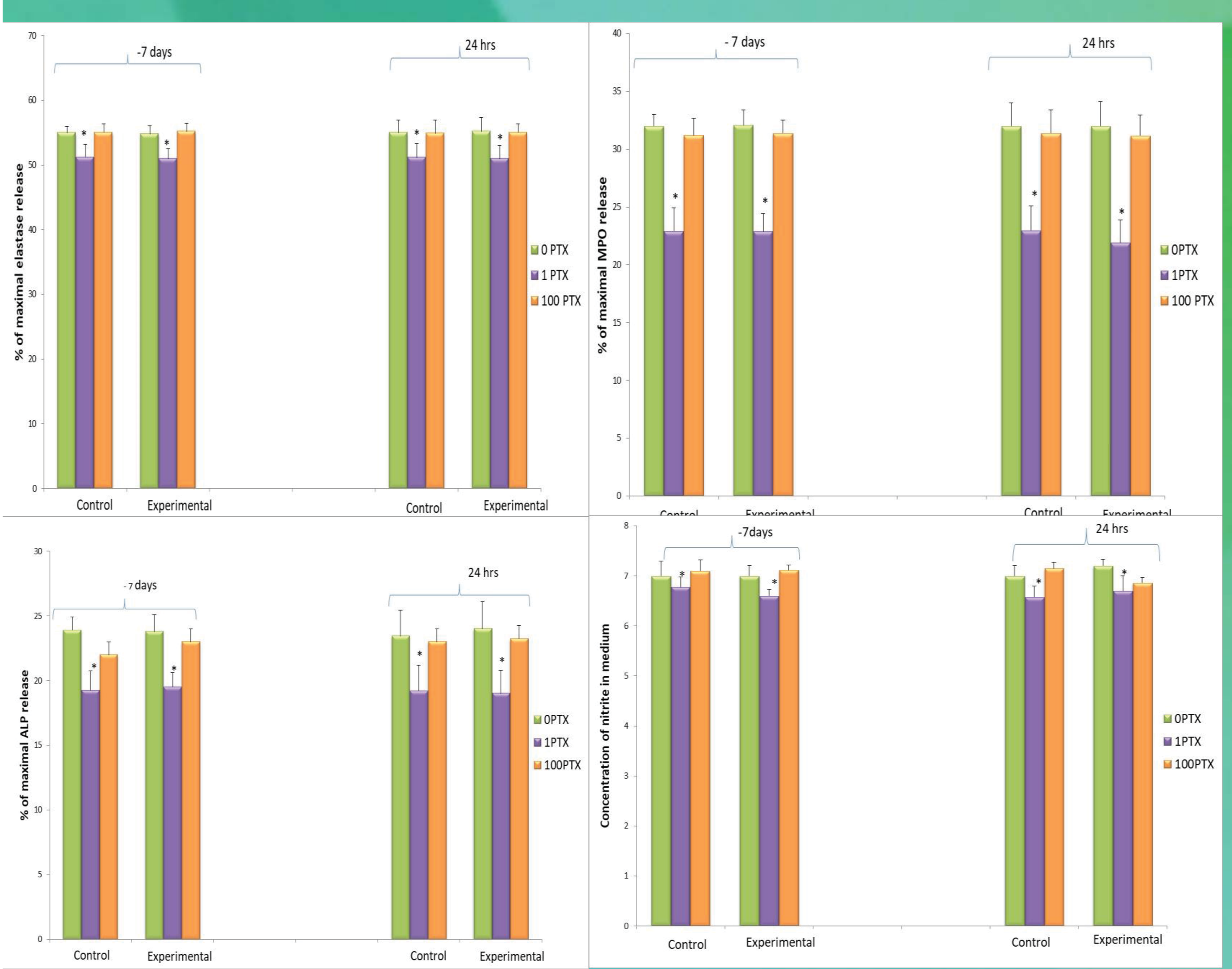

Figure 3. Activity of neutrophils isolated 7 days before and 24 hrs after implantation and treatment with two concentrations of PTX (1 and 100 μg/mL) in both groups: experimental and control after 30 min and 20 hrs incubation at 37°C and 5% CO_2. The neutrophil response to Ti implant insertion; A - elastase release from neutrophils, B - MPO release, C - ALP release, D - NO generation in the inflammatory phase of the repair process.

1. Mariani, E.; Lisignoli, G.; Borzi, R.M.; Pulsatelli, L. Biomaterials: Foreign Bodies or Tuners for the Immune Response? *International Journal of Molecular Sciences* 2019, 20, 636; doi:10.3390/ijms20030636
2. Yu PL, Van der Linden DS, Sugiato H, Anderson RC (2010) Antimicrobial peptides isolated from the blood of farm animals. *Animal Production Science*, 50(7), 660-669.
3. Cohn, J.; Bone, R.C. New strategies in nonantibiotic treatment of gram-negative sepsis. *Cleveland Clinic Journal of Medicine* 1992, 59, 608-615.

UTILITY OF THE PLATELET-ENDOTHELIAL CELL ADHESION MOLECULE 1 (PECAM-1) AS A MARKER OF PLATELET ACTIVITY IN THE FLOW CHAMBER MODEL OF THROMBOSIS IN ANIMAL AND HUMAN STUDY

Natalia Marcinczyk [1], Tomasz Misztal [2], Anna Gromotowicz-Popławska [1], Agnieszka Zebrowska [3], Tomasz Rusak [2], Piotr Radziwon [3,4], Ewa Chabielska [1]

[1] Department of Biopharmacy, Medical University of Bialystok, 15-222 Bialystok, Poland [2] Department of Physical Chemistry, Medical University of Bialystok, 15-089 Bialystok, Poland [3] Regional Centre for Transfusion Medicine, 15-950 Bialystok, Poland [4] Department of Haematology, Medical University of Bialystok, 15-276 Bialystok, Poland

Introduction

In our previous study, we introduced the platelet endothelial cell adhesion molecule 1 (PECAM-1)/thrombus ratio, which is a parameter indicating the proportion of PECAM-1 in a laser-induced thrombus in mice. Because PECAM-1 is an antithrombotic molecule, the higher the PECAM-1/thrombus ratio, the less activated platelets in thrombus are [1]. In this study, we used an extracorporeal model of thrombosis (flow chamber model) to verify its usefulness in the assessment of the PECAM-1/thrombus ratio in animal and human studies. Using the lipopolysaccharide (LPS)-induced inflammation model, we also evaluated whether the PECAM-1/thrombus ratio determined in the flow chamber (without endothelium) differed from that calculated in laser-induced thrombosis (with endothelium). Acetylsalicylic acid (ASA) was used as reference.

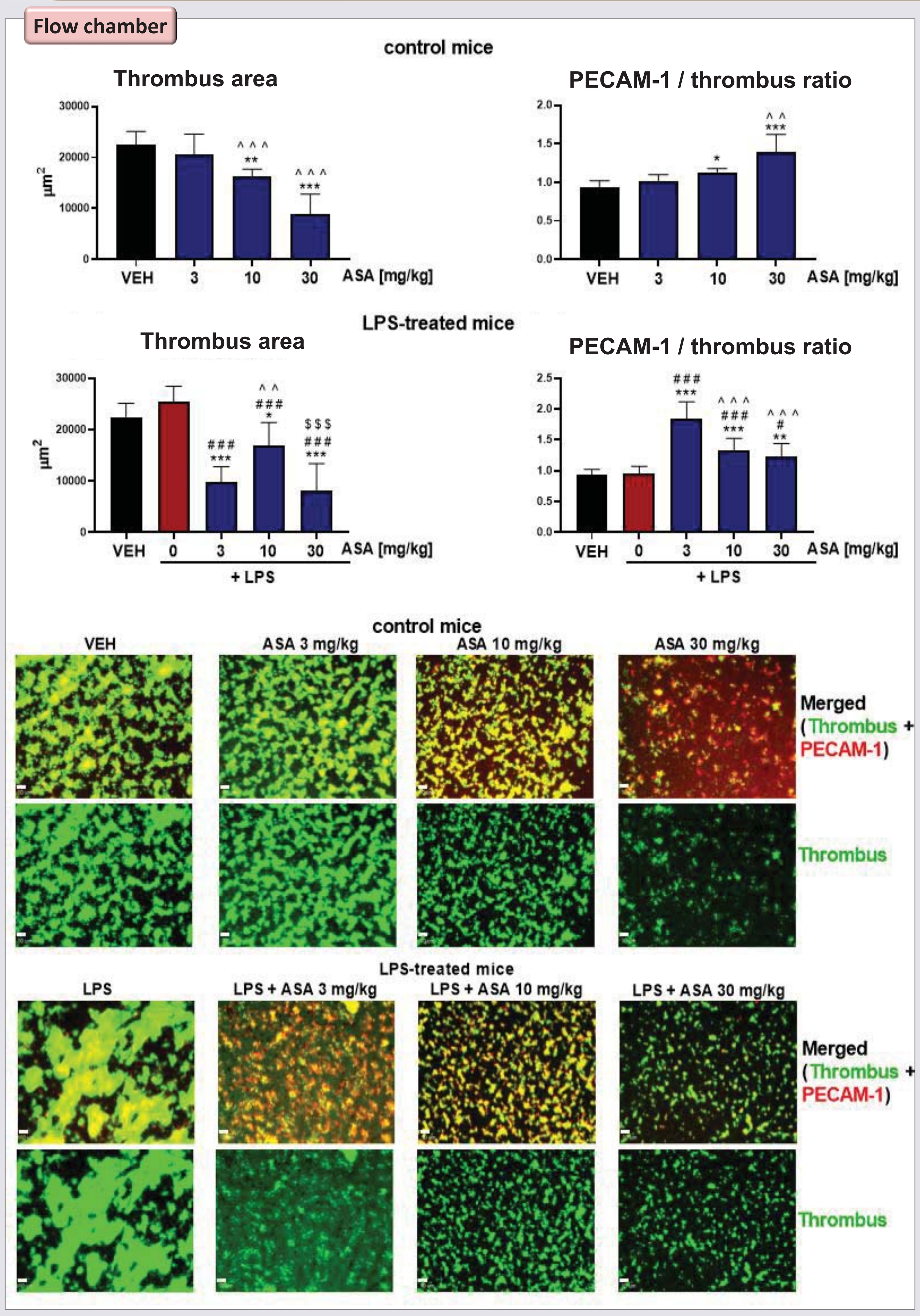

** $p < 0.05$, ** $p < 0.01$, *** $p < 0.001$ vs. VEH; # $p < 0.05$, ## $p < 0.01$, ### $p < 0.001$ vs. LPS; ^ $p < 0.05$, ^^ $p < 0.01$, ^^^ $p < 0.001$ vs. LPS + ASA 3 mg/kg; \$ $p < 0.05$, \$\$ $p < 0.01$, \$\$\$ $p < 0.001$ vs. LPS + ASA 10 mg/kg; n = 9–13; bar = 10 µm*

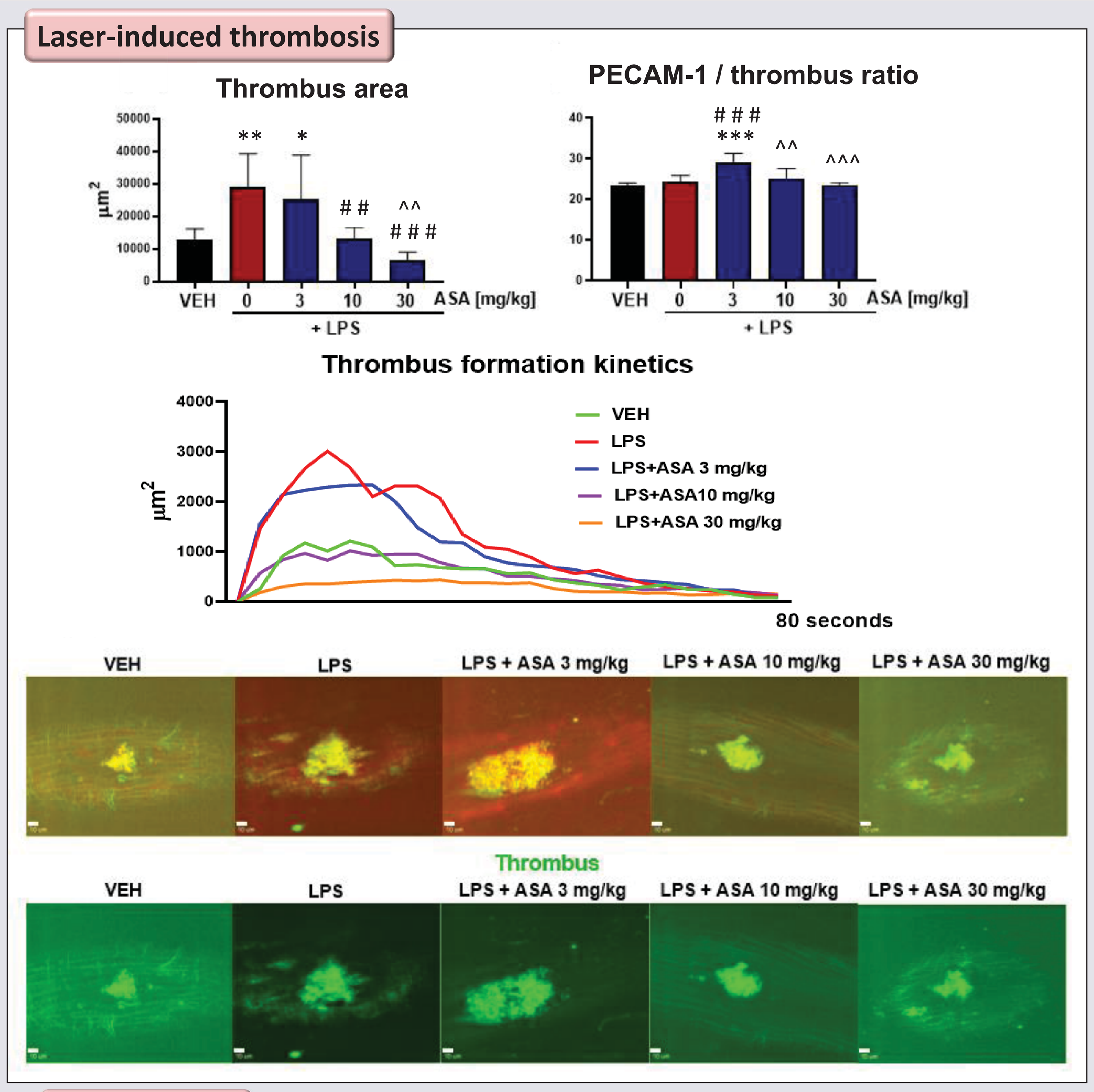

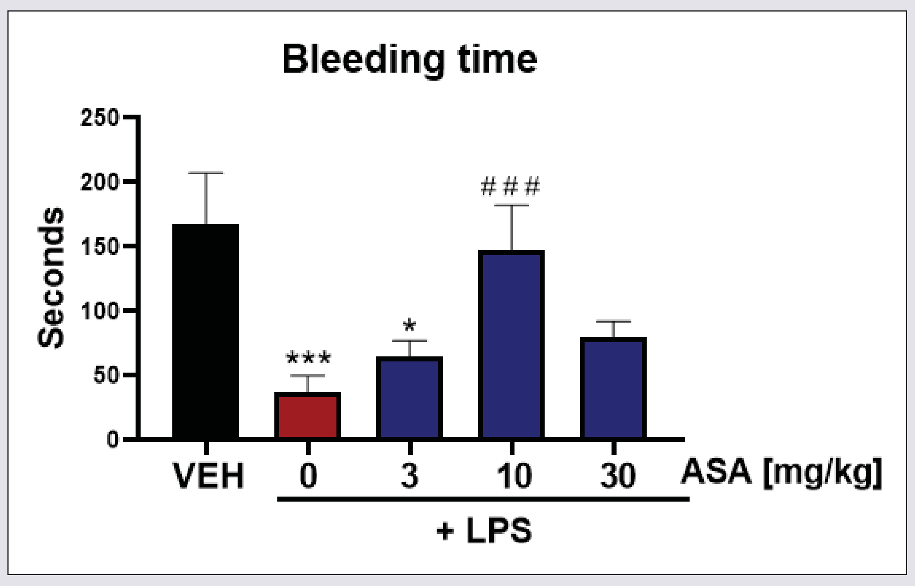

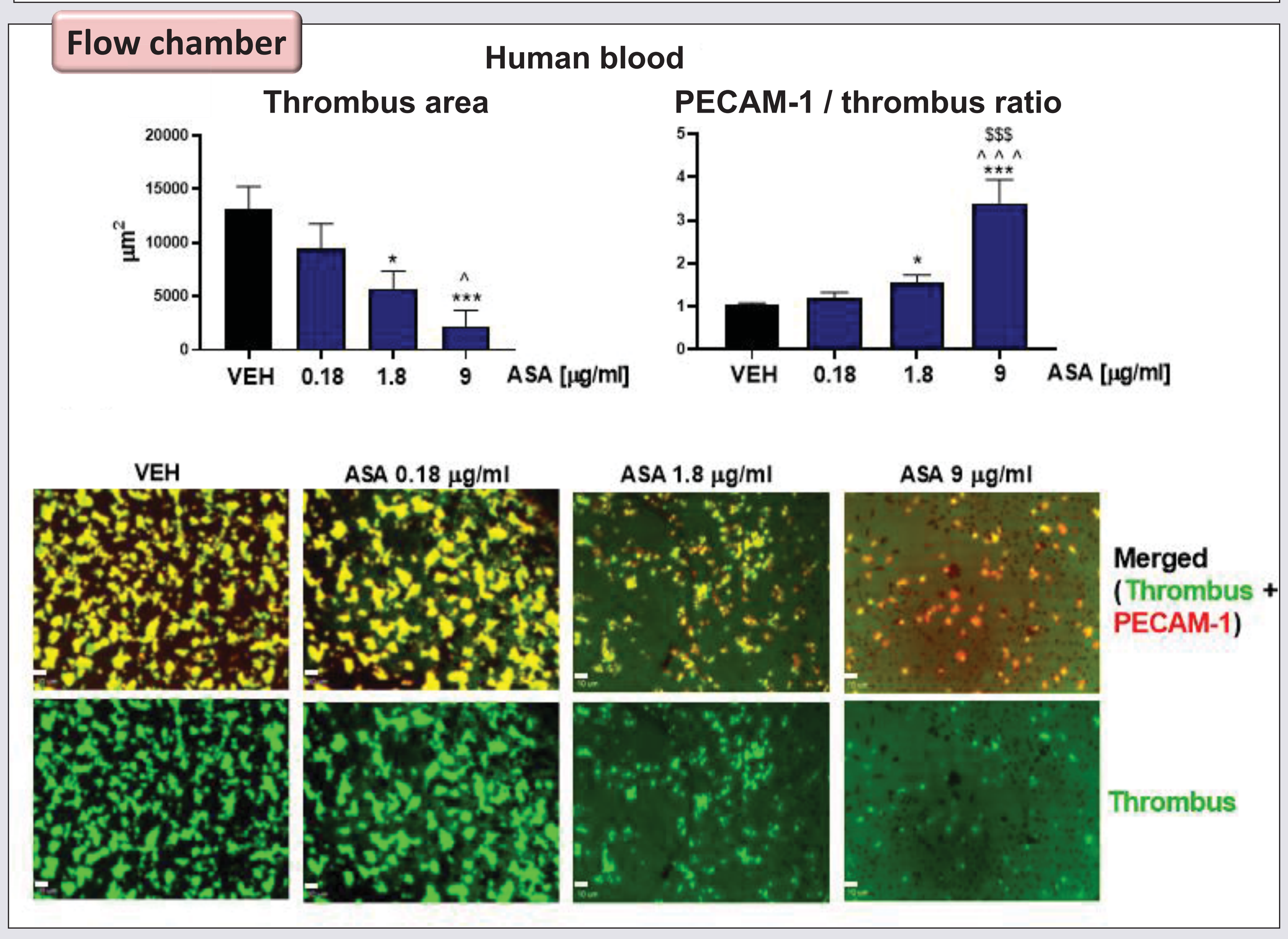

** $p < 0.05$, *** $p < 0.001$ vs. VEH; ^ $p < 0.05$, ^^^ $p < 0.001$ vs. ASA 0.18 µg/mL; \$\$\$ $p < 0.001$ vs. ASA 1.8 µg/mL; n = 7; bar = 10 µm*

Conclusions

- **ASA decreased the thrombus area while increasing the PECAM-1/thrombus ratio in control mice and humans in a dose-dependent manner in the flow chamber model.**
- **In LPS-treated mice, the PECAM-1/thrombus ratio decreased as the dose of ASA increased in both thrombosis models, but the direction of change in the thrombus area was inconsistent.**
- **PECAM-1/thrombus ratio more accurately describes the platelet activation status than commonly used parameters such as the thrombus area.**
- **PECAM-1 / thrombus ratio can be used in both human and animal studies.**

Materials and methods

Blood samples were collected from healthy volunteers using K_2EDTA (1.8 mg/mL). Male wild-type C57BL/6J mice (weighing 25–27 g) were anesthetized by intraperitoneally (i.p.) administering a single dose of ketamine (120 mg/kg) and xylazine (12.5 mg/kg) mixture. Blood samples were collected from the right heart ventricle with a 3.8% sodium citrate solution (1:10, v/v).

Inflammation was induced by single LPS (2 mg/kg) injection (i.p.). For the flow chamber experiment, blood samples were collected 30 min after LPS injection. In the laser-induced thrombosis, thrombus formation was induced 30 min after LPS injection.

ASA (Flectadol; Sanofi) in phosphate-buffered saline (PBS) was injected into the left femoral vein 5 min before blood collection or thrombosis induction. Mice that received ASA without LPS treatment were referred to as control mice.

Thrombus formation in flow chamber (*ex vivo, in vitro*). To inhibit coagulation, blood was treated with PPACK (40 µM). Then, the samples were supplemented with 3,3'-dihexyloxacarbocyanine iodide (DiOC6(3), 1 µM) and incubated (2 min at 37 °C) to stain platelets. For the human study, the blood samples were supplemented with ASA solution and incubated (3 min), then supplemented with 10 mM $CaCl_2$ and 3.37 mM $MgCl_2$ (for mouse blood, both at 3 mM concentration) and perfused through the chamber. PECAM-1 within thrombi was stained by topically applying 2 µL of Alexa Fluor 647-labeled PECAM-1 antibody on a thrombi-rich area and washed out after 5 minutes. End-stage measurements (including the surface area covered by the thrombus, referred to as the **thrombus area**) were performed by taking pictures using a confocal microscope. The area of fluorescence from platelet **PECAM-1** was divided by the thrombus area, and the value thus obtained was referred to as the **PECAM-1/thrombus ratio**.

Laser-induced thrombosis in mouse mesenteric vein and assessment of thrombus area and PECAM-1/thrombus ratio (intravital). Alexa Fluor 647-labeled PECAM-1 antibody (0.25 mg/kg) was injected into the femoral vein. To visualize the thrombus, DiOC6(3) (0.1 mM in 0.05 mL PBS) was intramuscularly injected. The mesentery vein was injured by a 532 nm argon-ion ablation laser. The thrombosis process was recorded for 80 s. One record was divided into 25 time points, and at each time point, the **thrombus area** was encircled. The thrombus area values obtained at each time point were added to estimate the final value. The area of **PECAM-1** fluorescence determined at a particular time point was then divided by the thrombus area at that time point. The values from one record were added to estimate the **PECAM-1/thrombus ratio**.

Determination of BT. A small tail segment (3 mm) was cut with a scalpel blade. Bleeding was monitored at 15-sec intervals by absorbing the bead of blood with filter paper. When no blood was observed on the paper, it was assumed that bleeding had stopped.

[1] Marcinczyk et al.: New approaches for the assessment of platelet activation status in thrombus under flow condition using confocal microscopy, Naunyn Schmiedebergs Arch Pharmacol. 2020.

This work was supported by Medical University of Bialystok. Grant number: SUB/2/DN/21/001/2226

LOW-DENSITY GRANULOCYTES AS A POTENTIAL MARKER REFLECTING INTENSITY OF INFLAMMATION IN PSORIASIS

W. DOMERECKA[1], I. HOMA-MLAK[1], R. MLAK[1], A. WILIŃSKA [2], T.MAŁECKA-MASSALSKA[1]
[1]Department of Human Physiology, Medical University of Lublin,
[2] Department of Clinical Genetics, Medical University of Lublin, Poland; domereckaweronika@gmail.com;

INTRODUCTION

Two populations of cells are observed in human peripheral blood, i.e. Polymorphonuclear Leukocytes (PMN), with their characteristic granular structure, and Peripheral blood mononuclear cells (PBMC). Low-density granulocytes (LDG) are neutrophils which, after separation by a density gradient, remain in the peripheral blood mononuclear fraction of PBMCs.

Post-inflammatory LDGs can damage endothelial cells and release a large amount of tumor necrosis factor (TNF) as well as type I and II interferons. They are characteristic of autoimmune diseases, including psoriasis, which occurs in about 2% of the population. The inflammatory process in the course of psoriasis is systemic and manifests itself mainly on the skin, but also affecting internal organs. The diagnosis and monitoring of the disease is based on the clinical picture. The assessment of disorders of other organs requires additional tests.

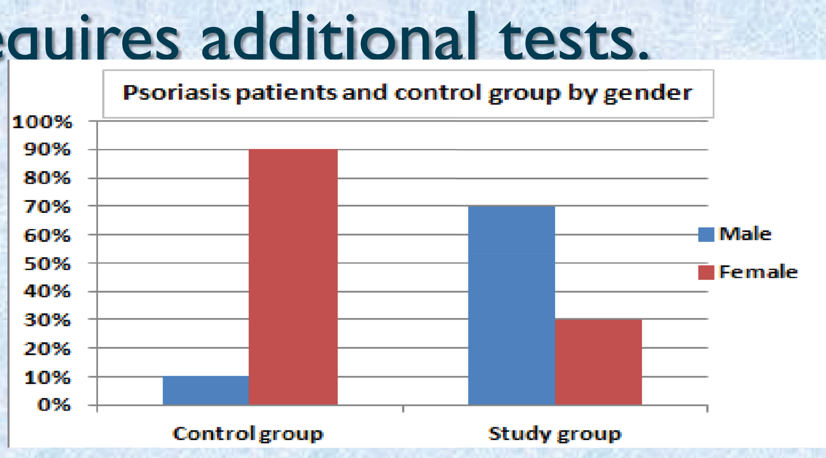

MATERIAL AND METHODS

40 patients from Chair and Department of Dermatology, Venerology and Paediatric Dermatology of Independent Public Clinical Hospital No. I in Lublin were included in the study. The study group consisted of 12 women and 28 men over the age of 18, who met the criteria for inclusion in the study. These were patients with diagnosed psoriasis (Table 1, column 2). The control group consisted of healthy individuals, represented by 20 volunteers over 18 years old, (Table 1, column 3). Venous blood samples of 10 mL each were collected from all subjects using disposable equipment. Then, within 2 hours of collection, blood concentrations of selected haematological and biochemical parameters were determined. LDG and neutrophils from other peripheral blood cells were separated by density gradient centrifugation with Ficoll. Then, using a flow cytometer, the immunophenotype of the isolated cells was assessed (using specific antibodies: CD15-FITC, CD14-PE, CD10-PE-Cy5). Cells with the following phenotype were considered LDG: CD15 + CD14-CD10 +.

		Total N = 60 Range/N (average/%)	
	Demographic data		
		Study group	Control group
1.	**Age (years)**	19-71 (43)	21-72 (49)
2.	**Male gender**	28 (70.9)	2 (10,0)
	Clinical data		
3.	**Smoking**	7 (17.5)	5 (16.7)
4.	**Time since psoriasis diagnosis (years)**	1.5-39.0 (15.0)	-
5.	**Accompanying chronic diseases** (including: pulmonary sarcoidosis, nephrolithiasis, inflammation of the duodenal mucosa, bronchial asthma, hypertension, hypercholesterolaemia, urinary tract infection, gout, diabetes, chronic heart failure, obesity, depression, hypothyroidism, degenerative spine disease, arthrosis , juvenile acne)	18 (58.1)	10 (33.3)
6.	**Cancers**	0	0

RESULTS

In the study, it was observed that in the PBMC fraction of patients with psoriasis, LDG cells appear in a much greater number, on average about 4 times higher than in healthy people from the control group. In patients suffering from psoriasis, it was on average about 1.46% of the PBMC population, while healthy donors had on average 0.38% of LDG ($p = 0.0182$). It is worth noting that in patients suffering from psoriasis, this population was up to approx. 17,7% of PBMCs, compared to healthy donors, whose maximum was approx. 1.7%. It was also shown that this population is characterized by an increased ability to release the MPO enzyme in psoriasis patients compared to healthy people (4,85% vs 0.67%; $p = 0.0042$). In sick patients, an increased activity of MPO is observed, on average about 7 times higher than in healthy

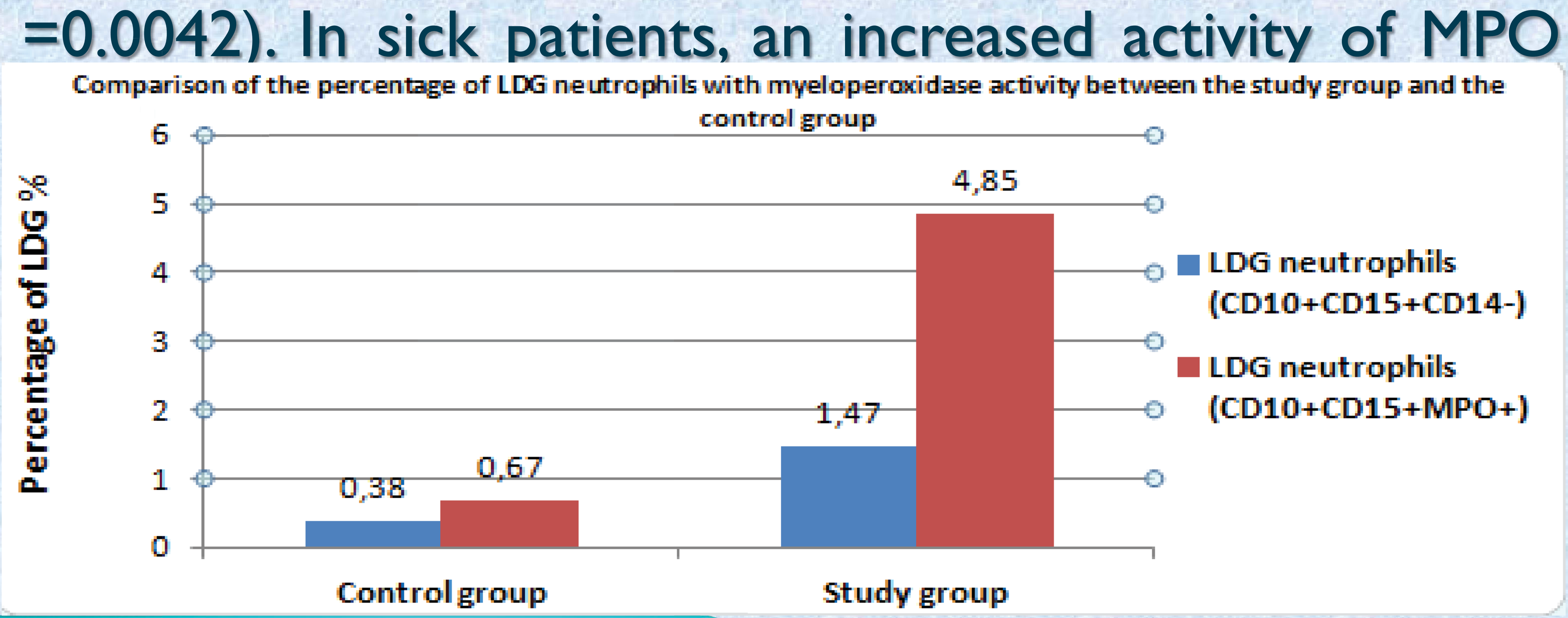

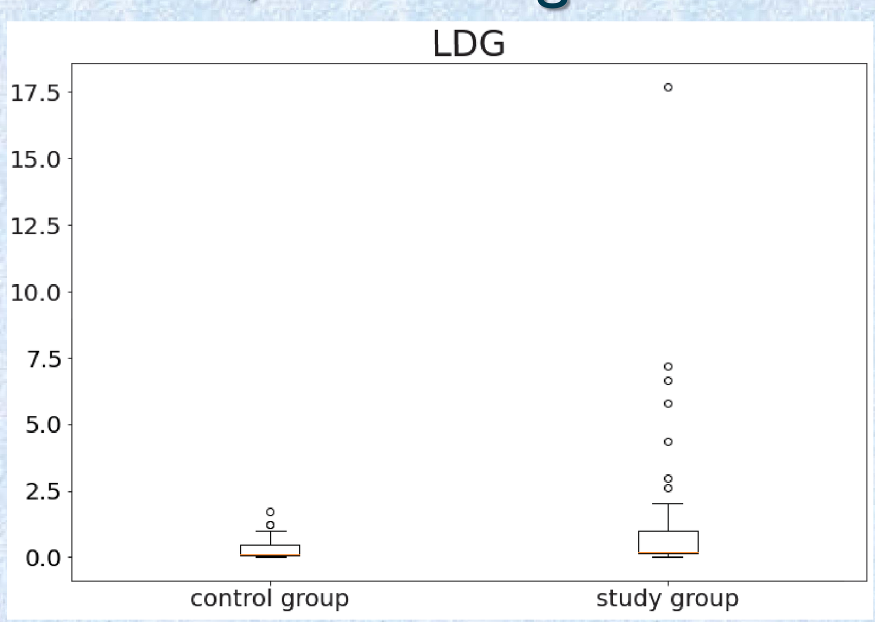

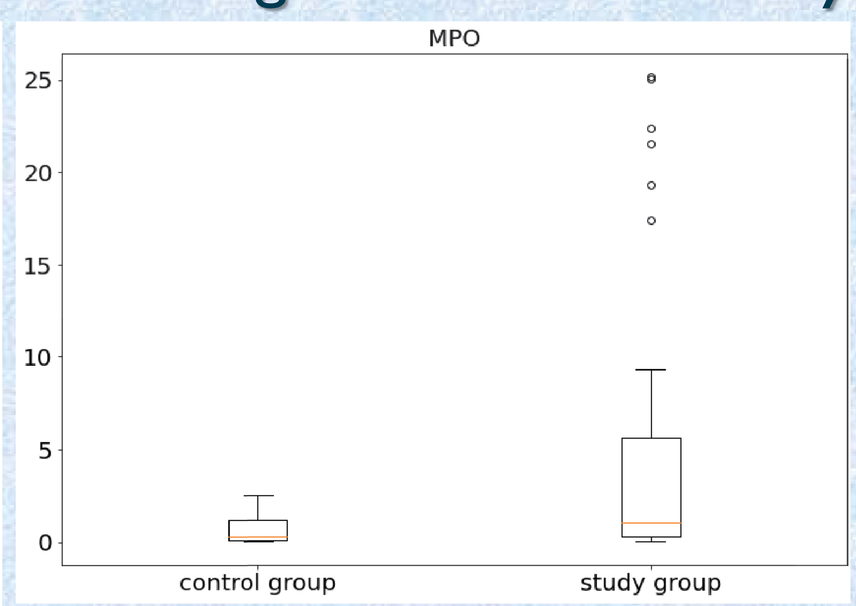

CONCLUSIONS

Flow cytometric analysis allowed to determine the percentage of neutrophils LDG based on the extracellular expression of antigens (CD10+ CD15+ CD14-) and intracellular (MPO+). The results obtained confirm the need for further studies involving a larger group of patients with psoriasis to assess the role of LDG cells as a factor in the development and severity of inflammation in these patients.

XXVIII Congress of the Polish Physiological Society

Gdańsk, September 15-17 2021

Poster book

SESSION VIII

ENDOCRINE REGULATIONS. CONTROL OF BODY WEIGHT

HONORARY PATRONAGE

Uniwersytet Gdański

Prof. dr Marcin Gruchała
Rector of the Medical University of Gdansk

Prof. dr Piotr Stepnowski
Rector of the University of Gdansk

WOJEWODA POMORSKI
DARIUSZ DRELICH

Dariusz Drelich
Governor of the Pomeranian Voivodeship

HONORARY PATRONAGE
Mayor of the City of Gdańsk

Aleksandra Dulkiewicz
Mayor of Gdansk

Mieczysław Struk
Marshal of the Pomeranian Voivodeship

PARTNER

PAN
POLSKA AKADEMIA NAUK

ANIMA LAB
animal facility and laboratory equipment • animal research models

FUNDACJA
LOTOS

Medical University of Gdansk
Department of Physiology

XXVIII Congress of the Polish Physiological Society

Gdańsk, September 15-17 2021

NICOLAUS COPERNICUS UNIVERSITY IN TORUŃ

Faculty of Medicine
Collegium Medicum in Bydgoszcz

LEPTIN, OMENTIN-1, MELATONIN AND VITAMIN D IN PATIENTS WITH CANCER OF LIP, ORAL CAVITY AND PHARYNX

Jarosław Nuszkiewicz, Marlena Budek, Karolina Szewczyk-Golec
Department of Medical Biology and Biochemistry, Faculty of Medicine, Ludwik Rydygier Collegium Medicum in Bydgoszcz
Nicolaus Copernicus University in Toruń, Bydgoszcz, Poland

INTRODUCTION AND OBJECTIVES

Tumors of the lip, oral cavity and pharynx (LOCP) are classified as cancers of the head and neck. LOCP neoplasms have been determined to account for approximately 6% of all tumors. In the course of LOCP neoplasms, the organism homeostasis is disturbed, leading to endocrine and metabolic changes. Adipose tissue hormones, known as adipokines, regulate metabolism, food intake and modulate inflammation. Melatonin and calcitriol, an active form of vitamin D, are hormones found to influence the synthesis and secretion of adipokines. They are also compounds with antioxidant activity. Clinicians point to the deficiency of both melatonin and vitamin D worldwide.

The aim of the study is to determine the concentration of melatonin, vitamin D and two adipokines, namely leptin and omentin-1, in patients diagnosed with LOCP cancer.

METHODS

The study group consisted of 25 patients with LOCP neoplasm and the control group consisted of 25 healthy subjects. Blood serum samples were obtained after collecting venous blood. $P < 0.05$ was considered as statistically significant.

Table 1. Anthropometric and demographic characteristic of patients with lip, oral cavity or pharyngeal cancer (LOCP) and healthy volunteers (control group). Each value is mean ± S.E.M. No statistically significant differences were observed.

Parameter	LOCP	Control group
n (male/female)	25 (15/10)	25 (11/14)
Age [yrs]	58.24 ± 1.29	55.36 ± 1.17
Body mass [kg]	72.53 ± 3.95	71.02 ± 2.22
Height [cm]	168.92 ± 1.84	169.88 ± 1.72
BMI [kg/m^2]	25.09 ± 0.99	24.50 ± 0.47
Current smoker (y/n)	7/18	4/21
Vitamin D supplementation (y/n)	5/20	8/17

REFERENCES

- Yeh, C.-M.; Su, S.-C.; Lin, C.-W.; Yang, W.-E.; Chien, M.-H.; Reiter, R.J.; Yang, S.-F. Melatonin as a potential inhibitory agent in head and neck cancer. Oncotarget 2017, 8, 90545–90556.
- Gómez-Moreno, G.; Guardia, J.; Ferrera, M.; Cutando, A.; Reiter, R. Melatonin in diseases of the oral cavity. Oral Dis 2010, 16, 242–247.
- Huang, Z.; Zhang, Y.; Li, H.; Zhou, Y.; Zhang, Q.; Chen, R.; Jin, T.; Hu, K.; Li, S.; Wang, Y.; et al. Vitamin D promotes the cisplatin sensitivity of oral squamous cell carcinoma by inhibiting LCN2-modulated NF-κB pathway activation through RPS3. Cell Death Dis 2019, 10, 936.
- Grant, W.B.; Moukayed, M. Vitamin D3 from Ultraviolet-B Exposure or Oral Intake in Relation to Cancer Incidence and Mortality. Curr Nutr Rep 2019, 8, 203–211.
- da Rocha, R.G.; Santos, E.M.S.; Santos, E.M.; Gomes, E.S.B.; Ramos, G.V.; Aguiar, K.M.; Gonçalves, B.R.; Santos, S.H.S.; De Paula, A.M.B.; Guimarães, A.L.S.; et al. Leptin impairs the therapeutic effect of ionizing radiation in oral squamous cell carcinoma cells. J Oral Pathol Med 2019, 48, 17–23.
- Ozsoy, S.; Besirli, A.; Unal, D.; Abdulrezzak, U.; Orhan, O. The association between depression, weight loss and leptin/ghrelin levels in male patients with head and neck cancer undergoing radiotherapy. Gen Hosp Psychiatry 2015, 37, 31–35.
- Li, D.; Zhao, X.; Xiao, Y.; Mei, H.; Pu, J.; Xiang, X.; Jiao, W.; Song, H.; Qu, H.; Huang, K.; et al. Intelectin 1 suppresses tumor progression and is associated with improved survival in gastric cancer. Oncotarget 2015, 6, 16168–16182.

RESULTS AND CONCLUSIONS

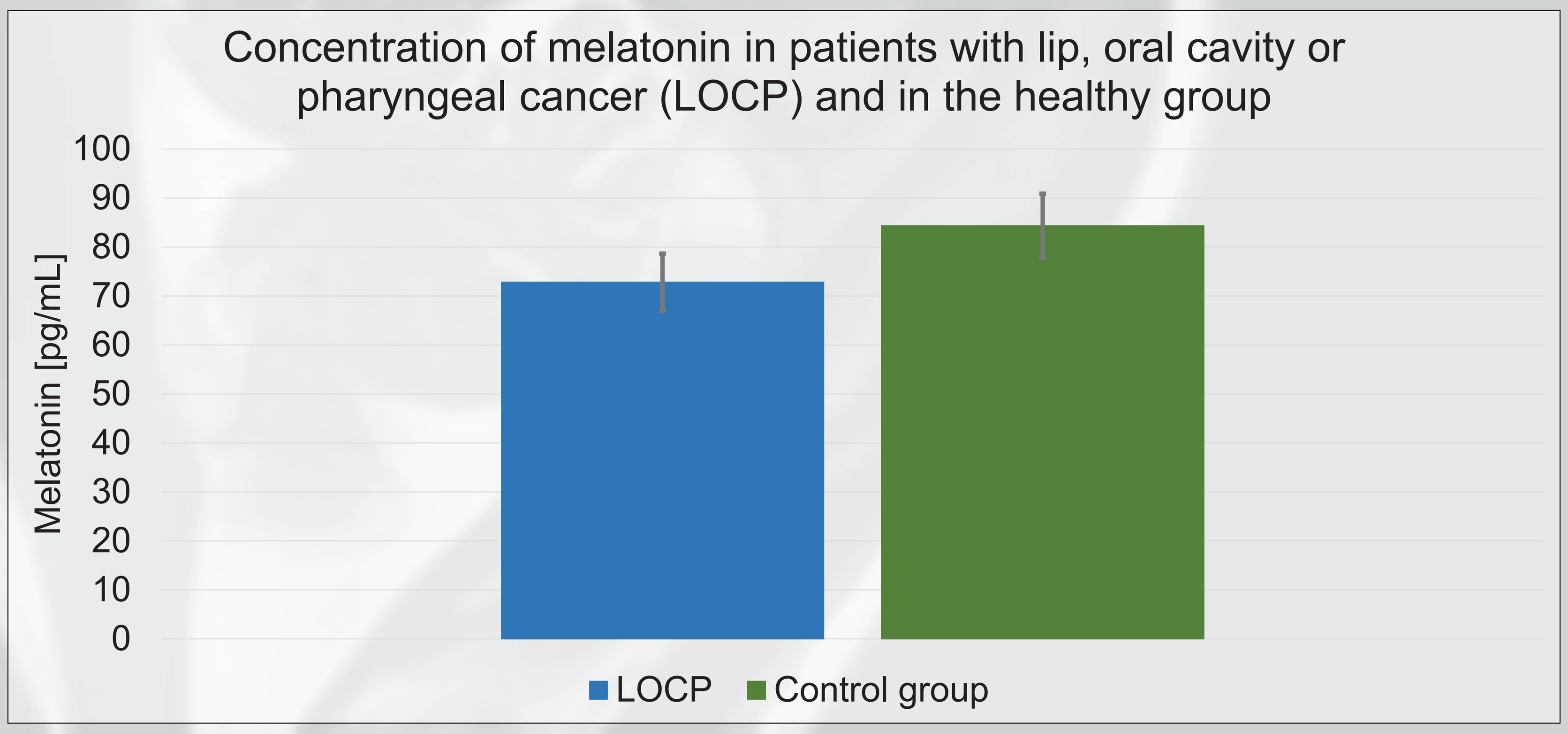

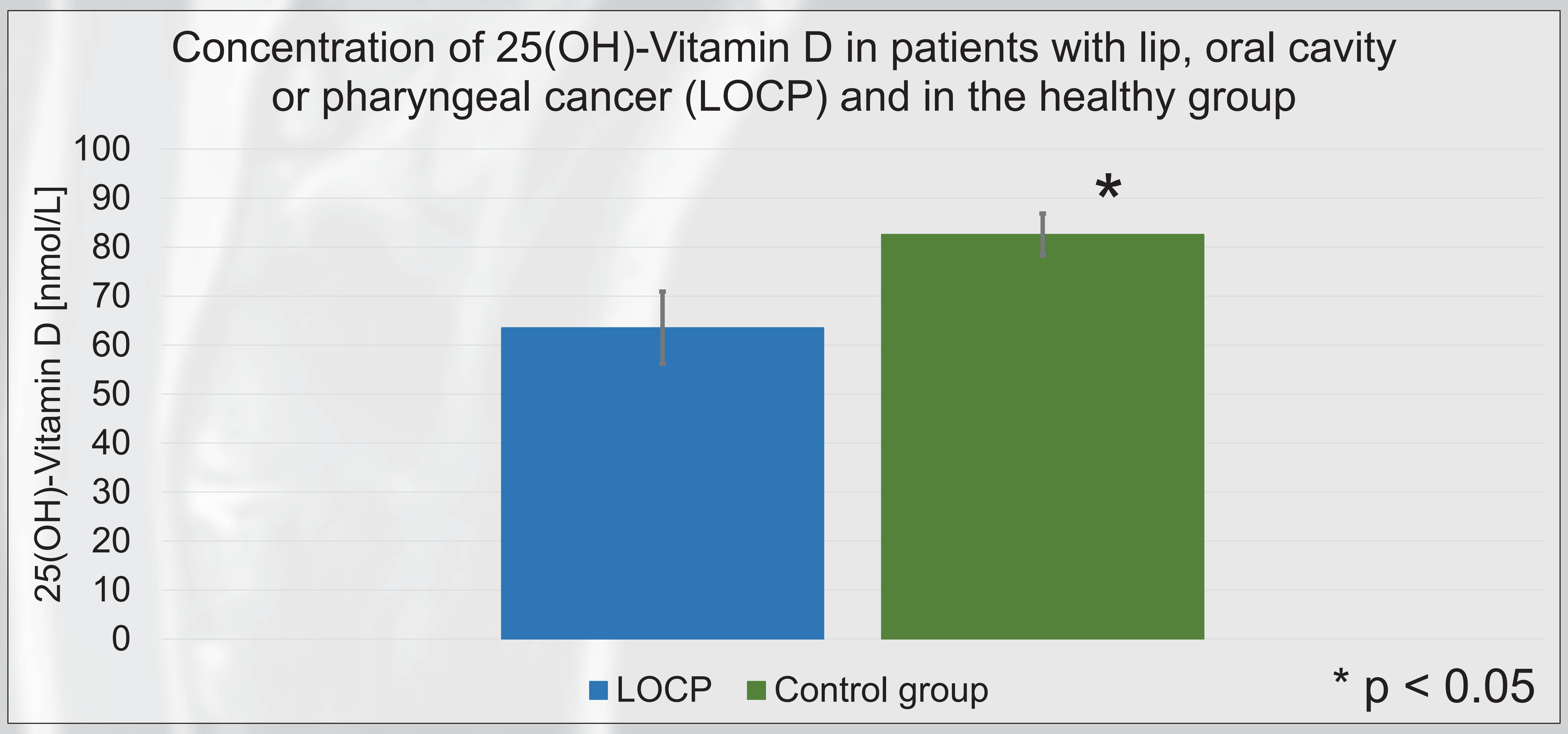

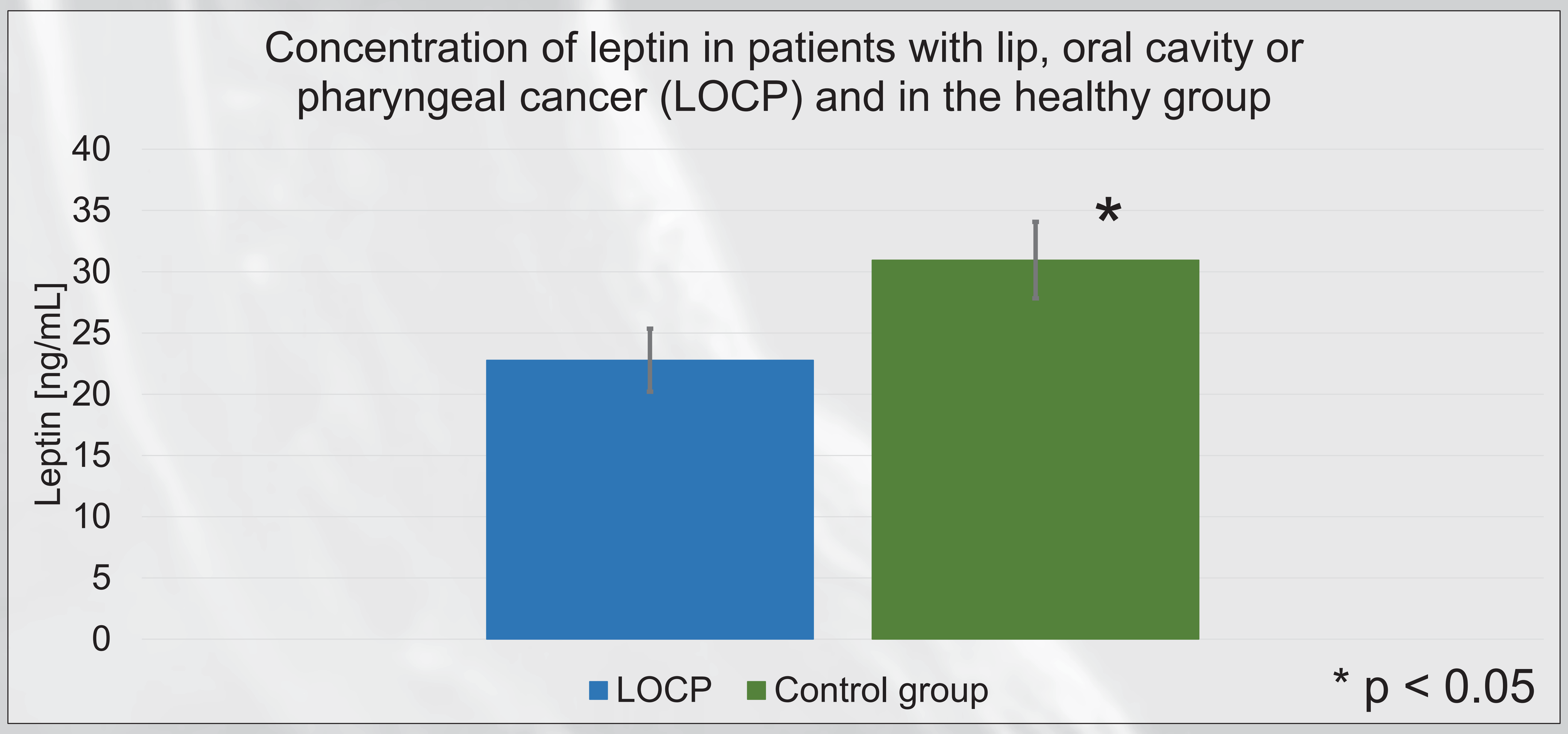

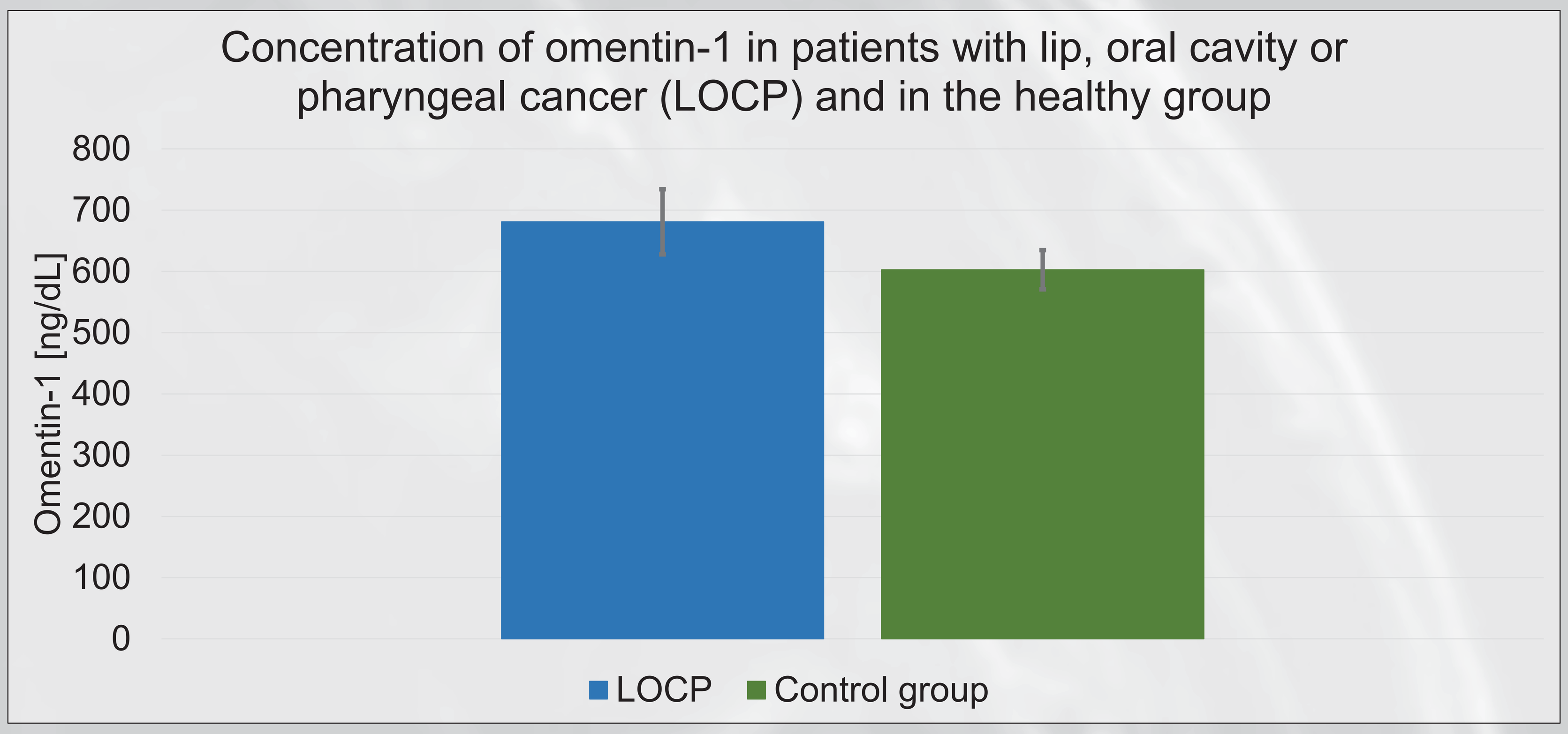

- In the group of patients with LOCP cancer, vitamin D deficiency was found. Vitamin D deficiencies should be treated with appropriate supplementation.
- A statistically significant lower level of leptin was observed among LOCP cancer patients. It is probably related to wasting by cancer and inadequate diet.

Cross-talk between thyroid hormones and vitamin D.

Elwira Smolińska-Fijołek[1], Justyna Wierzbicka[2], Michał Żmijewski[2]

[1]Department of Physiology, [2]Department of Histology, Medical University of Gdańsk
elwira.smolinska@gumed.edu.pl

The long-recognized "thyroid-skin conection" encompasses many layers of complexity and it has become a hot frontier in dermatoendocrinology. Thyroid disorders are known to involve all organ systems of the body and the skin is no exception. Cutaneous manifestations generally appear subsequent to the development of thyroid disease, but may be the first presenting sign or even precede the diagnosis by many years. However, the relationship between vitamin D and "thyroid-skin connection" has not been well elucidated.

The aim of the research was to analyze the *in vitro* effect of $1,25(OH)_2D_3$ on the keratinocytes and thyrocytes cells lines.

Material and Methods:

Cytotoxic and anti-proliferative activities of $1,25(OH)_2D_3$ against thyrocyte were tested. Gene expression profiling was performed by real-time qPCR on keratinocytes or thyrocytes treated with vitamin D.

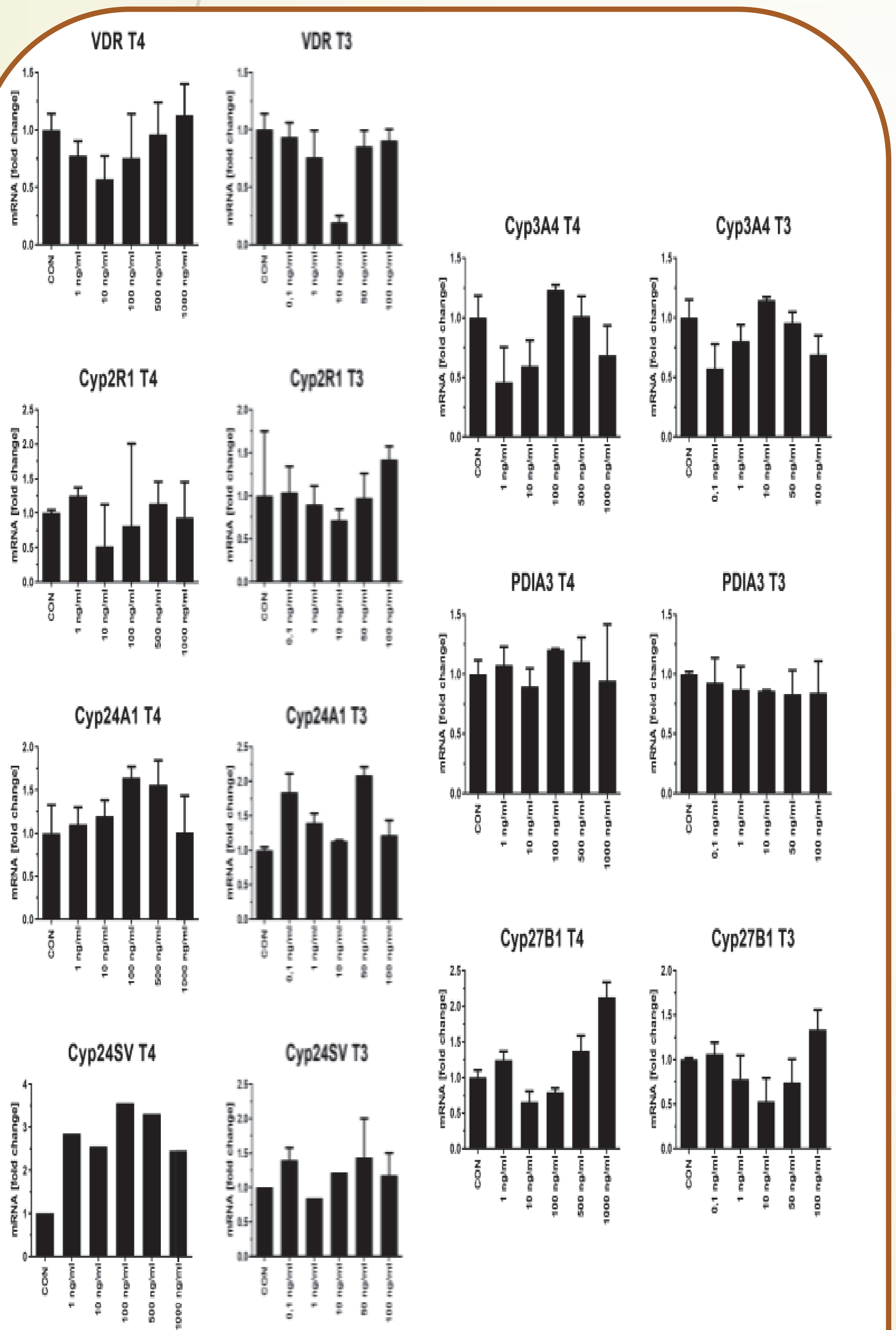

Effects of thyroid hormone (T3 or T4) on gene expression in HaCaT keratinocytes. Testing the effects of thyroid hormone on human keratinocytes transcriptional pattern, we not found that this compounds modulated of expression genes involved in vitamin D3 activation or metabolism.

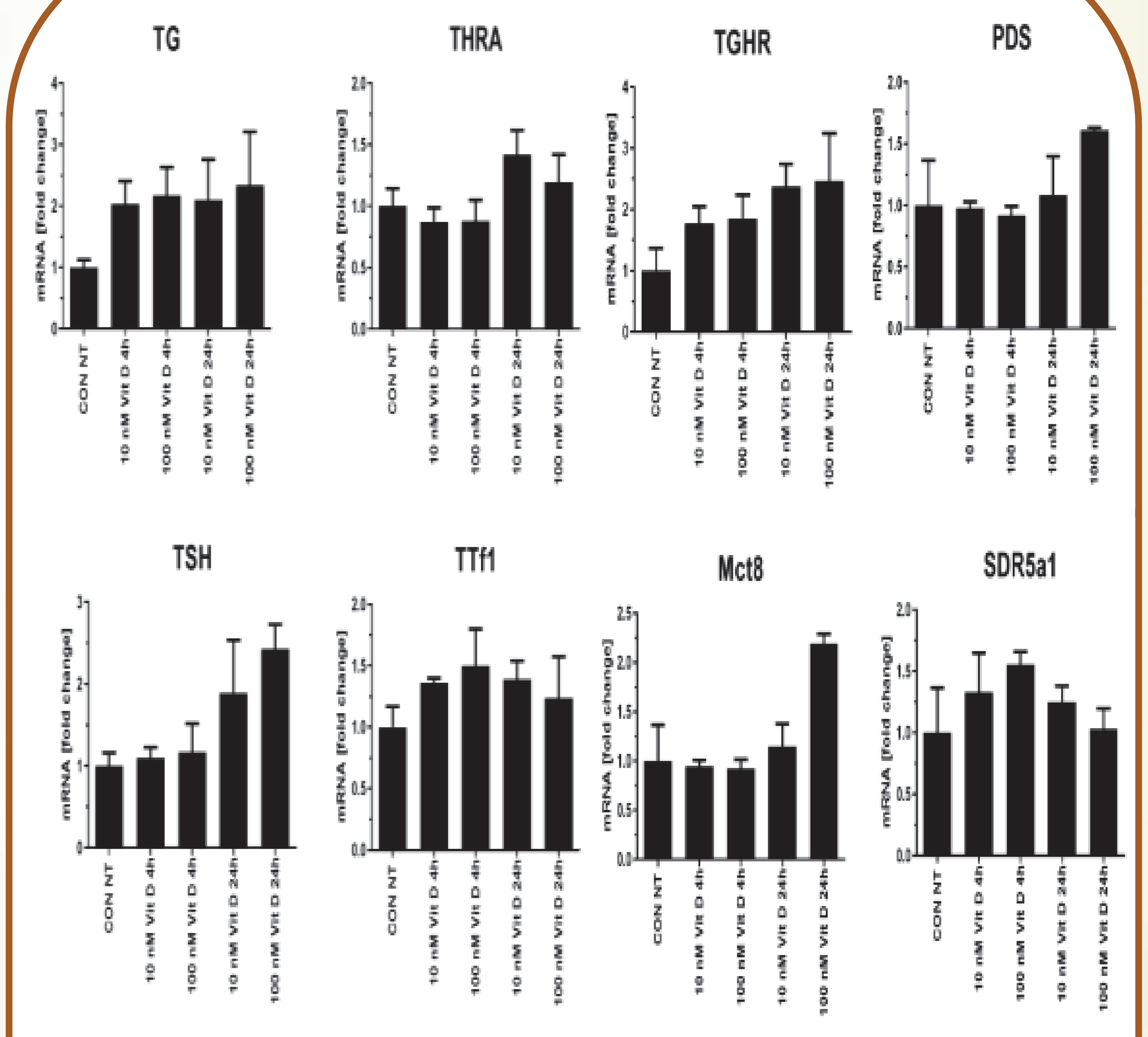

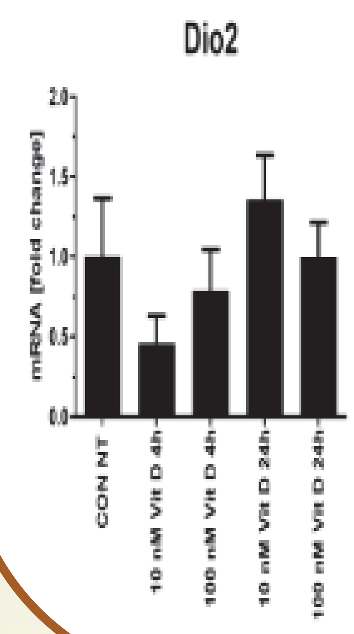

Effects of vitamin D on gene expression in K1 thyrocyte cells. Testing the effects of vitamin D on human thyrocyte transcriptional pattern, we found that this compound modulated of expression of receptors and enzymes responsible for thyroid hormone synthesis and activity.

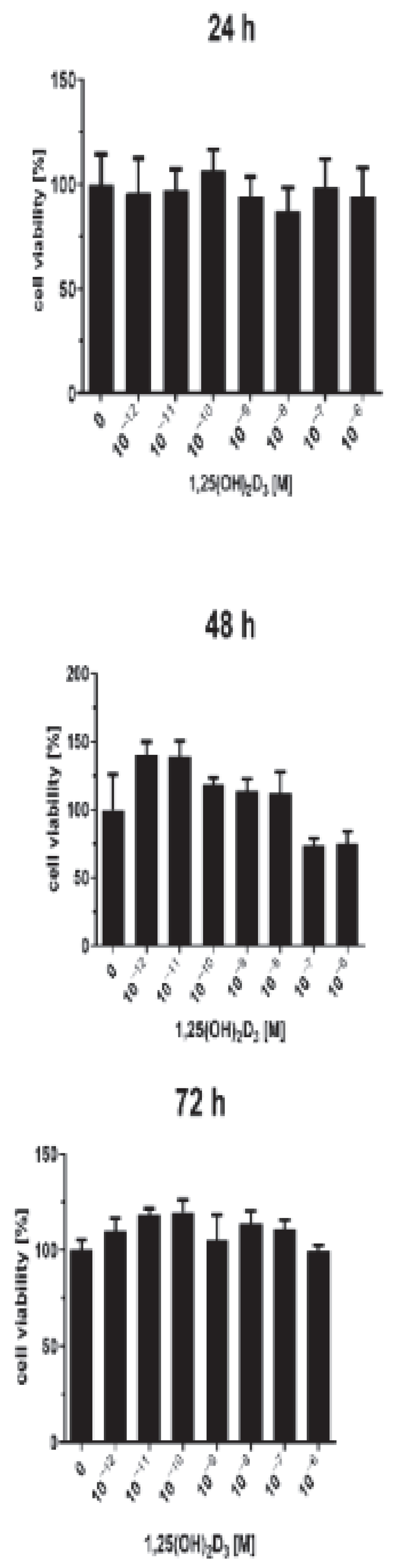

The effect of $1,25(OH)_2D_3$ on the cell viability and proliferation of thyrocytes. K1 thyrocytes cells lines were treated with serial dilutions) of $1,25(OH)_2D_3$. No remarkable cytotoxicity activity of vitamin D was observed in the range of tested concentrations in thyrocytes, while no inhibition of thyreocyte proliferation in a dose-dependent manner was demonstrated.

Conclusion:

Our results suggest that expression of genes involving in metabolism and intracellular activities of the thyroid hormones in skin and in thyroid follicular cell can be modulate by the vitamin D.

References: Kim D, 2017; Kriegel MA, 2010; Garcia-Serrano L, 2011; Antonini D, 2013, Słomiński AT, 2018

TNFRSF1A gene polymorphism (-610T>G, rs4149570) as a useful predictor of the development of malnutrition in patients with head and neck cancer.

Iwona Homa-Mlak[1], Radosław Mlak[1], Marcin Mazurek[1], Anna Brzozowska[2], Tomasz Powrózek[1], Teresa Małecka-Massalska[1]

1Department of Human Physiology, Medical University of Lublin, Poland;
2II Department of Radiotherapy, Center of Oncology of the Lublin Region St. John of Dukla, Poland

Introduction

Head and neck cancer (HNC) are 7th for the prevalence among malignancy in the world. The main treatment options include surgery, chemotherapy (CTH), radiotherapy (RT) or their combination [1, 2]. Malnutrition is the most frequently observed in gastrointestinal, HNC and lung cancer patients. Malnutrition, at the moment of diagnosis, is observed even in 52% of squamous cell carcinoma of the head and neck (SCCHN) Patients [2]. After treatment introduction percent of patients with malnutrition can increase even to 88% [2]. Occurrence of cancer malnutrition is associated with poor prognosis [1–3]. It is usually related with higher rate of toxicities associated with treatment (CTH and/or RT) and decreased quality of life (QoL) [1,2]. Manutrition in patients with cancer is associated with higher risk of morbidity and mortality. Many patients with malnutrition eventually develops cachexia [1–3]. According to guidelines of the European Society of Clinical Nutrition and Metabolism (ESPEN) cancer cachexia is chronic disease-related malnutrition (DRM) with coexisting inflammation [3]. Cachexia is usually accompanied by factors like neuropeptide-Y, hormones (leptin, insulin and glucagon) and excess of pro-inflammatory mediators (e.g. IL-1, IL-6, TNF-α). TNF-α is a pleotropic and pro-inflammatory cytokine mainly produced by activated macrophages. TNF-α plays one of the major role in the regulation of immune response, programmed cell death (e.g. apoptosis) and cytotoxicity. TNF-α is activated by a signal pathway through the two receptors: TNFRSF1A (CD120a,) and TNFRSF1B (CD120b) [4-6]. Some disorder of TNF receptor (TNFR) function and signaling can provide to inflammatory deregulation and consequently development of diseases [7].

Objectives

We postulate that SNP of TNFRSF1A (rs4149570) might be associated with higher risk of nutrition disorder occurrence. Identification of risk factor of malnutrition can help to prevent its development or at least minimize its consequences especially the development of chronic DRM and cachexia.

Methods and material

Assessment of nutritional status:

The medical examination included measurement of high and weigh of the patients, then BMI was calculated. Weight measurement was performed three times: before, during (IV-th week) and after treatment (VII-th week) (weight I, weight II and weight III respectively) and based on this BMI was calculated (BMI I, BMI II and BMI III respectively). The nutritional status of patients was assessed using NRS and SGA. Furthermore, in peripheral blood level of albumin, prealbumin and transferrin were determined (before treatment).

Determination of TNFRSF1A polymorphism:

DNA was isolated from peripheral blood using DNA Blood Mini Kit (Qiagen, Canada). Sequencing was performed using the primers for amplification by a standard protocol with BigDye Terminator kit v.3.1 cycle sequencing kit (Applied Biosystems) in the thermoblock 9700. Products of sequencing were purified (EX Terminator- A & A Biotechnology) and separated on the basis of capillary electrophoresis using Genetic Analyzer 3500 (Life Technologies). The results were analyzed using the software SeqScape v.3.0. Fig. 1 shows representative result of sequencing.

Results

Patient characteristics

The study included 74 patients with histologically confirmed, advanced HNC in stage III (28.38%) or IV (71.62%) according to the TNM classification. The median was 63 (range: 42-87 years). Men predominated in this study (81.08%). In 51.35% of patients tumor was located in the larynx and in 39.19% in the oropharyngeal. All patients received RT treatment (alone or combined with other types of treatment).

Factors Affecting the Risk of SGA Scale

The occurrence of the GG genotype of *TNFRSF1A* gene significantly increased (over 5.5 times) the risk of severe (C) malnutrition according to the SGA scale (53.12% vs.16.67%; OR = 5.67; p = 0.0015). On the other hand, GT heterozygote carriers had a significantly lower (more than 4-fold) risk of severe (C) malnutrition according to the SGA scale (17.14% vs 46.15%; OR=0.24; *p*=0.0100). Based on the multivariate analysis, it was found that M1 feature (HR=9.46; *p*=0.0308), stage IV according to TNM classification (HR=3.76; *p*=0.0168) and the GG genotype of the *TNFRSF1A* gene (HR=2.18; *p*=0.0419) were independent, unfavorable prognostic factors.

Variable		SGA					
		A	B and C	p OR [95%CI]	A and B	C	p OR [95%CI]
Gender	Male	11 (18.33%)	49 (81.67%)	0.0574	39 (65.00%)	21 (35.00%)	0.3348
	Female	6 (42.86%)	8 (57.14%)	3.34 [0.96-11.59]	11 (78.57%)	3 (21.43%)	0.33 [0.49-7.87]
Age [years]	≥ 65	9 (31.03%)	20 (68.97%)	0.1903	18 (62.07%)	11 (37.93%)	0.4184
	< 65	8 (17.78%)	37 (82.22%)	0.48 [0.16-1.44]	32 (91.43%)	13 (8.57%)	1.50 [0.55-4.04]
Histopathological diagnosis	Squamous-cell carcinoma	14 (20.29%)	55 (79.91%)	0.0648	45 (65.22%)	24 (34.78%)	0.2351
	Others	3 (60.00%)	2 (40.00%)	5.89 [0.89-38.73]	5 (100%)	-	5.92 [0.31-111.65]
Tumor location	Oropharyngeal	11 (37.93%)	18 (62.07%)	0.0178*	20 (68.97%)	9 (31.03%)	0.8366
	Others	6 (13.33%)	39 (86.67%)	0.25 [0.08-0.79]	30 (66.67%)	15 (33.33%)	0.90 [0.33-2.45]
	Larynx	5 (13.16%)	33 (86.84%)	0.0452*	26 (68.42%)	12 (31.58%)	0.8720
	Others	12 (46.15%)	24 (53.85%)	3.30 [1.02-10.61]	24 (66.67%)	12 (33.33%)	0.87 [0.35-2.44]
T stage	T4	1 (2.86%)	34 (97.14%)	0.0030*	19 (54.29%)	16 (45.71%)	0.0234*
	T1-3	16 (41.02%)	23 (58.97%)	23.65 [2.93-190.93]	31 (79.49%)	8 (20.51%)	3.26 [1.17-9.08]
N stage	N1-3	8 (17.02%)	39 (82.98%)	0.1137	29 (79.38%)	18 (21.62%)	0.1596
	N0	9 (33.33%)	18 (66.67%)	2.44 [0.81-7.35]	21 (77.77%)	6 (22.22%)	2.17 [0.74-6.41]
M stage	M1	-	1 (100%)	0.9646	-	1 (100%)	0.2593
	M0	17 (23.29%)	56 (76.71%)	0.93 [0.04-23.85]	50 (68.49%)	23 (31.51%)	6.45 [0.25-164.26]
Disease stage	IVA-IVC	6 (11.32%)	47 (88.68%)	0.0005*	29 (54.72%)	24 (45.28%)	0.0141*
	I-III	11 (52.38%)	10 (47.62%)	8.62 [2.58-28.79]	21 (100%)	-	35.71 [2.06-620.24]
Performance status (PS)	>1	5 (38.46%)	8 (61.54%)	0.1525	7 (53.85%)	6 (46.15%)	0.2501
	≤1	12 (19.67%)	49 (80.33%)	0.39 [0.11-1.41]	43 (53.09%)	18 (46.91%)	2.05 [0.60-6.94]
Alcohol consumption [no data n=5]	Yes	5 (17.24%)	24 (82.76%)	0.4428	16 (55.17%)	13 (44.83%)	0.0530
	No	10 (25.00%)	30 (75.00%)	1.60 [0.48-5.31]	31 (77.50%)	9 (22.50%)	2.80 [0.99-7.94]
Smoking status (ever) [no data n=5]	Smoker	10 (18.87%)	43 (81.13%)	0.2977	34 (64.15%)	19 (35.85%)	0.2075
	Non-smoker	5 (31.25%)	11 (68.75%)	1.95 [0.55-6.90]	13 (81.25%)	3 (18.75%)	2.42 [0.61-9.58]
Smoking status (currently) [no data n=11]	Current smoker	9 (18.37%)	40 (81.63%)	0.7458	30 (61.22%)	19 (38.78%)	0.2492
	Former smoker	1 (25.00%)	3 (75.00%)	1.48 [0.14-15.94]	4 (100%)	-	5.75 [0.29-112.89]
Concurrent C-RT	Yes	11 (33.33%)	22 (66.67%)	0.1460	21 (67.74%)	10 (32.26%)	0.9783
	No	8 (18.60%)	35 (81.40%)	0.46 [0.16-1.31]	29 (67.44%)	14 (32.56%)	0.99 [0.37-2.65]
TNFRSF1A genotype	TT	3 (42.86%)	4 (57.14%)	0.4912	6 (85.71%)	1 (14.29%)	0.3033
	GT and GG	14 (29.79%)	33 (70.21%)	0.56 [0.11-2.86]	44 (65.67%)	23 (34.33%)	0.32 [0.04-2.81]
	GG	2 (6.25%)	30 (93.75%)	0.0079*	15 (46.88%)	17 (53.12%)	0.0015*
	TT and GT	15 (35.71%)	27 (64.29%)	8.33 [1.74-39.83]	35 (83.33%)	7 (16.67%)	5.67 [1.94-16.49]
	GT	12 (34.28%)	23 (65.72%)	0.0339*	29 (82.86%)	6 (17.14%)	0.0100*
	GG and TT	5 (12.82%)	34 (87.18%)	0.28 [0.09-0.91]	21 (53.85%)	18 (46.15%)	0.24 [0.08-0.71]

Table 1. Impact of the clinical-demographic, nutritional and genetic factors on the SGA scoring.

Conclusions

Our study demonstrated that the pre-treatment NLR may be an independent, significant predictor of OM as well as prognostic factor in HNC patients undergoing RT. Large prospective and validation studies are warranted to confirm the optimal NLR cut-off value and its predictive significance in that group of patients.

References

1. Nicolini, A.; Ferrari, P.; Masoni, M.C.; Fini, M.; Pagani, S.; Giampietro, O.; Carpi, A. Malnutrition, anorexia and cachexia in cancer patients: A mini-review on pathogenesis and treatment. Biomed. Pharmacother. 2013, 67, 807–817, doi:10.1016/j.biopha.2013.08.005.
2. Gorenc, M.; Kozjek, N.R.; Strojan, P. Malnutrition and cachexia in patients with head and neck cancer treated with (chemo)radiotherapy. Reports Pract. Oncol. Radiother. 2015, 20, 249–258, doi:10.1016/j.rpor.2015.03.001.
3. Vanhoutte, G.; van de Wiel, M.; Wouters, K.; Sels, M.; Bartolomeeussen, L.; De Keersmaecker, S.; Verschueren, C.; De Vroey, V.; De Wilde, A.; Smits, E.; et al. Cachexia in cancer: what is in the definition? BMJ open Gastroenterol. 2016, 3, e000097, doi:10.1136/bmjgast-2016-000097.
4. Omatsu, H.; Kuwahara, A.; Yamamori, M.; Fujita, M.; Okuno, T.; Miki, I.; Tamura, T.; Nishiguchi, K.; Okamura, N.; Nakamura, T.; et al. TNF-α -857C>T genotype is predictive of clinical response after treatment with definitive 5-fluorouracil/cisplatin-based chemoradiotherapy in Japanese patients with esophageal squamous cell carcinoma. Int. J. Med. Sci. 2013, 10, 1755–1760, doi:10.7150/ijms.6749.
5. Sennikov, S. V; Vasilyev, F.F.; Lopatnikova, J.A.; Shkaruba, N.S.; Silkov, A.N. Polymorphisms in the tumor necrosis factor receptor genes affect the expression levels of membrane-bound type I and type II receptors. Mediators Inflamm. 2014, 2014, 745909, doi:10.1155/2014/745909.
6. Kalliolias, G.D.; Ivashkiv, L.B. TNF biology, pathogenic mechanisms and emerging therapeutic strategies. Nat. Rev. Rheumatol. 2016, 12, 49–62, doi:10.1038/nrrheum.2015.169.
7. Brenner, D.; Blaser, H.; Mak, T.W. Regulation of tumour necrosis factor signalling: live or let die. Nat. Rev. Immunol. 2015, 15, 362–374, doi:10.1038/nri3834.

THE IMPORTANCE OF LEPTIN AND LIPIDS IN SHEEP'S MILK FOR HUMAN HEALTH

E.MOLIK, Z.FLIS, E.MARCINIAK, H.PUSTKOWIAK

Department of Animal Nutrition and Biotechnology, and Fisheries, University of Agriculture in Krakow, Poland; Department of Genetics and Animal Breeding, and Ethology, University of Agriculture in Krakow, Poland; The Kielanowski Institute of Animal Physiology and Nutrition, Polish Academy of Sciences, Jablonna, Poland; corresponding author; rzmolik@cyf-kr.edu.pl

Introduction

Chronic metabolic disorders, referred to as "civilization diseases" are major public health problems. A measure of the high pro-health value of sheep's milk is i.a. more favorable fatty acid composition, such as conjugated linoleic acid (CLA). Metabolic hormones, in particular leptin, are also crucial bioactive factor in sheep's milk. The aim of the research was to determine the content of CLA and leptin in sheep's milk.

Methods

The fatty acid composition, with particular emphasis on conjugated linoleic acid (CLA) isomers, was determined using the methods described by Martial et al. (2005). Individual fatty acid methyl esters were identified by comparison to the standard mixture of (Supelco 37 component FAME Mix, Sigma-Aldrich Co.) and of CLA isomers (Sigma-Aldrich Co., St. Louis, MO). Milk samples were collected into sterile tubes containing EDTA and aprotinin (0.6TIU/ml of milk) and assayed for leptin concentrations using commercially available radioimmunoassay (RIA) kits.

Results

Changes in te leptin content in sheep's milk during lactation

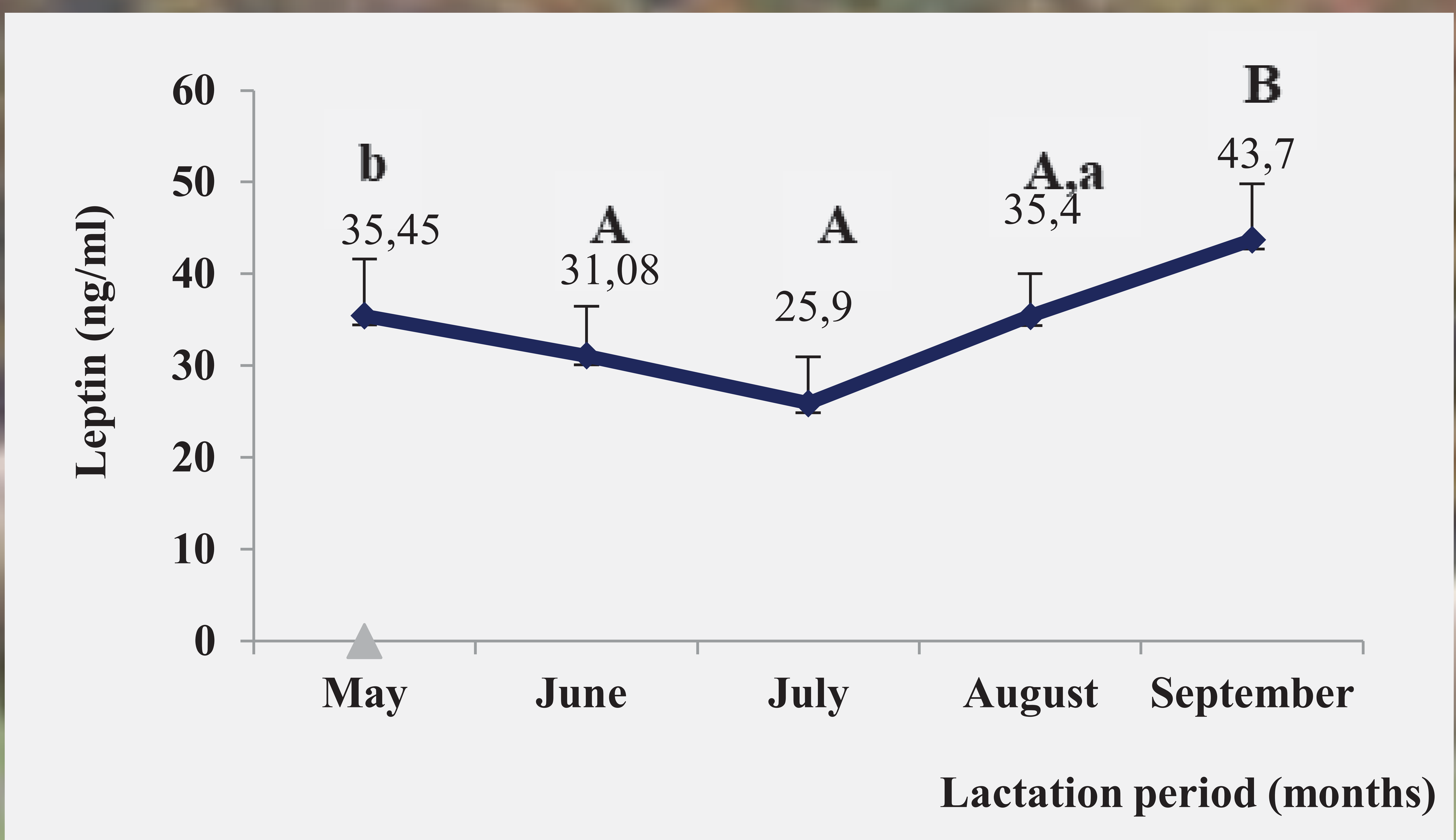

Changes in fat content in sheep's milk during lactation

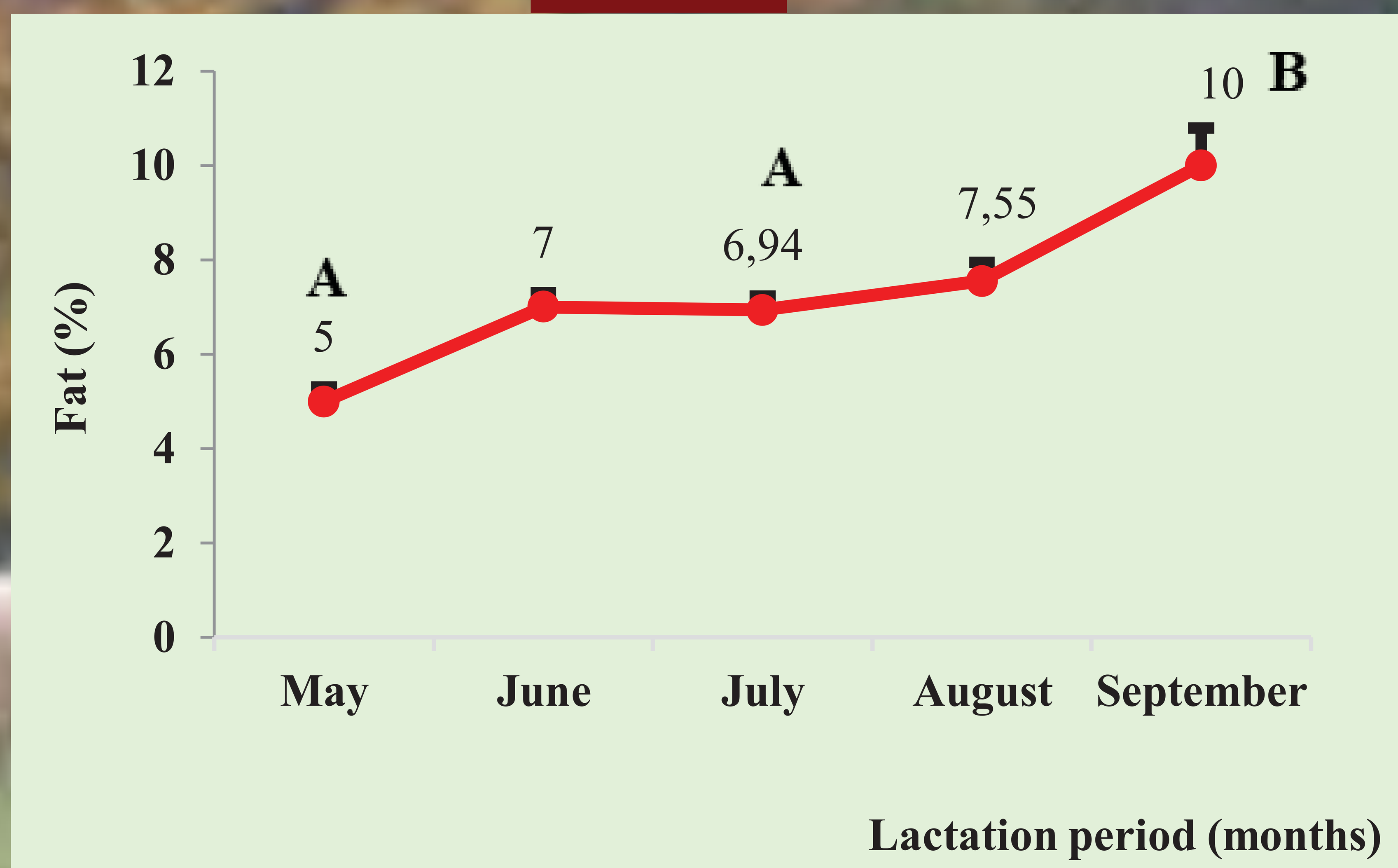

Changes in CLA content in sheep's milk during lactation

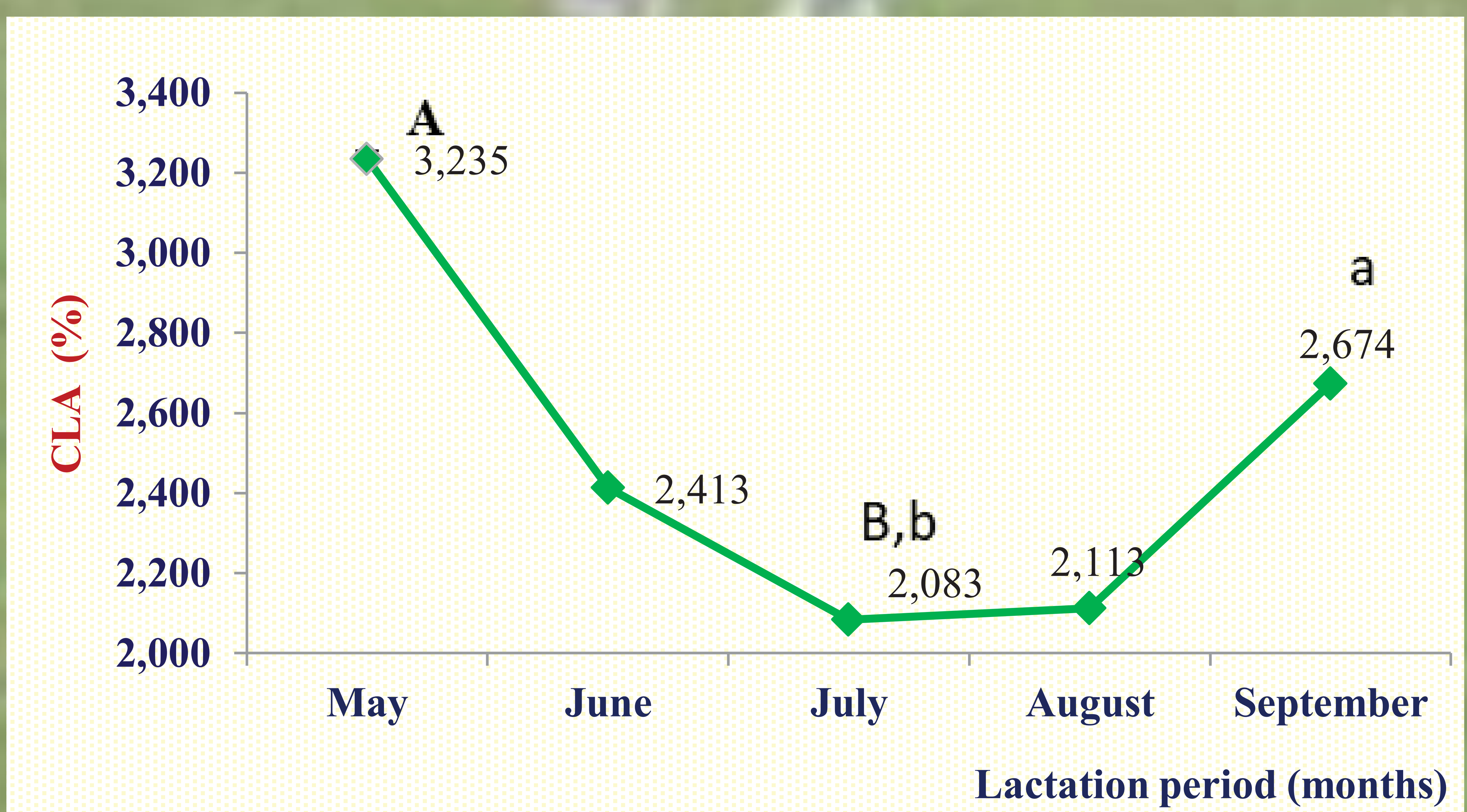

A, B – średnie różnią się istotnie przy P≤0,01

a, b – średnie różnią się istotnie przy P≤0,05

Conclusions

The obtained research results may allow the production of medicinal food from sheep's milk, which can be used in the prevention of many human diseases, including civilization diseases.

1. Molik E, Błasiak M, Pustkowiak H. Impact of Photoperiod Length and Treatment with Exogenous Melatonin during Pregnancy on Chemical Composition of Sheep's Milk. Animals, 2020, 10, 1721, doi:10.3390/ani10101721;
2. Molik E, Hell K, Staroń M, Flis Z. Znaczenie leptyny w zapoczątkowaniu i utrzymaniu laktacji u owiec. Przeg. Hodl., 2019, 5, 26-28;
3. Flis Z, Molik E. Importance of Bioactive Substances in Sheep's Milk in Human Health. Int. J. Mol. Sci., 2021, 22, 4364, doi:10.3390/ijms22094364.

REGULATORY EFFECT OF IRISIN ON CARDIAC FIBROBLASTS PROLIFERATION IS DEPENDENT ON GLUCOSE CONCENTRATION

Marta Drobnik[1], Małgorzata Gałdyszyńska[1], Jacek Szymański[2] And Paulina Radwańska[1]

[1]Laboratory of Connective Tissue Metabolism, Department of Pathophysiology, Medical University of Lodz, Łódź, Poland.
[2] Central Scientific Laboratory, Medical University of Lodz, Lodz, Poland.

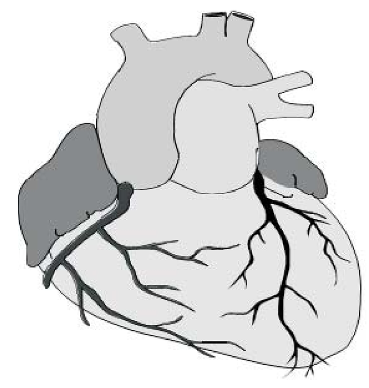

BACKGROUND:

Diffuse cardiac fibrosis within the heart in diabetics was reported. Cardiac fibroblasts increase collagen synthesis and accelerate proliferation in hyperglycaemic conditions.

Energetic status of the cells may influence on it function (extracellular matrix synthesis or proliferation). Glucose is not able to diffuse across cell membrane. Influx of glucose into the cells is dependent on glucose transporters. Two main types of glucose transporters were described: sodium-glucose-linked transporters (SGLT) and facilitated diffusion glucose transporters (GLUTs). GLUTs are the proteins containing 12 membrane spanning regions but both carboxy and amino terminals are localized intracellulary. GLUTs transports glucose across the plasma membrane by facilitating it diffusion.

Irisin, composed of 112 aminoacids, was described in 2012 as the hormone released from muscle cells. Augmentation of irisin concentration is linked with improvement of glucose homeostasis and reduction of insulin resistance. Irisin is also called as myokine and is released during exercise and is associated with elevated expenditure of energy. Except skeletal muscle and heart this myokine expression was also found in brain, liver, pancreas, stomach, and testis of rats. Irisin increases glucose uptake by human skeletal muscle. Elevated level of irisin was found in patients with type 2 of diabetes mellitus.

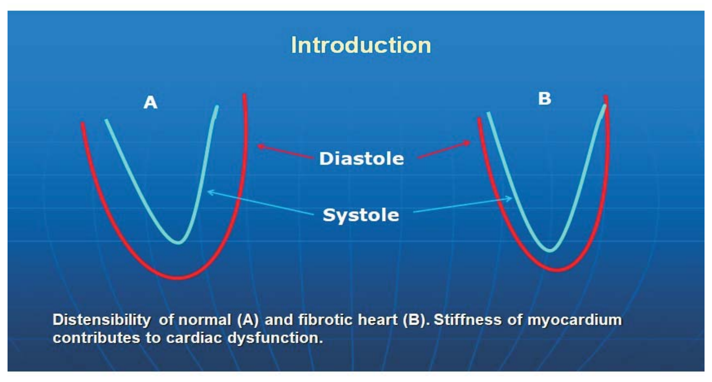

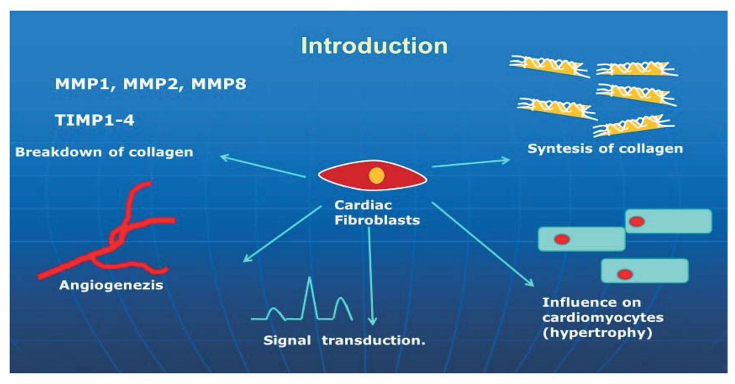

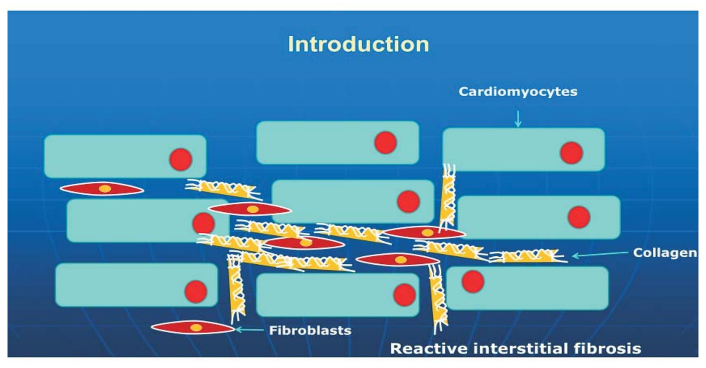

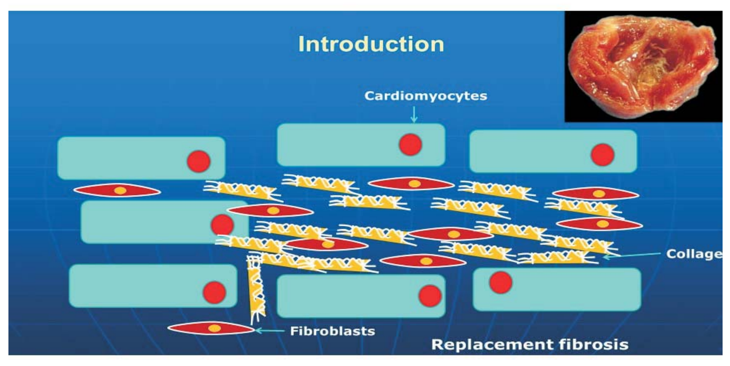

PURPOSE

1. The study is aimed at verification of hypothesis suggesting, that irisn may be involved in regulation of cardiac fibroblast proliferation.
2. Explanation whether concentration of glucose may influence on irisin effect.
3. Verification of GLUT 1, 3, 4 expression on cardiac fibroblasts surface was investigated.
4. Explanation whether irisin may change distribution of GLUTs across the cell membrane.

METHODS:

1. Human cardiac fibroblasts (ABM, Canada) on the plates coated with 10µg/cm2 type I collagen were applied for the sudy. Following concentrations of glucose were tested 1M (glu1) - hypoglycaemia, 5M (glu5) normoglycaemia and 25M (glu25) hypeglycaemia. Irisin was applied at concentrations: 10-7M, 10-8M and 10-9M.

2. Assessment of cell proliferation. The bromodeoxiuridine (BrdU) was incorporated to the newly synthetized DNA of proliferating cells.

3. Expression of GLUT 1, 3 and 4 was evaluated by flow cytometry. Before cytometry cells will be fixed and stained with antibody connected with FITC and then analyzed using a Cytometer CytoFLEX.

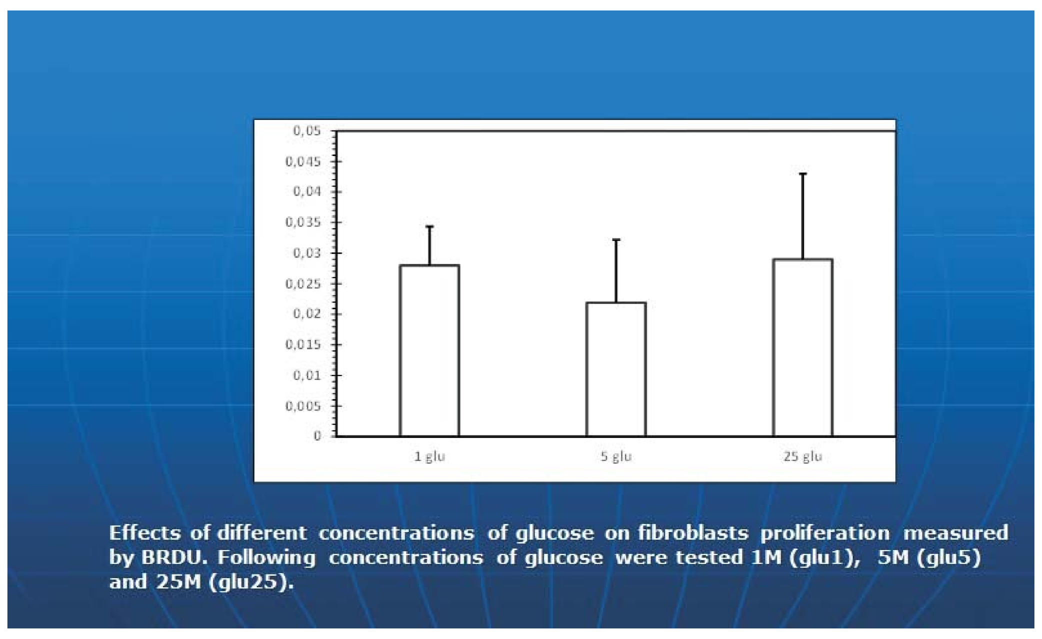

Effects of different concentrations of glucose on fibroblasts proliferation measured by BRDU. Following concentrations of glucose were tested 1M (glu1), 5M (glu5) and 25M (glu25).

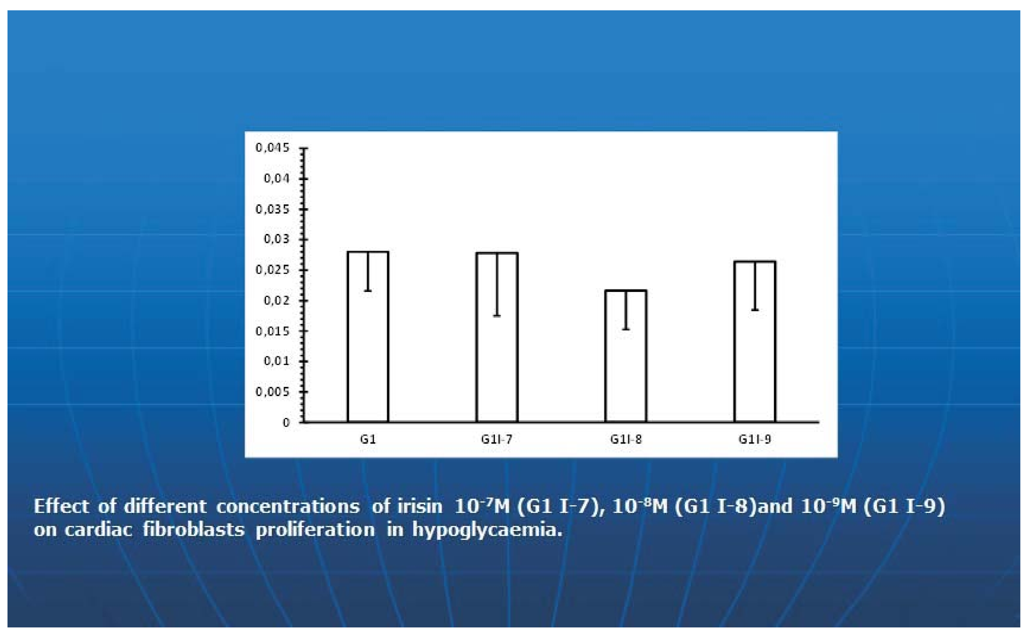

Effect of different concentrations of irisin 10^{-7}M (G1 I-7), 10^{-8}M (G1 I-8)and 10^{-9}M (G1 I-9) on cardiac fibroblasts proliferation in hypoglycaemia.

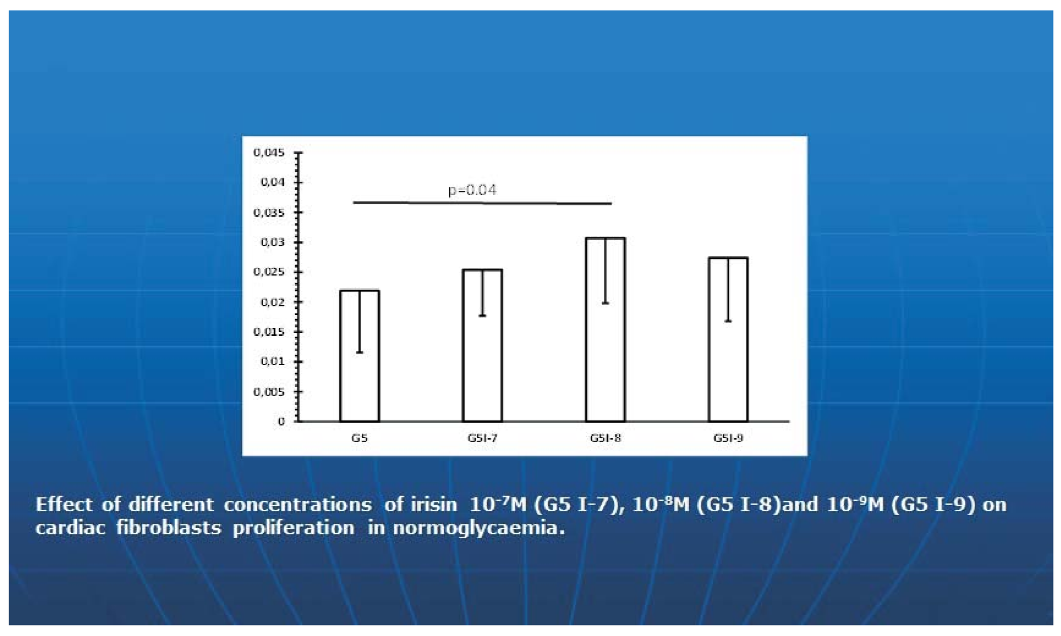

Effect of different concentrations of irisin 10^{-7}M (G5 I-7), 10^{-8}M (G5 I-8)and 10^{-9}M (G5 I-9) on cardiac fibroblasts proliferation in normoglycaemia.

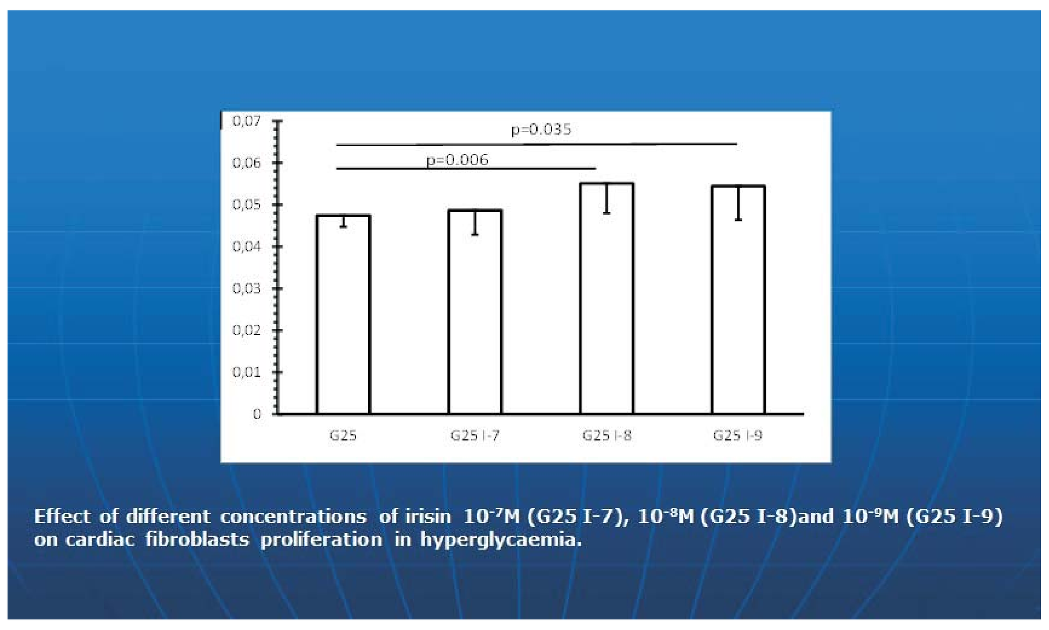

Effect of different concentrations of irisin 10^{-7}M (G25 I-7), 10^{-8}M (G25 I-8)and 10^{-9}M (G25 I-9) on cardiac fibroblasts proliferation in hyperglycaemia.

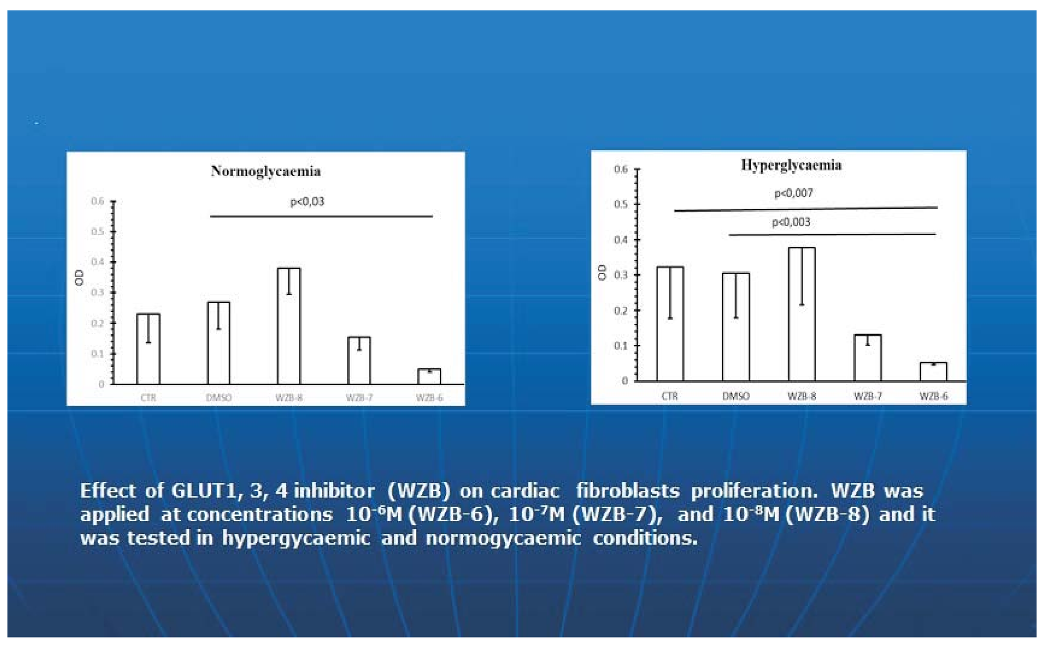

Effect of GLUT1, 3, 4 inhibitor (WZB) on cardiac fibroblasts proliferation. WZB was applied at concentrations 10^{-6}M (WZB-6), 10^{-7}M (WZB-7), and 10^{-8}M (WZB-8) and it was tested in hypergycaemic and normogycaemic conditions.

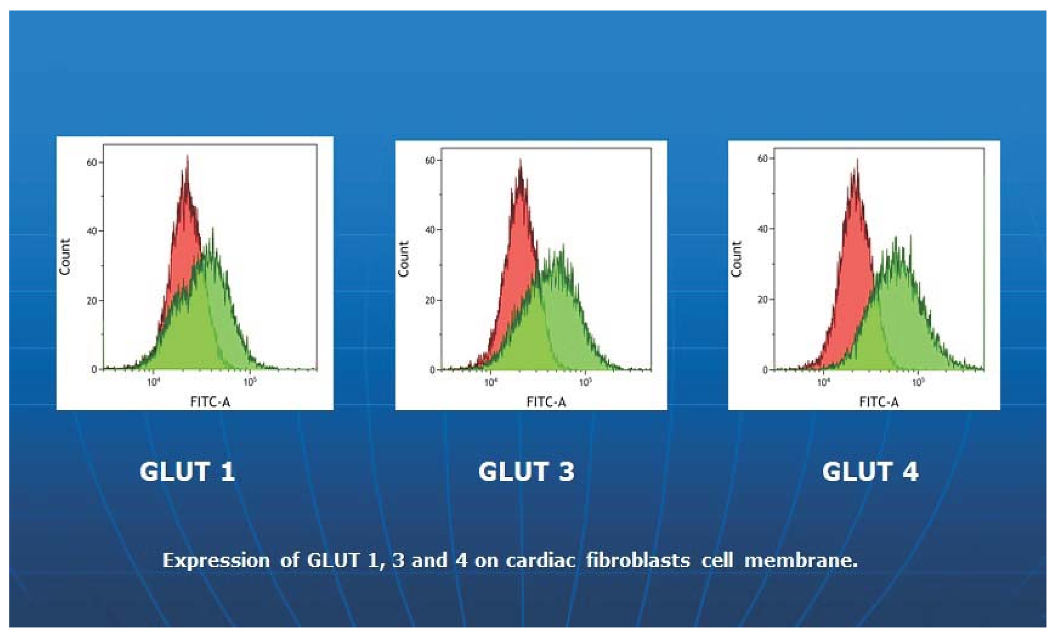

Expression of GLUT 1, 3 and 4 on cardiac fibroblasts cell membrane.

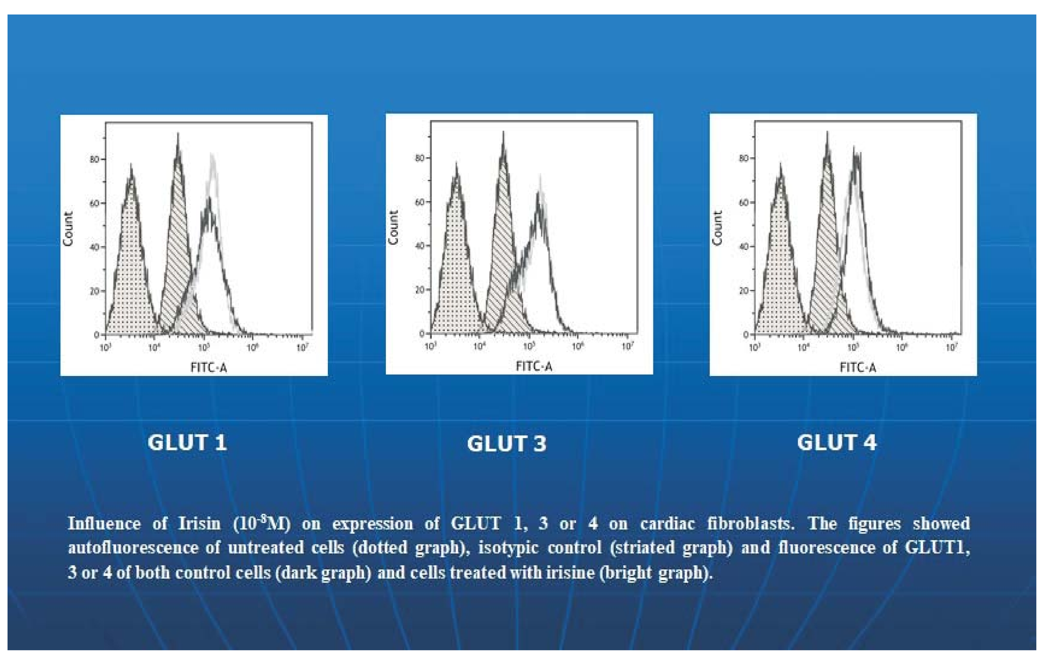

Influence of Irisin (10^{-8}M) on expression of GLUT 1, 3 or 4 on cardiac fibroblasts. The figures showed autofluorescence of untreated cells (dotted graph), isotypic control (striated graph) and fluorescence of GLUT1, 3 or 4 of both control cells (dark graph) and cells treated with irisine (bright graph).

CONCLUSION

Irisin in concentration dependent manner increases proliferation of cardiac fibroblasts. This effect is also determined by glucose concentration.

Expression of GLUT 1, 3 ,4 on cardiac fibroblasts was confirmed. The density of GLUT1, GLUT3 and GLUT4 is not dependent on irisin.

GLUTs1, 3, 4 blocker inhibits cardiac fibroblasts proliferation.

Explanation whether mechanism of irisin effect on fibroblast proliferation is dependent on modification of GLUT1, 3, 4 activity is planned.

MEDICAL UNIVERSITY OF LODZ

XXVIII Congress of the Polish Physiology Society
Gdańsk, 15-17 2021

Effect of N-acetylcysteine Supplementation on Fatty Acid Transporters in Adipose Tissue

Marta Wolosowicz[1], Mateusz Maciejczyk[2], Ewa Zebrowska[1], Bartlomiej Lukaszuk[1], Adrian Chabowski[1]

[1]Department of Physiology, Medical University of Bialystok, Poland
[2]Department of Hygiene, Epidemiology and Ergonomics, Medical University of Bialystok, Poland

INTRODUCTION / OBJECTIVES

Obesity is a systemic, multifactorial, and largely preventable disease, affecting, along with overweight, over a third of the world's population in the XXI century. Chronically elevated body mass index (BMI) is linked to the occurrence of a broad range of diseases, namely cardiovascular diseases, diabetes, musculoskeletal disorders, and cancers. The adipose tissue is a critical regulator of systemic energy homeostasis by acting as a caloric reservoir. Augmented oxidative stress in adipose tissue of obese subjects leads to insulin resistance, dysregulated adipokines secretion, inflammation, and increased protein carbonylation. Based on this, we aimed to check whether anti-oxidative agent – N-acetylcysteine (NAC) impacts fatty acid transporters expression in adipose tissue using a rodent model of a high-fat diet (HFD).

MATERIAL & METHODS

The experiment was carried out on 4-week-old Wistar rats. After six days of acclimatization to the trial conditions, the rodents were divided into four groups (n=10 per group): normal diet, normal diet + NAC, HFD, and HFD + NAC. The mRNA levels and protein expression of FAT/CD36, FABPpm, FATP1, and FATP4 were assessed using real-time PCR and Western Blot analyses. The level of lipids abundance (FFA, DAG, and TAG) was estimated by GLC.

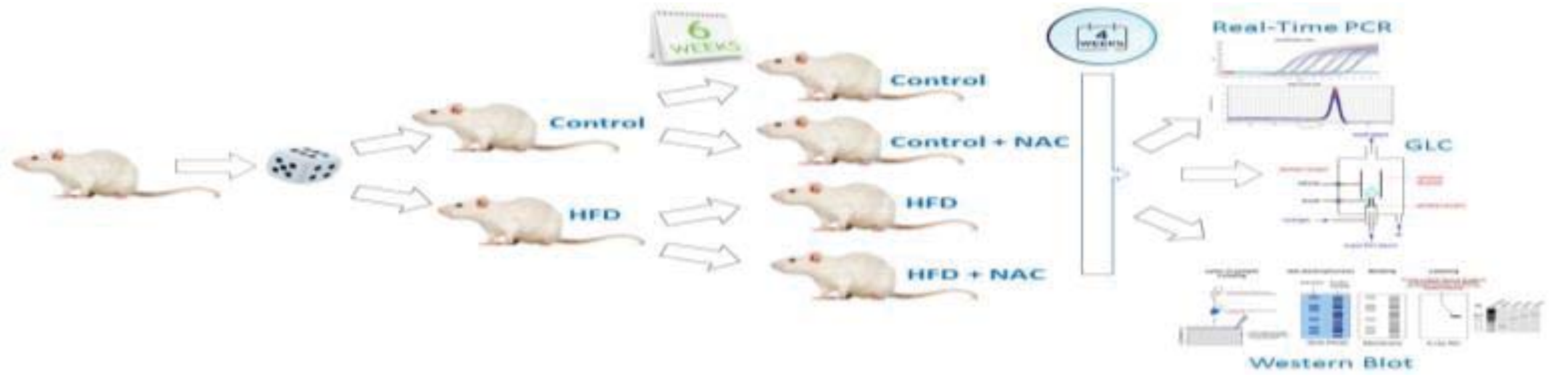

RESULTS

In visceral and subcutaneous adipose tissues statistically significant differences in the mRNA and protein levels of the long-chain fatty acid transporters have been found. Eight weeks of NAC treatment during the HFD regime resulted in a significant increase (p>0.05) in FATP1, FATP4, and FABPpm proteins expression in visceral and subcutaneous adipose tissue compared to the respective HFD. On the other hand there were observed a significant decrease (p>0.05) in FATP1, FATP4, FABPpm, and also in FAT/CD36 mRNA expressions in both adipose tissues. Interestingly, there were observed decrease in FFA, DAG, and TAG content in NAC+HFD groups compared to HFD, in visceral and subcutaneous adipose tissue.

SUMMARY / CONCLUSION

Our results revealed that NAC supplementation during the HFD regime promotes a decrease in the lipids pool in adipose tissue compared to HFD. Currently, studies are underway to identify the mechanisms involved in the observed phenomena.

RESULTS

The effects of NAC on the mRNA levels of FAT/CD36, FABPpm, FATP1, and FATP4 in the adipose tissues of HFD-fed rats

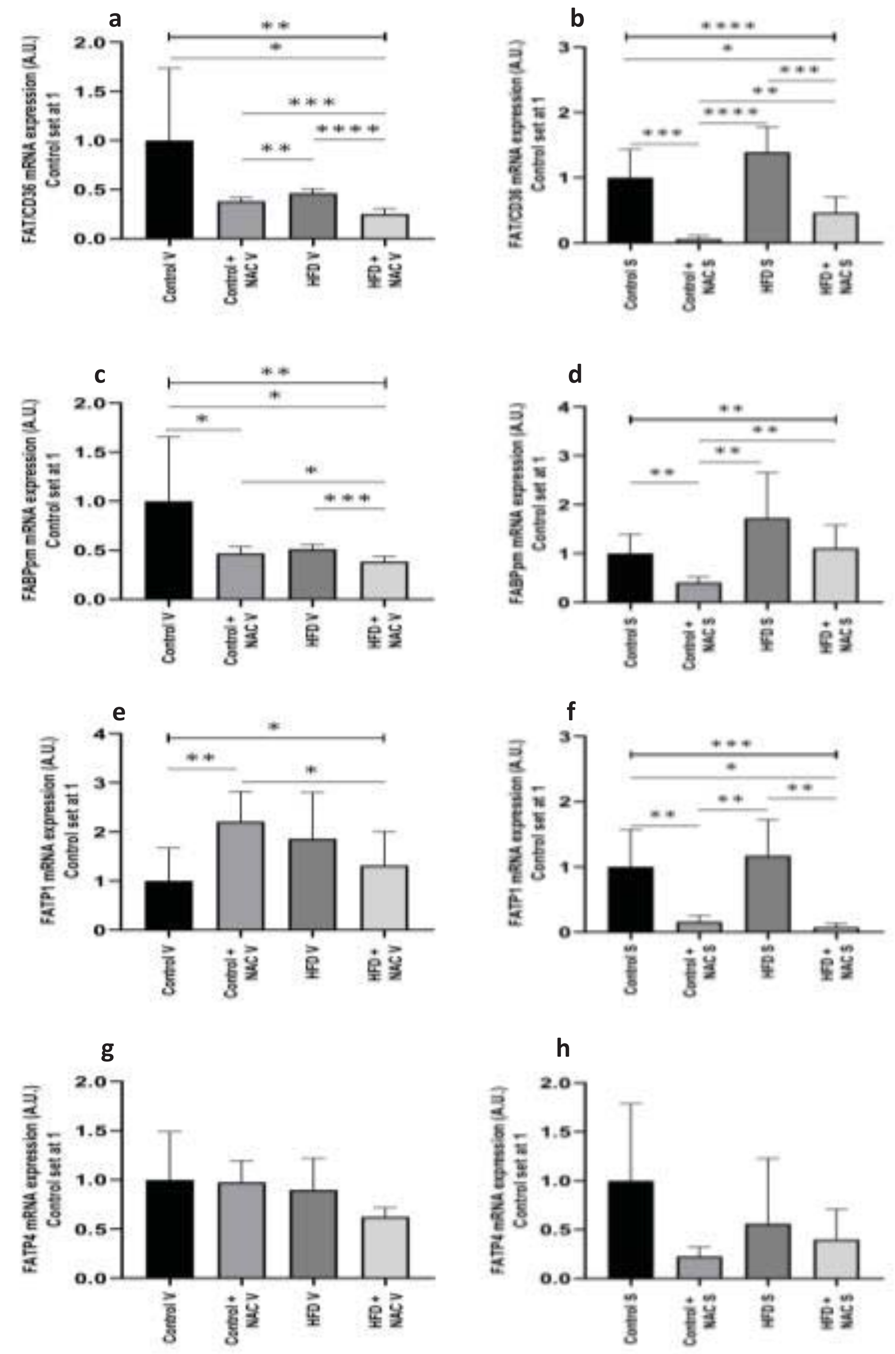

Figure 1. The effects of NAC on (**a**, **b**) FAT/CD36, (**c**, **d**) FABPpm, (**e**, **f**) FATP1, and (**g**, **h**) FATP4 mRNA expressions in adipose tissue during the HFD regime. Control V - control rats, visceral adipose tissue; Control +NAC V - control rats that received N-acetylcysteine, visceral adipose tissue; HFD V – high-fat diet-fed rats, visceral adipose tissue; HFD+NAC V – high-fat diet-fed rats that received N-acetylcysteine, visceral adipose tissue; Control S - control rats, subcutaneous adipose tissue; Control + NAC S – control rats that received N-acetylcysteine, subcutaneous adipose tissue; HFD S – high-fat diet-fed rats, subcutaneous adipose tissue; HFD+NAC S – high-fat diet fed rats that received N-acetylcysteine, subcutaneous adipose tissue;*p<0.05; **p<0.01; ***p<0.001; ****p<0.0001.

The effects of NAC on protein levels of FAT/CD36, FABPpm, FATP1, and FATP4 in the adipose tissue of HFD-fed rats

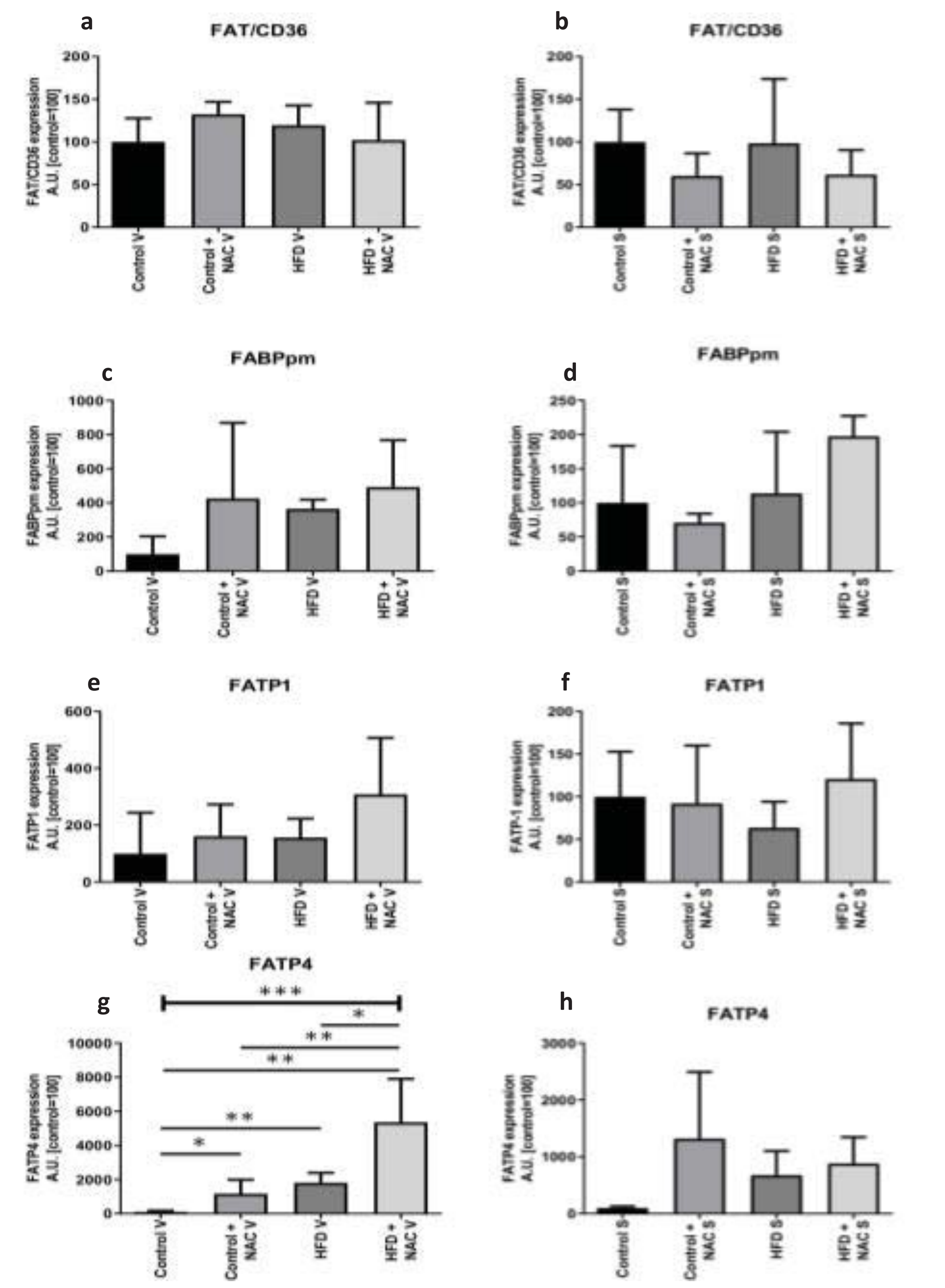

Figure 2. The effects of NAC on (**a**, **b**) FAT/CD36, (**c**, **d**) FABPpm, (**e**, **f**) FATP1, and (**g**, **h**) FATP4 protein expressions in adipose tissue during the HFD regime. Control V - control rats, visceral adipose tissue; Control +NAC V - control rats that received N-acetylcysteine, visceral adipose tissue; HFD V – high-fat diet-fed rats, visceral adipose tissue; HFD+NAC V – high-fat diet-fed rats that received N-acetylcysteine, visceral adipose tissue; Control S - control rats, subcutaneous adipose tissue; Control + NAC S – control rats that received N-acetylcysteine, subcutaneous adipose tissue; HFD S – high-fat diet-fed rats, subcutaneous adipose tissue; HFD+NAC S – high-fat diet fed rats that received N-acetylcysteine, subcutaneous adipose tissue;*p<0.05; **p<0.01; ***p<0.001; ****p<0.0001.

The effects of NAC on the adipose tissue's FFA, DAG, and TAG contents and compositions in the rats fed with the high-fat diet

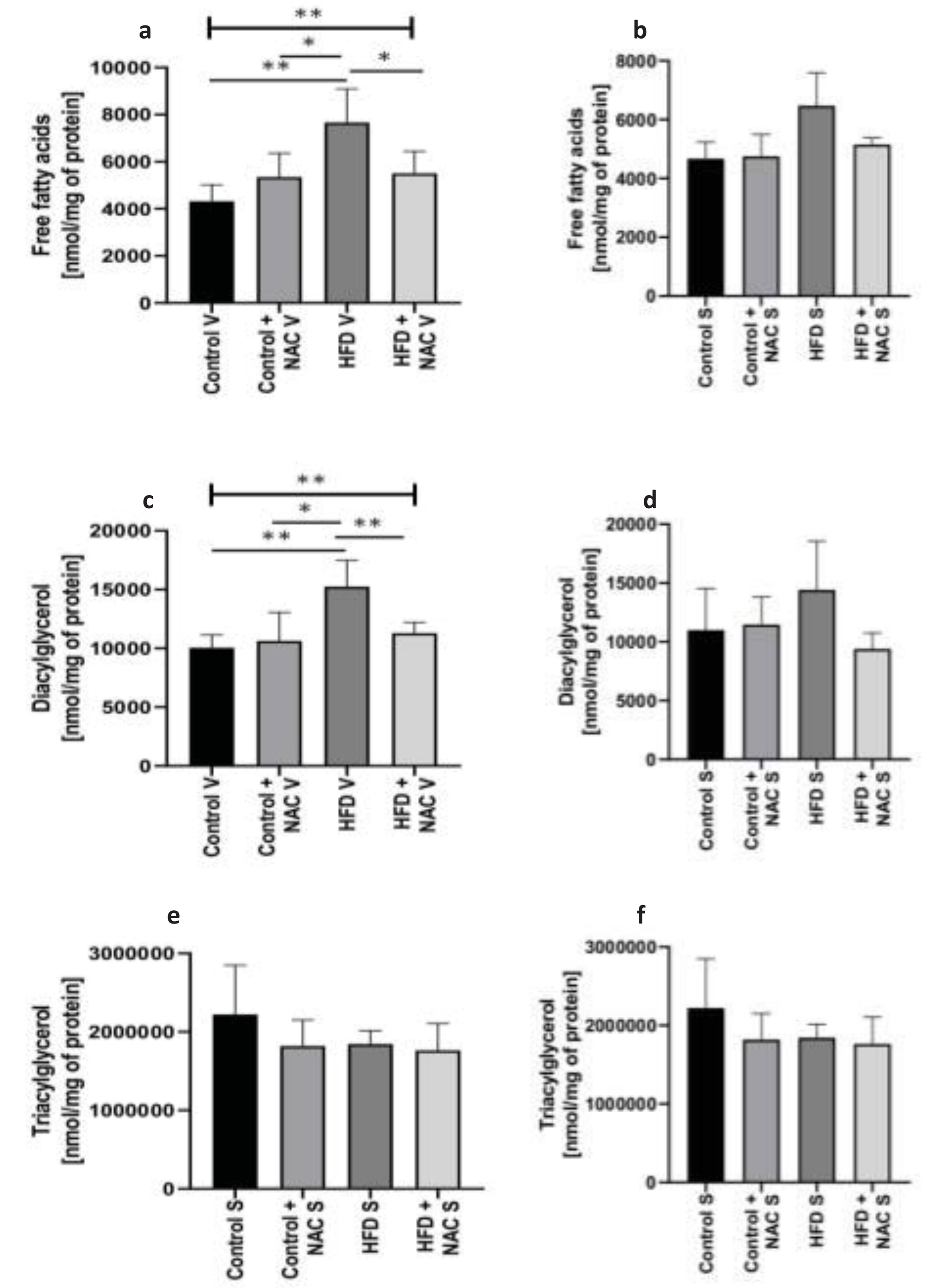

Figure 3. The effects of NAC on (**a**, **b**) FFA, (**c**, **d**) DAG, and (**e**, **f**) TAG content in adipose tissue. Control V - control rats, visceral adipose tissue; Control +NAC V - control rats that received N-acetylcysteine, visceral adipose tissue; HFD V – high-fat diet-fed rats, visceral adipose tissue; HFD+NAC V – high-fat diet-fed rats that received N-acetylcysteine, visceral adipose tissue; Control S - control rats, subcutaneous adipose tissue; Control + NAC S – control rats that received N-acetylcysteine, subcutaneous adipose tissue; HFD S – high-fat diet-fed rats, subcutaneous adipose tissue; HFD+NAC S – high-fat diet fed rats that received N-acetylcysteine, subcutaneous adipose tissue;*p<0.05; **p<0.01; ***p<0.001; ****p<0.0001.

REFERENCES

1) R. Buettner, K.G. Parhofer, M Woenckhaus et al., "Defining high-fat-diet rat models: metabolic and molecular effects of different fat types," *Journal of molecular Endocrinology*, 2006.
2) Q. Wu, A. Ortegon, B. Tsang et al.,"FATP1 is an insulin-sensitive fatty acid transporter involved in diet-induced obesity," *Molecular and cellular biology*, 2006.
3) P. Manna and S. Jain, "Obesity, Oxidative Stress, Adipose Tissue Dysfunction, and the Associated Health Risks: Causes and Therapeutic Strategies," *Metabolic syndrome and related disorders*, 2015.
4) G. Aldini, A. Altomare, G. Baron et al., "N-Acetylcysteine as an antioxidant and disulphide breaking agent: the reasons why," *Free radical research*, 2018.
5) P. Calzadilla, M. Gómez-Serrano, E. García-Santos et al., "N-Acetylcysteine affects obesity-related protein expression in 3T3-L1 adipocytes," *Redox report : communications in free radical research*, 2013.
6) L. M. Korou, G. Agrogiannis, C. Koros et al., "Impact of N-acetylcysteine and sesame oil on lipid metabolism and hypothalamic-pituitary-adrenal axis homeostasis in middle-aged hypercholesterolemic mice," *Scientific reports*, 2014.

CONTACT

marta.wolosowicz@umb.edu.pl

XXVIII Congress of the Polish Physiological Society

Gdańsk, September 15-17 2021

Poster book

SESSION IX

NEW INSIGHTS INTO CELLULAR FUNCTIONS

HONORARY PATRONAGE

Uniwersytet Gdański

Prof. dr Marcin Gruchała
Rector of the Medical University of Gdansk

Prof. dr Piotr Stepnowski
Rector of the University of Gdansk

WOJEWODA POMORSKI
DARIUSZ DRELICH

Dariusz Drelich
Governor of the Pomeranian Voivodeship

HONORARY PATRONAGE
Mayor of the City of Gdańsk

Aleksandra Dulkiewicz
Mayor of Gdansk

Mieczysław Struk
Marshal of the Pomeranian Voivodeship

PARTNER

PAN
POLSKA AKADEMIA NAUK

ANIMA LAB
animal facility and laboratory equipment • animal research models

FUNDACJA LOTOS

Medical University of Gdansk
Department of Physiology

Direct effect of Vit C on cell cycle and apoptosis gene and protein expression in cancer cells.

Natalia Respekta, Ewa L Gregoraszczuk

Laboratory of Physiology and Toxicology of Reproduction, Institute of Zoology and Biomedical Research, Jagiellonian University in Krakow, Poland.

What is known already The ovarian cancer has been at the forefront of diseases leading to the highest mortality among women. The main reason is the severity of the disease at diagnosis, the absence innovative therapies and lack of individual approach to the patient. Despite controversies regarding the role of Vit C in the prevention and treatment of cancer, many research showed the anticancer action of Vit C in ovarian cancer cells.

The purpose of the present study was to demonstrate the mechanism of action a high physiological or pharmacological doses of Vit C on selected parameters in ovarian cancer. We measured cells proliferation, membrane cell permeability, caspase-3 activity as an indicator of apoptosis through determining the dose-dependent effect of Vit C. Furthermore, the effect of 10 mM Vit C concentration were determined of cells morphology and expression selected genes and proteins of the cell cycle as well as apoptosis, oncosis and autophagy-dependent cell death in ovarian cancer granulosa and epithelial cells.

Additionally, we estimated the influence of cancer associated fibroblasts (CAFs) on the action of Vit C in ovarian cells.

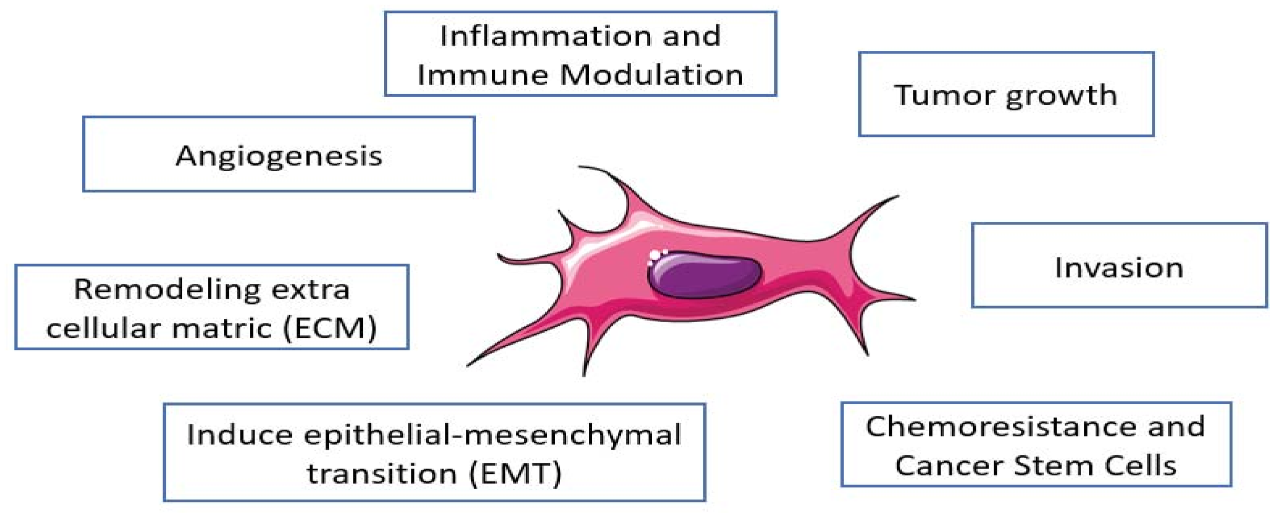

Functions of CAFs; modified; Subramanyam Dasari i wsp., (2018), Cancer Associated Fibroblasts: Naughty Neighbors That Drive Ovarian Cancer Progression; Cancers 10, 406 doi:10.3390/cancers10110406

MATERIAL & METHODS

https://cellbank.brc.riken.jp/cell_bank/CellInfo/?cellNo=RCB1154&lang=Ja

Human ovarian granulosa-like tumor cell line - KGN (Riken BRC, Kyoto, Japan).

Cells were routinely cultured in DMEM with 10% of calf serum.

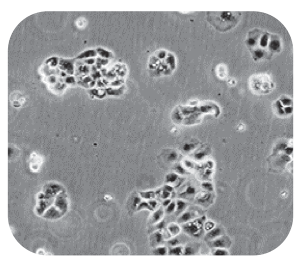

https://www.atcc.org/products/htb-161

Human ovarian epithelial carci- noma cell lines – OVCAR-3 (ATC, Manassas,VA, USA).

Cells were routinely cultured in RPMI with 15% of calf serum.

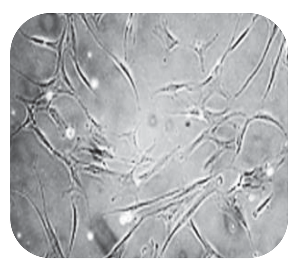

https://bioivt.com/primary-human-cancer-associated-fibroblasts-and-matched-normal-fibroblasts/

Cancer associated fibroblast – CAF (BIOIVT Elevating ScienceTM).

Cells were routinely cultured in DMEM with 10% of calf serum.

Cells were incubated for **1h** with Vit C in high physiological (**0.1 mM**) or pharmacologic concentrations (**0.5, 1, 10, 20 mM**). Alamar Blue assay, LDH assay and caspsese-3 assay was used for cytotoxicity effect.

Additionally, cells were incubated for **1h** with Vit C in **10 mM** concentration. Real - time PCR (qPCR) and Western blot analysis for measuring ccna2, cdk2, ccnd1, cdk4, as cell cycle protein and bcl-2, bax, caspase-3, p21 and p53 as parameters of apoptosis, and PARP. Moreover, qPCR analysis for measuring *UCP-2, CYCS* and ATP level as parametrs of oncosis and *ATG5, ATG7, BECN1* as autophagy-dependent cell death.

RESULTS

1. Cytotoxicity effects of Vit C – Alamar Blue, LDH and caspase-3 activity.

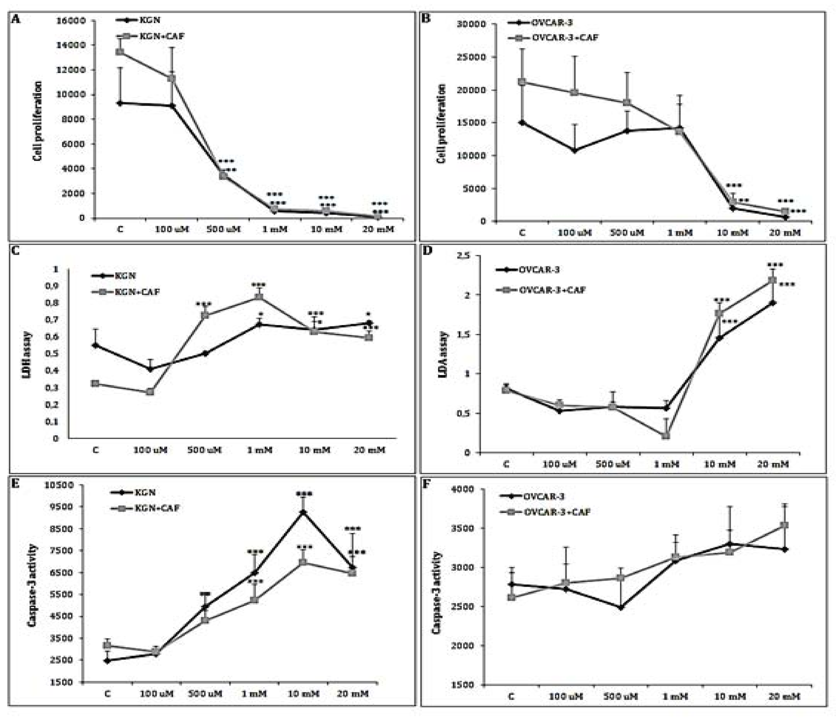

In granulosa cancer cells (KGN) Vit C in dose 500 µM to 20 mM decreased cell proliferation, but its increased membrane cell permeability and caspase-3 activity (Fig.1 A,C,E).

In epithelial cancer cells (OVCAR-3) Vit C in dose 10 mM and 20 mM decreased cell proliferation and increased membrane cell permeability (Fig.1 B, D). In all doses used, did not changed caspase-3 activity, as well as in CAF supplemented medium (Fig. 1 F).

3. Action of Vit C on the expression of selected cell cycle pathway: ccna2; cdk4; ccnd1; cdk2 in two types of ovarian cancer cells.

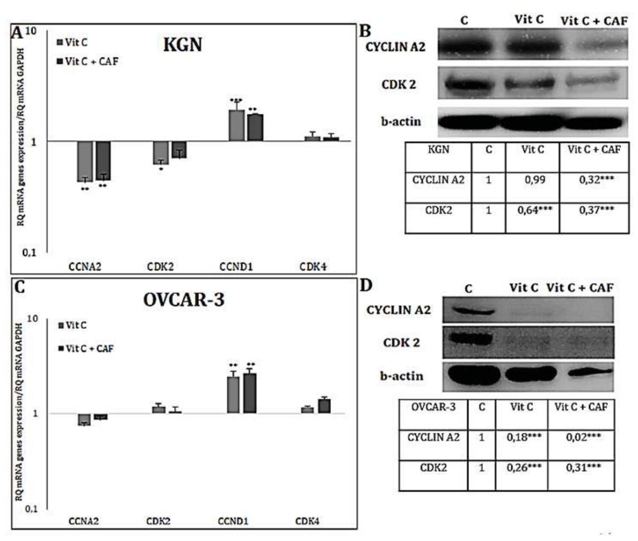

Both in KGN and OVCAR-3 Vit C in dose 10 mM decreased ccna2 and cdk2 expression (Fig. 3 B, D). Additionally, in KGN Vit C decreased *CCNA2* and *CKD2* gene expression (Fig. 3 A).

4. Action of Vit C on the expression of apoptosis pathway: bcl-2, bax, caspase-3, p21, p53 and PARP in two types of ovarian cancer cells.

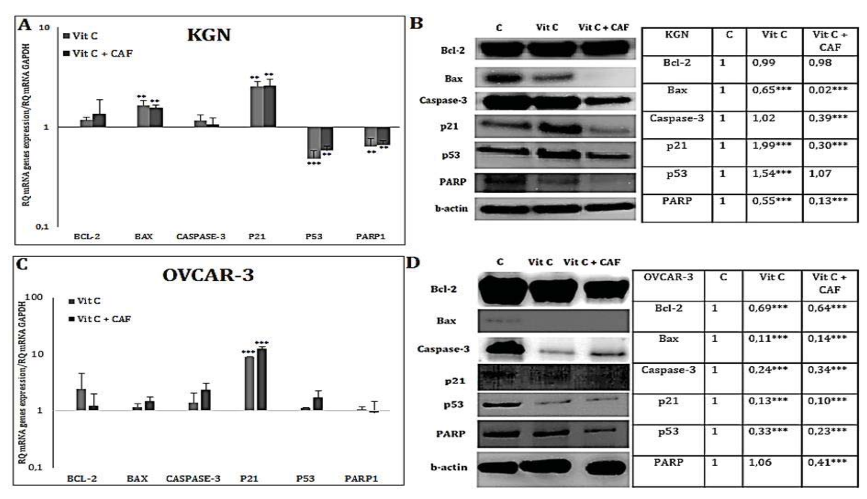

In KGN cells cultured with CAF supplemented Vit C in dose 10 mM decreased p21 which may be associated with CAF resistance to high vitamin concentrations (Fig. 4 B).

In OVCAR-3 Vit C in dose 10 mM decreased Bcl-2, proapoptotic protein Bax and caspase-3 (Fig. 4 D).

In both cell lines, Vit C inhibited PARP expression (Fig. 4. A-D). In addition, Vit C increased P21 gene expression. As a result, its may act to inhibit CDK2 activity lead to cell cycle phase disordes (Fig. 4 A – C).

In summary our results identify different types of cell death under the influence Vit C in pharmacological dose 10 mM :

1) in ovarian cancer cells Vit C in dose dependent manner decreased cells proliferation and ATP level, but its increased membrane cell permeability.
2) in ovarian granulosa cancer cells Vit C leads to apoptosis, which confirm our data and morphology observation.
3) in ovarian epithelial cancer cells Vit C leads to apoptosis in parallel with oncosis and autphagy-dependent cell death as research evidenced and morphology observation.
a) Vit C decreased proapoptotic and antyapoptotic genes and proteins expression and caspase-3.
b) Vit C increased oncosis and autophagy genes expression.
4) Vitamin C shows therapeutic potential as an inhibitor of PARP1 through reducing the level of PARP1 expression in two types of ovarian cancer.

2. Action of vitamin C on the morphology of ovarian cancer cells.

In cancer cells OVCAR-3 various types of cell death have been observed, such as apoptosis with the formation of apoptotic bodies (marked with a lightning), oncosis with the formation of characteristic vesicles (marked with an asterisk) and autophagy (marked with an arrow) with vacuolization of the cytoplasm (Fig. 2 B-C).

In cancer cells KGN most of the cells were apoptotic cells (Fig.2 E-F).

In cancer cells OVCAR-3 and KGN with CAF supplemented medium Vit C in dose 10 mM increased amount of cells stained with trypan blue (Fig.2 B'-C; E'-F') in compared to the control (Fig.2 A', D').

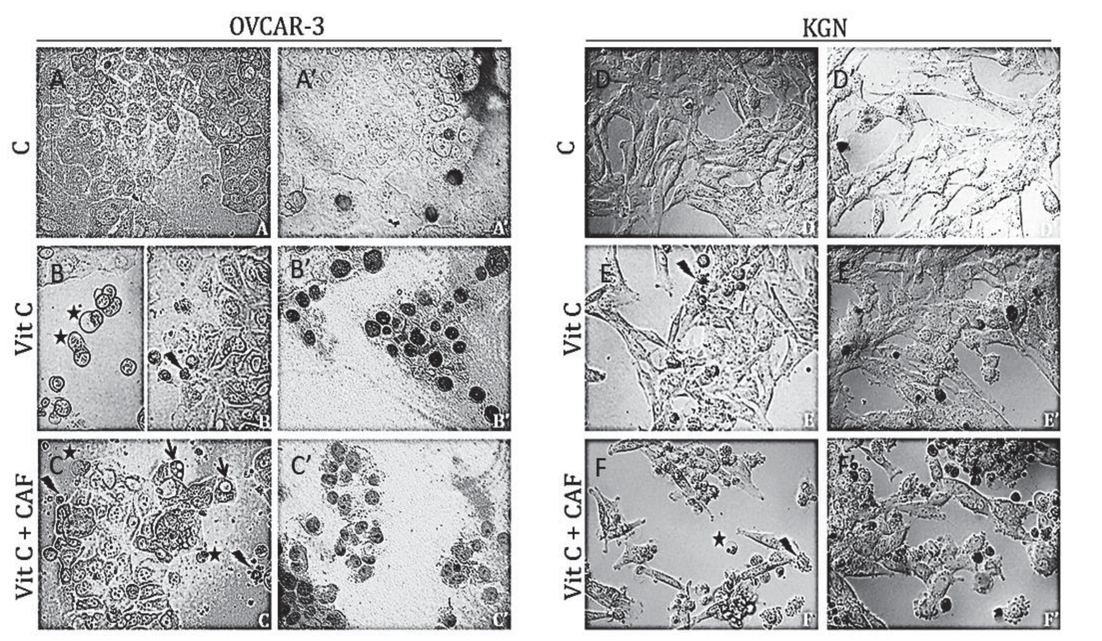

5. Action of Vit C on the expression of oncosis: *UCP-2, CYCS* and ATP level in two types of ovarian cancer cells.

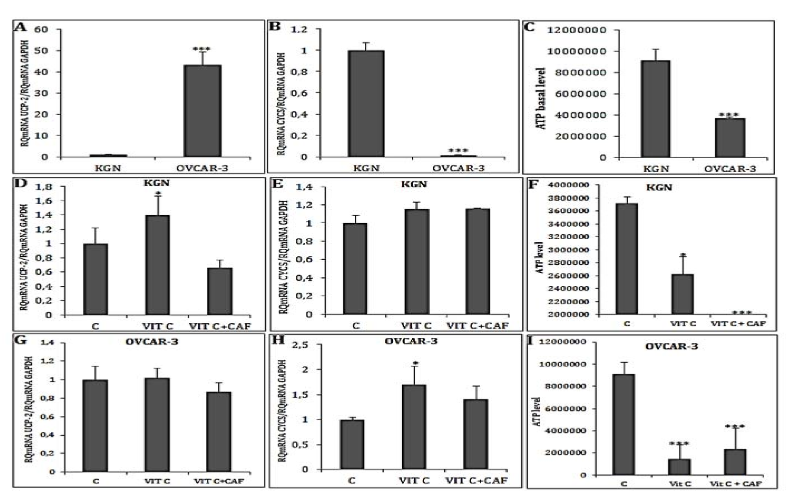

In OVCAR-3 cell line Vit C in dose 10 mM lead to overall increased *UCP-2* expression (Fig.5 A). Moreover, Vit C decreased *CYCS* expression (Fig.5 B). Cytochrome c has a crucial role in the intrinsic pathway of apoptosis. Also, Vit C decreased ATP level in comparision with KGN cell line (Fig. 5 C).

6. Action of Vit C on the expression of autophagy-dependent cell death : *ATG5, ATG7, BECN1* in two types of ovarian cancer cells.

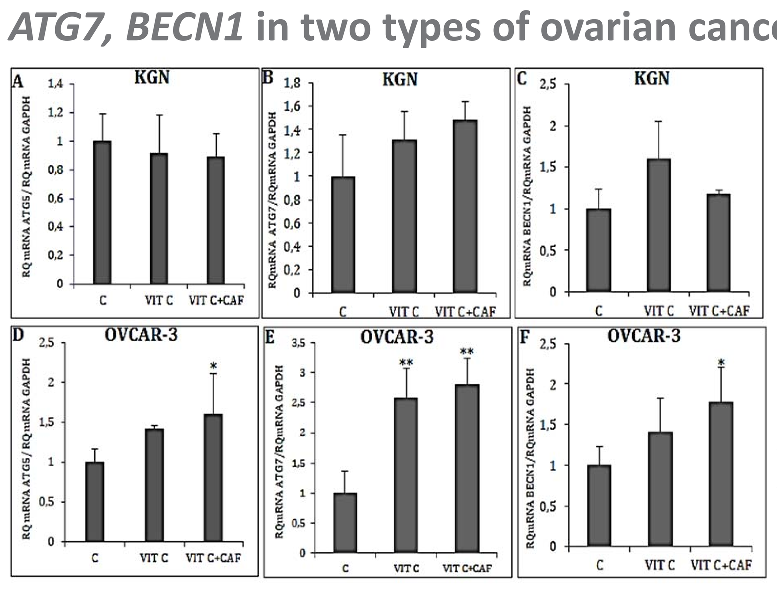

In KGN cells cultured in basal medium and CAF supplemented medium Vit C in dose 10 mM no effect on gene expression of autophagy-dependent cell death (Fig.6 A-C).

In OVCAR-3 cells cultured in basal medium and CAF supplemented medium Vit C in dose 10 mM increased *ATG7* expression (Fig. 6 E). Moreover, Vit C increased *ATG5* and *BECN1* expression in and CAF supplemented medium (Fig.6 D, F).

CONCLUSION

The results of the presented data will provide unique information about the molecular mechanism of cell death caused by vitamin C. Our research is the first to show different pathways of cell death in two types of ovarian cancer. The conducted research shows that the pathway of cell death is related to the type of the tumor.

Moreover, we checked that in the in vitro studies on cell lines it is necessary to take into account the participation of the tumor microenvironment and especially the cancer associated fibroblast.

The reduction of PARP expression also suggests the possible use of vitamin C as part of a combination therapy with PARP inhibitors. Most importantly, the administration of intravenous pharmacological doses of vitamin C may be considered as an adjunct to conventional therapy for ovarian cancer.

References

1. Gregoraszczuk E.L., Zajda K., Tekla J., Respekta N., Zdybał P., Such A. (2020), Vitamin C supplementation had no side effect in non-cancer, but had anticancer properties in ovarian cancer cells; International Journal of Vitamin and Nutrition Research 1–11
2. Blaszczyk W. i wsp. (2019), Vitamin C as a Modulator of the Response to Cancer Therapy; Molecules 24: 453
3. Subramanyam D. i wsp. (2018), Cancer Associated Fibroblasts: Naughty Neighbors That Drive Ovarian Cancer Progression; Cancers 10: 406
4. Ma Y., Chapman, J. i wsp. (2014), Cancer: High-dose parenteral Ascorbate enhanced chemosensitivity of ovarian cancer and reduced toxicity of chemotherapy; Science Translational Medicine 6

Sponsored partly by N18/DBS/000008

RELEASE OF INTERLEUKIN-6 IS DEPENDENT ON α2β1 INTEGRIN

Małgorzata Gałdyszyńska[1], Paulina Radwańska[1], Jacek Drobnik[1]
Department of Pathophysiology, Medical University of Lodz, Poland

INTRODUCTION

Cardiac fibroblasts constitute about 70% of cardiac cells and determine extracellular matrix metabolism. Moreover, cardiac fibroblast sense not only the biochemical stimuli but also the physical changes in the environment [1-3]. Cardiac fibrosis is a complex phenomenon, which is characterized by excessive synthesis and defective degradation of collagen, caused mainly by the action of activated cardiac fibroblasts. Accumulation of fibrous tissue increase rigidity of heart tissue [2, 3]. Cardiac fibrosis is typically accompanied by inflammation, which causes the secretion of pro-inflammatory cytokines, including interleukin-6 (IL-6) which binds to a receptor complex consisting of specific IL-6 binding protein (sIL-6R) and signal transducing molecule (gp130) [4-6]. IL-6 is well known to demonstrate profibrotic effects within the heart, however the final effect is strongly influenced by the duration of IL-6 elevation [6]. Chronic augmentation of IL-6 has been found to lead to cardiac hypertrophy and heart fibrosis[7].

AIM

The aim of the present study was to determine whether the stiffness of the environment of cardiac fibroblasts can influence the release of IL-6 and soluble IL-6 receptor (sIL-6). Moreover, it verify the role of integrin α2β1 activation and the kinases FAK and Src in regulation of cytokine release by fibroblasts.

METHODS

The research was conducted using stable cardiac fibroblast cell line, cultured on the polyacrylamide gels with different stiffness (soft gel E=2.23 ±0.8 kPa and stiff gel E=8.28 ±1.06 kPa), as well as on integrin α2β1 knockout animals (homozygous Itga2$^{tm1.1Tkun/tm1.1Tkun}$) and wild-type mice. Density of the α2β1 integrin was evaluated by flow cytometry and enzyme-linked immunosorbent assay. Level of mRNA of α2 integrin subunit was measured by qPCR. Concentrations of IL-6 and sIL-6R was measured by ELISA assay. Three inhibitors were used TCI-15 (α2β1 integrin inhibitor), AZM 475271 (Src kinase inhibitor) and FAK inhibitor 14 (FAK kinase inhibitor). To obtain the cells with low density of α2β1 integrin the expression of α2 integrin subunit was blocked by siRNA.

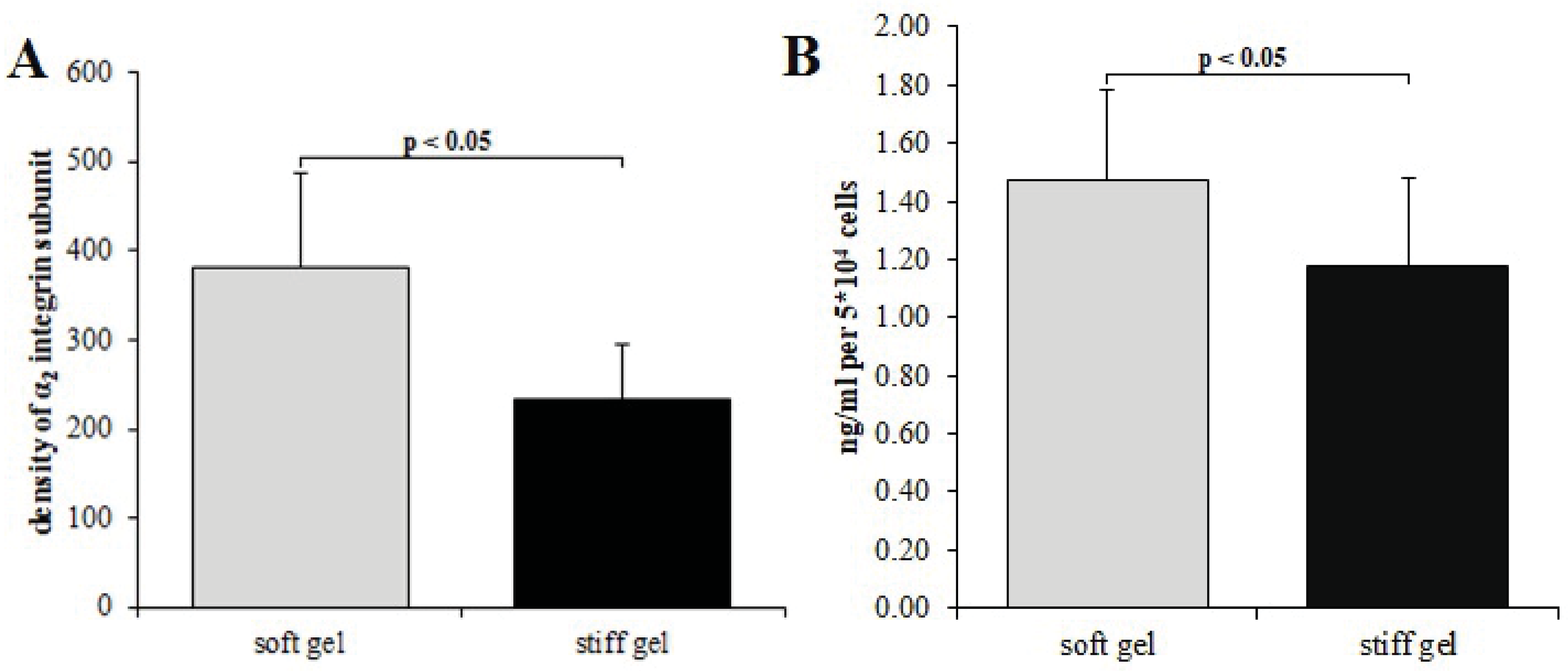

Figure 1. Density of α2 integrin subunit (A) and relative expression of ITGA2 gene (B) in cardiac fibroblasts cultured on soft and stiff gels. Each value represents a mean ± SD.

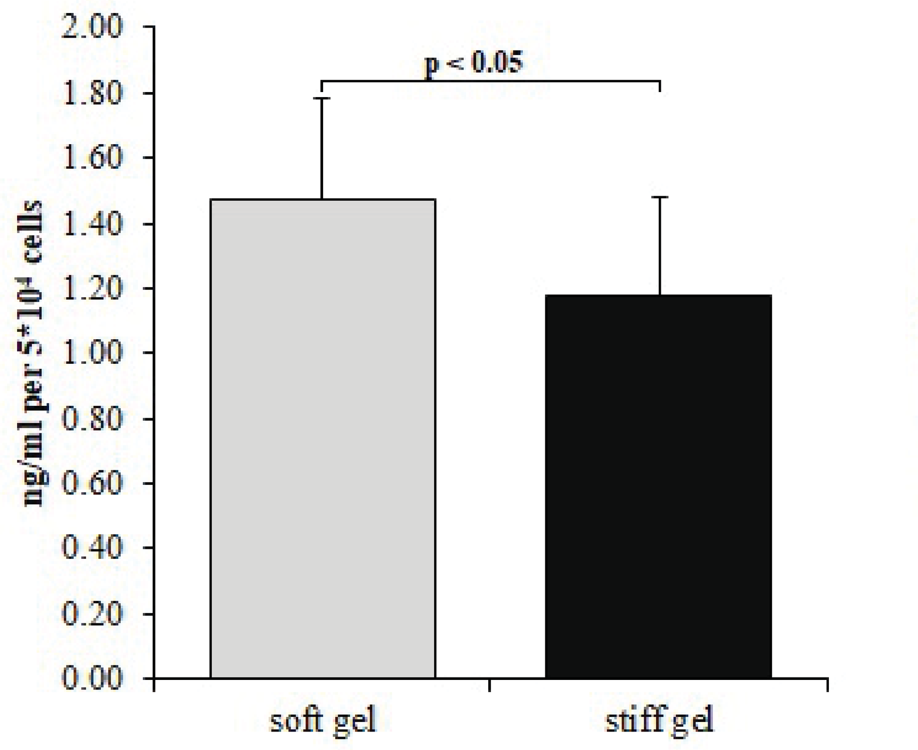

Figure 2. Content of IL-6 within cardiac fibroblast media cultured on soft and stiff gels after 96 hours. Each value represents a mean ± SD.

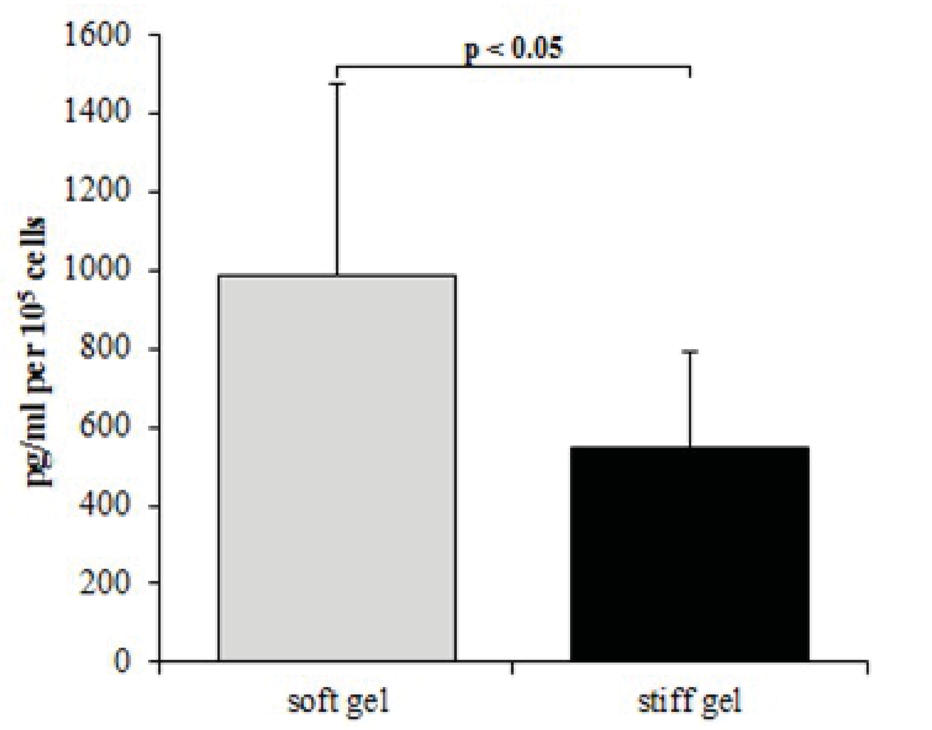

Figure 3. Content of integrin α2β1 in cardiac fibroblasts cultured on soft and stiff gels. Each value represents a mean ± SD.

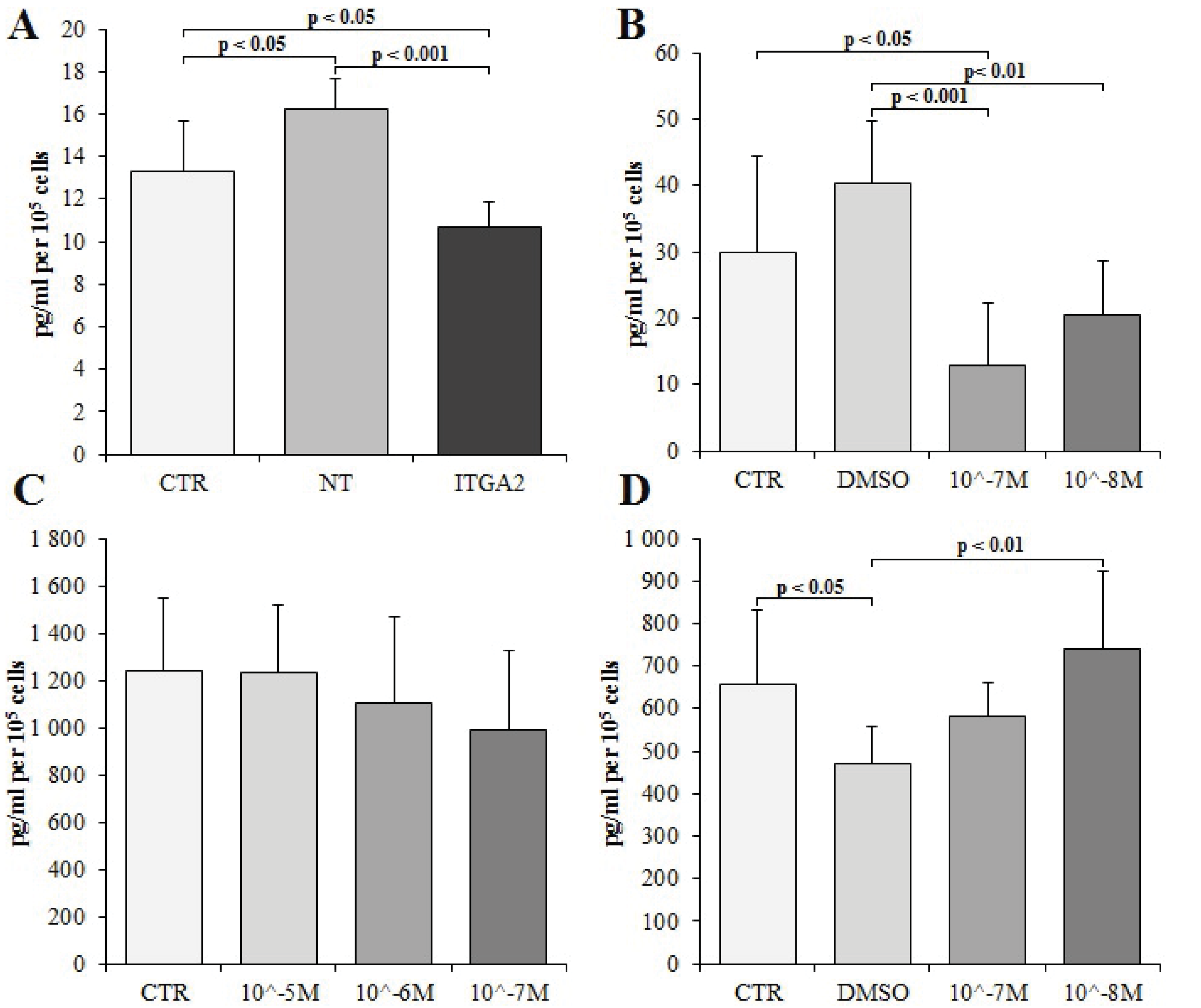

Figure 4. Level of IL-6 (A) in cardiac fibroblast after silencing of α2 integrin (ITGA2), in cells treated with non-targeting siRNA (NT) and untreated control (CTR). Effect (B) of TC-I 15 (α2β1 integrin inhibitor) applied at concentrations of 10-7 M (10^-7M) and 10-8 M (10^-8M), DMSO (TC-I15 solvent) and untreated control (CTR) on the IL-6 level in cardiac fibroblasts culture. Effect (C) of FAK 14 inhibitor (FAK kinase inhibitor) applied at concentrations of 10-5 M (10^-5M), 10-6 M (10^-6M), 10-7 M (10^-7M), and untreated control (CTR) on the IL-6 level in cardiac fibroblast culture. Effect (D) of AZM 475271 (Src kinase inhibitor) applied at concentrations of 10-7 M (10^-7M) and 10-8 M (10^-8M), DMSO (AZM 475271 solvent) and untreated control (CTR) on the IL-6 level in cardiac fibroblasts culture. Each value represents a mean ± SD.

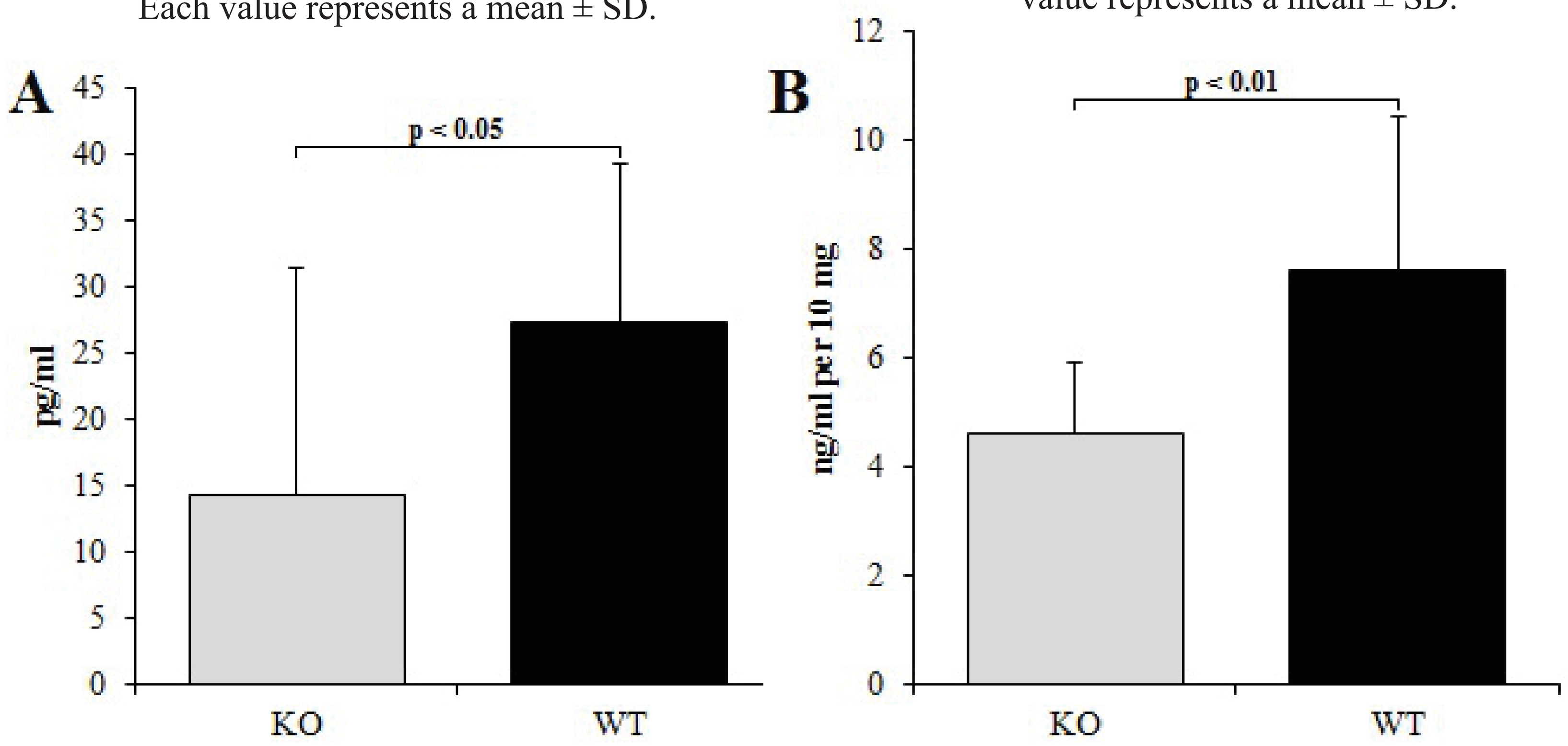

Figure 6. Content of IL-6 in serum (A) and heart (B) of α2 integrin deficient mice (KO) and wild type animals (WT). Each value represents a mean ± SD.

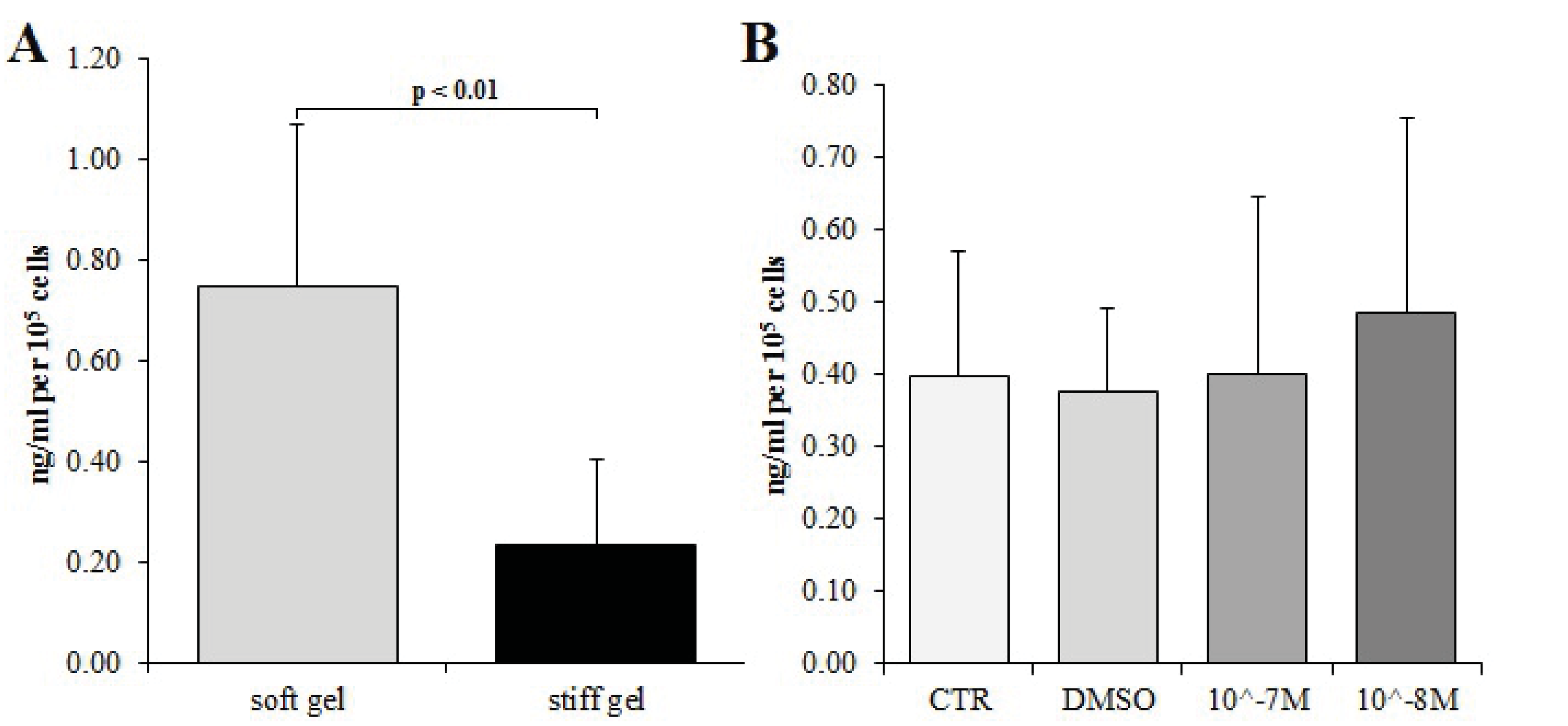

Figure 5. Content of sIL-6R in cardiac fibroblast media cultured on soft and stiff gels (A). Effect of TC-I 15 (α2β1 integrin inhibitor) applied at concentrations of 10-7 M (10^-7M) and 10-8 M (10^-8M), DMSO (TC-I15 solvent) and untreated control (CTR) on the sIL-6R level in cardiac fibroblast culture (B). Each value represents a mean ± SD.

CONCLUSION

The elevation of integrin α2β1 expression in cells cultured on soft substrate corresponds with increased levels of IL-6 in medium. Furthermore, our data suggests that integrin α2β1 exerts a regulatory effect on IL-6 release by cardiac fibroblasts. The signal is transmitted by Src kinase. The level of sIL-6R is not dependent on α2β1 integrin. All in all, integrin α2β1 could be considered as a target for anti-inflammatory therapy associated with heart conditions.

REFERENCES

1. Meléndez GC, McLarty JL, Levick SP, Du Y, Janicki JS, Brower GL Interleukin 6 mediates myocardial fibrosis, concentric hypertrophy, and diastolic dysfunction in rats Hypertension . 2010 Aug;56(2):225-31. doi: 10.1161/HYPERTENSIONAHA.109.148635.
2. Frangogiannis NG. Cardiac fibrosis: Cell biological mechanisms, molecular pathways and therapeutic opportunities. Mol Aspects Med. 2019 Feb;65:70-99. doi: 10.1016/j.mam.2018.07.001.
3. Kong P, Christia P, Frangogiannis NG. The pathogenesis of cardiac fibrosis. Cell Mol Life Sci. 2014 Feb;71(4):549-74. doi: 10.1007/s00018-013-1349-6.
4. Francis Stuart SD, De Jesus NM, Lindsey ML, Ripplinger CM. The crossroads of inflammation, fibrosis, and arrhythmia following myocardial infarction. J Mol Cell Cardiol. Feb 2016;91:114–22.
5. Mack M. Inflammation and fibrosis. Matrix Biol J Int Soc Matrix Biol. 2018;68–69:106–21.
6. Schaper F, Rose-John S. Interleukin-6: Biology, signaling and strategies of blockade. Cytokine Growth Factor Rev. Oct 2015;26(5):475–87.
7. González GE, Rhaleb N-E, D'Ambrosio MA, et al. Deletion of interleukin-6 prevents cardiac inflammation, fibrosis and dysfunction without affecting blood pressure in angiotensin II-high salt-induced hypertension. *J Hypertens*. Jan 2015;33(1):144–52.

The study was supported by the National Science Center Poland grant no. UMO-2015/17/B/NZ5/01382

WARSZAWSKI UNIWERSYTET MEDYCZNY
MEDICAL UNIVERSITY OF WARSAW
Zakład Medycyny Regeneracyjnej

CENTRUM BADAŃ PRZEDKLINICZNYCH
WARSZAWSKIEGO UNIWERSYTETU MEDYCZNEGO

The assessment of the proliferative potential of bronchoalveolar stem cells and alveolar type 2 cells isolated at various stages of bleomycin-induced lung injury

A.K. CIECHANOWICZ[1] , E. SUCHOCKI[1], S. LESZCZAK[1], W.X. LAY[1], J. PRADO PAULINO[1], C. LESZCZAK[1], M. KUCIA[1, 2] AND D.S. KRAUSE[3]

[1]Department of Regenerative Medicine, Center for Preclinical Research and Technology, Medical University of Warsaw, Warsaw, Poland; [2]Stem Cell Institute at James Graham Brown Cancer Center, University of Louisville, Louisville, KY, USA; [3]Departments of Laboratory Medicine, Cell Biology and Pathology and the Yale Stem Cell Center, Yale University School of Medicine, New Haven, USA; andrzej.ciechanowicz@wum.edu.pl

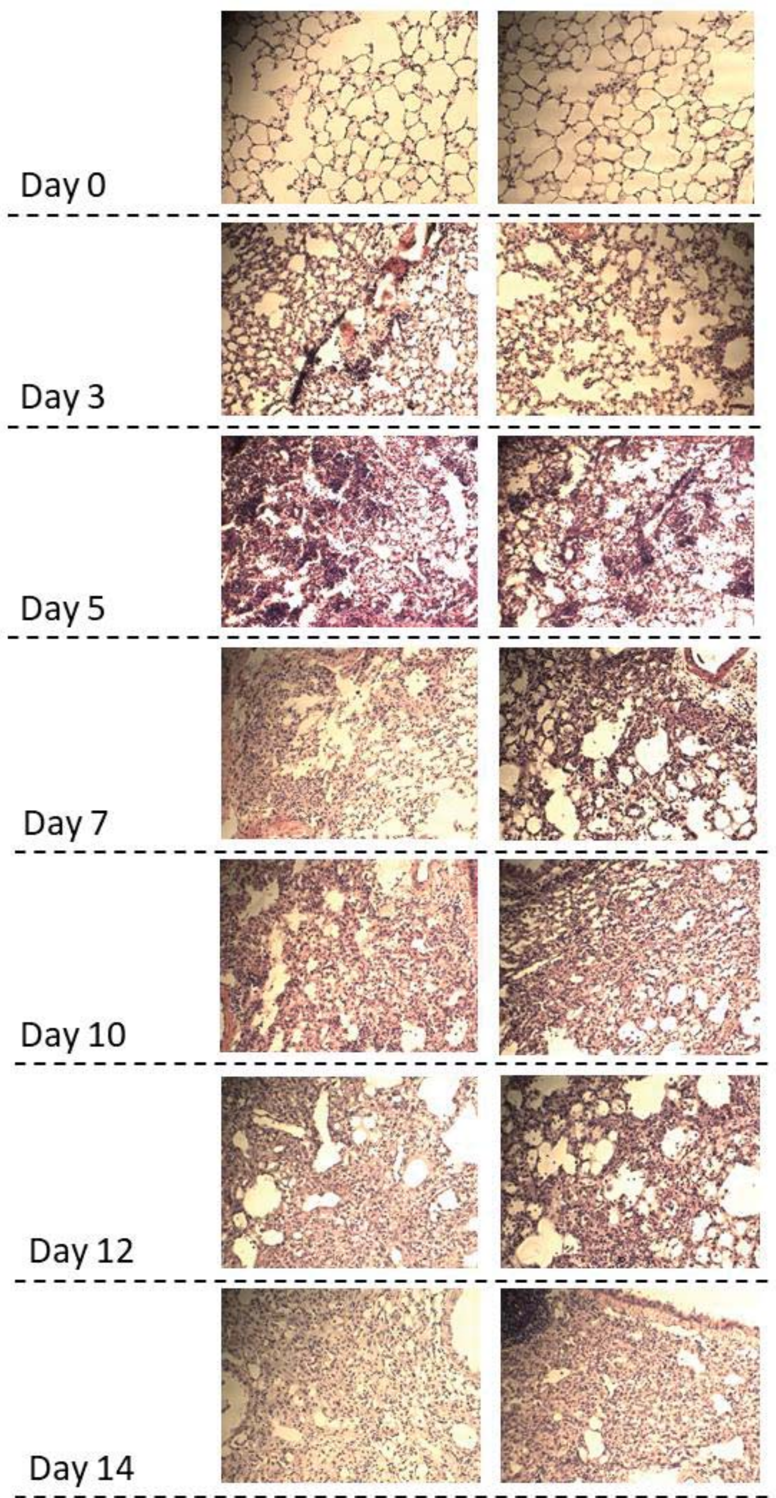

Figure 1. Representative lung tissue sections (stained H&E) after bleomycin-induced injury at various time points.

Introduction

The aim of the experiment is to assess the physiological ability of type II pneumocytes (AT2) and bronchopulmonary stem cells (BASCs) to proliferate and self-renew in response to bleomycin-induced lung damage. To achieve the intended goal, we isolated AT2 and BASC cells from lungs derived from C57BL/6J mice (experimental group exposed to lung injury, control group with healthy lungs, no injury). The isolated cells were cultured for organoid growth for 21 days followed by flow cytometric analysis.

The studies address gaps in our knowledge of lung repair and regeneration under pathological conditions. AT2 and BASC are rare subpopulations of lung cells that are directly responsible for the regeneration of small airways and alveoli. AT2 cells and BASCs are vulnerable to damage, which is the reason for slow and often inadequate lung regeneration. Therefore, it is necessary to develop an effective methodology for their isolation from damaged lungs, multiplication and their in vitro differentiation, and then implantation into the damaged organ.

The experiment assumes that both AT2 and BASCs isolated from damaged lungs at various stages of this lesion will differ in their activity, which will result in an increased number of organoids grown in the experimental group during active repair. These organoids should have a higher number of cells than in the control group. The material will be collected at multiple time points counted from the day the bleomycin is administered (i.e. on days 3, 5, 7, 10, 12 and 14), as well as the control group (i.e. on day 0).

Progressive lung damage may affect the proliferative potential and differentiation of lung stem cells in various ways. Determination of the stage of lung injury, in which the lung stem cells have the highest potential for differentiation and proliferation, can directly contribute to the development of the method of in vitro reproduction of pulmonary stem cells for later transplantation into the lungs for repair.

Materials and Methods

Studies were conducted on healthy 6-8 week old C57BL/6J mice. Placed for 2 minutes in a ventilated chamber, the animals inhaled anesthetic: isoflurane (5% in ambient air), and bleomycin (2.5 mg per kg. b. w.) suspended in 50 μl of saline was administrated intratracheally. Then, the mice were placed in a cage. On 3, 5, 7, 10, 12 and 14 days after bleomycin administration, the animals, after intraperitoneal anesthesia in the form of xylazine and ketamine, were sacrificed by cervical dislocation.

After they were sacrificed, mice underwent thoracotomy and right ventricular perfusion. The left lung lobe was tied off and processed for paraffin embedding. For analysis of paraffin embedded sections, the central parenchyma of the left lung lobe was analyzed in each animal from each time point. The part of right lobe was collected for Western blotting analysis and the remaining lung tissue was infused with Collagenase IV in DMEM followed by 1% low melting agarose. After cooling the agarose, the lung was digested and dissociated on a GentleMACS tissue dissociator. Then AT2 (CD31 negative, CD45 negative, Ep-CAM positive, Sca-1 negative) and BASCs (CD31 negative, CD45 negative, Ep-CAM positive, Sca-1 positive) were FACS sorted.

Sorted BASCs and AT2 cells were used for organoid assays according to previously described protocols (McQualter et al. 2010 and Teisanu et al. 2011) and revised by Joo-Hyeon Lee et al. (2014). Organoids were established from the same ammount of plated sorted cells (3 000 AT2 cells or 3 000 BASCs) and 100 000 MLG cells. Organoids were cultured for 21 days in 3D matrigel medium. Then, organoids were stained and analyzed with the use of flow cytometry.

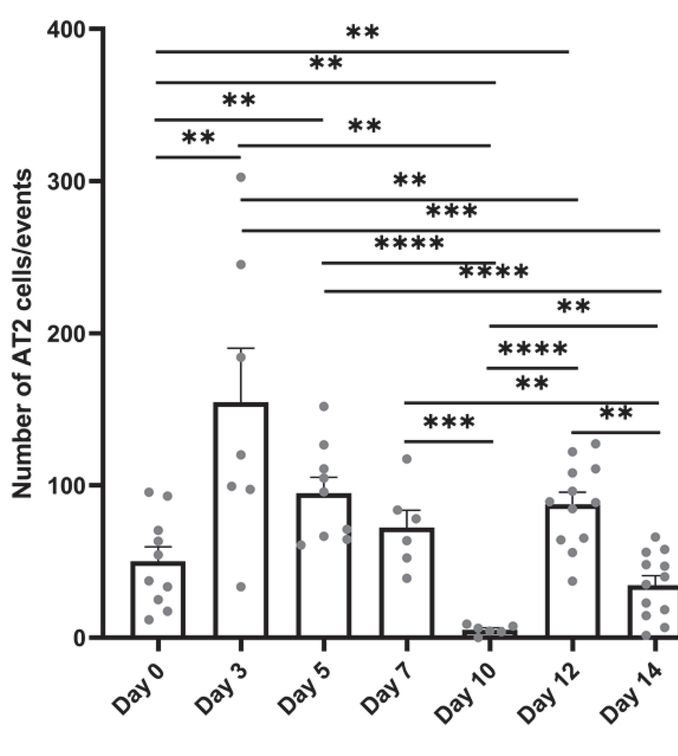

Figure 3. The quantification of type II pneumocytes obtained in culture of organoids established from isolated type II pneumocytes at various time points. Cells were identified using flow cytometry.

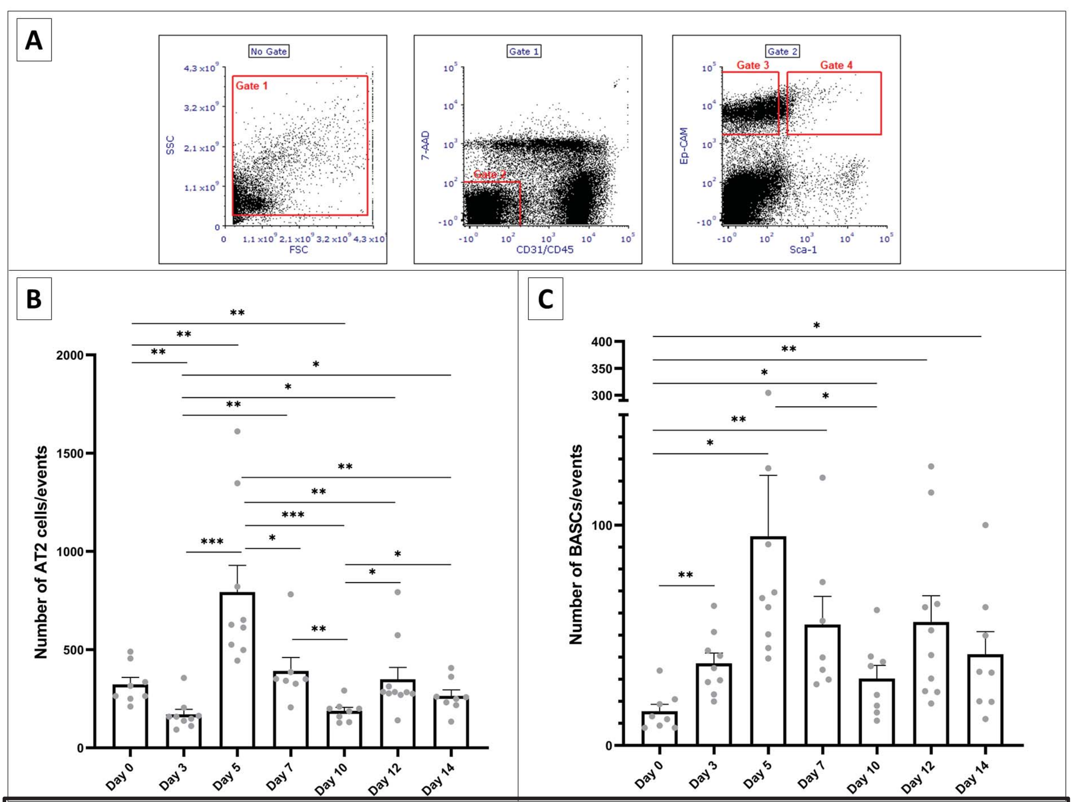

Figure 2. A) Gating strategy of FACS sorting and flow cytometry analysis; B) The quantification of type II pneumocytes present in murine lung at various time points. AT2 quantification has been carried out with the use of FACS. C) The quantification of BASCs present in murine lung at various time points. BASCs quantification has been carried out with the use of FACS.

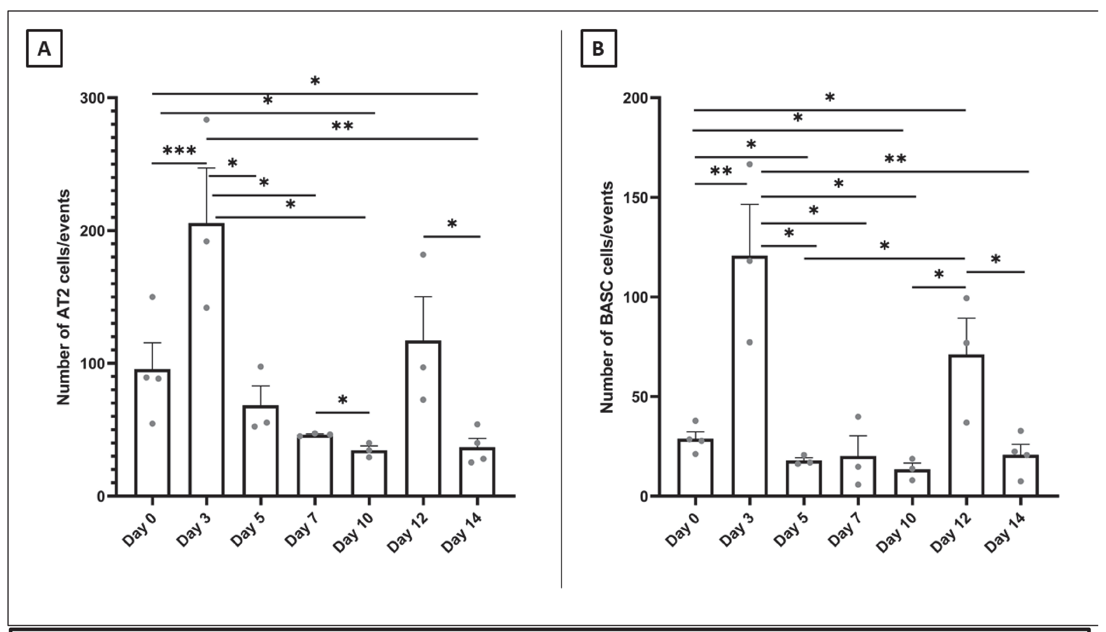

Figure 4. A) The quantification of Alveolar Type 2 cells obtained in culture of organoids established from isolated BASCs at various time points. Cells were identified using flow cytometry; B) The quantification of BASCs obtained in culture of organoids established from isolated BASCs at various time points. Cells were identified using flow cytometry;

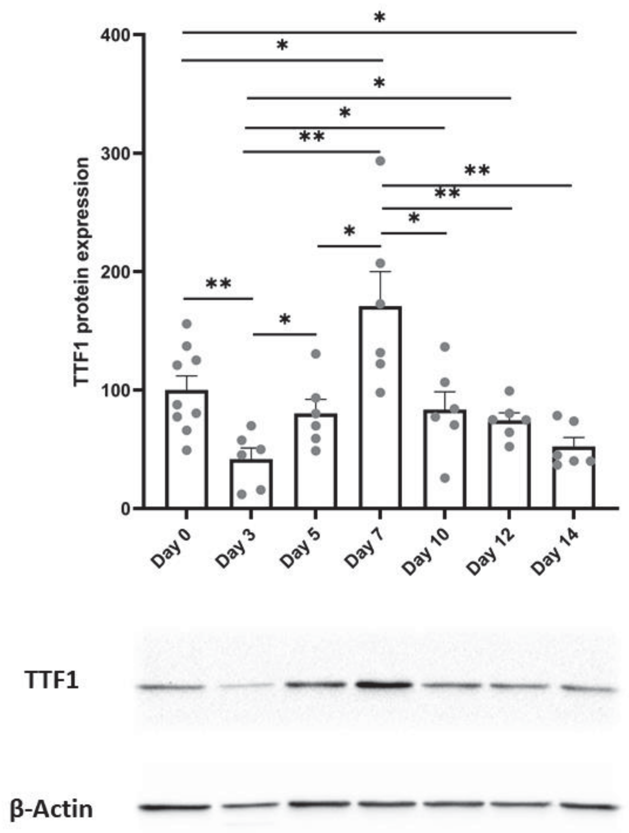

Figure 5. Upper panel: The graph shows the differences in TTF1 protein expression in the total lung tissue lysate at various stages of bleomycin-induced organ damage; Lower panel: Western blot visualisation of TTF1 protein expression in whole murine lung tissue lysate at various time points. The optical density of TTF1 protein has been normalized to β-Aktin;

Results and Discussion

FACS analysis showed a significant increase on the 5th day of the amount of AT2 and BASCs sorted . This indicates that cells up to day 4 from bleomycin-induced lung injury have the highest proliferative potential. To confirm this hypothesis, organoid cultures were established (from each collection point and from each cell type - AT2 and BASCs).

The organoid culture was carried out for 21 days with the 3D change of the medium every other day. After this time, the matrigel in which the organoids grew was harvested, and then the cells were recovered from the gel and then stained for subsequent cytometric analysis. Flow cytometric analysis confirmed the hypothesis that AT2 cells and BASCs isolated on the third day from bleomycin-induced damaged lung were characterized by the highest proliferative potential. In addition, it was decided to confirm these results by TTF1 protein expression (characteristic type II pneumocytes) and pro-SPC (characteristic AT2 and BASCs) in lung tissue collected at each time point.

Western blot analysis showed an increase in expression of TTF1 and pro-SPC proteins in group from day 7. The literature states that the newly formed AT2 and BASC cells begin to present characteristic TTF1 and pro-SPC proteins only from 2-3 days. That is why the increase in the expression of these proteins (in lung tissue) about 2 days after the observed increase in the number of AT2 cells and BASC on the 5th day, confirms the assumed hypothesis.

Conclusion

- Bleomycin-induced lung injury do influence on proliferative and self-renawal potential of type II pneumocytes and bronchoalveolar stem cells
- AT2 cells and BASCs in the first phase of lung injury present the highest proliferative potential and self-renewal ability.

This work was supported by the Harmonia NCN grant UMO-2014/14/M/NZ3/00475 and Miniatura NCN grant 2017/01/X/NZ3/00250.

miR-138-5p AS A PREDICTIVE FACTOR OF SEVERE ORAL MUCOSITIS IN PATIENTS WITH HEAD AND NECK CANCER UNDERGOING INTENSITY-MODULATED RADIATION THERAPY.

Radosław Mlak[1], Iwona Homa-Mlak[1],Tomasz Powrózek[1], Marcin Mazurek[1], Anna Brzozowska[2], Teresa Małecka-Massalska[1]

1Department of Human Physiology, Medical University of Lublin, Poland;

2II Department of Radiotherapy, Center of Oncology of the Lublin Region St. John of Dukla, Poland

Introduction

- Globally, the incidence of head and neck cancers (HNCs) is on the 6th location across all malignant neoplasms.[1]
- Radiotherapy (RT), widely used in the treatment of HNCs, causes numerous troublesome side effects. The most common and most serious complication of RT is oral mucositis (OM). Severe OM (grade ≥3) often forces the reduction of radiation doses or leads to treatment discontinuation, which significantly reduces its effectiveness. [2]
- Despite, that the introduction of the intensity-modulated radiation therapy (IMRT) technique led to the significant reduction of radiation reactions, most patients still develop OM.
- Interestingly, it was observed, that even patients receiving the same dose of radiation may develop various degrees of OM severity (probably due to patient variability at the molecular level).[4]
- miR-138 belongs to the group of small, non-coding RNAs responsible for the regulation of many different genes (Figure 1), including this involved in DNA repair mechanisms (e.g. ERCC1, ERCC2, PARP2). [5,6]

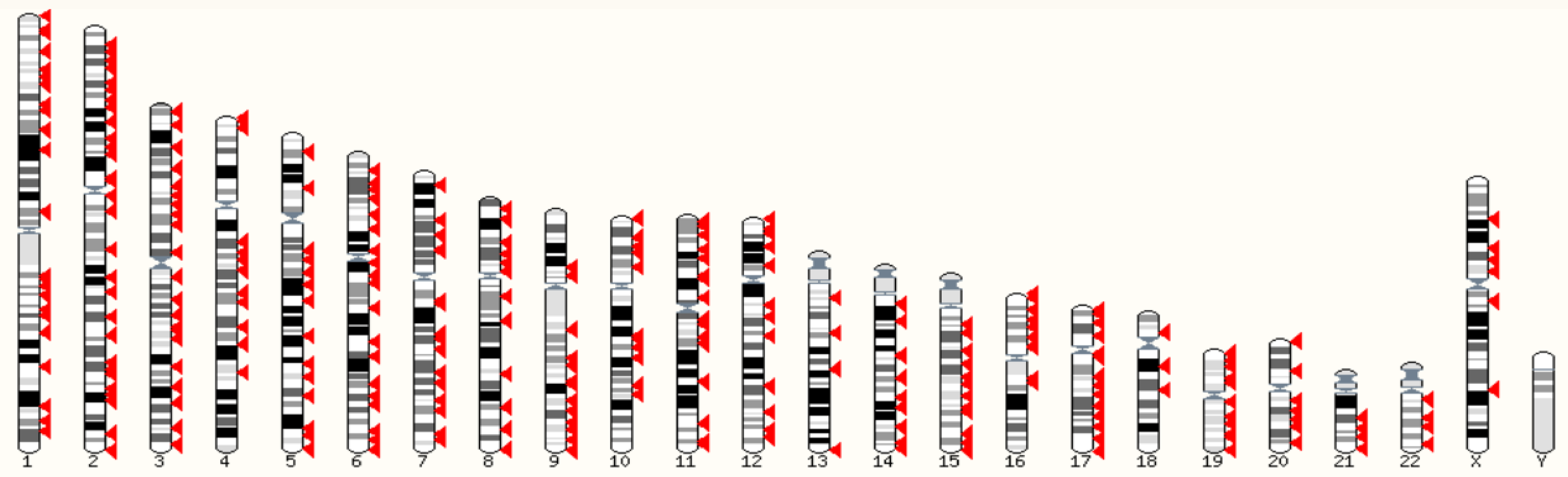

Figure 1. Locations of genes potentially regulated by miR-138-5p.[5]

Objectives

The aim of the study was to assess the relationship between pretreatment expression of the miR-138-5p and the occurrence of severe oral mucositis in patients with HNC subjected to IMRT.

Methods

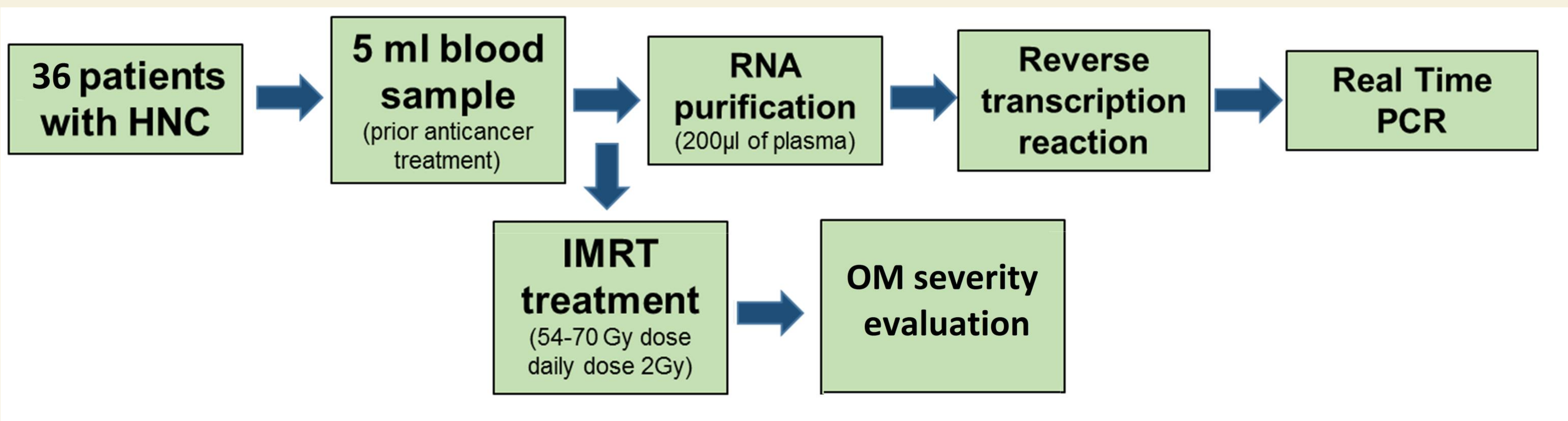

Figure 2. Flow chart of study design.

The level of miRNA 138-5p expression (Real Time PCR) was normalized by miRNA 26a-3p control reaction using 2-ΔΔCt and 2-ΔCt formulas. The MedCalc 15.8 software (MedCalc Software, Belgium) was used to perform statistical analysis of the results. In all analyses, statistical significance was established at p<0.05. Study design was presented in Figure 2.

Results

Characteristic of study group:

- The study group was dominated by men (86%).
- The median age of the patients was 63 years.
- According to the 7th edition of TNM, the dominant features were: T3 (53%), N + (67%) and M0 (100%).

Role of miR-138-5p expression as a predictive factor of more severe OM:

- We noted, that patients with severe OM (> grade 3) after 4, 5, 6, and 7 weeks of RT had significantly higher levels of pre-treatment expression of miR-138-5p.
- Pre-treatment miR-138-5p expression demonstrated to have a significant predictive value for weeks 4th to 7th of OM evaluation.
- The sensitivity and specificity of this biomarker were, respectively, in the 4th week: 100% and 86% (p<0.0001), in the 5th week: 86% and 79% (p=0.0012), in the 6th week: 100% and 86% (p<0,0001) and in the 7th week: 83% and 92% (p<0.0001) (Figure 3).

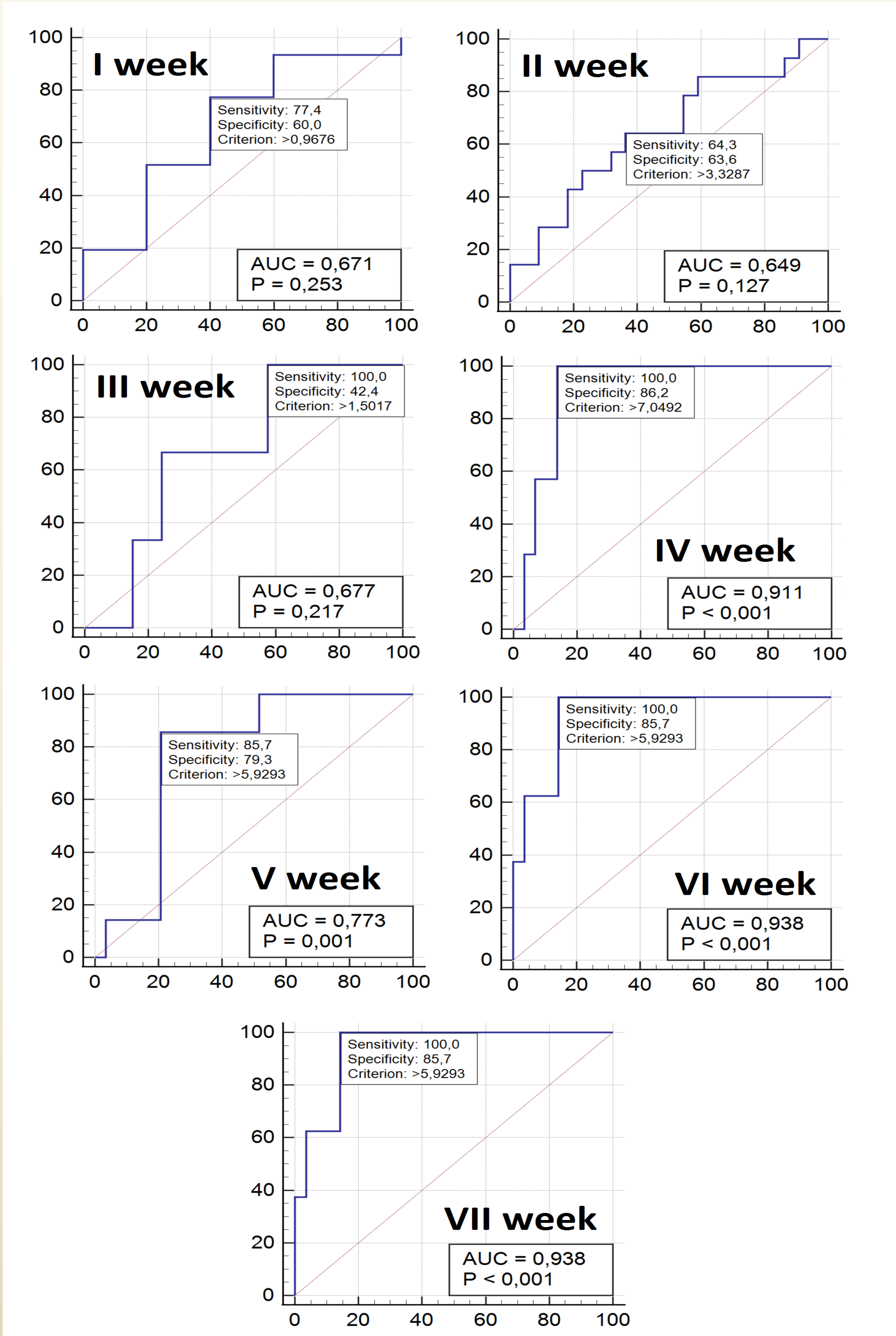

Figure 3. The assessment of miR-138-5p expression in predicting the occurrence of more severe OM in following weeks of IMRT using ROC analysis.

Conclusions

Pretreatment miR-138-5p expression is a promising biomarker, that may serve as a useful tool in the prediction of more severe OM in patients with HNCs undergoing IMRT

References

[1] Aupérin A. Epidemiology of head and neck cancers: An update. Curr Opin Oncol. 2020;32(3):178–86.
[2] Al-Mamgani, A.; Van Rooij, P.; Verduijn, G.M. The impact of treatment modality and radiation technique on outcomes and toxicity of patients with locally advanced oropharyngeal cancer. Laryngosc. 2013.
[3] Maria OM, Eliopoulos N, Muanza T. Radiation-Induced Oral Mucositis. Front Oncol. 2017;7(MAY).
[4] Yang DW, Wang TM, Zhang JB, Li XZ, He YQ, Xiao R, i wsp. Genome-wide association study identifies genetic susceptibility loci and pathways of radiation-induced acute oral mucositis. J Transl Med. 2020;18(1):1–1.
[5] Ensembl genome browser [Internet]. https://www.ensembl.org
[6] Wang Y, Huang JW, Li M, Cavenee WK, Mitchell PS, Zhou X, i wsp. MicroRNA-138 modulates DNA damage response by repressing histone H2AX expression. Mol Cancer Res. 2011;9(8):1100–11

XXVIII Congress of the Polish Physiological Society

Gdańsk, September 15-17 2021

Poster book

SESSION X

AGING

HONORARY PATRONAGE

Prof. dr Marcin Gruchała
Rector of the Medical University of Gdansk

Uniwersytet Gdański

Prof. dr Piotr Stepnowski
Rector of the University of Gdansk

WOJEWODA POMORSKI
DARIUSZ DRELICH

Dariusz Drelich
Governor of the Pomeranian Voivodeship

HONORARY PATRONAGE
Mayor of the City of Gdańsk

Aleksandra Dulkiewicz
Mayor of Gdansk

Mieczysław Struk
Marshal of the Pomeranian Voivodeship

PARTNER

PAN
POLSKA AKADEMIA NAUK

ANIMA LAB
animal facility and laboratory equipment • animal research models

FUNDACJA LOTOS

Medical University of Gdansk
Department of Physiology

S10.P1

ELASTASES IN THE DEVELOPMENT OF CHRONIC INFLAMMATION WITH AGE

S10.P1

L.M. SAMOKHINA1, V.V. LOMAKO2

1 GD "National Institute of Therapy of L.T. Malaya name of National Academy of Medical Sciences of Ukraine", Laboratory of Immuno-biochemical and Molecular Genetic Studies; Lyubov Malaya ave., 2a, Kharkiv, Ukraine, 61039; 2 Institute for Problems of Cryobiology and Cryomedicine of National Academy of Sciences of Ukraine, Department of Cryophysiology; st. Pereyaslavskaya, 23,Kharkiv, Ukraine, 61016.

Introduction

•Aging in most people is accompanied by the development of chronic inflammation, and this condition is a strong risk factor for appearance of multiple organ pathology, physical and cognitive impairment, and also leads to death. The mechanisms underlying of the inflammation regulation are not well understood [1]. It is known that certain environmental factors lead to the occurrence of oxidative stress and inflammation. Both are major factors in cellular aging, due to the release of inflammatory molecules, reactive oxygen species, and extracellular matrix components [2]. The development of inflammation is associated with the functioning of proteases. Neutrophil elastase causes inflammation mediated by the participation of the protease-activated receptor-2 and can destroy the components of the extracellular matrix. The elastase activity of human neutrophils leads to tissue destruction at various inflammatory diseases [3]. The neutrophil elastase is a serine elastase (EC 3.4.21.37) [4]. Endothelial cells are also capable of synthesizing elastase (endothelial elastase (EEl), cysteine or thiol elastase (EC 3.4.22)) and macrophages synthesize elastase (metalloelastase (MEl) or matrix metalloprotease 12) (EC 3.4.24.65)).

•The serum of human adults, compared with children, has a higher level of the total elastase activity (El) and a lower elastase inhibitory activity of α-1-proteinase inhibitor (EIA α-1-PI) [5]. In 6-months-old male rats, compared with 3-months-old, the EEl activity in the lungs, heart, and liver increases, that are caused by the influence of stress factors [6].

•**The aim of this work** was study of the El, EEl and MEl activity as well as EIA α-1-PI in the tissues of male rats of different ages.

Methods

•***Experiments on animals.*** The work was performed on white outbred rats (*Rattus norvegicus*) of different age (3-, 6-, and 24-months-old), obtained by the herd random breeding system, which were kept in a vivarium under natural light conditions on a standard diet *ad libitum* (n = 6 in each group). All animal experiments comply with the ARRIVE guidelines and was carried out in accordance with EU Directive 2010/63/EU for animal experiments.

•Tissue fragments were obtained after decapitation of animals. The liver perfusion was performed with cooled 0.15 M NaCl solution. The tissue samples of BC, lung, heart, liver and kidneys (300 mg) were washed with cooled physiological solution and homogenized in 3 ml Na-phosphate buffer pH 7.4 with cold, then centrifuged for 10 min at 5000g with PC-6 centrifuge (Dastan, Kazakhstan) at 4˚ C. They were stored at –20˚ C prior to analysis.

•***Determination of elastases activity and elastase inhibitory activity of alpha-1-proteinase inhibitor.*** The activity of elastases and EIA α-1-PI in nuclear-free fractions of the mentioned tissues was studied with highly sensitive enzyme method [3, 4]. On the measurements for optical density of the control samples there were calculated the activity of elastases and EIA α-1-PI in the investigated assays in U/ml with taking into account the protein concentrations in the samples, in U/mg protein. Protein concentration was found by Bradford method.

•***Reagents and equipment.*** In the work there were used horseradish peroxidase, elastase, phenylsulfonyl fluoride, monoiodacetate (ICN, USA), Ala-Ala (Fluka, Germany), ethylenediaminetetraacetate, bovine serum albumin (Russia), polystyrol stripplates (KIMA, Italy) and immune-enzyme photometer-analyser Humanreader 2106-1709 (Human, Germany).

•***Statistical analysis.*** The data were statistically processed with Student's t-test using Excel software 2003 (Microsoft, USA, 11.8412.8405 SP3).

Results

•The elastases activity changes in rats were tissue-specific. The El activity differed from EEl and MEl ones, which may indicate a significant contribution of serine elastase of neutrophilic origin to the manifestation of elastases total activity.

•The El activity increased in 6-months-old rats compared with 3 months of age in BC and decreased in ones in tissues of the lungs, heart, kidneys (p<0,001) (Fig. 1). The El activity in 24-month-old decreased compared with 6-months-old in BC, heart and liver and increased in kidneys as well as decreased in lungs, heart and liver and it increased in BC (p<0,01) and kidneys (p<0,001) compared with 3-months-old.

•The EEl activity in 6-months-old rats was higher compared with 3-months-old, in BC 3-months-old – no measurements, but in 24-months-old it decreased in BC, liver and kidneys compared with 6-months-old, in lung and heart 24-months-old – no measurements, and in the liver it was even lower than 3-months-old rats (Fig. 2).

•The activity of MEl was shown only in both 6- and 24-months-old animals and the differences are less pronounced in comparison with the El and EEl ones: it was significantly higher in BC (p<0,01) and lower in lungs (p<0,001) in 24-months-old rats compared with 6-months-old (Fig. 3).

•The EIA of α-1-PI increased significantly in 6-months-old rats compared with 3-months-old (p<0,01 in liver, p<0,001 in lungs, heart, kidneys), in BC 3-months-old – no measurements (Fig. 4). And in 24-months-old EIA of α-1-PI decreased compared with 6-months-old in all tissues as well as increased in the heart and decreased in liver compared with 3-months-old.

Importing Tables & Graphs

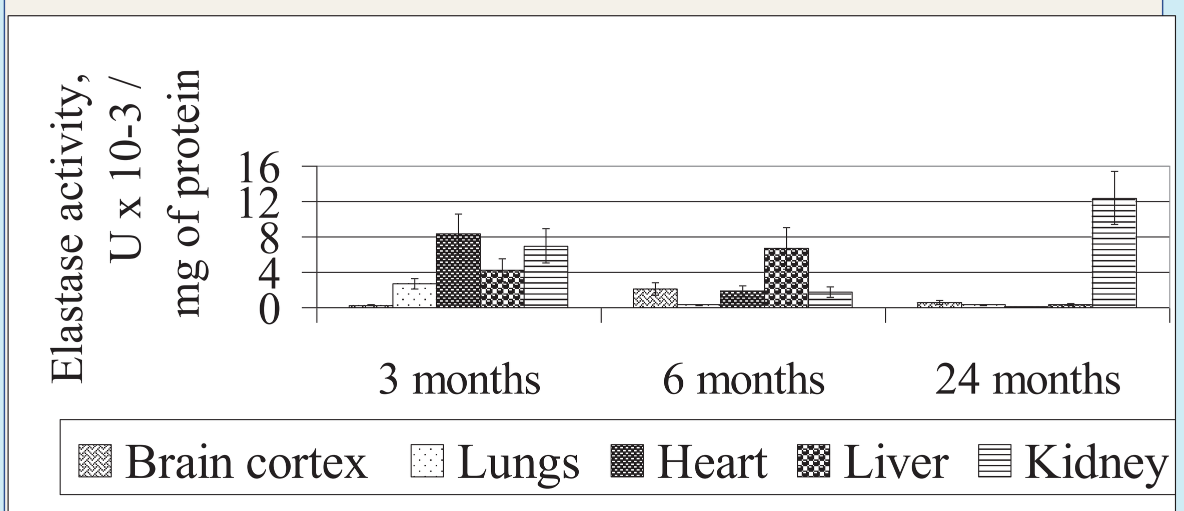

Fig.1 - Elastase activity in male rats

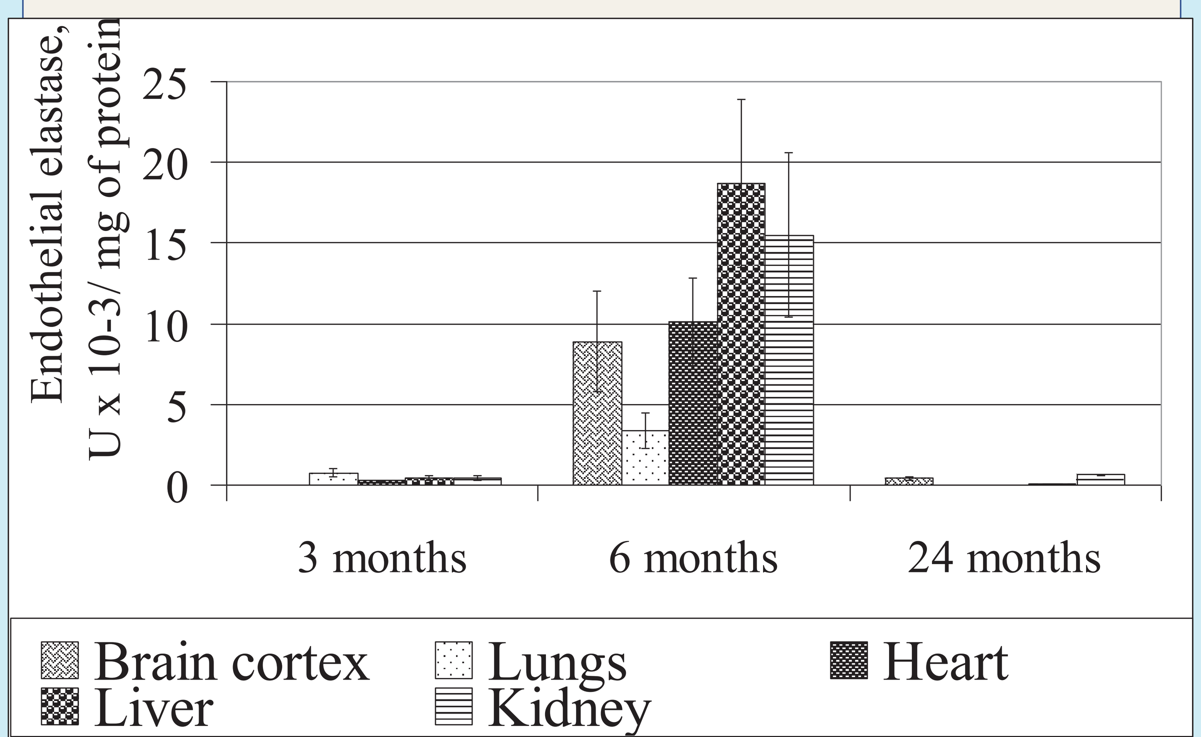

Fig.2 - Endothelial elastase activity in male rats

Importing Tables & Graphs

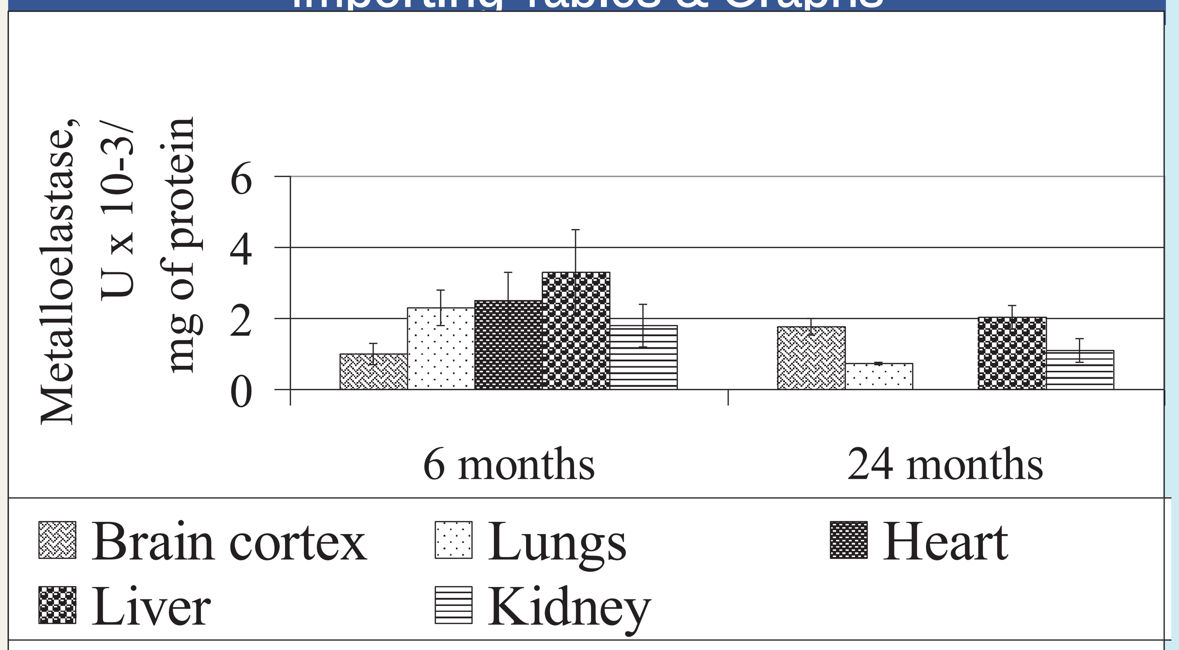

Fig.3 - Metalloelastase activity in male rats

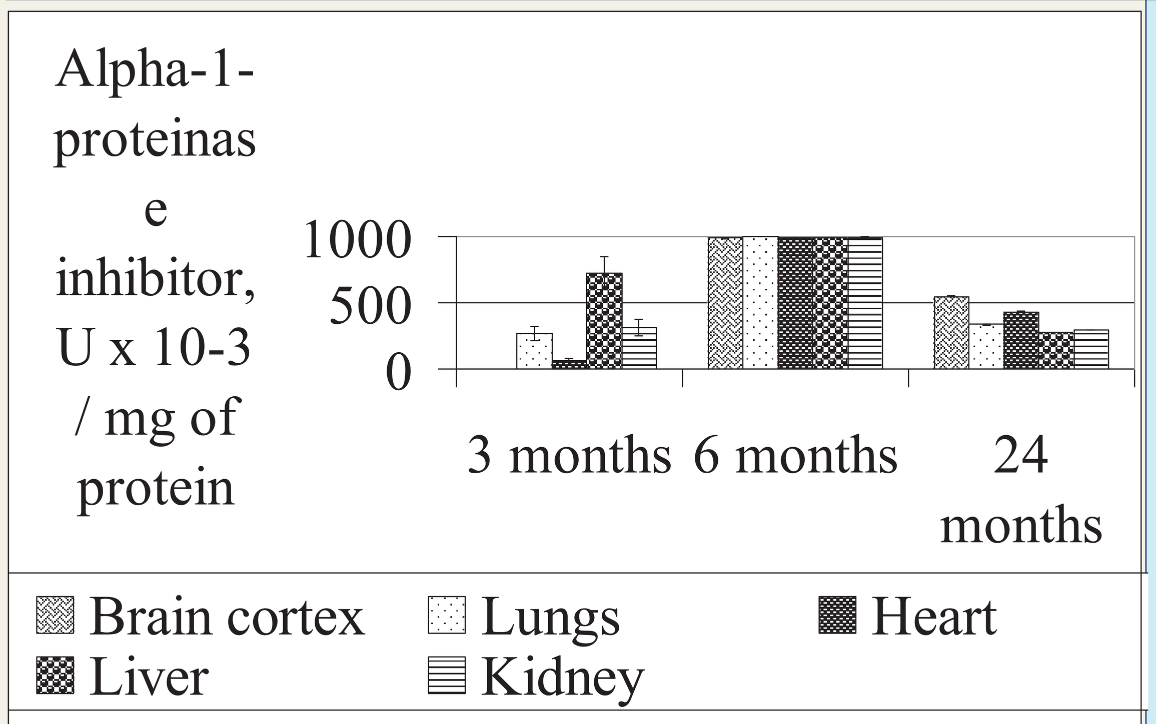

Fig.4 - Elastase inhibitory activity of alpha-1-proteinase inhibitor in male rats

Conclusion

•Aging depended as well as tissue-specific changes of the El, EEl and MEl as well as EIA of α-1-PI activity were observed in the male rats.

•1. The El activity decreased in 6- and 24-months-old rats may be the result of compensatory reserve loss. An increase of the El activity in BC in 6- and 24-months-old and kidney of 24-months-old may be due to a decrease in antioxidant protection and lead to the development of tissues destruction and vasoconstriction, as well as the inflammation.

•2. An increase in the EEl activity in 6-months-old rats as well as a decrease in 24-months-old can be considered as links of the body's compensatory response.

•3. The activity of MEl increased in BC of 24-months-old, as well as a decrease in the lungs may be a consequence of the oxidative stress development and pathological changes.

•4. The EIA of α-1-PI directly correlates with the EEl activity: it increased in 6-months-old rats and decreased in 24-months-old, and was below in the liver of 3-months-old.

References

•1. Serino A., Salazar G. (2018). Protective Role of Polyphenols against Vascular Inflammation, Aging and Cardiovascular Disease. Nutrients. 11(1), 53. doi: 10.3390/nu11010053.

•2. Zhao P., Lieu T. M., Barlow N., et al. (2015). Neutrophil Elastase Activates Protease-activated Receptor-2 (PAR2) and Transient Receptor Potential Vanilloid 4 (TRPV4) to Cause Inflammation and Pain. J Biol Chem. 290(22), 13875–13887. doi: 10.1074/jbc.M115.642736

•3. Samokhina L.M. (2014). E`nzimy` vazokonstrikczii i destrukczii: vliyanie tyazhely`kh metallov. Saarbrucken, Germaniya. ISBN: 978–3–659–63483–3.

•4. Samokhina L.M. (2015). Stress, gipertenziya i adaptacziya: e`nzimy` vazokonstrikczii i destrukczii v usloviyakh stressa, gipo– i gipertenzii: ritmicheskie kholodovy`e vozdejstviya. Saarbrucken, Germaniya. ISBN 978–3–659–33949–3.

•5. Samokhina L.M., Makyeyeva N.I. (2009). Akty`vnist` proteyinaz ta yih ingibitoriv u dorosly`h ta ditej. Ekspery`mental`na ta klinichna medy`cy`na. (3), 91-94.

•6. Samokhina L.M., Lomako V.V. (2015). Akty`vnist` endotelial`noyi elastazy` u shhuriv riznogo viku. Krovoobig ta gemostaz. (1-2), 140-141.

Contact Information

Lyubov M. Samokhina: lub.samokhina@gmail.com

S10.P2

S10.P2

AGE ASPECTS OF VASOCONSTRICTION DEVELOPMENT IN RATS

L.M. SAMOKHINA1, V.V. LOMAKO2

1 GD "National Institute of Therapy of L.T. Malaya name of National Academy of Medical Sciences of Ukraine", Laboratory of Immuno-biochemical and Molecular Genetic Studies; Lyubov Malaya ave., 2a, Kharkiv, Ukraine, 61039; 2 Institute for Problems of Cryobiology and Cryomedicine of National Academy of Sciences of Ukraine, Department of Cryophysiology; st. Pereyaslavskaya, 23,Kharkiv, Ukraine, 61016.

Introduction

Aging is considered to be the main risk factor for cardiovascular diseases (CVD) [1]. An increase in the rigidity of large arteries causes an increase in the systolic pressure and CVD risk and increases oxidative stress. Proteolytic enzymes play a special role in the processes described above. They are activated at the first stage of the mobilization of cellular protein reserve during the response to stress. A key mediator responding to the stress and associated CVD is the renin–angiotensin system (RAS), and angiotensin II (AII) is the most important and well-studied component of this system [2, 3]. AII plays a critical role in the regulation of the blood pressure and vascular tone. It is both a strong vasopressor and a promoter of a tissue remodeling in heart, arteries, and kidneys. Within a systemic blood flow, AII forms from angiotensin I (AI) with the involvement of angiotensin-converting enzyme (ACE). At the same time, the ACE-independent transformation of AI to AII in human tissues is controlled by chymase, kallikrein, cathepsin G, and elastase-2. AII can be also formed directly from angiotensinogen; this reaction is catalyzed by tonin, cathepsin G, or tissue plasminogen activator.

An AII-producing enzyme, chymase (EC 3.4.21.39) is present in the vascular tissues of humans, monkeys, dogs, and hamsters. Chymase from rabbits, rats, and mice cleaves AII into inactive fragments and is able to produce AII only at high AI concentrations. Under normal and pathological states also includes the modulation of inflammation, cardiomyocyte viability, the generation of reactive oxygen species, and the homeostasis of intracellular calcium. The last of these processes is connected with the activity of calpains representing Ca2+-dependent proteinases. Calpains (EC 3.4.22.17) often interact with caspases, lysosomal proteases, and endonucleases during apoptosis and represent the main cell-death factors [4]. Suppression of calpain activity promotes a reduction of the AII-induced hypertrophy of the left heart ventricle, vessel remodeling, increased perivascular inflammation, and tissue fibrosis [5]. An increase in the Ca2+ level in the organism initiates the contraction of smooth muscle cells in vascular walls, which results in hypertension [6]. The contractive function of cardiomyocytes, which associated with changes in the Ca2+ exchange may be controlled by tonin (EC 3.4.21.35), a kalikrein-like serine protease [3]. The effect of tonin results in a significant increase in blood pressure and heart rate. An increase in tonin activity is observed in elderly persons with reduced chymase activity; this fact is believed to be connected with noncoronary changes that enhance mechanical activity of the heart [7]. The understanding of fine mechanisms of aging with allowance for gender specificity may help to reduce the morbidity risk.

The purpose of this study was the evaluation of the activity of chymase, tonin, and calpains in tissues of rats of different ages.

Methods

The study was conducted on outbred albino rats (Rattus norvegicus) of different ages (3, 6, 8, and 24 months, n = 6 for each group). The rats were obtained with the herd random-breeding system. Prior the experiment, the rats were kept at animal facilities under natural light conditions on a standard ad libitum diet. Blood and tissue fragments were obtained after the decapitation of animals. Blood was collected in tubes, left for 10 min at room temperature, and then centrifuged at 5000 g for 15 min with a MPW-331 centrifuge (Mechanika Precyzyjna, Poland). The liver was perfused with a cold physiological solution for 5–10 min. Tissue samples (300 mg) of the cerebral cortex (CC), lungs, heart, liver, and kidneys were homogenized in 3 mL of 0.2 M Na–phosphate buffer (pH 7.2) at 4–6 oC and then centrifuged for 10 min at 6000 rpm and 4oC with a PC-6 centrifuge (Dastan, Kazakhstan). Blood serum (BS) samples and aliquots of 10% tissue homogenates were stored at –20oC until use.

The activity of chymase, tonin, and calpains in the BS and nucleus-free fractions of 10% tissue homogenates prepared from the CC, lungs, heart, liver, and kidneys was determined with highly sensitive (10–9 –10–10 g) enzymatic methods based on the cleavage of a complex of a protein substrate and marker enzyme (horseradish peroxidase) immobilized on a polystyrene surface [8, 9]. The optical density of the samples was measured at 490 nm. The chymase and tonin activity was expressed as E × 10–3 or nanomoles of substrate per minute; the calpains activity was expressed as mg/L of trypsin per 1 h. The following reagents and equipment were used un the study: horseradish peroxidase, 4–8 AII fragment, soybean trypsin inhibitor, protamine sulphate, aprotinin, bovine serum albumin (ICN, United States), trypsin (Spofa, Czechia), and other reagents (Reachim, Ukraine); polystyrene plates (KIMA, Italy), and an immunoenzyme Humanreader photometer (Human, Germany). The statistical treatment of data was carried out with the pairwise Student–Fisher test and the Excel software package (Microsoft, United States), as well as the nonparametric Mann-Whitney U-test.

Results

According to the results, the chymase activity in the kidneys of 6-month-old males decreased as compared to that in 3-month-old and remained low in 24-month-old. At the same time, this activity in the liver, BS, and CC tissues of 24-month-old increased, reaching the maximum level in the liver (Table 1).

The high chymase activity in 24-month-old may be evidence of the activation of the synthesis and/or release of chymase by liver mast cells and, in light of the species-specificity of chymase [4], may facilitate the development of vasodilatation, at least in CC tissues. The observed age-associated reduction of chymase activity in the kidneys in 6- and 24-month-old may provide local vasoconstriction. The energy exchange in cells becomes worse with age in parallel with disorders of the glucose and fatty acid metabolism; during aging, the amount of available ATP is reduced, and the chaperon activity changes, which may result in the accumulation of impaired proteins. This process is presumably manifested by a decrease in chymase activity, particularly in kidneys. The maximum chymase activity observed in the liver of 24-month-old can be considered a compensatory mechanism for the recovery of chymase activity in the organism via its synthesis and release by mast cells. Note that some publications describe other mechanisms, for example, aging in marmosets causes a decrease in the activity of cystathionine beta synthase, which is involved in the synthesis of hydrogen sulphide (H2S) [10]; this decrease in H2S production was observed. H2S can relax muscles and cause vasodilatation.

The tonin activity in 6-month-old exceeded that in 3-month-old, but it decreased with age in all studied tissues of 24-month-old, except in CC samples, in which no changes were observed (Table 2). Therefore, the tonin activity increases and then decreases, which most probably confirms the exhaustion of possibilities for its synthesis. At the same time, the tonin activity in the lungs decreases below the value determined at the age of 3 months, while the activity in the heart tissues remains at the level exceeding that in 3-month-old, i.e., it provides a high level of AII formation. Resistance to some stress types reaches the maximum in the early adult age but then decreases during aging, that is considered to be the result of a genetically programmed inactivation of stress-response mechanisms, which is not always associated with the accumulation of various impairments in the organism. The character of changes in tonin activity may determine the age-related development of stress reactions. For the heart and large arteries, such changes may initiate the process of proinflammatory tissue remodeling with the involvement of AII [11]. The structural reconstructions and functional changes that occur with aging include an increase in the rigidity of the heart and vascular tissues, systolic hypertension, and ventriculoarterial remodeling, which often are not clinically manifested.

6-month-old males showed an increase in calpain activity in the lungs, heart, liver, and kidneys; it was higher in 24-month-old as compared to 6-month-old in the CC, lungs, liver, and kidneys. The maximum level occurred in the lungs, which indicated the activation of calpain-dependent apoptogenic processes during aging. As compared to 3-month-old, the level of calpain activity in 24-month-old increased by ten times in the heart and liver tissues, 20 times in the kidneys, and 80 times in the lungs (Table 3). The aging of brain cells is associated with various bioenergetic disorders, adaptive neuroplasticity, anomalous activity of the neural network, the accumulation of modified molecules and organelles, inflammation, and impaired regulation of the neuronal Ca2+ homeostasis. Changes in the calcium concentration are directly connected with the activity of Ca2+-dependent proteinases (calpains), which increased in the CC tissues of 24-month-old rats. Aging causes oxidative stress and activates the stress-related signaling of the apoptosis in the skeletal muscles of mice [12]. The accumulation of aging cells may cause chronic inflammation, which, in turn, may lead to pathological changes in senior humans [13]. It is believed that factors related to stress resistance determine the difference in the lifespan and development of aging processes.

Importing Tables & Graphs

Table 1. Chymase activity in rats of different ages (E·10–4), M±SE

Tissue sample	3 month	6 month	24 month
Blood serum	–	0,020±0,006	0,12±0,03$^{2)*}$
Cerebral cortex	0,26±0,07	0,16±0,06	0,32±0,06$^{2)*}$
Lungs	0,15±0,04	0,19±0,06	0,20±0,08
Heart	0,14±0,05	0,10±0,03	0,20±0,08
Liver	0,17±0,05	0,17±0,04	1,28±0,42$^{1)*, 2)*}$
Kidneys	0,23±0,08	0,12±0,05$^{1)*}$	0,14±0,05$^{1)*}$

Here and in Tables 2 and 3: $^{1)*}$, statistically significant difference as compared to 3-month-old rats; $^{2)*}$, statistically significant difference as compared to 6-month-old rats, $p < 0.05$.

Importing Tables & Graphs

Table 2. Tonin activity in male rats of different ages ($E\cdot10^{-5}$), M ± SE

Tissue sample	3 month	6 month	24 month
Blood serum	–	0,422±0,105	0,384±0,121
Cerebral cortex	–	0,150±0,039	0,337±0,112$^{2)*}$
Lungs	0,050±0,004	0,362±0,090$^{1)*}$	4,152±1,350$^{1)*, 2)*}$
Heart	0,045±0,003	0,346±0,065$^{1)*}$	0,357±0,107$^{1)*}$
Liver	0,036±0,004	0,111±0,031$^{1)*}$	0,344±0,111$^{1)*, 2)*}$
Kidneys	0,035±0,002	0,162±0,040$^{1)*}$	0,763±0,254$^{1)*, 2)*}$

Table 3. Calpain activity in male rats of different ages, M ± SE (mg/L per hour)

Tissue sample	3 month	6 month	24 month
Blood serum	–	1,30±0,11	0,25±0,08$^{2)*}$
Cerebral cortex	0,34±0,12	0,61±0,17$^{1)*}$	0,55±0,18
Lungs	0,56±0,11	0,90±0,08$^{1)*}$	0,13±0,04$^{1)*, 2)*}$
Heart	0,25±0,07	1,11±0,22$^{1)*}$	0,50±0,16$^{1)*, 2)*}$
Liver	0,24±0,08	1,22±0,22$^{1)*}$	0,38±0,12$^{2)*}$
Kidneys	0,39±0,12	1,24±0,13$^{1)*}$	0,47±0,15$^{2)*}$

Conclusion

Changes in the activity of the studied proteinases are tissue-specific and depend on the age of animals. The chymase activity in BS, CC, and liver tissues of male rats increases up to the age of 24 months. Since the enzyme is species-specific, this may result in a decrease in vasoconstriction. The chymase activity decreased as compared to that in 3-month-old and remains lower in 24-month-old. The tonin activity in 6-month-old exceeds that in 3-month-old and decreases with age in 24-month-old in all of tissues, except for the CC, which is evidence of exhaustion of the possibilities for the synthesis; at the same time, the level of this activity in heart tissues remains higher than that in 3-month-old, i.e., it maintains a high level of AII formation. The calpain activity increases with age in 6-month-old (lungs, heart, liver, and kidneys) and then in 24-month-old (all tissues excepting the heart), reaching the maximum level in the lungs; this is indicative of more intensive apoptogenic processes.

References

1. Ungvari, Z., Tarantini, S., Kiss, T., et al., Endothelial dysfunction and angiogenesis impairment in the ageing vasculature, Nat. Rev. Cardiol., 2018, vol. 15, № 9, pp. 555–565. https://doi.org/10.1038/s41569-018-0030-z
2. Becari, C., Oliveira, E.B., and Salgado, M.C., Alternative pathways for angiotensin II generation in the cardiovascular system, Braz. J. Med. Biol. Res., 2011, vol. 44, № 9, pp. 914–919.
3. Damasceno, D.D., Lima, M.P., Motta, D.F., et al., Cardiovascular and eletrocardiographic parameters after tonin administration in Wistar rats, Regul. Pept., 2013, vol. 181, pp. 30–36.
4. Starodub, N.F., Samokhina, L.M., Koval', S.N., and Snegurskaya, I.A., Calpains: general characteristics and their role in various states of the organism, Ukr. Biokhim. Zh., 2014, № 1, pp. 5–20.
5. Letavernier, B., Zafrani, L., Nassar, D., et al., Calpains contribute to vascular repair in rapidly progressive form of glomerulonephritis: potential role of their externalization, Arterioscler., Thromb., Vasc. Biol., 2012, vol. 32, № 2, pp. 335–342.
6. Brule, C., Dargelos, E., Diallo, R., et al., Proteomic study of calpain interacting proteins during skeletal muscle aging, Biochimie, 2010, vol. 92, № 12, pp. 1923–1933.
7. Samokhina, L.M., Lazareva, S.A., and Volkov, V.I., The specific involvement of tonin and calpains in the heart failure processes, Dostizh. Biol. Med., 2007, № 1, pp. 14–17.
8. Samokhina, L.M., Enzimy vazokonstriktsii i destruktsii: vliyanie tyazhelykh metallov (The Effect of Heavy Metals on Vasoconstriction and Destruction Enzymes), Saarbrucken: LAP Lambert Academic, 2014.
9. Samokhina, L.M., Stress, gipertenziya i adaptatsiya: enzimy vazokonstriktsii i destruktsii v uloviyakh stressa, gipo- i gipertenzii. Ritmicheskie kholodovye vozdeistviya (Stress, Hypertension, and Adaptation: Vasoconstriction and Destruction Enzymes in Stress, Hypo- and Hypertension. Rhythmic Cold Effects), Saarbrucken: LAP Lambert Academic, 2015.
10. Lee, H.J., Gonzalez, O., Dick, E.J., et al., Marmoset as a model to study kidney changes associated with aging, J. Gerontol., A, 2019, vol. 74, № 3, pp. 315–324. https://doi.org/10.1093/gerona/gly237
11. Wang, M. and Shah, A.M., Age-associated pro-inflammatory remodeling and functional phenotype in the heart and large arteries, J. Mol. Cell Cardiol., 2015, vol. 83, pp. 101–111. https://doi.org/10.1016/j.yjmcc.2015.02.004
12. Belaya, I., Suwa, M., Chen, T., et al., Long-term exercise protects against cellular stresses in aged mice, Oxid. Med. Cell. Longevity, 2018, vol. 2018, art. ID 2894247. https://doi.org/10.1155/2018/2894247
13. Wei, W. and Ji, S., Cellular senescence: molecular mechanisms and pathogenicity, J. Cell Physiol., 2018, vol. 233, № 12, pp. 9121–9135. https://doi.org/10.1002/jcp.26956

Contact Information

Lyubov M. Samokhina: lub.samokhina@gmail.com

XXVIII Congress of the Polish Physiological Society

Gdańsk, September 15-17 2021

Poster book

SESSION XI

PHYSIOLOGY OF REPRODUCTION

HONORARY PATRONAGE

Uniwersytet Gdański

Prof. dr Marcin Gruchała
Rector of the Medical University of Gdansk

Prof. dr Piotr Stepnowski
Rector of the University of Gdansk

WOJEWODA POMORSKI
DARIUSZ DRELICH

Dariusz Drelich
Governor of the Pomeranian Voivodeship

HONORARY PATRONAGE
Mayor of the City of Gdańsk

Aleksandra Dulkiewicz
Mayor of Gdansk

Mieczysław Struk
Marshal of the Pomeranian Voivodeship

PARTNER

PAN
POLSKA AKADEMIA NAUK

ANIMA LAB
animal facility and laboratory equipment • animal research models

FUNDACJA LOTOS

Medical University of Gdansk
Department of Physiology

XXVIII Congress of the Polish Physiological Society

ELECTROMAGNETIC FIELD OF EXTREMELY LOW FREQUENCY INDUCES CHANGES IN THE RELATIVE ABUNDANCE OF *HSD17B2* AND *VDR* IN THE ENDOMETRIUM OF PIGS DURING THE PERI-IMPLANTATION PERIOD

Wiktoria Kozlowska[1], Ewa M Drzewiecka[1], Agata Zmijewska[1], Pawel J Wydorski[1], Anita Franczak[1]

[1]Department of Animal Anatomy and Physiology, Faculty of Biology and Biotechnology, University of Warmia and Mazury in Olsztyn, Oczapowskiego Str. 1A, 10-719 Olsztyn, wiktoria.kozlowska@uwm.edu.pl

Acknowledgments

This research was funded by the National Science Centre (Poland) [OPUS, grant number: 2017/25/B/NZ9/00090].
Wiktoria Kozlowska is a recipient of a scholarship from the Programme Interdisciplinary Doctoral Studies in Biology and Biotechnology [POWR.03.05.00-00-Z310/17], which is funded by the European Social Fund, “Development Program of the University of Warmia and Mazury in Olsztyn” [POWR.03.05.00-00-Z310/17], co-financed by the European Union under the European Social Fund from the Operational Program Knowledge Education Development.

Introduction

The extremely low-frequency electromagnetic field (EMF) originating from human-made sources becomes a part of the environment that may influence female reproduction. This study aimed also to determine the effect of the EMF (50 Hz, 2 h treatment duration) on *HSD17B2* and *VDR* mRNA transcript abundance in endometrial slices of pigs during the peri-implantation period (n = 5). To confirm the NGS results, the *HSD17B2* and *VDR* mRNA transcript abundances were determined with one-step Real-Time PCR with TaqMan probes.

It was hypothesized that EMF induces changes in *HSD17B2* and *VDR* mRNA transcript abundance in a pig endometrium during the peri-implantation period.

Material and methods

Endometrium collected from pigs (n = 5) during early pregnancy (days 15 to 16)

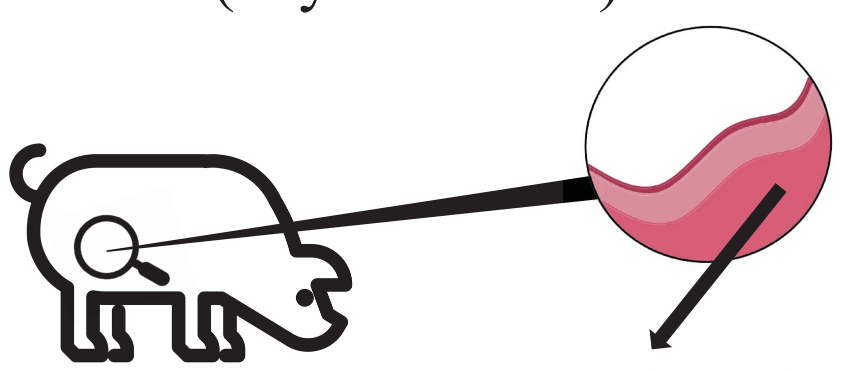

endometrial slices

1) Preincubation → 2 h
2) Incubation → 2 h

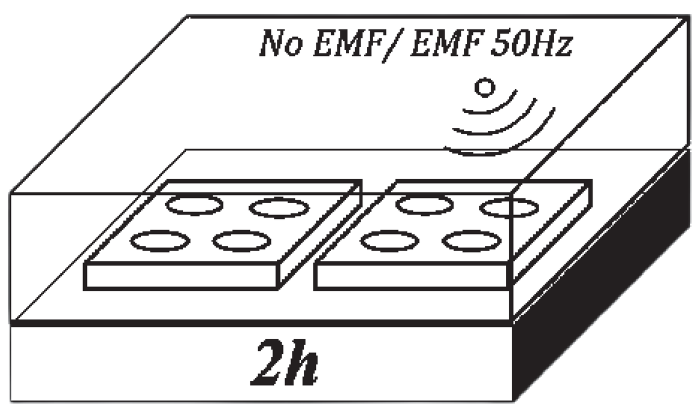

M199, 0,1% BSA, 1% antibiotics, 95% O_2, 5% CO_2, 37 °C

One-step Real-time PCR

Determination of ***HSD17B2*** and ***VDR*** mRNA transcript abundance

(reference genes: *ACTB*, *GAPDH*)

Results

Fig. 1.

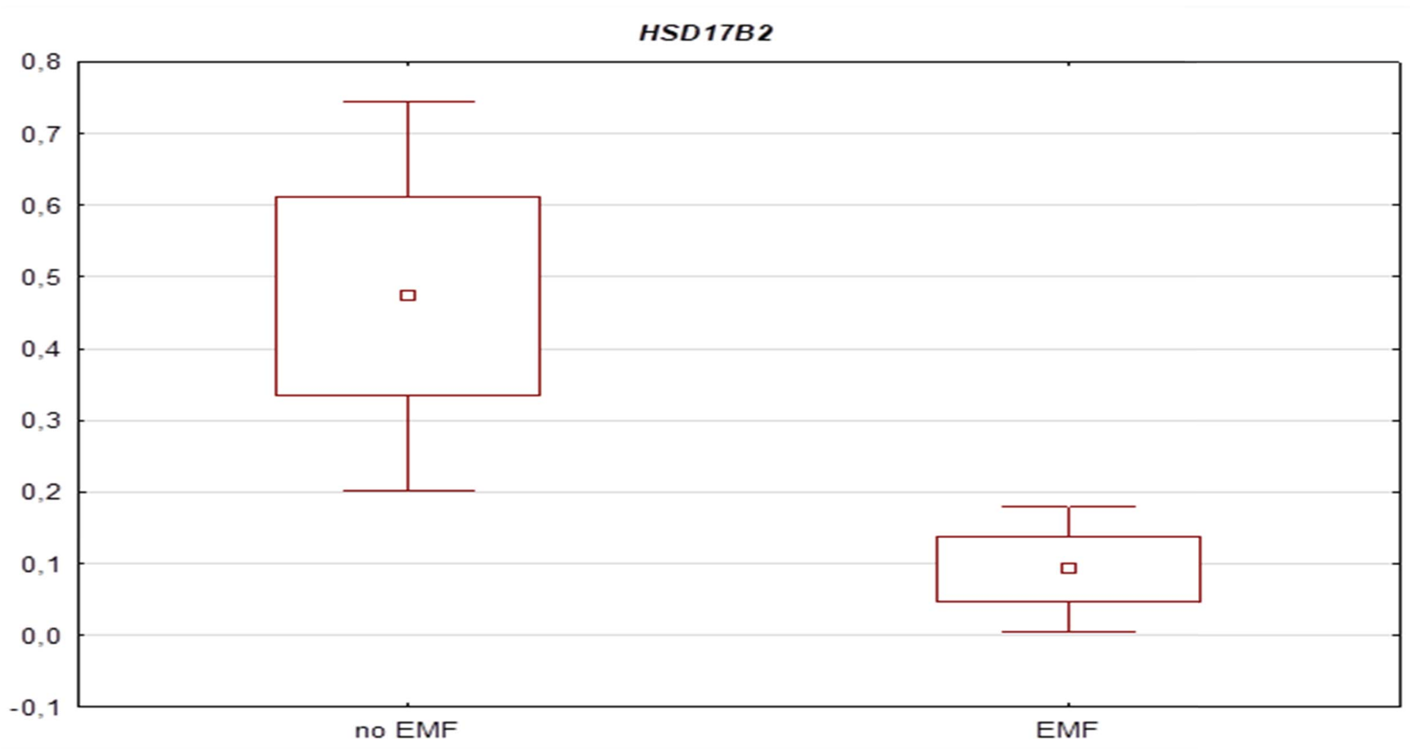

Fig. 2.

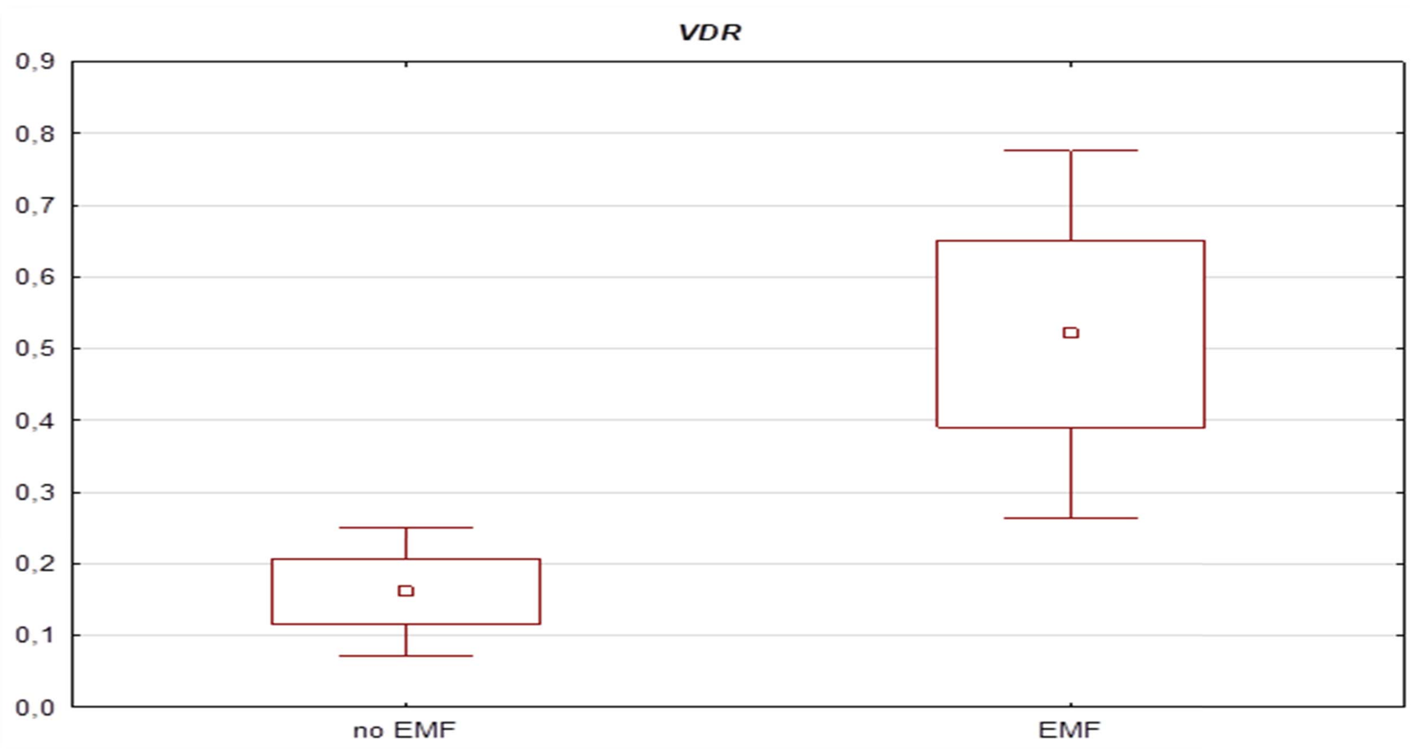

Fig. 1. The *HSD17B2* mRNA transcript abundance in endometrium exposed to EMF at 50 Hz for 2 h.

Fig. 2. The *VDR* mRNA transcript abundance in endometrium exposed to EMF at 50 Hz for 2 h.

Conclusions

The observed alterations in *HSD17B2* and *VDR* expression in the endometrium may lead to hyper-concentration of estrogens in the intra-uterine environment and induce cytotoxic effects on embryos during the peri-implantation period. These results could become a basis for further studies explaining the consequences of EMF treatment in the reproductive system.

SESSION XI

EFFECT OF VITAMIN D_3 ADMINISTRATION ON GLUCOSE AND INSULIN LEVEL, AND HOMA-IR INDEX IN RATS WITH LETROZOLE-INDUCED PCOS

M. GRZESIAK[1], K. KAMIŃSKA[1], O. FRĄCZEK[1], A. SZLAGA[2], A. MAŚLANKA[3], D. KLIMCZYK[3], P. SAMBAK[2], P. DZIUROWICZ[1], K. KNAPCZYK-STWORA[1], A. BŁASIAK[2], A.RAK[3]

[1]*Department of Endocrinology, Institute of Zoology and Biomedical Research, Jagiellonian University in Cracow, Cracow, Poland;*
[2]*Department of Neurophysiology and Chronobiology, Institute of Zoology and Biomedical Research, Jagiellonian University in Cracow, Cracow, Poland;*
[3]*Laboratory of Physiology and Toxicology of Reproduction, Institute of Zoology and Biomedical Research, Jagiellonian University in Cracow, Cracow, Poland*

E-mail: m.e.grzesiak@uj.edu.pl

INTRODUCTION

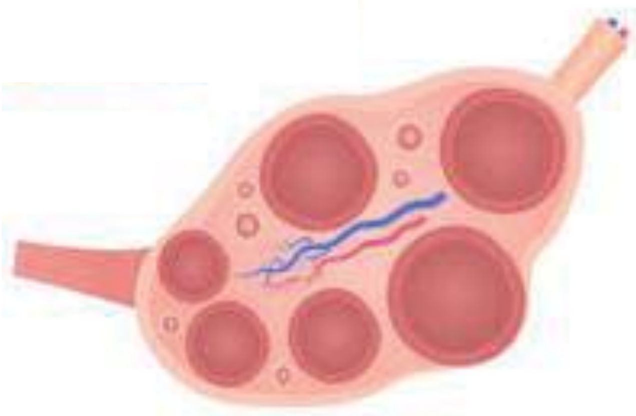

Polycystic ovary syndrome (PCOS) is characterized by:
- hyperandrogenism,
- olig-/anovulation,
- ovarian cysts,
- metabolic disorders, such as hyperinsulinemia and insulin resistance .

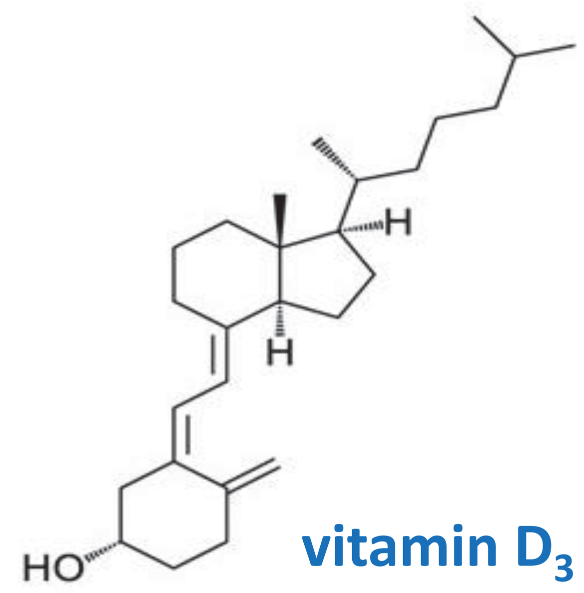

vitamin D_3

Decreased **vitamin D_3 (VD)** level was found among PCOS patients and beneficial effects of VD in PCOS treatment were reported.

OBJECTIVES

The aim of the present study was to examine the effect of VD administration on plasma glucose and insulin concentration, and homeostatic model assessment for insulin resistance (HOMA-IR) in rats with letrozole-induced PCOS.

MATERIAL & METHODS

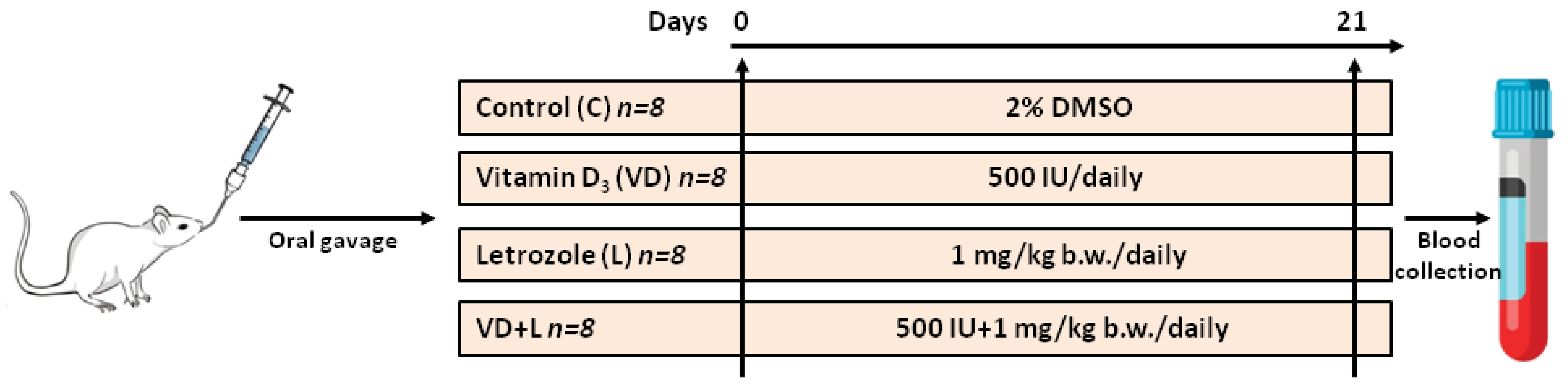

- **25OHD** (Total 25-OH Vitamin D ELISA Kit)
- **Fasting insulin** (Rat Insulin ELISA Kit)
- **Fasting glucose** (Rat Insulin ELISA Kit)
- **HOMA-IR index** (Zhang et al. 2020)

RESULTS

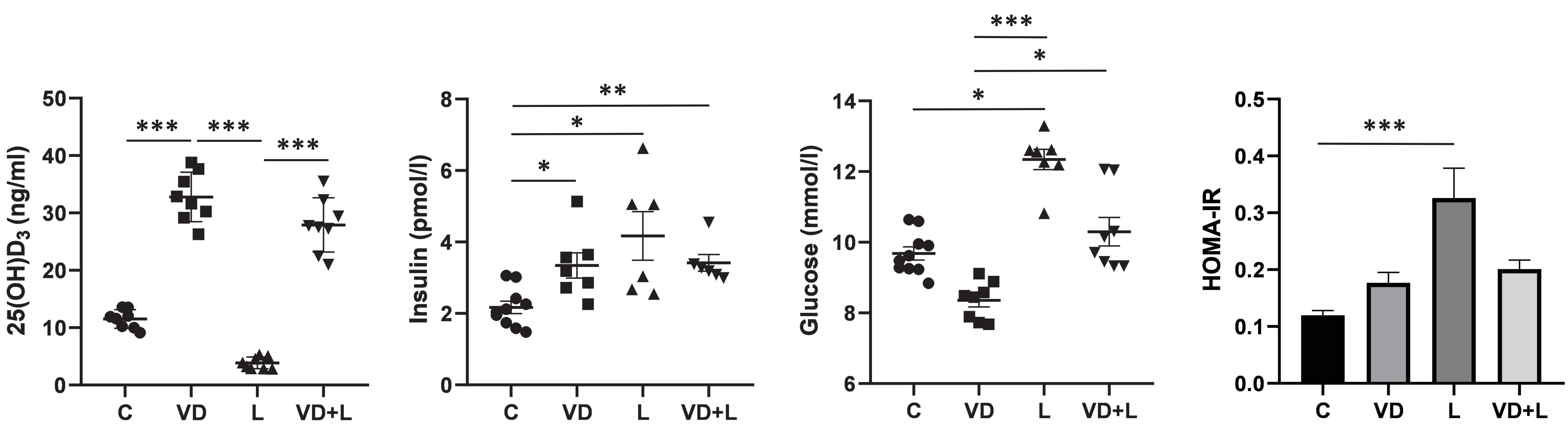

*P<0.05, **P<0.01, ***P<0.001; one-way ANOVA followed by Tukey *post hoc* test; data presented as the overall mean ± SEM

CONCLUSIONS

In the present study, we showed that VD significantly increased 25OHD level in the VD+L group in comparison to the group with induced PCOS. Futhermore, the tendency to decrease insulin and glucose concentration as well as HOMA-IR was found. Our results indicate that VD supplementation has a promising potential to improve metabolic parameters in PCOS, including insulin sensitivity. However, further studies on adequate VD dose are required.

REFERENCES

1. Grzesiak et al. *Altered vitamin D_3 metabolism in the ovary and periovarian adipose tissue of rats with letrozole-induced PCOS.* Histochem Cell Biol. 2021;155(1):101-116.
2. Zhang et al. *Berberine decreases insulin resistance in a PCOS rats by improving GLUT4: Dual regulation of the PI3K/AKT and MAPK pathways.* Regul Toxicol Pharmacol 2020;(110):104544.

Acknowledgements: funded by the Priority Research Area BioS, grant no. U1U/P03/DO/14.87

Protein expression and immunolocalisation of vaspin and GRP7878 receptor in human placenta of intrauterine growth restriction. Preliminary data.

Małgorzata Jurek [1], **Monika Dawid** [1], **Tomasz Milewicz** [2], **Piotr Pawlicki** [3], **Małgorzata Kotula-Balak** [4], **Agnieszka Rak** [1]

[1]Laboratory of Physiology and Toxicology of Reproduction, Institute of Zoology and Biomedical Research, Jagiellonian University in Krakow, Poland; [2] Department of Gynecological Endocrinology, Jagiellonian University Medical College, Poland; [3] Center for Experimental and Innovative Medicine, University of Agriculture in Krakow; [4] University Centre of Veterinary Medicine JU-UA, University of Agriculture in Krakow, Poland; *malgorzata99.jurek@student.uj.edu.pl*

INTRODUCTION

Intrauterine growth restriction (IUGR) is a serious pathological complication associated with compromised fetal development during pregnancy. IUGR is often linked with impaired placental development, structure and morphology, which in turn alter placental function and capacity of delivering nutrients to the fetus. Various factors including adipokines influence transfer of substances between maternal and fetal circulations. Vaspin (visceral adipose tissue-derived serine protease inhibitor) is known regulator of energy balance, it decreases food intake, promotes preadipocytes differentiation, improves insulin sensitivity and glucose tolerance, and plays an important role in female reproduction.

The aim of the present study was to investigate protein expression and immunolocalisation of vaspin and its receptor GRP78 in the maternal and fetal parts of the human placenta of healthy pregnant women (control) and with IUGR.

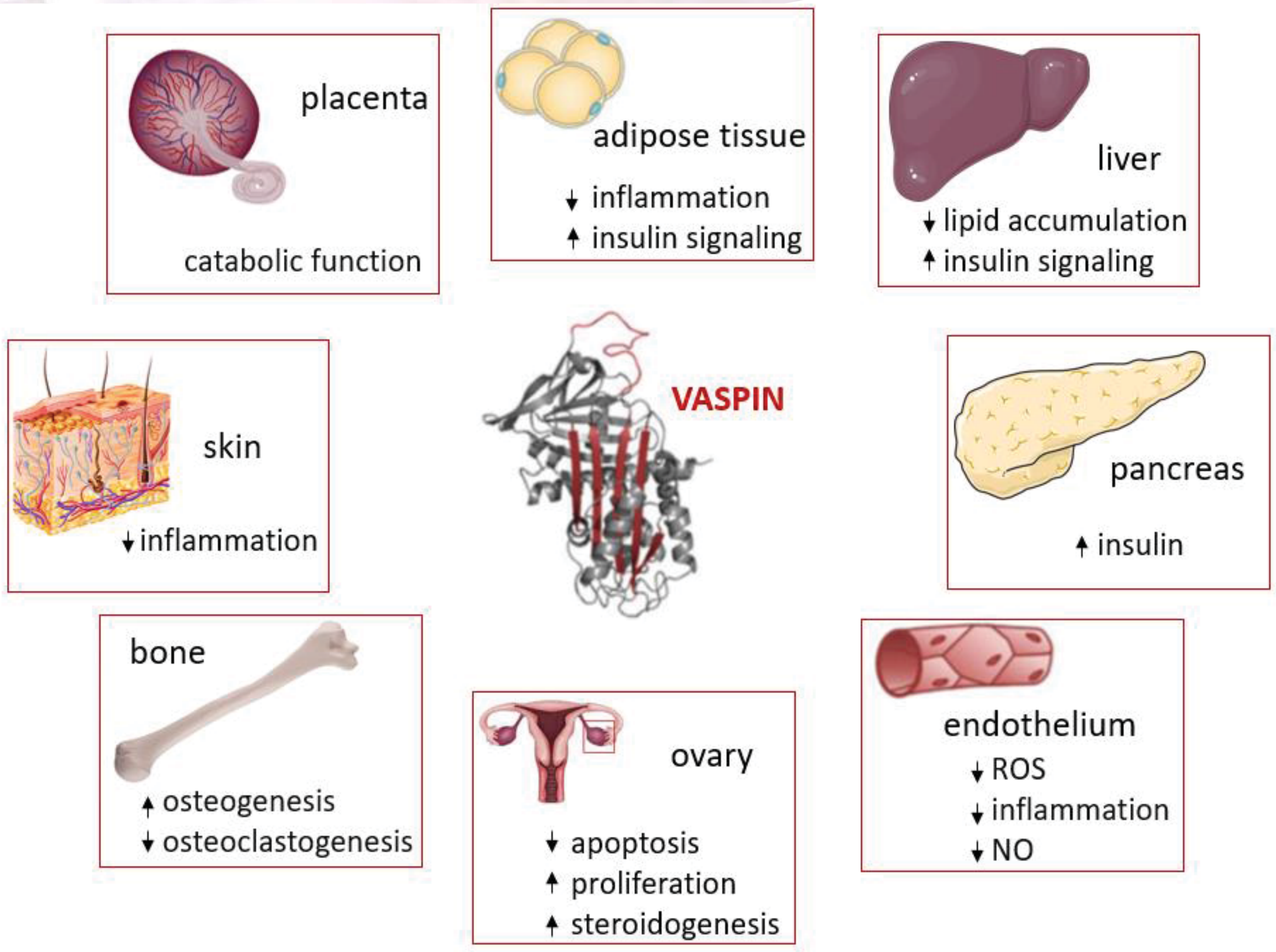

Fig 1. Expression and function of vaspin in various tissue.

MATERIAL AND METHODS

Placental tissue was collected in a gynaecological hospital in Krakow, Department of Gynecological Endocrinology, Jagiellonian University Medical College, Poland, where the clinical information on pregnancy outcomes was obtained. Western Blot and immunohistochemistry methods were used to analyze vaspin and GRP78 expression. Statistical analysis were carried out in GraphPad Prism 5 and a one-way ANOVA test ($p>0.05$).

RESULTS

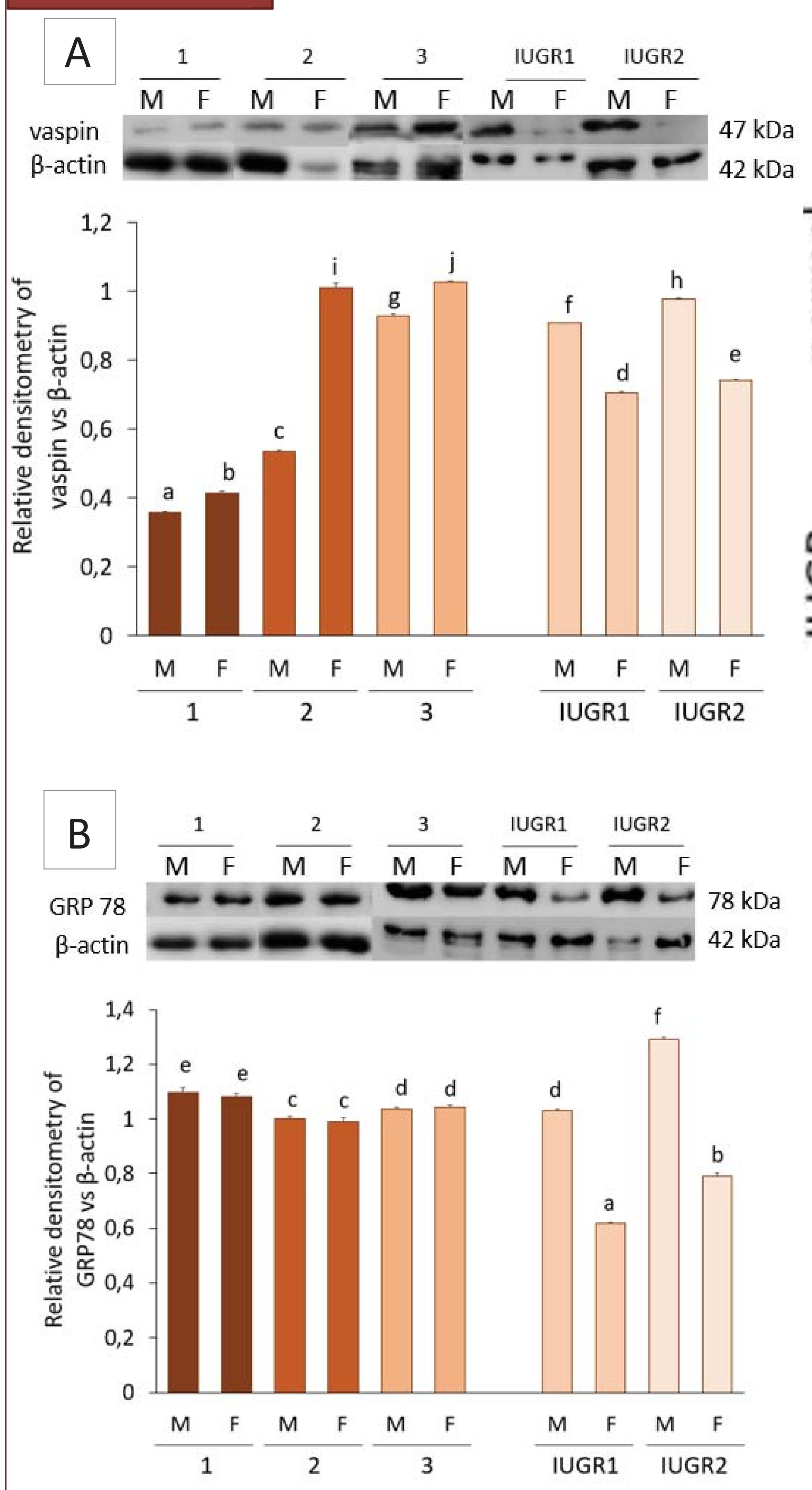

Fig 2. Protein expression of vaspin (A) and GRP78 (B) in human placenta – maternal (M) and fetal (F) part. Letters (a - j) denote statistical significance at the $p<0.05$ level.

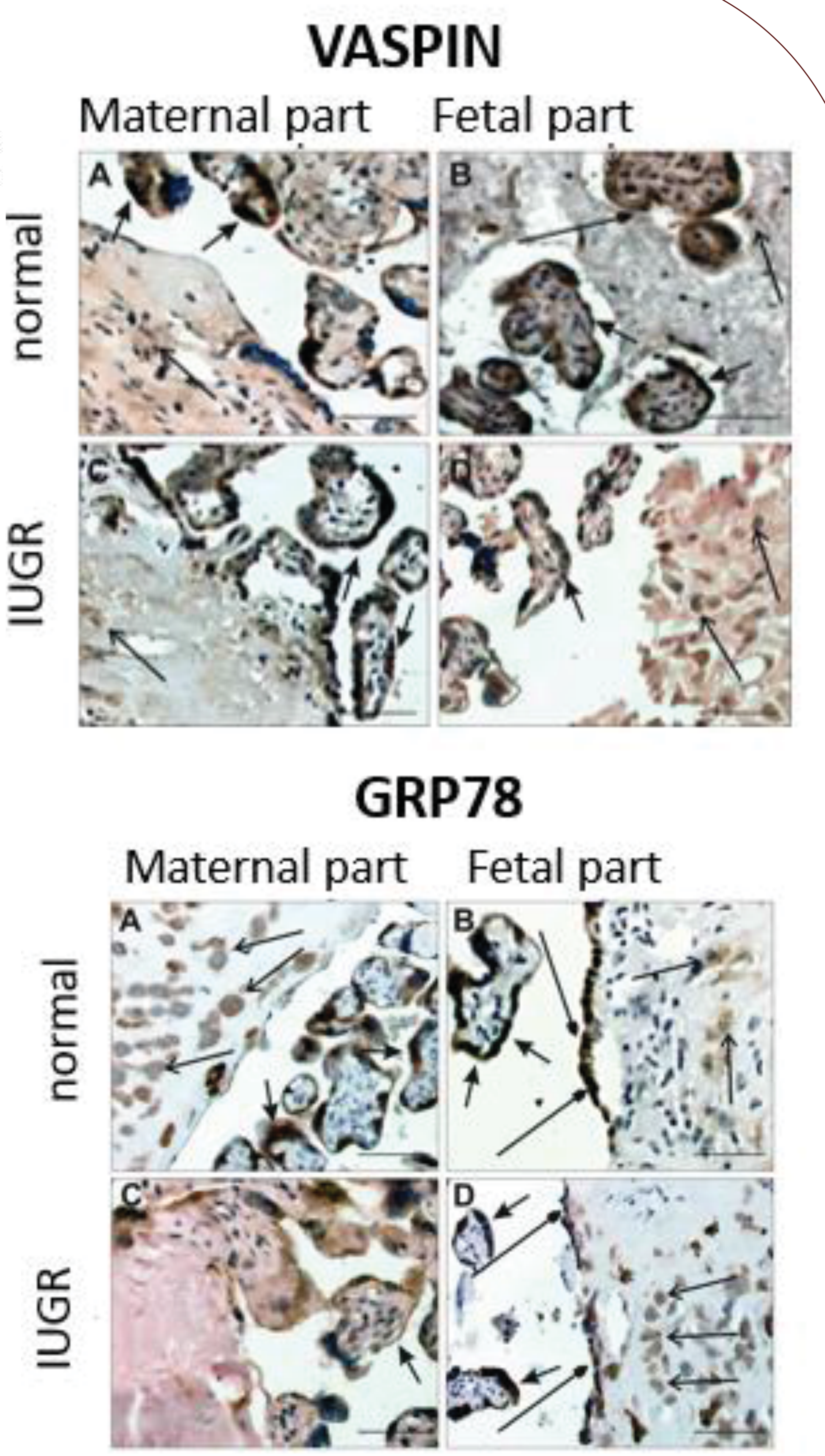

Fig 3. Immunolocalization of vaspin and GRP78 in maternal and fetal side presented by arrows in normal and IUGR placentas.

CONCLUSION

In conclusion, our study for the first time showed the immunoexpression and immunolocalisation of vaspin and GRP78 in the maternal and fetal parts of placentas from healthy and complicated by IUGR pregnancies, indicating vaspin as a new regulator in placenta cells. Interesting, protein expression of vaspin/GRP78 was significantly lower in the fetal part placenta of IGUR. Future studies will be necessary for understanding the role of vaspin on placenta physiology providing new insights into the pathology of IUGR.

References

1. Hida K. et al (2005) Visceral adipose tissuederived serine protease inhibitor: a unique insulin-sensitizing adipocytokine in obesity. Proceedings of the national academy of sciences 102(30), 10610-10615.
2. Weiner J., Zieger K., Pippel J., Heiker JT. (2018) Molecular mechanisms of vaspin action–from adipose tissue to skin and bone, from blood vessels to the brain. Protein Reviews–Purinergic Receptors, 1111; 159-188.
3. Kurowska P., Mlyczyńska E., Dawid M., Dupont J., Rak A. (2020a) Role of vaspin in porcine ovary: effect on signaling pathways and steroid synthesis via GRP78 receptor and protein kinase A†. Biol Reprod 26;102(6):1290-1305.

Supported by project „Diamond grant" DI201901104

Ministry of Education and Science

Analysis of changes in the proteomic profile of porcine corpus luteum during different stages of the estrous cycle: effects of PPAR gamma ligands

Kunicka Z. [1], Mierzejewski K.[1], Kurzyńska A.[1], Stryiński R.[2], Mateos J. [3], Carrera M. [4], Golubska M.[1]and Bogacka I.[1]

[1] Department of Animal Anatomy and Physiology, Faculty of Biology and Biotechnology, University of Warmia and Mazury in Olsztyn Poland; [2] Department of Biochemistry, Faculty of Biology and Biotechnology, University of Warmia and Mazury in Olsztyn, Poland; [3] Galapagos NV, Generaal de Wittelaan L11, Mechelen, Belgium; [4] Department of Food Technology, Marine Research Institute (IIM), Spanish National Research Council (CSIC), Vigo, Spain

INTRODUCTION

The corpus luteum (CL) is an essential structure for the mammalian reproduction. Disorders in the CL activity might be a cause of improper endometrium development, problems with the embryo implantation and early miscarriages. There are data suggesting that peroxisome proliferator-activated receptors (PPARs) can be engaged in the regulation of the CL functions. **The present study indicates the differences in the proteomic profile of the porcine CL during two stages of the estrous cycle: the mid-luteal phase (days 10-12) and late-luteal phase (days 14-16). The study also demonstrates changes in the CL proteome under the influence of PPARγ ligands (agonist – pioglitazone and antagonist – T0070907).**

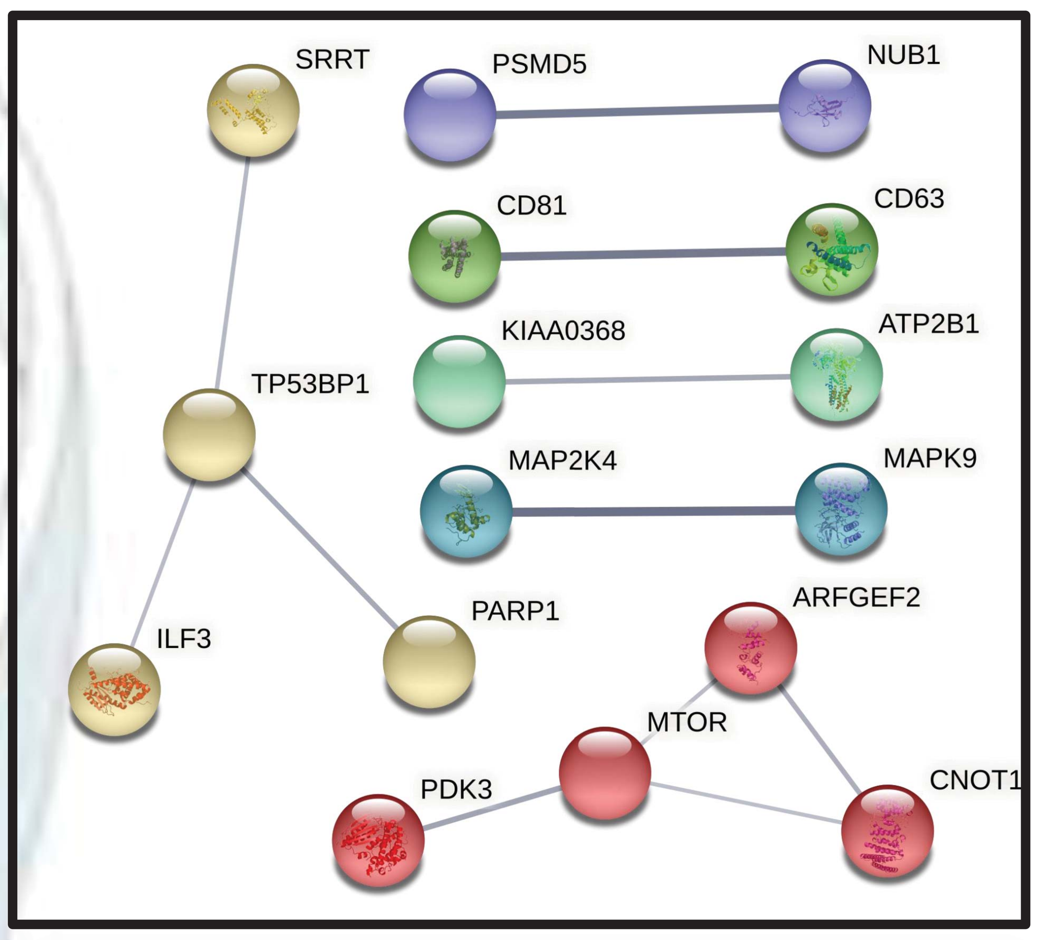

Figure 1. Protein–protein interaction network analysis of DRPs obtained after comparing the mid- with the late-luteal phase in the CL of *Sus scrofa domestica.*

MATERIAL AND METHODS

Corpus luteum explants in the mid- or late-luteal phase of the estrous cycle (n=4 for each group)

→

6 h *in vitro* incubation
- with PPARγ ligands (pioglitazone or T0070907 [10 µM])
- without treatment (control)

↓

protein extraction

←

trypsin + HIFU

↓

TMT 10 Plex labeling

→

LC-MS/MS

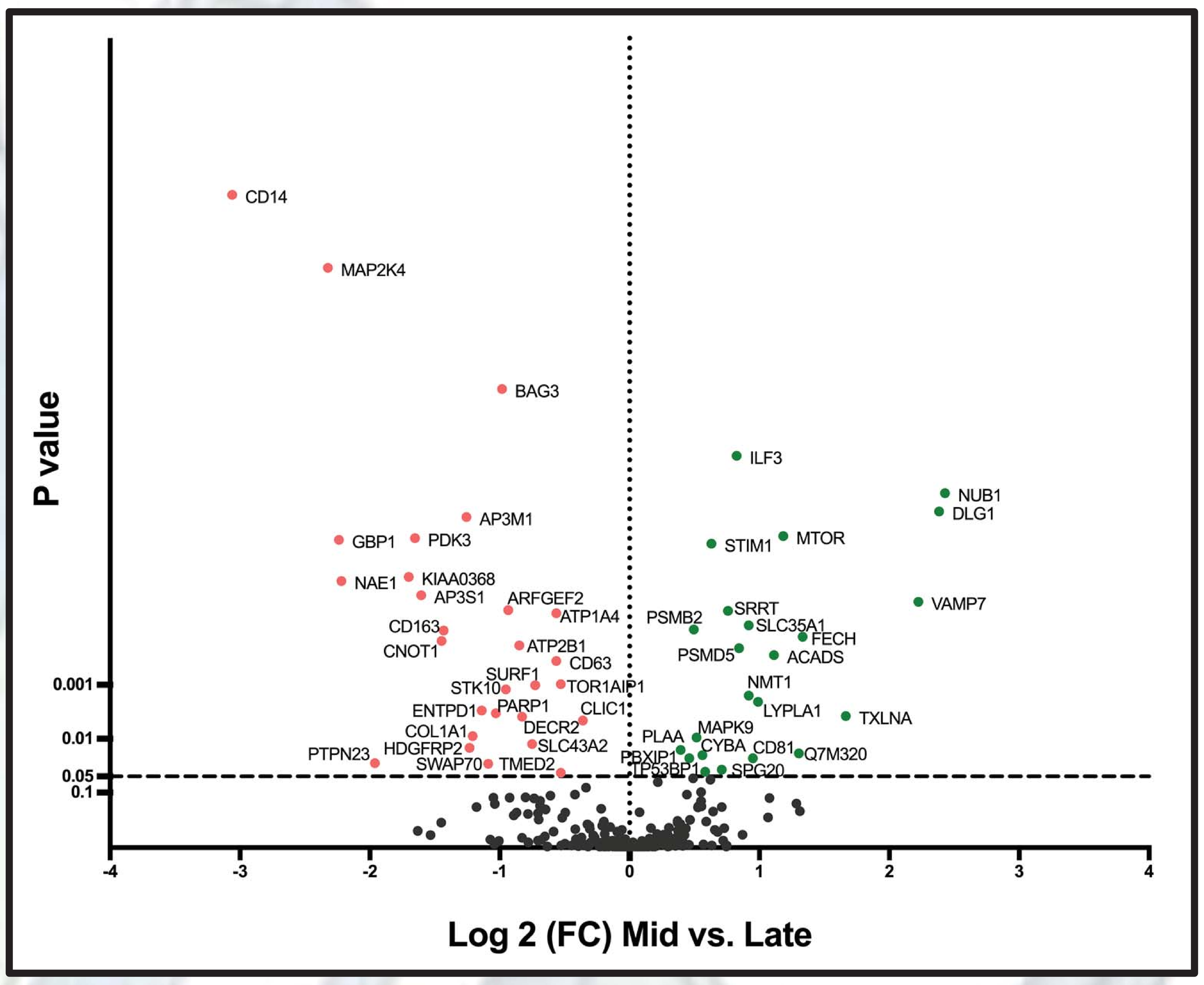

Figure 2. The Volcano plot representing DRPs obtained after comparing the mid- with the late-luteal phase in CL of *Sus scrofa domestica.* The proteins more abundant in the mid-luteal phase are towards the right (green color), the proteins more abundant in the late-luteal phase are towards the left (red color), and out of them the most statistically significant proteins are towards the top. FC = 1.5; p-value ≤ 0.05.

RESULTS

The comparative proteomic analysis revealed that certain proteins constitute a specific proteomic signature for each of the examined phase – 23 and 28 proteins for the mid- and late-luteal phase, respectively. Moreover, seven proteins were differentially regulated (DRPs) in the CL tissue treated with PPAR ligands. In the mid-luteal phase, one protein CAND1 was downregulated after T0070907 treatment. In the late-luteal phase, six DPRs were upregulated after CL treatment with pioglitazone: SPTAN1, GOLGB1, TP53BP1, MATR3, RRBP1 and SRRT. Three of them – SPTAN1, GOLGB1 and TP53BP1, were also upregulated in the CL treated with T0070907 during the late-luteal phase.

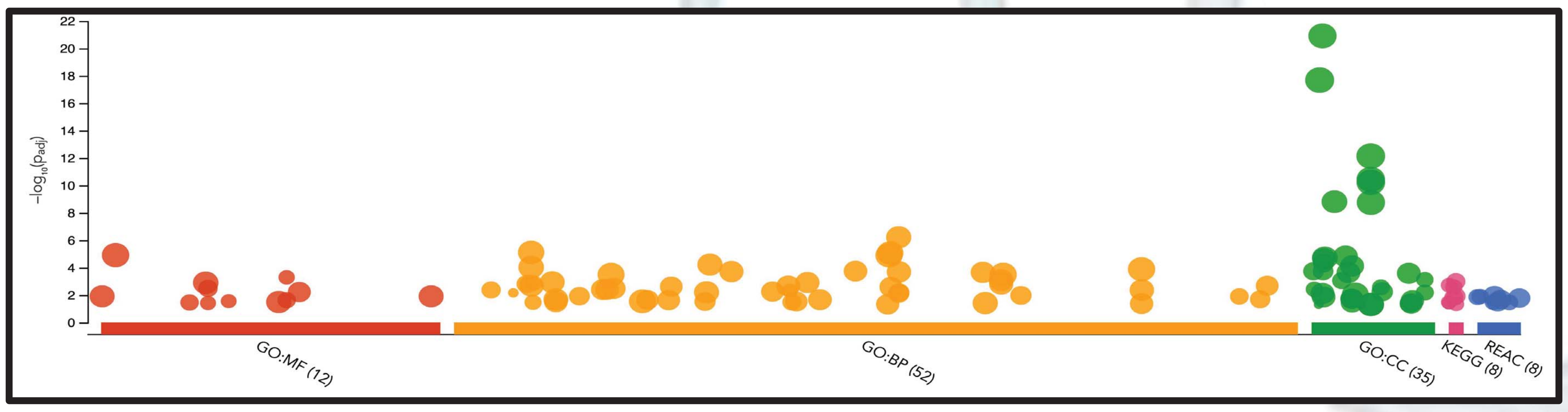

Figure 3. Manhattan plot illustrating the enrichment analysis results. The functional terms are grouped and color-coded by data sources, i.e., molecular function (MF) is in red, biological processes (BP) is in orange, and cellular components (CC) is in green etc.

CONCLUSION

- **Gene Ontology annotation indicated that identified DRPs were involved in protein metabolic process, catalytic activity, ion transport, peptide transport and nucleotide binding activity.**
- **The obtained results offer a broader insight into those which processes, apart from apoptosis and autophagy, may be responsible for the structural luteolysis of the porcine corpus luteum.**
- **The PPAR agonist (pioglitazone) had the greatest effect on changes in the CL proteome**

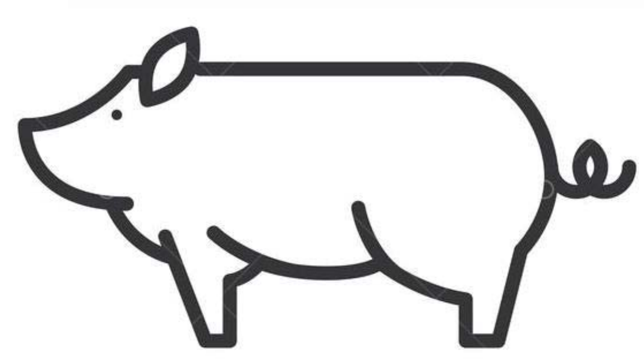

This research was funded by National Science Centre, Poland, grant no. 2017/27/N/NZ9/00907

TRANSCRIPTOMIC PROFILE OF OVIDUCTAL ISTHMUS IN PIGS ON DAYS 2 TO 3 OF PREGNANCY

M. MARTYNIAK[1*], E. WASZKIEWICZ[1], A. FRANCZAK[1], G. KOTWICA[1]
Department of Animal Anatomy and Physiology, Faculty of Biology and Biotechnology, University of Warmia and Mazury, Olsztyn, Poland;
*marcin.martyniak@uwm.edu.pl

INTRODUCTION AND OBJECTIVE

The proper activity of oviducts is crucial for fertilization, embryo development and its transfer to the uterus. It was hypothesized that the presence of embryos in the pig oviducts may evoke alterations in transcriptomic profile of oviductal isthmus.

METHODS

The transcriptomic profile of oviductal isthmus was determined in pigs on Days 2-3 of pregnancy and compared with the transcriptome of the tissue during Days 2-3 of the estrous cycle. The Porcine (V2) Expression Microarrays 8×60K were used. Different expressed genes (DEGs) were categorized in functional pathways.

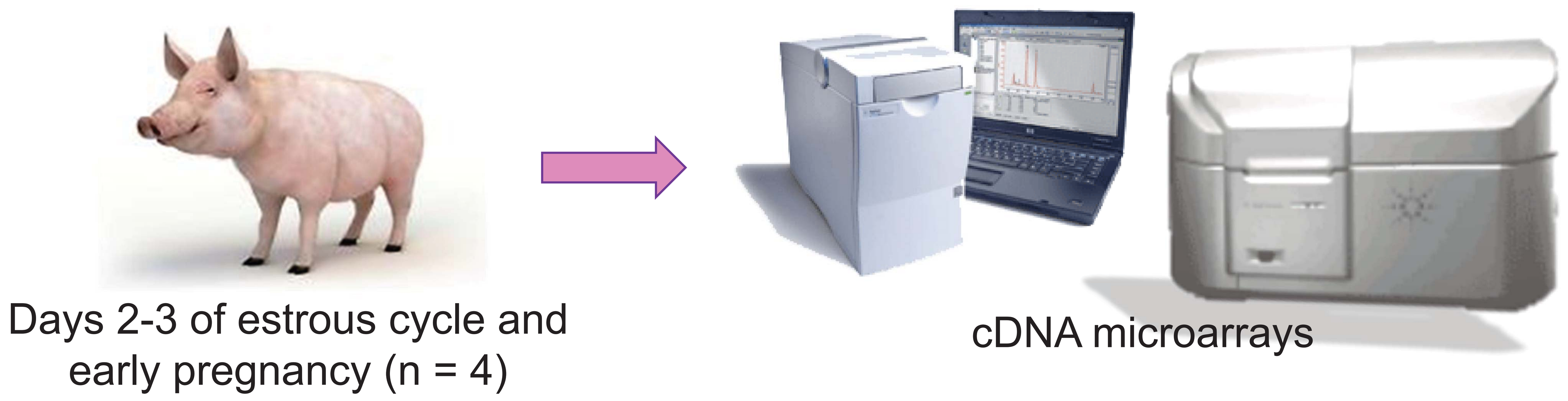

RESULTS AND CONCLUSION

The analysis indicated 1.91 % DEGs (P ≤ 0.05; Fold-change ≥ 2.0) in ampulla and isthmus from which 1.33 % was changed in isthmus (Fig. 1). Analysis of the relationships among DEGs in isthmus on Days 2-3 of pregnancy showed that altered genes are mainly involved in the regulation of endocrine and immune functions, signal transduction and molecule interaction (Fig. 2). The largest amount of DEGs was involved in environmental information processing.

Fig. 1. Number of affected genes in the ishmus.

Type of change	Isthmus	
	Number of affected genes	% of changed genes regarding number of sequences on microarray*
Up-regulated	274	0.44
Down-regulated	562	0.89
Sum	836	1.33

** assuming that the total number of sequences in the microarray is 62 976*

Fig. 2. Selected DEGs categoriezd in functional pathways.

	KEGG category	KEGG subcategory	KEGG pathways	*P*-value	Fisher exact	Altered genes
Up-regulated genes	Organismal Systems	Endocrine system	Oxytocin signaling pathway (ssc04921)	2,20E-01	9,70E-02	RGS2, CACNA2D2, KCNJ3, MYLK, MYL9
		Immune system	Leukocyte transendothelial migration (ssc04670)	2,80E-01	1,20E-01	CXCR4, RAP1A, CXCL12, MYL9
	Environmental Information Processing	Signaling molecules and interaction	Cytokine-cytokine receptor interaction (ssc04060)	2,20E-01	1,10E-01	CCL2, CXCR4, **TGFB3,** CXCL12, IFNGR1, GHR
		Signal transduction	TGF-beta signaling pathway (ssc04350)	3,50E-01	1,30E-01	**TGFB3**, DCN, MYC
			Jak-STAT signaling pathway (ssc04630)	3,90E-01	1,90E-01	**SOCS1**, MYC, IFNGR1, GHR
Down-regulated genes	Organismal Systems	Endocrine system	Progesterone-mediated oocyte maturation (ssc04914)	1,70E-01	6,60E-02	FZR1, RPS6KA3, HSP90AA1, CPEB3, ADCY6
			Oxytocin signaling pathway (ssc04921)	3,20E-01	1,70E-01	CDKN1A, ROCK1, ADCY6, **OXTR**, CACNB2, PPP3CA
			Prolactin signaling pathway (ssc04917)	4,90E-01	2,30E-01	**ESR1**, STAT3, CSN2
		Immune system	Leukocyte transendothelial migration (ssc04670)	1,60E-01	6,80E-02	ROCK1, AFDN, ESAM, ACTN2, CXCL12, PTPN11

It was concluded that the presence of embryos induces alterations in transcriptomic profile of selected genes (eg. TGFβ, OXTR, ESR1) which may be involved in regulation of reproductive processes in the porcine oviductal isthmus on Days 2-3 of pregnancy.

The study was funded by National Science Centre, Poland; Preludium Grant no. 2016/23/N/NZ9/02163

THE EFFECT OF SATURATED FATTY ACIDS ON GnRH-INDUCED GONADOTROPIN SECRETION FROM ANTERIOR PITUITARY CELLS OF PUBESCENT EWE LAMBS

N. SZYSIAK, A. FURMAŃCZYK-GNYP, B. SURÓWKA, B. SZYMCZAK, N. MINAKOW, U. KOSIOR-KORZECKA*
Department of Preclinical Veterinary Sciences, Faculty of Veterinary Medicine, University of Life Sciences in Lublin, Poland,
corresponding author: urszula.korzecka@up.lublin.pl

There are some reports showing that fatty acids may be involved in modulation of pituitary hormones secretion. Recently we found that in ewe lambs born to obese sheep carrying twins or triplets, high plasma level of saturated fatty acids (SFA) was in positive correlation with the delay in puberty. Delay in puberty in young ewes is correlated with high plasma palmitate and stearate level. Taking into account that the relationship between SFA and gonadotropin secretion from the ovine pituitary cells isolated from pubescent ewe lambs is not established, we resolved to study the direct effect of SFA on luteinizing hormone (LH) and follicle stimulating hormone (FSH) secretion stimulated with gonadotropin releasing hormone (GnRH *) in vitro*.

Aim of study

Our research was focused on studying the effect of SFA on GnRH-induced LH and FSH secretion by ovine pituitary gland. We also analysed the effect of saturated fatty acids on nitric oxide (NO) release and the relationship between NO and gonadotropin secretion under the influence of SFA.

Material and methods

Pituitary glands were isolated from 7 months old ewe lambs. Pituitary cells were cultured in McCoy 5A medium without GnRH and SFA (negative control), with GnRH only (positive control), with GnRH and 10^{-9}-10^{-3} M/l of the butyric (C4:0), caprylic (C8:0), lauric (C12:0), palmitic (C16:0) or stearic acid (C18:0), or with GnRH and 10^{-9}-10^{-3} M/l of the aforementioned SFA with L-arginine or L-NAME. After 2 or 6h of exposure to SFA followed by 2, 6, 12, 18, 24 or 30h incubation, the media for LH and FSH analysis were collected. Concurrently, NO release and the proliferation index of control and treated cells were determined.

Results

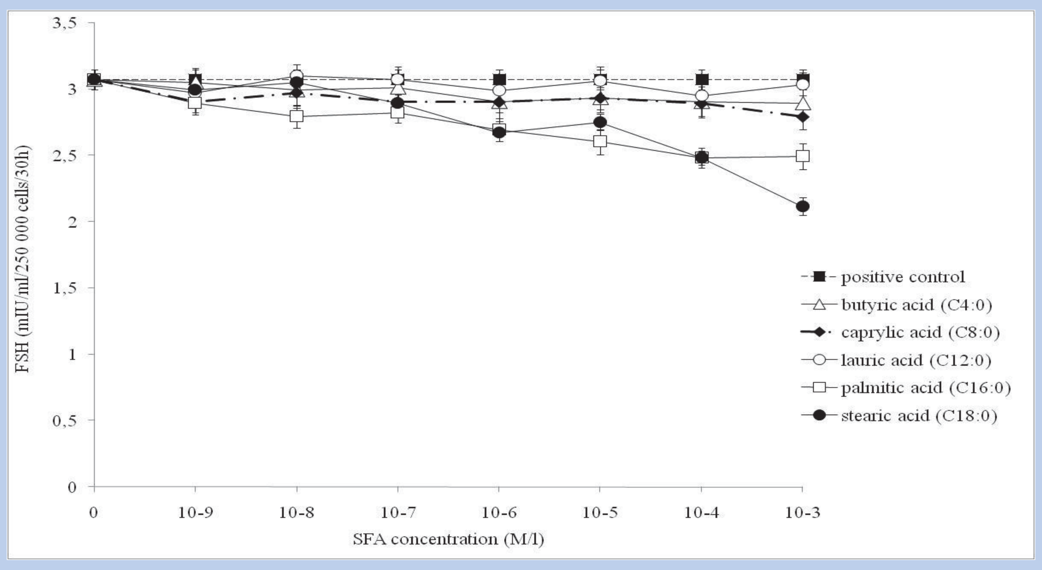

Fig.1. Changes in follicle-stimulating hormone secretion by ovine pituitary cells *in vitro* after 2-hour exposure to saturated fatty acids

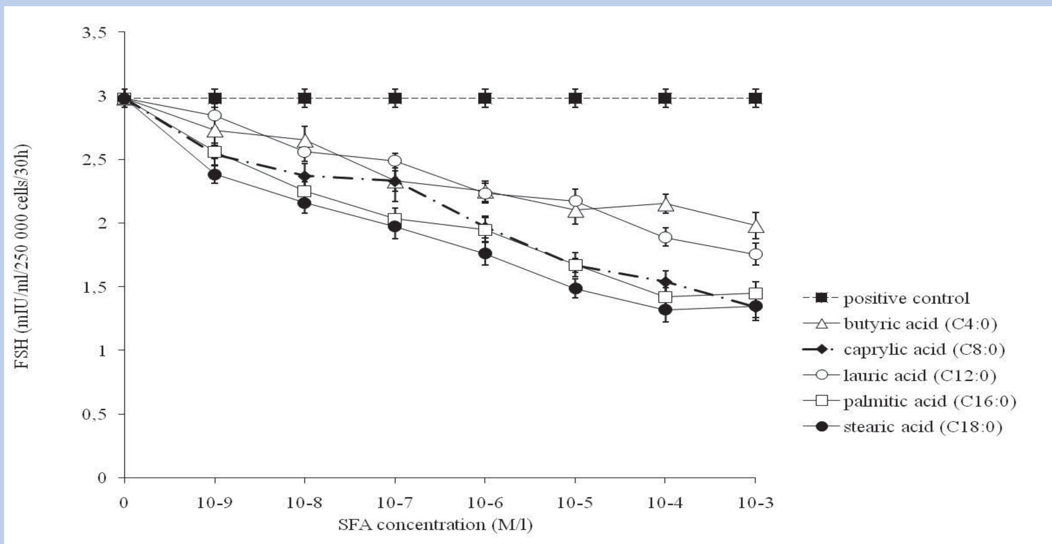

Fig.2. Changes in follicle-stimulating hormone secretion by ovine pituitary cells *in vitro* after 6-hour exposure to saturated fatty acids

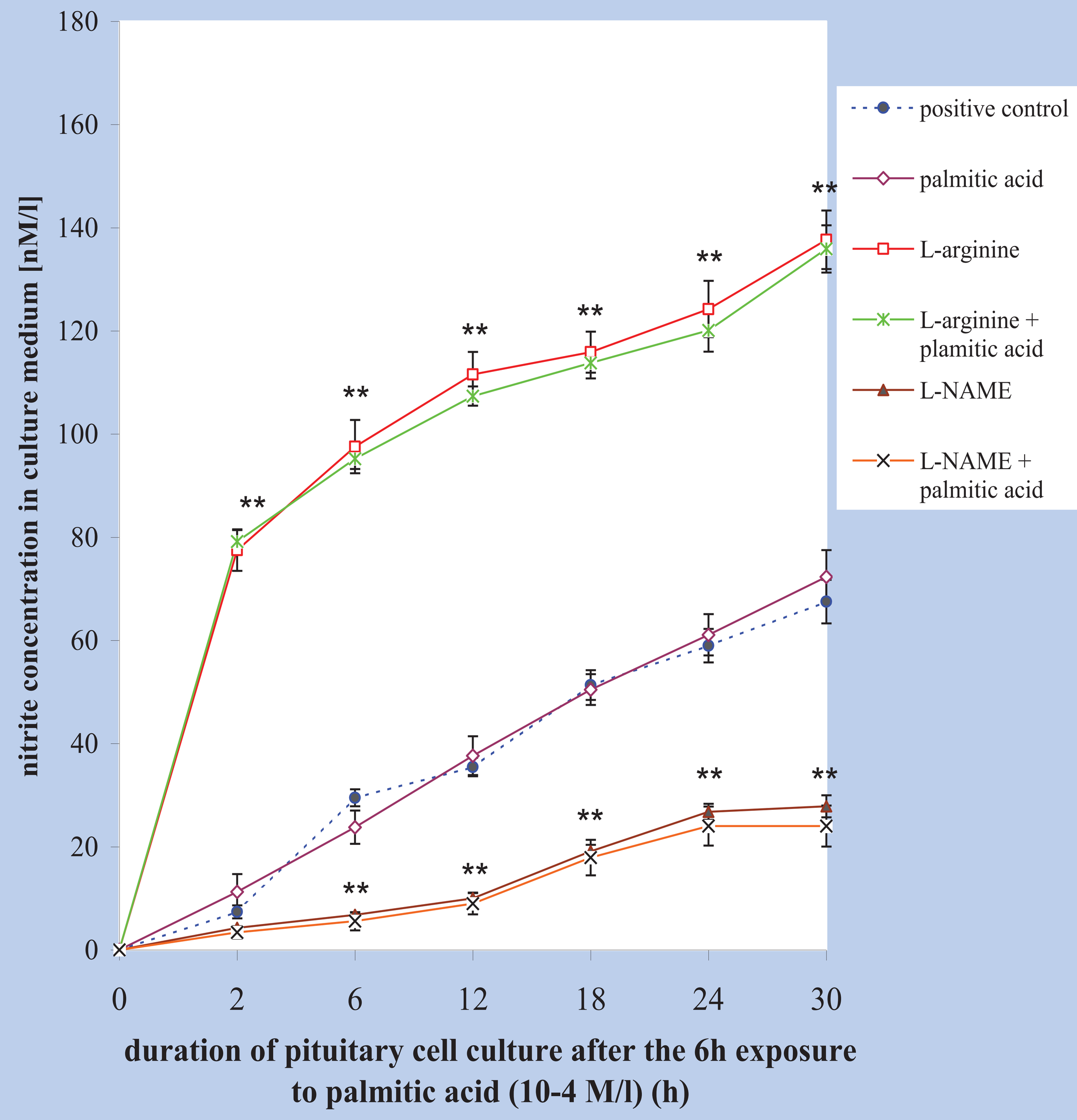

Fig.5. The effect of 6h exposure of ovine pituitary cells to palmitic acid (10^{-4} M/l) on NO release *in vitro.*
*- the significant (P≤0.05) difference in comparison to the positive control

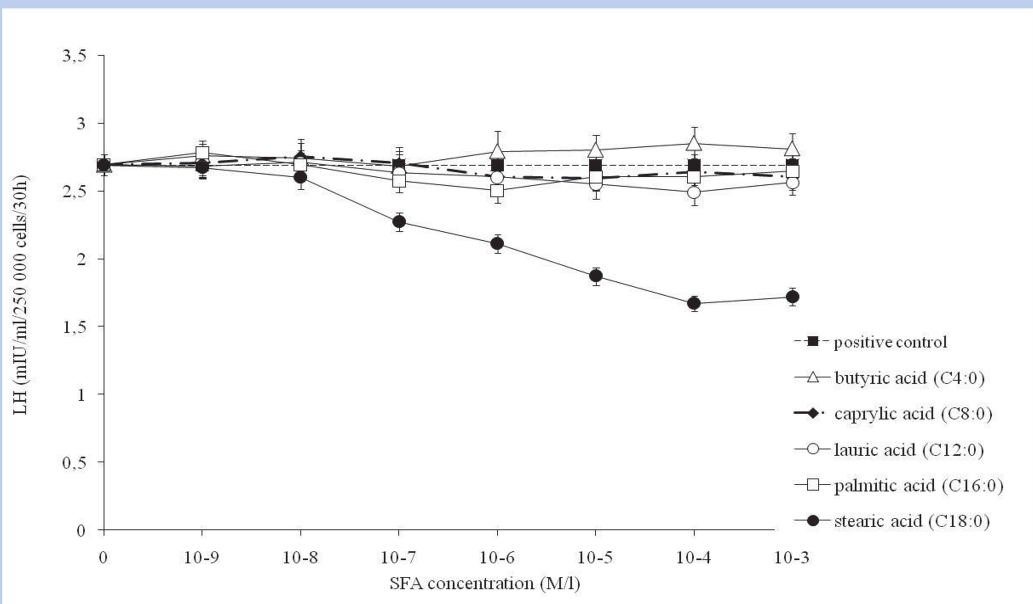

Fig.3. Changes in luteinizing hormone secretion by ovine pituitary cells *in vitro* after 2-hour exposure to saturated fatty acids

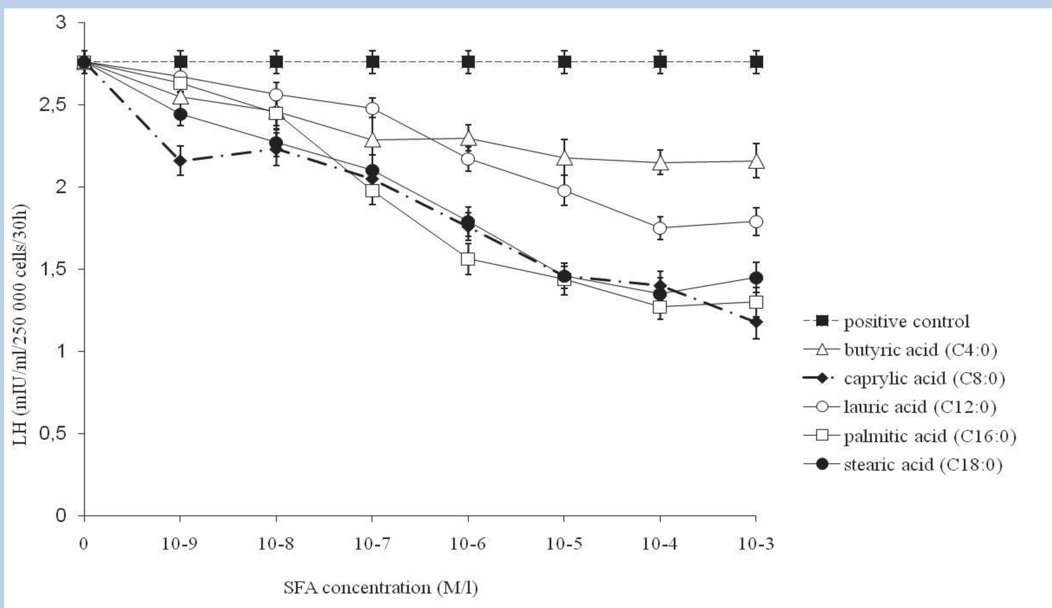

Fig.4. Changes in luteinizing hormone secretion by ovine pituitary cells *in vitro* after 6-hour exposure to saturated fatty acids

Conclusions

1. Saturated fatty acids (butyric (C4:0), caprylic (C8:0), lauric (C12:0), palmitic (C16:0) and stearic acid (C18:0)) reduced GnRH-induced LH as well as GnRH-induced FSH secretion from ovine pituitary cells *in vitro* in comparison to the positive control.
2. The most significant (P≤0.05) suppression in gonadotropin secretion was observed after the 6h exposure of cells to 10^{-3} M/l of caprylic acid, 10^{-4} M/l of palmitic acid and 10^{-4} M/l of stearic acid.
3. SFA used in the experiment did not change significantly NO release both in control and L-NAME or L-arginine treated ovine pituitary cells.
4. There was no significant correlation between gonadotropin secretion and NO release under the influence of SFA.

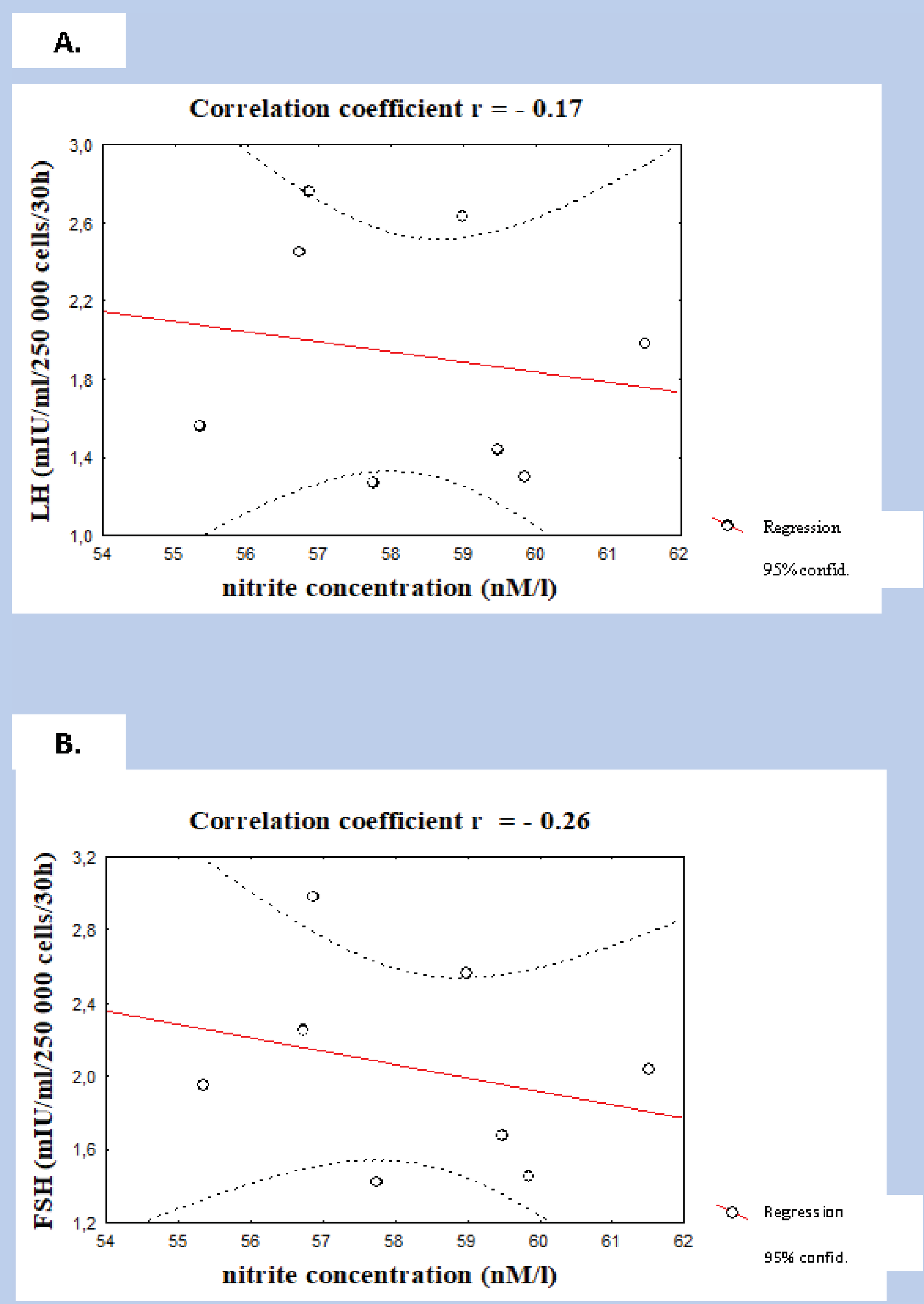

Fig. 6. Relationship between NO (expressed as nitrite concentration in culture medium) and GnRH-induced LH (A) or FSH (B) secretion from ovine pituitary cells after the 6h exposure to palmitic acid *in vitro.*

References
1. Briard N., Rico-Gomez M., Guillaume V., Sauze N., Vuaroqueaux V., Dadoun F., Le Bouc Y., Oliver C., Dutour A.: Hypothalamic mediated action of free fatty acid on growth hormone secretion in sheep. Endocrinology 1998, 139, 4811-4819.
2. Kosior-Korzecka U., Bobowiec R.: Leptin effect on nitric oxide and GnRH-induced FSH secretion from ovine pituitary cells *in vitro*. J. Physiol. Pharmacol. 2006, 57, 637-647.
3. Kosior-Korzecka U. The effect of leptin on LH secretion from ovine pituitary cells *in vitro*. In Hormonal changes and expression of leptin receptor mRNA in pituitary cells of sheep with ACTH induced ovarian cysts, U. Kosior-Korzecka. Lublin, University of Life Sciences in Lublin Publishing House, 2008, 36-39; 53 - 58.
4. Matsunaga N., Goka T., Nam K.T., Oda S., Ohneda A., Sasaki Y.: Inhibition of GH re leasing factor (GRF)-induced GH secretion by intraruminal infusion of volatile fatty acids (VFA) in sheep. Endocr. J. 1997, 44, 133-140.
5. Mattos R., Staples Ch.R., Thatcher W.W.: Effects of dietary fatty acids on reproduction in ruminants. Rev. Reprod. 2000, 5, 38-45.

Dietary supplementation with nettle induces apoptosis and affects folliculogenesis in the rabbit ovary

SESSION XI

K. KAMIŃSKA[1], K. KAPUSTA[1], S. PAŁKA[2], M. KMIECIK[2], J. ZUBEL-ŁOJEK[3], M. GRZESIAK[1]

[1]Department of Endocrinology, Institute of Zoology and Biomedical Research, Jagiellonian University in Cracow, Cracow, Poland;
[2]Department of Genetics, Animal Breeding and Ethology, University of Agriculture in Cracow, Cracow, Poland;
[3]Department of Animal Physiology and Endocrinology, University of Agriculture in Cracow, Cracow, Poland

Introduction

Nettle
(*Urtica dioica L.*) [3]

- Nettle is a herbaceous plant belonging to the family Urticaceae.
- Its leaves and roots contain flavonoids, phenolic acid, carotenoids, lectins, polysaccharides, sterols, lignans, vitamins and minerals [1].
- It has anti-proliferative, anti-inflammatory, antioxidant, antidiabetic actions [2].
- Clinical studies suggest beneficial effects of nettle supplementation on reproductive disturbances in women.

Aim

The aim of this study was to determine the effect of dietary supplementation with nettle on folliculogenesis in 12-week-old rabbit ovaries

Materials and Methods

20 rabbits ♀
5-week-old
(*A Termond White rabbit*)

I group (n=10) — Control diet

II group (n=10) — Diet with addition of 1% nettle

Slaughter at 12 weeks of age

Blood collection — *RIA analysis of steroid concentration*

Ovaries collection — *Histology, Immunohistochemistry, TUNEL assay, Western blot*

Results

Effect of nettle on ovarian histology

Treatment	Follicle number (mean ± SEM)				
	Primordial	Primary	Secondary	Early antral	Antral
Control	148,44 ± 52,09 ᵃ	5,7 ± 2,83 ᵃ	18,5 ± 8,62 ᵃ	4,0 ± 2,67 ᵃ	4,6 ± 1,12 ᵃ
Nettle	101,5 ± 22,82 ᵇ	10,83 ± 3,19 ᵇ	17,33 ± 5,92 ᵃ	0,83 ± 1,17 ᵇ	6,17 ± 1,94 ᵃ

(P< 0,05; Dunn's multiple comparison test).

Effect of nettle on plasma steroid concentrations

Treatment	Plasma		
	P4 (ng/ml)	T (ng/ml)	E2 (pg/ml)
Control	3,46 ± 0,28 ᵃ	0,16 ± 0,01 ᵃ	25,04 ± 0,53 ᵃ
Nettle	2,82 ± 0,18 ᵃ	0,20 ± 0,08 ᵃ	47,33 ± 1,22 ᵃ

(P < 0.05; Dunn's multiple comparison test).

Effect of nettle on ovarian cell apoptosis

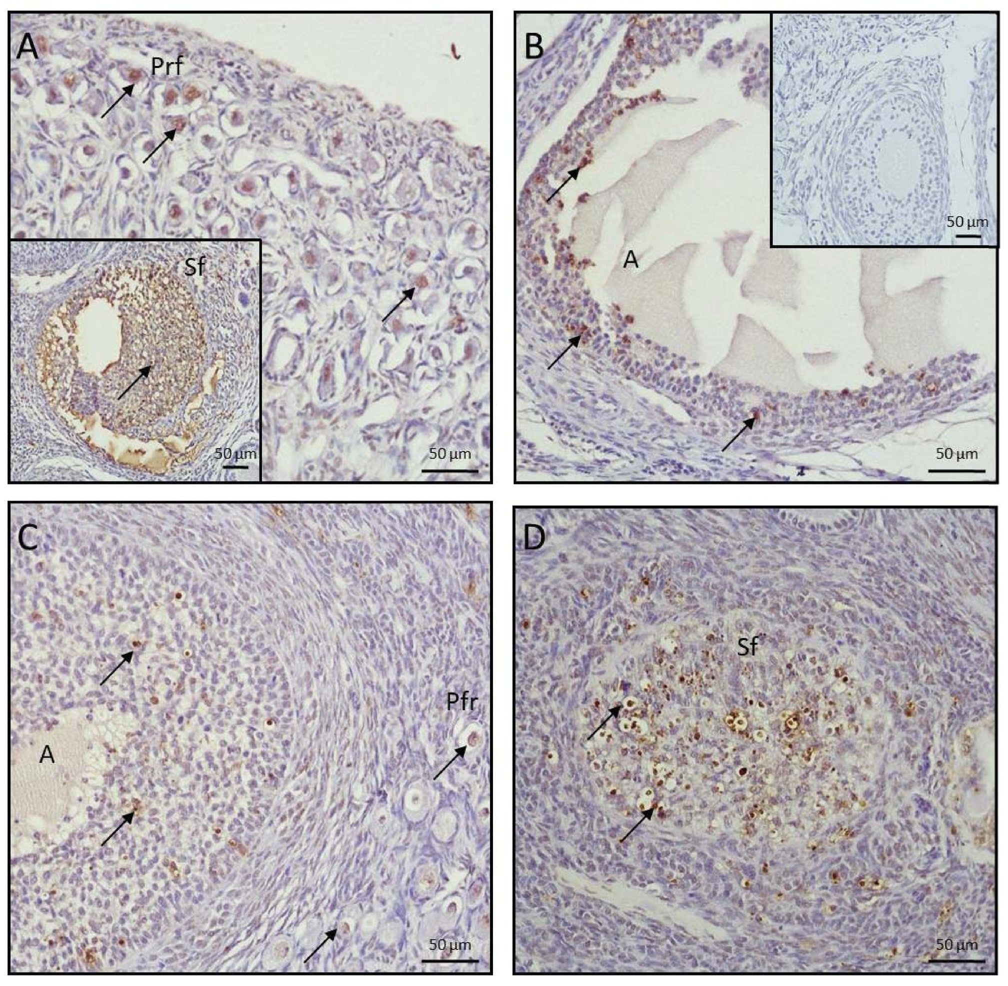

In situ **detection of apoptotic cells in ovaries obtained from 12-week-old rabbits of the control group (A, B) and fed with addition of nettle (C, D).** Arrows indicate apoptotic cells that are oocytes within primordial follicles (PrF) or granulosa cells in secondary (Sf) and antral (A) follicles. A negative control (B, inset).

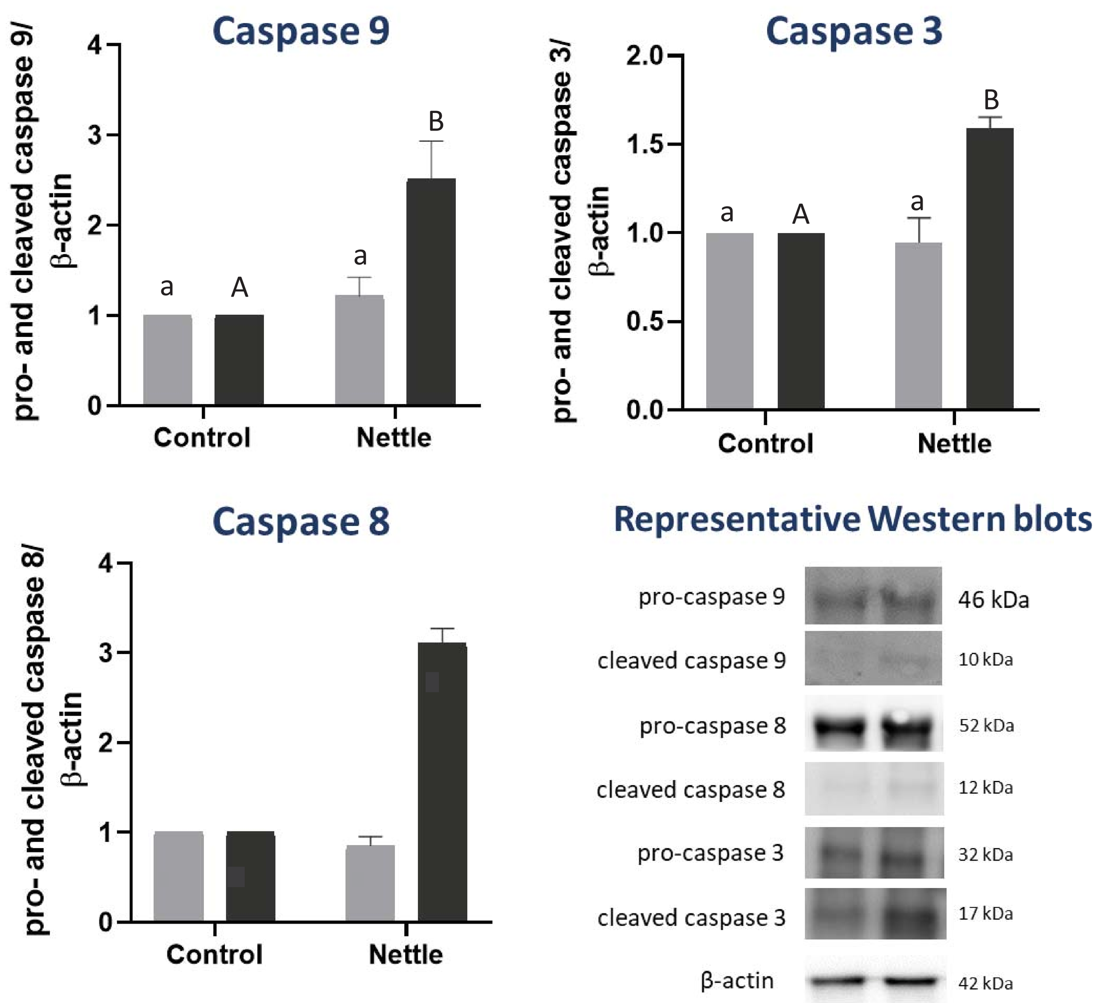

Western blot analysis of pro- and cleaved caspase 9, 8 and 3 protein abundance in ovaries obtained from 12-week-old rabbits of the control group and supplemented with nettle. Grey bars: pro-caspases, black bars: cleaved caspases.
(P < 0.05; Dunn's multiple comparison test).

Treatment	Atretic follicle number (mean ± SEM)		
	Primordial	Secondary	Antral
Control	59 ± 5,96 ᵃ	2,25 ± 0,63 ᵃ	1,25 ± 0,25 ᵃ
Nettle	54,75 ± 4,82 ᵃ	6,67 ± 0,88 ᵇ	0,75 ± 0,48 ᵃ

The number of atretic follicles in rabbit ovaries from the control group and supplemented with nettle. (P< 0,05; Dunn's multiple comparison test).

Effect of nettle on ovarian cell proliferation

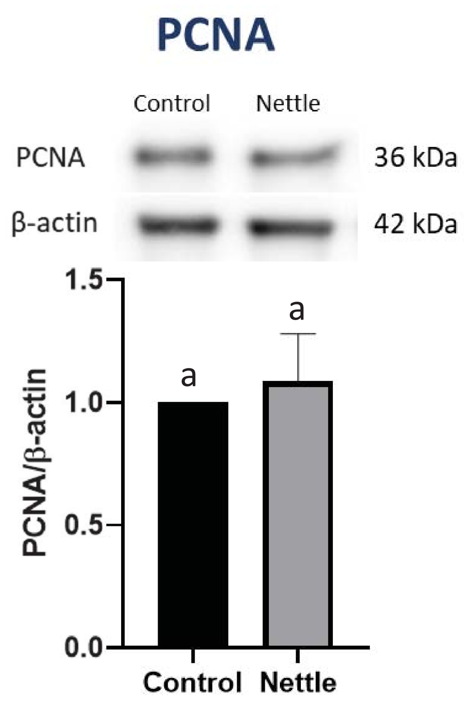

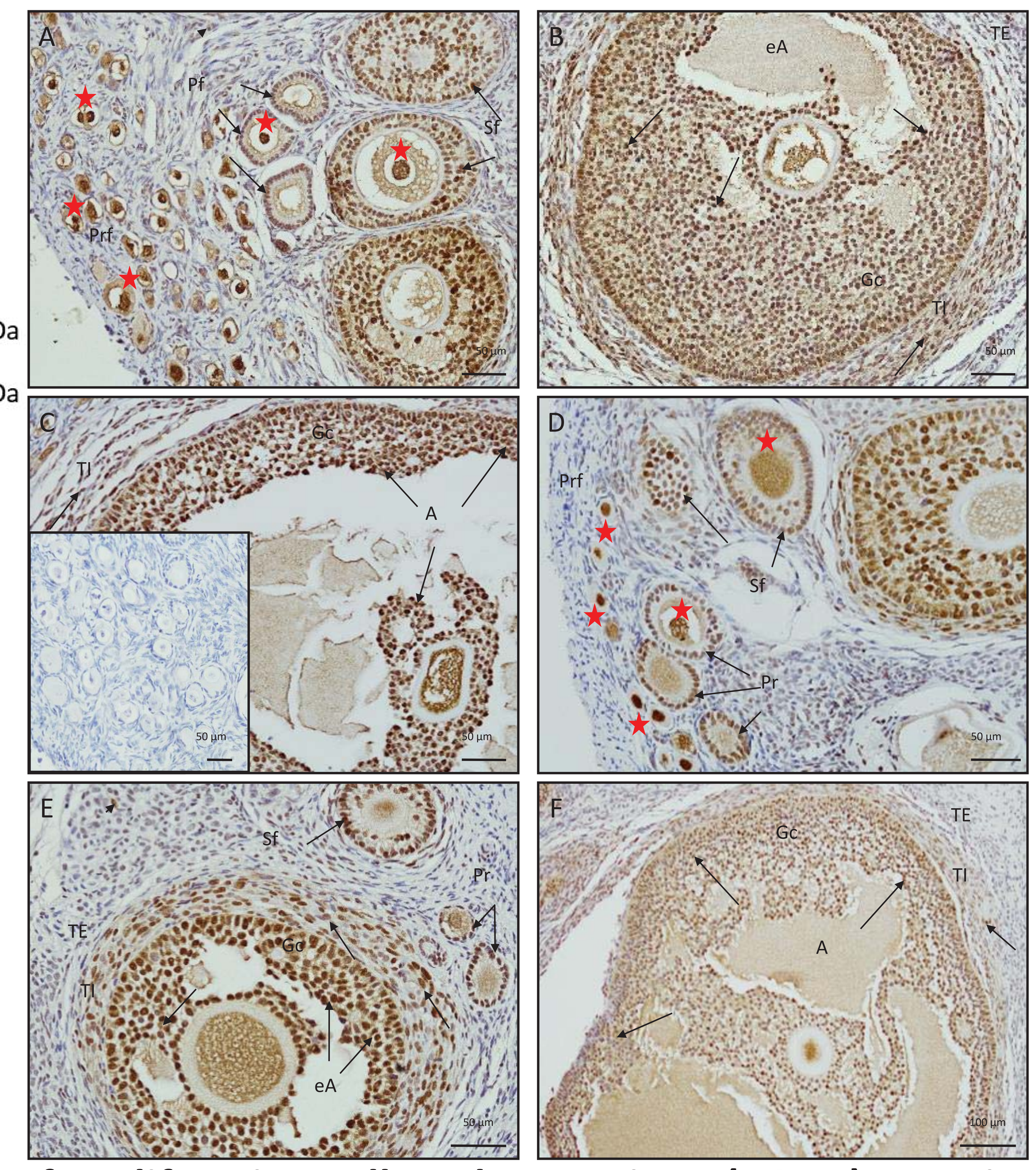

Western blot analysis of proliferating cell nuclear antigen (PCNA) protein abundance and immunohistochemical localization of PCNA-positive cells in ovaries obtained from 12-week-old rabbits of the control group (A-C) and fed with addition of nettle (D-F). Nuclear PCNA staining was observed in stroma cells (A, E; arrowheads), oocytes (red asterisks) of primordial (Pfr), primary (Pf) and secondary (Sf) follicles (A, D), in the granulosa cells (black arrows) of Pf, Sf, early antral (eA) and antral (A) follicles as well as theca interna cells (black arrows) of eA and A. Gc, granulosa cells; TI, Theca interna; TE, theca externa. A negative control (C, inset).
(P < 0.05; Dunn's multiple comparison test).

Conclusions

- Nettle affected follicle development in a stage specific manner and it seems to accelerate the initial recruitment of primordial follicles to growth and increase the artresia of secondary follicles.
- Nettle had an apoptotic effect in ovarian cells through the activation of caspase-mediated pathways.

REFERENCES: [1] Said AAH, Otmani ISE, Derfoufi S, Benmoussa A. Int J Pharm Pharmaceut Sci 2015;7:8-14; [2] Chrubasik JE, Roufogalis BD, Wagner H, *et al.* Phytomedicine 2007;14:423-55; [3] https://syberianhealth.com/pl/rosliny-lecznicze/urtica-dioica-l-89

CHEMERIN IMPACT ON DIFFERENTIALLY EXPRESSED GENES IN THE ENDOMETRIAL TRANSCRIPTOME OF PIGS DURING PERIIMPLANTATION PERIOD

K. BORS [1], G. KOPIJ [1], L. PAUKSZTO [2], M. KIEZUN [1], E. RYTELEWSKA [1], K. KISIELEWSKA [1], M. GUDELSKA [1], K. SZYMANSKA [1], K. DOBRZYN [1], E. ZAOBIDNA [1], J. JASTRZEBSKI [2], T. KAMINSKI [1], N. SMOLINSKA [1]

[1]Department of Animal Physiology and Anatomy; [2]Department of Plant Physiology, Genetics and Biotechnology; Faculty of Biology and Biotechnology, University of Warmia and Mazury, Olsztyn, Poland; kinga.bors@uwm.edu.pl

INTRODUCTION

Chemerin (CHEM) is one of many biologically active proteins secreted by the adipose tissue involved in the regulation of the energy homeostasis of the organism. In the present study, RNA-Seq was performed to investigate the expression of protein-coding (mRNAs) transcripts in the *in vitro* cultured porcine endometrial slices collected during implantation (days 15 to 16 of gestation) exposed to CHEM (400 ng/ml).

METHODS

To identify the expression profiles of the treated tissues, the cDNA libraries were performed by TruSeq Stranded Total RNA with Ribo-Zero H/M/R Kit (Illumina, USA) and the transcriptomes high-throughput sequencing was performed on the Illumina NovaSeq 6000 platform (Illumina, USA). All reads were trimmed to equal length (120 bp) and mapped to the pig reference genome with ENSEMBL annotation (Sscrofa11.1.99) using the STAR mapper v. 2.7.1a. To identify the differentially expressed genes (DEGs), we applied the DESeq2 method with correction of batch effect using Surrogate Variable Analysis library. To validate the obtained RNA-Seq results, eight DEGs were selected for Quantitative real-time PCR (qPCR) proceeded by cDNA synthesis using the same RNA as in the RNA-Seq.

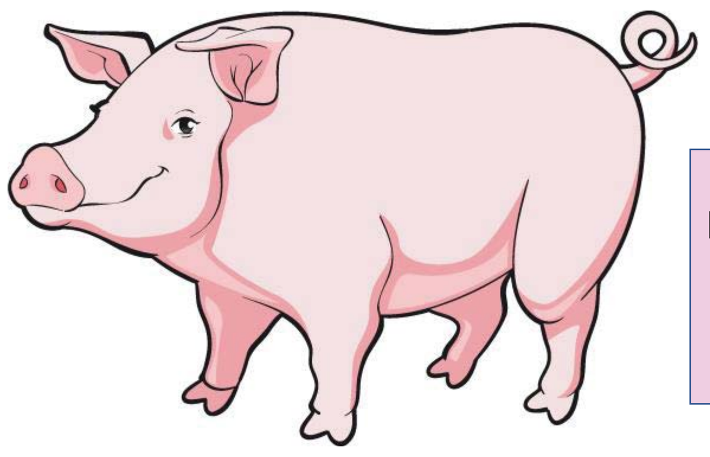

Porcine endometrium on 15 to 16 days of pregnancy (implantation) (n = 5) treated with CHEM → Total RNA isolation → RNA library preparation and High-throughput sequencing → Mapping reads to reference genome → Differentially expressed genes (DEGs)

RESULTS

In the current study, among all 130 DEGs, 58 were up-regulated and 72 were down-regulated in the CHEM-treated group. DEGs were assigned to 73 functional annotations. The products of above genes take part in many processes, important for the implantation, such as intense tissue remodeling, cell adhesion, angiogenesis, immune response and steroidogenesis. The qPCR expression patterns of all validated DEGs were in agreement with RNA-Seq results and confirmed the veracity of the high-throughput methods used in the present study.

CONSLUSIONS

CHEM affects the transcriptomic profile of the porcine endometrium, controlling the expression of various genes, including those involved in cell migration and adhesion process, angiogenesis, inflammation, and steroidogenesis. It can be assumed that CHEM may be essential to a proper course of gestation and embryo development.

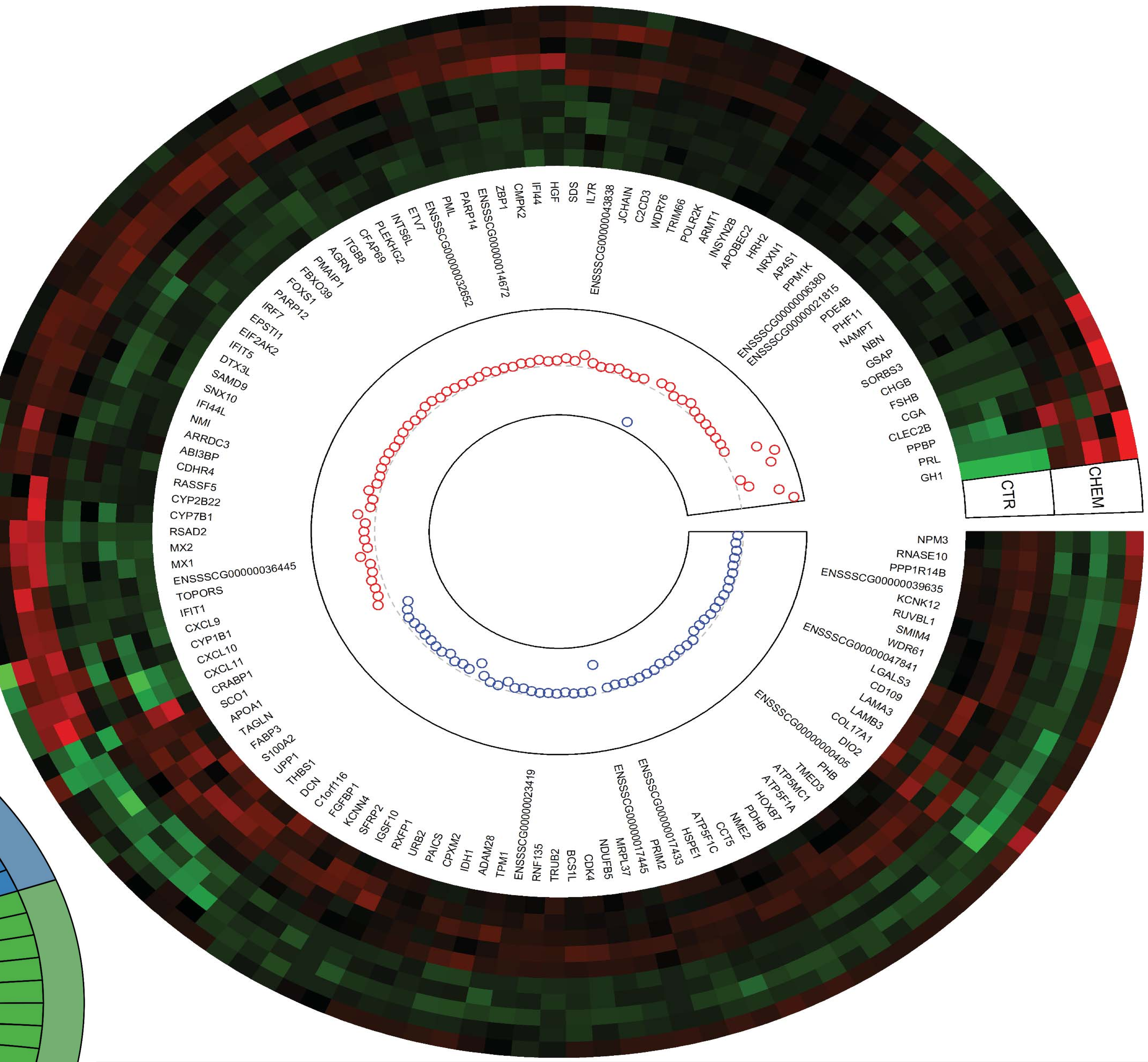

Fig. 1. Visualization of differentially expressed genes (DEGs) statistically significant (P-adjust < 0.05) in the impact of CHEM. The external circle represents the gene ID (gene names or ENSEMBL ID) of DEGs. Five tracks depict the normalized (Z-score; red-green scale) expression values for DEGs. The circles in the next track describe increased (red) and decreased (blue) expression (logFC) in the compared groups.

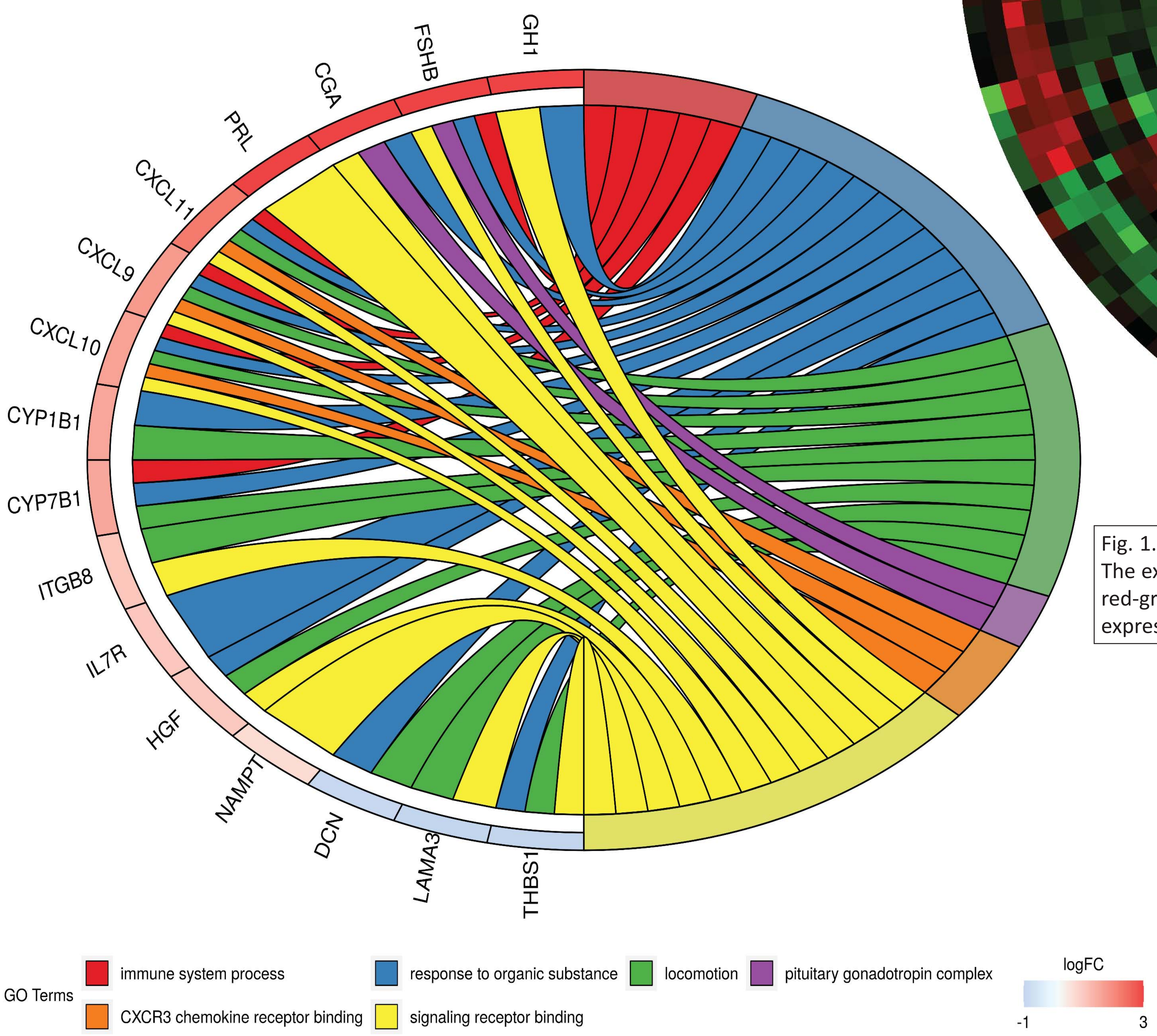

Fig. 2. Visualization of the differentially expressed genes (DEGs) statistically significant (P-adjust < 0.05) and their participation in the ontology terms detected during Gene Ontology (GO). The tracks show the pathways between the selected DEGs and GO terms evaluated in the endometrium treated with CHEM. Red links depict positive correlation and blue negative.

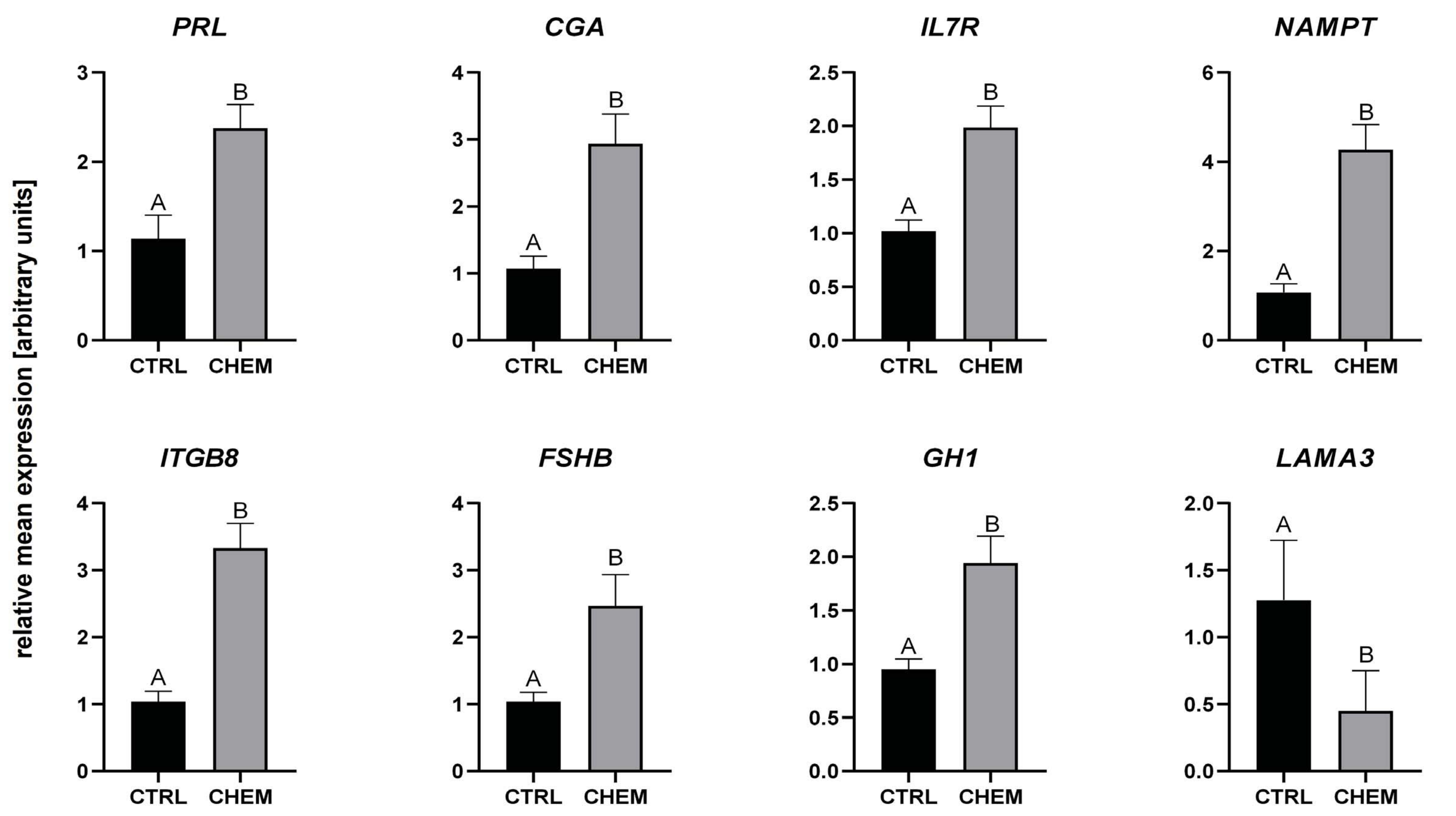

Fig. 3. Real-time PCR validation of the RNA-seq results for DEGs in the endometrium. Validation was performed for *PRL, CGA, IL7R, NAMPT, ITGB8, FSHB, GH1* and *LAMA3* genes with reference genes (*GAPDH* and *PPIA*) (p-value < 0.05). CTRL—samples from the control groups; CHEM—samples from the CHEM-treated groups.

This research was supported by National Science Centre (Projects No: 2017/25/B/NZ9/00040). Kinga Bors is a recipient of a scholarship from the Programme Interdisciplinary Doctoral Studies in Biology and Biotechnology (POWR.03.05.00-00-Z310/17), which is funded by the European Social Fund. "Development Program of the University of Warmia and Mazury in Olsztyn", POWR.03.05.00-00-Z310/17, co-financed by the European Union under the European Social Fund from the Operational Program Knowledge Education Development.

THE EFFECT OF TYPE 1 DIABETES AND HIGH FAT DIET ON THE EXPRESSION OF RECEPTOR FOR ADVANCED GLYCATION END-PRODUCTS (RAGE) IN MOUSE UTERUS

K. ZGLEJC-WASZAK[1], A. KORYTKO[1], J. WOJTKIEWICZ[1], K. WĄSOWICZ[2], J. K. JURANEK[1]

[1]University of Warmia and Mazury in Olsztyn, School of Medicine, Collegium Medicum, Department of Human Physiology and Pathophysiology, Warszawska 30, 10-082 Olsztyn, Poland

[2]University of Warmia and Mazury in Olsztyn, Faculty of Veterinary Medicine, Department of Pathophysiology, Oczapowskiego 13, 10-700 Olsztyn, Poland

corresponding author: kamila.zglejc@uwm.edu.pl

INTRODUCTION

The uterus is an essential organ for reproduction in mammals. A growing body of literature has shown that diabetes mellitus (DM) and high-fat diet (HFD) affect female reproductive functions. Moreover, DM and HFD are associated with a chronic low-grade inflammatory state that is involved in the development of associated metabolic complications. We hypothesize that hyperglycemic and high fat milieu may activate Advanced Glycation End-Products (AGEs) molecular pathway in mouse uterus. Receptor for Advanced Glycation End-products (RAGE) is involved in multiple processes related to host immunity, vascular regulation, and inflammatory damage in various disease states. Moreover, RAGE is expressed in nearly all tissues in mammals, with large quantities in lungs.

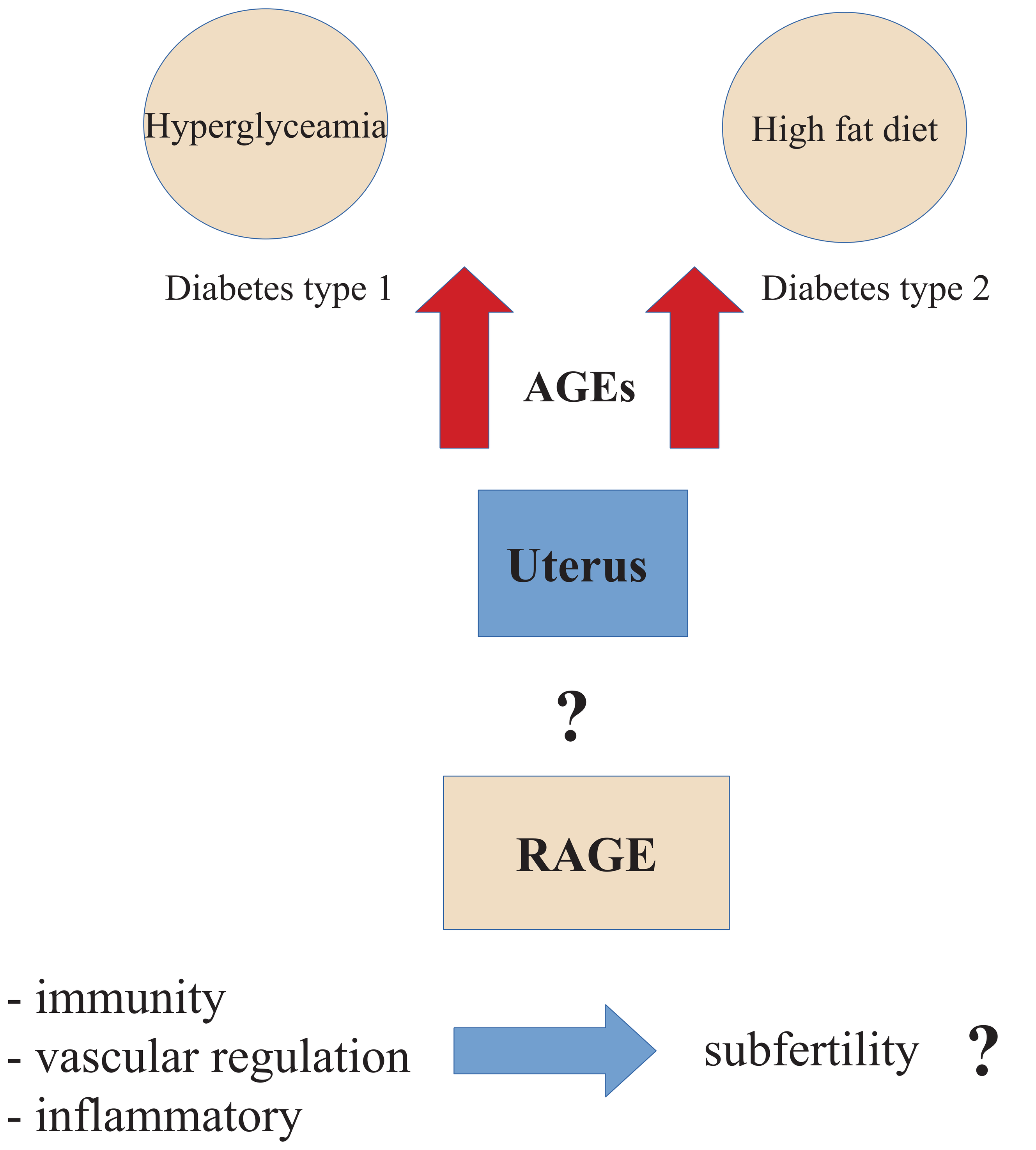

AIM

The aim of the study was to determine the expression of RAGE protein in uterine tissues harvested from female mice with DM1 and female mice fed HFD or normal diet.

METHOD

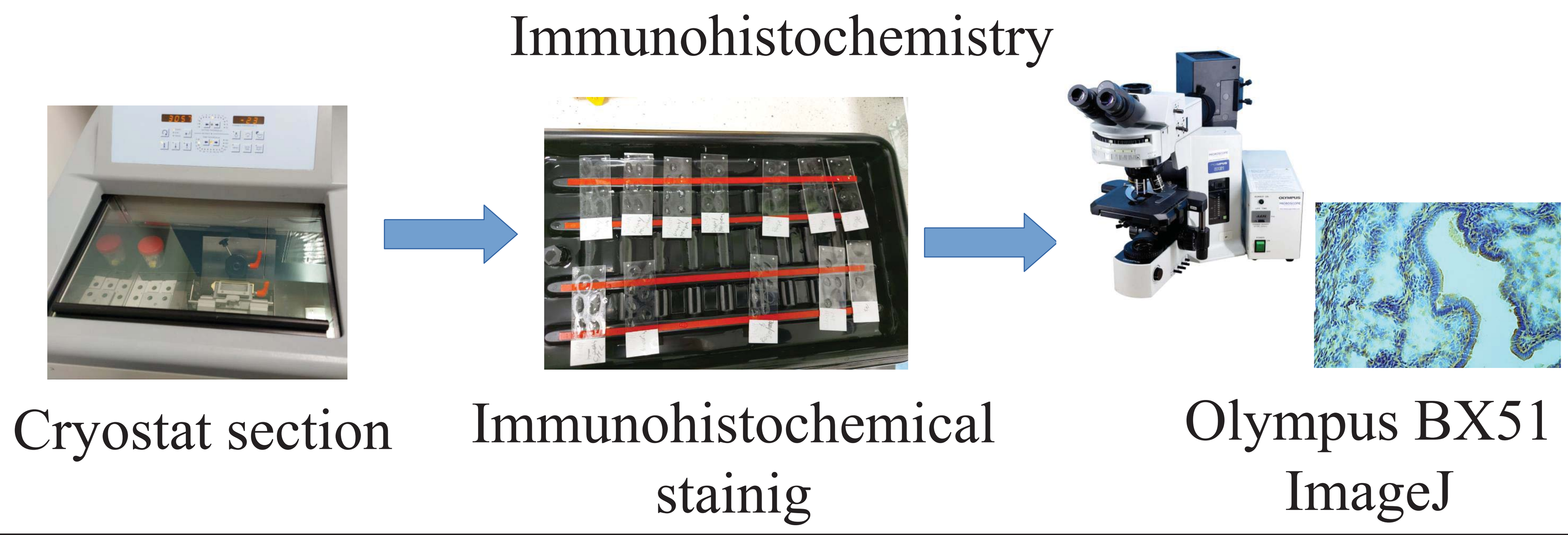

RESULTS

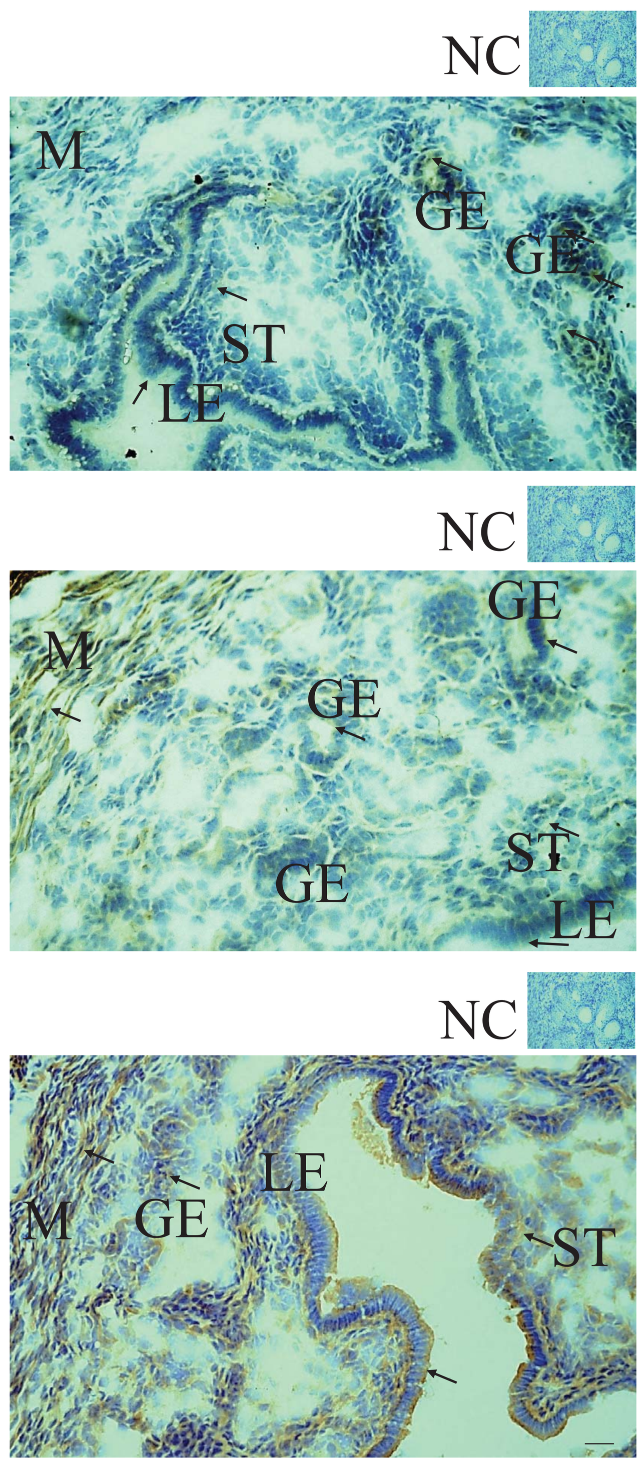

The localization of RAGE in the mouse uterus. Exemplary areas of immunoreactivity are marked with arrows. Pictures were taken at magnification ×400.

The presence and intracellular localization of RAGE protein in luminal epithelial (LE), stromal (ST), glandular epithelium (GE) and myometrium (M) cells was confirmed. NC – negative control, only goat serum.

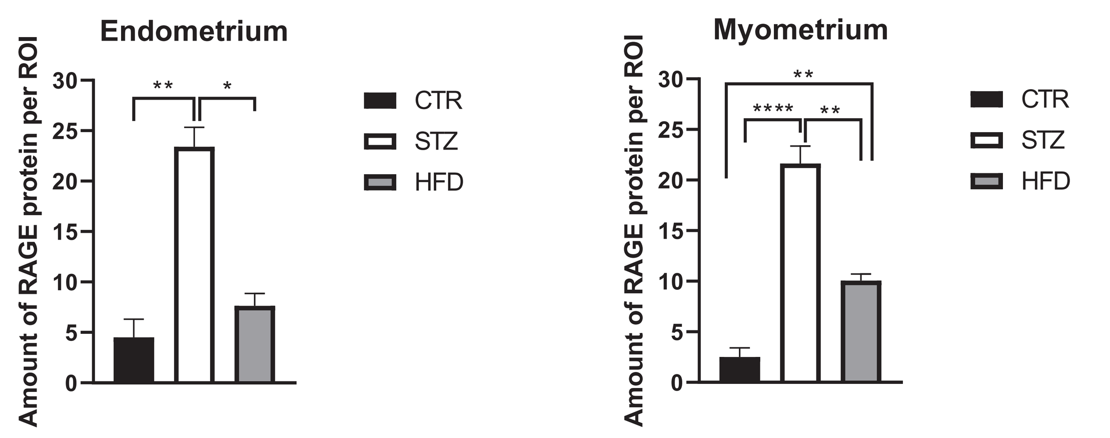

**** $P \leq 0.0001$, ** $P \leq 0.01$, * $P \leq 0.05$
Statistical analysis was performed by Student's t-test. The mean ± SEM is reported.

The highest expression of RAGE was observed in uterine tissues of STZ (DM1) mice. Myometrial expression of RAGE was increased in HFD in comparison to control group. CTR – control group.

CONCLUSIONS

- These data suggest the presence of an altered uterine environment in females with DM1 and HFD and indicate that elevated uterine level of RAGE may detrimentally impact endometrial and myometrial function during estrous cycle.

- We might speculate that DM 1 and HFD could modulate local immune system and activate the AGE-RAGE signaling pathway in uterine tissues during estrous cycle.

MATERIAL

♀

C57BL/6
n = 5
female mice fed normal diet *ad libitum* for 32 weeks (Labofeed B, Morawski, Poland) – control (CTR) mice

C57BL/6
n = 5
intraperitoneal injection of 50 mg/kg streptozotocin (STZ) diluted in PBS for 5 days; female mice fed normal diet *ad libitum* for 32 weeks (Labofeed B, Morawski, Poland) – STZ mice

C57BL/6
n = 5
female mice fed high fat diet (HFD) (ssniff EF R/M D12331 mod. – Surwit, ssniff Spezialdiäten GmbH, Soest, Germany) *ad libitum* for 32 weeks – HFD mice

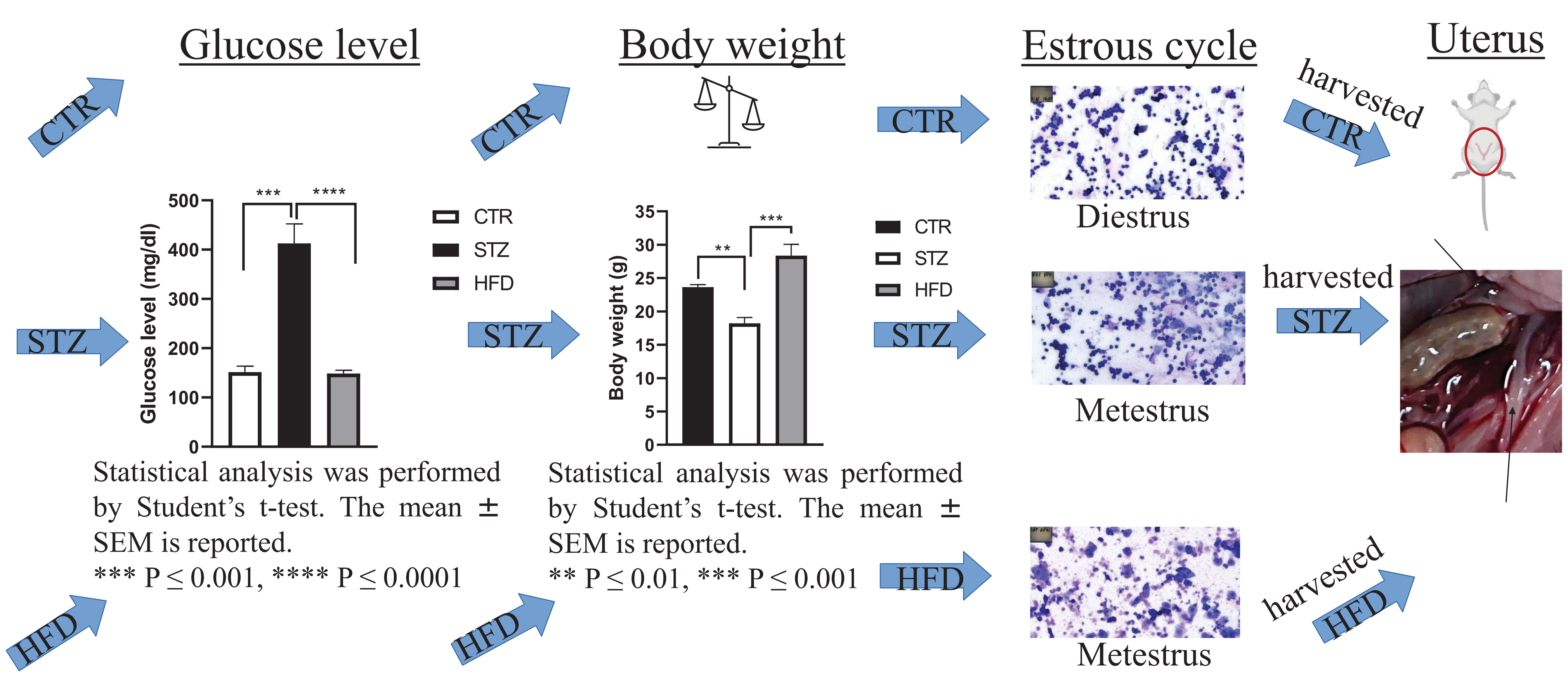

Statistical analysis was performed by Student's t-test. The mean ± SEM is reported.
*** $P \leq 0.001$, **** $P \leq 0.0001$

Statistical analysis was performed by Student's t-test. The mean ± SEM is reported.
** $P \leq 0.01$, *** $P \leq 0.001$

Funding by National Science Centre in Poland, UMO-2018/30/E/NZ5/00458

AQUAPORINS EXPRESSION IN REPRODUCTIVE TRACT OF THE BULL (BOS TAURUS) CHANGES WITH SEXUAL MATURITY. PRELIMINARY STUDY

Patrycja Oberska[1], Paulina Małkowska[1], Marta Grabowska[2]
Maciej Murawski[3], Dariusz Gączarzewicz[4], Andrzej Syczewski[5], Katarzyna Michałek[1]
[1]Department of Physiology, Cytobiology and Proteomics, West Pomeranian University of Technology in Szczecin, Poland; [2]Department of Histology and Developmental Biology, Pomeranian Medical University, Szczecin, Poland; [3]Department of Animal Nutrition, Biotechnology and Fisheries, University of Agriculture in Cracow, Poland; [4]Katedra Department of Animal Reproduction, Biotechnology and Enviromental Hygiene, West Pomeranian University of Technology in Szczecin, Poland; [5]Genetic and Animal Husbandry, Szczecin, Poland
Corresponding author: katarzyna.michalek@zut.edu.pl

XXVIII Congress of the Polish Physiological Society
Gdańsk, September 15-17, 2021
Session XI Physiology of reproduction

INTRODUCTION AND OBJECTIVES

Improving reproduction methods is associated with a constant need to search for new factors that not only significantly affect reproductive processes, but also create new possibilities when assessing male reproductive potential. Aquaporins (AQPs), which belong to a family of small (28-30 kDa), integral membrane proteins that facilitate the transport of water and other small molecules, seem to be particularly promising in this respect. To date, 13 AQPs (AQP0-AQP12) have been discovered in mammals. Almost all AQPs, except AQP6 and AQP12, are expressed in the male reproductive organs (Carrageta et al. 2020). At present, increasing evidence suggests that these proteins are involved in a number of processes responsible for the proper functioning of the male reproductive system and reproductive cell production. Despite enormous progress in knowledge in this field and presumably important role of AQPs in the development, maturation and function of male germ cells and in the production of high-quality semen, there is still little known about them in livestock, including cattle (Oberska and Michałek 2021). Hence, the aim of our research is to identify and analyze the expression of AQPs in the male reproductive system of cattle.

MATERIALS AND METHODS

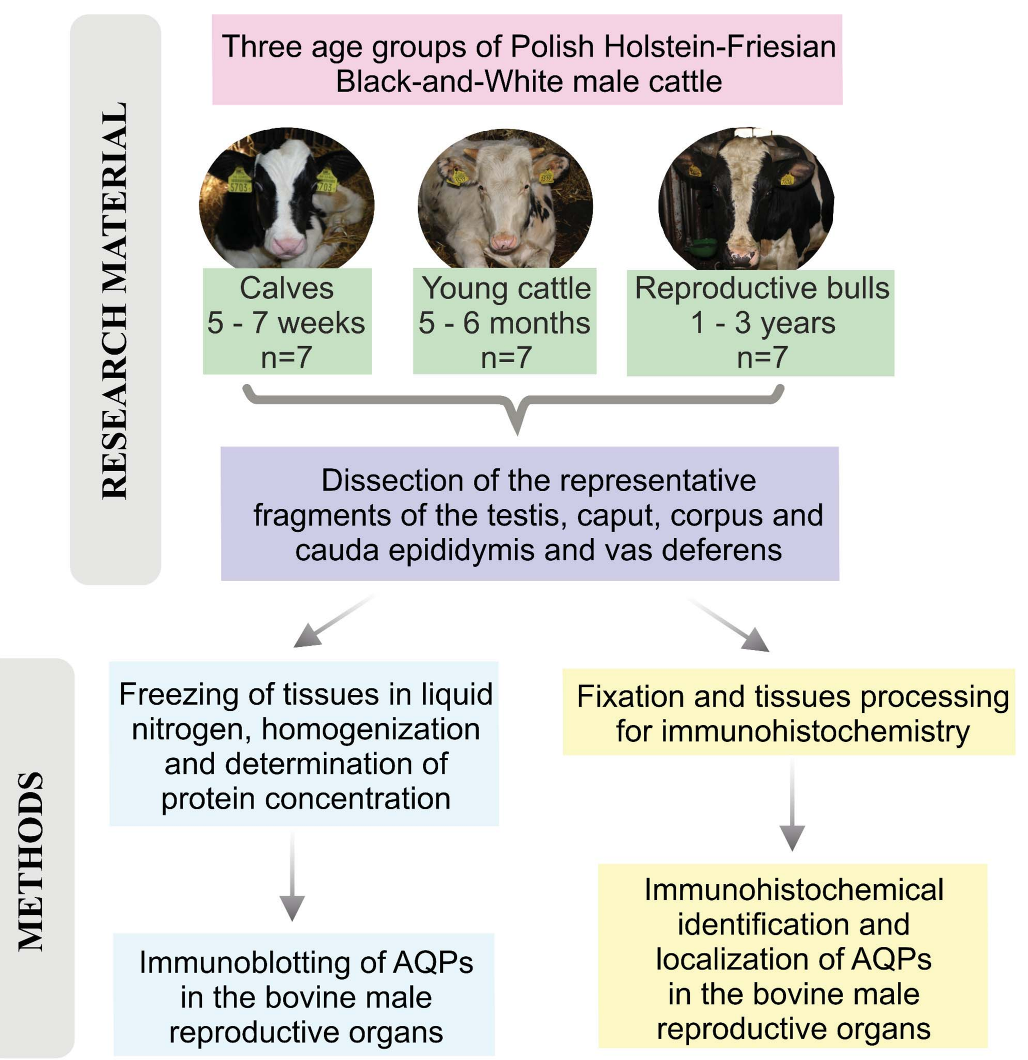

RESULTS

As a result of the studies carried out so far, the presence of AQP1, AQP3, AQP5, AQP7 and AQP9 in the bovine male reproductive organs has been confirmed. Moreover, it was observed that the expression of AQP3 and AQP7 in the bovine testis changed with growth and development of studied animals. The obtained results are shown in detail in Figure 1-3.

CONCLUSIONS

The obtained preliminary results seem to be very promising and suggest that AQPs are involved in the proper development of organs and the course of reproductive processes in male cattle. A detailed analysis of the localization and expression of AQPs in the male reproductive system will not only allow for complete understanding of the role of these proteins in the spermatogenesis, sperm maturation and semen production, but also may contribute to the improvement of the reproduction methods and estimation of the breeding value of bulls. Will the measurement of AQPs expression be considered in the future as a new and precise marker of the proper growth and development of the male reproductive system and the production of high-quality semen?

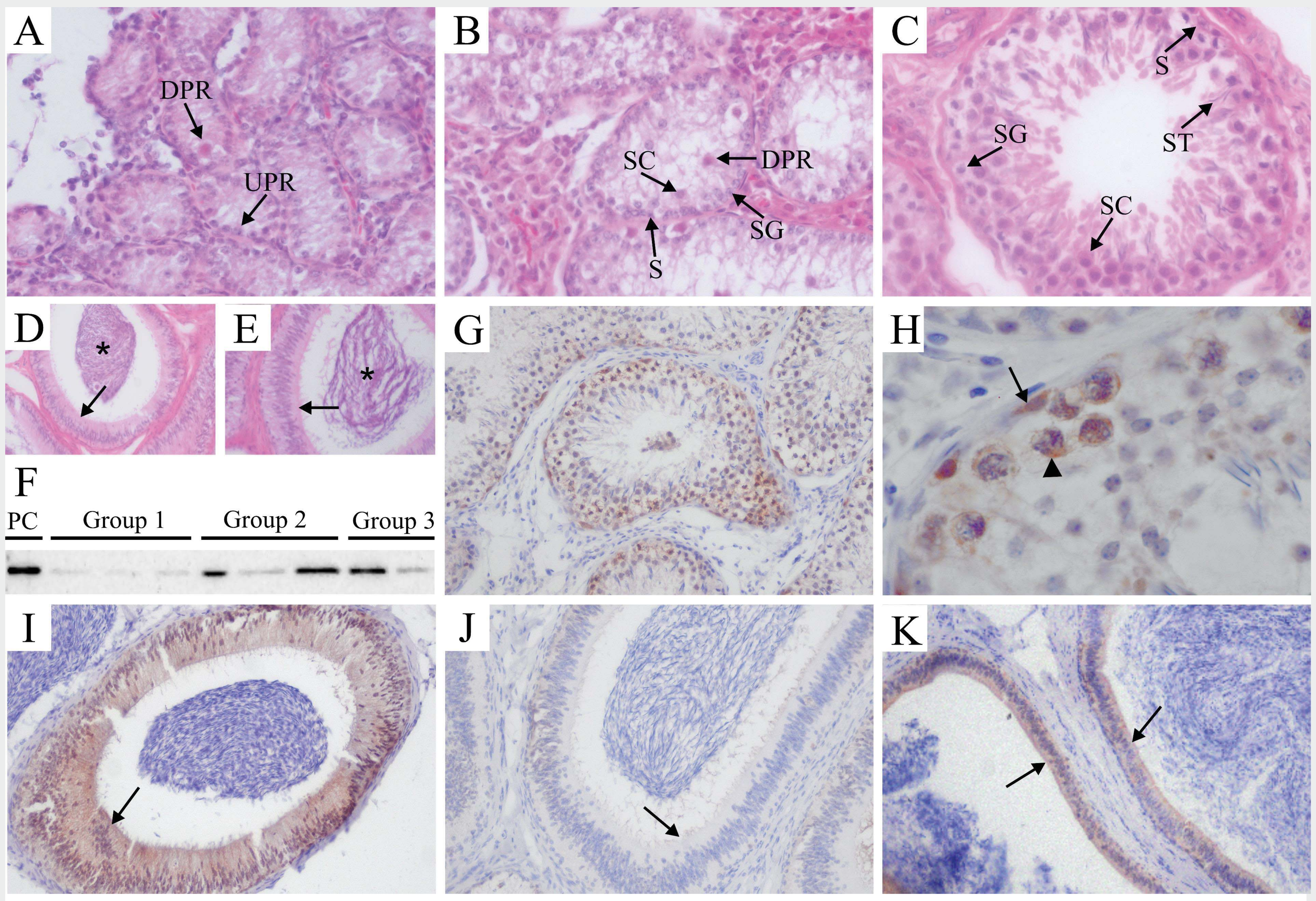

Figure 1. Morphology, expression and immunolocalization of AQP3 in the bovine male reproductive organs. Hematoxylin and eosin (H&E)-stained section of testicular seminiferous tubules of the calves (A), young cattle (B) and reproductive bulls (C). Note an increase in the diameter of the seminiferous tubules and the widening of their lumen with age of the studied animals. DPR, degenerating primordial cell; UPR, undifferentiated primordial cell; S, Sertoli cell; SG, spermatogonia; SC, spermatocyte; ST, spermatid. The caput (D) and corpus (E) epididymis of reproductive bulls stained with H&E showed a pseudostratified columnar epithelium (*arrows*). *Asterisks* indicate the plenty of the sperm cell in the epididymal lumen. Magnification: (A-C) ×400, (D, E) ×200. Results of Western blot analysis of AQP3 in the testicular homogenates from individuals of three age groups of cattle (F). AQP3 was detected as single band of 30 kDa in all three age groups, however, its protein expression varied with age of the tested animals. Group 1, calves aged 5 to 7 weeks; Group 2, young cattle aged 5 to 6 months; Group 3, reproductive bulls aged 1 to 3 years; PC, positive control (kidney cortex). AQP3 was observed in spermatogonia (*arrow*) and primary spermatocyte (*arrowhead*) within the seminiferous tubules of reproductive bulls (G, H). In reproductive bulls, AQP3 was also present in the pseudostratified epithelium (*arrows*) of the caput (I) and cauda (K) epididymis. AQP3 was not observed in the epithelium (*arrow*) of the corpus epididymis of reproductive bulls (J). Magnification: (G, I-K) ×200, (H) ×1000.

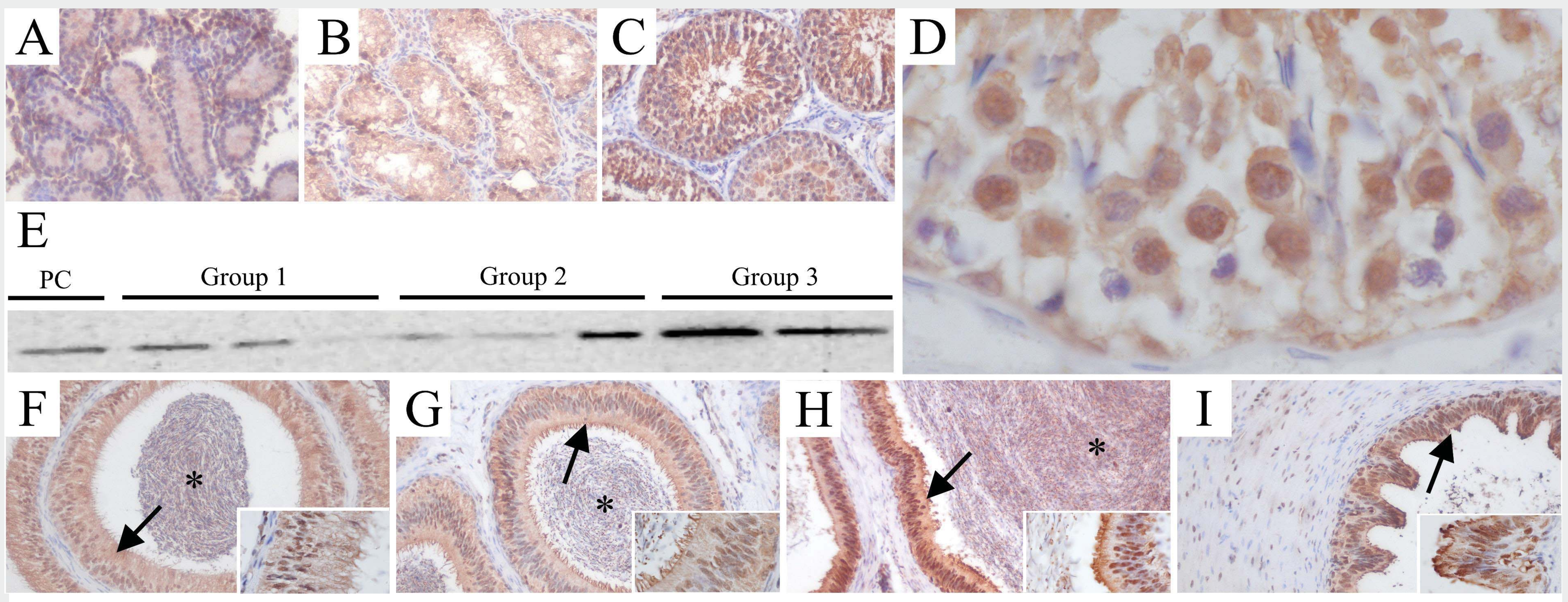

Figure 2. Immunolocalization and expression of AQP7 in the bovine male reproductive tract. AQP7 was observed in the seminiferous epithelium of the testis of the calves (A), young cattle (B) and reproductive bulls (C, D). Magnification: (A-C) ×200, (D) ×1000. Blot representing the single band of 30 kDa for AQP7 protein in the bovine testis (E). The presence of AQP7 was confirmed in the testicular homogenates from the studied animals, however, its expression level varied among three age groups of cattle. Group 1, calves aged 5 to 7 weeks; Group 2, young cattle aged 5 to 6 months; Group 3, reproductive bulls aged 1 to 3 years; PC, positive control (kidney cortex). In reproductive bulls, AQP7 was also present in the pseudostratified epithelium (*arrows*) of the caput (E), corpus (F) and cauda (H) epididymis, and in the sperm (*asterisks*) contained in the tubular lumen of the three epididymal regions. AQP7 was also expressed in the apical region of the principal cells (*arrow*) in the vas deferens of reproductive bulls (I). Magnification: (F-I) ×200, (Insets in F-I) ×1000.

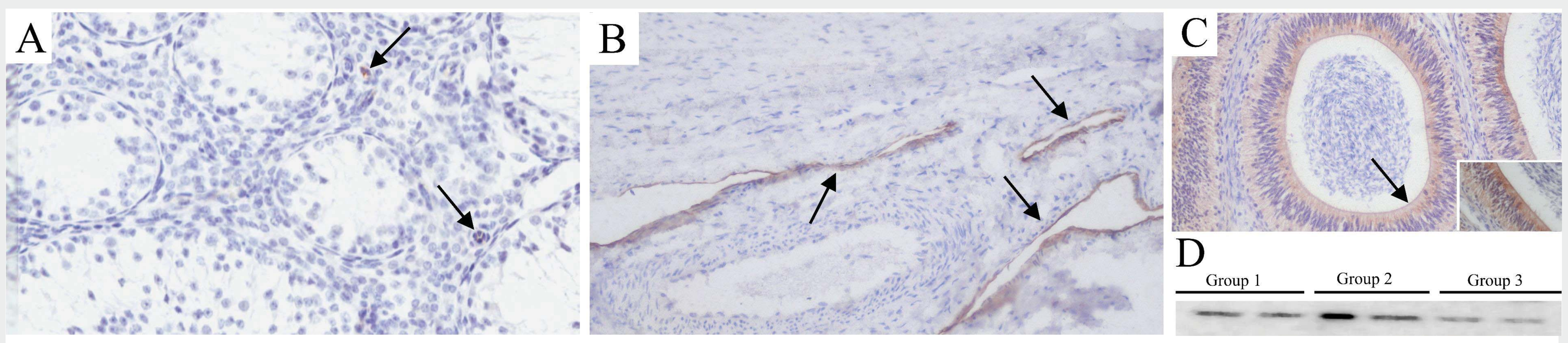

Figure 3. Immunolocalization of AQP1 and AQP5 and expression of AQP9 in the bovine male reproductive organs. In the young cattle, AQP1-immunoreactivity was detected at the level of the blood vessels (*arrows*) in the testis (A) and within caput epididymis (B). AQP5 was observed in the apical surface of the principal cells (*arrow*) in the corpus epididymis of the reproductive bulls (C). Magnification: (A, B) ×200, (C) ×400, (inset in C) ×1000. Blot showing the expression level of the AQP9 protein in the bovine testis (D). AQP9 was detected as single band of 32 kDa in all three age groups of studied animals. Group 1, calves aged 5 to 7 weeks; Group 2, young cattle aged 5 to 6 months; Group 3, reproductive bulls aged 1 to 3 years.

References: [1] Carrageta D.F. et al. 2020. Aquaporins and male (in)fertility: Expression and role throughout the male reproductive tract. Arch, Biochem. Biophys. 679:108222. **[2]** Oberska P., Michałek K. 2021. Aquaporins: new markers for male (in)fertility in livestock and poultry? Anim. Reprod. Sci. 231:106807.

IMPACT OF FETAL NUMBER ON ACUTE PHASE PROTEINS, CORTISOL AND HEMATOLOGICAL PARAMETERS IN EWES DURING THE PERIPARTURIENT PERIOD

Monika Greguła-Kania1, Urszula Kosior-Korzecka2, Konrad Kania3, Agata Hahaj-Siembida1,

1 Department of Animal Breeding and Biodiversity Conservation, Faculty of Animal Sciences and Bioeconomy,

2 Sub-Department of Pathophysiology, Department of Preclinical Veterinary Sciences, Faculty of Veterinary Medicine,

3 Department of BioPhysics, Faculty of Environmental Biology,

1,2,3 University of Life Sciences in Lublin, Lublin, Poland

corresponding-author: gregulakania@gmail.com,

Category: Reproduction

Introduction

An optimal transition requires a comprehensive understanding of the physiological events that occur during the periparturient period. Thus, the appropriate range of maternal APP concentrations should be determined to reflect the response to changes in homeostasis or disease as well as to reduce perinatal mortality. The objective of the study was to compare the plasma concentrations of SAA, Hp, Fb, and cortisol in healthy single- and twin-bearing ewes from 2 weeks before to 2 weeks after parturition. Moreover, pregnancies with more than one fetus are often accompanied by hematological disorders compared to single pregnancies. Thus, we determined hematological parameters in peripheral blood during the periparturient period to assess whether anemia develops and whether twin-lambing sheep are more sensitive to anemia during late pregnancy.

Materials and methods

We selected only healthy sheep and enrolled a total of 40 ewes of the prolific meat line BCP. The blood samples were obtained by jugular venipuncture and collected in sterile vacuum tubes, with EDTA as an anticoagulant, 14 and 7 days before parturition, a few hours after parturition, and finally 7 and 14 days after parturition. The ewes were classified into two research groups: females with single and twin pregnancy. We measured SAA, fibrinogen, haptoglobin and cortisol concentrations as well as hematology was performed.

- We measured SAA and cortisol concentrations in blood plasma with competitive inhibition enzyme-linked immunosorbent assay (ELISA) tests
- To determine the Hp concentration, we used a spectrophotometric method (Greguła-Kania et al., 2020; Wójcik et al., 2010)
- We analyzed the plasma Fb concentration based on a thrombin clottable assessment. We clotted 0.25 ml of the blood plasma with 0.5 ml of thrombin (20 U NIH/ml 0.9% NaCl) and incubated it for 25 min at room temperature. We transferred the fibrin clot into a new tube, mixed it with 1 ml of 10% NaOH solution, and heated it in a water bath at 80°C. Next, we added 3 ml of 10% Na_2CO_3 and 0.5 ml of Folin–Ciocalteu reagent. We prepared each sample in duplicate. Next, we measured the absorbance at 720 nm.

Results

1. We found a greater concentration of SAA, Hp, Fb, and cortisol in the periparturient period in twin- compared to single-bearing ewes. 2. There were no differences between single- and twin-bearing ewes for any hematological parameters.
3. The profile of APP changes was similar both in single- and twin-bearing females: an increase in SAA and Fb and a decrease in Hp concentrations.
4. The cortisol concentration did not change significantly.
5. With regard to hematological parameters, both single- and twin-bearing ewes exhibited trends typical for the periparturient period.
6. The values of all parameters were within the physiological range.

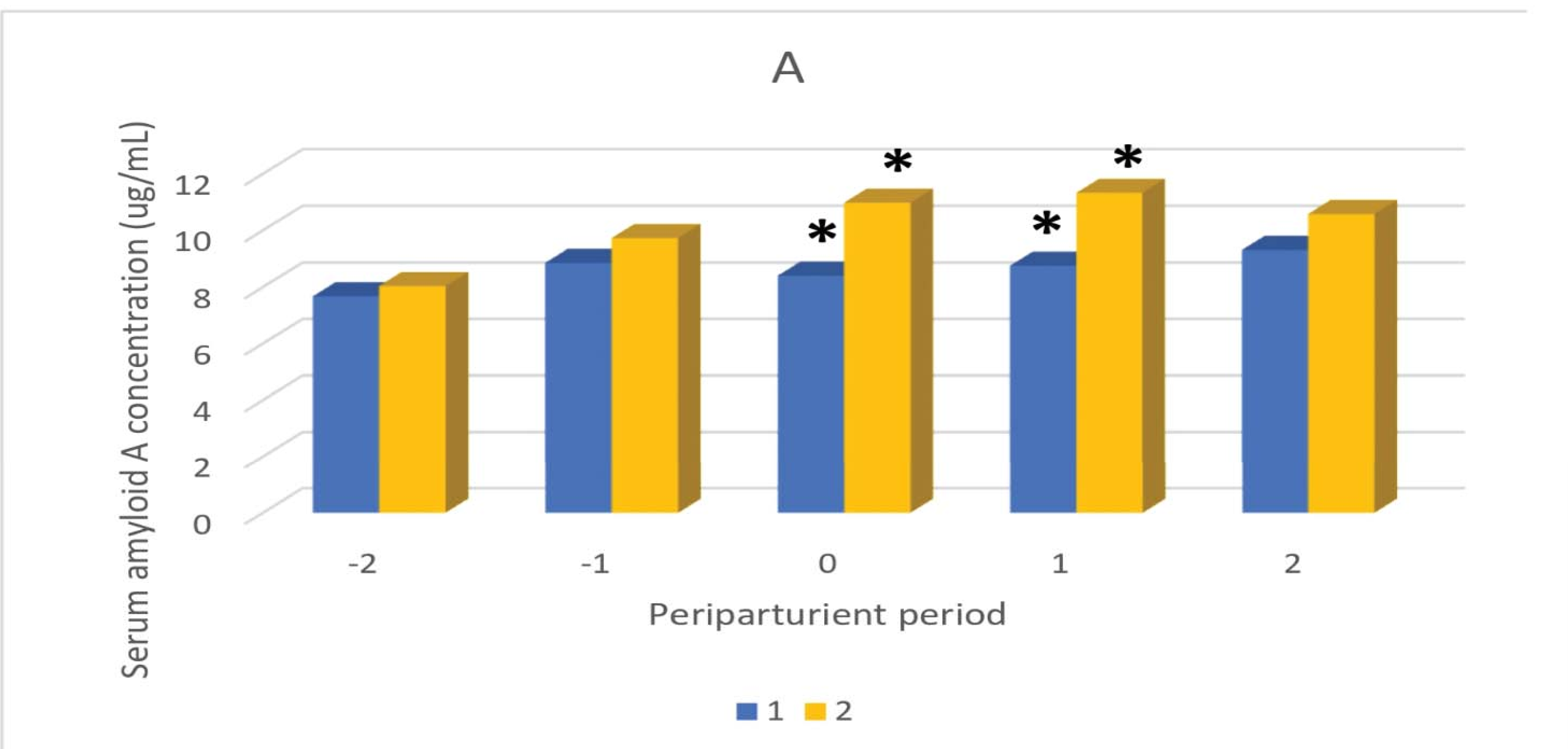

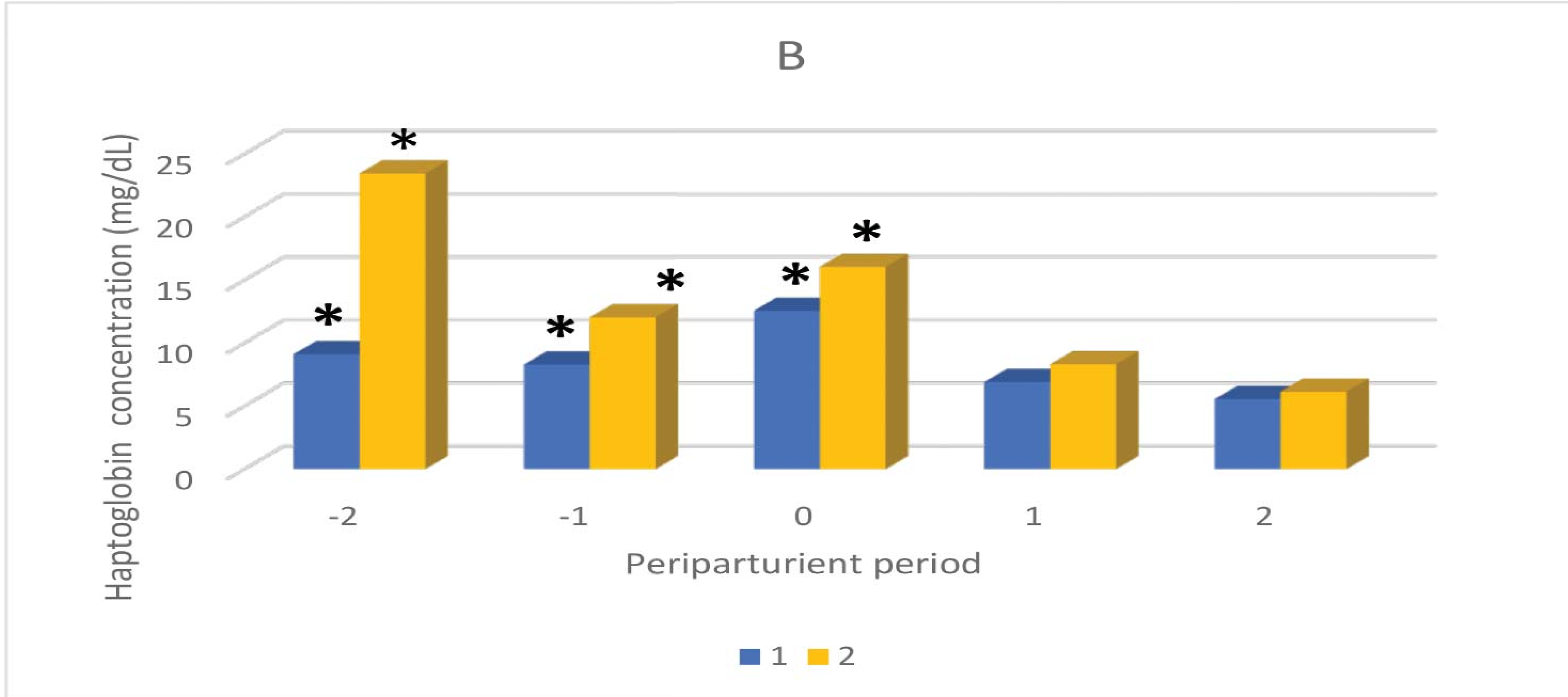

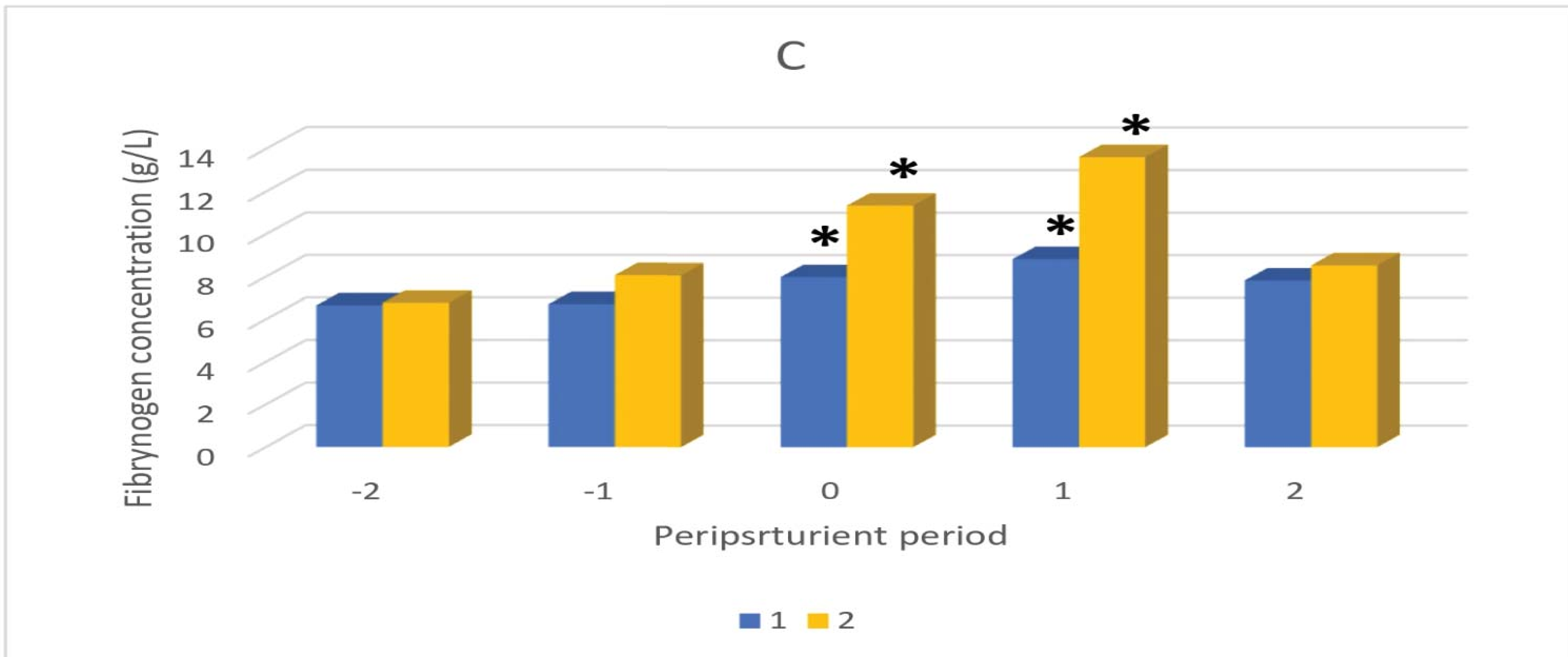

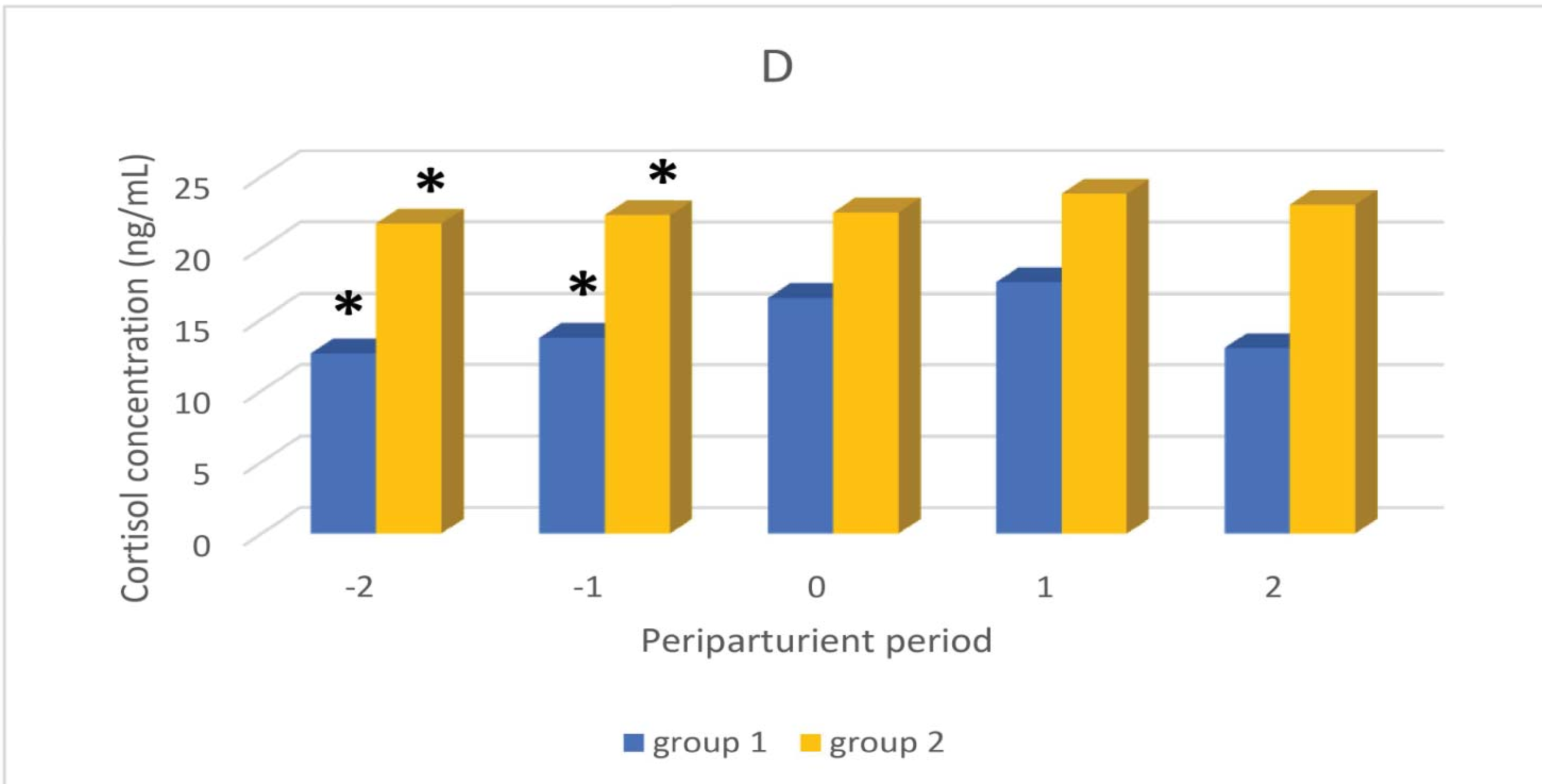

Fig 1. Changes in the concentration of serum amyloid A (SAA, µg/mL)(A), haptoglobin (Hp, mg/dL)(B), fibrinogen (Fb, g/L)(C), cortisol (ng/mL)(D) in blood plasma of ewes with one or two fetuses; The data are expressed as the mean; * indicate that means within singleton/twin with are significantly different (P< 0.05); (n = 40); Abbreviations: 1, single-bearing ewes; 2, twin-bearing ewes; -2, 2 weeks before parturition; -1, 1 week before parturition; 0, parturition; 1, 1 week after parturition; 2, 2 weeks after parturition.

Conclusions

-For the first was demonstrated time that the fetal number influences APP and cortisol concentrations in ewes during the periparturient period.
-Obtained results would facilitate the diagnosis of subclinical disorders and enable comparison of laboratory test results with different reference ranges for sheep in single and multiple pregnancy, respectively.
- There were no differences between single- and twin-bearing ewes for any hematological parameters. Neither single- or twin-bearing females were anemic

Referencies

SCaroprese, M., Albenzio, M., Annicchiarico, G., Sevi, A., 2006. Changes occurring in immune responsiveness of single- and twin-bearing Comisana ewes during the transition period. J. Dairy Sci. 89, 562–568. doi:10.3168/jds.S0022-0302(06)72119-1.
Jain, S., Gautam, V., Naseem, S., 2011. Acute phase proteins: As diagnostic tool. J. Pharm. Bioallied Sci. 3, 118–127. https://doi.org/10.4103/0975-7406.76489: 10.4103/0975-7406.76489.

CHEMERIN EFFECT ON STEROIDOGENESIS IN THE PORCINE UTERUS: AN *IN VITRO* STUDY

M. Gudelska, K. Dobrzyn, E. Rytelewska, K. Kisielewska, M. Kiezun, E. Zaobidna, K. Bors, G. Kopij, K. Szymanska, B. Kaminska, T. Kaminski, N. Smolinska

Department of Animal Anatomy and Physiology, Faculty of Biology and Biotechnology, University of Warmia and Mazury in Olsztyn, Poland

INTRODUCTION AND OBJECTIVES

Steroidogenesis is one of the most important processes which occur in the female reproductive system during both the oestrous cycle and early gestation. In pigs, besides the ovaries, placenta and other tissues, steroidogenesis process takes also place in the endometrium and myometrium. Chemerin belongs to the family of adipokines – hormones secreted by the adipose tissue. Chemerin exerts effects among others on energy homeostasis. Its receptors are present in the porcine uterus which suggests that this organ may be sensitive to the adipokine. Additionally, a growing body of evidence indicates the participation of chemerin in the regulation of reproductive system functions. The aim of this study was to determine the influence of chemerin (100 and 200 ng/mL) on steroidogenesis in the porcine endometrium, especially on the secretion of oestradiol (E_2), as well as on the expression of aromatase ($P450_{arom}$) and 3 beta-hydroxysteroid dehydrogenase (3βHSD) proteins during early gestation: on days 10 to 11 (the transuterine migration of embryos) and 12 to 13 (the maternal recognition of pregnancy).

METHODS

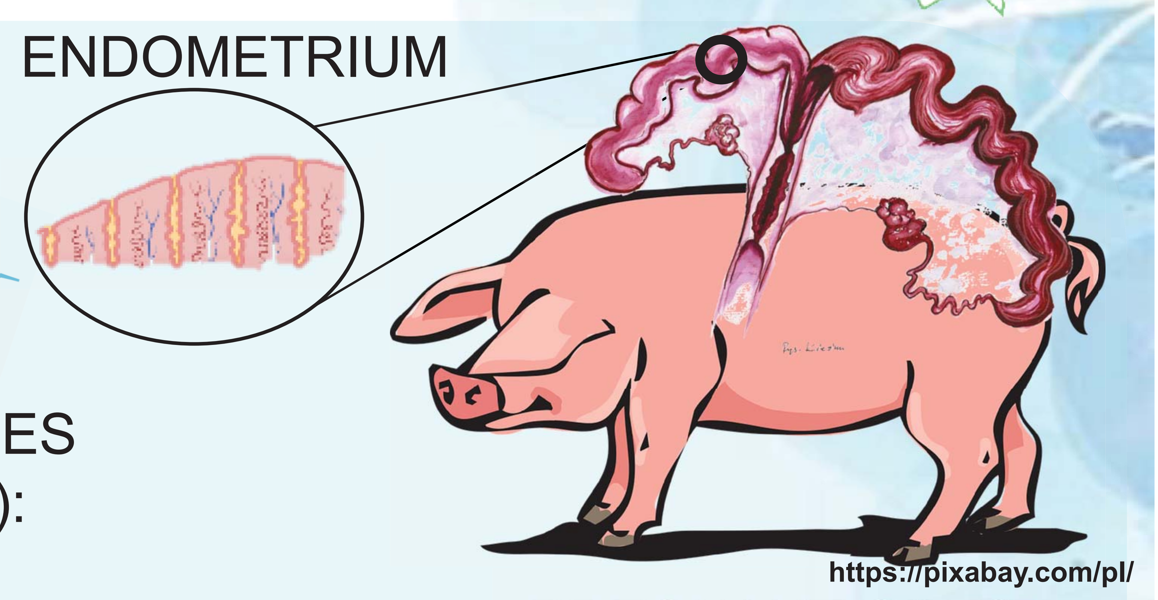

PREGNANT GILTS on days: 10 to 11 (the transuterine migration of embryos) and 12 to 13 (the maternal recognition of pregnancy)

ENDOMETRIAL SLICES INCUBATION (24h):

- CONTROL
- CHEMERIN 100 ng/mL
- CHEMERIN 200 ng/mL

WESTERN BLOT: $P450_{arom}$, 3βHSD

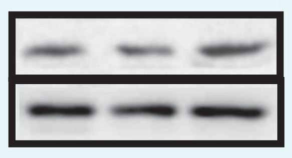

RADIOIMMUNOASSAY (RIA): E_2

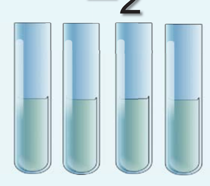

one-way ANOVA followed by the Duncan's *post-hoc* test (n=5)

RESULTS

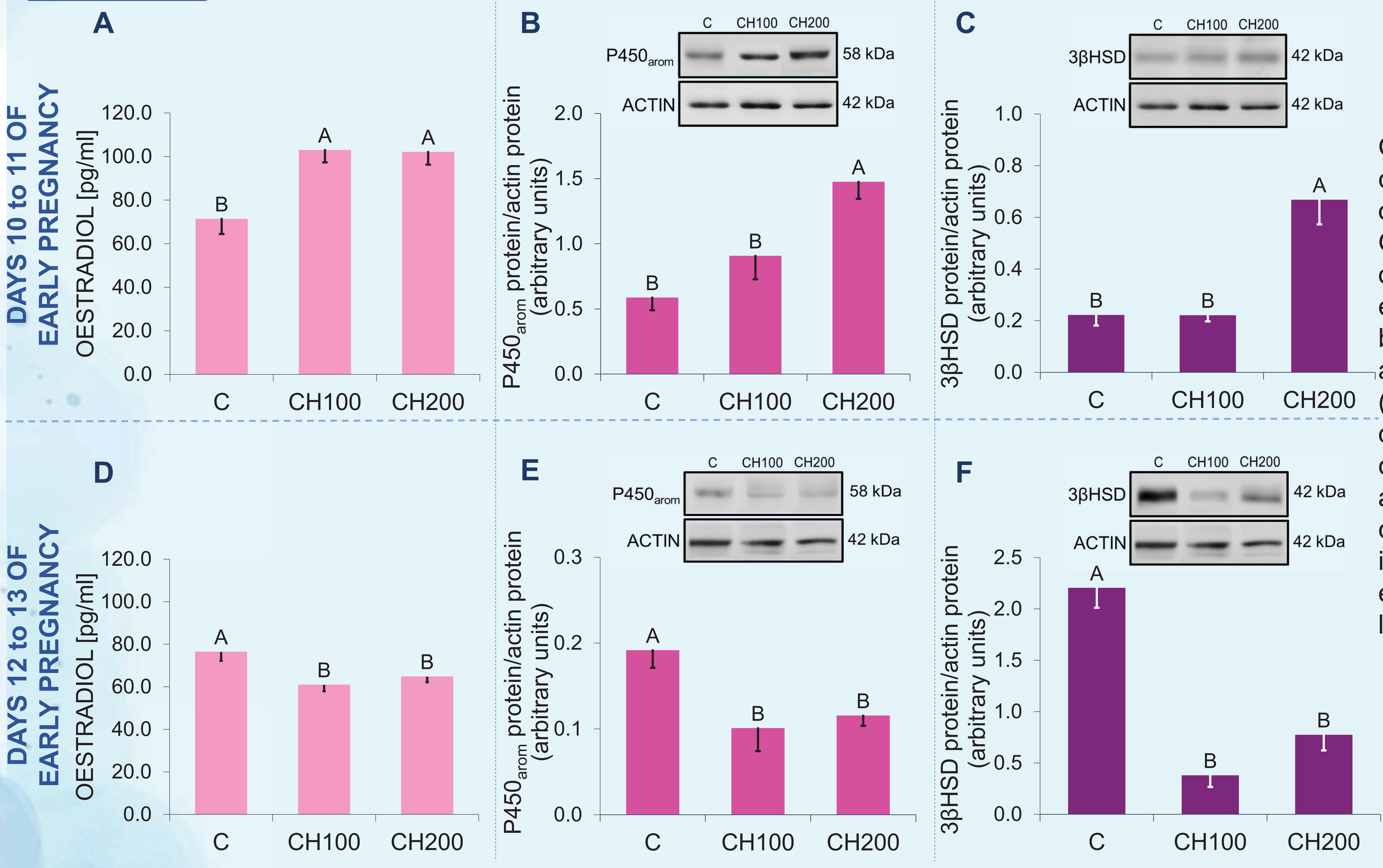

Obtained results showed that chemerin affects production of E_2 in the porcine uterus. On days 10 to 11 of pregnancy, chemerin enhanced the expression of both steroidogenic enzymes and E_2 secretion (Fig.1 A,B,C). However, on days 12 to 13 of gestation, chemerin reduced $P450_{arom}$ and 3βHSD proteins concentrations (Fig.1 E,F) in the *in vitro* incubated endometrial slices and E_2 levels in media (Fig.1 D).

Fig. 1. The impact of chemerin (100 and 200 ng/mL) on oestradiol (E_2) secretion and aromatase ($P450_{arom}$) and 3 beta-hydroxysteroid dehydrogenase (3βHSD) protein expression in the porcine endometrium on days 10 to 11 and 12 to 13 of pregnancy. The effect of chemerin (100 and 200 ng/mL) on the oestradiol (E_2) secretion and aromatase ($P450_{arom}$) and 3 beta-hydroxysteroid dehydrogenase (3βHSD) protein expression in the *in vitro* incubated endometrial explants on days 10 to 11 and 12 to 13 of pregnancy. The protein concentration was determined by the Western blot analysis; upper panels: representative immunoblots; lower panels: densitometric analysis of $P450_{arom}$/3βHSD protein relative to actin protein. Results are delineated as means ± SEM (n=5). Bars with different subscripts indicate statistically significant differences ($p<0.05$). E_2: oestradiol; $P450_{arom}$: aromatase; 3βHSD: 3 beta-hydroxysteroid dehydrogenase; C: control; CH100: chemerin 100 ng/mL; CH200: chemerin 200 ng/mL

CONCLUSIONS

The presented data indicate that uterine steroidogenesis in pigs may be dependent on chemerin presence. Moreover, the adipokine influence on E_2 production during crucial stages of pregnancy indicates that chemerin may be an important link between energy homeostasis and reproductive functions in pigs.

This research was supported by National Science Centre of Poland (project no. 2017/25/B/NZ9/00040)

marlena.gudelska@uwm.edu.pl

THE IMPACT OF CHEMERIN ON THE SECRETION OF CYTOKINES (IL-1β, IL-6) AND THE EXPRESSION OF CYTOKINE RECEPTORS (IL1R1, IL6R) BY THE PORCINE ENDOMETRIUM DURING THE OESTROUS CYCLE AND EARLY PREGNANCY

G.Kopij, M.Kiezun, E.Zaobidna, K.Dobrzyn, K.Kisielewska, E.Rytelewska, M.Gudelska, K.Bors, K.Szymanska, B.Kaminska, T.Kaminski, N.Smolinska

Department of Animal Anatomy and Physiology, Faculty of Biology and Biotechnology, University of Warmia and Mazury in Olsztyn, Poland

INTRODUCTION AND OBJECTIVES

Chemerin belongs to the group of adipokines involved in the regulation of energy homeostasis. Recent studies have demonstrated that chemerin participates in the regulation of uterine function. In the period of uterine receptivity, the endometrium produces many factors, i.a. cytokines, which are crucial for the proper course of the implantation process. The aim of this study was to investigate the impact of chemerin on the protein expression patterns of cytokine receptors (IL1R1, IL6R). We also aimed to examine the secretion of cytokines (IL-1β, IL-6) by the porcine endometrium under the influence of chemerin (100, 200 ng/mL).

MATERIAL AND METHODS

Tissues
- Endometrium
- 10-12 days of oestrous cycle
- 12-13 days of pregnancy

***In vitro* tissues culture**
- Medium 199
- Preincubation 2h
- Incubation with chemerin: 24h

Probes
- Media collection
- Protein isolation

Analisys
- ELISA test
- Western Blot

Statistical Analisys
- ONE WAY ANOVA and DUNCAN post hoc test. Data are reported as the means ± S.E.M., (n=5)

RESULTS

On days 10 to 12 of the oestrous cycle, chemerin decreased the expression of IL1R1. On days 12 to 13 of pregnancy, chemerin at the dose of 200 ng/mL decreased the expression of IL1R1 protein. Moreover, chemerin at the dose of 100 ng/mL caused an increase in IL6R protein expression on days 10 to 12 of the oestrous cycle. The stimulatory influence on IL6R protein expression was observed on days 12 to 13 of pregnancy after treatment with the adipokine at the dose of 200 ng/mL. On days 10 to 12 of the oestrous cycle the adipokine (200 ng/mL) stimulated the secretion of IL-1β and IL-6. On days 12 to 13 of pregnancy, the adipokine at the dose of 100 ng/mL enhanced, while at the higher dose depressed IL-1β release. Secretion of IL-6 by the endometrial tissues explant was decreased by chemerin on days 12 to 13 of pregnancy.

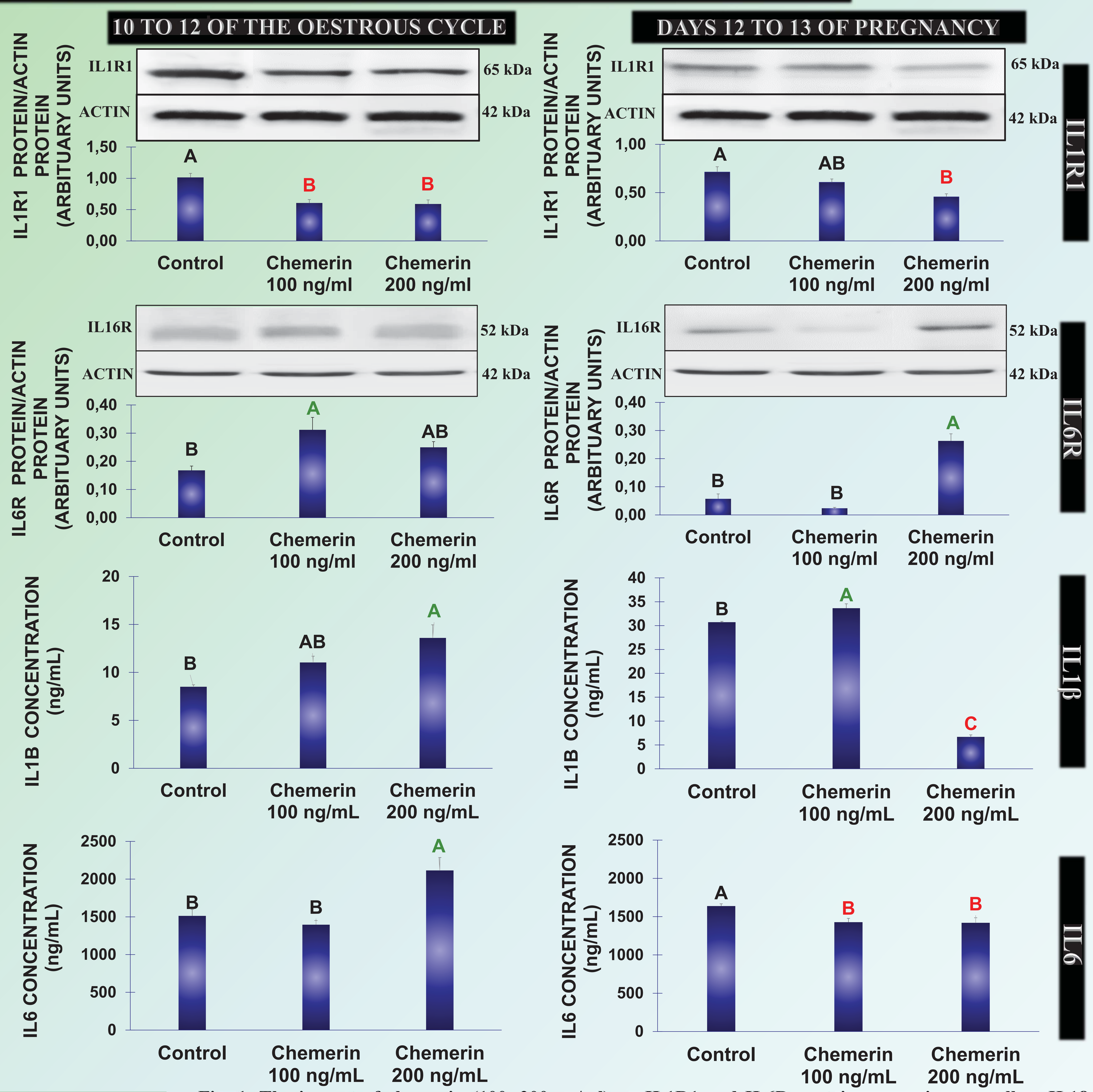

Fig. 1. The impact of chemerin (100, 200 ng/ml) on IL1R1 and IL6R protein expression as well as IL1β and IL6 secretion by the porcine endometrium on days 10 to 12 of the oestrous cycle and 12 to 13 days of pregnancy The results are reported as the mean ± standard error of the mean (n=5). Bars with different superscripts are significantly different. Capital letters indicate $p < 0.05$.

CONCLUSION

In conclusion, the influence of chemerin on IL1R1, IL6R protein expression as well as IL-1β, IL-6 secretion by endometrial explants was dependent on the dose of the adipokine and stage of the oestrous cycle or early pregnancy. Our results imply that chemerin may play an important role in the process of implantation in the pig.

The research was supported by National Science Centre (Projects No: 2017/25/BNZ9/00040).
Grzegorz.Kopij@uwm.edu.pl
XXVIII Congress of the Polish Physiological Society Gdańsk, September 15-17 2021

SESSION XI – PHYSIOLOGY OF REPRODUCTION

ADIPONECTIN AS A PROINFLAMMATORY FACTOR IN THE PORCINE ENDOMETRIUM DURING THE OESTROUS CYCLE AND IMPLANTATION: AN *IN VITRO* STUDY

M. KIEZUN, K. DOBRZYN, E. RYTELEWSKA, K. KISIELEWSKA, M. GUDELSKA, K. BORS, G. KOPIJ, K. SZYMANSKA, E. ZAOBIDNA, B. KAMINSKA, T. KAMINSKI, N. SMOLINSKA

Department of Animal Anatomy and Physiology, Faculty of Biology and Biotechnology, University of Warmia and Mazury in Olsztyn, Poland

INTRODUCTION AND OBJECTIVES

Adiponectin and its receptors are expressed in the human and porcine uterus. They play an important role in the regulation of reproductive processes [1]. We have previously reported that the adipokine affects uterine steroidogenesis and prostaglandin secretion [2]. These, with addition to the results of our preliminary studies of *in vitro* adiponectin effects on the porcine endometrial proteome with the use of mass spectrometry, prompt us to examine adiponectin role in the regulation of immunological processes occurring in this tissue. We hypothesized that adiponectin influences endometrial secretion of interleukins 1β (IL-1β) and 6 (IL-6), as well as their receptors, IL1R1 and IL-6R, protein expression.

METHODS

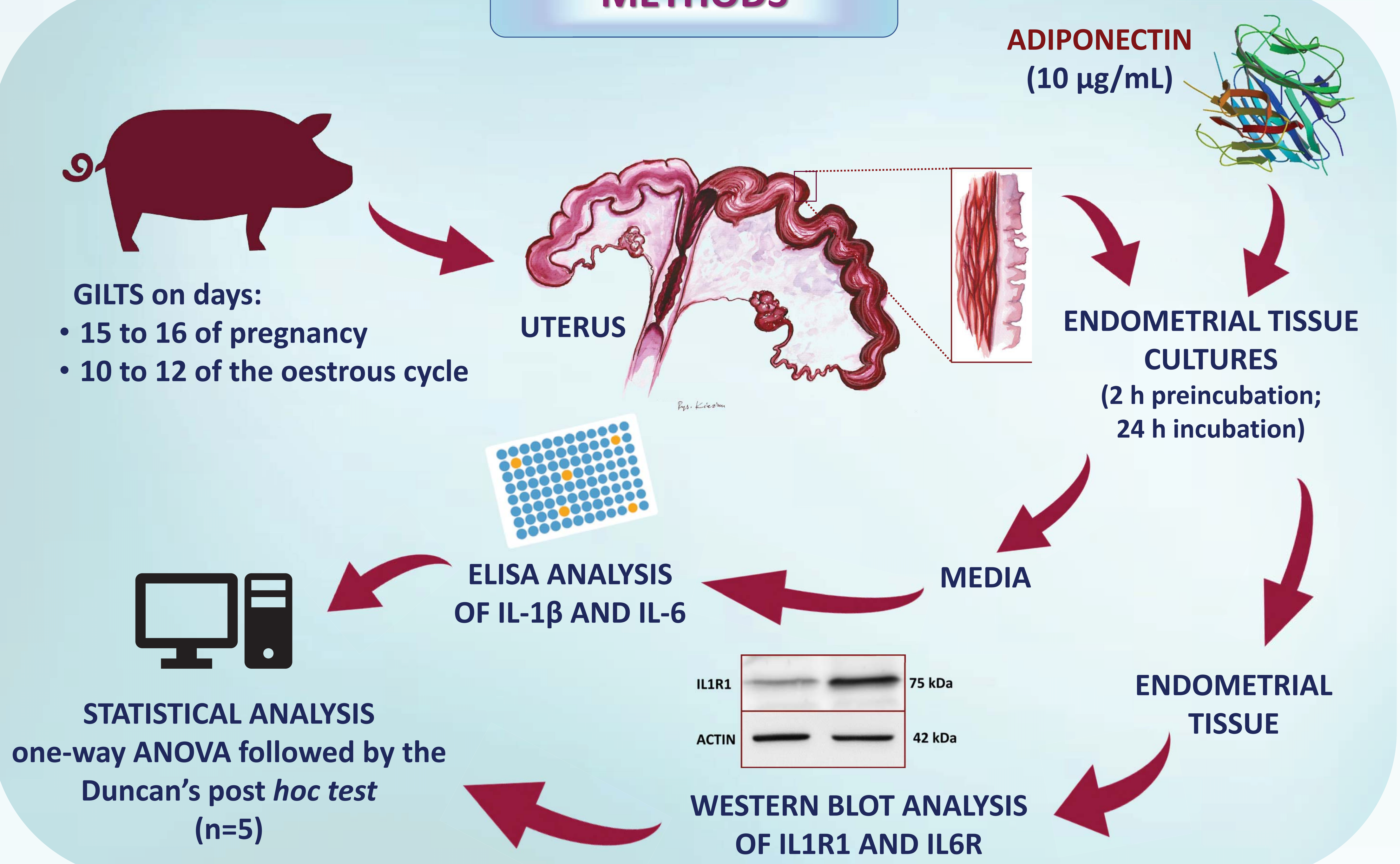

RESULTS

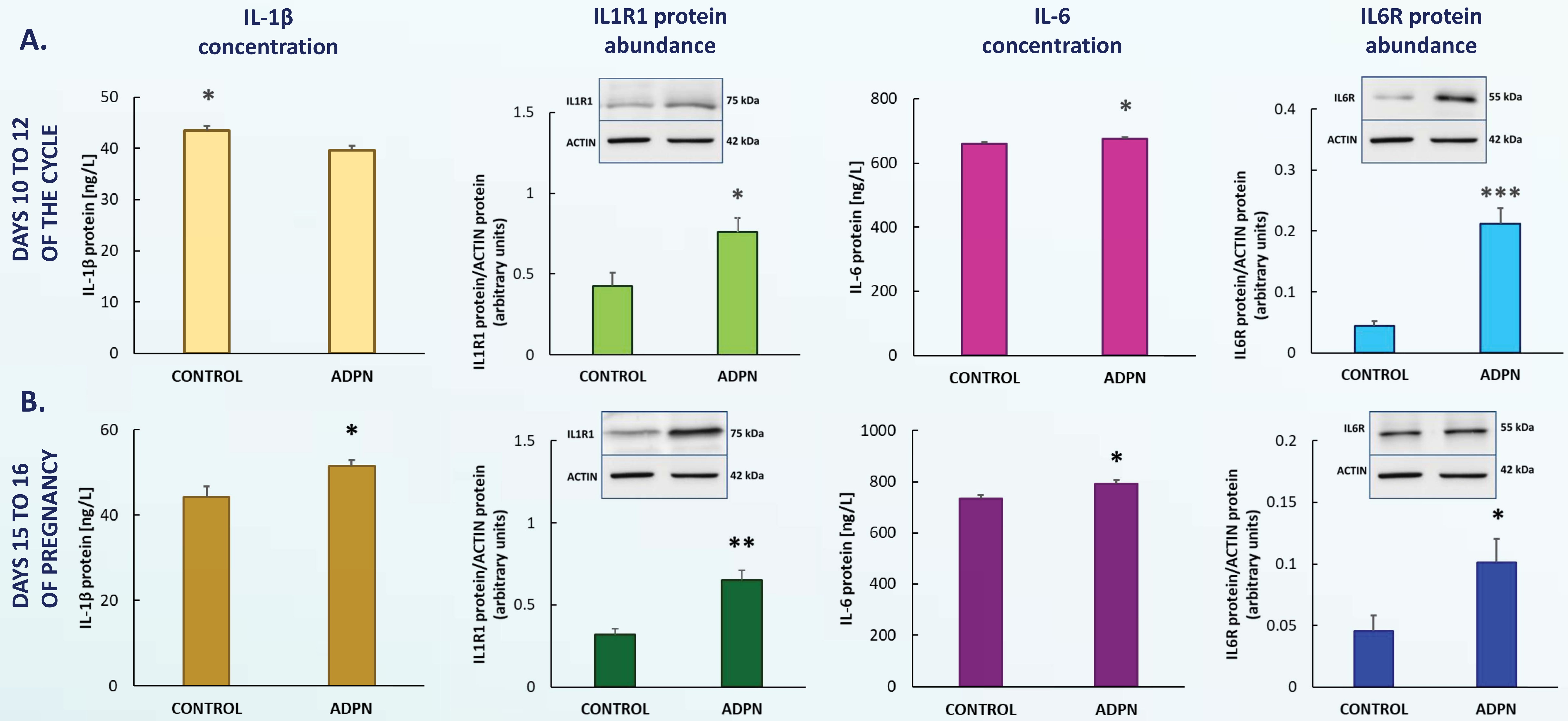

Figure 1. Adiponectin influence on IL-1β and IL-6 secretion as well as on IL1R1 and IL6R protein abundance in the *in vitro* cultured porcine endometrial tissue explants on days 10 to 12 of the oestrous cycle (A) and 15 to 16 of pregnancy (B). Results are expressed as means ± SEM (n=5). Data were analysed by t-Student's test. Bars with different superscripts are significantly different ($p<0.05$).

CONCLUSIONS

The obtained results suggest that **adiponectin may be an important factor regulating immunological processes in the endometrium** both during the oestrous cycle and at the stage of implantation. **Proinflammatory action adiponectin** in this tissue, especially at the window of implantation, **may affect the embryo-maternal communication and, as a result, embryo adhesion and implantation**.

REFERENCES

1. Dobrzyn K. et al. Adiponectin: A New Regulator of Female Reproductive System. Int J Endocrinol. 2018 Apr 29;2018:7965071.
2. Smolinska N. et al. Effect of adiponectin on the steroidogenic acute regulatory protein, P450 side chain cleavage enzyme and 3β-hydroxysteroid dehydrogenase gene expression, progesterone and androstenedione production by the porcine uterus during early pregnancy. J Physiol Pharmacol. 2016 Jun;67(3):443-56.

marta.kiezun@uwm.edu.pl

This research was supported by National Science Centre of Poland (projects no: 2011/03/B/NZ9/04187 and 2017/01/X/NZ9/00484)

THE INFLUENCE OF KETOGENIC DIET ON THE COURSE OF GESTATION AND BIOCHEMICAL COMPOSITION OF HIPPOCAMPAL FORMATION OF PREGNANT RATS

Z. Rauk[1], P. Szulc[2], W. Kosiek[1], Z. Setkowicz-Janeczko[1]
[1] Laboratory of Experimental Neuropathology, Institute of Zoology and Biomedical Research, Faculty of Biology, Jagiellonian University, Krakow, Poland;
[2] Faculty of Biochemistry, Biophysics and Biotechnology, Krakow, Poland

INTRODUCTION AND OBJECTIVES

Ketogenic diet (KD) is a high-fat, low-carbohydrate diet, used in the treatment of drug-resistant epilepsy, both in children and in adults, including pregnant women. The aim of this diet is to induce the state of ketosis and make the nerve cells use ketone bodies, such as acetoacetate and β-hydroxybutyrate (BHB), as a main source of energy, instead of glucose.

The main goal of this research was to determine the influence of KD application on the course of gestation and the biochemical composition of the brain of pregnant female rats.

https://www.ketchyketo.com/what-is-keto

METHODS

The group of 14 fertilized female Wistar rats was divided into 2 cohorts, obtaining normal diet (ND) or ketogenic diet (KD) ad libitum during the whole period of gestation. The body weight, blood level of glucose and ketone bodies as well as the food consumption were monitored on gestational day 0, 4, 15 and 20 (G0, G4, G15, G20). On the second day postpartum (P2) the number, sex and body weight of pups were assessed.

The brain tissue of females was analyzed using Fourier transform infrared microspectroscopy (FTIR), in order to assess the biochemical composition of the brain, especially hippocampal formation. The analysis was conducted for bands 1740cm^{-1}, 1360-1480cm^{-1}, 2924 cm^{-1}, 3012cm^{-1}, 2800-3000cm^{-1}, 1080 cm^{-1}, 1658cm^{-1} (carbonyl groups, cholesterol, saturated fatty acids, unsaturated fatty acids, lipid massif, phosphate groups, amide I).

REFERENCES

1. Miller, L. M., Dumas, P. (2006). Chemical imaging of biological tissue with synchrotron infrared light. *Biochimica et Biophysica Acta - Biomembranes*, *1758*(7), 846–857.

2. Chwiej, J., Skoczen, A., Janeczko, K., Kutorasinska, J., Matusiak, K., Figiel, H., Dumas P., Sandt C., Setkowicz, Z. (2015). The biochemical changes in hippocampal formation occurring in normal and seizure experiencing rats as a result of a ketogenic diet. *Analyst*, *140*(7), 2190–2204.

3. Gzieło, K., Janeczko, K., Węglarz, W., Jasiński, K., Kłodowski, K., Setkowicz, Z. (2020). MRI spectroscopic and tractography studies indicate consequences of long-term ketogenic diet. *Brain Structure and Function*, *225*(7), 2077–2089.

RESULTS AND CONCLUSIONS

The statistical analysis revealed a significantly higher ketone bodies blood level since the 4th day of gestation (Fig.1) and a lower glucose level in 20th day of gestation in KD fed rats than in control group (Fig.2). No significant differences were observed between the groups regarding the weight gaining during pregnancy, brain weight to body weight ratio in 2nd day postpartum, number of pups and the sex ratio of the brood. However, the pups' weight was significantly lower in KD fed group (Fig.3), despite the fact that KD fed rats appeared to consume significantly more calories per day (Fig.4).

The obtained results indicate **a negative influence of ketosis on the birth weight** and **a greater importance of diet composition than caloricity in fetus development**.

Fig.1 BHB blood level during the pregnancy

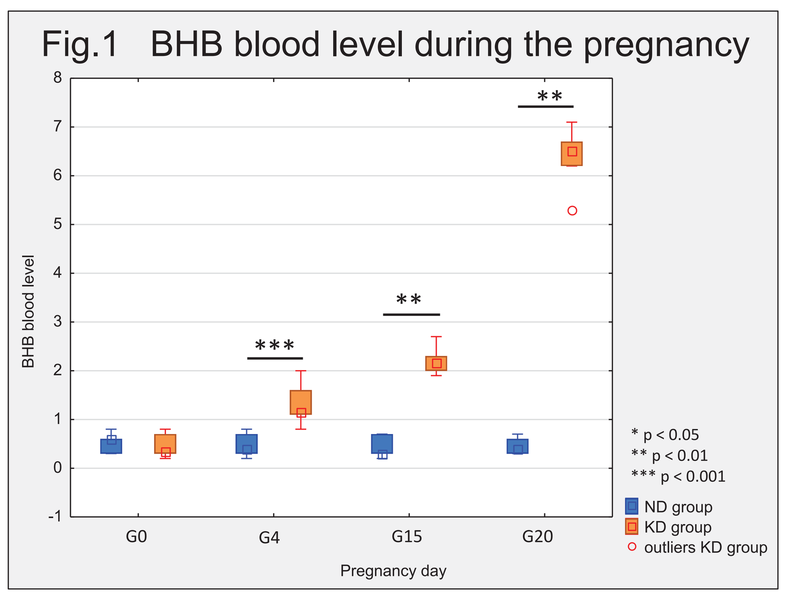

Fig.2 Glucose blood level [mg/dl] during the pregnancy

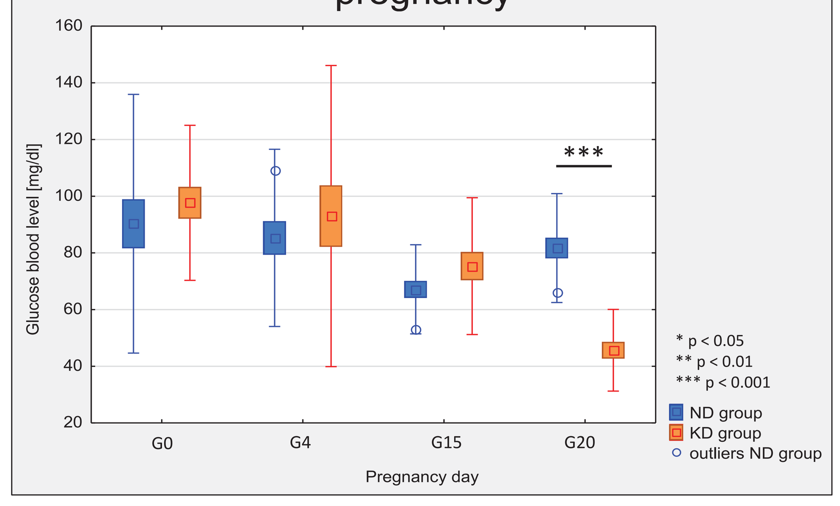

Fig.3 Pups' mean body mass in P2 [g]

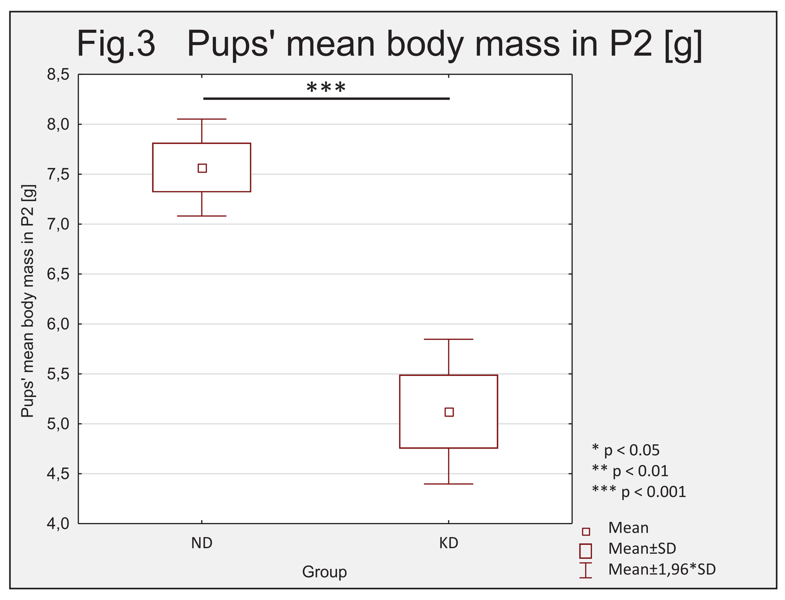

Fig.4 Mean calories intake/day [kJ] during the pregnancy

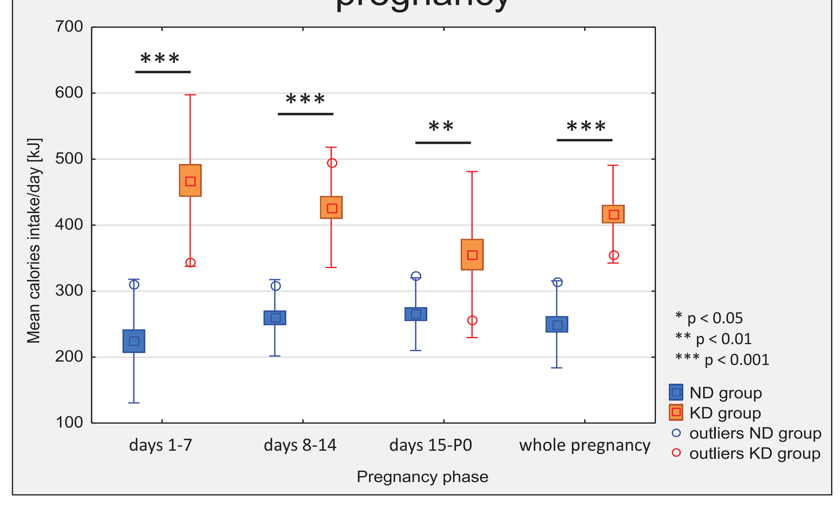

The FTIR analysis revealed an increased accumulation of unsaturated fatty acids (Fig. 5) and carbonyl groups in the hippocampus of rats fed with KD in comparison to ND group. Moreover, we have observed a higher accumulation of carbonyl groups (Fig. 6), unsaturated fatty acids and cholesterol in the white matter of rats in KD group than in ND group.

The aforementioned results suggest that **KD can affect the biochemical composition of hippocampus and white matter**, that may be of the importance for preventing the occurrence of epileptic seizures as well as for the development of connections between different brain areas.

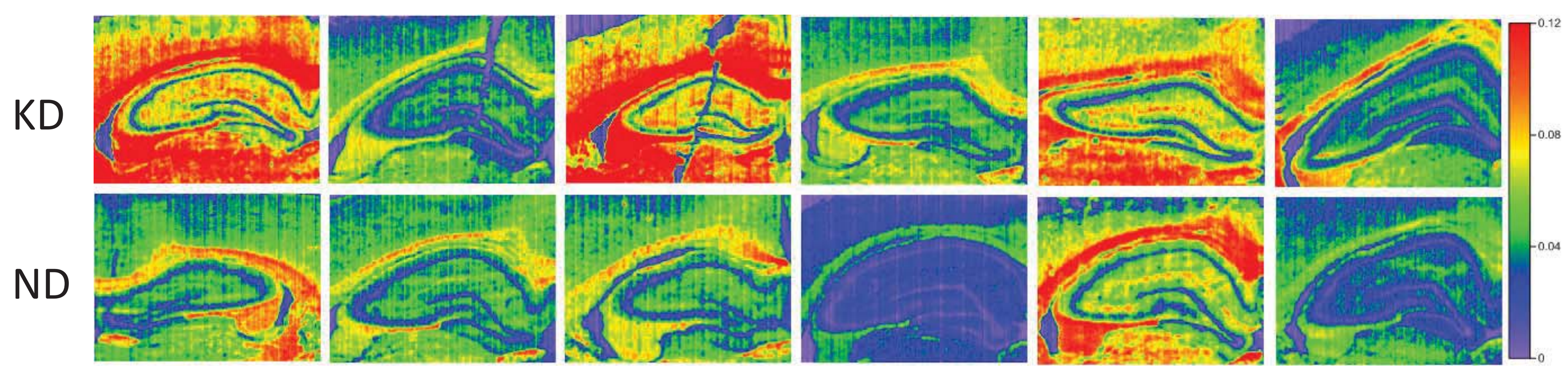

Fig. 5 Chemical map presenting the distribution of unsaturated fatty acids in the hippocampus of rats.

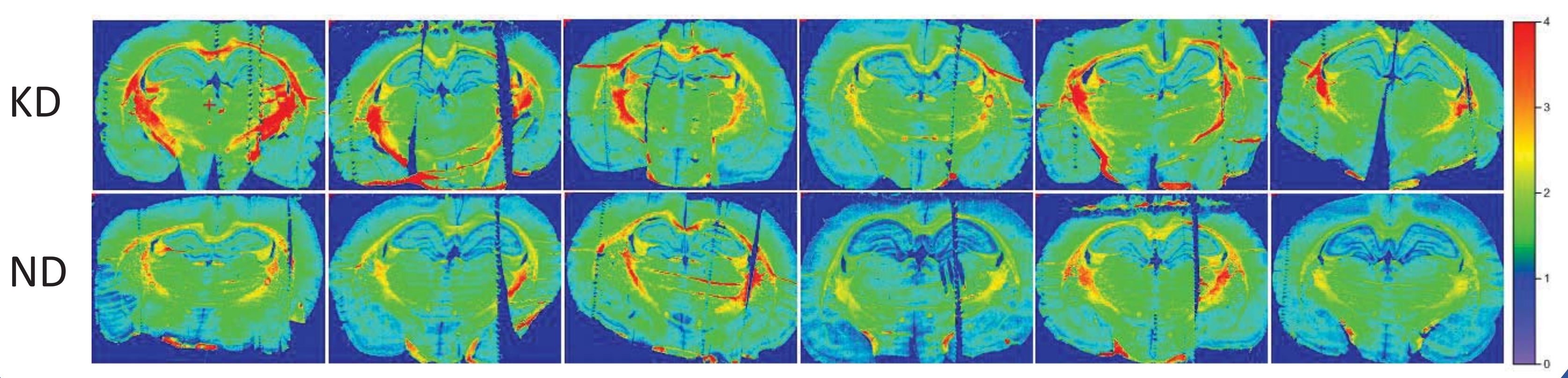

Fig. 6 Chemical map presenting the distribution of carbonyl groups in the white matter of rats.

XXVIII Congress of the Polish Physiological Society

VISFATIN GENE EXPRESSION IN THE PORCINE PITUITARY GLAND DURING THE OESTROUS CYCLE AND EARLY PREGNANCY

k.szymanska@uwm.edu.pl

K.SZYMANSKA[1], M.KIEZUN[1], E.ZAOBIDNA[1], K.DOBRZYN[1], E.MLYCZYNSKA[2], E.RYTELEWSKA[1], K.KISIELEWSKA[1], M.GUDELSKA[1], K.BORS[1], G.KOPIJ[1], B.KAMINSKA[1], AGNIESZKA RAK[2], N.SMOLINSKA[1], T.KAMINSKI[1]

[1]Department of Animal Anatomy and Physiology, Faculty of Biology and Biotechnology, University of Warmia and Mazury in Olsztyn, Poland
[2]Department of Physiology and Toxicology of Reproduction, Institute of Zoology and Biomedical Research, Jagiellonian University in Krakow, Poland

INTRODUCTION

Visfatin appears to be an energy sensor involved in the regulation of female fertility which creates a hormonal link integrating the control of energy homeostasis and reproduction. Visfatin expression in adipocytes can be affected by hormonal factors such as steroid hormones, tumor necrosis factor α, growth hormone and dexamethasone, while in the human granulosa cells by human chorionic gonadotropin and prostaglandin E_2. It is suggested that visfatin gene expression can be controlled by species-specific regulatory mechanism and the adipokine concentrations in human adipose tissue are affected by hormonal status related to pregnancy. We hypothesized that hormonal milieu connected with the specific phase of the oestrous cycle and period of pregnancy affects visfatin gene expression in the porcine pituitary.

RESULTS

During the oestrous cycle, the highest expression of visfatin gene was observed on days 10-12 and the lowest on days 17-19 (Fig. 1.). During pregnancy, visfatin gene expression was increased on days 12-13 and 27-28 in comparison to days 15-16 (Fig. 2.). Comparing visfatin gene expression throughout the early pregnancy with days 10-12 of the oestrous cycle, visfatin mRNA content during all periods of pregnancy was significantly lower (Fig. 3.).

CONCLUSIONS

The fluctuations in the expression levels of visfatin gene noticed during the oestrous cycle and early pregnancy may suggest their dependence on the hormonal milieu specific for the oestrous cycle and early pregnancy.

MATERIAL AND METHODS

EXPERIMENTAL ANIMALS:
- pigs on days of the oestrous cycle: 2 to 3, 10 to 12, 14 to 16 and 17 to 19,
- pigs on days of pregnancy: 10 to 11, 12 to 13, 15 to 16 and 27 to 28.

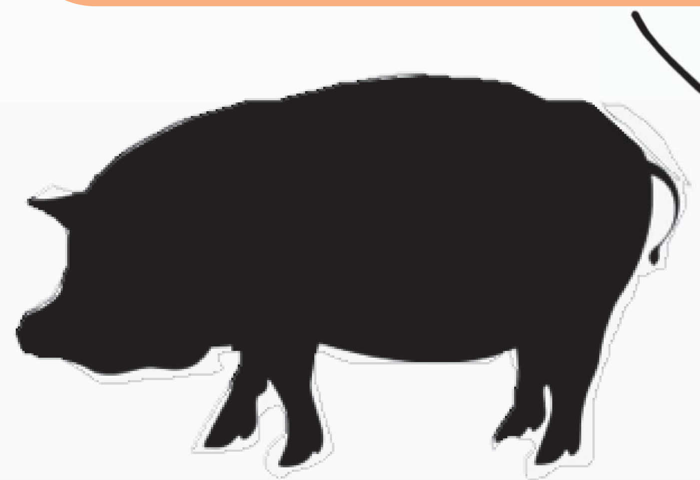

TISSUE EXPLANTS: anterior lobe of the pituitary

TISSUE COLLECTION

RNA ISOLATION and REVERSE TRANSCRIPTION

REAL-TIME PCR

STATISTICAL ANALYSIS: one-way ANOVA followed by Tukey's *post hoc* test. Data are reported as the mean ± S.E.M (n=5).

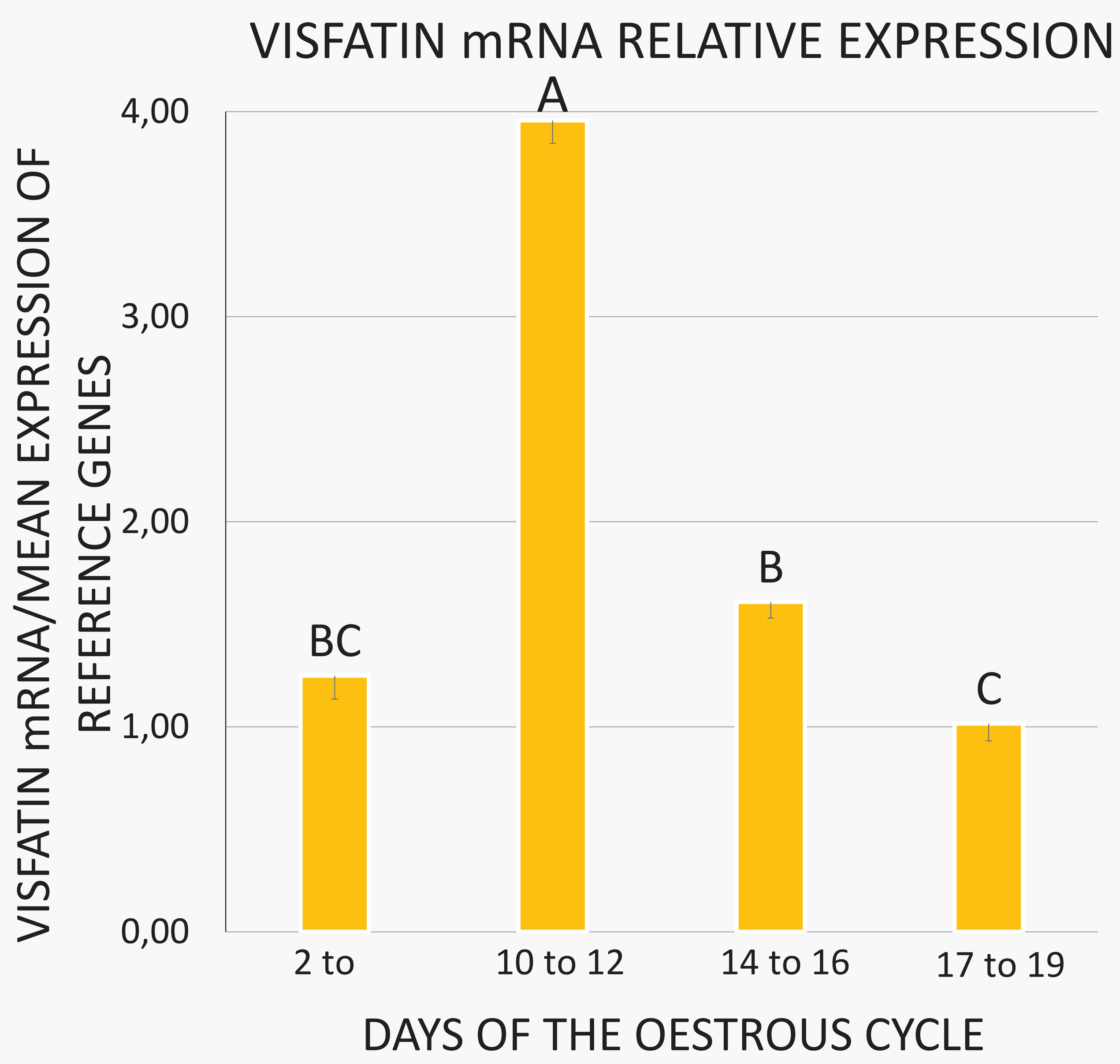

FIG. 1. Visfatin gene expression in the anterior lobe of porcine pituitary gland during the oestrous cycle. The results are reported as the mean ± standard error of the mean (n=5). Bars with different superscripts are significantly different.

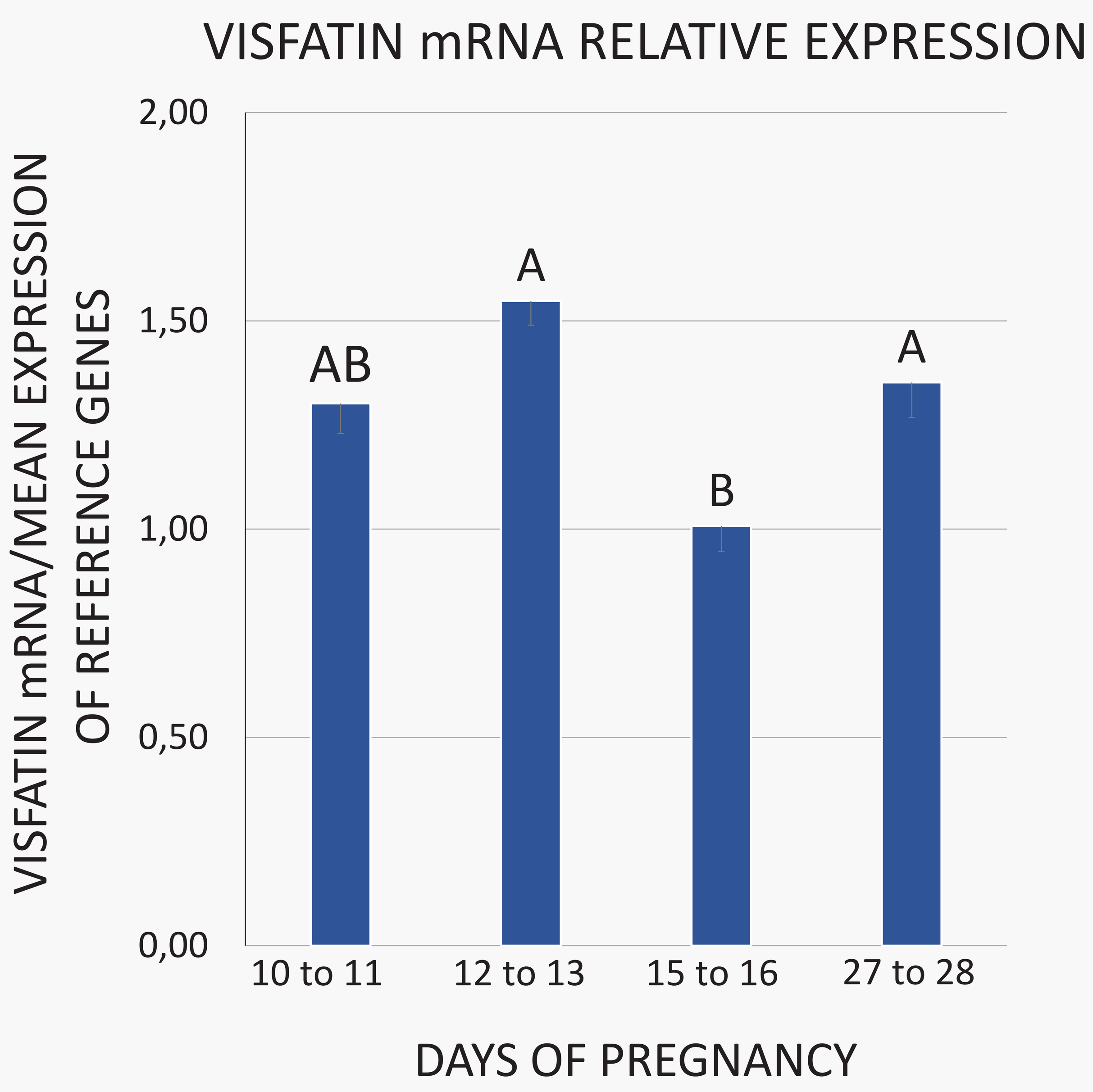

FIG. 2. Visfatin gene expression in the anterior lobe of porcine pituitary gland during pregnancy. The results are reported as the mean ± standard error of the mean (n=5). Bars with different superscripts are significantly different.

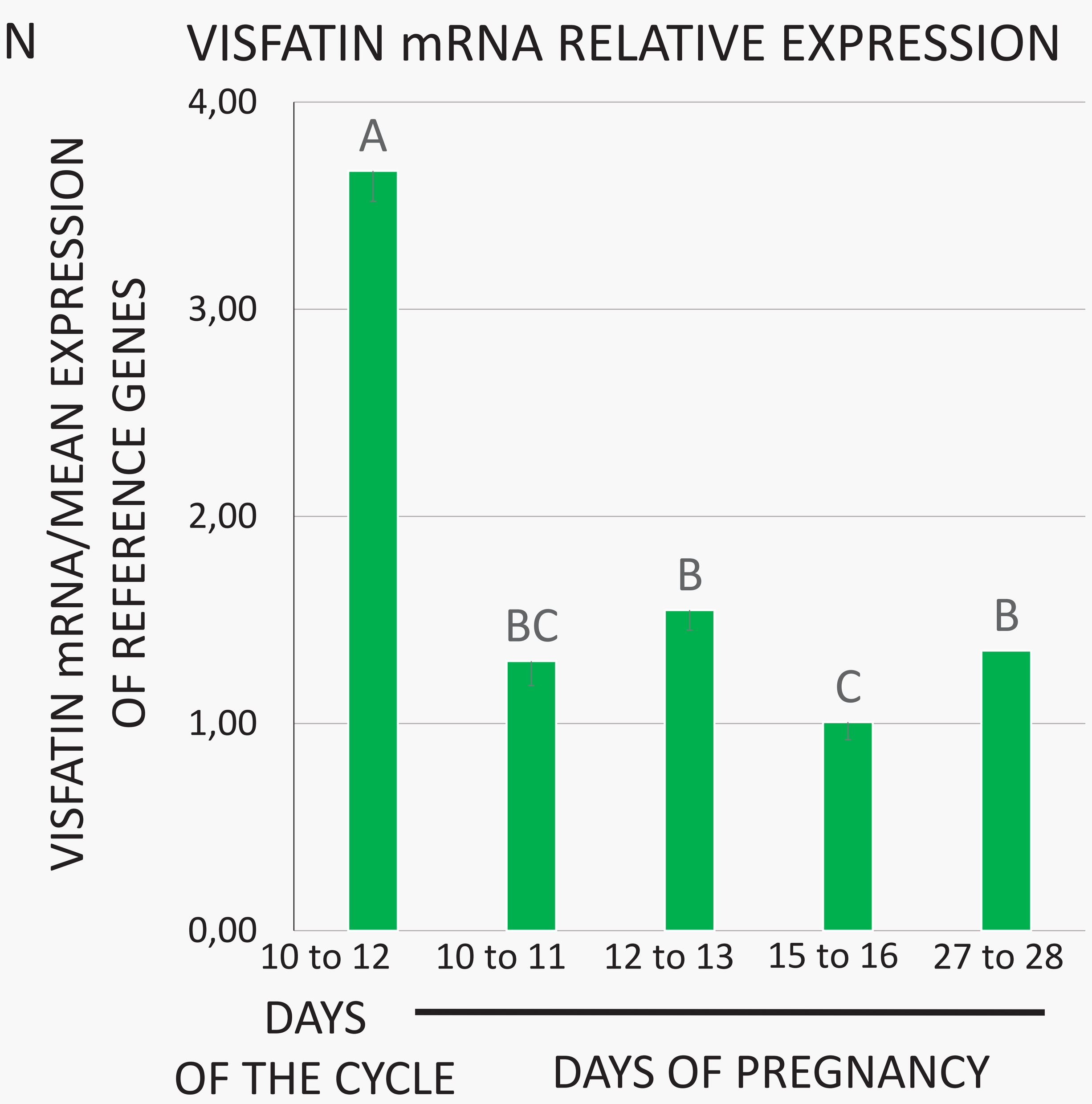

FIG. 3. Visfatin gene expression in the anterior lobe of porcine pituitary gland compared between early pregnancy and days 10 to 12 of the oestrous cycle. The results are reported as the mean ± standard error of the mean (n=5). Bars with different superscripts are significantly different.

The research was supported by National Science Centre (project no: 2018/31/B/NZ9/00781)

XXVIII Congress of the Polish Physiological Society

Gdańsk, September 15-17 2021

Poster book

SESSION XII

GASTROINTESTINAL PHYSIOLOGY AND PATHOPHYSIOLOGY,

PANCREAS AND LIVER

HONORARY PATRONAGE

Prof. dr Marcin Gruchała
Rector of the Medical University of Gdansk

Uniwersytet Gdański

Prof. dr Piotr Stepnowski
Rector of the University of Gdansk

WOJEWODA POMORSKI
DARIUSZ DRELICH

Dariusz Drelich
Governor of the Pomeranian Voivodeship

HONORARY PATRONAGE
Mayor of the City of Gdańsk

Aleksandra Dulkiewicz
Mayor of Gdansk

Mieczysław Struk
Marshal of the Pomeranian Voivodeship

PARTNER

PAN
POLSKA AKADEMIA NAUK

ANIMA LAB
animal facility and laboratory equipment • animal research models

FUNDACJA LOTOS

Medical University of Gdansk
Department of Physiology

GASTROINTESTINAL (GI) SAFETY AND EFFICACY OF NOVEL HYDROGEN SULFIDE-RELEASING NON-STEROIDAL ANTI-INFLAMMATORY DRUGS.

AUTHORS: ALEKSANDRA DANIELAK[1], URSZULA GŁOWACKA[1], KATARZYNA MAGIEROWSKA[1], DAGMARA WÓJCIK[1], JERZY HANKUS[2], MAŁGORZATA SZETELA[1], JAKUB CIESZKOWSKI[1], EDYTA KORBUT[1], ZBIGNIEW ŚLIWOWSKI[1], GRZEGORZ GINTER[1], JOHN L WALLACE[3], MARCIN MAGIEROWSKI[1]

[1] Department of Physiology, Jagiellonian University Medical College, Cracow, Poland; [2] Department of Pathomorphology, Jagiellonian University Medical College, Cracow, Poland; [3] Department of Physiology and Pharmacology, University of Calgary, Calgary, Canada.

GASTROINTESTINAL AND LIVER PHYSIOLOGY AND PATHOPHYSIOLOGY, PANCREAS AND LIVER

Narodowe Centrum Badań i Rozwoju

INTRODUCTION AND OBJECTIVES

Non-steroidal anti-inflammatory drugs (NSAIDs) play an important role in the therapy of numerous inflammatory diseases such as rheumatoid arthritis. However, they are also known to exert a numer of side effects affecting gastrointestinal (GI) tract, such as bleeding and ulcerations. Hydrogen sulfide (H2S) has been recently recognized as an anti-inflammatory and anti-oxidative gaseous messenger with important functions in the gastrointestinal (GI) tract. Both endogenous and egzogenous H2S released from chemical donors has been shown to afford protection against gastric mucosa damage induced by NSAIDs, ischemia/reperfusion or ethanol and to enhance the healing of gastric ulcers.

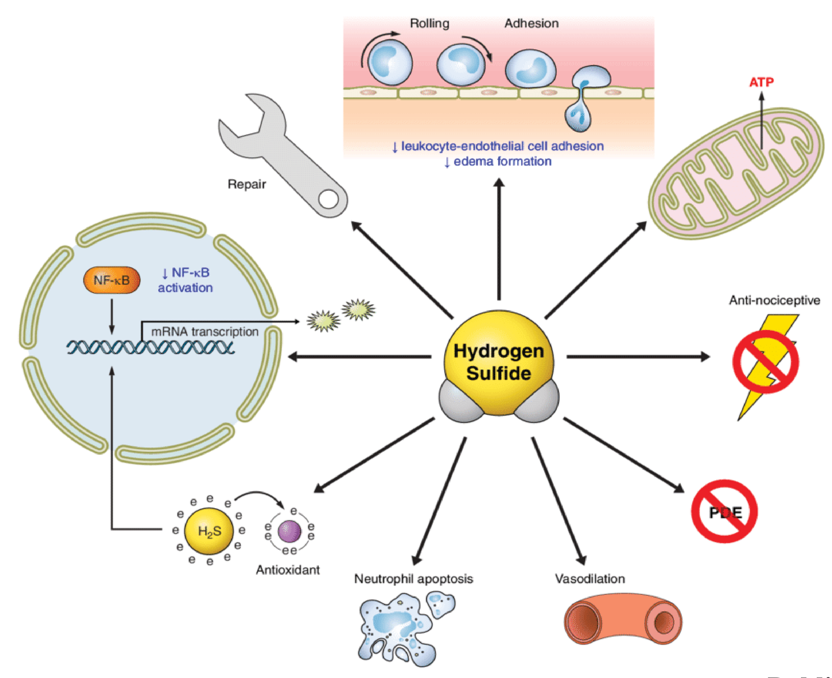

Published in doi: :10.1152/ajpgi.00169.2013

Based on these physiological properties of H2S a new class of H2S-relasing NSAIDs has been developed, among others H2S-releasing derivatives of ketoprofen (ATB-352) and acetylsalicylic acid (ATB-340).

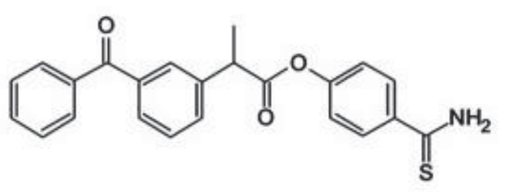

ATB-352
4-carbamothioylphenyl 2-(3-benzoylphenyl)propanoate
PubChem: 25065981

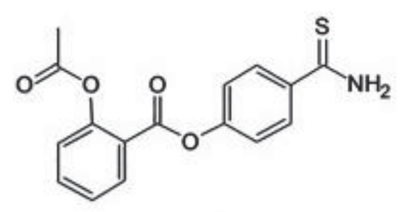

ATB-340
4-(5-thioxo-5H-1,2-dithiol-3-yl)phenyl 2-acetoxybenzoate
PubMed: 32848752

We aimed to evaluate the efficacy and GI safety of ATB-352 and ATB-340 as well as to investigate possible mechanisms underlying the activity of these novel compounds.

METHODS

35 Wistar rats were randomized to groups treated i.g. for 7 days with:

- DMSO + CMC (vehicle) - control group
- ATB-352 in a dose of 14 mg/kg
- Ketoprofen in a dose of 10mg/kg
- Aspirin (ASA) in a dose of 10mg/kg with or without ATB-352 or ketoprofen
- Omeprazol in a dose of 20mg/kg with or without ATB-352 or ketoprofen
- ATB-340 in doses of 2, 6, 12 and 24mg/kg

Further analysis:

Gastric and intestinal damage score was analized macro- and microscopically. Determination of intestinal microbiome profile was performed using next-generation sequencing.

RESULTS AND CONCLUSIONS

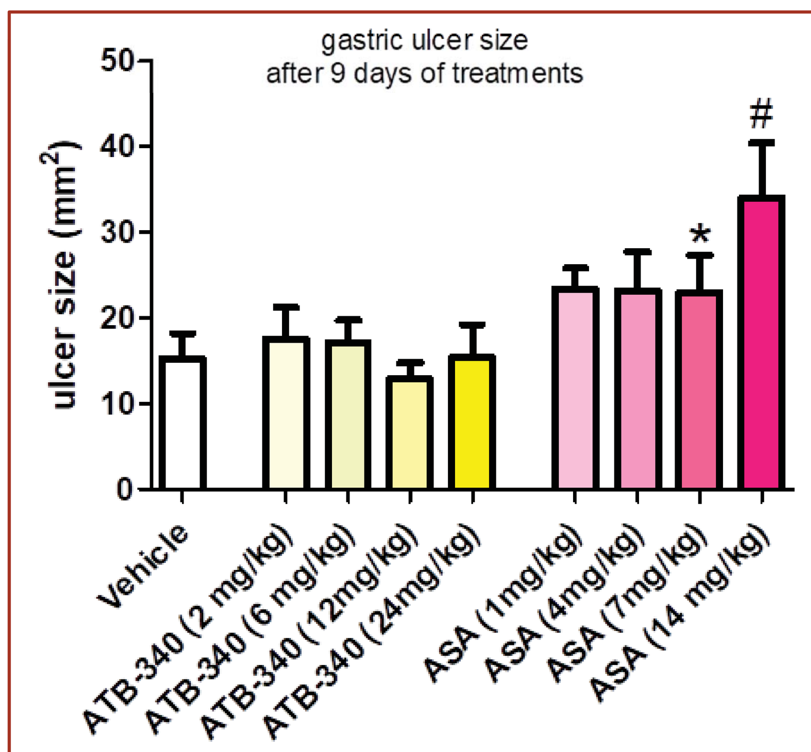

The healing of gastric ulcers was deteriorated after 9 days of ASA treatment, as reflected by significantly increased gastric ulcer size. In contrast to classic aspirin, ATB-340 did not affect gastric ulcer healing.

Gastric and intestinal toxicity of ATB-352 was significantly reduced when compared to ketoprofen. Co-administration of omeprazole reduced ketoprofen toxicity to the level of ATB-352 applied alone. Polypharmacy with aspirin further exacerbated ketoprofen- but not ATB-352-induced GI injury.

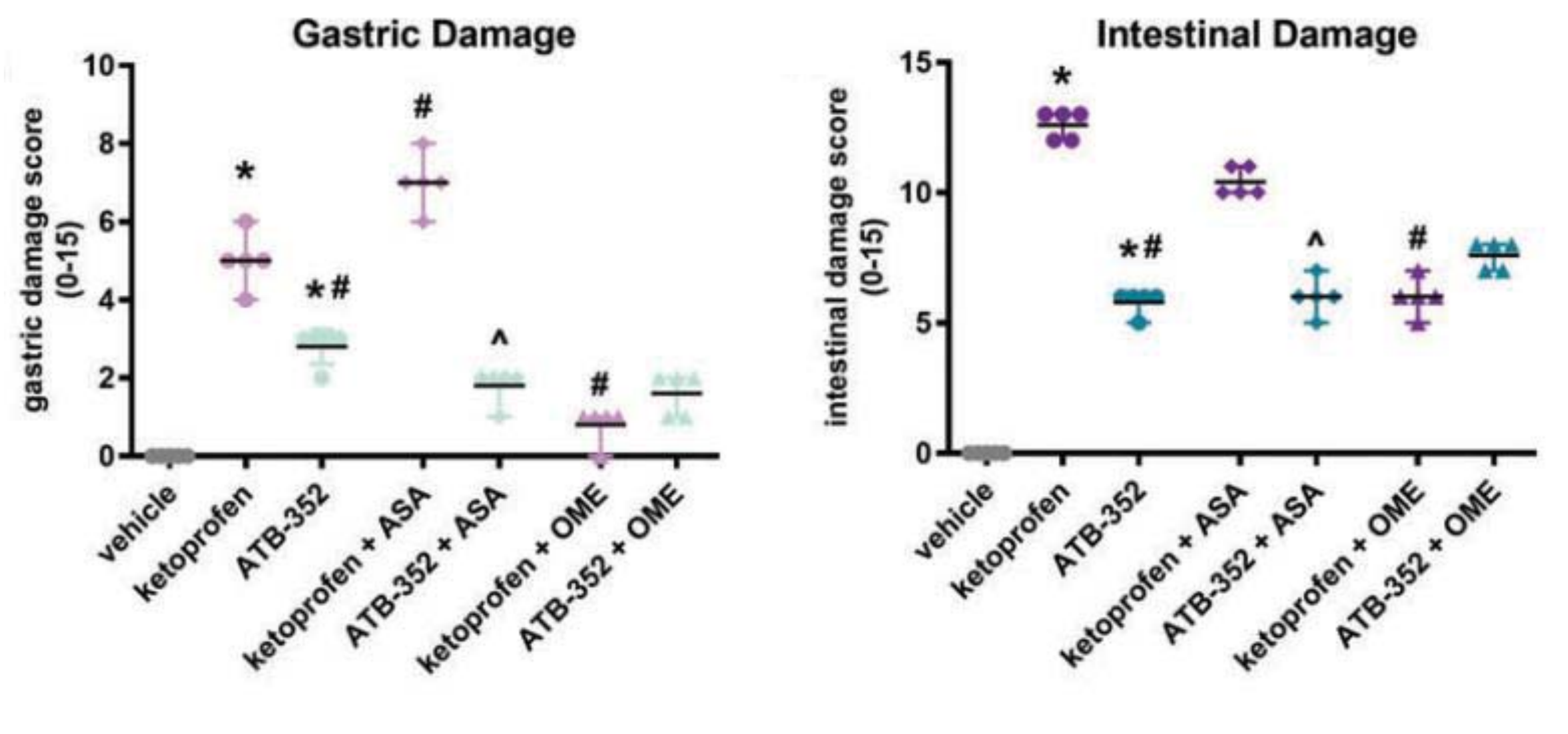

Published in doi: 10.1089/ars.2020.8240

Ketoprofen but not ATB significantly enhanced the percentage of Firmicutes and Bacteroidota. Ketoporfen in contrast to ATB decreased the level of Desulfobacterota being involved in H2S production.

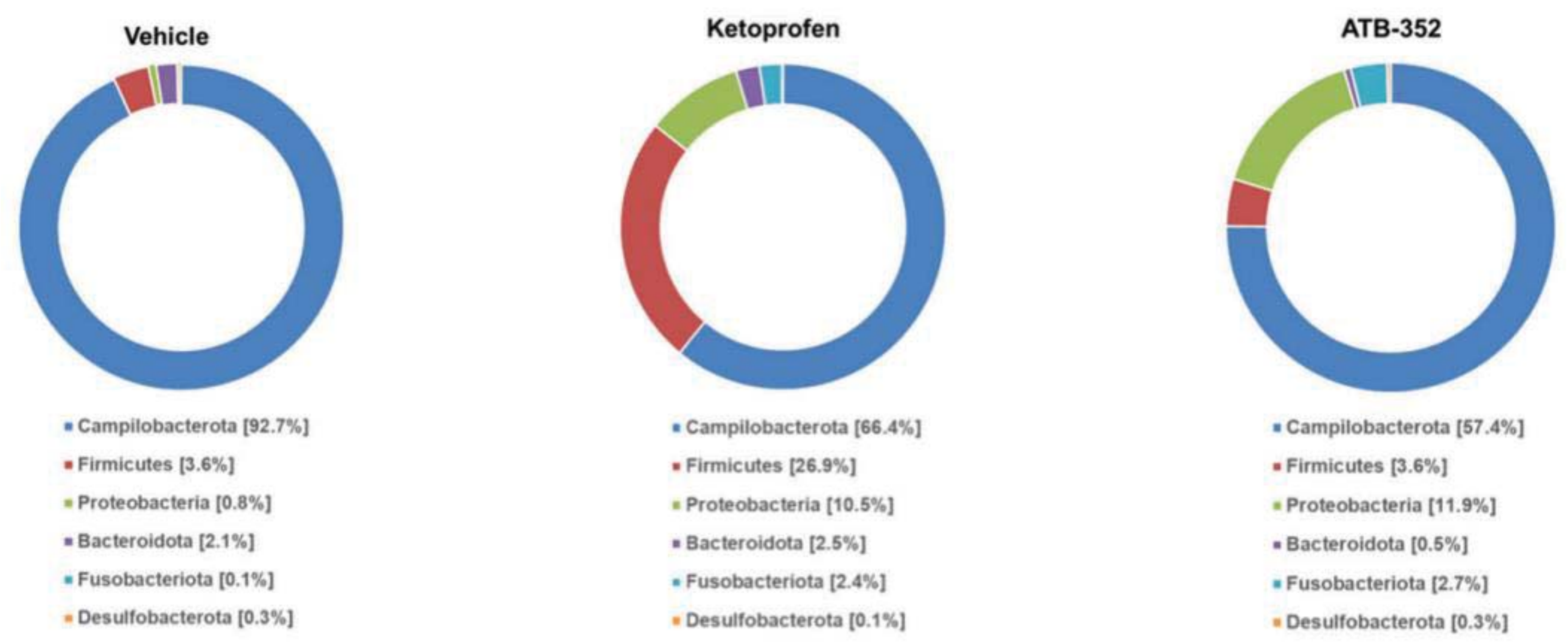

Published in doi: 10.1089/ars.2020.8240

Conclusions:

- ATB-352 presents increased GI safety than ketoprofen and doeas not require co-therapy with PPI to eliminate GI adverse effects.
- Enhanced safety of ATB-352 over ketoprofen could be due to lower impact on intestinal microbiota profile, being crucial for intestinal mucosal homeostasis.
- ATB-340, in contrast to aspirin, does not impair gastric ulcer healing.
- Novel H_2S-releasing NSAIDs including ATB-352 or ATB-340 seem to be promising alternative in therapies of GI disorders.

REFERENCES

- Glowacka, U., Magierowska, K., Wojcik, D., and Hankus, J., Szetela, M., Cieszkowski, J., et al. (2021). Microbiome Profile and Molecular Pathways Alterations in Gastrointestinal Tract by Hydrogen Sulfide-Releasing Non-steroidal Anti-inflammatory Drug (ATB-352). Insight into Possible Safer Polypharmacy. *Antioxid. Redox Signal.* 2020, 8240. doi:10.1089/ars.2020.8240
- Danielak A, Wallace JL, Brzozowski T, Magierowski M. (2021). Gaseous mediators as a key molecular targets for the development of gastrointestinal-safe anti-inflammatory pharmacology. *Front. Pharmacol.* doi: 10.3389/fphar.2021.657457.
- Chan M V., Wallace JL. Hydrogen sulfide-based therapeutics and gastrointestinal diseases: Translating physiology to treatments. *Am J Physiol - Gastrointest Liver Physiol.* 2013. doi:10.1152/ajpgi.00169.2013

ACKNOWLEDGEMENTS

Funding source: The National Centre for Research and Development (LIDER/9/0055/L8/16/NCBR/2017)

Opioid and cholinergic receptors interaction in rat intestine

Klaudia Jaszcza, Krystyna Pierzchała-Koziec

Department of Animal Physiology and Endocrinology, University of Agriculture in Kraków, Poland;

Corresponding author-email: rzkoziec@cyf-kr.edu.pl

Introduction

Enkephalins are short opioid peptides, which are also produced by the GI tract where they are formed in gastric and intestinal endocrine/nervous cells (ENS). Leu- and Met-enkephalin exist in the native, short form and total, extended proenkephalin (PENK) form. Both peptides are potent delta opioids receptor (DOR) agonists. Enterocytes and enteric nervous cells express muscarinic and cholinergic receptors as well as opioids receptors which may suggest that their interaction affects synthesis and release of many peptidergic hormones existing in GI tract. Ghrelin was found in the GI system and interaction with Met-enkephalin at the GI and CNS levels was suggested. Acetylcholine receptors (AChRs) in the gastrointestinal tract are represented by muscarinic and nicotinic receptors. Many anatomical and biochemical evidences indicate the opioidergic and cholinergic systems are co-localized and also act on the same neurons.

Aim of the study

The aim of this study was to evaluate the *in vitro* interaction of opioid and cholinergic receptors in the regulation of Met-enkephalin and ghrelin activity in the rat intestine.

Materials and methods

Materials
Male Wistar rats (n=24), divided into 4 groups:
1. Control group (injection of NaCl),
2. N group (3 mg/kg b.w. of naltrexone),
3. A group (5 mg/kg b.w. of atropine),
4. H group (5 mg/kg b.w. of hexamethonium).

Methods
The concentration of hormones, and proenkephalin mRNA expression were estimated from fragments of duodenum.

Results

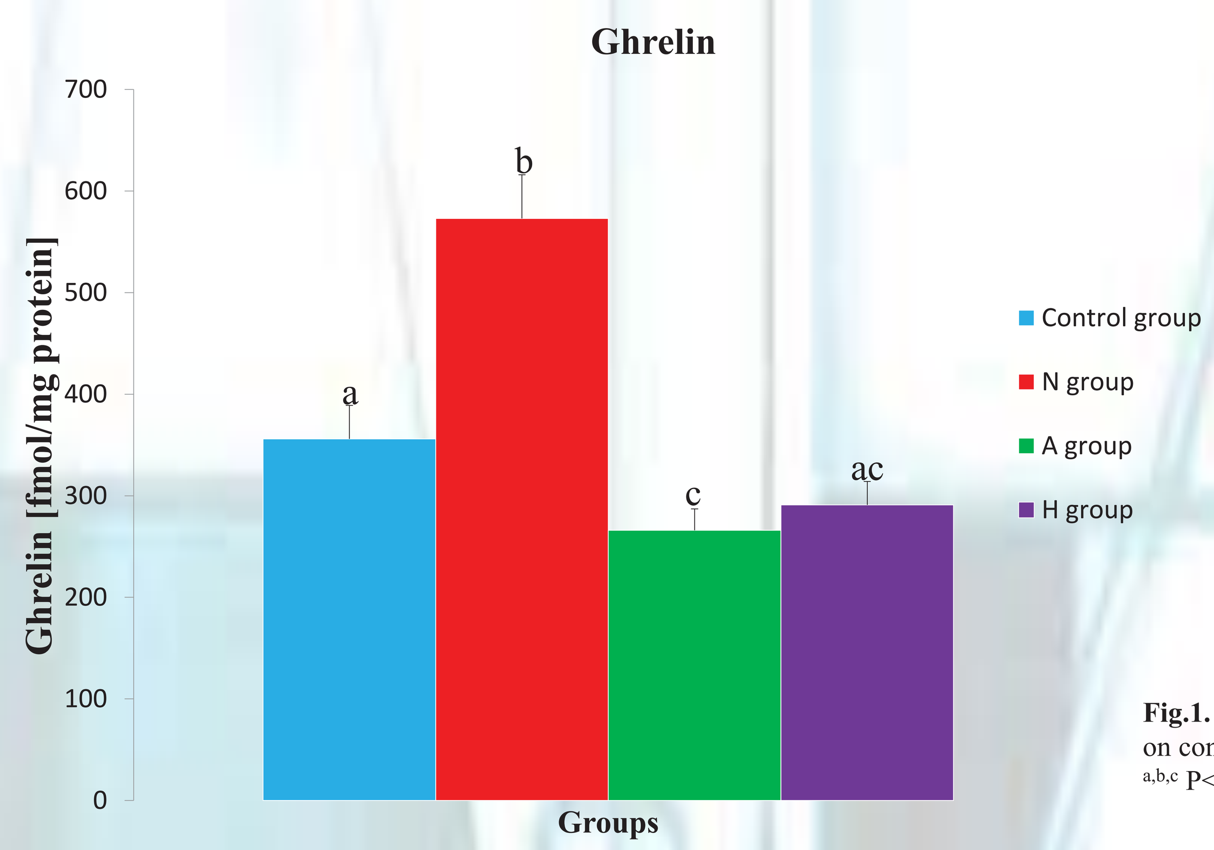

Fig.1. The effects of opioid and cholinergic receptors antagonist on concentration of ghrelin in the rat intestine (fmol/mg protein, x±SEM, a,b,c P<0.05)

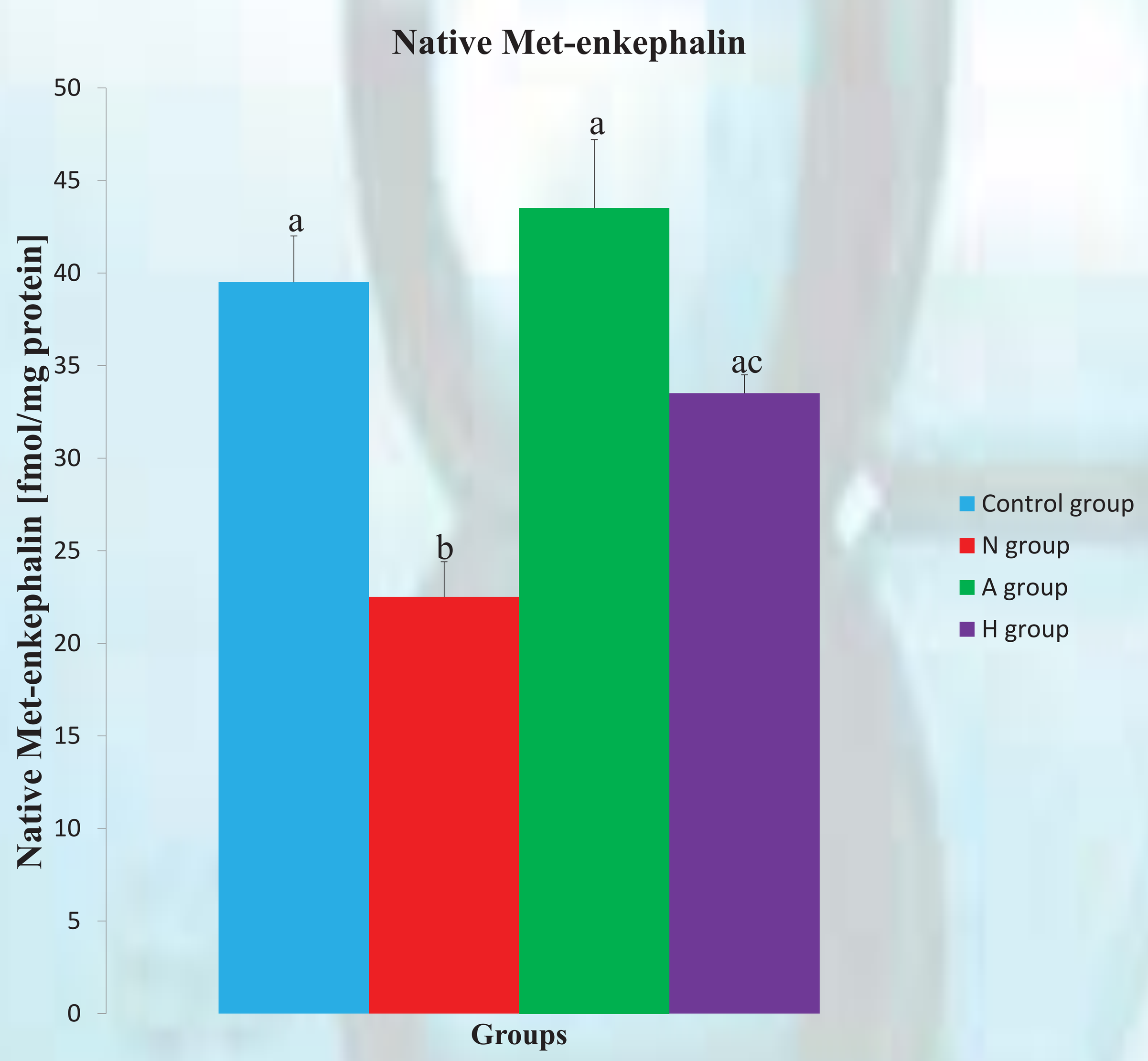

Fig.2. The effects of opioid and cholinergic receptors antagonist on concentration of native Met-enkephalin in the rat intestine (fmol/mg protein, x±SEM, a,b,c P<0.05)

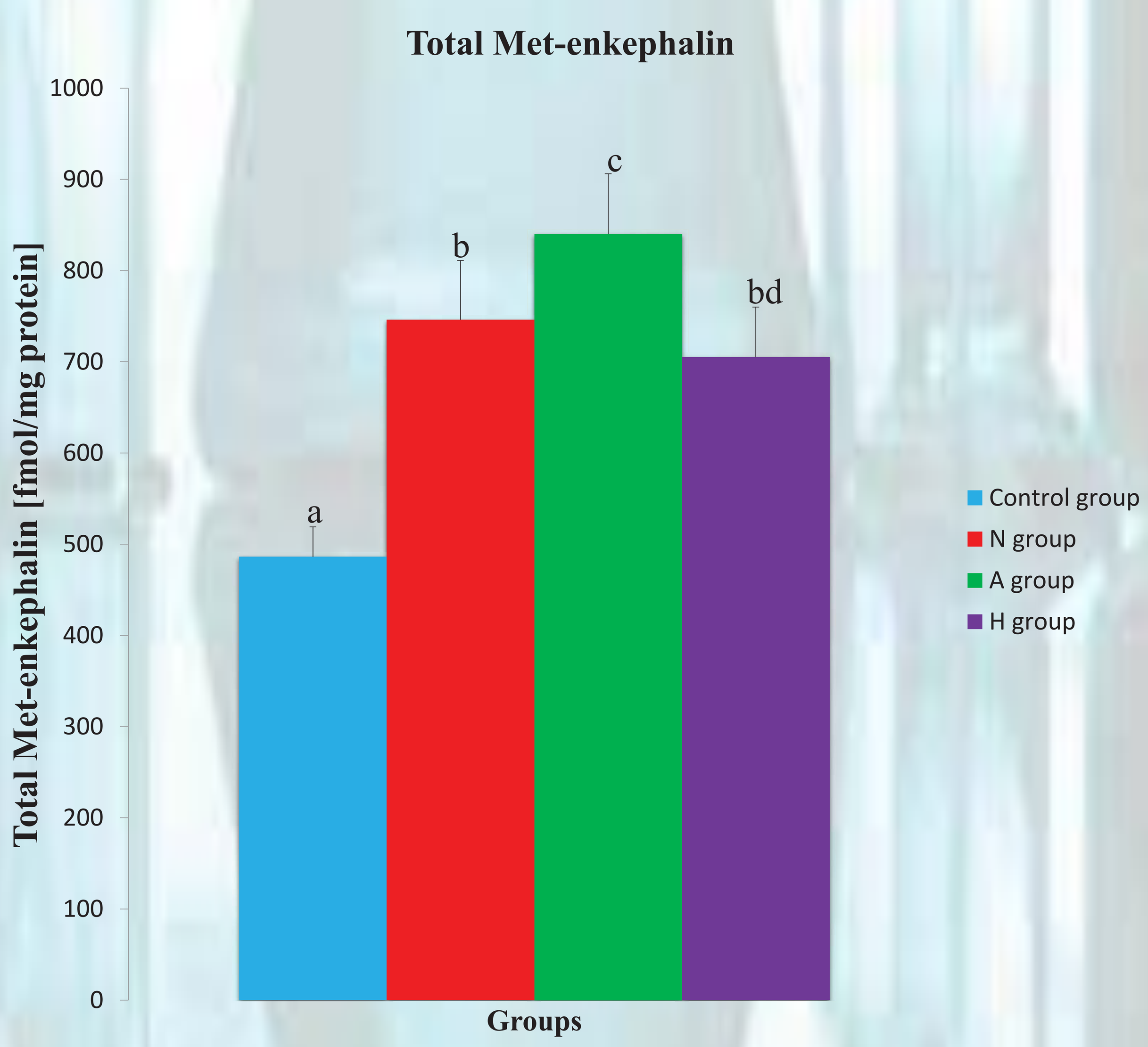

Fig.3. The effects of opioid and cholinergic receptors antagonist on concentration of total Met-enkephalin in the rat intestine (fmol/mg protein, x±SEM, a,b,c,d P<0.05)

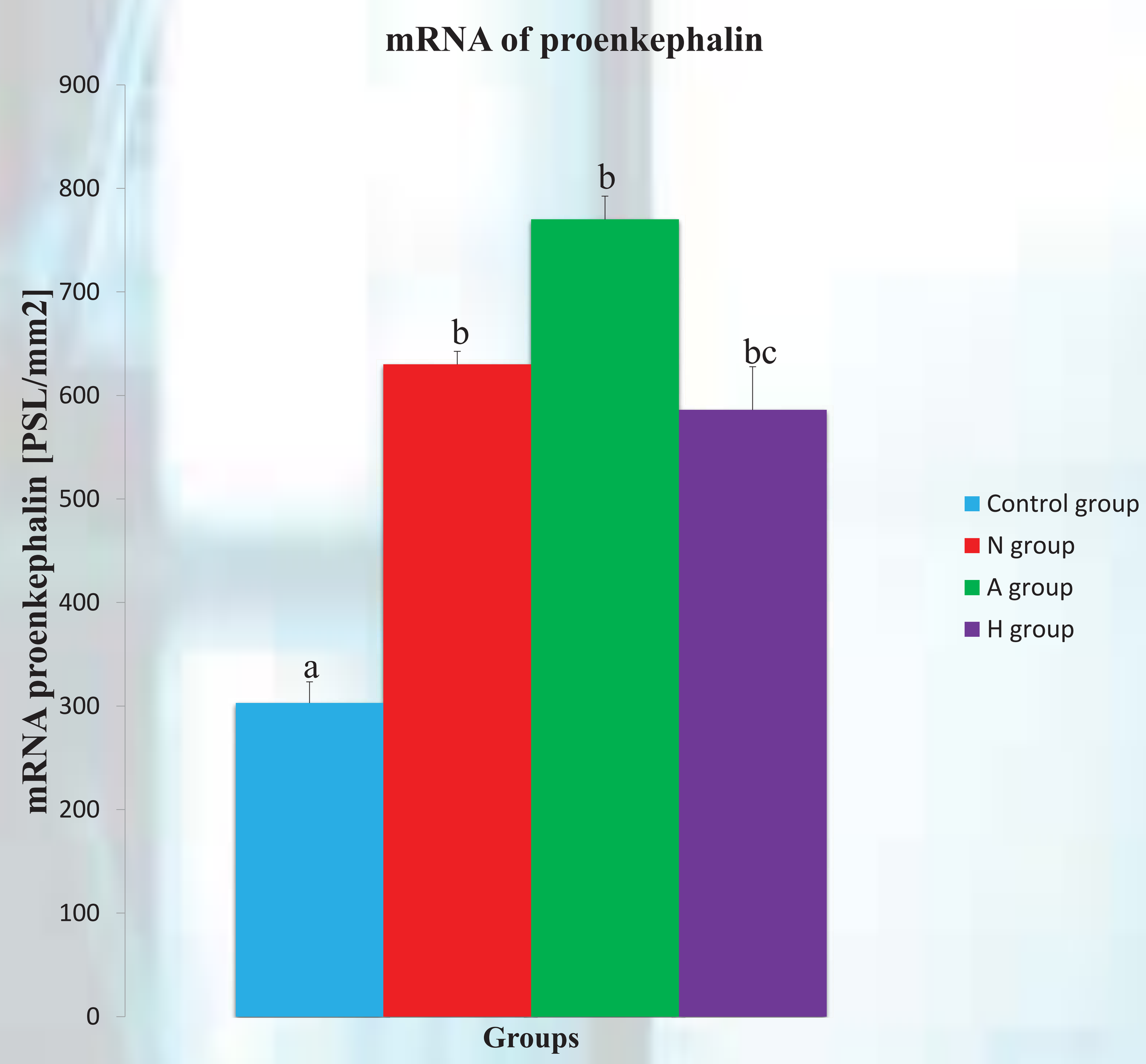

Fig.4. The effects of opioid and cholinergic receptors antagonist on mRNA of proenkephalin in the rat intestine (PSL/mm^2, x±SEM, a,b,c P<0.05)

Conclusion

The present study showed strong evidence for a bidirectional link delineating the relative contributions of neural (cholinergic) and endocrine (ghrelin and enkephalin) pathways in the regulating of gastrointestinal milieu.

Acknowledgments: *Research was financed by the Ministry of Science and Education, No Sub-020002-D015*

SILVER NANOPARTICLES AS DRUG DELIVERY PLATFORMS IN EXPERIMENTAL MODEL OF PERIODONTITIS

Karol P. Steckiewicz and Iwona Inkielewicz – Stępniak

karol.steckiewicz@gumed.edu.pl

Department of Pharmaceutical Pathophysiology, Medical University of Gdansk, Gdansk, Poland

www.gumed.edu.pl

Introduction

Periodontitis (PD) is inflammation of tissues surrounding the teeth, and it may be the cause of teeth loose. Currently treatment options for PD are limited thus novel therapeutic options are needed. Silver nanoparticles (AgNPs) may be interesting therapeutic agents in PD due to their synergistic anti-bacterial and anti-inflammatory properties. In this work we assessed AgNPs as drug delivery platforms in experimental model of periodontitis.

Material and methods

AgNPs conjugated with chlorhexidine and AgNPs conjugated with metronidazole were examined (Figure 1). HGF1 (human gingival fibroblast), hFOB1.19 (human foetal osteoblast), RAW264.7 (murine macrophages) cell lines were used to determine anti-inflammatory properties and safety of AgNPs. MTT assay was used to determine viability of the cells, commercially available ELISA tests were used to determine levels of pro-inflammatory cytokines levels (TNFα, IL1β, IL6, IL8)

Results

Cytotoxicity of AgNPs depended on the type of the drug and AgNPs concentration (Table 1). AgNPs conjugated with metronidazole were less toxic. In non-toxic concertation both types of AgNPs decreased production of pro-inflammatory cytokines by lipopolisacharyde stimulated murine macrophages . After stimulation with LPS, we observed increased levels cytokines. AgNPs-CHL in concentrations of 1.5 and 3 µg/mL significantly decreased levels of produces IL-1ß, Il-6 and TNFα cytokines. Interestingly, 3 µg/mL of AgNPs-CHL decreased TNFα concentration below level's produced by unstimulated control. AgNPs-PEG-MET in the con-centration of 10 µg/mL significantly decreased levels of IL-1ß and TNFα produced by stimulated RAW264.7 cells (Figure 2).

Conclusions

Silver nanoparticles may be safe and effective drug delivery platforms with anti-inflammatory properties to be used in periodontitis. Our findings needs to be evaluated in in vivo studies.

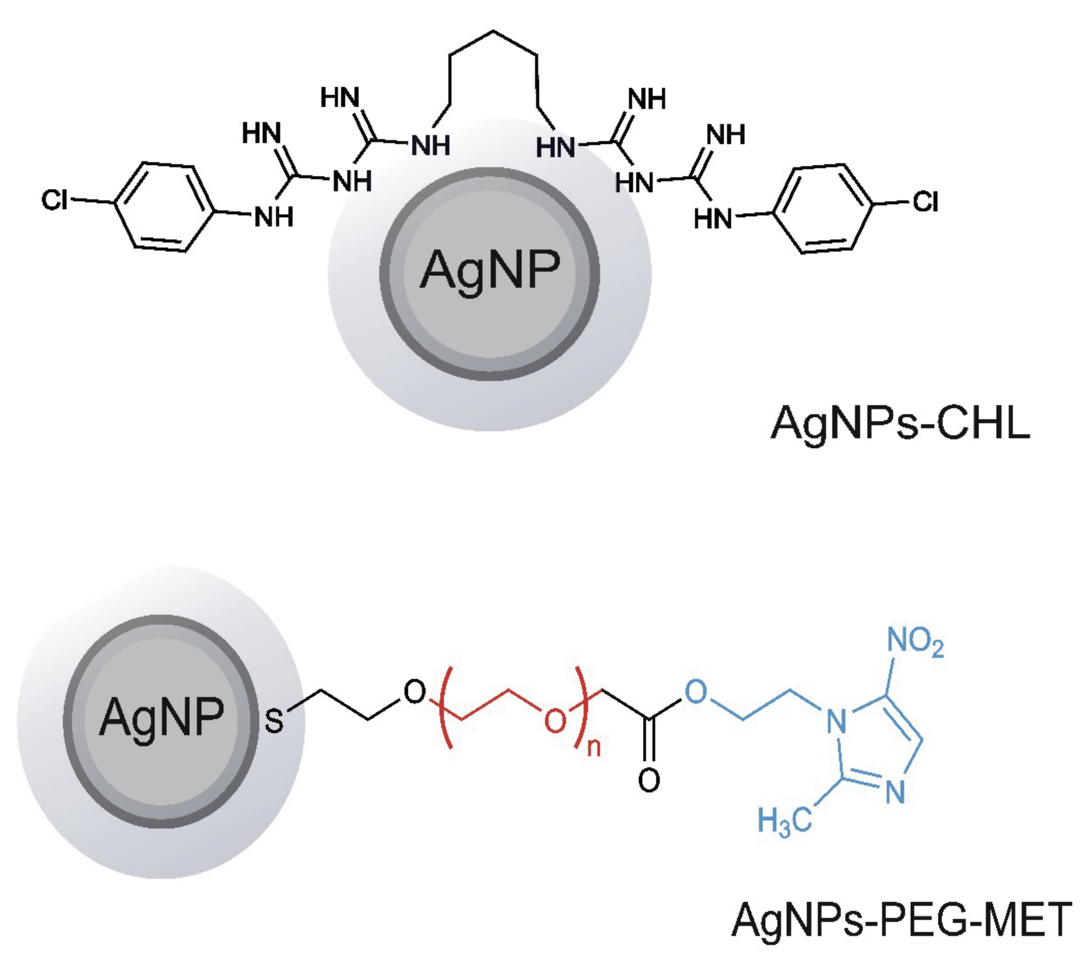

Figure 1. Nanoparticles' structures.

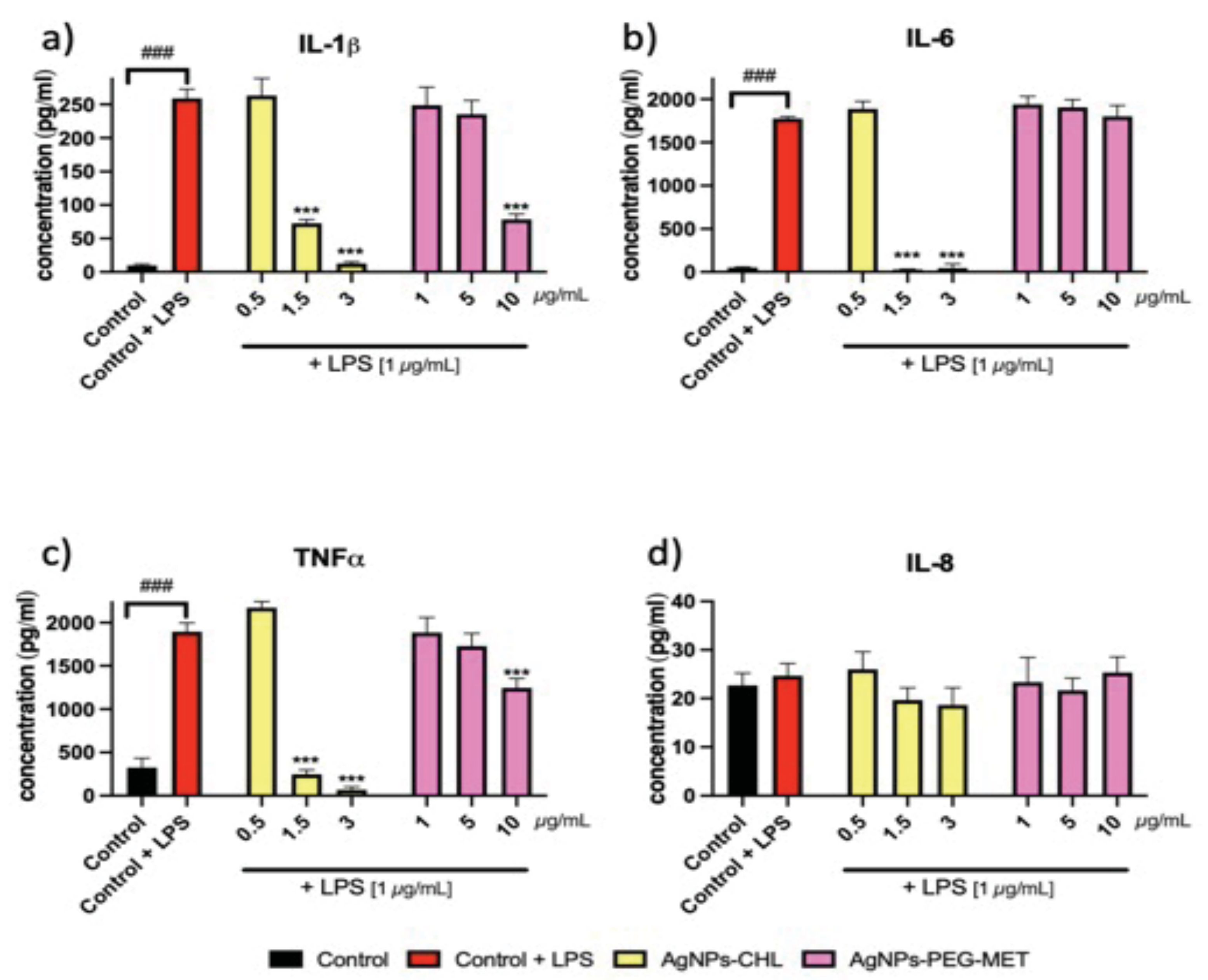

Figure 2. Effect of AgNPs-CHL and AgNPs-PEG-MET on cytokine secretion by RAW264.7 cells to medium. Cells were treated with AgNPs-drugs for 24h, and LPS (1 µg/mL) was used to stimulate inflammation. Secretion of a), IL-1ß secretion of b) IL-6, secretion of c) TNFα, secretion of d) IL-8. Data are presented as mean ± SD. ### p<0.001 (vs untreated control), *** p<0.001 (vs control treated with LPS).

Table 1. Half maximal inhibitory concertation IC50 for AgNPs-CHL and AgNPs-PEG-MET.

NPs type	hFOB1.19	HGF-1	RAW264.7
AgNPs-CHL	*2.332 µg/ml*	*2.246 µg/ml*	*8.425 µg/ml*
AgNPs-PEG-MET	*>10 µg/ml*	*>10 µg/ml*	*>10 µg/ml*

Bibliography

(1) Tonetti, M. S.et al.,Impact of the Global Burden of Periodontal Diseases on Health, Nutrition and Wellbeing of Mankind: A Call for Global Action. J. Clin. Periodontol. 2017, 44 (5), 456–462. (2) Zupancic, S. et al., Contribution of Nanotechnology to Improved Treatment of Periodontal Disease. Curr. Pharm. Des. 2015, 21 (22), 3257–3271 (3) Steckiewicz, K. P. et al., Shape-Depended Biological Properties of Ag_3PO_4 Microparticles: Evaluation of Antimicrobial Properties and Cytotoxicity in In Vitro Model — Safety Assessment of Potential Clinical Usage. Oxid. Med. Cell Longev 2019, 2019 (art id 6740325), 1–19.

Acknowledgments

We would like to thank Elzbieta Megiel and Piotr Cieciorski form University of Warsaw for nanoparticles synthesis. This work was supported by PRELUDIUM grant 2017/27/N/NZ7/0267 from the Polish National Science Center (NCN).

THE EFFECT OF INCREASED AND DECREASED H_2S BIOAVAILABILITY ON THE DEVELOPMENT OF BARRETT'S METAPLASIA

E.KORBUT[1], D.WÓJCIK[1], K.MAGIEROWSKA[1], V.JANMAAT[2], M.WIERDAK[1], T.BRZOZOWSKI[1], M.SZETELA[1], M.WHITEMAN[3], M.MAGIEROWSKI[1]

[1]Department of Physiology, Jagiellonian University Medical College, Krakow, Poland; [2]Department of Gastroenterology and Hepatology, Erasmus University Medical Center, Rotterdam, Netherlands; [3]University of Exeter, Exeter, The United Kingdom

GaMEG LAB

INTRODUCTION

Barrett's Esophagus (BE) is a pre-malignant condition characterized by the conversion of the normal esophageal squamous epithelium into metaplastic columnar epithelium. Hydrogen sulfide (H_2S), endogenously generated by cystathionine β-synthase (CBS) and cystathionine γ-lyase (CTH) contributes to the maintenance of gastrointestinal mucosa integrity. However, the role of H_2S-prodrugs in the pathogenesis of BE has not been elucidated.

OBJECTIVES

This study aimed to investigate the effect of chronic treatment with the slow-releasing H_2S donor, GYY4137, on BE progression *in vivo* and *in vitro*.

METHODS

***In vitro* studies:**

Human-derived esophageal keratinocytes (EPC2) with or without CRISPR/Cas9-induced CTH/CBS gene knock-outs (k/o) were treated with acidified bile mixture (BM), to induce clinically observed BE-like molecular profile and/or with GYY4137 and CTH inhibitor (PAG).

***In vivo* studies:**

Male Wistar rats with esophagogastroduodenal anastomosis (EGDA) were treated i.g. for 8 weeks with vehicle, GYY4137 (0.5-50 mg/kg) or CTH inhibitor (PAG,15 mg/kg). mRNA expression for BE-specific genes and proinflammatory targets was determined by real-time PCR. Serum content of 10 inflammatory-response markers and esophageal concentration of key modulators of important signaling pathways were determined by multiplex microbeads fluorescent assay.

RESULTS

***In vitro* studies:**

- GYY4137, PAG and CTH/CBS k/o did not affect EPC2 cell viability.

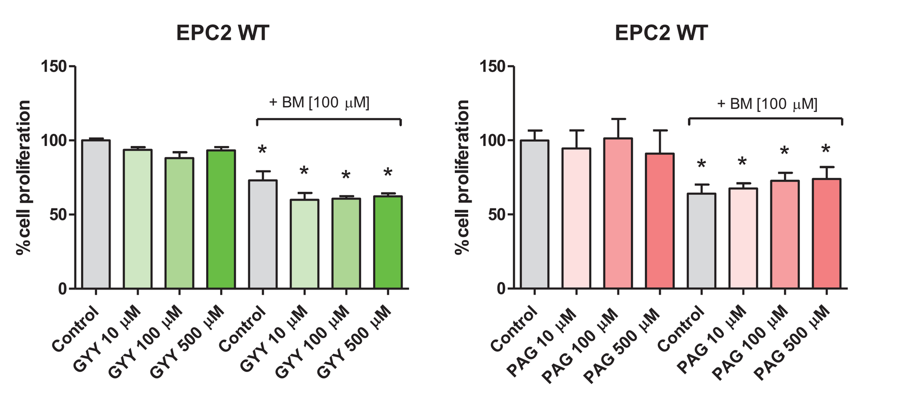

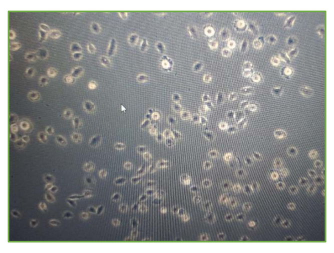

- BM treatment of CBS and CTH k/o EPC2 further enhanced molecular BE-specific alterations, similarly to the groups treated with PAG.

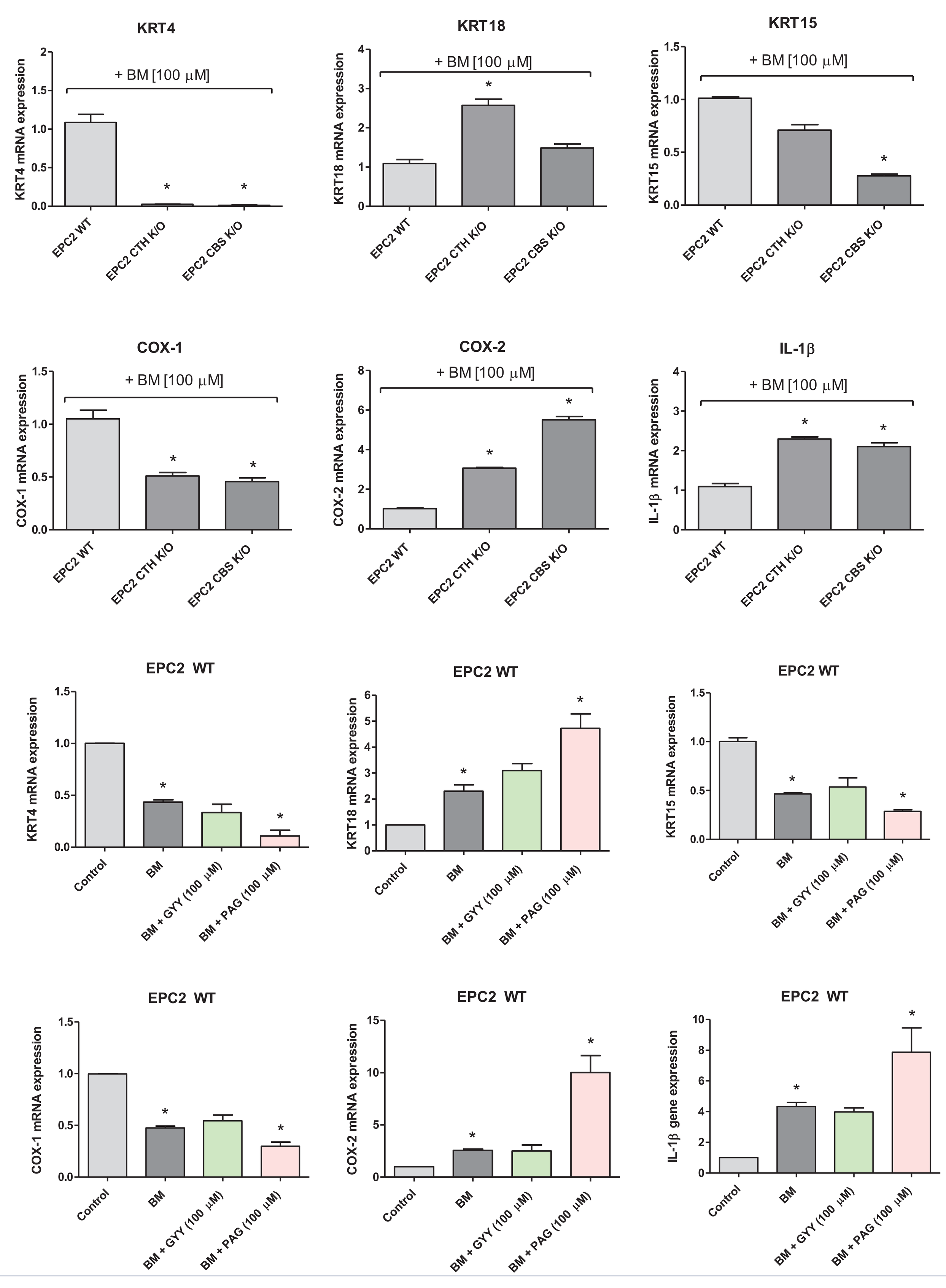

RESULTS

***In vivo* studies:**

- In animal model, daily treatment with GYY4137 dose-dependently reversed while PAG increased BE-specific targets expression as compared with vehicle.
- Furthermore, we observed decreased proinflammatory markers serum concentration and altered levels of transcription factors and kinase activities.

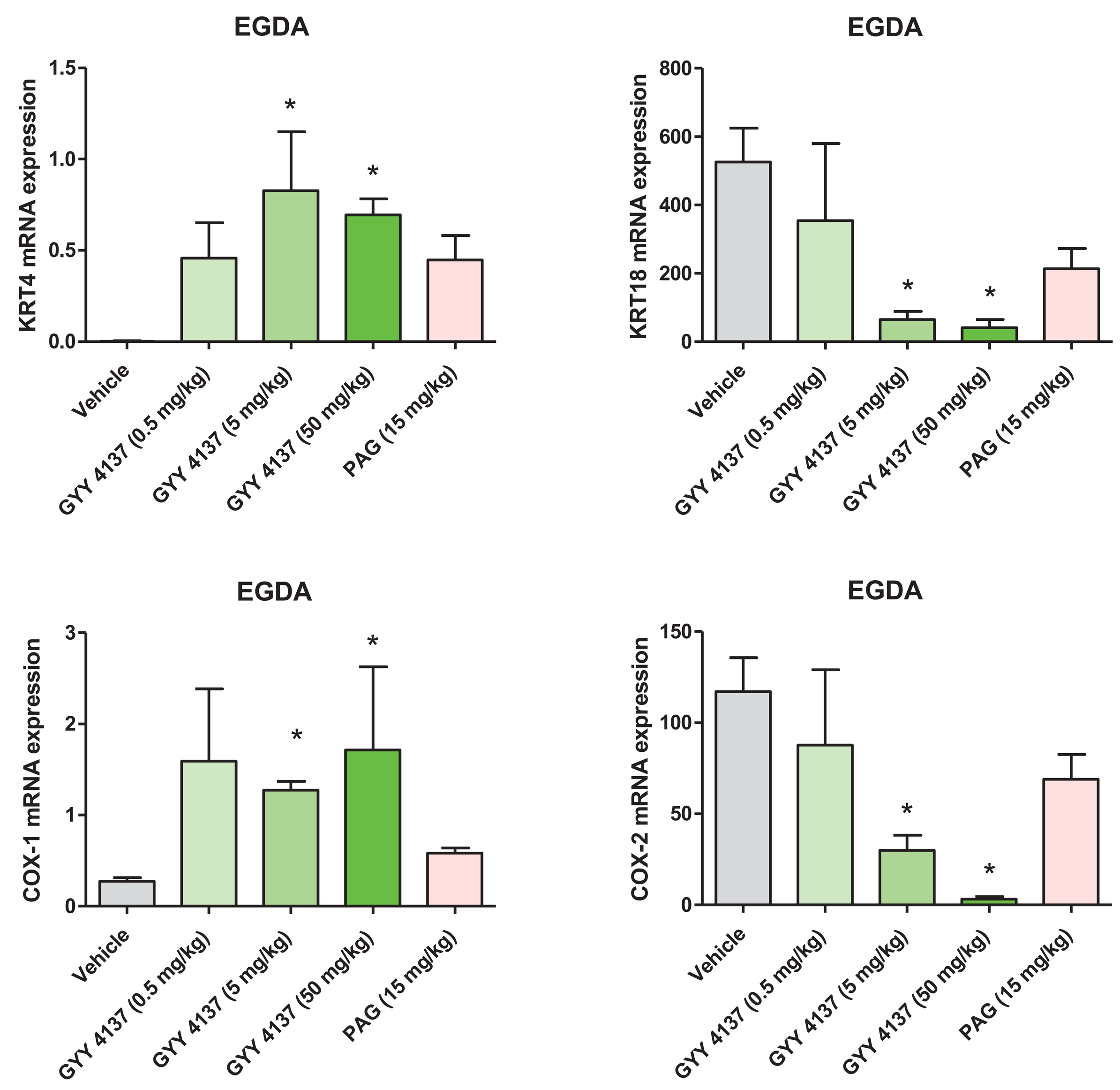

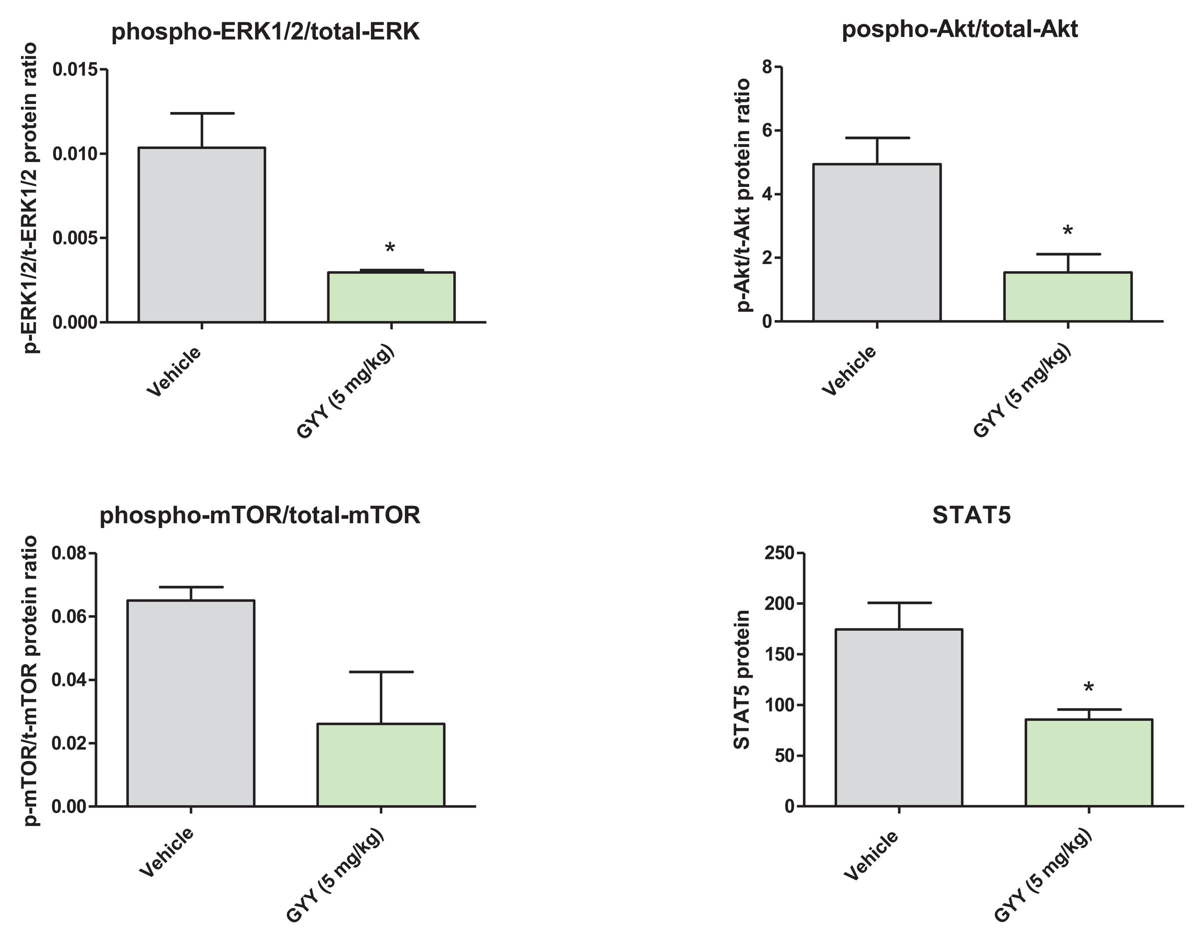

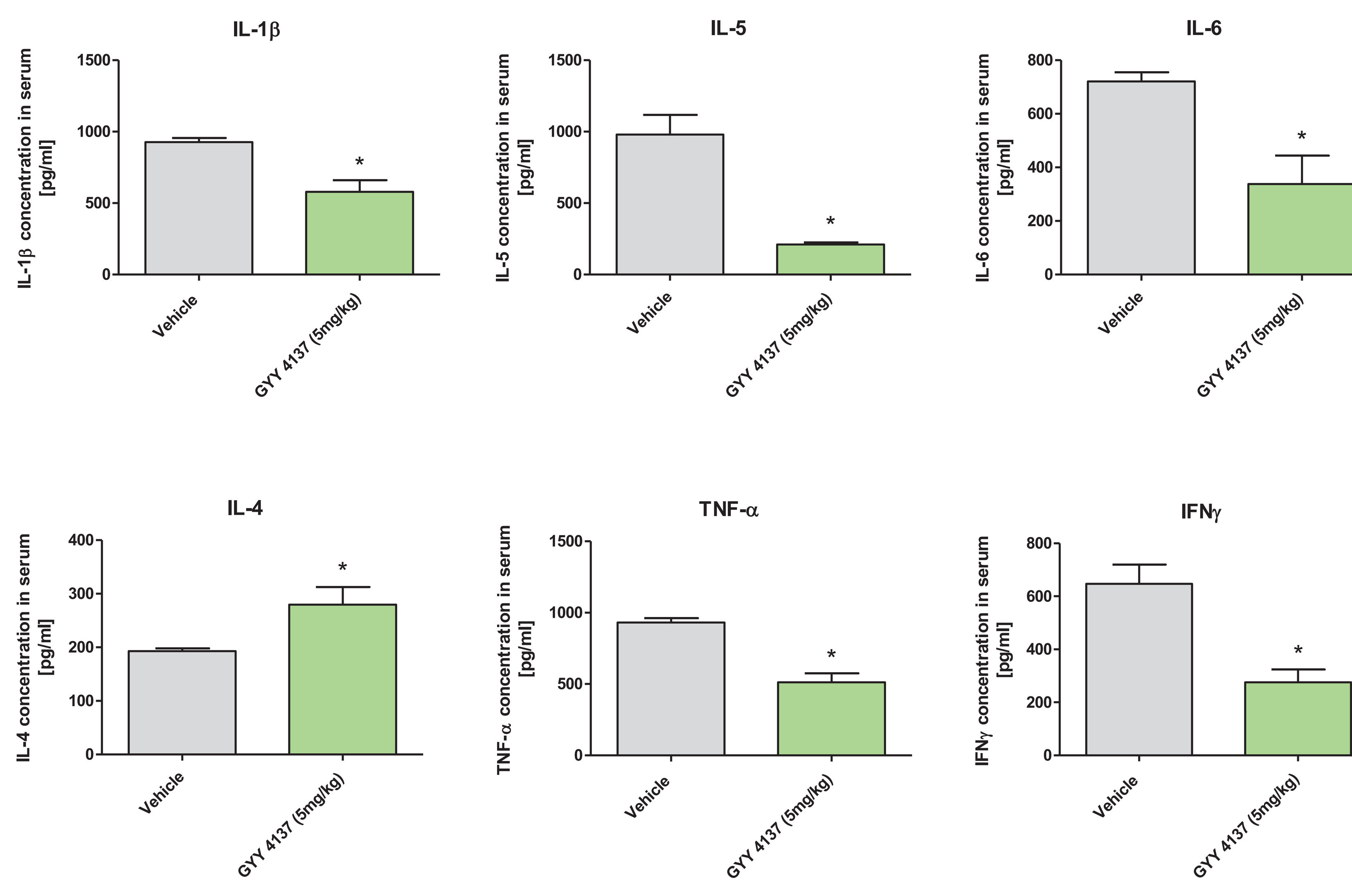

CONCLUSIONS

We conclude that H_2S produced endogenously or released from pharmacological tools could be involved in the inhibition of BE metaplasia development and its further progression due to downregulation of dysplasia-accelerating pathway and molecular pro-inflammatory signaling.

Contact: edyta.korbut@uj.edu.pl

Funding source: National Science Centre, Poland (UMO-2016/23/D/NZ4/01913).

THE EFFECT OF CARBON MONOXIDE (CO) RELEASED FROM PHARMACOLOGICAL DONORS ON THE DEVELOPMENT OF BARRETT'S ESOPHAGUS

KINGA KRUKOWSKA[1], DOMINIK BAKALARZ[1 2], DAGMARA WOJCIK[1], MATEUSZ WIERDAK[1], KATARZYNA MAGIEROWSKA[1], EDYTA KORBUT[1], ALEKSANDRA DANIELAK[1], TOMASZ BRZOZOWSKI[1], MARCIN MAGIEROWSKI[1]

[1] Department of Physiology, Jagiellonian University-Medical College, Cracow, Poland

[2] Department of Forensic Toxicology, Institute of Forensic Research, Cracow, Poland,

Corresponding author: kinga.krukowska@doctoral.uj.edu.pl, m.magierowski@uj.edu.pl

Introduction:

CO (carbon monoxide) is a cellular gaseous mediator produced via enzymatic activity of heme oxygenase (HMOX). This molecule has been shown to exert cytoprotective effects within gastrointestinal (GI) mucosa in low concentrations. On the other hand, Barrett's esophagus (BE) predisposes GI mucosa to the development of esophageal adenocarcinoma (EAC). There have been synthesized several CO releasing molecules (CORMs) so far, the effect of which is being widely studied [1].

Objective:

The evaluation of whether the chronic treatment with CORMs affects BE development and progression based on experimental *in vitro* and *in vivo* models.

Methods

In vivo	In vitro
I. **Male Wistar rats** with esophagogastroduodenal anastomosis (EGDA) subjected to a 8-week treatment i.g. with vehicle or with **CORM-2** (tricarbonyldichlororuthenium (II) dimer) in dose 0.2- 5 mg/kg	**EPC2** (human keratinocyte), **OE33, OE19** (cancer) cell lines subjected to a 3-day treatment with **CORM-A1** (0,05-1000μM)
II. The macroscopic evaluation of esophageal lesions/metaplasia index (**ELMI**)	
III. The evaluation of mRNA expression of: *KRT* gene family, *IL-1RA, SOCS3* by **qPCR**	

Results :

The **EMLI** score was decreased in gropus treated with CORM-2 as compared to the vehicle.

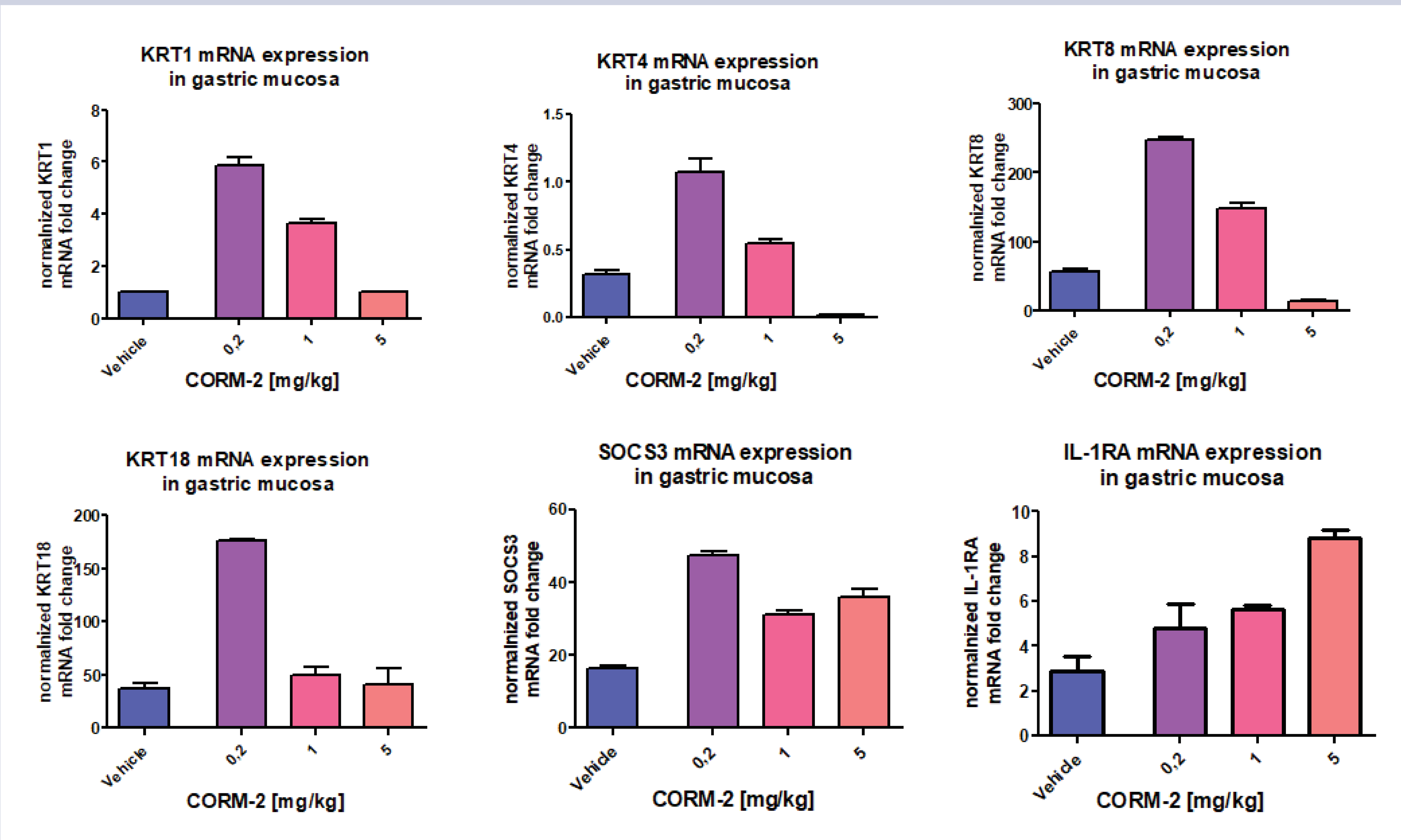

Graph 1. The mRNA expression of selected genes in rat's gastric mucosa , after 8-week treatment with CORM-2.

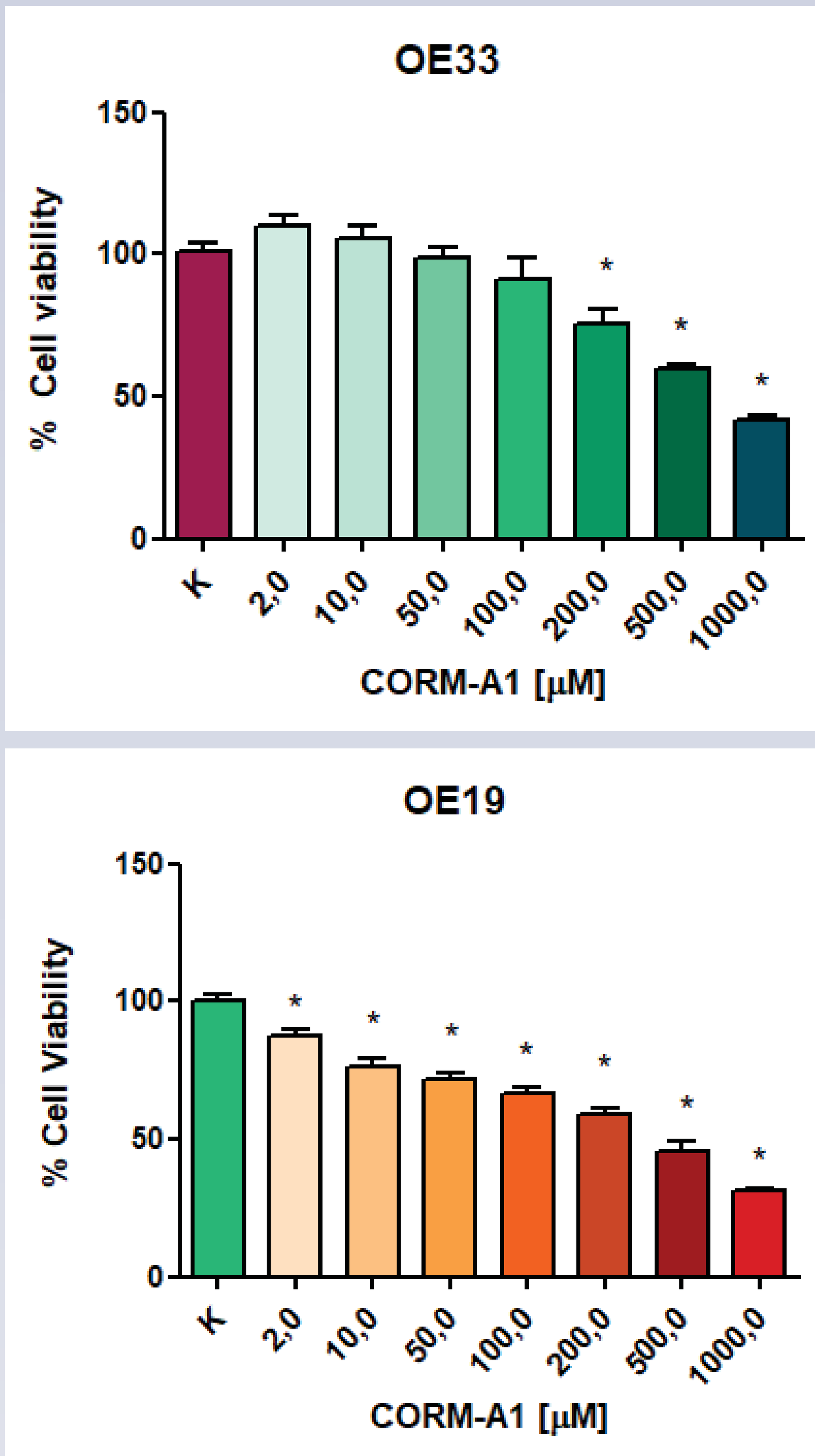

Graph 2. MTT assay of OE33 (above) and OE19 (below) cell line, treated with CORM-A1 for 3-days ($p<0,05$).

Conclusion: CO released from its pharmacological donors modulates the development and progression of BE due to the upregulation of anti-inflammatory response pathways within esophageal mucosa exposed to gastroesophageal reflux disease (GERD).

References:

[1] Ling K, Men F, Wang WC, Zhou YQ, Zhang HW, Ye DW. Carbon Monoxide and Its Controlled Release: Therapeutic Application, Detection, and Development of Carbon Monoxide Releasing Molecules (CORMs). J Med Chem. 2018 Apr 12;61(7):2611-2635.

[2] Motterlini R, Sawle P, Hammad J, Bains S, Alberto R, Foresti R, Green CJ. CORM-A1: a new pharmacologically active carbon monoxide-releasing molecule. FASEB J. 2005 Feb;19(2):284-6.

Funding source: National Science Centre, Poland (UMO-2019/33/B/NZ4/00616)]

MODULATION OF MITOCHONDRIAL ACTIVITY BY HYDROGEN SULFIDE-RELEASING AP-39 IN GASTROINTESTINAL PHYSIOLOGY AND PHARMACOLOGY.

Katarzyna Magierowska[1], Dagmara Wojcik[1], Dominik Bakalarz[1,2], Edyta Korbut[1], Zbigniew Sliwowski[1], Slawomir Kwiecien[1], Jakub Cieszkowski[1], Tomasz Brzozowski[1], Malgorzata Szetela[1], Matthew Whiteman[4], Marcin Magierowski[1]

[1]Department of Physiology, Jagiellonian University Medical College, Cracow, Poland; [2]Department of Forensic Toxicology, Institute of Forensic Research, Cracow, Poland; [3]University of Exeter, Exeter, The United Kingdom

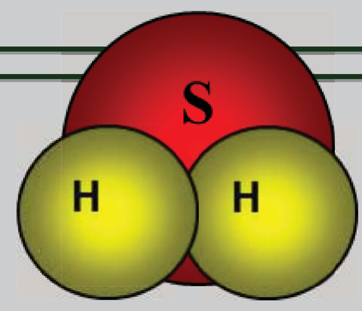

Background

Hydrogen sulfide (H_2S) is generated endogenously, H_2S is produced by cysthatione γ-lyase (CSE)/cystathionine β synthetase (CBS) and 3-mercaptopyruvate sulfurtansferase (3-MST). H_2S has been shown to accelerate the healing of chronic gastric ulcers and to prevent gastrointestinal (GI) tract against the drugs-induced toxicity.

Novel mitochondria-targeting H_2S-releasing compound [(10-oxo-10-(4-(3-thioxo-3H-1,2-dithiol-5yl)phenoxy)decyl) triphenylphosphonium bromide] (AP39) was developed allowing further investigation into detailed mechanisms of H_2S action.

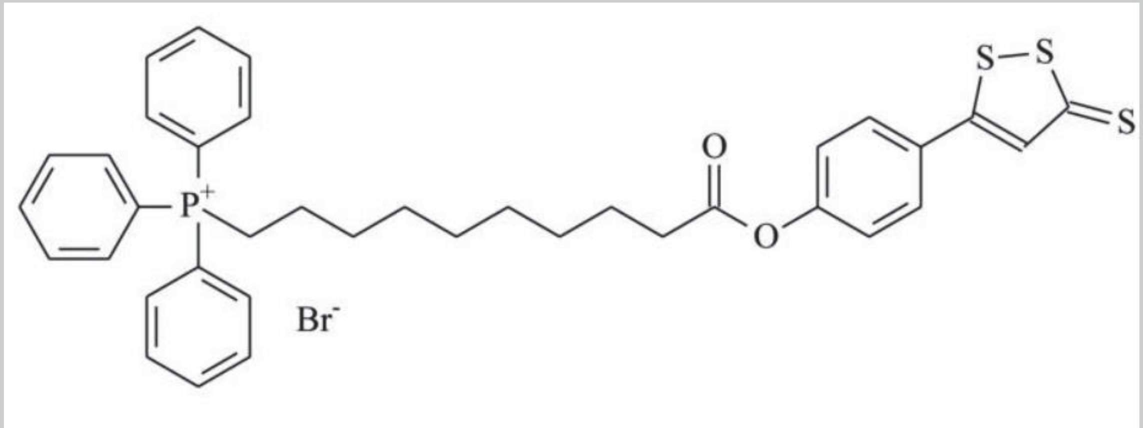

Chemical structure of mitochondria targeting H_2S-releasing AP39

Aim of the study

We aimed to determine the impact of H_2S released from AP39 within gastric mucosa exposed to acetylsalicylic acid (ASA).

Material and methods

- ✓ Male Wistar rats (average weight 250 g) were fasted for 24 h before the study.
- ✓ Gastric damage was induced by intragastric (i.g.) application of aspirin (ASA) in the dose of 125 mg/kg.
- ✓ 30 minutes before ASA application animals were pretreated with saline or AP39. 1 hour after gastric damage induction, animals were sacrified and stomachs were removed to determine gastric damage area by planimetry and samples were taken to prepare histological slides (stained with hematoxylin and eosin (H/E).
- ✓ Complex IV activity was assessed using the Complex IV Human Enzyme Activity Microplate Assay Kit.
- ✓ ERK, JNK, p38 phospho/total protein expression in gastric mucosa and content of TNF-β1 and TNF-β2 in serum was determined using Luminex micro beads fluorescent assays (Bio-Rad, Hercules, CA, USA) and Luminex MAGPIX System (Luminex Corp., Austin, TX, USA).

Results

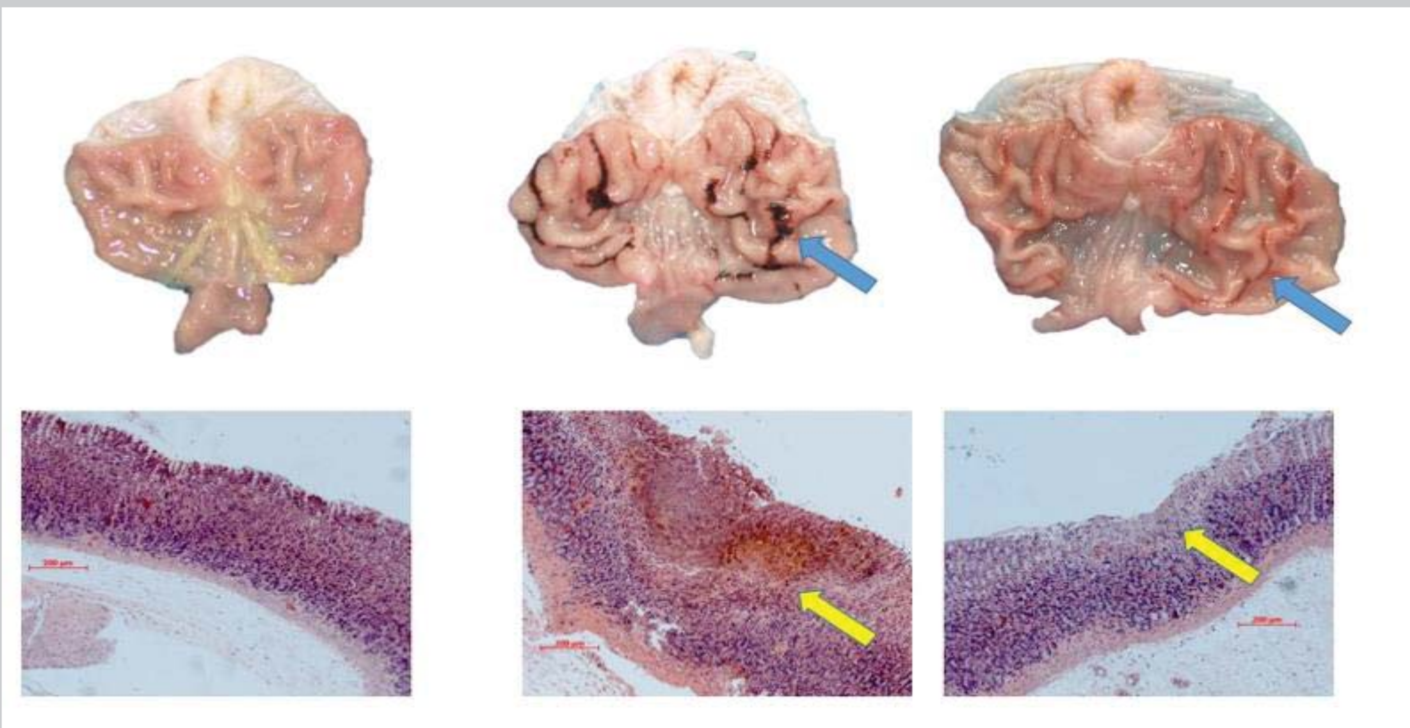

INTACT | VEHICLE | AP-39 (0,02 mg/kg i.g.)

+ ASA (125 mg/kg i.g.)

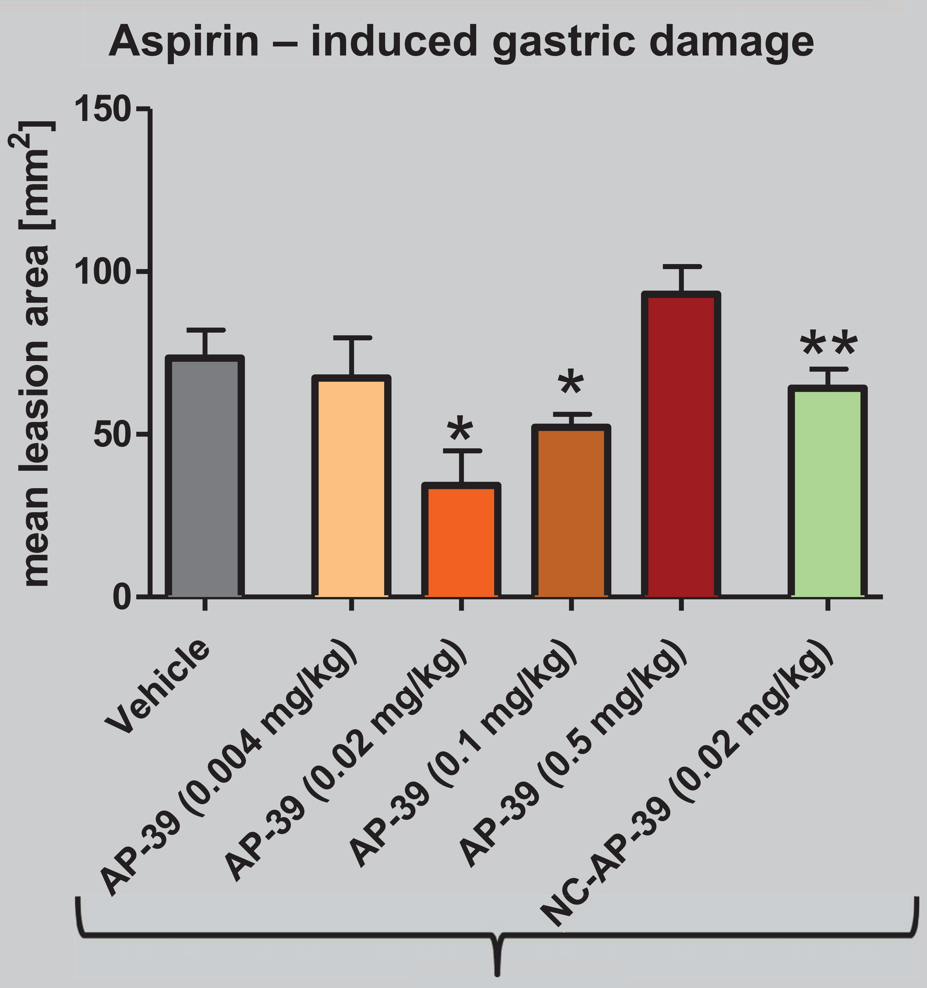

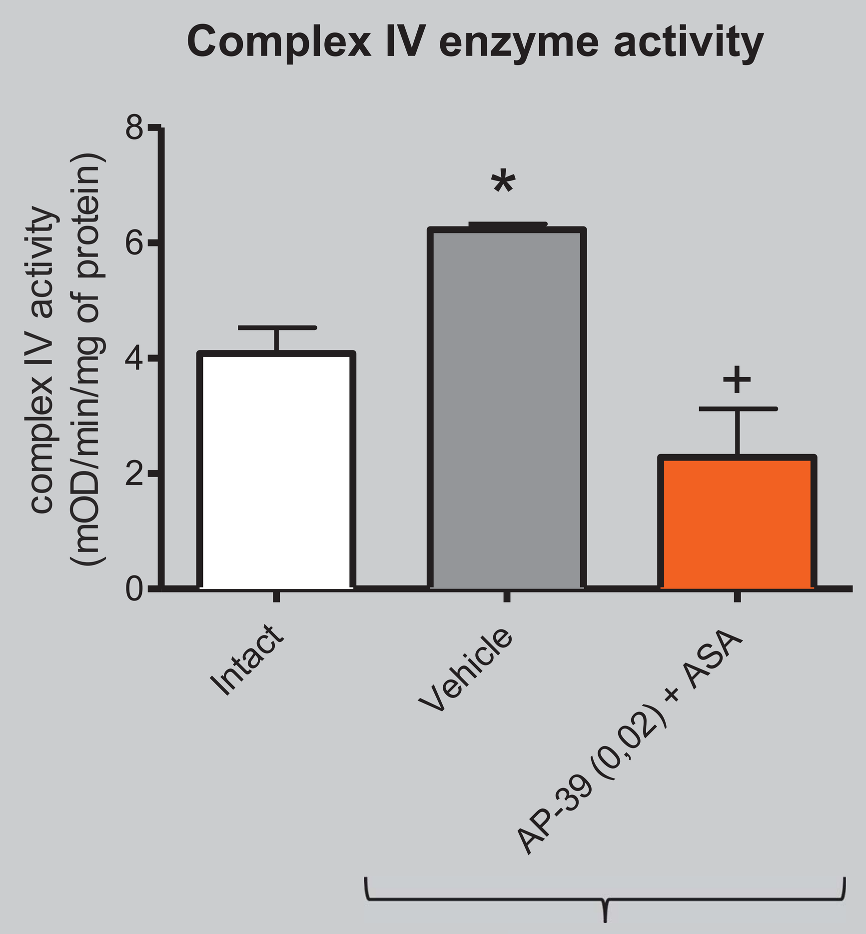

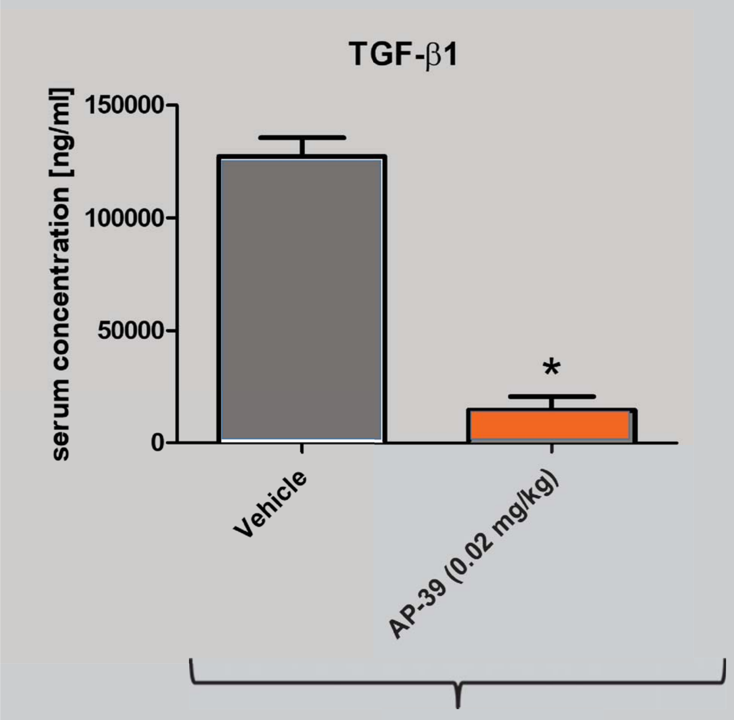

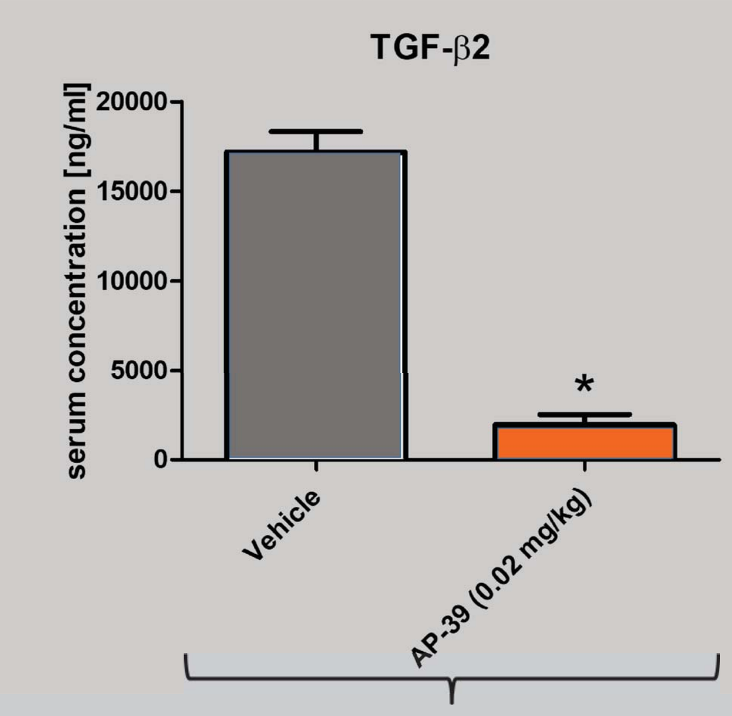

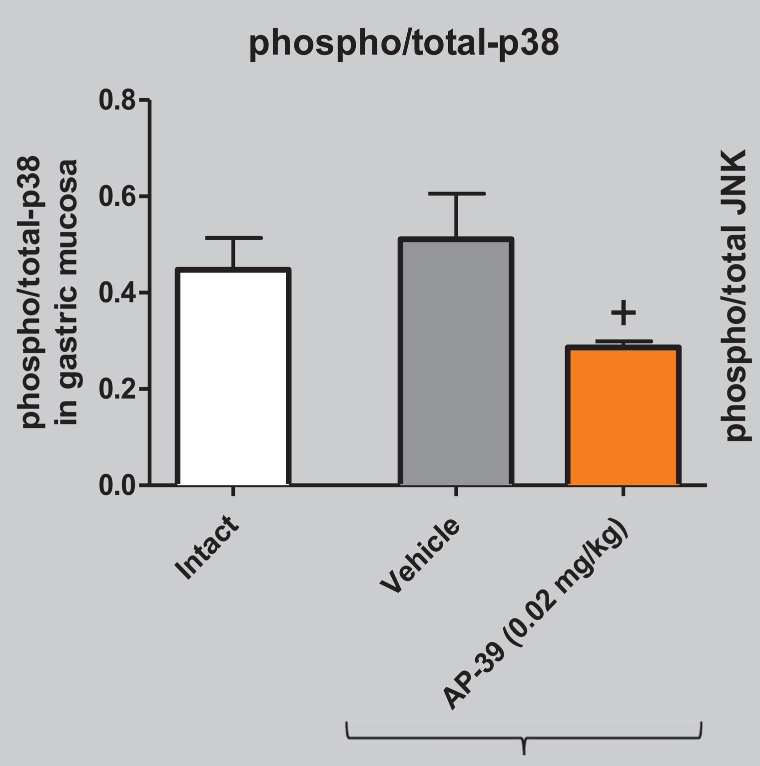

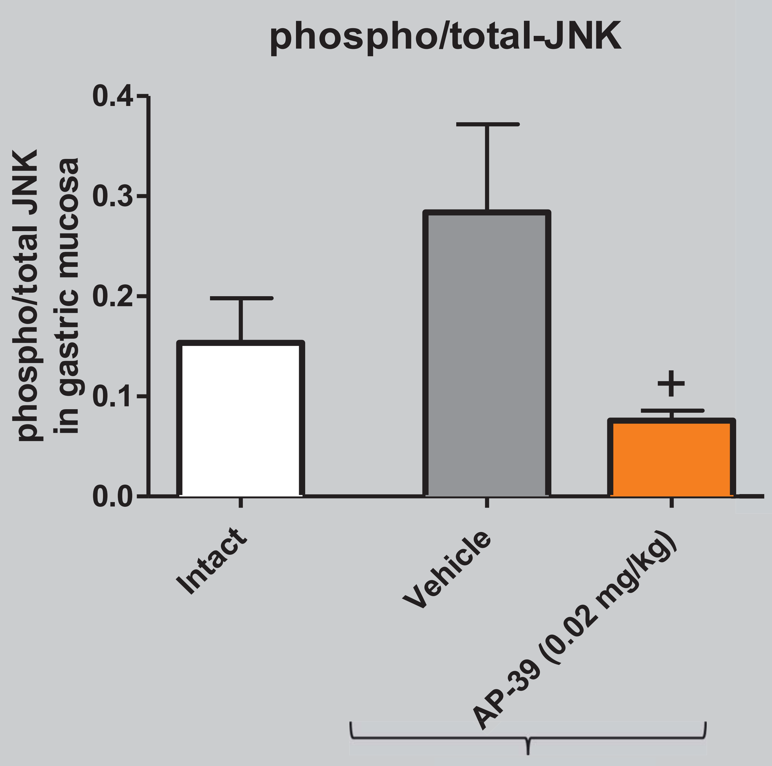

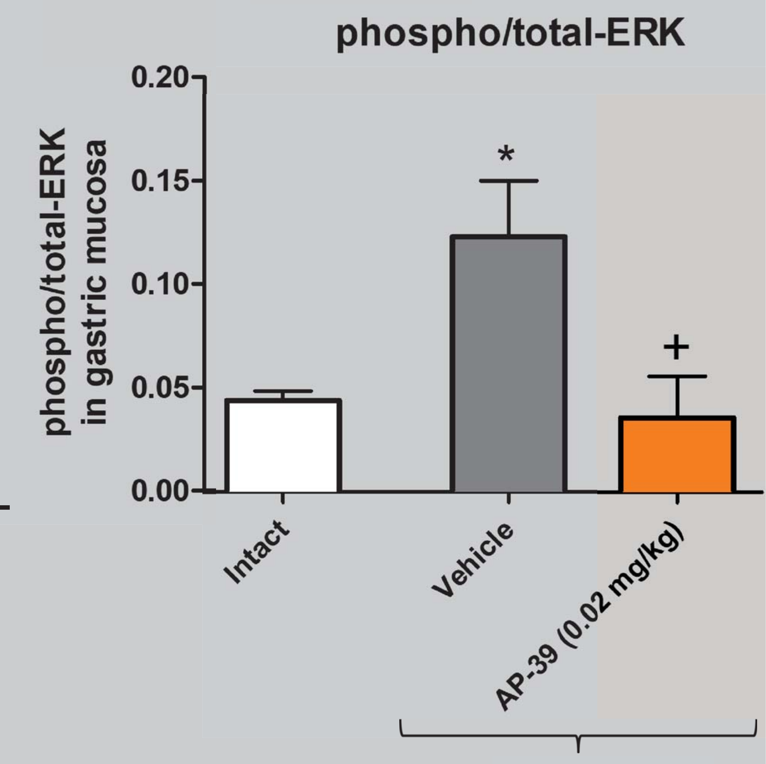

Conclusions

- ❑ H_2S released from AP39 directly into the mitochondria **prevents gastric mucosa** against ASA-induced injury
- ❑ H_2S released from AP39 **reversed the ASA-induced modulation of** complex IV activity
- ❑ AP39 - induced gastroprotection was accompanied by decreased serum content of TGF-β1 and TGF-β2
- ❑ The molecular mechanisms of AP39-gastroprotection is due to the **inhibiton of MAP kinases signalling pathway**

GaMEG LAB

E-mail: katarzyna.magierowska@uj.edu.pl

INTESTINAL ALKALINE PHOSPHATASE ATTENUATES THE EXACERBATION OF MURINE COLITIS IN VOLUNTARY EXERCISING OBESE MICE. INVOLVEMENT OF INTESTINAL MICROBIOTA, OXIDATIVE STRESS AND CYTOKINES

D. WOJCIK[1], M. HUBALEWSKA-MAZGAJ[1], M. SURMIAK[1], Z. SLIWOWSKI[1], A. WOJCIK[1], S. KWIECIEN[1], A. MAZUR-BIALY[2], J. BILSKI[2], T. BRZOZOWSKI[1]

[1] Department of Physiology, Faculty of Medicine, Jagiellonian University Medical College, Cracow, Poland;
[2] Department of Ergonomics and Exercise Physiology, Faculty of Health Sciences, Jagiellonian University Medical College, Cracow, Poland

JAGIELLONIAN UNIVERSITY
MEDICAL COLLEGE

This study was supported by National Science Centre in Poland within the framework of project grant (UMO-2015/19/B/NZ4/03130)

Introduction: Inflammatory bowel diseases (IBD) are chronic inflammatory disorders of the colon and small intestine, commonly described as Crohn disease and ulcerative colitis. Most IBD patients suffer from undernutrition, but have a higher ratio of abdominal fat than healthy, lean people. Visceral fat is the main source of pro-inflammatory cytokines. Intestinal alkaline phosphatase (IAP) is considered as an important brush border enzyme that acts by dephosphorylation of bacterial LPS. Administration of IAP in conjunction with voluntary exercise has been shown led to resolution of experimental colitis, but the changes in the oxidation status of the intestinal mucosa as well as the alteration in intestinal microbiota in IAP-treated mice with colitis remain unknown.

Methods: Animals fed a high-fat-diet (HFD) for 14-weeks were randomly assigned to exercise group maintained on in-cage spinning wheels (SW) for 7-weeks. Then mice were administered *i.g.* with IAP for 2-weeks followed by intrarectal administration of 2,4,6-trinitrobenzenesulfonic acid (TNBS). The macroscopic and microscopic changes in the colonic mucosa were expressed by disease activity index (DAI). The composition of intestinal microbiota was examined in stool samples by Next-Generation Sequencing (NGS) and proinflammatory markers in plasma were determined by Luminex.

- C57BL mice
  High Fat Diet
  14 weeks
- Voluntary exercise on SW, diets continued
  • 7 weeks
- IAP administration, diets and exercise continued
  • 2 weeks
- Colitis induction by intrarectal TNBS administration, diets and exercise continued
  • 5 days
- Mice sacrified, the colonic tissue collected, DAI assessment, macroscopic and microscopic assessment of the colon, intestinal microbiota examined, oxidative stress in colon and proinflammatory markers in plasma determined.

Fig.1. A flow chart presenting the experimental protocol and time duration of this study.

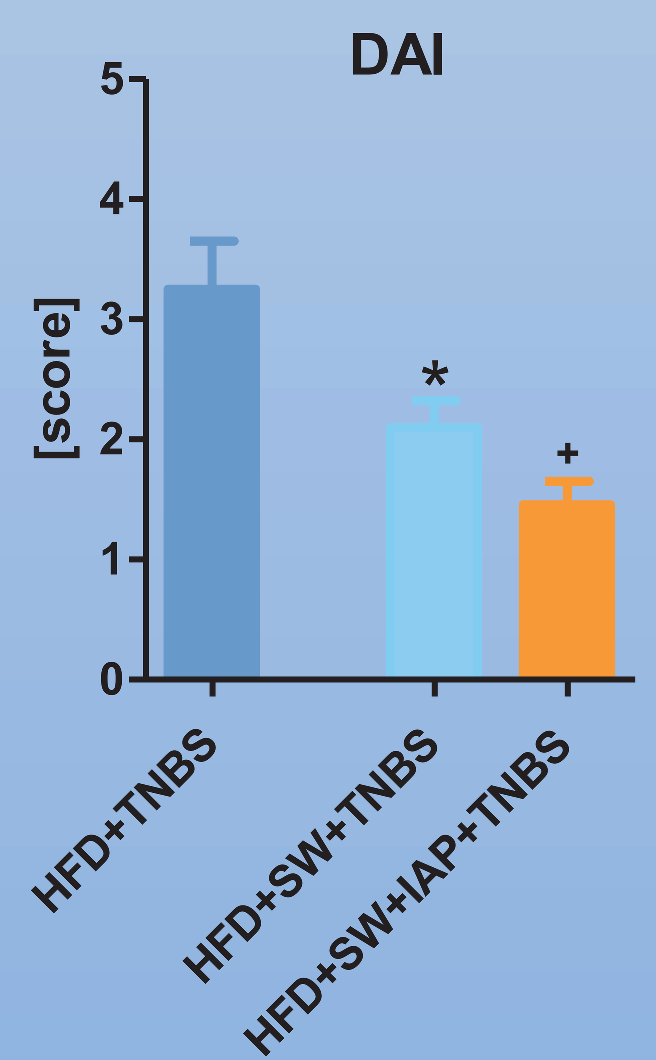

Fig.2. The effect of SW on DAI in mice fed HFD with TNBS colitis and with or without IAP administration. ‚*' indicates a significant change as compared to the respective values in group HFD+TNBS. ‚+' indicates a significant change as compared to the respective values in group: HFD+SW+TNBS (p<0.05).

Results: The intensity of colonic damage in sedentary TNBS mice was reduced when these mice had access to SW, and this effect in SW mice was potentiated by treatment with IAP. The lowest bacterial diversity was found in HFD fed mice with colitis but this effect was reversed by the combination of IAP and SW exercise. The combination of IAP administration and SW exercise reduced oxidative stress and plasma level of proinflammatory cytokines comparing to HFD sedentary mice.

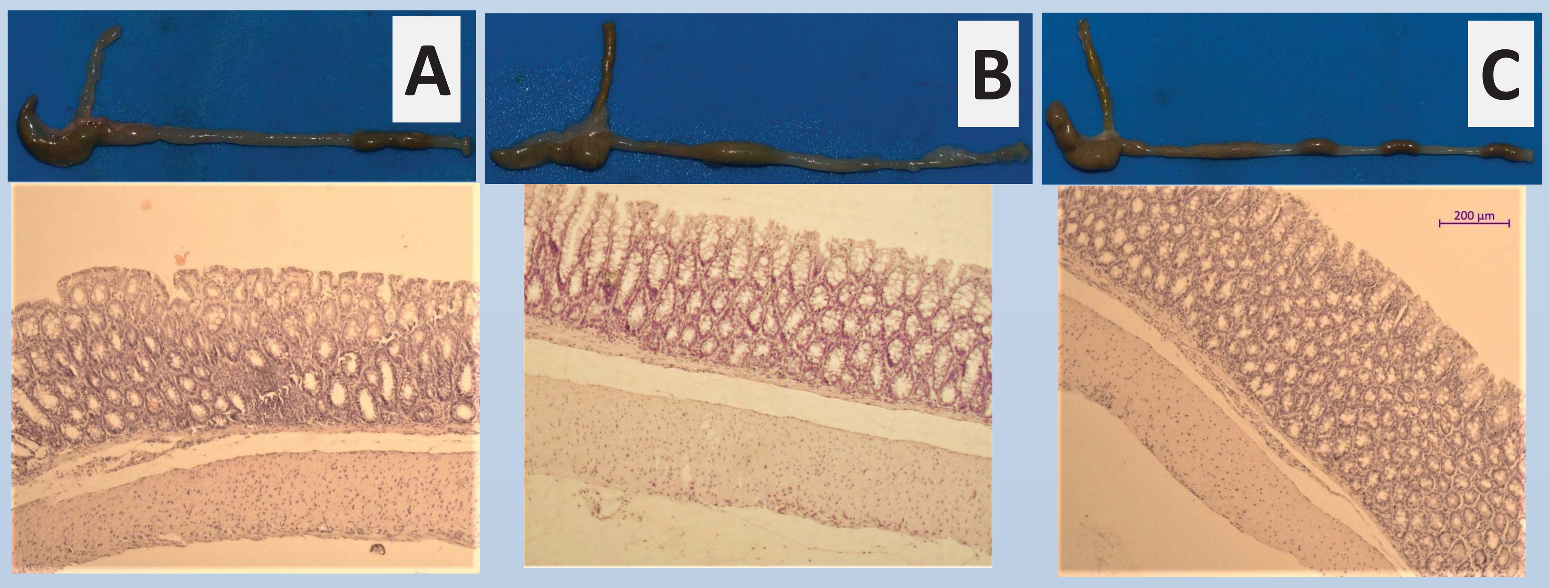

Fig.1. The representative macroscopic (upper) and microscopic (bottom) appearance of the colon obtained from: (A) an obese mouse with TNBS colitis, subjected to voluntary exercise and sacrificed at day 5 after the induction of colitis; (B) an obese mouse with IAP administration and sacrificed at day 5 after the induction of colitis; (C) an obese mouse with TNBS colitis and subjected to voluntary exercise, administered with IAP and sacrificed at day 5 after the induction of colitis.

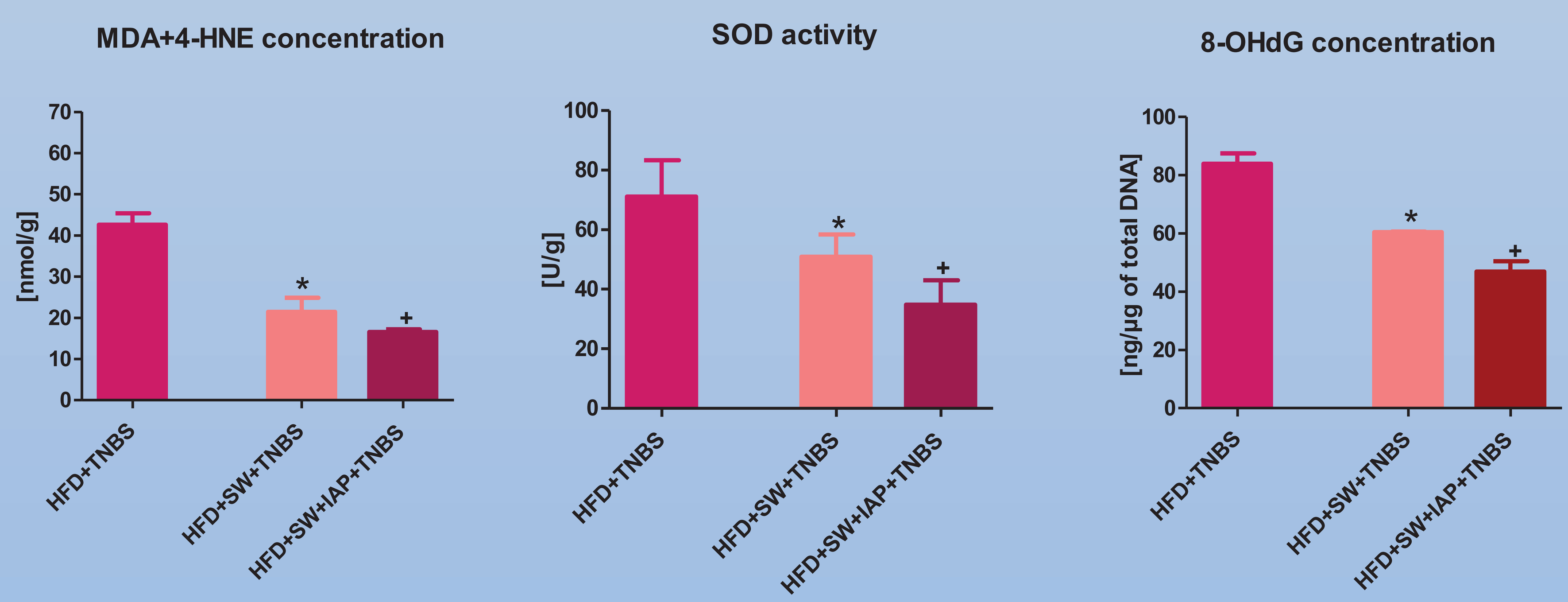

Fig.3. The effect of IAP administration on the MDA+4-HNE concentration, SOD activity and 8-OHdG concentration in the colonic mucosa HFD mice with SW and with TNBS colitis.
‚*' indicates a significant change as compared to the respective values in group HFD+TNBS.
‚+' indicates a significant change as compared to the respective values in group: HFD+SW+TNBS (p<0.05).

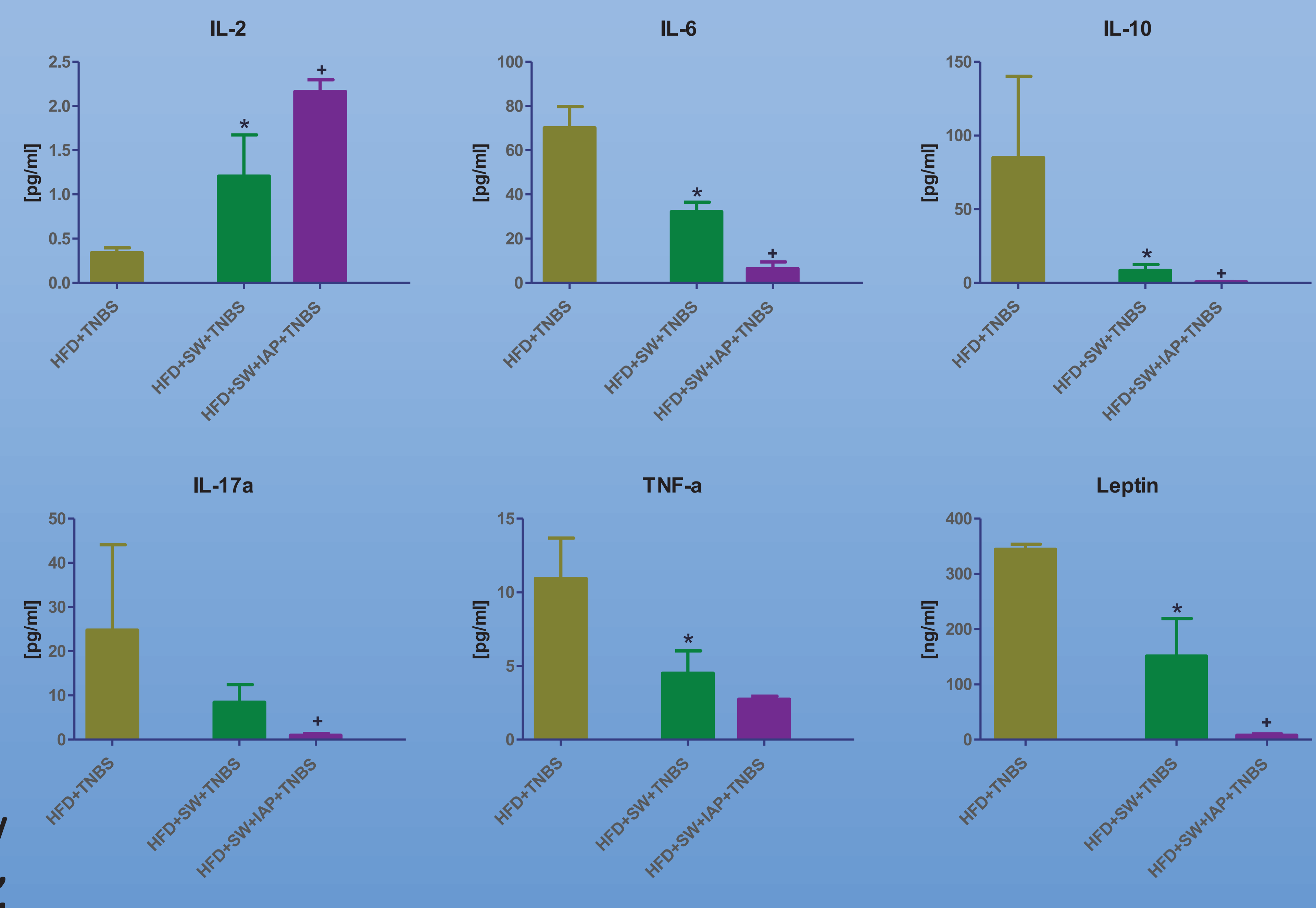

Fig.4. The effect of IAP administration on the IL-2, IL-6, IL-10, IL-17a, TNF-α and leptin concentration in plasma of HFD mice with SW and with TNBS colitis.
‚*' indicates a significant change as compared to the respective values in group HFD+TNBS.
‚+' indicates a significant change as compared to the respective values in group: HFD+SW+TNBS (p<0.05).

Conclusions: We conclude that the combination of IAP with voluntary exercise shows a beneficial effect on the course of experimental colitis, reducing inflammatory response, markers of oxidative stress and improving microbial diversity. Our data indicate a potential role of IAP and voluntary physical activity in the mechanism of resolution of intestinal disorders mediated by changes in colonic microbiota and attenuation of oxidative stress.

SPEXIN AS A MODULATOR OF HEPATOCYTE METABOLISM - *IN VITRO* STUDY

PAWEŁ A KOŁODZIEJSKI[1], MAŁGORZATA WOJCIECHOWSKA[2], NATALIA LECIEJEWSKA[1], MACIEJ SASSEK[1], LESZEK NOGOWSKI[1], KRZYSZTOF W NOWAK[1], HANNA KRAUSS[3], EMILIAN MAŁEK[4],KAROLINA MIELNIK[1], EWA PRUSZYŃSKA-OSZMAŁEK[1],
[1]Department of Animal Physiology, Biochemistry and Biostructure, Poznan University of Life Sciences, Poland; [2]Department of Mother and Child Health, Poznan University of Medical Sciences, Poznan, Poland; [3]Department of Medicine, the President Stanislaw Wojciechowski State University of Applied Sciences in Kalisz, Poland.; [4]Department of Preclinical Sciences and Infectious Diseases, Poznan University of Life Sciences, Poland; pawel.kolodziejski@up.poznan.pl ;

INTRODUCTION

The spexin is a novel highly conservative 14 amino acid peptide that was discovered in 2007 using bioinformatics methods (1). The biological activity of SPX is regulated via two isoforms of the galanin receptors - GALR2 and GALR3. To date, many positive effects of SPX on metabolism have been described. It was showed that SPX inhibits food intake, regulates fat tissue metabolism by effect on lipolysis and lipogenesis as well as regulates insulin secretion from pancreatic beta cells (2). Still, its role in the physiology of hepatocytes is known a little. However, based on the literature data from whole body in vivo studies as well as our previous studies, it may be concluded that SPX may be an important regulator in lipid metabolism in hepatocytes (3, 4).

In this study we decided to investigate the effect of SPX on hepatocyte metabolism in vitro.

MATERIAL AND METHODS

Using AML-12 and HepG2 cell lines we studied the effect of different doses of SPX on cell proliferation and viability, lipid accumulation and expression of genes involved in the development of non-alcoholic fatty liver disease (NAFLD).

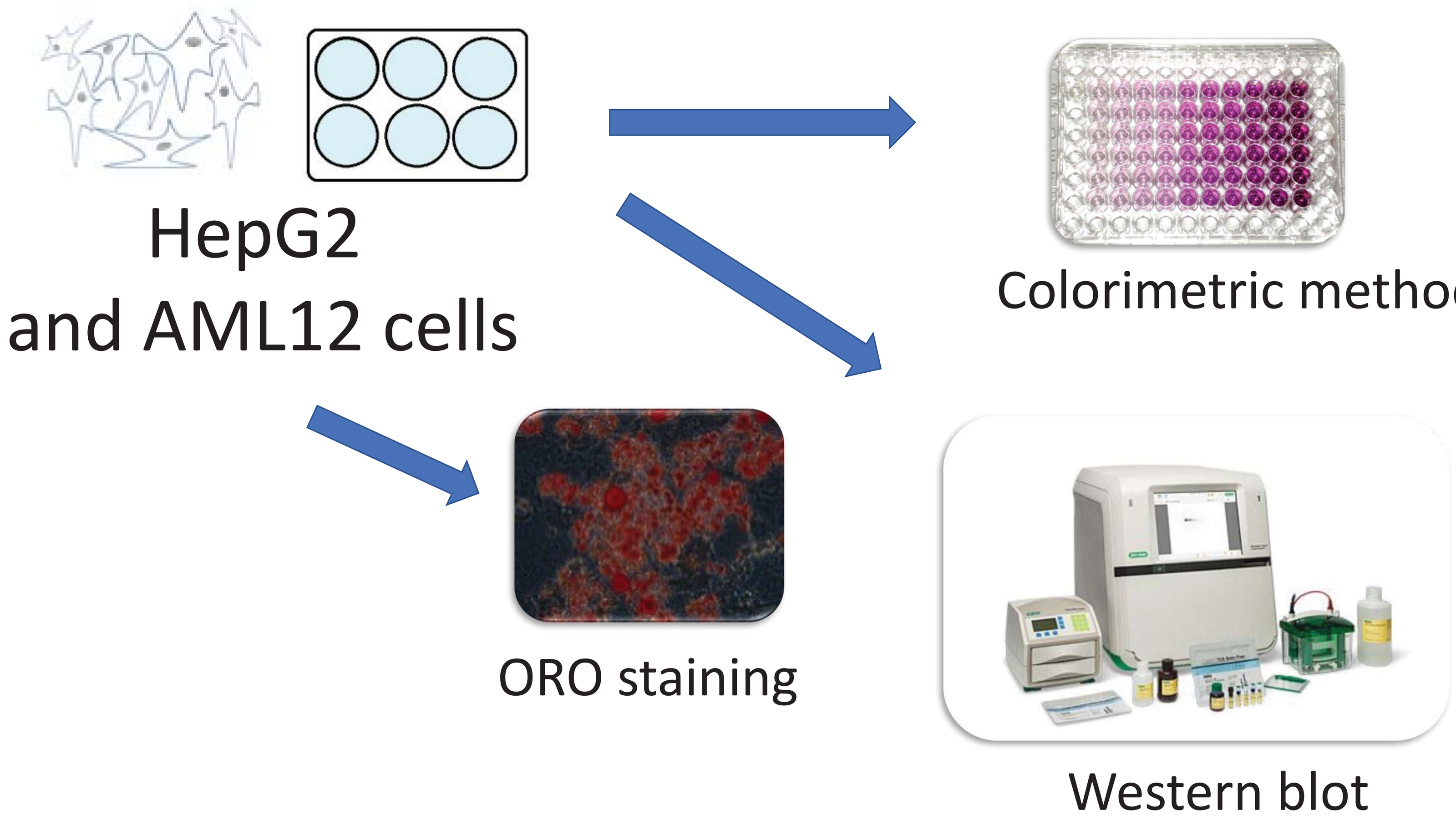

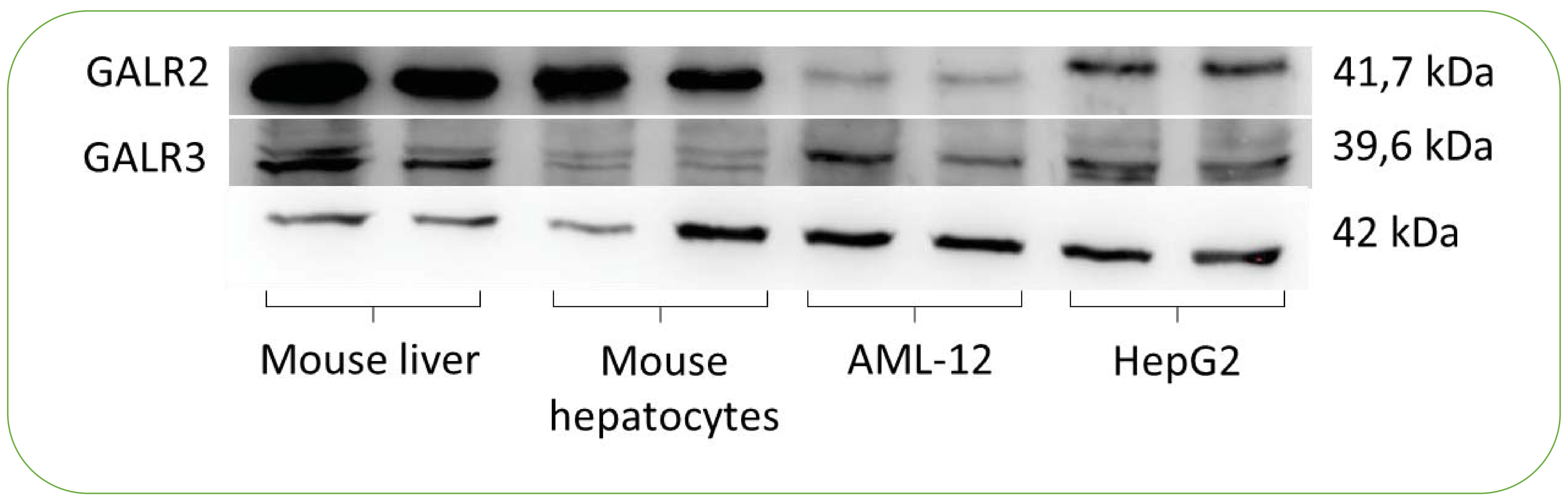

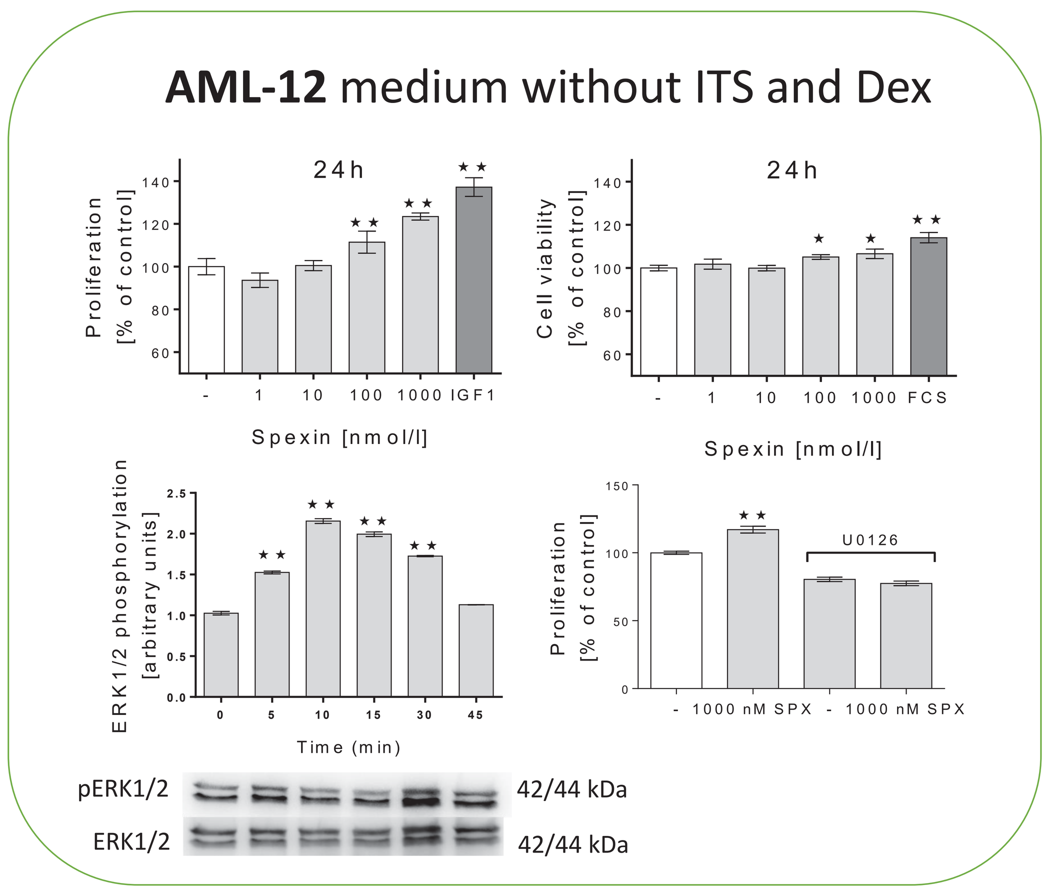

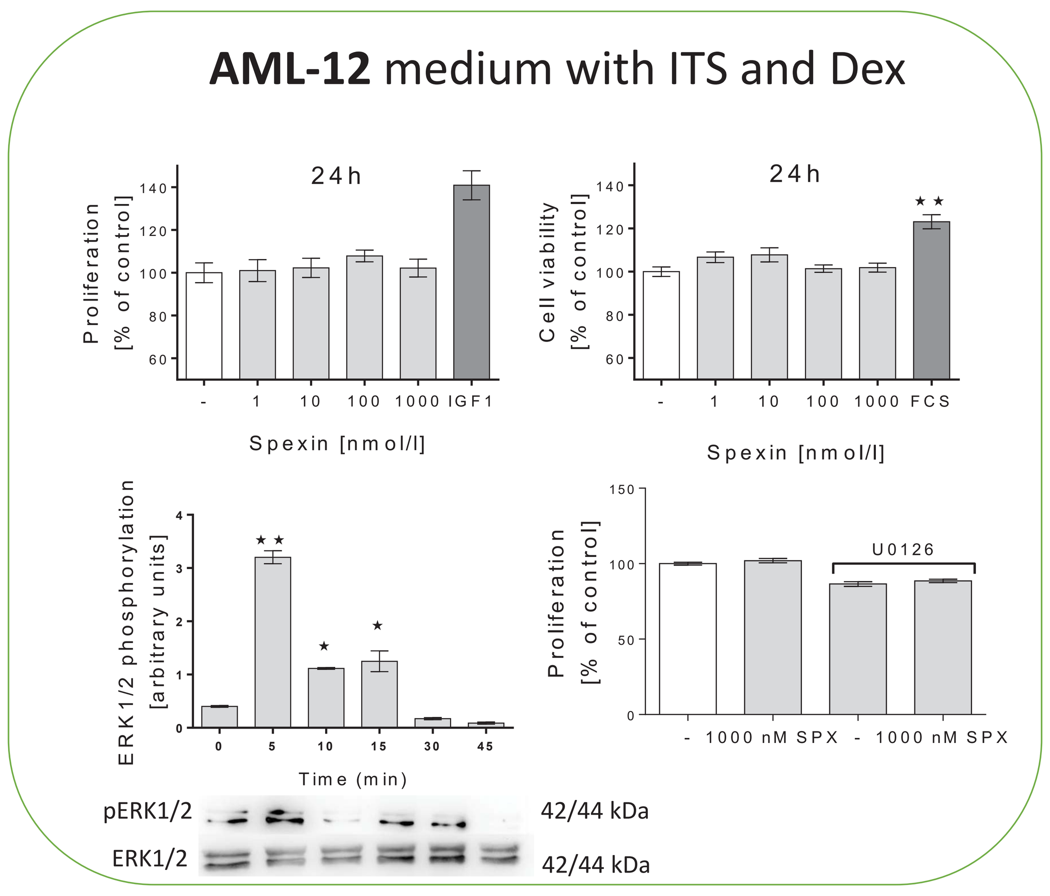

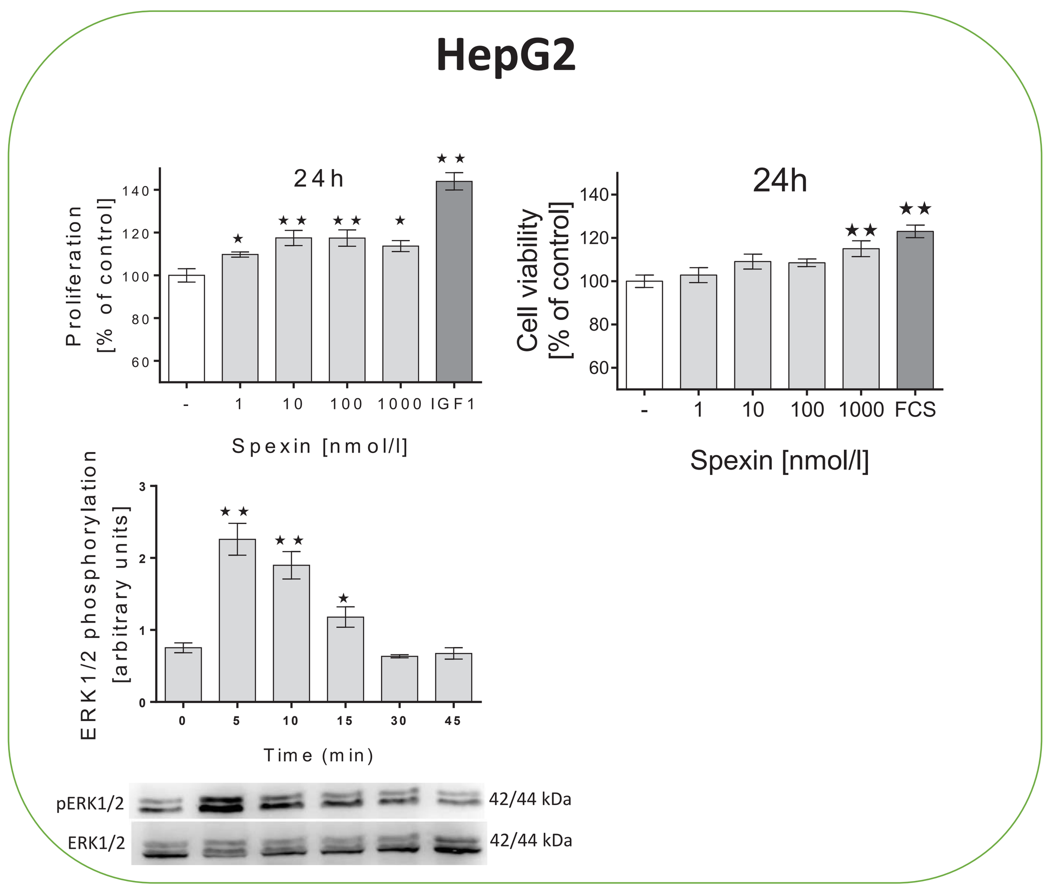

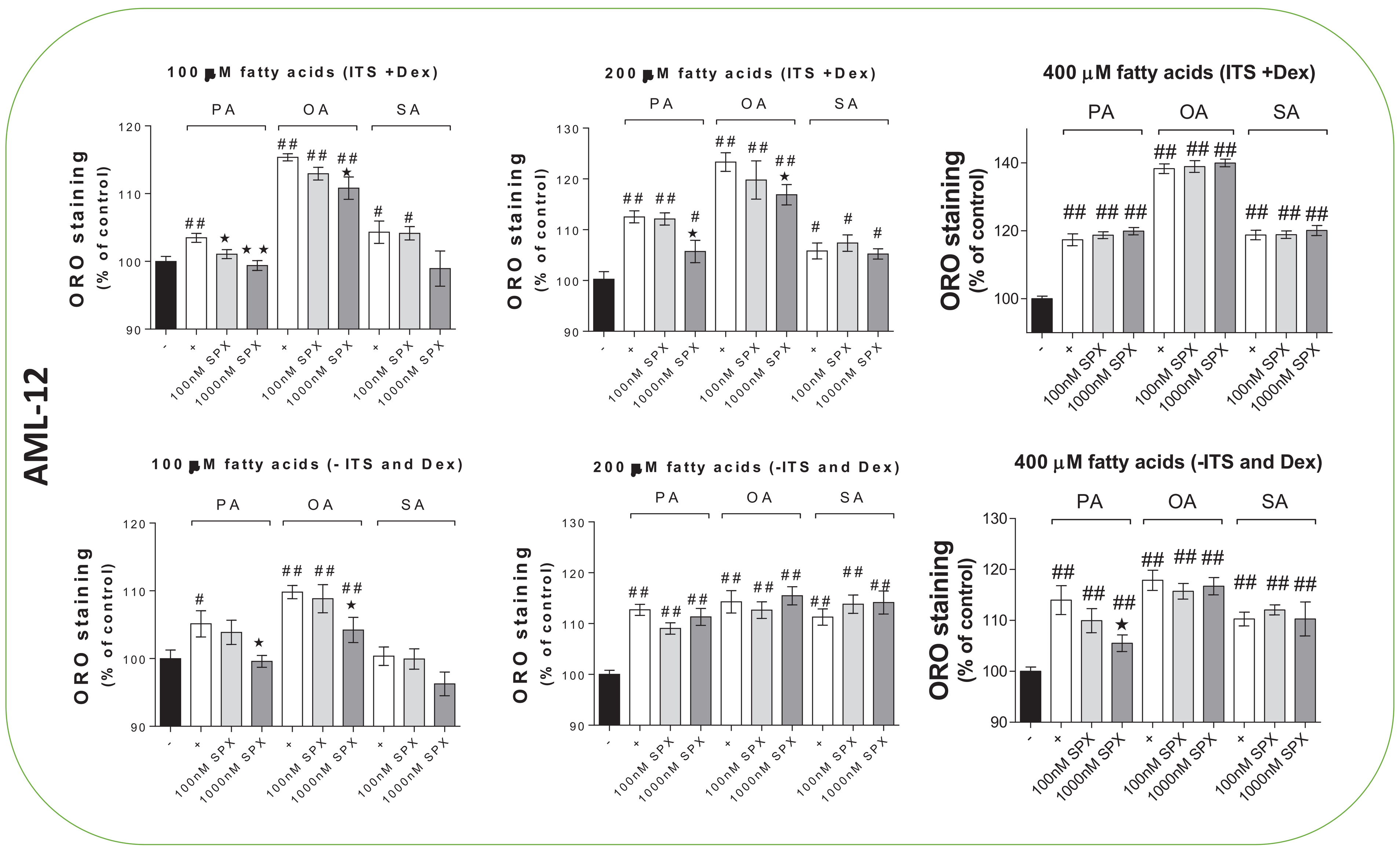

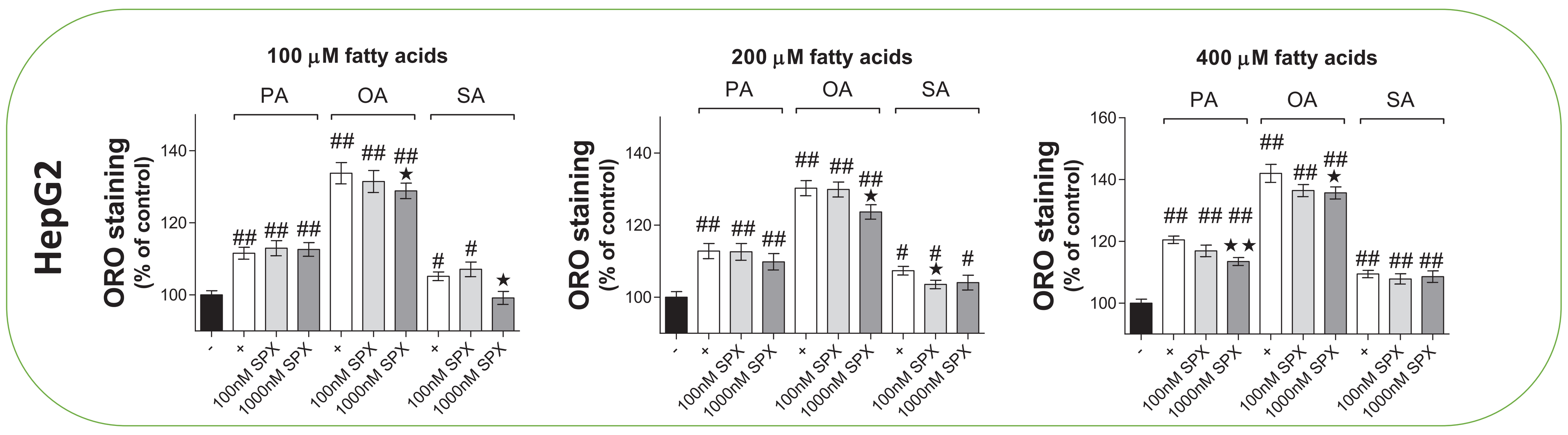

RESULTS AND CONCLUSION

We noted that SPX stimulates proliferation and cell viability of AML-12 and HepG2 cells increasing phosphorylation of ERK1/2 kinases. We also noted that SPX has the inhibitory effect on lipogenesis and this effect depends on the type of fatty acids. We summarize that SPX is a strong regulator of proliferation and fat metabolism of hepatocytes.

REFERENCES

1. O. Mirabeau, et al., Identification of novel peptide hormones in the human proteome by hidden Markov model screening. Genome Res. 17, 320–327 (2007).
2. P. A. Kolodziejski, et al., Spexin: A novel regulator of adipogenesis and fat tissue metabolism. Biochim. Biophys. Acta - Mol. Cell Biol. Lipids 1863 (2018).
3. P. A. Kolodziejski, et al., 30-Day spexin treatment of mice with diet-induced obesity (DIO) and type 2 diabetes (T2DM) increases insulin sensitivity, improves liver functions and metabolic status. Mol. Cell. Endocrinol. 536, 111420 (2021).
4. G. Jasmine, J. Walewski, D. Anglade, P. Berk, Regulation of Hepatocellular Fatty Acid Uptake in Mouse Models of Fatty Liver Disease with and without Functional Leptin Signaling: Roles of NfKB and SREBP-1C and the Effects of Spexin.

Acknowledgements:
The present research was supported by the National Science Centre, Poland (Grant No. 2015/19/N/NZ4/00572) and co-financed within the framework of the Ministry of Science.

THE NEW SYNTHETIC OXIDOVANADIUM(IV) COMPLEX WITH PYRIDINE DERIVATIVE'S DISRUPTS MITOCHONDRIAL MEMBRANE POTENTIAL AND INDUCES APOPTOSIS IN PANCREATIC CANCER CELLS

S. KOWALSKI[1], I. INKIELEWICZ-STĘPNIAK[1]

[1]Department of Pharmaceutical Pathophysiology, Faculty of Pharmacy, Medical University of Gdansk, Poland

www.mug.edu.pl

Introduction and objectives

While pancreatic cancer is a relatively rare type of cancer, it is the fourth leading cause of cancer-related death worldwide. Consequently, more than 80% of patients are diagnosed with metastatic stage, and surgical resection is not recommended. The current chemotherapeutic options are, unfortunately, minimally effective.

At the present time, there is a growing interest in metal-based anticancer agents. For example, metals are involved in electrolyte balance, oxygen transport, electron transfer, and catalysis. It have been demonstrated that synthetic vanadium complexes exhibit many biological activities including anti-cancer properties, however, cellular and molecular mechanisms still are not fully understood.

This investigation examined the potential effects of three newly synthesized oxidovanadium(IV) complexes with 2-amino-3-hydroxypyridine against pancreatic cancer cells.

Methods

We measured cytotoxicity by using 3-(4,5-dimethylthiazol-2-yl)-2,5-diphenyltetrazolium bromide, antiproliferative activity by bromodeoxyuridine assay and necrosis as well as late apoptosis by lactate dehydrogenase assay. Reactive oxygen species generation, apoptosis and mitochondrial membrane potential were determined by flow cytometry technique. Cells morphology was evaluated by using transmission electron microscope.

Results

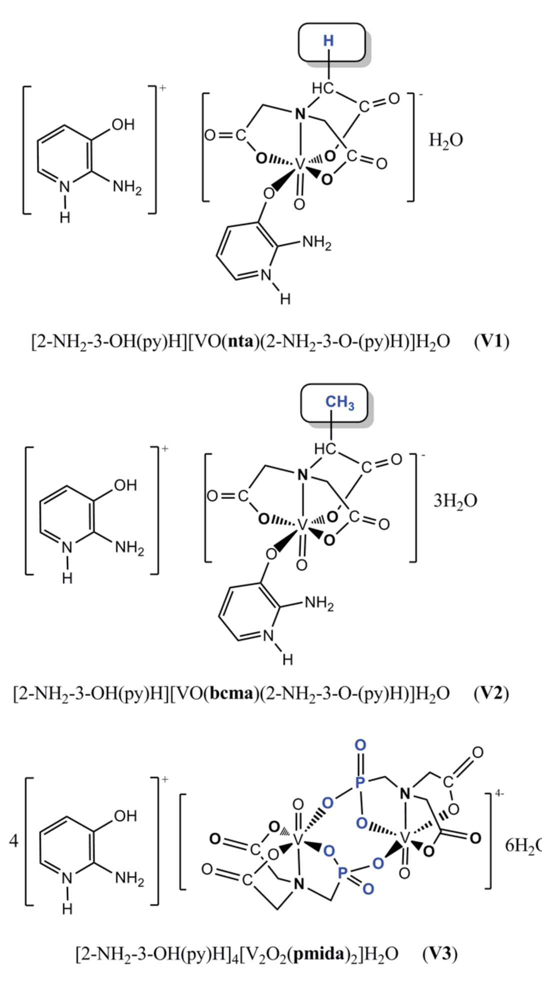

Figure 1. The chemical structures of V1–V3 complexes.

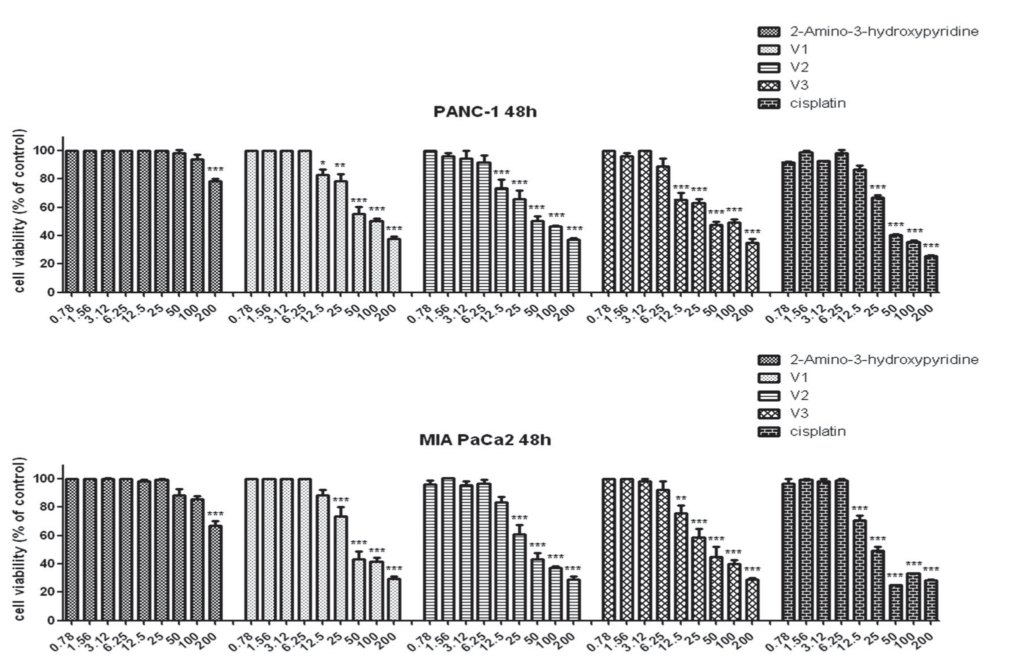

Figure 2. Cytotoxicity of vanadium complexes against pancreas ductal adenocarcinoma cell lines (PANC-1, MIA PaCa2). Cytotoxicity was measured as the cells viability using MTT assays. Cells were exposed to four vanadium complexes (V1-V3) in the range of 1 to 100 μM for 48 h. Data are mean ± SD of 3 separate determinations. *p<0.05; **p<0.01; ***p<0.001 as compared with untreated cells.

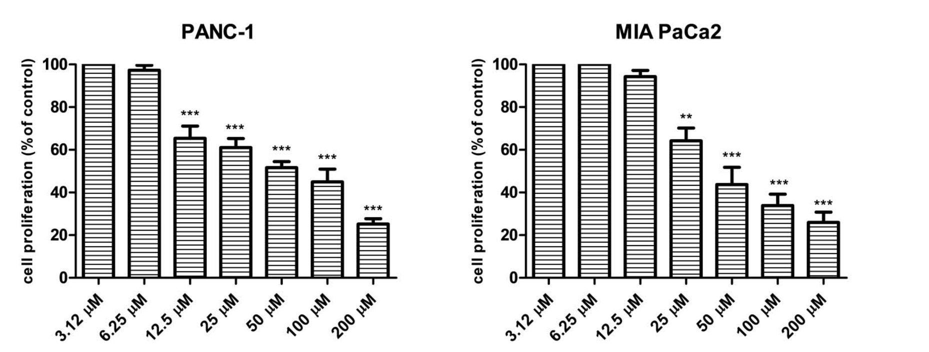

Figure 3. Antiproliferative effect of V3 against pancreas ductal adenocarcinoma cell lines PANC-1 and MIA PaCa2. Inhibition of PANC-1 and MIA PaCa2 cells proliferation was detected after 48h of treatment with vanadium compound. Data are mean ± SD of 3 separate determinations. **p<0.01; ***p<0.001 as compared with untreated cells.

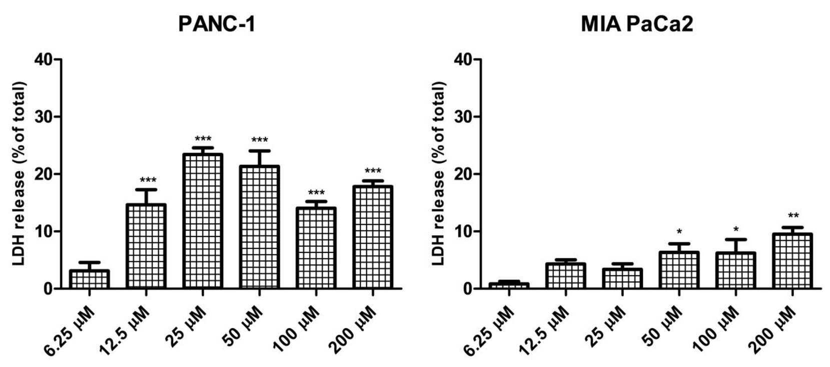

Figure 4. LDH release from PANC-1 and MIA PaCa2 cell lines after exposure to V3 complex. Cells were exposed to vanadium complex (V3 for 48 h. Data are mean ± SD of 3 separate determinations. *p<0.05; ** p<0.01; ***p<0.001, as compared with untreated cells.

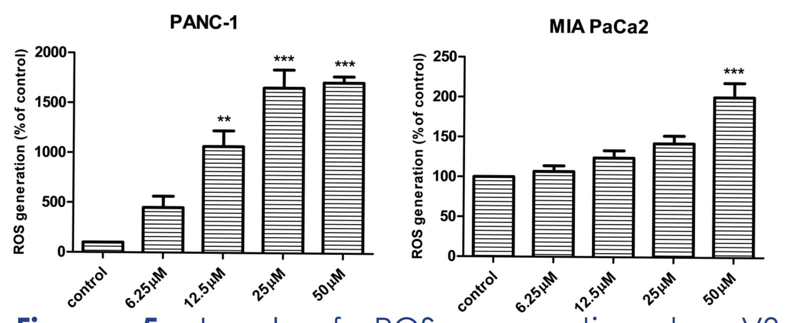

Figure 5. Level of ROS generation by V3 vanadium complex in PANC-1 and MIA PaCa2 cells after incubation for 48 h. Data are mean ± SD of 3 separate determinations. **p<0.01; ***p<0.001 as compared with untreated cells.

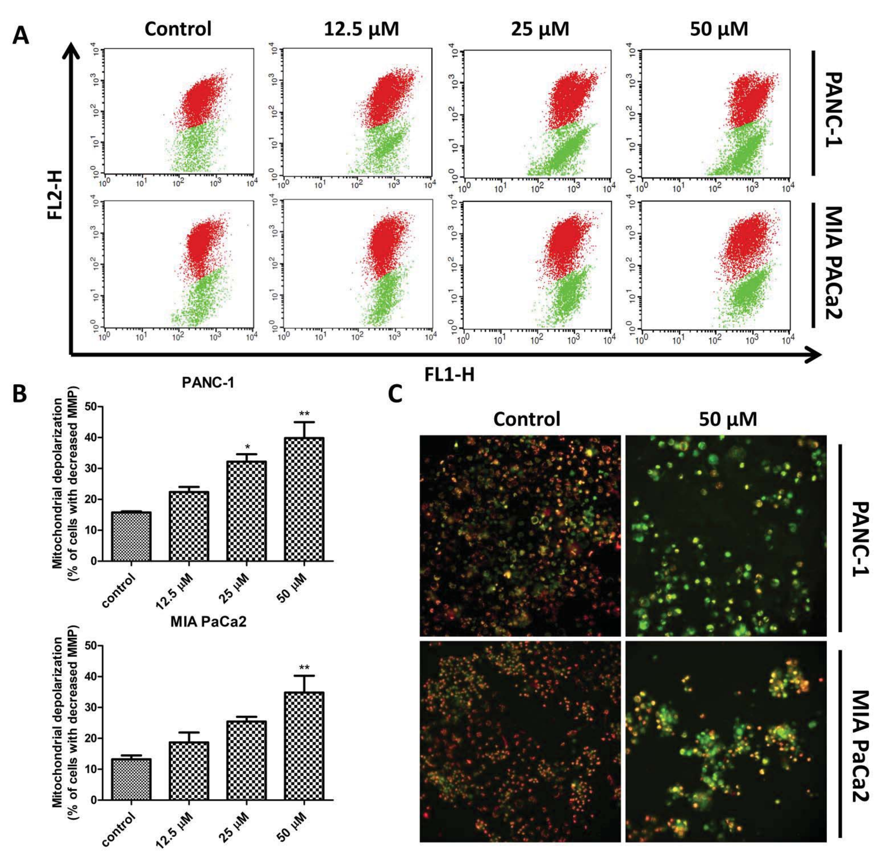

Figure 7. Mitochondrial membrane potential of PANC-1 and MIA PaCa2 cells after exposure to V3 complex. The analysis was performed by using flow cytometry and JC-1 fluorescent dye. (A) Representative bivariate histograms of the JC-1 staining in PANC-1 and MIA PaCa2 cells. (B) Percentage of cells with decreased MMP (green fluorescence population). (C) Representative images of JC-1 staining in PANC-1 and MIA PaCa2 cells. Cells were exposed to vanadium complex (V3) in the range of 12.5-50 μM for 48 h. Data are mean ± SD of 3 separate determinations. * p < 0.05; ** p < 0.01; as compared with untreated cells.

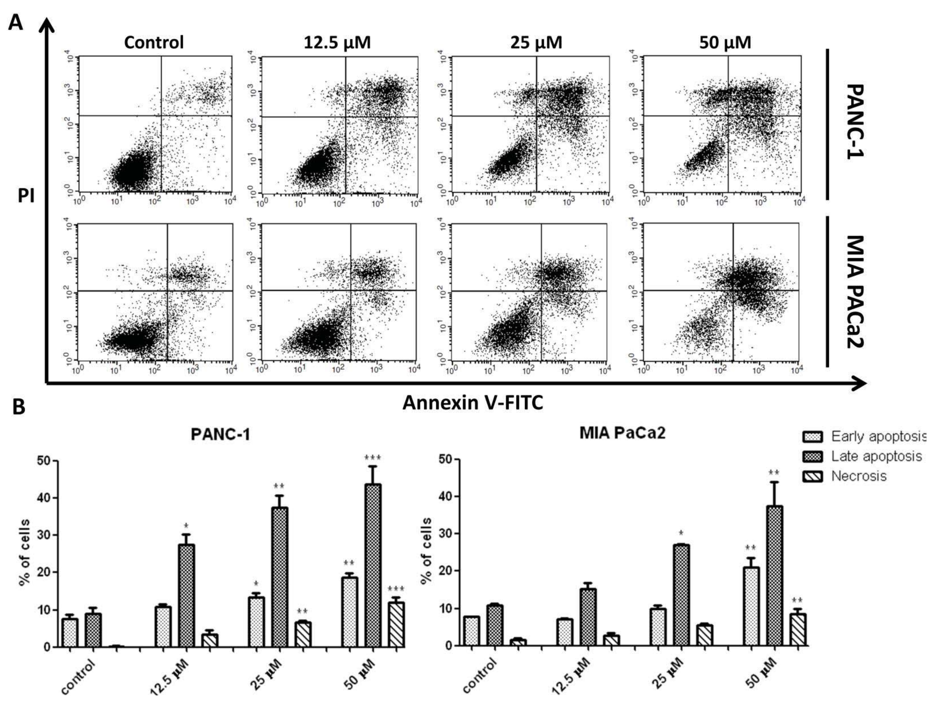

Figure 6. Apoptosis/Necrosis in PANC-1 and MIA PaCa2 cells after exposure to V3 complex. The analysis was performed by using flow cytometry. (A) Representative bivariate histograms of the Annexin V/PI staining in PANC-1 and MIA PaCa2 cells. (B) Percentage of apoptotic (Annexin V+/PI-), late apoptotic (Annexin V+/PI+) and necrotic cells (Annexin V-/PI+). Cells were exposed to vanadium complex (V3) in the range of 12.5-50 μM for 48 h. Data are mean ± SD of 3 separate determinations. * p < 0.05; ** p < 0.01; *** p < 0.001, as compared with untreated cells.

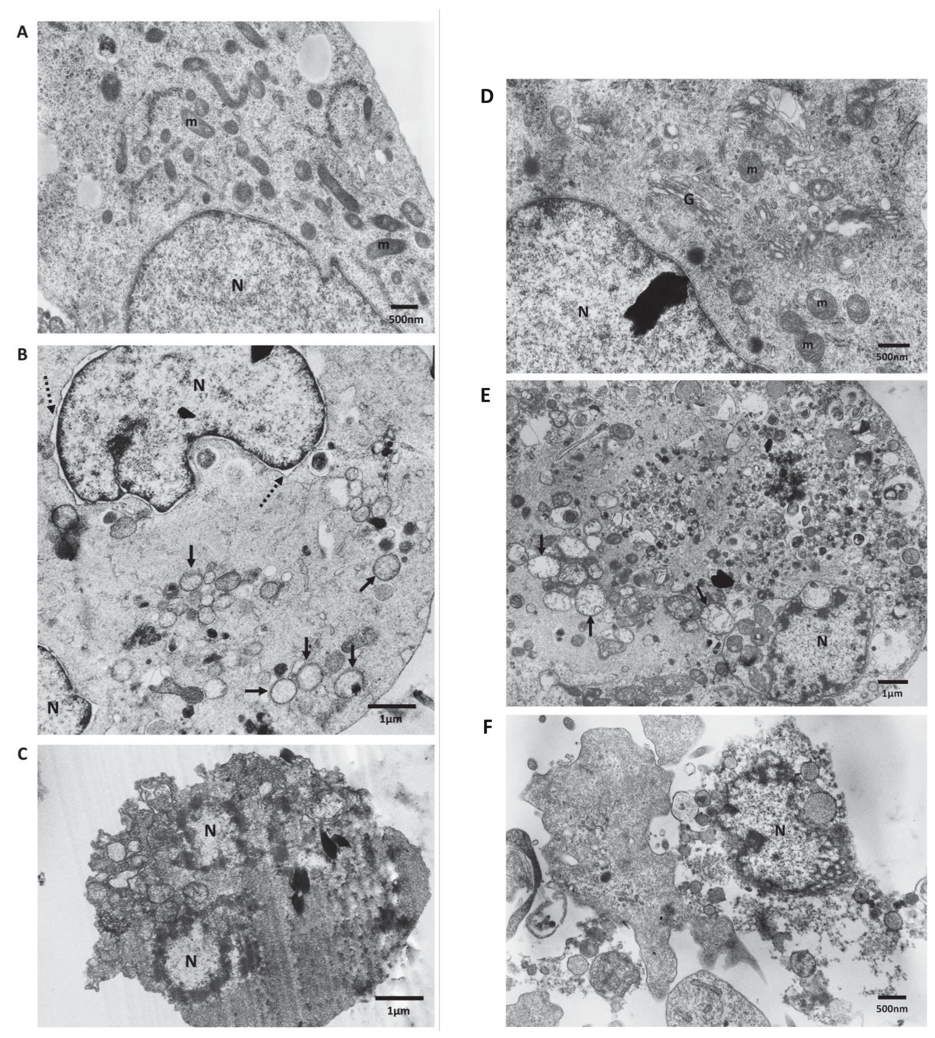

Figure 8. Ultrastructural features of MIA PaCa2 (A-B) and PANC-1 (D-F) cells incubated with vanadium complex: V3 for 48 h. (A,D) Control cell. (B) Cell treated with V3 complex (50 μM). Cell has swollen mitochondria with degraded cristae (black arrows) and dilated nuclear envelope (dashed arrows). (C) Cell treated with V3 complex (50 μM) shows apoptotic cell morphology with shrunk, condensed cytoplasm and characteristic fragmented nucleus. (E) Cell treated with V3 complex (25 μM). Cell has numerous swollen mitochondria with degraded cristae (black arrows). (F) Cell treated with V3 complex (50 μM) shows mature/late apoptotic cell morphology with large plasma membrane blebs and nuclear disintegration The scale bar (1 μm or 500 nm) is indicated at the bottom right of each image. (m) - mitochondria; (N) - nucleus; (G)- Golgi apparatus.

Conclusions

We have proven that oxidovanadium (IV) complexes show therapeutic potential in the pancreatic cancer therapy. The results of our research will help to understand the cellular mechanisms of the cytotoxic activity of the vanadium complexes and will allow a more effective design structure of new vanadium-based compounds in the future.

Literature

1. Miller, K.D.; Siegel, R.L.; Lin, C.C.; Mariotto, A.B.; Kramer, J.L.; Rowland, J.H.; et al. Cancer treatment and survivorship statistics, 2016. CA: Cancer J. Clin. 2016, 66, 271-289
2. Singh, D.; Upadhyay, G.; Srivastava, R.K.; Shankar, S. Recent advances in pancreatic cancer: biology, treatment, and prevention. BBA Rev. Cancer. 2015, 1856, 13-27
3. Bradford, S.S.; Cowan, J.A. From traditional drug design to catalytic metallodrugs: a brief history of the use of metals in medicine. Metallodrugs 2014, 1.1, 10-23

Identifier/Topic: GASTROINTESTINAL PHYSIOLOGY AND PATHOPHYSIOLOGY, PANCREAS AND LIVER

IMBALANCED DIET DURING PREGNANCY AFFECT GASTROINTESTINAL(GI) EXPRESSION OF THE ENZYMES INVOLVED IN ENDOGENOUS HYDROGEN SULFIDE(H_2S) BIOSYNTHESIS.

AUTHORS: U.GŁOWACKA[1],K.GAWLIŃSKA[2],D.GAWLIŃSKI[2],M. SZETELA[1],T.BRZOZOWSKI[1], M.FILIP[2], M. MAGIEROWSKI[1]

[1]Department of Physiology, Jagiellonian University Medical College, 31-531 Cracow, Poland

[2]Maj Institute of Pharmacology Polish Academy of Sciences, Department of Drug Addiction Pharmacology, 31-343, Kraków, Smętna Street 12, Poland

Contact author: urszula.glowacka@uj.edu.pl

BACKGROUND

The placenta plays a key role in the mother-fetus relationship, ensuring fetal homeostasis by regulating the flow of nutrients. According to the theory and developmental origins of health and disease (DOHaD), exposure to the harmful environment during critical periods of development and growth can have a significant impact on the health of offspring. An unbalanced diet during pregnancy and lactation increases the predisposition of offspring to develop diseases such as obesity, metabolic syndrome, diabetes as well as mental illness and possibly to affect gastrointestinal (GI) mucosal barrier integrity. Epigenetic regulation plays an important role in the period of early embryogenesis in mammals and enables organisms to adjust gene expression and function in response to the environment. On the other hand, hydrogen sulfide (H_2S) is an endogenous gaseous mediator produced in gastrointestinal (GI) tract by enzymatic activity of cystathionine-β-synthase (CBS), cystathionine-γ-lyase (CTH) or 3-mercaptopyruvate sulfurtransferase (MPST). This molecule exerts anti-inflammatory and vasodilatatory properties and its activity is important for the maintenance of gastric mucosal integrity. H2S also regulates epigenetic processes through acetylation and methylation of histones. We investigated based on animal experimental model, the effects of the maternal high-fat (HFD), high-sugar (HSD) mixed diet (HMD; rich in carbohydrates and fats) during pregnancy and lactation on the expression of CBS, CTH and MPST within GI mucosa of offspring. We observed that HFD ,HSD and MD modulated mRNA expression for H2S-producing enzymes in intestinal mucosa suggesting that possible dysregulation of physiological functions of GI mucosal barrier and its susceptibility to GI pathologies induced by imbalanced diet during pregnancy may involve altered activity of endogenous H_2S within GI tract.

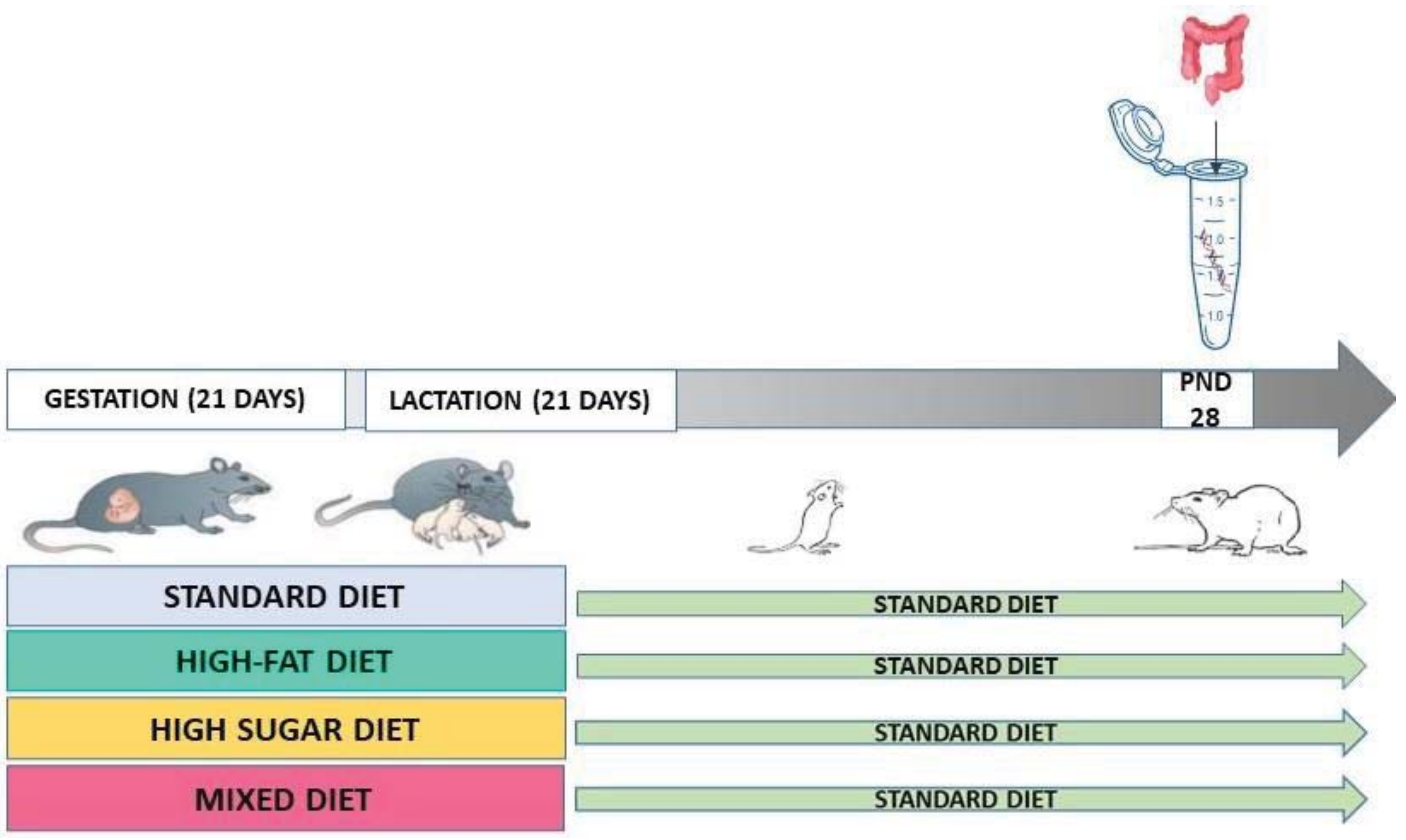

METHODS

The groups of individually housed pregnant females received standard diet (SD), high fat diet(HFD), high sugar diet (HSD) or miexed diet(MD). Dams were maintained ad libitum on these diets during the gestation (21 days) and lactation periods (21 days). At postnatal day (PND) 28 subset of offspring was sacrificed, and tissues were collected for molecular analysis. Expression level of mRNA in the intestine of rats fed diffrent diets were determined by real-time polymerase chain reaction (qRT-PCR). Results were analyzed using the $2^{-\Delta Ct}$ method. Statistical analysis was conducted using one-way Anova test with Dunnett's multiple comparison.

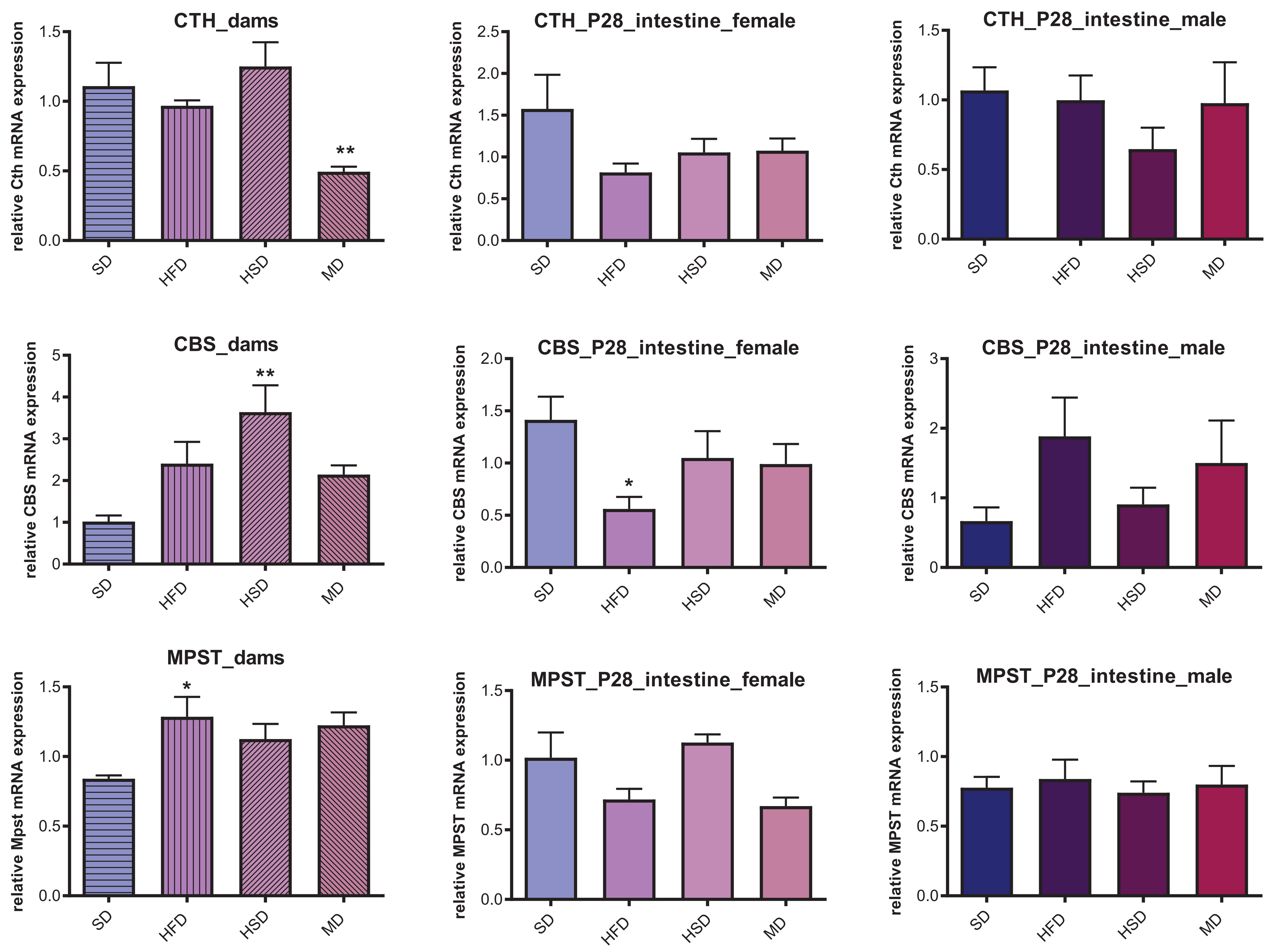

SUMMARY&CONCLUSION

- ✓ Our preliminary results showed that dams treated with HFD, HSD or MD exhibited changes in mRNA levels encoding enzymes responsible for the production of H2S.
- ✓ In dams fed during pregnancy and lactation with mixed diets, the expression of intestinal CTH was significantly reduced.
- ✓ We observed increased levels of CBS and MPST expression in the HSD and HFD treated groups, respectively.
- ✓ In the offspring in the female HFD group, CTH and CBS expression was decreased, coversely in male HFD group level of CBS was increased.

Funding sources: National Science Centre, Poland, UMO-2016/21/B/NZ4/00203

INFLUENCE OF IONIC AND THE ORGANIC COMPOSITION OF MICROELEMENTS ON THE PRESENCE OF *HELICOBACTER PYLORI* IN TAP WATER EVIDENCE FROM CRACOW

A. TARGOSZ[1], M. PLONKA[1], W. RECZYNSKI[2], M. JAKUBOWSKA[2], A. PTAK-BELOWSKA[1], U. SZCZYRK[1], M. STRZALKA[1], T. BRZOZOWSKI[1]

1. Department of Physiology, Faculty of Medicine, Jagiellonian University Medical College, Cracow, Poland
2. Department of Analytical Chemistry, AGH University of Science and Technology Faculty of Material Science and Ceramic, Poland

AGH

INTRODUCTION

Although the human stomach is the natural niche for *H. pylori* (*Hp*), this bacteria may need to survive outdoors to show widespread gastric infection. Drinking water is considered one of *Hp*'s external sources of survival. Using molecular techniques such as PCR, we traced the presence of *Hp* DNA in the drinking water, indicating that this aquatic environment may act as a reservoir for this bacterium.

AIM

1. Our goal was to determine the concentrations of selected ions and the possible correlation between the presence or absence of *Hp* in water samples.
2. We examined the relationship between twenty-six selected elements and the presence of *Hp* DNA in the tested water samples.
3. The following parameters were tested: total number of microorganisms at 22°C, color, pH of the water samples, conductivity at 25°C and concentration of sixteen ions and organic composition of microelements.

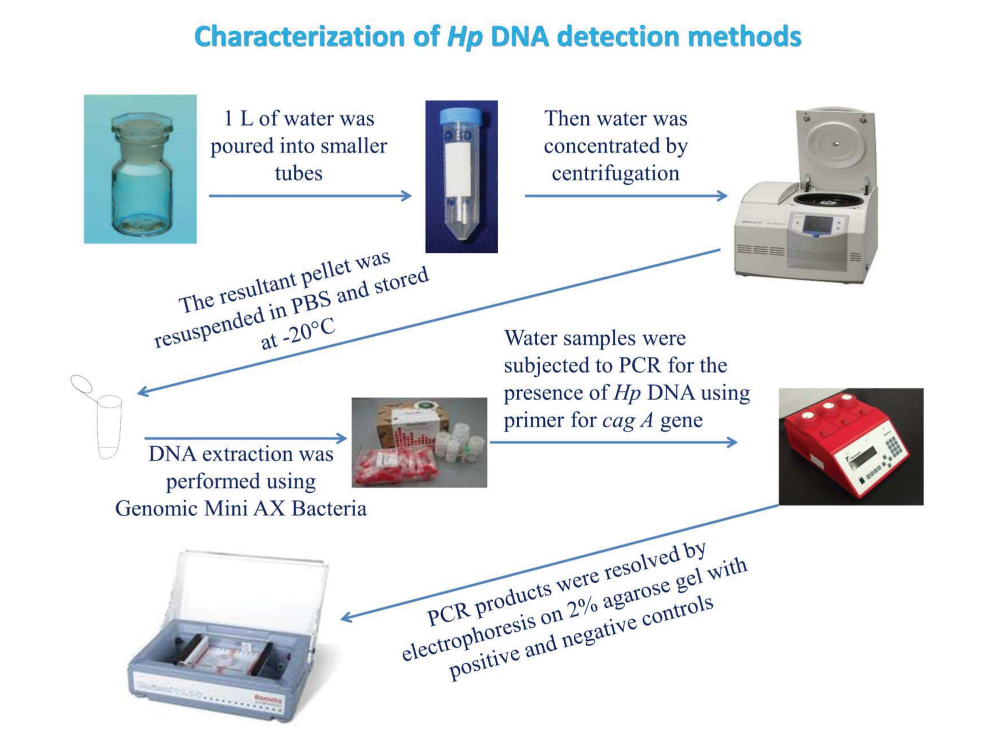

MATERIALS AND METHODS (I)

370 objects (water samples) from different municipal water distribution system from Cracow were collected

- 214 water samples from RABA river
- 38 water samples from SANKA river
- 87 water samples from RUDAWA river
- 40 water samples from DŁUBNIA river

Four rivers that supply water to Krakow

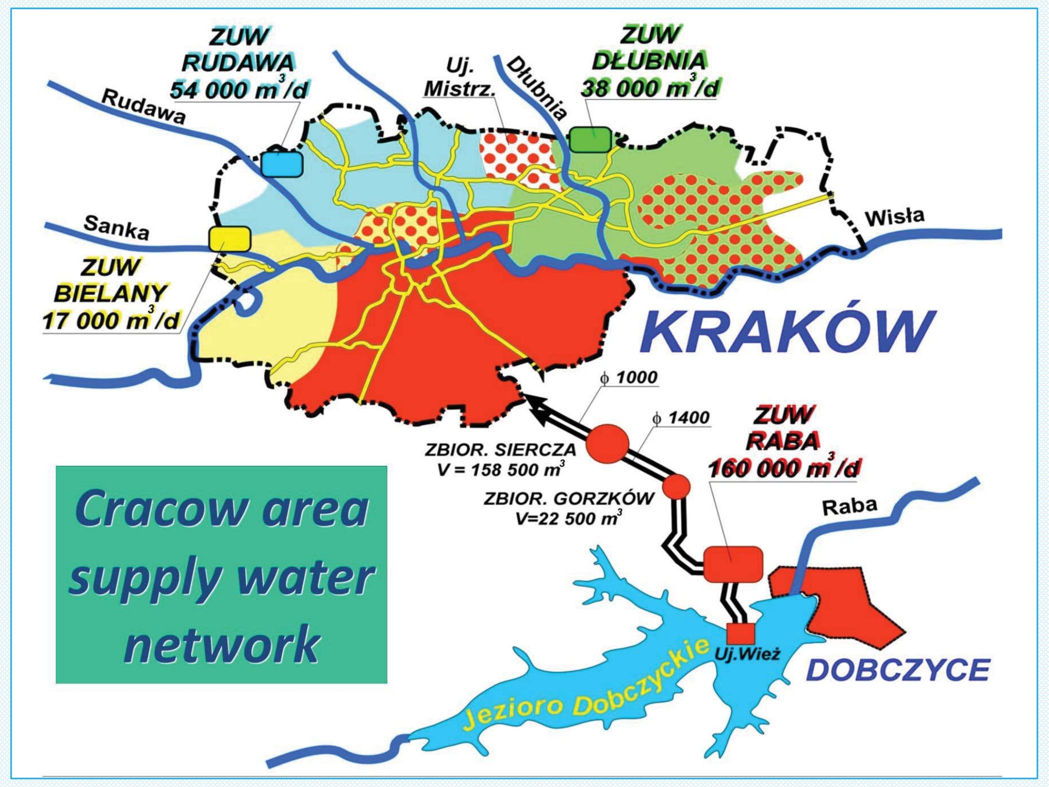

MATERIALS AND METHODS (II)

1. Water samples were subjected to PCR for the bacteria specific pathogenic *cag A* gene encoding the cytotoxic protein Cag A.
2. To denote ions the electroanalytical method AAS (atomic absorption spectrometry) has been employed.
3. Variables were marked in accordance with polish standards (PN) and ISO.
4. The strategy of multivariate data analysis was applied. Following algorithms were used: Principal component analysis (PCA), linear discriminant analysis (LDA).

RESULTS

Water network where *Hp* DNA was detected

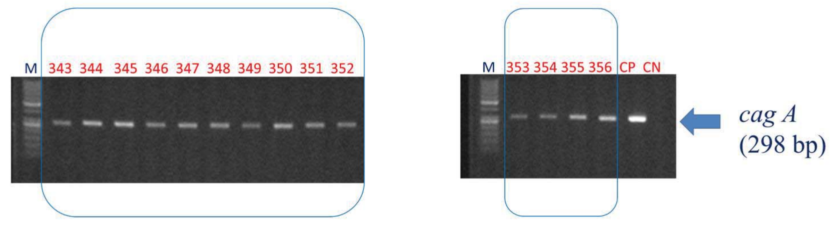

RESULTS

The data obtained from the tests show that 212 (55.96%) objects were *Hp* DNA positive. LDA was built for classifying objects based on fifteen variables: color, pH, chlorides, nitrites, phosphates, chlorates, sulphates, free chlorine, sodium, magnesium, total organic carbon, trichloromethane, bromodichloromethane, dibromochloroethane, sum trihalogenometanes (∑TMH) for which $p<0.05$.

RESULTS

On the basis of the water parameters tested, we can distinguish individual rivers, which are drinking water intakes for the city of Cracow and region

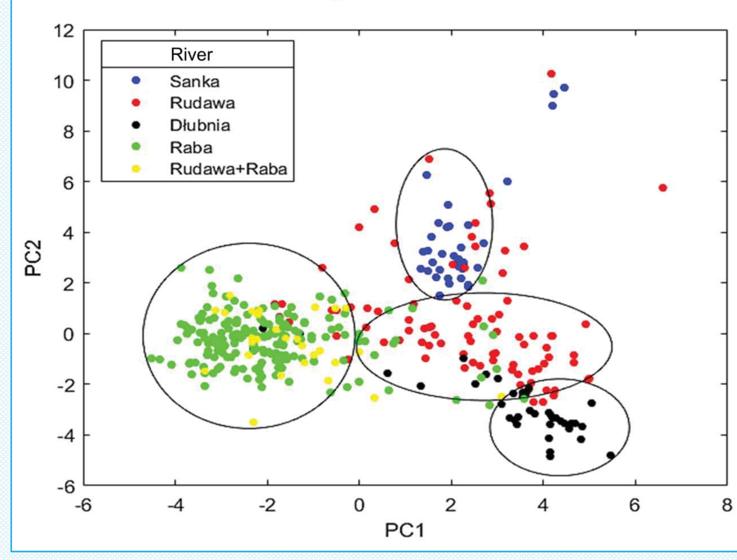

Figure shows a projection of objects (water samples) on PC1/PC2 from four different municipal water distribution system from Cracow.
The water samples with Raba and Raba + Rudawa are in the same area of the plane, they cannot be separated and constitute one group.
Subsets marked with ellipses.

RESULTS

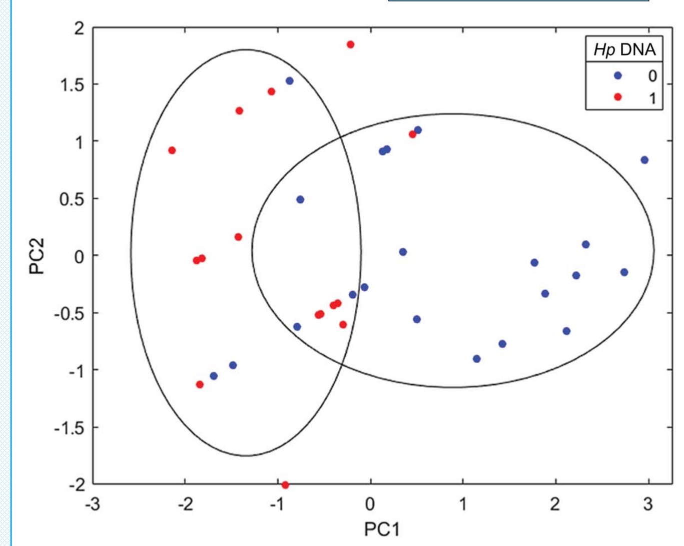

PCA analysis for Sanka river.
There are three selected variables ($p<0.05$): magnesium, trichloromethane, bromodichloromethane that differentiate water samples with *Hp* (1) DNA and without *Hp* (0) DNA

LDA analysis correctly differentiated 80.6% of the all samples from Sanka river, including 71.4% of the correct samples labeled *Hp* (0) DNA and 93.3% of the correct samples labeled *Hp* (1) DNA. Conclusion: on the basis of the three selected variables, LDA correctly recognizes *Hp* (1) DNA.

RESULTS

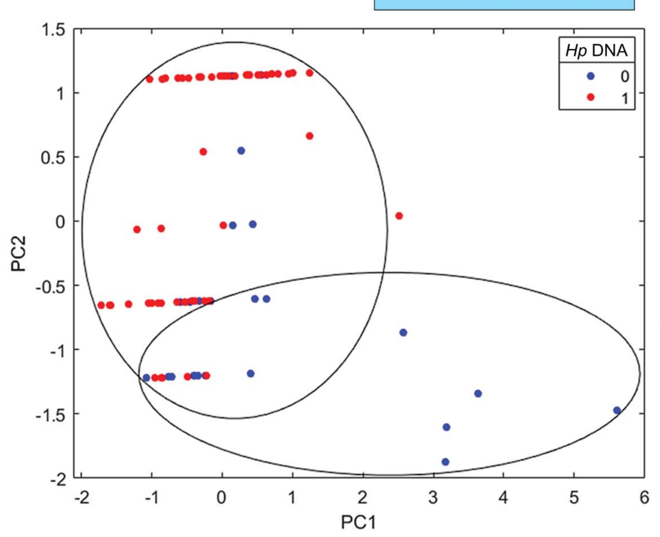

PCA analysis for Rudawa river.
There are three selected variables ($p<0.05$): color, nitrites, total organic carbon that differentiate water samples with *Hp* (1) DNA and without *Hp* (0) DNA

LDA analysis correctly differentiated 71.9% of the all samples from Rudawa river, including 31.2% of the correct samples labeled *Hp* (0) DNA and 94.7% of the correct samples labeled *Hp* (1) DNA. Conclusion: on the basis of the three selected variables, LDA correctly recognizes *Hp* (1) DNA.

RESULTS

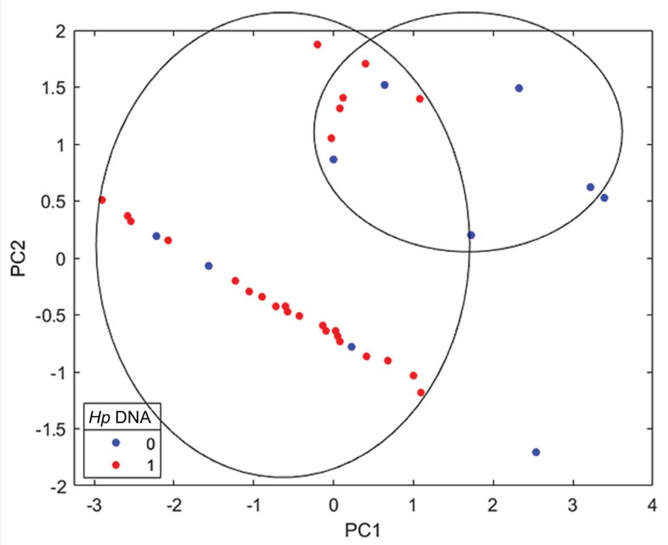

PCA analysis for Dlubnia river.
There are three selected variables ($p<0.05$): chlorites, phosphates, sulphates that differentiate water samples with *Hp* (1) DNA and without *Hp* (0) DNA

LDA analysis correctly differentiated 75.0% of the all samples from Dlubnia river, including 41.7% of the correct samples labeled *Hp* (0) DNA and 89.3% of the correct samples labeled *Hp* (1) DNA. Conclusion: on the basis of the three selected variables, LDA correctly recognizes *Hp* (1) DNA.

RESULTS

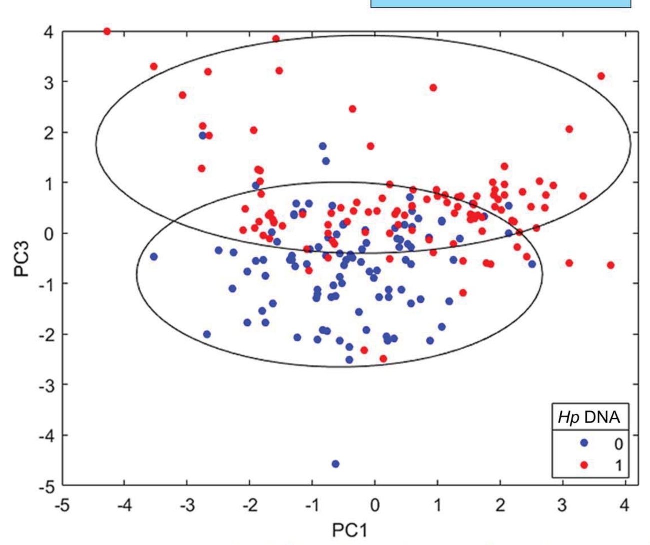

PCA analysis for Raba river.
There are ten selected variables ($p<0.05$): color, pH, phosphates, chlorates, free chlorine, sodium, total organic carbon, bromodichloromethane, dibromochloroethane, ΣTMH that differentiate water samples with *Hp* (1) DNA and without *Hp* (0) DNA

LDA analysis correctly differentiated 86.0% of the all samples from Raba river, including 84.3% of the correct samples labeled *Hp* (0) DNA and 87.5% of the correct samples labeled *Hp* (1) DNA. Conclusion: on the basis of the ten selected variables, LDA correctly recognizes *Hp* (1) DNA.

RESULTS

On the basis of the measured variables, it was possible to distinguish objects (water samples) containing *Hp* DNA from water samples containing no *Hp* DNA.

We believe that with these algorithms we can distinguish between objects with *Hp* DNA detection and those that do not detect *Hp* DNA in water samples.

CONCLUSIONS

1. The ionic and organic composition of the trace elements in the water can influence the presence of *Hp* DNA.
2. Thus, the determination of selected micronutrients can indirectly indicate and sometimes predict the presence of *Hp* in drinking water.
3. Based on the multivariate analysis, we conclude about the relationship between *Hp* DNA and ions.

Acknowledgements: The study was part of the project "Detection of *Hp* in drinking water samples. In what way is the water contaminated and what is the source of contamination?" Plonka, Targosz, Brzozowski. This work was supported by grant No 2011/01/B/NZ/01539

Influence of macrophages M1 (MF-M1) on kinases MAPK expression and apoptosis status of rat neoplastic hepatocytes incubated in 3D Quasi-Vivo System.

M. WÓJCIK [1] R.DORACZYŃSKA [2] A.KORGA-PLEWKO [3]

[1]Department of Preclinical Veterinary Sciences, Sub-Department of Pathophysiology, Faculty of Veterinary Medicine, University of Life Sciences in Lublin, Akademicka St. 12, 20-033 Lublin, Poland; [2]Department of Biophysics, Faculty of Environmental Biology, University of Life Sciences in Lublin, Akademicka St. 13, 20-950 Lublin, Poland; [3]Independent Medical Biology Unit, Medical University of Lublin, 8b Jaczewski Street, 20-090 Lublin, Poland)

Intoduction: Hepatocellular carcinoma (HCC) is a highly malignant tumor of humans, dogs and cats, with generally poor treatment outcomes. Targeting apoptosis represents a potent cancer treatment strategy as well as new methods with using of immunologically "trained" macrophages M1 (Mf-M1), which might directly or indirectly influenced on apoptosis pathways. Taking above into account we sought to analyze the mRNA expression of MAPK4, MAPK7 kinases and apoptosis status in rat neoplastic hepatocytes obtained from DEN-model of hepatocarcinogenesis additionally exposed to proinflammatory macrophages M1.

Materials and Methods: Wistar rats were divided into two groups: I - control (n=10) and II neoplastic (n=10). After 6 weeks of DEN administration, hepatocytes were isolated from both groups of animals by collagenase perfusion method. The blood mononuclear cells were isolated using Lymphoprep density-gradient centrifugation. Adherent cells were treated with β-glucan (BBG) at concentration of 10 μg/ml. The heaptocytes and Mf were put into the simple modular culture chambers with dynamic flow of culture medium (Quasi-Vivo System, Kirkstall Ltd., UK). cDNA samples were amplified using AmpliTaq Gold DNA polymerase and the Applied Biosystem 7500 RT PCR. After activation of DNA polymerase, with simultaneous deactivation of UNG, and after an initial denaturation of the matrix at 95ºC for 10 min, 45 cycles of a 2-stage PCR reaction was performed: I- denaturation at 95ºC for 30 s, II-annealing, elongation of DNA and degradation of the probe at 60ºC for 60 s.

A commercially available perfusion chamber bioreactor (Quasi-Vivo, QV500, Kirkstall, United Kingdom) was used to keep the cells under perfusion

Representative macroscopic features of the livers of PH/DEN model rats. Several white nodules were macroscopically observed following (DEN) treatment.

Results

As shown in Fig 1 and Fig.2, in comparison to control hepatocytes, mRNA expression of both kinases significantly elevated in DEN-obtained cells. Moreover, in such condition enhanced expression of kinases highly corelated with low percentage of apoptotic neoplastic cells. According to MKK7 kinase in neoplastic hepatocytes, non-stimulated macrophages had a greater effect on its expression, than stimulated one.

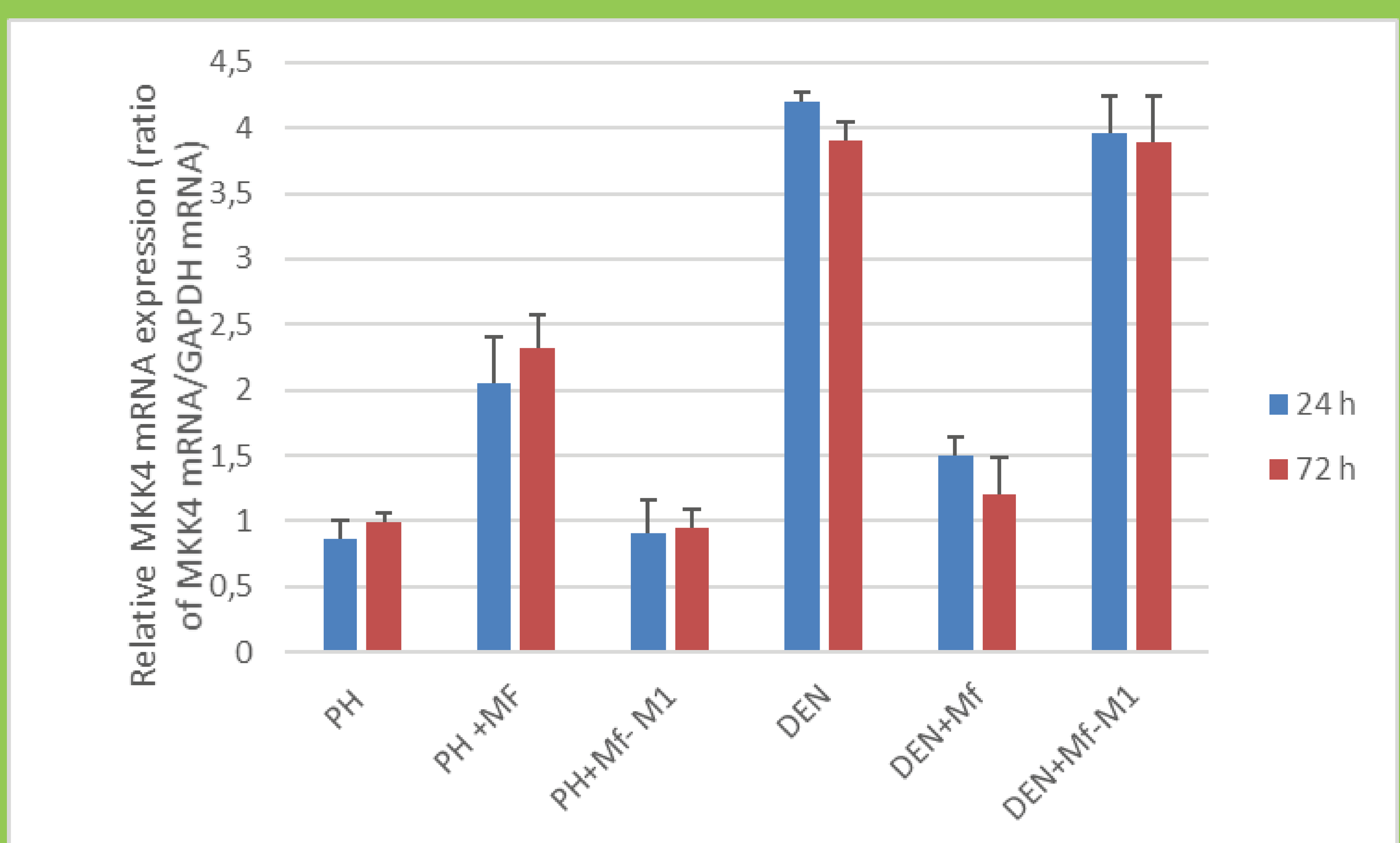

Expression of MKK4 mRNA in control and neoplastic hepatocytes in rats. (n=10, x±SD)

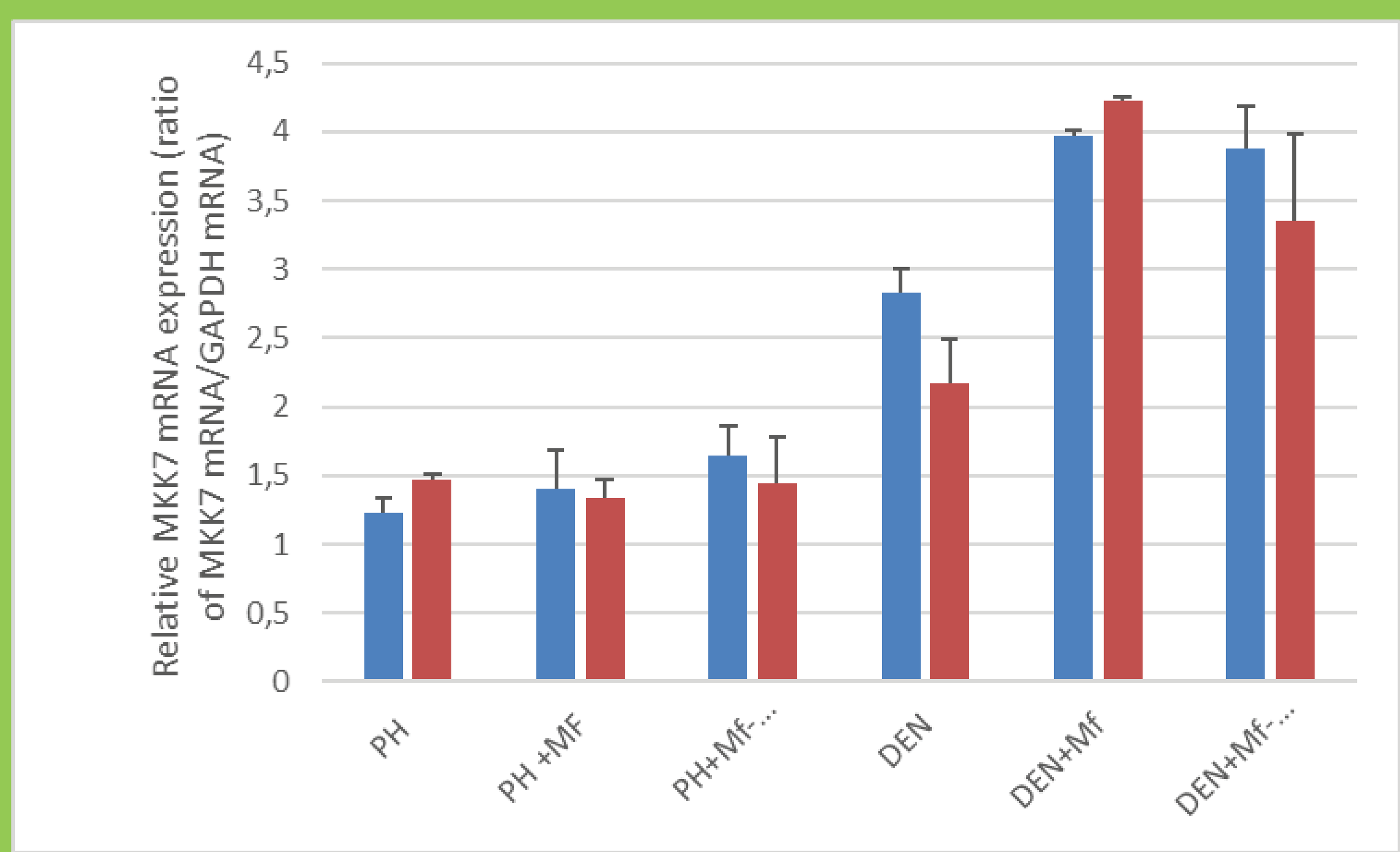

Fig.2 Expression of MKK7 mRNA in control and neoplastic hepatocytes in rats. (n=10, x±SD)

Conclussion

The obtained preliminary results indicate that, proinflammatory Mf-M1 can modulate the expression of MAPK4 and MAPK7 kinase, which are key regulatory factors of apoptosis process both in normal and neoplastic cells.

References

1. Guo Y, Wang W, Wang J, Feng J, Wang Q, Jin J et al. Receptor for activated C kinase 1 promotes hepatocellular carcinoma growth by enhancing mitogen-activated protein kinase kinase 7 activity. Hepatology 2013;57:140-51
2. Wójcik M, Wessely-Szponder J, Cichoż-Lach H, Celiński K, Bobowiec R.: In Vitro Proinflammatory Polarization of Macrophages Isolated from Hepatocarcinogenic Stage in Humans and Rats. In Vivo. 2016,11-12;30 (6):853-862.
3. Yoshida BA, Dubauskas Z, Chekmareva MA, Christiano TR, Stadler WM, Rinker-Schaeffer CW. Mitogen-activated protein kinase kinase 4/stress-activated protein/Erk kinase (MKK4/SEK1), a prostate cancer metastasis suppressor gene encoded by human chromosome 17. Cancer Res. 1999;59:5483-7

This study was supported by Grant no DEC-2014/15/B/Nz5/01587 from the National Science Centre, Poland.

ADMINISTRATION OF RIVAROXABAN IN THE COURSE OF ISCHEMIA/REPERFUSION-INDUCED ACUTE PANCREATATIS IN RATS ACCELERATES THE RECOVERY

M. MARAJ[1], P. CERANOWICZ[1], W. MACYK[2], J. CIESZKOWSKI[1], G. GINTER[1], B. KUŚNIERZ-CABALA[3], K. GAŁĄZKA[4], A. STEMPNIEWICZ[1], Z. WARZECHA[1]

[1]Department of Physiology, Faculty of Medicine, Jagiellonian University Medical College, Cracow, Poland;
[2]Department of Inorganic Chemistry, Faculty of Chemistry, Jagiellonian University, Cracow, Poland;
[3]Department of Diagnostics, Chair of Clinical Biochemistry, Faculty of Medicine, Jagiellonian University Medical College, Cracow, Poland; [4]Department of Pathomorphology, Faculty of Medicine, Jagiellonian University Medical College, Cracow, Poland; malgorzata.maraj@uj.edu.pl

MM acknowledges the fellowship with the project no. POWR.03.02.00-00-I013/16

Introduction:

Numerous studies emphasize the close interconnection between inflammation and coagulation [1–3]. Following the vessel damage the contact of tissue factor (TF) with the blood flow initiates the extrinsic coagulation cascade a series of reactions that lead to the conversion of prothrombin to thrombin. At the convergence of the intrinsic and extrinsic coagulation pathways lies factor X, which after activation generates about 1000 molecules of thrombin, a serine protease mainly associated with coagulative properties and its role in the proteolytic conversion of fibrinogen into fibrin. However, numerous studies go beyond hemostatic properties of thrombin and point to its activation of signaling pathways mediated via protease-activated receptors (PAR), which form the molecular connection between coagulation and inflammation. Rivaroxaban belongs to the group of novel anticoagulant drugs (NOACs) which does not target thrombin directly but via the inhibition of the factor Xa, a part of the prothrombinase complex essential for the conversion of prothrombin into thrombin [4].

Aim of the study:

The aim of the study was to investigate if administration of rivaroxaban, direct Xa factor inhibitor in the coagulation cascade, alleviates the severity of ischemia-reperfusion induced acute pancreatitis in rats.

Methods:

AP was induced with 30 min. ischemia and subsequent reperfusion in Wistar rats. Rivaroxaban in doses of 5, 20, 100 mg/kg was administered intragastrically once daily with the first dose 24 hours after the initiation of reperfusion. Histological, functional (blood low) and biochemical (serum level of lipase and amylase activity, D-dimer concentration, Il-1β) examinations were conducted 2, 5, 9 and 14 days from AP induction.

Results:

Influence of the treatment with rivaroxaban (RXB) on pancreatic morphological signs of pancreatic damage in the course of ischemia/reperfusion-induced acute pancreatitis (IR). RXB was given at a dose of 5, 20 or 100 mg/kg/day (RXB 5, RXB 20, or RXB 100).

Experimental groups		Edema (0–3)	Inflammatory Infiltration (0–3)	Vacuolization (0–3)	Necrosis (0–3)	Hemorrhages (0–3)
Control		0	0	0	0	0
I/R (6 h)		2–3	1–2	1	1	1–2
I/R (1 day)		2–3	3	1–2	1–2	2
I/R (2 days)	Saline	2	3	1	1–2	2
	RXB 5	2	3	1	1	2
	RXB 20	2	2–3	1	0–1	1–2
	RXB 100	2	2–3	1	0–1	1–2
I/R (5 days)	Saline	1–2	2	1	1	0–1
	RXB 5	1–2	2	1	1	0–1
	RXB 20	1	1–2	1	1	0–1
	RXB 100	1	1–2	1	1	0–1
I/R (9 days)	Saline	1	2	0–1	0	0–1
	RXB 5	0–1	1–2	0–1	0	0
	RXB 20	0–1	1	0	0	0
	RXB 100	1	2	0	0	1
I/R (14 days)	Saline	1	1	0–1	0	0
	RXB 5	0	0–1	0	0	0
	RXB 20	0	0–1	0	0	0
	RXB 100	1	1	0	0	0–1

Numbers represent the predominant histological grading in each experimental group.

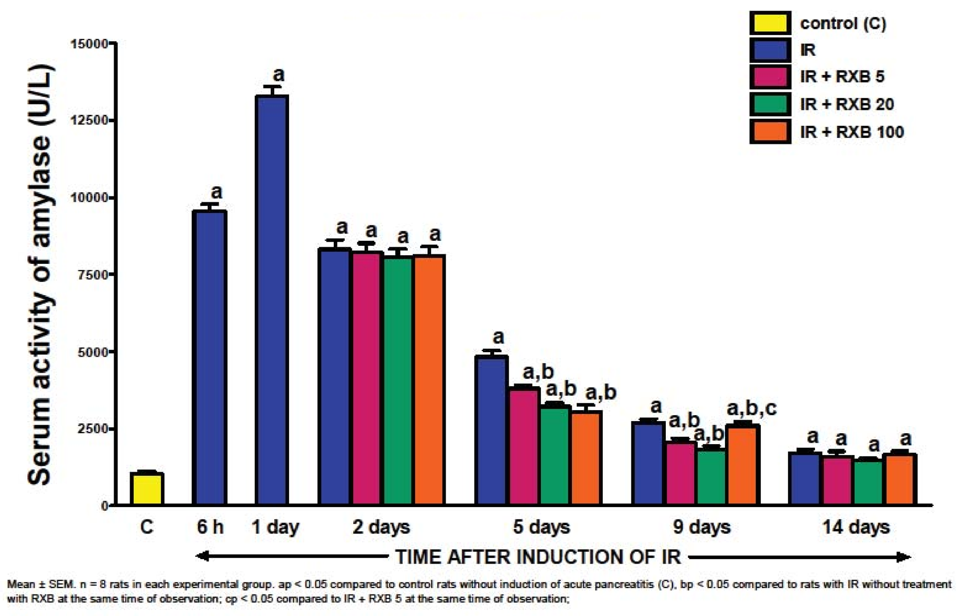

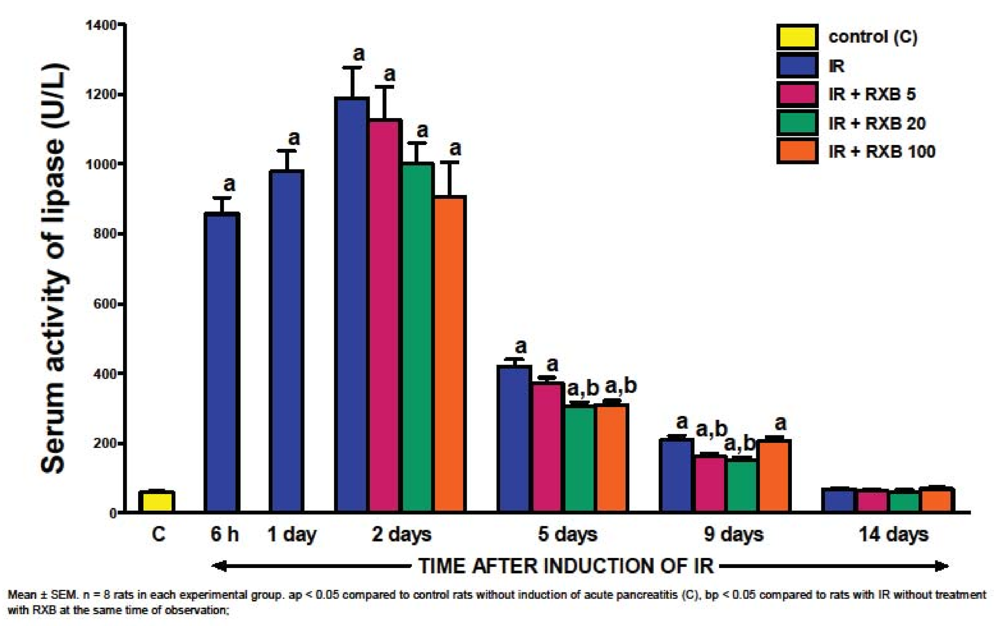

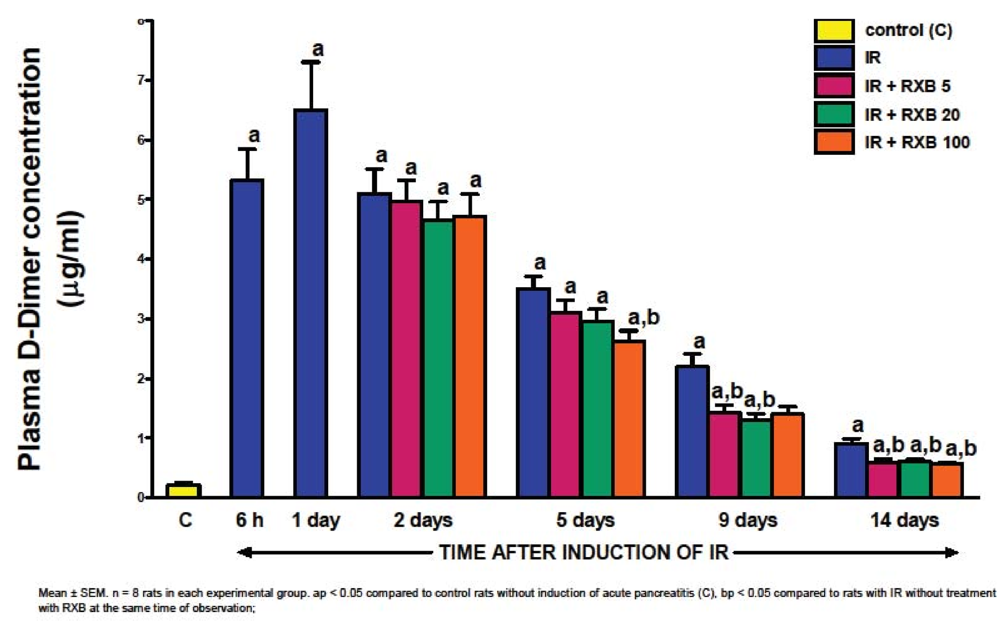

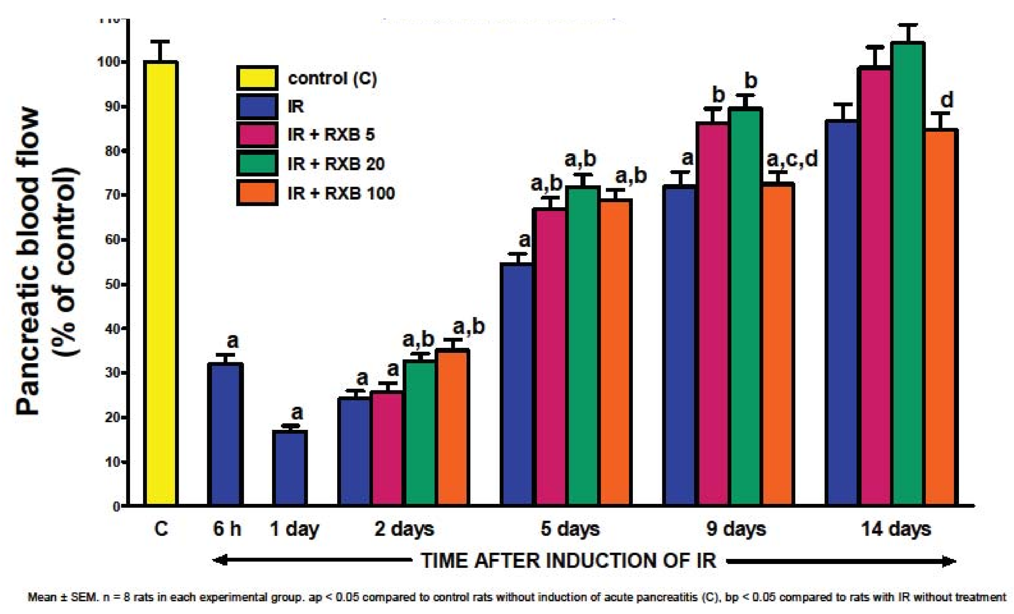

Conclusions:

Administration of RXB in the dose of 5 and 20 mg/kg limited the morphological damage of the pancreas such as edema, vacuolization of acinar cells, necrosis or the number of hemorrhages. Also the improvement in the pancreatic blood flow was observed. It was accompanied by the reduction of pancreatic enzymes amylase and lipase. Additionally, treatment with rivaroxaban decreased the concentration of interleukin 1β in the serum, as well as the drop in the D-Dimer level was recorded. Administration of rivaroxaban in the dose of 100 mg/kg led to the increased severity of damage of the pancreas and worse acute pancreatitis parameters as compared to lower doses. In some rats intestinal bleeding was observed.

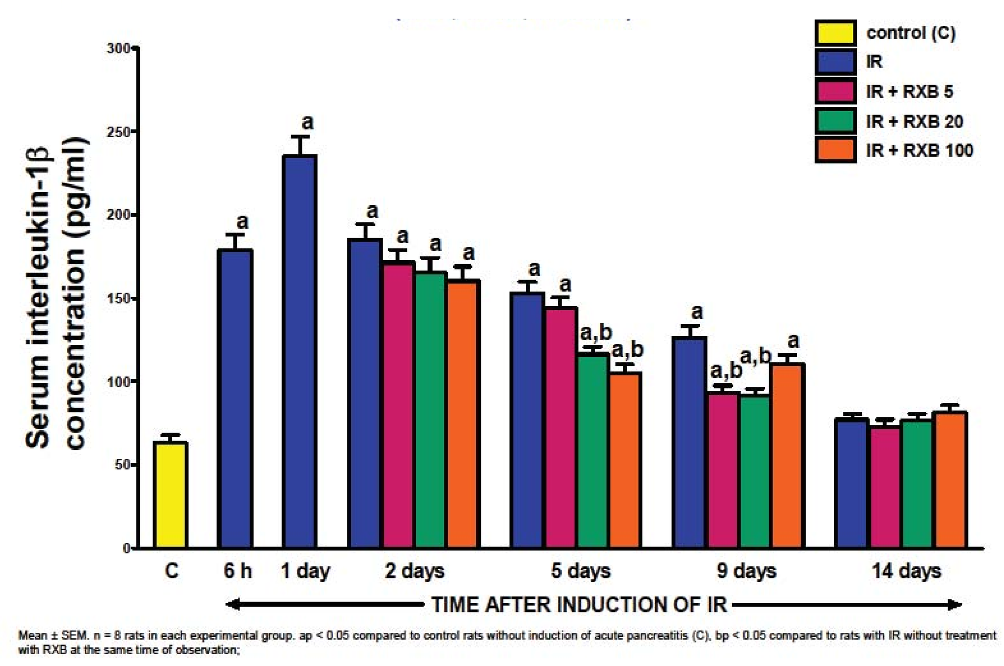

References

1. Dumnicka, P.; Maduzia, D.; Ceranowicz, P.; Olszanecki, R.; Drożdż, R.; Kuśnierz-Cabala B. The interplay between inflammation, coagulation and endothelial injury in the early phase of acute pancreatitis: Clinical implications. Int. J. Mol. Sci. 2017, 18, 1–25.
2. Foley, J.H.; Conway, E.M. Cross Talk Pathways between Coagulation and Inflammation. Circ. Res. 2016, 118, 1392–1408.
3. Jose, R.J.; Manuel, A. COVID-19 cytokine storm: the interplay between inflammation and coagulation. Lancet Respir. 2020, 8, e46–e47.
4. Cate, H.; Guzik, T.J.; Eikelboom, J.; Spronk, H.M.H. Pleiotropic actions of factor Xa inhibition in cardiovascular prevention: mechanistic insights and implications for anti-thrombotic treatment. Cardiovasc. Res. 2020.

XXVIII Congress of the Polish Physiological Society

Gdańsk, September 15-17 2021

Poster book

SESSION XIII

MULTI-OMICS PROSPECTIVES IN PHYSIOLOGY

HONORARY PATRONAGE

Uniwersytet Gdański

Prof. dr Marcin Gruchała
Rector of the Medical University of Gdansk

Prof. dr Piotr Stepnowski
Rector of the University of Gdansk

WOJEWODA POMORSKI
DARIUSZ DRELICH

Dariusz Drelich
Governor of the Pomeranian Voivodeship

HONORARY PATRONAGE
Mayor of the City of Gdańsk

Aleksandra Dulkiewicz
Mayor of Gdansk

Mieczysław Struk
Marshal of the Pomeranian Voivodeship

PARTNER

PAN
POLSKA AKADEMIA NAUK

ANIMA LAB
animal facility and laboratory equipment • animal research models

FUNDACJA LOTOS

Medical University of Gdansk
Department of Physiology

XXVIII Congress of the Polish Physiological Society

Gdańsk, September 15-17 2021

Poster book

SESSION XIV

PHYSIOLOGY MEETS ENGINEERING

HONORARY PATRONAGE

Uniwersytet Gdański

Prof. dr Marcin Gruchała
Rector of the Medical University of Gdansk

Prof. dr Piotr Stepnowski
Rector of the University of Gdansk

WOJEWODA POMORSKI
DARIUSZ DRELICH

Dariusz Drelich
Governor of the Pomeranian Voivodeship

HONORARY PATRONAGE
Mayor of the City of Gdańsk

Aleksandra Dulkiewicz
Mayor of Gdansk

Mieczysław Struk
Marshal of the Pomeranian Voivodeship

PARTNER

ANIMA LAB
animal facility and laboratory equipment • animal research models

Medical University of Gdansk
Department of Physiology

ASYMMETRIC PROFILE OF SPONTANEOUS SEQUENTIAL CHANGES OF BLOOD PRESSURE COUPLED WITH MONOTONIC CHANGES OF SUCCESSIVE HEARTBEATS IN UNRESTRAINED NORMOTENSIVE RATS.

Stanisław Zajączkowski & Tomasz H Wierzba

Department of Physiology, Medical University of Gdansk, Gdansk, Poland

INTRODUCTION

Intuitive assumption of relative regularity or even constancy of major hemodynamic variables stands in contrast to asymmetric distribution of spontaneous beat-to-beat changes of blood pressure (BP) and quantitative asymmetry in the deceleration and acceleration of heart cycles. An intriguing physiological phenomenon is occurrence of short periods of monotonic beat-to-beat changes of systolic blood pressure (SBP, increasing or decreasing runs) accompanied by unidirectional runs of RR intervals (RRi deceleration or acceleration).

AIM

The aim of the study was to assess the occurrence of spontaneous sequential changes in BP coupled with monotonic changes of intervals of successive heartbeats (RR intervals; RRi) in rats in resting conditions.

MATERIALS & METHODS

The experiments were performed on unrestrained male Wistar rats (N=11, 300 - 350g). ECG and systolic blood pressure (SBP) were recorded continuously at sampling rate 1,5 kHz. Sequences of 3 to 6 unidirectional changes of SBP and HR were identified. Frequency of the heart rate (HR) and SBP sequences was estimated to assess spontaneous baroreflex reactivity. Proportion of the SBP sequences coupled to the HR sequences was taken as an index of baroreflex sensitivity (BRS). Sequences of SBP increase or decrease were analyzed separately.

Two types of SBP sequences were discriminated: the **concordant**, in which SBP and RRi changed in the same direction (considered the baroreflex effect), and the **opposite** (regarded as a feed-forward cardiovascular setting), where changes of SBP coincided with inverse changes in RRi.

RESULTS

1. Mean SBP was 134 ± 5 mmHg and HR was 181 ± 6/min.
2. The sequences of an increase of SBP involved 10.1% of all cardiac cycles and were more frequent than its declining (7.4%).
3. RRi prolongation sequences (10.5%) were less frequent than those of RRi shortening.
4. Proportion of RRi sequences coupled with SBP-increase sequences was higher in the feed-forward sequences (↑SBP and ↓RRi) than in the concordant ones (↑SBP and ↑RRi).
5. In contrary, the feed-forward sequences of SBP decrease (↓SBP and ↑RRi) occurred less frequent than the opposite ones (↓SBP and ↓RRi).

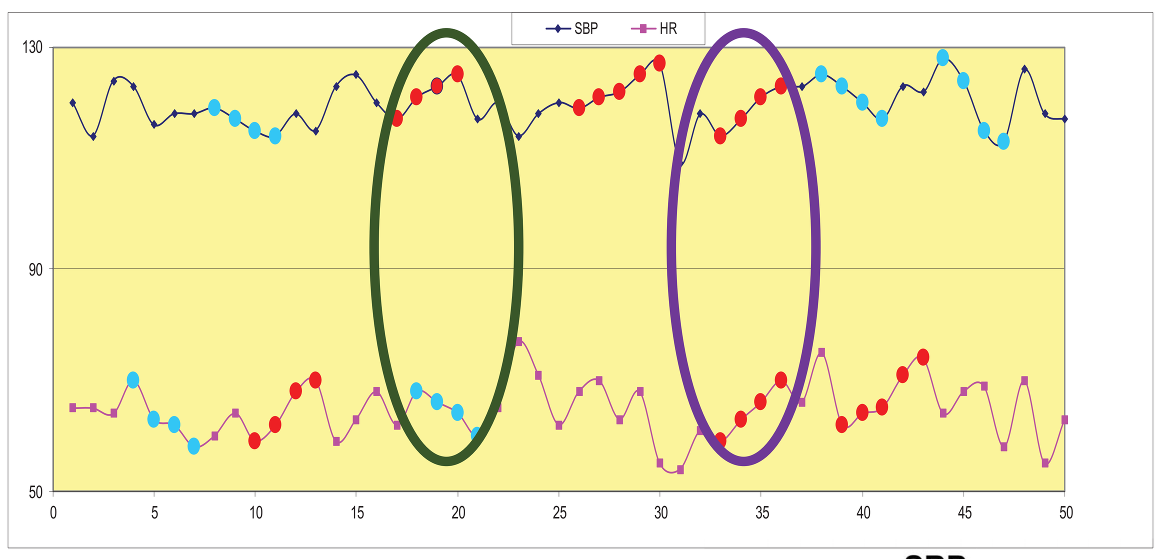

Unidirectional sequence of changes in blood pressure (SBP) and heart rate (HR). **Red** – increasing sequences **blue** – decreasing sequences. **Green** ring shows opposite (feed-forward) and **violet** ring shows concordant (baroreflex) sequences.

SBP

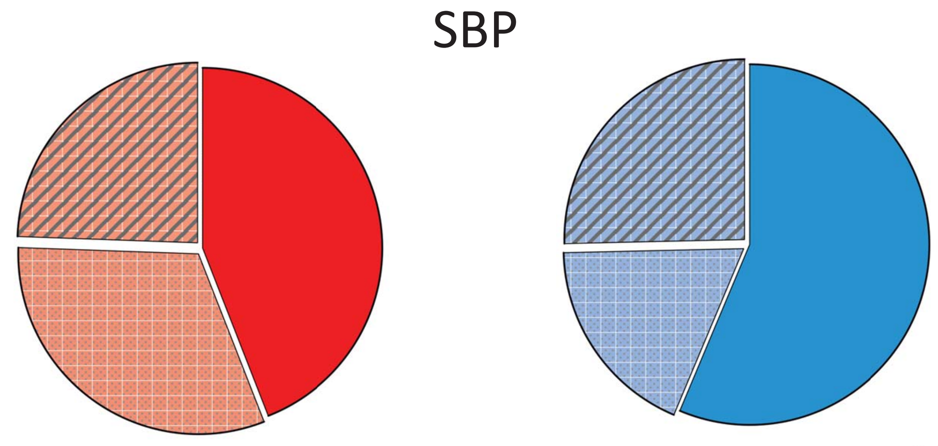

HR

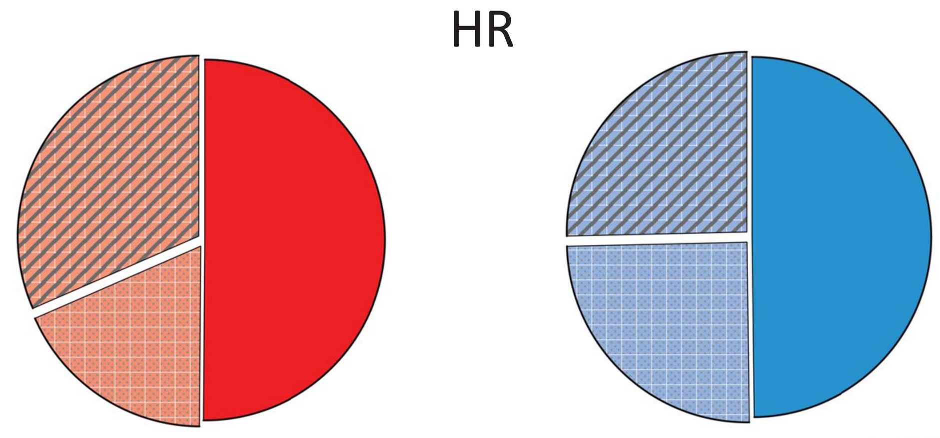

The sequences of SBP increase involved 10.1% of all cardiac cycles and were more frequent than its declining (7.4%). HR acceleration sequences (10.5%) were less frequent than those of HR deceleration.

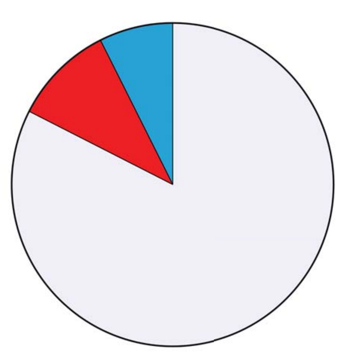

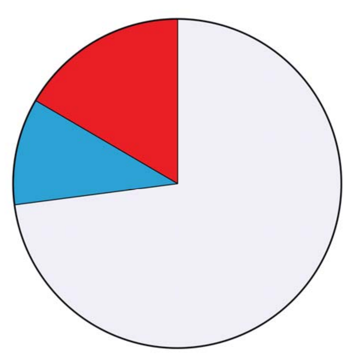

SUMMARY

Spontaneous variability of SBP and RRi have a well-determined irregularity. More frequent attempts to adjust high blood pressure are coordinated with an increased reflex control against its reduction. Analysis of the beat-to-beat fluctuations of SBP and RRi revealed non-random pattern of spontaneous hemodynamic oscillations. It is recommended, considering non-uniform profile of sequential beat-to-beat changes of RRi and SBP, that the sequences of either an increase or a decrease of SBP should be analyzes separately.

Supported by grant of the Medical University of Gdansk: 02-0036/07/261

TOMASZ H. WIERZBA, KRZYSZTOF MALINOWSKI, GRZEGORZ REDLARSKI

Department of Physiology, Medical University of Gdansk, Poland

IMPAIRED BLOOD PRESSURE REGULATION IN SHR RATS ASSESSED BY DETAILED ANALYSIS OF MONOTONIC RUNS OF BLOOD PRESSURE AND HEART RATE

Spontaneously hypertensive rats (SHR) represent experimental model corresponding to human hypertension of mostly neurogenic background. Observation of spontaneous fluctuations and coherence between major hemodynamic variables such as systolic blood pressure (SBP) and heart rate (HR) offers an advanced insight to the regulatory aspects of hypertension.

AIM OF THE STUDY

The study was performed to compare the occurrence of spontaneous sequential changes in SBP coupled with monotonic changes of intervals of successive heart cycles.

MATERIAL AND METHODS (1)

RATS:

- conscious male, previously instrumented (insertion of arterial line, ECG electrodes)
- spontaneously hypertensive; SHR; N=7; 306–344 g),
- their respective control; WKY; N=7; 302–355 g).

ECG and systolic blood pressure (SBP)
recorded at sampling rate 1.5 kHz.

MATERIAL AND METHODS (2)

Raw recording of SBP and HR

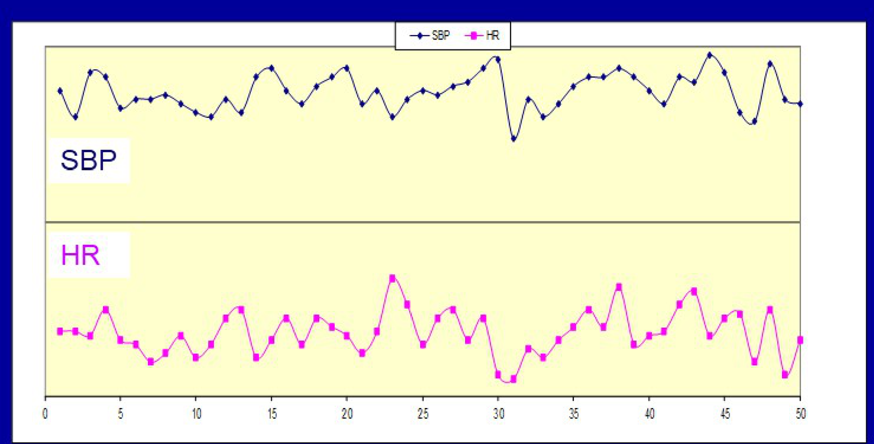

MATERIAL AND METHODS (3)

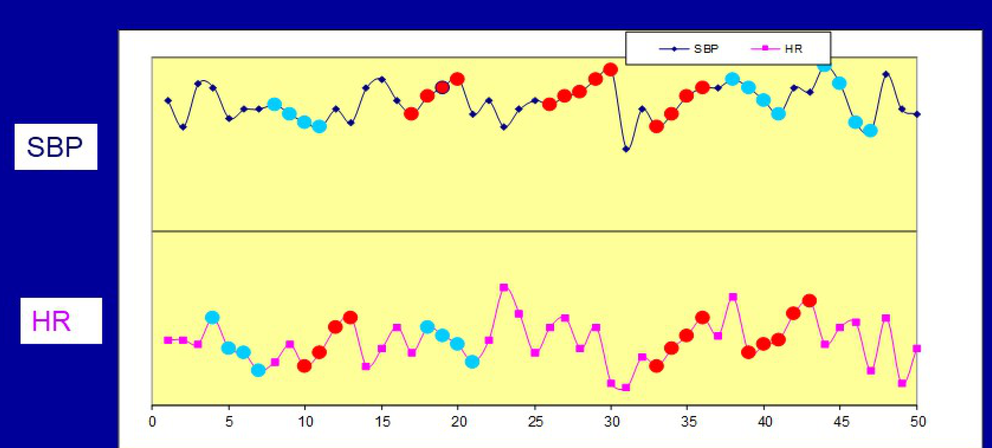

Sequences (Seq) of spontaneous increases or decreases of SBP and HR were identified.
For a sequence were taken from 3 to 6 consecutive unidirectional changes.

MATERIAL AND METHODS (4)

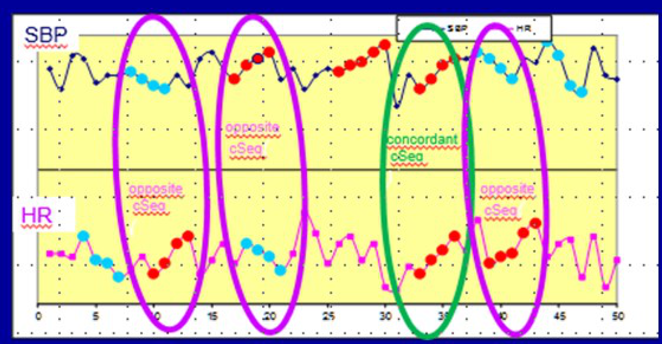

Two types of coupled (HR with SBP) sequences ere discriminated:

- the concordant, in which SBP and HR changed in the same direction (interpreted as a **feed-forward baroreflex setting**),
- the opposite (considered the **baroreflex effect**), where changes of SBP coincided with inverse changes in HR.

RESULTS (1)

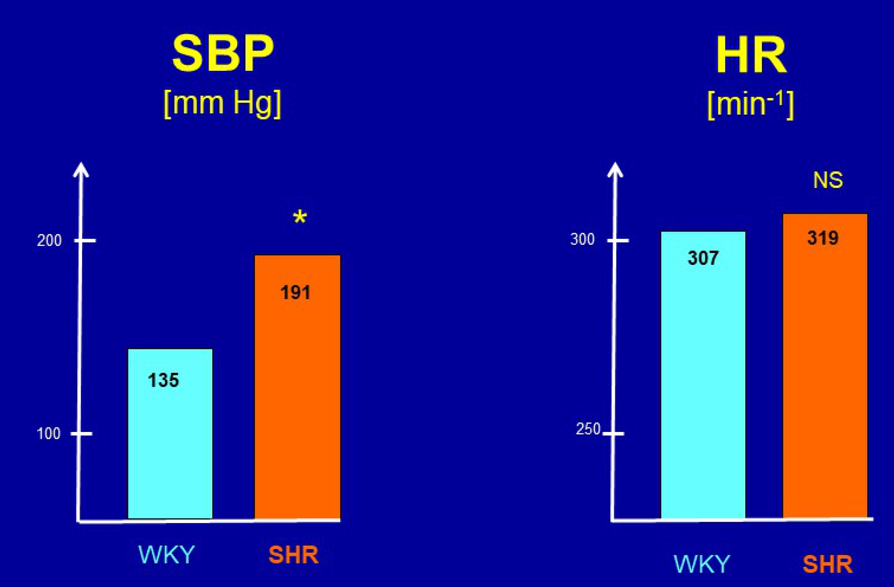

RESULTS (2)

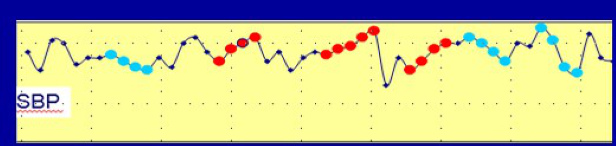

ΔSBP sequences frequency [Hz]

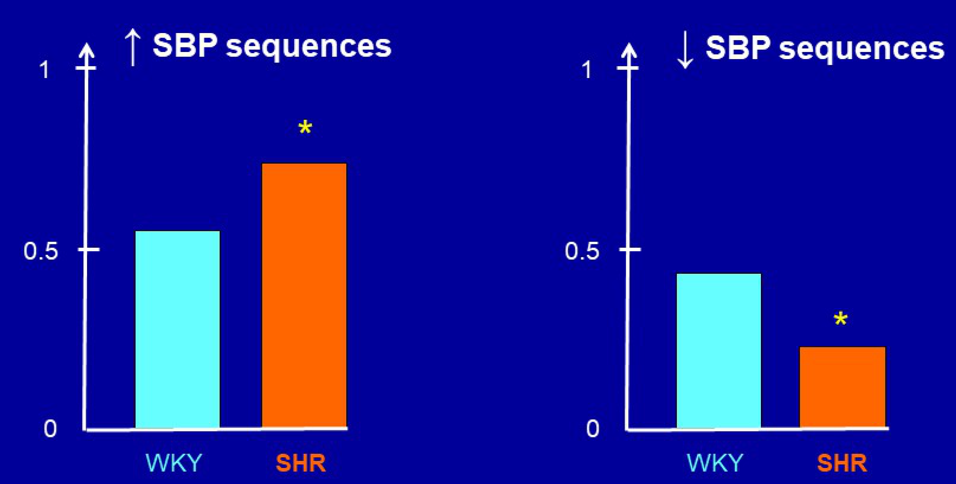

RESULTS (3)

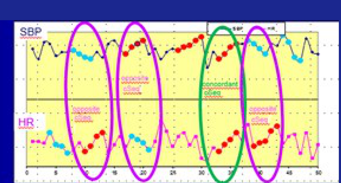

ΔHR sequences coupled with ΔSBP sequences
[% of all heart cycles]

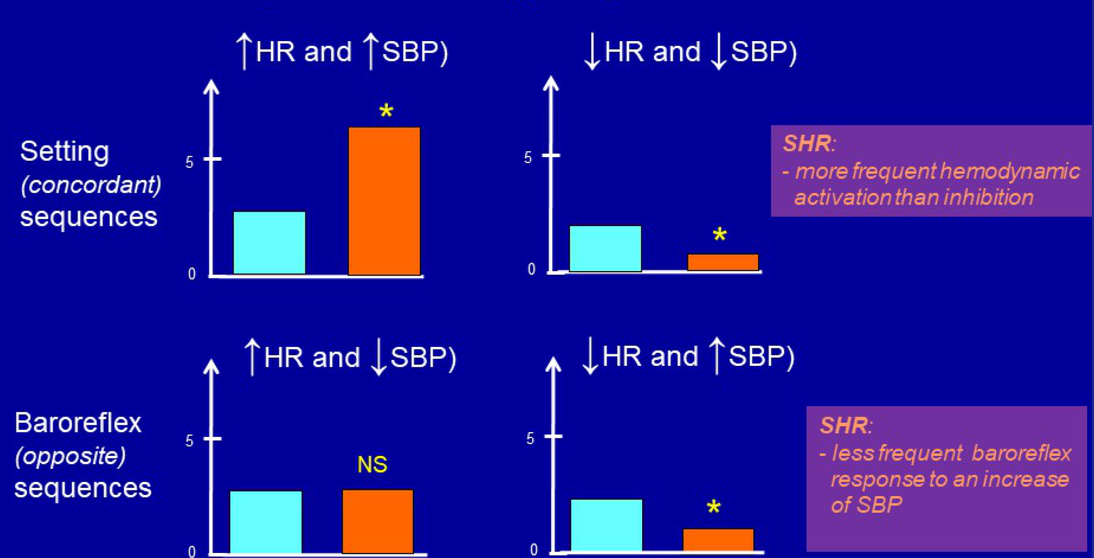

RESULTS (4)

Efficiency of coupled sequences (BEI) related to sequences of an increase or a decrease of SBP
[% all ↑SBP sequences or % all ↓SBP sequences]

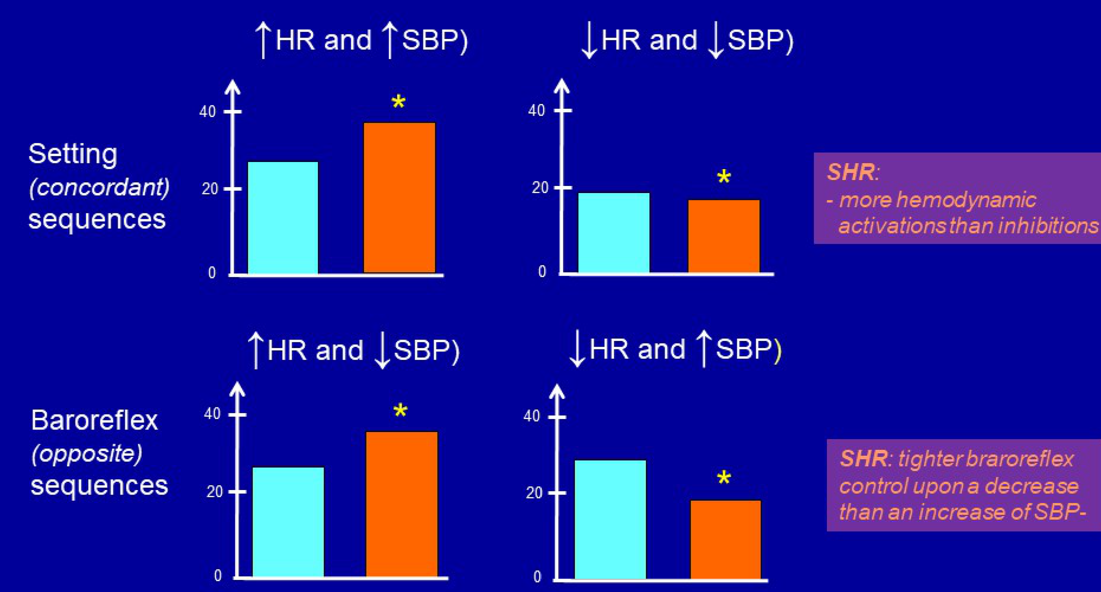

RESULTS (5)

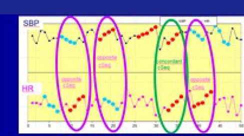

Beat-to beat latency of the regulatory (baroreflex related) HR responses to sequential changes of SBP [N of heart cycles]

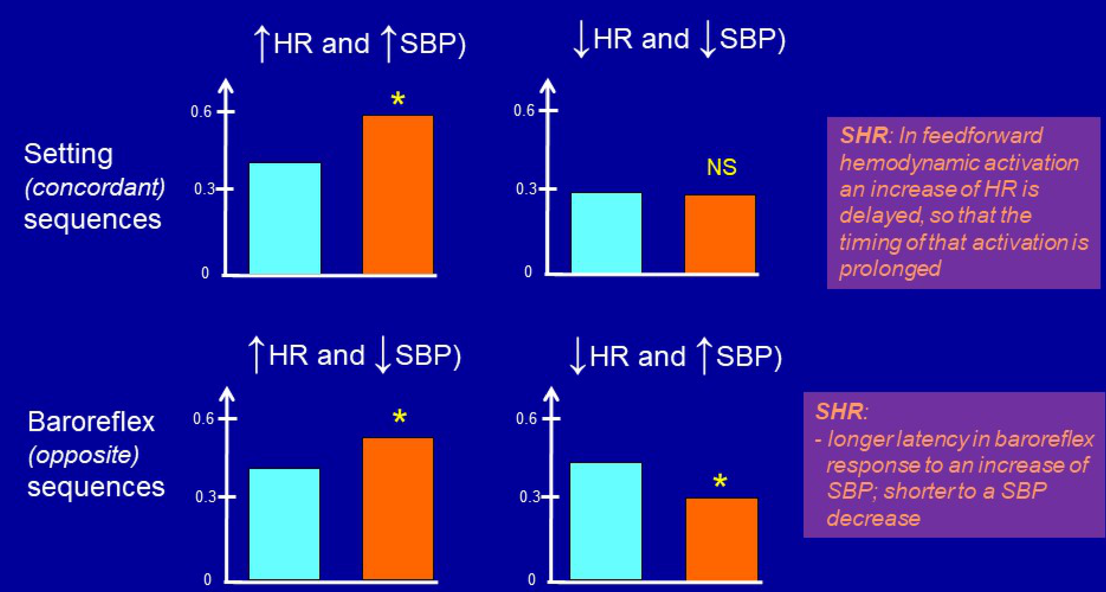

RESULTS (6)

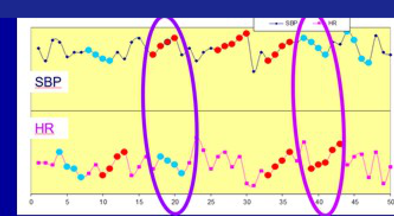

Spontaneous baroreflex sensitivity (BRS)

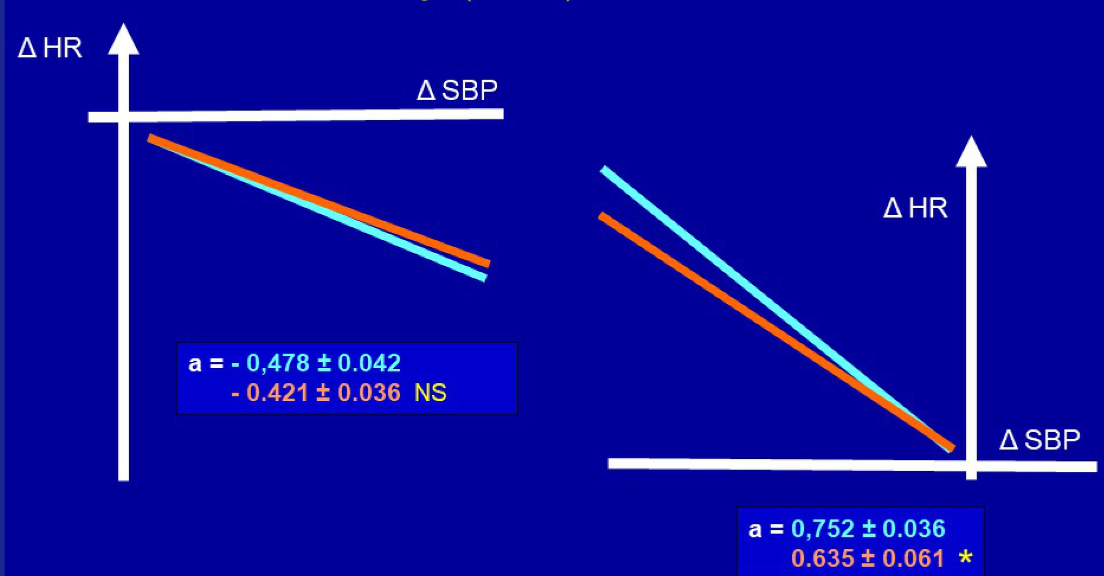

CONCLUSION

1. Our data indicate profound regulatory dysfunction in SHR rats.
2. The observed regulatory profile reflects reduced chance for the reflex correction of an increase in blood pressure, with impaired counter-regulatory defense against its decrease.
3. Moreover, an increased phase shift between the HR-response triggered by a change in SBP indictaes impaired neurogenic control upon the heart, that may promote sudden critical cardiovascular incidents.

HOW DATA SCIENCE MAY SUPPORT PHYSIOLOGICAL EXPERIMENTS? A REVIEW OF EXAMPLES AND POSSIBILITIES

AGNIESZKA SIENNICKA[1], B.PALECZNY[1], R.SEREDYŃSKI[1], M.PONDEL[2], M.WYCISZKIEWICZ[1], T.OKUPNIK[1], B.PONIKOWSKA[1]
[1]Wroclaw Medical University, Poland; [2]Wroclaw University of Economics and Business, Poland;
agnieszka.siennicka@umed.wroc.pl;

Where to look for „big" data?

Data science does not require large population of studied subjects. Nowadays – often a single experiment may serve as large dataset, as we use sensors collecting multiple parameters (heart rate, breathing rate, blood pressure, etc) with high sampling frequency in a synchronised way eg.:

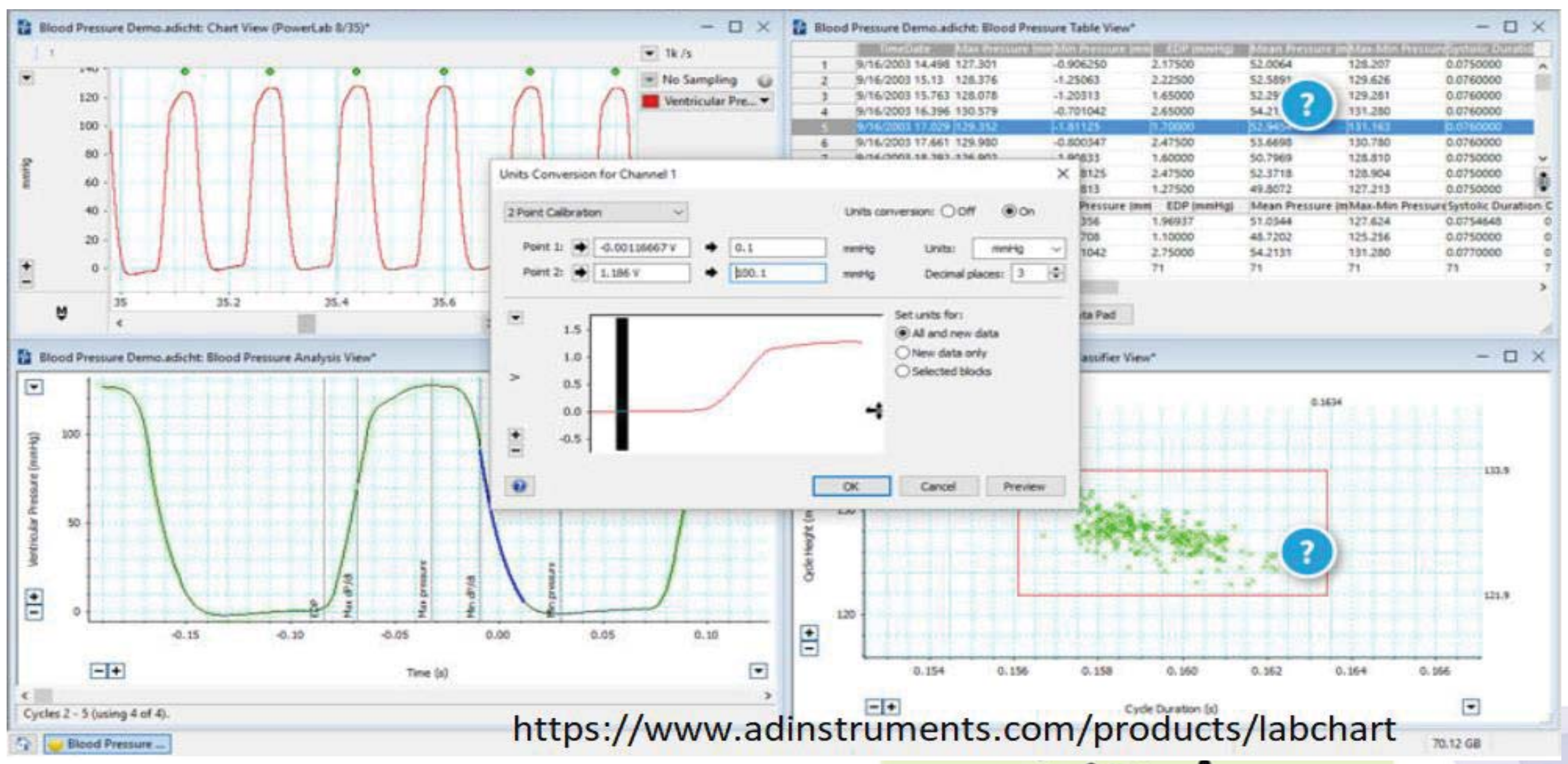

https://www.adinstruments.com/products/labchart

What are the options?

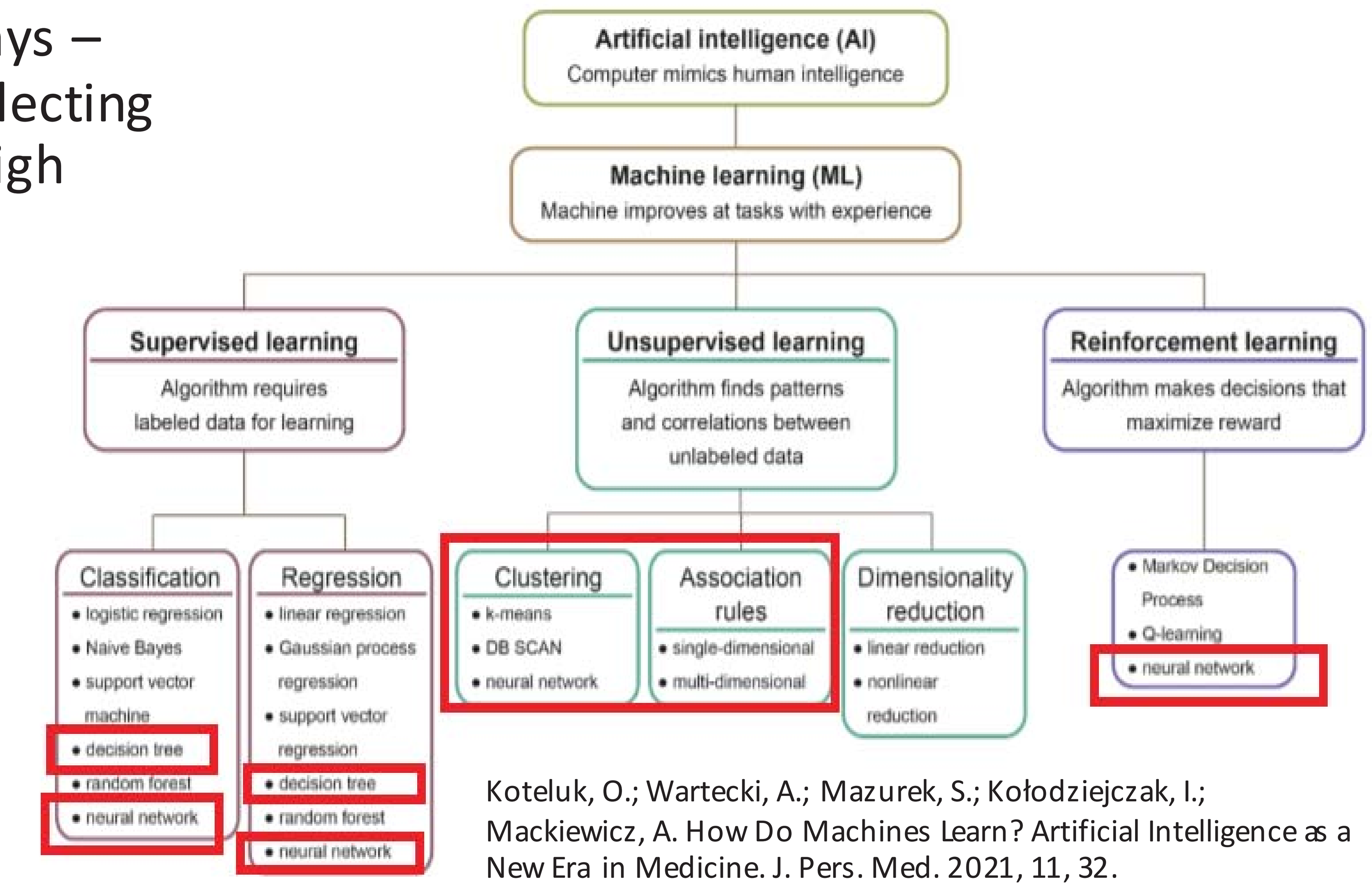

Koteluk, O.; Wartecki, A.; Mazurek, S.; Kołodziejczak, I.; Mackiewicz, A. How Do Machines Learn? Artificial Intelligence as a New Era in Medicine. J. Pers. Med. 2021, 11, 32. https://doi.org/10.3390/jpm11010032

Neural networks

In artificial neural networks (ANN), the model of an artificial neuron is used and it can be defined as follows: inputs, weights, input summation function, activation function, output. In the next step many neurons connect to each other to form a network. The network has to include: the inputs, through which external variables are provided and output that provide the final result of the computation. In the ANN, **the complex (extensive) relationships between dependent and independent variables can be observed, which cannot be predicted using other, classical models.** Thus, the artificial neural networks can be useful in prediction, classification, recognition and in associating data.

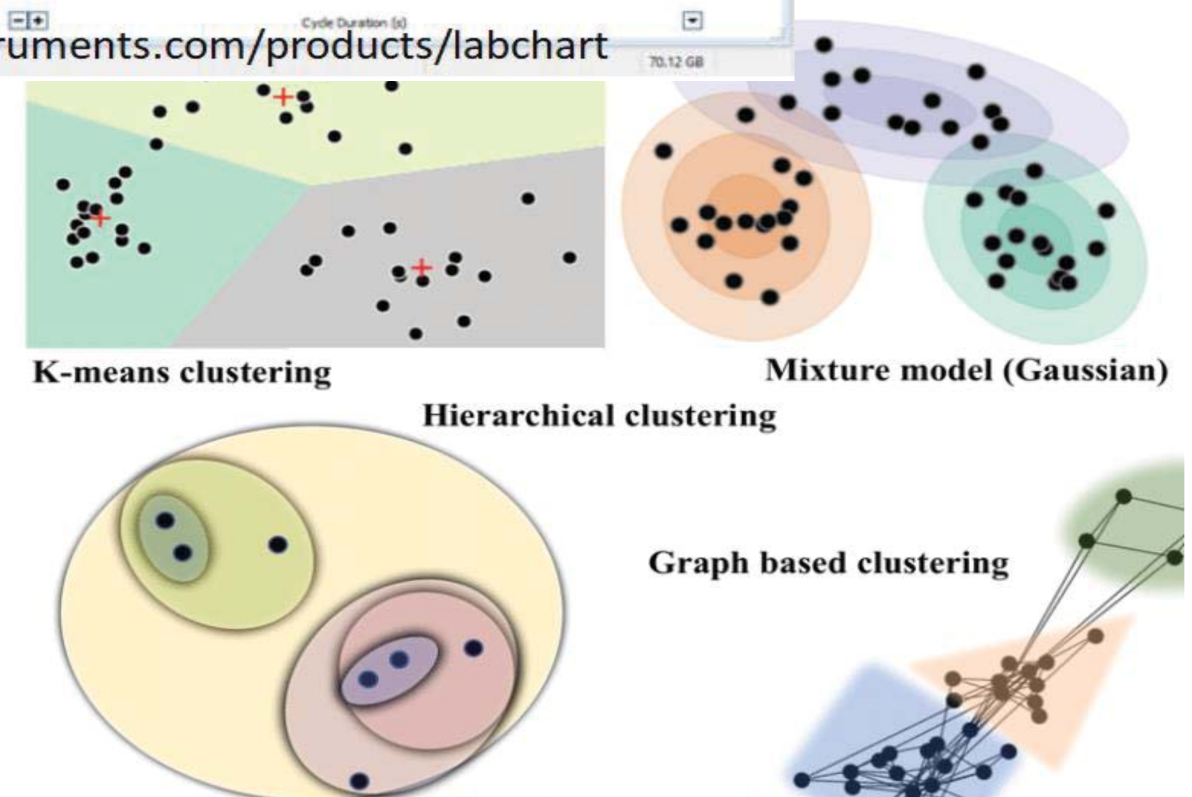

Khosla et al. (2019). Machine learning in resting-state fMRI analysis. Magnetic Resonance Imaging. 64. 10.1016/j.mri.2019.05.031.

Clustering algorithms

The first step to understand a data set is to group the examples. Grouping of unlabeled examples is called clustering which relies on unsupervised machine learning. **Grouping similar examples** require finding them. The similarity between examples may be measured by combining the examples' feature data into a metric, called a similarity measure. When each example is defined by one or two features, it's easy to measure similarity. For example, you can find similar books by their authors. As the number of features increases, creating a similarity measure becomes more complex. We'll later see how to create a similarity measure in different scenarios.
Clustering may be applied to divide examined subject but also to search within large datasets collected during a single study with multiple signals collected from one subject at the same time.

Association rules

Association rule is a technique of data mining using to identify patterns in large datasets. This procedure helps to discover **probability of relationships between two items** and is pivote to explain patterns which seem to be independent. Association rule contains two sections, an antecendent (if) which is an item found over the data and an consequent (then) which consists an item combined with an antecendent. This technique basing on support and confidence criteria which refers to the strong of correlation. Support exhibits how often item appears in the data and confidence indicates how many times if-then statements are found true, so represents frequence given rule works in practice. The rule may reveals big correlation for the reason that appears very often in the data (high support) and turns out much more less applied (low confidence). Converse situation is possible to occur as well.

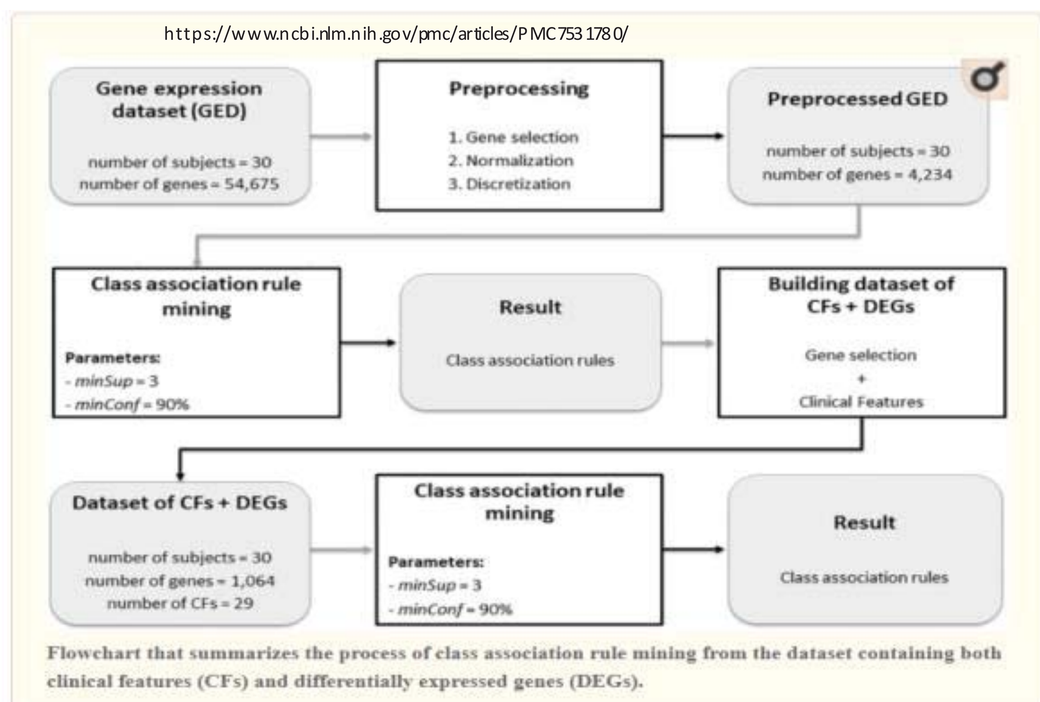

Flowchart that summarizes the process of class association rule mining from the dataset containing both clinical features (CFs) and differentially expressed genes (DEGs).

Veroneze R. et al., Using association rule mining to jointly detect clinical features and differentially expressed genes related to chronic inflammatory diseases, PLoS One. 2020; 15(10): e0240269.

OUR EXPERIENCES

We decided to employ machine learning (ML) for re-creation of the signal reflecting muscle sympathetic nerve activity (MSNA, which requires invasive measurement) based on physiological correlates of MSNA recorded noninvasively.
The applied methods included neural networks, decision trees and long short-term memory, which is an artificial recurrent neural network architecture linked to deep learning. Results are presented in a form of an oral presentation by Paleczny et al..

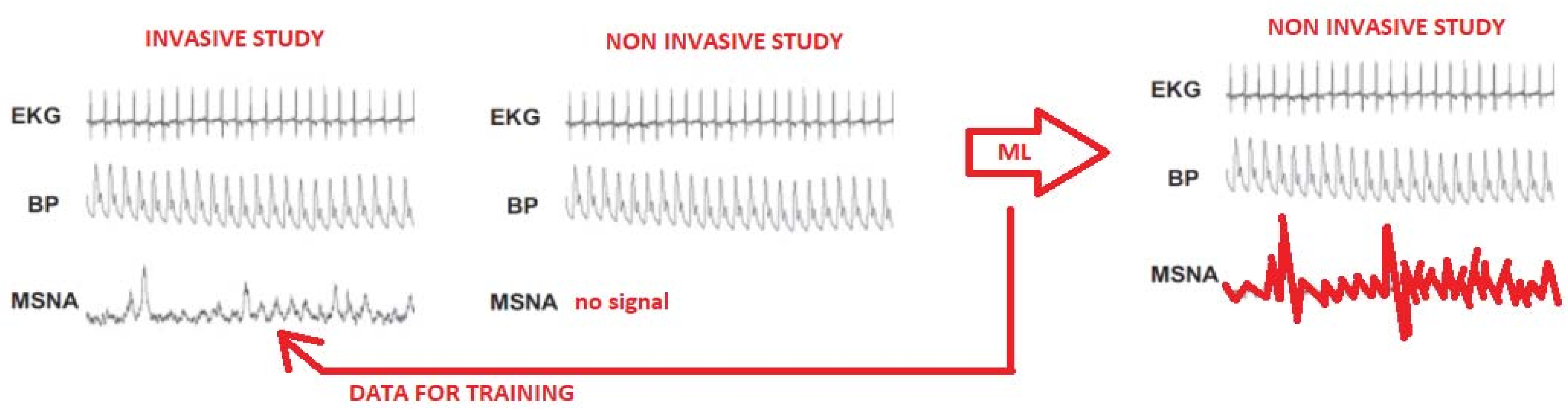

European Commission

Acknowledgements: This presentation results from a project: HeartBIT_4.0 – Application of innovative Medical Data Science technologies for heart diseases. Project has received funding from the European Union's Horizon 2020 research and innovation programme under grant agreement number 857446.

Cardiac and non-cardiac sources of T wave morphology

Karolina Rams, M.Ozimek, M.Andrzejewska, T.Buchner

Complex Systems Physics Division, Faculty of Physics, Warsaw University of Technology, Poland

Introduction

- When the morphology of the ECG is analyzed, there is often a tendency to interpret the observed symptoms as a sole result of electric activity of cardiac muscle, and to treat all the factors that modify the ECG as environmental noise, even if it is a symptom itself, as for pericarditis or P pulmonale.
- In order to circumvent these opinions, we have performed a thorough analysis of patients in THEW database – Holter ECG, 200 Hz sampling, 24h signals. Study group consists of 252 patients: 107 with LQTS syndrome and 145 healthy patients. Regarding the gender ratio, 61 females and 46 males were selected among the sick patients, and there were 74 females and 71 males among the healthy patients.
- Respective phase portraits, also referred to as clouds, were constructed based on the QT, RR, TQ intervals' lengths as well as the QRS and T amplitudes. Selected QT correction methods were applied to these datasets. A comparison between QT/RR and APD/DI phase portraits was created.

Methods

ECG processing algorithms

The Neurokit2 module, available in Python, was used to prepare the ECG signals for further processing, performing better than other traditional algorithms, e.g. Pan-Tompkins. Methods available in this module were also used so as to find the necessary waves' locations (Q,R,S and T). An innovative algorithm was proposed in order to compensate for the oversensitivity of these methods for the task of finding the R waves' locations. QT (APD), RR and TQ (DI) intervals as well as QRS and T waves' amplitudes were extracted from the processed signals.

QT correction methods

- Bazett's formula: $QT_C = \frac{QT}{\sqrt{RR}}$
- Fridericia's formula: $QT_F = \frac{QT}{\sqrt[3]{RR}}$
- Framingham formula: $QT_{LC} = QT + 0{,}154(1 - RR)$

Results

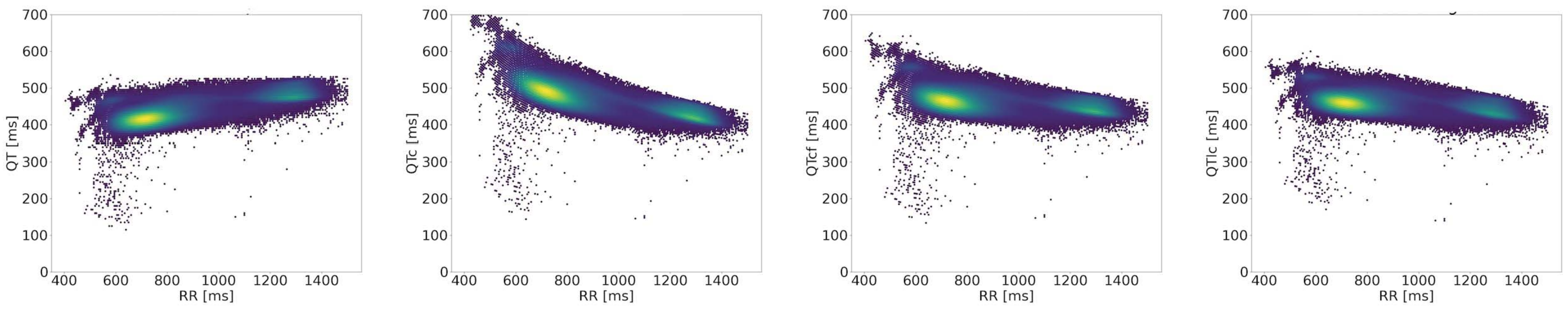

Fig. 1. QT-RR phase portraits for, uncorrected, Bazett's formula, Fridericia's formula and Framingham formula, LQTS individual

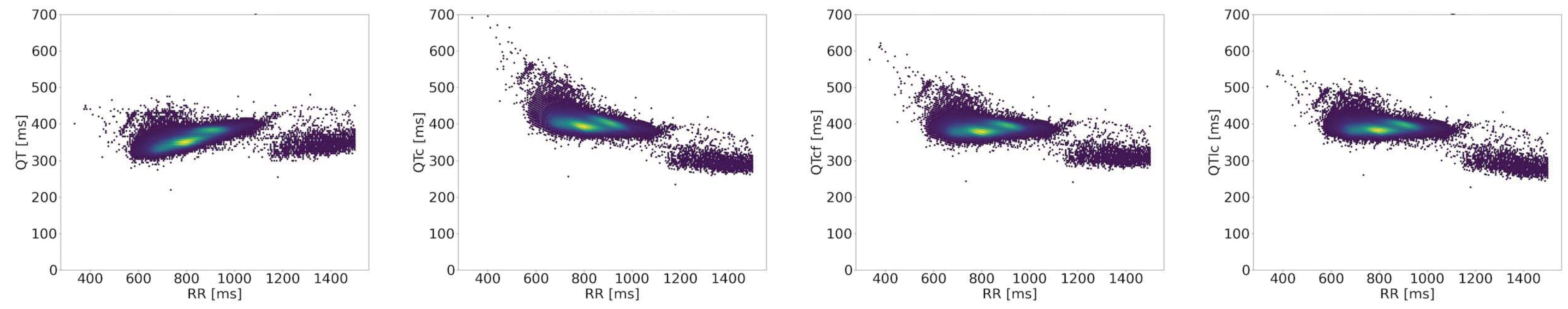

Fig. 2. QT-RR phase portraits for, uncorrected, Bazett's formula, Fridericia's formula and Framingham formula, normal individual

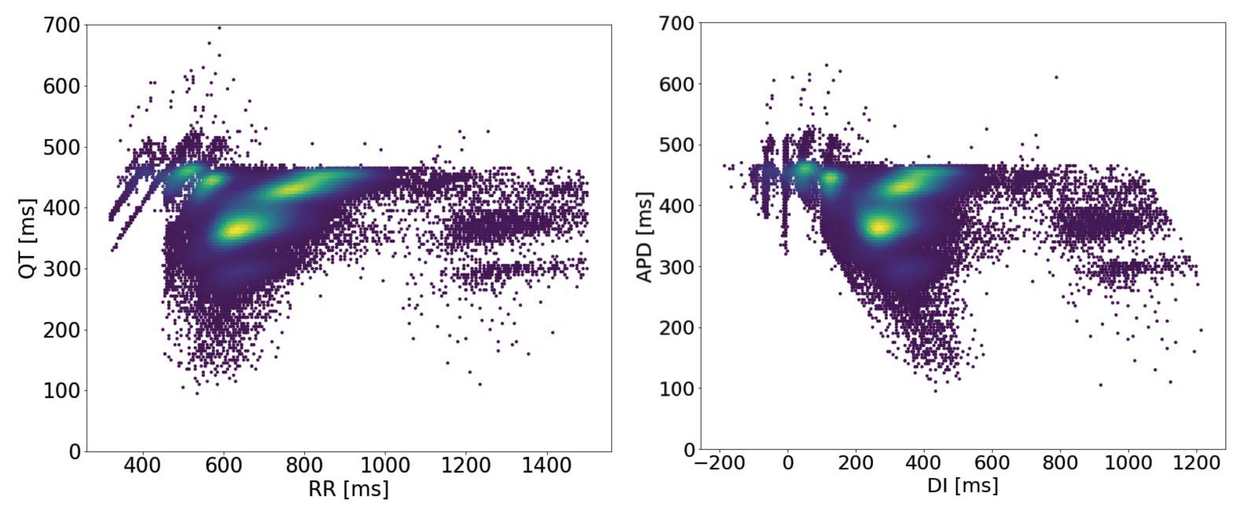

Fig. 3. Comparison of QT/RR cloud with ADF/DI cloud

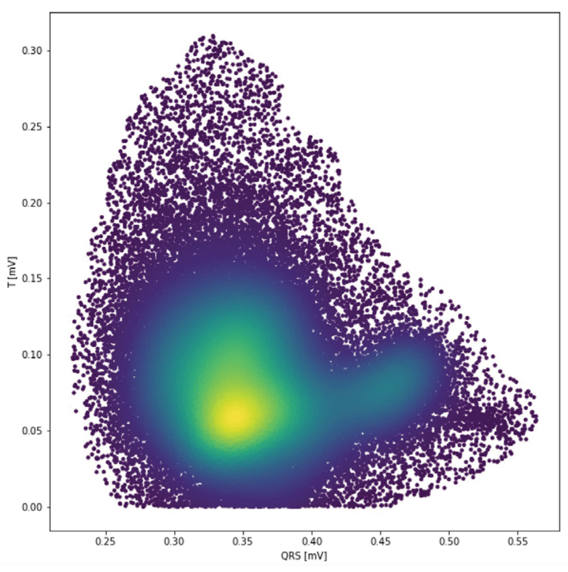

Fig. 4. Example QRS/T amplitude phase portrait

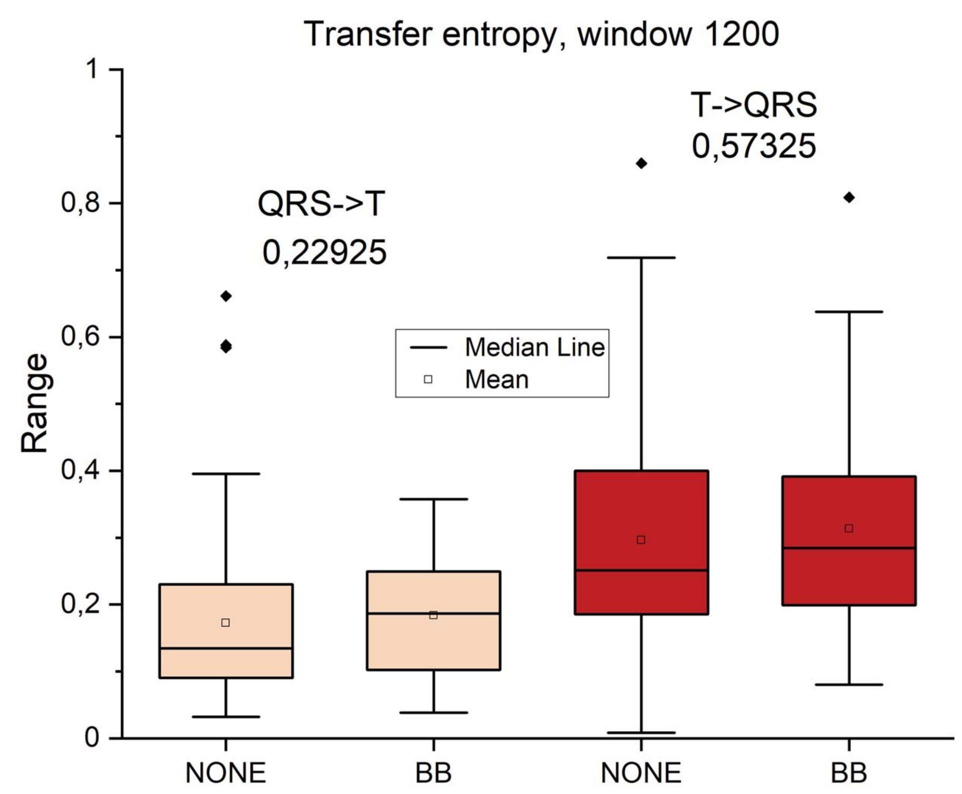

Fig. 5. Entropy flow between QRS and T

Summary

- As a result of visual analysis of the obtained clouds, we noticed an island-like structure occurring in many healthy and LQTS patients, which may indicate the day and night cycle, or a change in body position, which is responsible for the change in blood supply to the body under the electrodes. When body position changes, water can be considered an amplifier, and differences in hydration state and ionic content of hydrated fluids can affect measurements of bioelectrical impedance (BI) and hydrostatic weight (HW).
- The dominant role of the APD/DI relation on the whole QT and RR dynamics does not hold, as each of signals may exhibit a certain extent of its own dynamics. Of special importance are the QT increases at increasing HR, which correspond to the negative QT(RR) regression slope. They may appear as isolated islands in QT - RR plot.
- The amplitude of the T wave does not directly follow the amplitude of the QRS, so these two variables are to some extent statistically independent.
- The T wave possesses a different source of information, not necessarily related to both the interval and the amplitude of the QRS.
- The question of the origin of the observed changes, their relation to the position of the body and their potential clinical correlates is a matter of an ongoing study.
- These values indicate that the entropy flow between QRS and T exists. There is a noticeable asymmetry in the flow of information, meaning that T affects QRS more than vice versa. (Fig.5.)
- QT depends on RR and T amplitude, and these two values correspond to inotropic and chronotropic regulation.
- Inotropic regulation causes increased phosphorylation of channel proteins and ejection of more ions. Action potential increases, so the signal amplitude of a single ECG lead increases and the lead which is the difference of the two also increases. As a result, QT changes in two opposite directions. It increases because the amplitude of T increases, but shortens because RR shortens.

References

1. Shen Luo, Kurt Michler, Paul Johnston, Peter W. Macfarlane, „A comparison of commonly used QT correction formulae: The effect of heart rate on the QTc of normal ECGs", *Journal of Electrocardiology*, 2004, Pages 81-90, ISSN 0022-0736, https://doi.org/10.1016/j.jelectrocard.2004.08.030.
2. Starobin et al. METHOD AND SYSTEM FOR EVALUATING STABILITY OF CARDIAC PROPAGATION RESERVE. Number 20160287123. October 2016.
3. Baranowski R, Popławska W, Buchner T, Chojnowska L, Rydlewska-Sadowska W. Day-to-day reproducibility of Holter beat-by-beat analysis of repolarisation. Acta Cardiologica. 2003;58(3):185–189.

Faculty of Physics
WARSAW UNIVERSITY OF TECHNOLOGY

Research was funded by (POB Biotechnology and Biomedical Engineering) of Warsaw University of Technology within the Excellence Initiative: Research University (IDUB) program 1820/16/Z01/POB4/2021.

Heart rate dynamics irreversibility and information flow in type 1 LQTS patients under beta blocker treatment

Małgorzata Andrzejewska, M. Ozimek, J.J. Żebrowski, K. Rams, T. Buchner

Cardiovascular Physics, Complex Systems Physics Division, Faculty of Physics,

Warsaw University of Technology, Warszawa, Poland

Introduction

- Long QT syndrome is a genetically determined dysfunction of ion channels or the proteins that regulate them. This disease leads to serious symptoms, including fainting or losing consciousness. It can also cause sudden cardiac arrest. A prolonged QT interval can be acquired or congenital. The clinical course of the disease varies depending on which gene has been mutated. The most common types of LQTS are LQTS 1, 2 and 3. In the case of LQTS type 1, the mutation disrupts the slow potassium current. Symptoms of the disease most often occur during exercise, in contrast to, for example, LQTS2, where they are induced during increased catecholamine release.

- The basic diagnostic criterion for LQTS is the Schwartz criterion. In pharmacological treatment, beta blockers are used. In our research, we check whether they have an impact on non-linear parameters of heart rate variability, such as time irreversibility or information flow.

- Two databases from the THEW Project were used to provide the RR, QT and the DI intervals: E-HOL-03-0202-003 (202 ECG of healthy individuals) and E-HOL-03-0480-013 (480 ECGs of the Long QT Syndrome patients forming 4 subgroups by genotype).

- In this paper, we analyze two subgroups of those databases: 1. LQTS1 patients. This group consists of 63 patients (41 women). The range of age is limited to 18 – 50 years. 2. LQTS patients in general. 77 patients (47 women) aged 2 – 72 years.

- All signals were divided into non-overlapping windows of length 1200, and in all windows, we checked if the signal is mean-stationary. The numbers next to pairs of boxplots are responding p-values (U-Mann Whitney test).

Methods

Asymmetry indices

$$\Delta x = x_i - x_{i+1}$$

Porta's index P%

$$P\% = \frac{N(\Delta x^-)}{N(\Delta x \neq 0)} \cdot 100\%$$

Guzik's index G%

$$G\% = \frac{\sum_{i=1}^{N(\Delta RR^+)} \Delta x^{+2}(i)}{\sum_{i=1}^{N(\Delta RR)} \Delta x^2(i)} \cdot 100\%$$

Ehlers index E

$$E = \frac{\sum_{i=1}^{N(\Delta RR)} \Delta x^3(i)}{\left(\sum_{i=1}^{N(\Delta RR)} \Delta x^2(i)\right)^{3/2}}$$

Index D (Hou)

$$D = \sqrt{(P\% - 50)^2 + (G\% - 50)^2}$$

Transfer entropy

From target system $Y_j \Rightarrow$ time series y_n

Information generated by Y_j :

$$H_Y = -\sum p(y_n)\log(p(y_n))$$

Self entropy:

$$S_Y = \sum p(y_n|y_n^-)\, log\frac{p(y_n|y_n^-)}{p(y_n)}$$

New information:

$$N_Y = H(y_n|y_n^-)$$

$$H_Y = N_Y + S_Y$$

The effect of the past of one process on the current state of another can be assessed by transfer entropy:

$$T_{X\to Y} = \sum p(y_n, \boldsymbol{y}_n^-, \boldsymbol{x}_n^-)\, log\frac{p(y_n|\boldsymbol{x}_n^-, \boldsymbol{y}_n^-)}{p(y_n|\boldsymbol{y}_n^-)}$$

$$T_{X\to Y} = I(Y_n; X_n|\boldsymbol{X}_n^-) - H(Y_n|\boldsymbol{X}_n^-, \boldsymbol{Y}_n^-)$$

Visibility graphs

- **Visibility graphs methods** allows to study the probabilities of the appearance of certain repeating structures in the signal.
- Visibility algorithms map time series into network.
- Dynamic properties of time series may be described using graph-theoretical terms.
- These graphs are created by connecting nodes that meet a certain visibility criterion.
- For HRV analysis:
  Each bar ⟺ one RR interval.
  Each bar is the node of the graph.

Kullback-Leibler divergence (**KLD**) – the **distance between the in and out degree distributions**.

$$KLD[P_{out}(k)||P_{in}(k)] = \sum_k P_{out}(k) \cdot \ln\frac{P_{out}(k)}{P_{in}(k)}$$

Average edge overlap:

$$< o > = \frac{1}{K}\sum_{i,j} o_{ij},\ o_{ij} = \frac{1}{M}\sum_\alpha \alpha_{ij}^{[\alpha]}$$

K – total numer of pairs of nodes connected at least on one of the M nodes.

Interlayer mutual information $I_{\alpha,\beta}$:

$$I_{\alpha,\beta} = \sum_{k^{[\alpha]}}\sum_{k^{[\beta]}} P(k^{[\alpha]}, k^{[\beta]})log\frac{P(k^{[\alpha]}, k^{[\beta]})}{P(k^{[\alpha]})P(k^{[\beta]})}$$

$P(k^{[\alpha]}, k^{[\beta]})$ – joint probability of finding a node which has degree $k^{[\alpha]}$ and degree $k^{[\beta]}$ on layers α and β respectively.

Results

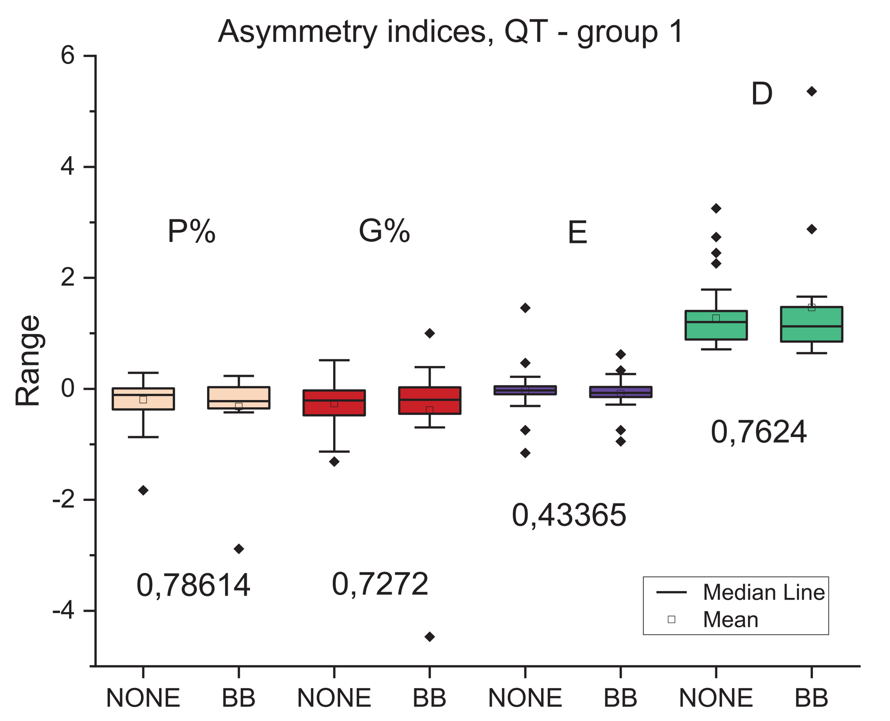

Fig. 1

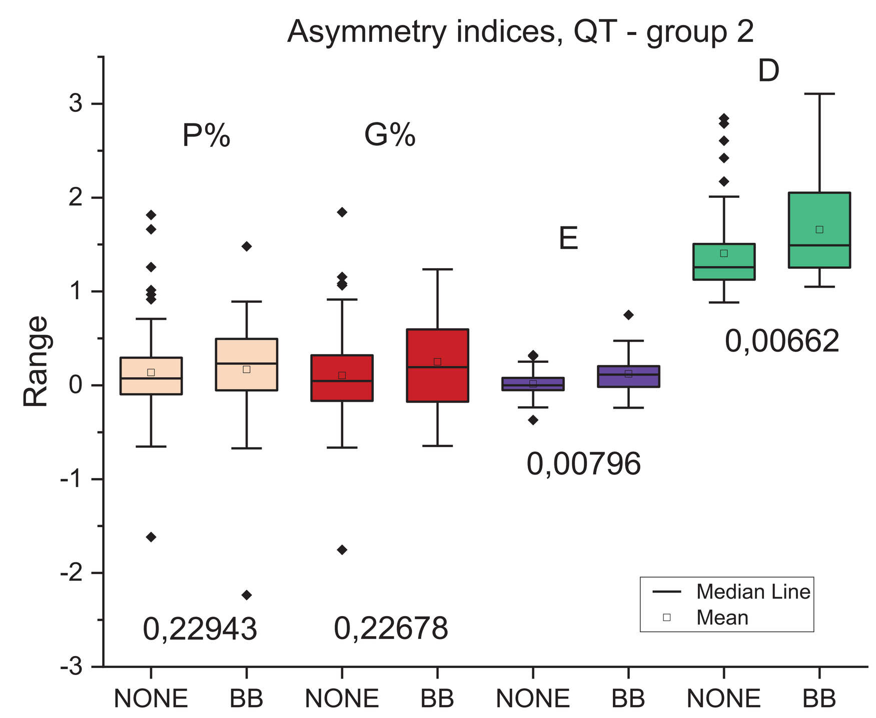

Fig. 2

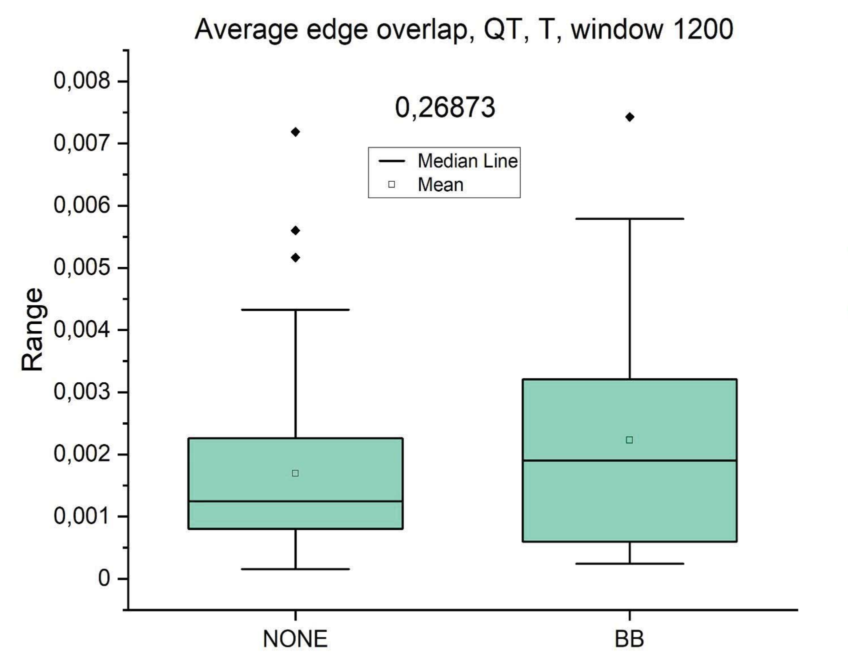

Fig. 3

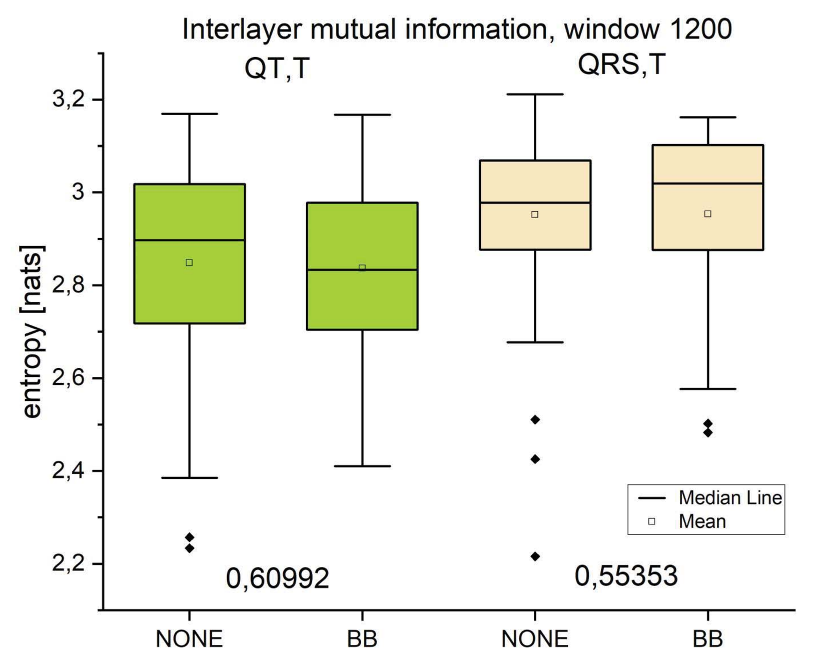

Fig. 4

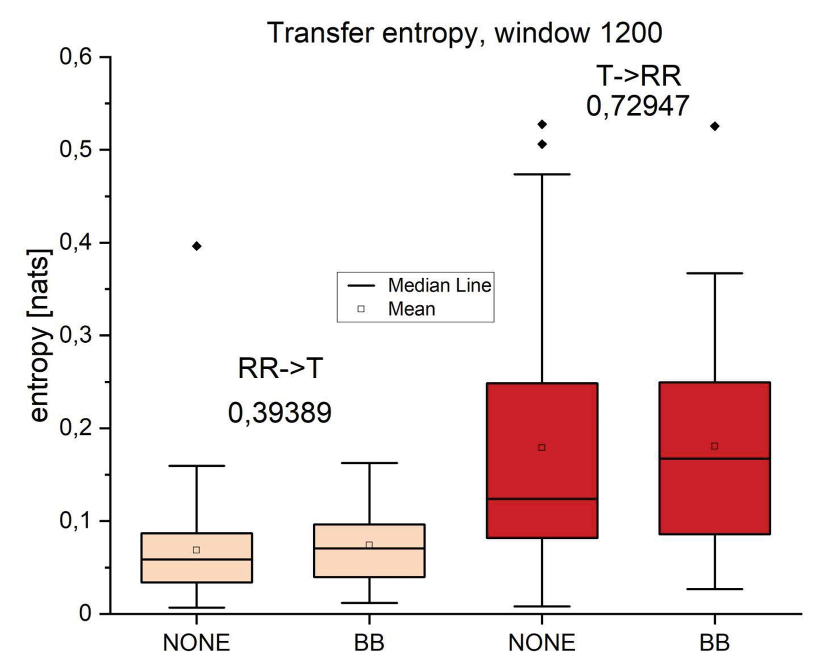

Fig. 5

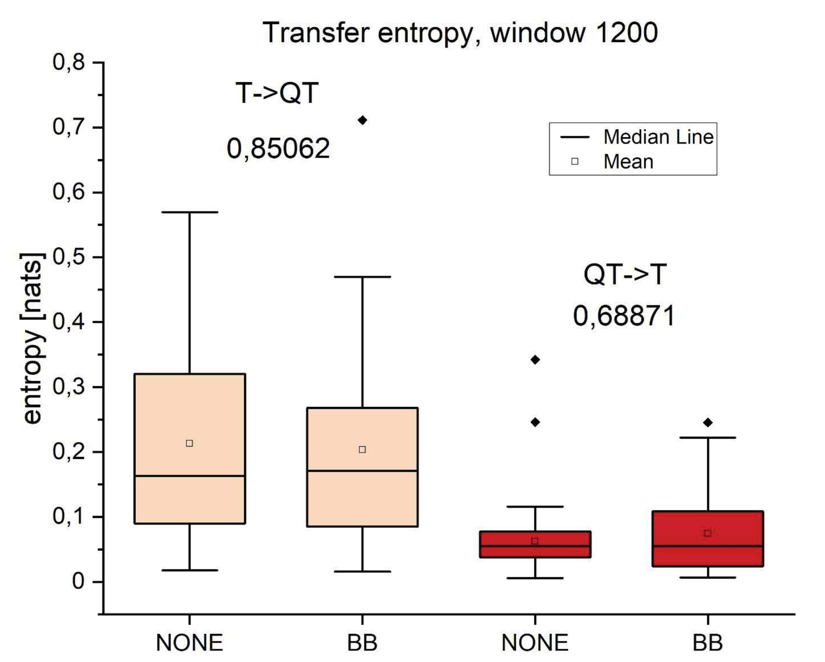

Fig. 6

Summary

- We observe no statistically significant difference between time irreversibility in LQTS1 group (Fig.1), however for broader group (Fig.2), patients taking BB are characterized by higher irreversibility (higher Ehlers and D index).

- The results for broader group (Figs 3 – 6) shows, that even if the characteristic of single variables are changed, the information flow and visibility graphs similarity is unchanged under BB treatment.

- Beta blockers therefore are not changing physiological network.

References

1. L. Lacasa, A. Nunez, E. Roldan, J.M.R. Parrondo and B. Luque, „Time series irreversibility: a visibility graph approach", Eur. Phys. J. B (2012) 85: 217
2. L. Chladekova, B. Czippelova, Z. Turianikova, I. Tonhajzerova, A. Calkovska, M. Baumert, M. Javorka: Multiscale time irreversibility of heart rate and blood pressure variability during orthostasis. *Psyhological Measurement*, 22:1747-1756, 2012
3. Lacasa, L., Nicosia, V. & Latora, V. Network structure of multivariate time series. *Sci Rep* **5**, 15508 (2015). https://doi.org/10.1038/srep15508
4. Luca Faes, Alberto Porta, Giandomenico Nollo, 'Information decomposition in bivariate systems: theory and application to cardiorespiratory dynamics', Entropy (special issue on "Entropy and Cardiac Physics") **17**, 277-303, 2015.

Wydział Fizyki
POLITECHNIKA WARSZAWSKA

Research was funded by (POB Biotechnology and Biomedical Engineering) of Warsaw University of Technology within the Excellence Initiative: Research University (IDUB) program 1820/16/Z01/POB4/2021.

XXVIII Congress of the Polish Physiological Society

Gdańsk, September 15-17 2021

Poster book

SESSION XV

MISCELLANEA

HONORARY PATRONAGE

Uniwersytet Gdański

Prof. dr Marcin Gruchała
Rector of the Medical University of Gdansk

Prof. dr Piotr Stepnowski
Rector of the University of Gdansk

WOJEWODA POMORSKI
DARIUSZ DRELICH

Dariusz Drelich
Governor of the Pomeranian Voivodeship

HONORARY PATRONAGE
Mayor of the City of Gdańsk

Aleksandra Dulkiewicz
Mayor of Gdansk

Mieczysław Struk
Marshal of the Pomeranian Voivodeship

PARTNER

PAN
POLSKA AKADEMIA NAUK

ANIMA LAB
animal facility and laboratory equipment • animal research models

FUNDACJA LOTOS

Medical University of Gdansk
Department of Physiology

The use of gaseous hydrogen in the treatment of Sars-Cov-2 virus infection

MD DSci Eng Krzysztof Piotr Michalak
Adam Mickiewicz University of Poznań, Physics Faculty, Poland
kmichalak@amu.edu.pl

Hydrogen (gaseous or saline) inhibits many of metabolic changes generated by Sars-Cov-2 virus in the cell. It is a possible therapeutic agent in the treatment of Severe Acute Resepiratory Syngrome. The seventh edition of Chinese Clinical Guidance for COVID-19 Pneumonia Diagnosis and Treatment issued by China National Health Commission recommended the inhalation of oxygen mixed with hydrogen gas (33.3% O2 and 66.6% H2), bringing H_2 to the forefront of contemporary therapeutic medical gas research. Graphs below present the POSSIBLE points of the positive effects of interaction of H_2 with ARDS cell metabolism reprogramming.

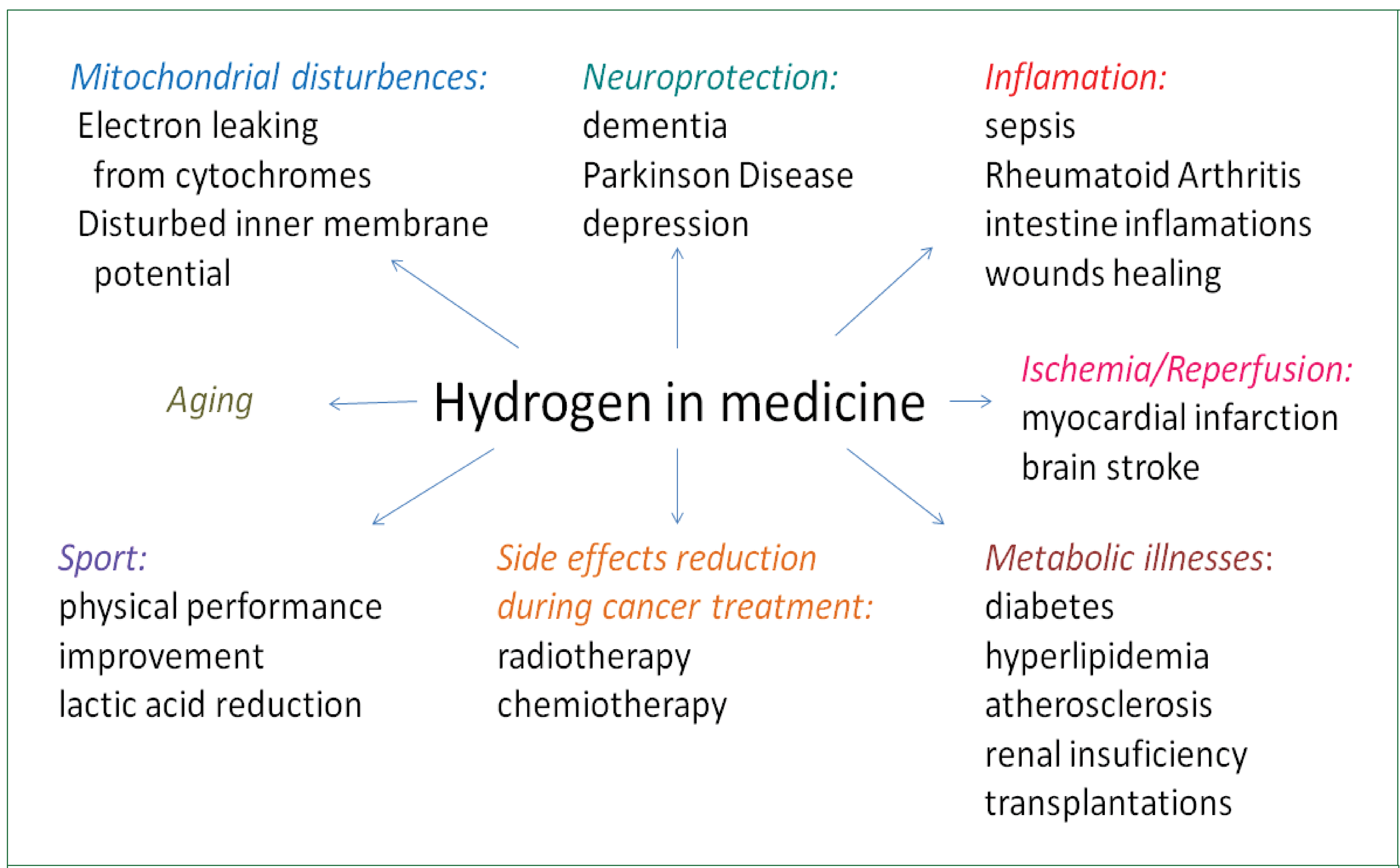

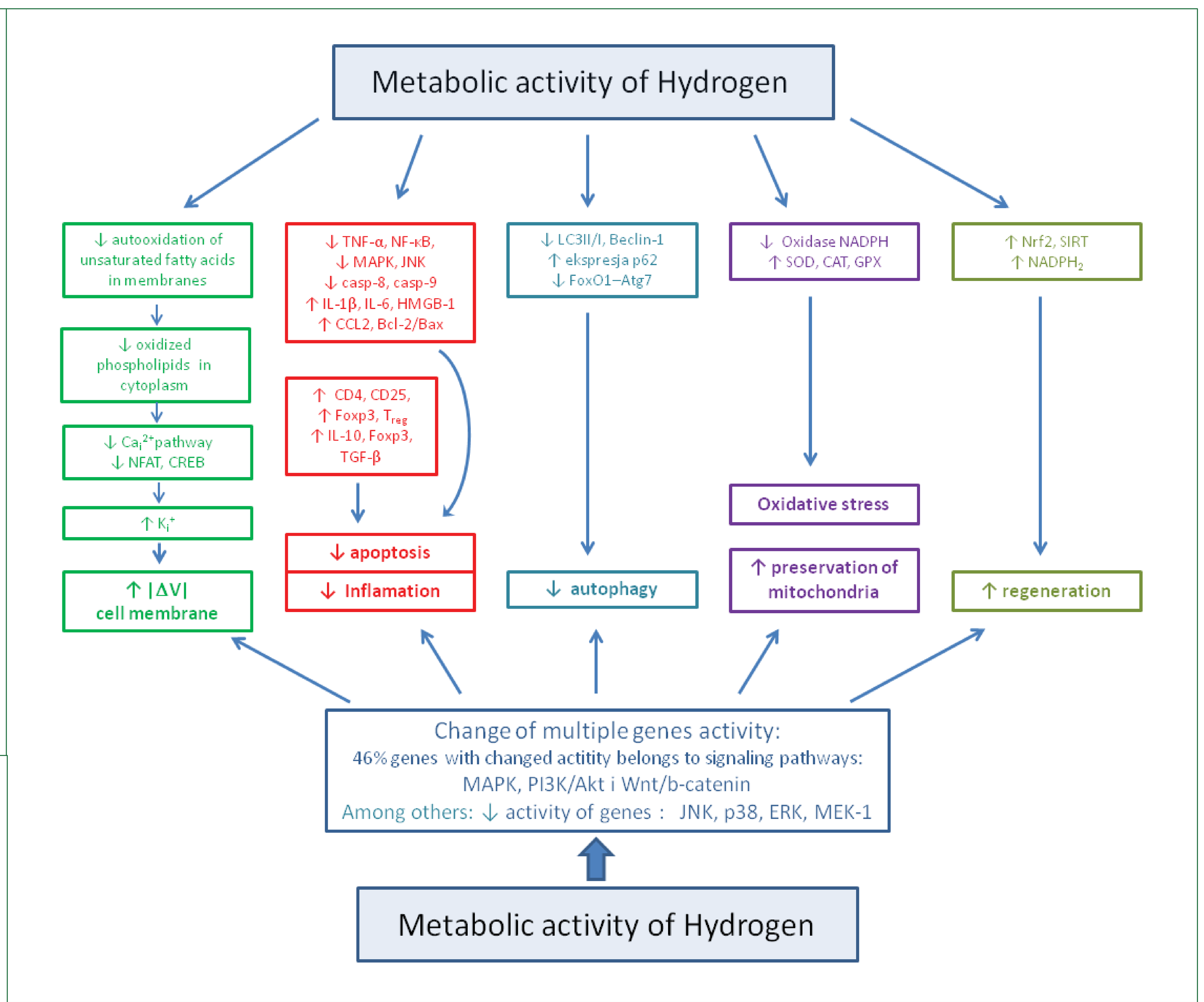

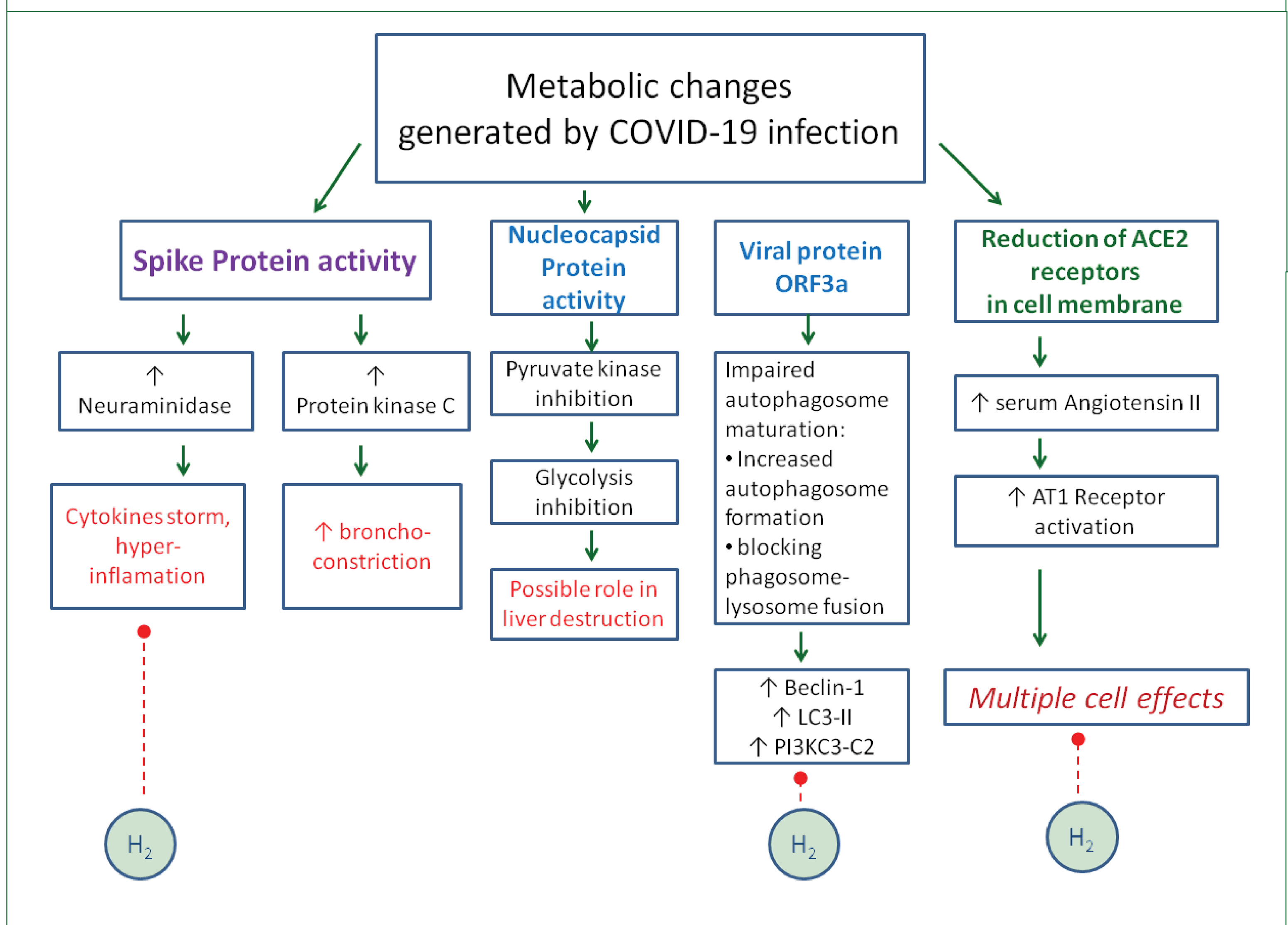

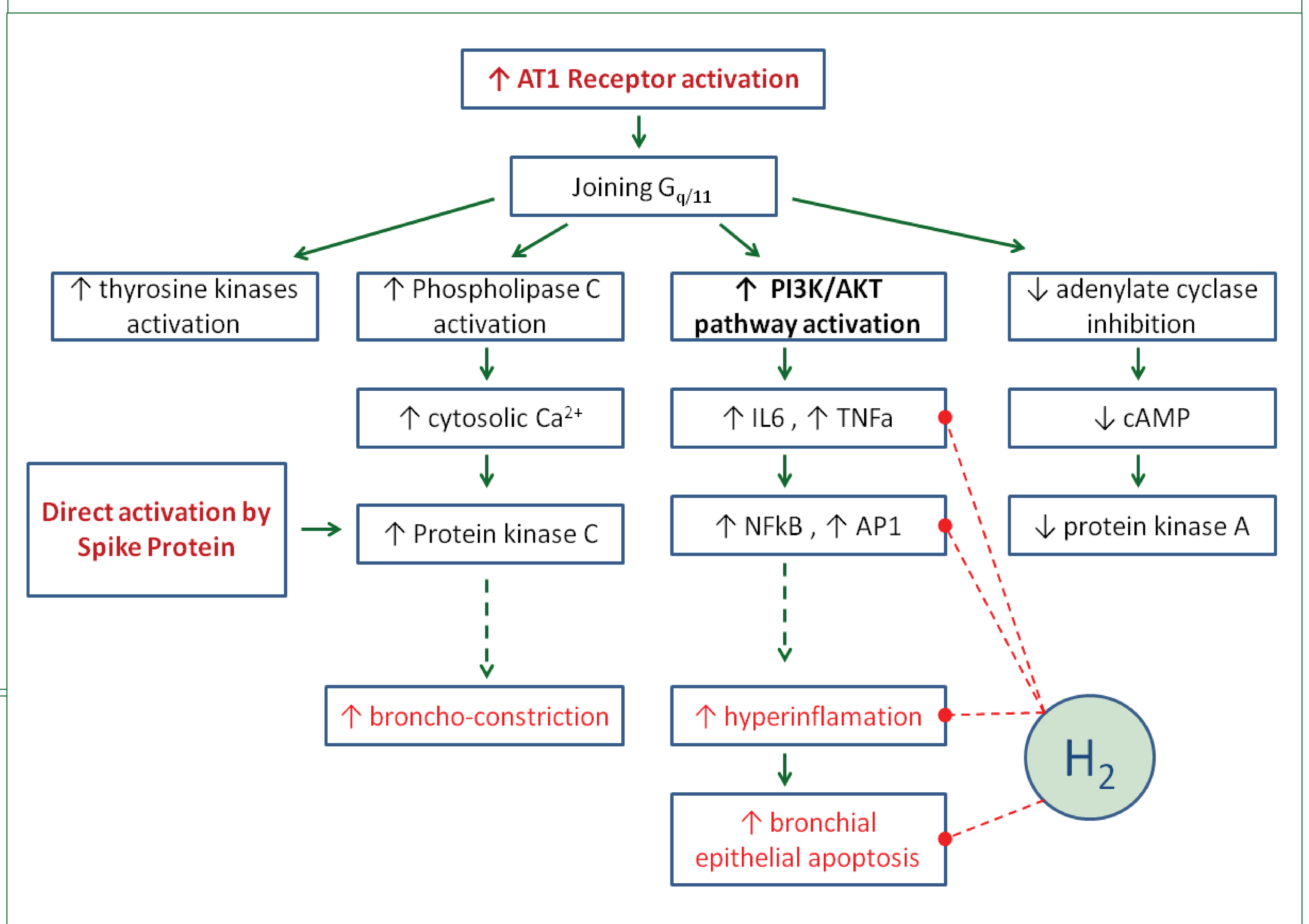

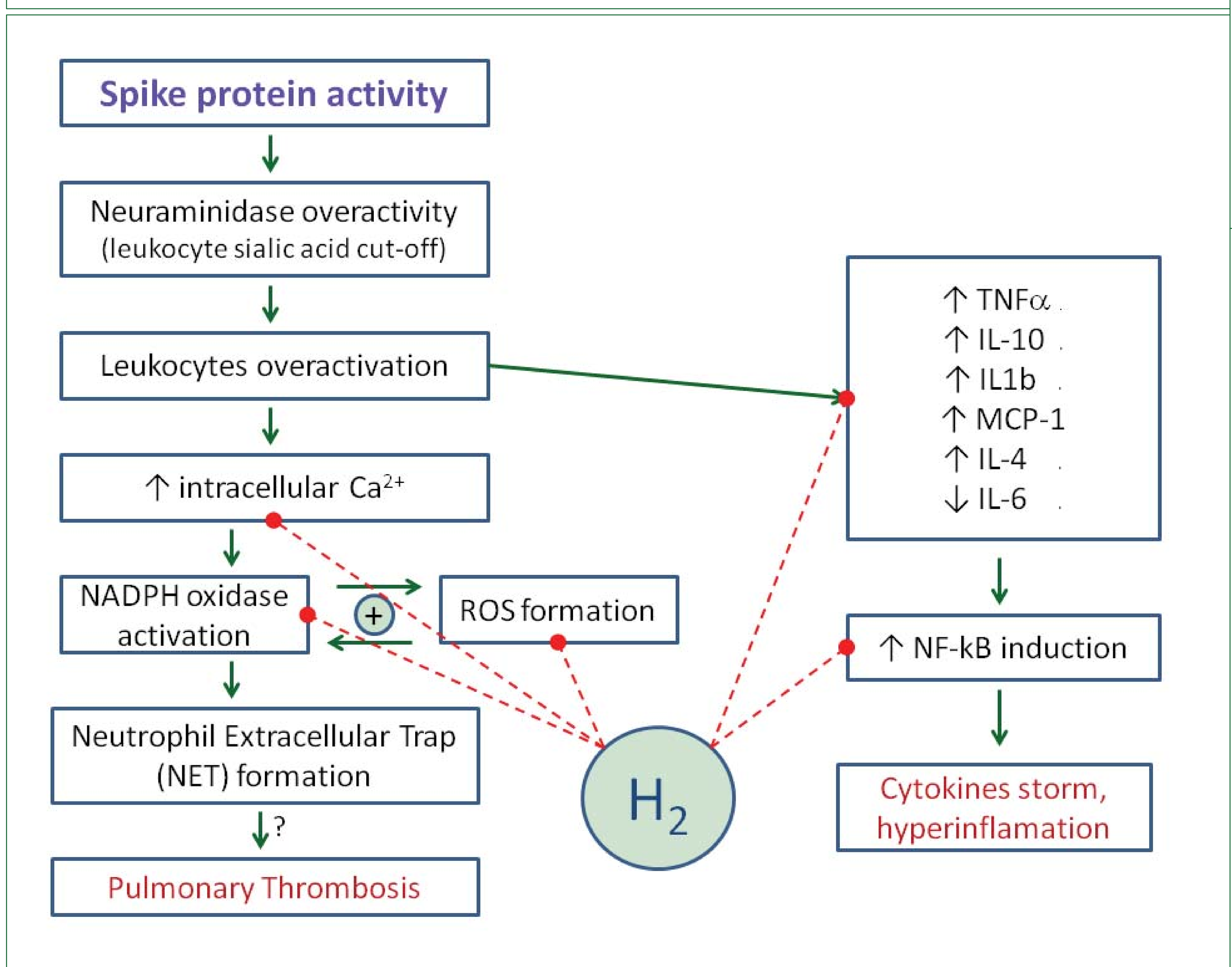

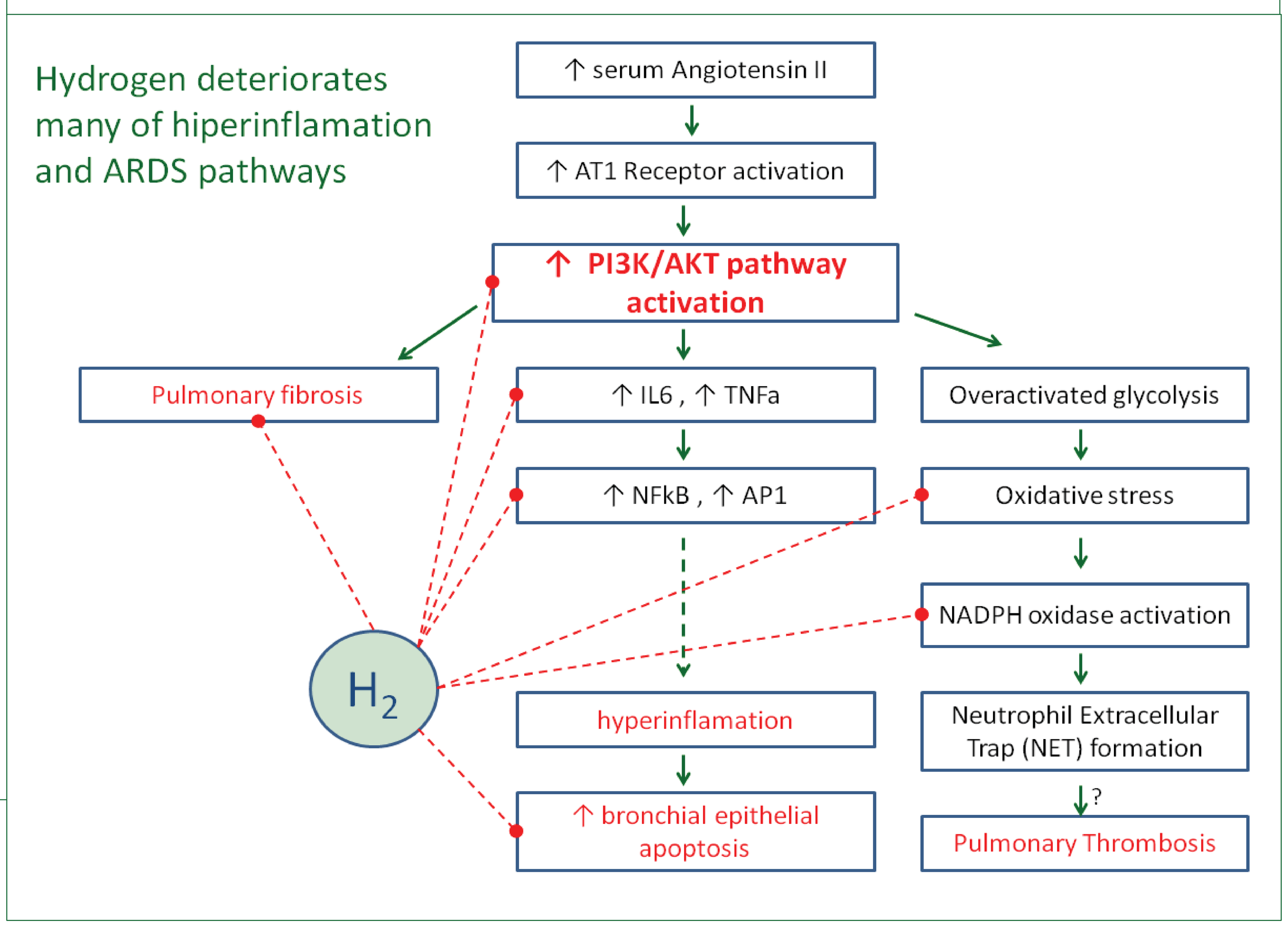

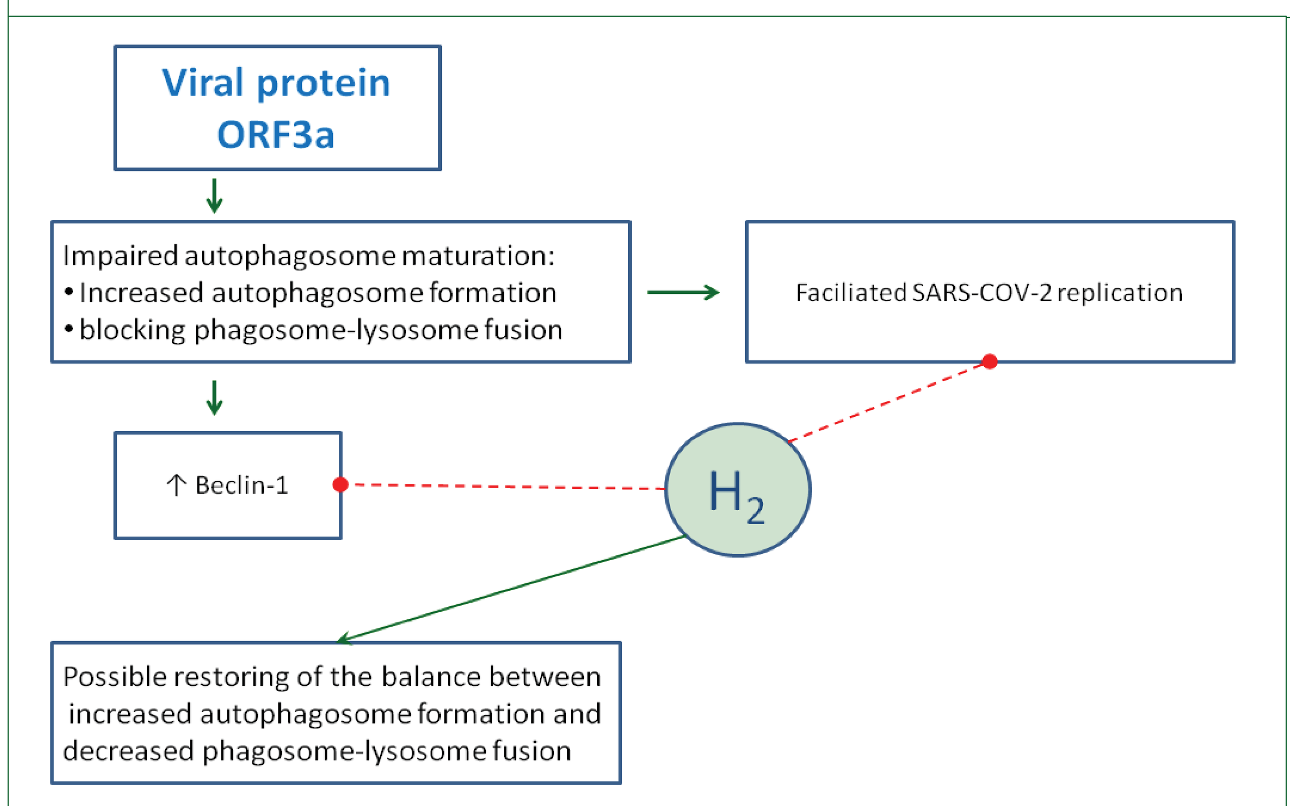

1.Formiga, R.O., et al., bioRxiv, 2021.
2.Zhang, X.W. and Y.L. Yap,. Theochem, 2004. **681**(1): p. 137-141.
3.Ostojic, S.M., Ther Adv Respir Dis, 2020. **14**: p. 1753466620951051.
4.Khezri, M.R., Hum Cell, 2021. **34**(2): p. 700-701.
5.Wei, W.Y., et al., Arch Virol, 2012. **157**(4): p. 635-45.
6.Liu, M., et al.,. FASEB J, 2007. **21**(7): p. 1586-96.
7.Jude, J.A., et al., Proc. Amer. Thor. Soc., 2008. **5**(1): p. 15-22.
8.Higuchi, S., et al., Clinical Science, 2007. **112**(8): p. 417-428.
9.Zhang, Z., et al., Brain Res Bull, 2021. **172**: p. 1-13.
10.Qu, Y., et al., Front Cell Dev Biol, 2021. **9**: p. 716208.
11.Okuyan, H.M., et al., Life Sci, 2021. **278**: p. 119596.
12.Fakhri, S., et al., Molecules, 2021. **26**(10).
13.Domdom, M.A., et al., Autophagy, 2020. **16**(12): p. 2276-2281.
14.Guo, X., Y. Zhu, and Y. Hong, Hypertension, 2020. **76**(2).
15.Zhuang, X., et al., Int Immunopharmacol, 2020. **81**: p. 106287.
16.Xun, Z.M., et al., Ann Agric Environ Med, 2020. **27**(3): p. 368-373.
17.Wang, S.T., et al., QJM, 2020..
18.Tamura, T., et al., J Clin Biochem Nutr, 2020. **67**(2): p. 214-221.
19.Tamura, T., et al., Shock, 2020. **54**(3): p. 377-385.
20.Slezak, J., et al., Curr Pharm Des, 2020.
21.Qi, B., et al., Curr Pharm Des, 2020.
22.Ohta, S., Curr Pharm Des, 2020.
23.Lu, H., et al., FASEB J, 2020. **34**(3): p. 4134-4146.
24.Ishihara, G., et al., Biochem Biophys Res Commun, 2020. **522**(4): p. 965-970.
25.Gvozdjakova, A., et al., Can J Physiol Pharmacol, 2020. **98**(1): p. 29-34.
26.Guan, W.J., et al., J Thorac Dis, 2020. **12**(6): p. 3448-3452.
27.Benoit, S.L., et al., Microbiol Mol Biol Rev, 2020. **84**(1).
28.Yan, M., et al., Int Immunopharmacol, 2019. **71**: p. 61-67.
29.Qiu, P., Y. Liu, and J. Zhang, Int J Biol Sci, 2019. **15**(6): p. 1261-1275.
30.Moon, D.H., et al., J Thorac Dis, 2019. **11**(4): p. 1519-1527.
31.LeBaron, T.W., et al., Molecules, 2019. **24**(11).
32.Iuchi, K., et al., Can J Physiol Pharmacol, 2019. **97**(10): p. 999-1005.
33.Cejka, C., S. et al.. Free Radic Res, 2019. **53**(3): p. 237-247.
34.Lu, W., et al., J Thorac Dis, 2018. **10**(6): p. 3232-3243.

The role of neurotensin and endomorphin pathways in the anti-inflammatory action of PK20 hybrid in mouse model of non-atopic asthma

E. Russjan[1], D. Zając[1], D. Sulejczak[2], P. Kleczkowska[3,4], K. Kaczyńska[1]

[1]Department of Respiration Physiology, Mossakowski Medical Research Institute, Polish Academy of Sciences, Warsaw, Poland
[2]Department of Experimental Pharmacology, Mossakowski Medical Research Institute, Polish Academy of Sciences, Warsaw, Poland
[3]Department of Pharmacodynamics, Centre for Preclinical Research, Medical University of Warsaw, Warsaw, Poland
[4]Military Institute of Hygiene and Epidemiology, Warsaw, Poland

category: **MISCELLANEOUS**

INTRODUCTION AND OBJECTIVES: Hybrid compounds, also referred to as chimeras or multifunctional drugs, are molecules which comprise at least two different structural elements. PK20 hybrid peptide, the subject of the present experiments, contains in its structure modified endomorphin-2 and neurotensin-like pharmacophores. Numerous reports have confirmed anti-inflammatory activity of endomorphin 2 **[1,2,3]**. In the case of neurotensin, the literature data are not conclusive, however, a part of them indicates beneficial effect of neurotensin in the course of inflammation **[4,5,6]**. In our previous studies, we have proven the anti-inflammatory activity of PK20 hybrid in a murine model of nonallergic asthma, through alleviating the influx of inflammatory cells into BALF, decreasing the activity of secretory phospholipase A_2 and the production of proinflammatory cytokines, mouse mast cell protease, malondialdehyde in lung tissue homogenates, as well as partially reducing airway hyperresponsiveness to metacholine nebulization **[7]**. However, the precise mechanism of PK20 action remains not clear. For this reason, in the present study, we have attempted to assess the contribution of opioid and neurotensin pharmacophores in the beneficial effects of the tested hybrid by using antagonistic compounds of particular receptors (opioid receptor antagonist naloxone hydrochloride and neurotensin receptor 1 (NTS1) antagonist SR 142948).

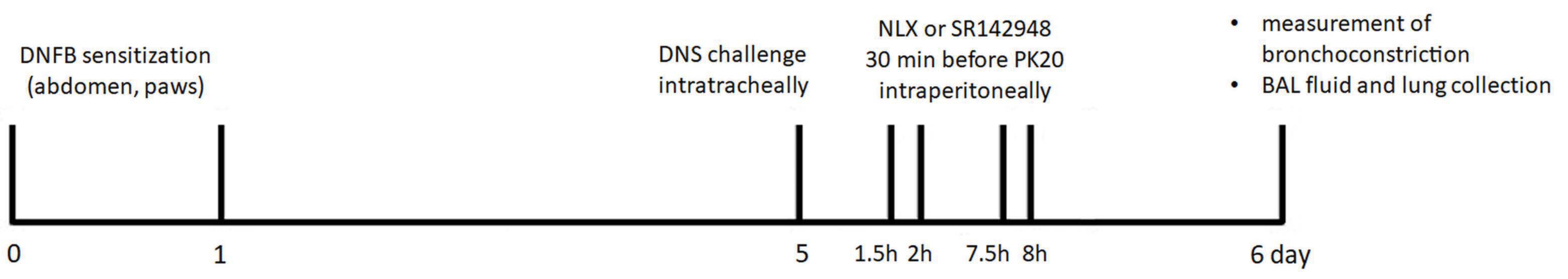

Fig. 1. Graphical scheme of the experimental asthma model

METHODS: Non-atopic asthma was induced in Balb/c mice on day 0 by skin sensitization with 0,5% dinitrofluorobenzene/vehicle (DNFB; dissolved in acetone:olive oil, 4:1) to shaved thorax skin (50 µl) and four paws (50 µl/paws). On day 1, DNFB/vehicle was applied only to the thorax (50 µl). On day 5, mice were challenged intratracheally with 50 µl of 0,6% dinitrobenzene sulfonic acid (DNS; water soluble cognate hapten of DNFB). The sensitization and challenge procedures were performed under anaesthesia induced by intramuscular injection of ketamine (70 mg/kg) and xylazine (10 mg/kg). 2 and 8 hours after induction of inflammation, PK20 hybrid, naloxone hydrochloride + PK20 hybrid, or SR 142948 + PK20 hybrid were administered intraperitoneally (antagonists were administrated thirty minutes before PK20 injection). After 24 hours, the airway responsiveness to increasing doses of methacholine was measured using whole-body plethysmograph. Afterward, mice were killed by intraperitoneal administration of pentobarbital sodium (150–200 mg/kg) and bronchoalveolar lavage fluid (BALF) and lung tissue were collected for further analyses (**Fig. 1**). In the study designed five experimental groups (according to the pattern: sensitization/challenge + treatment):

- CONTROL → vehicle/DNS + NaCl (physiological saline),
- DNFB/DNS → DNFB/DNS + NaCl,
- PK20 → DNFB/DNS + PK20,
- NLX+PK20 → DNFB/DNS + naloxone hydrochloride and PK20,
- SR 142948 + PK20 → DNFB/DNS + SR 142948 and PK20.

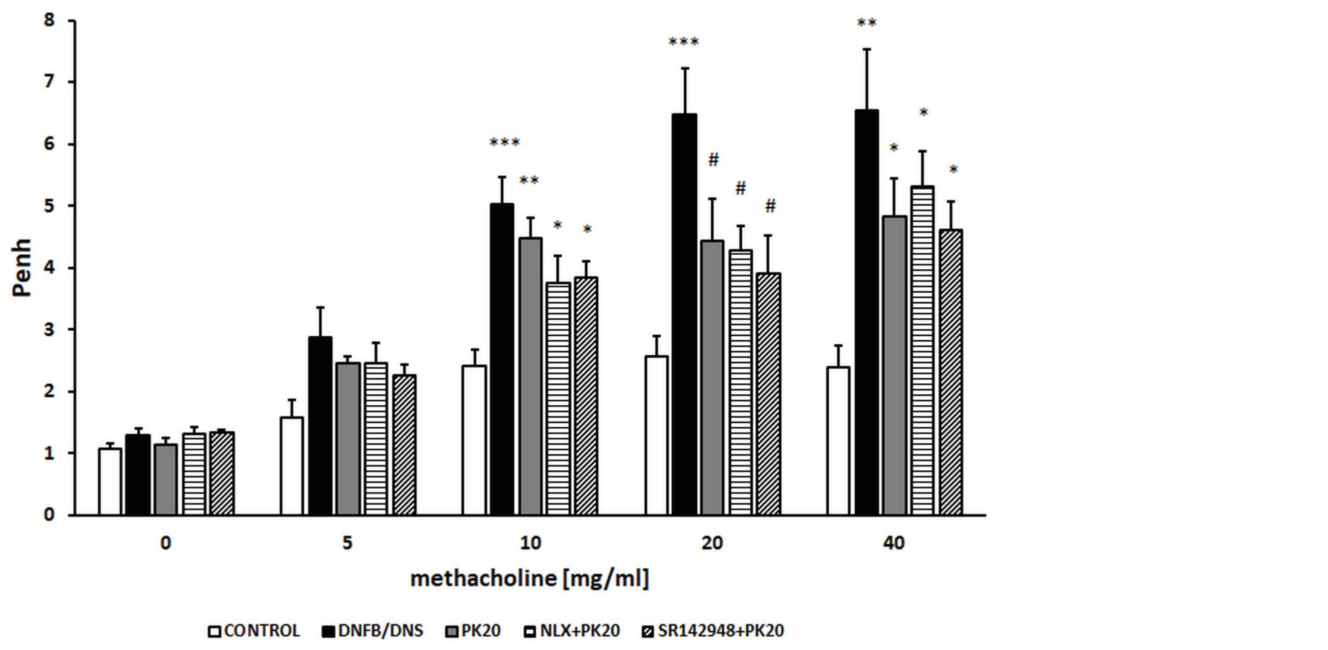

Fig. 2. Airway hyperresponsiveness showed as pause enhanced (Penh) in response to increasing doses of methacholine nabulization, 24 h after intratracheal DNS challenge. Effect of PK20 pretreatment with naloxone hydrochloride or SR 142948 compared to the group treated with the hybrid alone. N = 6–8 mice per group. The results are means ± SEM. * p < 0.05, ** p < 0.01, *** p < 0.001 vs. the control group, # p < 0.05 vs. the DNFB/DNS group.

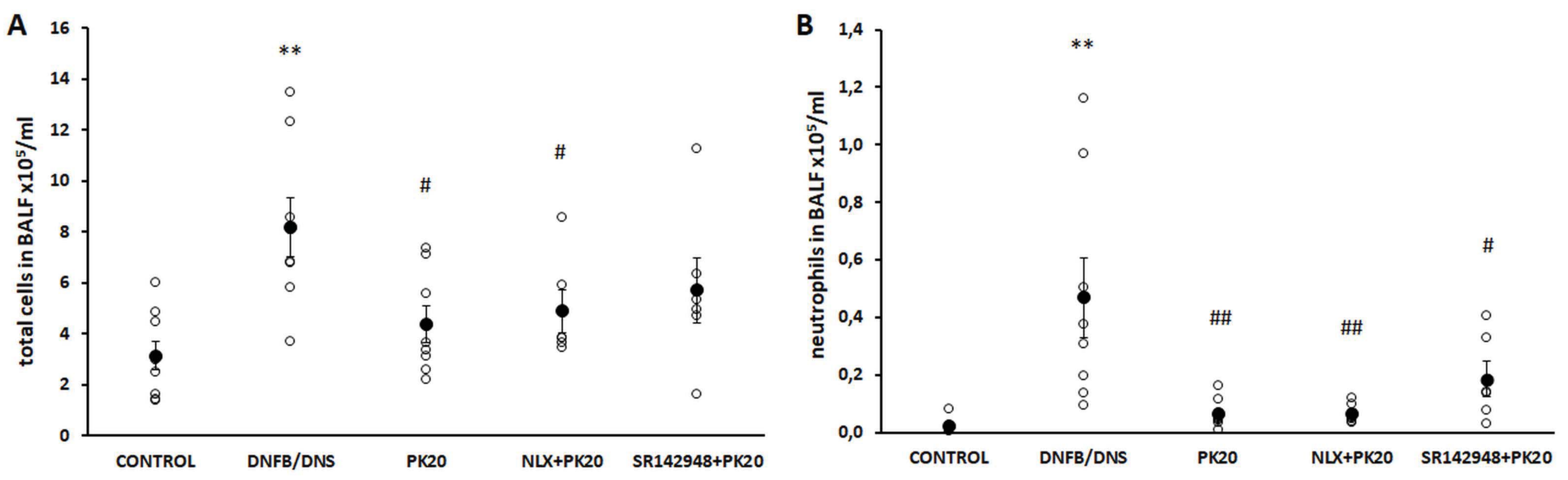

Fig. 3. Total number of inflammatory cells (A), including neutrophils (B) in BALF 24 h after intratracheal DNS challenge. Effect of PK20 pretreatment with naloxone hydrochloride or SR 142948 compared to the group treated with the PK20 hybrid solely. N = 6–9 mice per group. The results are means ± SEM. ** p < 0.01 vs. the control group, # p < 0.05, ## p < 0.01 vs. the DNFB/DNS group.

RESULTS: Intraperitoneal injection of naloxone hydrochloride or SR 142948 did not have an influence on the PK20 potential in reducing airway hyperresponsiveness, expressed as enhanced pause (Penh). There were no significant differences between the group of animals treated with the PK20 hybrid and mice pretreated with antagonistic compounds, using any of the methacholine doses. Only at the dose of 20 mg/mL, in all three tested groups, a statistically significant decrease in airway hyperresponsiveness compared to the DNFB/DNS animals was observed (**Fig. 2**). Administration of naloxone hydrochloride before PK20 injection did not adversely affect the inhibitory activity of PK20 on total inflammatory cell influx. However, pretreatment with a neurotensin receptor antagonist has weakened hybrid's action (**Fig. 3A**). In the case of neutrophils, their number was about 2.5 times higher in SR 142948 group, compared to the animals receiving the PK20 hybrid alone or pretreated with an opioid antagonist (**Fig. 3B**).

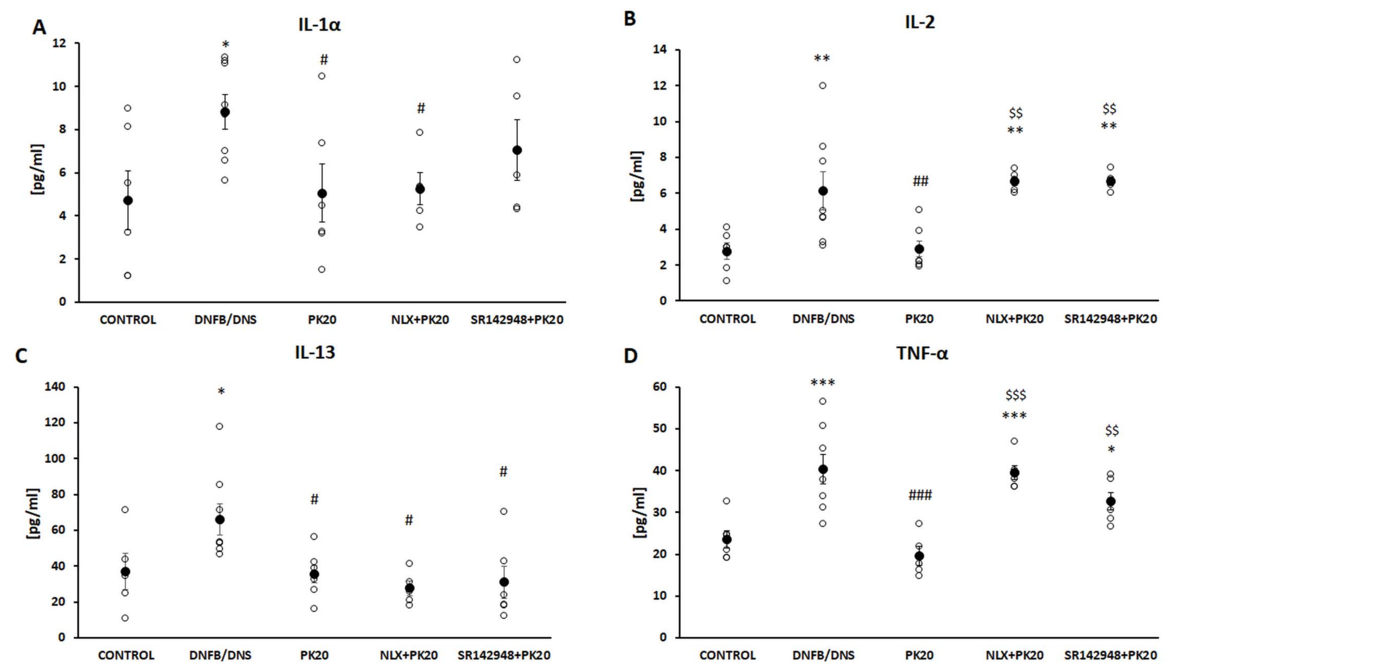

Fig. 4. Levels of proinflammatory cytokines: IL-1α (A), IL-2 (B), IL-13 (C), and TNF-α (D) in BALF 24 h after intratracheal DNS challenge. Effect of hybrid pretreatment with naloxone hydrochloride or SR 142948 compared to the group treated with the PK20 hybrid solely. N = 5–8 mice per group. The results are means ± SEM. * p < 0.05, ** p < 0.01, *** p < 0.001 vs. the control group, # p < 0.05, ## p < 0.01, ### p < 0.001 vs. the DNFB/DNS group. $$ p < 0.01, $$$ p < 0.001 vs. the PK20 hybrid group.

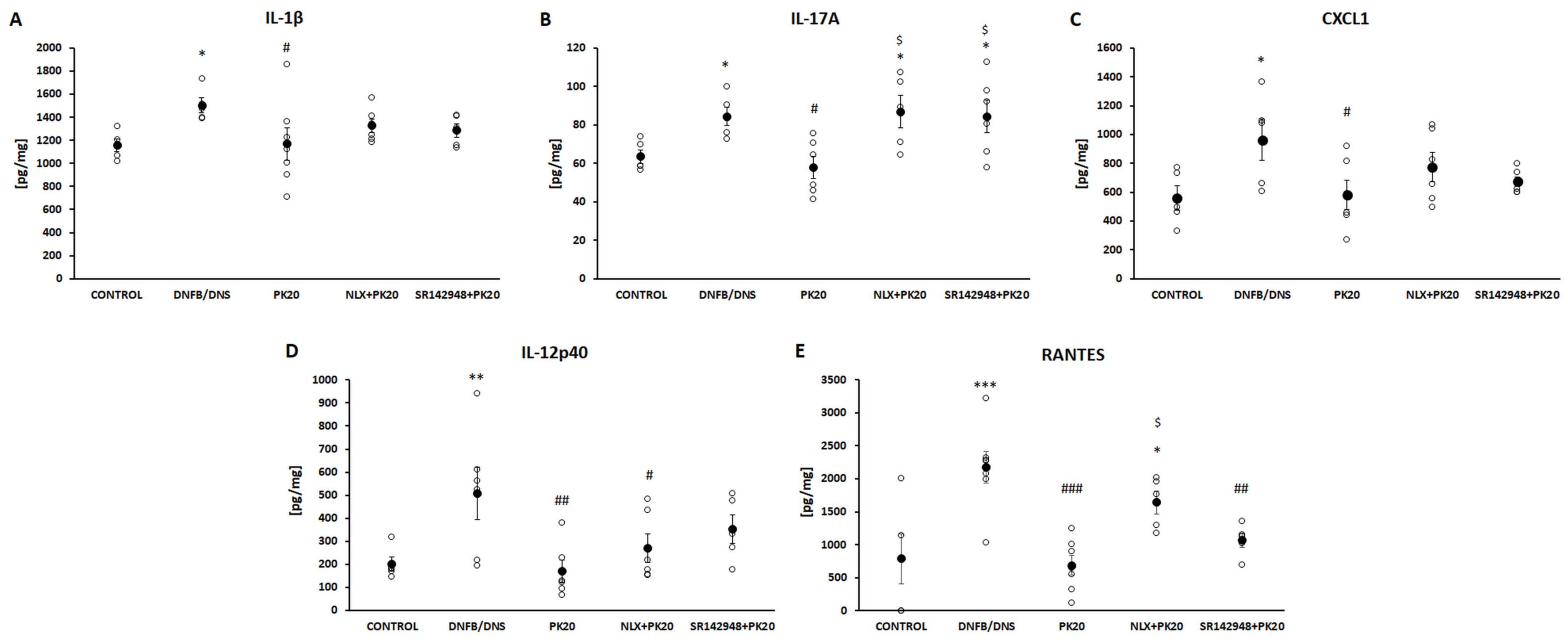

Fig. 5. Levels of pro-inflammatory cytokines: IL-1β (A), IL-17A (B), CXCL1 (C), IL-12p40 (D), and RANTES (E) in the lung, 24 h after intratracheal DNS challenge. Effect of hybrid pretreatment with naloxone hydrochloride or SR 142948 compared to the group treated with the PK20 hybrid solely. N = 5–7 mice per group. The results are means ± SEM. * p < 0.05, ** p < 0.01, *** p < 0.001 vs. the control group, # p < 0.05, ## p < 0.01, ### p < 0.001 vs. the DNFB/DNS group. $ p < 0.05 vs. the PK20 hybrid group.

Blockade of opioid or neurotensin receptors had a different effects on its anti-inflammatory activity in BALF cytokine studies (**Fig. 4**). In comparison to mice treated with PK20 alone, the level of IL-1α was higher in animals pretreated with SR 142948, but not in the group that received naloxone hydrochloride. The concentration of IL-13, in turn, was significantly lower in all three tested groups compared to the DNFB/DNS animals. For IL-2 and TNF-α, inhibition of both opioid and neurotensin receptor pathways blocked the anti-inflammatory effects of the hybrid. Analysis of proinflammatory cytokines in the lungs also did not lead to clear conclusions (**Fig. 5**). In the case of IL-17A, pretreatment with both SR 142948 or naloxone hydrochloride limited the activity of the PK20 hybrid. However, an inverse correlation was observed for the IL-1β and CXCL1. There were no significant differences between the antagonistic groups and PK20 group, irrespective of which receptor was blocked. In the IL-12p40 analysis, a significant decrease in the PK20 activity was due to the inhibition of NTS1 neurotensin receptors, while in the case of RANTES it was mainly the result of blockade of the opioid pathway. Pretreatment with naloxone hydrochloride or SR 142948 exhibited an adverse effect on the PK20 activity in the analysis of mouse mast cell protease (MCPT 1) concentration in lung tissue. This effect was especially noticeable for the opioid pathway inhibition (**Fig. 6A**). On the other hand, in the case of malondialdehyde (MDA), both opioid and neurotensin receptor antagonists did not have influence on the anti-inflammatory potential of the hybrid (**Fig. 6B**). For secretory phospholipase A_2 ($sPLA_2$) analysis, administration of SR 142948 eliminated the inhibitory action of PK20 on this enzyme, which may suggest a predominant role of neurotensin receptors in the observed effect (**Fig. 6C**).

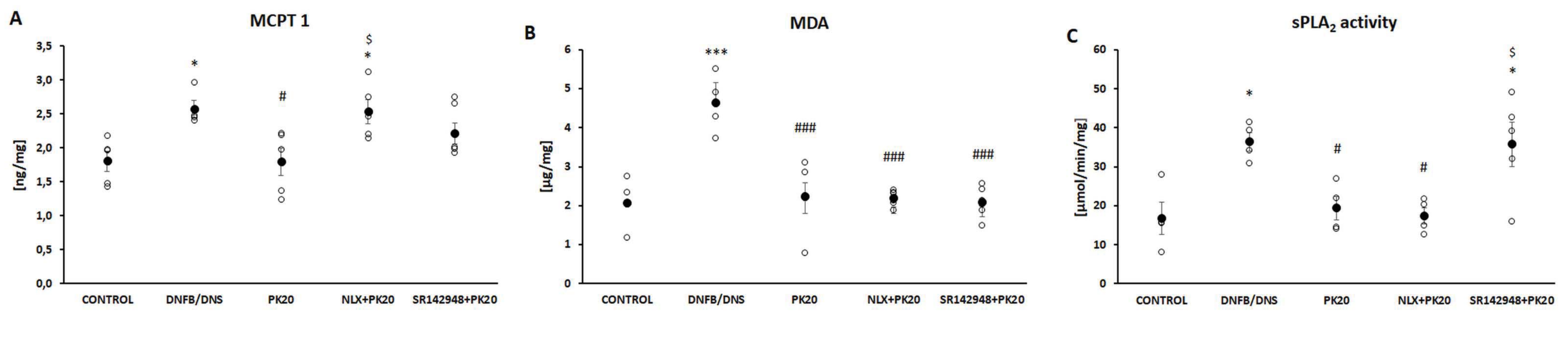

Fig. 6. Concentrations of (A) mouse mast cell protease (MCPT 1), (B) malondialdehyde (MDA), and (C) secretory phospholipase A_2 ($sPLA_2$) activity in the lung 24 h after intratracheal DNS challenge. Effect of hybrid pretreatment with naloxone hydrochloride or SR 142948 compared to the group treated with the PK20 hybrid solely. N = 4–6 mice per group. The results are means ± SEM. * p < 0.05, *** p < 0.001 vs. the control group, # p < 0.05, ### p < 0.001 vs. the DNFB/DNS group. $ p < 0.05 vs. the PK20 hybrid group.

CONCLUSIONS: Our study demonstrated that both endomorphin- and neurotensin-like parts of PK20 hybrid contribute to its biological effects. Furthermore, the full anti-inflammatory activity of PK20 requires simultaneous stimulation of both receptor pathways.

The authors have no conflicts of interests in relation to the present study.
The study was supported by a grant from National Science Centre, Poland, no. 014/13/B/NZ7/02247.

REFERENCES

[1] Jessop D.S. Endomorphins as agents for the treatment of chronic inflammatory disease. BioDrugs. 2006; 20(3):161-6.
[2] Straub R.H., Wolff C., Fassold A., Hofbauer R., Chover-Gonzalez A., Richards L.J., Jessop D.S. Antiinflammatory role of endomorphins in osteoarthritis, rheumatoid arthritis, and adjuvant-induced polyarthritis. Arthritis Rheum. 2008; 58(2):456-66.
[3] Anselmi L., Huynh J., Duraffourd C., Jaramillo I., Vegezzi G., Saccani F., Boschetti E., Brecha N.C., De Giorgio R., Sternini C. Activation of µ opioid receptors modulates inflammation in acute experimental colitis. Neurogastroenterol. Motil. 2015; 27(4):509-23.
[4] Piliponsky A.M., Chen C.C., Nishimura T., Metz M., Rios E.J., Dobner P.R., Wada E., Wada K., Zacharias S., Mohanasundaram U.M., Faix J.D., Abrink M., Pejler G., Pearl R.G., Tsai M., Galli S.J. Neurotensin increases mortality and mast cells reduce neurotensin levels in a mouse model of sepsis. Nat. Med. 2008; 14(4):392-8.
[5] Akcan A., Muhtaroglu S., Akgun H., Akyildiz H., Kucuk C., Sozuer E., Yurci A., Yilmaz N. Ameliorative effects of bombesin and neurotensin on trinitrobenzene sulphonic acid-induced colitis, oxidative damage and apoptosis in rats. World J. Gastroenterol. 2008; 14(8):1222-30.
[6] Moura L.I., Dias A.M., Suesca E., Casadiegos S., Leal E.C., Fontanilla M.R., Carvalho L., de Sousa H.C., Carvalho E. Neurotensin-loaded collagen dressings reduce inflammation and improve wound healing in diabetic mice. Biochim. Biophys. Acta. 2014; 1842(1):32-43.
[7] Russjan E., Andrzejewski K., Sulejczak D., Kleczkowska P., Kaczyńska K. Endomorphin-2- And Neurotensin- Based Chimeric Peptide Attenuates Airway Inflammation in Mouse Model of Nonallergic Asthma. Int. J. Mol. Sci. 2019; 20(23): 5935.

ANALYSIS OF ANTIOXIDANT ENZYMES IN PATIENTS WITH NEUROENDOCRINE NEOPLASMS OF THE LUNG, GASTROINTESTINAL TRACT AND PANCREAS

mgr Marlena Budek[1], mgr Jarosław Nuszkiewicz[1], dr hab. n. med. Karolina Szewczyk-Golec, prof. UMK[1]
[1] Department of Medical Biology and Biochemistry
Ludwik Rydygier Collegium Medicum in Bydgoszcz
Nicolaus Copernicus University in Toruń, Poland

Introduction and objectives

- Oxidative stress is an imbalance between the production and accumulation of reactive oxygen species (ROS) in cells and tissues, and the ability of the biological system to act as antioxidants [1]. Both in physiological and pathological states, the main source of ROS in a cell is mitochondria [2]. ROS production is elevated in cancer cells as a result of increased metabolic rate, gene mutations and relative hypoxia. Excess ROS is quenched by increasing the enzymatic and non-enzymatic antioxidant pathways. The increase in ROS contributes to several pathological conditions, including the promotion and progression of cancer, as they participate in various signaling pathways and induce mutations and DNA damage [3]. Cells use an antioxidant defense system primarily based on enzymatice components such as superoxide dismutases (SODs), catalase (CAT), and glutathione peroxidases (GPxs) to protect against ROS-induced cell damage [4]. One of the markers of oxidative stress is malonyldialdehyde (MDA), a marker of lipid peroxidation that results from the reaction of ROS with unsaturated fatty acids. It has a cytotoxic, mutagenic and carcinogenic effect. The increase in MDA is observed in cardiovascular, neurodegenerative, neoplastic and metabolic diseases [5]. However, there is no evidence that oxidative stress influences the initiation of neuroendocrine tumor (NET) formation. Therefore, research on oxidative stress in NET patients seems to be of great value.
- The aim of the study was to analyze the activity of antioxidant enzymes, namely –SOD type 1 (SOD1), CAT and cytosolic GPx (cGPx), and the concentration of MDA in the blood of patients with NEN of the lung, gastrointestinal tract and pancreas.

Methods

- The study included a group of 40 patients of the Prof. F. Łukaszczyk Oncology Center in Bydgoszcz diagnosed with pancreatic, gastrointestinal and lung NEN. The SOD1, CAT, and cGPx activities were measured in the erythrocytes, whereas the MDA concentration was assessed in both the erythrocytes and blood plasma. The spectrophotometric and kinetic methods were used to determine the measured parameters.

Results

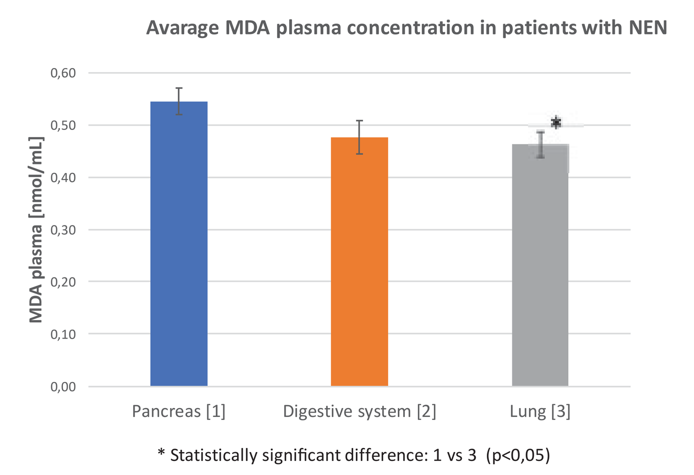

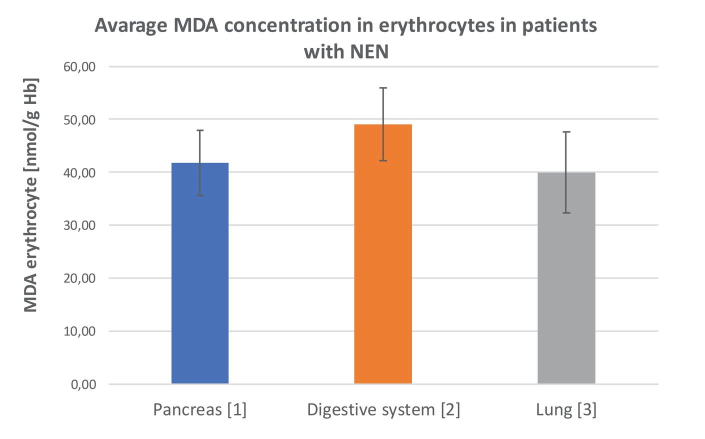

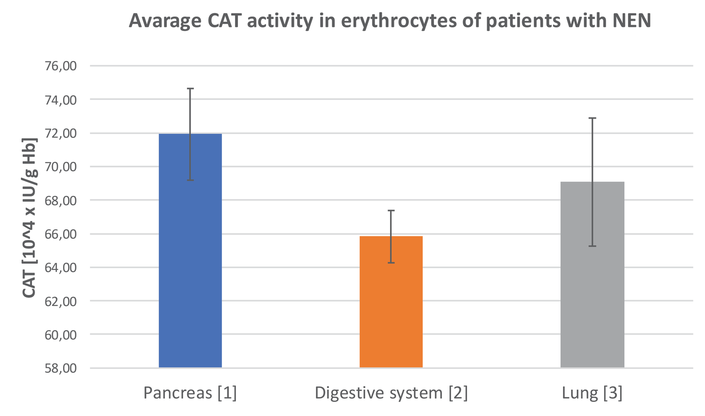

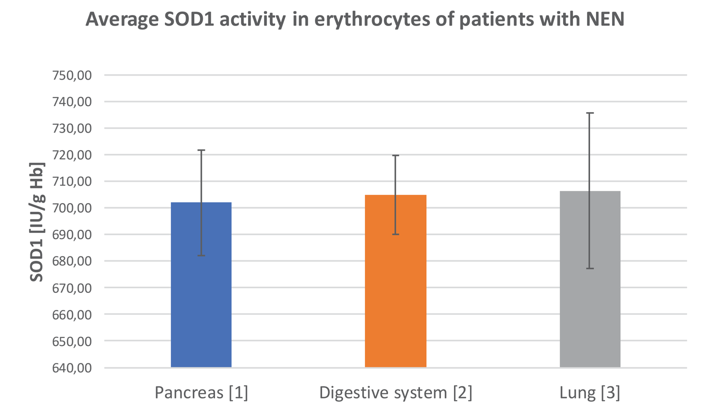

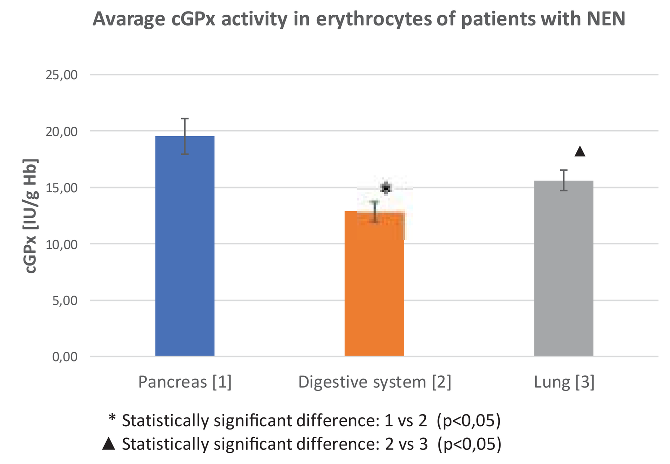

The activity of antioxidant enzymes (CAT, SOD1, cGPx) and the concentration of MDA in NENs of the pancreas, digestive system and lungs. The results are shown as average value and and standard error of measurement

Localization of NENs	Pancreas [1] n=15		Digestive system [2] n=15		Lung [3] n=10		p - value		
	Average value	SEM	Average value	SEM	Averag e value	SEM	1 vs 2	1 vs 3	2 vs 3
MDA plasma [nmol/mL]	0,55	0,02	0,48	0,03	0,46	0,02	-	$p<0,05$	-
MDA erythrocyte [nmol/g Hb]	41,76	6,13	49,08	6,89	39,98	7,63	-	-	-
CAT [10^4 x IU/g Hb]	71,94	2,74	65,85	1,55	69,10	3,82	-	-	-
SOD1 [IU/g Hb]	702,04	19,83	704,92	14,76	706,47	29,30	-	-	-
cGPx [IU/g Hb]	19,55	1,58	12,89	0,86	15,63	0,90	$p<0,05$	-	$p<0,05$

n-group size
SEM – standard error of the mean

Conclusions

- The abnormal oxidative state is one of the metabolic features of neuroendocrine neoplasms. The highest level of oxidative stress and the enhanced glutathione peroxidase response was observed in the patients with pancreatic NENs, which may be related to the aggressiveness of this tumor. Thus, glutathione-related antioxidant defense might show the strongest protective effect against pancreatic NENs.

Bibliography

1. Pizzino G, Gabriele N et al., *Oxidative Stress: Harms and Benefits for Human Health*, Oxid Med Cell Longev, 2017; 2017:8416763.
2. Kandola K, Bowman A, Birch-Machin MA, *Oxidative stress--a key emerging impact factor in health, ageing, lifestyle and aesthetics*, Int J Cosmet Sci, 2015; 37 Suppl 2:1-8.
3. Perillo B, Di Donato M et al., *ROS in cancer therapy: the bright side of the moon*, Exp Mol Med, 2020; 52(2):192-203.
4. Deponte M, *Glutathione catalysis and the reaction mechanisms of glutathione-dependent enzymes*, Biochim Biophys Acta, 2013; 1830(5):3217-66.
5. Lykkesfeldt J, *Malondialdehyde as biomarker of oxidative damage to lipids caused by smoking*, Clin Chim Acta, 2007; 380:50-8.

miR 511-5p EXPRESSION AS A PREDICTOR OF NUTRITIONAL STATUS DISORDERS IN PATIENTS TREATED WITH INTENSITY-MODULATED RADIATION THERAPHY DUE TO HEAD NECK CANCER.

Marcin Mazurek[1], Radosław Mlak[1], Iwona Homa-Mlak[1],Tomasz Powrózek[1], Anna Brzozowska[2], Teresa Małecka-Massalska[1]

1Department of Human Physiology, Medical University of Lublin, Poland;

2II Department of Radiotherapy, Center of Oncology of the Lublin Region St. John of Dukla, Poland

Introduction

- Cancers located in the head and neck area (HNC) predominantly occur in the pharyngeal, nasopharyngeal, laryngeal and oral regions.[1]
- Due to the fact that HNC patients are usually diagnosed in advanced stages of disease progression, radiation therapy (RT) has been the method of choice in clinical practice. The treatment using sole intensity-modulated radiotherapy (IMRT) allowed the reduction in the percentage of enteral feeding cases, compared to HNC patients treated with three-dimensional conformal radiation therapy (3DC-RT) (49% vs. 72%). [2]
- The malnutrition occurring during RT or C-RT treatment are observed in 44-88% of patients.[3]
- Similar disorders (imbalance between energy intake and expenditure due to conversion of balanced metabolism to catabolism), which result in the progressive loss of fat and muscle tissue underlie cancer cachexia, however, in this case, the inflammatory component seems to play a more important role. [3–5]
- Critical weight loss (CWL) is observed in 57% of patients with HNC undergoing RT (> 5% during RT from start until the 8th week or > 7.5% until the 12th week of treatment). [6,7]
- Monitoring of cancer cachexia biomarkers may allow finding patients with its higher risk, and indicate them as requiring special monitoring of nutritional status and implementation of timely treatment and thus prevent further development of this life-threatening condition.[8]
- However, based on a correlation between the expression of miR-511 and the inflammation, that has been demonstrated already by other authors, we concluded that this miRNA can be involved in the development of nutritional disorders. [9]

Objectives

The aim of the study was to assess the relationship between pretreatment expression of the miR-511-5p and the occurrence of nutritional status disorders in patients with HNC subjected to IMRT.

Methods

60 patients with HNC → IMRT treatment (54-70 Gy dose daily dose 2Gy) → 5 ml blood sample (prior anticancer treatment) → RNA purification (200µl of plasma) → Reverse transcription reaction → Real Time PCR

The level of miRNA 511-5p expression (Real Time PCR) was normalized in miRNA 26a-3p control reaction using 2-ΔΔCt and 2-ΔCt formulas. The MedCalc 15.8 software (MedCalc Software, Belgium) was used to perform statistical analysis of the results. In all analyses, statistical significance was established at p<0.05.

Results

Characteristic of study group:

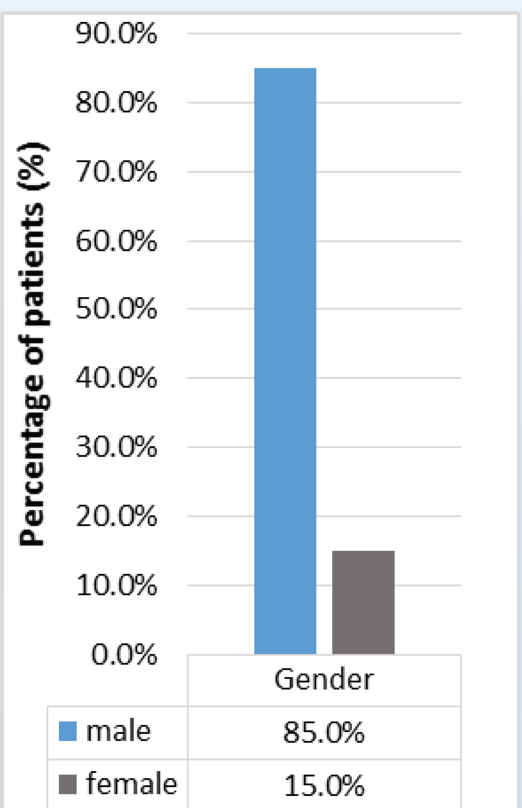

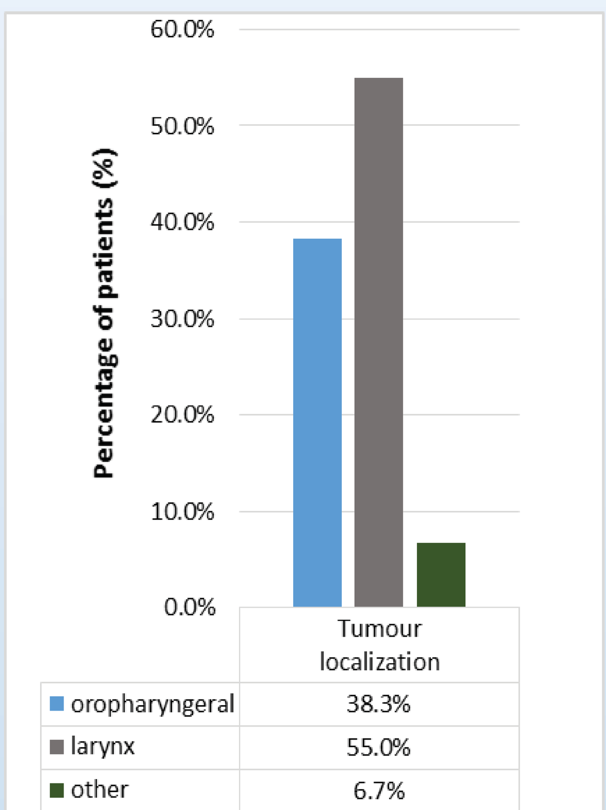

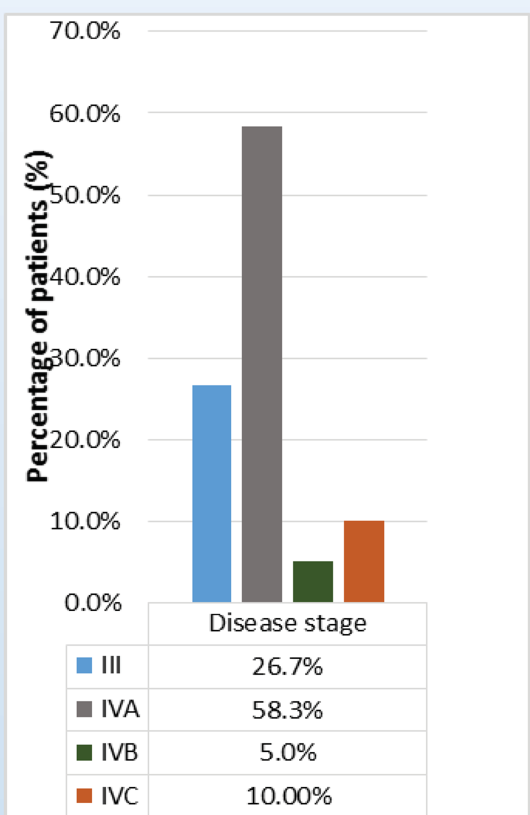

Comparisons of miR-511-5p expression depending on the nutritional status:

- Patients with moderate or severe malnutrition according to SGA showed significantly lower levels of miR511-5p expression compared to patients with normal nutritional status (0.93 vs 6.27; p = 0.0001).
- Patients with severe malnutrition showed significantly lower expression of the studied miR compared to those with normal nutritional status or moderate malnutrition (1.49 vs 0.68; *p* = 0.0251).
- Similarly, patients with CWL showed significantly lower levels of miR511-5p compared to patients without CWL (1.64 vs 0.51; *p* = 0.0025).

The assessment of miR-511-5p expression in predicting the occurrence of nutritional status conducted using ROC analysis with AUC calculation:

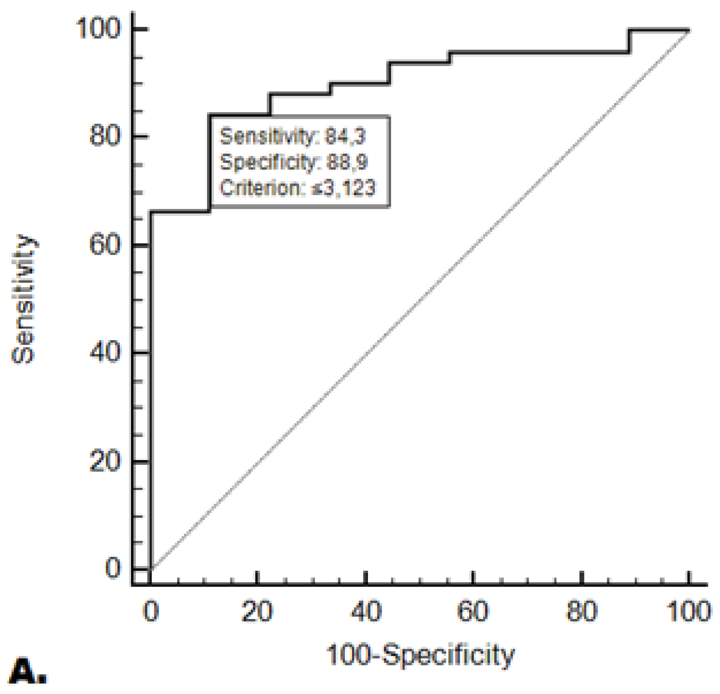

A.

The level of the studied miR expression was 84.3% sensitive and 88.90% specific in pre-dicting the occurrence of moderate to severe malnutrition (AUC = 0.90; p <0.0001).

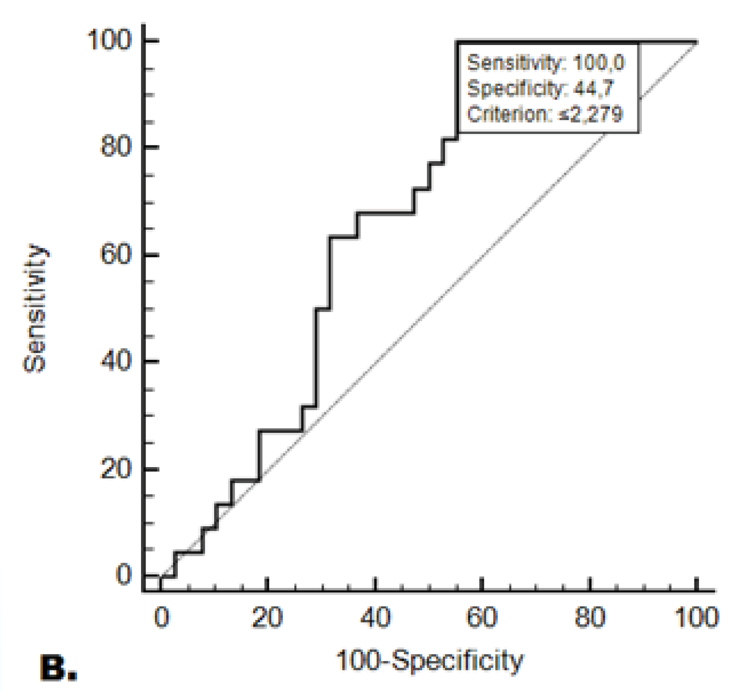

B.

Testing the level of miR511-5p expression enabled the prediction of severe malnutrition with 100% sensitivity and 44.7% specificity (AUC = 0.67; *p* = 0.0110).

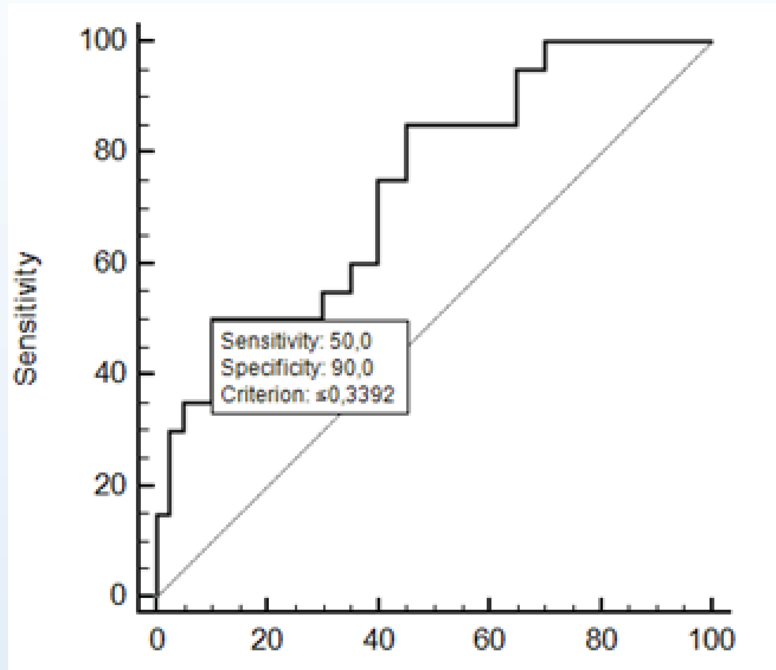

C.

The analysis of this biomarker conducted to predict CWL was characterized by the sensi-tivity of 50% and specificity of 90% (AUC = 0.74; p = 0.0003).

- The lower level of miR511-5p expression was associated with a significantly higher (over 37-fold) risk of moderate and severe malnutrition according to the SGA scale (OR = 37.33; *p* = 0.0013).
- Moreover, the lower level of the tested miR was associated with a 17-fold higher risk of severe malnutrition (OR = 17; *p* = 0.0084).
- In patients with low miR511-5p expression, the risk of developing CWL was more than 7 times higher (OR = 7.36; *p* = 0.0039).

Conclusions

Pretreatment miR-511-5p expression may be a useful parameter in the assessment of the risk of poor nutritional status in patients with HNC undergoing RT.

References

[1]Vigneswaran, N.; Williams, M.D. Epidemiologic trends in head and neck cancer and aids in diagnosis. Oral Maxillofac. Surg. Clin. North Am. 2014, 26, 123–141.
[2]Al-Mamgani, A.; Van Rooij, P.; Verduijn, G.M. The impact of treatment modality and radiation technique on outcomes and toxicity of patients with locally advanced oropharyngeal cancer. Laryngosc. 2013.
[3] Gorenc, M.; Kozjek, N.R.; Strojan, P. Malnutrition and cachexia in patients with head and neck cancer treated with (chemo)radiotherapy. Reports Pract. Oncol. Radiother. 2015, 20, 249–258.
[4]Meza-Valderrama, D.; Marco, E.; Dávalos-Yerovi, V. Sarcopenia, malnutrition, and cachexia: Adapting definitions and terminology of nutritional disorders in older people with cancer. Nutri. 2021, 13, 1–11.
[5] Ni, J.; Zhang, L. Cancer cachexia: Definition, staging, and emerging treatments. Cancer Manag. Res. 2020, 12, 5597–5605.
[6] Jager-Wittenaar, H.; Dijkstra, P.U.; Vissink, A. Critical weight loss in head and neck cancer - Prevalence and risk factors at diagnosis: An explorative study. Support. Care Cancer 2007, 15, 1045–1050.
[7]Langius, J.A.E.; Bakker, S.; Rietveld, D.H.F. Critical weight loss is a major prognostic indicator for disease-specific survival in patients with head and neck cancer receiving radiotherapy. Br. J. Cancer 2013, 109, 1093–1099.
[8] Cao, Z.; Zhao, K.; Jose, I.; Hoogenraad, N.J.; Osellame, L.D. Biomarkers for Cancer Cachexia: A Mini Review. Int. J. Mol. Sci. 2021, 22.
[9]Curtale, G.; Renzi, T.A.; Drufuca, L.. Glucocorticoids downregulate TLR4 signaling activity via its direct targeting by miR-511-5p. Eur. J. Immunol. 2017, 47, 2080–2089.

SILICON - A NOT-ESSENTIAL ELEMENT?

Institution: University of Applied Sciences in Nysa
Author: Marcin Błaszczyk
marcin.blaszczyk@pwsz.nysa.pl

Introduction: As it is well known, silicon is present in some plant tissues, in the skeletons of diatoms, etc. In trace amounts it is also present in the connective tissues of mammals (humans), most (which does not mean in a significant amount) in large arteries, in the aorta. This prompted a logical search for its role in the body. Initially, literally a few papers tried to analyze the subject experimentally. Then thousands of papers were written, almost always theoretical, describing the supposed physiological role of silicon, quoting each other, without adding any new information. It is even beginning to be listed in dietary publications as a micronutrient with a specified minimum daily intake. Nowadays, it has already come to listing silicon as an element necessary for the proper functioning of the body and to describing the symptoms of its deficiency (especially in cosmetological and dietary literature). In the flurry of unproven hypotheses, it is necessary to specific what is actually known about the indispensability of silicon.

Methods: Approximately 150 papers on the importance of silicon to human metabolism werte analysed. For obvious reasons, the list of references does not include numerous duplicate publications, only key ones for the topic.

Text: A review of papers on this topic from the last 15 years shows that the current state of knowledge definitely does not justify attributing such importance to it. The authors mostly refer to the work of R. Jugdaohsingh [1] and reproduce the same theses, taking them as facts. However, the author writes there that the importance of silicon is not actual, confirmed, but "strongly suggested," admitting that "The exact biological role(s) of silicon in bone health is still not clear, although a number of possible mechanisms have been suggested, including the synthesis of collagen and/or its stabilization, and matrix mineralization." Exactly the same claim, about involvement in collagen synthesis, is repeated by almost all other publications on the subject. However, collagen synthesis is well understood, it requires ascorbate, alpha-ketoglutaric acid and Fe^{3+} ions, interacting with proline dioxygenase, for proline hydroxylation (oxygen input). Silicon has no function in these processes. Furthermore, there is no known enzyme in human biochemistry that requires the presence of silicon (as in the case of zinc, nickel, magnesium, manganese, molybdenum, iron, cobalt).

In the context of silicon indispensability, silicon deficiency is currently described as manifesting itself in unspecified nail and hair problems (probably due to old folk medicine beliefs). It is even more incomprehensible to find the role of silicon in collagen synthesis since it is a protein absolutely essential for connective tissues but not for epidermis which synthesizes hair and nails. The effect of silicon on the synthesis of keratin proteins is never mentioned. Studies in the field of cosmetology and nutrition describing the "beneficial" effect of silicon supplements on the condition of hair and nails basically never have a control group, are blind/double-blind, but show a significant improvement in the condition of e.g. hair after a week or two of taking the supplement (this means a few mm of hair growth right next to the skin - a real improvement would not be noticeable earlier than after a few months).

The most serious, always cited, and one of the few experimental papers on which modern review papers are based, dates back 45 years [2, 3]. A study by K. Schwartz found that "day-old deutectomized cockerels fed a purified amino acid diet showed significantly retarded growth and development within 2 to 3 weeks. Chicks fed the same diet plus a silicon supplement showed 50 percent higher growth and normal development." However, as the previously cited R. Jugdaohsingh also writes: "these results have not been subsequently replicated, at least to the same magnitude and thus the essentiality of Si in higher animals remains questionable." [3] Another frequently cited study makes several conjectures about potential mechanisms. [4]

Currently, the greatest emphasis is on research related to bone health (BMD). Attempts are being made to show that silicon supplementation increases bone density. These studies are often methodologically questionable, most often written with the caveat that they were created through sponsorship by the manufacturer of a silicon-containing supplement. In addition, they produce contradictory results, e.g., that BMD increases after supplementation, or, in another paper, does not increase unless in estrogen deficiency (apparently the study is on targeted supplementation for postmenopausal women), still others show that silicon affects bone metabolism, but not bone density.[5, 6, 7] This raises the concern that more and more such papers will be produced to justify the claims of the manufacturers, rather than because of the real value of the research.

One of the most significant factors limiting the possibility of serious research is the extreme difficulty of achieving a silicon-deficient state in the body. [8] Silicon makes up 27.2% of the earth's crust and must of necessity be present, as a component of plant tissues, in every food, and is minimally passively absorbed from the intestines depending on chemical formulation (there are no mechanisms to prevent this, as it is rather chemically inert and not harmful in small doses).[9] It must therefore, of course, go into the blood, and from there - still according to the concentration gradient - to the connective tissues surrounding the blood vessels. Its widespread occurrence precludes a state of silicon "deficiency", which at the same time undermines the sense of research on its supplementation.

Another direction of hypothesis assumes a potential role of silicon in binding of hydroxyl groups of polyols related to metabolism of glycosaminoglycans and collagen in connective tissue, with effects on mineral absorption and metabolism. [10] However, there is no reliable study on this topic. Still other hypotheses speak of a potential role of silicon involving its influence on the expression of selected genes related to connective tissue metabolism. Preliminary studies have appeared on this subject, but they are also controversial, with a strong bias: it is not clear from them whether silicon is the factor, nor whether the effect is only on the selected genes studied, whether it is a natural mechanism or an artifact.

Therefore, review papers invariably conclude: "the specific biochemical or physiological functions of silicon, if any, are largely unknown although generally thought to exist." [11]

In this light, one wonders about the purposeful proliferation of these papers. The logical sequence in scientific descriptions is in the direction from observation, through hypothesis and research, to results and conclusions. In the case of silicon, it is assumed a priori that it has a physiological function. Hypotheses are repeated, but objective observations, reliable, scientific data are lacking, and despite a 50-year history of research, it has not even been possible to confirm the indispensability of silicon or to show any specific mechanism of its action. Perhaps such a role exists. But until it is demonstrated,

Conclusions:

As with all papers on silicon, it falls to conclude with the caveat that further research is needed. However, it is not a matter of "more publications" but rather "more specific research". Perhaps silicon has a role in human metabolism. But until it is demonstrated, it is not justified to claim that it exists, or to encourage its supplementation.

References:
1. Jugdaohsingh R., "Silicon and bone health." J Nutr Health Aging. 2007 Mar-Apr; 11(2): 99–110.
2. Schwarz K., Milne D.B., "Growth promoting effects of silicon in rats." Nature. 972;239:333–334.
3. Carlisle EM., "Silicon: an essential element for the chick." Science. 1972;178:619.
4. Carlisle EM., "Silicon as an essential trace element in animal nutrition." In: Evered D, O'Connor M, editors. Silicon Biochemistry Ciba Foundation Symposium 121. John Wiley and Sons Ltd.; Chichester: 1986. pp. 123–139.
5. So Young Bu et al.. "Effect of Silicon Supplementation on Bone Status in Ovariectomized Rats Under Calcium-Replete Condition" Biol Trace Elem Res . 2016 May; 171(1):138-44.
6. Michael H. Kogut "Silicon supplementation affects mineral metabolism but not bone density or strength in male broilers" PLoS One. **2020; 15(12): e0243007.**
7. Rodella L.F. et al., "A review of the effects of dietary silicon intake on bone homeostasis and regeneration." J Nutr Health Aging . 2014 Nov;18(9):820-6.
8. Lippard S.J., Berg J.M. "Principles of Bioinorganic Chemistry." Mill Valley, CA: University Science Books. 1944; p. 411.
9. N. Boqué et al. "Relative absorption of silicon from different formulations of dietary supplements: a pilot randomized, double-blind, crossover post-prandial study." Sci Rep. 2021; 11: 16479.
10. F.H. "Update on the possible nutritional importance of silicon", J Trace Elem Med Biol . 2014 Oct;28(4):379-82.
11. Martin K.R., "Silicon: The Health Benefits of a Metalloid"Met. Ions Life Sci. 13 (2013) 451-473

SPATIAL ORIENTATION IN ADOLESCENTS

KARAMAN PAGAVA[1], HELEN PHAGAVA[2]

[1]Department of Pediatrics and Adolescent Medicine, Tbilisi State Medical University, Tbilisi, Georgia
[2]Department of Epidemiology and Biostatistics, Tbilisi State Medical University, Tbilisi, Georgia

Spatial orientation and memory is very important for visually impaired persons. It is crucial for planning and adapting behaviour in regards to the environment.

The aim was to study spatial orientation in early and late blind adolescents.

Materials and Methods.

Participants n=16, 8 early blind (2 girls (12 and 17 years old) and 6 boys (10,10,10,11,11,17 yeas old) and 8 late blind adolescents (2 girls (12 and 19 years old) and 6 boys (10,14,15,18,18,19 years old). In total 4 girls and 12 boys, age range from 10 to 19.

Orientation in the locomotor space was studied in a closed room by means of changing location of the poles with toys. The changes were: 1) nothing; 2) 1 pole was moved closer to the center; 3) swapping 2 toys; 4) all poles moved closer to the center.
Orientation in the manipulatory space was studied using the rotatable table and changing placement of the toys on the table. The changes were: 1) nothing; 2) 1 toy was moved closer to the center; 3) swapping 2 toys. The participant had to make guess from 4 positions: 1) sitting in the initial position; 2) sitting in the initial position with table turned by 180 degrees; 3) sitting on the opposite side and getting there from the right; 4) sitting on the opposite side and getting there from the left.
There was music on when the change was being done and the investigator was producing extra noise to cover the real change.
Sequence of changes and positions (in case of manipulatory space exploration) was being produced randomly and prepared in advance on the special cards.
Participants had to explore, remember location and after the change, try to identify it. Performance as well as the strategy of the participants has been studied.
Responses were registered by the investigator. Video recording was performed. Before the study informed consent was obtained.

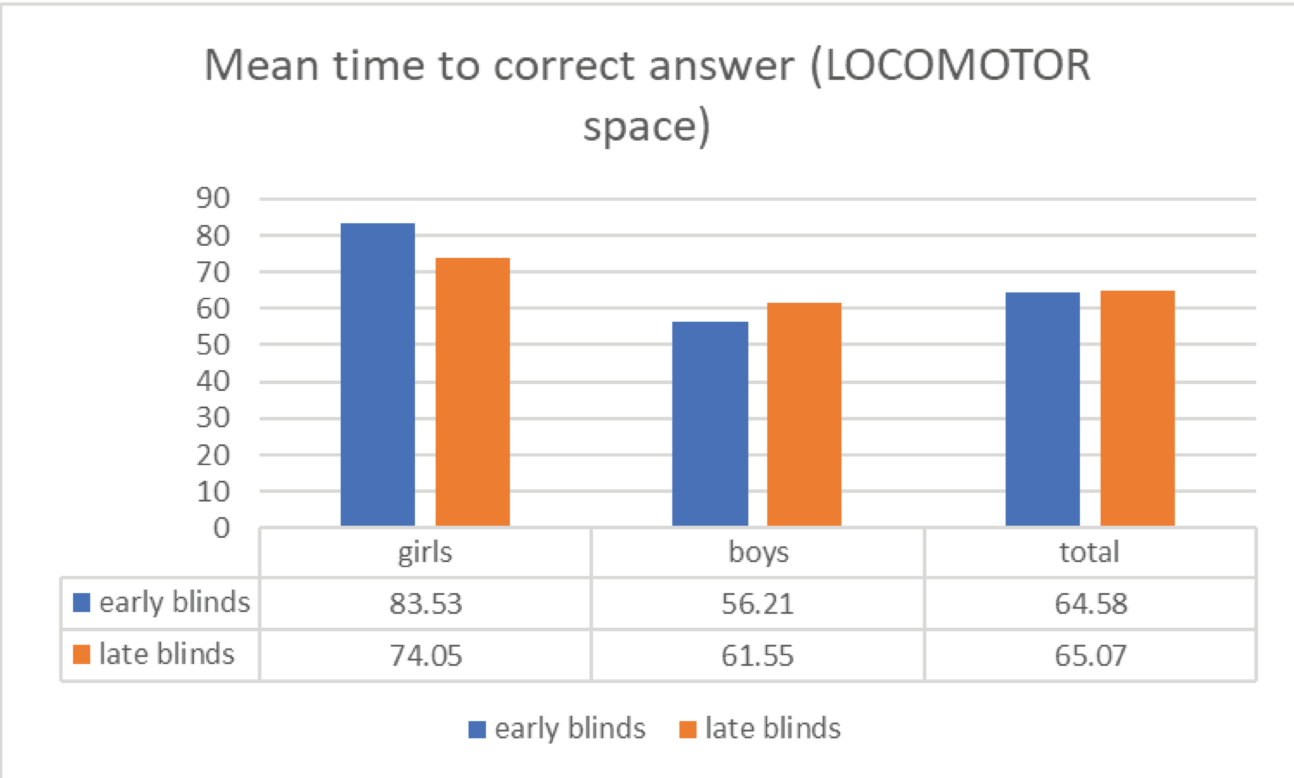

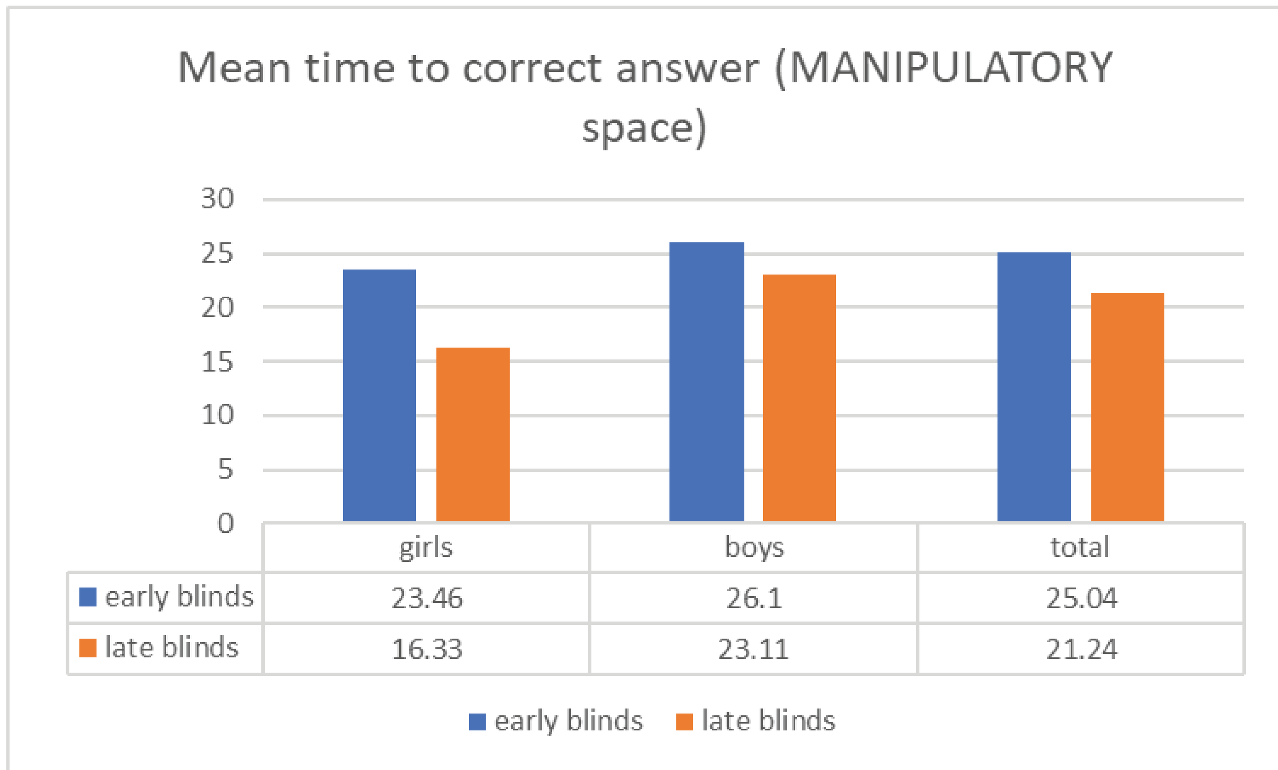

When studying locomotor space, it was found out that both the early and late blinds were better in detecting change when it consisted in swapping the objects. When studying manipulatory space, the most difficult to detect was moving the toy closer when the table was turned by 180 degrees.

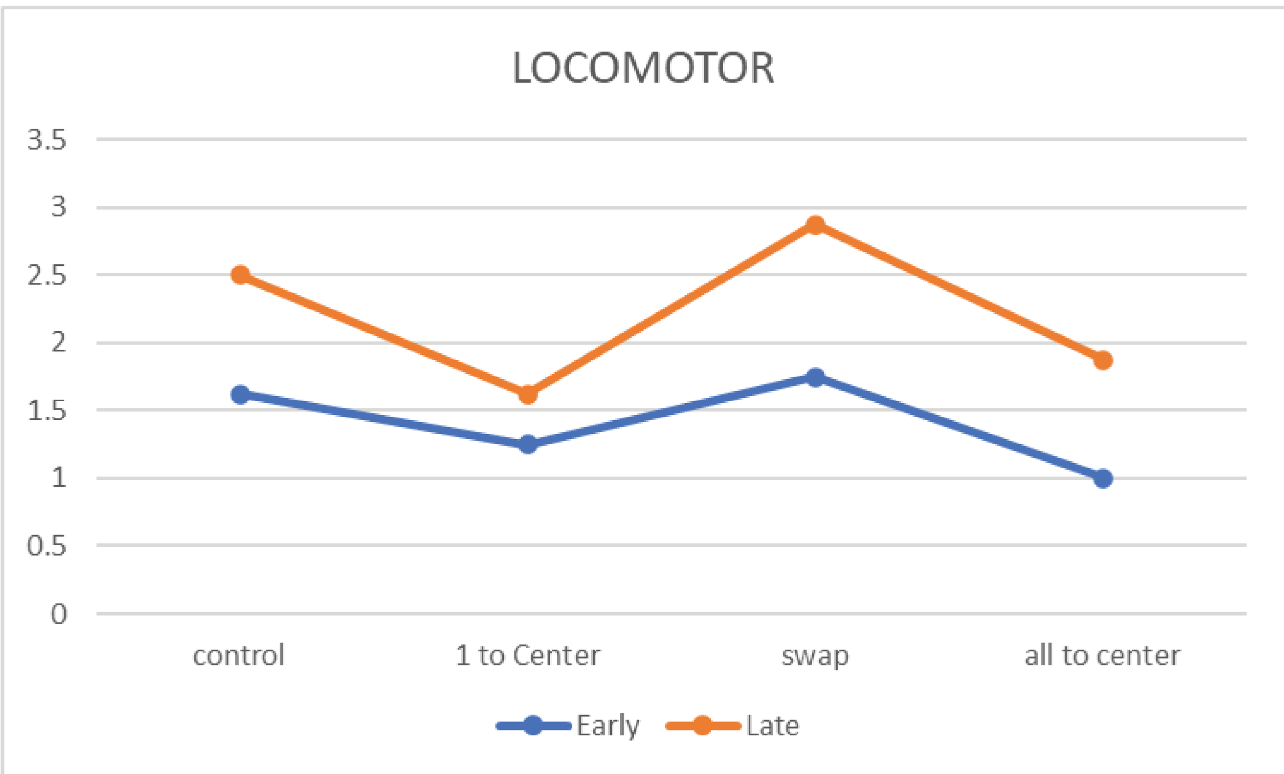

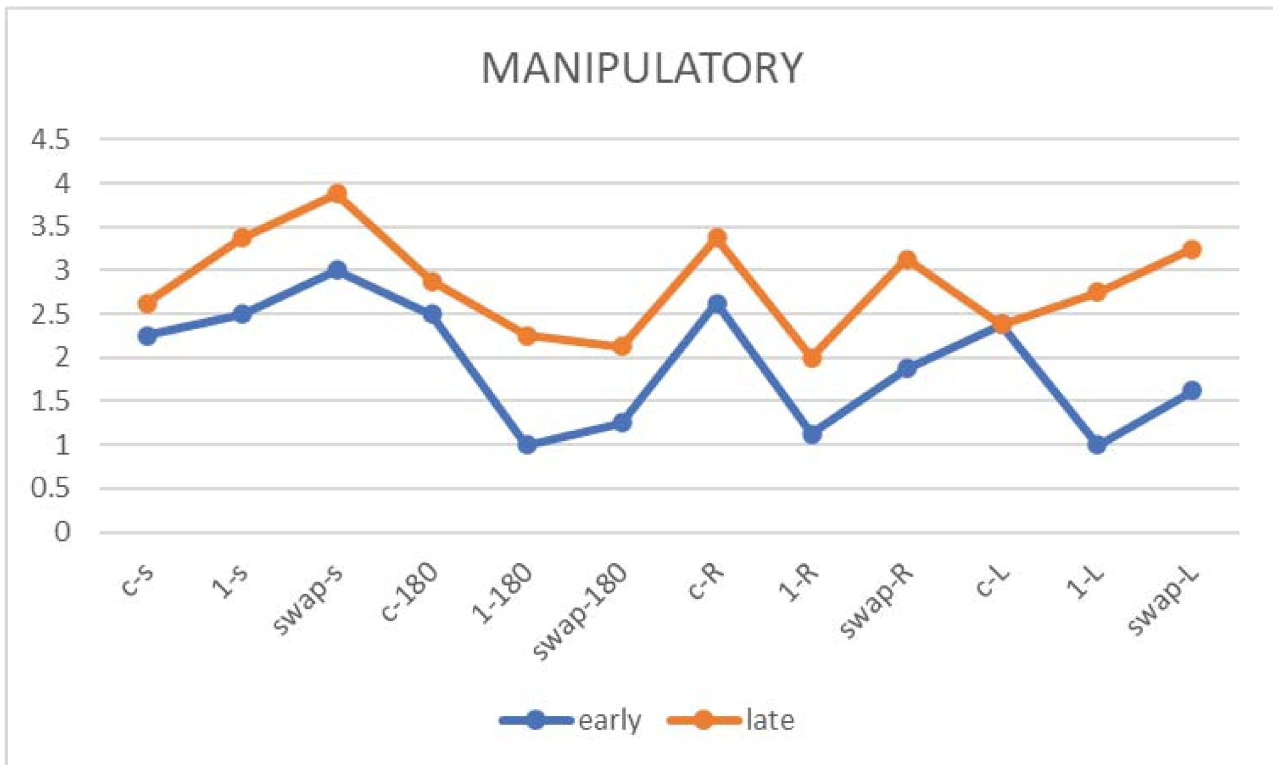

Frequency of correct answers

There was no difference in applied strategy. Both groups were using almost equally both "back and forth" and "cyclic" strategy of exploration.

Conclusion.
Findings have shown that the late blind adolescents show better spatial orientation in both, locomotor and manipulatory spaces.

References.
1. Gaunet F, Martinez JL, Thinus-Blanc C. Early-blind subjects' spatial representation of manipulatory space: exploratory strategies and reaction to change. Perception. 1997;26(3):345-66. doi: 10.1068/p260345. PMID: 9282231.
2. Gaunet F, Thinus-Blanc C. Early-blind subjects' spatial abilities in the locomotor space: exploratory strategies and reaction-to-change performance. Perception. 1996;25(8):967-81. doi: 10.1068/p250967. PMID: 8938009.

Acknowledgements: Prof. Catherine Thinus-Blanc, CNRS, France; James S. McDonnell Foundation

HOW VISION AFFECTS OUR TASTE SENSITIVITY?

Patrycja Redmer, Emilia Leszkowicz

Dept. Animal and Human Physiology, University of Gdańsk, Poland

There is little doubt that our perception of food and drink is affected by what we see. We hypothesised that visual influence on food perception is partially associated with changes in taste sensitivity thresholds, which was suggested by a study with congenitally blind people (Gagnon et al., 2013).

To test our hypothesis we studied the taste recognition threshold (concentration at which a given taste is recognized) under two conditions: in subjects (n=24, 18-45 years old) with (1) open eyes and (2) closed eyes. We expected that taste recognition thresholds would differ between those conditions. Five basic tastants: sweet (sucrose, 0.94-12.00 g/l), salty (sodium chloride, 0.34-2.00 g/l), sour (citric acid, 0.2-0.6 g/l), bitter (caffeine extract, 0.09-0.27 g/l) and umami (monosodium glutamate, 0.17-1.00 g/l) were dissolved in mineral water, and five sets of six different concentrations were prepared. The sensory testing was done in two conditions: first, when participants had their eyes open, and next, when they had their eyes closed.

Number of participants whose taste recognition threshold was lower in Eyes-open or Eyes-closed condition

	Bitter	Sweet	Salty	Sour	Umami
Eyes-open	5	8	7	5	9
Eyes-closed	13	14	13	9	6

Bitter taste recognition threshold

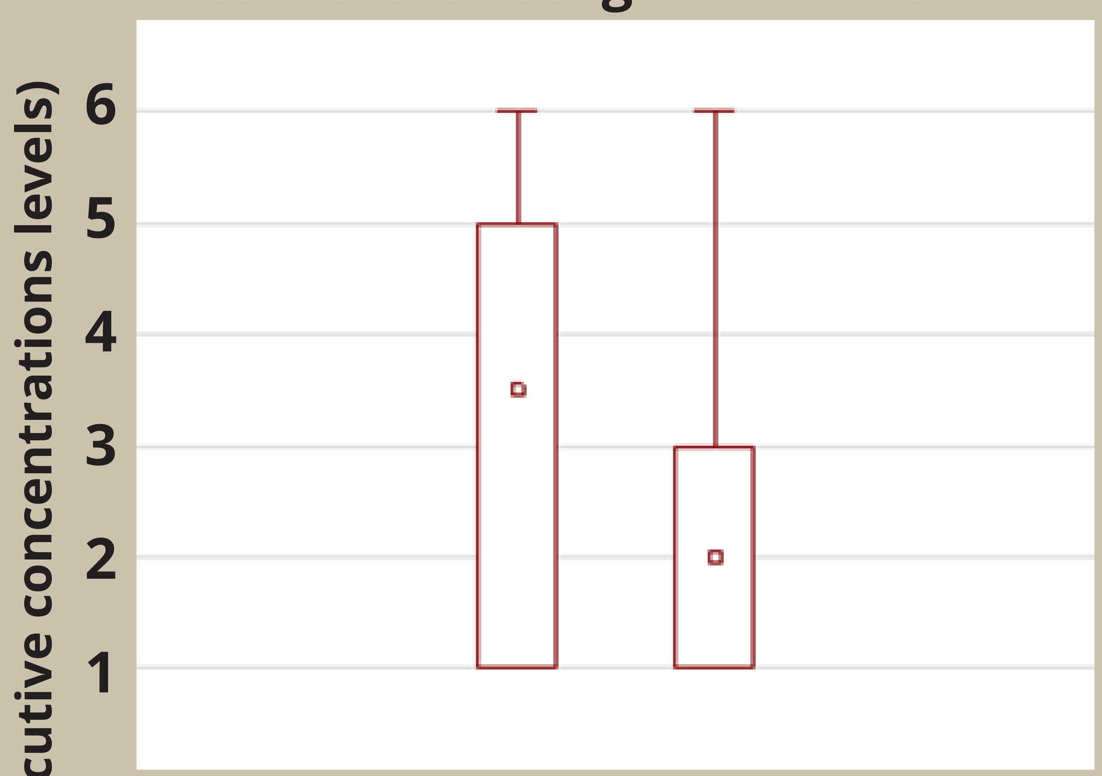

Sweet taste recognition threshold

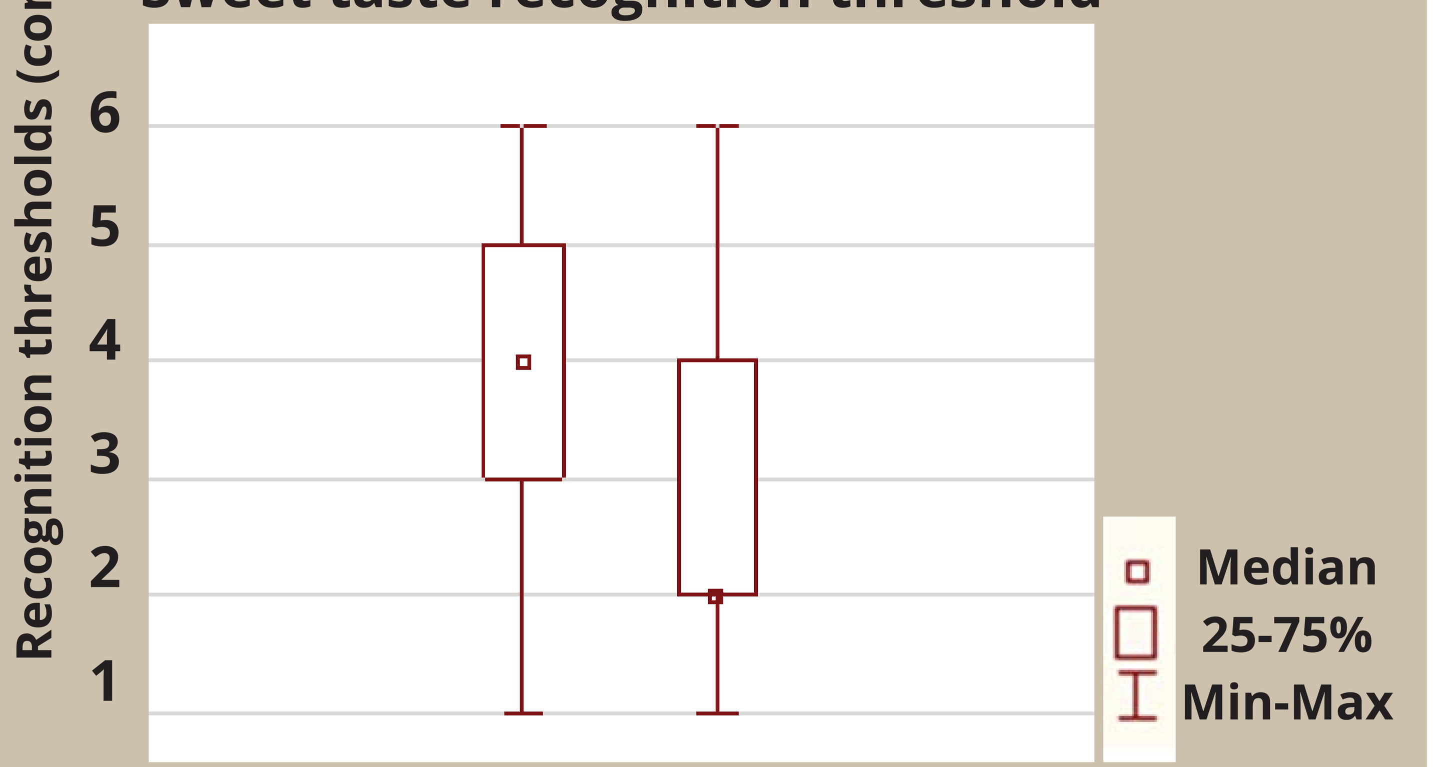

Bitter taste was recognized at lower concentrations in the closed-eyes than open-eyes condition (a Wilcoxon signed-rank test, the median open-eyes ranks were higher than the median closed-eyes ranks, T=19, Z=2.72, p=0.006). For sweet taste, there was a clear tendency to identify the taste at a lower concentration with eyes closed (14 subjects) than with eyes open (8 subjects), though the difference did not reach a significance level of p=0.05 (a Wilcoxon signed-rank test T=58.8, Z=1.74, p=0.08). Differences in recognition thresholds of salty, sour and umami tastes were less pronounced.

Our results suggest that vision may change taste recognition thresholds for some of the basic five tastes, particularly bitter and sweet, which could partially account for visual influence on taste perception. Yet, contrary to previous studies, taste sensitivity seems higher rather than lower when vision is not involved in taste perception. Further study is foreseen with a larger group of subjects to obtain more conclusive outcomes.

Gagnon L, Kupers R, Ptito M. Reduced taste sensitivity in congenital blindness. Chem Senses. 2013; 38(6): 509-517.